Proteomic Technology Applications For Fisheries Research

Joseph Banoub, Trevena Youssef, and Abanoub Mikhael

Science Branch, Newfoundland and Labrador Region
Fisheries and Oceans Canada,
Northwest Atlantic Fisheries Centre,
80 East White Hills Road,
St. John's, NL, Canada A1C 5X1

2022

Canadian Technical Report of
Fisheries and Aquatic Sciences 3465

Fisheries and Oceans Canada | Pêches et Océans Canada

Canada

Canadian Technical Report of Fisheries and Aquatic Sciences

Technical reports contain scientific and technical information that contributes to existing knowledge but which is not normally appropriate for primary literature. Technical reports are directed primarily toward a worldwide audience and have an international distribution. No restriction is placed on subject matter and the series reflects the broad interests and policies of Fisheries and Oceans Canada, namely, fisheries and aquatic sciences.

Technical reports may be cited as full publications. The correct citation appears above the abstract of each report. Each report is abstracted in the data base *Aquatic Sciences and Fisheries Abstracts*.

Technical reports are produced regionally but are numbered nationally. Requests for individual reports will be filled by the issuing establishment listed on the front cover and title page.

Numbers 1-456 in this series were issued as Technical Reports of the Fisheries Research Board of Canada. Numbers 457-714 were issued as Department of the Environment, Fisheries and Marine Service, Research and Development Directorate Technical Reports. Numbers 715-924 were issued as Department of Fisheries and Environment, Fisheries and Marine Service Technical Reports. The current series name was changed with report number 925.

Rapport technique canadien des sciences halieutiques et aquatiques

Les rapports techniques contiennent des renseignements scientifiques et techniques qui constituent une contribution aux connaissances actuelles, mais qui ne sont pas normalement appropriés pour la publication dans un journal scientifique. Les rapports techniques sont destinés essentiellement à un public international et ils sont distribués à cet échelon. II n'y a aucune restriction quant au sujet; de fait, la série reflète la vaste gamme des intérêts et des politiques de Pêches et Océans Canada, c'est-à-dire les sciences halieutiques et aquatiques.

Les rapports techniques peuvent être cités comme des publications à part entière. Le titre exact figure au-dessus du résumé de chaque rapport. Les rapports techniques sont résumés dans la base de données *Résumés des sciences aquatiques et halieutiques.*

Les rapports techniques sont produits à l'échelon régional, mais numérotés à l'échelon national. Les demandes de rapports seront satisfaites par l'établissement auteur dont le nom figure sur la couverture et la page du titre.

Les numéros 1 à 456 de cette série ont été publiés à titre de Rapports techniques de l'Office des recherches sur les pêcheries du Canada. Les numéros 457 à 714 sont parus à titre de Rapports techniques de la Direction générale de la recherche et du développement, Service des pêches et de la mer, ministère de l'Environnement. Les numéros 715 à 924 ont été publiés à titre de Rapports techniques du Service des pêches et de la mer, ministère des Pêches et de l'Environnement. Le nom actuel de la série a été établi lors de la parution du numéro 925.

Canadian Technical Report of Fisheries and Aquatic Sciences 3465

2022

Proteomic Technology Applications For Fisheries Research

By

Joseph Banoub,[1,2,3*] Trevena Youssef, [2]Abanoub Mikhael[3]

[1] Science Branch, NL Region, Fisheries and Oceans Canada, PO Box 5667

[2] Biochemistry Department, Memorial University of Newfoundland, St John's, Nl.

[3] Chemistry Department, Memorial University of Newfoundland, St John's, Nl.

Cat. No. Fs97-6/3465E-PDF ISBN 978-0-660-42187-2 ISSN 1488-5379

Correct citation for this publication:

Banoub, J., Youssef, T., Mikhael, A. 2022. Proteomic Technology Applications For Fisheries Research. Can. Tech. Rep. Fish. Aquat. Sci. 3465: xi + 668 p.

Table of Contents

Abstract

Banoub, J., Youssef, T., Mikhael, A. 2022. Proteomic Technology Applications For Fisheries Research. Can. Tech. Rep. Fish. Aquat. Sci. 3465: xi + 668 p.

Proteins perform many cellular functions, and the proteome, unlike the genome, changes dynamically and constantly. Proteomics is best defined as analysis of the entire set of proteins expressed at a defined time under specific conditions. Proteomics also includes studies of all the variants, post-translational modifications and the characterization of protein-protein interactions. The proteome integrates changes in gene expression, mRNA stability, post-translational modifications and protein turnover. By studying the whole proteome, potentially unforeseen responses can be observed, and new mechanistic hypotheses can be generated. Proteomics has been applied primarily to investigate the physiology, developmental biology and the impact of contaminants in fish model organisms, such as zebrafish, as well as in some commercial species produced in aquaculture, mainly salmonids and cyprinids.

Unfortunately, the lack of previous genetic information on most fish species has been a major drawback for a more general application of the different proteomic technologies currently available. In biological research, many teleosts of interest and with potential application in aquaculture hold unique physiological characteristics that cannot be directly addressed from the study of small laboratory fish models.

This technical report describes concise proteomic approaches that have been used to investigate diverse biological questions in model and non-model fish species.

Resumé

Banoub, J., Youssef, T., Mikhael, A. 2022. Proteomic Technology Applications For Fisheries Research. Can. Tech. Rep. Fish. Aquat. Sci. 3465: xi + 668 p.

Les protéines exercèrent de nombreuses fonctions cellulaires et contrairement au génome, le protéome change de manière dynamique et constante. La protéomique est définie comme l'analyse de l'ensemble des protéines exprimées à un moment défini par une cellule dans des conditions spécifiques. La protéomique comprend l'étude des variations, modifications post-traductionnelles et caractérisation des interactions protéine-protéine. Le protéome intègre les changements dans l'expression des gènes, stabilité de l'ARNm, modifications post-traductionnelles et renouvellement des protéines.

En étudiant l'ensemble du protéome, des réponses potentiellement imprévues peuvent être observées et de nouvelles hypothèses mécanistes peuvent être générées. La protéomique peut être appliquée pour étudier la physiologie, biologie du développement et l'impact des contaminants dans les organismes poissons modèles et espèces commerciales.

Le manque d'informations génétiques pour la plupart des espèces de poissons a été un inconvénient majeur pour une application plus générale des différentes technologies protéomiques disponibles. Dans la recherche biologique, de nombreux téléostéens d'intérêt ayant une application potentielle en aquaculture, possèdent des caractéristiques physiologiques uniques qui ne peuvent pas être directement comparés à partir de l'étude de petits modèles de poissons de laboratoire.

Ce rapport technique décrit les approches protéomiques concises utilisées pour étudier diverses questions biologiques des espèces de poissons modèles et non-modèles.

1. Introduction

Omics technology is an umbrella term for modern technologies like genomics, transcriptomics, proteomics and metabolomics. These techniques have received increasing recognition because of their potential to unravel novel mechanisms in biological science (Prasanna-Mohanty et al., 2019) The birth of the novel proteomics technology has provided a significant impetus and permitted great advances in structural and biofunctional protein studies. Proteomics research is the study of protein products expressed by the genome. The term 'proteome' originates from Protein, and it complements the genome. Indeed, proteomics arose as a leading technology following the post-genomic era because of the central role of proteins and protein-protein interactions in cell physiology.

Interestingly, the DNA/RNA-based functional genomic approaches, including all the physiological and pathological processes, did not provide information concerning protein expression levels (Brewis & Gadella, 2010) After unravelling the human genome project, researchers were disappointed to find that all the promises concerning our novel understating of life sciences were not as advanced as was hoped. The human genome sequences were not enough to elucidate genes' biochemical functions, so this was frustrating.

Following the hypothesis of "one gene = one protein," there should be at least ~20,000 nonmodified (canonical) human proteins. However, Wilkins *et al.* predicted that the average number of protein forms per gene could be three or more for humans (Wilkins et al., 1996a) Evidently, this does not fit into the dogma of 'one gene, one protein.' Consequently, it is not astonishing that the analysis of mRNA often does not reflect the protein content of the cell. This explains the lack of consensus in many correlation studies between mRNA and protein expression levels (Graves & Haystead, 2002) Unfortunately, there is an astonishingly high number of proteins (>300 000) that originate from a far lower number of protein-encoding genes (22,000–25,000 in humans) (Brewis & Gadella, 2010).

The generation of multiple protein forms typically arises from the two major steps: the processing of mRNA and the level of translation (Figure 1). The mRNA can be subjected to numerous structural modifications throughout the first step, such as alternative splicing, polyadenylation, and mRNA editing (insertion/deletion or deamination). These structural modifications result in producing several different protein isoforms which are formed from a single gene. After the translation process, the formed proteins are subjected to post-

translational modifications, which allow the fine-tuning of signalling pathways and networks within cells. There are at least 200 modifications that have been described in the literature. These modifications occur by lipid modification, glycosylation, phosphorylation, ubiquitination, and association with other proteins or different types of molecules. Also, post-translation modifications are caused by other essential sources of protein heterogeneity, such as proteolysis and compartmentalization. Disturbances to the latter can result in miso localization of proteins, leading to the disorder of cells and tissues (Conibear, 2020; Krishna & Wold, 1993).

A

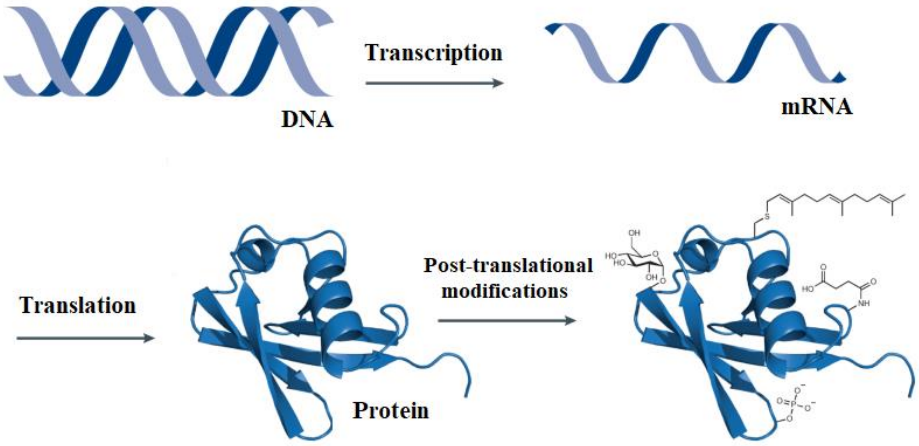

B

	AGA									UUA					AGC				
	AGG									UUG					AGU				
GCA	CGA						GGA			CUA				CCA	UCA	ACA			GUA	
GCC	CGC						GGC		AUA	CUC				CCC	UCC	ACC			GUC	UAA
GCG	CGG	GAC	AAC	UGC	GAA	CAA	GGG	CAC	AUC	CUG	AAA		UUC	CCG	UCG	ACG		UAC	GUG	UAG
GCU	CGU	GAU	AAU	UGU	GAG	CAG	GGU	CAU	AUU	CUU	AAG	AUG	UUU	CCU	UCU	ACU	UGG	UAU	GUU	UGA
Ala	Arg	Asp	Asn	Cys	Glu	Gln	Gly	His	Ile	Leu	Lys	Met	Phe	Pro	Ser	Thr	Trp	Tyr	Val	stop
A	R	D	N	C	E	Q	G	H	I	L	K	M	F	P	S	T	W	Y	V	

Figure 1. A. Schematic representation of the generation of proteins from DNA(Conibear, 2020).,B. The standard one-letter abbreviation for each amino acid is presented below its three-letter abbreviation (Alberts et al., 2002).

Proteomics research has been divided into three major studies: protein expression proteomics (or profiling proteomics), structural proteomics, and functional proteomics. Protein expression proteomics concerns the study of the differences in protein expression relating to physiological or (such as disease) or in response to experimental factors (Forné et al., 2009; Graves & Haystead, 2002) Structural proteomics deals with the characterization of protein-protein

interactions, which usually involve initially the elucidation of the tertiary structure of proteins, followed by studying the structure of either the protein complexes and/or proteins present in a specific cellular organelle. Functional proteomics is an important task and is regarded as a rather broad term for studying specific proteomic approaches dealing with the characterization of specific types of proteins and attempting to understand post-translational changes. This approach has also been described as targeted, restrictive, or directional proteomics. It is beneficial when addressing specific issues such as the study of phosphorylated proteins during motility activation in fish (Zilli et al., 2008a).

Unlike nucleic acids, proteins are an extremely diverse collection of compounds with respect to their chemical and physical properties. It is not astonishing to conceive that a field that allows "the systematic identification and characterization of proteins for their structure, function, activity and molecular interactions" (Peng et al., 2003) should be allowed to avail with a wide spectrum of novel methods that continue to be developed at a brisk pace. In general it is understood that proteomics research provides a very clear snapshot of the organism's state of being and, in principle at least, maps the entirety of its adaptive potential and mechanisms (Sveinsdóttir et al., 2012).

In this review, high-throughput, gel-free methods, mass spectrometry and tandem mass spectrometry (Peng et al., 2003), and protein arrays (Lee & Nagamune, 2004), hold great promises. The "classic or conventional proteomics approach" will be used to describe the process of two-dimensional electrophoresis (2DE) followed by protein identification via peptide mass fingerprinting of trypsin digests (PMF) which will remain the workhorse of most proteomics work, largely because of its high resolution, simplicity, and mass accuracy (Sveinsdóttir et al., 2012) Several studies on the advances and prospects of proteomics within various fields of study are available. Some recent ones include (J. S. Andersen & Mann, 2006; Balestrieri et al., 2008; Beretta, 2009; Bogyo & Cravatt, 2007; Drabik et al., 2007; Ikonomou et al., 2009; Issaq & Veenstra, 2008; Jorrín-Novo et al., 2009; Latterich et al., 2008; López, 2007; Malmström et al., 2007; Mamone et al., 2009; Premsler et al., 2009; M. P. W. Smith et al., 2009; J. Wang et al., 2006; Wilm, 2009; Diwan, 2021; H. Li et al., 2021; Natnan et al., 2021; Tsang et al., 2020; R. Xu et al., 2020; Forné et al., 2010; Giacometti et al., 2013; Martyniuk & Denslow, 2009a; Nessen et al., 2016).

In genral, proteomics will allow scientists to build and test better hypotheses, with the ultimate goal to find better solutions to challenges in agricultural sciences, medicine and environmental management. Also, we would like to reiterate that proteomics offers unique information on the expression, posttranslational modifications, interactions, organization, and functions of proteins.

In conclusion, proteomics research has emerged as a powerful tool for the study of biological systems and their dynamics in different conditions. Therefore, this technology has been increasingly used to address different questions related to fish biology during the last years.

1.1. General Clarifications on Proteomics

The proteome is the total set of proteins expressed by a genome in a cell, tissue, or organism. The study of the proteomes permits the association of distinct proteins or groups of proteins to a specific disease or toxic environmental exposure (Moseley et al., 2010; Wasinger et al., 1995; Wilkins et al., 1996b) These groups of expressed proteins can be used as biomarkers.

It is currently accepted that comparing the proteome (specific protein patterns) of any organism measured under stressed conditions versus unstressed controls allows the detection of definite changes to the protein expression and facilitates understanding of the fundamental modes of action (Blackstock & Weir, 1999) The proteome approach represents a significant paradigm shift in molecular biology. It targets a particular family of proteins that provides qualitative and quantitative views on the whole proteome, which is essential for the organism's life and function combined with transcriptomic and metabolomic data. This global protein information provides a truly comprehensive approach to understanding an organism's life cycle.

Conventional proteomics analysis usually targets proteins with a molecular mass >10 kDa. Analysis of peptides and small proteins with a molecular mass between 0.5 and 15 kDa is the subject of a related discipline termed ''peptidomics'' (Kennedy, 2002; Schulz-Knappe et al., 2001; Shekhar, 2017) Compared to established methods such as histology and clinical chemistry, the proteomics approach provides numerous valuable benefits, such as faster screening for toxic effects and the possibility to detect toxic effects at significantly lower doses (Domon & Aebersold, 2006; Kennedy, 2002) Moreover, when combined with conventional histopathology and clinical chemistry methods, proteomics allows one to gain new insights into toxic mechanisms and

distinguish between species-specific effects, thus providing a more accurate risk assessment (Kennedy, 2002).

In general, proteomics toxicological applications can be divided into two classes (Kennedy, 2002) The first class is the investigative study to identify new molecular targets for the various toxic substances and to provide insights into their mechanisms of action. The second class is concerned with screening and predictive toxicology, which measures the specific protein expression patterns changes. This second class permits the identification of toxicological biomarkers and compounds which responsible for their appearance and study structure-activity relationships (SARs) within a group of chemical compounds (Kennedy, 2002).

The field of proteomics ranges from ”global” to ‘‘targeted’’ modes of protein analysis. In the global analysis mode, the main aim is to identify a maximum number of proteins, whereas the ‘‘targeted’’ mode offers the opportunity to look at sub-proteomes; for example, proteins in organelles, the nucleus, or proteins that are part of signalling pathways. It is essential to note that one important and measurable attribute of a protein is its quantity within a limited cell volume. Hence, measuring the concentration difference between the highest and lowest abundance proteins (also defined as dynamic range) can reach ten orders of magnitude (Lipton et al., 2002; Nesatyy & Suter, 2008) As a result, the design and completion of any proteomics experiment should consider the dynamic concentration range needed, which should be adjusted in the experimental protocol. This will achieve the optimal separation of the proteins and increase their chance of identification (Nesatyy & Suter, 2008; Wu & Han, 2006) In addition to a vast dynamic range, other aspects contribute to the difficulties in analyzing the proteome. For example, amino acids, which are the building blocks of proteins, can also be subjected to post-translational modifications (PTMs), such as phosphorylation and glycosylation. These PTMs affect the protein polarity, hydrophobicity, pI, the protein’s three-dimensional structure, and its affinity to ligands (Nesatyy & Suter, 2008) Moreover, proteins are constantly being synthesized and degraded, adding time as another dimension to the problem of understanding signalling pathways in a cell or organism. The challenges mentioned above encountered when trying to characterize very complex protein mixtures were met by significant improvements in separation techniques, mass spectrometry, and bioinformatics, as described below (Nesatyy & Suter, 2008).

1.2. **Mass Spectrometry-Based Proteomics**

Mass spectrometry-based comparative proteomics and their approaches, advances and applications have been used extensively in fisheries research over the last decades. It offers rapid and sensitive qualitative and quantitative protein characterization combined with separation techniques such as electrophoresis and liquid chromatography. The following section will provide in-depth details about different proteomic methodologies that have been used in fisheries research.

In this review, we will focus mainly on using the classical MS-proteomic approach, which starts with the two-dimensional gel electrophoresis (2-DGE) followed by protein identification via peptide mass fingerprinting of trypsin digests (Figure 2). In this approach, after extracting the proteins from specific fish tissue, these proteins are separated by two-dimensional gel electrophoresis (2DGE). Any protein of interest can be excised from the gel and degraded by trypsin or other suitable enzymes. Mass spectrometry (MS) analyzes the resulting peptides, which creates a valuable peptide mass fingerprint for protein identification (Sveinsdóttir et al., 2012; C. Xu et al., 2019) Additionally, peptides can be selected for tandem mass spectrometry (MS/MS) to support the protein identification and sequencing process. In general, proteomic structures characterization using mass spectrometry techniques offers an unique advantage of providing an assumption-free determination of the stoichiometries present in the analyte, while the peak intensities inform on the relative abundance of each species in solution. Electrophoresis and MS-based proteomics will be discussed in detail in the following section.

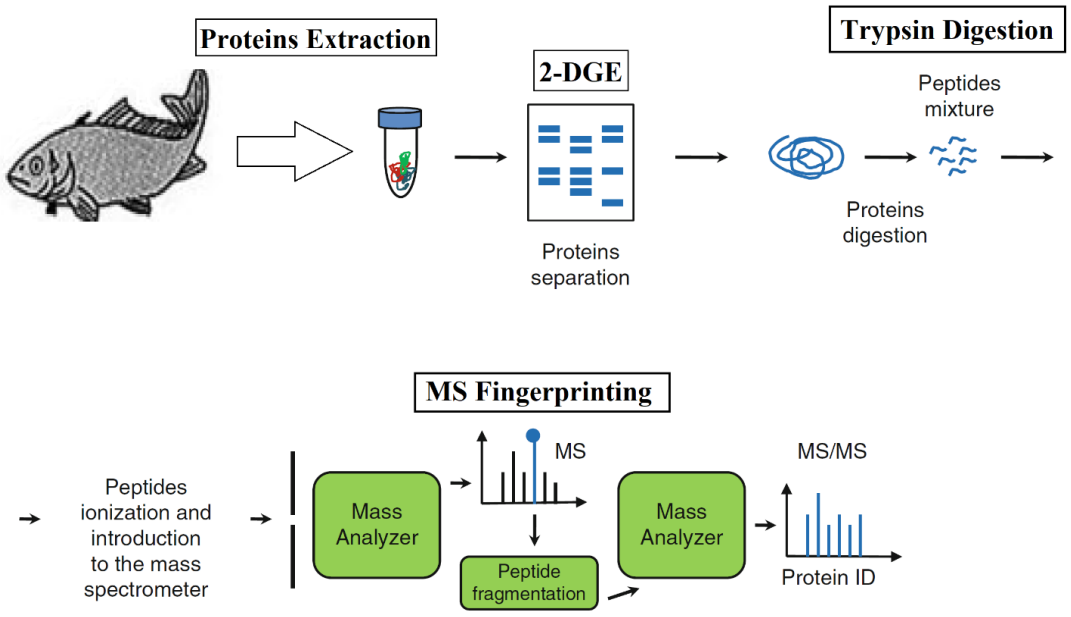

Figure 2. Schematic representation of the classical MS-proteomic approach (C. Xu et al., 2019).

1.2.1. 2-Dimensional Gel Electrophoresis (2-DGE)

The two-dimensional gel electrophoresis is a powerful tool that simultaneously separates hundreds or even thousands of proteins (Görg et al., 2000) 2-DGE generally separates a complex mixture of proteins based on their isoelectric point (pI) in the horizontal dimension and their masses in the vertical dimension (Figure 3). It should be noted that the conventional or the most used 2-DGE type in proteins separation is sodium dodecyl sulphate-polyacrylamide gel electrophoresis (SDS-PAGE). The resulting protein spots can be visualized through staining and analyzed by any 2-DGE available commercial image analysis software such as Progenesis SameSpots (Nonlinear Dynamics), PDQuest (Bio-Rad Laboratories), and DeCyder (GE Healthcare). This analysis is useful in comparing the abundance of individual proteins from different samples, from which upregulation or downregulation of these proteins can be detected.

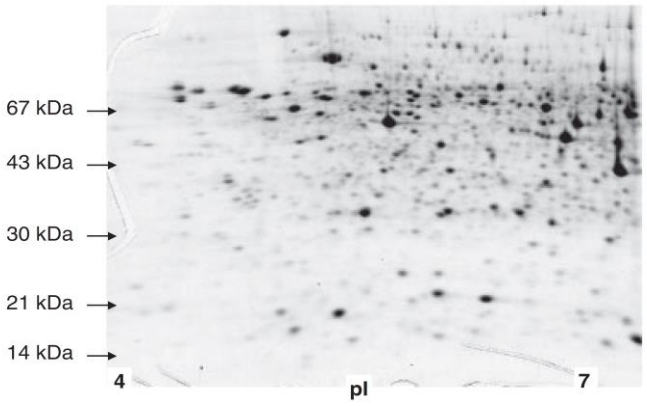

Figure 3. A two-dimensional electrophoresis protein map of rainbow trout (Oncorhynchusmykiss) liver proteins with pI between 4 and 7 and molecular mass about 10–100 (Sveinsdóttir et al., 2012).

Gel-to-gel variation due to running time and separation in 2D gel electrophoresis is an obstacle in comparing spots among gels. Different gel electrophoresis (DIGE) was developed to reduce this variation. A single gel is used to compare protein abundance in control and treatment samples (Ünlü et al., 1997; Westermeier & Marouga, 2005) In this technique, control, treatment, and a pooled internal standard are labelled and/or tagged with three different fluorophores (e.g. cyanins 2, 3, and 5) (Figure 4). It should be noted that the pooled internal standard is composed of all possible detectable proteins in the experiment prepared by mixing equal aliquots from the control and the treatment samples. This standard is added to the control and treatment protein mix before the electrophoresis separation.

The use of three different dyes, which fluorescing at different wavelengths, allows the identification of differentially expressed proteins on the same gel. This identification can be accomplished by overlaying different fluorescent images (McNamara et al., 2010; Robotti & Marengo, 2018; Westermeier & Marouga, 2005).

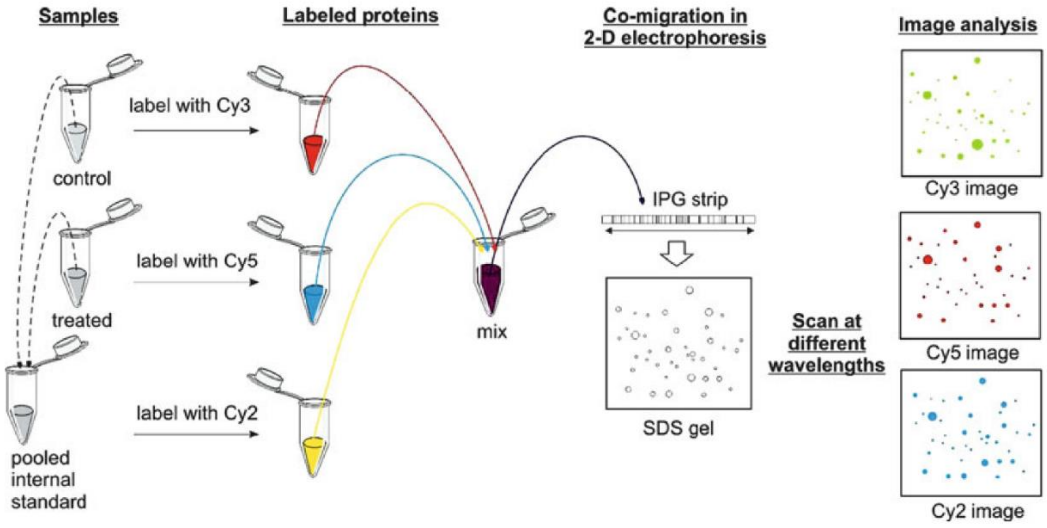

Figure 4. Schematic representation of 2-D difference gel electrophoresis in one gel (Westermeier & Marouga, 2005).

1.2.2. Proteomics Strategies

To date, various efficient and effective MS-based proteomics strategies have been developed to tackle different biological and analytical challenges. Protein identification via MS is usually carried out in the form of whole-protein analysis ('top-down' proteomics) or analysis of enzymatically or chemically produced peptides ('bottom-up' proteomics), as shown in Figure 5 (C. Chen et al., 2020; Ghahremani et al., 2016; Han et al., 2008).

1.2.2.1. Top-Down Proteomics

In top-down proteomics, the extracted proteins are analyzed directly without previous enzymatic digestion. Proteins are usually separated by liquid chromatography followed by their identification (amino acid sequencing) through their fragmentation in a tandem mass spectrometry experiment (LC-MS/MS) (Han et al., 2008; Piñeiro et al., 2010a; Priyadharshini & Teran, 2020).

1.2.2.2. Bottom-Up Proteomics

The 'Bottom Up" proteomics approach aims at identifying biological markers in a given proteome. This proteomic approach usually uses two-dimensional gel electrophoresis (2-DGE), which allows the extraction of the individual protein analyte. The gel-based separation procedure

is the most suitable approach for species whose protein sequences are unknown, including many fish. In addition, the 2-DE gels themselves can be analyzed by programs such as Progenesis and PDQuest (Carrera, Piñeiro, et al., 2020). This has been traditionally the technique selected for the separation of proteins samples (Rabilloud & Lelong, 2011) Finally,the obtained peptides are identified by tandem mass spectrometry techniques such as LC-MS/MS and MALDI-TOF-MS/MS (Han et al., 2008; Piñeiro et al., 2010a; Priyadharshini & Teran, 2020, Figure 5).
The identification of the formed peptides is conducted by comparison of the MS/MS spectra of the peptides obtained with orthologous protein sequences from related species or by *de novo* MS/MS sequencing (Carrera et al., 2007, Figure 5).

1.2.3. Peptide Mass Fingerprinting (PMF)

The identification of proteins through the peptide mass fingerprinting (single-stage MS) necessitates the presence of the entire genomic and/or proteomic data of the studied species, such as in the case of Zebrafish (*Danio rerio*) (Forné et al., 2010; Nessen et al., 2016; C. Xu et al., 2019).

Unfortunately, accurate identification in fish proteomics studies is sometimes problematic due to the lack of available proteins sequences for these species in the database. In this case, any available nucleotide data and/or sequence can be used to identify the protein sequence tentatively. However, this method's success will depend on the quality and the length of the available nucleotides sequence. Also, it should be noted that peptides from the fingerprinting MS-spectrum can be selected for further fragmentation by tandem mass spectrometry creating peptide fragment fingerprinting (PFF) (Forné et al., 2010; Nessen et al., 2016; C. Xu et al., 2019).

The sequence identification of peptides is performed by comparing the experimentally obtained MS/MS spectra against all available fragmentation spectra in the database (Figure 6). The fragmentation spectra for a specific peptide sequence are unique and differentiate between isomass peptides with a different amino acid sequence. The peptide mass fingerprinting is beneficial in the accurate identification of unknown protein sequences. Besides identifying protein sequence (Qualitative analysis), MS-Based proteomics is also helpful in quantitating proteins. Changes in a specific protein quantity and/or MS- peak intensity due to a specific condition experienced by an organism are useful in biomarker proteins identification (C. Chen et al., 2020; Giacometti et al., 2013; Nessen et al., 2016; C. Xu et al., 2019).

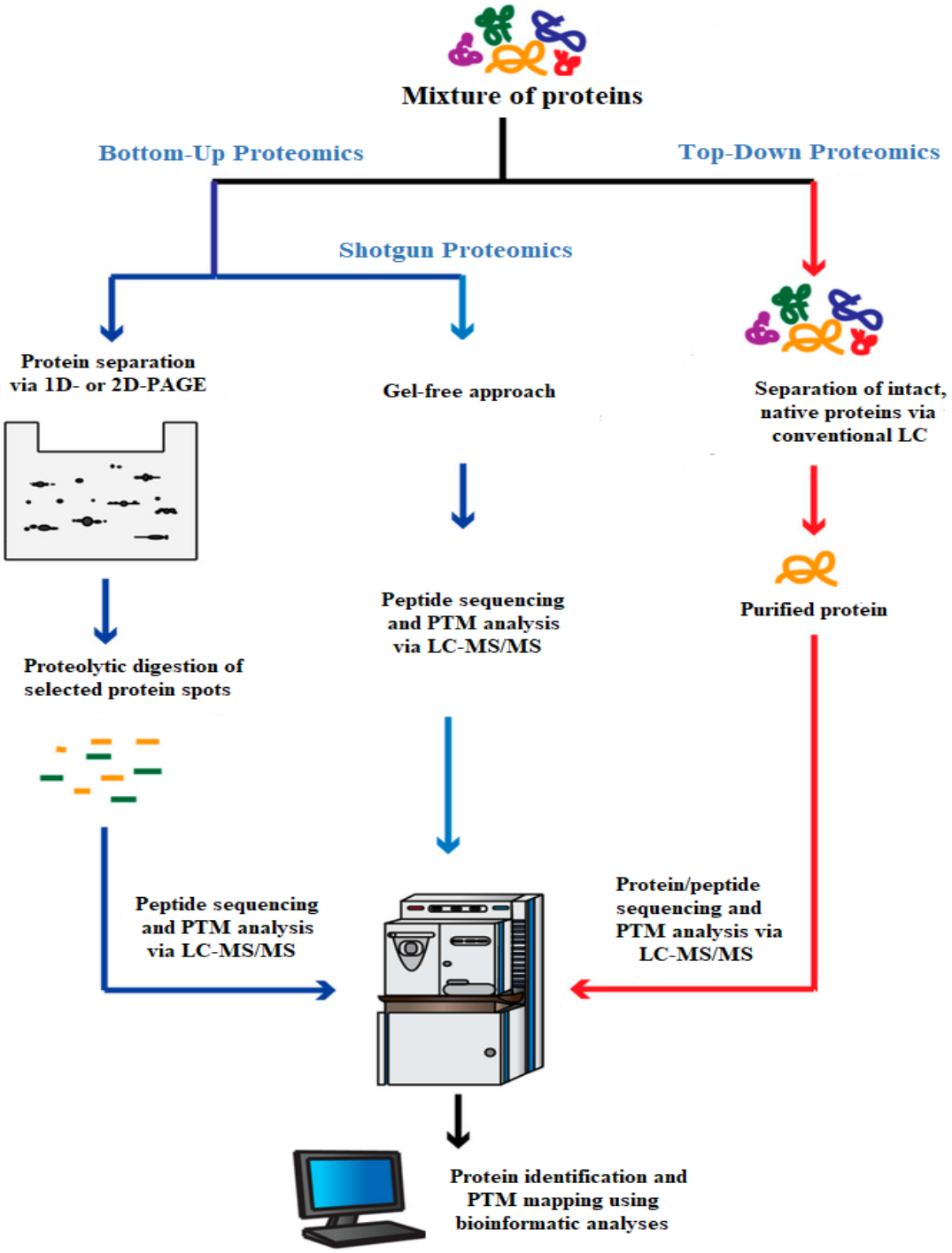

Figure 5. A schematic comparing the "top-down" and "bottom-up" approaches used in proteomic studies. 1D, one dimensional; 2D, two dimensional; LC, liquid chromatography; MS/MS, tandem mass spectrometry; PTM, post-translational modification. (Ghahremani et al., 2016).

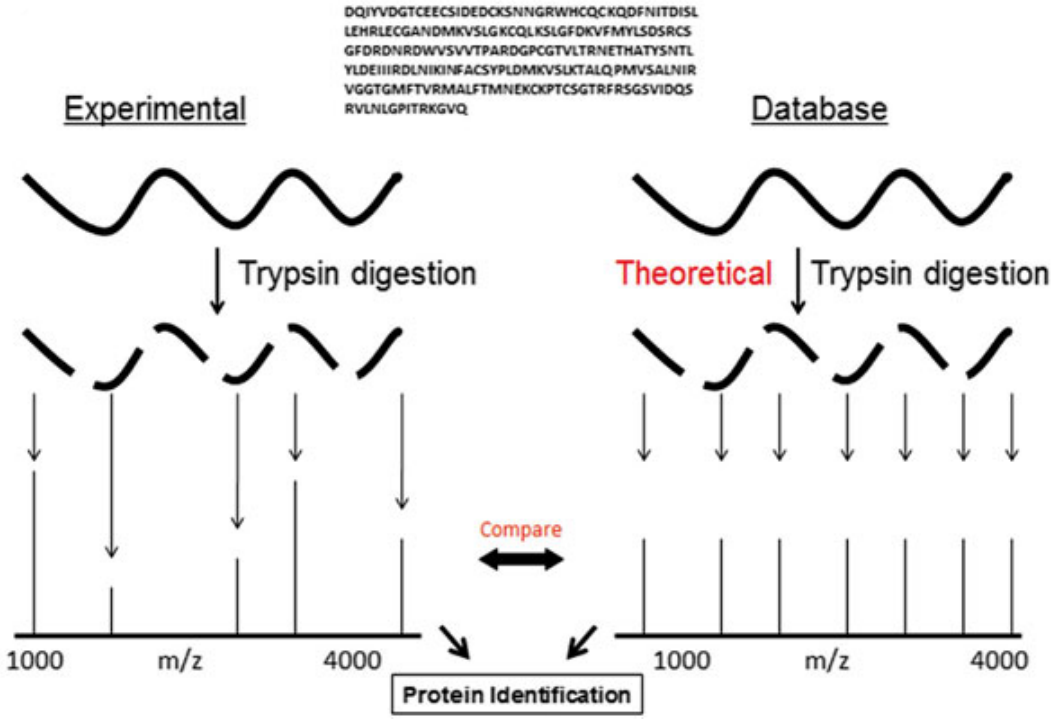

Figure 6. A peptide mass fingerprinting: In the MALDI-TOF-MS, one peak corresponds to one peptide, and many peaks correspond to many peptides, either from one protein or more proteins. Database searches of the MALDI-MS spectra usually identify that single protein or those proteins through a process named peptide mass fingerprinting(C. Xu et al., 2019).

1.2.4. Shotgun Proteomics

In other cases, the extracted proteins can be digested directly without any separation step (gel-free approach), and the formed peptides are separated by multi-dimensional liquid chromatography coupled to a mass spectrometer. This approach is called multi-dimensional protein identification (MudPit) and/or shotgun proteomics. In this approach, the complex peptide mixture is first separated according to their charge by strong cation exchange chromatography (SCX), followed by their separation according to their hydrophobicity by reverse phase chromatography prior to the MS analysis (Han et al., 2008; Piñeiro et al., 2010a; van Vliet, 2014; Yu et al., 2010).

The protein spots of interest resulting from the 2-DGE analysis can be excised from the gel followed by its in-gel digestion using a specific protease enzyme. The resulting peptide mixture can be further analyzed by mass spectrometry. As mentioned before, in all analytical approaches,

the resulting mass spectra allow protein identification through the use of search engines and/or software.

The MS analysis depends on the ionization of the peptide mixture to gas-phase ions that a mass analyzer can separate according to their m/z ratio. The most common used soft ionization techniques in MS-based proteomics are electrospray (ESI) and matrix-assisted laser desorption ionization (MALDI), which successfully ionize peptides mixture without prior derivatization. The resulting MS-spectrum is a peptide mass fingerprinting which is useful in confirming the corresponding protein identity through matching with a database (Chaurand et al., 2008; C. Xu et al., 2019), as shown in Figure 6.

Database searching programs, like SEQUEST, X! Tandem, or Mascot (Eng et al., 1994; Perkins et al., 1999), allow the tentative identification of presumed peptide sequences based on the obtained fragmentation spectra, and additional software programs, such as Percolator, are used to validate the identification (Käll et al., 2007).

When the protein is not present in the database, then the peptides must be sequenced de novo (Shevchenko et al., 1997), either manually or using programs such as PEAKS and DeNovoX (Ma et al., 2003) This approach has been successfully used in the de novo sequencing of some fish allergens, such as parvalbumins and shrimp arginine kinases (Carrera et al., 2007, 2010a; Ortea et al., 2009).

Targeted proteomics refers to monitoring relevant peptide biomarkers, and it has become a recognized methodology to detect selected proteins with significant accuracy, reproducibility, and sensitivity (Borràs & Sabidó, 2017) In targeted proteomics, the MS analyzer is focused on detecting only the peptide/s chosen by selected/multiple-reaction monitoring (SRM/MRM) (Aebersold et al., 2016) Monitoring appropriate transitions (evens of precursor and fragment ions m/z) represents a common analysis for detecting and identifying peptide biomarkers. These techniques are selective, sensitive, highly reproducible, with a high dynamic range and an excellent signal-to-noise (S/N) ratio (Carrera, Piñeiro, et al., 2020; Lange et al., 2008).

1.2.5. Protein Quantitation Approaches

When protein quantification is deemed necessary, the methods of choice is the stable isotope labelling (stable isotope labelling by/with amino acids in cell culture, SILAC) (Ong et al., 2002); isotope tagging by chemical reaction, such as isobaric tags for relative and absolute

quantitation (iTRAQ), tandem mass tag (TMT) and difference gel electrophoresis (DIGE) (Mateos et al., 2015; Robotti & Marengo, 2018; Stryiński et al., 2019); stable isotope incorporation via enzyme reaction (i.e., ^{18}O) (López-Ferrer et al., 2006); and label-free quantification (i.e., measuring the intensity of the peptides at the MS level) (Mueller et al., 2007).

After matching the obtained peptides and proteins by alignment software programs like BLAST (https://blast.ncbi.nlm.nih.gov/), it is possible to select relevant peptide biomarkers to be used in the subsequent phases, (Carrera, Piñeiro, et al., 2020). As mentioned before, there are two types of protein quantitation approaches, label-free quantitation and label-based quantitation techniques. The Label-free method is fast, cheap, and can be accomplished either by spectral counting or the measurement of ion intensity (or the chromatographic peak area), as demonstrated in Figure 7. The proteins are quantified based on the total tandem mass spectra number that correlates peptides to a specific protein in spectral counting. According to Washburn et al., the abundance of a specific protein is directly proportional to the number of its matched peptides (Sokolowska et al., 2013; C. Xu et al., 2019).

In the MS Precursor Ion Intensity Approach, proteins are quantified by calculating the peak area of extracted ion chromatogram of a particular peptide at a normalized elution time (extracted ion chromatogram) compared with another sample (Lam et al., 2016; C. Xu et al., 2019) The label-based absolute quantitation (AQUA) approach depends on using synthetic peptides or proteins with stable isotopes such as ^{13}C, ^{15}N, ^{18}O, or ^{2}H, which are added to the sample as an internal labelled standard before performing the MS-analysis. These synthetic peptides and/or proteins are labelled with stable isotopes in one or more of their amino acids. The difference in the isotopic distribution pattern and mass between labelled and unlabelled peptides are helpful for quantitation purposes (Figure 8) (Sokolowska et al., 2013; C. Xu et al., 2019).

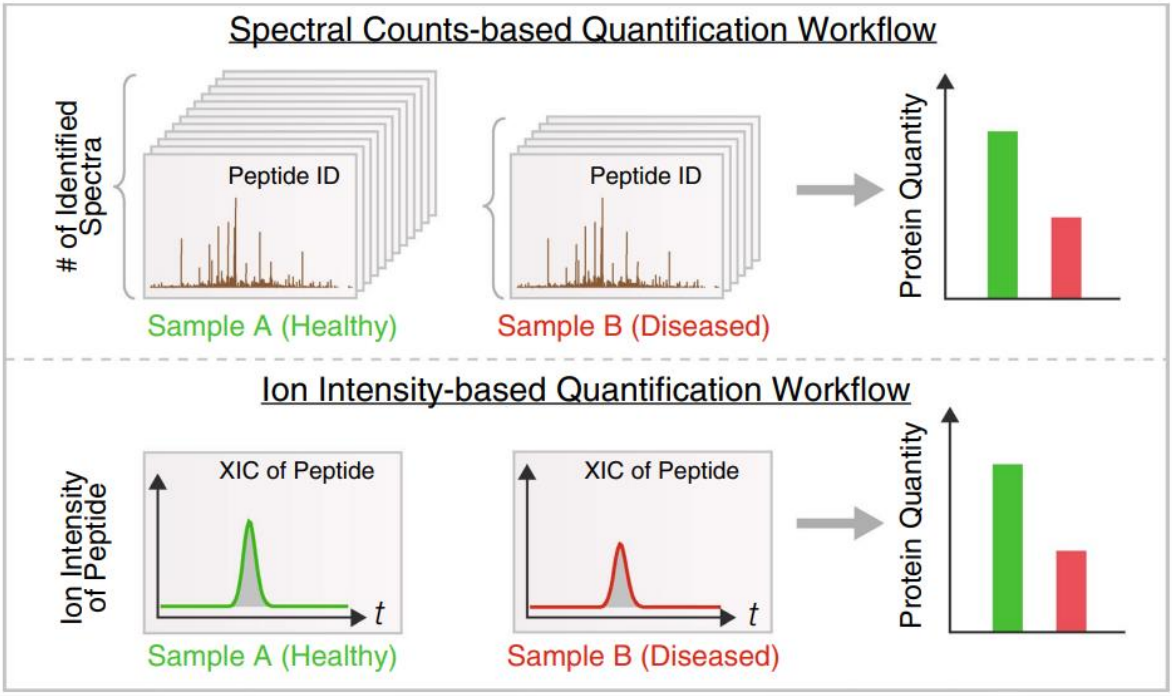

Figure 7. Label-free quantification in proteomics studies. Two common approaches are based on spectral count (top) and ion intensity (bottom)(Lam et al., 2016).

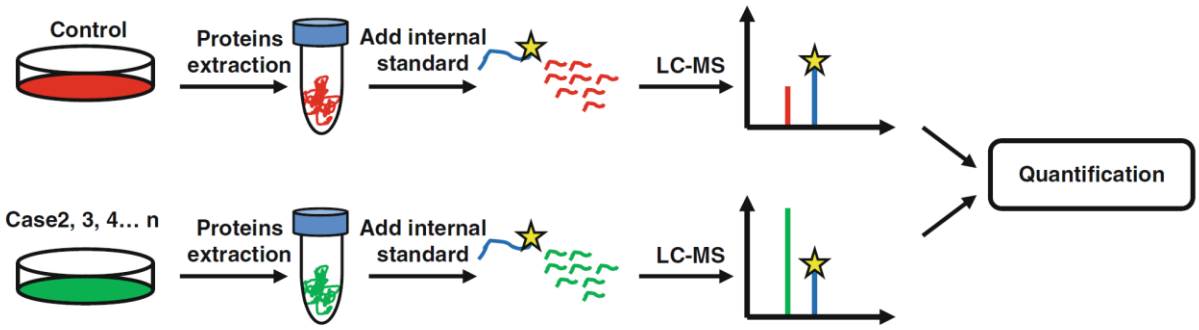

Figure 8. MS-based protein quantification strategies via stable isotope labelling (C. Xu et al., 2019).

One of the most important technique to identify the change in protein quantity during biological modifications is isobaric tags for relative and absolute quantification (iTRAQ) and tandem mass tags (TMT) (Figure 9). In this method, peptides quantitation depends on the low mass region peaks of the reporter ion in the tandem mass spectra. Different peptide samples are labelled by different isobaric tags with the same mass but differ in their isotopic enrichment with

^{13}C, ^{15}N, and ^{18}O atoms. For this reason, the labelled peptide ions will appear as one peak in the full MS-scan. However, when this peak is selected for fragmentation, it will produce different low-mass reporter ions based on their isotopic composition. The low *m/z* reporter fragment ion intensities are used to quantify the same peptide from different samples (Sokolowska et al., 2013; C. Xu et al., 2019).

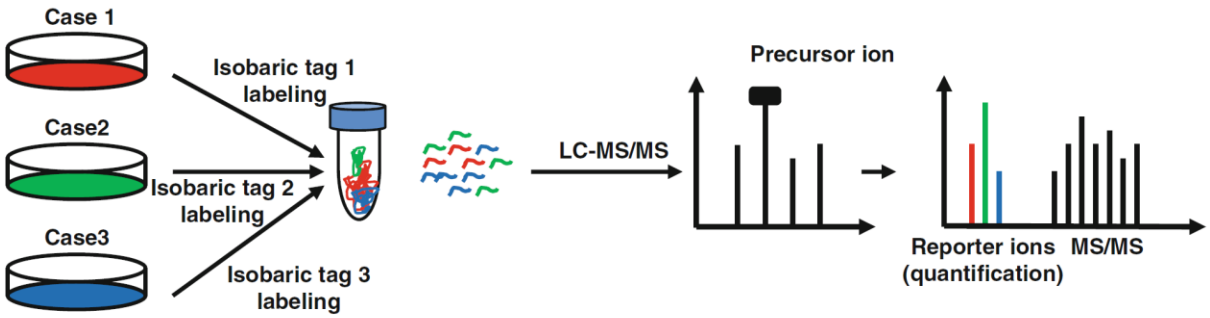

Figure 9. MS-based protein quantification strategies using stable isotope labelling(C. Xu et al., 2019).

Label-free or label methods, tandem mass approach, and database construction and search engines can study proteomic responses in fish. Many non-gel-based approaches in quantitative proteomics offer limited information on post-translational modifications essential for protein function, for example, protein methylation or phosphorylation (Martyniuk & Denslow, 2009b).

1.3. **Post-Script**

The following sections present some applications of proteomic technologies to fisheries research. Please note that according to Google Scholar, there are approximately about 20,700 results. And accordingly, writing a report to cover all these applications would be a Gargantuan task and not within the given mandate. We have chosen, for this reason, to present each pertinent example of the proteomic applications with a short introduction, results and conclusion. In this text, each individual section contains a brief description of the proteomic application with emphasis placed on the principle of detection. Much of the context presented herein was obtained from the open-source literature and is an introduction to the proteomic field application to fisheries science. Annex 1, containing all the supplementary tables, is found at the end of this report.

2. Fish and Shellfish Reproduction Proteomics

The sperm-egg recognition system has been studied in marine invertebrates such as sea urchins, starfish, clams, oysters, abalones, sea snails and worms (Vacquier & Swanson, 2011; Wilburn & Swanson, 2016) This greater diversity of species-specificity gamete interactions during fertilization was advocated as an excellent way to elucidate diverse questions that remain open in reproductive biology (Klinovska et al., 2014; M. R. Romero et al., 2019) sperms are highly differentiated cells that possess marked genetic, cellular and functional differences from other cell types. Indeed, sperm has a vital role in fertilization, embryonic development, and heredity (Oliva et al., 2009) In this work, it was predicted that as sperm cell, was transcriptionally inert, and this is why it was chosen as the ideal candidate for proteomic analyses (Gur & Breitbart, 2008; Karr, 2007; M. R. Romero et al., 2019).

Most sperm cell proteomic research studies have focused on external fertilizer models, such as ascidian *Ciona intestinales* (Bayram et al., 2016; McDonough et al., 2016a; Nakachi et al., 2011), the *red abalone Haliotis rufescens* (Palmer et al., 2013), the Pacific oyster *Crassostrea gigas* (Kingtong et al., 2013), the king scallop *Pecten maximus* (Boonmee et al., 2016) and the marine mussels *Mytilus edulis* (Bartel et al., 2012; Diz et al., 2012) and *M. galloprovincialis* (M. R. Romero et al., 2019; Y. Zhang et al., 2015) The characterization of seminal fish proteins determined by conventional approaches has been published extensively (Ciereszko, 2008; Ciereszko, A.; Glogowski, J.; Dabrowski, 2011; P. Li et al., 2009).

The semen of most teleost fish seems to be better suited for proteomic studies than higher vertebrates due to its simplicity. Seminal plasma is a secretory product of the testes and spermatic duct (Ciereszko, 2008; Ciereszko et al., 2017b; Lahnsteiner, 2003; Lahnsteiner et al., 1993, 1995).

Recently, the subject of state-of-the-art mass spectrometry proteomics studies of fish semen was reviewed (Ciereszko et al., 2012) In this overview of primary proteomic methodologies and recent advances in proteomic studies of fish semen, particular emphasis was placed on the relationship between blood and seminal proteins, sperm and seminal plasma proteins and changes in the semen proteome following cryopreservation. Specifically, a vast amount of information was presented on the proteome of rainbow trout (*Oncorhynchus mykiss*) and carp (*Cyprinus carpio*), two worldwide essential aquaculture species (Ciereszko et al., 2017b).

Fish, unlike mammals, do not possess accessory glands are the seminal plasma composition reflects only testicular and spermatic duct activity. This is why the composition of the seminal fish plasma is not affected by the variable participation of accessory gland secretions in semen. Also, seminal fish plasma is characterized by low protein concentrations (less than 1-2 mg ml^{-1}), allows better detection of proteins and short-term storage for cryopreservation (Ciereszko et al., 2017b; Ciereszko, A.; Glogowski, J.; Dabrowski, 2011) The spermatozoa of teleost fish are distinct from those of higher vertebrates. They are characterized by a very simplified structure (Jamieson, 1991) Compared to mammals, their size is small and lacks an acrosome. Likewise, during external fish fertilization, the spermatozoa are immotile in the spermatic duct. When external fertilization occurs in water, the sperm motility period is very brief. As such, only the activation of sperm movement can be distinguished as a physiological phenomenon (Scott & Baynes, 1980) In contrast, this is contrary to mammals subjected to capacitation, acrosome reaction and penetration of the egg envelopes (Ciereszko et al., 2017b; Zilli et al., 2017).

In our review, whenever the "Proteomic Approach" is mentioned, we specifically allude to the following steps used for this analytical application, which can be summarized are as follows (Figure10):

- The 2-DGE separation of proteins.
- The extraction from the gel and digestion of proteins into peptides by sequence-specific endopeptidases (usually
  trypsin).
- The measurement of the exact molecular weight of the digested peptides using sophisticated mass spectrometry techniques.
- The identification of proteins through peptide mass fingerprinting, using information obtained from protein and DNA sequence databases, often by the in silico digestion of sequences in genomic databases.
- The use of advanced bioinformatics for data analysis.

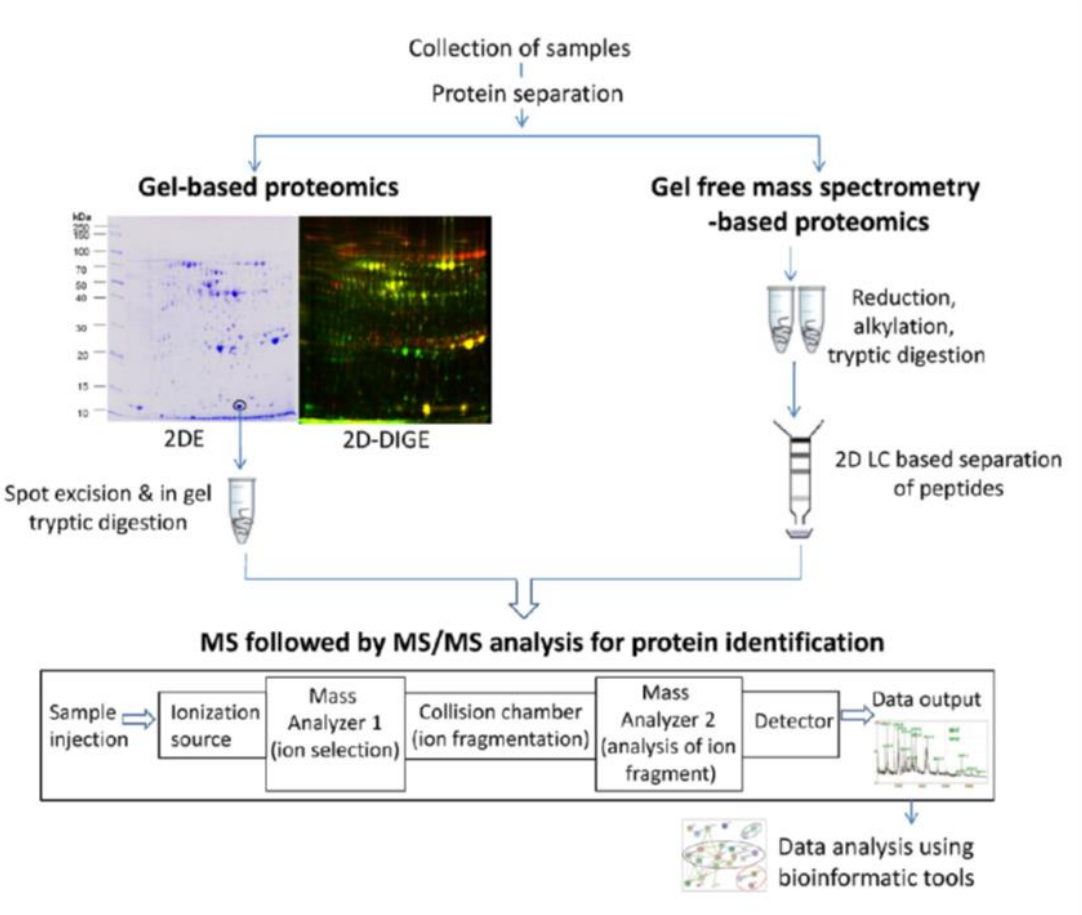

Figure 10. Schematic presentation of proteomic research methodology (Ciereszko et al., 2017a).

2.1. **Mussels Sperm Proteomics**

The study of the mechanisms of the formation of new species is of particular interest in marine ecosystems. These occur due to the absence of obvious barriers to gene flow, which is also relevant for organisms subjected to a prolonged period of larval dispersion. Numerous marine species release their gametes into seawater, so fertilization occurs externally. For this reason, the marine mussel *Mytilus edulis* complex species is an excellent model to study the mechanisms underlying species formation (Palumbi, 1994; M. R. Romero et al., 2019) Fertilization of mussels occurs externally, provided that the sperm cells released must show specific adaptations for survival. In order to achieve fertilization, a sperm must come into contact with an egg and interact with it appropriately. The interactions between sperm and egg during the fertilization process are mediated at each step by proteins. Therefore, various mussel

sperm represent excellent targets to study the molecular mechanisms of reproductive isolation (Lessios, 2011; McDonough et al., 2016b; Palumbi, 1994; M. R. Romero et al., 2019; Swanson & Vacquier, 2002).

During gamete interaction, there is growing evidenc suggesting that multiple protein complexes are involved in concert (Dun et al., 2011; Redgrove et al., 2011; M. R. Romero et al., 2019) It is proposed that species differences in these proteins are key factors that lead to species-specific fertilization and reproductive isolation. When prezygotic barriers fail, interspecies hybrids can occur. When this happens, postzygotic barriers play an essential role in the preservation of species integrity (Lessios, 2011; McDonough et al., 2016b; Palumbi, 1994; M. R. Romero et al., 2019; Swanson & Vacquier, 2002) It should be understood that the role of postzygotic mechanisms is less studied and remain contentious (Corbett-Detig et al., 2013; Orr & Presgraves, 2000; M. R. Romero et al., 2019) It seems evident that gametes are key cell targets in investigating the molecular mechanisms underlying reproductive isolation.

A deep transcriptome sequencing (RNA-seq) of mature male gonads of both *Mytilus edulis* and *M. galloprovincialis* raised in a typical environment were studied, and a 2-DGE, HPLC-MS/MS-based proteome analysis of sperm was initiated. This study provided clear evidence of extensive variation in the mature male gonad transcriptome and sperm proteome in these two mussel species. The transcriptome analysis provided a preliminary list of proteins with sperm-specific functions. These latter functions were connected to sperm-egg interaction, the acrosome reaction, spermatogenesis and motility. It should be noted that the proteome analysis offered evidence of an overrepresentation of mitochondrial proteins and especially candidate protein spots identified by MS, as well as contrasting differential expression in isoforms of many proteins, as shown in Table 1 (M. R. Romero et al., 2019).

Table 1. Transcripts (loci) showing significant differences (FDR 1% at isotig level) in expression of mature male gonad tissue between Mytilus edulis (mussels from Swansea, E) and M. galloprovincialis (mussels from Vigo, G), with GO or protein name terms associated with the search term string "SPERM" OR "FERT*" and a prediction that they have a signal peptide (SP) or a transmembrane (TM) domain in their sequences, this later information coming from SignalP 4.1, TMHMM 2.0 and InterProScan 5.0 analysis. Transcripts were functionally annotated using Blast2GO against UniProt-SwissProt database [all organisms], but protein names below are derived by checking against the nrNCBI[Mollusca] protein database. The numbers of significant isotigs from each locus (FDR 1%) with higher expression levels in M. edulis compared to M. galloprovincialis (E < G) and vice-versa (G > E) are also displayed (M. R. Romero et al., 2019).*

Transcript #	Gene name	Protein name (nrNCBI [Mollusca])	Function	SP, TM	N. *Isotigs* E > G	N. *Isotigs* G > E
Locus_2854	Iap2	Apoptosis 2 inhibitor [*C. gigas*]	Spermatogenesis, acrosome reaction	TM	1	2
Locus_3972	Tmbim6	Bax inhibitor-1 protein [*M. galloprovincialis*]	Spermatogenesis, acrosome reaction	TM	3	2
Locus_9050	Bre-4	Beta-1,4-*N*-acetylgalactosaminyltransferase bre-4 [*C. gigas*]	Sperm-egg interaction	TM	0	1
Locus_1384	CtsB	Cathepsin B [*C. ariakensis*]	Spermatogenesis, acrosome reaction	SP, TM	2	2
Locus_175	CtsL	Cathepsin L [*C. gigas*]	Spermatogenesis, acrosome reaction	SP, TM	3	2
Locus_2547					0	2
Locus_587	CtsL2	Cathepsin L2 cysteine protease [*P. fucata*]	Spermatogenesis, acrosome reaction	TM	1	1
Locus_6135	Cdc42	Cell division cycle 42 [*Mytilus* sp. ZED-2008]	Sperm capacitation, acrosome reaction	TM	1	0
Locus_24960	Cht3	Chitinase-3 [*H. cumingii*]	Sperm-egg interaction	TM	0	3
Locus_6902	Cdyl2	Chromodomain Y-like protein 2 [*C. gigas*]	Spermatogenesis	TM	0	1
Locus_1290	Cng	Cyclic nucleotide-gated channel rod photoreceptor sub. alpha [*C. gigas*]	Spermatogenesis	TM	0	1
Locus_1433	Dnal1	Dynein light chain 1, axonemal, partial [*C. gigas*]	Sperm motility	TM	0	1
Locus_2552	Eif4g2	Eukaryotic translation initiation factor 4 gamma 2 [*C. gigas*]	Spermatogenesis	SP, TM	1	2
Locus_5126	Ggnbp2	Gametogenetin-binding protein 2 [*C. gigas*]	Spermatogenesis	TM	1	3
Locus_134	Hsp90	Heat shock protein 90 [*M. galloprovincialis*]	Spermatogenesis	TM	1	1
Locus_22899	Prdm9	Histone-lysine *N*-methyltransferase PRDM9 [*C. gigas*]	Spermatogenesis	TM	0	1
Locus_18746	Suv39h2	Histone-lysine *N*-methyltransferase SUV39H2 [*C. gigas*]	Spermatogenesis	TM	1	1
Locus_6027	Hya	Hyaluronidase [*C. gigas*]	Sperm-egg interaction	SP, TM	1	0
Locus_1259	Irs	Insulin-related peptide receptor [*P. fucata*]	Spermatogenesis	SP, TM	1	6
Locus_12988					1	1
Locus_5663	Ift172	Intraflagellar transport protein 172 homolog, predicted [*A. californica*]	Sperm motility	TM	2	2
Locus_2244	Imp2	Mitochondrial inner membrane protease subunit 2 [*C. gigas*]	Spermatogenesis	TM	1	2
Locus_10336	Nphp1	Nephrocystin-1 [*C. gigas*]	Spermatogenesis	SP, TM	0	2
Locus_9945	Pmca	Plasma membrane calcium ATPase [*P. fucata*]	Sperm motility	TM	2	4
Locus_1143	Phb	Prohibitin [*O. tankahkeei*]	Spermatogenesis	TM	1	1
Locus_1157	Phb2	Prohibitin-2-like, predicted [*A. californica*]	Spermatogenesis	TM	0	1
Locus_19017	Pc1	Prohormone convertase 1 [*H. diversicolor* sup.]	Sperm-egg interaction, sperm capacitation, sperm motility	SP, TM	0	2
Locus_2686	Psma2	Proteasome subunit alpha type-2 [*C. gigas*]	Sperm capacitation, acrosome reaction	TM	0	1
Locus_29609	Rarb	Retinoic acid receptor beta [*C. gigas*]	Spermatogenesis	SP, TM	0	3
Locus_29136	Ropn1	Ropporin-1-like protein [*C. gigas*]	Spermatogenesis, sperm motility	TM	0	1

Locus_815	Sqstm1	Sequestosome-1 [*C. gigas*]	Spermatogenesis	TM	0	1
Locus_9081	Slc6a5	Sodium- and chloride-dependent glycine transporter 2 [*C. gigas*]	Sperm motility	TM	1	2
Locus_3269	Slc9c1	Sodium/hydrogen exchanger 10 [*C. gigas*]	Spermatogenesis, sperm motility	TM	2	2
Locus_29004	Spatc1	Speriolin [*C. gigas*]	Spermatogenesis	TM	1	5
Locus_13213	Spa17	Sperm surface protein Sp17 [*C. gigas*]	Spermatogenesis, sperm-egg interaction, sperm capacitation, acrosome reaction	TM	0	1
Locus_12286	Spag1	Sperm-associated antigen 1 [*C. gigas*]	Sperm-egg interaction	TM	1	1
Locus_1176	Srsf4	Splicing factor, arginine/serine-rich 4 [*C. gigas*]	Spermatogenesis	SP, TM	1	1
Locus_10277					0	1
Locus_18976	Samd7	Sterile alpha motif domain-containing protein 7 [*C. gigas*]	Spermatogenesis	TM	1	1
Locus_1959	Slc26	Sulfate transporter-like, predicted [*A. californica*]	Sperm motility	TM	2	2
Locus_4801	Cct2	T-complex protein 1 (TCP-1) subunit beta [*C. gigas*]	Sperm-egg interaction	TM	1	0
Locus_586	Cct4	T-complex protein 1 (TCP-1) subunit delta [*C. gigas*]	Sperm-egg interaction	TM	0	2
Locus_1374	Cct5	T-complex protein 1 (TCP-1) subunit epsilon [*C. gigas*]	Sperm-egg interaction	–	4	3
Locus_24738	Cct7	T-complex protein 1 (TCP-1) subunit eta [*C. gigas*]	Sperm-egg interaction	TM	0	1
Locus_22131	Cct3	T-complex protein 1 (TCP-1) subunit gamma [*C. gigas*]	Sperm-egg interaction	TM	0	2
Locus_25048					2	2
Locus_36832					0	1
Locus_20775	Cct8	T-complex protein 1 (TCP-1) subunit theta [*C. gigas*]	Sperm-egg interaction	TM	2	1
Locus_188	Cct6a	T-complex protein 1 (TCP-1) subunit zeta [*C. gigas*]	Sperm-egg interaction	–	1	0
Locus_8047	Thbs1	Thrombospondin-1 [*C. gigas*]	Sperm-egg interaction	SP, TM	0	2
Locus_29534					0	1
Locus_17402	Ubc8	Ubiquitin-conjugating enzyme E2–24 kDa [*C. gigas*]	Spermatogenesis	TM	1	0
Locus_39229	M3	vitelline coat lysin M3 [*M. edulis*]	Sperm-egg interaction	SP	1	1
Locus_25485					0	1
Locus_24	M6	vitelline coat lysin M6 [*M. edulis*]	Sperm-egg interaction	SP	1	2
Locus_30388					0	2
Locus_3846	Zfr	Zinc finger RNA-binding protein [*C. gigas*]	Spermatogenesis	TM	1	0
Locus_1040	Zan	Zonadhesin [*C. gigas*]	Sperm-egg interaction	TM	1	0
Locus_1240					1	2
Locus_1570					1	1
Locus_2570					0	1

The obtained results showed that the existence of candidate sperm proteins in *M. edulis* and *M. galloprovincia* were good targets for further genomic analysis of reproductive barriers between closely related species (M. R. Romero et al., 2019).

For *M. edulis*, these candidate proteins were the ones relating to sperm motility, ATP reserves, and ROS production in *M. edulis.* Whereas *M. galloprovincia* included the proteins relating to sperm motility, the acrosome reaction, capacitation and sperm-egg interaction. It

was concluded that proteins and their corresponding genes are excellent targets in further genomic analysis of reproductive barriers between these closely related species (M. R. Romero et al., 2019).

2.2. New Opportunities in Fish Reproductive Research

Few Proteomic studies on fish semen have been reported and are listed in Table 2. One of the first proteomic applications was studying through profiling the proteomics effects of cryopreservation on sea bass proteins (Ciereszko et al., 2012; Zilli et al., 2005).

Table 2. Proteomic studies of fish semen(Ciereszko et al., 2012).

Study	Reference	No. of identified proteins
Effects of cryopreservation on sea bass proteins	(Zilli et al., 2005)	3
Cryopreservation of carp semen	(P. Li, Hulak, Koubek, et al., 2010)	11
Sperm motility initiation in Sparids	(Zilli et al., 2008b)	5
Testis proteome of wild and cultured (F1) Senegalese sole	(Forné et al., 2009)	58
Comparative proteomics of sturgeon gonads	(Keyvanshokooh et al., 2009)	48
Protein profiles of sturgeon sperm	(P. Li, Hulak, Rodina, et al., 2010)	22

2.2.1. Fish Seminal Plasma Proteomics

The seminal plasma of fish is designed to provide an optimal environment for the storage of spermatozoa before spawning. Seminal plasma proteins have been designed to play an important role in sperm protection, and some of these proteins were identified as apolipoproteins (Dietrich, Adamek, et al., 2014; Nynca et al., 2010), transferrin (Wojtczak, Dietrich, et al., 2007; Wojtczak et al., 2005), and proteinase inhibitors (Mak, Mak, Olczak, Szalewicz, Glogowski, Dubin, Wątorek, et al., 2004; Wojtczak, Całka, et al., 2007a). These proteins were isolated and characterized in straightforward conventional studies. Therefore, an in-depth analysis of the seminal plasma proteome would be indispensable for a better understanding of the complexity of seminal fish proteins and the selection of protein candidates for more detailed studies (Ciereszko et al., 2017a).

The proteomics of rainbow trout and seminal carp plasma has been described by using the shotgun proteomics approach (Nynca, Arnold, Fröhlich, Otte, Flenkenthaler, et al., 2014) and (Dietrich, Arnold, Nynca, et al., 2014) Therefore, the use of a combination of protein

fractionation by one-dimensional gel electrophoresis and high-performance liquid chromatography coupled to electrospray ionization mass spectrometry and MS/MS extended significantly previous findings, which were restricted due to the limited number of proteins identified (P. Li, Hulak, Koubek, et al., 2010; Shaliutina et al., 2012) This resulted in the creation of a catalogue of 152 rainbow trout seminal plasma proteins and 186 carp seminal plasma proteins. The major seminal plasma proteins of both species are shown in Table 3. Please note that there is substantial overlap in the composition of the significant proteins between these studies. This suggests that fish general protective mechanisms are well conserved. Conversely, some proteins appear to be species-specific (e.g. precerebellin-like protein in rainbow trout) (Table 3). Nevertheless, it should be emphasized that protein concentration can change depending on the season or handling of fish (Ciereszko et al., 1996, 2004, 2017a).

Table 3. The most abundant seminal plasma proteins in carp (Dietrich, Arnold, Nynca, et al., 2014)) and rainbow trout (Ciereszko et al., 2017a; Nynca, Arnold, Fröhlich, Otte, Flenkenthaler, et al., 2014).

Carp		Rainbow trout	
Protein	**Quantitative value**	**Protein**	**Quantitative value**
Transferrin variant G	1033	Transferrin precursor	2764
Transferrin variant C	1000	Complement C3	548
Complement C3-H1	377	Alpha-1-antiproteinase-like protein precursor	200
Complement C3-S	152	present[a]	
Alpha-1 antitrypsin	274	present[a]	
14 kDa lipoprotein	133	Apolipoprotein A-II	304
Warm-temperature-acclimation-related-65 kDa -protein	82	Hemopexin-like protein	426
Apolipoprotein A-1	72	Apolipoprotein A-I-1-precursor	717
Heat shock protein HSP 90-alpha	69	Apolipoprotein A-I-2-precursor	298
Retinol binding protein	80	Precerebelin-like protein precursor	114
		Serum albumin 1 protein	615
		Serum albumin	457

BOLD proteins are classified as the most abundant in carp blood plasma based on Scaffold's "Quantitative value." The "Quantitative value" provides normalized spectral counts based on the total number of spectra identified in each sample. Identified but not abundant.

2.2.2. Seminal Plasma and Shotgun Proteomics

Although the fish semen is composed of seminal plasma and spermatozoa, it should be understood that the biochemical basis of sperm-specific physiology cannot be achieved without resorting to any proteomic studies. It has been proposed that during reproduction, the sperm of cyprinids and salmonids differ in structure, the complement of nuclear proteins, metabolism, mechanism of sperm activation, and parameters of sperm movement (Billard, 1992; Billard R. et al., 1995; Jamieson, 1991). Due to both species' essential commercial value, a plethora of sperm proteomic studies has been described by (Nynca, Arnold, Fröhlich, Otte, Flenkenthaler, et al., 2014) and (Dietrich, Arnold, Fröhlich, et al., 2014). These studies significantly complement previous findings, which had a limited number of identified proteins (Forné et al., 2009; P. Li et al., 2013; P. Li, Hulak, Koubek, et al., 2010; P. Li, Li, et al., 2010) The shotgun proteomics approaches of the seminal plasma performed with a combination of protein fractionation by one-dimensional gel electrophoresis and high-performance liquid chromatography-electrospray ionization tandem mass spectrometry allowed the creation of a catalogue of rainbow trout sperm proteins (206 proteins) and carp sperm proteins (348 proteins). The major sperm proteins of both species are shown in Table 4 (Dietrich, Arnold, Fröhlich, et al., 2014).

Table 4. The most abundant sperm proteins in carp (Dietrich, Arnold, Fröhlich, et al., 2014) and rainbow trout (Ciereszko et al., 2017a; Nynca, Arnold, Fröhlich, Otte, Flenkenthaler, et al., 2014).

Carp		Rainbow trout	
Protein	**Quantitative value**	**Protein**	**Quantitative value**
Tubulin beta 2	313	The dense outer fibre of sperm tail protein 3	185
Tubulin alpha 6	204	Tubulin alpha chain, testis-specific	662
Dynein heavy chain	220	Beta-actin	66
Creatine kinase	144	Creatine kinase	1318
Heat shock protein HSP 90 alpha	133	Valosin containing protein	50
Valosin containing protein	112	Glucose-regulated protein 78 kDa	45
NKEF-B Natural killer enhancer factor	86	14-3-3C1 protein	104
S-adenosylhomocysteine hydrolase	94	14-3-3C2 protein	113
Heat shock 60 kDa protein, mitochondria	85	14-3-3 protein beta/alpha-1 14-3-3	198
ATP synthase subunit beta, mitochondrial	106	14-3-3 protein beta/alpha-2	168
Heat shock 70 kDa protein 5	91		

The "Quantitative value" was used for the quantitative analysis of protein abundance in sperm. The "Quantitative value" provides normalized spectral counts based on the total number of spectra identified in each sample.

Among the identified 348 carp spermatozoa proteins, 124 matched the sperm proteins identified in the rainbow trout. Also, as expected, several main abundant proteins were present in both species, such as creatine kinase, tubulin, valosin-containing protein and glucose-regulated protein (Table 5) (Dietrich, Arnold, Fröhlich, et al., 2014).

It is interesting to note that many high abundance proteins were different between the two species. Also, note that the natural killer cell enhancing factor (NKEF), belonging to the peroxiredoxin and adenosylhomocysteinase families, which was abundant in carp, were also present in low concentration in the rainbow trout sperm (Nynca, Arnold, Fröhlich, Otte, & Ciereszko, 2014; Nynca et al., 2015a) These differences reflect the specificity difference between carp and rainbow trout sperm biology (Dietrich, Arnold, Fröhlich, et al., 2014).

Needless, to say that the fish proteomic studies of fish are hampered due to the poor annotation of transcriptomics databases. The lack of fully sequenced rainbow trout and typical carp genome hampered the success in sequence-homology searching of the database. For example, the NCBI database generated on 2013.10.31 contained only 7065 and 2279 entries for *O. mykiss* and *C. carpio*, respectively. Nowadays, a French consortium sequenced and analyzed the rainbow trout genome (O. mykiss), which constitutes the first published salmonid genome (Berthelot et al., 2014) Recently, using a whole-genome shotgun strategy and combining data from several next-generation sequencing platforms, high-quality genome assembly *for C. carpio* was produced (P. Xu et al., 2014) The annotation of the contigs of carp scaffolds was only added recently. It is important to note that poor annotation of databases is still a significant problem for the proteomic studies of most fish species (Dietrich, Arnold, Fröhlich, et al., 2014).

Table 5. Proteins common for carp seminal plasma and spermatozoa (Dietrich, Arnold, Fröhlich, et al., 2014).

	Identified proteins	**GI number**	**Molecular mass**
1	tubulin beta 2c (zgc:55461) [Danio rerio])	gi|123232717 (+1)	50 kDa
2	PREDICTED: dynein heavy chain 5, axonemal [Danio rerio]	gi|326679792	525 kDa
3	brain creatine kinase (Zgc:154095) [Danio rerio]	gi|115313427 (+2)	43 kDa
4	heat shock protein HSP 90-alpha [Danio rerio]	gi|113681112 (+2)	85 kDa
5	valosin containing protein [Danio rerio]	gi|122891315 (+5)	89 kDa
6	NKEF-B [Cyprinus carpio]	gi|209977950 (+2)	22 kDa
7	Ahcy protein [Danio rerio]	gi|182890144 (+3)	48 kDa
8	Ldhb protein [Danio rerio]	gi|28277619 (+3)	36 kDa
9	ADP-ribosylation factor 1 like [Danio rerio]	gi|28279265 (+3)	21 kDa
10	beta-actin 1 [Hemibarbus mylodon]	gi|147742803 (+14)	42 kDa
11	O-linked N-acetylglucosamine (GlcNAc) transferase (UDP-N-acetylglucosamine:polypeptide-N-acetylglucosaminyl transferase) [Danio rerio]	gi|190340092 (+8)	117 kDa
12	proteasome subunit alpha type-3 (Zgc:114044) [Danio rerio]	gi|66911343 (+1)	28 kDa
13	malate dehydrogenase, mitochondrial (Zgc:64133) [Danio rerio]	gi|31419562 (+1)	35 kDa
14	puromycin-sensitive aminopeptidase [Danio rerio]	gi|255683531	98 kDa
15	Rab1a protein [Danio rerio]	gi|182889992 (+4)	22 kDa
16	transferrin variant G [Cyprinus carpio]	gi|189473165	73 kDa
17	PREDICTED: filamin-A [Danio rerio]	gi|189535920	269 kDa
18	putative glyceraldehyde-3-phosphate dehydrogenase [Cyprinus carpio]	gi|56709493	33 kDa
19	Pvalb6 protein [Danio rerio]	gi|182889304 (+3)	12 kDa
20	proteasome subunit alpha type-1 (Zgc:92726) [Danio rerio]	gi|50369319 (+1)	29 kDa
21	constitutive heat shock protein 70 [Hypophthalmichthys molitrix]	gi|296409582	71 kDa
22	Thyroid hormone receptor interactor 13 [Danio rerio]	gi|34784059 (+2)	48 kDa
23	RecName: Full=Proteasome subunit alpha type-7; AltName: Full=Proteasome subunit alpha 4	gi|12229928 (+5)	28 kDa
24	Triosephosphate isomerase B Tpi1b protein [Danio rerio]	gi|156230739 (+2)	27 kDa
25	Ubiquitin-like modifier activating enzyme 1 [Danio rerio]	gi|38173709 (+1)	118 kDa

26	glutathione S-transferase rho [Cyprinus carpio]	gi|112901127	26 kDa
27	Dipeptidylpeptidase 3 [Danio rerio]	gi|49899818 (+1)	82 kDa
28	Ubiquitin-conjugating enzyme E2 variant 2 [Danio rerio]	gi|37046870 (+2)	16 kDa
29	14-3-3 protein beta/alpha-A Ywhab1 protein [Danio rerio]	gi|126631813 (+3)	28 kDa
30	Acetyl-Coenzyme A acetyltransferase 1 (acetoacetyl Coenzyme A thiolase) [Danio rerio]	gi|50925330 (+2)	44 kDa
31	S-phase kinase-associated protein 1 [Danio rerio]	gi|37748746 (+2)	19 kDa
32	proteasome subunit beta type-6 [Danio rerio]	gi|18859271 (+1)	24 kDa
33	Ras-related C3 botulinum toxin substrate 1 (rho family, small GTP binding protein Rac1) [Danio rerio]	gi|27882091 (+5)	22 kDa
34	phosphoglycerate mutase 1 [Danio rerio]	gi|220678284 (+4)	29 kDa
35	RecName: Full=Proteasome subunit beta type-1-A; AltName: Full=20S proteasome beta-6 subunit A; Short=B6-A	gi|17380207 (+1)	26 kDa
36	muscle cofilin 2 [Danio rerio]	gi|37681759 (+1)	19 kDa
37	alcohol dehydrogenase [Danio rerio]	gi|16565980 (+2)	40 kDa
38	Proteasome (prosome, macropain) subunit, alpha type, 2 [Danio rerio]	gi|66267588 (+1)	26 kDa
39	phosphoglycerate kinase Pgk1 protein (unnamed protein product) [Danio rerio]	gi|259685081 (+3)	45 kDa
40	Glutamic-oxaloacetic transaminase 1, soluble [Danio rerio]	gi|160773417 (+5)	46 kDa
41	Ubiquitin-conjugating enzyme E2L 3 [Danio rerio]	gi|48735248 (+1)	18 kDa
42	10-formyltetrahydrofolate dehydrogenase [Danio rerio]	gi|196174733 (+1)	100 kDa
43	methionine adenosyltransferase 2 subunit beta (Zgc:110308) [Danio rerio]	gi|60688479 (+2)	36 kDa
44	glutathione peroxidase 4b [Cyprinus carpio]	gi|237930378	19 kDa
45	RecName: Full=L-lactate dehydrogenase A chain; Short=LDH-A	gi|17369409 (+5)	36 kDa
46	EF-hand domain (C-terminal) containing 2 [Danio rerio]	gi|220941673	86 kDa
47	ribose 5-phosphate isomerase A (ribose 5-phosphate epimerase) [Danio rerio]	gi|220679087	30 kDa
48	Aldoaa protein [Danio rerio]	gi|182891262 (+5)	40 kDa
49	14 kDa apolipoprotein [Cyprinus carpio]	gi|385865216	16 kDa
50	proteasome subunit beta type-3 [Danio rerio]	gi|193788711 (+1)	23 kDa
51	Hypoxanthine phosphoribosyltransferase 1 [Danio rerio]	gi|28277932 (+2)	25 kDa
52	H1 histone [Carassius auratus]	gi|37731906	19 kDa
53	Lsm6 protein [Danio rerio]	gi|182888802 (+3)	9 kDa
54	Tyrosine 3-monooxygenase/tryptophan 5-monooxygenase activation protein, beta polypeptide like [Danio rerio]	gi|37748232 (+2)	28 kDa
55	Ubiquitin specific protease 14 (tRNA-guanine transglycosylase) [Danio rerio]	gi|27882361 (+1)	55 kDa

56	Heat shock protein 5 [Danio rerio]	gi|39645428 (+1)	72 kDa
57	Aldose reductase; Si:dkey-180p18.9 protein [Danio rerio]	gi|50604191 (+2)	37 kDa
58	Muscle-type creatine kinase CKM2 creatine kinase M3-CK [Cyprinus carpio]	gi|4027929	43 kDa
59	methionine adenosyltransferase II alpha a [Danio rerio]	gi|376341473	44 kDa
60	RecName: Full=Triosephosphate isomerase A; Short=TIM-A; AltName: Full=Triose-phosphate isomerase A	gi|123889553 (+9)	27 kDa
61	Chromosome segregation 1-like[Danio rerio]	gi|30962883 (+3)	110 kDa
62	nucleoside diphosphate kinase B Nme2 protein [Danio rerio]	gi|197247050 (+2)	17 kDa
63	glutathione S-transferase mu [Cyprinus carpio]	gi|112901117	26 kDa
64	novel protein similar to vertebrate ubiquitin carboxyl-terminal esterase L3 (ubiquitin thiolesterase) (UCHL3, zgc:109963) [Danio rerio]	gi|169158616 (+3)	26 kDa

2.2.3. Proteomic and Metabolomic Insights into the Functions of the Male Reproductive System in Fishes

Proteomics and metabolomics are emerging and powerful tools to unravel the complex molecular mechanisms regulating reproduction in male fish. So far, numerous proteins and metabolites have been identified that provide us with valuable information to conduct a comprehensive analysis on seminal plasma and spermatozoa components and their functions. These analyses have allowed a better understanding of the blood-testis barrier functions, the molecular mechanisms underlying spermatogenesis, spermatozoa maturation, motility signalling, competition, and the mechanism of cryodamage to sperm structure and functions. To extend, proteins that undergo posttranslational modification, such as phosphorylation and oxidation in response to spermatozoa motility activation and cryopreservation, respectively, have been identified (Dietrich et al., 2019).

Proteomic studies identified potential proteins that can be used as biomarkers for sperm quality and freezability to enable the control of artificial reproduction and improve methods for long-term preservation (cryopreservation) of sperm.The different proteins expressed in the spermatozoa of neomales and normal males can also provide new insights into the development of methods for separating X and Y fish sperm and changes in the protein profiles in haploid and diploid spermatozoa will provide new perspectives to better understand the mechanism of male polyploidy (Dietrich et al., 2019).

Overall, the knowledge gained by proteomic and metabolomic studies is important from basic to applied sciences for the development and/or optimization of techniques in controlled fish reproduction (Dietrich et al., 2019)

2.3. Shotgun Proteomics of Rainbow Trout Ovarian Fluid

This study was responsible for generating the first protein catalogue of rainbow trout Ovarian fluid (OF) using the shotgun approach (one-dimensional electrophoresis (1-DE) pre-fractionation combined with LC-ESI-MS/MS) (Nynca et al., 2015b). This study permitted the identification of 54 rainbows OF proteins that were not previously reported in the fish ovarian fluid (Supplementary Table S1). Once more, the lack of a fully sequenced rainbow trout genome hampered the success of sequence homology searching of databases. For the records, the National Center for Biotechnology Information (NCBI) *Oncorhynchus mykiss* database contains

approximately 110- fold fewer proteins (7065) than the NCBI *Homo sapiens* database (78 6331;http://www.ncbi.nlm.nih.gov/protein/?term=homo+sapiens). Moreover, the large amounts and multiple forms of vitellogenin present in trout of mask and hinder the successful identification of other less abundant proteins (Nynca et al., 2015b).

In this section, the present study confirmed the presence of putative markers of oocyte quality (different forms of vitellogenin, apolipoproteins A-I-1 and mannose-binding lectin) reported by previous studies of the proteome of rainbow trout OF (Bobe & William Goetz, 2001; Rime et al., 2004) and found additional proteins that had not been reported earlier for trout OF.

A detailed list of all proteins identified in the present study is provided in the supplementary material Supplementary Table S1, together with their accession number, molecular mass, sequence coverage and number of unique peptides assigned to each protein (Nynca et al., 2015b).

In order to understand the remaining of this review, it is important to understand what "Gene Ontology" (GO) means. The major bioinformatics initiative termed GO was created to unify the representation of gene and gene product attributes across all species. It also refers to a formal representation of a body of knowledge within a given domain (Nynca et al., 2015b). The GO allows users to describe a gene/gene product in detail, considering three main aspects: its molecular function, the biological process in which it participates, and its cellular location. For this reason rom the 54 OF proteins, 28 were classified according to the term 'biological process,' and 33 proteins were signed to the term 'molecular functions.' The GO analysis for the proteins were assigned to the 'biological process' group revealed that most of the OF proteins were involved in the metabolic process (43%), followed by transport (26%) and then response to stimulus (26%; Figure 11*A*) (Nynca et al., 2015b).

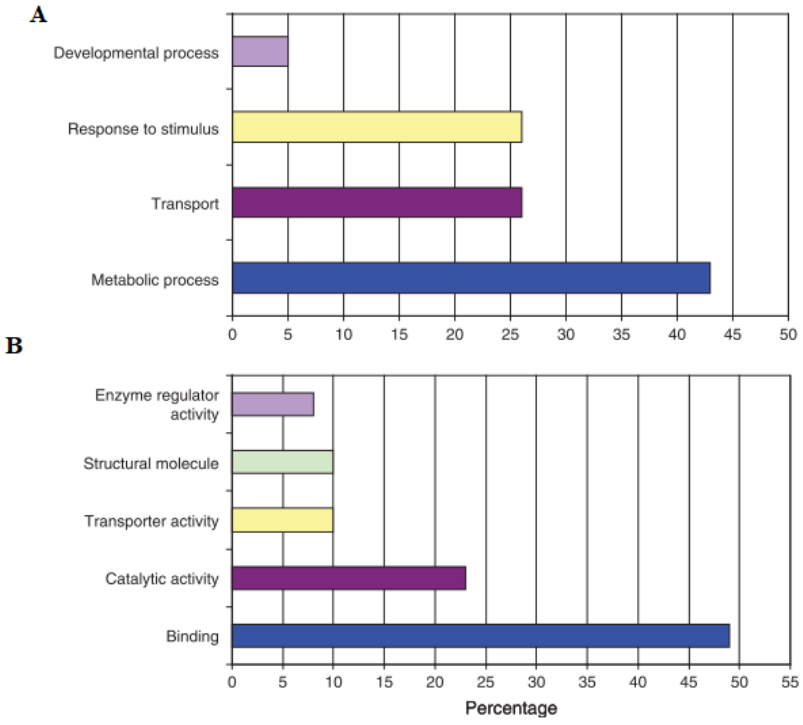

Figure 11. Bar graphs showing the rainbow trout ovarian fluid proteome in terms of (A) biological process and (B) molecular function (Nynca et al., 2015b).

It was found that the proteome of trout ovarian fluid consisted of diverse proteins participating in lipid binding and metabolism, carbohydrate and ion transport, innate immunity, maturation and ovulation processes. Most trout ovarian fluid proteins correspond to follicular fluid proteins of higher vertebrates, but 15% of the proteins were found to be different, such as those related to the immune system (precerebellin-like protein), proteolysis (myeloid cell lineage chitinase), carbohydrate and lipid binding and metabolism (vitellogenins), cell structure and shape (vitelline envelope protein gamma) and a protein with unknown functions (UPF0762 protein C6orf58 homologue) (Nynca et al., 2015b).

The GO analysis of the 'molecular function' group revealed that most of these proteins (49%) were implicated in binding (mostly ions (45%), lipids (23%) and carbohydrates (18%)), followed by catalytic functions (Fig. 11*B*). The proteins were also grouped into five functional categories based on the information generated by GO annotations and proposed for purple sea urchin (Dheilly et al., 2013) and sea star (Franco et al., 2011) coelomic fluid (Dheilly et al., 2013).

Polyclonal antibodies against rainbow trout seminal plasma transferrin, PGDS and a1-antiproteinase cross-reacted with trout OF proteins separated by SDS-PAGE (Figure 12). The migration rates of the main bands reflected molecular masses of these proteins obtained by proteomic methods (see Supplementary Table S1) and published results (Nynca, Dietrich, et al., 2011a; Nynca, Słowińska, et al., 2011). Additional bands of low migration rates presumably represent complexes of the α1-antiproteinase with target proteins (Mak, Mak, Olczak, Szalewicz, Glogowski, Dubin, Wątorek, et al., 2004; Wojtczak, Całka, et al., 2007b).

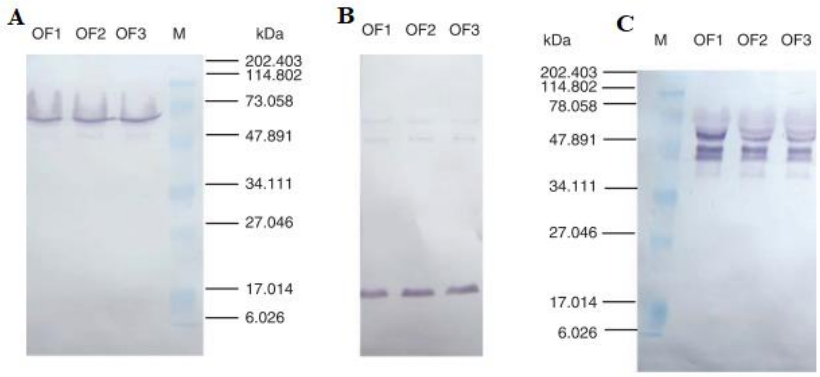

Figure 12. Cross-reactivity between polyclonal antibodies against (A) transferrin, (B) prostaglandin D synthase and(C) a1-antiproteinase and ovarian fluid samples (OF1, OF2, OF3). M, molecular mass marker (202.403–6.026 kDa) (Dheilly et al., 2013).

The present study could help in decoding the biological function of these proteins and in the discovery of potential biomarkers of oocyte quality.

2.4. Post-Ovulatory Ageing and Egg Quality: a Proteomic Analysis of Rainbow Trout Coelomic Fluid

In fish, oocyte post-ovulatory ageing is generally associated with egg quality decrease. During this period, the eggs are held in the body cavity, where they bath in a semi-viscous liquid known as coelomic fluid (CF). In addition, the CF components are assumed to play a role in maintaining the oocyte fertility and in developmental competence (egg quality). Nevertheless, CF proteome composition remains poorly studied (Rime et al., 2004).

The present study examined the rainbow trout CF proteome associated with egg quality decrease and the resulting oocyte post-ovulatory ageing. Accordingly, the usual proteomics

approach was used (2-DGE, MALDI-TOF-MS and MALDI-TOF/TOF-MS/MS to analyze the proteome of rainbow trout (*Oncorhynchus mykiss*). Consequently, a first experiment was conducted using CF pools originating from 17 females sampled at ovulation and 7, 14 and 21 days later. Similarly, the second set of CF pools originating from 22 females sampled 5 and 16 days following ovulation (Rime et al., 2004). It is well known that the post-ovulatory ageing of ovulated oocytes in the abdominal cavity of salmonids is associated with a progressive egg viability decrease that may last 2–3 weeks (Aegerter & Jalabert, 2004; Nomura M, Sakai K, 1974). In addition, it is known that post-ovulatory ageing is associated with an increased occurrence of morphological abnormalities (Aegerter & Jalabert, 2004).

In the present study, the number of alevins reaching yolk-sac resorption without exhibiting any obvious morphological abnormality (Living a Normal Embryo Rate, LNER) was used to estimate egg quality for all female at each post-ovulatory sampling time. However, it was shown, that only monitoring the embryonic survival was not sufficient to fully estimate the developmental competence of ovulated oocytes. In both experiments a strong and significant decrease in the developmental competence was observed for holding times longer than 5 (experiment 2) or 7 (experiment 1) days (Figure 13, Table 6). Thus, LNER decreased from 70 to 30% between 7 and 14 days post-ovulation (experiment 1) and from 76 to 14% between 5 and 16 days post-ovulation (experiment 2). These observations are in total agreement with previous studies performed on rainbow trout and other salmonids at 12°C (Aegerter & Jalabert, 2004; Rime et al., 2004; Springate et al., 1984).

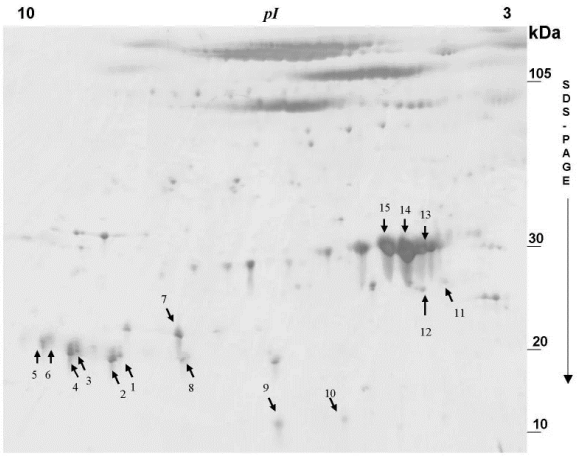

Figure 13. Two-dimensional gel of rainbow trout coelomic fluid Silver stained 2D-PAGE of coelomic fluid 21 days (D21) after ovulation. Proteins (40 µg) were loaded. Protein spots marked

with arrows were excised from 2D gels for MALDI-TOF-MS analysis (the numbering of spots corresponds to table 6) (Rime et al., 2004).

Table 6. List of proteins identified in coelomic fluid during post ovulation ageing. The spot identification # corresponds to Figure 13. SwissProt accession numbers and corresponding protein names are shown (Rime et al., 2004).

Identification	Protein name	Accession No. (SwissProt)
1	Vitellogenin	AAB02176
2	Vitellogenin	AAB02176
3	Vitellogenin	AAB02176
4	Vitellogenin	AAB02176
5	Vitellogenin	AAB02176
6	Vitellogenin	AAB02176
7	No match	
8	No match	
9	No match	
10	No match	
11	Lectin	AAM21196
12	Lectin	AAM21196
13	Apolipoprotein A I-1	AAB96972
14	Apolipoprotein A I-1	AAB96972
15	Apolipoprotein A I-1	AAB96972

Approximately 200 protein spots possessing molecular mass around 10–105 kDa and isoelectrical 3–10 p*I* were detected in CF samples. While undetected at the time of ovulation, several protein spots exhibited a progressive and strong accumulation in CF during post-ovulatory ageing. After silver-staining and MALDI-TOF-MS analysis, some of these protein spots were identified as lipovitellin II fragments (Rime et al., 2004). Also, it was found that about 20 spots appeared between ovulation and 21 days post-ovulation. More specifically, 8 protein spots were characterized by a strong accumulation during post-ovulatory ageing (Figure 14). Their abundance exhibited a 260% increase between 7 and 21 days post-ovulation (Figure 14E).

Similar observations were made in a second experiment using CF pools originating from 22 females sampled 5 and 16 days following ovulation (Figure 15). For this second experiment, the measured abundance exhibited a 500% increase between 5 and 16 days post-ovulation (Figure 15C).

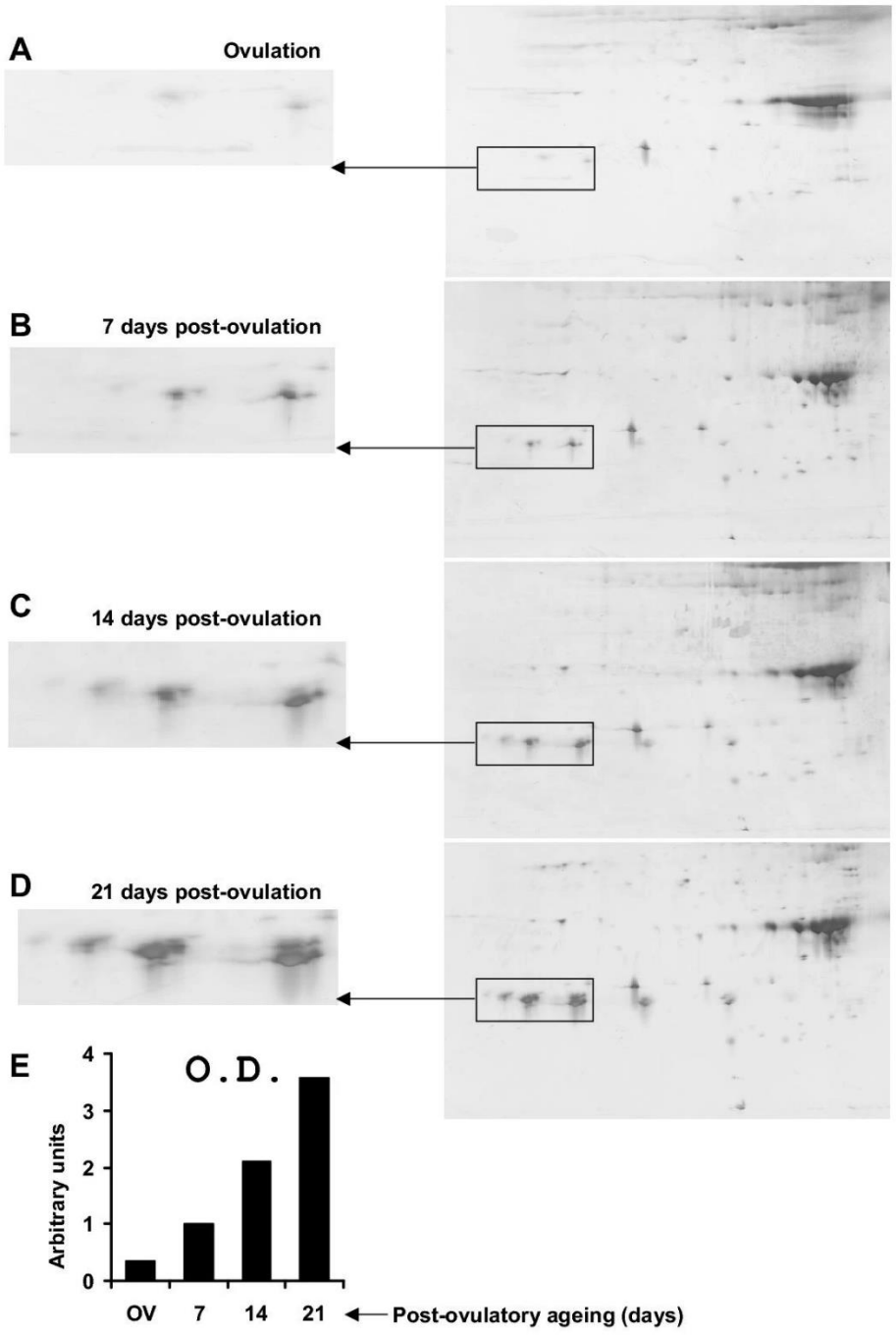

Figure 14. Two-dimensional gel analysis of rainbow trout coelomic fluid during post-ovulatory ageing Two-dimensional gel of rainbow trout coelomic fluid pools originating from 17 females sampled at the time of ovulation (A) and on day 7 (B), day 14 (C) and day 21 (D) after ovulation. Each sample (40 µg) was separated by IEF using a non linear immobilized pH 3–10 gradient for separation in the first dimension combined with SDS-PAGE 12% – 14% gradient gel in the second dimension. Optic density (OD, arbitrary units) of spots shown on the left panel is plotted on the graph (E). OD was arbitrarily set to 1 at 7 days postovulation (Rime et al., 2004).

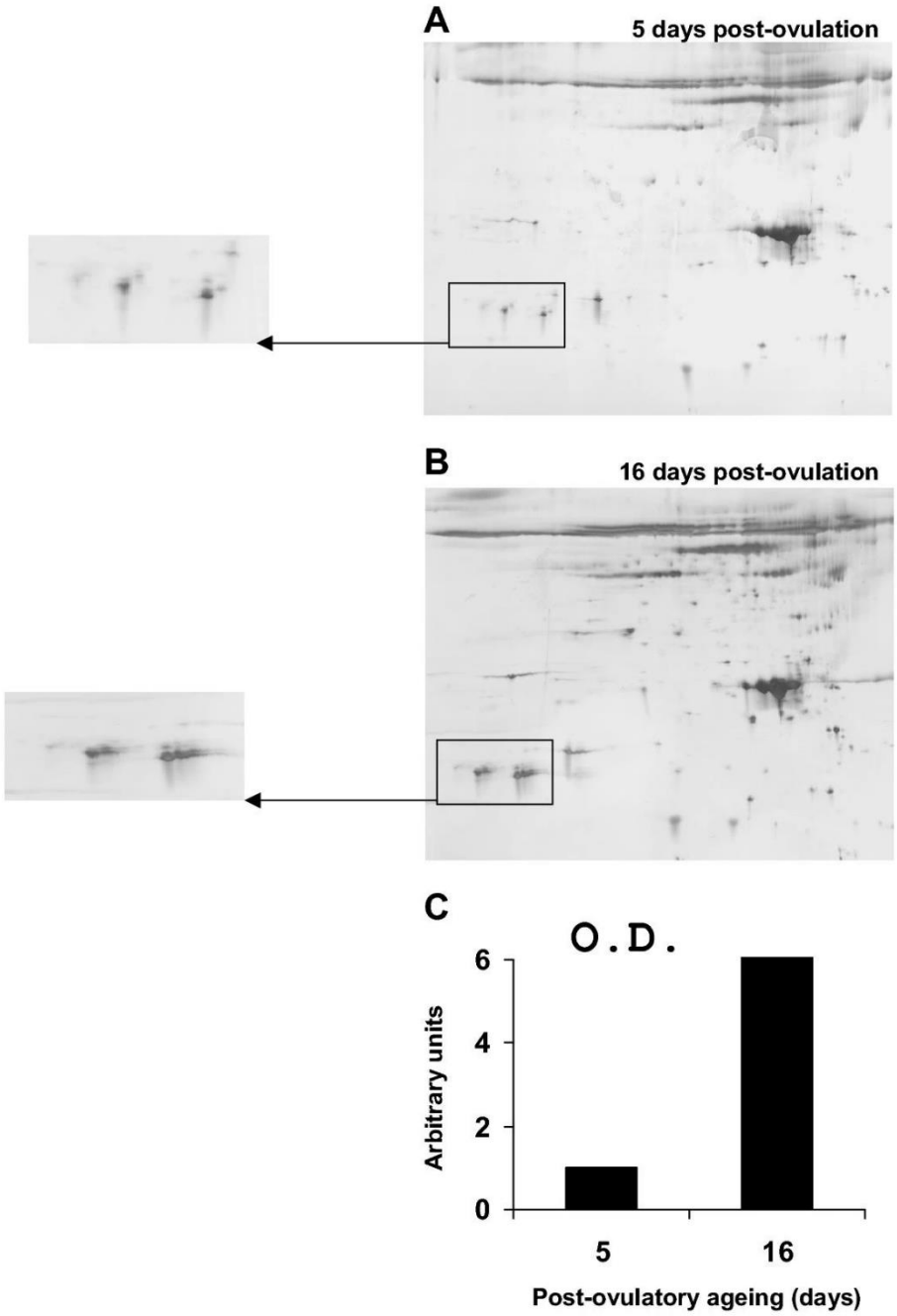

Figure 15. Two-dimensional gel analysis of rainbow trout coelomic fluid at 5 and 16 days post-ovulation Two-dimensional gel of rainbow trout coelomic fluid pools originating from 22 females sampled on day 5 (A) and day 16 (B) after ovulation. Each sample (40 µg) was separated by IEF using a non linear immobilized pH 3–10 gradient for separation in the first dimension com- bined with SDS-PAGE 12 – 14% gradient gel in the second dimension. Optic density (OD, arbitrary units) of spots shown on the left panel is plotted on the graph (C). OD was arbitrarily set to 1 at 5 days post-ovulation (Nomura M, Sakai K, 1974).

Together, these observations show that postovulatory ageing is associated with the apparition of several proteins or protein fragments in coelomic fluid. The strong accumulation of some of these spots is consistent with the increase of CF protein concentration reported in the literature (Lahnsteiner, F., Weismann, T. & Patzner, 1999; Rime et al., 2004).

In conclusion, this study suggests that egg protein fragments accumulate in the CF during the post-ovulatory period and could therefore be used to detect egg quality defects associated with oocyte post-ovulatory ageing.

2.5. **Proteomics of Early Zebrafish Embryos**

Zebrafish (*D. rerio*) has become a powerful and widely used model system for analyzing vertebrate embryogenesis and organ development. While genetic methods are readily available in zebrafish, protocols for proteomics analysis (2D-gel electrophoresis and MALDI-TOF-MS analysis) need to be developed (Link et al., 2006).

As a prerequisite to carry out proteomic experiments with early zebrafish embryos, this study developed a method to remove the yolk from large batches of embryos efficiently. This study enabled high-resolution 2D gel electrophoresis and improved Western blotting considerably. In addition, detailed protocols for proteomics analysis in zebrafish from sample preparation to mass spectrometry (MS), include a comparison of databases for MS identification of zebrafish proteins. The provided protocols for proteomic analysis of early embryos enable research to be taken in novel directions in embryogenesis (Link et al., 2006).

Also, this study indicated that western blotting analysis improved significantly when using the deyolking method. The evaluation of mass spectrometry-based database searches revealed that the combination of two publicly available databases yields a good identification rate. It is finally desired that the developed method herein coud be used to facilitate the proteomics study of zebrafish embryos to analyze fundamental developmental processes (Link et al., 2006).

2.6. **Identification of the Potential Bioactive Proteins Associated with Wound Healing Properties in Snakehead Fish *(Channa striata*) Mucus**

The main objective of this study was to identify the potential proteins in the *C. striata*'s mucus, which are the main players to wound healing enhancement. In this study, the mucus of *C. striata* was analyzed using a proteomic approach (Kwan & Ismail, 2018). The proteins were

seperated using a liquid fractionation system prior to MS analysis with the state-of-the-art high-resolution LTQ-Orbitrap Velos Pro mass spectrometer was used to identify the proteins available in the sample. The data generated were then compared with the Uniprot *Actinopterygii* database to identify the proteins and PTMs available. The complete protein profile (list of bioactive proteins) and the post-translational modifications (PTMs) were highlighted. Moreover, the post-translational modifications (PTMs) identified allowed to complement the protein list to better understand those proteins. Fifty-three and 120 unique proteins in the crude mucus sample and the fractionated sample were identified, respectively (Kwan & Ismail, 2018).

Interesting proteins such as histones, ribosomal proteins, protein S100, heat shock protein, proteolytic enzymes, heparin cofactor II and a group of uncharacterized proteins were identified and discussed thoroughly. Besides, 39% of the proteins identified were post-translational modified. Methylation, hydroxylation, acetylation, ubiquitin and biotinylation were the PTMs detected (Kwan & Ismail, 2018).

In conclusion the proteins and PTMs profiling of the *C. striata* mucus serve as a preliminary report and foundation for future in-depth exploration of the species. These results serve as a fundamental preliminary report on the mucus of *C. striata*, which provides insights for harvesting the bio-active proteins for possible drug production and medication purposes in the future.

2.7. **Proteome Reference Map of the Skin Mucus of Atlantic Cod (*Gadus morhua*) Revealing Immune Competent Molecules**

A recent study on the effect of fish skin mucus on the soluble proteome of *Vibrio salmonicida* has indicated that there was an up-regulation of proteins involved in both general motility and oxidative stress responses. On the other hand, the fish host response usually depends on the components of the skin mucus, which reacts to the pathogen and orchestrates the immune response. A recent study showed that Koi herpesvirus (KHV), which is a highly contagious virus that causes significant morbidity and mortality in common carp (Cyprinus carpio), a common pathogen of carp, uses skin as its primary portal of entry (Rajan et al., 2011; Uttakleiv Ræder et al., 2007a., Haenen et al., 2004; Hartman et al., 2013; Hedrick et al., 2000).

With the help of novel bio-imaging techniques, it was established that the virus attached to the skin surface only in the sites where mucus was manually removed. This suggests that the intact

mucus surface offers strong protection to the host from infection. The information available on a host-mucosal-pathogen paradigm with respect to infection and disease susceptibility has been compelling enough to further characterize these components, primarily from the host mucus (Costes et al., 2009; Rajan et al., 2011).

Characterization of the mucus from fish skin has been approached from different angles, which includes the focus on the various proteases present in the skin mucus (Firth et al., 2000; Salles et al., 2007). However, little research work was done on the Atlantic cod skin mucosa. Although, a recent study on cod skin mucus proteases revealed that serine proteases are more predominant than metalloproteases and that overall protease activity was less than some freshwater fish and hagfish (Firth et al., 2000). Therefore, a different and more comprehensive approach is needed to characterize the general skin mucosal proteome. Targeting skin mucosa for proteome-based studies also helps in identifying biomarkers, some of which may be employed in non-invasive protocols for fish disease diagnosis (Rajan et al., 2011).

For these reasons, the skin mucosal proteome of Atlantic cod (*Gadus morhua*) was mapped using a proteomics approach (2D PAGE and LC-ESI-MS/MS). Here, the skin mucus from naive cod was run on 2D gels, followed by identifying spots using LC-ESI-MS/MS. In addition, the selected vital immune-competent genes were subsequently cloned. The representative 2D gel profiles of the mucosal proteome are shown in Figure. 16. The 15% gels and 10% gels (Figure. 16A and B respectively) together were used to identify a broad range of proteins, of which 67 spots were excised and identified by LC-ESI-MS/MS analysis. The majority of the mucosal proteins are in the pH 4-8 range (Figure. 16A and B). The 2D gels yielded considerable reproducibility for the mucus samples from individual fish (Figures.16A and B) (Rajan et al., 2011).

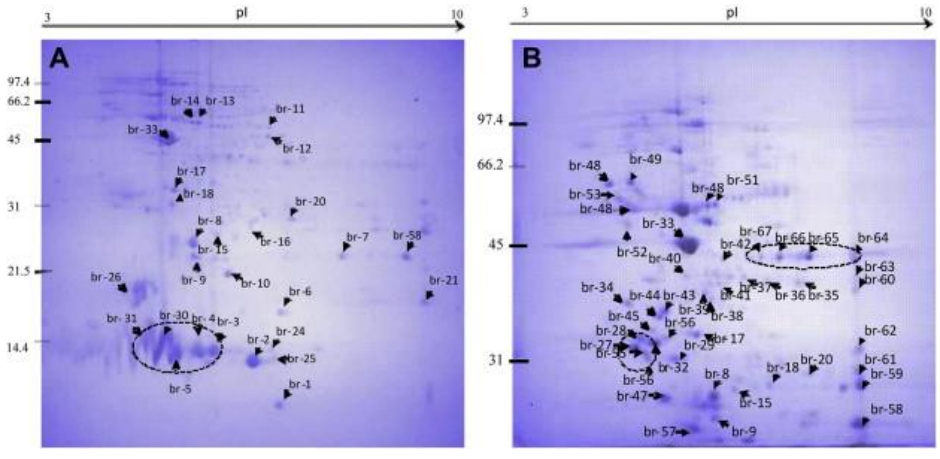

Figure 16. 2D gels of Atlantic cod skin mucosal proteins. (1A) 15% 2D reference gel (17 cm) stained with Coomassie blue G. The circled portion within the gel shows galectin-1 isoforms. (1b) 10% 2D gel (17 cm) stained with Coomassie blue G. The circled portions within the gels show serpin isoforms (br-64, br-65, br-66, br-67) and 14-3-3 isoforms (br-27, br-28, br- 55, br-56). Molecular weight is indicated in kDa (Rajan et al., 2011).

The LC-ESI-MS/MS approach proved to be more useful than MALDI-TOF/TOF-MS/MS analysis in identifying a considerable number of proteins in this study. Preliminary search of the designated peptides against the protein databases yielded few direct protein hits except for proteins like g-type lysozyme and apolipoprotein 1A. However, queries over the dbEST resources returned several EST matches for cod with a high score. The protein spots identified along with their features are listed in Supplementary Table S2. The identified proteins were clustered into 8 groups based on gene ontology classification for biological process. Most of the proteins identified from the gel are hitherto unreported for cod. Galectin-1, mannan binding lectin (MBL), serpins, cystatin B, cyclophilin A, FK-506 binding protein, proteasome subunits (alpha-3 and -7), ubiquitin, and g-type lysozyme are considered immune competent molecules (Rajan et al., 2011).

Supplementary Table S2 shows MASCOT scores and accession numbers for a cod EST or a direct protein hit from cod or other species. The Table also lists the pI and MW observed from the 2D gel profiles for each protein and their isoforms. The proteins are grouped into 8 different clusters based on biological process annotation, as shown in Figure 17 (Rajan et al., 2011).

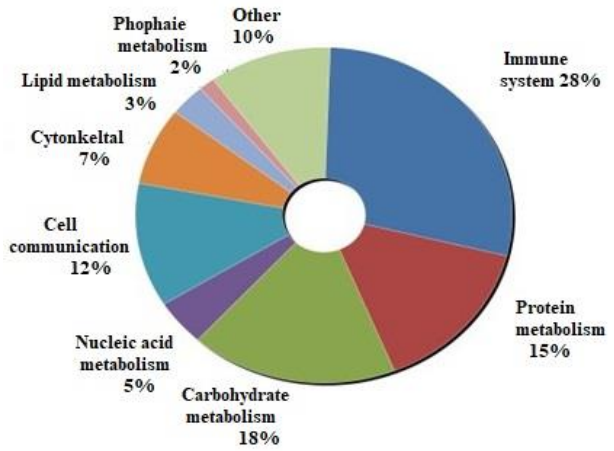

Figure 17. Classification of protein spots from the mucus of Atlantic cod identified through LC-ESI-MS/MS. The spots identified were clustered into different categories based on gene ontology category: biological process (Rajan et al., 2011).

As expected, several spots were identified as immune-related proteins. In addition, proteins like 14-3-3 and proteasome subunit types which are indirectly involved in immune response, and other proteins wherein immunological roles may be debated were identified. Considering these factors, Table 7 lists the different unique proteins that may be immune-relevant and possibly natural components of the mucus. The information, however, is based primarily on mammalian studies (Rajan et al., 2011).

Table 7. Unique proteins identified from the 2D gels of the mucus of Atlantic cod - a literature-based distinction of their immune potential, secretory nature and affiliation to mucosa (Rajan et al., 2011).

Protein	Immune function[a]	Secreted[a]	Reported in mucus[a]
Ubiquitin	✓	✓	✓
Galectin−1	✓	✓	✓
Nucleoside diphosphate kinase	✓	✓	✓
G-type lysozyme	✓	✓	✓
Cofilin-2	✓	x	x
6-Phosphogluconate dehydrogenase	x	x	✓
Citrate synthase	x	x	✓
Alpha enolase	x	x	✓
Rab-7	✓	x	x
Beta actin	x	x	✓
FK-506 binding protein	✓	x	x
Cyclophilin A	✓	✓	✓
Cystatin B	✓	✓	✓
Mannan binding lectin	✓	✓	✓
14-3-3 protein	✓	✓	✓
Apolipoprotein 1A	✓	✓	✓
Fatty acid binding protein	x	x	✓
Transaldolase	x	x	✓
Leukocyte elastase inhibitor	✓	✓	✓
Tropomyosin	x	x	✓
Proteasome subunit alpha type 3	✓	x	✓
Proteasome subunit alpha type 7	✓	x	✓
Calreticulin	✓	x	✓
Glyceraldehyde-3-phosphate dehydrogenase	x	x	✓
Glutathione transferase pi	✓	x	✓

[a] Unless mentioned as separate references, the information is based on UniProt data (www.uniprot.org) for individual proteins.

The mucosal proteins from naive fish were identified primarily by similarity searches across various cod EST databases. The identified proteins were clustered into eight groups based on gene ontology classification for biological processes. Finally, five of the aforementioned proteins were cloned, and their tissue distribution was analyzed by RT-PCR.

2.8. Proteomic Identification of Rainbow Trout Blood Plasma Proteins and their Relationship to Seminal Plasma Proteins

Fish represent the earliest class of vertebrates possessing the elements of both innate and acquired immunity, with a highly developed innate immune response and less developed adaptive immune response compared to higher vertebrates (Nynca et al., 2017).

The characterization of rainbow trout blood proteome contributes to the characterization of the fish immune mechanisms and pathways. A quantitative comparison of blood and seminal proteomes allowed to determine the origin of seminal fish plasma (SP) proteins and characterize their relationship to blood plasma (BP) proteins (Nynca et al., 2017).

This study provided the first in-depth analysis of the rainbow trout SP proteome, identifying a total of 152 proteins. The major proteins of rainbow trout SP, such as transferrin, apolipoproteins, complement C3, serum albumin, hemopexin-like protein, α1-antiproteinase-like protein, and precerebellin-like protein, are members of the acute phase protein family. However, the relationship of these proteins to their blood counterparts has not yet been analyzed (Nynca, Dietrich, et al., 2011b; Nynca et al., 2017).

The present study is one of the largest dataset published to date, which allows the characterization of the fish BP proteome, which contains a total of 119 identified proteins. The usual proteomics approach (LC-ESI-MS/MS and 2D DIGE) was applied to compare rainbow trout seminal (SP) and blood plasma (BP) proteomes. The comparison of SP and BP proteomes, combined with the bioinformatic analysis, highlighted a prevalent acute phase responses signalling pathway modulated by the proteins more abundant in SP. Moreover, this study provided the first in-depth analysis of the trout BP proteome, with a total of 119 proteins identified. The major proteins of rainbow trout BP were recognized as acute-phase proteins. Analysis of BP proteins indicated that acute phase response signalling, the complement system, LXR/RXR and FXR/RXR activation and the coagulation system are the top canonical pathways. The 54 differentially abundant proteins identified in SP are involved in a variety of signalling pathways, including

protein ubiquitination, liver X receptor/retinoid X receptor (LXR/RXR) and farnesoid X receptor (FXR)/RXR activation, cell cycle and acute phase signalling (Nynca et al., 2017).

These findings may indicate the prevalence of acute-phase signalling pathways in trout SP and its essential role in protecting spermatozoa and reproductive tissues. In contrast to mammals, most SP proteins resemble those of BP in trout, which reflects a close relationship between both body fluids in fish (Nynca et al., 2017).

In the present study, SDS-PAGE pre-fractionation combined with nano-LC-ESI-MS/MS-based identification was used to generate an inventory of the most prominent rainbow trout BP proteins. Moreover, LC-ESI-MS/MS and 2D DIGE followed by MALDI-TOF/TOF-MS/MS analysis allowed to identification and quantitatively compare the SP and BP proteomes. Also, Polyclonal antibodies against SP transferrin (TF) and PGDS (Nynca, Arnold, Fröhlich, Otte, & Ciereszko, 2014)were used to confirm the identity of these proteins and to qualitatively assess their abundance in SP and BP (Figure 18) (Nynca et al., 2017).

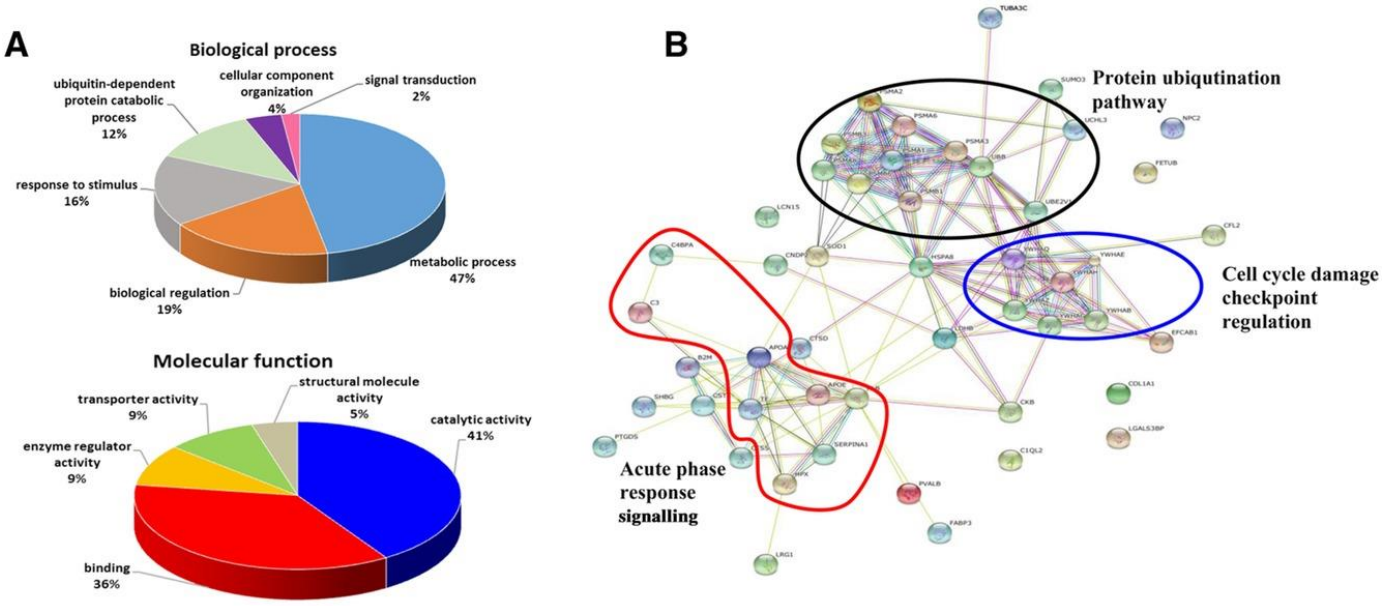

C

Top canonical pathways	p-value	Molecular and cellular functions	p-value
Protein ubiquitination pathway	1.70E-11	Cell death and survival	2.65E-03 – 2.20E-07
FXR/RXR activation	6.30E-10	Molecular transport	2.62E-03 – 8.77E-07
LXR/RXR activation	1.46E-08	Lipid metabolism small molecule biochemistry	2.62E-03 – 9.51E-07
Cell cycle: G2/M DNA damage checkpoint regulation	1.11E-07		
Acute phase response signaling	1.46E-07	Protein degradation	2.39E-03 – 1.46E-06

Figure 18. Functional analysis of identified proteins enriched in SP. (A) Ontology analysis. (B) STRING protein-protein interaction network. The figure was produced using STRING evidence view. Proteins in the black, blue and red circles belong to the ubiquitination, cell cycle damage checkpoint regulation and acute phase response signalling pathways, respectively. (C) Signalling pathways and functions of proteins enriched in SP (Ingenuity Pathway Analysis) (Nynca et al., 2017).

Contrary to what has been observed in higher vertebrates, there is a high level of similarity between BP and SP proteins in fish. The most abundant proteins common to SP and BP were almost identical. This is in agreement with previous data indicating that most rainbow trout seminal proteins are antigenically related to serum proteins (Loir et al., 1990; Nynca et al., 2017).

Moreover, these findings confirmed that the individual major proteins in trout SP, including protease inhibitors (α1-antiproteinase and fetuin-B-like protein) and TF (Nynca, Słowińska, et al., 2011). These proteins are suggested to be transported to the semen from the blood and/or partially synthesized and secreted by reproductive tract cells. Their immune-histochemical staining was found in reproductive tissues (within the testis in Sertoli Leydig cells, as well as in the efferent duct) and liver. The presence of an abundance of blood proteins in fish SP is likely related to the absence of the epididymis and accessory glands, which in mammals are the main source of seminal fluid proteins (Nynca et al., 2017).

On the other hand, some proteins seem to be specific to milt, including PGDS, which was identified only in the rainbow trout SP (Nynca, Dietrich, et al., 2011c). It has to be underlined that most of the enriched proteins identified in this study are known to be intracellular spermatozoal proteins, which indicates that they likely originate from damaged sperm and somatic cells of the reproductive system. The leakage of those proteins could occur during prolonged storage of semen in the reproductive tract, possible injures related to maintenance and handling of fish and the extraction of milt from the fish. However, there is little likelihood that these proteins are biologically active. This should be taken into account during analyses of protein functions in semen (Nynca et al., 2017).

This study enhances knowledge of the blood origin of trout SP proteins and understanding of fish reproductive biology. Our results provide new insight into blood proteins specifically essential for fish physiology and innate immunity. The mass spectrometry data are available via ProteomeXchange with the identifier PXD005988 and DOI 10.6019/PXD005988 (Nynca et al., 2017).

2.9. **Proteomic Characterization of Seminal Plasma from Alternative Reproductive Tactics of Chinook Salmon (*Oncorhynchus tswatchysha*)**

Chinook salmon (*Oncorhynchus tshawytscha*) males represent an example of male alternative reproductive tactics, which possess diverse reproductive strategies known to increase sexual selection. Furthermore, Chinook salmon (*Oncorhynchus tshawytscha*) are external fertilizers that display sneak-guard alternative reproductive tactics. The larger hooknose males dominate mating positions, while the smaller jack males utilize sneak tactics to fertilize (Gombar et al., 2017).

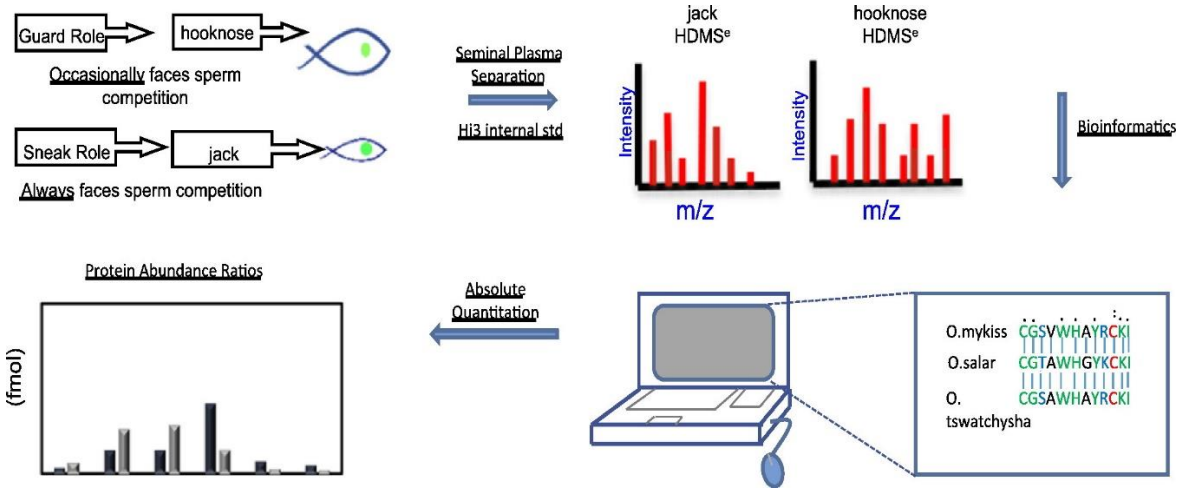

Figure 19. Schematic studies of seminal plasma proteome for Chinook salmon alternative reproductive tactics (Gombar et al., 2017).

Although poorly understood, previous studies have suggested that differences in spermatozoa quality may play a critical role in sperm competition. While seminal plasma has been shown to play an essential regulatory role in sperm competition in many species, little is known about the protein composition of the seminal plasma of salmon (Gombar et al., 2017).

Therefore, seminal plasma isolated from Chinook salmon's two alternative reproductive tactics (small sneaky jacks and large dominant hooknoses) was analyzed by label-free quantitative mass spectrometry employing data-independent acquisition and ion mobility separation. The following scheme represents the strategy used in this work (Gombar et al., 2017).

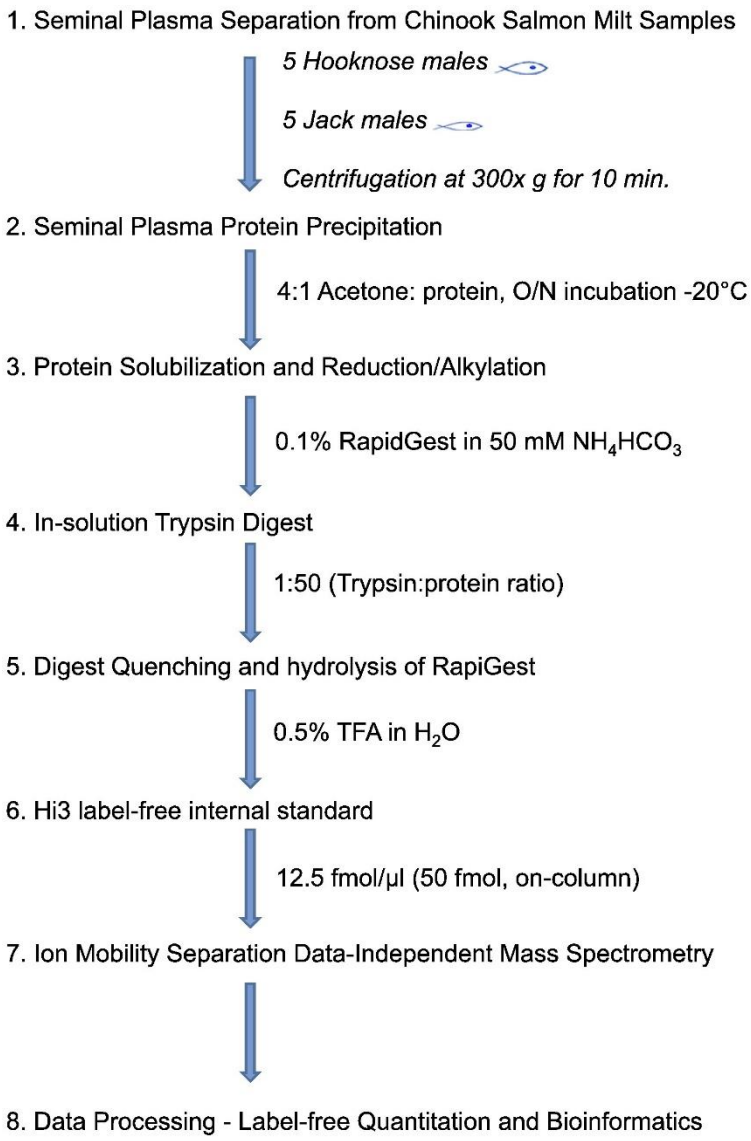

Figure 20. Schematic workflow of seminal plasma sample preparation and proteomic analysis. Seminal plasma was extracted from milt by centrifugation, and proteins were prepared for mass spectrometry analysis using RapiGest solubilization and in-solution trypsin digestion (Steps 1–5). Label-free internal standards (Hi3) were added to each sample for absolute quantitation (Step 6). Samples were analyzed by UPLC ion-mobility data-independent mass spectrometry (Step 7), and the data was processed using Progenesis-QI (Step 8). Statistical analysis was performed to determine significant differences in protein abundance (Step 8) (Gombar et al., 2017).

This analysis provided the largest proteome data set of the seminal plasma from salmon and was the first to examine protein abundance differences between male alternative reproductive tactics. In addition, the quantitative proteomics data obtained provided insight into possible unique

mechanistic aspects of Chinook salmon alternative reproductive tactics utilized for sperm competition and fertilization success (Gombar et al., 2017). A total of 345 proteins were identified in all biological replicates analyzed, including many established seminal plasma proteins that may serve as future biomarkers for Chinook salmon fertility and sperm competition (Table 8).

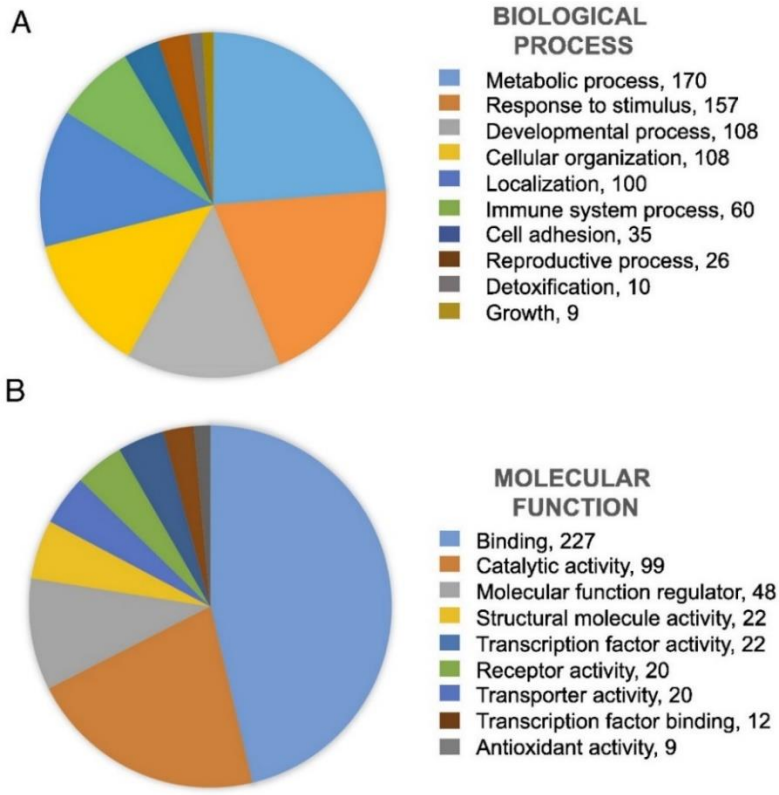

Figure 21. Gene ontology of seminal plasma proteins identified in Chinook salmon (Oncorhynchus tswatchysha) jack and hooknose seminal plasma. A) Gene ontology mapped for seminal plasma proteins in relation to biological processes. B) Gene ontology mapped for seminal plasma proteins concerning molecular function. Gene ontology terms are shown in adjacent legend with a corresponding number of matching proteins (Gombar et al., 2017).

Moreover, this study elucidated statistically significant protein abundance differences between hooknose and jack male tactics. Proteins involved in membrane remodelling, proteolysis, hormonal transport, redox regulation, immunomodulation, and ATP metabolism were among the proteins reproducibly identified at different levels and represent putative factors influencing sperm competition between jack and hooknose males. This study represents the largest seminal plasma proteome from teleost fish and the first reported for Chinook salmon (Gombar et al., 2017).

Table 8. Significant seminal plasma proteins list, that may serve as future biomarkers for Chinook salmon fertility and sperm competition (Gombar et al., 2017).

Accession	Peptide count	Unique peptides	Confidence score	Anova (p)	Max fold change	Highest mean condition	Lowest mean condition	Description
NP_001017750.1;AAA91212.1	4	4	20.1806	4.20E-07	2.8550924	Jack	Hooknose	actin gamma-enteric smooth muscle [Danio rerio]
AAG30018.1	4	4	20.9844	4.39E-06	2.5191646	Hooknose	Jack	putative collagen alpha 1 partial [Oncorhynchus mykiss]
P03946.2	5	5	25.2499	1.44E-09	2.3504658	Hooknose	Jack	Superoxide dismutase [Cu-Zn]
ACH70899.1;CDQ66597.1	20	20	103.3611	2.12E-06	2.2878186	Hooknose	Jack	adenylate kinase 1-1 [Salmo salar]
CDQ96259.1	19	19	124.8091	2.38E-08	2.2454468	Hooknose	Jack	spidroin-1-like [Salmo salar]
AAF04305.2	21	21	150.76	4.11E-05	2.1636602	Jack	Hooknose	precerebellin-like protein [Oncorhynchus mykiss]
XP_014067707.1;CDQ79014.1	80	80	575.0588	1.23E-09	2.1396367	Hooknose	Jack	RNA-binding motif protein, X chromosome-like isoform X1 [Salmo salar]
ACN10110.1;ACN12459.1	7	7	46.4545	3.21E-11	2.0755929	Hooknose	Jack	Beta-2-glycoprotein 1 precursor [Salmo salar]
CDQ62262.1	9	9	46.8825	1.67E-15	2.0643791	Hooknose	Jack	E3 ubiquitin-protein ligase KEG-like [Salmo salar]
XP_014063047.1;CDQ67409.1	23	23	121.7746	5.76E-07	2.0184025	Jack	Hooknose	L-lactate dehydrogenase B chain [Salmo salar]
XP_013993786.1;CDQ57040.1	10	10	71.5254	1.02E-07	1.996803	Jack	Hooknose	ARF GTPase-activating protein GIT2-like isoform X5 [Salmo salar]
ACJ25982.1	4	4	24.4738	3.48E-07	1.9580766	Jack	Hooknose	sex hormone-binding globulin beta [Oncorhynchus tshawytscha]
XP_014008493.1;CDQ88795.1	6	6	35.521	2.82E-07	1.8867544	Jack	Hooknose	cGMP-inhibited 3',5'-cyclic phosphodiesterase A-like isoform X3 [Salmo salar]
CDQ91547.1	30	30	183.1699	1.90E-05	1.8802113	Hooknose	Jack	Creatine kinase B-type [Salmo salar]
CDQ92643.1	28	28	185.2306	3.52E-11	1.8397571	Hooknose	Jack	Apolipoprotein C-I precursor [Salmo salar]
ACI33424.1	7	7	33.8396	2.37E-11	1.8206803	Hooknose	Jack	Lumican precursor [Salmo salar]
CDQ82094.1	7	7	45.6921	2.50E-05	1.8044188	Jack	Hooknose	ubiquitin carboxyl-terminal hydrolase 44-like [Salmo salar]
ACH70915.1; CDQ58363.1;XP_005157650.1;NP_5710072	11	11	73.7719	9.01E-05	1.7645079	Jack	Hooknose	creatine kinase-2 [Salmo salar]
XP_014065278.1;CDR00465.1	15	15	83.0884	9.36E-07	1.7160816	Hooknose	Jack	semaphorin-4F-like [Salmo salar]
Q6UFZ3.1;XP_005737827.1	11	11	59.8259	1.58E-05	1.6984079	Jack	Hooknose	14-3-3 protein gamma-1; Short=Protein 14-3-3G1
AAH45970.1	9	9	53.5333	7.27E-09	1.6913926	Jack	Hooknose	Proteasome (prosome macropain) subunit alpha type 4 [Danio rerio]
CDQ58627.1	11	11	69.0896	7.40E-10	1.6167305	Hooknose	Jack	transcription factor Sox-19a-like [Salmo salar]

CAA37852.1;P24722.1	9	9	73.2986	1.75E-10	1.6095784	Hooknose	Jack	creatine kinase [Oncorhynchus mykiss]
CDQ56006.1	16	16	98.7473	1.92E-08	1.5891365	Hooknose	Jack	tubulin beta-5 chain [Salmo salar]
XP_003199201.2	90	90	726.3129	9.90E-07	1.5606457	Hooknose	Jack	trans-Golgi network integral membrane protein 2 [Danio rerio]
CDQ84911.1	97	97	717.6975	6.93E-07	1.538138	Jack	Hooknose	seizure 6-like protein [Salmo salar]
CDQ81599.1;XP_003443802.1	8	8	50.9949	6.50E-09	1.5178415	Hooknose	Jack	SH3 domain-binding glutamic acid-rich-like protein 3 [Salmo salar]
NP_958892.1	18	18	134.5518	2.33E-09	1.5150201	Hooknose	Jack	tyrosine 3-monooxygenase/tryptophan 5-monooxygenase activation protein theta polypeptide b [Danio rerio]
ACH85299.1	17	17	96.6843	2.83E-06	1.5048479	Hooknose	Jack	proteasome (prosome macropain) subunit beta type 5 partial [Salmo salar]

2.10. **Proteomic Profiling of Salmon Skin Mucus for the Comparison of Sampling Methods**

As already indicated in this review article, the epidermal mucus protects fish against harmful environmental factors and the loss of physiological metabolites and water. Indeed, epidermal mucus is an efficient barrier between the fish and the biosphere. The integrity of the skin mucus is thus of vital importance for the welfare and survival of the fish. It has been established that excreted proteins and small molecules in the mucus can mirror the health status of the fish. It is a valuable matrix for monitoring stress, pathogen exposure, and nutritional effects. Several methods for sampling epidermal mucus from different fish species have been described, but information about their efficiency or on the comparability of mucus analyses is lacking (Fæste et al., 2020).

The present study sampled skin mucus from farmed Atlantic salmon by three methods: absorption, wiping with tissue paper, and scraping with a blunt blade. The mucus proteome was analyzed by the usual conventional proteomics approach as follows. The in-solution digested salmon skin mucus samples were analyzed using an ultra-high pressure liquid chromatography system (Dionex Ultimate 3000 UHPLC) coupled via a nano-electrospray ion source (nESI) to a Q Exactive Hybrid Quadrupole-Orbitrap high-resolution mass spectrometer (HRMS) (ThermoScientific, Bremen, Germany) (Fæste et al., 2020).

Protein identification in the analyzed skin mucus samples was based on a set threshold of at least two peptides per protein that have been detected with a minimum of 90% probability. Under these conditions, the proteomic analysis delivered on average 747 (+-18%) identified proteins per sample for absorbed, 961 (+-15%) for scraped, and 991 (+-3%) for wiped mucus of Atlantic salmon, showing that the latter was the most consistent sampling method (Table 9). The comparison of samples taken from the same fish by two methods indicating the ratios of protein numbers of 1.1 for wiping versus scraping (Group 1), 1.3 for scraping versus absorption (Group 2), and 1.4 for wiping versus absorption (Group 3). The yield of positively identified proteins was thus comparable for wiped and scraped mucus, and significantly lower for absorbed mucus (Fæste et al., 2020).

Table 9. Number (N) of identified proteins and spectra in salmon skin mucus samples collected by different sampling methods (Fæste et al., 2020).

Sampling Method	Fish No.*	N of identified proteins per sample	N of identified spectra per sample	Total number of spectra per sample	Spectrum identification rate
Absorbed	1	761	3676	21,477	0.17
Absorbed	2	479	1978	15,019	0.13
Absorbed	3	876	5122	23,998	0.21
Absorbed	4	769	3814	23,899	0.16
Absorbed	5	886	4821	24,030	0.20
Absorbed	6	709	3259	23,077	0.14
Scraped	3	1018	5449	25,306	0.22
Scraped	4	1024	5344	25,144	0.21
Scraped	6	1018	5327	25,186	0.21
Scraped	7	1032	5446	25,189	0.22
Scraped	8	1036	5855	25,499	0.23
Scraped	9	638	2189	25,158	0.09
Wiped	1	1012	6300	24,960	0.25
Wiped	2	955	5612	24,712	0.23
Wiped	5	998	6251	24,906	0.25
Wiped	7	1008	6522	24,821	0.26
Wiped	8	957	5451	24,337	0.22
Wiped	9	1016	5336	25,256	0.21
Absorbed¤		747 ± 135; 18%	3778 ± 1034; 27%	21917 ± 3211; 15%	0.17 ± 0.03; 17%
Scraped¤		961 ± 145; 15%	4935 ± 1241; 25%	25247 ± 124; 1%	0.20 ± 0.05; 25%
Wiped¤		991 ± 25; 3%	5912 ± 460; 8%	24832 ± 277; 1%	0.24 ± 0.02; 8%

* Identical numbers indicate that samples were collected from the same fish, on both lateral sides.
¤ Mean values with SD and %CV.

The results for fish 9 were of notably lower performance in protein numbers and spectrum identification rate (Table 9), suggesting that this sample could be considered as an outlier. It was, however, not excluded from subsequent data analyses. The measured protein contents, numbers, compositions and the observed data quality were compared between sampling methods. In total, 1192 proteins were identified in the mucus samples of the present study under the observation of the thresholds set for peptide numbers and probability (Supplementary Table S3). Of these, 1013 proteins were detected in mucus obtained by all three sampling methods (Figure. 22a). Several high-abundance proteins such as serum albumin (P21848) (Table 10) were measured with similar signal intensities (mean normalized TIC) indifferently sampled mucus. Such proteins were localized in the upper left corner of graphics that sorted the complete protein set with regard to the mean normalized TIC per protein and sampling method, and by increasing variation coefficients between the sampling methods (Figure. 22b, the position of P21848 is indicated) (Fæste et al., 2020).

Table 10. Most abundant proteins in salmon skin mucus samples, ranked according to their relative mean normalized TICprotein,total (Fæste et al., 2020).[¤]

Protein	Homologs	UniProt Accession No.[&]	Rel. $TIC_{protein,total}$ (%)	RPA*		
				Absorbed	Scraped	Wiped
Deoxyribonuclease	3	B5XGV3	13.2	0.60	0.09	0.31
Actin, cytoplasmic 1	1	O42161	3.66	0.33	0.31	0.36
Histone H2A	4	B5X851	3.26	0.43	0.23	0.34
Fast myotomal muscle actin 2	1	B5DG40	2.67	0.36	0.29	0.35
Cofilin-2	5	B5XB84	2.26	0.36	0.28	0.36
Keratin, type II cytoskeletal 8	1	B5X320	1.79	0.05	0.77	0.18
Elongation factor 2	2	C0H9N2	1.43	0.15	0.41	0.44
Serum albumin 2	1	Q03156	1.42	0.57	0.14	0.29
Serum albumin 1	1	P21848	1.38	0.56	0.15	0.29
Heat shock cognate 70 kDa prot.	2	B5DFX7	1.35	0.37	0.35	0.28
Serotransferrin-1	1	B5X2B3	1.23	0.55	0.18	0.27
Tubulin alpha chain	4	B5DH01	1.22	0.13	0.36	0.51
Glutathione S-transferase P	3	B5XGZ2	1.17	0.38	0.26	0.36
Peptidyl-prolyl cis–trans isom.	NB[#]	B5DG94	0.93	0.24	0.42	0.34
Gelsolin (Fragment)	1	C0PU67	0.89	0.35	0.33	0.32
Alpha-enolase	2	B5X1B	0.83	0.45	0.24	0.31
L-lactate dehydrogenase B chain	2	B5X4K4	0.83	0.40	0.23	0.37
Tropomyosin alpha-3 chain	2	C0H9C0	0.75	0.36	0.39	0.25
Actin, adductor muscle	1	B5XFZ3	0.71	0.14	0.26	0.60
Transketolase	1	B5X4R7	0.70	0.19	0.46	0.35
Triosephosphate isomerase	1	B5DGL3	0.68	0.40	0.25	0.35
Disulfide-isomerase A3	2	B5X1H7	0.66	0.18	0.67	0.15
14-3-3 protein beta/alpha-1	2	B5XF08	0.61	0.27	0.34	0.39
Peroxiredoxin-1	2	B5XBY3	0.57	0.45	0.26	0.29
Malate dehydrogenase	2	B5X2Q1	0.56	0.34	0.36	0.30
Anterior gradient protein 2 hom.	1	Q2V6Q8	0.53	0.21	0.51	0.28
Heat shock protein hsp90 beta	1	Q9W6K6	0.51	0.04	0.58	0.38
Profilin	4	B5X5I8	0.50	0.28	0.44	0.28
Histone H2B	1	B5XEY5	0.50	0.38	0.36	0.26

¤ Rel. $TIC_{protein,total}$: cut-off for inclusion into list at ≥0.5%; values of homologous proteins were combined.
& Accession number of the most abundant protein homolog is given.
* RPA: relative protein abundance; values representing the highest RPA and RPA ≥ 0.4 are underlined.
# NB: nucleotide BLAST: no matched homologs according to comparison with NCBI nucleotide collection by BLAST search.

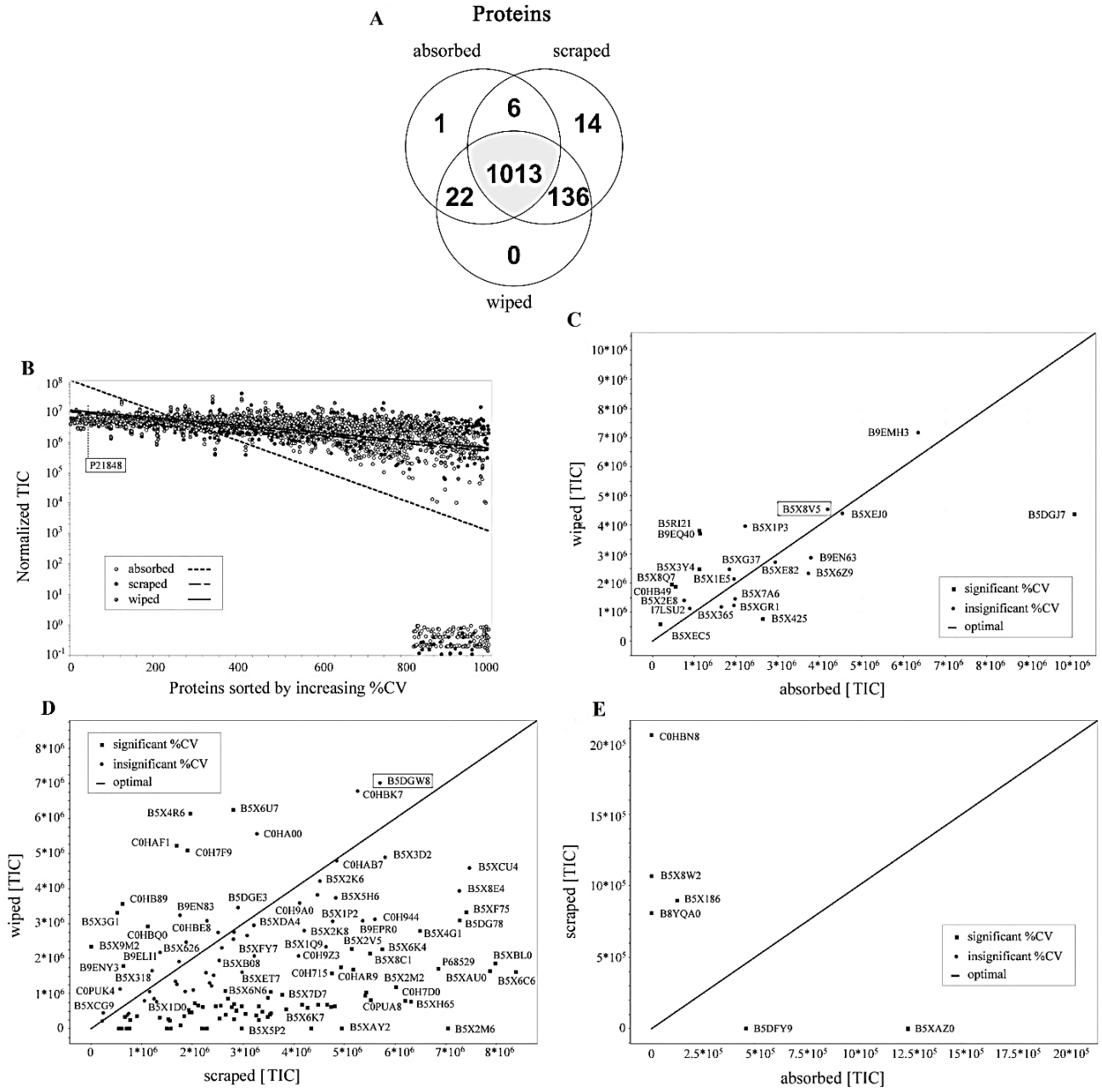

Figure 22. (A) Venn diagram showing shared and specific proteins obtained by the three sampling methods; (B) Complete protein set (1192) with mean normalized TIC and regression line for each sampling method, sorted by increasing variation coefficient (%CV) of TIC values between the methods; (C) Scatterplot showing significant and insignificant differences in the mean normalized TIC obtained by absorbed vs wiped, (D) wiped vs scraped, and (E) absorbed vs scraped sampling methods for all detected proteins. Proteins described in more detail in Fig. 23 are boxed (Fæste et al., 2020).

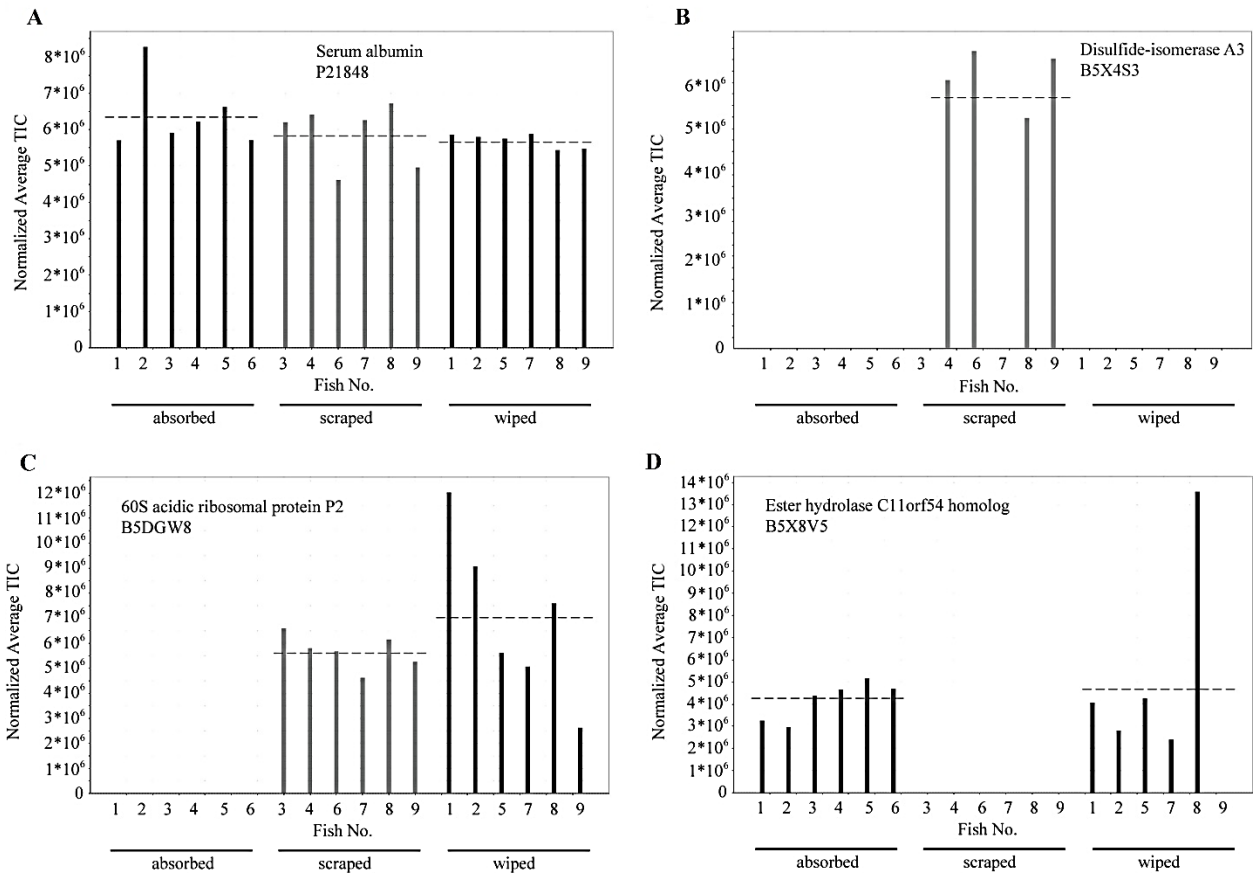

Figure 23. Examples for proteins detected (A) with comparable abundance by all sampling methods (serum albumin); (B) only in scraped samples (disulphide-isomerase A3); (C) both in scraped and wiped samples with insignificant %CV (60S acidic ribosomal protein P2); both in absorbed and wiped samples with insignificant %CV (ester hydrolase C1) (Fæste et al., 2020).

Furthermore, functional annotation and classification of the identified proteins was performed. The results showed that the three skin mucus sample types differed qualitatively as well as quantitatively. The absorbed mucus was the least tainted by proteins resulting from damage inflicted to the fish epidermis by the sampling procedure (Fæste et al., 2020).

Wiped mucus showed a better protein yield than absorbed and delivered a larger proteome of identifiable proteins, with less contamination from epithelial proteins than observed for scraped mucus. It is recommended that future research of mucus, should use the absorption method, where it is essential that the mucus is devoid of proteins from the underlying epithelium. Also, the wiping method, is recommended when protein yield is crucial or when the proteome of the outer epithelium is of interest (Fæste et al., 2020).

The proteins identified in skin mucus samples obtained by using the three sampling methods were sorted according to their roles in different physiological processes with the aid of GO. The detected proteins could be grouped into the nine general biological functions "*Cellular compartment organization or biogenesis*," "*Cellular process*," "*Localization*," "*Biological regulation*," "*Response to stimuli*," "*Developmental process*," "*Multicellular organismal process*," "*Metabolic process*," and "*Immune system process*". The sampling method had only little influence on the distribution of the identified proteins by biological function. Although it was found that the identified proteins were identical for scraped and wiped mucus, the absorbed mucus contained a higher percentage of proteins belonging to the "*Metabolic process*" and a lower percentage of proteins belonging to "*Biological regulation*" (Table 11). Independently of the sampling method, most of the identified proteins were connected to the "*Cellular process*," and the least to the "*Immune system process*" (Fæste et al., 2020).

Table 11. Typical peptide markers differentiating between mucus sampling methods (Fæste et al., 2020).

Sampling method	Access. No.	Protein name[&]	Peptide[¤]	MW [Da]	z
Scraped	B5X4S3	Disulfide-isomerase A3	IFKDGEDAGAYDGPR	1609.73	+3
			EATNPLVAQEEK	1328.67	+3
	B5X3B8	Acetyl-CoA acetyltransf. mitochondr.	IVGHMVHALK	1103.63	+3
			GKPDVVVSEDEEWR	1643.78	+3
abs./wip.	B9EMH3	Actin-rel. pr. 2/3 com. S5	AFAVGGLGSIVR	1146.65	+2
			GFEKPSDNSSAILLQWHEK	2185.08	+3
	B5X8V5	Ester hydrol. C11orf54 h	SLALGGTFLIQK	1246.73	+2
			ITDVGGVPYLVPLVK	1568.92	+2
	B9EN63	DJ-1 (Class I gatase-like)	QGPYDVVFLPGGALGAQHLSESPAVK	2636.37	+3
			DVYLVPDASLEDARK	1689.86	+2
	B5X6Z9	Lambda-crystallin	EIDGFALNR	1033.52	+2
			TITVIGSGLIGR	1185.71	+2
scrap./wip.	B5DGW8	60S acidic ribos. prot. P2	ILESVGIEADNTR	1415.72	+2
			NVEEVIAQGYGK	1305.66	+2
	B5X3D2	Splic-fac., Arg/Ser-rich 5	LNEGVVEFASYSDLK	1669.81	+2
			DAEDAVYELDGK	1323.58	+2
	B5XCU4	U1 small nucl. rib.nucl.pr	LNHTIYINNLNEK	1584.82	+3
			SMQGFPFYDKPMR	1602.74	+3
	C0HBK7	DnaJ hom. sub. A mem 2	VSLEDLYNGK	1136.57	+2
			EISFAYEVLTNPEKK	1766.91	+2

[&] Proteins with relatively high abundances (no significant differences) in all samples obtained with one method or for two sampling methods in pairwise comparisons. [¤] Typical peptide, no missed cleavages.

From the total 1192 proteins identified, 13, 521 or 322 proteins were recognized by LC-ESI-MS/MS with or without upstream 2D gel electrophoresis (Easy & Ross, 2009; Provan et al.,

2013; Valdenegro-Vega et al., 2014). Among the skin mucus proteins characterized, a range of defence molecules was also identified; this included the antimicrobial histones (H1, H2A, H2B, H3), heat shock proteins (hsp10, hsp70, hsp90 beta), complement factors (C1, C1Q C6, D), proteasome subunits, lysozyme, cathepsins (B, D, H, K, M, S, Z), calreticulin, superoxide dismutase and peroxiredoxin. These and other defensive proteins are important for maintaining the primary protective barrier of fish, and some functionalities have previously been described (Easy & Ross, 2009; Fæste et al., 2020; Hellio et al., 2002; Patel & Brinchmann, 2017; Provan et al., 2013; Valdenegro-Vega et al., 2014). It should be mentioned that the identities of the defensive proteins in the skin mucus analysis are essential, especially as changes in their expression levels changes, when fish are exposed to stress (Easy & Ross, 2009; Fæste et al., 2020; Guardiola et al., 2014; Jurado et al., 2015a; Rajan et al., 2013; Ross et al., 2000; Valdenegro-Vega et al., 2014).

In this context, the histone-derived peptides detected in the present study were found with relatively high robotic process automation (RPA) in all mucus samples. They might have been released from cells to the extracellular space as a result of cell damage in samples collected by a harsh method such as scraping. However, the considerably high abundances of histones in absorbed mucus samples suggested that histone proteins could at least partially have been secreted intentionally into the mucus. Secreted histones can act as endogenous danger signals that activate the immune system and cause cytotoxicity (Fæste et al., 2020; Silk et al., 2017). Furthermore, Various proteases in the mucus perform defensive tasks but are also involved in the remodelling of tissues, cells and mucus structures and are therefore regulated by protease inhibitors such as the observed metalloproteinase inhibitor, elastase inhibitor, Kunitz-type protease inhibitor and plasminogen activator inhibitor (Rajan et al., 2013; Sanahuja & Ibarz, 2015a).

In addition, several proteins were identified in the skin mucus samples, such as. serine/threonine-protein phosphatase, members of the 14-3-3 family, Rho GDP-dissociation inhibitor (1, 2) and Rab GDP dissociation inhibitor (beta), are involved in signal transduction processes and might also be useful biomarkers of increased physiological activity. The metabolic enzymes such as transketolase, enolase and aldolase are possibly required for maintaining the epithelial layers (Cordero et al., 2017; Fæste et al., 2020; Jurado et al., 2015a; Pérez-Sánchez et al., 2017; Saleh et al., 2018; Sanahuja & Ibarz, 2015a). Also, the considerable amount of serum albumin detected in all samples, independently of the sampling method, could be a result of

secretion or leakage from the plasma, while hemoglobin could have been released from red blood cells and diffused into the mucus (Fæste et al., 2020; Valdenegro-Vega et al., 2014).

The overall difference in the proteome compositions of the differently sampled skin mucus were studied in more detail by KEGG-based analysis of proteins belonging to the 26S proteasome complex. While the core particle components of the proteasome were most abundant in absorbed mucus, regulatory particle components and proteasome-interacting proteins occurred more frequently in scraped and/or wiped mucus (Fæste et al., 2020). Also, it was recently shown that extracellular proteasomes exported by human primary cell cultures, consisted exclusively of 20S core particle subunits with no attached regulatory particles. The presumed presence of unregulated proteasome CP could provide the mucus with a capacity to degrade proteins irrespectively of their ubiquitination status and thus might have defensive functions (Ben-Nissan & Sharon, 2014; Fæste et al., 2020; Kulichkova et al., 2017). This study indicated that contrary to the different extracellular proteasomes described in humans, the catalytic β subunits specific for the immunoproteasome CP in salmon mucus, could be involved in removing damaged proteins during stress conditions (Fæste et al., 2020).

In conclusion, the combined results of this study prove the importance of choosing a mucus sampling protocol with respect to the intended purpose of the planned experiment. Scraped mucus and, to a much lesser degree, wiped mucus contained intracellular proteins that were released by abrasion during sampling. In contrast, the proteome of the absorbed mucus contained mainly proteins that had diffused from the mucosal layer into the receiving tissue paper. Accordingly, the variation in protein consistency between samples was lowest for absorbed but increased for wiped, and the highest for scraped samples (Fæste et al., 2020).

2.11. **Proteomic Profile of the Skin Mucus of Farmed Gilthead Seabream (*Sparus aurata*)**

As described ealier, fish skin mucus is the first line of defence against infections, and it discriminates between pathogenic and commensal bacterial strains. Mucus composition varies amongst fish species and is influenced by endogenous and exogenous factors. This study describes the first proteome map of the epidermal mucus of farmed gilthead seabream (*Sparus aurata*) (Jurado et al., 2015b).

In this study, an integrative proteomic approach was used by combining a label-free procedure (LC-ESI-MS/MS) with the classical 2-DGE-PMF-ESI-MS/MS methodology. The

identified mucosal proteins were clustered in four groups according to their biological functions. Structural proteins (actins, keratins, tubulins, tropomyosin, cofilin-2 and filamin-A) and metabolic proteins (ribosomal proteins, proteasomal subunits, NACA, VCP, histones, NDPK, transferrin, glycolytic enzymes, ATP synthase components, beta-globin, Apo-A1 and FABP7) were the best represented functional categories (Tables 12 and 13) (Jurado et al., 2015b).

Table 12. Proteins in the skin mucus of S. aurata identified by tandem MS. MS/MS-derived peptide sequence data were used for a BLAST analysis in which the search was restricted to the class Actinopterygii. Proteins are shown match completely with the sequenced peptide (Jurado et al., 2015b).

Protein[a]	Sequence ID[a]	UniProt[a]	PM[b]	Sample[c]	Score[d]	Expect [e]
Structural proteins: cytoskeleton and extracellular						
Alpha-actin, partial [Deltistes luxatus]	gb|AEO79977.1|	H6DA56	1, 1	1, 2	75.3	2.0E− 16
Skeletal alpha-actin [Sparus aurata]	gb|AAF22646.1|	Q9PTJ5	1, 1	1, 2	60.4	2.0E −11
Actin-related protein 3 [Perca flavescens]	gb|ADX97138.1|	F1C778	1	1	48.1	4.0E −08
Beta-actin [Sparus aurata]	gb|AAK63074.1|	Q90Z11	7, 7	1, 2	99.0	7.0E− 16
Beta actin isoform 2a, partial [Sparus aurata]	gb|AFA25665.1|	H6UWY4	1, 1	1, 2	96.5	2.0E− 23
B-actin [Pagrus major]	dbj|BAA89429.1|	Q9PTU4	1	1	84.6	7.0E− 20
Beta-actin, partial [Oreochromis niloticus]	gb|ABK20357.1|	A0FKD6	1	2	33.3	3.0E− 03
Keratin, type I cytoskeletal 13 [Oncorhynchus mykiss]	ref|NP_001117848.1|	Q8JFQ6	1	2	42.2	2.0E− 05
Keratin, type I cytoskeletal 13-like [Oreochromis niloticus]	ref|XP_003442600.1|	N.E.	1	1	39.2	2.0E− 04
Type I keratin-like protein [Sparus aurata]	gb|ACN62548.1|	C0LMQ3	1, 1	1, 2	53.7	4.0E− 09
Type I keratin isoform 1 [Solea senegalensis]	dbj|BAF56913.1|	A4UYK3	2, 3	1, 2	43.9	5.0E− 06
PREDICTED: keratin, type I cytoskeletal 13-like [Maylandia zebra]	ref|XP_004556558.1|	N.E.	1	2	37.1	7.0E− 04
Keratin, type II cytoskeletal 8 [Epinephelus coioides]	gb|AEG78360.1|	F6KMI6	1, 1	1, 2	43.5	7.0E− 06
Keratin type II [Epinephelus coioides]	gb|AEG78338.1|	F6KMG4	1, 1	1, 2	52.8	6.0E− 09
Type II keratin E3, partial [Gillichthys seta]	gb|ACO57583.1|	C1J0K3	1, 1	1, 2	51.5	2.0E− 08
Type II keratin E3-like protein [Sparus aurata]	gb|AAT44423.1|	Q4QY72	1	2	34.6	4.0E− 03
Keratin [Poecilia reticulata]	gb|AAD47884.1|AF172645_1	Q9PW53	1	1	30.8	6.9E− 02
Keratin 18 [Epinephelus coioides]	gb|ACE06742.1|	B3GPH2	1	2	52.4	1.0E− 10
Alpha-tubulin [Sparus aurata]	gb|AAP89018.1|	Q7T1F8	2	1	59.2	7.0E− 11
Beta tubulin [Chionodraco rastrospinosus]	gb|AAG15329.1|AF255955_1	Q9DFS7	1, 2	1, 2	57.1.5	3.0E− 10
Uncharacterized protein LOC767806 [Danio rerio]	ref|NP_001070241.1|	Q08CC8	1	1	57.1	3.0E− 10
PREDICTED: collagen alpha-1(I) chain-like isoform X1 [Maylandia zebra]	ref|XP_004572575.1|	N.E.	1	1	73.6	2.0E− 15

Filamin-A-like [Oreochromis niloticus]	ref|XP_003454305.1|	N.E.	1	1	60.9	2.0E− 11
Metabolism						
Protein metabolism						
Ribosomal protein L8 [Sander lucioperca]	gb|AEE81293.1|	F6KH17	1, 1	1, 2	52.8	7.0E− 09
Ribosomal protein L11 [Perca flavescens]	gb|ABW06869.1|	A8HTH7	1	1	46.4	7.0E− 07
40S ribosomal protein Sa-like protein [Sparus aurata]	gb|AAT44424.1|	Q4QY71	1,1	1, 2	56.2	6.0E− 10
40S ribosomal protein S7 [Oncorhynchus mykiss]	ref|NP_001117902.1|	Q2YHL9	1	1	71.5	6.0E− 15
40S ribosomal protein S3 [Salmo salar]	gb|ACI67536.1|	B5X9L6	1	2	44.8	3.0E− 06
60S ribosomal protein L7A [Siniperca chuatsi]	gb|AAY79207.1|	Q2KL19	1, 1	1, 2	51.1	2.0E− 08
60S ribosomal protein L24 [Gillichthys mirabilis]	gb|AAG13295.1|AF266175_1	Q9DFQ7	1	2	42.2	2.0E− 05
60S ribosomal protein L19 [Epinephelus coioides]	gb|ADG29150.1|	D6PVQ5	1	2	59.2	5.0E− 11
20S proteasome beta 6 subunit [Pagrus major]	gb|AAP20145.1|	Q6Y267	1	1	64.3	1.0E− 12
NAC alpha, partial [Oryzias melastigma]	gb|AEB71553.1|	I1SSG5	1	2	48.6	2.0E− 07
Valosin containing protein [Oncorhynchus mykiss]	ref|NP_001117982.1|	Q1M179	1, 1	1, 2	57.1	4.0E− 10
DNA metabolism						
Histone H2A-like [Oreochromis niloticus]	ref|XP_003451178.1|	N.E.	2, 2	1, 2	71.9	9.0E− 16
Histone h2a.x [Perca flavescens]	gb|ADX97213.1|	F1C7F3	2, 1	1, 2	90.1	2.0E− 21
Histone H4-like [Oreochromis niloticus]	ref|XP_003460383.1|	P62796	2, 1	1, 2	41.4	3.0E− 05
Nucleoside diphosphate kinase [Sparus aurata]	gb|ACF75416.1|	B5APB7	1, 1	1, 2	56.6	3.0E− 10
Carbohydrate metabolism						
Alpha-1 enolase-1 [Salmo trutta]	gb|AAG16310.1|	N.E.	2, 1	1, 2	56.6	3.0E− 12
Enolase [Epinephelus bruneus]	gb|AEB31337.1|	F5BZS7	1	2	49.8	7.0E− 08
Fructose-bisphosphate aldolase [Epinephelus coioides]	gb|ACL98138.1|	B9V3W3	1	1	44.8	2.0E− 08
Glyceraldehyde 3-phosphate dehydrogenase [Pagrus major]	dbj|BAB62812.1|	Q90WD9	3, 1	1, 2	81.2	4.0E− 18
Triose phosphate isomerase [Polypterus ornatipinnis]	dbj|BAD17930.1|	Q76BC6	1	2	51.5	2.0E− 08
Triose phosphate isomerase [Amia calva]	dbj|BAD17915.1|	Q76BE1	1	2	43.1	1.0E− 05
Energy metabolism						
ATP synthase subunit alpha, mitochondrial precursor [Psetta maxima]	emb|CAY56619.1|	C4QUY7	1	2	70.6	5.0E− 15
ATP synthase beta-subunit [Pagrus major]	dbj|BAF37105.1|	A0PA13	1, 1	1, 2	61.7	7.0E− 12
Beta globin [Sparus aurata]	gb|ABE28021.1|	Q1PCB2	1, 1	1, 2	43.1	9.0E− 06
Lipid metabolism						
Apolipoprotein A-I [Sparus aurata]	sp|O42175.1|APOA1_SPAAU	O42175	3, 4	1, 2	74.4	6.0E− 18
Stress response						
Heat shock cognate 70 kDa [Carassius auratus]	dbj|BAC67185.1|	Q801X8	2, 2	1, 2	71.9	7.0E− 15
Superoxide dismutase [Cu-Zn] [Xiphias gladius]	sp|P03946.2|SODC_XIPGL	P03946	1	1	53.7	3.0E− 11
Signal transduction						

PREDICTED: 14-3-3 protein beta/alpha-1-like [Oryzias latipes]	ref|XP_004070571.1|	H2M383	1, 1	1, 2	46.0	1.0E− 08
Serine/threonine-protein phosphatase 2A 65 kDa regulatory subunit A beta isoform [Salmo salar]	gb|ACN58639.1|	C0PUA0	1	1	57.5	2.0E− 10

[a] Protein name, sequence ID and UniProt database ID of the record with the highest score retrieved by BLAST. N.E.: No entry in UniProt.
[b] PM: Number of MS/MS derived peptides from samples 1, and/or 2 that match exactly the protein sequence.
[c] Sample(s) in which the protein has been identified.
[d] Maximum score obtained in BLAST analysis by a peptide matching this protein.
[e] Number of times we would expect to obtain an equal or higher score by chance.

Table 13. Proteins identified by coupled PMF and MS/MS (Jurado et al., 2015b).

SN[a]	Protein[b]	Organism[b]	UniProt ID[b]	Symbol[c]	Score[d]	Expect[e]	PM[f]	PF[f]	SC %[f]	Mass (kDa)	p*I*
Structural proteins: cytoskeleton and extracellular											
201	Alpha-actin 4	*Rachycentron canadum*	E9L834	ACTA	572	2.4E − 52	11	5	41	42.3	5.22
203	Beta actin	*Acipenser transmontanus*	B6E4I1	ACTB	279	4.9E − 23	10	5	37	42.1	5.30
105	Beta-actin	*Tetraodon nigroviridis*	Q4SMI4	ACTB	508	6.1E − 46	12	8	43	42.9	5.57
106	Beta-actin (Fragment)	*Gobio gobio*	G8A4Z9	ACTB	397	7.7E − 35	7	5	45	30.0	5.33
119	keratin, type I cytoskeletal 13-like	*Oreochromis niloticus*	I3JS53	CYT1L	229	4.9E − 18	7	3	11	49.0	5.68
122	Type I cytokeratin, enveloping layer, like	*Oreochromis niloticus*	I3JS53	CYT1L	224	1.5E − 17	11	3	17	49.0	5.68
107	Type II cytokeratin	*Danio rerio*	Q9PUB5	KRT5	462	2.4E − 41	18	4	32	58.5	5.34
108	Type II keratin E3 (Fragment)	*Gillichthys mirabilis*	C1J0K	KRT	52	2.4E − 00	3	2	11	34.1	4.83
215	Coactosin-like protein	*Tetraodon nigroviridis*	Q4SKB8	COTL1	89	4.5E − 01	3	2	16	16.2	4.92
125	Cofilin-2	*Tetraodon nigroviridis*	Q4RP95	COF2	229	4.9E − 18	4	3	18	18.8	6.82
110	Tropomyosin4-2	*Takifugu rubripes*	Q805C2	TPM4-2	93	1.8E − 04	7	1	30	28.4	4.58
Metabolism											
Protein metabolism											
113	Proteasome subunit alpha type	*Oryzias latipes*	H2L6P7	PSMA	283	1.9E − 23	9	3	43	29.7	6.07
115	Proteasome subunit alpha type	*Tetraodon nigroviridis*	Q4SRB7	PSMA5	407	7.7E − 36	9	5	41	26.5	4.74
116	Proteasome subunit alpha type	*Gasterosteus aculeatus*	G3PZP3	PSMA4	353	1.9E − 30	7	4	32	29.5	5.34
120	Proteasome subunit alpha type	*Oreochromis niloticus*	I3JJY5	PSMA	704	1.5E − 65	9	7	52	25.9	5.99
123	Proteasome subunit beta type	*Danio rerio*	Q6DHI9	PMSB2	242	2.4E − 19	6	2	27	22.7	6.1
Other metabolism pathways											
218	Brain-type fatty acid binding protein	*Epinephelus coioides*	A8HG12	FABP	96	1.0E − 04	3	2	25	14.9	6.17
219	Brain-type fatty acid binding protein	*Epinephelus coioides*	A8HG12	FABP	118	6.1E − 07	3	2	25	14.9	6.17
109	Glyceraldehyde-3-phosphate dehydrogenase	*Pagrus major*	Q90WD9	GAPDH	114	1.5E − 06	12	1	40	36.4	6.36

128	Nucleoside diphosphate kinase	*Sparus aurata*	B5APB7	NDPK	236	9.7E − 19	4	3	26	17.1	6.42
101	Transferrin	*Sparus aurata*	F2YLA1	TF	720	3.9E − 67	26	6	40	76.1	5.93
102	Transferrin	*Sparus aurata*	F2YLA1	TF	491	3.1E − 44	14	6	30	76.1	5.93
Stress response											
211	Peroxiredoxin 1	*Sparua aurata*	G0T332	PRDX1	119	4.9E − 07	5	2	29	22.1	6.30
212	Peroxiredoxin 2	*Sparus aurata*	G0T333	PRDX2	232	2.4E − 18	6	4	38	21.9	5.79
104	Stress protein HSC70-1	*Seriola quinqueradiata*	B6F133	HSC70-1	1020	3.9E − 97	25	7	37	71.4	5.23
127	Superoxide dismutase [Cu-Zn] (Fragment)	*Sparus aurata*	Q571Q7	Cu/Zn SOD	89	5.2E − 04	2	2	28	6970	5.41
103	Warm temperature acclimation-related 65 kDa protein	*Sparus aurata*	C0L788	WAP65	394	1.5E − 34	20	6	41	49.7	5.41
Signal transduction											
124	Phosphatidylethanolamine-binding protein 1	*Takifugu rubripes*	H2UXL0	PEBP1	172	2.4E − 12	3	2	13	21.1	5.65
118	Rho GDP dissociation inhibitor (GDI) alpha	*Danio rerio*	Q6P3J2	ARHGDIA	268	6.1E − 22	3	2	20	23.1	5
112	Tyrosine 3-monooxygenase/tryptophan 5-monooxygenase activation protein, beta polypeptide like	*Gasterosteus aculeatus*	G3NHX0	YWHABL	69	5.4E − 02	6	1	21	29.6	4.65

[a] Spot number in reference 2-DE gel.
[b]Protein name, organism and UniProt ID of the first hit returned by Mascot search, except for spots 105, 119, 122, 125, 112, 124, and 215 in which the first in the list was an unidentified protein. In these cases, the protein name that is shown is the first identified protein after a BLAST search performed in the UniProt page.
[c] Protein symbol as UniProtKB/Swiss-Prot database.
[d] MOWSE score based on MS data. Protein scores greater than 68 are significant ($p < 0.05$). SN 108 have a score below 68 but two fragmented peptides from this spot match with high score with this protein.
[e] Number of times we would expect to obtain an equal or higher score by chance.
[f] PM: Number of non redundant matching peptides. PF: Number of fragmented peptides matching the protein. SC: % of sequence coverage.

In addition, this study also identified proteins involved in stress response (WAP65, HSPC70, Cu, Zn-SOD, and PRDX1 and PRDX2) and signal transduction (PP2A 65 kDa regulatory subunit, 14-3-3 protein beta/alpha, tyrosine 3-monooxygenase/tryptophan 5-monooxygenase activation protein, RhoGDI and PEBP1). Interestingly, most of the identified proteins addressed different aspects of the innate immune response (Jurado et al., 2015b). Furthermore, this study analyzed bacterial peptides which were identified in the skin mucus of healthy *S. aurata*. These results revealed that genera belonging to the Lactobacillales order constitute the most abundant microorganism populations in this habitat (Jurado et al., 2015b).

2.12. **Proteomic Identification of Rainbow Trout Sperm Proteins**

Proteomics represents a powerful tool for the analysis of fish spermatozoa, since these cells are transcriptionally inactive. The aim of the present study was to generate an inventory of the

most prominent rainbow trout sperm proteins by SDS-PAGE pre-fractionation combined with nano- LC-ESI-MS/MS-based identification (Nynca, Arnold, Fröhlich, Otte, & Ciereszko, 2014).

This study provides the first in-depth analysis of the rainbow trout sperm proteome, with a total of 206 identified proteins. It was found that rainbow trout spermatozoa are equipped with functionally diverse proteins related to energetic metabolism, signal transduction, protein turnover, transport, cytoskeleton, oxidative injuries, and stress and reproduction (Nynca, Arnold, Fröhlich, Otte, & Ciereszko, 2014). The availability of a catalog of rainbow trout sperm proteins provides a crucial tool for the understanding of fundamental molecular processes in fish spermatozoa, for the ongoing development of novel markers of sperm quality and for the optimization of short- and long-term sperm preservation procedures. The MS data are available at ProteomeXchange with the dataset identifier PXD000355 and DOI 10.6019/PXD000355 (Nynca, Arnold, Fröhlich, Otte, & Ciereszko, 2014).

2.13. **Characterization of the Intact Rainbow Trout Vitellogenin Protein**

Vitellogenin (VTG) is a protein produced by the liver of oviparous animals. The plasma level of VTG is a sensitive test used to screen wildlife for the biological effects of exposure to such chemicals in both fields and *in vitro* studies (Banoub et al., 2003; Denslow et al., 1999; Holmes et al., 1997). VTG is the major precursor to the egg-yolk proteins of oviparous vertebrates (H. R. Andersen et al., 1999; Banoub et al., 2003).

VTG is a large serum phospholipid-glycoprotein composed of 1644 amino acid residues, containing lipovitellin I (LVI, positions: 16–1088), phosvitin (PV, positions: 1089–1145) and lipovitellin II (LVII, positions: 1146–1659). The complete structure of rainbow trout VTG is shown. Rainbow trout Vtg has recently been sequenced by the conventional cDNA nucleotide approach (Figure 24) (Banoub et al., 2003).

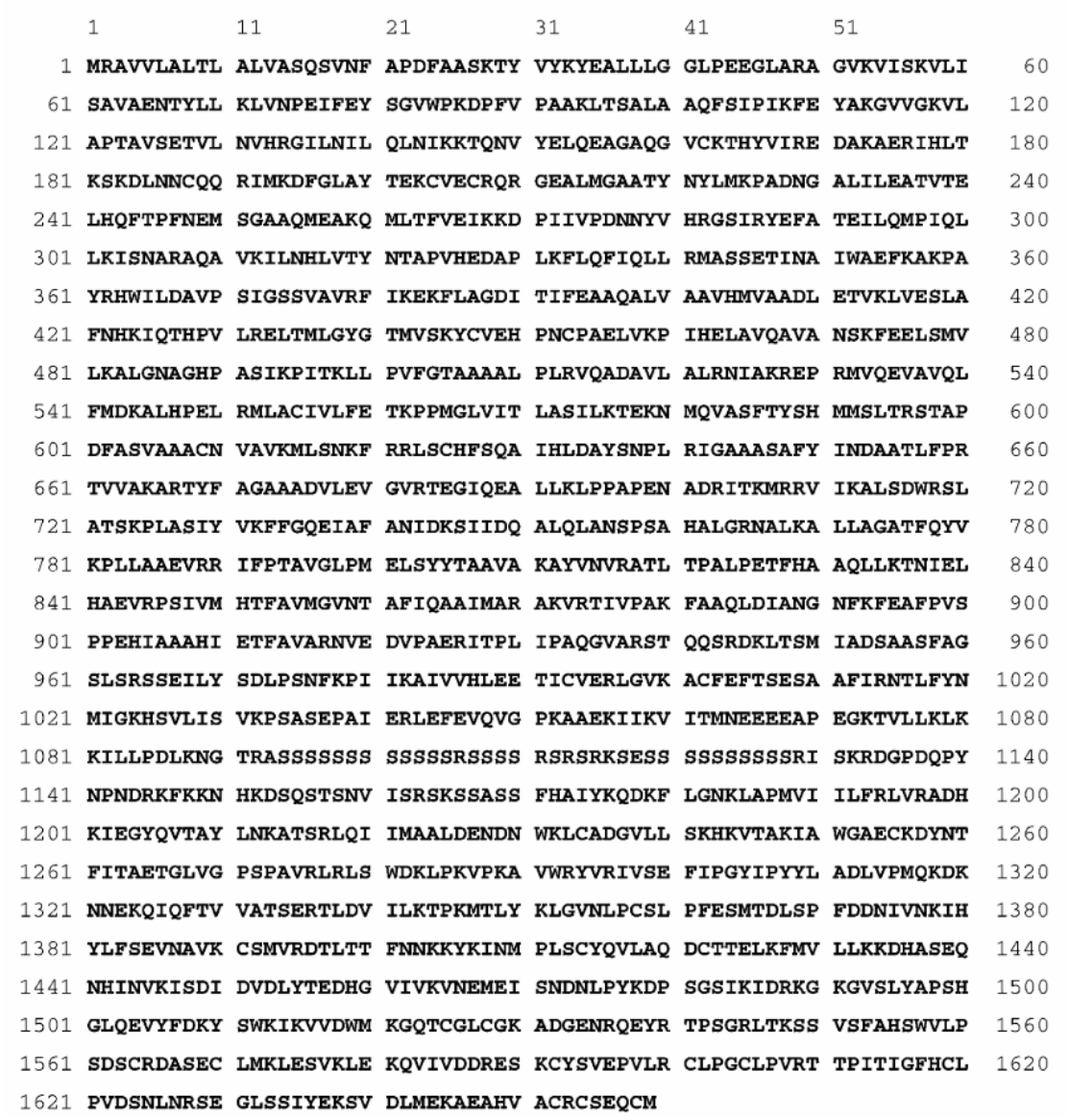

	1	11	21	31	41	51	
1	MRAVVLALTL	ALVASQSVNF	APDFAASKTY	VYKYEALLLG	GLPEEGLARA	GVKVISKVLI	60
61	SAVAENTYLL	KLVNPEIFEY	SGVWPKDPFV	PAAKLTSALA	AQFSIPIKFE	YAKGVVGKVL	120
121	APTAVSETVL	NVHRGILNIL	QLNIKKTQNV	YELQEAGAQG	VCKTHYVIRE	DAKAERIHLT	180
181	KSKDLNNCQQ	RIMKDFGLAY	TEKCVECRQR	GEALMGAATY	NYLMKPADNG	ALILEATVTE	240
241	LHQFTPFNEM	SGAAQMEAKQ	MLTFVEIKKD	PIIVPDNNYV	HRGSIRYEFA	TEILQMPIQL	300
301	LKISNARAQA	VKILNHLVTY	NTAPVHEDAP	LKFLQFIQLL	RMASSETINA	IWAEFKAKPA	360
361	YRHWILDAVP	SIGSSVAVRF	IKEKFLAGDI	TIFEAAQALV	AAVHMVAADL	ETVKLVESLA	420
421	FNHKIQTHPV	LRELTMLGYG	TMVSKYCVEH	PNCPAELVKP	IHELAVQAVA	NSKFEELSMV	480
481	LKALGNAGHP	ASIKPITKLL	PVFGTAAAAL	PLRVQADAVL	ALRNIAKREP	RMVQEVAVQL	540
541	FMDKALHPEL	RMLACIVLFE	TKPPMGLVIT	LASILKTEKN	MQVASFTYSH	MMSLTRSTAP	600
601	DFASVAAACN	VAVKMLSNKF	RRLSCHFSQA	IHLDAYSNPL	RIGAAASAFY	INDAATLFPR	660
661	TVVAKARTYF	AGAAADVLEV	GVRTEGIQEA	LLKLPPAPEN	ADRITKMRRV	IKALSDWRSL	720
721	ATSKPLASIY	VKFFGQEIAF	ANIDKSIIDQ	ALQLANSPSA	HALGRNALKA	LLAGATFQYV	780
781	KPLLAAEVRR	IFPTAVGLPM	ELSYYTAAVA	KAYVNVRATL	TPALPETFHA	AQLLKTNIEL	840
841	HAEVRPSIVM	HTFAVMGVNT	AFIQAAIMAR	AKVRTIVPAK	FAAQLDIANG	NFKFEAFPVS	900
901	PPEHIAAAHI	ETFAVARNVE	DVPAERITPL	IPAQGVARST	QQSRDKLTSM	IADSAASFAG	960
961	SLSRSSEILY	SDLPSNFKPI	IKAIVVHLEE	TICVERLGVK	ACFEFTSESA	AFIRNTLFYN	1020
1021	MIGKHSVLIS	VKPSASEPAI	ERLEFEVQVG	PKAAEKIIKV	ITMNEEEEAP	EGKTVLLKLK	1080
1081	KILLPDLKNG	TRASSSSSSS	SSSSSRSSSS	RSRSRKSESS	SSSSSSSSRI	SKRDGPDQPY	1140
1141	NPNDRKFKKN	HKDSQSTSNV	ISRSKSSASS	FHAIYKQDKF	LGNKLAPMVI	ILFRLVRADH	1200
1201	KIEGYQVTAY	LNKATSRLQI	IMAALDENDN	WKLCADGVLL	SKHKVTAKIA	WGAECKDYNT	1260
1261	FITAETGLVG	PSPAVRLRLS	WDKLPKVPKA	VWRYVRIVSE	FIPGYIPYYL	ADLVPMQKDK	1320
1321	NNEKQIQFTV	VATSERTLDV	ILKTPKMTLY	KLGVNLPCSL	PFESMTDLSP	FDDNIVNKIH	1380
1381	YLFSEVNAVK	CSMVRDTLTT	FNNKKYKINM	PLSCYQVLAQ	DCTTELKFMV	LLKKDHASEQ	1440
1441	NHINVKISDI	DVDLYTEDHG	VIVKVNEMEI	SNDNLPYKDP	SGSIKIDRKG	KGVSLYAPSH	1500
1501	GLQEVYFDKY	SWKIKVVDWM	KGQTCGLCGK	ADGENRQEYR	TPSGRLTKSS	VSFAHSWVLP	1560
1561	SDSCRDASEC	LMKLESVKLE	KQVIVDDRES	KCYSVEPVLR	CLPGCLPVRT	TPITIGFHCL	1620
1621	PVDSNLNRSE	GLSSIYEKSV	DLMEKAEAHV	ACRCSEQCM			

Figure 24. The complete sequence of rainbow trout vitellogenin, entry Q92093 on the Swiss Prot database (Banoub et al., 2003).

This research work focused on the protein characterization of the intact protein and its derived tryptic and cyanogen bromide peptides by matrix-assisted laser desorption/ionization and electrospray ionization mass spectrometry. The molecular mass of the intact protein was found to be 183127 Da. A large number of unidentified peptide ions encourage further structural analysis to propose possible sequence variants and post-translational modifications (Banoub et al., 2003).

2.14. Characterization and *De Novo* Sequencing of Atlantic Salmon Vitellogenin Protein by Tandem Mass Spectrometry

It has been established that some toxic chemicals known as "xenobiotic estrogens" are present in the environment. These toxic chemicals act as hormone mimics and interfere with the reproductive status of vertebrates through effects ranging from alterations in reproductive hormone plasma levels to sterility (Banoub et al., 2004; Gronen et al., 1999; Maclatchy & van der kraak, 1995; Wade et al., 1997).

Xenobiotic estrogens have a strong tendency to cocentrate in the upper food chain due to their lipophilic nature and, hence, tend to accumulate in fish due to the high dose exposure found in some aquatic ecosystems. Furthermore, plasma levels of VTG have been shown to be a sensitive test to screen wildlife for the biological effects of exposure to such chemicals in both fields and *in-vitro* studies (H. R. Andersen et al., 1999; Banoub et al., 2004; Denslow et al., 1999; Sumpter & Jobling, 1995).

VTG is the major precursor to the egg-yolk proteins of oviparous vertebrates. VTG's molecular weight can vary between 160 kDa and 600 kDa, depending on the species. The gene for VTG expression is found in both females and males and is activated in the liver by exposure to estrogen or estrogen-mimicking compounds. Normally, in mature females, VTG is produced by the liver in response to endogenous circulating estrogens, and is taken up by the developing oocyte through receptor-mediated endocytosis, where it is further cleaved (Banoub et al., 2004).

When males synthesize it, VTG is exported into the blood, where it remains until it is degraded by plasma proteases or is cleared out by the kidneys. VTG is usually undetectable in the plasma of males and immature females. The response to exposure to estrogen or estrogen mimics in males is neither as rapid nor as strong as in mature females, but, as males normally have no VTG, its expression serves as a good biomarker for xenobiotic chemicals (Banoub et al., 2004).

In the present study, characterization of intact Atlantic salmon VTG was effected MALDI-TOF-MS and tandem mass spectrometry (MALDI-TOF/TOF-MS/MS). Tryptic digest peptides were analyzed in order to obtain a peptide mass fingerprint (Banoub et al., 2004).

De novo sequencing of the tryptic peptides used by ESI-MS and low-energy CID-MS/MS analysis (Banoub et al., 2004). The molecular mass of the intact protein was found to be 187335 Da. A total of 14 tryptic peptides were sequenced and compared with the complete rainbow trout

VTG and the partial Atlantic salmon VTG sequences found in the Swiss-Prot database (Banoub et al., 2004).

De novo sequencing by CID MS/MS of 11 Atlantic salmon tryptic digest peptides with selected precursor ions at *m/z* 788.24, 700.20, 794.75, 834.31, 889.28, 819.79, 865.27, 843.81, 572.20, 573.66 and 561.68 showed high homology with the known sequence of rainbow trout VTG. The last two precursor peptide ions, found at *m/z* 573.66 and *m/z* 561.68, also specifically matched the known portion of the Atlantic salmon VTG sequence (Banoub et al., 2004).

Finally, three tryptic precursor peptide ions found at *m/z* 795.18, 893.28 and 791.05, provided product-ion spectra, indicated that they were exclusive to the unsequenced portion of the Atlantic salmon VTG (Banoub et al., 2004).

2.15. **Absolute Quantification of Atlantic Salmon and Rainbow Trout Vitellogenin by the 'Signature Peptide' Approach using electrospray ionization tandem mass spectrometry**

VTG, a phosphoglycolipoprotein, is synthesized in the liver of oviparous animals in response to circulating estrogens. Depending on the species, its molecular weight may vary from 200 to 500 KDa. In sexually mature females, VTG is secreted into the bloodstream and is incorporated into the oocyte by receptor-mediated endocystosis, where it is further cleaved. The exact functions of these proteins are still uncertain. However, it is generally accepted that these proteins are finally hydrolyzed into a free amino acid pool, which serves as the primary nutritional source for the developing embryo (Cohen et al., 2006a).

This work presented a very simple method for absolute quantification of plasma vitellogenin from both rainbow trout and Atlantic salmon. Plasma samples obtained from control and βestradiol-induced fish were digested with trypsin. A characteristic 'signature peptide' was selected and analyzed by HPLC coupled to an electrospray quadrupole-time-of-flight tandem mass spectrometer, using a deuterated homolog peptide as an internal standard. The hybrid tandem mass spectrometer was operated in a 'pseudo' selected reaction-monitoring mode in which three diagnostic product ions were monitored for identification and quantification purposes. The reproducibility (coefficient of variation ~5%) and sensitivity (limit of quantification (LOQ) of 0.009 mg/ml) achieved by this simple assay allow it to be considered as an alternative to immunological assays (Cohen et al., 2006a).

2.16. *De Novo* Sequencing of Atlantic Cod Vitellogenin Tryptic Peptides by Tandem Mass Spectrometry: Similarities with Haddock Vitellogenin

VTG is a protein produced by the liver of oviparous animals in response to circulating estrogens. Recently, the plasma Vtg levels in female fish were investigated by our research group for their use in the fisheries and aquaculture industry as a prospective indicator for assessing the reproductive status of fish stocks. Note that the amino acid sequence of the protein of Atlantic cod (*Gadus morhua*) was not yet available in either the protein or DNA sequence databases (Cohen et al., 2005a).

In this study, Atlantic cod vitellogenin was characterized using a 'bottom-up' mass spectrometric approach. VTG synthesis was induced 'in vivo' with β-estradiol and subjected to trypsin digestion for characterization by MALDI-TOF-MS and tandem mass spectrometry (Cohen et al., 2005a).

A peptide mass fingerprint was obtained, and 'de Novo sequencing of the most abundant tryptic peptides was performed by MALDI-TOF/TOF-MS/MS (Cohen et al., 2005a). As a result of these experiments, the sequences of various tryptic peptides have been elucidated. The database search has shown that Atlantic cod vitellogenin shares a series of common peptides with the two different known vitellogenin sequences of haddock, a closely related species. These findings allowed to propose that Atlantic cod might also co-express at least two distinct forms of vitellogenin (Cohen et al., 2005a).

2.17. Quantification of Greenland Halibut SerumVitellogenin

This work focuses on the sequential s teps involved in developing a technique for quantifying Greenland halibut vitellogenin, a serum protein biomarker, using a comprehensive mass spectrometric approach. In the first phase of this study, in-gel trypsin digestions of serum proteins separated by 2-DGE and MALDI-TOF-MS (Cohen et al., 2009a).

A characteristic band around a molecular mass of 185 kDa, present in the mature female specimens but absent in the male samples, was identified as vitellognin according to the peptide mass fingerprint obtained by MALDI-TOF-MS. Subsequently, MALDI- and ESI-MS/MS analyses were performed on the digest of the vitellogenin band for de novo sequencing (Cohen et al., 2009a).

From these studies, a characteristic 'signature' peptide (sequence: FFGQEIAFANIDK) was selected from a list of candidate peptides as a surrogate analytical standard used for quantification purposes. Sample preparation for vitellogenin quantification consisted of a simple one-step overnight trypsin digestion. Samples were spiked with an isotopologue signature peptide standard and analyzed by HPLC coupled in-line to an electrospray quadrupole-hexapole-quadrupole tandem mass spectrometer, operated in selective reaction monitoring mode. Transitions [(m/z 750.0→1020.4 and 750.0→1205.4) and (754.8→1028.6 and 754.8→ 1213.2)] were monitored for the signature peptide and the internal standard, respectively. Samples obtained from the field showed that vitellogenin levels were in accordance with fish maturity determined by macroscopic examination of the gonad, proving this technique suitable for measuring vitellogenin as a serum protein biomarker for reproductive maturity in female fish (Cohen et al., 2009a).

In conclusion, this novel signature peptide approach using liquid chromatography/mass spectrometric technique allowed measuring serum levels of Greenland halibut vitellogen. This technique is currently being used in our laboratories to measure vitellogenin levels in samples obtained by commercial and research vessels operating in the northwest Atlantic, off the coasts of Newfoundland and Labrador (Cohen et al., 2009a).

2.18. **Proteomic Characterization of Vitellogenins from three Species of South American Fresh Water Fish**

VTGs are glycolipophosphoproteins synthesized by oviparous vertebrates as yolk proteins precursors. These proteins have been studied for their role in reproduction and endocrine disruption (Urdaneta et al., 2018).

This study reports the first proteomic study towards the characterization of VTG from *Pseudoplatystoma fasciatum*, *Piaractus brachypomus* and *Colossoma macropomum*. Male specimens of each of the three fish species were estradiol-induced (experimental) and non-induced (control). The initial VTG characterization was made by 2-DGE protein gel electrophoresis of both groups. The identification of the high molecular weight spots, presumed to be VTGs, was assessed by MALDI-TOF-MS analysis (Urdaneta et al., 2018).

A post-translational modification study was performed by differential staining of 2-DGE gels in order to visualize phosphoproteins and glycoproteins. It was established that the plasma

samples from the three species, induced with estrogen, showed three high molecular weight spots with variable isoelectric points. The post-translational modifications indicated that Vtgs from *P. brachypomus* and *C. macropomum* presented a phosphorylated and glycosylated subunit, while the same subunit in *P. fasciatum* was only glycosylated. This characterization will help in the development of reliable immunoassays, which could be used for studies of endocrine disruption or for the improvement of artificial spawning by uncovering the time of fish maturation or sex determination (Urdaneta et al., 2018).

2.19. **Skin Mucus and Venon from the *Scorpaena plumieri* Fish**

As mentioned previously, it is well lnown that skin mucus plays a major role in preventing the colonization by parasites, bacteria and fungi (Balasubramanian S., Baby Rani P., Arul Prakash A., Prakash M.* & Department, 2012; Jones, 2001). In fact, antibacterial activity against a broad range of infectious pathogens has been described in epidermal fish mucus (Borges et al., 2018; Hellio et al., 2002; Ramos et al., 2012). Therefore, mucous secretion has been considered a key component of fish innate immunity mechanisms and the first line of defence against pathogens (Borges et al., 2018; Ingram, 1980).

The spotted scorpionfish *Scorpaena plumieri* is one of the most venomous fish in the Atlantic Ocean, being responsible for many accidents on the Brazilian coast. The representatives of this species use their venom to protect themselves against potential predators. They possess a primitive venom apparatus formed by 13 dorsal, 3 anal and 2 pelvic fin spines associated with venomous glandular tissue, which is no more than a grouping of secretory cells, within long grooves located in the anterior portion of these spines, which are covered by a mucous-rich integumentary sheath (Borges et al., 2018; Russell, 1965).

In this study, a large number of proteins, including classical and non-classical toxins, were identified in the venomous apparatus and the skin mucus extracts of the *Scorpaena plumieri* fish through the shotgun proteomic approach. The biological activities observed upon envenomation by *Scorpaena plumieri* fish was linked to both the venom and the skin mucus.

Consequently, 885 proteins were identified: 722 in the Venomous Apparatus extracts (*Sp-VAe*) and 391 in the Skin Mucus extract (*Sp-SMe*), with 494 found exclusively in *Sp-VAe*, being named *S. plumieri* Venom Proteins (Sp-VP), while 228 were found in both extracts (Figure 25). The majority of the many proteins identified were not directly related to the biological activities

reported here. Nevertheless, some were classified as toxins/potentially interesting molecules: lectins, proteases and protease inhibitors were detected in both extracts, while the pore-forming toxin and hyaluronidase were associated with Sp-VP (Table 14) (Borges et al., 2018).

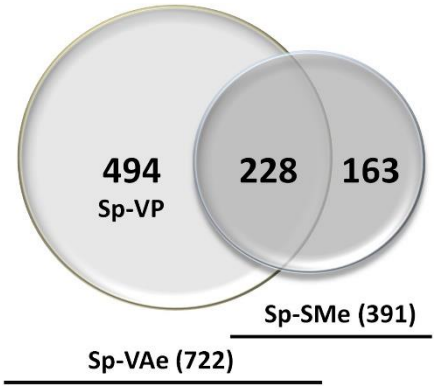

Figure 25. Venn Diagram. Number of proteins found in extracts from the venomous apparatus (Sp-VAe) and from the skin mucus (Sp-SMe). Proteins found exclusively in Sp-VAe were named Sp-VP: S. plumieri Venom Proteins (Borges et al., 2018).

Table 14. Summary information on potentially interesting toxins/proteins found in Sp-VP and Sp-SMe (Borges et al., 2018).

Classification	Protein name	FC	Sp-VP	Sp-SMe	Fish species	molecular function/function of homologous proteins (*)
Cytolysins	Tx alpha-subunit # §	5	v		*Synanceia horrida*	Pore-formation toxins
					Scorpaenopsis oxycephala	
					Sebastapistes strongia	
					Dendrochirus zebra	
					Pterois antennata	
	Tx beta-subunit # §	5	v		*Scorpaenopsis oxycephala*	Pore-formation toxins
					Sebastapistes strongia	
			v		*Notothenia coriiceps*	
	Cytolysin Src-1-like #	5	v		*Notothenia coriiceps*	Pore-formation toxins
Enzymes	Aspartyl aminopeptidase # (6)	6		v	*Notothenia coriiceps*	Metallopeptidase/Cystein-type
	Probable aminopeptidase NPEPL1 #	6		v	*Notothenia coriiceps*	Metalloexopeptidase
	Putative aminopeptidase W07G4.4 #	6	v	v	*Notothenia coriiceps*	Metalloexopeptidase
	Thimet oligopeptidase-like #	6	v		*Notothenia coriiceps*	Metalloendopeptidase
	Bleomycin hydrolase #	6	v	v	*Notothenia coriiceps*	Cystein peptidase

	Calpain small subunit 1 #	6	v	v	*Notothenia coriiceps*	Cystein-type endopeptidase
	Cathepsin B #	6		v	*Epinephelus coioides*	Cystein-type endopeptidase
					Notothenia coriiceps	
	Cathepsin D #	6		v	*Notothenia coriiceps*	Aspartic-type endopeptidase
					Chionodraco hamatus	
	Dipeptidyl peptidase 3 #	6		v	*Notothenia coriiceps*	Serine-protease
	Prolyl endopeptidase-like #	6		v	*Notothenia coriiceps*	Serine-protease
	Serine protease ami-like #	6	v		*Notothenia coriiceps*	Serine-peptidase
	Trypsin, partial §	6	v		*Totoaba macdonaldi*	Serine- protease
	Cytosolic non-specific dipeptidase #	6	v	v	*Notothenia coriiceps*	Carboxypeptidase
	Coagulin factor II §	6/7	v		*Oplegnathus fasciatus*	Serine -protesase (Gel –forming protein)
	Hyaluronidase #	1.1	v		*Pterois antennata*	Hyaluronon glucosaminidase
					Pterois volitans	
					Notothenia coriiceps	
	Alpha anti-plasmin #	6	v		*Notothenia coriiceps*	Serine-endopeptidase inhibition
	kunitz-type protease inhibitor 1 #	6	v		*Notothenia coriiceps*	Serine-endopeptidase inhibition
	pregnancy zone protein §	6	v	v	*Pundamilia nyererei* *Takifugu rubripes* *Clupea harengus*	Serine-protease inhibitor
	Hibernation-specific plasma protein HP-55-like §	6	v	v	*Larimichthys crocea*	Serine-protease inhibitor
	Anti-thrombin III §		v	v	*Pundamilia nyererei*; *Cynoglossus semilaevis*; *Larimichthys crocea*	Serine-protease inhibitor
	Cystatin-B #	6	v		*Anoplopoma fimbria*	Cystein-type endopeptidase inhibition
	Fetuin b #	6		v	*Perca flavescens*	Cystein-type endopeptidase inhibition
	Histidine-rich glycoprotein-like 3 #	6	v		*Notothenia coriiceps*	Cystein-type endopeptidase inhibition
Adhesion molecules	Intelectin-2-like partial 3 #	3.1	v		*Notothenia coriiceps*	Carbohydrate binding
	Lily-type lectin 3 #	3.1		v	*Epinephelus coioides*	Carbohydrate binding
	Mannose-specific lectin-like 3 #	3.1		v	*Notothenia coriiceps*	Carbohydrate binding
	Nattectin partial 3 #	3.1		v	*Epinephelus bruneus*	Carbohydrate binding
	Putative F-type lectin 3 #	3.1	v		*Perca flavescens]*	Carbohydrate binding
	Skin mucus lectin 3 #	3.1	v		*Platycephalus indicus*	Carbohydrate binding
	Serum amyloid p-component 3 #	3.1	v		*Perca flavescens*	Carbohydrate binding
	Fucolectin §	3.1	v		*Pundamilia nyererei*	Carbohydrate binding
	Lactose-binding lectin l-2-like §	3.1	v		*Fundulus heteroclitus*	Carbohydrate binding
	CD209 antigen-like -lectin §	3.1	v		*Sinocyclocheilus grahami*	Carbohydrate binding
	L-rhamnose-binding lectin CSL1-like lectin §	3.1	v		*Larimichthys crocea*	Carbohydrate binding
	Beta-galactoside-binding lectin-like –lectin §	3.1	v		*Austrofundulus limnaeus*	Carbohydrate binding

Others	Aflatoxin B1 aldehyde reductase like #	1.1	v		*Notothenia coriiceps*	Oxiredutase
	Olfactomedin-like protein 3 partial #	10	v		*Notothenia coriiceps*	Proangiongenic factor
	Peptidoglycan recognition protein L2 #	10	v		*Sebastes schlegelii*	*N*-acetylmuramoyl-L-alanine amidase
	Tributyltin binding protein type 1b #	5	v		*Epinephelus bruneus*	Detoxification
	Saxitoxin and tetrodotoxin binding protein §	5	v	v	*Kryptolebias marmoratus*; *Nothobranchius furzeri*	Detoxification

(v) Fragments found in: Sp-VP (*S. plumieri* Venom Proteins) and/or Sp-SMe (*S. plumieri* Skin Mucus extract); (#) found through peptide-spectrum matches; (§) found through de novo sequencing; (FC) functional group according to Figure 26; (*) Information retrieved from Databases (Uniprot/NCBIsystem).

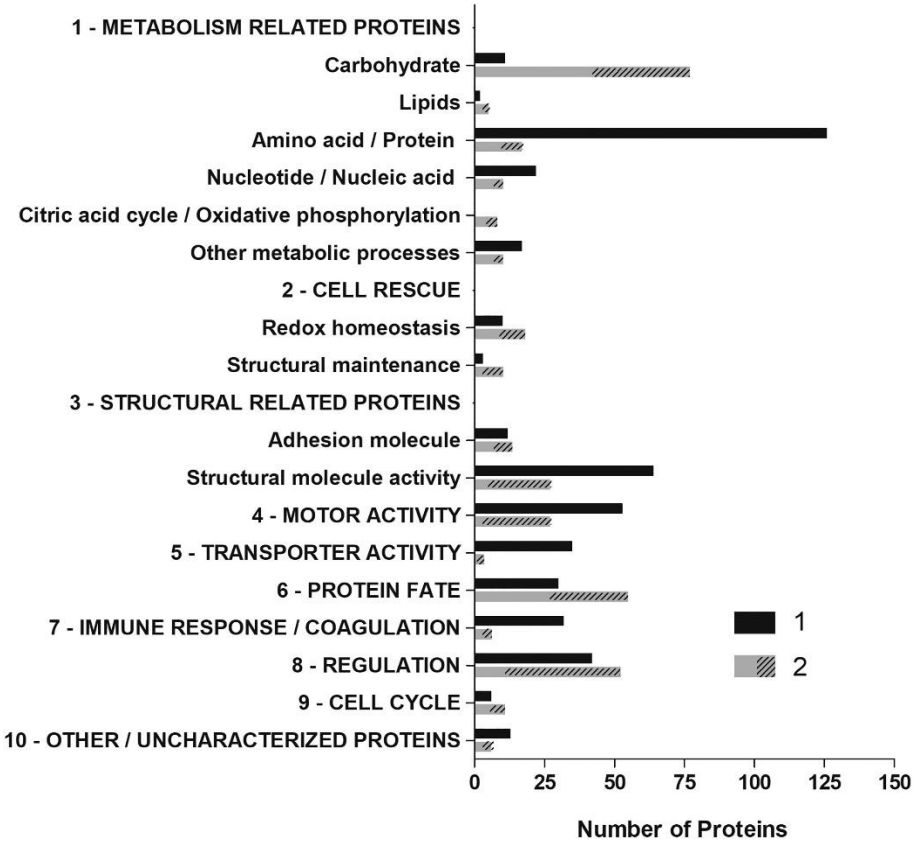

Figure 26. Distribution of identified proteins. Proteins were manually clustered into ten groups (1−10) according to similarities found through blast analysis in Uniprot/SwissProt. (1) Sp-VP (S. plumieri Venom Proteins): proteins found exclusively in Sp-VAe; (2) Sp-SMe: skin mucus proteins, including those also found in Sp-VAe (patterned area) (Borges et al., 2018).

Proteolytic and anti-microbial activities were linked to both extracts, while the main toxic activities, cardiovascular, inflammatory, hemolytic and nociceptive, were elicited only by Sp-VAe. This study provided a clear picture of the composition of the skin mucus and the venom. It also showed that the classic effects observed upon envenomation are produced by molecules from the venomous gland. The obtained results add to the growing catalogue of scorpaeniform fish venoms and their skin mucus proteins (Borges et al., 2018).

In conclusion, this study indicated that many proteins, including classical and non-classical toxins, were identified in the venomous apparatus and the skin mucus extracts of the *Scorpaena plumieri* fish. It was shown that the toxic effects observed upon envenomation are elicited by molecules originating from the venomous gland. These results add to the growing catalogue of *scorpaeniform* fish venoms and their skin mucus proteins – so scarcely explored compared to terrestrial animals' venoms and bioactive components of terrestrial animals (Borges et al., 2018).

2.20. **Combined Proteomic and Transcriptomic Investigation of Fish Venom Composition Uusing Barb Tissue from the Blue Stingray (*Neotrygon kuhlii*)**

Venom systems are important ecological innovations that have evolved independently on many occasions throughout the animal kingdom. Venoms are bioactive secretions utilized for various functions, such as defence, competitor deterrence or predation (K. Baumann et al., 2014; Casewell et al., 2013; Fry et al., 2009). Little is known about the composition of venoms present in bony and cartilaginous fishes. In contrast to snakes, fishes appear to use their venom systems to protect themselves from predation primarily. It is interesting to note that fish venoms remain almost completely unstudied despite a large number of different species. In part, this is due to the inherent nature of fish venoms, in that they are highly sensitive to heat, pH, lyophilization, storage and repeated freeze-thawing. Fish venoms are also heavily contaminated with skin mucus, which makes proteomic study difficult (K. Baumann et al., 2014).

This study describes a novel protein-handling protocol used to remove mucus contamination, which depended on using ammonium sulphate and acetone precipitation. The validation of this approach was based on using barb venom gland tissue protein extract from the blue-spotted stingray *Neotrygon kuhlii*. Accordincly, the protein extract was analyzed by the traditional proteomics approach (1-DGE and 2-D GE gels (K. Baumann et al., 2014). The venom

composition of *N. kuhlii* of the cleaned venom protein extract was subjected to proteomics analyses by the and shotgun LC-ESI-MS/MS sequencing approach (Figure 27), (K. Baumann et al., 2014).

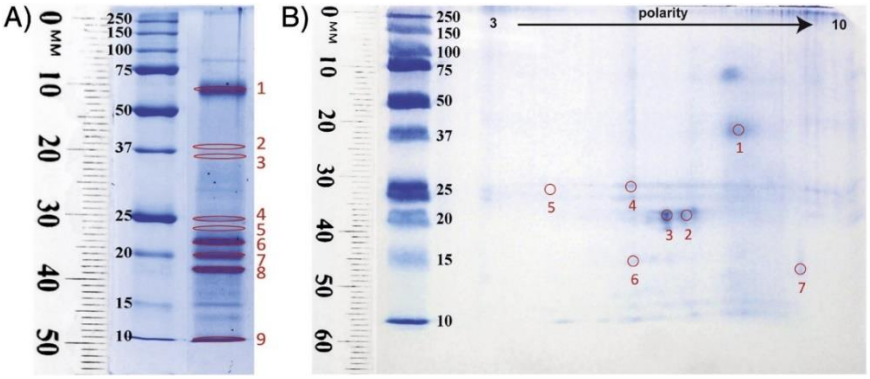

Figure 27. 1D and 2D SDS-PAGE gel profiles of N. kuhlii barb venom protein extract. A) 1D SDS-PAGE gel profile highlighting the bands that were selected for in-gel digestion and protein identification. B) 2D SDS-PAGE gel profile highlighting the spots that were selected for in-gel digestion and protein identification. The numbers in each gel refer to the proteins displayed in Table 15. The gels were stained with Colloidal Coomassie Brilliant Blue G250(K. Baumann et al., 2014).

Table 15. Protein types identified in the barb venom gland extract of N. kuhlii (K. Baumann et al., 2014).

rotein type	1D bands	2D spots	Shotgun	UniProt match	Known functions
60S acidic ribosomal protein			✔	K4GJD9	Elongation in protein synthesis (UniProt)
ATP synthase	5	1, 2, 3, 4, 6	✔	Q9PTY0	Generating ATP
Coronin			✔	F1QDY7	Actin binding protein
Cystatin	9	6	✔	Q28988, J7FQE8	Cysteine proteinase inhibition
Cytochrome C	9		✔	Q6DKE1	Electron carrier activity (UniProt)
Ferritin			✔	Q801J6	Important in iron homeostasis (UniProt)
Galectin	1, 4, 5, 6, 7, 8, 9	3, 4, 6, 7	✔	H2UTD9	Apoptotic, pro-/anti-inflammatory
Ganglioside GM2 activator	8	2, 3	✔	K4FYQ1	Unknown activity
Glutathione S-transferase mu		4, 5		Q9TSM5	Cellular detoxification
Haemoglobin subunit alpha	2, 4, 5, 6, 7, 8, 9	1, 2, 3, 4, 5, 7	✔	P56691	Antimicrobial
Leukocyte elastase inhibitor	2, 3, 9	1	✔	R0LF52	Inflammation
Nucleoside diphosphate kinase		7	✔	G3HBD3	Regulatory functions
Peroxiredoxin 6	1	2, 3, 4		K4FY71	Antioxidant functions
Transaldolase	3	1	✔	Q28H29	Glucose metabolism
Type III intermediate filament	9	1	✔	P23729	Structural

Voltage-dependent anion channel	4		✔	Q9IA66	Diffusion of small hydrophilic molecules (UniProt)

To underpin the annotation of venom proteins detected by proteomics, the authors generated a venom gland transcriptome for *N. kuhlii*. Next-generation sequencing of this transcriptome resulted in 2.95 million reads, representing 1.47 million read pairs, with a mean read length of ~160 bp. The transcriptome assembly resulted in 4584 contigs with an N50 of 602 bp. GO-term annotations of the assembled transcriptome revealed a variety of putative functions for the protein-encoding genes detected (Figure 28) (K. Baumann et al., 2014).

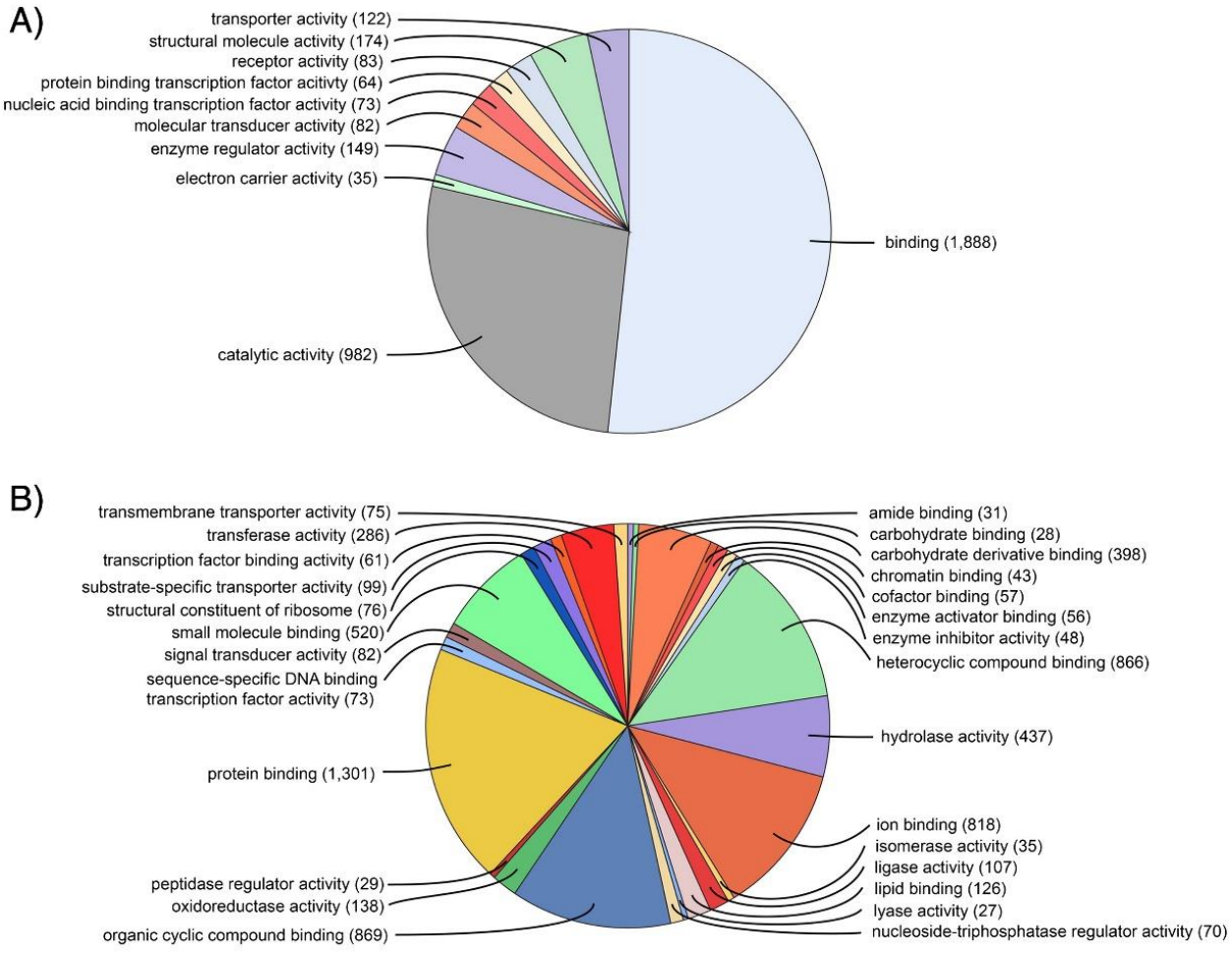

C)

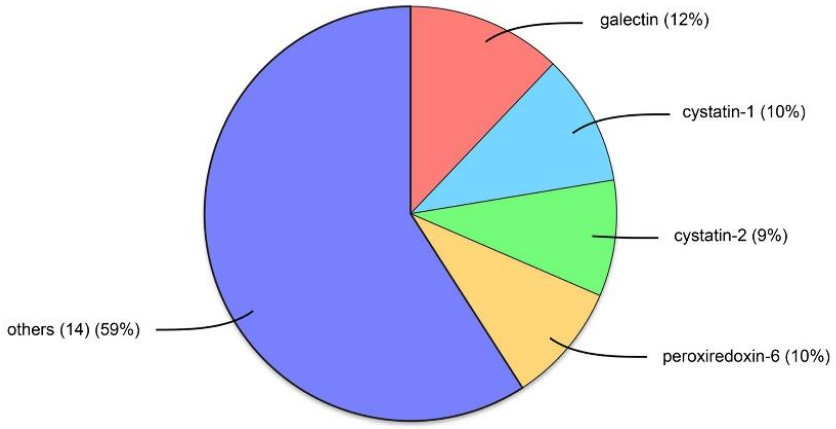

Figure 28. GO-term classification of the assembled and annotated N. kuhlii venom gland transcriptome. A) Level 2 and B) level 3 GO-term analysis of the annotated contigs. C) The relative abundance of proteins in the N. kuhlii venome (venom proteome) is calculated by transcriptomic expression levels (K. Baumann et al., 2014).

Level 2 molecular functions were dominated by genes associated with 'binding' and 'catalytic' activity, with both categories representing 79% of all annotated contigs (Figure 28A). Level 3 molecular functions were inherently more diverse, although, notably, predicted protein functions such as 'protein binding' and 'hydrolase activity were well-represented (19% and 7%, respectively) (Figure 28B) (K. Baumann et al., 2014).

The venom gland transcriptome supported the protein annotation. The composition of the *N. kuhlii* venom sample revealed a variety of protein types that were completely novel to animal venom systems. Notably, none of the detected proteins exhibited similarity to the few toxin components previously characterized from fish venoms, including those found in other stingrays. Putative venom toxins identified here included cystatin, peroxiredoxin and galectin (K. Baumann et al., 2014).

In conclusion, this study represents the first combined survey of the gene and protein composition from the venom apparatus of any fish, and our novel protein handling method will aid the future characterization of toxins from other unstudied venomous fish lineages (K. Baumann et al., 2014).

2.21. 2-D DIGE Analysis of Senegalese Sole (*Solea senegalensis*) Testis Proteome in Wild-Caught and Hormone-Treated F1 Fish

The Senegalese sole (*Solea senegalensis*) F1 is a flatfish of high commercial interest, but reproduction in captivity is not yet controlled. After several years of conditioning in captivity, spontaneous ovulation and egg fertilization by wild-caught broodstock can be observed (Anguis & Cañavate, 2005). However, under some rearing conditions, males from the F1 generation show lower plasma levels of 11-KT than wild fish and produce less sperm, and this is often associated with the complete absence of egg fertilization (Agulleiro et al., 2006; Anguis & Cañavate, 2005; Cabrita et al., 2006; Forné et al., 2009; Porta et al., 2006).

To gain insights on the molecular mechanisms that showed altered sperm production of the F1 testis, the authors used the proteomics approach to compare the protein profiling of the testis of wild-caught males at the spermiation stage with that of F1 males showing different stages of germ cell development after hormone treatment *in vivo* (Forné et al., 2009). Therefore, it was found that the 11-KT plasma levels and sperm production of sole F1 males were enhanced by using GnRHa implants during the reproductive season, although levels were still lower than those observed in wild fish (Agulleiro et al., 2007). It was also suggested that GnRHa in combination with 11-ketoandrostenedione (OA, natural precursor of 11-KT), transiently increased plasma 11-KT to levels similar to those measured in wild fish and stimulated germ cell development (Forné et al., 2009). However, the GnRHa 1 OA treated fish produced 6-fold less sperm than GnRHa-treated males, although the spermatozoa were approximately twice as motile as those produced by the other groups. These observations suggest that treatment of sole F1 males with GnRHa 1 OA, although able to stimulate germ cell differentiation, may inhibit sperm production (Forné et al., 2009). These results contribute to identifying proteins associated with spermatogenesis not previously described in teleosts, and suggest potential mechanisms that may be involved in the poor reproductive performance of Senegalese sole F1 males (Forné et al., 2009). The proteome profile of the F0Mat testis was considered the protein phenotype which hormone-treated F1 fish would have to reach since wild-caught males produce more sperm and show higher fertilization rates than F1 males (Anguis & Cañavate, 2005).

The proteomics approach to investigate the testis proteome employed the 2-D DIGE technology since it allows detection of protein spots with higher sensitivity than conventional 2-DE methods, and also allowed a more accurate quantification of differences in protein abundance

(Matranga et al., 2005; Rime et al., 2004; Zilli et al., 2005; Ziv et al., 2008). 2D-DIGE technology involves labeling samples with different CyDyes (Cy2, Cy3, and Cy5) that excite and emit at different wavelengths, allowing two separate samples and an internal control to be separated and detected together on one gel.

Protein identification was based on *de novo* peptide sequencing by ESI-MS/MS, using two different software packages, and further confirmation by database searching and calculation of experimental and in silico *M*r and p*I* data, which increased the confidence level to identify differentially expressed proteins (Forné et al., 2009). Furthermore, *de novo* identification of these proteins by MS/MS revealed that proteins implicated in oxidoreductase activity, protein catabolism, formation of the zona pellucida receptor, cytoskeleton organization, and lipid binding and metabolism were regulated in the F1 testes as germ cell development progressed. However, distinct isoforms or PTMs of some of these proteins and proteins involved in iron and glucose metabolism and ATP production expressed at lower levels in the testes of F1 males than in wild fish regardless of the hormone treatment (Forné et al., 2009) (Figure 29).

Furthermore, this study showed that from a total of about 1500 spots, 1014 could be quantified in the experiments. A total of 58 of these spots showed significant differences between the groups analyzed, and 45 of them were products of 31 different genes (Forné et al., 2009) (Figure 29).

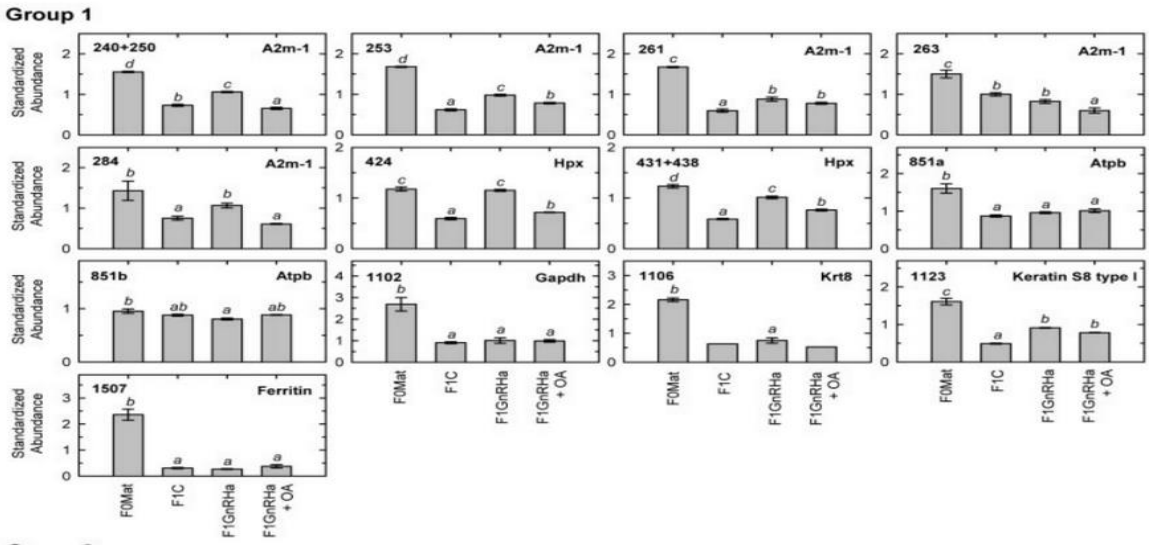

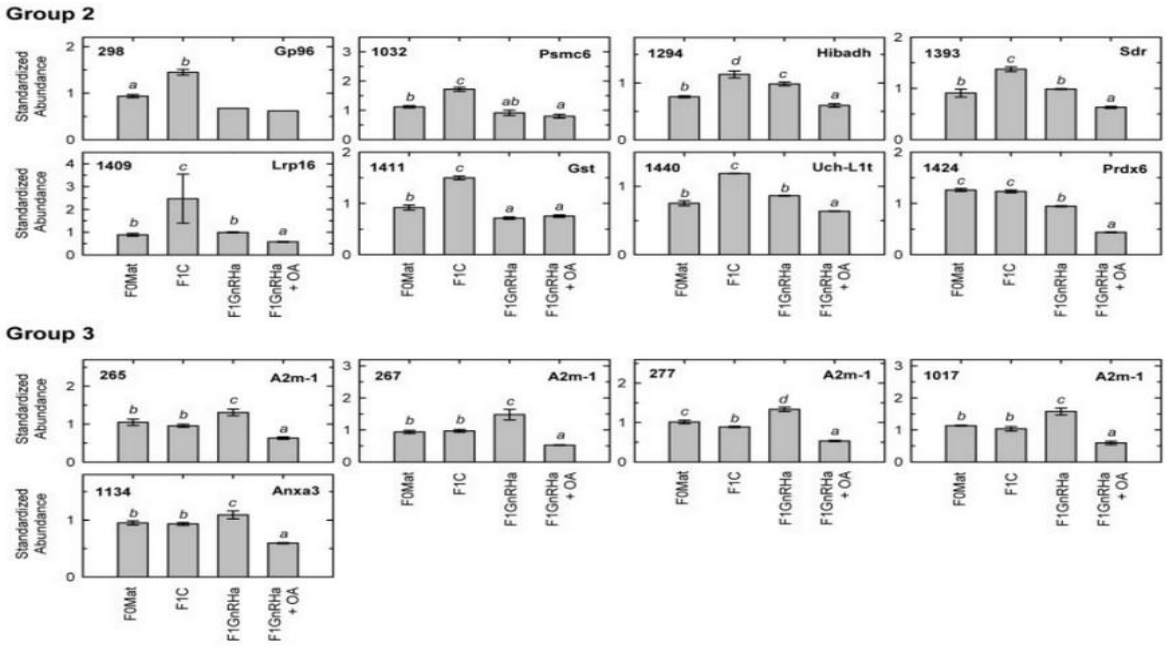

Figure 29. Differentially expressed proteins in the testis of wild-caught Senegalese sole during spermiation (F0Mat) and in the F1 testis after treatment of fish with saline (F1C), GnRHa (F1GnRHa), or GnRHa 1 OA (F1GnRHa 1 OA).Proteins were classified into six groups according to the expression pattern. The figure shows the first three groups. Values are the mean 6 SEM of the standardized abundance of each spot. Values with different superscript are significantly different (ANOVA, p,0.05).

Considering the changes in the cytological profile of the samples analyzed, it is likely that up-regulation and down-regulation of different proteins are associated with different stages of cell differentiation and function of the testis. A relevant feature of the set of differential proteins identified was that many of them were represented by several differential spots, such as A2m-1 (10 spots), hemopexin (Hpx, 4 spots), and keratin (three spots), and adenosine triphosphate (ATP) synthase b subunit (Atpb), peroxiredoxin 6 (Prdx6), and Krt18, that were represented by two spots each. Interestingly, in some cases, there were different regulation patterns depending on the testis's developmental stage. These observations are similar to those reported for mammals (Paz et al., 2006) and underline the complex post-transcriptional and post-translational regulatory mechanisms of gene expression that possibly occur during fish spermatogenesis (Forné et al., 2009).

In summary, this study identified 24 differentially expressed proteins in the testis of Senegalese sole F1 fish compared with wild-caught males showing higher sperm production and fertilization rates. Proteins involved in cytoskeletal organization and catabolic processes as well

as in redox or antioxidant activity were identified in high proportions. In addition, proteins not previously described in the teleost testis were also found. However, for some of these proteins, there was an elevated number of different isoforms and/or PTMs, which possessed very different expression profiles depending on the developmental stage of the testis, which underlines the complex regulatory mechanisms of protein function that probably occur during teleost spermatogenesis (Forné et al., 2009).

The obtained data suggest that this study indicated that there were alterations in protease inhibition, iron and glucose metabolism, and protection against oxidative stress, which may be mechanisms underlying the low production and poor fertilization capacity of the sperm produced by sole F1 males. The role of these mechanisms and their endocrine regulation should be investigated in the future to understand the physiological basis of the production of viable sperm in Senegalese sole and possibly in other farmed flatfish (Forné et al., 2009).

2.22. **Proteomic Analysis of Epidermal Mucus from Sea Lice–Infected Atlantic Salmon, *Salmo salar L*.**

Sea lice, *Lepeophtheirus salmonis*, infection is one of the biggest challenges faced by the aquaculture industry in the North Atlantic region. The sea lice cause a substantial loss to the industry every year, and the transfer of sea lice infestation from farmed fish to wild fish is of great concern (Provan et al., 2013). It is now accepted that the life cycle of the salmon louse can be followed by observing the chalimus larvae molting in incubators and by morphometric cluster analysis, it was established that there are only two chalimus instars: chalimus 1 (comprising the former chalimus I and II stages which are not separated by a molt) and chalimus 2 (the former chalimus III and IV stages which are not separated by a molt). Consequently the salmon louse life cycle has only six post-nauplius instars, as in other genera of caligid sea lice and copepods in general. These findings are of fundamental importance in experimental studies as well as for interpretation of salmon louse biology and for control and management of this economically important parasite (Hamre et al., 2013).

Recently, it was established that healthy diets that contain immunostimulants and other functional ingredients usually strengthen the immune response of the Atlantic salmon (*Salmo salar*) and thereby reduce the sea lice, *Lepeophtheirus salmonis* infection levels. Such diets can be

used to supplement other treatments and will potentially reduce the need for delousing and medication (Provan et al., 2013).

In this study, a sea lice infection trial was conducted on fish with an average weight of 215 g. One control diet and four experimental diets containing functional ingredients were produced. The diets were fed to salmon for four weeks before infection with sea lice copepodids. Fish mucus is a complex material and functions as mechanical protection against the environment. It also contains enzymes, antibacterial agents and other immune-related compounds (Easy & Ross, 2009; Fast et al., 2002; Firth et al., 2000; Provan et al., 2013). Mucus is seen as a promising biological matrix for biomarker identification (Provan et al., 2013).

When lice had developed to chalimus II, 88 fish per diet were examined for lice loads. The mucus samples from fish fed the different diets were taken before and after lice infection. Tandem mass spectrometry-based proteomics was used to characterize the protein composition in the epidermal mucus of Atlantic salmon and to identify quantitative alterations in protein expression. The workflow involved in LC-ESI-MS/MS analysis and identification of putative biomarkers is illustrated in Figure. 30 (Provan et al., 2013).

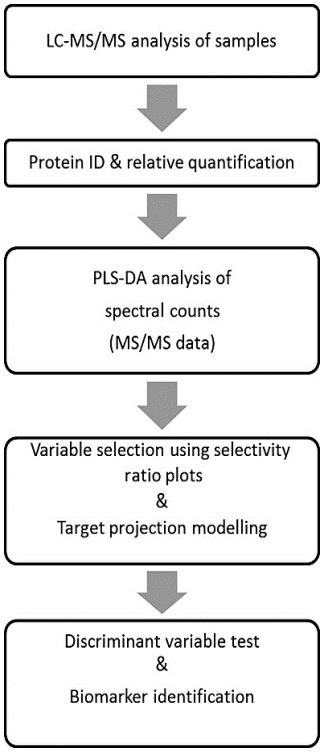

Figure 30. Workflow for LC-MS/MS analysis of epidermal mucus samples and multivariate analysis of normalized spectral count data (Provan et al., 2013).

The mucus samples were analyzed from six fish in each of the five diet groups (control + diets B–E) before sea lice infection. Analysis of the LC-MS/MS data revealed a total of 323 proteins that were expressed in mucus. A total of 118 proteins were present in samples from all groups. A number of these common proteins were altered in expression levels in mucus samples from fish-fed diets with functional feeds. In particular, the protein peptidyl-prolyl cis transisomerase, an immunophilin, was downregulated in the mucus of all fish fed functional feeds. This downregulation was detected through the calculation of fold change values from the spectral count data for each protein (Tables 16, 17, and 18) (Provan et al., 2013).

Multivariate analysis of quantitative LC-MS/MS data (spectral count values) facilitates both visualization of the data and the identification of proteins with significantly altered expression levels, related to infection. PCA plots (Figure. 31) were generated of the entire data set (CC vs. LL vs. HL). This revealed the existence of four outliers (two samples in LL and two samples in HL (Provan et al., 2013).

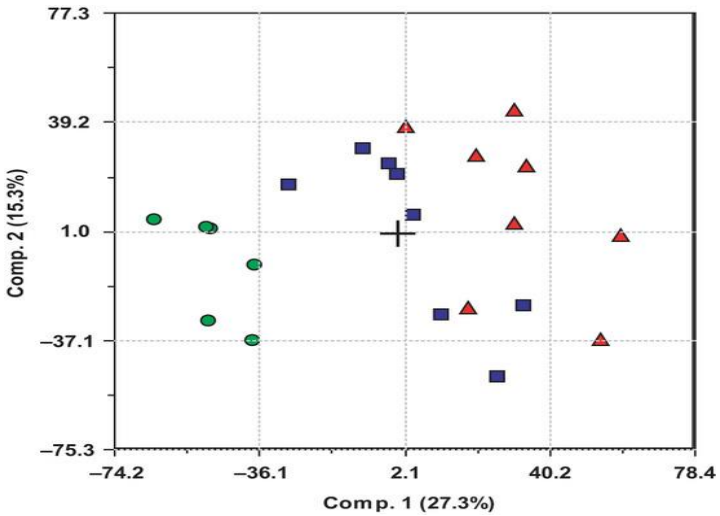

Figure 31. PCA score plot of samples from controls (CC, green circles), low lice levels (LL, blue squares) and high lice levels (HL, red triangles) (Provan et al., 2013).

Table 16. Selected proteins with SR values above the statistical boundary selected by the DIVA test. Samples from control (CC) vs low lice levels (LL) (Provan et al., 2013).

Protein name	Amino acids	Accession number	Selectivity ratio value
RecName: Full = Glyceraldehyde-3-phosphate dehydrogenase	335-aa protein	GI:6016082	4.872
Elongation factor 1-alpha oocyte form [Salmo salar]	461-aa protein	GI:223648646	4.647
elongation factor 1 alpha [Salmo salar]	461-aa protein	GI:185136154	3.811
ATP synthase subunit alpha, mitochondrial [Salmo salar]	528-aa protein	GI:213512628	2.146
Galectin-3 [Salmo salar]	271-aa protein	GI:209732232	2.131
Nascent polypeptide-associated complex subunit alpha [Salmo salar]	213-aa protein	GI:209730306	1.996
Rho GDP-dissociation inhibitor 1 [Salmo salar]	205-aa protein	GI:209148544	1.975
Proteasome subunit alpha type-2 [Salmo salar]	234-aa protein	GI:209732674	1.841
Adenylyl cyclase–associated protein 1 [Salmo salar]	467-aa protein	GI:213513451	1.736
SH3 domain–binding glutamic acid-rich-like protein 3 [Salmo salar]	91-aa protein	GI:209731122	1.706
Glyceraldehyde-3-phosphate dehydrogenase [Salmo salar]	335-aa protein	GI:221222316	1.635
14-3-3 protein beta/alpha-2 [Salmo salar]	244-aa protein	GI:209733710	1.429
RecName: Full = Serum albumin 2; Flags: Precursor	608-aa protein	GI:543792	1.238
Elongation factor 2 [Salmo salar]	858-aa protein	GI:213511398	1.220

Proteasome subunit beta type-1-A [Salmo salar]	237-aa protein	GI:209732446	1.197
Glucose-6-phosphate isomerase [Salmo salar]	553-aa protein	GI:223647970	1.193
Argininosuccinate synthase [Salmo salar]	412-aa protein	GI:209734100	1.118
Fructose-bisphosphate aldolase A [Salmo salar]	363-aa protein	GI:223647884	1.073
transketolase-like protein 2 [Salmo salar]	626-aa protein	GI:213511480	1.022
Elongation factor 1-alpha 1 [Salmo salar]	462-aa protein	GI:223649464	0.981

Table 17. Selected proteins with SR values above the statistical boundary selected by the DIVA test. Samples from control (CC) vs high lice levels (HL) (Provan et al., 2013).

Protein identification	Amino acids	Accession number	Selectivity ratio value
6-Phosphogluconate dehydrogenase, decarboxylating [Salmo salar]	483-aa protein	GI:223648108	5.737
Proteasome subunit beta type-1-A [Salmo salar]	237-aa protein	GI:209732446	5.230
Rho GDP-dissociation inhibitor 1 [Salmo salar]	205-aa protein	GI:209148544	4.277
Heat shock cognate 70-kDa protein [Salmo salar]	663-aa protein	GI:209155490	3.590
Elongation factor 1-alpha, oocyte form [Salmo salar]	461-aa protein	GI:223648646	3.554
alcohol dehydrogenase class 3 [Salmo salar]	376-aa protein	GI:224747157	3.299
Profilin-2 [Salmo salar]	143-aa protein	GI:209735284	3.072
elongation factor 1 alpha [Salmo salar]	461-aa protein	GI:185136154	2.875
tubulin, alpha 8 like 3-2 [Salmo salar]	450-aa protein	GI:197632605	2.804
disulfide-isomerase A3 precursor [Salmo salar]	491-aa protein	GI:209156144	2.795
Elongation factor 2 [Salmo salar]	858-aa protein	GI:223647986	2.693
Elongation factor 2 [Salmo salar]	858-aa protein	GI:213511398	2.678
transketolase-like protein 2 [Salmo salar]	626-aa protein	GI:213511480	2.590
RecName: Full = Glyceraldehyde-3-phosphate dehydrogenase	335-aa protein	GI:6016082	2.521
Fructose-bisphosphate aldolase A [Salmo salar]	363-aa protein	GI:223647884	2.503
Argininosuccinate synthase [Salmo salar]	412-aa protein	GI:209734100	2.450
Cystathionine gamma-lyase [Salmo salar]	405-aa protein	GI:223648092	2.425
Glyceraldehyde-3-phosphate dehydrogenase [Salmo salar]	335-aa protein	GI:221222316	2.373
Nascent polypeptide-associated complex subunit alpha [Salmo salar]	213-aa protein	GI:209730306	2.057
Proteasome subunit alpha type-2 [Salmo salar]	234-aa protein	GI:209732674	1.922

Tubulin alpha chain [Salmo salar]	450-aa protein	GI:209155464	1.814
60S ribosomal protein L7 [Salmo salar]	245-aa protein	GI:209734288	1.707
disulfide-isomerase A3 precursor [Salmo salar]	493-aa protein	GI:223647886	1.689
beta-actin [Oncorhynchus mykiss]	375-aa protein	GI:8886013	1.670
Galectin-3 [Salmo salar]	271-aa protein	GI:209732232	1.659
Adenylyl cyclase-associated protein 1 [Salmo salar]	467-aa protein	GI:213513451	1.641
Lysyl-tRNA synthetase [Salmo salar]	569-aa protein	GI:224613430	1.595
RecName: Full = Serum albumin 2	608-aa protein	GI:543792	1.551
RecName: Full = Heat shock cognate 70-kDa protein	651-aa protein	GI:232285	1.550
Elongation factor 1-alpha 1 [Salmo salar]	462-aa protein	GI:223649464	1.522
RecName: Full = Retinol-binding protein 4-B	176-aa protein	GI:267585	1.479
ATP synthase subunit alpha, mitochondrial [Salmo salar]	528-aa protein	GI:213512628	1.466
Heterogeneous nuclear ribonucleoprotein A1 [Salmo salar]	384-aa protein	GI:223673171	1.453
transient receptor potential cation channel subfamily V member 1 [Salm salar]	804-aa protein	GI:213514830	1.429
Glucose-6-phosphate isomerase [Salmo salar]	553-aa protein	GI:223647970	1.361
14-3-3A1 protein [Oncorhynchus mykiss]	246-aa protein	GI:185134456	1.357
Eukaryotic translation initiation factor 3 subunit H [Salmo salar]	344-aa protein	GI:221220796	1.326
Pyruvate kinase muscle isozyme [Salmo salar]	524-aa protein	GI:224587654	1.321
14-3-3 protein beta/alpha-1 [Salmo salar]	250-aa protein	GI:209737118	1.311
ribosomal protein L22 [Salmo salar]	129-aa protein	GI:198285529	1.222
Anterior gradient protein 2 homolog precursor [Salmo salar]	171-aa protein	GI:209734700	1.216
RecName: Full = Serum albumin 1	608-aa protein	GI:113581	1.207
Lysozyme g [Salmo salar]	192-aa protein	GI:209734070	1.173
Tubulin beta-1 chain [Salmo salar]	445-aa protein	GI:223672699	1.172
L-Lactate dehydrogenase B chain [Salmo salar]	334-aa protein	GI:213514660	1.168
heat shock protein hsp90 beta [Salmo salar]	722-aa protein	GI:185132934	1.099
40S ribosomal protein SA [Salmo salar]	317-aa protein	GI:209735958	1.086
T-complex protein 1 subunit theta [Salmo salar]	546-aa protein	GI:213511620	1.085
Tropomyosin alpha-3 chain [Salmo salar]	246-aa protein	GI:223647762	1.075
ATP synthase H+ transporting mitochondrial F1 complex beta [Salmo salar]	495-aa protein	GI:198285477	1.051

Actin-related protein 3 [Salmo salar]	418-aa protein	GI:223649212	1.046
Eukaryotic translation initiation factor 5A-1 [Salmo salar]	157-aa protein	GI:221219086	1.037
Ran-specific GTPase-activating protein [Salmo salar]	208-aa protein	GI:213511046	1.021
nucleolin [Oncorhynchus mykiss]	255-aa protein	GI:7417424	1.0

Table 18. Selected proteins with SR values above the statistical boundary selected by the DIVA test. Samples from low lice levels (LL) vs high lice levels (HL) (Provan et al., 2013).

Protein	Amino acids	Accession number	Selectivity ratio value
RecName: Full = Heat shock cognate 70-kDa protein; Short = HSP70	651-aa protein	GI:232285	1.385
alpha-1-antiproteinase-like protein precursor [Oncorhynchus mykiss]	426-aa protein	GI:185132174	−1.018
Heat shock cognate 70-kDa protein [Salmo salar]	663-aa protein	GI:209155490	1.394
NHP2-like protein 1 [Salmo salar]	128-aa protein	GI:209733540	0.963
T-complex protein 1 subunit theta [Salmo salar]	546-aa protein	GI:213511620	1.568
Eukaryotic translation initiation factor 5A-1 [Salmo salar]	157-aa protein	GI:221219086	1.051
Complement component C6 precursor [Salmo salar]	940-aa protein	GI:223647842	−1.34
Heterogeneous nuclear ribonucleoprotein A1 [Salmo salar]	384-aa protein	GI:223673171	1.168

In conclusion, it was found that tte putative biomarkers identified were associated with functional feed intake and with sea lice infection have been identified and can form the basis for strategic validation experiments with selected functional feeds (Provan et al., 2013).

3. Fish Health and Immunology Proteomics

The vertebrate immune function necessitates coordinating a complex set of regulatory processes and signalling pathways. In teleost fishes, these processes are regulated by the immediate innate response to pathogenic offence, which is governed by cellular and humoral components (Bird et al., 2007; Causey et al., 2018; Magnadóttir, 2006; Secombes, 2016). For example, the conserved cytokines IL-1β, IL-8 and tumour necrosis factor α (TNFα) each activate nuclear factor kappa-light-chain enhancer of activated B cells (NF-κB) signalling pathways to regulate early inflammatory responses to bacterial infection. These are followed by the acute phase response (APR), defined by the production of plasma proteins such as complement system components,

cerebellin-like proteins, lectins, haptoglobin and ferritin (Figure. 32) (Bayne et al., 2001; Bayne & Gerwick, 2001; Zou & Secombes, 2016).

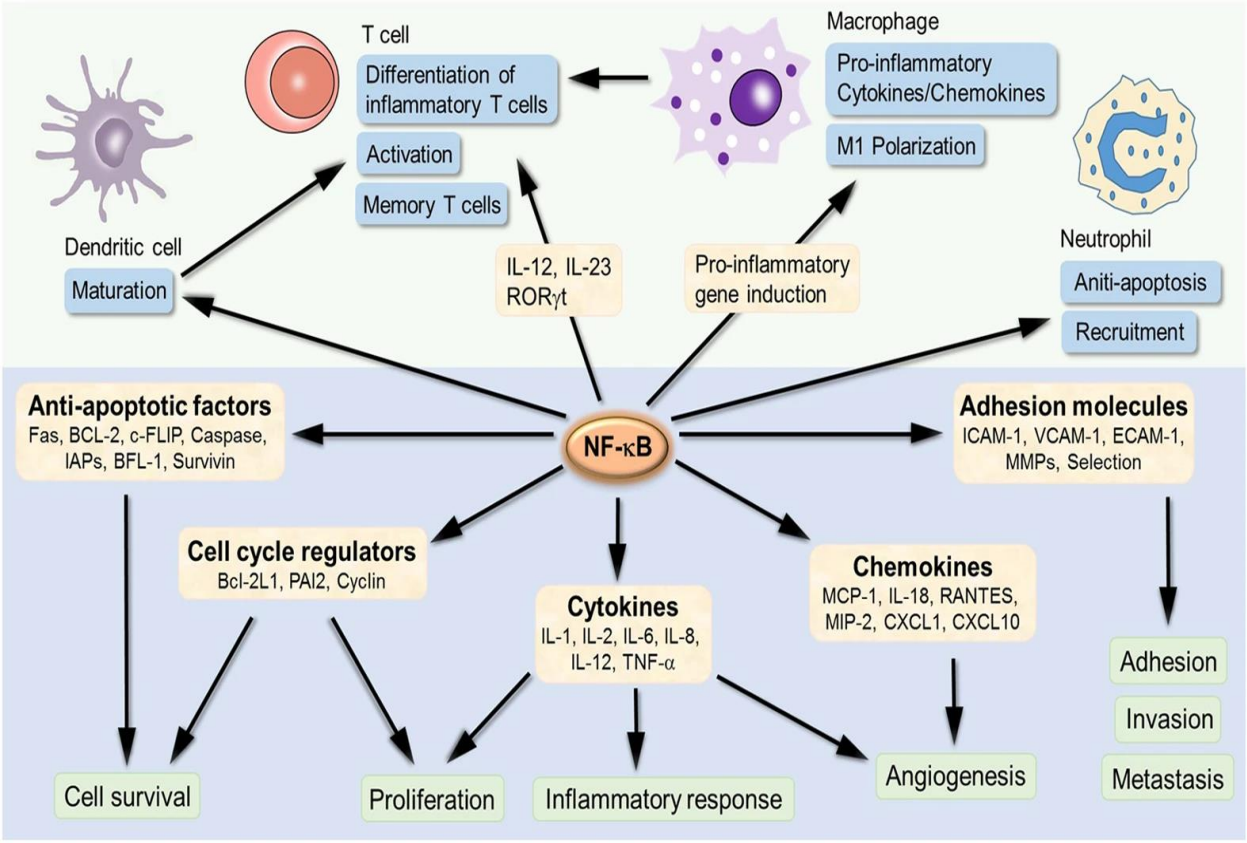

Figure 32. NF-κB target genes involved in inflammation development and progression. NF-κB is an inducible transcription factor. After its activation, it can activate transcription of various genes and thereby regulate inflammation. NF-κB targets inflammation not only directly by increasing the production of inflammatory cytokines, chemokines and adhesion molecules but also by regulating the cell proliferation, apoptosis, morphogenesis and differentiation (T. Liu et al., 2017).

The teleost fishes' innate immune response originates primarily in the lymphoid organs such as the head, kidney, and spleen and various mucosal-associated sites (e.g. gills, gut, skin and nostrils) (Gomez et al., 2013; Z. Xu et al., 2013). In addition, the humoral innate immune components comprise an extensive range of receptors and molecules that are soluble in plasma and other body fluids. These latter consist of cytokines, APR proteins, antimicrobial peptides and protease inhibitors (Causey et al., 2018; Magnadóttir, 2006).

On the other hand, the successful establishment of the aquaculture venture production industries mainly depends on the efficient development of farming techniques, the mass production of fish fry and fingerling, the stabilization of marketing status, and the support of surrounding industries. Unfortunately, the major limiting factors affecting the aquaculture industries are mainly caused by infectious diseases. These fish diseases could be caused by bacteria, viruses, protists, helminths, oomycetes, fungi, and other disease-causing pathogens. The resulting severe mortality and morbidity caused by infectious diseases lead to huge economic losses. Lately, the aquaculture industries have adopted modern pathogen-control techniques to maintain healthy stocks to enhance production. These techniques frequently consist of antibiotics and chemicals, which lead to the unplanned consequence of producing multidrug-resistant pathogens. In general, fish mucus acts as a physiological and immunological barrier for maintaining normal fish physiology and conferring defence against pathogens infection. It is recognized that the biochemically defensive roles of fish skin are largely attributed to fish mucus components which expression varies in response to various stresses (Jurado et al., 2015a; Y. Xiong et al., 2020a).

3.1. Antimicrobial Peptide Epinecidin-1 and Proteomic and Functional Analysis of Zebrafish

The antimicrobial peptides (AMPs) are considered evolutionarily conserved, natural defensive weapons and they are secreted by prokaryotes, plants, and invertebrates, which play essential roles in the innate immune response (Hancock & Scott, 2000). The AMP epinecidin-1 was found to be an effective antimicrobial agent against various pathogens, including Gram-positive bacteria (such as *Micrococcus luteus, Staphylococcus aureus, and S. aureus subsp)* and Gram-negative bacteria (such as *Vibrio alginolyticus and V. vulnificus*) (Hancock & Lehrer, 1998; T. C. Huang & Chen, 2013; Pan et al., 2007, 2012; Sawyer et al., 1988). Epinecidin-1 exists as an alpha-helical AMP, which causes cell lysis by forming pores in bacterial membranes (T. C. Huang & Chen, 2013).

Notwithstanding the extensive investigation of the effects of AMPs on pathogens, the interactions between AMPs and host cells have not been studied extensively (Diamond et al., 2009; T. C. Huang & Chen, 2013; Y. Huang et al., 2010; Lai & Gallo, 2009). This section presents the proteomic and functional analysis of zebrafish after the administration of antimicrobial peptide

epinecidin-1. This was accomplished in order to understand the underlying antimicrobial molecular mechanisms study of epinecidin-1 (T. C. Huang & Chen, 2013).

The identification of the associated antimicrobial proteins was achieved by comparing the "shotgun" proteomics approach " between the epinecidin-1 injected and control zebrafish. The identification of the differentially expressed proteins was achieved by 2DE coupled to LC-ESI-MS/MS (Figure 33, and Table 19) (T. C. Huang & Chen, 2013).

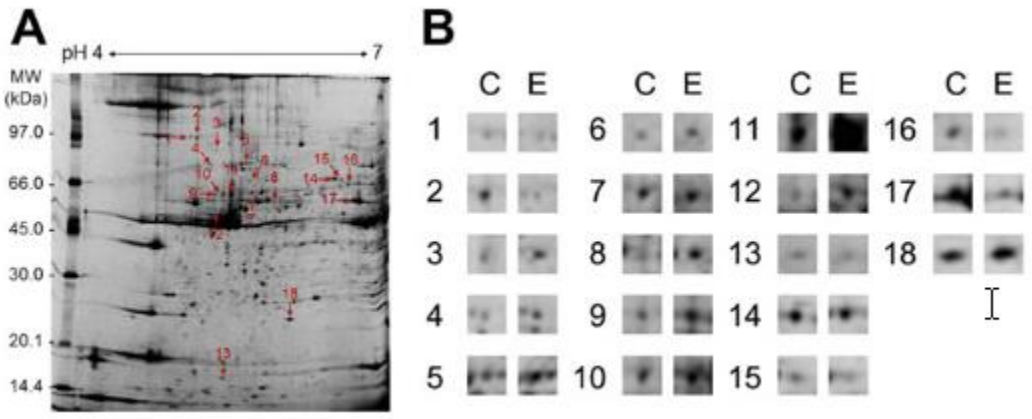

Figure 33. Proteomic analysis showing alterations in the protein profile of epinecidine-1- treated zebrafish(T. C. Huang & Chen, 2013).

Table 19. Proteins differentially expressed upon epinecidine-1 treatment in zebrafish, as identified by LC-ESI-MS/MS(T. C. Huang & Chen, 2013).

Spot[a]	Protein name	Accession No.[b]	Gene name	Score[c]	Matched peptide[d]	Mr[e]	pI[f]	Fold[g]
1	Pleckstrin homology domain-containing family H member	Q00IB7	plekhh1	28	1	159,944	6.43	-1.7
2	Pleckstrin homology domain-containing family H member	Q00IB7	plekhh1	26	1	159,944	6.43	-1.6
3	E3 ubiquitin-protein ligase Siah2	Q7SYL3	siah21	29	1	34,471	6.48	1.7
4[h]	Heat shock cognate 71 kDa	Q90473	hspa8	75	2	70,930	5.18	1.4
5[h]	Tropomyosin alpha-1 chain	P13104	tpma	561	12	32,703	4.7	1.6
6	Sphingosine 1-phosphate receptor 2	Q9I8K8	s1pr2	28	1	41,749	9.18	1.4
7[h]	Keratin, type II cytoskeletal 8	Q6NWF6	krt8	310	8	57,723	5.15	1.4
8[h]	Glial fibrillary acidic protein	Q58EE9	gfap	81	1	51,218	5334	1.6
9	Solute carrier family 25 member 35	A3KPP4	slc25a35	43	1	32,264	9359	3.2

10[h]	Glial fibrillary acidic protein	Q58EE9	gfap	91	2	51,218	5.34	2
11[h]	Glial fibrillary acidic protein	Q58EE9	gfap	157	3	51,218	5.34	1.4
12[h]	Actin, cytoplasmic 1	Q7ZVI7	actba	54	1	41,740	5.3	2.2
13	Twisted gastrulation protein homolog 1-B	Q98SR9	twsg1b	27	1	24,523	5.41	1.5
14	Hemopexin	Q6PHG2	hpx	608	18	50,994	6.14	-1.7
15	Hemopexin	Q6PHG2	hpx	126	4	50,994	6.14	-1.7
16	Hemopexin	Q6PHG2	hpx	120	7	50,994	6.14	-1.9
17	Sodium-coupled monocarboxylate transporter 1	Q3ZMH1	slc5a8	55	2	66,315	6.23	-1.3
18[h]	Protein DJ-1	Q5XJ36	park7	322	12	19,751	5.84	2.3

[a] Protein spot number according to Figure 10.
[b] Protein accession number according to the SwissProt database.
[c] Score according to the MASCOT database.
[d] Number of peptide masses matching the top hit from MS-Fit PMF.
[e] Theoretical molecular weight (Mr) according to protein sequence.
[f] Theoretical pI according to protein sequence.
[g] Protein expression fold change between epinecidin-1-injected and PBS-injected fish.
[h] Protein expression was verified by qPCR.

The expression data were also subjected to Ingenuity Pathway Analysis (IPA) was used to construct a protein-protein interaction network. Accordingly, it was postulated that epinecidin-1 regulates cellular ubiquitination, as ubiquitin was identified by IPA as the hub protein in the top network composed of molecules with the most associated functions (Figure 34) (T. C. Huang & Chen, 2013).

Moreover, several differentially expressed proteins were identified and were validated by real-time quantitative RT-PCR. The changes in expression of *HSPA8*, *GFAP*, *PARK7*, AND *TPMA* mRNA were consistent with those of the encoded proteins 12 h after epinecidin-1 injection (T. C. Huang & Chen, 2013).

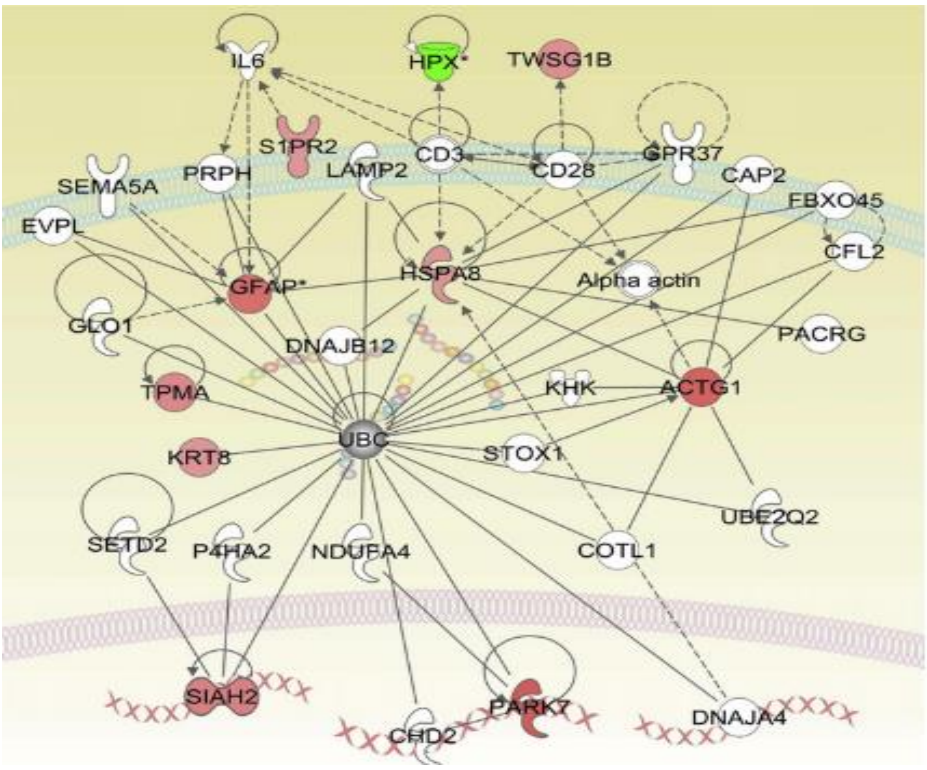

Figure 34. Network analysis of differentially expressed proteins was performed using the Ingenuity Pathways Analysis (IPA) software. Proteins highlighted in red were identified as up-regulated, and those highlighted in green were found to be down-regulated in epinecidine-1 treated zebrafish(T. C. Huang & Chen, 2013).

Gene Ontology (GO) analysis showed that a quarter of identified proteins were localized to the cytoskeleton. In addition, half of the identified proteins were involved in molecule binding; It was also found that over a fifth were involved in developmental processes, while another fifth were involved in the regulation of biological processes (Figure 35) (T. C. Huang & Chen, 2013).

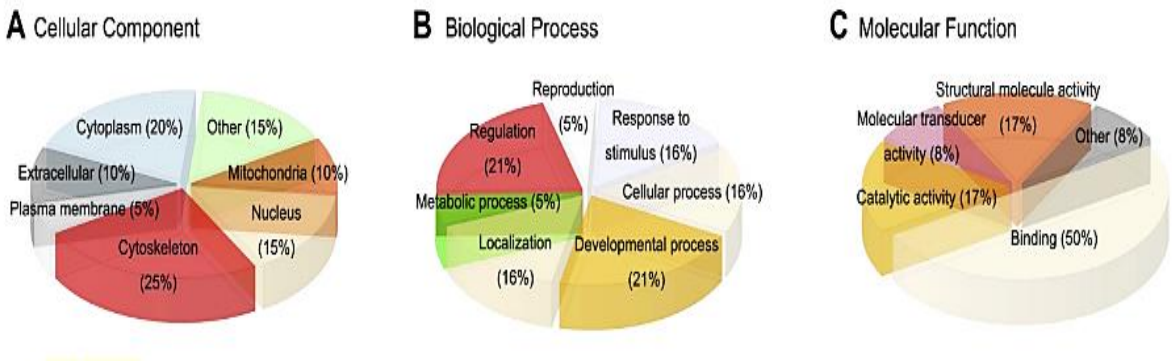

Figure 35. Gene ontology (GO) analysis of proteins differentially expressed in epinecidine-1-treated zebrafish. The GO (A) cellular component, (B) biological process, and (C) molecular function annotations were classified using STRAP software. The percentage of proteins for each class is shown as represented in the pie chart (T. C. Huang & Chen, 2013).

The expression data were subjected to the Ingenuity Pathway Analysis (IPA), and the results were used to construct a protein-protein interaction network. Accordingly, it was postulated that epinecidin-1 regulates cellular ubiquitination, as ubiquitin was identified by IPA as the hub protein in the top network composed of molecules with the most associated functions. The IPA of the canonical pathways network suggested a potential role of epinecindin-1 in the cytoskeletal assembly and organization. This finding implies that epinecidin-1 can stabilize the cytoskeleton network in host cells, thereby promoting resistance to bacterial infection (T. C. Huang & Chen, 2013).

3.2. **Differentially Expressed Proteins in Gill and Skin Mucus of Atlantic Salmon (*Salmo salar*) Affected by Amoebic Gill isease**

As indicated previously, mucus can be considered as an excellent biological matrix which contains the majority of the proteins produced in the gill and skin. Amoebic gill disease (AGD) is caused by the protozoan amoeba species *Neoparamoeba perurans.* This disease affects salmonids worldwide and induces excessive mucus production in the gills and skin (Valdenegro-Vega et al., 2014).

The limited knowledge of the immune response to AGD was obtained through gene expression studies (Bridle, Morrison, & Nowak, 2006; Bridle, Morrison, Cupit Cunningham, et al., 2006; Morrison et al., 2006; Pennacchi et al., 2014; Young et al., 2008), antibody response (Taylor et al., 2010; Villavedra et al., 2010; Vincent et al., 2008, 2009) and histopathology (Adams & Nowak, 2003, 2004). Also, *N. perurans* infection promotes the expression of pro-inflammatory cytokines such as interleukin -1b (Bridle, Morrison, & Nowak, 2006; Bridle, Morrison, Cupit Cunningham, et al., 2006; Morrison et al., 2007; Young et al., 2008) in areas of the gill affected by the parasite.

It was expected that attempts to discover the host immune response to AGD using the new proteomics research tools would provide further insight. Accordingly, gill and skin mucus samples were obtained from Atlantic salmon (*Salmo salar*) fish, which were infected with *N. perurans* on

four successive occasions. The characterization and proteins extraction of the broad pattern of proteins was performed by SDS-PAGE. The protein content of gill mucus samples obtained from diseased and control fish ranged between 1.0 and 1.3 mg/mL, indicating marked heterogeneity in the protein bands (Figure 36), with little consistency between AGD-affected and AGD naïve mucus proteins (Valdenegro-Vega et al., 2014).

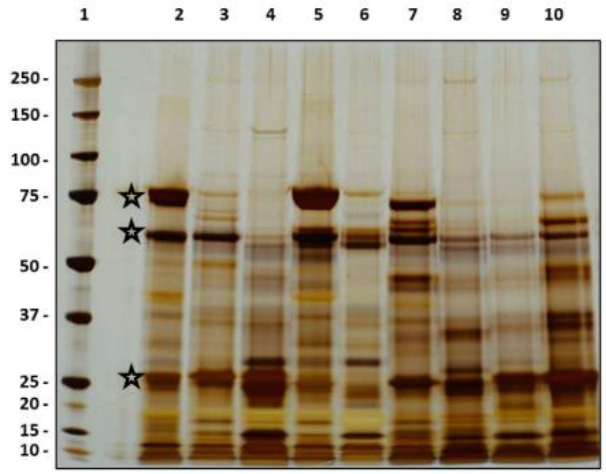

Figure 36. Protein extractions from Atlantic salmon (Salmo salar) gill mucus resolved by Bis-Tris 4e12% NuPAGE and silver stained. Each lane contains a similar protein yield amount (~4 mg per lane) after dialysis and lyophilisation. Lane 1 MWM, lanes 2e6: gill mucus samples from AGD-naïve fish, lanes 7e10: gill mucus from AGD- affected fish. Stars indicate bands that were excised and subjected to in-gel digestion for identification by nanoLC/MS (Valdenegro-Vega et al., 2014).

Nano-HPLC-ESI-MS/MS analysis was used to identify the proteins in the gill and skin mucus of Atlantic salmon affected by AGD. A total of 186 and 322 non-redundant proteins were identified in gill and skin mucus respectively, Also, based on stringent filtration criteria, and statistics it was found that 52 gill and 42 skin mucus proteins were differentially expressed in mucus samples from AGD-affected fish (Table 23) (Valdenegro-Vega et al., 2014).

These diagnostic proteins were identified based on two or more distinct matching peptide sequences, similar to the number of mucus proteins identified in a previous gel-free proteomics analysis (Provan et al., 2013; Valdenegro-Vega et al., 2014). Nevertheless, non-redundant protein groups' presence was characterized as follows: 15% of gill and 21% of skin mucus proteins were specifically identified only in mucus samples from AGD affected fish. It should be noted that the mucus of the naïve salmon serum contained serum albumin and serotransferrin, which have been

previously identified in the analyses of mucus (Easy & Ross, 2009; Provan et al., 2013). In particular, serum albumin can account for a high proportion of the total protein in mucus (Table 20) (Panicker et al., 2010; Valdenegro-Vega et al., 2014).

By generating protein-protein interaction networks, some of these proteins formed part of the cell to cell signalling and inflammation pathways, such as C-reactive protein, apolipoprotein 1, granulin, cathepsin, angiogenin-1 (Valdenegro-Vega et al., 2014).

In addition to proteins that were entirely novel in the context in the host response to *N. perurans*, our results have confirmed the presence of protein markers in mucus that have been previously predicted based on modified mRNA expression, such as anterior gradient-2 protein, annexin A-1 and complement C3 factor (Table 20) (Valdenegro-Vega et al., 2014).

In summary, this study allowed the identification of a series of proteins expressed in the mucus of AGD-affected Atlantic salmon. It was found that some of these proteins are related to inflammation and IL-1b expression, which is upregulated in this disease (Bridle, Morrison, & Nowak, 2006; Bridle, Morrison, Cupit Cunningham, et al., 2006; Morrison et al., 2006; Pennacchi et al., 2014; Young et al., 2008). Other proteins, such as as AG-2, have already been shown in cells of the gills of salmon infected by *N. perurans* and their mRNA expression levels have been characterized (Morrison & Nowak, 2008; Nowak et al., 2013; Valdenegro-Vega et al., 2014).

Table 20. Proteins significantly and differentially abundant in the skin mucus of AGD-affected Atlantic salmon. NanoLC-MS/MS identified proteins. Proteins with P < 0.05 and fold change >2.0 are in bold letters. SPC C, Spectral count Control group; SPC D, spectral count diseased (AGD) group; FC, fold change (Valdenegro-Vega et al., 2014).

#	Description	Accession numbers	SpC C	SpC D	FC	*P*-value	Q-value
1	Acidic leucine-rich nuclear phosphoprotein 32 family member A (*Danio rerio*) and family member B (*Salmo salar*, *Danio rerio*)	ACN11434.1, ACM08449.1, AAI65448.1, ACN12741.1, CAG01930.1, NP_997768.2	0	1.5	>1.5	0.002	0.035
2	Actinin alpha 4 (*Danio rerio*)	NP_955880.1	1.3	3.9	3.0	0.007	0.088
3	Actin-related protein 3 (*Salmo salar*, *Esox lucius*)	ACI69786.1, ACO13358.1	0	0.8	>0.8	0.019	0.110
4	Alanyl-tRNA synthetase, cytoplasmic (*Salmo salar*)	NP_001133550.1	2.0	5.4	2.7	0.017	0.110
5	Aminopeptidase B (*Salmo salar*, *Osmerus mordax*), Arginyl aminopeptidase (*Danio rerio*)	ACN10761.1, NP_001002741.1, ACO08981.1	0	1.8	>1.8	0.014	0.110
6	Anterior gradient-2-like protein 1 (*Salmo salar*), Anterior gradient protein 2 homolog precursor (*Salmo salar*, *Esox lucius*), Anterior gradient homolog 2 (*Xenopus laevis*, *Danio rerio*)	ABB96968.1, ACI69433.1, ABB96969.1, ACM09796.1, ACI67616.1, ACO13414.1, AAI52145.1, CAM56358.1	6.9	10.5	1.5	0.036	0.172
7	APEX nuclease 1 (*Salmo salar*)	NP_001135227.1	0	1.2	>1.2	0.008	0.091
8	Barrier-to-autointegration factor (*Oncorhynchus mykiss*, *Salmo salar*, *Esox lucius*, *Osmerus mordax*)	ACO07632.1, ACI69910.1, ACO13844.1, ACM08201.1, ACI66267.1, ACO08277.1, ACO09060.1	0	1.8	>1.8	0.001	0.028
9	Betaine-homocysteine methyltransferase (*Salmo salar*)	NP_001133157.1	1.2	2.9	2.4	0.018	0.110
10	Carbonic anhydrase II (*Oncorhynchus mykiss*), carbonic anhydrase (*Salmo salar*)	NP_001117693.1, ACN10477.1	5.7	1.8	-3.1	0.015	0.110
11	Cathepsin H precursor (*Salmo salar*), Cathepsin H precursor (*Salmo salar*)	ACI66855.1, ACI66895.1	0	1.6	>1.6	0.009	0.093
12	Cleavage and polyadenylation specificity factor subunit 5 (*Salmo salar*, *Esox lucius*, *Danio rerio*, *Oncorhynchus mykiss*)	ACO14322.1, CAF99562.1, ACM08683.1, ACM08212.1, AAI65427.1, ACN12771.1, CAN88764.1, ACM09751.1, ACO08099.1, XP_001921533.1, ACI68139.1	0	1.0	>1.0	0.019	0.110
13	Coactosin-like 1 (*Ictalurus punctatus*, *Salmo salar*)	ABC75560.1, ACN12230.1, CAF98914.1	0.4	1.9	4.7	0.027	0.148
14	Complement C3 group (*Oncorhynchus mykiss*, *Salmo marmoratus*)	AAB05029.1, ACF75925.1	13.6	7.0	-1.9	0.003	0.046
15	Complement component C9 (*Oncorhynchus mykiss*)	NP_001117898.1, CAA29037.1	3.9	0.4	-9.9	<0.001	0.014
16	Cystathionine gamma-lyase inhibitor (*Oncorhynchus mykiss*), Cystathionine gamma-lyase (*Salmo salar*)	NP_001118157.1, ACN10804.1	0.4	2.0	5.0	0.015	0.110
17	Cystatin precursor (*Salmo salar*)	ACI66857.1, ACI68640.1, ACN12429.1, ACI68292.1, ACI66239.1, ACI69177.1	0	2.4	>2.4	<0.001	0.006
18	Deoxyribonuclease gamma precursor (*Salmo salar*)	ACI70073.1, ACI69566.1	18.8	29.5	1.6	0.029	0.150
19	Eukaryotic translation initiation factor 4H (*Salmo salar*, *Danio rerio*, *Osmerus mordax*)	NP_001133347.1, NP_991258.1, ACO10072.1, ACN10439.1	0.6	2.7	4.6	0.011	0.103
20	Eukaryotic translation initiation factor 5A-1 (*Salmo salar*, *Esox lucius*)	ACI34012.1, ACO14228.1, ACM08851.1, ACM08204.1	1.3	3.3	2.5	0.038	0.172

21	FAM139A (*Salmo salar*)	ACN60260.1	0	1.3	>1.3	0.019	0.110
22	Fructose-bisphosphate aldolase A (*Osmerus mordax, Esox lucius, Salmo salar, Oryzias latipes, Epinephelus coioides, Danio rerio*), aldolase A (*Danio rerio*), aldolase (*Ictalurus punctatus*)	ACO09344.1, ACO14552.1, NP_001133180.1, AAN04476.1, NP_001133181.1, AAO25766.1, BAD17895.1, ACL98138.1, NP_998380.1, AAQ94593.1, ACN10700.1	1.7	4.9	3.0	0.018	0.110
#	Description	Accession numbers	SpC C	SpC D	FC	*P*-value	Q-value
23	Glutamate dehydrogenase 1, mitochondrial precursor (*Salmo salar*)	ACN10920.1	0	23.1	>2.31	<0.001	0.006
24	Glutathione transferase omega-1 (*Salmo salar, Oncorhynchus mykiss*)	ACN10920.1	0	2.5	>2.5	<0.001	0.006
25	Guanine nucleotide binding protein (G protein), beta polypeptide 2-like 1 (*Danio rerio, Salmo salar, Osmerus mordax, Esox lucius, Oreochromis niloticus, Anoplopoma fimbria, Danio rerio*), receptor for activated protein kinase c (*Pagrus major, Dicentrarchus labrax, Oncorhynchus mykiss, Sander vitreus, Paralichthys olivaceus, Oreochromis mossambicus, Platichthys flesus*), activated protein kinase C (*Epinephelus akaara*)	NP_571519.1, ACN11311.1, CAG01204.1, ACO09909.1, AAP20196.1, ACO14497.1, ABI26262.1, NP_001118140.1, ABX90099.1, AAT35603.1, ACQ58047.1, ACN12499.1, AAQ91574.1, AAP40018.1, CAE53390.1	0	1.4	>1.4	0.009	0.091
26	Hemoglobin subunit alpha (*Salmo salar, Misgurnus anguillicaudatus*)	ACN12417.1, ACN12305.1, ACN12747.1, ACO08777.1, ACQ59075.1, ACO08865.1, BAC20295.1, ACO13595.1, ACO07584.1, AAB24975.1, ACO07564.1, 1708181A, ACO07614.1, ACO13254.1, ACN12759.1, BAC20294.1, ACQ58404.1, ACO08140.1, ACQ57918.1, AAK12633.1, ACO14036.1, ACO14182.1, ABJ98630.1, ACN12658.1, CAA65949.1, AAM93258.1, ACN12527.1, ACN12414.1, ACO08002.1, ACO07580.1, CAA65946.1, ACI68793.1, ACN12530.1	23.5	13.9	-1.7	0.002	0.035
27	Hemoglobin subunit beta (*Salmo salar, Oncorhynchus mykiss, O.masou formosanus, O. nerka*)	ACI68214.1, ACM08711.1, ACI68343.1, ACI69922.1, ACH70759.1, ACI68603.1, ACI66413.1, ACN12210.1, ACN12791.1, ACN12547.1, ACN12702.1, ACI66980.1, ACO07576.1, ACO07923.1, 1009195A, ABY21329.1, ACO08038.1, ACO08017.1	44.6	12.1	-3.7	0.007	0.084
28	Keratin 12 (*Oncorhynchus mykiss*)	CAD20811.1	5.3	11.3	2.2	0.001	0.020
29	Keratin type I (*Epinephelus coioides, Sparus aurata, Oncorhynchus mykiss*)	ACL98136.1, CAG13267.1, ACN62548.1, NP_001117826.1	0	2.1	>2.1	0.011	0.102
30	Major vault protein (*Salmo salar*)	ACN10921.1	1.2	5.7	4.7	0.001	0.021
31	Myeloperoxidase precursor (*Salmo salar*)	ACN60208.1	15.8	9.8	-1.6	0.015	0.110
32	Myosin-9 (*Salmo salar*)	ACN60211.1, CAF91216.1, CAG06107.1, XP_001920024.1	0	0.6	>0.6	0.019	0.110
33	PREDICTED: similar to nonmuscle myosin heavy chain (*Danio rerio*)	XP_001920004.1, CAG10783.1, XP_683046.3, CAE30366.1, CAF92169.1	0	0.7	>0.7	0.018	0.110

34	Proteasome subunit beta type 1-A (*Salmo salar*, *Oncorhynchus mykiss*, *Carassius auratus*, *Danio rerio*, *Osmerus mordax*,*Gillichthys mirabilis*, *Anoplopoma fimbria*, *Esox lucius*) 20S proteasome beta subunit (*Pagrus major*, *Cirrhinus molitorella*) , proteasome beta-subunit C5 (*Danio rerio*)	ACO07867.1, AAZ73764.1, ACO09437.1, ACI68289.1, AAG13340.1, AF266220_1, ACO08500.1, ACO08383.1, ACQ58517.1, CAG11005.1, AAT68124.1, XP_001921270.1, ACQ58613.1, ACO13854.1, ACI67092.1, ACO07486.1, AAP20145.1, ACO07501.1	1.3	3.5	2.7	0.034	0.168
35	Ribosomal protein L4 (*Danio rerio*, *Oncorhynchus mykiss*, *Salmo salar*), 60S ribosomal protein L4-A (*Salmo salar*, *Osmerus mordax*)	CAK04710.1, CAC43331.1, ACM09838.1, CAC44155.1, ACH70798.1, ACM08761.1, ACO09148.1, CAN88105.1	0.7	2.7	3.8	0.037	0.172
36	Ribosomal protein S7 (*Solea senegalensis*, *Epinephelus coioides*, *Danio rerio*, *Takifugu rubripes*), 40S ribosomal protein S7 (*Oncorhynchus mykiss*, *Danio rerio*, *Salmo salar*, *Fugu rubripes*, *Perca flavescens*, *Oncorhynchus mykiss*, Ictalurus punctatus)	BAF45895.1, ACH73065.1, CAG01472.1, NP_957046.1, CAA64412.1, ACO08212.1, ACI66988.1, ACI66768.1, ABU54857.1, ACN12304.1, ACI66314.1, NP_001117902.1, ACI67293.1	0.5	2.1	4.0	0.034	0.168
37	S100-A16 (*Salmo salar*)	NP_001134817.1	0.4	3.5	9.7	0.001	0.019
38	Serum albumin 1and 2 precursor (*Salmo salar*)	spQ03156, ALBU2_SALSA, spP21848, ALBU1_SALSA	140.6	109.4	-1.3	0.005	0.074
39	SH3 domain-binding glutamic acid-rich-like protein 3 (*Salmo salar*)	ACI66430.1	0	3.1	>3.1	0.001	0.024
40	Tubulin beta-2C chain (*Salmo salar*)	NP_001134313.1, NP_001133265.1, ABQ59661.1	1.9	0.4	-5.1	0.029	0.150
41	Tumor-associated calcium signal transducer 2 precursor (*Salmo salar*)	ACI69332.1, NP_001134932.1, ACI67643.1, ACI68675.1	0	1.3	>1.3	0.004	0.057
42	Unnamed protein product (*Danio rerio*)	CAR80295.1	30.0	19.2	-1.6	0.020	0.110

3.3. **Proteomic Profiling of Yellow Catfish (*Pelteobagrus fulvidraco*) Skin Mucus in Response to *Edwardsiella ictalurid* Infection**

All studies involving the characterizations of skin mucus in different species (Atlantic cod (*Gadus morhoa*) (Easy & Ross, 2009; Rajan et al., 2011, 2013; Y. Xiong et al., 2020b), Atlantic salmon (*Salmo salar*)(Easy & Ross, 2009), European sea bass (*Dicentrarchus labrax*)(Cordero et al., 2015a), large yellow croaker (*Pseudosciaena crocea*)(Ao et al., 2015) and gilthead seabream (*Sparus aurata*) (Cordero et al., 2016a; Pérez-Sánchez et al., 2017; Sanahuja & Ibarz, 2015b), have shown that fish mucus is composed mainly of glycoproteins and water (Y. Xiong et al., 2020c).

Fish mucus mainly comprises the glycoprotein mucins, which possess a high molecular mass (~106 kDa) (Jurado et al., 2015a). Fish mucus also contains lipids, ions and multiple enzymes, some of which are typically immune-relevant factors with well-established biological functions. These enzymes include lectins, lysozymes, calmodulin, immunoglobulins, complement molecules, serotransferrin, C-reactive proteins, proteolytic enzymes, and antimicrobial peptides (Ángeles Esteban, 2012; Brinchmann, 2016; Ellis, 2001; Fast et al., 2002; Vasta et al., 2011; Y. Xiong et al., 2020c). In addition, fish mucus contains other molecules such as heat shock proteins and superoxide dismutase found in some fish species, although their roles in mucus remain investigated (Brinchmann, 2016).

It is essential to mention that the fish mucus composition varies significantly among different fish species when exposed to diverse stressors (Sanahuja & Ibarz, 2015b). Several protein components from the mucus of yellow catfish were separated by gel electrophoresis, and Cyclophilin A (CYPA) was identified as a typical chemokine with vigorous chemotactic activity (Dawar et al., 2016).

The Yellow catfish (*Pelteobagrus fulvidraco*) is an important aquaculture species that are sensitive to bacterial infection caused by the gram-negative bacteria *Edwardsiella ictalurid* (Dong et al., 2015; Zhou et al., 2017). In order to delineate the difference in protein compositions of yellow catfish skin mucus before and after *E. ictaluri* infection. A comparison study was performed between the proteomic profiles of the skin mucus of *E. ictaluri*-infected yellow catfish and healthy fish (Y. Xiong et al., 2020c).

Identification of the peptides was achieved by reverse-phase nanoflow HPLC-ESI-MS (Y. Xiong et al., 2020c). Furthermore, LC-MS/MS analysis was measured with a triple TOF-MS/MS instrument and, using the MaxQuant software, retrieved a total of 385711 spectra corresponding

to 54443 queries in terms of yellow catfish genome data, which resulted in 5874 peptide hits. Removal of redundant peptides obtained 4727 unique peptides that actually represent 918 non-redundant proteins (Figure 37A). Furthermore, similar numbers of proteins (*ca*. 770) were retrieved from six skin samples and importantly, a total of 613 proteins were obtained from three replicates of control samples (C1, C2 and C3, each with three fish), and 631 were common in three *E. ictaluri*-infected samples (P1, P2 and P3, each with three fish), highlighting sufficient coverage of proteomic map (Figure 37 B) (Y. Xiong et al., 2020c).

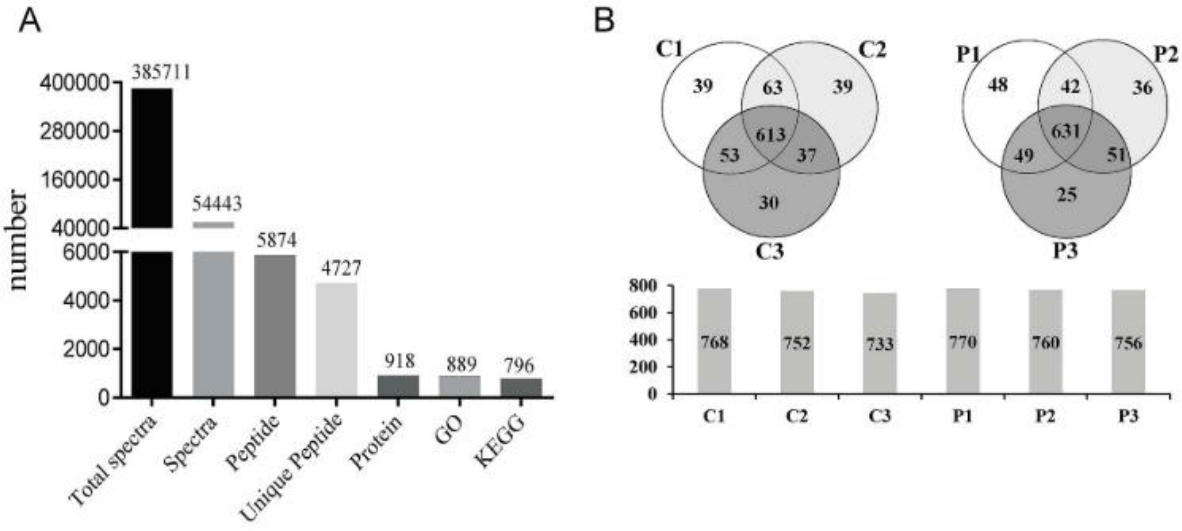

Figure 37. Summary information of the skin mucus proteome analysis. (A) Statistics of proteomic sequencing and annotation. Total spectra: the number of the mass spectra; Spectra: the number of mass spectra after quality control; Unique peptide: specific peptide in a group of proteins. (B) VENN diagram illustrating the number of standard and unique proteins per group. C1, C2 and C3 indicate three control groups, and E. ictaluri-infected groups are indicated by P1, P2, P3. Total number of proteins of each group is shown(Y. Xiong et al., 2020c).

Comparison of protein abundance between *E. ictaluri*-infected samples and mock-infected samples identified a total of 133 differentially expressed proteins (DEPs), including 76 up-regulated proteins (Table 21). and 57 down-regulated proteins (Table 22). These DEPs are classified into four groups based on their predicted biological functions: 1) structure-related proteins, such as many subunits or isoforms of actin, keratins, tubulin and tropomyosin; 2) metabolic proteins, mainly involving three subsets: DNA/RNA metabolism, protein metabolism and Carbohydrate metabolism; 3) signal transduction-related proteins, like protein LZIC, cytokine

receptor-like proteins; 4) immune-related proteins, including aerolysin-like protein isoform (L. L. Chen et al., 2018), apolipoprotein A-I-1-like (Johnston et al., 2008; Pridgeon & Klesius, 2013), and complement components C3 (Brinchmann, 2016; Y. Xiong et al., 2020c).

Consistently, it was noted that significant proliferation of mucus-secreting goblet cells and CYPA-expressing cells are formed outside the yellow catfish skin after *E. ictaluri* infection, which indicates an enhanced immune response to *E. ictaluri* infection. Mostly, the expressed proteins appeared to have multiple functions. For example, hemoglobin subunit beta (which belongs to the immune-related proteins in Table 22) participates in oxygen transport and exerts antimicrobial properties in skin mucus (Seo et al., 2014; Ullal et al., 2008).

Table 21. Detailed up-regulated proteins in response to E. ictaluri infection (Y. Xiong et al., 2020c).

Protein name[a]	Gene name	GI number[a]	FC[b]	*P* value[b]	T/(U)[c]	Score[d]
Structural protein						
F-actin-capping protein subunit alpha-2-like	capza1a	XP_027002575.1	1.33	0.017	10/(10)	286.57
actin-related protein 2/3 complex subunit 1A-A-like isoform X2	zgc:86896	XP_027034631.1	2.16	0.005	4/(4)	18.56
keratin, type II cytoskeletal 8-like	krt8	XP_027000312.1	1.37	0.000	20/(16)	323.31
keratin, type I cytoskeletal 50 kDa-like	krt50	XP_027011376.1	1.28	0.013	21/(11)	323.31
keratin, type I cytoskeletal 18	krt18	XP_027001042.1	2.07	0.047	10/(10)	236.78
keratin, type I cytoskeletal 13-like	LOC108257051	XP_027011380.1	1.90	0.008	17/(14)	189.38
keratin, type I cytoskeletal 18-like	LOC108266441	XP_027013129.1	2.80	0.005	5/(5)	33.12
tubulin beta-4B chain-like isoform X2	zgc:55461	XP_027021318.1	1.84	0.004	14/(1)	7.28
tubulin-folding cofactor B	tbcb	XP_026994762.1	2.31	0.044	2(2)	6.91
acidic leucine-rich nuclear phosphoprotein 32 family member B-like isoform	anp32b	XP_026988631.1	3.26	0.010	2(1)	11.96
tropomyosin alpha-4 chain-like isoform X10	tpm3	XP_026999752.1	1.55	0.005	8/(1)	179.58
tropomyosin alpha-4 chain-like isoform X2	tpm1	XP_026998469.1	1.41	0.000	9/(6)	172.91
protein LZIC	lzic	XP_027026104.1	3.17	0.019	2/(2)	35.78
parvalbumin alpha	pvalb3	XP_026993337.1	8.72	0.001	3/(2)	10.28
Metabolism						
Protein metabolism						
40S ribosomal protein S12	rps12	XP_027027195.1	1.60	0.036	4/(4)	34.80
60S ribosomal protein L30	rpl30	XP_027031661.1	4.68	0.031	4/(4)	15.50
40S ribosomal protein S10	rps10	XP_027003144.1	2.06	0.006	2/(2)	7.05
40S ribosomal protein S23	rps23	XP_027023449.1	2.23	0.047	1/(1)	5.06
heterogeneous nuclear ribonucleoprotein A0	hnrnpa0	XP_026991341.1	2.02	0.027	6/(6)	22.44
histone H3-like	h3	XP_027007152.1	1.42	0.041	7/(7)	105.00
proteasome subunit alpha type-5	psma5	XP_027011660.1	1.24	0.050	9/(9)	323.31
proteasome subunit alpha type-2	psma2	XP_027031459.1	1.40	0.042	10/(1)	176.28
proteasome subunit alpha type-4	psma4	XP_027029172.1	1.40	0.041	5/(5)	171.99
26S proteasome regulatory subunit 10B	psmc6	XP_026998168.1	1.59	0.014	7/(7)	73.83
proteasome subunit beta type-8	psmb8	XP_027012277.1	1.87	0.016	4/(4)	38.81
26S proteasome non-ATPase regulatory subunit 14	psmd14	XP_027027280.1	1.45	0.027	4/(4)	28.96
proteasome subunit alpha type-6 isoform X1	psma6a	XP_026990497.1	1.61	0.015	4/(2)	24.37
26S proteasome non-ATPase regulatory subunit 8	psmd8	XP_027030611.1	3.27	0.019	4/(4)	19.64
26S proteasome non-ATPase regulatory subunit 13-like	psmd13	XP_027016670.1	2.05	0.011	6/(6)	17.01
glycogen phosphorylase, brain form	pygb	XP_026998832	6.42	0.040	4/(4)	11.05
elongation factor 2	eef2	XP_027025384.1	1.25	0.018	22/(14)	323.31
elongation factor 1-delta-like isoform X7	eef1db	XP_027021881.1	1.98	0.035	2/(1)	3.98
triosephosphate isomerase	tpi1b	XP_027003965.1	1.22	0.028	11/(11)	219.42

kininogen-1 isoform X2	kng1	XP_027014484.1	1.39	0.040	6/(6)	124.18
peroxiredoxin-1	prdx1	XP_027012595.1	2.16	0.011	5/(4)	121.78
N(G),N(G)-dimethylarginine dimethylaminohydrolase 1 isoform X1	ddah1	XP_027027030.1	1.34	0.036	8/(8)	116.41
regulating synaptic membrane exocytosis protein 4	rims4	XP_027002953.1	4.57	0.006	1/(1)	4.38
protein-glutamine gamma-glutamyltransferase K-like	tgm1	XP_027016067.1	2.46	0.014	3/(3)	3.08
brain-specific angiogenesis inhibitor 1-associated protein 2-like protein 1	baiap2l1b	XP_026994852.1	1.48	0.041	1/(1)	2.38
PDZ and LIM domain protein 1-like	pdlim1	XP_026992147.1	2.16	0.003	6/(6)	20.78
hyaluronan-binding protein 2-like	habp2	XP_027021414.1	4.77	0.009	4/(4)	8.64
Carbohydrate metabolism						
carbonic anhydrase-like	cahz	XP_026998648.1	1.59	0.001	11/(11)	323.31
l-lactate dehydrogenase B chain	ldhb	XP_027016173.1	2.33	0.009	7/(6)	149.46
adenosine kinase-like	adka	XP_027030695.1	3.28	0.010	5/(5)	14.65
l-lactate dehydrogenase A chain-like	ldha	XP_027028964.1	5.01	0.006	6/(5)	6.74
lambda-crystallin homolog isoform X2	cryl1	XP_027020142.1	1.41	0.036	3/(3)	6.15
mth938 domain-containing protein isoform X2	aamdc	XP_027002394.1	2.20	0.028	1/(1)	2.56
DNA and RNA metabolism						
asparagine--tRNA ligase, cytoplasmic	nars1	XP_026988852.1	1.26	0.042	10/(10)	314.56
cold-inducible RNA-binding protein B-like isoform X5	cirbpa	XP_027006457.1	1.36	0.004	4/(4)	236.41
Signal transduction						
14-3-3 protein zeta/delta-like	ywhaz	XP_027013202.1	1.25	0.002	15/(13)	323.31
protein S100-A1-like	s100a10b	XP_026999586.1	1.51	0.044	2/(2)	20.50
cytokine receptor-like factor 3	crlf3	XP_027027728.1	1.90	0.001	1/(1)	2.22
Immune-related proteins						
serotransferrin-2-like isoform X2	tfa	XP_026993067.1	1.71	0.001	24/(24)	323.31
aerolysin-like protein isoform X2	aep1	XP_026993987.1	1.45	0.002	17/(17)	323.31
cyclophilin A	cypa	XP_026995231.1	1.23	0.002	5/(5)	323.31
hemopexin-like	hpx	XP_026998048.1	1.40	0.002	17/(17)	323.31
apolipoprotein A-I-1-like	apoa1b	XP_027017964.1	1.83	0.000	16/(16)	323.31
polyubiquitin-like	isg15	XP_026995943.1	2.65	0.028	2/(2)	7.46
hemoglobin subunit beta-like	ba1	XP_027024025.1	1.59	0.031	8/(1)	323.31
hemoglobin subunit alpha-like	hbaa1	XP_027024026.1	2.06	0.000	8/(3)	323.31
cystatin-B-like	cst14a	XP_027030842.1	2.25	0.000	6/(2)	319.07
complement C3-like	c3	XP_026992187.1	2.22	0.005	30/(13)	273.23
immunoglobulin M heavy chain	ighv	AER10487.1	3.67	0.003	11/(11)	179.84
intelectin-like	itln3	XP_027018872.1	3.62	0.001	5/(5)	125.26
alpha-2-macroglobulin-like	a2ml	XP_027031049.1	5.80	0.003	10/(8)	64.02
interferon-induced 35 kDa protein	ifi35	XP_027035171.1	2.13	0.014	5/(5)	32.66
histidine-rich glycoprotein-like	ahsg1	XP_027025429.1	1.45	0.006	4/(4)	32.28
protein phosphatase 1 regulatory subunit 7	ppp1r7	XP_026993046.1	3.19	0.033	4/(4)	31.22
BCL2/adenovirus E1B 19 kDa protein-interacting protein 2-like isoform X3	bnip2	XP_027029075.1	2.50	0.003	2/(2)	30.16
plasma protease C1 inhibitor-like isoform X1	serping1	XP_027002018.1	5.32	0.034	7/(7)	21.38
serum amyloid P-component-like	LOC108276003	XP_027034716.1	4.02	0.009	3/(3)	13.33
haptoglobin	hp	XP_027008872.1	2.46	0.014	1/(1)	9.99
glutathione peroxidase 1-like isoform X2	gpx1a	XP_027011612.1	2.22	0.000	1/(1)	4.41
thioredoxin reductase 3	txnrd3	XP_027002866.1	12.16	0.021	3/(3)	25.35
Others						
uncharacterized protein LOC113651703	–	XP_027016353.1	2.88	0.000	4/(4)	142.53
uncharacterized protein LOC113656729	–	XP_027023908.1	3.09	0.018	2/(2)	20.85

[a] Protein name and GI database ID of the record with the highest score retrieved by BLAST.
[b] Up-regulated expressed proteins were picked using a foldchange (FC) > 1.2 measurement (P-Value < 0.05) between the E. ictaluri infected group and control group.
[c]Total matched peptides (T) against total unique peptides (U).
[d]Maximum score obtained in BLAST analysis by total peptides matching this protein.

Table 22. Detailed down-regulated proteins in response to E. ictaluri infection (Y. Xiong et al., 2020c) .

Protein name[a]	Gene name	GI number[a]	FC[b]	*P* value[b]	T/(U)[c]	Score[d]
Structural proteins						
actin, alpha cardiac muscle 1	actc1c	XP_026991826.1	0.76	0.010	11/(2)	94.79
protein POF1B isoform X2	pof1b	XP_027033124.1	0.33	0.011	2/(2)	3.02
LOW QUALITY PROTEIN: annexin A1	anxa1a	XP_026997148.1	0.82	0.005	3/(3)	53.77
sorting nexin-1-like	snx1a	XP_027029151.1	0.15	0.031	6/(6)	9.28
band 4.1-like protein 3 isoform X9	epb41l3a	XP_027006376.1	0.26	0.001	1/(1)	2.23
Metabolism						
Protein metabolism						
60S ribosomal protein L27a isoform X2	rpl27a	XP_027016714.1	0.42	0.036	1/(1)	3.09
26S proteasome non-ATPase regulatory 6	psmd6	XP_027032118.1	0.31	0.015	3/(3)	15.11
ubiquitin-conjugating enzyme E2 variant 1-like isoform X2	ube2v1	XP_027032390.1	0.36	0.039	2/(1)	2.29
elongation factor 1-alpha	ef1a	XP_027031345.1	0.81	0.025	19/(19)	323.31
arfaptin-1 isoform X2	arfip1	XP_026989827.1	0.28	0.001	4/(4)	12.48
coatomer subunit gamma-2	copg2	XP_027016156.1	0.39	0.044	4/(4)	9.93
betaine--homocysteine S-methyltransferase 1-like	bhmt	XP_027008516.1	0.78	0.019	18/(18)	323.31
bifunctional epoxide hydrolase 2-like	ephx2	XP_027028213.1	0.82	0.042	25/(25)	323.30
***trans*-3-hydroxy-l-proline dehydratase**	l3hypdh	XP_027004736.1	0.36	0.022	1/(1)	2.49
protein ADP-ribosylarginine hydrolase-like	adprh	XP_027014854.1	0.59	0.005	6/(6)	29.91
ELMO domain-containing protein 2	elmod2	XP_027001865.1	1.48	0.041	1/(1)	2.38
acidic leucine-rich nuclear phosphoprotein 32 family member E	anp32e	XP_027031820.1	0.58	0.050	3/(3)	61.07
Carbohydrate metabolism						
D-dopachrome decarboxylase-A-like	ddt	XP_027034651.1	0.34	0.041	3/(3)	8.53
alpha-endosulfine-like	ensab	XP_027005667.1	0.27	0.019	2/(1)	7.88
creatine kinase B-type	ckba	XP_026997838.1	0.82	0.016	9/(5)	323.31
glutamine--fructose-6-phosphate aminotransferase [isomerizing] 1	gfpt1	XP_027007135.1	0.47	0.032	11/(11)	140.06
glutamine--fructose-6-phosphate aminotransferase [isomerizing] 2-like	gfpt2	XP_027009250.1	0.40	0.009	9/(9)	68.48
6-phosphogluconate dehydrogenase, decarboxylating	pgd	XP_027026350.1	0.57	0.028	10/(10)	122.73
6-phosphogluconolactonase-like	pgls	XP_027023671.1	0.34	0.003	5/(5)	28.30
DNA and RNA metabolism						
arginine--tRNA ligase, cytoplasmic	rars	XP_027019591.1	0.62	0.027	3/(3)	9.15
histidine--tRNA ligase, cytoplasmic	hars	XP_027020984.1	0.34	0.044	5/(5)	5.88
zinc-binding protein A33-like isoform X1	a33	XP_026992436.1	0.25	0.040	3/(3)	5.96
eukaryotic translation initiation factor 2 subunit 2	eif2s2	XP_027023248.1	0.43	0.031	1/(1)	3.61
eukaryotic translation initiation factor 6	eif6	XP_027002954.1	0.19	0.000	1/(1)	3.00
deoxynucleoside triphosphate triphosphohydrolase SAMHD1-like	samhd1	XP_026996669.1	0.58	0.005	12/(7)	219.95
probable ATP-dependent RNA helicase DHX4	dhx40	XP_027027213.1	0.50	0.003	1/(1)	2.71
ADP-ribosylation factor 1-like	arf1	XP_026992509.1	0.15	0.001	3/(2)	32.22
bolA-like protein 2	zgc:112271	XP_027025314.1	0.27	0.015	2/(2)	3.43
Signal transduction						
rab GDP dissociation inhibitor beta	gdi2	XP_027007352.1	0.78	0.046	21/(21)	323.31
ictacalcin-like	icn	XP_027009134.1	0.72	0.023	4/(4)	323.31
protein S100-A11-like	s100a11	XP_027010782.1	0.48	0.012	3/(3)	107.20
neuroblast differentiation-associated protein AHNAK-like	LOC108270732	XP_027032430.1	0.27	0.010	2/(2)	21.49
LOW QUALITY PROTEIN: neuroblast differentiation-associated protein AHNAK	ahnak	XP_026991257.1	0.62	0.005	9/(9)	323.31
Immune-related proteins						
calpastatin	cast	XP_027008421.1	0.72	0.002	24/(24)	323.31
heat shock protein HSP 90-alpha	hsp90a.2	XP_027021967.1	0.64	0.033	21/(8)	323.31
ATP-citrate synthase isoform X2	aclya	XP_027016865.1	0.81	0.017	7/(2)	20.74
dual specificity mitogen-activated protein kinase kinase 6 isoform X4	map2k6	XP_027016243.1	0.60	0.011	4/(4)	6.08
mitogen-activated protein kinase 1-like isoform X2	mapk1	XP_027016872.1	0.13	0.028	2/(2)	7.24
thimet oligopeptidase isoform X2	thop1	XP_027025795.1	0.34	0.017	4/(4)	14.73
thioredoxin-like protein 1	txnl1	XP_026988865.1	0.36	0.027	4/(4)	26.59
thioredoxin	zgc:56493	XP_027001599.1	0.63	0.040	1/(1)	40.79

thioredoxin-like	txn	XP_027034119.1	0.78	0.033	4/(4)	161.35
probable E3 ubiquitin-protein ligase HERC4 isoform X2	herc4	XP_027005893.1	0.62	0.000	1/(1)	2.78
spectrin alpha chain, non-erythrocytic 1 isoform X6	sptan1	XP_026995816.1	0.81	0.034	23/(23)	124.03
calpain-2 catalytic subunit-like	capn2b	XP_027024371.1	0.70	0.019	21/(19)	323.31
calpain-3-like isoform X2	casp3b	XP_027028040.1	0.70	0.016	24/(24)	323.31
calpain-1 catalytic subunit-like	zgc:55262	XP_027034021.1	0.66	0.008	22/(22)	323.31
caspase-3-like	casp3b	XP_026991353.1	0.26	0.022	4/(4)	39.07
prothymosin alpha	ptma	XP_027003134.1	0.74	0.012	1/(1)	27.98
Others						
uncharacterized protein LOC113638704	–	XP_026995926.1	0.34	0.000	13./(9)	323.31
uncharacterized protein LOC113647380 isoform X2	–	XP_027009887.1	0.79	0.010	11/(11)	285.96
uncharacterized protein LOC113650581	–	XP_027014804.1	0.68	0.020	15/(5)	249.56

[a] Protein name, and GI database ID of the record with the highest score retrieved by BLAST.
[B] Down-regulated expressed proteins were picked using a foldchange (FC) < 0.83 measurement (*P*-Value < 0.05) between the *E. ictaluri* infected group and control group.
[C] Total matched peptides (T) against total unique peptides (U).
[d] Maximum score obtained in BLAST analysis by total peptides matching this protein.

In addition, 5 novel yellow catfish proteins were identified as DEPs, including 2 up-regulated proteins (XP_027016353.1, XP_027023908.1) and 3 down-regulated proteins (XP_026995926.1,XP_027009887.1, XP_027014804.1).

In conclusion, it is evident that the proteomic data provides excellent systematic protein information permitting the comprehension of the biological function of the yellow catfish skin mucus in response to bacterial infection (Y. Xiong et al., 2020c).

3.4. Plasma Proteomic Analysis of Zebrafish Following Spring Viremia of Carp Virus Infection

A proteomics study on adult zebrafish challenged with the spring viremia carp virus (SVCV) was performed by straightforward LC-MS/MS analysis. This study permitted the identification of novel biomarkers and the establishment of the plasma protein profile in SVCV-infected zebrafish. A total of 3062 proteins were identified. It was found that 137, 63, and 31 proteins were present respectively in blood samples harvested at 1, 2 and 5 days post-SVCV infection (Table 23). These altered host proteins were classified based on their biological function: 23 proteins under the response to stimulus term were identified. Interestingly, at the top of the up-regulated proteins during SVCV infection were the proteins of the vitellogenin family (VTG) and the grass carp reovirus-induced gene (Gig) proteins (Table 23) (Medina-Gali et al., 2019).

Table 23. List of the top 20 most abundant proteins detected in the plasma of zebrafish control. The average value and standard deviation of % emPAI values are indicated concerning the total protein of the sample (n=5). UNIPROT(Medina-Gali et al., 2019).

UNIPROT	Gene	Description	*emPAI*, %
Q803Z5	*hbaa1*	Hbaa1 protein OS = *Danio rerio* GN = hbaa1 PE = 2 SV = 1	20,951 ± 8944
B3DG37	*ba1*	Ba1 protein OS = *Danio rerio* GN = ba1 PE = 1 SV = 1	20,698 ± 18,108
Q1JQ69	*hbaa1*	Hbaa1 protein OS = *Danio rerio* GN = hbaa1 PE = 1 SV = 1	18,152 ± 9388
Q6ZM17	*si:ch211-5k11.8*	Novel protein similar to zebrafish hemoglobin alpha-adult 1 (Hbaa1) OS = *Danio rerio* GN = si:ch211-5k11.8 PE = 1 SV = 1	12,932 ± 7539
Q1RM32	*ba1*	Ba1 globin OS = *Danio rerio* GN = ba1 PE = 2 SV = 1	7781 ± 9731
Q7SZV9	*hbaa1*	Novel alpha-globin OS = *Danio rerio* GN = hbaa1 PE = 3 SV = 1	7347 ± 8852
Q90485	*ba2*	Hemoglobin subunit beta-2 OS = *Danio rerio* GN = ba2 PE = 1 SV = 3	6179 ± 8280
Q6XG62	*icn*	Protein S100 OS = *Danio rerio* GN = icn PE = 1 SV = 1	0,344 ± 0128
A0A0R4IKF0	*apoa1b*	Uncharacterized protein OS = *Danio rerio* GN = apoa1b PE = 1 SV = 1	0,245 ± 0205
A3FKT8	*icn2*	Protein S100 OS = *Danio rerio* GN = icn2 PE = 1 SV = 1	0,213 ± 0160
Q6DGK4	*zgc:92880*	Zgc:92880 OS = *Danio rerio* GN = zgc:92880 PE = 2 SV = 1	0,127 ± 0047
Q5BJC7	*si:ch211-5k11.6*	Si:xx-by187g17.5 OS = *Danio rerio* GN = si:ch211-5k11.6 PE = 2 SV = 1	0,125 ± 0001
B3DFP9	*apoa2*	Uncharacterized protein OS = *Danio rerio* GN = apoa2 PE = 1 SV = 1	0,123 ± 0093
Q7ZVF9	*actbb*	Actin, cytoplasmic 2 OS = *Danio rerio* GN = actbb PE = 2 SV = 2	0,121 ± 0032
Q7ZVI7	*actba*	Actin, cytoplasmic 1 OS = *Danio rerio* GN = actba PE = 2 SV = 2	0,120 ± 0032
Q7SXL4	*nme2b.2*	Nucleoside diphosphate kinase OS = *Danio rerio* GN = nme2b.2 PE = 1 SV = 1	0,116 ± 0062
Q9DDU5	*gstp1*	Glutathione S-transferase pi OS = *Danio rerio* GN = gstp1 PE = 1 SV = 1	0,114 ± 0055
B2GS08	*actb1*	Bactin1 protein OS = *Danio rerio* GN = actb1 PE = 2 SV = 1	0,110 ± 0009
Q6ZM13	*si:ch211-5k11.6*	Novel alpha globin OS = *Danio rerio* GN = si:ch211-5k11.6 PE = 1 SV = 1	0,094 ± 0039
X1WGM1	*si:dkey-108k21.12*	Histone H4 (Fragment) OS = *Danio rerio* GN = si:dkey-108k21.12 PE = 1 SV = 1	0,092 ± 0011

Real-time RT-PCR evaluation of samples from internal organs verified that SVCV infection-induced VTG and gig2 gene expression was already present at day one post-infection. Western blot analysis revealed the presence of VTG protein only in the blood of SVCV-infected fish. It is important to point out that this was the first proteomic study that revealed the involvement of Vtg proteins in adult fish response to viral challenge. It also highlighted the role of Gig proteins as essential factors in antiviral response in fish. This work provides valuable, relevant insight into virus-host interaction and the identification of molecular markers of fish response to the virus (Johnson & Brown, 2011; Medina-Gali et al., 2019).

3.5. **Proteomic Analysis of Skeletal Deformity in Diploid and Triploid Rainbow Trout (*Oncorhynchus mykiss*) Larvae**

Two-dimensional gel electrophoresis (2-DGE) followed by MALDI-TOF MS, MALDI-TOF/TOF-MS/MS analyses and database searching were used to compare protein expression

profiles of normal phenotype and deformed phenotype in diploid and heat-shocked rainbow trout **(*Oncorhynchus mykiss*)** larvae (Babaheydari et al., 2016).

After manual examination of the results obtained by automated spot detection and matching, over 500 protein spots with molecular masses between approximately 5–100 kDa and pI values between about 4–8 were identified. Based on the results from the statistical analoid deformed lyses, five protein spots were found to differ significantly in abundance between diploid normal larvae (DNL) and diploid deformed larvae (DDL) (Table 24) (Babaheydari et al., 2016).

Table 24. Protein spots with significantly altered abundance between diploid normal larvae (DNL) and diploid deformed larvae (DDL) of rainbow trout(Babaheydari et al., 2016).

Spot number	Accession number[a]	Protein identification (species)	Functional category	Fold change[b]	MS/MS score	SC[c]	Experimental pI/MW (kDa)	Theoretical pI/MW (kDa)	PM[d]	Anova (P-value)
Proteins increased in abundance in DDL										
1	gi | 156972295	Creatine kinase isoform a, partial (*Hippoglossus hippoglossus*)	Metabolism	+ 3.2	175	10%	5.4/10.5	6.86/27.492	2	1.484e-009
Proteins decreased in abundance in DDL										
2	gi | 238814310	Apolipoprotein A-II precursor (*Oncorhynchus mykiss*)	Metabolism	− 1.7	349	32%	5.2/9.2	6.30/15.641	3	4.289e-006
3	gi | 115509	Calmodulin (*Electrophorus electricus*)	Calcium binding	− 1.7	240	22%	3.8/10.8	4.09/16.799	2	9.914e-007
4	gi | 185132822	Apolipoprotein A-I-2 precursor (*Oncorhynchus mykiss*)	Metabolism	− 1.7	306	14%	4.4/23	5.10/29.661	4	3.388e-004

[a] NCBInr ID accession number.
[b] Change in abundance in DDL relative to DNL.
[C] Percentage of sequence coverage.
[d] Number of peptides matched.

The main goal of this proteomic screening approach was to obtain a better understanding of the changes that occurred in the protein expression patterns associated with skeletal deformities in both diploid and triploid rainbow trout larvae (Babaheydari et al., 2016). It was found that triploidy was induced through the application of heat shock of 28 ºC post-fertilization in an aquarium. After five days of hatching, the identities of the normal (non-deformed) proteins and

deformed specimens were established after two-dimensional electrophoresis and mass spectrometry of deyolked larvae (Babaheydari et al., 2016).

Among the identified protein spots from diploids, it was found that creatine kinase levels increased in larvae with skeletal deformities. Whereas the levels of apolipoprotein A-I-2, apolipoprotein A-II and calmodulin were found to be decreased in deformed fish. Also, the five protein spots that were identified following heat-shock fish were as follows: apolipoprotein A-I-2, apolipoprotein A-II, parvalbumin, myosin light chain 1-1 and nucleoside diphosphate kinase, their levels appeared to decrease in the deformed larvae. The presence of these last five protein spots indicates that the alteration of deformed fish can explain the molecular mechanisms that are involved in the development of skeletal malformations in diploid and triploid fish.

Furthermore, these results could potentially be used to reveal the possible adverse effects of suboptimal rearing conditions on rainbow trout larvae which could be considered to reduce skeletal deformities (Babaheydari et al., 2016).

3.6. **Changes in the Proteome of Sea Urchin *Paracentrotus lividus coelomocytes* in Response to LPS Injection into the Body Cavity**

The immune system of the echinoderms (sea urchins) is far from being well understood and is dedicated to perform a variety of functions. Specifically, the echinoderm immune system is composed of various cells in a heterogeneous population, both at the morphological and functional levels. Their profile can vary between species in terms of morphology, abundance, size, role and physiology. Four subpopulations of immune cells are known; these are the phagocytes, vibratile cells, colourless and red spherule cells (Hirano, 2016; L. C. Smith et al., 2006) which were described in *Strongylocentrotus purpuratus* (purple sea urchin) and in *Paracentrotus lividus* species (Arizza et al., 2007; Inguglia et al., 2020; Matranga et al., 2005; Pinsino & Matranga, 2015).

It is also known that the coelomocytes, cells that circulate in the coelomic fluid, also mediate immune responses through phagocytosis and encapsulation of non-self-particles in addition to the production of antimicrobial molecules. The non-self-molecules are usually pathogen-associated molecular patterns (PAMPs), and their receptors are termed pattern-recognition receptors (PRRs) (Chiaramonte et al., 2019; Chiaramonte & Russo, 2015). These PRRs receptors are localized in the immune cells and the body fluid as soluble factors (Buckley &

Rast, 2012; Gay & Gangloff, 2007; Satake & Sekiguchi, 2012). The most common PAMPs are bacterial cell wall components, such as lipopolysaccharide (LPS), peptidoglycans (PGN) and lipopeptides, flagellin, DNA double-stranded RNA (Mogensen, 2009).

Recently, it was suggested that the molecular analysis of immune functions of the sea urchin was quite complex and was regulated by a complement system that possessed multiple alternative pathways and diverse activators (L. C. Smith et al., 2006). Also, the immune system of the sea urchin was found to include multiple sets of lectins, proteins with different antimicrobial activities, Toll-like receptors and associated signalling protein (Chiaramonte & Russo, 2015). Flow cytometry-based studies in PAMP-challenged *P. lividus* coelomocytes indicated an increase in ROS production and the number of phagocytic cells (A. Romero et al., 2016).

In order to study the molecular mechanisms and the cellular processes of the sea urchin, which are activated in response to the immune stimulation, sea urchins *P. lividus* were treated with the bacterial lipopolysaccharide (LPS; *Escherichia coli;*) and coelomocytes were collected at different time-points (1, 3, 6 and 24 hours. Using label-free tandem mass spectrometry, the authors identified a number of proteins that were differently modulated, following LPS injection at 1, 3, 6 and 24 hours after treatment (Figure 38). This MS/MS analysis also allowed to measure the coelomocyte proteome's modulation and identify cellular pathways, such as endocytosis and phagocytosis.

The present study has also confirmed that the LPS treatment modulates various cellular processes such as cytoskeleton reorganization and stress and energetic homeostasis (Inguglia et al., 2020). Further analysis of these results allowed the identification of protein clusters by STRING analysis and protein pathways based on the KEGG database, which is affected by bacterial LPS treatment (Inguglia et al., 2020). Recently, a similar shotgun mass spectrometry analysis was recently used to describe a number of proteins with possible immune function in the purple sea urchin.

In conclusion, it was established that LPS could set off an immune response in the sea urchins *P. lividus*, inducing cytoskeleton reorganization, which affects the appearance of HSP clusters and histone proteins and promotes the activation of the endocytosis and phagocytosis pathways (Inguglia et al., 2020).

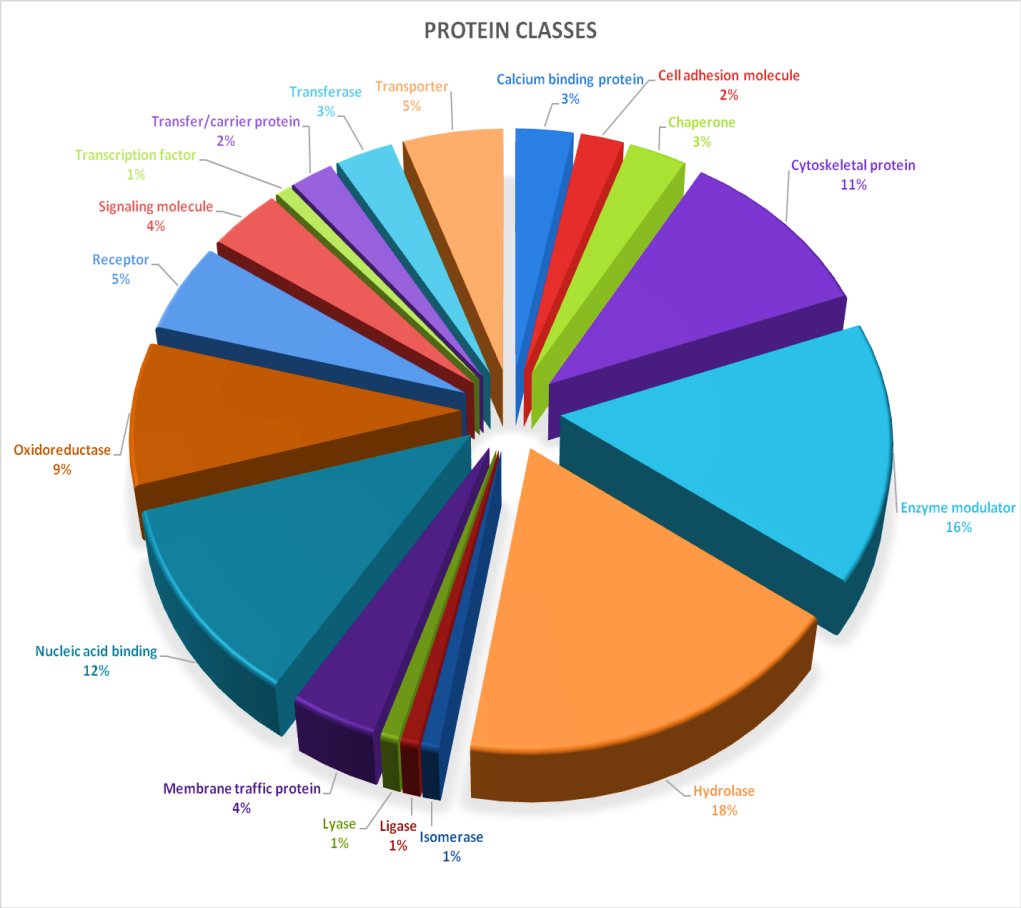

Figure 38. Protein classes identified by mass spectrometry. Proteins identified by Mass Spectrometry were examined using Panther (Protein Analysis Through Evolutionary Relationships, Version 13.1). A total of 137 protein was recognized and divided into eighteen classes: calcium-binding protein, cell adhesion molecule, chaperone, cytoskeletal protein, enzyme modulator, hydrolase, isomerase, ligase, lyase, membrane traffic protein, nucleic acid binding, oxidoreductase, receptor, a signalling molecule, transcription factor, transfer/carrier protein, transferase, transporter (Inguglia et al., 2020).

3.7. **Proteomic Analysis of Zebrafish (*Danio rerio*) Infected with Infectious Spleen and Kidney Necrosis Virus**

Iridovirus infections remain a severe problem in aquaculture industries worldwide. This infectious spleen and kidney necrosis virus (ISKNV) (genus *Megalocytivirus*, family *Iridoviridae*) has caused significant economic losses among freshwater fish in different Asian countries. The ISKNV virion comprises a single, linear dsDNA molecule of 111, 362 bp, encoding 125 potential open reading frames (ORFs). The ISKNV virion has recently been classified as the type species of the genus *Megalocytivirus* in the family Iridovidae (J. G. He et al., 2001; X. P. Xiong et al., 2011).

To investigate the molecular mechanism of iridoviral pathogenesis, the differential proteome from the spleen of ISKNV-infected zebrafish was investigated through a conventional top-down proteomics analysis which used 2-DEG followed by MALDI-TOF-MS analysis. The resulting peptides were analyzed by MALDI-TOF/TOF-MS/MS analysis and database searches (X. P. Xiong et al., 2011).

From the 39 spots, 35 were identified. Furthermore, it was found that from these 35 identified proteins, 15 were upregulated, whereas the remaining 20 proteins were downregulated by the ISKNV infection (Table 25). The results of identification together with the expression-level differences obtained with ImageMaster analysis are presented in Table 25 (X. P. Xiong et al., 2011).

Table 25. Differentially expressed protein spots in ISKNV-infected zebrafish identified by MALDI-TOF or MALDI-TOF/TOF(X. P. Xiong et al., 2011).

Spot no.[a]	Protein name[b]	Gene name	NCBI Accession No.	Theoretical Mr/pI[c]	Mascot Score	Sequence coverage (%)	Peptides matched	Ratio (I/C)[d]
1	Fatty acid binding protein 3	FABP3	gi|23308625	14,872.7/5.74	85	23	7	C
2	Fatty acid binding protein 6	FABP6	gi|50344806	14,397.3/6.59	82	24	3	0.39 ± 0.01
3	Beta-1-globin	BA1	gi|18858329	16,378.2/7.7	112	70	17	0.20 ± 0.02
4	Actin, cytoplasmic 1	ACTBA	gi|18858335	42,074/5.30	159	13	3	3.2 ± 0.16
5	Ferritin	ZGC:92066	gi|50539816	20,278.9/5.26	256	62	16	0.11 ± 0.04
6	Actin, cytoplasmic 1	ACTBA	gi|18858335	42,068/5.3	78	24	6	2.24 ± 0.3
7	Proteasome activator subunit 2	PSME2	gi|50540284	22,571.6/6.1	99	21	9	4.49 ± 0.6
8	Actin, cytoplasmic 1	ACTBA	gi|18858335	42,068/5.30	249	34	14	2.33 ± 0.32
9	Glyceraldehyde 3-phosphate dehydrogenase	GAPDH	gi|47085833	36,084.1/6.55	407	72	22	2.26 ± 0.07
10	Rho GDP dissociation inhibitor (GDI) alpha	ARHGDIA	gi|39645438	23,175/5.00	122	32	10	0.34 ± 0.12
12	GTP-binding nuclear protein Ran	RAN	gi|18859307	24,616/6.60	156	18	4	0.44 ± 0.06
13	GTP-binding nuclear protein Ran	RAN	gi|18859307	24,616/6.60	394	33	9	0.35 ± 0.02
14	Methylthioadenosine phosphorylase	MTAP	gi|41054629	30,827.4/5.99	94	23	6	0.32 ± 0.1
15	Glutathione S-transferase M	GSTM	gi|47086689	36,084.1/6.55	450	65	32	0.41 ± 0.01
16	Carbonic anhydrase	CAHZ	gi|18858379	28,659.5/7.12	344	54	8	0.42 ± 0.1
17	hypothetical protein LOC322453	ZGC:66382	gi|41054557	27,046/4.94	189	53	17	2.62 ± 0.25
18	Actin, cytoplasmic 1	ACTBA	gi|113271	42,068/5.30	138	29	10	2.52 ± 0.25
19	Bactin1 protein	BACT	gi|28279111	42,068/5.30	392	44	22	2.03 ± 0.12
20	Anxa1c protein	ANXA1C	gi|79153964	31,700/5.92	75	24	5	0.32 ± 0.2
21	JMJD7-PLA2G4B protein-like	ZGC:101699	gi|292613527	62,700/5.04	174	52	18	0.28 ± 0.09
22	Tubulin alpha 6	TUBA8L4	gi|37595424	50,687/4.93	101	41	14	2.78 ± 0.14
23	Phosphoglucomutase 1	PGM1	gi|41056111	61,090/5.74	208	30	18	0.21 ± 0.04
24	3-oxoacid CoA transferase 1b	OXCT1B	gi|116004513	58,094/6.74	117	32	13	0.5 ± 0.02
26	Uroporphyrinogen decarboxylase	UROD	gi|18859531	41,618.1/6.05	298	61	33	0.37 ± 0.07
27	4-Hydroxyphenylpyruvate dioxygenase	ZGC:56326	gi|41054723	44,004.6/6.21	320	47	24	0.20 ± 0.06
28	4-Hydroxyphenylpyruvate dioxygenase	ZGC:56326	gi|41054723	44,004.6/6.21	370	57	24	0.18 ± 0.02

30	Aldehyde dehydrogenase family 9 member A1-A	ALDH9A1A	gi|41393103	55,225.9/6.18	343	49	23	0.49 ± 0.01
31	Glyceraldehydes-3-phosphate dehydrogenase	GAPDH	gi|47085833	36,426/6.55	245	21	11	3.29 ± 0.6
32	Peroxiredoxin 2	PRDX2	gi|50539996	21,837.2/5.93	138	42	11	0.48 ± 0.02
33	HSC70 protein	HSC70	gi|1865782	71,131.3/5.18	222	18	13	0.47 ± 0.05
34	Proteasome activator subunit 1	PSME1	gi|18859279	28,194.7/6.85	159	39	13	2.6 ± 0.5
35	Ferritin	ZGC:173593	gi|68357884	20,268.9/5.65	166	37	13	0.42 ± 0.6
36	Tropomyosin 4	TPM4	gi|47085929	28,598/4.63	293	50	19	3.9 ± 0.9
37	Major capsid protein (ISKNV)	MCP	gi|19881411	49,580.7/5.86	152	26	12	I
38	Annexin A2a	ANXA2A	gi|38566042	38,114.8/7.56	92	18	8	2.26 ± 0.17

[a] Spot no. is the sample spot protein number.
[b] Accession no. is the MASCOT result of MALDI-TOF or MALDI-TOF/TOF searched from the NCBInr database.
[c] Predicted molecular mass and p*I* based on the ORF.
[d] Relative protein expression in infected/control samples. (I) Protein expression detected only in infected samples; (C) protein expression detected only in control samples.

The altered host proteins were classified into 13 categories based on their biological processes: cytoskeletal protein, stress response, lipoprotein metabolism, ubiquitin-proteasome pathway, carbohydrate metabolism, signal transduction, proteolysis, ion binding, transport, metabolic process, catabolic process, biosynthesis, and oxidation-reduction (X. P. Xiong et al., 2011).

Moreover, 14 corresponding genes of the differentially expressed proteins were validated by RT-PCR. Western blot analysis further demonstrated the changes in α-tubulin, β-actin, HSC70, and major capsid protein (MCP) during infection. β-Actin was selected for further study via co-immunoprecipitation analyses, which confirmed that the cellular β-actin interacts with the MCP protein of ISKNV in the infected zebrafish. These findings provide insight into the interactions between iridoviruses (especially ISKNV) and host and the mechanism and pathogenesis of ISKNV infections (X. P. Xiong et al., 2011).

3.8. **Proteome Profiling Reveals Immune Responses in Japanese Flounder (*Paralichthys olivaceus*) Infected with *Edwardsiella tarda***

The complete genome sequence of *E. tarda* EIB202 has been determined, and it was inferred that this bacterium harbours an array of antibiotic-resistance determinants. This means that this pathogen is well prepared to face the antibiotic cocktail that will be delivered in the aquaculture ecosystem. It has been established that the liver is an essential organ for bacterial pathogen attacks in fish (L. Wang et al., 2017).

Based on the recent genome and transcriptome published research of the Japanese flounder (Bioproject ID PRJNA73673) (Shao et al., 2017), the present study's main goal was to identify Japanese flounder liver proteins that are altered in response to bacterial infection. The differential proteomic response of the Japanese flounder liver to *Edwardsiella tarda* infection was examined using isobaric tags for relative and absolute quantitation (iTRAQ) labelling followed by liquid chromatography-tandem mass spectrometry (LC-MS/MS) (L. Wang et al., 2017).

A total of 3290 proteins were identified and classified into categories related to biological processes (51.4%), molecular function (63.6%), and cellular components (57.7%). Kyoto encyclopedia of genes and genomes (KEGG) database enrichment analysis indicated that the complement, the coagulation cascade pathways and the mineral absorption pathway were significantly enriched (Table 26).

It was established that several upregulated proteins were related to bacterial infection and host immunity, especially the complement factors. Also, it was found that the complement system consisted of more than 35 serum and cell surface proteins that play crucial roles in innate and adaptive immune immunity (Table 26) (Sunyer & Lambris, 1998).

Table 26. Differentially expressed proteins are associated with the immune response and other biological processes (L. Wang et al., 2017).

		Protein name	Score	Coverage	Peptide	Fold change (mean ± SD)	MRM Fold change
Complement and coagulation cascades pathway							
XP_019949090		complement component C4	943	17.3	16	1.237 ± 0.097	1.93
XP_019965009		complement component C7	114	11.3	5	1.488 ± 0.276	
XP_019955087		complement component C8 beta	397	19.3	7	1.209 ± 0.130	1.20
XP_019937550		complement component C9	1729	35.3	13	1.273 ± 0.167	
XP_019960470		complement factor H precursor, partial	1015	17.5	13	1.341 ± 0.130	
XP_019940984		putative complement factor Bf/C2	962	19.1	10	1.309 ± 0.200	
XP_019939505		beta-2-glycoprotein 1-like (C4BP)	56	3	1	1.495 ± 0.304	
XP_019960575		C4b-binding protein alpha chain-like	183	3.3	1	1.310 ± 0.217	
XP_019962614		interferon regulatory factor 3 variant 1	99	5.1	2	1.301 ± 0.880	
ACY70392		serum lectin isoform 3	1382	61.1	5	1.511 ± 0.135	
ACB59380		progranulin type I	269	7.2	1	1.617 ± 0.388	
XP_019935276		Haptoglobin	251	27.5	6	2.172 ± 0.672	
XP_019953144		heat shock protein 90 beta	3235	36.8	21	0.821 ± 0.118	
XP_019952778		heat shock protein 70 protein 4-like	585	20.8	11	0.747 ± 0.184	
XP_019959679		Kininogen (Fragments)	464	12.8	3	0.593 ± 0.307	
		Unknown protein	743	16.4	21	1.247 ± 0.237	
Mineral absorption pathway							
XP_019949085		metalloreductase STEAP4-like	1241	34.9	9	1.239 ± 0.321	
XP_019965890		Ferritin, middle subunit	51	34.1	1	1.625 ± 0.334	1.25
XP_019935778		Ferritin, heavy subunit	71	19.6	14	1.832 ± 0.280	
AAF33233		transferrin	204	15.7	2	0.625 ± 0.102	0.75
Biosynthesis and metabolism							
XP_019958255		H1 histone, partial	137	10.6	2	1.425 ± 0.327	
XP_019965661		H1 histone, like	154	10.2	2	1.374 ± 0.123	
XP_019969491		glyceraldehyde-3-phosphate dehydrogenase	852	17.8	5	4.278 ± 1.953	
XP_019941327		Peroxiredoxin-4-like	338	17.3	9	1.265 ± 0.074	1.56
XP_019968978		natural killer enhancing factor (Peroxiredoxin-1)	226	10	4	1.115 ± 0.091	
XP_019969518		cathepsin D	1475	28	8	1.229 ± 0.028	
Cytoskeleton-related proteins							
XP_019411630		actin, alpha skeletal muscle B-like isoform 1	3268	47.2	13	1.233 ± 0.145	
NP_001001409		actin, alpha, cardiac muscle 1a	4209	49.1	15	1.201 ± 0.149	
XP_019943289		myosin regulatory light chain 2, smooth muscle minor isoform-like	477	40.1	5	1.387 ± 0.241	
XP_019964547		alpha-actinin-1-like	5290	55.5	16	0.830 ± 0.128	
XP_019936640		Profilin-2 (negative regulation of actin filament polymerization)	289	25.9	3	0.720 ± 0.242	
XP_019937463		catenin delta-1-like	338	17.3	9	0.686 ± 0.201	
XP_019948040		cytoskeleton-associated protein 4-like	226	10	4	0.732 ± 0.351	
XP_019944878		Keratin, type I cytoskeletal 18-like	1269	15.9	3	1.533 ± 0.118	2.66

The functions of the complement system included microbial killing, phagocytosis, inflammatory reactions, complex immune clearance, and antibody production (Boshra et al., 2006). Among the differentially expressed proteins, those involved in mediating complement cascade (e.g. complement component C7, C8, C9, complement factor H, complement factor Bf/C2) and mineral absorption (e.g. ferritin, STEAP-4) were most significantly upregulated during infection. Subsequently, five significantly upregulated (C4, C8 beta, ferritin middle subunit, PRDX4-like and KRT18) and one significantly downregulated (transferrin) candidate immune proteins were validated by multiple reactions monitoring ESI-MS/MS analysis using the multiple reaction monitoring (MRM) mode (L. Wang et al., 2017).

Furthermore, changes in expression of 15 proteins of the complement component and mineral absorption pathways were validated at the transcriptional level using quantitative real-time PCR (qPCR). The transcriptional levels of four transcription factors (p21Ras, Rab-31-like, NF-κB, STAT3) were also investigated by qPCR following infection with *E. tarda* (L. Wang et al., 2017).

In conclusion, This study contributes to understanding the defence mechanisms of the liver in fish. Also, it indicated clearly that the fish livers were involved in the immune response against *E. tarda* infection at the protein level. This study results indicate how important it is to understand the evolution of this system and the development of new strategies in fish health management (L. Wang et al., 2017).

3.9. **Proteomic Profiling of Zebrafish Challenged by Spring Viremia of Carp Virus Provides Insight into Skin Antiviral Response.**

The skin proteome profiling of zebrafish following infection with the spring viremia of carp virus **(**SVCV) has helped elucidate the molecular mechanism of local mucosal immunity in fish. Skin hemorrhagic disease in cyprinid species is caused by infection with SVCV. Nevertheless, the molecular mechanism of this skin immune response remains unclear at the protein level (R. Liu et al., 2020).

The differential proteomics of the zebrafish (*Danio rerio*) resulting skin response to SVCV infection was examined by isobaric tags for relative and absolute quantitation and quantitative polymerase chain reaction (qPCR) assays. The skin proteins from zebrafish were separated by SDS-polyacrylamide gel, and the skin proteins were determined by iTRAQ MS analysis. Digested

proteins analysis was performed with MS/MS analysis which permitted the identification of peptide length distribution of the proteins in the skin and establishing the upregulated and down-regulated proteins. A total of 3999 proteins were identified, of which 320 and 181 proteins were differentially expressed at 24 and 96 h post-infection, respectively (Tables 27 and Supplementary S4) (R. Liu et al., 2020).

Table 27. Representative immune-related differentially expressed proteind proteinpressed proteinpressed proteinpressed proteins in the skin of zebrafish infected with spring viremia of carp virus (R. Liu et al., 2020).

		Fold change					
Accession	*otein*	*Score*	*Covera ge*	*(24/96 h)*	*MW/kDa*	*pl*	*Peptide sequence*
Q918V0	Parvalbumin 2	983.73	58.72	0.53/0.96	11.61	4.68	LFLQNFSAGAR, AFLSAGDSDGDGK
Q7ZT36	Parvalbumin 3	658.18	37.61	0.52/0.88	11.54	4.64	LFLQNFSAGAR, IGVDEFASLVKA
Q6IMW7	Parvalbumin 4	897.92	33.94	0.60/0.83	57.79	7.03	AFAIIDQDK, LFLQNFK, IGIDEFAALVKA, AADSFNHK
F1RDE6	Phospholipid-transporting ATPase	30.22	1.85	3.14/1.97	126.51	6.80	NLLLLGATAIEDR, IWVLTGDK
Q7T3A4	Ras-related protein Rab-	163.14	14.50	1.84/1.61	22.44	9.38	LLIIGDSGVGK, LQVWDTAGQER, FFETSAK
A4QNU4	Rh type C	22.86	1.43	1.38/1.75	53.61	5.67	GFWCGPK
Q803H1	RNA-binding motif	48.60	2.87	1.88/2.65	58.29	10.24	L
Q6DG30	Serpin peptidase inhibitor Glade B member 1	36.25	2.63	1.12/1.36	103.18	7.90	VQVLELPYVK
093598	Signal transducer and activator of transcription la	167.87	12.82	1.22/1.02	86.80	5.87	AASDPEAQIPWNR
E9QB13	Sodium channel protein type 4 subunit alpha B	41.72	0.78	0.65/0.83	56.92	4.65	FMGNLRQK, ERPCPPGWYK
BOR068	Sodium/potassium-transporting ATPase subunit alpha	715.22	26.24	2.21/1.05	112.67	5.35	VFLAEQTDVPILK
B6RD09	Solute carrier family 12	74.33	1.93	2.19/1.12	21.10	8.54	VFILGDQETK, FEDTITPFR
Q6NXIO	Solute carrier family 25 member 4	441.73	30.87	0.59/0.91	32.67	9.73	DFLAGGVAAAISK, TAVAPIER, EFTGLGNCVAK, AAYFGIYDTAK
Q6NYQ0	Tropomyosin 1	1290.62	30.99	1.14/1.18	125.85	9.03	LLTAEEVATK, RIQLVEEELDRAQER, AADESER
Q6DHU6	Troponin I skeletal fast 2a 3	70.74	13.64	0.52/0.90	19.72	9.22	SLVLSITK, EVVDTAAAK, VVDLQGK
Q6POT7	Troponin T 3b	75.33	25.88	0.37/0.75	27.27	9.60	ALSNGSQYSSYLQK, ALSNMGSQYSSYLQK, PDGDKVDFDDIQKK

Q7T3D0	Tumor necrosis factor alpha-induced protein 8-like protein 3	21.29	3.47	0.56/1.02	23.19	5.77	ICDGINK
Q803K5	Tumor protein D52-like	28.75	9.09	1.29/1.08	112.88	6.34	LGISPLSEIK, HAAELK
FIQSEI	Uncharacterized protein	2952.19	27.12	0.27/0.26	223.24	5.67	IEEAGGATAAQIEMNK,
E7FBU7	Uncharacterized protein	37.27	2.80	1.76/1.71	123.07	6.19	EPEVLSTMATIVNK
Q567J7	Zgc:111997	45.50	11.01	1.51/2.03	38.71	5.55	TASPQVSLLQK, TSTLNVKPEEWK, ESGIVPVFK

GTP, guanosine triphosphate; MW, molecular weight.

The expression levels of 16 selected immune-related differentially expressed proteins (DEPs) were confirmed by qPCR analysis. Additionally, following enrichment analyses by the "Gene Ontology" (GO) and Kyoto Encyclopedia of Genes and Genomes (KEGG)," it was revealed that DEPs were significantly associated with complement, inflammation, and antiviral response. The protein-protein interaction network of the cytoskeleton-associated proteins, ATPase-related proteins, and parvalbumins from DEPs was shown to be involved in skin immune response. The results of this study will provide a scientific reference for elucidating the mechanism of mucosal skin immunity of fish by viral infection (R. Liu et al., 2020).

3.10. Comparative Proteomic Analysis of Lysine Acetylation in Fish CIK Cells Infected with Aquareovirus

The grass carp (*Ctenopharyngodon idellus*), a commercial freshwater cultured species, usually get infected by grass carp reovirus (GCRV), which induces severe hemorrhages in fingerlings and yearlings (Guo et al., 2017). To understand the molecular pathogenesis of host cells during GCRV infection, intensive proteomic quantification analysis of lysine acetylation in *Ctenopharyngodon idella* kidney (CIK) cells was performed (Guo et al., 2017).

In order to recognize whether the lysine acetylation level of cell proteins could be influenced by GCRV infection, Western blotting analyses were achieved with infected or mock-infected cells using the pan anti-acetyllysine and anti-β-actin antibodies.

Figure 39A indicates a comparison between the protein profiles of infected and mock-infected cells. Both profiles showed enhanced and reduced protein bands detected at their lysine acetylation level under the same expression level of β-actin, suggesting that the lysine acetylome of host proteins were changed in response to GCRV infection. This was followed by performing combined dimethylation labelling mass spectrometry-based quantitative proteomics to comparatively quantify the detailed changes of lysine acetylome towards GCRV infection in CIK cells. The scheme of the experimental workflow is illustrated in Figure 39B (Guo et al., 2017).

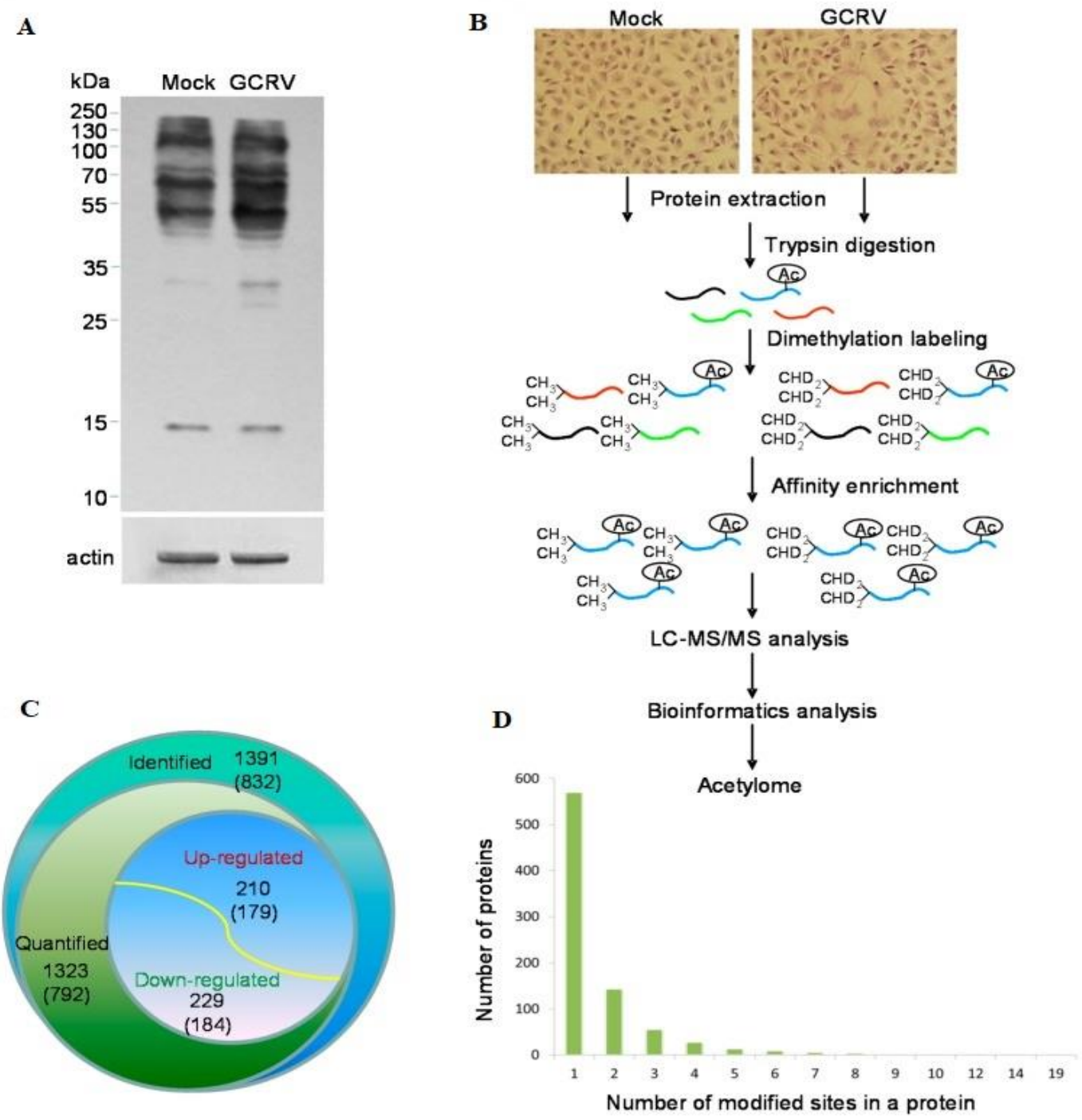

Figure 39. *Proteome-wide identification of lysine acetylation sites and proteins in CIK cells in response to grass carp reovirus (GCRV) infection. (A) Lysine acetylation in GCRV infected or mock-infected cells as analyzed by Western blotting, β-actin was used as loading control; (B) Experimental strategy used to identify and quantify acetylated lysine sites in CIK cells in response to GCRV infection; (C) Number of identified and quantified lysine-acetylated sites and proteins. The up-regulated and down-regulated sites and proteins were also indicated. The number of proteins was shown in brackets; (D) Distribution of acetylated proteins based on their number of acetylation sites* (Guo et al., 2017) .

In addition, the most identified peptides were distributed in length between 7 and 19, which agree with the property of tryptic peptides. The further quantitative result showed that 1391 lysine acetylation sites in 832 proteins were identified, of which 1323 sites in 792 proteins were quantifiable (Supplementary Table S5) These identified proteins were involved in various biological functions, diverse cellular processes and distributed in multiple subcellular compartments (Guo et al., 2017).

It has been suggested that histone proteins are thought to be lysine-acetylated. However, the identified in this present work in the previous report were predominantly non-histone proteins(Allfrey et al., 1964). Among these acetylated proteins, 210 sites in 179 proteins displayed a greater than or equal to 1.5-fold increased expression, and 229 sites in 184 proteins displayed a lesser than or equal to 1.5-fold decreased expression in response to GCRV infection (Figure 39C) (Guo et al., 2017).

Bioinformatics analysis showed that differentially expressed lysine-acetylated proteins are involved in diverse cellular processes and associated with multifarious functions, suggesting that extensive intracellular activities were changed upon viral infection. In addition, extensive alterations on host–protein interactions at the lysine acetylation level were also detected. Further biological experiments showed that the histone deacetylases (HDAC) inhibitor suberoylanilide hydroxamic acid (SAHA) could significantly suppress the GCRV replication. According to the authors of this study, this was the first example to reveal that the proteome-wide changes in host cell acetylome by a aquatic virus infection.

The results provided in this study laid a basis for further understanding the host response to aquareovirus infection in the post-translational modification aspect by regulating cell lysine acetylation conducive to viral replication (Guo et al., 2017).

3.11. iTRAQ Analysis of Gill Proteins from the Zebrafish (Danio rerio) Infected with Aeromonas hydrophila

The aim of this study was to determine the gill immune response against the infection caused by the marine Gram-negative bacteria *Aeromonas hydrophila*. The differential proteomes of the zebrafish gill response were identified using isobaric tags for relative and absolute quantitation (iTRAQ) labelling, followed by liquid chromatography-tandem mass spectrometry (LC-MS/MS) (A. Lü et al., 2014).

A total of 1338 proteins were identified and classified into categories primarily related to the cellular process (15.36%), metabolic process (11.95%) and biological regulation (8.29%). Of these, 82 differentially expressed proteins were reliably quantified by iTRAQ analysis, 57 proteins were upregulated, and 25 proteins were downregulated upon bacterial infection. Following gene ontology (GO) enrichment analysis, it was found that approximately 33 (8.8%) of the differential proteins in gills were involved in the stress and immune responses, as shown in Figure 40 (A. Lü et al., 2014).

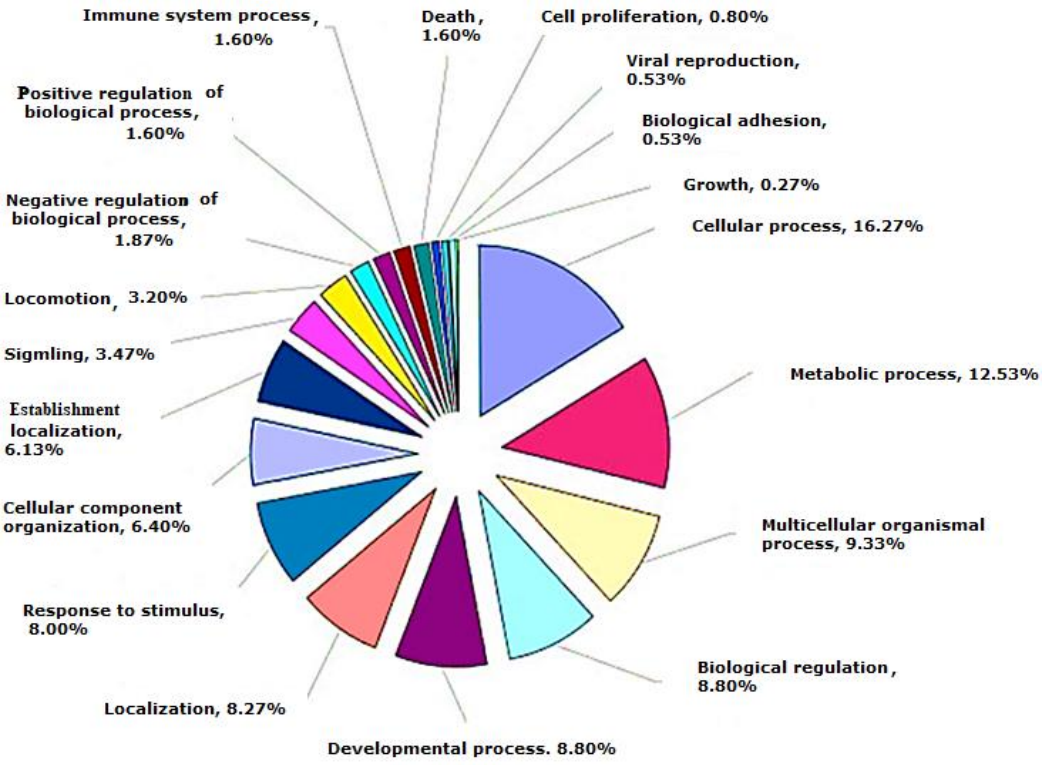

Figure 40. Gene ontology (GO) analysis of differentially expressed proteins in gills. A total of 82 proteins were identified as differentially expressed by iTRAQ analysis. Shown above is the classification of these proteins in different categories based on biological processes (A. Lü et al., 2014).

Several upregulated proteins were observed, such as complement component 5, serpin peptidase inhibitor clade A member 7, annexin A3a, histone H4, glyceraldehyde 3-phosphate dehydrogenase, creatine kinase, and peroxiredoxin. These protein expression changes were further validated at the transcript level using microarray analysis.

Moreover, complement and coagulation cascades, pathogenic *Escherichia coli* infection and phagosome were the significant pathways identified by KEGG enrichment analysis. This is the first report on the proteome of fish gills against *A. hydrophila* infection, which contributes to understanding the gills' defence mechanism fish (A. Lü et al., 2014).

.

3.12. High-Throughput Proteomic Profiling of the Rainbow Trouts Livers Following Gram-Negative Bacteria Aeromonas salmonicida Infection

A high-throughput proteomics approach was used to determine the role of the rainbow trouts (*Oncorhynchus mykiss*) liver in defense responses to bacterial infection with *Aeromonas salmonicida*, the causative agent furunculosis (Causey et al., 2018).

The trout possess multifaceted functions involved in innate immunity, metabolism, and growth. For these reasons, in this study the liver tissue was chosen as it serves a dual role, supporting host defense and in parallel and driving the metabolic adjustments that promote effective immune function. While past studies have reported mRNA responses to *A. salmonicida* in salmonids, the impact of bacterial infection on the liver proteome remains uncharacterized in fish (Causey et al., 2018).

The experimental design of this study is summarized in Figure 41 High-throughput proteomic analysis of rainbow trout liver was initiated comparing controls to bacterial-challenged (48 h post-infection of *Aeromonas salmonicida*. The validation of the systematic immune response to *A.salmonicida* challenge was verified by quantitative PCR gene expression profiling. It indicated a strong transcriptional upregulation of the pro-inflammatory cytokines *IL-1β* and *TNF-α2* in the head kidney. Specifically, it was established that IL-1β and TNF-α2 increased by approx. 105- and 8.1-fold, respectively, in the infected compared to controls (Causey et al., 2018).

The strong response of these immune markers in the head kidney is consistent with a systematic immune response to *A. salmonicida* infection. In addition, a markedly enlarged spleen in the infected fish indicated a clinical sign of bacterial infection rainbow trouts (*Oncorhynchus mykiss*) (Causey et al., 2018).

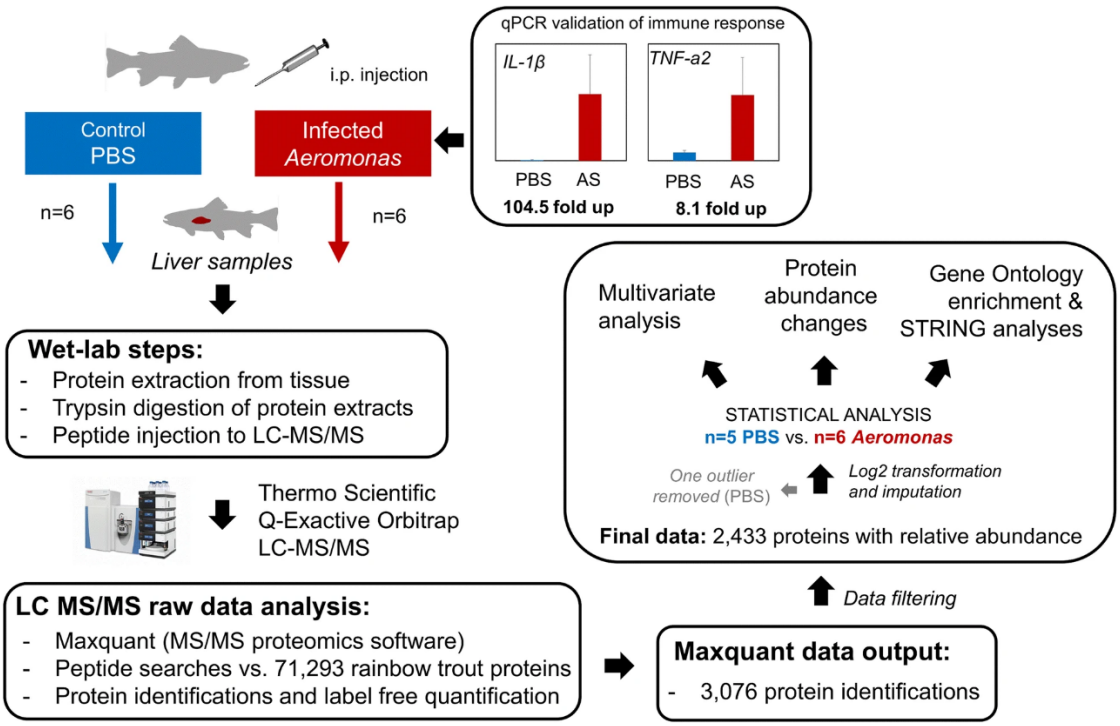

Figure 41. Summary of experimental study design (Causey et al., 2018).

The rainbow trout were injected with *A. salmonicida* or PBS (control), and the livers were extracted 48 h later. The HPLC-ESI-MS/MS proteomic analysis was performed with a high-resolution_hybrid quadrupole-Orbitrap mass spectrometer. A label-free method was used for protein abundance profiling, which revealed a strong innate immune response and evidence to support the parallel rewiring of metabolic and growth systems. It was found that the 3076 proteins were initially identified against all proteins (n = 71,293 RefSeq proteins) were annotated in a single high-quality rainbow trout reference genome, of which 2433 were maintained for analysis post-quality filtering (Supplementary Table S6) (Causey et al., 2018).

Among the 2433 proteins, 109 showed significant differential abundance following *A. salmonicida* challenge, including many upregulated complement systems and acute phase response proteins, in addition to molecules with putative functions that may support metabolic re-adjustments. Furthermore, there were novel expansions in the complement system due to gene and whole-genome duplication events in salmonid evolutionary history, including eight C3 proteins showing differential changes in abundance.

To sum it up, this study provided a high-throughput proteomic examination of the trout liver in response to bacterial challenge. It also revealed novel diagnostic protein biomarkers for the host defence response and evidence of metabolic remodelling in conjunction with activation of innate immunity (Causey et al., 2018).

3.13. Proteome Analysis Reveals a Role of Rainbow Trout Lymphoid Organs during Yersinia ruckeri Infection Process

Yersinia ruckeri is the causative agent of enteric redmouth disease in salmonids. The Head, kidney and spleen are major lymphoid organs of the teleost fish where antigen presentation and immune defense against microbes occur. There is an urgent need to understand the protein changes in the host lymphoid organs in response to *Y. ruckeri* infection. The present study describes the proteome alteration in the head kidney and spleen of the rainbow trout following *Y. ruckeri* strains infection. The organs were analyzed after 3, 9 and, 28 days post-exposure with a shotgun proteomic approach (Kumar et al., 2018).

The lack of information on how protein changes in the host lymphoid organs in response to *Y. ruckeri* infection has been addressed by the following study. The main objective of the present study was to identify and quantify rainbow trout lymphoid organ proteomic expression profiles in response to infection with biotype 1 and biotype 2 Y. ruckeri strains by SWATH-MS (Sequential Windowed Acquisition of All Theoretical Mass Spectra), a label-free quantitative proteomic approach (Kumar et al., 2018).

Gene Ontology (GO) annotation and protein-protein interaction were projected using bioinformatic tools. It was found that 34 proteins from the head kidney and 85 proteins from the spleen were differentially expressed in rainbow trout during the *Y. ruckeri* infection process. These included lysosomal, antioxidant, metalloproteinase, cytoskeleton, tetraspanin, cathepsin B and c-type lectin receptor proteins (Tables 28 and Supplementary S7). Some immune-related proteins such as lysozyme C, thioredoxin, chemotaxis, precerebellin-like protein, cathepsin B, C type lectin B and tetraspanin were strongly up-regulated in infected rainbow trout, which are essential to defence mechanisms against *Y. ruckeri* infection, and add new insights into the antibacterial activities in rainbow trout (Kumar et al., 2018).

*Table 28. List of top up- and down-regulated spleen proteins of rainbow trout in response to Yersinia ruckeri strains. (**Full table is presented in Supplementary Table S7**) (Kumar et al., 2018).*

Accession UniProt	Protein	Number of quantified Peptides	Function	Spleen control in response to strain	3 dpe	9 dpe	28 dpe
LYSC2_ONCMY	Lysozyme C II	6	Lysozyme activity	CSF007-82	4.6*	11.8	3.7
				7959-11	3.0*	6.6	3.5
Q60FB6_ONCMY	NADPH oxidase cytosolic protein p40phox	6	Phagocytosis	CSF007-82	3.0*	2.6	1.5
				7959-11	3.0*	2.2	1.3
Q60FB5_ONCMY	NADPH oxidase cytosolic protein p67phox	4	Phagocytosis	CSF007-82	2.7*	2.2	−1.3
				7959-11	3.1*	2.1	−1.4
C1BHL9_ONCMY	Ras-related C3 botulinum toxin substrate 2	2	Phagocytosis /GTPase activity	CSF007-82	7.3*	5.4*	3.6
				7959-11	5.2*	4.9*	3.4
C1BH85_ONCMY	Thioredoxin	5	Antioxidant defence	CSF007-82	3.2*	4.8	3.6
				7959-11	2.8*	2.6	3.1
W8W0Y8_ONCMY	Glutathione peroxidase	5	Anti-oxidant activity	CSF007-82	1.9	1.3	1.6
				7959-11	2.2*	1.9	1.4
Q92004_ONCMY	Beta-2-microglobulin	4	Glycoprotein binding	CSF007-82	2.2	4.1*	2.0
				7959-11	1.7	3.0*	2.1
Q9DFJ1_ONCMY	Chemotaxin (Fragment)	5	Neutrophil chemotactic activity	CSF007-82	4.9*	3.6	1.5
				7959-11	4.2*	3.0	1.3
A0A060X145_ONCMY	Tetraspanin	2	Cell surface receptor signaling pathway	CSF007-82	4.0*	4.5*	3.7*
				7959-11	2.9*	5.2*	3.2*
B5X4P4_SALSA	Cathepsin B	2	Cysteine-type endopeptidase activity	CSF007-82	2.3	3.8*	2.6*
				7959-11	1.5	2.9*	2.6*
B9ENC0_SALSA	Cellular nucleic acid-binding protein	5	Nucleic acid binding	CSF007-82	5.4*	7.2*	5.7*
				7959-11	4.5*	7.1*	4.3*
C1BEZ5_ONCMY	C6orf115	2	Protein folding	CSF007-82	3.0*	4.0*	2.8*
				7959-11	2.5*	2.5*	2.2*
C1BH21_ONCMY	Dynein light chain 1, cytoplasmic	3	Microtubule-based process	CSF007-82	2.0	2.9*	2.4*
				7959-11	1.7	2.9*	2.1*
B5X1B5_SALSA	Alpha-enolase	2	Glycolytic process	CSF007-82	3.1*	3.0*	2.4*
				7959-11	3.2*	2.9*	1.8
C1BHS7_ONCMY	Protein S100	2	Calcium ion binding	CSF007-82	−1.3	−1.5	−1.1
				7959-11	−2.4*	−1.4	1.2

Fold change (infected vs control) was statistically analyzed in Y. ruckeri CSF007-82 (biotype 1) and 7959-11 (biotype 2) infected and control rainbow trout samples (n = 27). *Denotes statistically significant difference according to both ANOVA and post hoc Tukey's HSD with FDR-adjusted p-value < 0.05 and fold change <−2 or >+ 2.

The findings of this study regarding the immune response at the protein level offer new insight into the systemic response to *Y. ruckeri* infection in rainbow trout. This proteomic data facilitate a better understanding of host-pathogen interactions and response of fish against *Y. ruckeri* biotype 1 and 2 strains. Protein-protein interaction analysis predicts carbon metabolism, ribosome and phagosome pathways in the spleen of infected fish, which might be helpful in understanding biological processes and further studies in the direction of pathways (Figure 42) (Kumar et al., 2018)

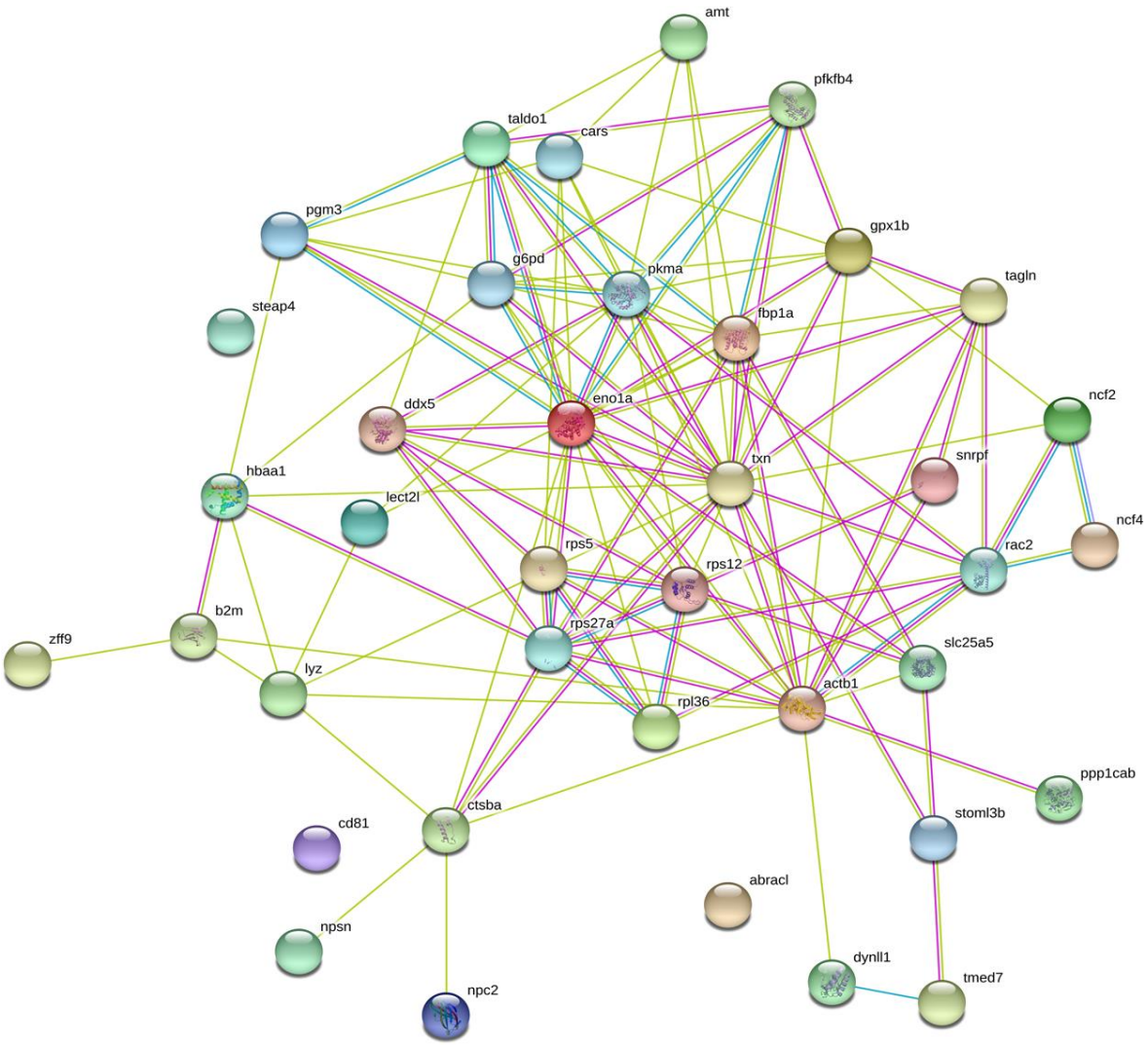

Figure 42. The protein-protein interaction network of 38 up-regulated spleen proteins excluding uncharacterized proteins (Kumar et al., 2018).

In this network, nodes are proteins, lines represent the predicted functional associations, and the number of lines represents the strength of predicted functional interactions between proteins. The yellow lines represent examining evidence, the purple lines represent experimental evidence, and the light blue lines represent database evidence. It is interesting to note that recently, RNA-seq analysis was used to detect the changes in gene expression following *Y. ruckeri* strain H01 challenge of Amur sturgeon (*Acipenser schrenckii*) (S. Li et al., 2017). Although this type of research is precious, it may not accurately reflect the exact protein expression as post-translational modifications cannot be determined by mRNA analysis (Kumar et al., 2018; S. Li et al., 2017).

3.14. Immune Relevant Molecules Identified in the Skin Mucus of Fish Using -Omics Technologies

This review will provide an overview of immune-relevant molecules in fish skin mucus. The skin of fish is continuously exposed to the water environment. Unlike that of terrestrial vertebrates, it is a mucosal surface with a thin epidermis of live cells covered by a mucus layer. The mucosa plays an important role in keeping the homeostasis of the fish and preventing entry of invading pathogens (Brinchmann, 2016).

Also, this review provides an overview of proteins, RNA, DNA, lipids and carbohydrates found in the skin mucus of studied species. Proteins such as actin, histones, lectins, lysozyme, mucin, and transferrin have extracellular immune relevant functions, other molecules including complements molecules, heat shock molecules and superoxide dismutase present in mucus show differential expression during pathogen challenge in some species, but their functions in mucus, if any, need to be shown. RNA, DNA, lipids, carbohydrates and metabolites in mucus have been studied to a limited extent in fish, the current knowledge is summarized, and knowledge gaps are pointed out (Brinchmann, 2016).

3.15. Development of Liquid Chromatography-Tandem Mass Spectrometry Methods for the Quantitation of *Anisakis simplex* Proteins in Fish

The parasite *Anisakis simplex* is present in many marine fish species that are directly used as food or in processed products. The *anisakid* larvae infect mostly the gut and inner organs of fish but have also been shown to penetrate into the fillet. For this major reason, human health can be

at risk, either by contracting anisakiasis through the consumption of raw or undercooked fish or by sensitization to *anisakid* proteins in processed food (Fæste et al., 2016).

A number of different methods for detecting *A. simplex* in fish and products thereof have been developed, including visual techniques, PCR for larvae tracing, and immunological assays for the determination of proteins. The recent identification of a number of anisakid proteins by mass spectrometry-based proteomics has laid the groundwork for developing two quantitative liquid chromatography-tandem mass spectrometry methods for the detection of *A. simplex* in fish that are described in the present study. Both the label-free semi-quantitative nLC-nESI-Orbitrap-MS/MS (MS^1) and the heavy peptide-applying absolute-quantitative (AQUA) LC-TripleQ-MS/MS (MS^2)use unique reporter peptides derived from *anisakid* hemoglobin and SXP/RAL-2 protein as analytes (Table 29) (Fæste et al., 2016).

Table 29.Simplex peptides were detected in fractions of HILIC-LC-MS/MS (Fæste et al., 2016).

Fraction no.	Protein; gi-number[a]	URP[b]	*m/z*; z[c]	Nematode species[d]
2	Phosphofructokinase; gi:323575365	FGVLDILEDVK	624.34; 2	Ascaris suum
	Adenylate kinase isoenzyme; gi:324524542	YGLTHLSSGDLLR	477.91; 3	*Ascaris suum*
	Peptidylprolyl isomerase-3; gi:158591678	IVMELFSDVVPK	688.87; 2	*Brugia malayi*
3	Hemoglobin; gi:428230092	LFAEYLDQK	563.76; 2	*Anisakis pegreffi*
		HSWTTIGEEFGHEADK	615.24; 3	
		HMFEHYPVNK	440.19; 3	
		DDIHLPQAQWHEFWK	650.61; 3	
		ETFDAYTHELMAR	528.55; 3	
	SXP/RAL-2 protein; gi:155676678	DAFAALAQTFK	591.80; 2	*Anisakis simplex*
		IVQTFESLPPAVK	714.90; 2	
		EVLAAQQAAEEEHK	776.87; 2	
		ADAELTAIADDASLTLAAK	930.47; 2	
	Glutamate dehydrogenase; gi:324509349	GFLGPGIDVPAPDMGTGER	943.45; 2	*Ascaris suum*
		VIGEAANGPTTPAADK	756.38; 2	
		DIVHSGLEYSMQK	502.91; 3	
	14-3-3 protein; gi:324527518	SQQSYQEAFDIAK	757.85; 2	*Ascaris suum*
		KVTELGAELSNEER	787.89; 2	
	Fructosebisphosphate aldolase; gi:324514307	VTEQTLAFVYK	649.84; 2	*Ascaris suum*
	Ani s 9; gi:157418806	QLAAAFQALDPAVK	721.89; 2	*Anisakis simplex*
	Nucleoside diphosphate kinase; gi:324531155	TFIAIKPDAVQR	679.88; 2	*Ascaris suum*
		LMLGATNPLASNPGTIR	863.46; 2	
	Malate dehydrogenase gi:324505349	DVIIWGNHSSTQFPDAK	638.98; 3	*Ascaris suum*
	Glycogen phosphorylase; gi:324501938	GIAQVENVANIK	628.35; 2	*Anisakis simplex*
		ARPEYMLPVNMYGNVEK	1005.98; 2	

	Glutathione-S-transferase; gi:1254920	LIFHQAGVQFEDHR	566.28; 3	*Ascaridia galli*
	Phosphoenolpyruvate carboxykinase; gi:307762034	RPEGVPLVFESR	693.37; 2	*Loa loa*
	Phosphoglycerate mutase; gi:324504802	VAYDALIGGIGEK	653.35; 2	*Ascaris suum*
		VATYDLLPPMSSAGVADK	917.95; 2	
	Tropomyosin; gi:350285785	AQEDLSTANSNLEEK	824.88; 2	*Anisakis simplex*
	Rab GDP dissociation inhibitor; gi:324507378	NNYYGGESASLTPLEQLFEK	1130.53; 2	*Ascaris suum*
4	transketolase-1; gi:308257950	KIDSDIEGHPTPR	488.91; 3	*Caenorhabditis remanei*
	hemoglobin; gi:428230092	HREGYTAADV	458.89; 3	*Anisakis pegreffi*
	SXP/RAL-2 protein; gi:155676678	KEVLAAQQAAEEEHKK	603.65; 3	*Anisakis simplex*
	Ani s 11-like protein; gi:323575365	GPLPIGGPGPVVSGSGIGR	837.46; 2	*Anisakis simplex*

[a] gi-number: genInfo nucleotide sequence identifier in the NCBI GenBank.
[b] Unique reporter peptides with mass peak signal intensities >5 × 10^7 are underlined.
[c] Positively charged peptide ions.
[d] *Anisakis simplex* peptide identified by homology to nematode protein in the NCBI database.

Standard curves in buffer and salmon matrix showed detection limits at 1g/mL and 10g/mL for $MS^1$and 0.1g/mL and 2g/mL for MS^2. Preliminary method validation included the assessment of sensitivity, repeatability, reproducibility, and applicability to incurred and naturally-contaminated samples for both assays (Fæste et al., 2016). By further optimization and full validation in accordance with current recommendations, the LC-MS/MS methods could be standardized and used generally as confirmative techniques for the detection of *A. simplex* protein in fish (Fæste et al., 2016).

3.16. Influence of *Moraxella sp*. Colonization on the Kidney Proteome of Farmed GiltheadS Breams (*Sparus aurata,* L.)

Moraxella spp. is Gram-negative diplococci that morphologically and phenotypically resemble the *Neisseria spp*. These diplococci are strictly aerobic, oxidase-positive, catalase-positive, DNAse-positive and asaccharolytic. At present, the presence of *Moraxella sp*. in the internal organs of fish is not considered detrimental for fish farming. However, it was established that bacterial colonization of internal organs typically affects fish wellness and decreases growth rate, stress resistance, and immune response (Addis et al., 2010).

Recently, internal organ colonization by *Moraxella sp* has been reported by farmers concerning the slow growth, poor feed conversion, and low average weight increase of fish farmed

in offshore floating sea cages. For this reason, it is only logical to analyze whether the presence of these opportunistic bacteria deserves further investigations for elucidating incidence and impact on fish metabolism (Addis et al., 2010).

A total of 960 gilthead sea breams (*Sparus aurata*, L.), collected along 17 months from four offshore sea cage plants and two natural lagoons in Sardinia, were studied. The gilhead sea breams were subjected to the routine microbiological examination of internal organs throughout the production cycle. It was found that thirteen subjects (1.35%) were positive for *Moraxella sp*. in the kidney (7), brain (3), eye (1), spleen (1), and perivisceral fat (1) (Addis et al., 2010).

In order to investigate the colonization and the influence of *Moraxella sp*., positive and negative kidney samples were subjected to a differential proteomics study by means of 2-D PAGE and mass spectrometry. The differential analysis of protein expression among tissue maps of *Moraxella*-positive and negative kidneys revealed the differential expression of several protein spots. In particular, ten spots were prominently upregulated in Moraxella-positive tissue and reproducibly under expressed in negative tissues (Figure 43, in white) (Addis et al., 2010).

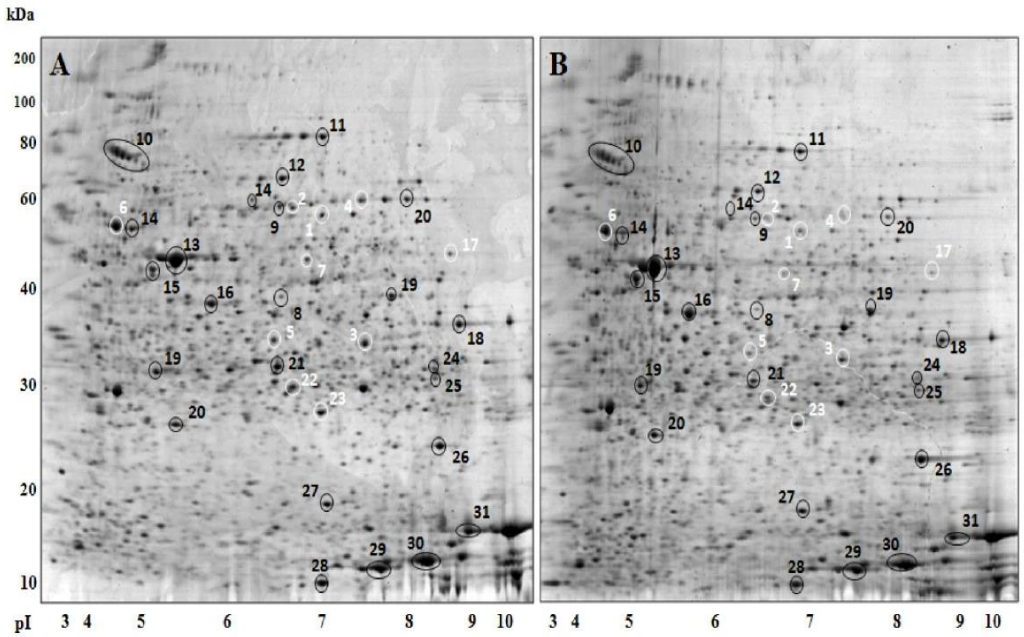

Figure 43. 2-D PAGE map of Moraxella spp. positive (A) and negative (B) kidney tissue. Circled, numbered spots indicate all spots identified in this work, ordered following the increase in expression upon Moraxella sp. colonization. The ten spots most significantly upregulated in positive kidney are indicated in white. Protein identifications corresponding to spot numbers are reported in Table 30 (Addis et al., 2010).

These spots were subjected to MALDI-TOF-MS and by Nano-ESI-QqTOF-MS/MS for identification, producing the following matches: mitochondrial alanine aminotransferase, mitochondrial aldehyde dehydrogenase, mitochondrial dihydrodipicolinate synthase, mitochondrial methylmalonate semialdehyde dehydrogenase, mitochondrial ATP synthase beta subunit, mitochondrial Acyl-CoA-dehydrogenase, S-adenosylhomocysteine hydrolase, and peroxiredoxins (Addis et al., 2010). Interestingly, seven out of ten spots with a statistically significant upregulation in *Moraxella*-positive kidney produced identifications corresponding to mitochondrial enzymes (Table 30) (Addis et al., 2010).

It was concluded that the *Moraxella sp*., which infected the kidneys, displayed a concerted upregulation of several mitochondrial enzymes compared to negative tissues, reinforcing previous observations following lipopolysaccharide (LPS) challenge in fish. This means that the presence of *Moraxella sp.* in farmed sea bream kidneys is able to induce proteome alterations, similar to those described following LPS challenges in other fish species. In conclusion, this study revealed that *Moraxella sp*. might be causing metabolic alterations in fish and provided indications on proteins that could be investigated as markers of infection by Gram-negative bacteria within farming plants (Addis et al., 2010).

Table 30. Proteins identified in sea bream kidney tissue (Addis et al., 2010).

N.	Protein	Acc. no.	Species	Pred. mass	Pred. pI	Sc.	QM (%c.)	FC	*p*
1	**Alanine aminotransferase, mt**	gi|37783307	*S. aurata*	62091	8.54	527	26(23)	**2.3**	**0.0016**
2	**Aldehyde dehydrogenase, mt**	gi|118503	*E. caballus*	54532	5.7	76	2(4)	**3.3**	**0.0005**
3	**Dihydrodipicolinate synthase, mt**	gi|47208001	*T. nigroviridis*	34365	8.17	100	9(5)	**1.6**	**0.0001**
4	**Methylmalonate semialdehyde dehydrogenase, mt**	gi|47230188	*T. nigroviridis*	57397	7.06	410	10(12)	**2.3**	**0.0005**
5	**Dihydrodipicolinate synthase, mt**	gi|47208001	*T. nigroviridis*	34365	8.17	110	9(6)	**2.2**	**0.0006**
6	**ATP synthase, beta subunit, mt**	gi|47605558	*C. carpio*	55327	5.05	1432	76(46)	**1.5**	**0.005**
7	**S-adenosyl-homocysteine hydrolase**	gi|178277	*H. sapiens*	48254	6.03	156	7(6)	**2.6**	**0.0104**
8	Phosphoenolpyruvate carboxykin.	gi|24637098	*S. aurata*	14574	5.61	48	1(9)	<1.5	>0.05
9	*Antiquitin*	gi|61742178	*A. schlegelii*	55832	5.88	369	9(13)	*1.71*	*>0.05*
10	*Wap65*	gi|119393859	*A. schlegelii*	49162	5.40	250	11(10)	*1.86*	*>0.05*
11	*Transferrin*	gi|34329603	*A. schlegelii*	76152	6.38	418	12(9)	*2.69*	*>0.05*
12	Transferrin	gi|33113484	*P. major*	76146	5.72	206	6(6)	<1.5	>0.05
13	Beta actin	gi|33526989	*M. albus*	42110	5.31	752	41(45)	<1.5	>0.05
14	ATP synthase, mt	gi|66773080	*D. rerio*	55080	5.25	1546	79(47)	<1.5	>0.05
15	Cytoplasmic actin	gi|13699190	*L. japonicum*	42137	5.30	777	57(42)	<1.5	>0.05
16	Beta actin	gi|49868	*M. musculus*	39446	5.78	557	59(28)	<1.5	>0.05
17	**Acyl-Co A dehydrogenase, mt**	gi|47209002	*T. negroviridis*	39802	6.08	211	4 (11)	**1.9**	**0.0117**
18	Fructose-biphosphate aldolase B	gi|1703243	*S. aurata*	40190	8.43	664	25(20)	<1.5	>0.05
19	Electron transfer flavopr. alpha, mt	gi|47225813	*T. nigroviridis*	35017	7.64	406	14(26)	<1.5	>0.05
20	PEBP superfamily	gi|47221502	*T. nigroviridis*	21069	6.89	393	20(27)	<1.5	>0.05
21	*Carbonic anhydrase*	gi|56554783	*P. americanus*	28512	5.22	64	4(10)	*2.21*	*>0.05*
22	**Peroxiredoxin**	gi|47220267	*T. nigroviridis*	22280	5.44	313	24(22)	**2.5**	**0.0025**
23	**Peroxiredoxin family protein**	gi|93211500	*P. maxima*	22063	5.58	364	21(32)	**1.6**	**0.05**
24	Enoyl-CoA hydratase short chain	gi|12805413	*M. musculus*	31636	8.51	224	13(12)	<1.5	>0.05
25	*Glutathione S-transferase*	gi|34014736	*S. aurata*	24748	8.51	205	10(28)	*1.6*	*>0.05*
26	Nucleoside diphosphate kinase	gi|10121713	*G. mirabilis*	17214	8.52	299	39(48)	<1.5	>0.05
27	*Cu/Zn superoxide dismutase*	gi|62550923	*S. aurata*	6979	5.41	545	25(68)	*1.8*	*>0.05*
28	Alpha-2 globin	gi|99122203	*S. aurata*	15887	8.79	96	11(6)	<1.5	>0.05
29	Beta globin	gi|91260232	*S. aurata*	16308	7.82	158	7(18)	<1.5	>0.05
30	Alpha-2 globin	gi|99122203	*S. aurata*	15887	8.79	466	23(41)	<1.5	>0.05
31	Beta globin	gi|91260232	*S. aurata*	16308	7.82	367	10(47)	<1.5	>0.05

N, spot number; Acc. no., accession number; Pred. mass, predicted mass; Pred. pI, predicted pI; Sc, score; QM (%c.), Queries matched (% coverage); FC, fold change.
Protein identifications were performed both by MALDI-MS and nano-HPLC-nano-ESI-Q-TOF-MS/MS. Proteins with fold change > 1.5 and P < 0.05 are in bold. Proteins with fold change > 1.5 and *p* > 0.05 are in italics.

3.17. **Proteomic and Functional Analysis of Zebrafish after Administration of the Antimicrobial Peptide Epinecidin-1**

The antimicrobial peptides (AMPs) play important roles in innate immunity. Epinecidin-1, an AMP isolated from *Epinephelus coioides*, possesses antibacterial activity against *Vibrio vulnificus* in zebrafish. This study's main goal was to identify the associated antimicrobial proteins affected by epinecidin-1 treatment and to unravel the underlying antimicrobial molecular mechanisms of epinecidin-1. For this reason, the authors analyzed the proteome changes following epinecidin-1-treated zebrafish using the conventional proteomic approach (2DE electrophoresis coupled to tandem mass spectrometry analysis). Several differentially expressed proteins were identified, some of which were validated by real-time quantitative RT-PCR (Table 19 and Figure 33) (T. C. Huang & Chen, 2013).

The differentially expressed proteins were mapped onto Ingenuity Pathway Analysis canonical pathways, to construct a possible protein-protein interacting network regulated by epinecidin-1. This network suggested a potential role of epinecindin-1 in cytoskeletal assembly and organization (T. C. Huang & Chen, 2013).

These findings imply that epinecidin-1 may stabilize the cytoskeleton network in host cells, thereby promoting resistance to bacterial infection (T. C. Huang & Chen, 2013).

3.18. **Skin Mucus Proteome Map of European Sea Bass (*Dicentrarchus labrax*)**

Skin mucus is known to be the first barrier in the fish defense. In this study, the proteins from skin mucus of European sea bass (*Dicentrarchus labrax*) were identified by 2DE followed by LC-MS/MS (Cordero et al., 2015b).

A draft sequence of the European sea bass (*D. labrax*, ID 13489) genome was recently published (Tine et al., 2014). However, only 2420 *D. labrax* proteins were registered in the NCBI database, whilst the fully sequenced and well-annotated zebrafish (*Danio rerio*, ID 7955) genome had 81 527 protein entries. As already indicated in this review, when working with species with less annotated genomes, the homology-driven proteomics become the only major tool permitting the characterization of the proteomes (Jurado et al., 2015b).

Consequently, this study permitted the identification of a wide range of proteins in skin mucus of *D. labrax* (Figure 44, and Supplementary Tables S8) (Cordero et al., 2015b).

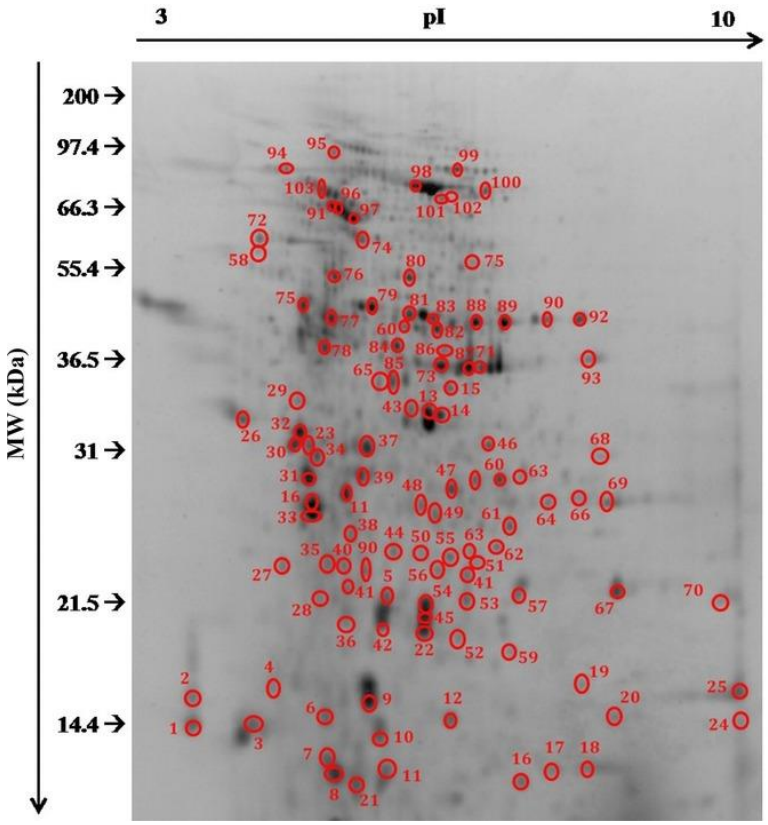

Figure 44. D. labrax skin mucus 2DE map. Two hundred µg of proteins were loaded on 17 cm, 3–10 nonlinear IPG strips. Second dimension was a 12.5% polyacrylamide vertical gel. Red circles and numbers show analysed protein spots (Cordero et al., 2015b).

The identified proteins could be remains of dead cells from the skin surface or the proteins actively secreted to function in the mucus. The authors focus on the proteins associated with several immune pathways in fish from all the identified proteins in the proteome map. Proteins found include apolipoprotein A1, calmodulin, complement C3, fucose-binding lectin, lysozyme and several caspases (Cordero et al., 2015b).

It should be pointed out that this was the first skin mucus proteome study and further transcriptional profiling of the identified proteins done on this bony fish species. This not only contributes knowledge on the routes involved in mucosal innate immunity but also establishes a non-invasive technique based on locating immune markers with potential use for prevention and/or diagnosis of fish diseases (Cordero et al., 2015b).

3.19. Liver Tumors in Wild Flatfish: a Histopathological, Proteomic, and Metabolomic Study

Fish play host to viral, bacterial, and parasitic diseases in addition to non-infectious conditions such as cancer. The National Marine Monitoring Programme (NMMP) provides information to the U.K. Government on the health status of marine fish stocks (Stentiford et al., 2005).

An aspect of this work relates to the presence of tumors and other pathologies in the liver of the offshore sentinel flatfish species, dab (*Limanda limanda*). Using internationally agreed quality assurance criteria, tumors and pre-tumors are diagnosed using histopathology (Stentiford et al., 2005).

The current study has expanded upon this work by integrating these traditional diagnostic approaches with utilizing modern technologies to analyze proteomic and metabolomic profiles of selected lesions (Stentiford et al., 2005).

In this study, the authors have used surface-enhanced laser desorption/ionization (SELDI-TOF-MS/MS), and electrospray ionization Fourier transform ion cyclotron resonance tandem mass spectrometry (ESI-FTICR-MS/MS) technologies (for both proteomic and metabolomic analyses, respectively) to tumor and non-tumor samples resected from the liver of dab (Stentiford et al., 2005).

This combined approach has demonstrated how these technologies are able to identify protein and metabolite profiles that are specific to liver tumors. The proteomic study yielded rich information on the abundance of peptides and small proteins (2–15 kDa). The metabolome was measured using ESI-FTICR-MS/MS, which benefits from the ultrahigh mass resolution and accuracy (Stentiford et al., 2005).

In addition, using histopathology helped the classification of “analysis groups”. It permitted the elimination of spurious samples (e.g., those containing parasite infections), which could confuse the interpretation of the “omic” data. As such, the pathology laboratory plays a central role in collating information relating to particular specimens and in establishing sampling groups relative to specific diagnostic questions (Stentiford et al., 2005).

The data obtained allowed to establish that wild fish can be used as effective models for environmental carcinogenesis research, particularly by combining traditional approaches based on histopathology with emerging proteomic technologies. In particular, the authors highlighted the

importance of incorporating quality assured histopathological methods, for pre-selection of particular trial groups, before further analyzing using proteomic approaches (Stentiford et al., 2005).

In conclusion, this pilot study showed that it was possible to use proteomics technologies for the analysis of both protein and metabolite profiles of liver tumor samples resected from wild fish and collected under the National Marine Monitoring Program (NMMP) of the United Kingdom (Stentiford et al., 2005).

3.20. **Effect of Fish Skin Mucus on the Soluble Proteome of *Vibrio salmonicida* Analysed by 2-DGE and Tandem Mass Spectrometry**

Vibrio salmonicida is the causative agent of cold-water vibriosis in farmed marine fish species. Adherence of the pathogenic bacteria to the mucosal surfaces is considered to be the first step in the infective processes, and the proteins involved in this process are regarded as virulence factors. The ability of bacteria to adhere to host surfaces is considered necessary for successful colonization, and thereby eliciting of the disease. As bacterial colonization is required for pathogenicity, genes involved in bacterial colonization have been regarded as virulence genes (Uttakleiv Ræder et al., 2007b).

External and internal epithelial surfaces of fish are covered with a mucus layer protecting environmental factors like microorganisms, toxins, pollutants, acidic pH and hydrolytic enzymes. Secretory mucins are the major constituents of the mucus layer in which several biochemical compounds have been identified: lysozyme(Fletcher & White, 1973), antimicrobial peptides (Cole et al., 1997)and antibodies (Fletcher & White, 1972; Uttakleiv Ræder et al., 2007b).

This study involved the growth of the Gram-negative bacteria *V. salmonicida* in the presence of 15 mg mucus protein/mL medium and in the absence of mucus in the medium. It was found that the added mucus had virtually no effect on either the growth rate or the final growth yield (Uttakleiv Ræder et al., 2007b).

As already mentioned several times before, it is more difficult to perform correct annotation of the protein mass fingerprint search utilizing MS, especially for organisms in which their genome is not fully sequenced. For this reason, sequencing organisms like *V. salmonicida* required using tandem MS/MS sequencing analysis (Uttakleiv Ræder et al., 2007b)

Therefore, identity of *V. salmonicida* protein spots was achieved by BLAST search using MS/MS ions data or de novo predicted peptide sequences. Proteins differing in intensity were

distinguished by analysing protein spot density on the gel images. Most of the proteins were located in the range of pH 4–7 (Figure 45) (Uttakleiv Ræder et al., 2007b).

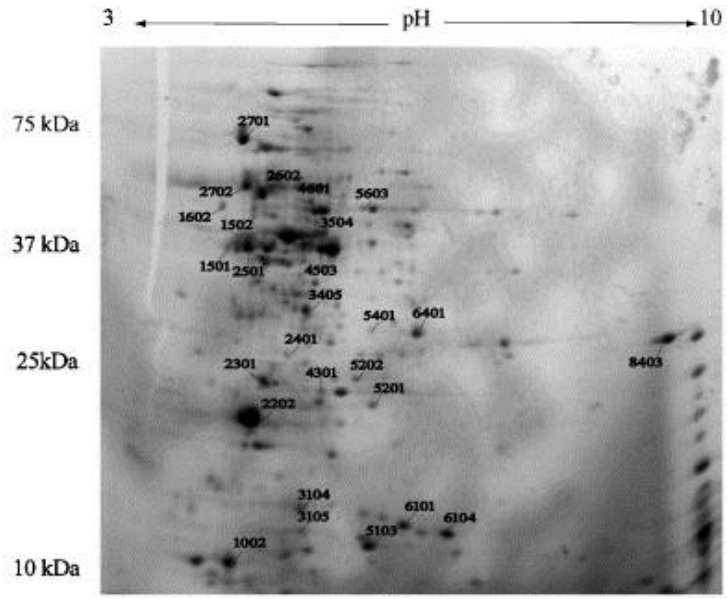

Figure 45. 2-DE image of the total soluble protein extract of V. salmonicida LFI 315. The protein extract was separated on a 13 cm nonlinear pH 3–10 IPG strip, followed by separation on 12% SDS-polyacrylamide gel. Numbers indicate annotated protein spots (see Supplementary Table S9). The protein load was 200 mg (Uttakleiv Ræder et al., 2007b).

Fifty proteins displayed increased spot intensity while 25 proteins demonstrated reduced intensity, when comparing cells grown in the presence and absence of skin mucus proteins. Spots demonstrating significant difference in intensity were processed for protein identification by matching against relevant databases. Successfully annotated protein spots are indicated (Figure 45 and Supplementary Table S9) and the protein identities (Uttakleiv Ræder et al., 2007b).

A comparison in the global protein expression profile of *V. salmonicida*, grown with and without the presence of fish skin mucus in the synthetic media, was affected. The increased levels of proteins involved in motility, oxidative stress responses, and general stress responses were demonstrated as an effect of growth in the presence of mucus compared to non-mucus-containing media (Uttakleiv Ræder et al., 2007b).

Enhanced levels of the flagellar proteins FlaC, FlaD, and FlaE indicate increased motility capacity. In contrast, enhanced levels of the heat shock protein DnaK and the chaperonin GroEL

indicate a general stress response. In addition, it was found that the peroxidases, TPx, Grx, and AhpC, involved in the oxidative stress responses, were induced by mucus proteins. The addition of mucus to the culture medium did not significantly alter the growth rate of *V. salmonicida*. An analysis of mucus proteins suggests that the mucus layer harbours a protein species that potentially possesses catalytic activity against DNA and a protein with iron-chelating activity.

In conclusion, this study represented the first *V. salmonicida* proteomic analysis. It provided specific insight into the proteins necessary for the bacteria to challenge the skin mucus barrier of the fish (Uttakleiv Ræder et al., 2007b).

4. Fish Ecotoxicological Proteomics

It is well known that the chemical analysis of any environmental samples whose primary goal is to assess the pollution status of a specific ecosystem is a nightmare. Indeed, the chemical analysis is incredibly complicated by the complexity of the mixture and by the very low toxicity thresholds of the analytes present. This is why in reality, a proteomics approach must be used that will be capable of detecting the subtle changes in the level and structure of the individual proteins within the whole proteome, which changes in response to the altered surroundings. In addition to identifying new protein biomarkers, it can also help provide insight into underlying mechanisms of toxicity (Nesatyy & Suter, 2008).

Undeniably, the application of proteomics as an indispensable research tool for ecotoxicological investigations has significantly risen in the last two decades. Proteomics provides valuable knowledge and facilitates the interpretation of ecotoxicological mechanisms and to the definition of new biomarkers (Dowling & Sheehan, 2006a; Monsinjon & Knigge, 2007; Pampanin et al., 2014; Qiao et al., 2016; Sánchez et al., 2011; Song et al., 2016). Despite being a comparatively new field, proteomics applications have spread from microorganisms and plants to invertebrates and vertebrates, gradually becoming an established technology used in environmental research (Nesatyy & Suter, 2008).

Ecotoxicological proteomic research activity has tremendously benefitted from the advances in mass spectrometric instrumentation and techniques. The currently available mass spectrometry ecotoxicological proteomic techniques serve as powerful and sensitive tools for protein detection. It is interesting to point out, that some of these MS approaches do not include

sample fractionation prior to analysis; and it becomes extremely simple to achieve initial proteome characterization of the sample material and identify its high abundant proteins (HAPs). To this aim, proteomic, metabolomic and transcriptomic approaches have been applied to farmed and wild fish biofluids and tissues, such as serum, liver, muscle and other organs, with differing degrees of success.

Environmental proteomics has been established as a powerful tool for producing hypotheses regarding how the environment affects the biology of marine organisms. Proteomics study the changes in the abundance of proteins and their post-translational modifications resulting from unknown cellular effects caused by environmental stressors like changes in thermal, osmotic, and anaerobic conditions. In general, proteomic analyses have permitted the characterization of the biological effects of pollutants. It also allowed the identification of comprehensive and pollutant-specific sets of biomarkers, especially those highlighting post-translational modifications.

Furthermore, proteomic analyses of infected organisms have underlined the broader changes occurring during immune responses and how the same pathways are attenuated during the maintenance of symbiotic relationships (Tomanek, 2011).

Finally, proteomic changes occurring during the early life stages of marine organisms emphasize the importance of signalling events during development in a rapidly changing environment. Changes in proteins functioning in energy metabolism, cytoskeleton, protein stabilization and turnover, oxidative stress, and signalling are common responses to environmental change (Tomanek, 2011).

4.1. Can Proteomics Contribute to the Biomonitoring of Aquatic Pollution?

World aquatic pollution is one of the greatest world environmental evils, and developing new biomonitoring tools for its control represents a significant challenge.

Recently, proteomics science has emerged as a powerful environmental monitoring tool that created a vast array of protein biomarkers. Concerning marine environmental monitoring, it has been established that bivalves are the preferred organisms that can be used to assess organic and inorganic pollutants. This is why the bivalves proteome has been intensively studied, and it was demonstrated that heavy metal pollution and organic chemicals are the main cause that alters the degradation of the structural protein of tissues of molluscs.

Similarly, pollution causes structural changes to other proteins involved in stress oxidative metabolism such as glutathione and enzymes as catalase, superoxide dismutase or peroxisomes, which are overexpressed in response to contaminants. It is essential to mention that metabolic proteins can also be used as pollution biomarkers (López-Pedrouso et al., 2020).

Nevertheless, for monitoring freshwater pollution, a great variety of fish and crustaceans can be used in proteomics analyses. In fish species, proteins involved in stress oxidative such as heat shock family or proteins from lipid and carbohydrate metabolism were proposed as candidate biomarkers. On the contrary, for crustaceans, there is a lack of proteomic studies individually assessing the contaminants (López-Pedrouso et al., 2020).

Emerging contaminants and new environmental threats necessitate the development of new approaches and identifying novel biomarkers. The following figure indicates the advantages and drawbacks of proteomic pollution biomonitoring (Figure 46) (López-Pedrouso et al., 2020).

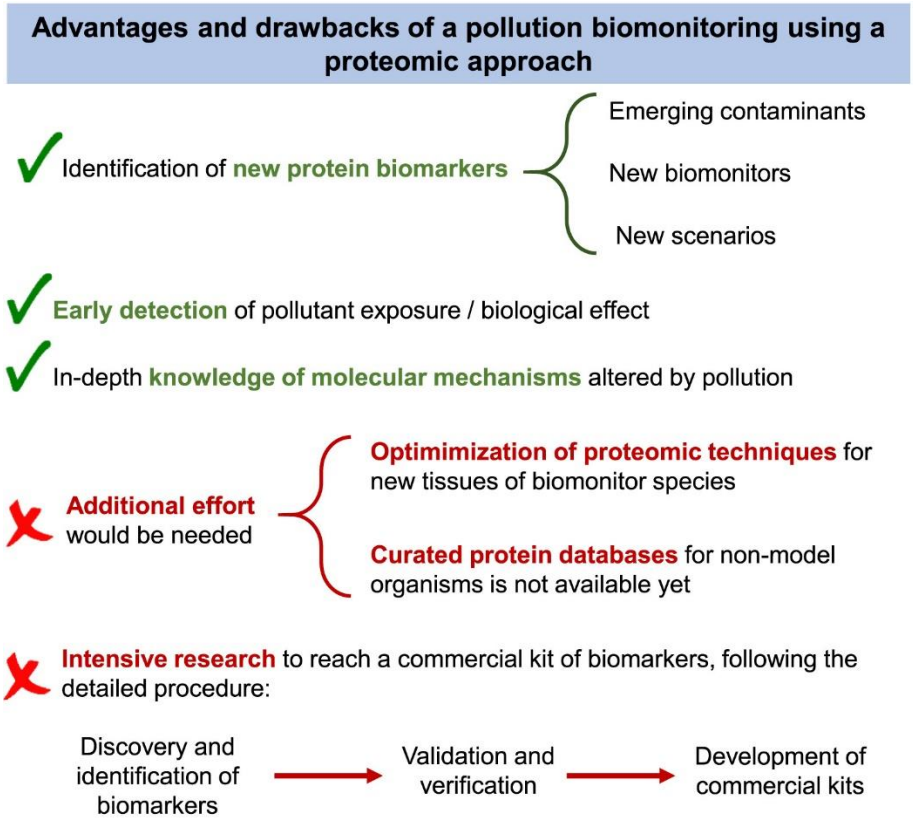

Figure 46. Advantages and drawbacks of pollution biomonitoring from a proteomic point of view (López-Pedrouso et al., 2020).

Consequently, the proteomic approach is the most dynamic and fast-developing methodology that permits field analysis and helps to decipher protein expression. Indeed, protein biomarkers represent the best valuable tool for the early detection of pollutant exposure and even effect evaluation. However, it is essential to say that the establishment of biomonitoring protocols necessitates a great effort due to the seasonal and spatial variability of communities as well as individual variability. Moreover, novel scenarios emerging from contaminants and new threats will require proteomic technology for a systematic search of protein biomarkers and a greater knowledge at the molecular level of those cellular pathways induced by contamination (López-Pedrouso et al., 2020).

4.2. Effect of Copper Nanoparticles Exposure in the Physiology of the Common Carp (*Cyprinus carpio*): Biochemical, Histological an Proteomic Approaches

Copper nanoparticles (Cu-NPs) are serious water pollutants, but their impact on performance on teleosts remains poorly understood. The present study depicted the impact of Cu-NPs exposure in the physiology of the common carp using biochemical, histological and proteome analysis.

Following exposure of freshwater juvenile carps (*Cyprinus carpio*) to two different doses (20 and 100 mg/L) of Cu-NPs for seven days, it was established that the activity of the oxidative stress enzymes: catalase (CAT), superoxide dismutase (SOD), and glutathione-S-transferase (GST), were significantly increased in the kidney, liver and gills of the treated groups when compared to the control (Gupta et al., 2016).

Similarly, the histological analysis revealed that after exposure, disruption of the secondary lamellae of gills, liver damage with pyknotic nuclei and that several proteins were down-regulated. These proteins were consisted of the heavy ferritin chain, rho guanine nucleotide exchange factor 17-like, cytoglobin-1 and up-regulation of diphosphomevalonate decarboxylase and selenide & water dikinase-1 (Gupta et al., 2016).

As expected, the histological tissue analysis after the exposure corroborates the present findings. The two-dimensional gel electrophoresis of the liver identified several differentially expressed proteins after the exposure is shown in Figure 47 (Gupta et al., 2016). Taken together, the present results suggest that short-term exposure to Cu-NPs elicits oxidative stress in the common

carp even at an eco-relevant concentration observed in the environment as a pollutant (Gupta et al., 2016).

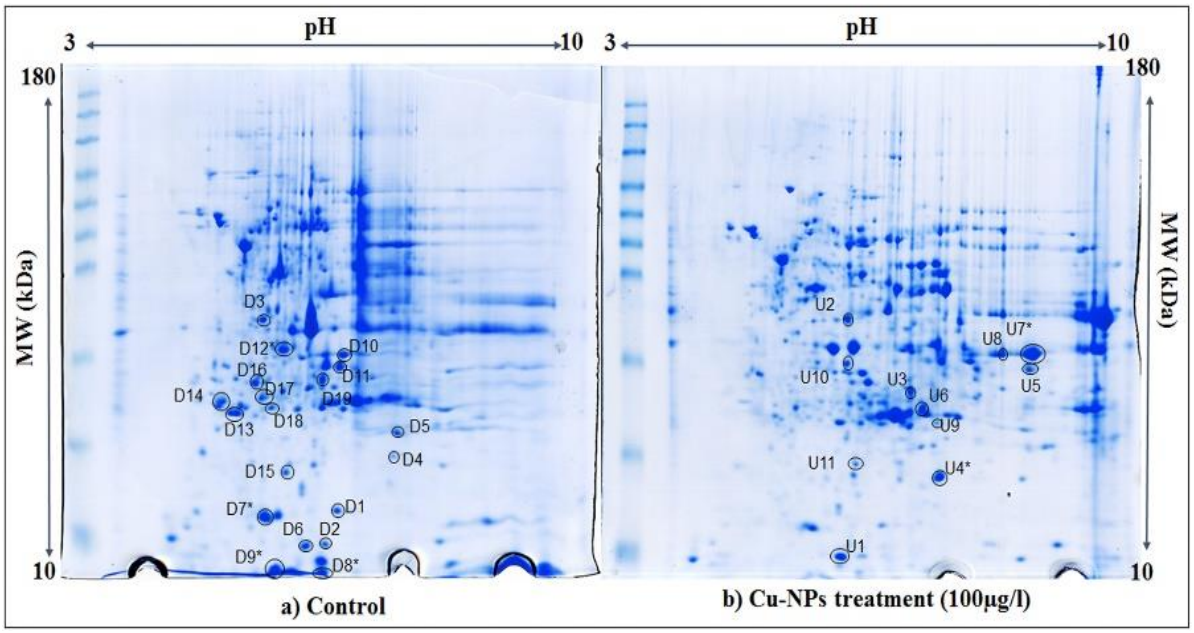

Figure 47. Representative two-dimensional electrophoresis gels of common carp liver (n = 3) following exposure to Cu-NPs for 7 days. (Note: The spots chosen for MALDI-TOF/TOF) (a) Control and (b) Cu-NPs 100mM exposed groups. The coomassie stained 2D-gels from control and treated groups were compared with the Image Master 2D Platinum (GE-Healthcare) system. Spots indicated by circles were found to be up-regulated (U) and down-regulated (D) across the two groups. Spots were: Selenide, water dikinase 1 (UR1), ferritin heavy chain (DR1), rho guanine nucleotide exchange factor 17-like (DR2), Cytoglobin-1 (DR3) and Diphosphomevalonate decarboxylase (DR4) (Gupta et al., 2016).

Table 31. List of identified protein spots from liver tissue of common carp (Gupta et al., 2016).

Sample	Protein name	Score	Molecular weight in kDa	Calculated pI
DR1	ferritin heavy chain	87	20,450	5.26
DR2	PREDICTED: rho guanine nucleotide exchange factor 17-like	43	146,858	6.03
DR3	Cytoglobin-1	37	20,010	5.22
DR4	Diphosphomevalonate decarboxylase	29	45,084	5.97
UR1	Selenide, water dikinase 1	37	43,408	5.65

4.3. **Study of the Plasma Proteome of Atlantic Cod (*Gadus morhua*): Effect of Exposure to Two PAHs and their Corresponding Diols**

It has been established that the presence of polycyclic aromatic hydrocarbon (PAH) contamination in the marine environment represents a major risk to marine life and humans. In this study, plasma samples from Atlantic cod (*Gadus morhua*) were analyzed by the shotgun mass spectrometry approach in order to investigate the plasma proteome response to exposure to single PAHs (naphthalene or chrysene) and their corresponding metabolites (dihydrodiols) (Skogland Enerstvedt et al., 2017).

The plasma protein identification and relative abundance indicated the presence of 369 proteins (780 unique peptides) were identified from the analysis of 51 female (GSI < 1) plasma samples. These 369 proteins were identified and ranked according to their relative abundance. The levels of 12 proteins were found significantly altered in PAH exposed fish and are proposed as new biomarker candidates. Eleven proteins were upregulated, primarily immunoglobulin components, and one protein was downregulated (antifreeze protein type IV.) The uniformity of the upregulated proteins suggests a triggered immune response in the exposed fish (Skogland Enerstvedt et al., 2017).

An overview of the plasma profile is shown in Figure 48, and a complete list of all identified proteins is provided as Supplementary Table S10. The top 2 relatively abundant proteins are both apolipoproteins (i.e. 14 kDa apolipoproteins and predicted apolipoprotein A-I) and represent 51% of the total amount of identified proteins. Further, the top 10 relative abundant proteins represent 64% of the identified proteins. Due to the shotgun MS approach applied, these identified proteins can be categorized as HAPs of the Atlantic cod (female, GSI < 1) plasma proteome. The top 20 HAPs were ranked by the NSAF calculated relative abundance and their GO characteristics are reported in Table 32 (Skogland Enerstvedt et al., 2017).

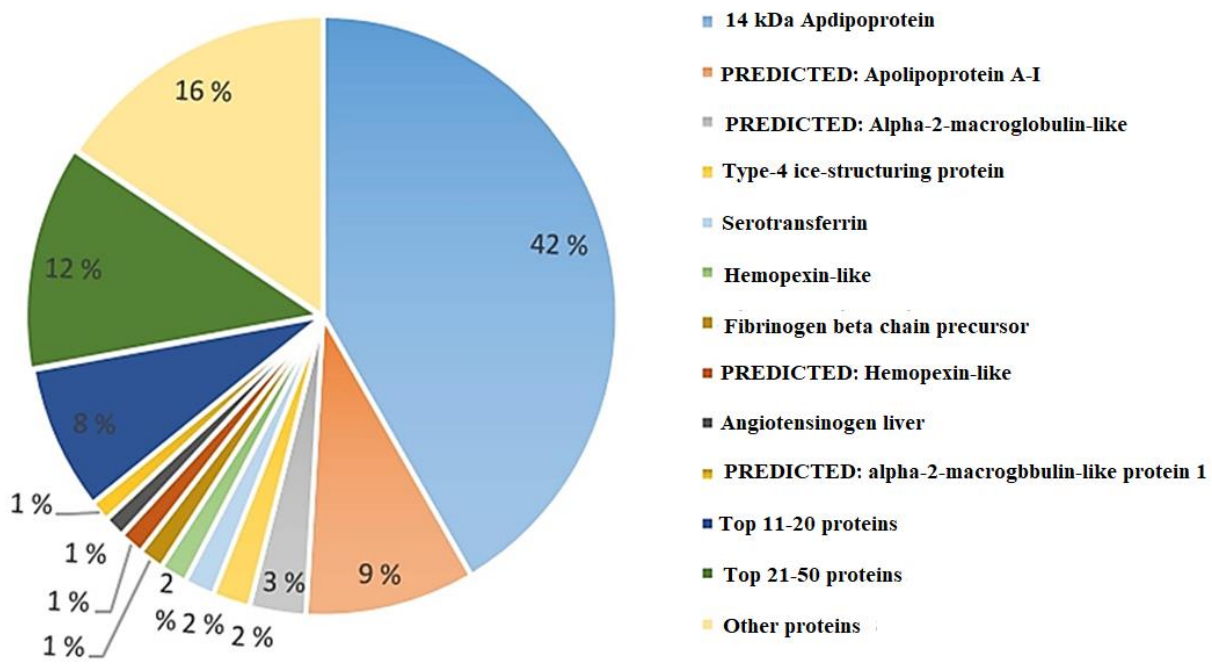

Figure 48. Overview of the plasma protein profile of female Atlantic cod (gonad somatic index < 1, n = 51) identified by shotgun mass spectrometry analysis. Protein relative abundance was calculated according to (Zybailov et al., 2006) and is reported as %. The 10 most abundant proteins are reported individually, while the remaining proteins are grouped as the top 11 to 20 most abundant proteins (top 11–20), the top 21 to 50 most abundant proteins (top 21–50) and the remaining proteins numbered 51 to 369 (other proteins) (Skogland Enerstvedt et al., 2017).

Biological processes and molecular functions associated with these proteins, together with the cellular component that they derived from, are shown in Figure 49. Since there is currently no-GO information for the 14 kDa apolipoprotein (top 1 HAP), this could not be included in the GO distribution charts. Overall, the results provide valuable knowledge for future studies of the Atlantic cod plasma proteome and generate grounds for establishing new plasma protein biomarkers for environmental monitoring of PAH-related exposure (Skogland Enerstvedt et al., 2017).

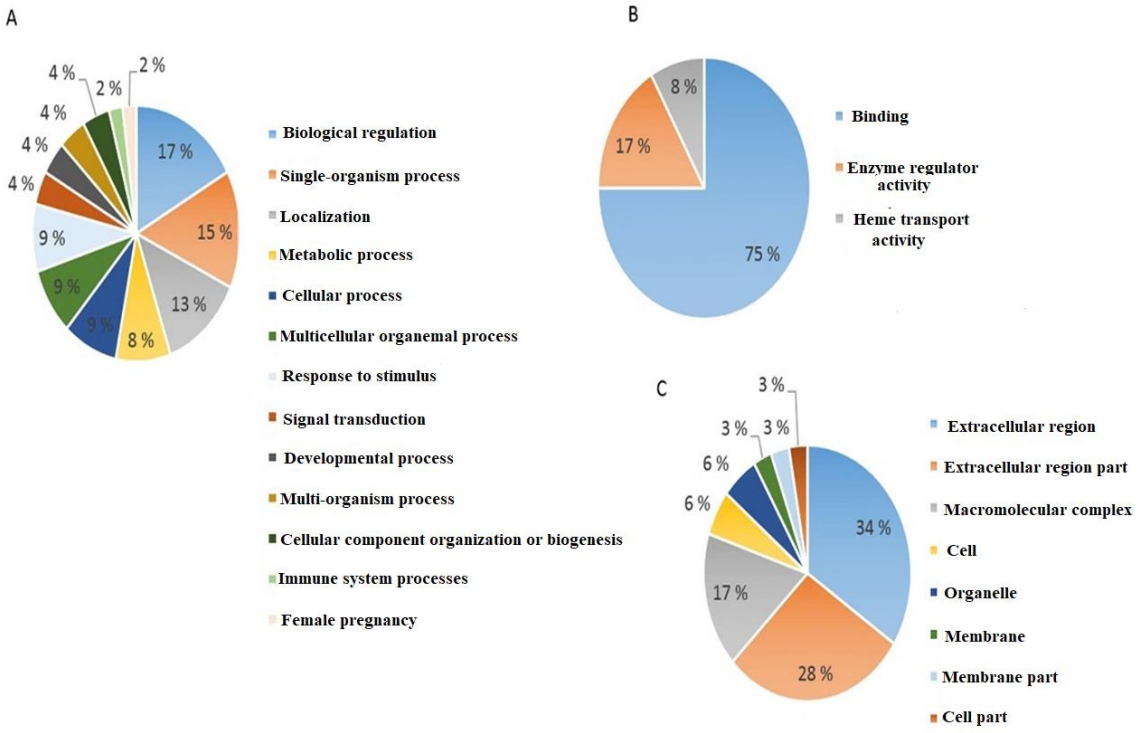

Figure 49. Characteristics of the top 20 high abundant proteins in plasma of Atlantic cod females (gonad somatic index < 1, n = 51). Gene ontology distribution according to: biological processes (A), molecular functions (B) and cellular components (C), results based on the UniProt homolog search (Skogland Enerstvedt et al., 2017).

Table 32. Top 20 high abundant proteins identified in plasma of Atlantic cod females (gonad somatic index < 1, n = 51), calculated according to Zybailov et al. (2006). Proteins are ranked according to their relative abundance, and their respective gene ontology (GO) information of biological processes and molecular function, and the cellular component which they are derived from is reported. The accession numbers behind the protein homolog identities and GO information is given as Supplementary material (Table S10) (Skogland Enerstvedt et al., 2017).

	Protein identification	Biological processes	Molecular function	Cellular component
#1	14 kDa apolipoprotein, partial	information not available	information not available	information not available
#2	PREDICTED: apolipoprotein A-I	cholesterol metabolic process; lipid transport; lipoprotein metabolic process	lipid binding	high-density lipoprotein particle
#3	PREDICTED: alpha-2-macroglobulin-like, partial	regulation of endopeptidase activity	peptidase inhibitor activity; serine-type endopeptidase inhibitor activity	extracellular exosome; extracellular space
#4	Type-4 ice-structuring protein	response to freezing	information not available	extracellular region

#5	Serotransferrin, partial	ion transport; iron ion homeostasis	metal ion binding	extracellular space
#6	hemopexin-like protein, partial	cellular iron ion homeostasis; cellular response to estrogen stimulus	heme transporter activity; metal ion binding	cell; extracellular region
#7	fibrinogen beta chain precursor	platelet activation; protein polymerization; signal transduction	metal ion binding	fibrinogen complex
#8	PREDICTED: hemopexin-like	cellular iron ion homeostasis; cellular response to estrogen stimulus	heme transporter activity; metal ion binding	cell; extracellular region
#9	angiotensinogen	regulation of systemic arterial blood pressure by renin-angiotensin; vasoconstriction	information not available	extracellular space
#10	PREDICTED: alpha-2-macroglobulin-like protein 1, partial	regulation of endopeptidase activity	peptidase inhibitor activity; serine-type endopeptidase inhibitor activity	extracellular exosome; extracellular space
#11	PREDICTED: hemopexin	cellular iron ion homeostasis; cellular response to estrogen stimulus	heme transporter activity; metal ion binding	cell; extracellular region
#12	immunoglobulin light chain L1 region J-C, partial	B cell differentiation; B cell receptor signaling pathway; complement activation, classical pathway; defense response to bacterium; innate immune response; phagocytosis, engulfment; phagocytosis, recognition; positive regulation of B cell activation	antigen binding; immunoglobulin receptor binding	blood microparticle; external side of plasma membrane; immunoglobulin complex, circulating; plasma membrane
#13	No homolog found	information not available	information not available	information not available
#14	PREDICTED: alpha-2-macroglobulin-like	regulation of endopeptidase activity	peptidase inhibitor activity; serine-type endopeptidase inhibitor activity	extracellular exosome; extracellular space
#15	PREDICTED: alpha-2-macroglobulin-like	female pregnancy; negative regulation of complement activation, lectin pathway; stem cell differentiation	calcium-dependent protein binding; enzyme binding; growth factor binding; interleukin-1/8 binding; peptidase inhibitor activity; protease binding; receptor binding; serine-type endopeptidase inhibitor activity; tumor necrosis factor binding	blood microparticle; extracellular exosome
#16	hemopexin	cellular iron ion homeostasis; cellular response to estrogen stimulus	heme transporter activity; metal ion binding	cell; extracellular region
#17	PREDICTED: apolipoprotein C-I-like	lipid catabolic process; lipid transport; lipoprotein metabolic process	lipid binding	chylomicron; very-low-density lipoprotein particle
#18	PREDICTED: complement C1q-like protein 2	negative regulation of ERK1 and ERK2 cascade; negative regulation of fat cell differentiation; negative regulation of fibroblast proliferation	identical protein binding	collagen trimer; extracellular space
#19	PREDICTED: complement C3-like	information not available	information not available	information not available

#20	PREDICTED: apolipoprotein A-IV-like	cholesterol metabolic process; lipid transport; lipoprotein metabolic process	lipid binding	high-density lipoprotein particle

4.4. Alterations in the Atlantic Cod (*Gadus morhua*) Hepatic Thiol-Proteome After Methylmercury Exposure

Methylmercury is a persistent environmental contaminant that has a potent affinity toward thiol groups and can directly bind proteins via available cysteine residues. In this study, Atlantic cod (*Gadus morhua*) liver samples were fractionated using activated thiol sepharose (ATS) to isolate the hepatic proteins containing free/reactive cysteines. This group of proteins is of special interest when studying the physiological effects attributed to methylmercury (MeHg) exposure (Karlsen et al., 2014).

In the present study, following ATS fractionation of the Atlantic cod hepatic thiol-proteome, two-dimensional (2-D) gel electrophoresis comparison allowed to assess the effects of MeHg. Thirteen of the 35 spots, initially identified to differ between treatments, were subsequently analyzed by MALDI-TOF-MS for protein identification (Table 33), and functional annotation. Also, 13 proteins were identified when searching cod-specific databases with acquired mass spectrometry data (Karlsen et al., 2014).

Among the identified thiol-containing proteins, some of which were known to respond to MeHg treatment were identified as follows: constituents of the cytoskeleton, proteins involved in oxidative stress responses, protein synthesis, protein folding, and energy metabolism. Furthermore, methylmercury appeared to affect the hematological system of Atlantic cod heme metabolism/turnover, which creates significantly altered levels of hemoglobin and hemopexin in livers (Karlsen et al., 2014).

Table 33. Differentially Expressed Hepatic Thiol-Proteins Identified With MALDI-ToF MS and MS/MS (Karlsen et al., 2014).

Spot number	Fold change	*p* Value (t-test)	Number of peptides, MS (MS/MS)[a]	Mascot score	Coverage (%)[b]	Protein identity
51	0.61	0.0123	10 (2)	207	73	Hemoglobin, subunit β
53	0.44	0.0018	5 (2)	100	40	Hemoglobin, subunit β
66	1.35	0.0097	11 (1)	92	18	T-complex protein, subunit β
75	1.48	0.0009	7 (1)	62	23	Hydroxyphenylpyruvate dioxygenase

141	1.90	0.0331	18 (1)	127	38	Asparginyl-tRNA synthetase
179	4.09	0.0112	6 (1)	80	28	Hydroxypyruvate isomerase
313	1.43	0.0037	25 (3)	293	39	Heat shock protein 70 kD (HSP70)
328	0.35	0.0215	5 (1)	127	25	Hemopexin
341	2.12	0.0019	24 (3)	232	51	Tubulin, β-chain
343	2.16	0.0003	1 8 (1)	213	47	Tubulin,β-chain
345	1.51	0.0016	10 (2)	128	36	Tubulin, α-chain
346	1.28	0.0235	14 (3)	305	43	Tubulin, α-chain
373	4.53	1.9E-6	8	65	21	DnaJ homolog (HSP40)

[a] Number of tryptic peptides and MS/MS spectra (in parentheses) matching the [b] amino acid sequence. [b] Sequence coverage.

4.5. Study of the Bile Proteome of Atlantic Cod (Gadus morhua): Multi-Biological Markers of Exposure to Polycyclic Aromatic Hydrocarbons

As a developing field in ecotoxicological research and for environmental monitoring purposes, the proteomic approach was used to explore the bile of Atlantic cod (*Gadus morhua*): as a new matrix for monitoring and identifying the source of contaminants in the aquatic environment(Karim et al., 2011), PAH metabolites present in bile are well-known biological markers of exposure in fish, and their investigation is recommended by the ICES (International Council for the Exploration of the Sea) and the OSPAR Convention (Convention for the Protection of the Marine Environment of the North-East Atlantic) for monitoring purposes (Pampanin et al., 2014).

The development of analytical strategies for fish bile is encouraged by the need for more sensitive and informative markers (e.g. capable of tracking the PAH composition of contamination sources) and strengthened by recent results in both fish genomics and proteomics.

The following study represents preliminary testing for discovering new sensitive biomarkers in the form of expressed proteins affected by PAH exposure (i.e. PAH-protein adducts), Juvenile Atlantic cod from Idsefjord (Stavanger, Norway) acclimated for two weeks prior to exposure. After this period, they were exposed to 1 ppm HDF200 base oil, a mud lubricant used in the past in the Tampen area (Norwegian sector of the North Sea). This HDF200 base oil has been prohibited in Norway since 1993. Due to the low amount of available base oil, the exposure was done through the dispersion of oil droplets in the water flow of the exposure tank. In addition, one tank contained control fish, which only received fresh seawater. The experiment was carried out for 30 days in a continuous flow system (CFS) (Sanni et al., 1998). As a positive

control, fish were injected subcutaneously. As a positive control, fish were injected subcutaneously (sc) with benzo[a]pyrene (BaP) (1 mg kg_1 body weight) (Pampanin et al., 2014).

The protein biomarkers were identified using LC-ESI-MS and MS/MS analyses. Through multivariate analyses, the overall proteome was revealed to be a sensitive multi-biological marker of exposure to PAHs. A total of 177 proteins (289 unique peptides) were identified in the bile of Atlantic cod. Protein homologs were identified running a BLASTp search (NCBI) representing the bile proteome of the studied Atlantic cod. Analysis showed that 39 of the identified peptides contained BaP and 30 contained pyrene modifications. Twenty-four unique proteins, i.e. specific protein expressed in at least four samples in a group but absent in the other groups, were found (6 in the control group and 4 in the exposed groups (Pampanin et al., 2014).

Table 34. Selected proteins with selectivity ratio (SR) values above the statistical boundary selected by the DIVA test (Pampanin et al., 2014).

Treatment group	Regulation after treatment	Protein identification	Entry	Selectivity ratio value
HDF200 base oil	Down-regulated	Myeloperoxidase	GENSCAN00000038569	−0.997
	Down-regulated	Serotransferrin	GENSCAN00000019236	−1.165
Benzo[*a*]pyrene	Up-regulated	Hemoglobin alpha chain	GENSCAN00000001677	0.401
	Up-regulated	Uncharacterized protein	GENSCAN00000026681	0.529
	Down-regulated	Saxitoxin and tetrodotoxin-binding protein	GENSCAN00000057737	−0.417
	Down-regulated	Alpha-2 macroglobulin-like	GENSCAN00000008741	−0.440
	Down-regulated	Pleiotopic regulator 1	GENSCAN00000030172	−0.527
	Down-regulated	No homolog	GENSCAN00000073085	−0.628
	Down-regulated	Predicted protein	GENSCAN00000056740	−0.770
	Down-regulated	Serotransferrin	GENSCAN00000019236	−0.853
	Down-regulated	Actin beta	GENSCAN00000005268	−0.400

In addition to plasma albumin, other physiological functions proteins which were altered by the PAHs exposure were detected. These included hemoglobin, which is involved in oxygen transport from gills to all peripheral tissues. Moreover, saxitoxin and tetrodotoxin-binding proteins were also detected, which are involved in toxin transporter activity. Also, the pleiotropic regulator 1 protein, a component of the PRP19-CDC5L, was detected. This complex protein forms the spliceosome and is required for activating pre-mRNA splicing. Finally, actin beta is a member of the actin family was detected (Pampanin et al., 2014)

4.6. **Proteomic Analysis of Sockeye Salmon Serum as a Tool for Biomarker Discovery and New Insight into the Sublethal Toxicity of Diluted Bitumen**

It has been established that the swimming performance of juvenile sockeyes (*Oncorhynchus nerka*) are affected by exposure to diluted bitumen (dilbit). This is why there is a continuous search for biomarkers of dilbit exposure, which permit the monitoring of-risk pacific salmon stocks. For this reason, a study of the serum proteome of sockeye exposed to a sub-lethal and environmentally concentration of dilbit was achieved.

This protoeomic study used isobaric tags for the relative and absolute quantitation (iTRAQ). It also included a range of experimental conditions, which allowed the proper identification of biomarkers across time (1 and 4 wk) and exercise level (at rest and following a swim test) (Alderman et al., 2017).

Over 500 of a total of 513 proteins were quantified by iTRAQ in all 8 sera pools (Supplementary Table S11). Among these proteins, 188 were “unnamed” or “uncharacterized” protein entries in NCBI, accounting for 37% of the quantified portion of the proteome. All but 5 of these unnamed entries were successfully identified in Blast2GO (Supplementary Table S11) and are used throughout the main text and tables. The average protein sequence coverage was 20.4% and ranged from 1 to 84%. The average number of identified peptides per protein was 15.8 and ranged from 2 to 184. The average number of unique peptides per hit was 6.9 and ranged from 2 to 58 (Alderman et al., 2017).

It was found that the abundance of 24 proteins which were identified and quantified in the sockeye serum after dilbit exposure, were significantly altered irrespective of time and exercise. These were the proteins associated with immune and inflammatory responses, coagulation, and iron homeostasis. Also, an increase in creatine kinase (CK) activity in serum was confirmed using iTRAQ analysis.

The combination of 4 wk dilbit exposure and a swim test had a greater effect on the serum proteome than either treatment alone, including a marked increase in tissue leakage proteins, suggesting that aerobic exercise exacerbates the serum proteome response to dilbit, and the increased cellular damage could impede exercise recovery.

In conclusion, this study provided a foundation for the development of biomonitoring tools for salmon stock assessments and offers new insights into the sub-lethal toxicity of crude oil exposure in fish (Alderman et al., 2017).

4.7. **Proteome Profiles in Medaka (*Oryzias melastigma*) Liver and Brain Experimentally Exposed to Acute Inorganic mercury**

Mercuric chloride (HgC_{l2}) is the most toxic form of inorganic mercury in freshwater and marine ecosystems as it readily forms organomercury complexes with proteins (Lorscheider et al., 1995).

In this study, model marine fishes medaka (*Oryzias melastigma*) were acutely exposed to a high concentration of $HgCl_2$ (1000_g/L) for 8 h, and mercury accumulation in the liver and brain was examined after the exposure. The protein expression profiles of the liver and brain of exposed and non-exposed medaka were also analyzed using the proteomic approach, and the altered expression proteins were identified using matrix-assisted laser desorption/ionization tandem time-of-flight mass spectrometry analysis (M. Wang et al., 2011).

The results showed that this acute exposure enhanced mercury accumulation in both livers and brains. Comparison of the two-dimensional electrophoresis protein profiles of the $HgCl_2$-exposed and non-exposed group revealed an altered protein expression, which was quantitatively detected in 20 spots in the brain and 27 in the liver. This series of identified proteins were involved in oxidative stress, cytoskeleton assembly, signal transduction, protein modification, metabolism and other related functions (e.g. immune response, ion regulation and transporting) (M. Wang et al., 2011).

4.8. **Proteomic Sstudy of the Effects of Microcystin-LR on Organelle and Membrane Proteins in Medaka Fish Liver**

Cyanobacteria produce the microcystin-leucine-arginine toxin (MC-LR) during bloom in water reservoirs. MC-LR usually targets fish liver and inhibits the protein phosphatases PP1 and PP2A, leading to diverse cellular. For this reason, the study of the effects of MC-LR on the liver of the medaka fish (*Oryzias latipes*) was affected by a proteomics approach. Accordingly, the phosphorylation and expression states of proteins in the medaka liver following exposure to MC-LR by gavage were analyzed by 2D gels (Figure 50) (Malécot et al., 2009).

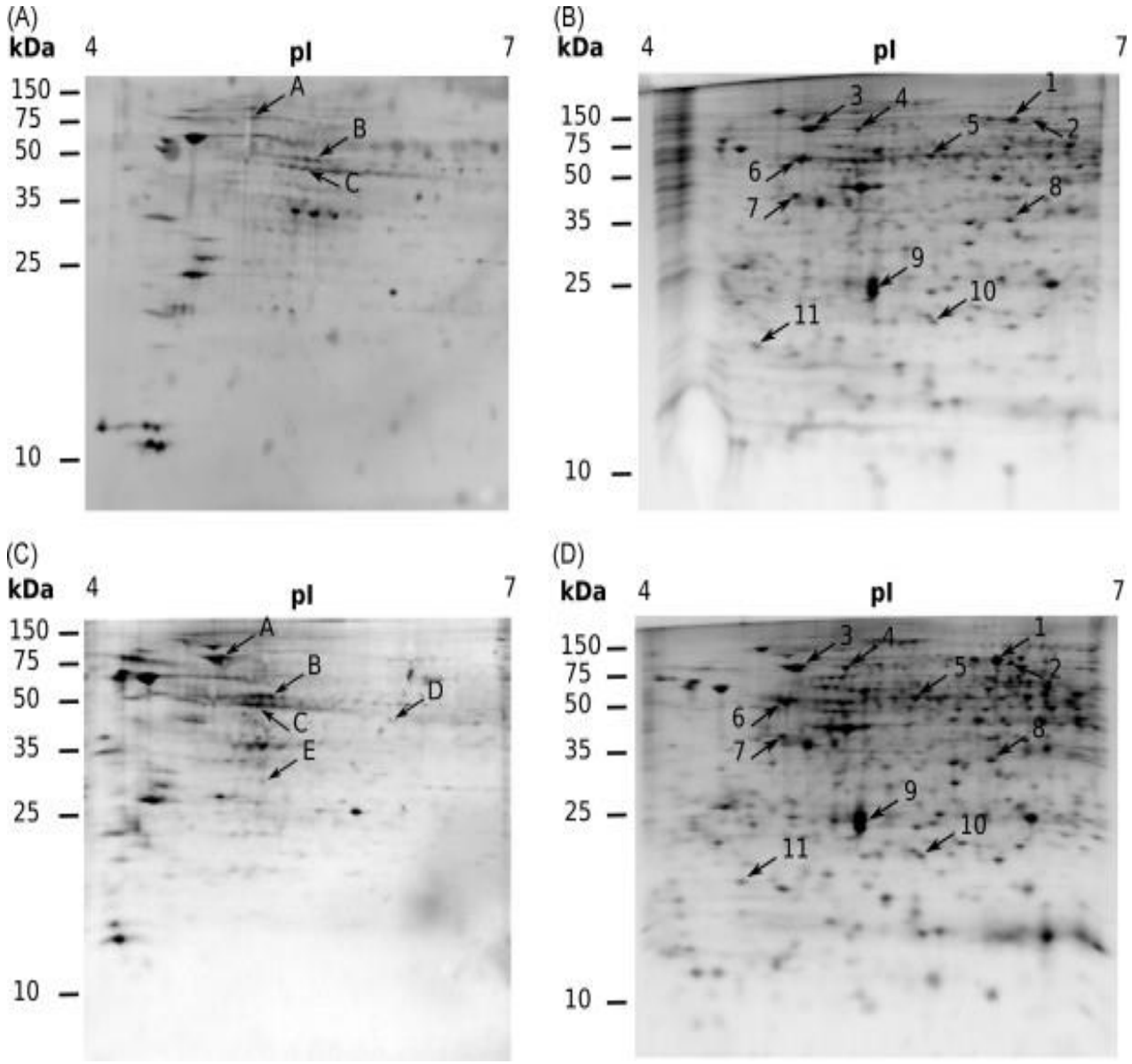

Figure 50. Gels comparison of controls and treated samples. (A and B) Gels from control samples were stained respectively for phosphorylated and all proteins. (C and D) Gels from treated samples were stained respectively for phosphorylated and all proteins. On the four gels are indicated the spots corresponding to identified proteins. Spots numbered with letters are spots with significant statistical phosphorylation variations, and spots with numbers have significant statistical expression variations (Malécot et al., 2009).

It was determined that about 460 spots were counted on gels stained for all proteins (Figure 50 B and D) versus 150 on gels stained for phosphorylated proteins (Figure 50 A and C). This shows that about 30% of the proteins in the membrane and organelle fraction of the liver were

phosphorylated. In addition, differences were detected between gels from the livers of MC-LR-treated fish and control fish. Also, it was noted that many spots displayed different fluorescence signal intensities and consequently different volumes in the two sets. Thus, some proteins apparently displayed different levels of phosphorylation.

Furthermore, the SYPRO gels showed observed modifications that reflect either changes at diverse levels leading to RNA or protein synthesis or stabilities, as well as post-translational protein modifications. Our experiments lasted long enough to comprise all these types of events. Protein spots from the gels corresponding to MC-LR- treated were digested overnight, and the desalted peptides were then analyzed by electrospray mass spectrometry (ESI-MS) (Supplementary Table S12).

The sequencing of these digested peptides was achieved by MS/MS analysis using a hybrid quadrupole time-of-flight (ESI-QqTOF-MS/MS) instrument (Malécot et al., 2009).

To sum it up, it was found that seventeen proteins were identified to be modulated in response to MC-LR treatment. Eight of which were never reported, these were shown to be involved in MC-LR effects: prohibitin, fumarylacetoacetate, protein disulphide isomerase A4 and A6, glucose-regulated protein 78 kDa, 40S ribosomal protein SA, cytochrome b5, and ATP synthase mitochondrial d subunit. These proteins are responsible for protein maturation or in response to oxidative stress. This work highlights the role of organelles in protein processing and the complex cooperation associated with oxidative stress (Malécot et al., 2009).

4.9. Metabolic Changes in Medaka Fish Inducied by Cyanobacterial Exposures in Mesocosms: an Integrative Approach Combining Proteomics and Metabolomics Analyses

In the past decades, cyanobacterial blooms were found to cause serious threats to aquatic organisms and the functioning of aquatic ecosystems. It is also known that cyanobacteria produce a wide range of potentially bioactive secondary cyanotoxin metabolites. The microcystins genus is a prominent member of the freshwater cyanobacteria family, which causes harmful algal bloom-forming and toxin-producing genus in continental aquatic ecosystems that also present a potential risk to aquatic organisms. Also, microcystis is known to produce various bioactive peptides, the microcystins (MCs) that are highly hepatotoxic (Sotton et al., 2017).

For these reasons, the proteomic approach was used to target and monitor the fish response to a cyanobacteria bloom. Therefore, the identities search of the proteinaceous and metabolic changes was initiated to assess the fish exposed to an MC-producing or a non-MC-producing cyanobacterial bloom. This search will support known toxicological knowledge on MC and shed light on fish-cyanobacteria ecotoxicology in natural environments (Sotton et al., 2017).

Medaka fish (*Oryzias latipes*) were exposed for 96 hours either to an MC-producing or to a non-MC-producing strain of *Microcystis aeruginosa*. The cellular, proteome and metabolome changes following exposure to cyanobacteria were characterized in the fish livers. Therefore, a multi-tool approach that combined histology, proteomic and metabolomic analyses was performed on males and females medaka fish (*Oryzias latipes*) exposed for 4 days to environmentally relevant concentrations of an MC-producing (Mcy) or a non-MC-producing bloom (N-mcy) of *Microcystis aeruginosa* (Sotton et al., 2017).

LC-ESI-Q-qOF-MS and MALDI-TOF-MS of the MC-producing strain (Mcy) and the non-MC-producing strain (N-mcy) respectively allowed the detection of a total of 59 and 41 metabolites (Table 35 and Figure 51). Only one metabolite, acutyphicin, was detected in both strains using LC-ESI-QqTOF-MS. However, MALDI-TOF-MS analysis showed that both strains shared 16 other metabolites, including aeruginosins (n = 2), anabaenopeptins (n = 2), radiosumin and 11 uncharacterized metabolites. For the 9 MC variants, 3 were detected only by LC-ESI-QqTOF-MS, and another 3 by MALDI-TOF-MS, while 3 MC variants were detected by both analytical methods. In addition to MCs, other cyanobacterial secondary metabolites include cyanopeptolins (n = 6) (Sotton et al., 2017).

Table 35. Chemodiversity of the experimental cyanobacterial strains revealed by LC-ESI-Q-TOF-MS and MALDI-TOF analyses(Sotton et al., 2017) .

Peptide classes	N-mcy (PMC 570.08)	Mcy (PCC 7820 strain)
Uncharacterized metabolites	+(20)	+(22)
Microginins	+(8)	+(2)
Microcystins	–	+(9)
Aeruginosins	+(3)	+(6)
Anabaenopeptins	+(4)	+(3)
Cyanopeptolins	+	+(6)
Cyclamids	–	+(5)
Acutiphycins	+	+
Cryptophycins	+(2)[#]	–
Aeruginoguanidins	–	+[#]
Comnostins	+[#]	–
Micropeptins	–	+[#]
Mozamides	–	+[#]

Oscillatoxins	–	+#
Radiosumins	+#	+#

The signs "+" or "–" refer to the detection or not of the different peptides classes in each strain. The numbers in brackets relate to the number of compounds and/or variants detected for each peptide class in each strain. The sign "#" refers to an annotation performed thanks to molecular mass estimated using MALDI-TOF analysis, without ESI-MS/MS confirmation.

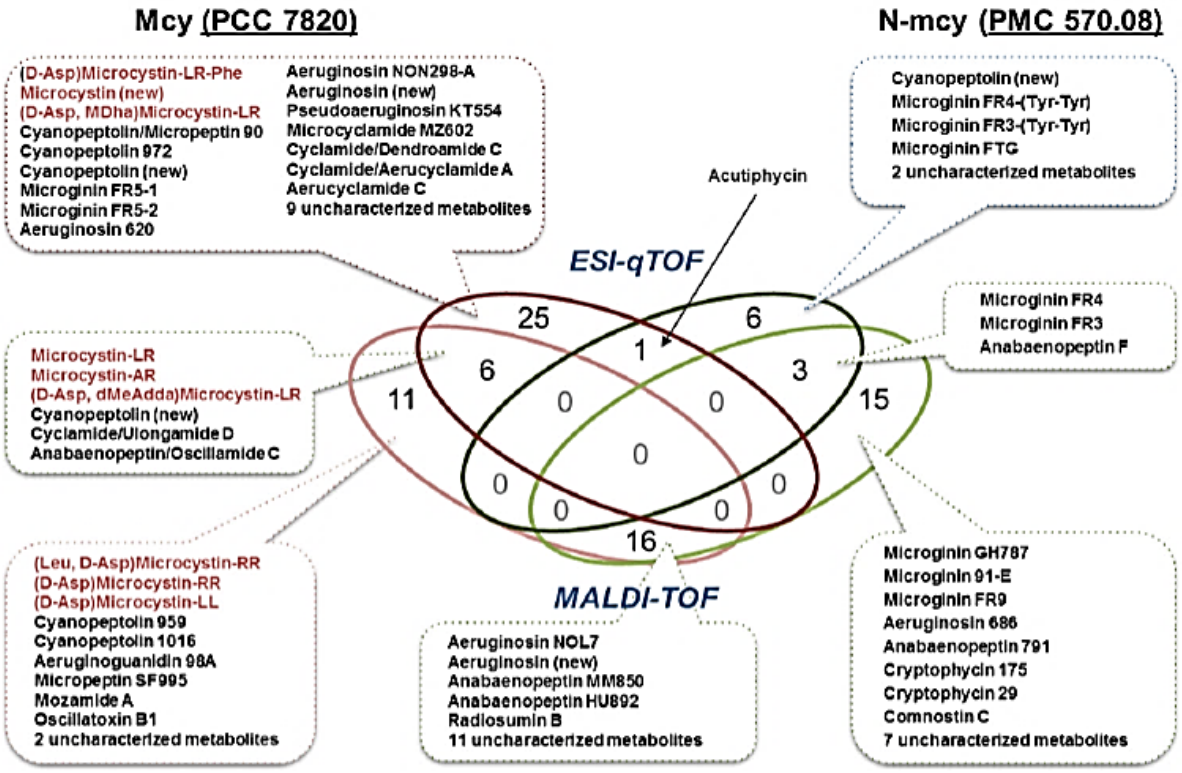

Figure 51. Venn diagram of the chemodiversityrevealed by LC-ESI-Q-TOF-MS and MALDI-TOF in experimental cyanobacterial strains(Sotton et al., 2017) .

A total of 468 and 809 proteins were respectively identified in male and female medaka livers. The quantitative proteomic analysis based on iTRAQ ratios suggested differential expression (log2 (|fold-change|) > 0.3) for 134 proteins. In the female fish, it was found that the number of dysregulated proteins was about 5-fold higher than in males (respectively104 females- and 19 males). Also, it appeared that there were11 common proteins which were dysregulated in both males and females but with specific dysregulation patterns according to the gender and the treatment (Figure 52).

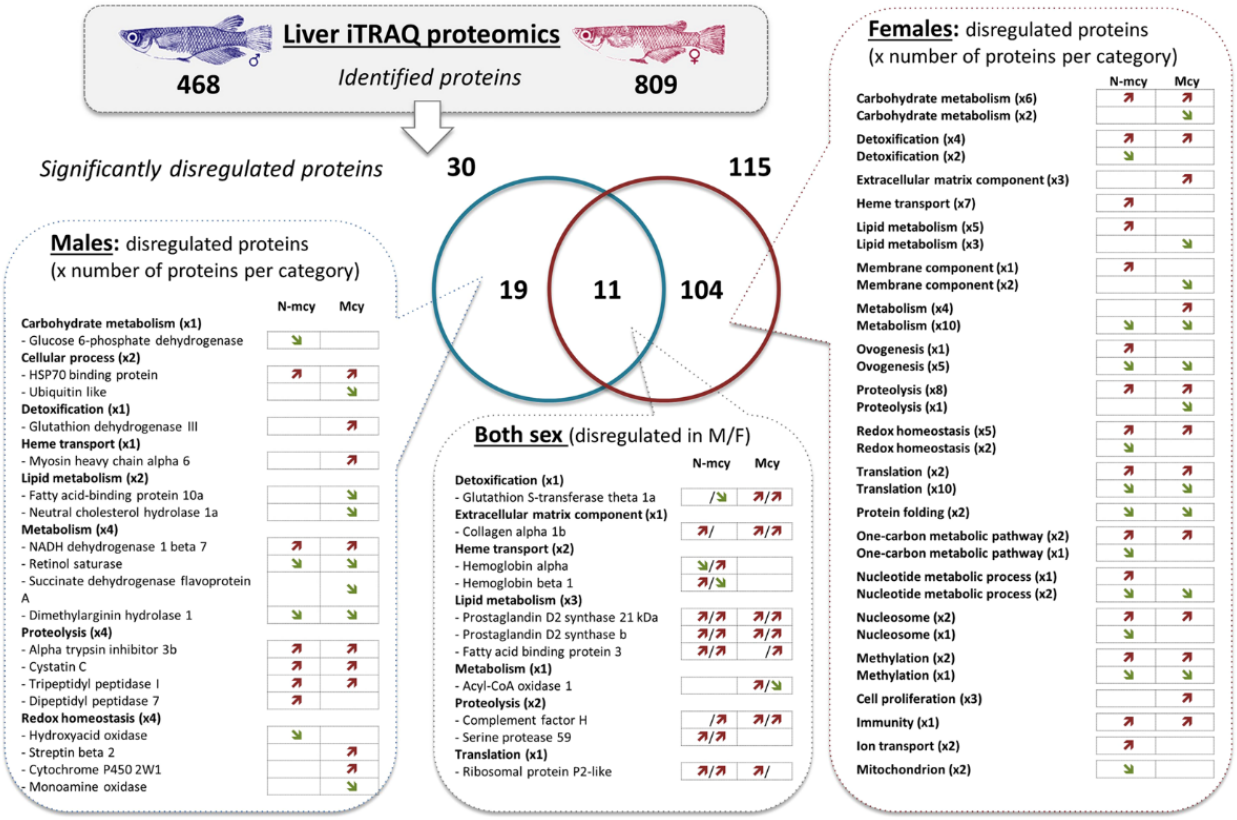

Figure 52. Proteome dysregulations of fish exposed to MCs producing and non-producing strains of cyanobacteria were revealed by iTRAQ proteomic analysis. The dysregulated proteins (log2 (|fold-change|) > 0.3 compared to control fish) were shown. The red and green arrows correspond to up and down-regulated proteins, respectively (Sotton et al., 2017).

Likewise, the N-mcy treated male fishes express three dysregulated proteins that were involved specifically in carbohydrate metabolism, redox homeostasis, and proteolysis processes. Whereas 25 other proteins detected in the female fishes belonged to the detoxification, redox homeostasis, one-carbon metabolic pathway, nucleosome, mitochondrion, ion transport, nucleotide metabolic process, oogenesis, membrane components, lipid metabolism and heme transport (Sotton et al., 2017).

The results obtained in this study concluded that short-term exposure to cyanobacteria (producing or not MCs) created sex-dependent molecular changes in medaka fish without causing any cellular alterations. Generally, following cyanobacterial exposure, it was established that the molecular entities involved in stress response were specifically lipid metabolism and developmental processes. These last two processes displayed the most contrasted changes.

Furthermore, the present study indicates that the proteomic and metabolomic analyses are helpful tools to verify previous information and to additionally bring new horizons concerning the molecular effects of cyanobacteria on fish (Sotton et al., 2017).

4.10. **Proteomic and Phosphoproteomic Analysis of Cellular Responses in Medaka Fish (*Oryzias latipes*) Following Oral Gavage with Microcystin-LR**

Chronic and subchronic toxicity resulting from exposure to microcystins (MCs) receives increasing attention due to the risk of bioaccumulation of these toxins by aquatic animals, including fish. In this work, it was decided to use an alternative way of introducing the toxin into fish; that is by gavage (force-feeding). This gavage was accomplished by using tritiated MC-LR, which permitted quantifying the quantification of the toxin incorporated into fish (Mezhoud et al., 2008).

Consequently, medaka fish were given 5 mg/fish (1 g) MC-LR, which resulted in severe pathological changes in the hepatocytes after 24 h; however, no mortality was observed. Similar experiments using 10 mg/g MC-LR led to a 75% mortality within 4 h. These data mean that the dose 5 mg/g MC-LR can be considered as a toxic interesting upper limit for experimentation in the used condition (Mezhoud et al., 2008).

The mechanisms of action of MCs that target the liver involves modifications of protein phosphorylation resulting from phosphatases 1 and 2A inhibition. Therefore, studying phosphoprotein modifications by using a specific phosphoprotein stain Pro-Q Diamond in fish liver contaminated with MC-leucine–arginine (MC-LR), the most toxic MC, should help dissect disturbed signalling and metabolic networks (Mezhoud et al., 2008).

MC-LR radiolabeling confirmed that the main target of the cyanotoxin is the liver that was reached relatively early as detected by radioactivity in liver samples after 3 h. However, 24 h treatment was necessary to observe hepatocyte morphological alterations by histopathologic examination. To further understand the mechanisms underlying these hepatocyte alterations, a proteomic study was performed on the cytosolic fractions of medaka livers 2 h after MC-LR gavage, which should be enough to provide information on early responses comparable to those obtained in balneation experiments. The identified proteins were modulated either in phosphorylation or in expression and were involved in cell structure alteration or other biological processes such as apoptosis, necrosis and tumorigenesis (Mezhoud et al., 2008).

Since the radiolabeling experiment indicated that MC-LR liver content reached its maximum 3 h after gavage, the authors used a similar treatment duration for the ESI-MS/MS proteomic study. Eighteen and 20 medaka fish were force-fed with water (control) or water contaminated with MC-LR (treated), respectively. After 2 h contamination, livers were extracted, pooled, and a cytosolic fraction was prepared. Image analysis was performed on gels loaded with samples from fishes exposed or not to MC-LR for comparison. Figure 53 shows a 2-D pattern obtained after the separation of 200 mg proteins (Mezhoud et al., 2008).

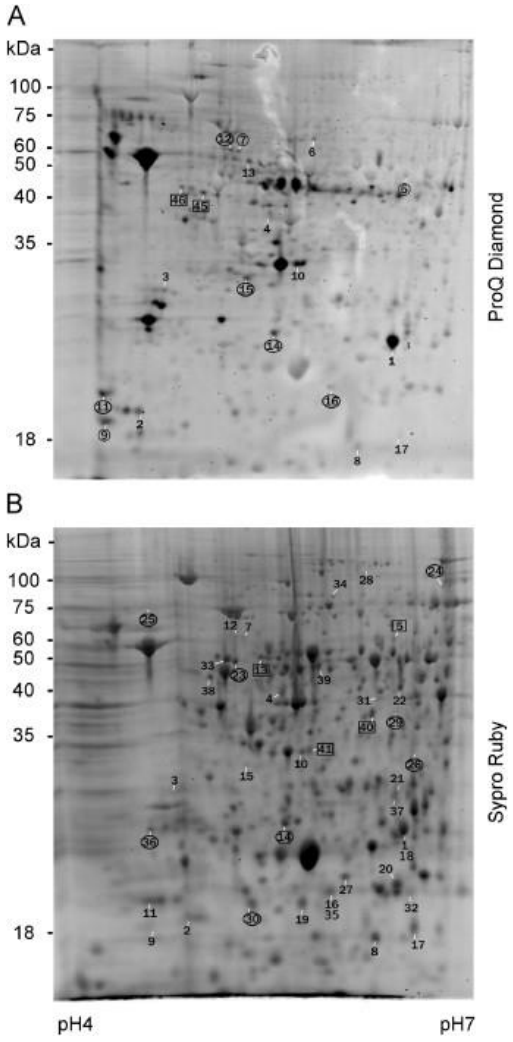

Figure 53. Serial detection of phosphoproteins and total proteins from medaka hepatocyte cytosolic fraction in a 2-DE gel using sequential staining. (A) Gel stained with Pro-Q Diamond phosphoprotein dye. (B) The same gel was stained with Sypro Ruby dye. Protein spots selected for identification were discriminated by the Student t-test and Mann–Whitney test (pp0.05). Numbers inside circles; spots selected from Student t-test only; numbers inside squares; spots selected from Mann–Whitney test only (Mezhoud et al., 2008).

This proteomics study was limited to liver cytosolic proteins of contaminated animals showed that several proteins were up or down-regulated either in quantity or in phosphorylation, or both. Some of them had been previously detected as modified in balneation experiments, but new molecules were identified as involved in signal transduction pathways activated by the toxin. In addition, in the conditions (Mezhoud et al., 2008).

4.11. **Proteomic Modification in Gills and Brains of Medaka Fsh (*Oryzias melastigma*) After Exposure to a Sodium Channel Activator Neurotoxin, Brevetoxin-1**

The marine dinoflagellate *Karenia brevis* is a microscopic, single-celled, photosynthetic organism belonging to the genus *Karenia*. During coastal blooms, *Karenia brevis* produces lipid-soluble polyether toxins (brevetoxins, PbTxs) which are accumulated by shellfish and cause massive fish kills, bird deaths, and marine mammal mortalities (Bossart et al., 1998; Flewelling et al., 2005).

It was established that the massive fish kills were caused due to the depletion of oxygen during biomass decomposition. Similarly, fish kills could be attributed to the accumulation of PbTxs via direct ingestion by *K. brevis* cells or by feeding on contaminated prey, as well as the absorption of toxins across the gill membranes (Pierce & Henry, 2008). It has been suggested that the biological mode of action of the brevetoxins (PbTxs) appears to be produced by absorption across the fish gill membranes. PbTxs cause their acute toxic effects through an ion-channel mediated pathway in neural tissue. However, the exact biochemical mechanism concerning PbTxs neurotoxicity in neural tissue and gas-exchange organs has not been resolved (Tian et al., 2011).

As already mentioned before, the uses of the newer global techniques, such as proteomics, offer novel strategies and excellent tools that can be used for toxicological studies such as the investigation of the cellular responses to toxicants (Dowling & Sheehan, 2006b). In this study, the medaka fish were exposed to a PbTx-1 concentration of 6 µg/L for 2 days, and the protein profiles of the gill and brain were analyzed using the proteomic approach (Tian et al., 2011).

Comparison of the 2-DGE gels of the exposed and non-exposed medaka fish gills indicated a total of 14 protein spots from the PbTx-exposed medaka fish gills, which were found to be significantly altered in abundance (percentage volume ≥ 1.5, $p < 0.05$). Also, one protein spot

disappeared in the PbTx-exposed treatment among these altered proteins, eight protein spots were significantly downregulated, and five were noticeably upregulated (Figure 54) (Tian et al., 2011).

Thirteen protein spots were successfully identified (and all the matched proteins came from the NCBI database for fish species. It is important to indicate that six protein spots (1, 2, 5, 6, 7 and 8) were involved in cell structure; two (spots 9 and 12) were concerned with metabolism, one participating in lipid binding and the other in the carbohydrate metabolism; and five proteins (spots 3, 4, 10, 11 and 13) were involved in signal transduction, mostly in calcium ion binding (Tian et al., 2011).

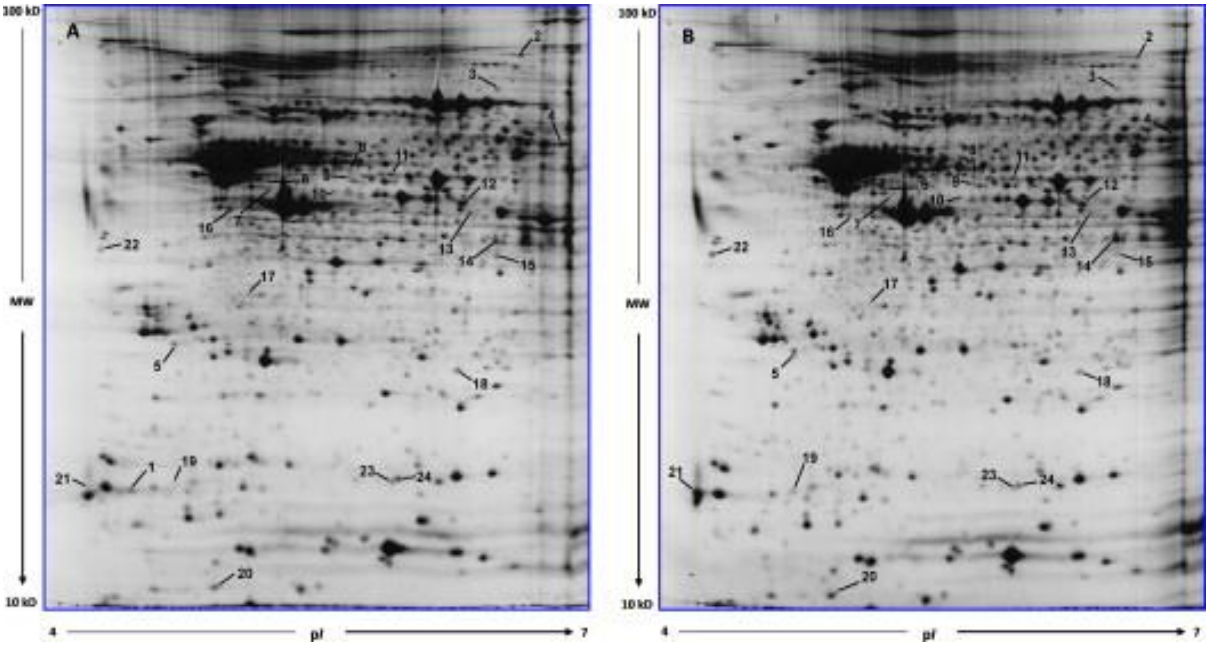

Figure 54. Representative 2-DE gels of brain proteins in the medaka fish after 2 d exposure to PbTx-1. (A) Control and (B) 6 μg/L. The soluble proteins from medaka fish brains were separated using 2-DE and visualized with colloidal Coomassie G-250 staining. The protein spots altered by PbTx-1 exposure are labelled with numbers. The molecular weights (MW) and pI scales are indicated. Each gel is representative of three independent replicates (Tian et al., 2011).

In conclusion, thirteen gill and twenty brain proteins were identified using MALDI-TOF-MS and MALDI-TOF/TOF-MS/MS. These proteins were categorized into diverse functional classes such as cell structure, macromolecule metabolism, signal transduction, and neurotransmitter release. These findings can help to elucidate the possible pathways by which aquatic toxins affect marine organisms within target organs (Tian et al., 2011).

4.12. **Proteomic Changes in the Liver of *Channa striatus* in Response to High-Temperature Stress**

The present study investigated the proteomic changes in the liver of murrel *Channa striatus* exposed to high-temperature stress. Fishes were exposed to 36°C for 4 days, and liver proteome changes were analyzed using gel-based proteomics (2DE, MALDI-TOF-MS) (Table 36) and validation by transcript analysis (Mahanty et al., 2016).

This study showed an increased abundance of two sets of proteins, the antioxidative enzymes superoxide dismutase (SOD), which include ferritin, cellular retinol-binding protein (CRBP), glutathione-*S*-transferase (GST), chaperones HSP60 and the protein disulphide isomerase (which was validated by transcript analysis). Further, gene expression analysis in the fishes exposed to thermal stress for longer durations (30 days experimental exposure in the laboratory and for 30 days beyond, taking Channa collected from a hot spring runoff at 36–38°C); indicated the upregulation of levels of *sod*, *gst*, *crbp*, and *hsp60* at eight-, 2.5-, 2.4-, and 2.45-fold, in the hot spring runoff fish (Mahanty et al., 2016).

Pathway analysis indicated that the upregulations of the antioxidant enzymes and molecular chaperones were induced by the transcription factor Nrf2 (nuclear factor erythroid 2-related factor 2). And, in conclusion, it appears that chronic heat stress is associated with SOD, CRBP, GST, and chaperones HSP60 (Mahanty et al., 2016).

Table 36. Proteins identified in the liver proteome of Channa striatus by MALDI-TOF/TOF-MS Spot (Mahanty et al., 2016).

Spot no.	MASCOT score	Sequence coverage (%)	Theoretical pl value	Protein identified	Species	Accession no.	Fold change	p-value	Peptides matched
CHL-1	46	28	5.60	Superoxide dismutase	*Lates calcarifer*	E7DRM9	↑ 57.92	0.00001	21/52
CHL-2	93	13	5.56	Ferritin	*Salmo salar*	C0H718	↑ 44.84	1.95×10^{09}	3/18
CHL-3	52	15	6.09	Cellular retinol-binding protein	*Danio rerio*	Q8UVG6	↑ 15.62	1.6×10^{46}	3/15
CHL-4	215	13	8.85	Glutathine-Stransferase	*Channa punctata*	E6Y3H0	↑ 11.98	9.9×10^{-11}	4/23
CHL-5	185	8	5.48	Hsp60	*Paralichthys olivaceus*	AOELV5	↑ 11.97	0.0006	5/55
CHL-6	155	10	5.40	Hsp60	*Carassius auratus*	GOGC54	↑ 8.19	9.9×10^{-11}	6/60
CHL-7	74	9	5.40	Protein disulfide isomerase	*Salmo salar*	DOQELO	↑ '9.02	3.3×10^{-10}	5/45
CHL-8	118	6	5.76	Protein disulfide isomerase	*Gasterosteus aculeatus*	G3NVG1	↑ 6.82	7.8×10^{-10}	3/49
CHL-9	196	10	5.76	Protein disulfide isomerase	*Gasterosteus aculeatus*	G3NVG1	↑ 5.53	3.1×10^{-139}	2/22
CHL-10	80	5	5.68	3-Hydroxyanthranilate 3,4-dioxygenase	*Osmerus mordax*	C1 BJQ4	↑ 7.88	0.0001	2/30
CHL-11	42	4	8.40	Malate dehydrogenase	*Danio rerio*	0.7T334	↑ 6.71	0.0002	2/34
CHL-12	83	6	8.51	Glyceraldehyde 3 phosphate dehydrogenase	*Esox lucius*	C1 BX93	↑ 6.54	0.0003	2/33
CHL-13	165	10	8.69	Glyceraldehyde 3 phosphate dehydrogenase	*Oplegnathus fasciatus*	B5AAJ5	↑ 5.79	0.0002	5/34
CHL-14	152	4	6.27	Fumarylacetoacetase	*Osmerus mordax*	C1 BJG5	↑ 5.44	0.0003	2/45

CHL-15	45	2	7.18	δ-1-Pyrroline-5-carboxylate dehydrogenase, mitochondrial	*Danio rerio*	F1 R9W9	↑4.91	8.6×10^{49}	2/46
CHL-16	89	6	6.11	Phosphoglycerate kinase	*Acipenser baerii*	Q76BD4	↑3.96	8.8×10^{47}	3/48
CHL-17	355	6	5.99	Enolase	*Tetraodon nigroviridis*	0.4TBD1	↑9.10	0.0001	3/49
CHL-18	1198	34	5.09	ATP synthase β	*Tetraodon nigroviridis*	Q4S324	↑2.98	2.3×10^{47}	23/52
CHL-19	637	28	5.30	Actin, cytoplasmic1	*Salmo salar*	B5 x 872	↑9.36	5.4×10^{46}	12/38
CHL-20	660	32	5.29	β-Actin	*Misgumus anguillicaudatus*	A11GU7	↑13.46	4.2E-11	12/32
CHL-21	76	10	5.08	β-Actin, cytoplasmic	*Psetta maxima*	A0F027	↑8.28	1.8×10^{46}	5/36
CHL-22	814	25	5.29	β-Actin	*Misgurnus anguillicaudatus*	A11GU7	↑4.17	0.00007	12/32
CHL-23	76	13	6.57	Hemoglobin-β	*Oncorhynchus mykiss*	C1BEM6	↑41.42	1.2×10^{46}	4/15
CHL-24	219	18	6.57	Hemoglobin-β	*Oncorhynchus mykiss*	C1BEM6	No Change	0.18	5/15
CHL-25	95	13	6.57	Hemoglobin-β	*Oncorhynchus mykiss*	C1 B EM6	No Change	0.11	5/18
CHL-26	1819	18	6.57	Hemoglobin-β	*Oncorhynchus mykiss*	C1BEM6	No Change	0.23	5/15

The up (↑) and down (↓) arrows indicate high and low abundance of protein spots.

4.13. Proteomic Analysis of Environmental Stress Response

Thousands of man-made chemicals are annually released into the environment by agriculture, transport, industries, and other human activities. It is well known that the chemical analysis of any environmental samples whose main goal is to assess the pollution status of a specific ecosystem is a nightmare. Indeed, the chemical analysis is greatly complicated by the complexity of the mixture and by the very low toxicity thresholds of the analytes present. This is why in reality, a proteomics approach must be used to detect the subtle changes in the level and structure of the individual proteins within the whole proteome; these changes are caused by the response to the altered surroundings. In addition to identifying new protein biomarkers, it can also help to provide an insight into underlying mechanisms of toxicity. Despite being a comparatively new field with a number of caveats, proteomics applications have spread from microorganisms and plants to invertebrates and vertebrates, gradually becoming an established technology used in environmental research (Nesatyy & Suter, 2008).

This review article highlights recent advances in the environmental proteomics field, mainly focusing on experimental approaches with the potential to understand toxic modes of action and to identify novel ecotoxicological biomarkers (Nesatyy & Suter, 2008).

4.14. Proteomics Analysis of Zebrafish Larvae Exposed to 3,4-Dichloroaniline Using the Fish Embryo Acute Toxicity Test

The zebrafish (*Danio rerio*) is a small teleost fish selected for use during (eco)toxicological studies. International organizations such as ISO and OECD have published specific guidelines for its use in the ecotoxicological assessment of environmental toxicants, such as the Fish Embryo Acute Toxicity (FET) test, OECD n_ 236 guidelines. As a positive control, this protocol uses the aniline pesticide 3,4-dichloroaniline (DCA), which is toxic to fish species at early life stages. Nevertheless, despite using DCA, little is known about the FET test's molecular mechanisms (Vieira et al., 2020).

As a result, this study was devised to investigate changes in zebrafish larvae exposed to DCA (4 mg/L) for 96 hours. Following a gel-free proteomics analysis, 24 proteins were detected in both treated and non-treated groups were identified as significantly affected by DCA exposure, and, when considering group-specific entities, 48 proteins were exclusive to DCA (group-specific proteins) while 248 were only detected in the control group. Furthermore, it was established that

the proteins modulated by DCA treatment were involved in the metabolic processes, especially lipids and hormone metabolism (e.g., Apoa1 and Apoa1b and vitelogenins), in addition to the developmental processes and organogenesis (e.g., Myhc4, Acta2, Sncb, and Marcksb) (Vieira et al., 2020).

Therefore, the results presented here may provide a better understanding of the relationships between molecular changes and phenotype in zebrafish larvae treated with DCA, the reference compound of the FET test (Vieira et al., 2020).

4.15. **Proteomic Analysis of Hepatic Tissue in Adult Female Zebrafish (*Danio rerio*) Exposed to Atrazine**

The herbicide Atrazine (ATZ) is a contaminant of freshwater ecosystems. In the present study, two-dimensional gel electrophoresis and MALDI-TOF-MS combined with histopathological analysis were used to show and detect the hepatic damage in adult female zebrafish (*Danio rerio*) exposed to ATZ. Eight female adult fish (8) were reared in 3 l each solution in an aquarium, and three separate aquaria were used for each treatment. Control female fish were raised in rearing water with 0.1% acetone without ATZ. Whereas female adult zebrafish (8) were exposed toATZ at concentrations of 10 and 1000 lg/l in water containing 0.1% acetone (Jin et al., 2012).

The 2D Gel electrophoresis showed 600 hepatic protein spots, which were visualized with silver staining and most of the proteins' molecular weights ranged from 20 to 70 kD and pH 4–9. The representative 2-DE protein profiles obtained from livers of solvent control 10 and 1000 lg/l ATZ-treated zebrafish are shown in Figure 55 (Jin et al., 2012).

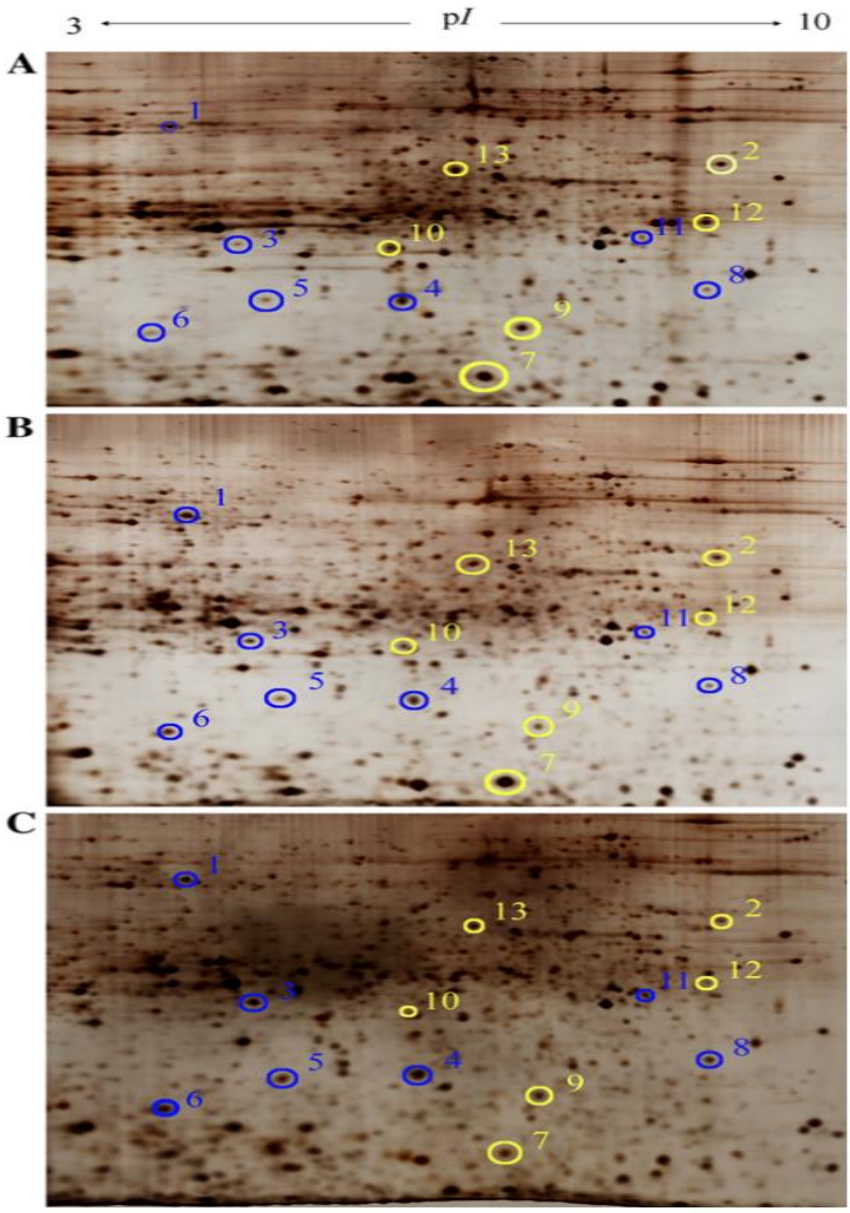

Figure 55. Representative 2-DE protein profiles resolved from hepatic tissues of control adult female zebrafish (a), adult female zebrafish exposed to 10 lg/l ATZ (b), and adult female zebrafish exposed to 1000 lg/l ATZ (c) for 14 days. Proteins were solubilized from zebrafish livers and separated in the first dimension by IEF using Immobiline Dry strips (24 cm), pH 3–10. Separation in the second dimension was performed using 12.5% constant gels, followed by silver staining. Differentially expressed proteins (upregulated: 1, 3, 4, 5, 6, 8, 11; downregulated: 2, 7, 9, 10, 12, 13) were excised from gels and identified by MALDI-TOF-MS (Jin et al., 2012).

Examination of Figure 55 indicates that the protein-distribution patterns of control and exposed fish were similar. However, the intensities of some proteins were influenced significantly

in the liver of the exposed ATZ zebrafish. For example, three proteins (spots 3, 6, and 11) were upregulated >2-fold in the liver after low or high concentrations of ATZ treatment. Three (spots 4, 5 and 8) and one (spot 1) proteins were upregulated >2-fold after 1000 and 10 lg/l of ATZ treatment, respectively. In addition, two proteins (spots 12 and 13) were downregulated <2-fold in liver after ATZ treatment. Three proteins (spots 2, 7, and 10) and one protein (spot 9) were downregulated <2-fold after 1000 and 10 lg/l ATZ exposure, respectively. All of the altered protein spots were submitted for identification using MALDI-TOF-MS analysis and the NCBI nonredundant database. The peptide mass fingerprint spectra profile of spot 1 is shown in Figure 56. In general, the proteins could be identified according to the peptide fragments resulting from digestion by trypsin and matched with the theoretical standard spectra of proteins in the public (Jin et al., 2012).

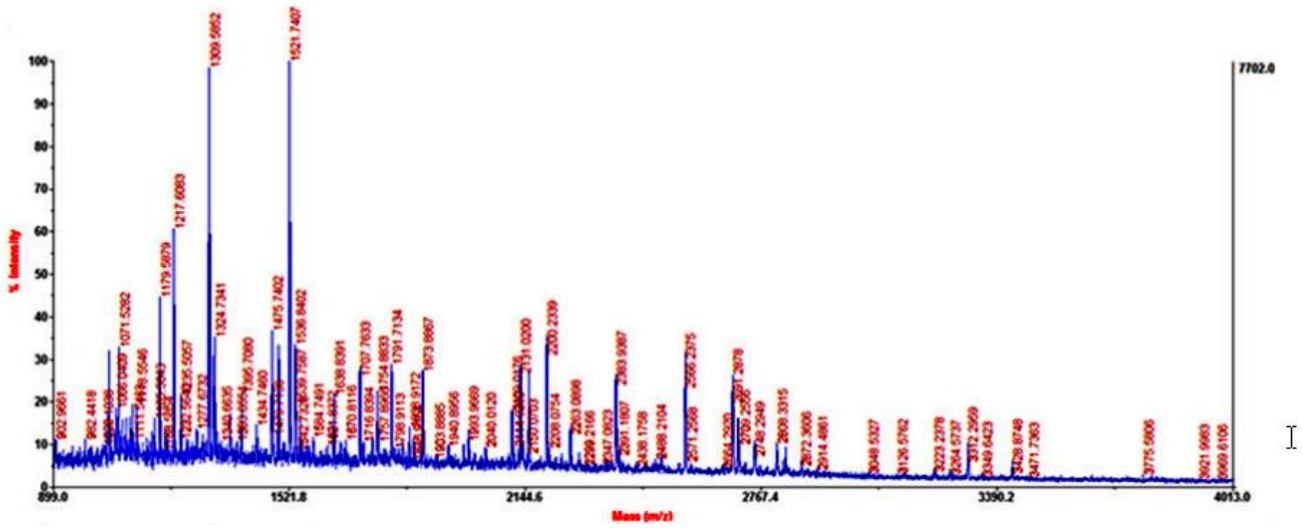

Figure 56. Sliver-stained spot no. excised and destained, followed by enzymatic digestion. Peptides were analyzed with MALDI-TOFMS. After baseline correction, peak deisotoping, and peak detection, the spot was identified as the protein of 4-Hydroxyphenylpyruvate dioxygenase. The fragments of m/z 1071.5283 (FGFEPLAYK), 1217.6082 (QIHTEYSALR), 1309.5852 (NNHFGFGAGNFK), 1324.7352 (EPLFRDPLLPK), 1395.7068 (SIVVTNYEETIK), 1521.7402 (SLFEAIEKDQDAR), 1745.8834 (GAAVLKEPWVEQDAGGK), 1873.8875 (GLEFLSAPDNYYESLR),2109.0183 (FWSIDDKQIHTEYSALR), 2131.0193 (GLEFLSAPDNYYESLREK), and 2566.2371 (YAIVQTYGDTTHTFVEYLGPYK) are included in the identification (Jin et al., 2012).

This study showed that these changed proteins were associated with various cellular biological processes, such as response to oxidative stress, oncogenesis, etc. The results demonstrated that ATZ comprehensively influenced a variety of cellular and biological processes in zebrafish. The information presented in this study will be helpful in fully understanding the mechanism of the potential effects induced by ATZ in fish (Jin et al., 2012).

4.16. **The Effect of Environmental Salinity on the Proteome of the Sea Bass (*Dicentrarchus labrax L.*)**

The European sea bass, *Dicentrarchus labrax L.*, tolerates a range of salinities from freshwater to hyper-saline. The present work aimed to investigate whether there were changes in the sea bass gill and intestinal epithelial proteome, which altered during acclimation from seawater into freshwater, and, tentatively, to identify differentially expressed proteins. These patterns could provide useful biomarkers of freshwater transition (Ky et al., 2007).

Therefore, to investigate the differences in protein expression, fish were reared in both freshwater and seawater. After 3-month acclimation, gill and intestine epithelia were collected, and the soluble protein was extracted. To this end, high-resolution two-dimensional gel electrophoresis (2-DE) separated the proteins according to their isoelectric point, and molecular weights were determined with mass spectrometry (MS). Specific proteins were identified from the Actinopterygian class. In addition, transcript abundances of some identified proteins were evaluated by RT-PCR (real-time polymerase chain reaction) to investigate their regulatory effect during osmotic acclimation. It was established that all 362 spots were differentially expressed in the gills and intestines of fishes reared in seawater compared to those from freshwater. Fifty differential protein spots were excised from a colloidal Coomassie-stained gel. Nine different protein spots were identified unambiguously by mass spectrometry and database searching (Ky et al., 2007).

Among the six proteins over-expressed in gill cells in seawater, five were cytoskeleton proteins and one was the aromatase cytochrome P450. In gill cells under freshwater conditions, the two over-expressed proteins identified were the prolactin receptor and the primary histocompatibility complex class II b-antigen. In intestinal cells under freshwater conditions, the Iroquois homeobox protein Ziro5 was upregulated over ninefold. The expression of these proteins, their possible direct

or indirect roles in the adaptation of D. labrax to salinity, and their correspondences with a previous study are discussed (Ky et al., 2007).

This study constitutes the first differential proteomic display approach on the response to changes in salinity by sea bass. 2-DE coupled with MALDI-TOF MS analysis on gills and intestine allowed the identification of proteins involved (Table 37), directly or undirectly, in cell functions related to osmoregulation, such as cell structure modification, immune system and development responses (Ky et al., 2007).

The study also showed the complementary nature of the proteomic approach compared to that of the transcriptome (Boutet et al. 2006). Indeed, three cases were found: (i) same molecules with both approaches, such as the cytoskeleton element in the same tissue and under the same water conditions; (ii) molecules found only by proteomics, such as PRL-R and aromatase cytochrome P450; and (iii) molecules found only by the transcriptomics, such as the well-known osmoregulated co-transportor Na+K+ ATPase alpha 4 (Ky et al., 2007).

Identified proteins involved in the osmoregulatory cascade, and which are regulated at both transcriptomic and proteomic levels, seem to be good candidate genes involved in physiological and morphological changes in the osmotic response. A further step would be to inquire into the functions of the identified proteins in the osmoregulatory process. The localization of these proteins and their transcripts from osmoregulatory organs during osmotic acclimation should be investigated. In addition, the regulatory elements of identified proteins offer an interesting route to search for polymorphisms responsible for individual fluctuations in acclimation to variations in salinity (Ky et al., 2007).

Table 37. Protein spots isolated from 2-D gels identified by MALDI-TOF mass spectrometry combined with searches in the MASCOT database restrained to Actinopterygii (Ky et al., 2007).

Protein name (species)	Accession (Swiss prot)	Protein function	Spot no.	Expression factor (SW/FW)	Tissue	MASCOT score	Sequence coverage	MW (theor/exp)
Tubulin a *(Brachydanio rerio)*	042271_BRARE	Cytoskeleton	28	SW-specific	Gills	121	26	0.98
Iroquois homeobox protein ZiroS *(8rachydanio rerio)*	090YM9_BRARE	Development	544	0.1	Intestine	59	28	2.33
Actin, cytoplasmic 2 *(Takifugu rubripes)*	ACT82_FUGRU	Cytoskeleton	417	4.8	Gills	116	33	1.09
Prolactin receptor *(Sparus aurata)*	Q9DFUO_SPAAU	Osmoregulation	257	0.3	Gills	85	31	2.71
Actin-like protein 3 *(Takifugu rubripes)*	ARP3_FUGRU	Cytoskeleton	148	2.9	Gills	99	18	1.06
MHC class II ft-antigen (fragments) *(Salmo sa/ar)*	A1Y9R3_SALSA	Immune system	618	0.4	Gills	79	48	1.13
Cytochrome P450 aromatase *(Oreothromis mossambicus)*	Q9W6M1_0REMO	Reproduction	36	2.1	Gills	87	23	2.64
Tubulin *a* (fragment) *(Notothenia coriiceps)*	Q9DF58_9PERC	Cytoskeleton	509	2.0	Gills	111	28	0.89
Actin *a,* cardiac *(Takifugu rubripes)*	ACTC_FUGRU	Cytoskeleton	529	1.8	Gills	85	20	1.09

4.17. A Proteomics Approach Reveals Divergent Molecular Responses to Salinity in Populations of European Whitefish (*Coregonus lavaretus*)

Osmoregulation is a vital physiological function for fish, as it helps maintain a stable intracellular concentration of ions in environments of variable salinities. A study on the freshwater species, the European whitefish (*Coregonus lavaretus*), was initiated to investigate the molecular mechanisms underlying salinity tolerance. It was also devised to examine whether these molecular mechanisms differed between genetically similar populations that spawn in freshwater (FW) vs. brackish (BW) water environments (Papakostas et al., 2012).

A common garden experiment involving 27 families in two populations and five salinity treatments was conducted. This experiment was to monitor in each studied populations the phenotypic and proteomic responses during early development, from fertilization till hatching. It was found that salinity had a highly significant effect on the fertilization success and the survival of the FW whitefish. Whereas, BW whitefish performed nearly equally in all salinity treatments.

Proteins were isolated using standard sodium dodecyl sulphate (SDS)- based extraction method and digested in-solution. The proteins were identified by label-free shotgun quantitative proteomics method using Nano-LC-ESI-MS/MS. The protein quantification was based on both unique and 'razor' peptides. 'Razor' peptides have been defined as shared peptides that are most sparingly associated with the group that has the highest number of identified peptides (Cox & Mann, 2008; Nesvizhskii & Aebersold, 2005). The use of both unique and 'razor' peptides for protein quantification are suggested to be a good compromise between unequivocal peptide assignment and more accurate quantification (Cox et al., 2011; Cox & Mann, 2008). After removing contaminants and reverse hits (Supplementary Table S13), a total of 1500 proteins and protein groups were quantified (Papakostas et al., 2012).

These proteins were identified on the basis of 8160 highly confident peptides, of which 6696 were unique (Supplementary Table S13). The mean sequence coverage was 22.32% (all peptides), 15.74% (unique peptides) or 18.67% ('razor' and unique peptides that were used for quantification). On average, each protein was quantified by 5.44 peptides. Overall, 73 (q-value = 0.18) and 42 (q-value = 0.31) proteins were differentially expressed between salinity treatments in FW and BW whitefish, respectively (Papakostas et al., 2012).

Of these proteins, only six were common to both populations. In the FW whitefish, most of the significant proteins (61) were overexpressed in 10 ppt salinity, and only 12 were under expressed.

Similarly, in BW whitefish, most of the significant proteins (34) were over expressed in 10 ppt, and only eight were under expressed (Figure 57) (Papakostas et al., 2012).

It was concluded that each studied populations displayed severely different phenotypic and proteomic responses to salinity. The response obtained for the freshwater-spawning whitefish showed a significantly higher mortality rate with higher salinity treatments. It was also recognized that the ion calcium involved in osmotic stress sensing, had a fundamental role in the observed proteomic responses (Papakostas et al., 2012).

On the other hand, brackishwater spawning fish were capable of viable osmoregulation, which was modulated by cortisol, an important seawater-adaptation hormone in teleost fish.

In conclusion, it was found that several identified proteins played key roles in osmoregulation, most importantly the highly conserved cytokine and the tumour necrosis factor. Also, it was established that the calcium receptor activities were also associated to salinity adaptation (Papakostas et al., 2012).

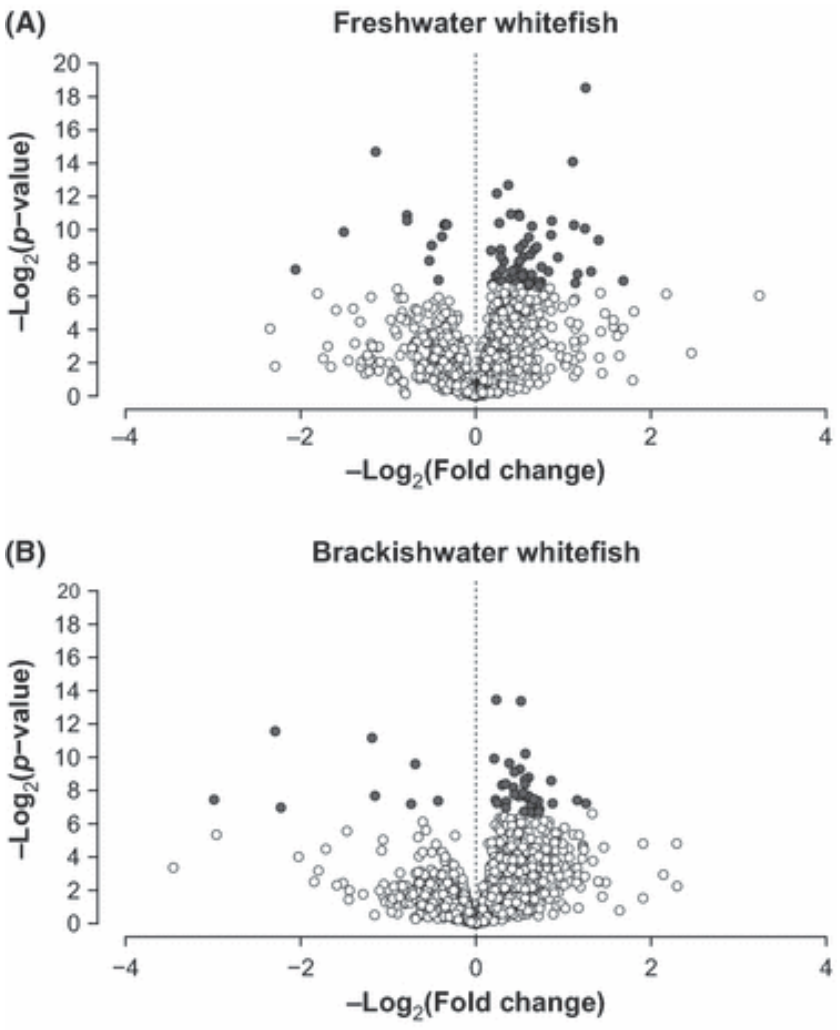

Figure 57. Scatter plots showing the distribution of the protein expression measurements for the 1500 quantified proteins in the two whitefish populations, according to the -log2 P value of the ANOVA test and the -log2 fold change in expression between the 0 ppt and 10 ppt salinities. Dark circles indicate proteins with P < 0.01, and positive fold changes represent upregulation in higher salinity. (A) In the brackishwater whitefish, 34 proteins were significantly upregulated and eight significantly downregulated in 10 ppt salinity. (B) Likewise, freshwater whitefish had 61 and 12 proteins significantly up- and downregulated in 10 ppt salinity, respectively (Papakostas et al., 2012).

These results imply that individuals from these populations are most likely adapted to their local environments, even though the baseline level of genetic divergence between them is low (FST = 0.049). They also provided excellent clues for choosing candidate loci for studying the molecular basis of salinity adaptation in other species. In conclusion this approach provided an example of how

proteomic methods can be successfully used, to obtain novel insights into the molecular mechanisms behind adaptation in non-model organism (Papakostas et al., 2012).

4.18. Proteomic Analysis of Fathead Minnows (*Pimephales promelas*) Fish Exposed to Individual Insecticides and a binary mixture

The health and reproductive status of aquatic organisms can be negatively impacted by exposure to organophosphate (OP) and pyrethroid insecticides (Baldwin et al., 2009; Biales et al., 2011; Dutta et al., 2006). Permethrin is a type 1 pyrethroid pesticide known to reduce the open state of the brain's Na+ channels, resulting in the nervous system's hyperactivity (Toshio, 1992). In addition, permethrin is a suspected endocrine disruptor. Similarly, terbufos is an OP insecticide/nematicide, which is highly toxic to freshwater fish species. Generally, OP pesticides, are acetylcholinesterase (AChE) inhibitors known to reduce plasma, brain and red blood cell (RBC) cholinesterase activity. Although these two classes of insecticides are the most heavily used and highly toxic to fish, the molecular mechanisms underlying the toxic effects of sub-lethal exposure to these pesticides are unclear (Biales et al., 2011).

The current work aims to identify and compare differentially expressed proteins in brains of male fathead minnows (*Pimephales promelas*) exposed for 72 h to permethrin (7.5_g/L), terbufos (57.5_g/L) and a binary mixture of both. As a result, it was possible to identify 24 differentially expressed proteins among all of the treatment groups that were exposed to terbufos, permethrin, and to the binary mixture of both relative to unexposed control organisms. Fifteen of these proteins were clearly identified using LC–ESI-MS/MS (Biales et al., 2011).

Little overlap in differentially expressed proteins was observed among treatments. However, proteins involved in glycolysis, hypoxia, the UPS and cytoskeletal dynamics were seen in all three groups suggested a potential role of these cellular activities in pesticide toxicity. Moreover, many of these processes have been previously associated with neuropathologies, such as sporadic Parkinson’s disease (PD) (Biales et al., 2011).

Table 38. Functional annotation clusters for identified proteins calculated using DAVID software (Biales et al., 2011).

Mixture			
Annotation cluster 1	Enrichment score: 1.94		
	Term	*p*-value	Fold enrichment
	IPR016040:NAD(P)-binding domain	0.002	37.9
	Genes		
	GAPDH		
	LDHB4		
	VAT1		
	GO:0016491~oxidoreductase activity	0.004	9.5
	Genes		
	GAPDH		
	LDHB4		
	VAT1		
	P4HB		
Annotation cluster 2	Enrichment score: 1.09		
	Term	*p*-value	Fold enrichment
	GO:0006091~generation of precursor metabolites and energy	0.004	26.1
	Genes		
	ATP6V1AL		
	LDH-B4		
	GAPDH		
Terbufos			
Annotation cluster 1	Enrichment score: 0.87		
	Term	*p*-value	Fold enrichment
	GO:0009056~catabolic process	0.013	12.3
	Genes		
	Hexokinase 1		
	PGK1		
	Proteasome 26S subunit		

The results of the current work demonstrate that both permethrin and terbufos, acting independently, are capable ofeliciting a proteomic response in the brains of fathead minnows exposed for 72 h. The proteomic response to the binary mixture was largely different from that observed in either of the individual exposures. Of the 12 proteins found to be differentially expressed in the mixture exposure, ten were unique to the mixture (Figure 58) (Biales et al., 2011).

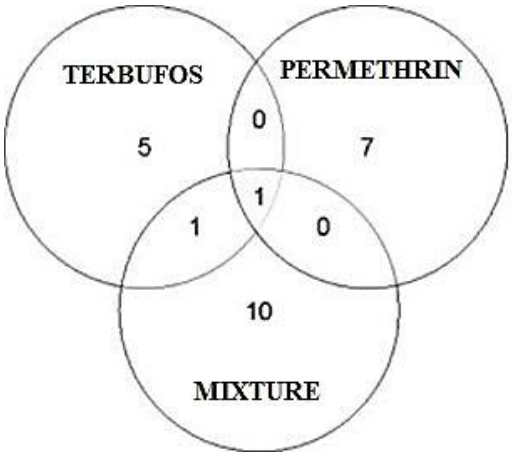

Figure 58. Venn diagram of differentially expressed proteins. Proteins were identified as differentially expressed relative to control through a Dunnett's test (p≤0.05)(Biales et al., 2011).

Although it was established that it was impossible to generate a useable PES for terbufos, it was also found that it was possible to generate the PES for permethrin between control and permethrin-exposed individuals with an accuracy of 87.5%. The present work clearly indicates that the PES can be useful in characterizing environmental exposures of non-target aquatic organisms to permethrin. In addition, it will give to environmental risk assessors a valid means of reducing the complexity of real-world exposure scenarios (Biales et al., 2011).

4.19. **Liver Proteomics of Gilthead Sea Bream (*Sparus aurata*) Exposed to Cold Stress**

The gilt-head (sea) bream (*Sparus aurata*) is a fish of the bream family *Sparidae* found in the Mediterranean Sea and the eastern coastal regions of the North Atlantic Ocean. This species is very sensitive to low temperatures, which causes fasting and reduced growth performances. For this reason, it became essential to understand and optimize specific aquaculture practices for the winter period (Ghisaura et al., 2019).

It should be understood that when farmed sea breams live in outdoor tanks and in floating sea cages, for prolonged exposure to temperatures below 13 °C, they are unable to avoid this thermal stress and results in a decrease in activity (Ibarz et al., 2003), growth delay (TORT et al., 1998), metabolic depression (Sanahuja et al., 2019; Sánchez-Nuño, Eroldogan, et al., 2018) and reduced feed consumption. (Ibarz, Padrós, et al., 2010). Additional physiological alterations comprise the hepatic functionality, in which the liver becomes steatosic and whitish due to a large deposition of lipids, as

well as reduced efficiency of adaptive immunity with increased susceptibility to infections (winter syndrome or winter disease) and alteration of the main redox pathways (Abram et al., 2017; Ibarz et al., 2005, 2007; Sánchez-Nuño, Sanahuja, et al., 2018).

In order to study the impact of cold on fish metabolism and their development, an 8 week feeding trial was carried out on gilthead seabream juveniles reared in a Recirculated Aquaculture System (RAS). This system permitted to change the temperature ramp in two phases of four weeks each: a cooling phase from 18 °C to 11 °C and a cold maintenance phase at 11 °C (Ghisaura et al., 2019).

It was noted that along with the whole trial, the sea breams experienced several changes in their liver protein abundance. These occurred mostly during the cooling phase when catabolic processes were mainly observed, including protein and lipid degradation, together with a reduction in protein synthesis and amino acid metabolism. A decrease in protein mediators of oxidative stress protection was also seen. Liver protein profiles changed less during cold maintenance, but pathways such as the methionine cycle and sugar metabolism were significantly affected (Ghisaura et al., 2019).

The liver protein profiles were assessed with a shotgun proteomics workflow based on filter-aided sample preparation (FASP) and liquid chromatography-electrospray-mass spectrometry (LC-ESI-MS and MS/MS) followed by label-free differential analysis. This study showed that a total of 42 proteins showed statistically in abundance at t_1 *vs* t_0 (and are listed in Table 39) (Ghisaura et al., 2019).

Table 39. Sea bream liver proteins undergoing significant changes along the whole trial (t_2 vs t0). RNSAF > 0.5 or < −0.5; p value < 0.05; FDR multiple comparison test <0.1 (Ghisaura et al., 2019).

Accession number	Protein name	R_{NSAF} t1/t0
	Increased proteins	
Q4RBW9	Proteasome subunit beta type-2	2.0501
B3F9U6	Hemoglobin beta chain	1.7291
Q1PCB2	Beta globin	1.6826
P86232	Ezrin (Fragments)	1.5108
P11748	Hemoglobin subunit alpha	1.3526
K7GAK5	Tubulin beta-7 chain	0.9969
Q4S3J3	GTP-binding nuclear protein Ran	0.8656
Q91060	Tubulin alpha chain	0.8281
M9P052	Lysosomal acid lipase	0.8276
Q4RVS0	ATP synthase F(0) complex subunit B1, mitochondrial	0.7537
L5M3T4	GTP-binding protein SAR1a	0.707
Q4S798	Nucleolin isoform X2 (Fragment)	0.6757
H2MYW8	Fumarylacetoacetase	0.6599
J7FII7	Glutathione S-transferase (Fragment)	0.6588
G9I0G6	Transferrin	0.6428
S4S3W7	Phosphoglucomutase 1 (Fragment)	0.5869

I3JSE9	Formimidoyltransferase-cyclodeaminase-like	0.5706
G1QD60	H3 histone (Fragment)	0.5705
H2LS09	Nucleolin isoform X1	0.5106
Decreased proteins		
Q0GPQ8	Cytochrome P450 2P11	−0.5457
A0A060VGE8	Cytochrome oxidase subunit II	−0.5506
W5LDH9	Uricase	−0.584
G3PTX7	Endoplasmic reticulum resident protein 27	−0.5926
H0YZD0	Electron transfer flavoprotein subunit alpha, mitochondrial	−0.6356
W5N925	Protein disulfide-isomerase (Fragment)	−0.6434
H2RKV3	Malic enzyme	−0.6595
M4AX90	Peroxisomal 2,4-dienoyl-CoA reductase-like	−0.6643
Q27HS3	Vascular smooth muscle alpha-actin (Fragment)	−0.6784
Q4RKE4	Fatty acid-binding protein, heart-like	−0.7223
Q8JHC5	Metallothionein (Fragment)	−0.7259
F1Q6E1	4-hydroxyphenylpyruvate dioxygenase	−0.7963
A0A060WA9	Adenosylhomocysteinase B	−0.8248
M4VQF0	Glyceraldehyde-3-phosphate dehydrogenase	−0.8662
M4AAN9	Phosphate carrier protein, mitochondrial-like isoform X1	−0.8739
F7DQ24	11-cis retinol dehydrogenase-like	−0.92
F7FYK5	40S ribosomal protein SA-like	−1.0889
A0A060YQH0	Aspartate aminotransferase, cytoplasmic-like	−1.1398
B5X8Y0	Cofilin-2	−1.2505
H2VEH5	Peptidyl-prolyl cis-trans isomerase	−1.2816
B9EN58	Thioredoxin	−1.841
G3HK42	60S ribosomal protein L30	−2.441
G3UYV7	40S ribosomal protein S28 (Fragment)	−2.7022

Indeed, numerous metabolic pathways were affected, and these are reported in Supplementary Table S14. KEGG pathways were mainly related to carbon metabolisms such as amino acid metabolism, including phenylalanine, tyrosine and cysteine and methionine metabolisms. Other general pathways that encompass metabolic pathways and carbon metabolism were also statistically significant (FDR<0.05). Amino acid metabolism plays an important role in fish metabolism for protein synthesis, glucose formation, and energy (Ghisaura et al., 2019).

These results provide novel insights on the dynamics and extent of the metabolic shift occurring in sea bream liver with decreasing water temperature, supporting future studies on temperature-adapted feed formulations. The mass spectrometry proteomics data of this study has been deposited to to the ProteomeXchange Consortium via the PRIDE partner repository with the dataset identifier PXD011059 (Ghisaura et al., 2019).

This study indicated that when sea bream liver are exposed to decreasing water temperature, it was found that the protein makeup of undergoes several changes, These changes induce a metabolic shift enabling adaptation to changed environmental conditions. Also, maintenance of low but continuous temperatures seems to affect protein levels to a lesser extent, such as in methionine metabolism (Ghisaura et al., 2019).

Gaining a greater knowledge of sea bream metabolic changes to cold adaptation might be of use to fish farmers for the development of specific aquaculture practices aimed at mitigating the negative effects of cold on fish growth, including the design of novel feed formulations for the winter season (Ghisaura et al., 2019).

4.20. **Altered Expression of Metabolites and Proteins in Wild and Caged Gold Fish Exposed to Wastewater Effluents**

The constant world population growth has led to an increased environment global discharge of wastewater. It is known that not all contaminants are fully removed during the wastewater remedial treatment. These compounds are exemplified by pharmaceuticals and personal care products (PPCPs), which without doubt negatively affect the aquatic ecosystems. After use or disposal, PPCPs often end up in wastewater, which then undergoes a multi-step treatment process at municipal wastewater treatment plants (WWTPs) to remove solids, bacteria, and nutrients. WWTPs, however, do not remove all chemical contaminants. It was established that PPCPs can also bioaccumulate and can cause adverse health effects and behavioural changes in the exposed fish (Simmons et al., 2017).

In order to assess whether caged fish could be used as a surrogate for resident wild fish and to assess the impact of PPCPs on wild goldfish, caged goldfish were placed in a marsh affected by discharges of wastewater effluents. (Cootes Paradise, Lake Ontario, Canada). It is interesting to note that goldfish are known to be a highly resilient species, and as such, have proven highly successful as invaders of Great Lakes ecosystems (Nathan et al., 2015; Simmons et al., 2017).

The untargeted shotgun proteomics approach was used to identify the plasma proteins. The plasma was collected from resident wild fish and from caged goldfish in the marsh for three weeks. This was followed by an analysis of the plasma proteome of both wild fish and caged fish. This analysis showed significant changes in the expression of over 250 molecules that were related to liver necrosis, accumulation and synthesis of lipids, synthesis of cyclic AMP, and to the quantity of intracellular calcium in fish from the wastewater-affected marsh. Among the plasma proteins detected in the caged male goldfish, it was observed that the expression of 36 proteins were significantly different in at least one exposure location in CPM compared to the reference site JH (Figure 59) (Simmons et al., 2017).

Furthermore, the PPCPs that were detected in the plasma of caged and wild fish from the CPM location appeared to have had subtle molecular level effects, which resulted in altered behaviour

of the plasma metabolome and proteome responses in caged goldfish near the WWTP outfall and the CPM2 and CPM1 locations permitted the prediction of the responses in wild goldfish. The observed changes in protein expression and metabolite concentrations suggested liver necrosis and altered lipid metabolism. The expression of plasma proteins in caged goldfish agreed well with those in the wild goldfish, suggesting that the proteomics approaches and caged surrogates is a useful way to predict the molecular effects of contaminants in wild fish (Simmons et al., 2017) .

Ultimately, the molecular responses observed in these robust fish can be used as likely conservative predictors of the potential effects of PPCPs and wastewater effluents on other wild fish species. These findings suggested the need of future studies that focus on the mechanisms underlying metabolic disruption in fish exposed to wastewater effluents (Simmons et al., 2017).

			CPM1		CPM2		CPM3	
Symbol	Name	NCBI Accession Number	Log2(FC)	p-value	Log2(FC)	p-value	Log2(FC)	p-value
Aftph	Aftiphilin	CDQ90298.1	1.3398	0.0840	0.9438	0.1663	0.9616	0.3223
Ankrd12	Ankyrin repeat domain-containing protein 12	XP_005751611	-0.3306	0.4157	-1.0392	0.0925	-1.0392	0.0925
Ash1l	Histone-lysine N-methyltransferase	XP_003966329	-2.1063	0.0611	-1.0906	0.0850	-0.4282	0.2584
Atad2b	ATPase family AAA domain-containing protein 2B	AAW82445.1	-0.0733	0.2752	-0.0796	0.2613	-0.1773	0.0102
Brd1	Bromodomain-containing protein 1	XP_698063.5	2.6465	0.0011				
Btd	Biotinidase	XP_004073869	-2.3530	0.0078	-0.0672	0.7855		
C3	Complement C3	BAA36618.1	0.3364	0.0249	-0.0230	0.8971	-0.2418	0.2116
Chmp6	Charged multivesicular body protein 6	ACO09124.1	1.4989	0.0791	1.2470	0.2029	1.1647	0.1555
Cracr2a	EF-hand calcium-binding domain-containing protein 4B	XP_005805973	0.0152	0.9725	0.7374	0.0141	-0.6697	0.3628
Cyp51a1	Lanosterol 14-alpha demethylase	CDQ67700.1	-1.6909	0.0781	-0.4367	0.3302	-1.6909	0.0781
Daam1	Disheveled-associated activator of morphogenesis 1	XP_004541887	-0.0525	0.8470	0.1344	0.5305	-0.5285	0.0950
Dab2ip	Disabled homolog 2-interacting protein	XP_003976523	-1.5858	0.0920	-1.5858	0.0920	-0.3229	0.4717
Epdr1	Mammalian ependymin-related protein 1	AAB40068.1	-0.9388	0.0140	0.4635	0.0022	-0.0784	0.7044
Epm2a	Laforin, isoform 9	CDQ80564.1	2.0074	0.3223	2.3361	0.0791	1.3535	0.3223
Fetub	Fetuin-B	ABA33614.1	0.0907	0.2643	-0.1724	0.0376	-0.5017	0.0000
Fgg	Fibrinogen gamma chain	ABD83891.1	0.2229	0.2677	0.3162	0.0100	-0.2098	0.2499
Fn1	Fibronectin	AAU14809.1	1.6460	0.0111	0.2799	0.6182	-0.5854	0.3223
Hbb	Hemoglobin subunit beta	P02140.1	3.4162	0.0000	3.2752	0.0000	3.3314	0.0000
Hbe1	Hemoglobin subunit epsilon	0606173B	-3.3963	0.0000	-3.3963	0.0000	-3.3963	0.0000
Hpx	Hemopexin	BAD98538.1	-0.3167	0.0000	-0.4065	0.0000	-0.2872	0.0000
Ifi44	Interferon-induced protein 44	AAP20189.1	1.6710	0.0469	1.7527	0.0491	1.3617	0.1302
Iglc6	Ig lambda-6 chain C region	BAB90987.1	-0.3079	0.0872	-0.3931	0.0661	0.0473	0.6738
Il10rb	Interleukin-10 receptor subunit beta	ABJ97307.1	0.7637	0.3223	2.6225	0.0012		
Myo5c	Unconventional myosin-Vc	CAG05565.1	0.3535	0.2569	-0.0415	0.9145	-1.9834	0.0640
Nphs1	Nephrin	CAG12048.1	0.3930	0.0262	0.1591	0.4757	0.1789	0.3015
Or52k1	Olfactory receptor 52K1	CAG09001.1	0.1047	0.3384	0.2079	0.0772	-0.2994	0.0182
Psme4	Proteasome activator complex subunit 4	XP_004077490	0.0660	0.4604	0.0653	0.3722	0.1919	0.0080
Serpina1	Alpha-1-antitrypsin	AAA73954.1	-0.2322	0.0674	-0.3847	0.0304	-0.3144	0.0228
Serpina5	Plasma serine protease inhibitor	AGO58874.1	-0.2489	0.1900	0.6049	0.0000	-0.0794	0.6424
Smyd2	N-lysine methyltransferase SMYD2	DAA01312.1	2.0448	0.0955			1.1213	0.3223
Snrnp25	U11/U12 small nuclear ribonucleoprotein 25 kDa protein	XP_003442116	-1.0079	0.0005	-0.9440	0.0006	-0.5276	0.0156
Sptbn1	Spectrin beta chain, non-erythrocytic 1	CAG13137.1	1.9156	0.0989	1.8807	0.3223		
Taf2	Transcription initiation factor TFIID subunit 2	CAF95588.1	-0.4629	0.3282	-1.8733	0.0928	-1.8733	0.0928
Tf	Serotransferrin	P80426.1	0.4175	0.0050	0.6721	0.0012	0.3570	0.0075
Usp39	U4/U6.U5 tri-snRNP-associated protein 2	XP_003975010	1.2085	0.0276	0.9418	0.0611	0.6728	0.0984
Znf500	Zinc finger protein 500	CAG00059.1	-0.5077	0.0714	-0.5119	0.0694	-0.7805	0.0193

Figure 59. List of proteins with symbol, name, function (if known), fold change (log_2(FC)), and p-value that were differentially expressed in goldfish plasma for each caging location in CPM compared to expression at the reference site, JH. Red bars indicate increased expression while green bars indicate decreased expression. The size of the bar represents the magnitude of the difference(Simmons et al., 2017).

4.21. **Proteome Response of Goldfish (*Carassius auratus*) Under Multiple Stress Exposure: Effects of Pesticide Mixtures and Temperature Increase**

The following study was achieved to test that aquatic systems can be subjected to multiple stressors, such as exposure to pollutant cocktails and to elevated temperatures. For this reason, goldfish (*Carassius auratus*) were acclimated to two different temperatures (22 and 32 ºC) for 15 days. After which they were exposed for 96 h to a cocktail of herbicides and fungicides (S-metolachlor, isoproturon, linuron, atrazine-desethyl, aclonifen, pendimethalin and tebuconazole) at two environmentally relevant concentrations (Table 40) (Gandar et al., 2017).

Table 40. Composition and characteristics of the two mixtures of pesticides: LD and HD for total concentrations of 8.4 µg L^{-1} and 42 µg L^{-1}, respectively. $LC_{50\text{-}96h}$: concentration which causes 50% mortality at 96 h of exposure. CLP classification of chemical risk in aquatic system (CE 1272/2008): C1 = very toxic; C2 = toxic; ND = no data; NC = not concerned (Gandar et al., 2017).

Chemicals	Family	Use	$LC_{50\text{-}96h}$ fish (mg L^{-1})	CLP classification	Mixture concentrations (µg L^{-1})	
			(min-max)	(acute/chronic)	LD	HD
S-Metolachlor	chloroacetanilide	herbicide	1.23 − 12	C1/C1	2.4	12.0
Linuron	urea	herbicide	3.15 − 31.1	C1/C1	2.0	10.0
Isoproturon	substituted urea	herbicide	18 − 54.41	C1/C1	1.2	6.0
Tebuconazole	triazole	fungicide	4.4	NC/C2	1.2	6.0
Aclonifen	diphenyl ether	herbicide	0.67	C1/C1	0.8	4.0
Atrazine-desethyl	triazine	herbicide	ND	ND	0.4	2.0
Pendimethalin	dinitroaniline	herbicide	0.138 − 0.418	C1/C1	0.4	2.0
Total concentrations					8.4	42.0

Prior to the pesticide exposure, fish were gradually acclimatized during 15 days to the experimental temperatures of 22 and 32◦C (Figure 60A). Twelve fish were used for each condition of pesticides x temperature (Figure 60B). Temperature, pH, conductivity and oxygen concentration were assessed on a daily basis (Figure 1C) (Gandar et al., 2017).

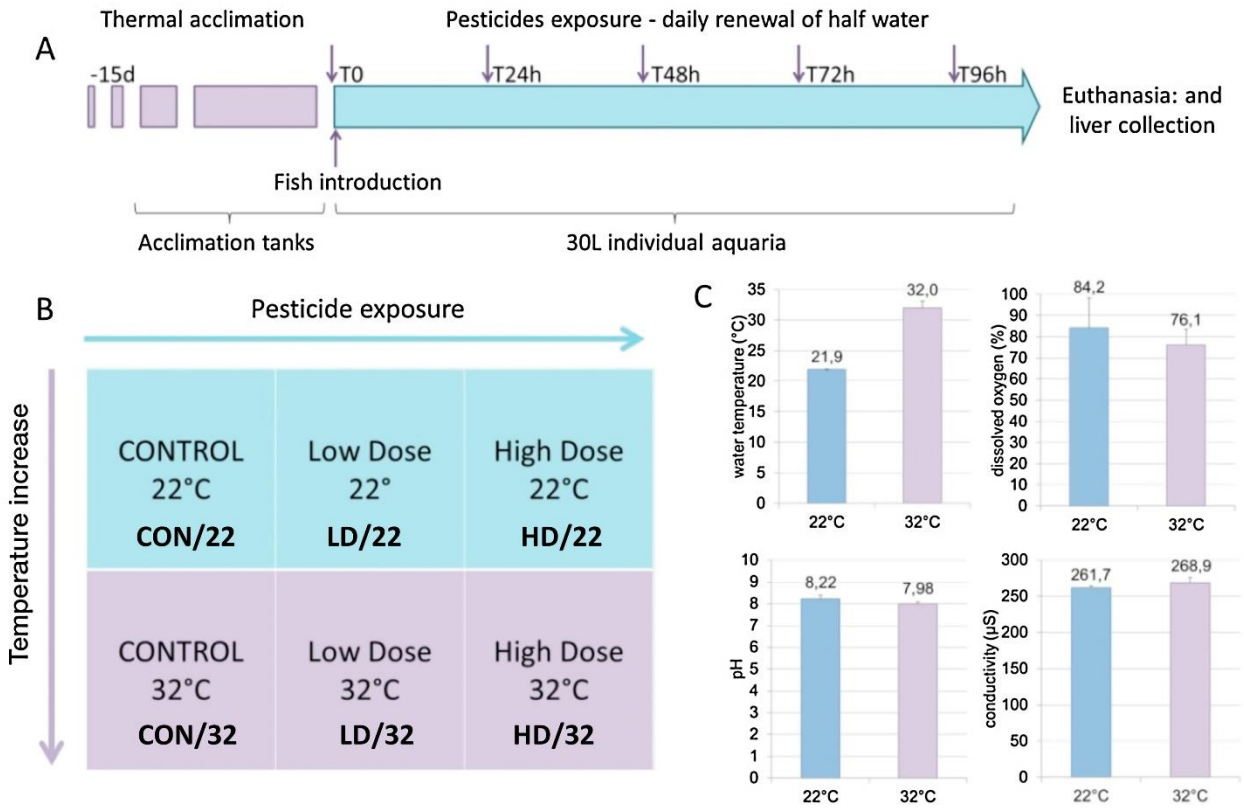

Figure 60. Effects of pesticide exposure and rising temperature on liver proteome response of an aquatic fish species, Carassius auratus: experimental design. (A) Timeline of the experiment: fish were acclimated during 15 days to experimental temperature in collective tanks, and then exposed to pesticides for 96 h in 30L individual aquaria. Fish wereeuthanized and liver collected at the end of the experiment. (B) Experimental design: fish were exposed at two temperatures (22 and 32◦C) to a mixture of seven commonpesticides at different concentrations: CONTROL (total concentration = 0 _g L−1), Low Dose (total concentration = 8.4 _g L−1) and High Dose (total concentration = 42 _g L−1).N = 12 fish for each thermal × exposure condition. (C) Measures of some water physico-chemical parameters in each thermal condition: water temperature (◦C), dissolvedoxygen (%), pH and conductivity (_S). Measures were realized daily in each aquarium. Mean ± SD (Gandar et al., 2017).

The molecular response in liver was assessed by conventional-proteomics and the identified proteins were integrated using pathway enrichment analysis software to determine the biological functions involved in the individual or combined stress responses and to predict the potential deleterious outcomes. The proteins were hydrolyzed and extracted using sonication. The supernatants were transferred in HPLC vials and infused into the nano LC-ESI-MS/MS analysis (Gandar et al., 2017).

The pesticide mixtures elicited pathways involved in cellular stress response, carbohydrate, protein and lipid metabolisms, methionine cycle, cellular functions, cell structure and death control, with concentration- and temperature-dependent profiles of response (Gandar et al., 2017) .

In addition, it was established that combined temperature increase and cocktail pesticide exposure affected the cellular stress response. The effects of the oxidative stress were more marked and there was a deregulation of the cell cycle via apoptosis inhibition. Moreover a decrease in the formation of glucose by liver and in ketogenic activity, was also observed in this multi-stress condition. The decrease in both pathways could reflect a shift from a metabolic compensation strategy to a conservation state (Gandar et al., 2017).

This study permitted to establish that: (I) that environmental cocktails of herbicides and fungicides, induced important changes in the pathways involved in metabolism, cell structure and cell cycle, with possible deleterious outcomes at higher biological scales and (II) that increasing temperature could affect the response of fish to pesticide exposure (Gandar et al., 2017).

4.22. **Proteomic Response to Sublethal Cadmium Exposure in a Ssentinel Fish Species, *Cottus gobio***

In order to gain a more detailed toxicological comprehension, proteomics approaches can complement data acquired at higher levels of biological organization. The present study aimed at evaluating the toxicity of short-term cadmium (Cd) exposure in the European bullhead *Cottus gobio*, a candidate sentinel species (Dorts et al., 2011).

Several enzymatic activity assays (citrate synthase, cytochrome c oxidase, and lactate dehydrogenase) were carried out in the liver and gills of fish exposed to 0.01, 0.05, 0.25, and 1 mg Cd/L for 4 days. Exposure to high Cd concentrations significantly altered the activity of these enzymes either in the liver and/or in gills (Dorts et al., 2011).

The 2D-DIGE (Figure 61) technique allowed the identification of proteins differentially expressed in tissues of fish exposed to either 0.01 or 1 mg Cd/L. Fifty-four hepatic protein spots and 37 branchial protein spots displayed significant changes in abundance in response to Cd exposure (Dorts et al., 2011).

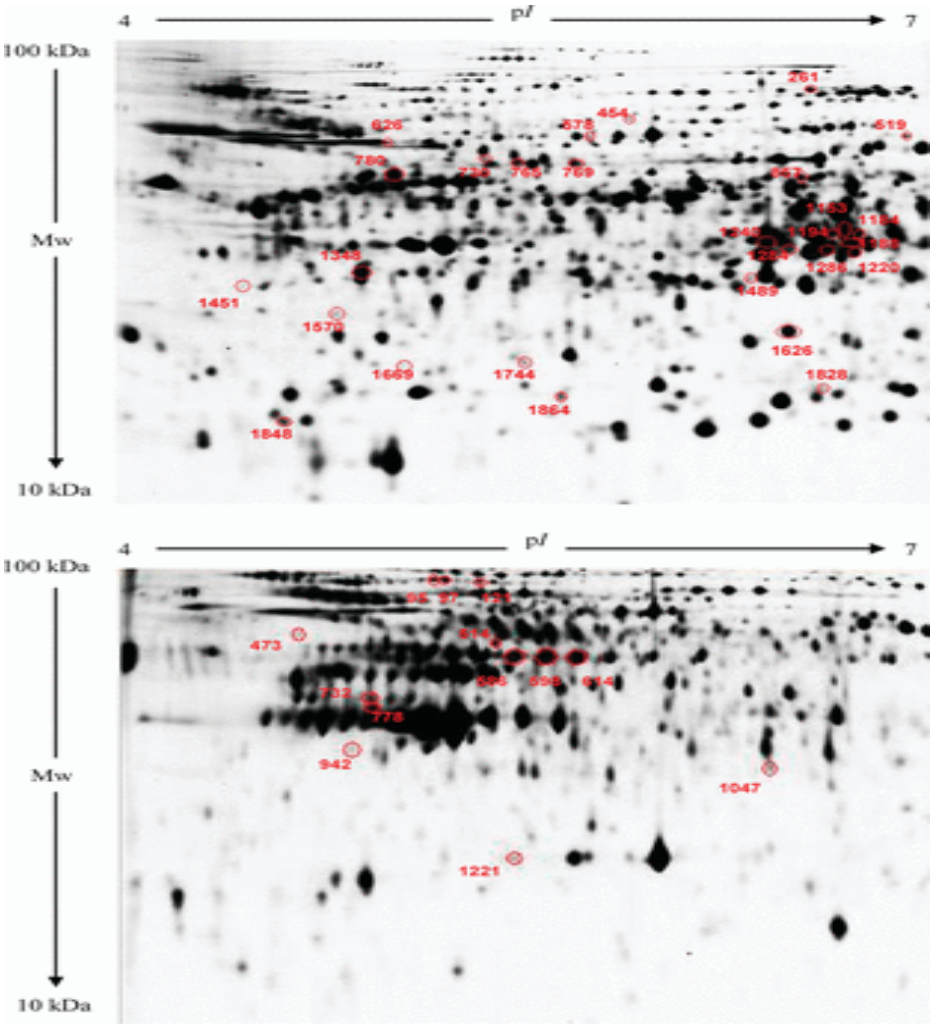

Figure 61. Representative 2D gels showing the protein expression profiles obtained from (top) liver and (bottom) gills of C. gobio exposed for 4 days to Cd. Proteins of the samples obtained for the different experimental conditions were differentially labeled with Cy3 and Cy5. An internal standard composed of equal amounts of each sample and labeled with Cy2 was added.Labeled samples (25 µg of each of the Cy3 and Cy5 labeled samples and of the Cy2 labeled internal standard) were loaded on 24 cm pH 4-7 IPG strips and subjected to IEF. Proteins were further separated by SDS-PAGE (10%) in the second dimension. Numbers allocated by the DeCyder software indicate spots with significant changes in intensity (p < 0.05) (n) 3) (Dorts et al., 2011).

A total of 26 and 12 different proteins were identified using nano LC-MS/MS in liver (Table 41) and gills, respectively. Most of these proteins were successfully identified and validated through the Peptide and Protein Prophet of Scaffold software. The identified differentially expressed proteins can be categorized into diverse functional classes, related to metabolic process, general stress response, protein fate, and cell structure for instance. In this study, it was found that short-term

exposure to Cd induced significant alterations in the activities of various enzymes, such as lactate dehydrogenase (LDH), and in the hepatic and branchial protein expression profiles of a no model species with few genomic sequences available in databases (Dorts et al., 2011).

The wide range of proteins affected suggests that Cd has profound effects on various biological processes, such as metabolic process, general stress response, protein fate, and cell structure. The function of these proteins can provide new clues on the molecular mechanisms by which Cd induce toxicity in liver and gill tissues. The results not only further our knowledge of the effects of Cd on fish, but also provide a global view of changes in cell responses to Cd in a sentinel fish species (Dorts et al., 2011).

Table 41. Detailed List of Protein Identified by Nano LC−MS/MS Differentially Expressed in Liver of C. gobio Following Cd Treatment (Dorts et al., 2011).

spot no.	accession no.[a]	protein name	species	matching peptides	theorical pI/M_w (kDa)	fold change[b]	
						0.01 vs 0 mg/L	1 vs 0 mg/L
Metabolic process							
857	Q19A30	Aldehyde dehydrogenase family 9 member A1	*Oryzias latipes*	2	6.7/54	−1.08[d]	1.03
1194	Q4RVN6	6-phosphogluconate dehydrogenase, decarboxylating	*Tetraodon nigroviridis*	4	5.9/53	−1.22[c]	−1.4[d]
519	Q4RSD6	Histidine amonia-lyase	*Tetraodon nigroviridis*	3	5.9/77	−1.38[c]	1.05
1184	C3KJ67	Cystathionine gamma-lyase	*Anoplopoma fimbria*	6	6.2/45	−1.17[d]	−1.07
1220	C3KIF6	4-hydroxyphenylpyruvate dioxygenase	*Anoplopoma fimbria*	2	6.3/45	−1.18[d]	−1.04
1286	Q7ZUW8	Aspartate aminotransferase	*Danio rerio*	3	6.5/46	−1.12[c]	1.05
730	Q7SXW7	Phosphoglucomutase 1	*Danio rerio*	2	6.1/58	1.79[d]	1.39[c]
769	Q7SXW7	Phosphoglucomutase 1	*Danio rerio*	5	6.1/58	1.17[d]	1.17[d]
765	Q7SXW7	Phosphoglucomutase 1	*Danio rerio*	2	6.1/58	1.45[d]	1.24
261	B5 × 348	Iron-responsive element-binding protein 1	*Salmo salar*	4	6.2/100	−1.16[c]	1
1240	Q4SPX4	Phosphoglycerate kinase	*Tetraodon nigroviridis*	2	7.0/44	−1.5[c]	−1.27
	C1BJG5	Fumarylacetoacetase	*Osmerus mordax*	4	6.3/50	−1.5[c]	−1.27
1188	Q90WD9	Glyceraldehyde 3-phosphate dehydrogenase	*Pagrus major*	2	6.4/36	−1.16[c]	−1.05
	C3KIA2	Betaine-homocysteine S-methyltransferase 1	*Anoplopoma fimbria*	3	5.9/41	−1.16[c]	−1.05
1153	Q90WD9	Glyceraldehyde 3-phosphate dehydrogenase	*Pagrus major*	2	6.4/36	−1.11[c]	1.05
	Q6P2 V4	Homogentisate 1,2-dioxygenase	*Danio rerio*	5	6.2/50	−1.11[c]	1.05
1284	Q4SPX4	Phosphoglycerate kinase	*Tetraodon nigroviridis*	4	7.0/44	−1.22[d]	−1.14[c]
	C1BJG5	Fumarylacetoacetase	*Osmerus mordax*	2	6.3/50	−1.22[d]	−1.14[c]
General stress response							
626	B6F134	Stress protein HSC70−2	*Seriola quinqueradiata*	14	5.3/71	1.11[c]	1.27[e]

578	A9CD13	Glucose regulated protein 75	*Sparus aurata*	4	5.6/69	1.56[d]	1.32[c]
1864	C3KJR7	Thioredoxin-dependent peroxide reductase, mitochondrial precursor	*Anoplopoma fimbria*	3	7.1/27	−1.16[c]	−1.19[d]
Protein repair and proteolytic pathways							
1828	Q92047	Protein-L-isoaspartate (d-aspartate) O-methyltransferase 1	*Danio rerio*	3	6.1/25	−1.29[d]	−1.06
1348	C7SFR6	Cathepsin D	*Paralichthys olivaceus*	5	6.0/43	1.55[d]	1.35[c]
1848	C3UWD7	Cathepsin B	*Lutjanus argentimaculatus*	3	5.7/36	1.48[e]	1.31[d]
454	C0H8W2	Autophagy-related protein 7	*Salmo salar*	3	5.6/79	1.21[c]	1.17[c]
Cytoskeleton							
1744	C3KHQ3	F-actin-capping protein subunit beta	*Anoplopoma fimbria*	7	5.5/31	1.28[c]	1.25[c]
1669	C3KHQ3	F-actin-capping protein subunit beta	*Anoplopoma fimbria*	1	5.5/31	1.35[c]	1.22[c]
1451	C0LMQ3	Type I keratin-like protein	*Sparus aurata*	2	5.0/36	−1.06	−1.41[c]
1570	Q5BL39	Tubulin, beta 4	*Xenopus tropicalis*	2	4.8/50	7.1[d]	2.87[c]
Other functions							
1489	Q4SBV7	Ribosomal protein large P0-like protein	*Tetraodon nigroviridis*	2	5.4/34	−1.33[c]	1.05
1626	C3KJK4	Phenazine biosynthesis-like domain-containing protein 1	*Anoplopoma fimbria*	6	6.0/32	−1.12[c]	1.02
780	B1GS20	Warm temperature acclimation related-like 65 kDa protein	*Harpagifer antarcticus*	3	5.3/49	1.22[c]	1.04

[a] Accession number in UniProt/TrEMBL.
[b] Values >1 indicate up-regulation and <1 indicate down-regulation.
[c] $p < 0.05$.
[d] $p < 0.01$.
[e] $p < 0.001$.

4.23. **Alterations to Proteome and Tissue Recovery Responses in Sole Fish Liver Caused by Short-Term Combination Treatment with Cadmium and Benzo[a]pyrene**

The fundamental mechanisms of fish cellular detoxification and elimination of xenobiotics are extremely complex and depend on multiple factors. These are determined by the contaminant (class and doses), biological species, affected tissue and cell types. The complexity of these mechanisms in fish whole tissue and organs poses an important hindrance to environmental toxicology, especially when multiple contaminants are involved (P. M. Costa et al., 2010).

The present study goals were to investigate the effects and responses of Cd and B[a]P in the sole (*Solea senegalensis*) whole-liver tissue, combining proteomics, histology and cytology as screening tools. It was intended to unravel our understanding of the mechanisms of joint exposure to Cd and B[a]P and to determine the resulting consequences in the hepatic parenchyma (P. M. Costa et al., 2010).

The differential expression of cytosolic proteins was assessed by two-dimensional electrophoresis 2D, which showed twenty-four proteins that were selected for protein identification. Eleven of these twenty-four spots were analyzed by MALDI-TOF-MS (Table 42) and identified using the NCBI nrProtein database. The individual spot was excised and trypsin digested, followed by *de novo* sequencing by MS/MS analysis with electrospray ionization tandem mass spectrometry (P. M. Costa et al., 2010).

It was found that individual exposure of cadmium and B[a]P respectively induced hepatocyte apoptosis and Kupfer cell hyperplasia. It was also noted that apoptosis was triggered through distinct pathways. Furthermore, individual exposure to cadmium and B[a]P caused upregulation of different anti-oxidative enzymes such as peroxiredoxin and glutathione peroxidase, respectively. It was also found that combined exposure with cadmium and B[a]P impaired induction of the anti-oxidative enzymes and inhibited apoptosis. The regulation factors of nine out of 11 of the different identified proteins revealed antagonistic or synergistic effects between Cd and B[a]P at the prospected doses after 24 h of exposure (P. M. Costa et al., 2010).

Table 42. Protein identification summary after de novo sequencing using ESI-ITMS/MS and peptide sequence database search with Protein–Protein Blast plus relative regulation factors over control (± standard deviation) for each identified protein (P. M. Costa et al., 2010).

							Regulation factors over control		
Protein ID	**Abbreviation**	**UniProt Accession**	**Taxa database** [a]	**Score**	***e*-value**	**N° matched peptides**	**Cd**	**Cd + B[a]P**	**B[a]P**
1-cys Peroxiredoxin	1-cysPrx	B5X838	1,2,3	36.7	4.0×10^{-5}	2	0.64 ± 0.44	0.30 ± 0.44	−0.21 ± 0.16
Apolipoprotein A-IV3	ApoA-IV3	Q5KSU2	2,3	29.1	8.7×10^{-1}	6	−0.20 ± 0.27	0.54 ± 0.23	−0.25 ± 0.18
Beta-actin	β-actin	Q1HHC7	1,2,3	37.1	3.0×10^{-5}	5	−0.51 ± 0.10	0.91 ± 0.50	0.46 ± 0.28
Cathepsin L	CatL	P79722	1,2,3	90.1	4.0×10^{-19}	4	0.61 ± 0.07	0.40 ± 0.06	0.13 ± 0.07
Cell division cycle 48	CDC48	A5JP17	1	30.3	4.0×10^{-3}	2	−0.39 ± 0.10	−0.44 ± 0.11	−0.52 ± 0.04
Glutathione peroxidase	Gpx	Q802G1	2,3	28.6	1.2×10^{0}	2	0.30 ± 0.17	0.76 ± 0.10	1.42 ± 0.32
Histone H4	H4	H4	2,3	35.0	1.5×10^{-2}	2	1.93 ± 0.98	0.08 ± 0.32	−0.50 ± 0.05
Metallothionein I	MT1	MT1	1,2,3	38.8	8.0×10^{-3}	3	−0.38 ± 0.14	−0.51 ± 0.04	−0.50 ± 0.07
Phosphatidylethanolamine-binding protein	PEBP	B5DGG2	2,3	37.5	2.0×10^{-2}	3	−0.48 ± 0.03	−0.54 ± 0.06	0.35 ± 0.14
Tissue metalloproteinase inhibitor 2	TIMP2	B5XCZ1	1,2,3	46.9	4.0×10^{-6}	1	0.13 ± 0.21	0.52 ± 0.48	0.40 ± 0.54
Trypsin	Trypsin	Q5XUG5	1,2,3	24.8	1.7×10^{-1}	5	0.46 ± 0.06	0.68 ± 0.17	0.12 ± 0.23

[a] nrNCBI database taxa from which peptides were matched: 1-Order Pleuronectiformes; 2-Class Actinopterygii; 3-Phylum Chordata.

4.24. Comparative Proteomics of Kidney Samples from Puffer Fish *Takifugu rubripes* Exposed to Excessive Fluoride

This study involves challenging a good fluorotic fish model, *Takifugu rubripes*, with excessive water fluoride. Using proteomics analysis, it was possible to assess protein expression changes in the fish kidney samples. The authors randomly placed respectively16 fishes into the control and the treated groups that were raised in softwater alone (F^- = 0.4 mg/L) or with sodium fluoride of 35 mg/L for 3 days, respectively (J. Lu et al., 2010).

The proteins of the fish kidneys were profiled by two-dimensional electrophoresis. In total, 547 ± 4 and 516 ± 5 protein spots in the control and the treated groups were detected, respectively. And 453 spots were matched on the 2-DE images after being visualized by Bio-Safe™. Compared with the control group, the differential image analysis showed 247 spots with a significant density change (32 up-regulated spots and 215 down-regulated spots, $p < 0.01$) in the fluoride-treated group (J. Lu et al., 2010).

Previous SDS-PAGE study showed that the molecular mass of most proteins in the medaka fish midgut ranges between 20–120 kDa. In this work, MALDI-TOF-MS analysis allowed the detection of 547 and 516 protein spots in control and the treated groups, respectively. Among them, 32 protein spots showed significant alteration ($p < 0.05$) between the fluoride-treated and the control groups and 22 differentially expressed protein spots. PMF (peptide mapping fingerprint) of 22 protein spots ($p < 0.01$) were identified by MASCOT (J. Lu et al., 2010).

Table 43. The list of up-and down-regulated proteins in the fluoride-treated group (group A) compared with the control group (group B) (J. Lu et al., 2010).

Spot no.	Protein description	Accession no.	Species	Theoretical		Peptides matched	Sequence coverage	Up or down regulation ($p < 0.01$)
				Mr (kDa)	pI			
K1	Parathyroid hormone-likeprotein	gi184309999	Takifugu rubripes	12.5	9.6	3/11	33%	↑
K2	Unknown protein	gi14633116	Takifugu rubripes	215.3	9.1	9/61	6%	↓
K3	Hypothetical protein	gib 131887391	Danio rerio	37.7	7.7	6/19	23%	↑
K4	ATP synthase, H^+ transporting, mitochondrial FO complex, sub-unit b, isoform 1	gi154400426	Takifugu rubripes	28.3	9.2	9/121	46%	↓
K5	PREDICTED: similar to hCG20426	gi1125845177	Danio rerio	47.9	8.7	11/104	27%	↓

K6	Polymerase (DNA-directed), delta interacting protein 2	gib 156914925	Takifugu rubripes	43.4	8.7	6/31	21%	↓
K7	Lysyl hydroxylase 2	gil 153792754	Takifugu rubripes	88.2	6.3	6/48	14%	↑
K8	Chromosome segregation protein SMC1 homolog	T30534	Takifugu rubripes	143.5	6.7	8/38	9%	↓
K9	Non-neuronal tryp-tophan hydroxylase 1.	Q6IWN2_FUGRU	Takifugu rubripes	55.6	6.4	10/66	23%	↑
K10	Hypothetical protein	gi166472678	Danio rerio	59.6	6.5	14/84	29%	↑
Kll	Hypothetical protein	Q4VBKO_BRARE	Danio rerio	55.1	5.3	12/75	35%	↑
K12	Eukaryotic translation initiation factor 3, sub-unit 6	gi137681791	Danio rerio	53.0	6.2	11/64	34%	↑
K13	Novel protein similar to type I cytokeratin, enveloping layer.	Q1LXJ8_BRARE	Danio rerio	43.1	5.2	22/209	43%	↑
K14	Hypothetical protein	gil 125837507	Danio rerio	17.6	7.9	7/37	34%	↓
K15	ASPIC	gib 148839326	Taldfugu rubripes	69.6	5.5	8/58	19%	↓
K16	Novel protein containing an ATP synthase E chain domain	gib 148724895	Danio rerio	8.3	6.3	4/28	56%	↓
K17	Chromosome 17 open reading frame 27	Q8UWL7_FUGRU	Takifugu rubripes	49.6	5.9	37/88	10%	↓
K18	rCG23467, isoform CRA_a	gi1149063941	Taldfugu rubripes	223.6	5.6	25/71	17%	↑
K19	Gag-pol fusion polyprotein	gi123194332	Takifugu rubripes	231.5	9.1	14/57	8%	↓
K20	Calponin 3, acidic	gil41054309	Danio rerio	36.9	5.7	8/34	24%	↓
K21	Suppressor of cytokine signaling 3	gil118344630	Takifugu rubripes	23.0	8.8	8/115	47%	↓
K22	Piwi-like 2	gil124286793	Danio rerio	117.0	9.0	23/121	27%	↓

Among these identified proteins, nine were up-regulated and 13 were down-regulated. (SM Table 1 lists 22 proteins identified from the databases derived from *Takifugu rubripes* and *Danio rerio*, the NCBI non-redundant database, MSDB and UniProtKB/TrEMBL. Moreover, Figures 62–64 show the PMF of partial proteins (J. Lu et al., 2010).

Consistent with their previously annotated functions, these proteins appear to be involved in the biological functions associated with fluorosis. These results will greatly advance one's understanding of the effects of fluoride exposure on the physiological and biochemical functions of *takifugu* kidney as well as the toxicological mechanism of fluoride-causing fluorosis in both fish and humans (J. Lu et al., 2010).

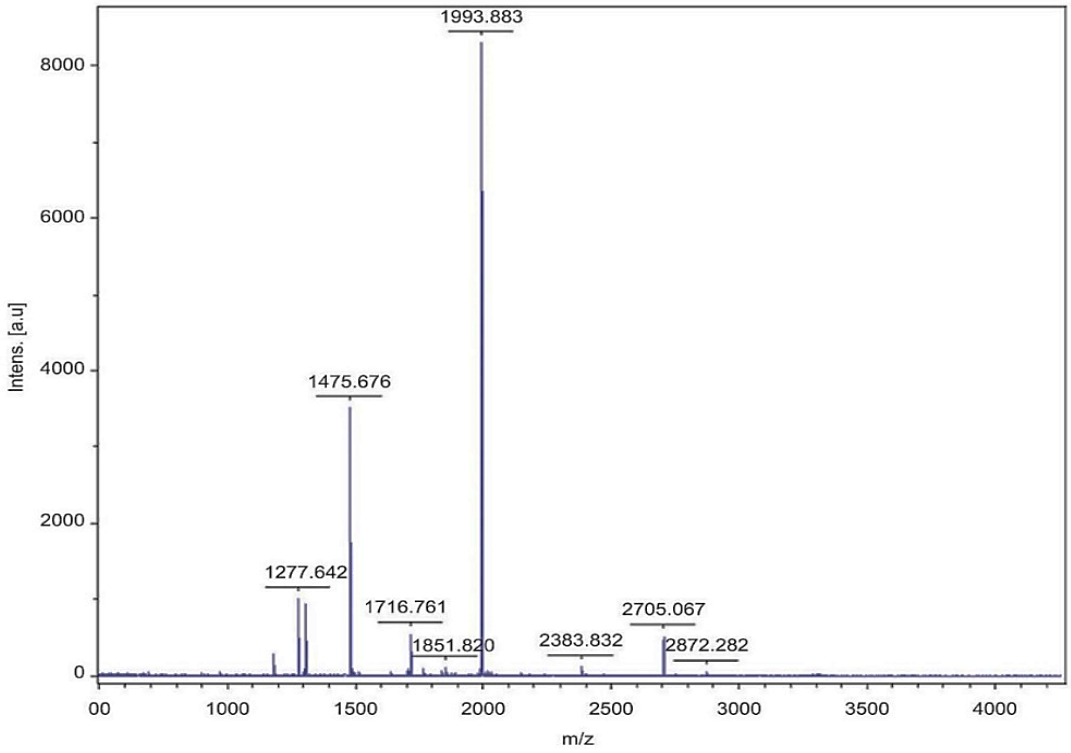

Figure 62. PMF of K2 protein spot (Unknown protein, gi|4633116) (J. Lu et al., 2010).

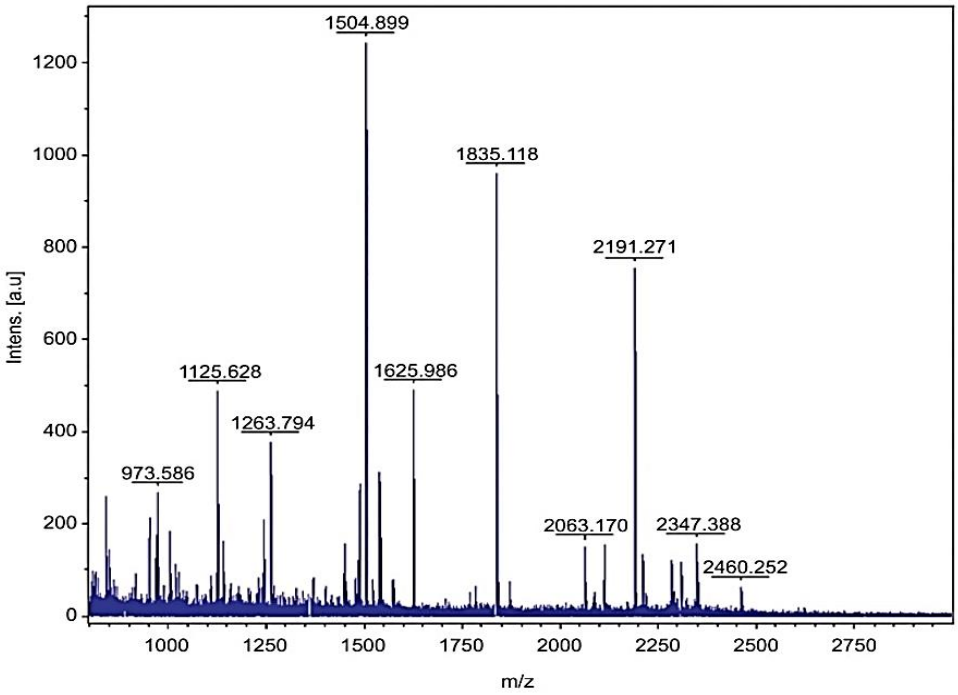

Figure 63. PMF of K4 protein (ATP synthase, H^+ transporting, mitochondrial F0 complex, sub-unit b, isoform 1, gi|54400426) (J. Lu et al., 2010).

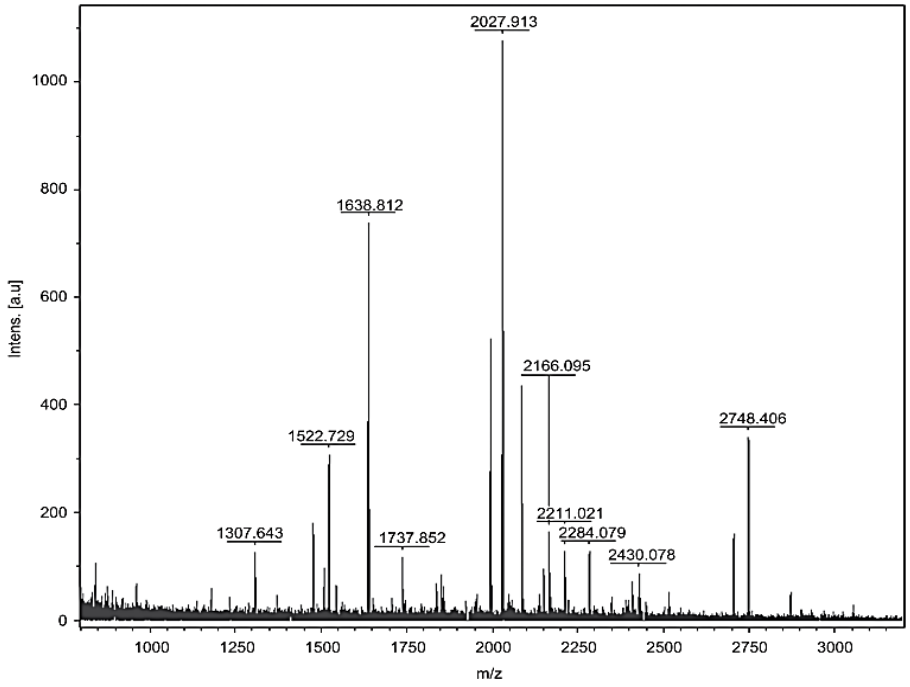

Figure 64. PMF of K12 protein spot (eukaryotic translation initiation factor 3, sub-unit 6, gi|37681791)(J. Lu et al., 2010).

4.25. **Influence of Acute Cadmium Exposure on the Liver Proteome of a Teleost fFsh, Ayu (*Plecoglossus altivelis*)**

Cadmium (Cd) is a toxic heavy metal that causes the disruption of a variety of physiological processes. This study's main goal was to investigate the proteomic alteration of the ayu (*Plecoglossus altivelis)* liver after acute exposure to Cd in order to identify differentially expressed proteins that could represent useful biomarkers under Cd stress. The Ayu specimen (20–25 g/fish) were acclimatized to laboratory conditions for two weeks and fed with commercial pellets for two weeks. The Ayu fishes were exposed to 5.0 ppm Cd (as CdCl2_H2O) prepared in water (X. J. Lu et al., 2012).

Proteins extracted from liver samples were separated via 2-DE. About 540 protein spots on average per gel were visualized using Coomassie brilliant blue G-250 staining and PDQuest 2-D analysis software. Overall, 27 spots were recognized as differentially expressed in livers between Cd-treated and control groups. It was found that in the control 2D, spots 1–11 and 27 were up-regulated in the livers of the Cd-treated ayu, whereas spots 12–26 were down-regulated.

The altered protein spots were excised and analyzed by MALDI-TOF–MS and MALDI-TOF/TOF-MS/MS. There were 23 spots that were successfully identified by Mascot search. These proteins were mainly implicated in biological processes, including oxidative stress response, metal metabolism and function, methylation, and so on. The protein expression intensity of each differential spot was assessed by total integrated optical density in Cd-treated and healthy control groups (Figure 65) (X. J. Lu et al., 2012).

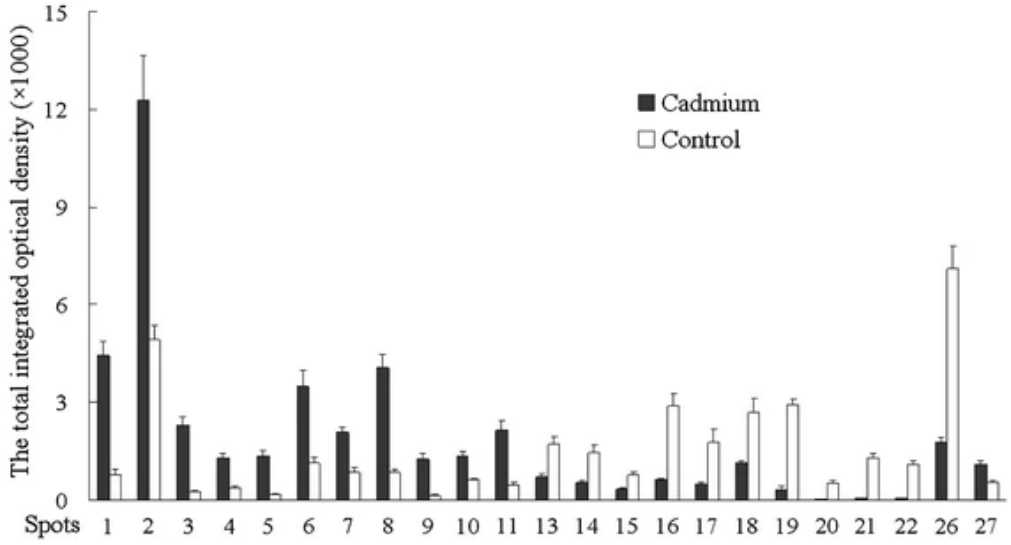

Figure 65. The protein quantities of the spots in Cd-treated and healthy control groups. The total integrated optical density was calculated by PDQuest software, and proteins were identified by matrix assisted laser desorption ionization time-of-flight tandem mass spectrometry (MALDI-TOF–MS/MS). Each bar represents the mean ± SEM of the results from four ayu (X. J. Lu et al., 2012).

Twenty-three altered protein spots were successfully identified. These proteins were involved in oxidative stress response, metal metabolism, methylation. The altered expression of many proteins that were involved in the characteristic response to acute Cd exposure suggested that they followed known mechanisms of toxicity resulting from Cd exposure. The up-regulation of liver Hsp70, Gst, and Aldh were observed in acute Cd-treated ayu. Also, it was found that Gst and Aldh can catalyze the detoxification of lipid-derived toxic aldehydes to reduce their potential damage. The increased expression of Aldh has been found in fishes under environmental stresses such as, low temperature (Ibarz, Martín-Pérez, et al., 2010), environmental pollutants (Williams et al., 2003), and osmotic stress (J. Chen et al., 2009). This study identified two up-regulated spots (5 and 11) in the acute Cd-treated group as Aldh. Acute Cd exposure induces the up-regulation of Aldh, which is possibly complementary to the Gst pathway for the antioxidant process (X. J. Lu et al., 2012).

In addition, genes were chosen for real-time PCR (RT–PCR) analysis with respect to their biological significance related to the Cd exposure, and to the degree of sequence information available for the PCR primer design, and their fold change in the proteomic experiment (X. J. Lu et al., 2012).

The effect of Cd stress on the mRNA expression of 60S acidic ribosomal protein P0 (Rplp0), heat shock protein 70 (Hsp70), apolipoprotein A-I (Apoa1), betaine-homocysteine S-methyltransferase (Bhmt), 2-oxo-4-hydroxy-4-carboxy-5-ureidoimidazoline decarboxylase (Prhoxnb), transferrin (Trf), and 18S ribosomal RNA (18S rRNA) genes was tested by RT–PCR subsequently.The mRNA expression of 60S acidic ribosomal protein P0, heat shock protein 70, apolipoprotein A-I, betaine homocysteine S-methyltransferase, parahox cluster neighbor and transferrin, was subsequently determined by real-time PCR. The mRNA expression of these genes was consistent with proteomic results (X. J. Lu et al., 2012).

These findings enrich our knowledge on the influence of Cd toxicity on teleost fish, and maybe worthy of further investigation to develop biomarkers (X. J. Lu et al., 2012).

4.26. Mass Spectrometry-Based Detection of Common Vitellogenin Peptides Across Fish Species for Assessing Exposure to Estrogenic Compounds in Aquatic Environments

Uncountable chemicals that mimic hormones and mode of action disturb the endocrine functions of exposed oceans organisms, known as endocrine-disrupting chemicals (EDCs). These are usually present in very low concentrations in the aquatic systems and paradoxically affect the metabolic, developmental, and reproductive functions in exposed fish and wildlife (P. He et al., 2019).

VTG is the precursor of egg yolk, and it blood transports protein and lipid from the liver to the growing oocytes. Normally, VTG is only found in the blood or hemolymph of female fishes. However, it can also be found in environmentally affected males. For this reason, VTG can be used as a biomarker in vertebrates exposed to environmental estrogens that stimulate elevated levels in males and females. VTG is classified as a glycolipoprotein, and belongs to several lipid transport protein families (P. He et al., 2019).

The objectives of the present study are to identify common VTG peptides from different fish species, and to demonstrate the potential of liquid chromatography-tandem mass spectrometry (LC-MS/MS) as an effective method for the detection of VTG from multiple fish species. Mass spectrometric quantification is based on identification of particular peptides from VTG protein following enzymatic digestion with synthetic isotope-labeled peptides as standards (Simon et al., 2010). To date, mass spectrometry-based methods have been successfully established for VTG quantification in fathead minnow (*Pimephales promaelas*) (Wunschel et al., 2005), zebrafish (*Danio rerio*) (F. Yang et al., 2015), Greenland halibut (*Reinhardtius hippoglossoides*) (Cohen et al., 2009b), Atlantic cod (*Gadus morhua*) (Cohen et al., 2005b), Atlantic salmon (*Salmo salar*) and rainbow trout (*Oncorhynchus mykiss*) (Cohen et al., 2006b).

It was predicted that large proteins with the same function must share a high degree of sequence homology across species (Dayhoff et al., 1983). This implies that different species VTG protein most probably share common peptide sequences. Accordingly, the ultimate goal of this study was to develop by using with LC-ESI-MS and LC-ESI-MS/MS shotgun approach based quantification method which targets a specific set of VTG peptides resulting from trypsin enzymatic hydrolysis of purified VTG from three different fish species namely: fathead minnow, largemouth bass, and killifish. Fourteen peptides were identified to be common for all three fish

species; the m/z values for these peptides and their putative sequences are listed in Table 44 (P. He et al., 2019).

Table 44. Common VTG peptides present in fathead minnow, largemouth bass, and killifish, identified using non-targeted analysis by LC-Q-TOF/MS/MS (P. He et al., 2019).

m/z	***z***	**Peptide sequence**
399.7220	2	DPAVPATK
402.2438	2	TIDIITK
418.2424	2	ALHPELR
441.7876	2	ITPLLPTK
472.2949	2	IENILLTK
531.7354	2	DLNQCQER
545.2647	2	NPALSESTDR
551.3116	2	TEGIQEALLK
552.7886	2	ELPIQEYGR
565.8508	2	FVELIQLLR
572.8643	2	FIELIQLLR
619.8962	2	GILNILQLNLK
670.8756	2	ISDAPAQVAEVLK
683.9424	2	GILNILQLNLKK

Two peptides (ALHPELR and FIELIQLLR) were identified as common fragments of digested VTG protein isolated from three different fish species, and their product ion scan is shown in Figure 66. This was followed by optimizing the MS/MS analysis by using the selected reaction monitoring mode for the detection of these two peptides. in trypsin-digested plasma from female fish (positive control), estrogen-exposed male fish (test sample), and unexposed male fish (negative control) using two of the same species used for identifying the common peptides (*P. promelas, and M. salmoides*) and one new species (*Ameiurus nebulosus*) that was not included during the selection of peptides (P. He et al., 2019).

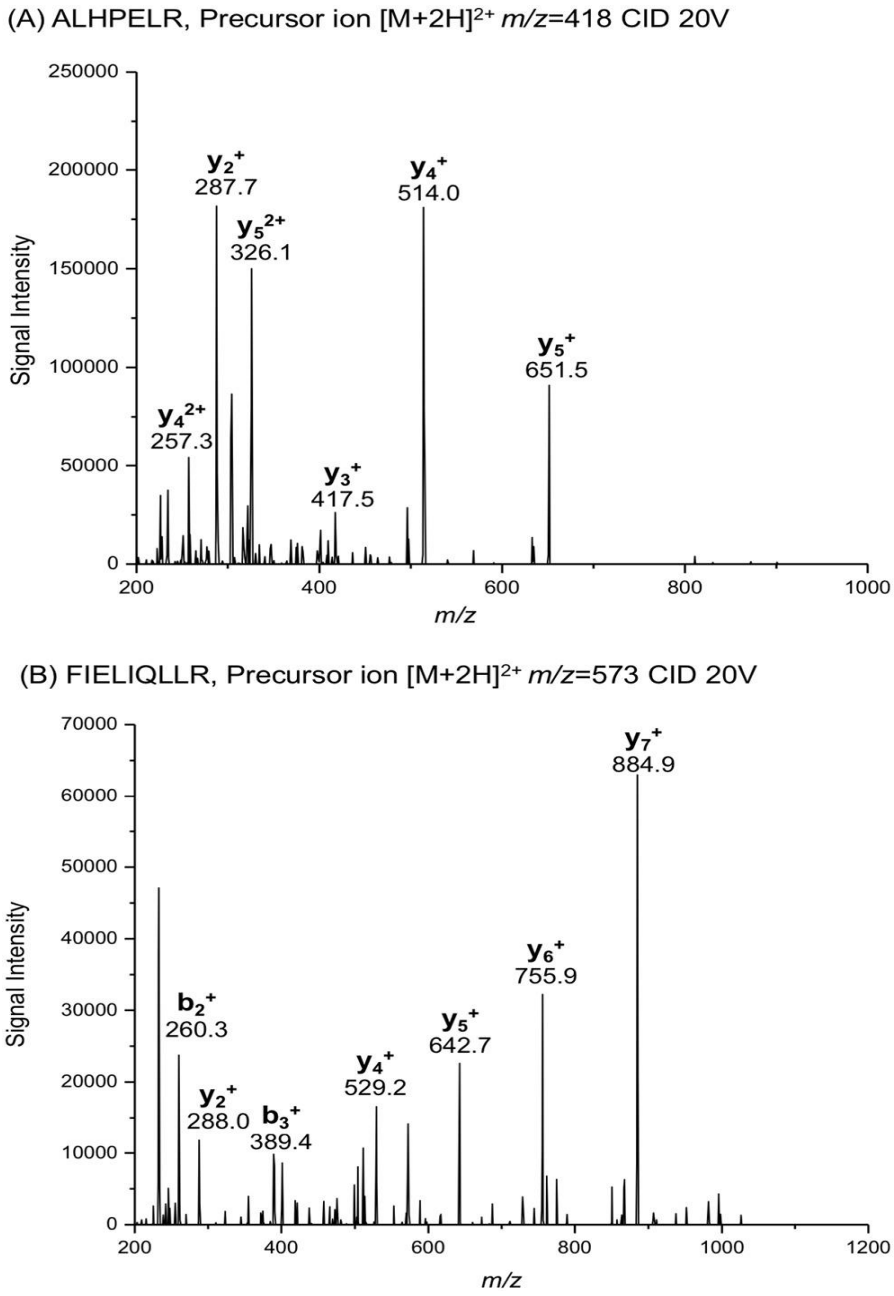

Figure 66. (A) Product ion spectra of doubly charged ALHPELR at m/z *418 by targeted analysis using LC-MS/MS, the Y_2^+, Y_4^+, and Y_5^{2+} were used as diagnostic ions; (B) Product ion spectra of doubly charged FIELIQLLR at* m/z *573 by targeted analysis using LC-MS/MS, the Y_5^+, Y_6^+, and Y_7^+ were used as diagnostic ions* (P. He et al., 2019).

Results from this study demonstrate the potential of LC-MS/MS as an effective cross species method to detect VTG in fish, which can be an alternative analytical technique for assessing endocrine disruption in multiple fish species (P. He et al., 2019).

4.27. **Proteomic Responses to Ocean Acidification in the Brain of Juvenile Coral Reef Fish**

It is general knowledge that we shall witness an increase in CO_2 levels in our oceans and that it will cause dire consequences to the physiology and behavior of marine fishes. A vital fish survival mechanism in response to chemical alarm cues (CAC) is to cause the conspecific organisms substantial individual variation in the extent of behavioral impairment. Studying the response to a change in environmental condition on the molecular level of an organisms can provide insight into the broad response of a tissue to this change. Some molecular processes might change to acclimate to the new condition and prevent the need of a change on the physiological, behavioral or whole organism level. On the other hand, some molecular patterns will be the underlying processes to the whole organism's physiological changes in response to the environmental alteration (Madeira et al., 2017; Tsang et al., 2020).

The whole brain of juvenile fish transcriptomic data has shown the importance of parental phenotypic variation in the response to elevated CO_2. A novel study was reported on the genome-wide proteomic responses of this variation in the brain of 5-week-old spiny damselfish, *Acanthochromis polyacanthus*. For this reason, a comparison of accumulation of the brain proteins of juvenile *A. polyacanthus* from two different parental behavioral phenotypes (sensitive and tolerant) was held. This study was done by comparing experimentally fishes exposed to short-term, long-term and inter-generational elevated CO_2 levels (Tsang et al., 2020).

Proteins from whole brain tissue were extracted along with DNA and RNA with a Qiagen AllPrep DNA/RNA Mini Kit. This was followed by protein digestion and iTRAQ Labeling. The iTRAQ labelling permits for the relative comparison of protein accumulation across a maximum of eight labeled samples. The labelled pool of peptides was fractionated with strong cation exchange chromatography, and a total of 15 peptide fractions were analyzed through three technical replicates a Nanospray ESI- Q Exactive-MS instrument with electrospray potential of 1.5 kV operating with data acquisition in the positive ion mode. The ten most intense ions above a $2e^4$ threshold and carrying multiple charges were selected for fragmentation using higher collision dissociation (HCD) (Tsang et al., 2020).

This study used offspring from two breeding pairs from each parental phenotype (Tolerant and Sensitive) within each of the two parental CO_2 treatments (Control © and elevated CO_2). Offspring clutches from each breeding pair were then placed into different experimental conditions

resulting in a total of four treatment groups for each parental behavioral phenotype (T and S) (Tsang et al., 2020).

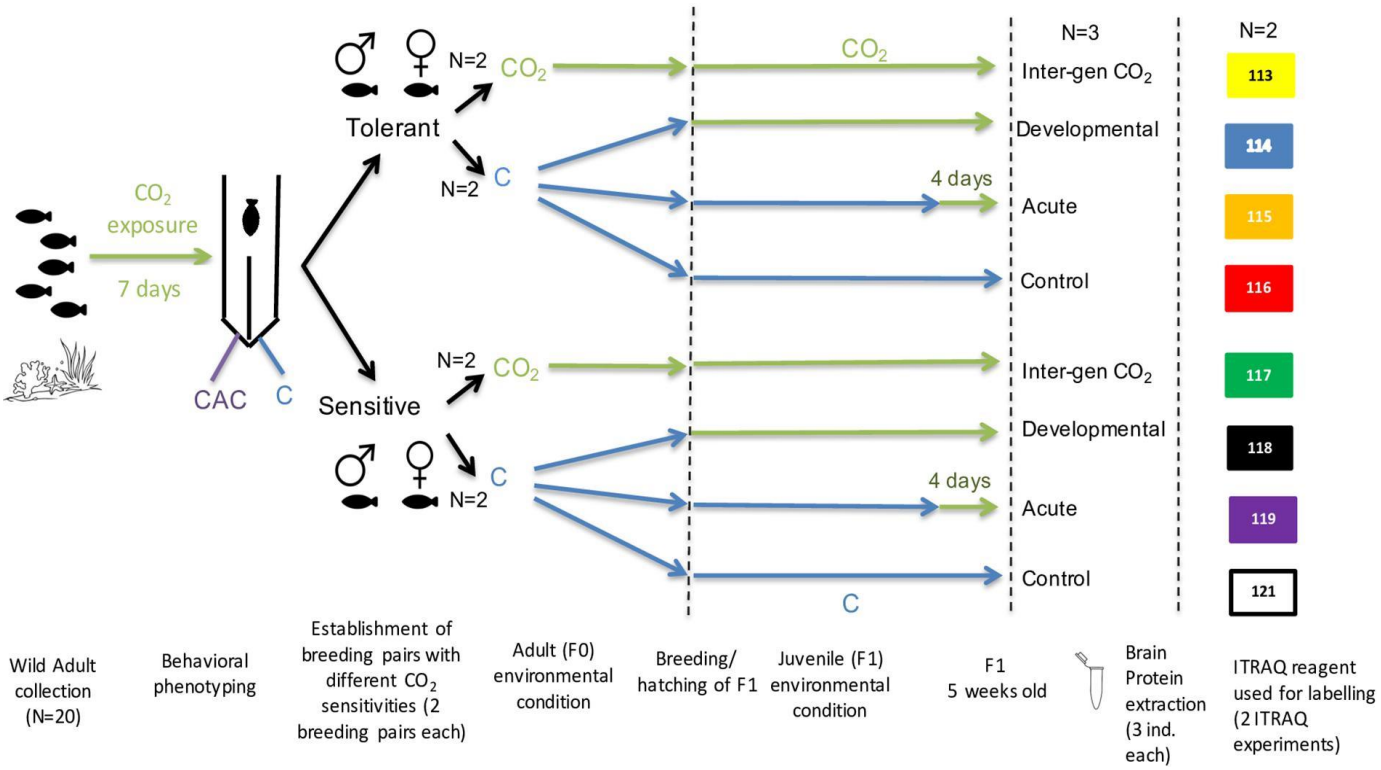

Figure 67. Schematic of experimental design from wild adult fish collection, behavioural testing, environmental CO_2 exposure treatments and Proteome iTraq experimental design (Tsang et al., 2020).

The results showed a marked differential accumulation of key proteins related to stress response and epigenetic markers with elevated CO_2 exposure. Furthermore, proteins related to neurological development and glucose metabolism were also differentially accumulated particularly in the long-term developmental treatment, which might be critical for juvenile development (Tsang et al., 2020).

By contrast, exposure to elevated CO_2 in the parental generation resulted in only three differentially accumulated proteins in the offspring, revealing the potential for intergenerational acclimation (Tsang et al., 2020).

Lastly, a distinct proteomic pattern in juveniles was found in response to the behavioral sensitivity of parents to elevated CO_2, even though the behavior of the juvenile fish was impaired regardless of parental phenotype. Our data shows that developing juveniles are affected in their

brain protein accumulation by elevated CO_2, but the effect varies with the length of exposure as well as due to variation of parental phenotypes in the population (Tsang et al., 2020).

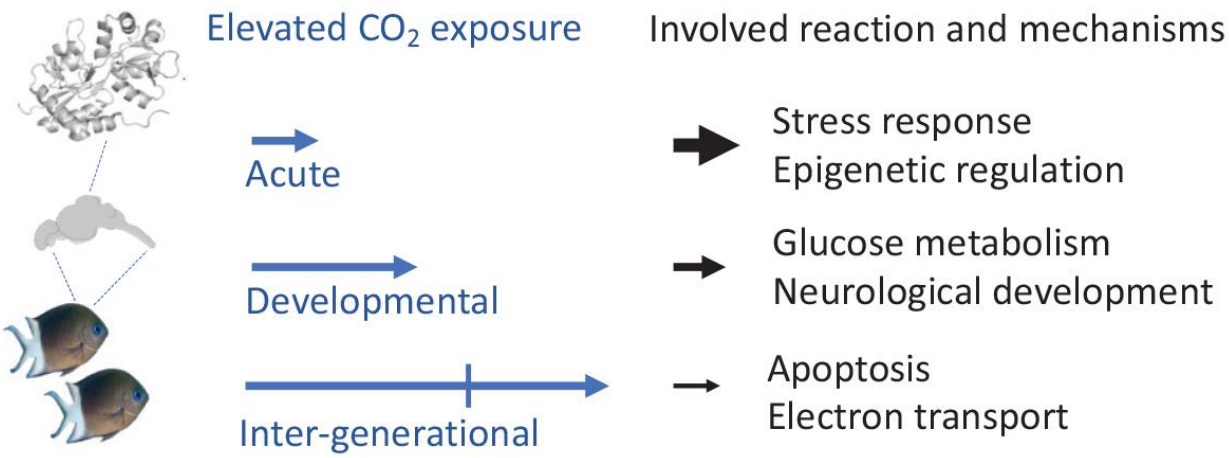

Figure 68. Functional proteome response to varying length of elevated CO_2 exposure in fish brains (Tsang et al., 2020).

4.28. The Proteome of Atlantic Herring (*Clupea harengus L.*) Larvae is Resistant to Elevated pCO_2

The new state-of-the-art expression proteomic technology is becoming a useful tool that allow the assessment of global change and in analyzing the environment's sublethal influence on organisms and their adaptation to the environment (DIZ et al., 2012; Görg et al., 2004). The proteome, which is the expressed protein complement of the genome, varies among tissues and over time. It also represents the final and stable product of many redundant gene expression processes. This means that the final protein level becomes the close approximation of the organism response (Campos et al., 2012; López-Barea & Gómez-Ariza, 2006; Maneja et al., 2014 ., Lacerda & Reardon, 2009).

It is well known that elevated anthropogenic pCO_2 delays the growth and impairs the otolith structure and function in the larvae of some fishes. These effects may concurrently alter the larva's proteome expression pattern. To test this hypothesis, Atlantic herring larvae were exposed to ambient (370 µatm) and elevated (1800 µatm) pCO_2 for one month. The proteome structure of the larvae was examined using a 2-DE and mass spectrometry (Maneja et al., 2014).

The 2-DE analysis of herring larvae samples permitted the identification of over 649 proteins. The quality and the number of protein spots visualized on the 2-DE gels were distinct

and the edges of the spots were clear (Figure 69). The majority of proteins in the larvae were visualized in the acidic region of the gel (pI 3 to 7) and were of low-molecular-weight, ranging between 40 and 10 kDa. It was noted that when a less stringent threshold criterion for the spot intensity (i.e. 1.5-fold) was used, it became possible to the assessment of the effect of pCO_2 on the proteome of herring larvae. This means that a difference between the control and treatment groups could be observed. However, this difference between the groups consisted of only 10 down-regulated and 9 up-regulated proteins (Maneja et al., 2014).

All of the 19 differentially expressed proteins were identified by MALDI-TOF-MS using PMF strategy, and the correct molecular structures were analyzed by MALDI-TOF/TOF-MS/MS sequencing. Alas, only 12 differentially expressed proteins were identified with high confidence. The remaining seven expressed proteins could not be identified due to the lack of sequenced genomic information for Atlantic herring. The identified proteins are listed in Table 45 and marked on the gel image in Figure 69. Most of the up-regulated protein spots were identified as muscle proteins, while down-regulated proteins were involved in metabolism (Maneja et al., 2014).

Table 45. List of identified and differentially expressed protein of the Atlantic herring larvae (Clupea harengus L.) in response to elevated pCO_2 (Maneja et al., 2014).

Spot[a]	Putative identification[b]	Total protein score[c]	Peptide count[d]	Homology to protein (NCBI accession no. and species name)[e]	Fold change	*p*-value
1316	Actin	399 (100)*	13	gi|37903435 *Danio rerio*	−1.4	0.0008
1030	Actin	492 (100)	16	gi|37903435 *Danio rerio*	−1.5	0.002
1398	ATP synthase subunit alpha	113(99.9)*	4	gi|40386586 *Amphimedon queenslandica*	1.5	0.015
1485	ATP dependent helicase CHD1	65*	17	gi|269969347 *Gallus gallus*	1.4	0.003
1496	Actin	321 (100)*	13	gi|345322034 *Ornithorhynchus anatinus*	−1.9	0.013
1562	Prohibitin	371 (100)*	9	gi|213515458 *Salmo salar*	−1.8	0.013
1584	Beta-actin, partial	192 (100)	5	gi|374413852 Sardina pilchardus	−1.5	0.004
1770	ATP synthase subunit alpha, mitochondrial	101 (99.9)*	12	gi|116325975 *Danio rerio*	1.9	0.038
1825	Spectrin beta chain, brain1 like	65*	31	gi|345481110 *Nasonia vitripennis*	1.4	0.014
2480	NADP-dependent malic enzyme, mitochondrial	62*	10	gi|346716344 *Sus scrofa*	1.7	0.029
2533	Putative 5′ nucleotidase	66*	8	gi|190702164 *Glyptapanteles flavicoxis*	−1.4	0.017
1611	Actin, aortic smooth muscle-like isoform1	549 (100)*	16	gi|297301436 *Macaca mulatta*	−1.8	0.005

[a]The assigned spot number.
[b] Name of the putatively identified protein.
[c] The in-house MASCOT Total protein score obtained through searching against the Herrings NCBI and Metazoan NCBI database (MASCOT score >69 is considered significant).

[d] Number of matched peptides.
[e] Genbank accession number.
[*] The protein is identified by the Metazoan NCBI database.

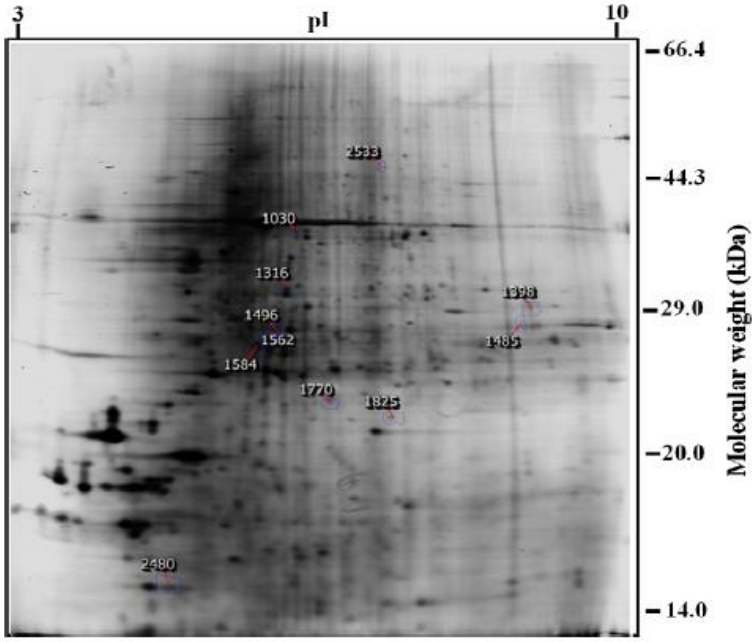

Figure 69. A typical proteome map of the Atlantic herring (Clupea harengus L.) larvae obtained from standard 2-DE analysis. The marked protein spots were identified using MALDI-TOF-MS and MS/MS analyses (Maneja et al., 2014).

There was a minor discrepancy between the theoretical MW and pI and those obtained experimentally from the gel. However, the PMF and MS/MS results suggested that this could be due to the low sequence coverage of the analyzed peptide fragments in the database, which is common in non-model species (Kültz et al., 2007; Maneja et al., 2014).

In conclusion, it was established that the length of herring larva were marginally shorter in the elevated pCO_2 treatment compared to the control. The proteome structure was also different between the control and treatment, but only slightly. In addition, it was observed that the expression of a small number of proteins was altered by a factor of less than 2-fold at elevated pCO_2. This comparative proteome study indicated that the proteome of herring larvae is resilient to elevated pCO_2 (Maneja et al., 2014).

4.29. **Effects of Increased CO_2 on Fish Gill and Plasma Proteome of the Atlantic Halibut (*Hippoglossus hippoglossus*)**

Marine organisms are constantly exposed to ocean acidification and warming. The increased levels of atmospheric CO2 cause these two stressor agents. While the effects of temperature on fish have been studied at length over the last century, the long-term effects of modest CO_2 exposure and the combination of both stressors are almost entirely unknown (K. B. de Souza et al., 2014).

A proteomics approach was used to evaluate the conflicting physiological and biochemical changes that may occur upon exposure to these two stressor agents. For this reason, gills and blood plasma of Atlantic halibut (*Hippoglossus hippoglossus*) were exposed to temperatures of 12^{o}C (control) and 18^{o}C (impaired growth) in combination with control (400 µatm) or high-CO_2 water (1000 µatm) for 14 weeks (K. B. de Souza et al., 2014).

The proteomic shotgun analysis was performed using 2DE followed by Nanoflow LC-ESI-MS/MS using an LTQ-Orbitrap. It was established that high-CO_2 treatment induced the up-regulation of the immune system-related proteins, specifically the plasma proteins complement component C3 and the fibrinogen b chain precursor in both temperature treatments (K. B. de Souza et al., 2014).

On the other hand, changes in the gill proteome for the high-CO_2 (18 ^{o}C) group were related to increased energy metabolism proteins such as ATP synthase, malate dehydrogenase, malate dehydrogenase thermostable, and fructose-1,6-bisphosphate aldolase). In addition. Gills from fish exposed to high-CO_2 at both temperature treatments showed changes in proteins associated with increased cellular turnover and apoptosis signalling annexin 5, eukaryotic translation elongation factor 1c, the receptor for protein kinase C, and putative ribosomal protein S27 (K. B. de Souza et al., 2014).

This study indicates that moderate CO_2-driven acidification, alone and combined with high temperature, can elicit biochemical changes that may affect fish health (K. B. de Souza et al., 2014).

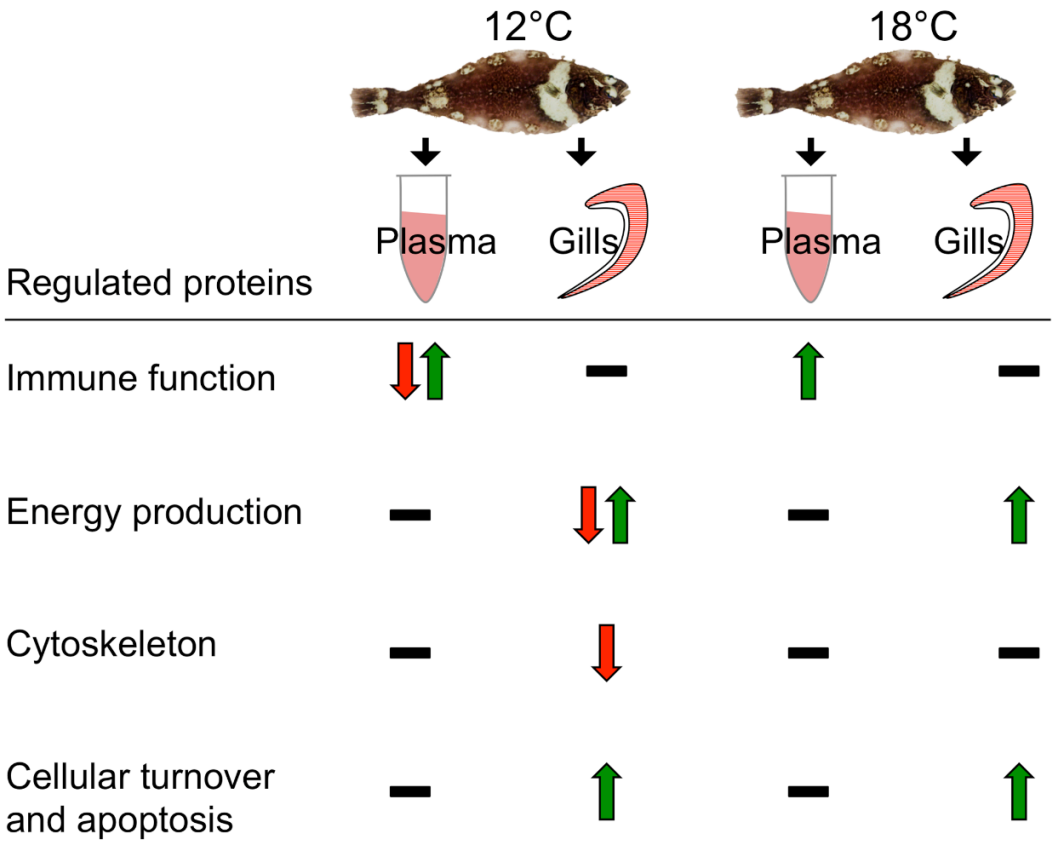

*Figure 70. Schematic summary about analyzed gills and blood plasma of Atlantic halibut (*Hippoglossus hippoglossus*) exposed to temperatures of 12°C (control) and 18°C (impaired growth) in combination with control (400 µatm) or high-CO_2 water (1000 µatm) for 14 weeks. The proteome analysis was performed using (2DE) followed by Nanoflow LC-MS/MS. The main systems affected are listed. Green arrows represent up-regulation, red arrows represent down-regulation, and black dashes represent no protein regulation (K. B. de Souza et al., 2014).*

4.30. **Proteomic Response to Elevated PCO_2 Level in Eastern Oysters (*Crassostrea virginica*): Evidence for Oxidative Stress**

It is well known that estuaries are subjected to extreme fluctuations in CO_2 levels due to exposure of CO_2 production by the resident biota and by the gas exchange with the atmosphere and open ocean waters. Elevated partial pressures of PCO_2 decrease the pH of estuarine waters, which eventually change and affect the extracellular and intracellular pH levels of estuarine organisms (e.g., mollusks), which compromise their limited capacity for pH regulation (Tomanek et al., 2011).

Eastern oysters, *Crassostrea virginica*, are common bivalve mollusks that serve as ecosystem engineers in western Atlantic estuaries (Gutiérrez et al., 2003). This work describes the proteomic changes associated with exposure to elevated PCO_2 in the mantle tissue of eastern oysters (*Crassostrea virginica*) following 2. weeks of exposure to control (~39.Pa PCO2) and hypercapnic (~357.Pa PCO2) conditions (Tomanek et al., 2011).

To attain this quest, a proteomics approach consisting of 2D, MALDI-TOF-MS and MALDI-TOF/TOF-MS/MS analyses was deemed an excellent tool to provide insights into elevated *P*CO2 environmental stress causing changes in the global protein expression. This latter certainly reflects the changes in protein synthesis, post-translational modifications or degradation (Tomanek et al., 2011). Peptide mass fingerprints (PMFs) obtained by MALDI-TOF/TOF-MS/MS analysis permitted the sequencing of the separated proteins (Tomanek et al., 2011).

It was found that exposure to high PCO_2 resulted in a significant proteome shift in the mantle tissue, with 12% of proteins (54 out of 456) differentially expressed under the high PCO_2 compared with control conditions. Furthermore, 54 differentially expressed proteins were measured. However, only 17 proteins were properly identified. These identified proteins consisted of two main functional categories: those upregulated in response to hypercapnia and associated with the cytoskeleton (e.g., several actin isoforms) and those associated with oxidative stress (e.g. superoxide dismutase and several peroxiredoxins as well as the thioredoxin-related nucleoredoxin). This indicates that exposure to high PCO_2 induces oxidative stress and suggests that the cytoskeleton is a major target of oxidative stress (Tomanek et al., 2011).

In addition, it was suggested that oxidative stress and changes in the expression of cytoskeleton-related proteins, elevated *P*CO2 also resulted in upregulation of mitochondrial malate dehydrogenase. This latter is a ribosomal protein and a proteasome subunit that reflects elevated PCO2 and/or reduced pH, altering the energy metabolism, protein synthesis, and degradation in oysters (Glickman & Ciechanover, 2002; Kossinova et al., 2008; Tomanek et al., 2011).

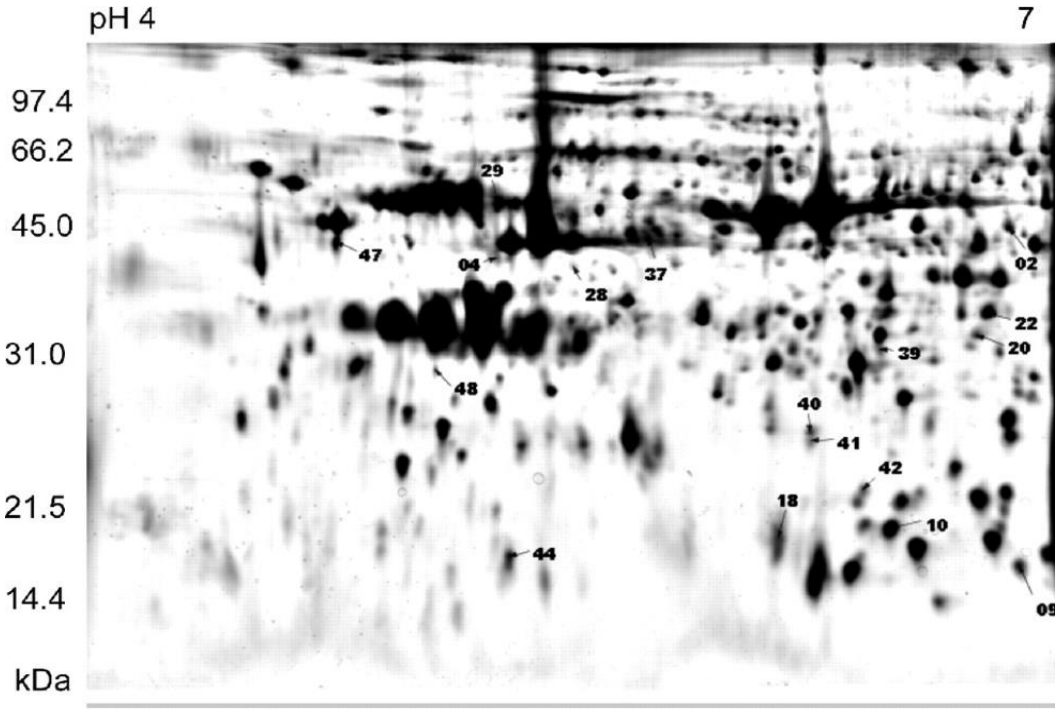

*Figure 71. A composite gel image (or proteome map) of twenty 2-D gel images of eastern oyster (*Crassostrea virginica*) mantle tissue exposed to normal and elevated CO_2 levels for 2 weeks. The image represents the mean pixel volume for each of the 456 detected protein spots. The numbers correspond to proteins that significantly changed in abundance in response to treatment conditions and identified by tandem mass spectrometry (Tomanek et al., 2011).*

Table 46. Protein identifications and fold changes with hypercapnia treatment in mantle tissue of the eastern oyster, Crassostrea virginica (Tomanek et al., 2011).

Spot ID	Protein ID	*M*, (kDa) estimated	pI estimated	*M*, (kDa) predicted	pI predicted	GenBank ID	MOWSE score	Peptide matches	Sequence coverage (%)	Mean normalized volume		Ratio	Functional category
										39 Pa P_{CO2}	357 Pa P_{CO2}		
2	Calponin 2	52.00	6.90	33.80	6.60	gi1164568905	47	2	4	0.129± 0.007	0.168± 0.011	1.305	Cytoskeleton
4	Actin	47.00	5.30	41.80	5.30	gi132423714	74	2	7	0.107± 0.016	0.181± 0.012	1.688	Cytoskeleton
9	Actin depolymerization factor-1 (ADF)	11.00	6.90	17.30	7.60	giI31904714	51	2	13	0.163± 0.011	0.252± 0.016	1.546	Cytoskeleton
10	Peroxiredoxin-5	14.00	6.50	19.60	8.30	gi1152818317	141	4	32	0.365± 0.006	0.453± 0.024	1.241	Oxidative stress
18	Cu, Zn-superoxide dismutase	14.00	6.10	16.00	6.10	gi122598381	114	2	6	0.214± 0.015	0.329± 0.017	1.539	Oxidative stress
20	Receptor of activated kinase C	35.00	6.80	35.00	7.00	gi131906094	115	4	23	0.084± 0.005	0.111± 0.007	1.315	Cell signaling
22	Mitochondria! malate dehydrogenase	37.00	6.80	35.00	8.40	gi1152813302	105	3	13	0.239± 0.009	0.314± 0.016	1.315	Energy metabolism
28	(mMDH) Actin	45.00	5.50	41.70	5.30	gi131905164	44	2	9	0.021± 0.003	0.050± 0.005	2.298	Cytoskeleton
29	Collagen type 6, cc6	57.00	5.30	25.50	6.80	gi184142151	64	2		0.5950 0.032	0.412± 0.027	0.694	Extracellular matrix
37	Actin	50.00	5.80	41.80	5.30	gi122598136	51	2	12	0.112± 0.033	0.260± 0.045	2.321	Cytoskeleton
39	Thioredoxin peroxidase	32.00	6.50	25.00	8.40	gi113488586	82	2		0.066± 0.004	0.1160 0.010	1.751	Oxidative stress
40	Peroxiredoxin 2	23.00	6.30	22.30	7.60	gi1164571416	240	4	23	0.082± 0.008	0.049± 0.005	0.601	Oxidative stress
41	Peroxiredoxin 2	23.00	6.25	22.30	7.60	gi1164571416	240	4	23	0.0330 0.005	0.093± 0.009	2.778	Oxidative stress
42	Rap-1b precursor	17.00	6.40	20.80	6.40	911189407780	134	2	4	0.086± 0.005	0.042± 0.007	0.490	Cell signaling
44	Nucleoredoxin	12.00	5.30	45.20	9.40	gi114580680	143	5	18	0.166± 0.016	0.293± 0.040	1.770	Oxidative stress
47	40S ribosomal protein SA	50.00	4.80	33.50	5.20	gi131900908	235	4	15	0.127± 0.015	0.180± 0.010	1.417	Cell adhesion
48	Proteasomep type 3	30.00	5.00	23.00	5.40	gi1164584631	117	3	18	0.024± 0.004	0.097± 0.015	4.013	Protein degradation

Relative molecular masses (M_r) and isoelectric points (pi) are estimated according to the spots' position on the proteome map (Fig. 1). Ratios of hypercapnia/normcapnia are the mean levels of expression (abundance) under hypercapnic treatment relative to the normcapnia control treatment [values <1.0 (>1.0) indicate a decrease (increase) in protein abundance].

4.31. Application of Genomics and Proteomics for Study of the Integrated Response to Zinc Exposure in a Non-Model Fish Species, the Rainbow Trout

The onset of DNA array technology and proteomics has transformed molecular biology by allowing the analysis of cellular events. Recently, DNA array technology has revolutionized transcriptome analysis, enabling semi-quantitative expression studies of thousands of genes in response to a variety of conditions (Heller et al., 1997; Schena et al., 1998; Welford et al., 1998). There is substantial interest in using DNA arrays in toxicological studies for the analysis of cellular response mechanisms to a particular toxicant (Hogstrand et al., 2002).

In the present study, rainbow trouts (*Oncorhynchus mykiss*) were exposed to sublethal concentrations of waterborne zinc for up to 6 days. This study reports the use of a *Fugu rubripes* gill cDNA array to identify genes involved in response to zinc exposure in rainbow trout (*Oncorhynchus mykiss*) gill. It is important to understand that *Fugu rubripes* has been designated as a genetic model organism, which draft sequence is known, covering 90% of the Fugu genome. The obtained cDNA array revealed differentially expressed genes related to energy production, protein synthesis, paracellular integrity, and inflammatory response (Hogstrand et al., 2002).

Protein profiling investigations involve the separation of complex protein mixtures followed by the analysis of those proteins that exhibit altered expression. Analysis may continue with the identification of the proteins of interest transcriptomic approaches offer a powerful tool for the analysis of complex, integrated responses, providing insight into the cellular mechanisms of toxicant action, putative means of detoxification, and potential modes of acclimation to environmental zinc, However, protein, and not mRNA, is the functional unit of the cell. Post-translational modifications and degradation of proteins mean that the cellular phenotype may differ considerably from that predicted by analysis of transcription (Abbott, 1999).

The 2D separation was limited to 355 individual proteins that were present in three out of four pooled gill samples. This analysis indicated the presence of seven unique proteins that were diagnostic for zinc exposure (Table 47) (Hogstrand et al., 2002).

On the other hand, it was shown that zinc suppressed the appearance of four proteins. The standardized data collection procedure also allowed the comparison of protein abundance between zinc exposed and control gills. The unique seven proteins were found to have a two-fold increase in peak intensity upon zinc exposure, whereas suppressed four showed the reverse trend of a two-fold lower protein abundance in the zinc-exposed fish (Hogstrand et al., 2002).

Table 47. Unique and differentially expressed proteins in rainbow trout gill upon exposure to zinc, as determined by SELDI analysis (Hogstrand et al., 2002).

Response to	Molecular	Chip distribution			Exchanger beta
Zn(II) exposure	**mass (Daltons)**	**SAX**	**WCX**	**IMAC**	
Unique to Zn(II)	1618		*		No database matches
exposed fish					
	6343			*	No database matches
	6911		*		No database matches
	18731			*	*Brachydanio rerio* transcriptional regulator
					(Acc. no. P52161)
	58374		*		No database matches
	70301		*		*Oncorhynchus mykiss* complement 3-1
					fragment (Acc. no. P98093)
	84275		*	*	No database matches
Unique to controls	7763	*			*Cyprinus carpio* insulin-like growth factor
					(precursor) (Acc. no. Q90325)
	11543		*		No database matches
	37470		*		No database matches
	85486		*		No database matches
Up-regulated by	6964			*	No database matches
Zn(II) exposure					
	27442			*	*Sparus aurata* Apolipoprotein A-I
					(precursor) (Acc. no. O42175)
	37658			*	*Cyprinus carpio* Proto-oncogene protein c-fos
					(Acc. no. P79702); *Brachydanio rerio*
					developmental signalling molecules
					(Acc. nos. P51029; P51028); *Astyanax mexicanus*
					Retinal homeobox protein (Acc. No. Q9I9D5)
	83936		*	*	*Brachydanio rerio* cytosolic phospholipase A2
					(Acc. no. P50392)
	85080	*	*	*	*Oncorynchus mykiss* Na^+/H^+ exchanger â
					(Acc. no. Q01345)
	88369	*	*		No database matches
	96152	*			No database matches
Down-regulated	12185	*	*		*Cyprinus carpio* ovarian cystatin
by Zn(II) exposure					(Acc. no. P35481)
	54826	*	*	*	*Brachydanio rerio* growth regulator
					(Acc. no. P58781)
	60427	*		*	*Fugu rubripes* glucose-6-phospate dehydrogenase
					(Acc. no. P54996)
	95594	*	*	*	*Brachydanio rerio* developmental growth regulator
					(Acc. no. Q9W7J1)

*Represents the peaks presence on a chip.

The determination of the identity of these proteins was performed by SELDI-TOF-MS in combination with database (SWISS-PROT) search. Fig. 1 illustrates population of proteins with a molecular mass between 5 and 10 kDa present in zinc-exposed (Fig. 72A) and control gills (Fig. 72B) at 24 h. Conventional SELDI-TOF-MS analysis yielded seven proteins that were

consistently present only in zinc-exposed gills, and four proteins unique to gills from control fish. A further 11 proteins were differentially regulated. Identification of these proteins by bioinformatics proved difficult in spite of detailed information on molecular mass, charge and zinc-binding affinity (Hogstrand et al., 2002).

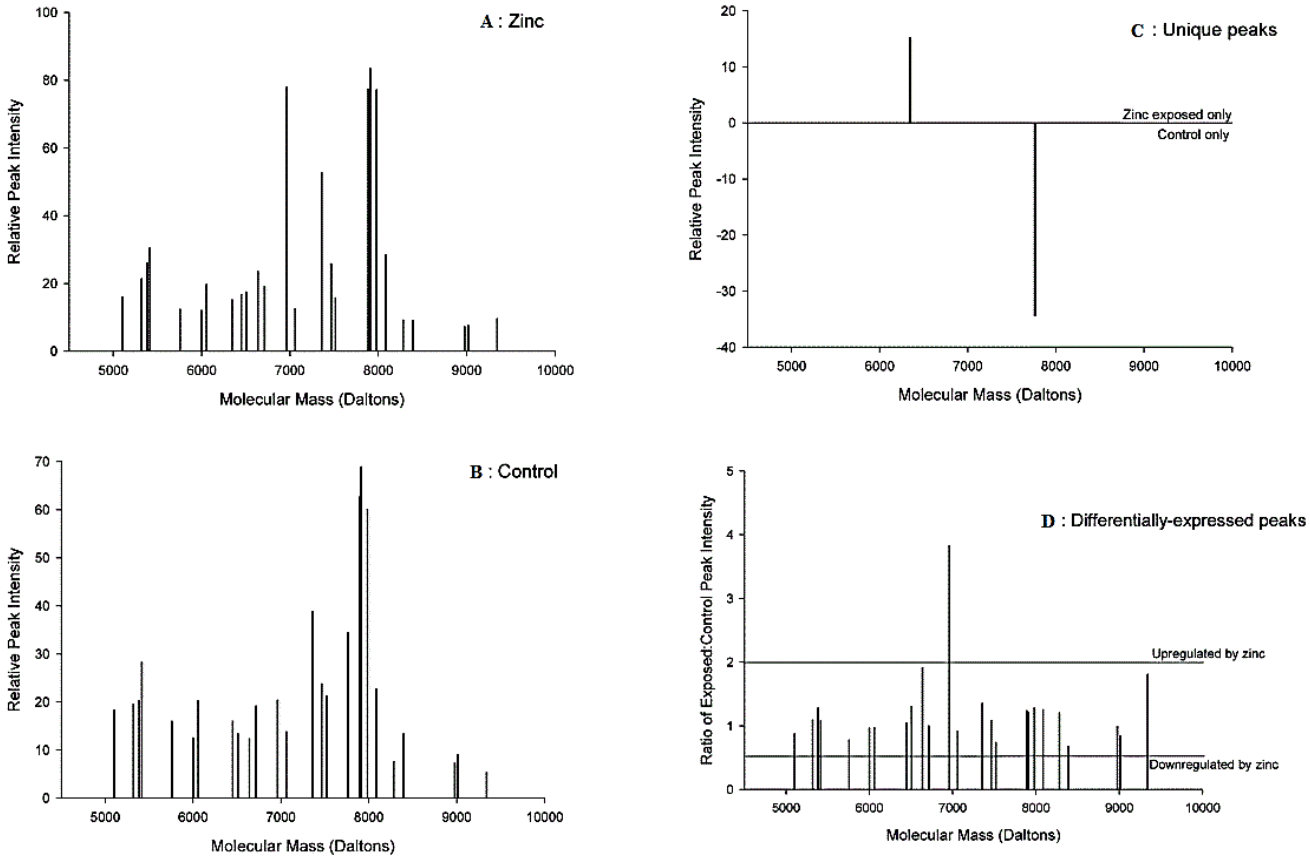

Figure 72. An example of protein analysis using SELDI. Protein peaks from zinc-exposed gills (A) are compared to identically processed samples from control gills (B). Subtraction of commonly occurring peaks reveals uniquely induced (present in zinc-exposed gills only) or repressed (present in control gills only) proteins (C). Quantitative analysis of exposed vs. control gills reveals proteins with altered expression levels (D). The example shown is a composite analysis of proteins with mass between 5 and 10 kDa occurring on immobilized metal affinity, weak cationic exchange, and strong anionic exchange surface affinity chips after 24 h of zinc exposure (Hogstrand et al., 2002).

4.32. Application of a Label-Free, Gel-Free Quantitative Proteomics Method for Ecotoxicological Studies of Small Fathead Minnows Fish

Although two-dimensional electrophoresis (2D-GE) remains the basis or many ecotoxicoproteomic analyses, newer non-gel-based methods are beginning to be applied to overcome throughput and coverage limitations of 2D-GE (Ralston-Hooper et al., 2013).

The overall objective of this presented research was to apply a comprehensive, liquid chromatography−tandem mass spectrometry (LC-MS/MS)-based proteomic approach to identify and quantify differentially expressed hepatic proteins from female fathead minnows exposed to fadrozole, a potent inhibitor of estrogen synthesis (Ralston-Hooper et al., 2013).

Female fathead minnows were exposed to 0 (control), 0.04, and 1.0 μg of fadrozole/L of water for 4 days, and proteomic analysis was performed. Proteins were extracted and digested, and proteolytic peptides were separated via high-resolution one- or two-dimensional (1-D or 2-D) ultrapressure liquid chromatography (UPLC) and analyzed by tandem mass spectrometry (Ralston-Hooper et al., 2013).

Following ID gel separation, 782 unique proteins and 3419 peptides were identified. Following LC-ESI-MS/MS analysis it was noted that 173 proteins had more than one peptide match per protein, whereas 309 had only one peptide match (Figure 73A). The coefficient of variation (CV) for the internal standard (yeast alcohol dehydrogenase) across the four quality control (QC) pools during the 2-day analysis had an average of 6.9%. Furthermore, the internal standard expression level across all 15 samples was an average 8.9%, suggesting excellent analytical reproducibility (Ralston-Hooper et al., 2013).

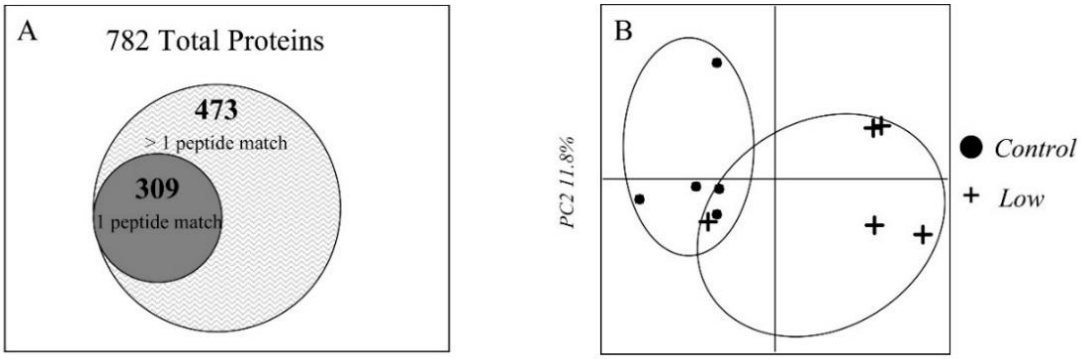

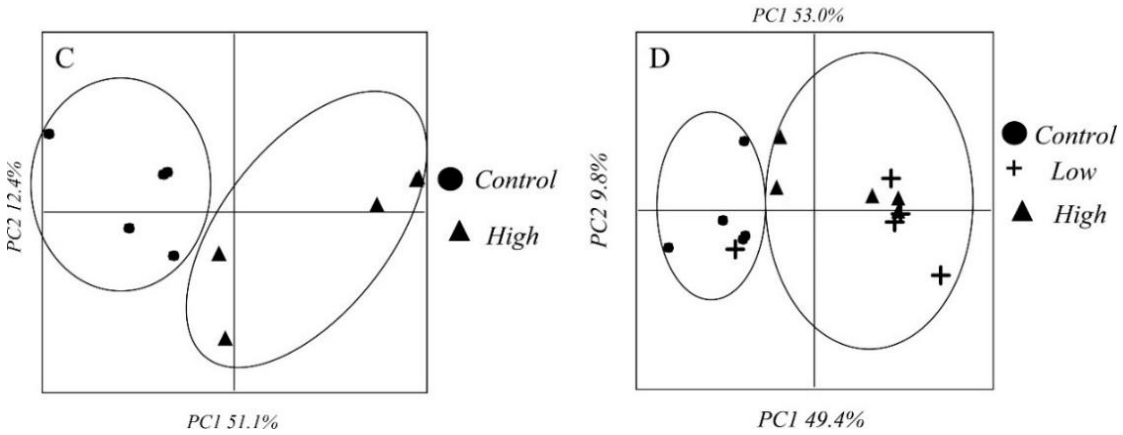

Figure 73. (A) Venn diagrams of the total number of proteins identified by a nonlabeled, gel-free proteomics method (LC-ESI-MS^e). (B−D) Principal component analysis (PCA) to visualize treatment effects as well as biological variability of (B) control vs low dose,(C) control vs high dose, and (D)all treatments (Ralston-Hooper et al., 2013).

Figure 74 establishes the excellent reproducibility and alignment of the product ion peptides across treatment, based on extracted ion chromatograms of selected expressed ions at low (Figure 74C) and high levels (Figure 74A) as well as peptides that were unchanged due to treatment (Figure 74B). Average protein intensity CVs for the individual treatments were 37.6%, 57.1%, and 44.3% for the control, 0.04, and 1.0 μg/L treatments, respectively (Ralston-Hooper et al., 2013).

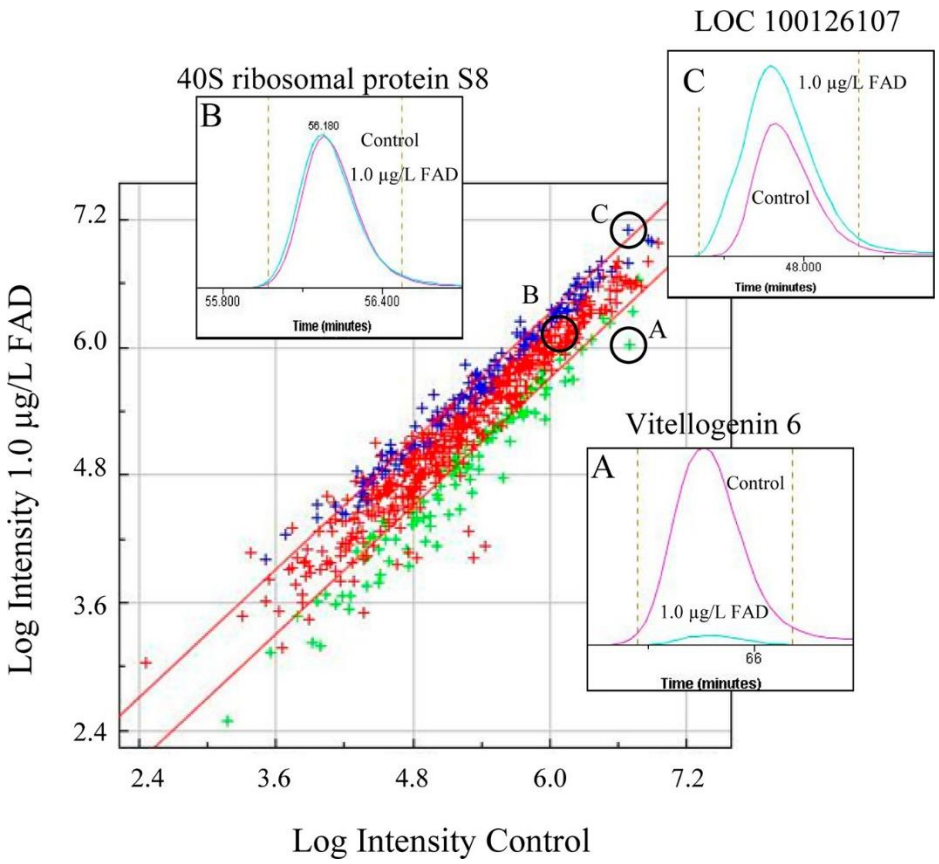

Figure 74. Scatter plot of the log transformed HPLC-MS peak areas of tryptic peptides from proteins of Fathead minnows exposed to 1.0 µg/L fadrozole (y-axis) versus control (x-axis). Red crosses (+) indicate peptides associated with proteins that did not show significant change in expression whereas dark blue crosses (+) indicate those proteins that were up-regulated (greater than 2.0 fold mean change) in fadrozole-exposed fish relative to control. Green crosses (+) represent proteins that were down-regulated in the fadrozole-exposed fish. Extracted ion chromatograms are shown for selected peptides to illustrate the reproducibility and alignment of peptides that are expressed at high (C − Predicted protein LOC 100126107) and low levels (A− Vitellogenin 6) in the fadrozole-exposed fish (light blue peaks) relative to controls (magenta peaks), as well as peptides that that did not show changes in expression (B − 40 S ribosomal protein S8) (Ralston-Hooper et al., 2013).

2D gel separation using the control versus 0.04 µg/L FAD dose comparison showed that 312 proteins had greater than an absolute 2-fold mean change value when compared to the controls. From these 312 proteins, 242 were also significant (p-value <0.05). 93 were downregulated and 152 were upregulated. PCA analysis performed on all identified proteins revealed distinct separation between control and 0.04 µg/L FAD dose samples, with the exception of one treatment sample that clustered among the control samples (Figure 73B). When multidimensional LC-ESI-

MS/MS analysis (2-D) was performed, an average increase of 1.9× in the number of identified proteins was observed. Differentially expressed proteins in fadrozole exposures were consistent with changes in liver function, including a decline in concentrations of vitellogenin as well as other proteins associated with endocrine function and cholesterol synthesis. Mass spectra were searched against the National Center for Biotechnology Information (NCBI) ray-finned fish (Actinopterygii) database, resulting in the identification of 782 unique proteins by single-dimension UPLC (Ralston-Hooper et al., 2013).

Table 48. Differentially Expressed Hepatic Proteinsa between Control and Fadrozole-Exposed Female Fathead Minnows (Ralston-Hooper et al., 2013).

NCBI ref no.	protein[b]	species	peptide match	*p*-value	*x*-fold change
1.0 µg/L FAD Dose					
XP_693881.4	VTG (predicted)	*D. rerio*	**1**	<0.001	–5.6
NP_001116082.2	VTG 6	*D. rerio*	**24**	<0.001	–4.8
NP_001038362.2	VTG 1	*D. rerio*	**8**	<0.001	–3.2
NP_001038378.1	VTG 2, isoform 1	*D. rerio*	**11**	<0.001	–2.0
NP_001118072.1	ZP2	*Oncorhynchus mykiss*	**1**	0.395	–10.7
NP_955893.1	HSD17B2	*D. rerio*	**2**	0.203	–1.7
NP_001007393.1	PGRM1	*D. rerio*	**4**	0.005	2.0
XP 003199447.1	CNBP or SREBP (predicted)	*D. rerio*	**3**	0.04	1.8
0.04 µg/L FAD Dose					
XP_693881.4	VTG (predicted)	*D. rerio*	**1**	0.118	–2.6
NP_001116082.2	VTG 6	*D. rerio*	**24**	0.012	–2.3
NP_001096141.1	VTG 7	*D. rerio*	**3**	0.004	–2.1
NP_001118072.1	ZP2	*O. mykiss*	**1**	0.506	–9.2
NP_955893.1	HSD17B2	*D. rerio*	**2**	0.236	–1.4
NP_001007393.1	PGRM1	*D. rerio*	**4**	0.009	2.1
XP 003199447.1	CNBP or SREBP (predicted)	*D. rerio*	**3**	0.001	2.4

[a]>2.0-fold change.
[b]VTG, vitellogenin; ZP2, zona pellucida glycoprotein 2.3; HSD17B2, hydroxysteroid dehydrogenase-like protein 2; PGRM1, membrane-associated progesterone receptor component 1; CNBP or SREBP, cellular nucleic acid-binding protein or sterol regulatory element-binding protein.

Overall, these results demonstrate that a gel-free, label-free proteomic analysis method can successfully be utilized to determine differentially expressed proteins in small fish species after toxicant exposure (Ralston-Hooper et al., 2013).

4.33. **Proteomic Analysis of Bllood Cells in Fsh Exposed to Chemotherapeutics**

Proteomics technology is increasingly used in ecotoxicological studies to characterize and monitor biomarkers of exposure. The present study aims at identifying the long-term effects of malachite green (MG) exposure on the proteome of peripheral blood mononuclear cells (PBMC)

from the Asian catfish, *Pangasianodon hypophthalmus*. A common (0.1 ppm) concentration for therapeutic treatment was applied twice with a 72 h interval. PBMC were collected directly at the end of the second bath of MG (T1) and after 1 month of decontamination (T2) (Pierrard et al., 2012).

Analytical 2D-DIGE gels were run (Figure 75), and a total of 2551 ± 364 spots were matched. Among them, MG induced significant changes in abundance of 116 spots with no recovery after one month of decontamination. Using LC-MS/MS (Table 49) (Pierrard et al., 2012) and considering single identification per spot, we could identify 25 different proteins. Additionally, MG residues were measured in muscle and in blood, indicating that leuco-MG has almost totally disappeared after one month of decontamination (Pierrard et al., 2012). This work highlights the long-term effects of MG treatment on the PBMC proteome from fish intended for human consumption (Pierrard et al., 2012).

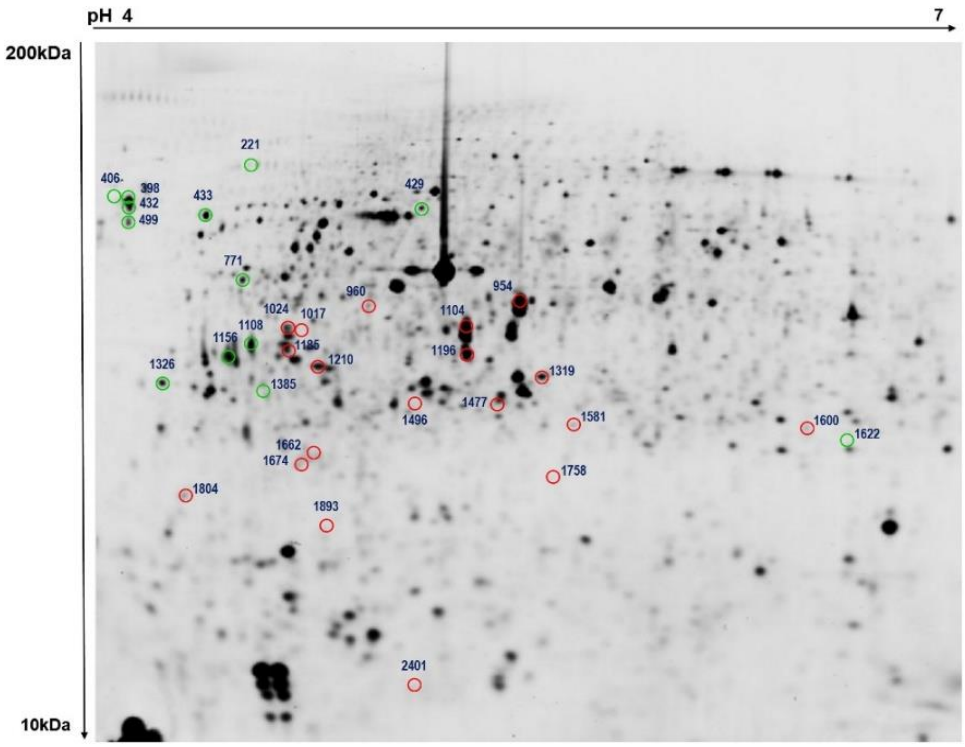

Figure 75. Representative 2D gels showing the protein expression profiles obtained from PBMC isolated from Pangasianodon hypophthlmus in vivo exposed to the classic MG treatment. Proteins were separated by 24 cm 4–7 NL IPG-Strips and loaded on SDS-PAGE (8–13% acrylamid) gels. Identified spots allocated by the De Cyder software showed significant changes in intensity (Anova 2 condition 1 value, $p<0.05$; interactions value, $1 \leq p \geq 0.05$) that are common for both sampling times (Pierrard et al., 2012).

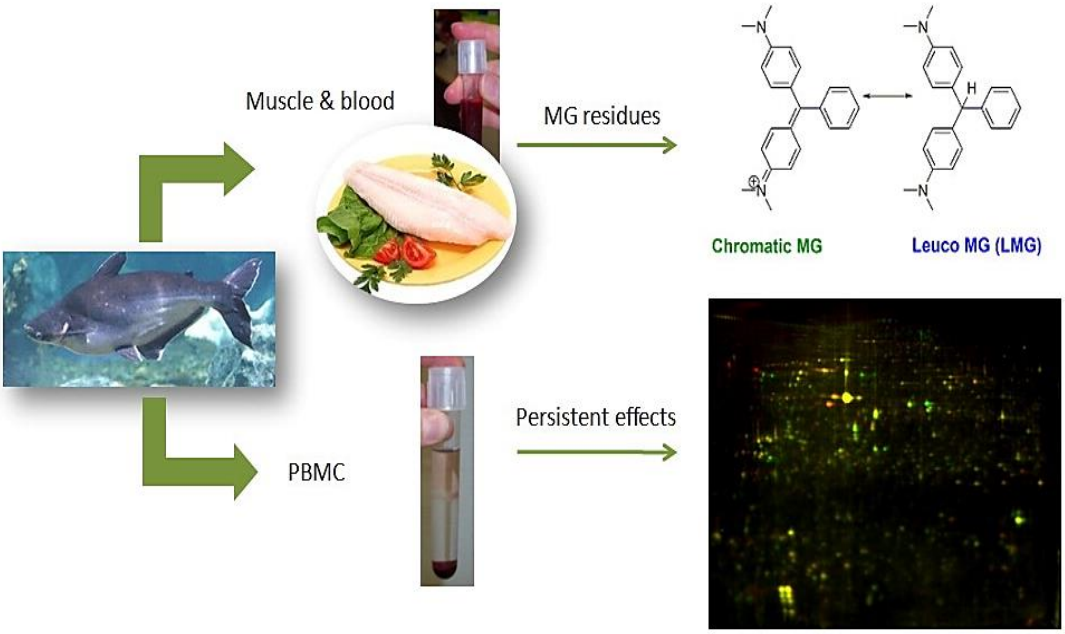

Figure 76. Schematic summary about evaluating the impact of malachite green (MG) treatment in peripheral blood mononuclear cells (PBMC) of the Asian catfish, Pangasianodon hypophthalmus *(Pierrard et al., 2012).*

Table 49. Detailed list of protein spots identified by nano LC-MS/MS differentially expressed in PBMC of P. hypophthalmus following 0.1 ppm MG treatment (T1) and after one month of decontamination (T2), selected following an ANOVA 2 filter (MG treatment $p \leq 0.05$; no interaction between MG treatment and sampling time $p \geq 0.05$) (Pierrard et al., 2012).

Spot No.	Accession No.[a]	Protein name	Species	Matching peptides	Theoretical pI/Mw (kDa)	Fold change[b] T1	Fold change[b] T2	ANOVA 2 MG	ANOVA 2 Interaction
Glycolytic pathway									
1319	Q6PC12	Enolase 1	*Danio rerio*	2	6.2/47	1.84	2.27	0.018	0.86
1600	Q90WD9	Glyceraldehyde-3-phosphate dehydrogenase	*Solea senegalensis*	3	6.4/36	1.42	1.33	0.042	0.61
Cytoskeleton									
954	Q6NWK7	Tuba1 protein (Tubulin, alpha 1, like)	*Danio rerio*	2	4.9/50	1.19	1.30	0.033	0.73
1804	C0H808	Tubulin beta-1 chain	*Salmo salar*	6	4.8/50	1.02	1.19	0.025	0.073
960	C0H808	Tubulin beta-1 chain	*Salmo salar*	9	4.8/50	1.47	1.63	0.043	0.79
2401	Q7SXW6	Actin-related protein 2-A (Actin-like protein 2-A)	*Danio rerio*	4	6.3/45	1.52	1.12	0.019	0.16
1156	Q803M1	Novel protein similar to vertebrate tropomyosin 1 (Alpha) (TPM1, zgc:77592) (Tropomyosin 3)	*Danio rerio*	2	4.8/29	− 1.16	− 1.29	0.048	0.16
1108	Q803M1	Novel protein similar to vertebrate tropomyosin 1 (Alpha) (TPM1, zgc:77592) (Tropomyosin 3)	*Danio rerio*	3	4.8/29	− 1.20	− 1.30	0.0016	0.48
1662	Q7SXP1	Capping protein (Actin filament) muscle Z-lin	*Danio rerio*	2	5.7/31	1.46	2.22	0.014	0.34
Molecular chaperones									
398	Q6DI13	Calreticulin like	*Danio rerio*	4	4.3/48	− 1.91	− 1.99	0.024	0.94
406	Q6DI13	Calreticulin like	*Danio rerio*	2	4.3/48	− 1.64	− 1.82	0.048	0.89
432	Q6DI13	Calreticulin like	*Danio rerio*	2	4.3/48	− 1.94	− 2.44	0.019	0.66
499	Q6DI13	Calreticulin like	*Danio rerio*	3	4.3/48	− 2.02	− 1.96	0.02	0.83
433	B0S564	Proline 4-hydroxylase, beta polypeptide (Protein disulfide isomerase; thyroid hormone binding protein p55) (P4HB)	*Danio rerio*	3	4.5/57	− 4.02	− 5.84	0.031	0.89
771	P47773	Heat shock cognate 71 kDa protein	*Ictalurus punctatus*	2	5.2/71	− 1.26	− 1.50	0.031	0.44
429	Q803B0	Heat shock 60 kD protein 1 (Chaperonin)	*Danio rerio*	7	5.6/61	− 1.52	− 2.83	0.039	0.35
1581	B5RI17	Chaperonin containing TCP1, subunit 3 - T-complex protein 1 subunit gamma	*Salmo salar*	3	6.3/60	1.31	2.32	0.0013	0.052
1024	A5H1I2	Glucose-regulated protein 94	*Paralichthys olivaceus*	3	4.7/92	1.45	1.28	0.019	0.34
Ubiquitin proteasome system (UPS)									
1210	Q4V918	Proteasome subunit alpha type	*Danio rerio*	5	4.9/24	1.34	1.40	0.04	0.95
1017	B5X5I0	26S protease regulatory subunit 6A	*Salmo salar*	4	5.1/48	1.40	1.18	0.013	0.34
Regulators of Ras super family									
1893	Q802W6	Rho GDP dissociation inhibitor (GDI) alpha	*Danio rerio*	2	5.0/23	1.03	2.39	0.027	0.11
1496	C1BJZ6	Rab GDP dissociation inhibitor beta	*Osmerus mordax*	2	5.4/51	1.34	1.41	0.0025	0.7
221	Q4SGG0	Chromosome undetermined SCAF14596, whole genome shotgun sequence	*Tetraodon nigroviridis*	2	8.4/200	− 1.80	− 1.65	0.0013	0.72
mRNA Splicing									
1674	A4QP67	Heterogeneous nuclear ribonucleoprotein D	*Danio rerio*	2	5.7/36	1.20	1.48	0.0001	0.052

1185	Q6NYU8	Heterogeneous nuclear ribonucleoprotein A/B	*Danio rerio*	2	5.8/37	1.53	1.18	0.013	0.25
1758	Q7SXP4	Serine/arginine-rich splicing factor 1A (Sfrs1 protein)	*Xenopus laevis*	2	10.3/32	1.41	1.69	0.0073	0.44
1385	Q5RKQ0	Pre-mRNA-splicing factor SPF27 (BCAS2 homolog)	*Danio rerio*	3	4.7/26	− 1.05	− 1.34	0.011	0.06
DNA replication									
1326	Q9PTP1	Proliferating cell nuclear antigen (PCNA)	*Ictalurus punctatus*	2	4.5/24	− 1.45	− 1.91	0.014	0.47
Other functions									
1104	C1K7M3	Annexin A4	*Ictalurus punctatus*	4	5.3/36	1.66	2.01	0.012	0.81
1196	C1K7M3	Annexin A4	*Ictalurus punctatus*	5	5.3/36	1.83	1.95	0.0057	0.95
1477	C1K7M3	Annexin A4	*Ictalurus punctatus*	4	5.3/36	1.42	2.02	0.005	0.33
1622	Q803M6	Protein tyrosine phosphatase, non-receptor type 6 (Ptpn6)	*Danio rerio*	3	7.9/67	− 1.27	− 1.29	0.045	0.95

[a] Accession number in UniProt/TrEMBL.
[b] Values > 0 indicate up-regulation, and < 0 indicate down-regulation.

5. Aquaculture Proteomics

The rising percentage of seafood production worldwide has been delivered from the aquaculture industry, which importance has increased due to the restricted commercial overfishing. For this reason, there has been an increased interest in improving the quality and certification of seafood products in order to guarantee their safety, quality, authenticity, and nutritional benefits (Moreira et al., 2021).

As already mentioned, proteomics technology has shown to be a capable tool for unravelling the biological, physiological and ecological traits of seafood products, thus improving the cost-effectiveness and sustainability of aquaculture. Certainly, seafood production and shellfish farming can directly benefit from the proteomics technologies, which permitted the search for biomarkers .and for the detection of shellfish contamination, health, quality, safety and nutritional value (Gomes et al., 2017a).

Needless to say, shellfish consumption has been encouraged due to the low content of saturated fat, considerable levels of omega-3 polyunsaturated fatty acids, high-quality animal proteins, vitamins, such as B12 and C, and minerals such as Fe, Mn, P, Se, and Zn (T. Morais et al., 2020).

One of the main constraints in aquaculture production is the constant threat of the farmed fish vulnerability to diseases, which occur as a result of husbandry practices and external factors like pollution, climate changes. Without any doubt, it is primordial to better understand and characterize the intervenient culprit in a disease outbreak, which will cause huge economic losses. High-throughput proteomics technology is an important characterization tool, especially in pathogen identification and identifying the virulence mechanisms related to host-pathogen interactions in disease research. Aquaculture proteomics important role is also maximized by its holistic approach to understanding pathogenesis processes and fish responses to external factors like stress or temperature, making it one of the most promising tools for fish pathology research (Moreira et al., 2021).

5.1. Proteomic Strategies to Evaluate the Impact of Farming Conditions on Food Quality and Safety in Aquaculture Products

This section reports an elegant review that presents the primary applications of various proteomic strategies to evaluate the impact of farming conditions on food quality and safety in

aquaculture products. As mentioned before, aquaculture is a quickly growing sector that represents 47% of total fish production. This review examines the following topics involving food quality, dietary management, fish welfare, stress response, food safety, and antibiotic resistance. These topics were studied by proteomic techniques and strategies which were successfully applied. The review concludes by outlining future directions and potential perspectives (Carrera, Piñeiro, et al., 2020).

The following figure shows the proteomic approaches used for discovery and targeted proteomics, with their corresponding workflows (Carrera, Piñeiro, et al., 2020).

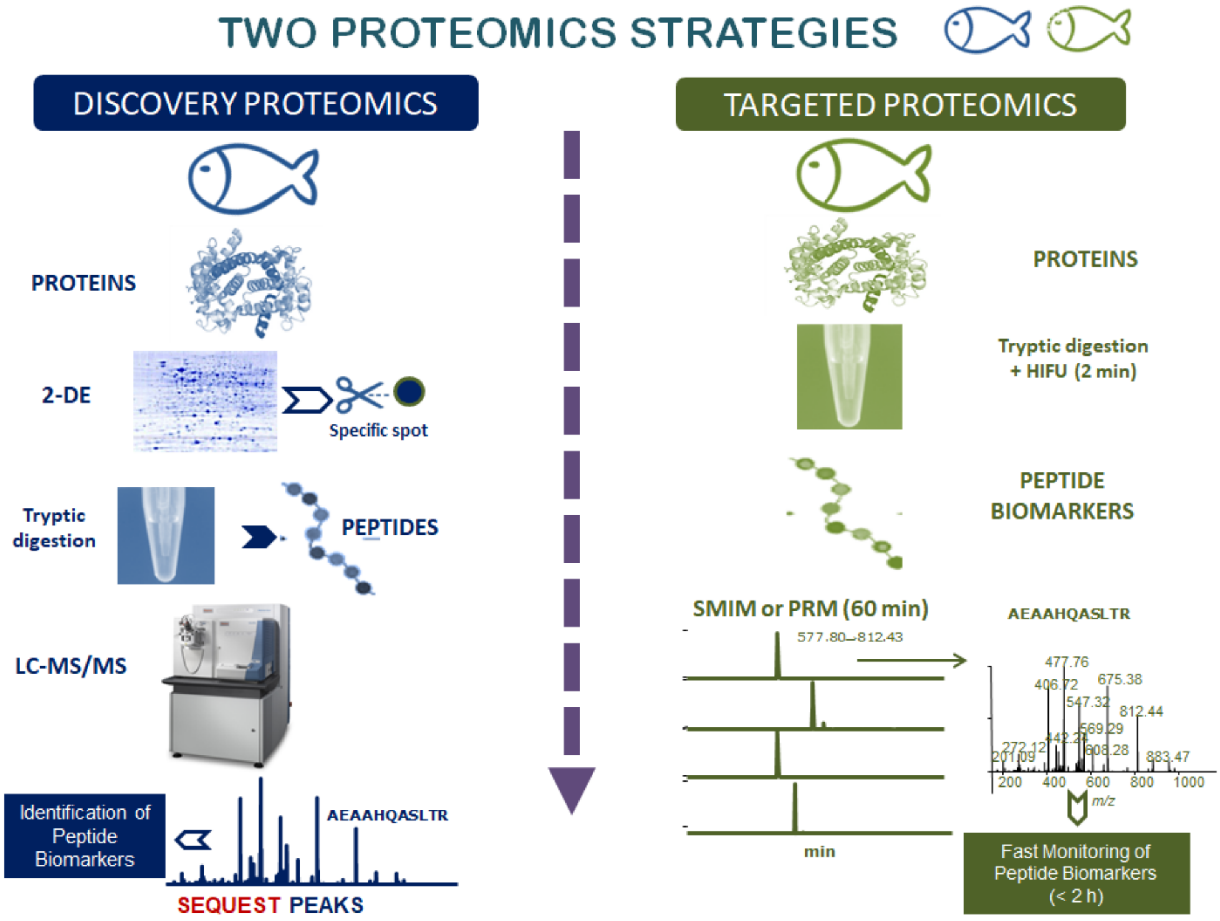

Figure 77. Workflow of proteomics: discovery and targeted proteomics (Carrera, Piñeiro, et al., 2020).

The discovery proteomics approach (also knowm as the Bottom-Up Approach) aims at identifying biological markers in a given proteome. This approach usually uses two-dimensional gel electrophoresis (2-D DE), which allows the extraction of the individual protein analytes; this has been traditionally the technique selected for the separation of proteins samples (Rabilloud & Lelong, 2011). Please note that the gel-based procedure is the most suitable approach for species whose protein sequences are unknown, including many fish. In addition, the 2-DE gels themselves can be analyzed by programs such as Progenesis and PDQuest (Carrera, Piñeiro, et al., 2020). The proteins of the sample are separated, proteolyzed with enzymes such as trypsin or Glu-C and the peptides obtained are subsequently identiufed by tandem mass spectrometry (MS/MS). The identification is performed by comparison of the MS/MS spectra of the peptides obtained with orthologous protein sequences from related species or by *de novo* MS/MS sequencing (Carrera et al., 2007).

In the gel-free approaches, also known as "Target Approach or s"hotgun proteomics", the proteins are directly digested in the extract with a selected enzyme. The obtained mixture of peptides is subsequently analyzed by liquid chromatography (LC) coupled to tandem mass spectrometry (LC-MS/MS) (Carrera, Ezquerra-Brauer, et al., 2020; Wolters et al., 2001). It is possible to perform multidimensional LC separations, combining, for example, strong anion/cation exchange chromatography (SA/CX) and reverse phase (RP) chromatography (Gao & Yates, 2019).

Database searching programs, like SEQUEST, X! Tandem, or Mascot (Eng et al., 1994; Perkins et al., 1999), allow the tentative identification of presumed peptide sequences based on the obtained fragmentation spectra, and additional software programs, such as Percolator, are used to validate the identification (Käll et al., 2007). When the protein is not present in the database, then the peptides must be sequenced de novo (Shevchenko et al., 1997), either manually or using programs such as PEAKS and DeNovoX (Ma et al., 2003). This approach has been successfully used in the de novo sequencing of some fish allergens, such as parvalbumins and shrimp arginine kinases (Carrera et al., 2007, 2010a; Ortea et al., 2009).

When protein quantification is deemed necessary, the methods of choice include metabolic stable isotope labelling (such as stable isotope labelling by/with amino acids in cell culture, SILAC) (Ong et al., 2002); isotope tagging by chemical reaction, such as isobaric tags for relative and absolute quantitation (iTRAQ), tandem mass tag (TMT) and difference gel electrophoresis (DIGE) (Mateos et al., 2015; Robotti & Marengo, 2018; Stryiński et al., 2019); stable isotope incorporation via

enzyme reaction (i.e., ^{18}O) (López-Ferrer et al., 2006); and label-free quantification (i.e., measuring the intensity of the peptides at the MS level) (Mueller et al., 2007). After matching the obtained peptides and proteins by alignment software programs like BLAST (https://blast.ncbi.nlm.nih.gov/), it is possible to select relevant peptide biomarkers to be used in the subsequent phase, namely, targeted proteomics (Carrera, Piñeiro, et al., 2020).

Targeted proteomics refers to monitoring relevant peptide biomarkers, and it has become a recognized methodology to detect selected proteins with significant accuracy, reproducibility, and sensitivity (Borràs & Sabidó, 2017). In targeted proteomics, the MS analyzer is focused on detecting only the peptide/s chosen by selected/multiple-reaction monitoring (SRM/MRM) (Aebersold et al., 2016). Monitoring appropriate transitions (evens of precursor and fragment ions m/z) represents a common analysis for detecting and identifying peptide biomarkers. These techniques are selective, sensitive, highly reproducible, with a high dynamic range and an excellent signal-to-noise (S/N) ratio (Carrera, Piñeiro, et al., 2020; Lange et al., 2008).

5.2. Potential Use of Proteomics in Shellfish Aquaculture: From Assessment of Environmental Toxicity to an Evaluation of Seafood Quality and Safety

Proteomic technology was used to identify shellfish species in search of differentially regulated proteins and to characterize biologically active proteins. Indeed, proteomics technology was primarily used to instigate the alterations of the proteome that impact shellfish quality and safety, concerning *the* impact of contaminants, climate change, algal toxins, pathogens, allergens, processing and storage, with further repercussion to human health (Akaike, 2015; Carrera et al., 2013; Gomes et al., 2017a; Piñeiro et al., 2010b; Rodrigues et al., 2012). Nevertheless, the use of large-scale proteomics in shellfish farming is still in its infancy, and the lack of information at the genome level for most of the shellfish cultured species is still a major limiting factor in aquaculture proteomics, making protein identification a challenging task (Gomes et al., 2017a).

With this in mind, this section will focus on how advanced and throughput proteomic tools have been demonstrated to be very useful. The use of the proteomic tools also allowed to assess the toxicity related to environmental contamination b and determine the safety and quality of shellfish food. An overview of the different proteomic approaches was addressed regarding the limitations inherent to such methods, new approaches, and future challenges (Gomes et al., 2017a).

5.3. **Aquaculture Main Shellfish Species**

In the past five decades, global fisheries and aquaculture have grown steadily, and seafood consumption per capita has increased from an average of 9.9 kg in the 1960s to 22.45 kg in 2012 (FAO 2020). Molluscan shellfish have traditionally been a significant component of world aquaculture (H. Yang et al., 2016).

Shellfish aquaculture includes the raising of molluscs and crustaceans, both of freshwater and marine origin (H. Yang et al., 2016). The bivalve molluscs are the most commonly cultured and widely distributed types of shellfish. The different species intended for human consumption consist of mussels, clams and oysters: which are generally farmed in shallower coastal areas, exploiting bottom and hanging/pole-farming systems. *Mytilus edulis* (blue mussel) and *Mytilus galloprovincialis* (Mediterranean mussel) is the principal cultured mussel species. In addition, Blue mussels are broadly distributed in European waters, extending from the White Sea, Russia as far as south to the Atlantic coast of Southern France. The green-lipped mussel (*Perna canaliculus*) has been harvested for human consumption since the beginning of human habitation in New Zealand (Gomes et al., 2017b).

The cosmopolitan and ubiquitous family of clams *Veneridae* is distributed across all oceans, from intertidal flats to deep-sea areas, colonizing all types of soft bottoms, including over 680 living species worldwide. In general, the clam *venerids burrow* grows in muddy or sandy habitats but can also colonize mangrove zones, coastal lagoons, estuaries, bays, surf zones and the deep sea. The hard-shell clam, *Mercenaria mercenaria,* is mainly harvested in both the Atlantic and Pacific oceans; whereas, *Chamalea gallina*, the common clam, occurs in the Mediterranean Sea and the Atlantic Ocean (Gaspar et al., 2013; Gomes et al., 2017c).

The most commonly oyster farmed species include the Eastern oyster (*Crassostrea virginica*), the Pacific oyster (*Crassostrea gigas*), the Belon oyster (*Ostrea edulis*), and the Sydney rock oyster (*Saccostrea glomerata*). It should be pointed out that *C. gigas* is native to the Pacific coast of Asia, and it has become the oyster of choice for cultivation in North America, Australia, Europe and New Zealand because of its rapid growth and tolerance to different environmental conditions (H. Yang et al., 2016).

Nonetheless, the shellfish aquaculture also includes a wide variety of freshwater and marine crustacean species, such as: decapods, crustaceans, including crayfish, crabs, lobsters, prawns and shrimps (H. Yang et al., 2016).

5.4. Shellfish Safety Proteomic Applications

This excellent review, furthermost presents all health risks associated with seafood safety are usually related to anthropogenic contamination of the environment where the organisms come from. It is well accepted that infectious disease outbreaks such as typhoid fever, hepatitis and salmonellosis and poisoning by methylmercury, heavy metals and organochlorine compounds are directly related to the unsafe consumption of shellfish, acting as vectors of chemicals, toxins and pathogens derived from human activities (Gomes et al., 2017c; Mahaffey, 2004; Rippey, 1994; Sivaperumal et al., 2007; A. G. Smith & Gangolli, 2002). Additionally, it is well accepted that intensive or super-intensive use of aquaculture systems are usually associated with different factors such as heavy stocking densities and the use of certain feed, chemicals and drugs, which are also responsible for potentially unsafe shellfish production and for a negative impact on the surrounding environment (Gomes et al., 2017c).

For these reasons, proteomics is an affordable tool not only for environmental research but also for food science, offering a snapshot of the organism's state and mapping the entirety of its adaptive potential and mechanisms. In fact, it may provide valuable insight into the health status of shellfish; the stress or contamination levels at the breeding place (Gomes et al., 2017c; Paerl & Otten, 2013).

5.5. Characterization and Expression Analysis of Myogenin Gene in White Muscle of Chinese Mandarin Fish (*Siniperca chuatsi*)

Myogenin, is a transcriptional activator protein encoded by the MYOG gene. Myogenin is a muscle-specific basic-helix-loop-helix (bHLH) transcription factor involved in the coordination of skeletal muscle development myogenesis and repair. Myogenin is a member of the MyoD family of transcription factors. Also, myogenin plays a crucial role in myoblast differentiation and maturation (Chu et al., 2014).

In the present study, the myogenin gene structure and expressional patterns in *Siniperca chuatsi* were characterized. Sequence analysis indicated that the myogenin shared a similar structure and the conserved bHLH domain with other vertebrate myogenin genes (Chu et al., 2014). Sequence alignment and phylogenetic analysis showed that *Siniperca chuatsi* myogenin shared homologous with *Epinephelus coioides*, *Sparus aurata*, *Takifugu rubripes* and *Salmo salar* (Chu et al., 2014).

Whole-mount in situ hybridization (WMISH) is a common technique used for visualizing the location of expressed RNAs in embryos. In this process, synthetically produced RNA probes are first complementarily bound, or "hybridized," to the transcripts of target genes (Education, 2021). Whole-mount *in situ* hybridization revealed that myogenin expression was first detected in the gastrula stage embryos and high levels of expression at the 24 somite stage (Chu et al., 2014). After the 24 somite stage, myogenin expression began to decrease in the anterior somites where somatic cells were differentiated. Further, the muscle structural gene, MyHC, and myogenin, are concomitantly expressed during *S. chuatsi* embryonic development as assayed with whole-mount *in situ* hybridization (Chu et al., 2014).

In the adult fish, myogenin showed the highest levels of expression in the brain compared with the kidney, spleen, liver, heart and white muscles. This present research work on the myogenin gene from the mandarin fish provides useful information for fish molecular biology and fish genomics fish. Also, it provides useful information on fish molecular biology and fish genomics (Chu et al., 2014).

The complete genomic sequence of the myogenin spanned approximately 3.3 kb (Gene bank accession no. HQ724299), including 0.35 kb 5'-flanking sequence and 2.5 kb transcriptional unit followed by 0.45 kb 3' flanking sequence (Figure 78). The myogenin gene sequence contains three exons and two introns. The three exons were named as exon I, exon II and exon III with nucleotides of 537 bp, 96 bp and 120 bp, respectively, and the two introns, named intron 1 and intron 2, are of 803 bp and 95 bp each. The 5' promoter region analyzed with DNA star revealed that it contains two putative E-box sites (CAnn TG), a MEF-2 (myocyte enhancer factor-2) binding site (TAAATTTA) and a MEF3 (myocyte enhancer factor-3) binding site (TCAGGTTT). The two E boxes were located at 184 and 170 bp, while MEF2 and MEF3 at 238 and 359 bp upstream of the ATG starting codon, respectively (Chu et al., 2014).

Comparison of the *S. chuatsi* myogenin promoter sequences with other two fish species, *Sparus aurata* (EF462192) and *Epinephelus coioides* (HM190251) is presented in Figure 79. The nucleotide sequence and location of the regulatory elements are highly conserved among the three fish species (Figure 79) (Chu et al., 2014).

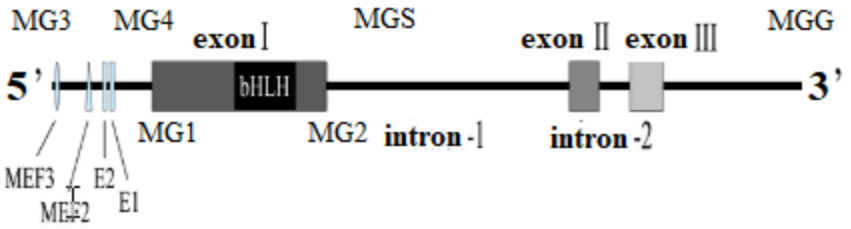

Figure 78. Genomic structure of S. chuatsi myogenin gene which contains 3 exons separated by 2 introns. The conserved basic Helix-loop-helix domain is located in the exon 1. The two putative E-boxes, the MEF2 and MEF3 binding sites are indicated in the promoter. The two E-boxes are located at 170 and 184 bp, while the MEF2 and MEF3 binding sites are located at 238 and 259 bp upstream from the ATG start codon. The full-length open reading frame is 735 bp with deduced amino acids of 250 AA (Gene bank accession # HQ724299) (Chu et al., 2014).

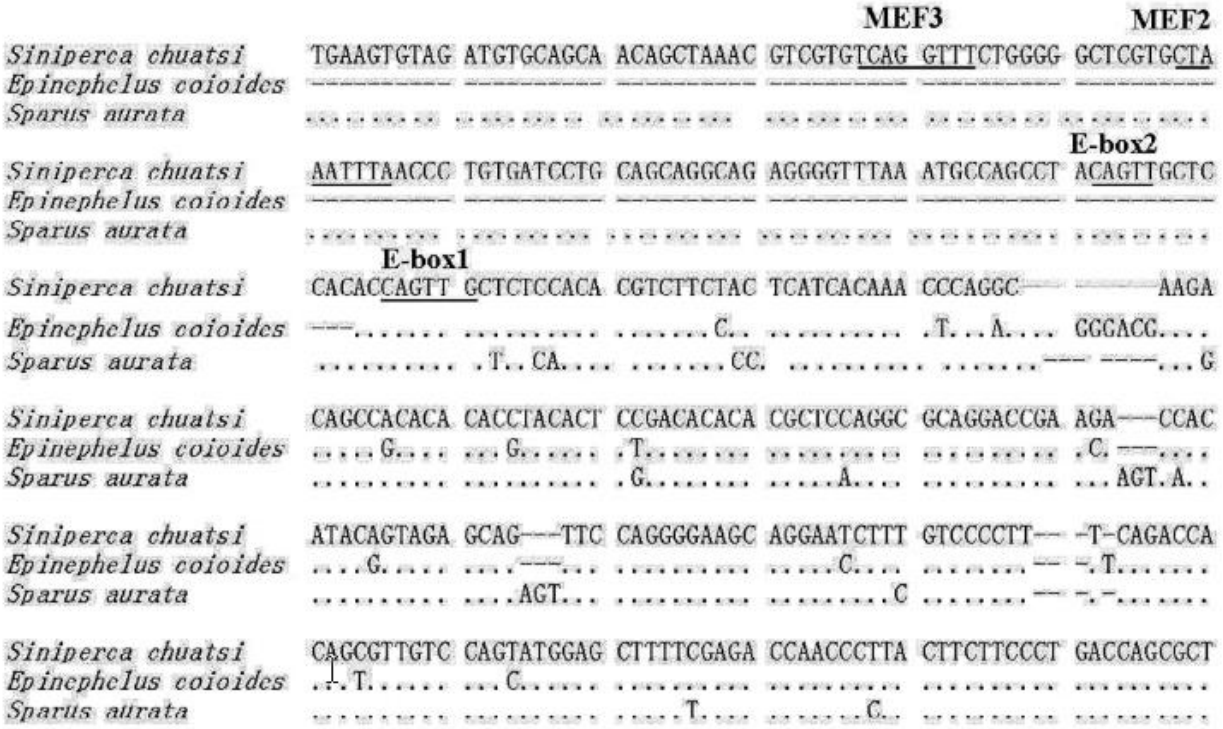

Figure 79. Comparison of the S. chuatsi myogenin promoter sequences with other fish species, Sparus aurata (EF462192) and Epinephelus coioides (HM190251). The two E-boxes, E-box 1 (CAGTTG) and E-box 2 (CAGTTG), MEF2 (CTAAATTTAA) and MEF3 (CAGGGTTT) binding sites are underlined. The nucleotide sequence and location of the regulatory elements are highly conserved among the three fish species (Chu et al., 2014).

5.6. **Comparison of *S. chautsi* Myogenin Protein Sequence and Phylogenetic Relations to Other Vertebrates**

The *S. chautsi* myogenin gene encodes a protein of 250 amino acids. The BLAST analysis of myogenin sequences of 16 species in the Gene bank revealed that the bHLH domain in the first exon of these myogenins was highly conserved among the species analyzed (Figure 80). The phylogenic analysis revealed that among the teolest species, *S. chautsi* myogenin had the highest sequence identity with myogenin from *Epinephelus coioides*, followed by *Sparus aurata, Takifugu rubripes, Salmo salar* and *Danio rerio*. The other vertebrate myogenin sequences were fallen into a group, including mammalians and reptile species, while the amphibians were in the middle (Figure 81) (Chu et al., 2014).

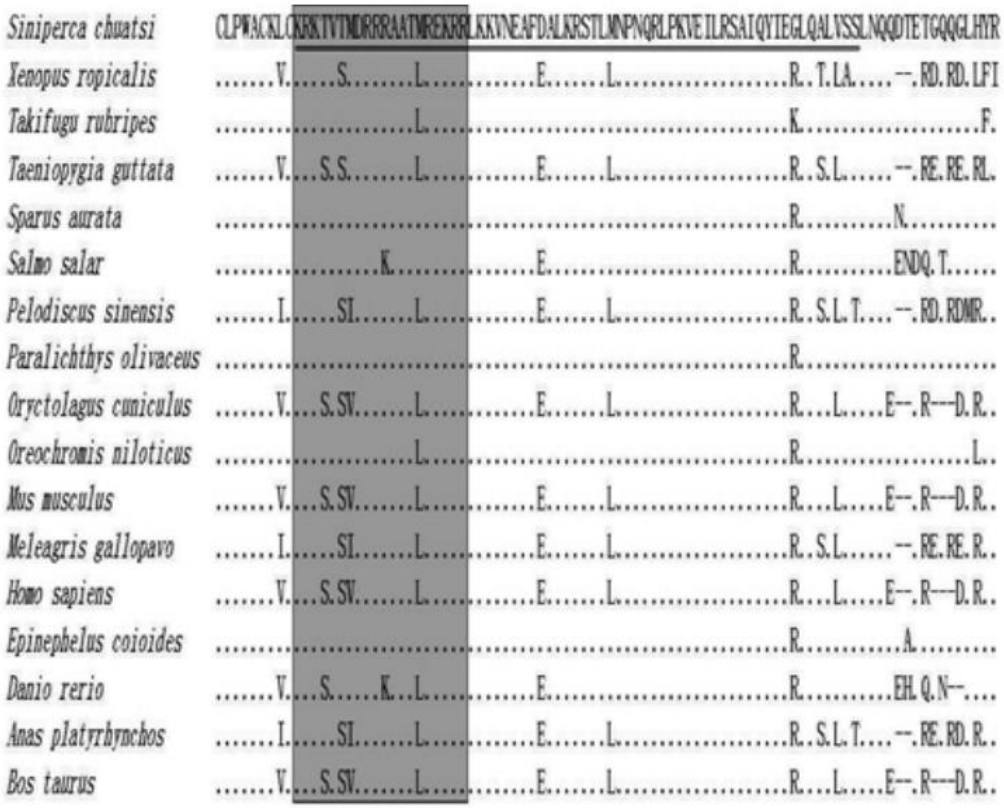

Figure 80. Protein sequence comparison of myogenin from 16 vertebrates. The highly conserved basic helix-loop-helix domains are underlined, and the basic regions are marked in square box. The conserved residues are indicated by dots. The Gene bank accession number for the selected vertebrate myogenin proteins are: Epinephelus coioides (HM190251), Sparus aurata (EF462192), Oreochromis niloticus (GU246725), Paralichthys olivaceus (EF144128), Takifugu rubripes (AY566282), Danio rerio (CAQ14920), Xenopus (Silurana) tropicalis (CAJ82458), Taeniopygia

guttata (XP_002195870), Salmo salar (NP_001117072), Pelodiscus sinensis (BAJ53267), Oryctolagus cuniculus (ACN53836), Mus musculus (NP_112466), Meleagris gallopavo (AAT39143), Anas platyrhynchos (ADG85647), Bos Taurus (BAE93440), and Homo sapiens (NP_002470) (Chu et al., 2014).

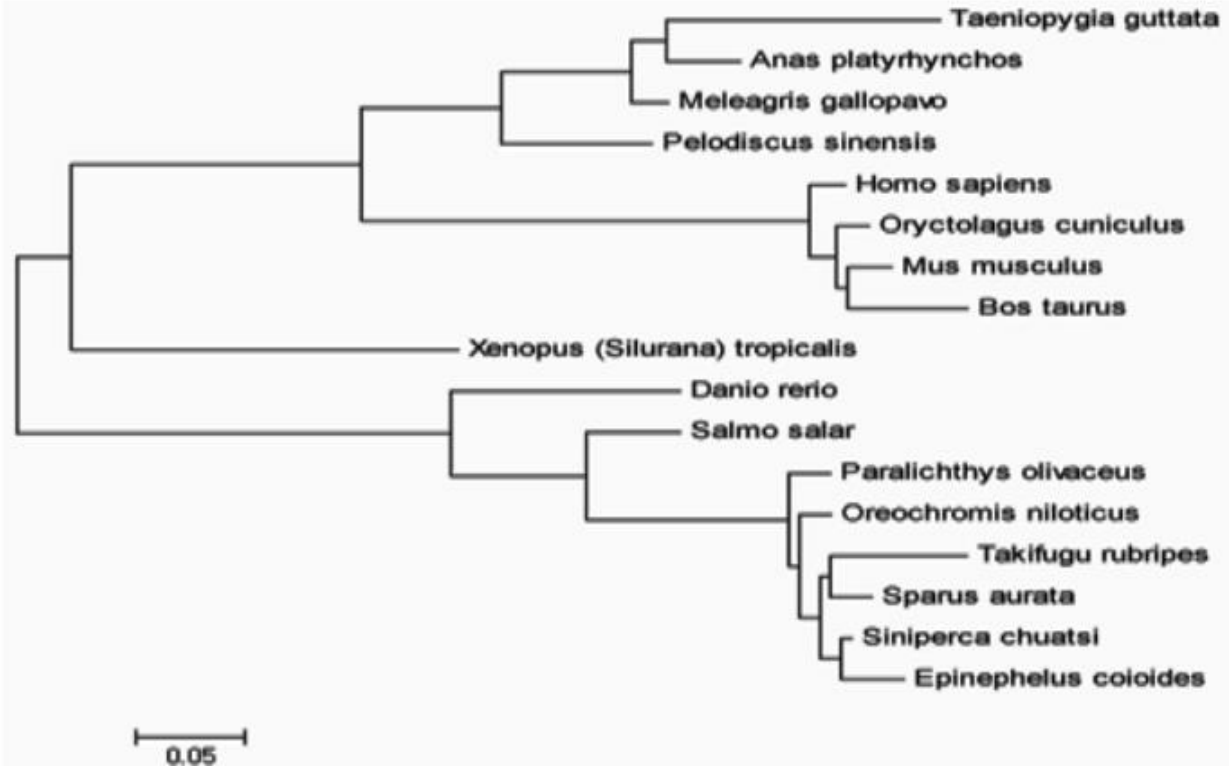

Figure 81. Phylogenetic analysis of the S. chuatsi myogenin gene sequence relative to myogenin genes from other vertebrates. The deduced protein sequences were searched from Gene bank same as in Figure 80 and the phylogenetic tree was constructed with the neighbor-joining method in MEGA version 3.0 based on Poisson-corrected pairwise distances between protein sequences. Note S. chuatsi, Epinophelus coioides, Sparus aurata and Taklfugu rubripos are in the same branch (Chu et al., 2014).

5.7. **Proteomics: Methodology and Application in Fish Processing**

This excellent review discusses all fish food matrix are in large part constructed of proteins. Furthermore, the construction of the food matrix, both on the cellular and tissue-wide levels, is regulated and brought about by proteins. This is why proteomics is a tool that can be of great value to the food scientist, revealing valuable insight into the composition of the raw materials; the quality involution within the product before, during, and after processing or storage; and the interactions

of the proteins with one another, with other food components, or with the human immune system after consumption (Vilhelmsson et al., 2007).

5.7.1. Antemortem Metabolism and Postmortem Quality in Trout

The feasibility of substituting fishmeal in rainbow trout *(Oncorhynchus mykiss* diets with protein from plant sources was studied by 2DE-based proteomics techniques (Martin, Vilhelmsson, & Houlihan, 2003; Vilhelmsson et al., 2004). The various quality characteristics of fillet and body were also measured (de Francesco et al., 2004; Papini et al., 2004). Among the findings obtained, it was shown that cooked trout, that had been fed the plant protein diet, possessed higher hardness, lower juiciness, and lower odor intensity than those fed the fishmeal-containing diet. This clearly demonstrate the effect of antemortem metabolism on the product texture (Vilhelmsson et al., 2007).

Additionally, the amount and composition of free amino acids in the fish flesh was significantly affected by the diet, as was the postmortem development of the free amino acid pool. It is interesting to note that the diets were formulated to have a nearly identical amino acid composition. Once more, these results indicate that the altered postmortem proteolytic activity of the plant protein–fed fish when compared to the fishmeal-fed ones (Vilhelmsson et al., 2007).

This study investigated the liver proteome, as the liver is the primary organ of the fish's key metabolic pathways. This study identified a number of metabolic pathways sensitive to plant protein substitution in rainbow trout feed. For example, the pathways involved in cellular protein degradation, fatty acid breakdown, and NADPH metabolism are indicated in Table 50 (Vilhelmsson et al., 2007).

Table 50. Commercially or Scientifically Important Fish and Seafood Species and the Availability of Protein and Nucleotide Sequence Data as of June 7, 2004, (Vilhelmsson et al., 2007).

	Protein Sequences	Nucleotide Sequences		Protein Sequences	Nucleotide Sequences
Actinopterygii (ray-finned fishes)	77,396	1.586,862	*Tetraodontiformes* (puffers and	29,387	305,449
Elopomorpha	1,215	1,473	Pufferfish *(TaJujitsu rubripes)*	948	89,901
Anguilhfonnes (eels and morays)	966	1,354	Green pufferfish *(Tetmodonnigroviridis)*	28.149	215.158
European eel *(Anguilla anguilla)*	114	199	*Zeifonnes* (dories)	171	57
Clupeonzotpha	180	337	John Dory *(Zeus faber)*	34	29
Clupeifortnes (herrings)	180	337	*Scomaenifonnes* (scorpionfisheq flatheads)	634	1.388
Atlantic herring *(Clupea harengus)*	29	35	Redfish *(Sebastes marines)*	3	7
European pilchard *(Sardina pilchardus)*	17	44	Lumpsucker *(Cyclopterus lumpus)*	3	14
Ostariophysii	21,562	771,661			
Cyprinifonnes (carps)	18.890	722,727	*Chondrichthyes* (cartilagenous fishes)	2,389	2,224
Zebrafish *(Danio rerio)*	13.659	704,204	*Carcharhiniformes* (ground sharks)	480	399
Silurtfonnes (catfishes)	1,674	47,635	Lesser spotted dogfish *(Scyliorhirzus*	208	104
Channel catfish *(Ictalunts punctatus)*	532	35,240	Blue shark *(Prionace glauca)*	8	4
Protacanthopterygii	4.392	257,953	*Lamnifonnes* (mackerel sharks)	178	239
Salmontfonnes (salmons)	4,230	257,923	Basking shark *(Cetorhinus maximus)*	16	16
Atlantic salmon *(Salmo :War)*	686	90,577	*Rajiformes* (skates)	275	304
Rainbow trout *(Oncorhynchus mykiss)*	1,480	159,907	Thorny skate *(Raja radiata)*	39	6
Arctic chart *(Salvelinus alpinus)*	90	251	Blue skate *(Raja bads)*	1	0
Paracanthoptetygii	1.880	2,335	Little skate *(Raja erinacea)*	162	152
Gadifonnes (cods)	1.445	1,528			
Atlantic cod *(Gadus morhua)*	905	936	*Mollusca* (mollusks)	11,229	35,187
Alaska pollock *(Theragra chalcogramma)*	124	136	*Bivalvia*	3.072	15.926
Saithe *(Pollachius Wrens)*	16	26	Blue mussel *(Mytilus edulis)*	535	591
Haddock *(Melattogramtnus aeglefinus)*	56	61	Bay scallop *(Argopecten irradians)*	99	2,106
Lophiifonnes (anglerfishes)	197	82	*Gastropods*	7,036	17.484
Monkfish *(Lophius piscatorius)*	6	9	Common whelk *(Buccimun undatum)*	4	15
Acanthopterygii	45.732	550.100	Abalone *(Haliotis tubercultua)*	*11*	158
Percifonnes (perch-likes)	9,532	60,715	*Cephalopoda*	931	1,490
Gilthead sea bream *(Spares arras)*	139	325	Northern European squid *(Loligo forbesi)*	30	39
European sea bass *(Dicentmchus labrar)*	150	264	Common cuttlefish *(Sepia of cinal's)*	52	44
Atlantic mackerel (Scomber scombrus)	8	23	Common octopus *(Octopus vulgaris)*	58	79
Albacore *(Thunnus alalunga)*	40	124			
Bluefin tuna *(Thunnus thynnus)*	85	178	*Crustacea* (crustaceans)	6,295	24.638
Spotted wolffish *(Anarhichas minor)*	30	16	*Caridea*	689	916
Beryciformes *(sawbellies)*	345	181	Northern shrimp *(Pandalus borealis)*	11	8
Orange roughy *(Hoplostethus atlanticus)*	0	12	*Astacidea* (lobsters and crayfishes)	646	3,507
Pleurotzectiformes (flatfishes)	957	7,392	American lobster *(Homers atnericanus)*	160	2,140
Atlantic halibut *(Hippoglossus hippoglossus)*	38	699	European crayfish *(Astacus astacus)*	26	11
Witch *(Glyptocephalus cynoglossus)*	5	22	Langoustine *(Nephrops norvegicus)*	18	18
Plaice *(Pleuronectes platessa)*	50	216	*Brachyura* (short-tailed crabs)	556	1.213
Winter flounder *(Pseudopleuronectes atnericanus)*	131	1,347	Edible crab *(Cancer pagunts)*	34	7
Turbot *(Scophthalmus marimus)*	49	112	Blue crab *(Callinectes sapidus)*	*Is*	30

Table 51. Protein Spots Affected by Dietary Plant Protein Substitution in Rainbow Trout as Judged by 2DE and Their Identities as Determined by Trypsin Digest Mass Fingerprinting (Vilhelmsson et al., 2007).

Spot Reference No.	PH	MW (kDa)	Normalized Volume Diet FM[a]	Normalized Volume Diet PP100[a]		Fold Difference	P
Downregulated							
128	6.3	66	303 ± 57	60 ± 19	Vacuolar ATPase β-subunit	5	0.026
291	6.4	42	521 ± 37	273 ± 30	β-ureidopropionase	2	0.004
356	6.3	38	161 ± 37	44 ± 19	Transaldolase	4	0.031
747	5.6	43	101 ± 19	19 ± 11	β-actin	2	0.040
760	6.3	39	41 ± 6	21±5	ND[b]	2	0.040
766	4.8	27	12 ± 1	6 ± 1	ND	2	0.004
Uperegulated							
81:7	4.4	82	9 ± 4	47 ± 8	"Unknown protein"	5	0.007
87	5.7	75	58 ± 14	262 ± 21	Transferrin	5	<
138	5.5	67	99 ± 16	267 ± 39	Hemopexin-like	3	0.009
144	5.4	63	26 ± 6	265 ± 66	L-Plastin	10	0.018
190	5.9	54	6 ± 2	50 ± 9	Malic enzyme	9	0.018
199	5.9	53	60 ± 16	156 ± 13	Thyroid hormone receptor	3	0.020
275	6.1	45	1 ± 0.6	11 ± 0.6	NSH[b]	9	<
387	5.6	35	97 ± 3	251 ± 49	Electron transferring flavoprotein	3	0.035
389	5.8	35	192 ± 45	414 ± 54	Electron transferring flavoprotein	2	0.027
399	6.8	33	59 ± 12	130 ± 10	Aldolase B	2	0.028
457	4.7	29	26 ± 7	57 ± 5	14-3-3 B2 protein	2	0.021
461	4.7	27	75 ± 9	190 ± 12	Proteasome alpha 2	3	0.004
517	4.4	22	15 ± 6	135 ± 29	Cytochrome *c* oxidase	9	0.013
539	4.9	19	7 ± 3	18 ± 3	ND	3	0.033
551	4.1	17	40 ± 11	143 ± 28	ND	4	0.018
563	5.2	15	814 ± 198	3762 ± 984	Fatty acid binding protein	5	0.039
639	6.4	84	10 ± 6	28 ± 5	NSH	3	0.047
648	6.1	55	17 ± 5	154 ± 46	Hydroxymethylglutaryl-CoA synthase	9	0.040
678	5.3	48	26 ± 7	69 ± 15	Proteasome 26S	3	0.044
746	4.4	46	45 ± 13	107 ± 15	ATPase subunit 4 "similar to catenin"	2	0.012
754	4.1	15	6 ± 2	36 ± 4	ND	7	<0.001
761	6.1	36	44 ± 21	204 ± 34	Transaldolase	5	0.006
764	6.2	65	0	102 ± 17	NSH	>10	N/A
770	5.0	21	4 ± 1	18 ± 4	ND	4	0.026

[a]Values are mean normalized protein abundance (-± SE). Data were analyzed by the Student's t test (n = 5). In diet FM, protein was provided in the form of fishmeal; in diet PP100, protein was provided by a cocktail of plant product with an equivalent amino acid composition to fishmeal.
[b]INSH = no significant homology detected; ND = identity not determined.

The liver proteome of the rainbow trout *(Oncorhynchus mykiss)* attained an identification rate of about 80% using a combination of search algorithms that included the open-access Mascot program (Pappin et al., 1999) and a licensed version of Protein Prospector MS-Fit (Clauser et al., 1999), searching against both protein databases and a database containing all salmonid nucleotide sequences. In those cases where both the protein and nucleotide databases yielded results, a 100% agreement was observed between the two methods (Vilhelmsson et al., 2007).

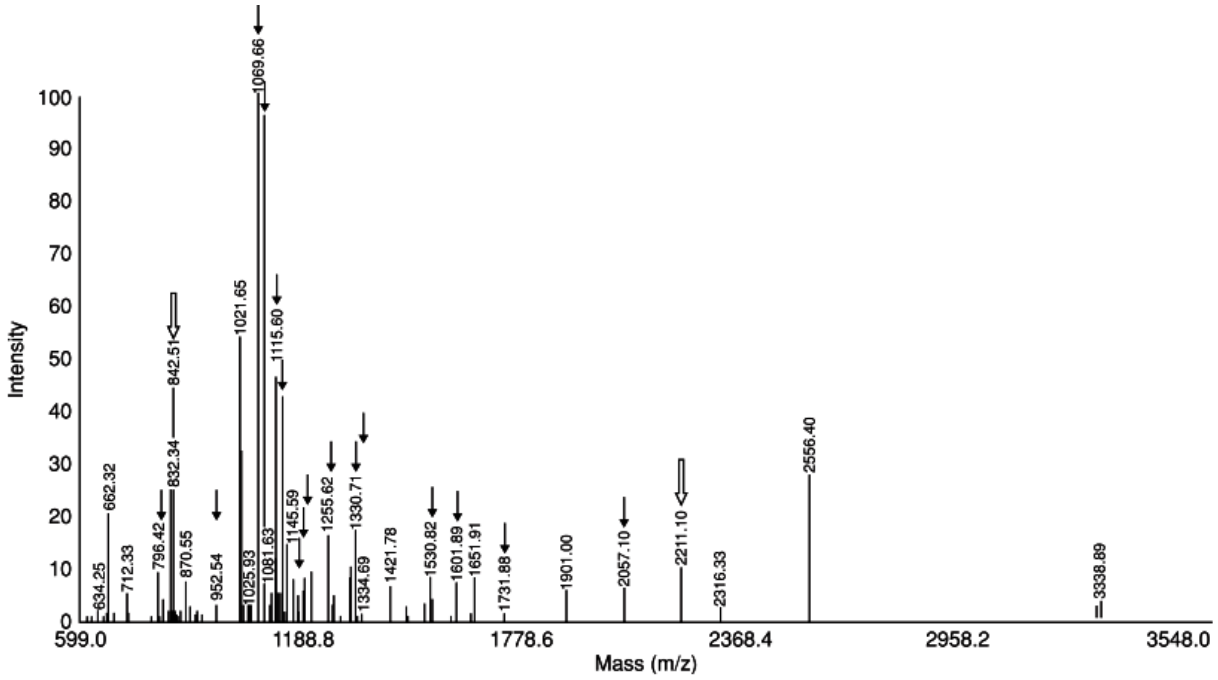

Figure 82. A trypsin digest mass spectrometry fingerprint of a rainbow trout liver protein spot, identified as apolipoprotein A I-1 (S. Martin, unpublished). The open arrows indicate mass peaks corresponding to trypsin self-digestion products and were, therefore, excluded from the analysis. The solid arrows indicate the peaks that were found to correspond to expected apolipoprotein A I-1 peptides (Vilhelmsson et al., 2007).

5.8. **Tracking Quality Changes Using Proteomics**

An excellent text book by Hui and collaborators describe postmortem degradation of fish muscle as a tenacious problem in the seafood industry, especially during the chilled storage step. This deleterious effect changes the fish muscle texture in becoming tenderized. Although, this

phenomenon has been primarily attributed to autolysis of muscle proteins, the specifics of this protein degradation are still somewhat in the dark (Hui et al., 2006).

However, degradation of myofibrillar proteins by calpains and cathepsins (Ladrat et al., 2000; Ogata et al., 1998) and degradation of the extracellular matrix by the matrix metalloproteases and matrix serine proteases, which are capable of degrading collagens, proteoglycans and other matrix components (Lødemel & Olsen, 2003; Woessner, 1991), are thought to be among the main culprits. Irrespective of the degradation mechanism, it is clear that these quality changes are species-dependent (Papa et al., 1996; Verrez-Bagnis et al., 1999) and furthermore appear to display seasonal variations (Ingolfsdottir et al., 1998; Ladrat et al., 2000).

As with postmortem protein degradation during storage, autolysis during processing seems to be somewhat specific. Indeed, the myosin heavy chain of the Atlantic cod was shown to be significantly degraded during the processing of "salt fish" *(bachalhau)*, whereas actin was less affected (Thorarinsdottir et al., 2002). Problems of this kind, where differences are expected to occur in the number, molecular mass, and pH of the proteins present in a tissue, are well suited to investigation using 2DE-based proteomics (Hui et al., 2006).

It is also worth noting that protein isoforms other than proteolytic ones, whether they be encoded in structural genes or brought about by posttranslational modification, usually have a different molecular weight or pH and can, therefore, be distinguished on 2DE gels. Thus, specific isoforms of myofibrillar proteins, many of which are correlated with specific textural properties in seafood products, can be observed using 2DE or other proteomic methods (Hui et al., 2006; Martinez et al., 1990; Piñeiro et al., 2003).

5.9. **Postmortem Protein Degradation as a Tool to Estimate the Postmortem Interval (PMI).**

There have been few proteomic studies linking the antemortem protein metabolism with the postmortem quality in fish and seafood. However, considering the substantial importance of protein degradation and the quality and processability of fish and seafood, it is anticipated that the potential for the application of proteomics will increase in this field of study (Zissler et al., 2020).

This section provides a systematic review of the literature to evaluate the current research status of protein degradation-based postmortem interval (PMI) estimation. In this review, special attention was given to the applicability of the proposed approaches/methods in routine forensic practice. For this reason, the authors presented a systematic review of the literature on protein

degradation in tissues and organs of animals and humans. They searched the scientific databases Pubmed and Ovid, and Google Scholar. This enabled the consideration of several degradation patterns of over 130 proteins from 11 different tissues, studied with well-established and proteomic approaches. Although the comparison between studies was complicated by the heterogeneity of study designs, tissue types, methods, proteins and outcome measurement, this review provided clear evidence for high explanatory power of protein degradation analysis in forensic PMI analysis. This review states that although few approaches have yet exceeded a basic research level, it is anticipated the applicability of a protein degradation-based PMI estimation method will become in future, routine forensic practice (Zissler et al., 2020).

5.10. Can Antemortem Proteomics Shed Light on Gaping Tendency

Farmed fish, when compared to the wild catch, are subjected to gaping. This is a phenomenon caused by the cleavage of the matrix proteases of myocommatal collagen cross-links, which results in the weakening and rupturing of connective tissue (Børresen, 1992; Foegeding, 1996). Obviously. Gaping is a very serious quality issue in the fish processing industry. Irrespective of the obvious visual defect, gaping is responsible for the difficulties faced during mechanical skinning and slicing of the fish (Love, 1997).

Gaping is caused by the weakening of collagen, and it is facilitated by low pH. Furthermore, well-fed aquaculture fish tend to yield flesh of comparatively low pH, which has tendencies to gape (Einen et al., 1999; Foegeding, 1996). This indicates a major problem for the aquaculture industry, particularly with rare fish species with a high natural gaping tendency, such as the Atlantic cod. Gaping tendency varies considerably among wild fish caught in different areas (Love et al., 1974), and thus, it is conceivable that gaping tendency can be controlled with dietary or other environmental manipulations (Hui et al., 2006).

Once more, proteomics and transcriptomics, with their capacity to monitor multiple biochemical processes simultaneously, are methodologies eminently suitable to finding biochemical or metabolic markers that can be used for predicting features such as gaping tendendency of different stocks reared under different dietary or environmental conditions (Hui et al., 2006) .

5.11. Species Authentication Proteomics

It is well known that food authentication is an area of growing importance, both economically and from a public health standpoint. Taking into account the large differences in the market value of and the increased prevalence of processed products on the market, it is perhaps not surprising that species authentication is fast becoming an issue of supreme commercial importance (Mazzeo & Siciliano, 2016).

Along with other molecular techniques, such as DNA-based species identification (Mackie et al., 1999; Martinez et al., 2001; Sotelo et al., 1993) and isotope distribution techniques for determining geographical origin (Campana & Thorrold, 2001), proteomics are proving to be a powerful tool in this area, particularly for addressing questions on the health status of the organism, stresses or contamination levels at the place of breeding, and postmortem treatment (Martinez & Jakobsen Friis, 2004).

Recently, (Martinez et al., 2003) reviewed the proteomic methodology for species authentication in foodstuffs. As, already indicated many times in this review article, unlike genomic, the proteome is not a static entity, and it can change between tissues and with environmental conditions. This means that proteomics can potentially yield more information than genomic methods, possibly indicating freshness and tissue information in addition to species. In many cases, the proteomes of even closely related fish species can be easily distinguishable by eye from one another on 2D gels (Figure 83), indicating that diagnostic protein spots may be used to distinguish closely related species (Hui et al., 2006).

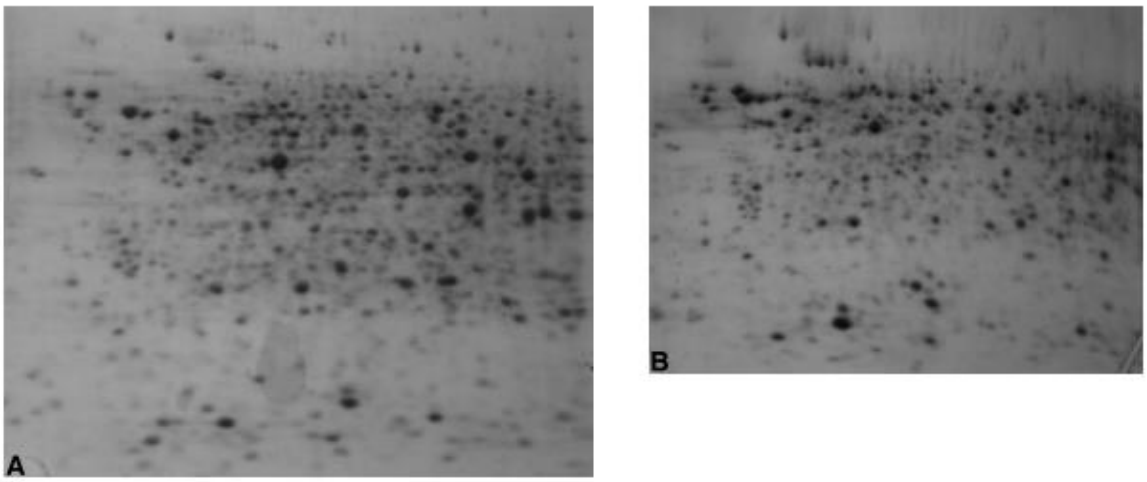

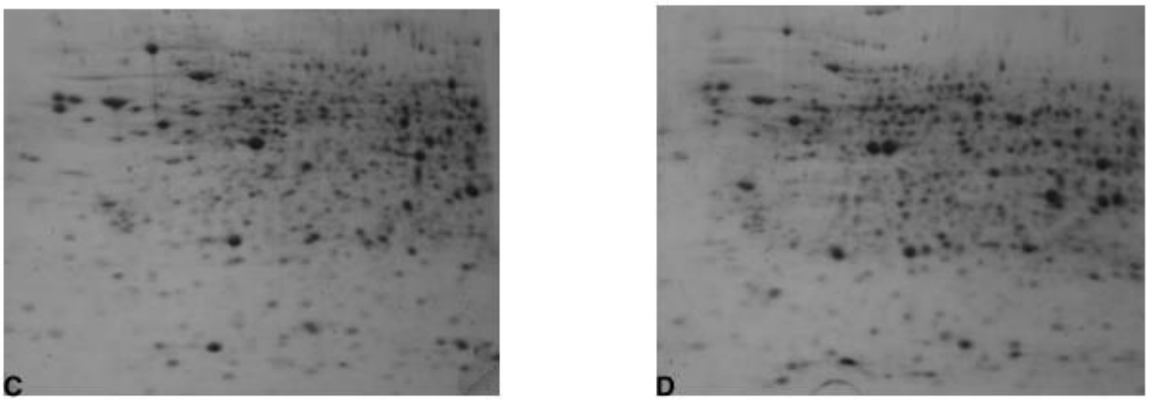

*Figure 83. 2DE liver proteome maps of four salmonid fish (S. Martin and O. Vilhelmsson, unpublished). Running conditions are as in Figure 18.2. **A**. Brown trout (Salmo trutta), **B**. Arctic charr (Salvelinus alpinus), **C**. rainbow trout (Oncorhynchus mykiss), **D**. Atlantic salmon (Salmo salar)(Hui et al., 2006).*

2DE-based methods have been used to distinguish various closely related species, such as the gadoids species and several flatfishes (Piñeiro et al., 1998, 1999, 2001) Similarly, it was possible to distinguish by 2D gels, between Cape hake *(Merluccius capensis)* and the European hake *(Merluccius merluccius)* from other closely related species by the presence of a particular protein spot. This latter spot was identified by means of nano-electrospray ionization mass spectrometry, as nucleoside diphosphate kinase (Piñeiro et al., 2001).

Similarly, it was possible to distinguish between three species of European mussels, *Mytilus edulis*, *Mytilus galloprovincialis* and *Mytilus trossulus*. It was found that *M. trossulus* could be distinguished from the other two species on foot extract 2D gels by a difference in a tropomyosin spot. This difference was due to a single T to D amino acid substitution (López et al., 2002). In addition, the authors went further and attempted to identify not only the species present, but also their relative ratios in mixtures of several fish species and muscle types (Martinez & Jakobsen Friis, 2004).

5.12. **Protein Changes as Robust Signatures of Fish Chronic Stress: a Proteomics Approach to Fish Welfare Research**

In order to improve the welfare standards of aquaculture practices, it is essential to prevent stress by optimizing the fish stress response and by quantification of the stress level. Fish stress

response is characterized by a cascade of physiological responses that, in turn, induce further changes at the whole animal level. These physiological responses can either increase fitness or impair welfare. Nonetheless, monitoring this dynamic process has relied on indicators that are only a snapshot of the stress level experienced. However, proteomics, allow an unbiased approach for the discovery of potential biomarkers for stress monitoring (Raposo De Magalhães et al., 2020).

In this study, the Gilthead seabream (*Sparus aurata*) was chosen as a model to evaluate three chronic stress conditions, namely overcrowding, handling and hypoxia. These three stress conditions were chosen in order to evaluate the potential of the fish protein-based adaptations, as reliable signatures of chronic stress, in contrast to the commonly used hormonal and metabolic indicators (Raposo De Magalhães et al., 2020).

The results of this study indicated a broad spectrum of biological variation regarding cortisol and glucose levels. It was shown that the level values of cortisol and glucose rose higher in net-handled fish. Therefore the potential pattern of stressor-specificity became very clear, as the level of response varied markedly between a persistent (crowding) and a repetitive stressor (handling) (Raposo De Magalhães et al., 2020).

Gel-based proteomics analysis of the plasma proteome also revealed that net-handled fish had the highest number of differential proteins, compared to the other trials. Mass spectrometric analysis, followed by gene ontology enrichment and protein-protein interaction analyses, characterized these biological variations (chronic stress) as humoral components of the innate immune system and key elements of the response to stimulus (Raposo De Magalhães et al., 2020).

Overall, this study represents the first screening of reliable signatures of physiological adaptation to chronic stress in fish, allowing the future development of novel biomarker models to monitor fish welfare (Raposo De Magalhães et al., 2020).

5.13. **Proteome Analysis of Pyloric Ceca: a Methodology for Fish Feed Development?**

This study evaluated if the change in the protein source of fish feed, from conventional fish meal to alternative sources of protein, will affect traits such as fish growth, quality, and feed utilization. 2D gel electrophoresis-based proteomics was used to investigate the feed effects on fish by analyzing the protein changes in the fish gut. Hence, the workflow was used to study the effect of substituting fish meal in fish feed by alternative protein sources. Rainbow trout divided into five groups were fed for 72 days with feeds varying in protein composition (Wulff et al., 2012).

Table 52. Main Protein Source and Proximate Composition and Energy Content of the Five Types of Fish Feed (Wulff et al., 2012).

feed	protein source (%)	dry matter (%)	protein (%)	fat (%)	carbohydrate (%)	ash (%)	gross energy (kcal/kg)	metabolic energy (kcal/kg)
A	fish meal: 61	91.7	45.7	27.7	10.7	7.6	5760	5186
B	fish meal: 36	93.0	41.5	28.5	15.5	7.5	5580	4587
C	fish meal: 36 blood meal: 8	93.4	40.3	28.0	17.6	7.5	5690	4694
D	fish meal: 18 pea protein: 18	92.7	42.4	27.4	16.6	6.3	5643	4619
E	fish meal: 18	92.3	41.0	28.7	16.7	6.0	5784	4763

When feed enters the gastrointestinal system, the pyloric ceca (PC) (accounting for 70% of the gut) is after the stomach the first organ in contact with the feed. When the feed is changed, the PC is therefore challenged and has to adapt to handle the new feed components (Wulff et al., 2012).

The 2D gel electrophoresis proteins extracted from the pyloric ceca were separated and allowed to measure the abundance of more than 440 protein spots. Ultimately, the expression of 41 protein spots was found to change due to differences in feed composition (Wulff et al., 2012).

Tandem mass spectrometry analyses allowed the identification of 31 proteins. This series of identified proteins included proteins involved in digestion (trypsinogen, carboxylic ester hydrolase, and aminopeptidase). The many expression changes indicated that the trout, when adapting to differences in feed formulation, alter the protein composition of the gut (Wulff et al., 2012).

5.14. Effects of Genotype and Dietary Fish Oil Replacement with Vegetable Oil on the Intestinal Transcriptome and Proteome of Atlantic Salmon (*Salmo salar*)

There have been no study implemented on the use of dietary vegetable oil (VO) in order to reduce dependency on fish oil (FO) in aquaculture ventures. Thus, alternative feeds and breeding strategies are needed in order to reduce the dependency on fish oil (FO) and better utilization of dietary vegetable oil (VO). Regardless of the central role of the intestine in maintaining body homeostasis and health, the molecular response of replacement of the dietary FO by VO has been little investigated (S. Morais et al., 2012).

In this study, the authors employed transcriptomic and proteomic analyses to study the effects of dietary VO in two family groups of Atlantic salmon selected for flesh lipid content, 'Lean' or 'Fat'. It was established that metabolism, mainly of lipid and energy, was the functional category most affected by diet. Similarly, important effects were also measured in ribosomal proteins and signalling. It was found that the long-chain polyunsaturated fatty acid (LC-PUFA) biosynthesis pathway, which is assessed by fatty acid composition and gene expression, was influenced by the genotype (S. Morais et al., 2012).

In addition, the authors indicated that the intestinal tissue contents of docosahexaenoic acid, were equivalent in Lean salmon fed either a FO or VO diet. Likewise, the expression of LC-PUFA biosynthesis genes was up-regulated in VO-fed fish in Fat salmon. In addition, the dietary VO increased the lipogenesis of Lean fish, assessed by expression of FAS, while no effect was observed on β-oxidation. Although the transcripts of the mitochondrial respiratory chain were down-regulated, it was determined that perhaps there was less active energetic metabolism in fish fed VO. In contrast, dietary VO up-regulated genes and proteins involved in detoxification, antioxidant defence and apoptosis, which could be associated with higher levels of polycyclic aromatic hydrocarbons in this diet (S. Morais et al., 2012).

Regarding genotype, the following pathways were identified as being differentially affected: proteasomal proteolysis, response to oxidative and cellular stress (xenobiotic and oxidant metabolism and heat shock proteins), apoptosis and structural proteins particularly associated with tissue contractile properties. Genotype effects were accentuated by dietary VO (S. Morais et al., 2012).

Table 53. Proteins differentially regulated by diet (S. Morais et al., 2012).

Spot No	Protein ID	Accession No. (NCBInr)	Theoretical Mw (KDa)/pI	Protein Score[a]	No. Matched peptides (MS/MS)[b]	Best score peptide	VO/FO Lean	VO/FO Fat	p-value
1136	Epoxide hydrolase 2 (EPHX2)	gb|ACI33129.1|	54.2/5.52	84	1	GGLFVGLPDEIPR	1.23	1.40	0.0190
1148	Hemopexin-like protein* (HPX)	emb|CAA92147.1|	50.4/5.61	169	1	VHLDAITSDDAGNIYAFR	1.32	1.56	0.0002
1151	Hemopexin-like protein* (HPX)	ref|NP_001104617.1|	51.0/6.18	161	1	VHLDAITSDDAGNIYAFR	1.38	1.54	0.0001
2683	Peroxiredoxin 1 (PRDX1)	gb|ACI67145.1|	22.0/6.42	757	8	SISTDYGVLKEDEGIAYR	1.14	1.09	0.0310

3168	2-peptidylprolyl isomerase A (PPIA)	ref|NP_001135161.1|	17.5/7.61	101	1	VYFDITIGDTPAGR	−1.46	−1.18	0.0170
3243	Myosin light chain smooth muscle isoform (MYL)	ref|NP_998803.1|	16.9/4.47	100	2	EAFLLFDR	−1.23	−1.11	0.0490
3331	similar to H2A histone family, member J (H2A)	ref|XP_001521566.1|	13.3/10.84	74	1	AGLQFPVGR	−1.58	−1.18	0.0250
3334	Histone H2A** (H2A)	emb|CAA25528.1|	13.7/10.88	37	1	AGLQFPVGR	−1.48	−1.18	0.0210
3445	Galectin 2 (LGALS2)	gb|ACN10131.1|	14.8/5.93	314	2	SGASSFSINIGHDSDNYALHFNPR	1.17	1.15	0.0170

[a] The protein score probability limit (where $P < 0.05$) is 73.
[b] Peptides with confidence interval above 95% were considered.
* Equivalent to warm-temperature-acclimation-related-65 kDa-protein.
**Same protein identification obtained by MS/PMF (peptide mass fingerprinting): Score = 76; 7 peptides matched.
Only reliable identifications of Actinopterygii, obtained by mass spectrometry (MALDI-TOF-MS/MS) analysis and searches in MASCOT, NCBI and ExPASy (Mw/pI) databases are shown. Expression ratios between fish fed VO and FO diets are given for each family group, as well as p-value for diet (two-way ANOVA, DeCyder V7.0).

5.15. **Dietary Creatine Supplementation in Gilthead Seabream (*Sparus aurata*): Comparative Proteomics Analysis on Fish Allergens, Muscle Quality, and Liver**

Fish flesh quality depends on the energetic skeletal muscle state. Delaying energy depletion through diet supplementation contributes to preserving muscle quality traits and on modulation of the fish allergens. Indeed, food allergies cause a serious public health problems worldwide. Needless to say that fish allergies are on top of the eight more allergenic foods. Parvalbumins is known to be the main fish allergen (Schrama et al., 2018).

This study has tried to produce a low allergenic farmed fish, with improved muscle quality in controlled artificial conditions. This was done by supplementing the commercial fish diet with different creatine percentages. The supplementation of fish diets with specific nutrients were supposed to reduce the expression of parvalbumin. For this reason, the authors investigated the effects of these supplemented diets on fish growth, physiological stress, fish muscle status, and parvalbuminmodulation (Schrama et al., 2018).

Data from zootechnical parameters were used to evaluate fish growth, food conversion ratios and hepatosomatic index. Furthermore, the physiological stress responses were assessed by

measuring cortisol releases and muscle quality analyzed by rigor mortis and pH. Also, parvalbumin, creatine, and glycogen concentrations in muscle were also determined. Comparative proteomics was used to look into changes in the muscle and liver tissues at the protein level (Schrama et al., 2018).

The results obtained suggested that the supplementation of commercial fish diets with creatine does not affect farmed fish productivity parameters or either muscle quality. Moreover, the effect of higher concentrations of creatine supplementation revealed a minor influence in fish physiological welfare. Differences at the proteome level were detected among fish fed with different diets. This study also showed the presence of differential muscle proteins expression identified as tropomyosins, beta enolase, and creatine kinase among others. With respect to liver several proteins involved in the immune system, cellular processes, stress, and inflammation response were modulated (Schrama et al., 2018).

In conclusion and regarding the parvalbumin modulation, the tested creatine percentages added to the commercial diet had no effect at all on the expression of this protein. Nonetheless, the use of proteomics tools showed to be very sensitive to infer about changes of the underlying molecular mechanisms regarding fish responses to external stimulus. Accordingly, this study provided a holistic and unbiased view on fish allergens and muscle quality (Schrama et al., 2018).

5.16. **Proteomic Sensitivity to Dietary Manipulations in Rainbow Trout**

It has been suggested that the in-farmed fish changes in dietary protein sources. With respect of the substitution of fish meal with other protein sources, it can have metabolic consequences. This presented study uses the proteomics approach to study the protein profiles of livers of rainbow trout that have been fed two diets containing different proportions of plant ingredients. For this reason, the authors used both diets control (C) and soy (S) containing fish meal and plant ingredients and synthetic amino acids. However, diet S had a greater proportion of soybean meal. A feeding trial was performed for 12 weeks at the end of which, growth and protein metabolism parameters were measured (Martin, Vilhelmsson, Médale, et al., 2003).

It was established that protein growth rates were not different in fish fed different diets. However, protein consumption and protein synthesis rates were higher in the fish fed the diet S. Fish fed diet S had lower efficiency of retention of synthesized protein. Furthermore, ammonia

excretion was increased as well as the activities of hepatic glutamate dehydrogenase and aspartate amino transferase (ASAT) (Martin, Vilhelmsson, Médale, et al., 2003).

Interestingly, no differences were found in free amino acid pools in either liver or muscle between diets. Protein extraction followed by high-resolution two-dimensional electrophoresis, coupled with gel image analysis, allowed the identification and expression of hundreds of protein. The individual proteins of interest were then subjected to further analysis leading to protein identification by trypsin digest fingerprinting control (C) and soy (S) (Martin, Vilhelmsson, Médale, et al., 2003).

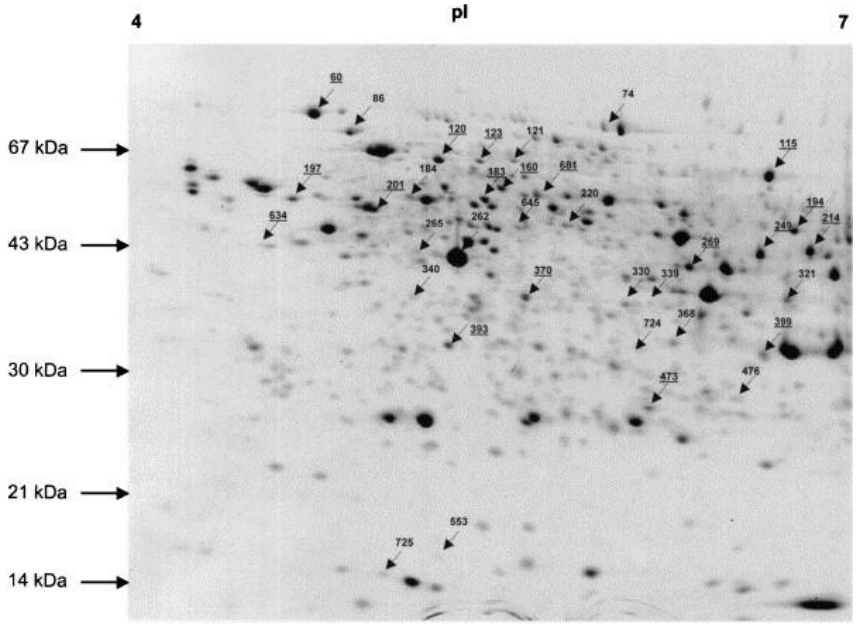

Figure 84. Two-dimensional gel of rainbow trout liver proteins (fish S3). A total liver protein extract was separated by charge between pI 4 and 7, second dimension was by size on a gradient 10–15% gel. The proteins were located by staining with colloidal coomassie blue G250. Proteins marked by arrows were found to be differentially expressed as a result of dietary manipulation, the corresponding number is the spot reference number. Underlined protein numbers were positively identified by trypsin digest fingerprinting (Martin, Vilhelmsson, Médale, et al., 2003).

During this study, 800 liver proteins were analysed for expression pattern, of which 33 were found to be differentially expressed between diets C and S. Seventeen proteins were positively identified after database searching (Martin, Vilhelmsson, Médale, et al., 2003).

Proteins were identified from diverse metabolic pathways, demonstrating the complex nature of gene expression responses to dietary manipulation revealed by proteomic characterization (Martin, Vilhelmsson, Médale, et al., 2003).

Table 54. Results from peptide mass fingerprinting of protein spots excised from the 2DE gels (Martin, Vilhelmsson, Médale, et al., 2003).

Reference spot	p*I*	kDa	Identities by MS-Fit followed by BLASTx					Identities by Mascot			
			Salmonid sequence	MS-Fit Mowse score	Protein	Species identified	Accession no.	Protein	Species identified	Accession no.	Mascot score
60^{C}	4.9	85	BG933954	1.4×10^{-4}	HSP108	*Salmo salar*	AF387865	HSP108	*Gallus gallus*	AF387865	201
115^{C}	6.8	67	CA343417	1.6×10^{5}	Transketolase	*Xenopus laevis*	AAF67194	*N*-ethylmaleimide-sensitive factor	*Homo sapiens*	15314649	82
120^{C}	5.5	66	BX081803	2.3×10^{5}	HSP70	*Oncorhynchus mykiss*	P08108	HSP70	*Oncorhynchus mykiss*		108
123^{C}	5.6	66	CA044261	4.6×10^{4}	HSP70	*Oncorhynchus mykiss*	P08108	HSP70	*Xiphophorus maculatus*		115
160^{C}	5.7	59	AJ295231	1.3×10^{4}	Nitric oxide synthase	*Oncorhynchus mykiss*	CAC82808				
183^{C}	5.7	55	AJ272373	3.0×10^{10}	Simple type II Keratin k8	*Oncorhynchus mykiss*	CAC45060	Simple type II Keratin k8	*Oncorhynchus mykiss*	CAC45060	88
194^{C}	6.8	54	CA375586	3.3×10^{5}	Selenium binding protein 2	*Rattus norvegicus*	NP_543168	Occludin-like protein	*Drosophila melanogaster*		81
197^{S}	4.8	53	CA386490	7.5×10^{3}	HSP108	*Xenopus laevis*	AAO21339	HSP108	*Gallus gallus*	AF387865	193
201^{C}	5.2	52	CA350990	8.6×10^{7}	Beta tubulin	*Notothenia coriiceps*	AAG15317	Beta tubulin	*Haliotis discus*		95
214^{C}	6.9	51	BX080834	3.5×10^{3}	Adenosylhomocysteinase 2	*Xenopus laevis*	O93477	Adenosylhomocysteinase 2	*Xenopus laevis*	O93477	85
249^{C}	6.7	47	CA363453	6.6×10^{7}	Homogentisate 1,2-dioxygenase	*Mus musculus*	XP_147229	–	–		
269^{C}	6.5	45	BG934321	6.4×10^{7}	Phosphogluconate dehydrogenase	*Homo sapiens*	AAH00368	–	–		
321^{C}	6.8	39			–	–		–	–		
370^{S}	5.6	36	CA039103	5.0×10^{4}	Hypothetical ORF	*Saccharomyces cerevisiae*	NP_014422	Protein Phosphatase 2A catalytic chain	*Xenopus laevis*		114
393^{C}	5.5	33						Apo A I-1	*Oncorhynchus mykiss*	AAB96972	148
399^{SBM}	6.8	33	AF067796	4.8×10^{4}	Aldolase B	*Salmo salar*	AAD11573	Aldolase B	*Salmo salar*	AAD11573	82
330^{SBM}	6.2	30	BG933866	2.5×10^{-3}	–	–		–	–		
473^{FM}	6.4	28	BX076136	2.5×10^{4}	Hypoxanthine guanine phosphoribosyl transferase	*Gallus gallus*	AJ697	Hypoxanthine guanine phosphoribosyl transferase	*Homo sapiens*		75

485	5.4	25	BX074107	2.8×10^{4}	Apo A I-1	*Oncorhynchus mykiss*	AAB96972				
487	5.3	25	CA386629	1.6×10^{7}	Apo A I-2	*Oncorhynchus mykiss*	AAB96973	Apo A I-2	*Oncorhynchus mykiss*	AAB96973	87
553^{SBM}	5.4	17			–	–		–	–		
634^{SBM}	4.8	42			–	–		Glucose regulated protein precursor (GRP 78)	*Gallus gallus*	Q90593	447
681^{FM}	5.9	57	CA361952	1.0×10^{5}	Pyruvate kinase	*Takifugu rubripes*	BAC02918	–	–		

The superscript following the reference spot number indicates if the spot is increased in abundance after being fed the diet. Using MS-Fit, if unannotated cDNA sequences were identified, this sequence was used to search GenBank using BLASTx to show the protein the cDNA encodes, if a significant hit is obtained. All digests were also searched using Mascot search program. (–) indicates no homology for this protein. ^{C} and ^{S} indicate which diet the protein is more abundant.

5.17. **Metabolic Molecular Indicators of Chronic Stress in gilthead Seabream (*Sparus aurata*) Using Comparative Proteomics**

This study's main goal was to identify the possible metabolic, molecular indicators of chronic stress in gilthead seabream *Sparus aurata*. For this reason, two potential stressful conditions were tested: repeated handling and crowding at high stocking density. Also, gilthead seabream was kept under optimized rearing conditions as control fish (Alves et al., 2010).

The cortisol was measured as the primary stress indicator, and the liver proteome of stressed fish, was compared to that of control fish by using comparative proteomics. It was found that the plasma cortisol levels of the sea bream repeatedly handled and crowded at high stocking density were significantly higher than in the undisturbed control fish (Alves et al., 2010).

2D analysis indicated the presence of a total of 560 spots were detected. The statistical analysis revealed a differential expression in about 50% of all detected proteins. As usual the spots with greater than 2-fold or lower than 0.5-fold changes were identified by liquid chromatography-tandem mass spectrometry (LC-MS/MS) (Table 55) (Alves et al., 2010).

This series of proteins were identified as fatty acid-binding protein (lipid transport and antioxidant role), heat shock cognate protein (chaperoning), calmodulin (Ca2+ signaling), mitochondrial porine voltage-dependent anion channel (lipid oxidation), glutamine synthetase (ammonia metabolism), cofilin and beta-tubulin (cytoskeleton), hemoglobin and several other proteins involved in carbohydrate metabolism (triose-phosphate isomerase, pyruvate dehydrogenase, glyceraldehyde 3-phosphate dehydrogenase, alfa-enolase) were differentially expressed in fish under chronic stress (Alves et al., 2010).

Some of these proteins may be used in the future as chronic stress and/or part of a panel of welfare biomarkers after validation studies using RT-PCR and ELISA assays (Alves et al., 2010).

Table 55.Main identified proteins by LC–MS/MS. The identification was made by peptide fragment fingerprinting (PFF) in the option MS/MS Ion Search from the bioinformatics application Mascot. The PFF was made in the non redundant NCBInr data base for the Actinopterygii taxonomic level (p-valueb1E−05) (Alves et al., 2010).

Spot no.	Protein (species)	GI number[a]	Mw_{th}/pI_{th}[b] (Mw_{exp}/pI_{exp}[c])	Sequence coverage (%)[d]	# matched peptides (*E*-value < 0.05)[e]	Best peptide match: sequence, charge state, *E*-value[f]	Combined Mowse score[g]
0103	Calmodulin (*Oncorhynchus sp.*)	gi|71664	16.70/4.09 (18.00/4.10)	10	2	VFDKDGNGYISAAELR, 2+, 9.2*E*− 06	89
1204	Triose-phosphate isomerase (*Acipenser brevirostrum*)	gi|15149246	27.10/6.30 (25.00/4.60)	9	1	VVLAYEPWAIGTGK, 2+, 5.30*E*− 04	59
2308	Beta-tubulin (*Danio rerio*)	gi|82658236	50.10/4.81 (33.00/5.72)	39	31	GHYTEGAELVDSVLDVVR, 2+, 2.7*E*− 12	922
2403	Glutamine synthetase (*Bostrychus sinensis*)	gi|20799646	42.0/5.75 (42.50/5.80)	25	6	RLTGHHETSNNINEFSAGVANR, 3+, 7.1*E*− 07	255
2415	Pyruvate dehydrogenase (*Danio rerio*)	gi|47085923	39.60/5.78 (35.00/5.60)	5	1	VFLLGEEVAQYDDGAYKVSR, 3+, 2.50*E*− 02	46
2612	Heat shock cognate protein 70 (*Oryzias latipes*)	gi|157278337	76.58/5.80 (73.00/5.48)	43	28	SINPDEAVAYGAAVQAAILSGDK, 2+, 3.8*E*− 10	1156
4308	Glyceraldehyde 3-phosphate dehydrogenase (*Pagrus major*)	gi|15146358	36.38/6.36 (36.00/6,67)	50	18	VPVADVSVVDLTCR, 2+, 8.3*E*− 07	529
4408	Alfa-enolase (*Acipenser baerii*)	gi|98979415	47.47/5.95 (49.00/6.45)	47	28	SGETEDTFIADLVVGLCTGQIK, 2+, 4.1*E*− 10	1274
5104	Voltage-dependent anion channel I (*Tetraodon nigroviridis)*	gi|47221743	30.65/6.53 (31.00/6.50)	41	11	SENGLEFTSTGSANTETSK, 2+, 1.9*E*− 12	500
5203	Cofilin (*Tetraodon nigroviridis*)	gi|47225287	18.86/6.82 (18.40/5.50)	15	3	YALYDATYETK, 2+, 1.50*E*− 03	108
6102	Fatty acid binding protein (*Tetraodon nigroviridis*)	gi|47222259	13.40/6.32 (10.00/6.80)	29	1	MISSENFDDYMK, 2+, 6.9*E*− 05	68
7129	Hemoglobin (*Pagrus major*)	gi|37778990	15.81/8.55 (12.00/8.33)	7	1	SADIGAEALGR, 2+, 2.4*E*− 06	84

[a] GI number — NCBI accession number. [b] Mw_{th}/pI_{th} — Theoretical molecular weight and isoelectric point. Mw_{th} is given in kDa.
[c] Mw_{exp}/pI_{exp} — Experimental molecular weight and isoelectric point. Mw_{exp} is given in kDa.
[d] Sequence coverage (%) — percentage of the entire protein covered by matched peptides.
[e] # matched peptides (*E*-value < 0.05) — number of peptides matched to entry with significative *E*-value (when *E*-value < 0.05).
[f] Best peptide match with the lower *E*-value: sequence, charge state and *E*-value.
[g] Combined Mowse score — a non-probabilistic protein score, derived from the ions score.

5.18. Use of Emerging Genomic and Proteomic Technologies in Fish Physiology

Post-genomic research such as proteomics have contributed in creating a vast greater knowledge about the human genome and those of other species. Indeed, genomic strategies, together with those that look at the proteome of cells and tissues, are likely to revolutionize scientific research over the coming years (Parrington & Coward, 2002). The ease with which novel and homologous genes can be isolated using the new databases and technologies, and the ability to study the expression of thousands of genes simultaneously at a global cellular level will be the major factors in this revolution. Genomic information is already being used to further our understanding of physiology and gene evolution in fish. Furthermore, the highly compact pufferfish (*Takifugu rubripes*) genome is being used extensively as a model to interpret those of tetrapods (Parrington & Coward, 2002).

Currently, studies of the fish genome are limited to gene evolution and to a much lesser extent, environmental toxicology. However, as interpretation of fish genomes gathers pace, we are likely to see the increasing involvement of other key areas such as reproduction, growth, pathology of disease, and flesh development/quality. Here, the authors present some of the advanced genomic technologies currently available and discuss how these might influence our knowledge of fish biology reserved (Parrington & Coward, 2002).

The other main area where proteomic technologies may be expected to transform fish physiology research is in identifying novel signaling proteins and homologues of known proteins in a variety of fish species (Parrington & Coward, 2002).

A variety of fish species are the subject of genome initiatives. As part of these initiatives, EST (expressed sequence tag) databases, cDNA databases, and DNA arrays are being created based on many different tissues from a range of species. These include model species such as zebrafish, medaka *Oryzias latipes* (Temminck and Schlegel) and pufferfish, but also commercially important species such as Atlantic salmon *Salmo salar* (L.) and tilapia *Oreochromis niloticus* (L.) (Parrington & Coward, 2002).

Generation of these resources can be expected to transform our ability to identify important new proteins involved in fish tissue and cellular mechanisms as it will allow the rapid isolation of novel proteins along with homologues shown to be important in other species. It will be thus possible to generate a range of antibodies, fluorescent probes, and other molecular tools that can be used to study these proteins' physiological function (Parrington & Coward, 2002).

One potential drawback that might hamper the future exploitation of some fish genomes is that owing to genome duplication on the fish lineage (though there is still some debate on this issue (Robinson-Rechavi et al., 2001), many gene families appear to be typically half the size in land vertebrates than they are in fish (Meyer & Málaga-Trillo, 1999). This might be a factor that impedes the analysis and accurate interpretation of fish genomes (Parrington & Coward, 2002).

5.19. **Proteome Analysis of a Single Zebrafish Embryo Using Three Different Digestion Strategies Coupled with Liquid Chromatography-Tandem Mass Spectrometry**

Zebrafish is a powerful model to analyze vertebrate embryogenesis and organ development. Although a number of genes have been identified to specify embryonic development processes, only a few largescale proteomic analyses have been reported in regard to these events to date (Lin et al., 2009).

Here the total proteins of a single embryo were analyzed by urea-, sodium deoxycholate (SDC)-, and performic acid (PA)-assisted trypsin digestion strategies coupled to capillary liquid chromatography-tandem mass spectrometry (CapLC–ESI-MS/MS) identification. In total, 509 and 210 proteins were detected from the embryos at 72- and 120 hours post-fertilization (hpf), respectively, with a false identification rate of less than 1%. Approximately 95% of those proteins could be observed by combining the urea- and SDC-assisted digestion strategies, suggesting that these two methods are more effective than the PA-assisted method (Lin et al., 2009).

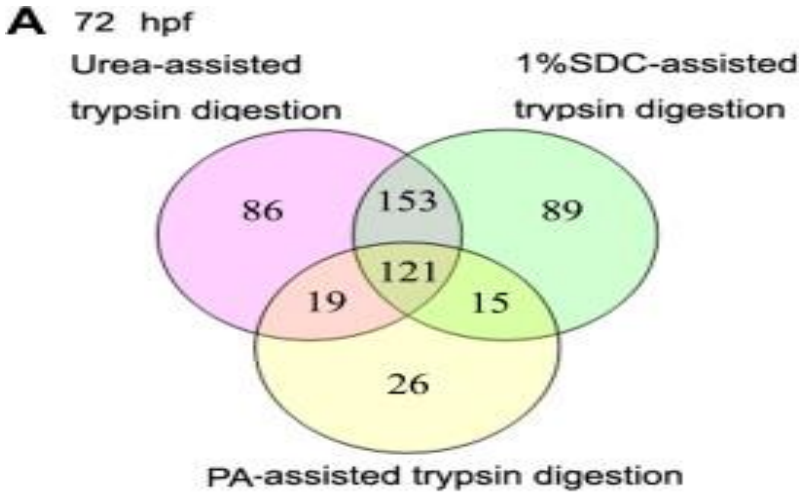

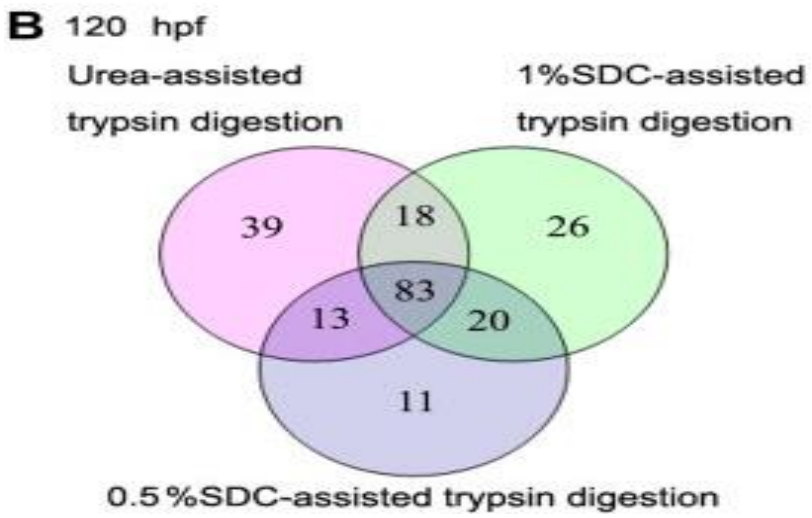

Figure 85. Comparison of protein identification results from three digestion methods. (A) In total, 509 proteins were identified in the single zebrafish embryo proteome at 72 hpf (379, 378, and 181 proteins from the urea-, SDC-, and PA-assisted digests, respectively). (B) In total, 210 proteins were identified at 120 hpf (153, 147, and 127 proteins from the urea-, 0.5% SDC-, and 1% SDC-assisted digests, respectively) (Lin et al., 2009).

The following Figure 86 shows three MS/MS spectra of the same tryptic peptide (IEDEQSLGAQLQK, precursor *m/z* 729.9, 2+) from the three digests of zebrafish embryos at 72 hpf. Figure 86A and C show the spectra of the peptides from the urea and PA digestion strategies, respectively, and Figure 86B shows the spectrum of the peptide from the SDC method. It was found that, compared with Figure 86A and C, the peptide detected in SDC digest has a larger number of y-fragment ions with an excellent signal/noise ratio (Figure 86B). This result indicates that the SDC method is able to efficiently digest proteins and facilitate protein identification from zebrafish embryos, allowing large-scale proteome analysis of zebrafish larvae (Lin et al., 2009).

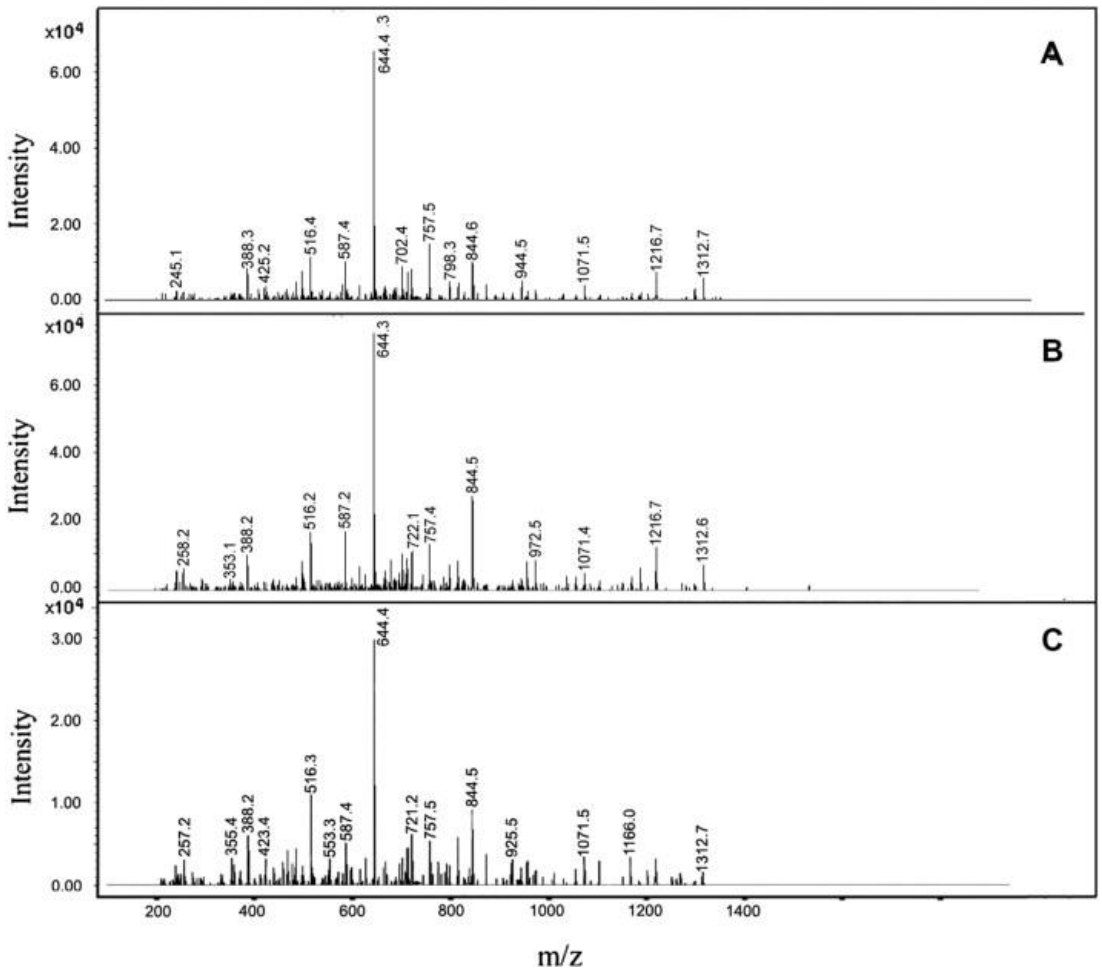

Figure 86. LC–ESI-MS/MS spectra of the tryptic peptide IEDEQSLGAQLQK (precursor m/z 729.9, 2+) identified in the samples prepared by three different digestion methods: (A) urea assisted tryptic digestion; (B) SDC-assisted tryptic digestion; (C) PA-assisted digestion (Lin et al., 2009).

Compared with 0.5% SDC, 1% SDC was more effective in identifying proteins in zebrafish embryos. In addition, the authors found that removal of the predominant yolk proteins could significantly improve protein identification efficiency (Lin et al., 2009).

In conclusion, this study represents the first overview of the protein expression profile of a single zebrafish embryo at 72 or 120 hpf. More important, this single individual proteome methodology could be applied to multiple development stages of wide-type or mutant embryos, providing a simple and powerful way to further our understanding of embryonic development (Lin et al., 2009).

5.20. **A Proteomics and Other Omics Approach in the Context of Farmed Fish Welfare and Biomarker Discovery**

The rapid and intensive growth of aquaculture over the last decade poses a tremendous challenge to this industry to comply with the latest guidelines established to minimize its negative effects on the environment, animal welfare and public health (Raposo de Magalhães et al., 2020).

Farmed fish welfare has become one of the main priorities towards sustainable aquaculture production, with several initiatives launched by the European Union within the framework of the 2030 agenda. It is clear that an unbiased and reliable way to access farmed fish welfare needs to be implemented due to the lack of reliable indicators and standardized methods that are used at present (Raposo de Magalhães et al., 2020).

In this review, the authors attempted to address the status quo of animal and fish welfare definition in particular, describing the methods and assays currently used to measure it. In addition, they explained why they believed these antiquated methods were unreliable and why there is an urgent need to establish new ones that will promote productivity and consumer's acceptance of farmed fish (Raposo de Magalhães et al., 2020).

The establishment of a new type of welfare biomarkers using cutting-edge technologies like proteomics and other omics technologies is proposed as a solution to this issue. In conclusion, this study provided a brief description of these new methodologies, describing how each of these novel methodologies could improve our scientific knowledge and the role they can play in farmed fish welfare biomarker discovery (Raposo de Magalhães et al., 2020).

5.21. **Proteome Analysis of Abundant Proteins in Two Age Groups of Early Atlantic Cod (*Gadus morhua*) Larvae**

The protein expression profiles of two different age groups of Atlantic cod larvae, at 6 days post-hatch (dph) and 24 dph, were compared using 2-dimensional electrophoresis and MALDI-TOF-MS analysis (Sveinsdóttir et al., 2008).

It is noteworthy to mention that in cod hatcheries, the life stage of the cod larvae under study, usually covers the first feeding period, which is generally characterized by high mortality. Despite visible morphological and functional changes in larvae from 6 to 24 dph, the pattern of abundant proteins was largely conserved (Sveinsdóttir et al., 2008).

High-resolution 2DE revealed the protein expression profile of soluble proteins during the early development of cod larvae. On average, 374 (373.67±25.42 s.d.) protein spots in the 6 dph larval group and 428 (428.33±2.52 s.d.) spots in the 24 dph larval group were observed (Figure 87) (Sveinsdóttir et al., 2008).

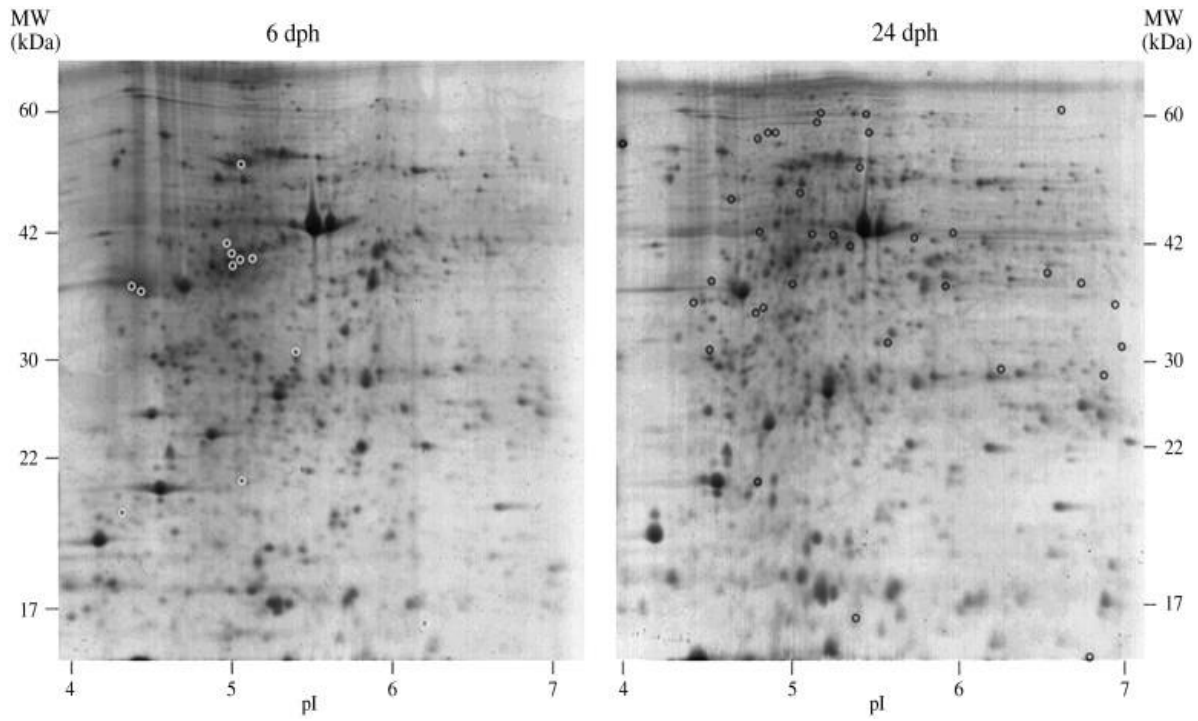

Figure 87. Average gels of protein extracts from 6 dph and 24 dph cod larvae showing temporal expression of proteins during early larval development. The spots circled (white) on the protein profile from 6 dph larvae were only detected in this age group whereas circled spots (black) on the protein profile from 24 dph larvae were only expressed in that group (Sveinsdóttir et al., 2008).

Thirty four protein spots were selected for identification based on abundance and temporal expression criteria. Protein spots were unambiguously identified by PMF using MALDI-TOF-MS. Fourteen protein spots were selected for confirmation of their identities and for sequencing by LC-MS/MS analysis. It was noted that the highly abundant protein spots showed constant expression during the early larval development (Table 56). Moreover, five protein spots were identified as α-actin, showing the highest similarity to α-actin from the following fishes; Atlantic cod (spots 393, 423), Estuary cod (*Epinephelus coioides*) (spots 470, 1341) and gilthead seabream (spot 339). Protein spot 979 had the highest identity with zebrafish myosin light chain 2. Also, four protein

spots were identified as tubulins, and these were most similar to tubulin from chum salmon (*Oncorhynchus keta*) (spot 234), Atlantic cod (spots 253, 259) and zebrafish (spot 1541).

Other protein spots identified displayed similarity to Atlantic cod glycerol-3-phosphate dehydrogenase (spot 1338), common carp (*Cyprinus carpio*), ATP synthase (spot 299) and zebrafish prohibitin (spot 773) (Sveinsdóttir et al., 2008).

Table 56. Identification of abundant protein spots showing constant expression during the early larval period (Sveinsdóttir et al., 2008).

Spot number	Accession number	Protein identification (*species*)	MM/pI		PM	SC (%)
			Theoretical	Observed		
234	P30436	α-Tubulin chain (*Oncorhynchus keta*)	50.0/4.92	53.8/5.25	16	35
253	Q9PUG4	β-2 tubulin (*Gadus morhua*)	50.0/4.71	52.9/5.19	13	23
259	Q9PUG4	β-2 tubulin (*Gadus morhua*)	50.0/4.71	52.5/5.0	35	58
299	Q9PTY0	ATP synthase subunit β, mitochondrial (*Cyprinus carpio*)	55.3/5.0	549.7/5.12	17	38
339	Q9PTJ5	Skeletal α-actin (*Sparus aurata*)	42.2/5.28	43.7/5.48	9	27
393	Q78AY8	Fast skeletal muscle α-actin (*Gadus morhua*)	42.3/5.23	43.6/5.57	13	28
423	Q78AY8	Fast skeletal muscle α-actin (*Gadus morhua*)	42.3/5.23	43.6/5.38	14	38
470	Q5IGP9	α-actin (*Epinephelus coioides*)	37.0/5.57	42.1/5.32	30	55
773	Q7T1D8	Prohibitin (*Danio rerio*)	29.7/5.28	28.8/5.37	5	18
774		No identification		29.0/4.68		
979	O93409	Myosin, light polypeptide 2, skeletal muscle (*Danio rerio*)	19.0/4.68	20.6/4.68	9	50
1338	Q6GUQ0	Glycerol-3-phosphate dehydrogenase (*Gadus morhua*)	38.7/5.47	38.2/5.91	10	37
1341	Q5IGP9	α-actin (*Epinephelus coioides*)	37.0/5.57	23.2/6.16	7	20
1541	Q6P5N0	α-Tubulin, 8 like 2 (*Danio rerio*)	50.8/4.97	54.2/5.33	17	40

Results from PMF are shown.
The Mascot search program was used to search the NCBI database.
MM/pI: Molecular mass and isoelectric point;
PM: the number of peptides matched; SC: the percentage of sequence coverage.

Interestingly, more than half of the proteins identified in the present study corresponded to different isoforms of the same proteins. The keratins showed the most pronounced developmental stage specific expression pattern. Type II keratins were more dominant in younger larvae and type I keratins in the older larval group (Sveinsdóttir et al., 2008).

In addition, four isoforms of the fast skeletal muscle α-actin, 3 isoforms of β-2 tubulin and 2 isoforms of α-actin were detected. The presence of the different isoforms could well originate by encoding by different genes or most probably generated by post-translational modifications (PTMs)

of the same gene product. Once more, we reiterate that the PTMs are largely overlooked by studies based on mRNA detection (Sveinsdóttir et al., 2008).

In conclusion, this study indicates the importance of the proteome approach to understanding the cellular mechanisms underlying fish development (Sveinsdóttir et al., 2008).

6. Aquaculture Fish Diet Proteomics

One of the main goals of the aquaculture industry is the production of fish possessing an optimal growth performance and health status (Babaheydari et al., 2016; Rodrigues et al., 2012). Also, the prevention of chronic stress exposure is of the utmost importance in cultured systems, a stress is known to have harmful impacts on the welfare and performance of farmed fish (Naderi et al., 2017; Santos et al., 2010).

6.1. Proteomic Analysis of Muscle Tissue from Rainbow Trout (*Oncorhynchus mykiss*) Fed Dietary β-Glucan

This study's main goal was to examine the changes in muscle proteome of the rainbow trout which were fed a dietary β-glucan. The experimental diets contained 0 (control), 0.1% and 0.2% β-1,3/1,6 yeast glucan. The feeding of larvae consisted on nine times per day feeding with their respective diets over two months (Ghaedi et al., 2016).

It was found that the percentage of body weight gain and feed efficiency of fish which were fed 0.2% diet was significantly higher than those of fish fed the control and 0.1% diets. This was followed by proteomics analysis of the control and 0.2% fed fish, thus proteins muscle tissue were analyzed using two-dimensional electrophoresis and mass spectrometry (Ghaedi et al., 2016).

The authors excised and identified the spots that differed significantly in abundance between control and β-glucan fed fish. Out of 8 protein spots showing differential expression, the authors were capable to identify 7 spots. Two protein spots that were found to be increased in abundance in the β-glucan treated rainbow trout corresponded to tropomyosin alpha-1 chain (spot 1) and slow myotomal muscle tropomyosin (spot 2). The five spots that were down-regulated with dietary β-glucan supplementation were identified as different forms of myosin: myosin light polypeptide 3-2 (spot 3), myosin light chain 1 (spots 4 and 5), fast myosin light chain 2 (spot 6) and myosin heavy chain (spot 7) (Ghaedi et al., 2016).

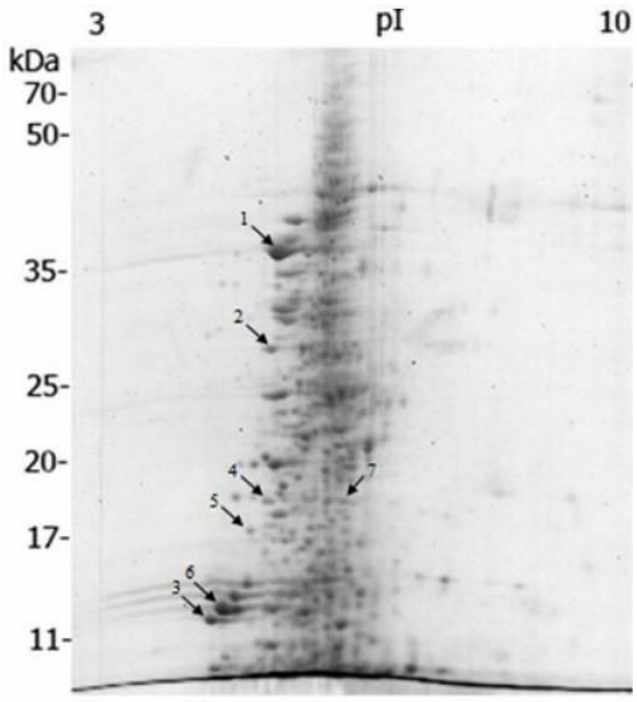

Figure 88. 2-DE map of muscle proteins of rainbow trout (Oncorhynchus mykiss), prepared by linear wide-range immobilized pH gradients (pH = 3-10, 17 cm; BioRad, USA) in the first dimension and on 12% SDS-PAGE for the second dimension. Proteins were stained with colloidal coomassie brilliant blue G-250. Labeled spots indicate identified proteins with significant altered expression profile after dietary β-glucan treatment . (Ghaedi et al., 2016).

Table 57. Protein spots with significantly altered abundance between muscle from control and β-glucan fed rainbow trout (Ghaedi et al., 2016).

Spot number	Accession number[a]	Protein identification (species)	Fold change[b]	Mascot score	SC[c]	PM[d]
Proteins increased in abundance in the β-glucan fed rainbow trout						
1	gi|185132405	Tropomyosin alpha-1 chain (*Salmo salar*)	+1.3	420	21%	5
2	gi|3063940	Slow myotomal muscle tropomyosin (*Salmo trutta*)	+1.3	76	3%	1
Proteins decreased in abundance in the β-glucan fed rainbow trout						
3	gi|197632465	Myosin, light polypeptide 3-2 (*Salmo salar*)	-1.9	440	41%	6
4	gi|185134620	Myosin light chain 1 (*Oncorhynchus mykiss*)	-1.6	149	11%	2
5	gi|185134620	Myosin light chain 1 (*Oncorhynchus mykiss*)	-1.7	139	11%	2
6	gi|185134779	Fast myosin light chain 2 (*Oncorhynchus mykiss*)	-1.5	384	24%	4
7	gi|806511	Myosin heavy chain (*Cyprinus carpio*)	-1.4	263	3%	3

[a] NCBInr ID accession number, [b] Change in abundance in β-glucan fed rainbow trout relative to control,
[c] Percentage of sequence coverage, and
[d] Number of peptides matched

It was found that the altered expression of structural proteins in fish fed β-glucan was related to higher growth rate in rainbow trout. These findings provide basic information to understand possible mechanisms of dietary β-glucan contribution to better growth in rainbow trout (Ghaedi et al., 2016).

6.2. **Vegetable Based Fish Feed Changes Protein Expression in Muscle of Rainbow Trout (*Oncorhynchus mykiss*)**

Aquaculture of carnivore fish species relies heavily on the feed production composed of protein and lipid obtained from limited resources. Consequently, the development of alternative feeds should be able to replace fish meal and oil, with alternatives obtained from vegetable origin (Glencross et al., 2007). It is reasonable to expect that such a change in feed ingredients will affect the metabolic pathways in fish (Jessen et al., 2012).

This study consisted of analyzing two groups of rainbow trout which were fed different diets for 12 weeks, with a traditionally control diet (C) (based on marine oil and protein) and a diet (V) based exclusively on vegetable products. Both groups were fed with 42% protein and 26% fat. The 2-DE comparison of the fish muscle revealed 39 spots that were significantly different between the two feeding groups C (n=8) and V (n=7) (Jessen et al., 2012).

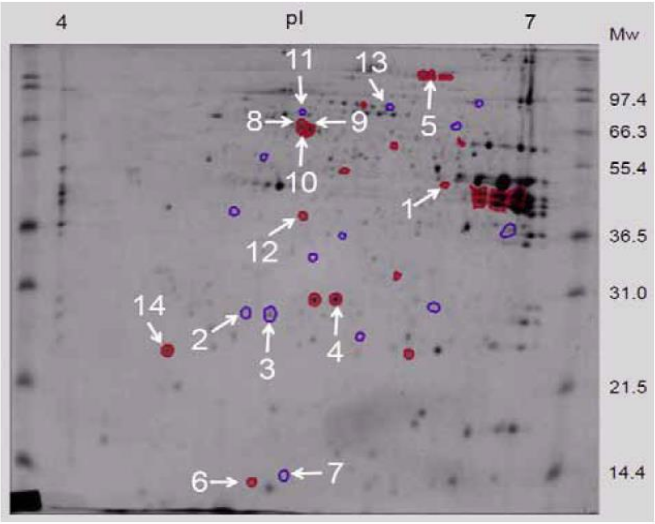

Figure 89. Muscle protein expression differences in rainbow trout fed the two type of feed. Proteins(39) of interest based on Student t-test (P<0.05) are marked. The 2-DE gel is a representative gel of water soluble proteins from rainbow trout muscle. Mw is given i kDa (Jessen et al., 2012).

It was found that the major part (25 spots) out of the 39 spots, represented up-regulated proteins, whereas 14 spots represented down-regulated proteins in fish from the V group. The provisionally identified spots (14) are indicated by numbers in the gel (Figure 89) and given by name, function, and direction of expression change in fish from the V group in Table 58 (Jessen et al., 2012).

In conclusion, this study proved that intake of the vegetable based diet, among others, influenced the expression of muscle proteins involved in lipid binding/transport, protein turnover, and binding of different ions (Jessen et al., 2012).

Table 58. Identified differential expressed proteins in fish feed the two type of feed (Jessen et al., 2012).

No.	Protein name	Effect[1] of vegetable based feed	Function
1	6-phosphogluconate dehydrogenase	↑	Pentose shunt
2-32	Apolipoprotein A-I-1 precursor	↓	Lipid/cholesterol transport
4	Carbonic anhydrase	↑	One-carbon metabolic process
5	eEF1A2 binding protein-like	↑	Protein synthesis (translation)
6	Fatty acid-binding protein	↑	Lipid binding and transport
7	Fatty acid-binding protein	↓	Lipid binding and transport
8-9	Hemopexin-like protein	↑	Metal binding
10	T-complex protein 1 subunit theta	↑	Protein folding
11	Thimet oligopeptidase	↓	Proteolysis
12	Selenoprotein J	↑	Selenium binding
13	Transferrin 1	↓	Iron binding
14	Translationally-controlled tumor protein	↑	Calcium binding; microtubule stabilization

[1] Arrow pointing up shows up-regulated protein expression in fish fed the vegetable based diet, and *vice versa*.
[2] Proteins in **bold** were among those also correlating to the textural attributes.

6.3. **Proteomic Analysis of Rainbow Trout (*Oncorhynchus mykiss, Walbaum*) Sserum after Administration of Probiotics in Diets**

The response of the rainbow trout (*Oncorhynchus mykiss*, Walbaum) fed a probiotics diet was investigated by examining the acute phase response (APR) of the serum proteome (Brunt et al., 2008).

Proteomic analysis by two-dimensional electrophoresis (2D) followed by mass spectrometry was used to detect APR-related proteins in rainbow trout serum following feeding with diet containing probiotics *Aeromonas sobria* (GC2) and *Bacillus sp*.(JB-*1)*. The acute phase response (APR) has been defined as a rapid, orchestrated, physiologically induced response to tissue

injury, infection, neoplasia, trauma and stress (H. Baumann & Gauldie, 1994; Brunt et al., 2008; Jensen et al., 1997).

2D gel profiles of pre-and post-stimulus rainbow trout serum with probiotic GC2 is shown in Fig. 1. The number of spots detected on the gels varied from 156 to 220 between the six replicates. The detected proteins had molecular masses of between 125 and 5 kDa, and pI's between 4 and 7. It is important to understand that proteins are considered to be differentially expressed between the two groups on the following criteria: (1) there was >±2-fold difference in the spot abundance between pre-and post-stimulus fish and (2) the change was consistent in all replicate the analysis for each group of fish (Brunt et al., 2008).

In all individual fish that were treated with GC2, three proteins were increased (Pt1, Pt2 and Pt3) as shown in Figure 90. One low molecular weight protein, Pt2 (15 kDa, pI 5.2), exhibited a > 3-fold increase in volume between pre- and post-treated fish. Figure 91 shows the mean normalised volume value of the increased proteins from the pre- and post-treated fish (Brunt et al., 2008).

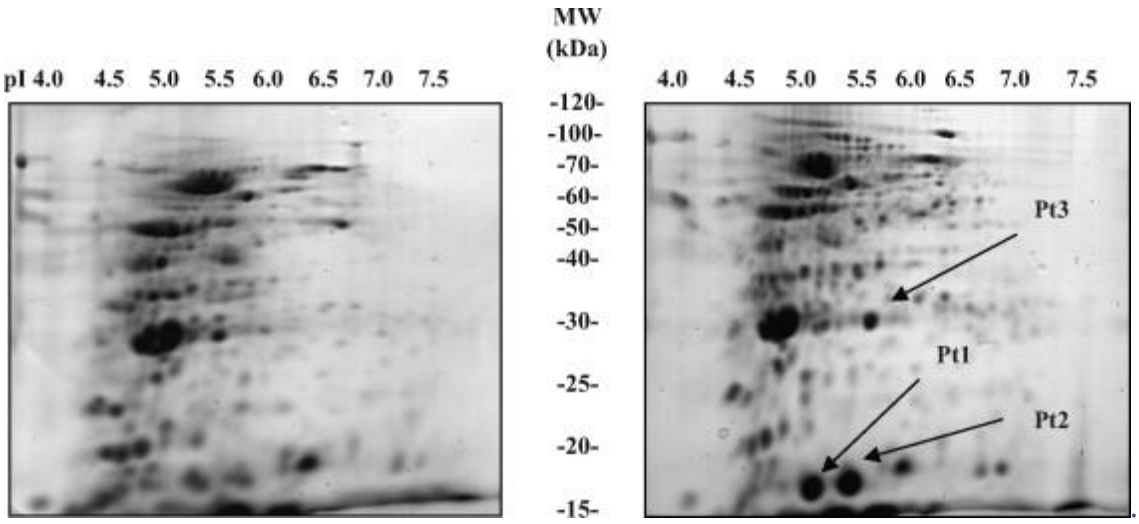

Figure 90.Two-dimensional PAGE of serum taken from a rainbow trout before stimulus (control, left) and of serum from the same rainbow trout after treatment with probiotic GC2 for 14 days (right). Presumptive acute phase response in fish is indicated by arrows (Brunt et al., 2008).

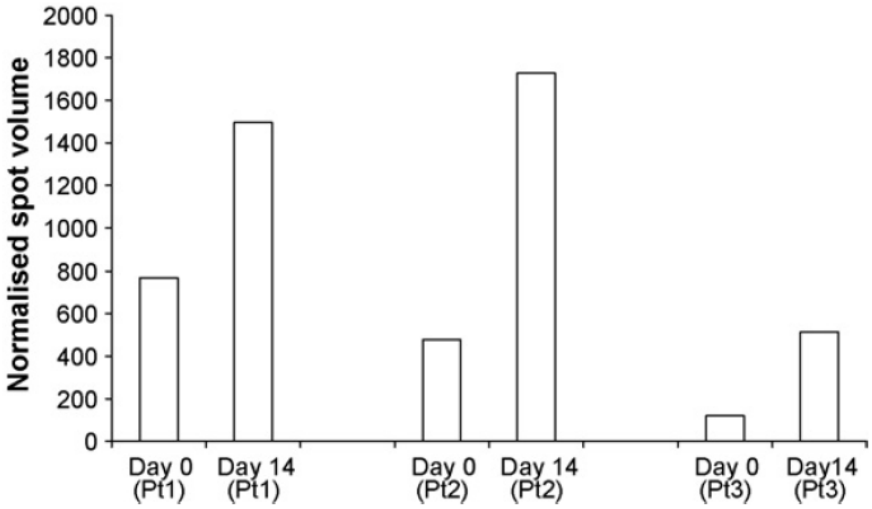

Figure 91. Changes in normalised spot volumes of Pt1, Pt2 and Pt3 preand post-stimulus with probiotic GC2 after 14 days (Brunt et al., 2008).

In comparison, rainbow trout that were treated with JB-1, two proteins (Ptc and Ptd) with molecular weights of 74 and 30 kDa and pI's of 5.9 and 5.5, respectively were consistently induced (Figure 92). The low molecular weight proteins Pta and Ptb (12 kDa, pI 6–6.4) were consistently altered in treatmen groups. Thus, protein Pta reduced in volume in treatment groups, and the protein Ptb was undetectable in all probiotic fed trout serum (Figure. 93) (Brunt et al., 2008).

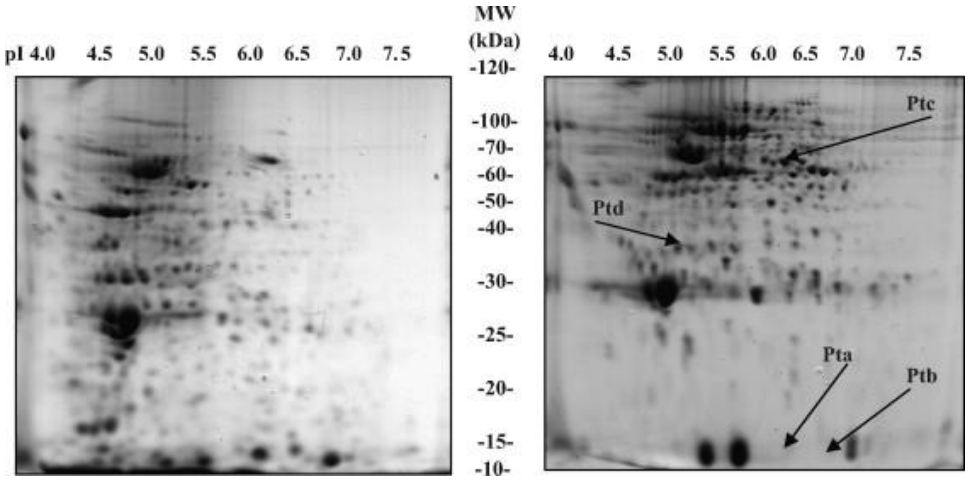

Figure 92. Two-dimensional PAGE of serum taken from a rainbow trout before stimulus (control, left) and of serum from the same rainbow trout after treatment with probiotic JB-1 for 14 days (right). Presumptive acute phase response in fish is indicated by arrows (Brunt et al., 2008).

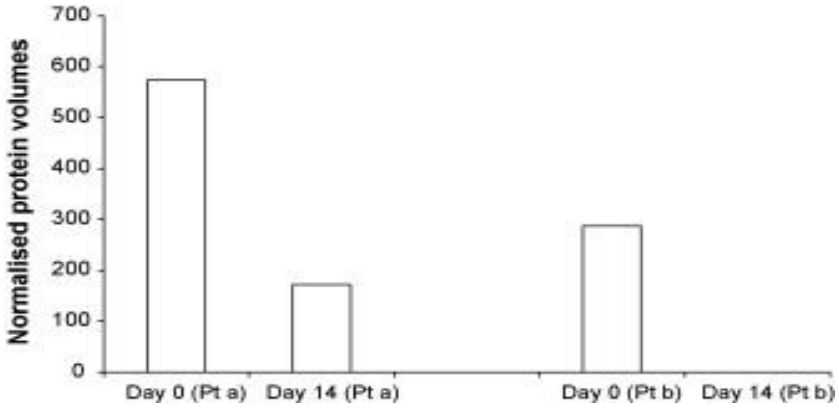

Figure 93. Changes in normalised spot volumes of Pta and Ptb pre- and post-stimulus with probiotic JB-1 after 14 days (Brunt et al., 2008).

Protein spots of interest were manually excised, subjected to in-gel digestion and MALDI-TOF-MS analysis. Three candidate proteins, Pt1, Pt2 and Pt3, were putatively identified as NADH dehydrogenase, dystrophin and mKIAA0350, respectively (Table 59). However, none of these were positively identified as rainbow trout proteins. Conversely, proteins Ptc and Ptd which were induced following use of JB-1 (see were identified as transferrin and EnsangP0000001, respectively (Table 59). Furthermore, these were identified as Rainbow trout proteins in the Mascot database ($P < 0.05$). Moreover, protein Ptb which disappeared subsequent to JB-1 treatment demonstrated homology with rainbow trout hemoglobin, expectation 0.000. Finally, the nearest match to the down-regulated protein, Pta, was an unnamed protein from Mus musculus (Brunt et al., 2008).

Table 59. Mascot™ database identification of proteins whose levels change following probiotic treatment (Brunt et al., 2008).

Spot ID	Expression	p*I*	Molecular weight (kDa)	Protein		Expectation
Pt1	↑	5.3	15	NADH dehydrogenase	*Catharus dryas*	0.098
Pt2	↑	5.7	15	Dystrophin Dp260-1	*Homo sapiens*	0.331
Pt3	↑	5.5	33	Similar to mKIAA0350	*Rattus norvegicus*	0.022
Pta	↓	6.0	12	Unnamed protein	*Mus musculus*	0.082
Ptb	↕	6.4	12	Haemoglobin IV beta chain	*Oncorhynchus mykiss*	0.000
Ptc	I	5.9	74	Transferrin	*O. mykiss*	0.000
Ptd	I	5.5	30	EnsangP0000001	*Anopheles gambiae*	0.001

↑ Indicates an increase in spot volume, ↓ decrease in spot volume, ↕ disappearance of spot and I induced spot.

In conclusion, this study established that three candidate proteins increased following use of GC2. These were identified by MS and as NADH dehydrogenase, dystrophin and mKIAA0350.

Conversely, one of the proteins, which were induced following use of JB-1 was identified as transferrin (Brunt et al., 2008).

6.4. **Dietary Lysine Imbalance Affects Muscle Proteome in Zebrafish (*Danio rerio*)**

Lysine (Lys) is an indispensable amino acid (AA) in vegetable protein sources of fish feeds. It has been proven that inadequate dietary Lys availability restrict the protein synthesis, accretion and growth of fish. In order to further elucidate the role of Lys imbalance on fish growth, it was decided to study the myotomal muscle proteome of juvenile zebrafish (*Danio rerio*). Quadruplicate groups of 8 fish were fed either a low-Lys [Lys(−), 1.34 gk^{-1}], medium/control (Lys, 2.47 gk^{-1}) or high-Lys [Lys(+), 4.63 gkg−1] diet (Table 60) (de Vareilles et al., 2012).

Table 60. Ingredient and chemical composition of the three experimental diets (de Vareilles et al., 2012; Gómez-Requeni et al., 2011).

Ingredient (%)	Control	Lys(−)	Lys(+)
Fish meal	20.60	20.60	20.60
Corn gluten 176/07	13.25	13.25	13.25
Wheat gluten 225/07	13.25	13.25	13.25
Wheat starch 143/07	19.86	19.87	19.83
Fish oil[a]	11.80	11.80	11.80
Vitamin mix[b]	2.00	2.00	2.00
Mineral mix [c]	0.60	0.60	0.60
Betafine (Choline chloride)[d]	0.40	0.40	0.40
Inositol[e]	0.03	0.03	0.03
KH_2PO_4 (22.5 %)	1.28	1.28	1.28
NaH_2PO_4 (22.5 %)	1.28	1.28	1.28
AA mix full[f]	14.22	0	0
AA mix Lys−[g]	0	14.21	0
AA mix Lys+[h]	0	0	14.25
Taurine	1.43	1.43	1.43
Proximate composition (%)			
Dry matter	90.70	92.20	91.90
Crude protein	45.40	45.60	45.80
Crude fat	14.40	15.30	14.70
Ash	5.00	5.00	4.90

[a]NorSeaOil O1/07, Norsildmel, Norway
[b]Provided per kg of feed: vitamin D_3, 3,000 I.E.; vitamin E, 160 mg; thiamin, 20 mg; riboflavin, 30 mg; pyridoxine–HCl, 25 mg; vitamin C, 200 mg; calcium pantothenate, 60 mg; biotin. 1 mg; folic acid, 10 mg; niacin, 200 mg; vitamin B_{12}, 0.05 mg; menadion bisulphite, 20 mg
[c]Provided per kg of feed: magnesium, 56 mg; potassium, 450 mg; zinc, 90 mg; iron, 56 mg; manganese, 11 mg; copper, 5.6 mg
[d]Betafin BCR, Finnsugar Bioproducts, Finland
[e]Danisco Animal Nutrition, Finland
[f]AA mix full provided in g/100 g: Asn, 9.12; Gln, 13.30; Ser, 5.34; Gly, 7.67; His, 2.23; Arg, 6.79; Thr, 4.37; Ala, 6.50; Pro, 4.46; Tyr, 2.43; Val, 4.95; Met, 3.20; Ile, 4.46; Leu, 7.57; Phe, 4.08; Lys, 9.72; Cys, 1.65; Trp, 2.17
[g]AA mix Lys− provided in g/100 g: Asn, 10.12; Gln, 14.76; Ser, 5.92; Gly, 8.51; His, 2.48; Arg, 7.54; Thr, 4.85; Ala, 7.22; Pro, 4.95; Tyr, 2.69; Val, 5.49; Met, 3.55; Ile, 4.95; Leu, 8.40; Phe, 4.52; Cys, 1.83; Trp, 2.20

[h]AA mix Lys+ provided in g/100 g: Asn, 6.99; Gln, 10.19; Ser, 4.09; Gly, 5.88; His, 1.71; Arg, 5.21; Thr, 4.40; Ala, 4.98; Pro, 3.42; Tyr, 1.86; Val, 3.79; Met, 2.45; Ile, 3.42; Leu, 5.80; Phe, 3.12; Lys, 29.26; Cys, 1.26; Trp, 2.15

Comparative 2D-DIGE analysis of the trunk myotomal muscle, using the BVA module of DeCyder software (GE Healthcare) applied to the resulting gel images, each one representing a biological quadruplicate of each experiment condition, enabled the detection and quantification of 527±11 (mean±S.E.M.) protein spots across all spot maps, covering a molecular mass range of ~10 to 150 kDa and pI values between 4 and 7 (Figure. 94) (de Vareilles et al., 2012).

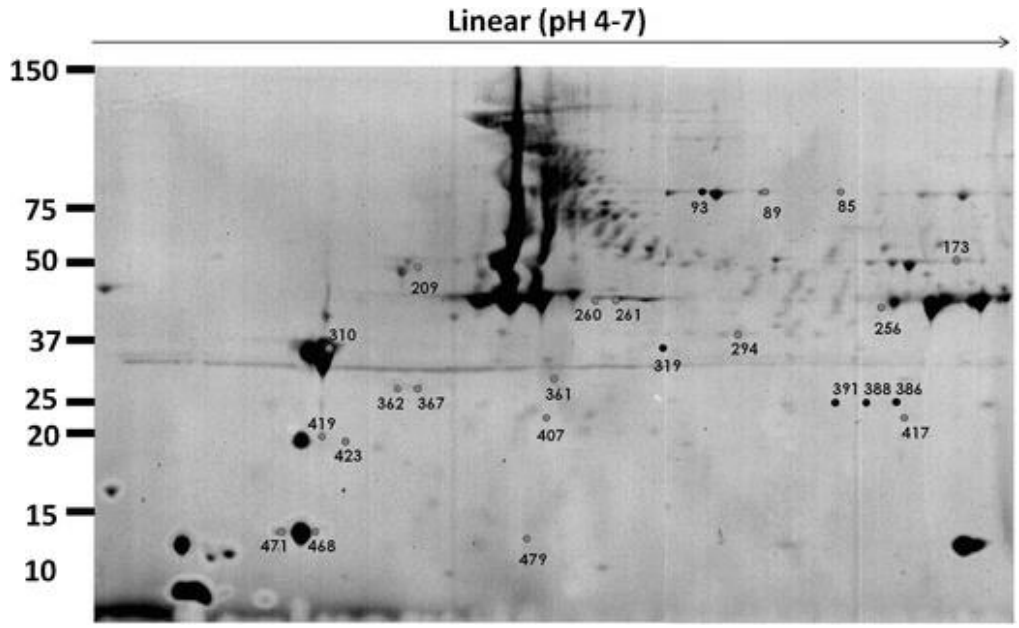

Figure 94. 2-D PAGE of 300 µg skeletal muscle protein (whole extraction) from a mix of zebrafish fed lysine deficient and lysine enriched experimental diets, performed on 11 cm ImmobilineTM Drystrip pH 4–7 (GE Healthcare) and 13.3×8.7 cm 12 % Bis–Tris Criterion™ XT Precast Gels (Bio-Rad), and stained with Colloidal Coomassie Blue, G-250. Numbered spots represent significantly differentially expressed protein spots ($p<0.05$, Student's t test; $|fold\text{-}change|>1.2$) between treatments, selected for sequencing. Light grey circles are positively identified spots. Black circles are unidentified protein spots (de Vareilles et al., 2012).

Accordingly, the fish growth was monitored from 33 to 49 days post-fertilization (dpf) and the trunk myotomal muscle proteome of Lys (−) and Lys (+) treatments were screened by 2D-DIGE and MALDI-TOF-MS. Protein spots of interest were manually excised, subjected to in-gel digestion and MALDI-TOF-MS analysis. The 24 protein spots whose expression was significantly affected by dietary Lys content, we excised and subjected to in-gel tryptic digestion, 18 of which

were successfully identified, corresponding to 11 proteins (Table 61). Sixteen spots matched proteins involved in the cytoskeletal network and the contractile apparatus of skeletalmuscle, 11 of which were more abundant in Lys (−) fish [myosin-binding protein H-like (MyBP-H, spots 85, 89 and 93), fast skeletal myosin heavy chain (myhc4, spot 294), fast skeletal myosin light chains (myl1, spots 419 and 423; mylz2, spots 468 and 471), tropomyosin alpha 1 chain (tpma, spot 310) and alpha actin (spots 260 and 261)] and 5 of which were less abundant [fast skeletal muscle myosin heavy chain (myhz1, spot 256), F-actincapping protein subunit beta (capzb, spot 361) and alpha actin fragments (spots 367, 407 and 479)] (Table 61; Figures. 94 and 95). In addition to structural proteins, significant increases in abundance in the skeletal muscle of Lys (−) zebrafish were also found for proteins involved in energy metabolism [betaenolase (glycolytic pathway; spot 173) and mitochondrial ATP synthase beta s ubunit-like (oxidative phosphorylation; spot 209)] (Figures. 94 and 95; Table 61). The remaining identified peptides are indicated in the following table (de Vareilles et al., 2012).

Table 61. Protein spots with significantly altered abundance between muscle from Lys(−) and Lys(+) zebrafish (de Vareilles et al., 2012).

Spot #	Protein identification	Accession #[a]	Fold change[b]	S.C. (M.P.M.)[c]	pI/kDa		Score (PMF) [d]	P.M.[e]	Best P.M. p-value[f]
					Observed	Theoretical			
Proteins increased in abundance in fish fed Lys(−) diet									
85	myosin-binding protein H-like	gi|153945848	1.77	20 (11)	6.35/79.50	5.39/57.57	(84)	n.a.	n.a.
89	myosin-binding protein H-like	gi|153945848	1.96	30 (17)	6.20/75.69	5.39/57.57	82	3	KPGNFDGGVYSCR
									7.94E-07
260	actin, alpha 1b, skeletal muscle	gi|70778800	1.55	35 (10)	5.66/41.95	5.29/42.20	(79)	n.a.	n.a.
261	actin, alpha, cardiac muscle 1b	gi|28277651	1.90	40 (11)	5.72/41.95	5.23/42.3	63	2	QEYDEAGPSIVHR
									3.16E07
294	fast skeletal myosin heavy chain 4	gi|33088009	1.44	34 (12)	6.15/34.46	5.70/40.88	42	1	DAQLHLDDAVR
									6.31E-05
310	tropomyosin alpha-1 chain	gi|18859505	1.57	62 (26)	4.78/32.01	4.70/32.76	68	2	KLVIVEGELER
									3.16E-06
419	fast skeletal myosin alkali light chain 1	gi|41053385	1.72	60 (9)	4.72/19.57	4.63/20.98	238	4	ATYDDYVEGLR
									5.01E-08
423	fast skeletal myosin alkali light chain 1	gi|41053385	1.74	29 (6)	4.80/19.10	4.63/20.98	28	1	EAFLLFDR
									3.98E-03
468	myosin, light polypeptide 2, skeletal muscle	gi|18859049	2.26	95 (24)	4.72/11.68	4.68/18.97	259	3	NICYVITHGEEKEE
									2.00E-12
471	myosin, light polypeptide 2, skeletal muscle	gi|18859049	1.73	85 (9)	4.60/11.68	4.68/18.97	326	4	NICYVITHGEEKEE
									2.00E-12
173	beta-enolase	gi|47551317	1.95	43 (14)	6.84/52.34	6.25/47.84	(99)	n.a.	n.a.
209	mitochondrial ATP synthase beta subunit-like	gi|66773080	1.90	48 (27)	5.08/48.62	5.25/55.08	194	3	IPVGPETLGR
									5.01E-07
Proteins decreased in abundance in fish fed Lys(−) diet									
256	fast skeletal myosin heavy polypeptide 1	gi|8698685	1.49	38 (22)	6.55/38.97	5.52/48.69	128	2	DAQLHLDDAVR
									2.00E-10
367	actin, alpha, cardiac muscle 1b	gi|28277651	1.46	25 (7)	5.04/26.95	5.23/42.30	119	2	SYELPDGQVITIGNER
									1.58E-11
407	actin, alpha 1b, skeletal muscle	gi|70778800	1.22	28 (10)	5.46/22.69	5.29/42.20	46	1	GYSFVTTAER
									2.00E-05
479	actin, alpha 1b, skeletal muscle	gi|70778800	2.00	32 (13)	5.38/11.12	5.29/42.20	59	1	AGFAGDDAPR
									1.26E-06
361	F-actin-capping protein subunit beta	gi|41053959	1.37	31 (9)	5.51/27.62	5.70/30.95	80	2	KLEVEANNAFDQYR
									2.00E-07
362	apolipoprotein A-I precursor	gi|18858281	1.43	64 (27)	5.00/27.62	5.06/30.24	32	1	IAPHTQDLQTR
									6.31E-04
417	Pdlim7 protein	gi|45709024	1.20	50 (12)	6.62/21.60	6.97/23.51	77	3	LEGPACFIPNDR
									2.51E-06

All searches were performed against the *Danio rerio* NCBInr database. Experimental molecular weights and isoelectric points were estimated from the position of the spots in the gels; theoretical molecular weights and isoelectric points were calculated based on the best result's sequence

[a]NCBInr RefSeq accession number

[b]Fold-change of protein abundance between treatments

[c]Percentage of sequence coverage and number of mass peaks matched to sequence

[d]Ion score obtained in MSMS ion search (significant when above 31, $P < 0.05$). When no reliable MSMS data are available, the protein score from PMF is given (significant when above 59, $P < 0.05$)

[e]Number of significant peptide matches in MSMS ion search (ion score > 31; E value <0.05)

[f] p value was calculated as $10^{-0.1 \times \text{score}}$, where "score" is the ion score of the best matched peptide

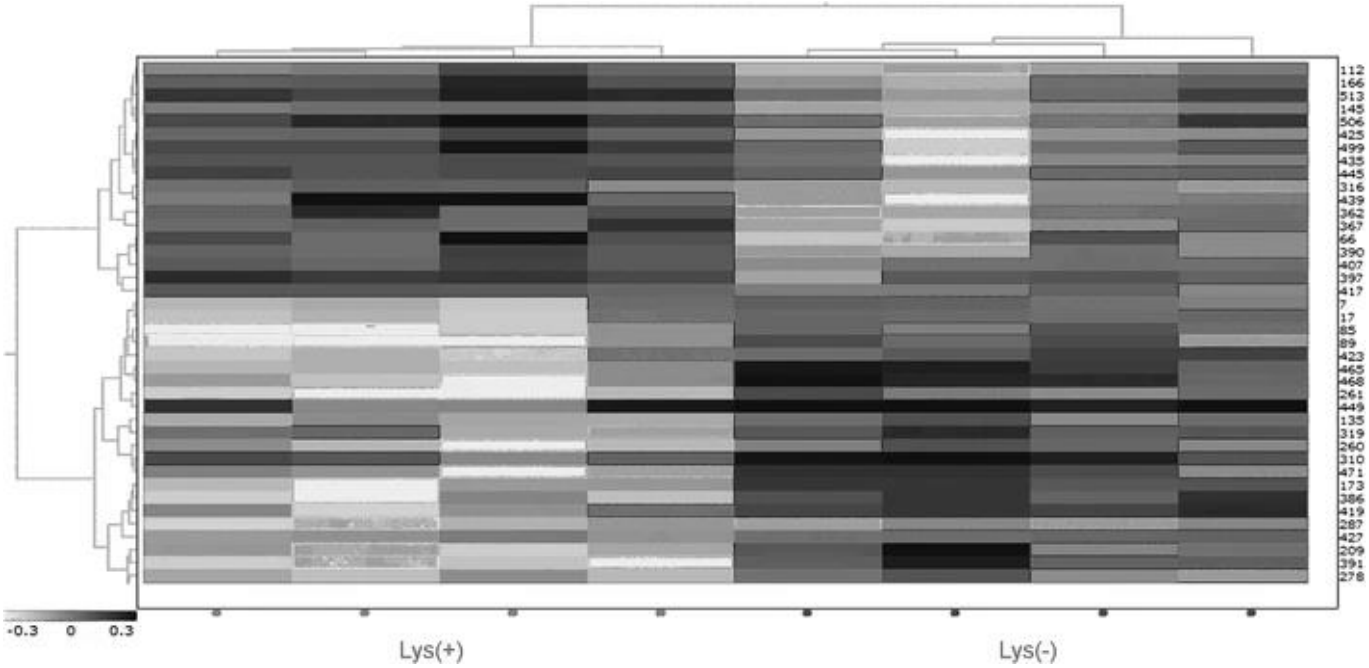

Figure 95. Heat map showing relative abundance of identified proteins for all samples. Spots were grouped using Euclidian distance by agglomerative hierarchical clustering (complete linkage method). Only spots present in more than 80 % of spot maps and with p value lower than 0.05 (Student's t test) were included. Light shades indicate a lower than average expression of protein spots and dark shades indicate a higher than average expression. Samples from Lys(+) treatment are labelled in light grey and from Lys(−) treatment in black. Numbers refer to spot IDs (de Vareilles et al., 2012).

Finally, apolipoprotein A-I precursor (Apo A-I, lipid transport; spot 362) and a protein belonging to the PDZLIM protein family, Pdlim7 (spot 417) whose members are reported to act as signal mediators in various cellular processes such as migration, signal transduction and differentiation, showed an increased abundance in the trunk myotomal muscle of juvenile zebrafish fed the Lys enriched diet, Lys (+). It was found that the growth rate was negatively affected by diet Lys (−). In addition, out of 527±11 (mean ± S.E.M.) protein spots detected (~10–150 kDa and 4–7 pI value), 30 were over-expressed and 22 under-expressed in Lys (−) fish (|fold-change|>1.2, p value <0.05). Furthermore, it was found that the higher myosin light chains abundance and the other myofibrillar proteins in Lys (−) fish pointed to increased sarcomeric degradation, indicating a higher protein turnover for supplying basal energy saving metabolism rather than growth and muscle protein accretion. Another interesting observation was that the Lys deficiency most probably induced a higher feeding activity; this was reflected in the over-expression of beta enolase and mitochondrial ATP synthase. Contrarily, in the faster growing fish [Lys (+)], the over-expression of apolipoprotein A-I, F-actin capping protein and Pdlim7 point to increased energy storage as fat and enhanced muscle growth, particularly by mosaic hyperplasia (de Vareilles et al., 2012).

In conclusion, this study presented the effects of a dietary Lys imbalance on the growth of zebrafish reared under best practice laboratory protocols. It also permitted to gain a deeper insight into how a dietary Lys level can affect the white skeletal trunk muscle of juvenile zebrafish. A decrease in growth rate in fish fed with a Lys deficient diet was found when compared to fish fed with diets with a theoretically non-deficient Lys profile. Furthermore, the analysis of the muscle indicated that the decreased growth rate observed in the Lys (−) pointed to an enhanced catabolism of the myofibrillar apparatus induced by the dietary AA deficiency or imbalance. This deficiency may have induced a higher feeding activity in these fish for compensatory reasons, and perturbed normal transport of cholesterol and energy storage (de Vareilles et al., 2012).

On the other hand, the higher growth rate observed in fish fed an enriched-Lys diet seems to reflect an active hyperplasic growth and enhanced skeletal muscle development. This would make Lys one of the factors that might regulate the process of hyperplasia in fish skeletal muscle and thus be of particular importance to optimise muscle growth in aquaculture (de Vareilles et al., 2012).

This study, without any doubts have proven the usefulness of the novel screening molecular approaches such as 2D-proteomics as a hypothesis-generating approach in modern biology (de Vareilles et al., 2012).

6.5. **Impact of High Dietary Plant Protein With or Without Marine Ingredients in Gut Mucosa Proteome of Gilthead Seabream (*Sparus aurata*, L.).**

The gut mucosa plays a crucial role in the digestion and absorption of nutrients, and in the immune defence. It has been established that fishmeal replacement by plant sources usually have an impact on the intestinal status at both digestive and immune level, which may compromise relevant, productive parameters, such as feed efficiency, growth or survival. For these reasons and in order to evaluate the long-term impact of total fishmeal replacement on the intestinal mucosa, it became important to study the gut mucosa proteome in fish fed with a fishmeal-based diet, against plant protein-based diets with or without alternative marine sources inclusion (Estruch et al., 2020). In this study, three different diets were assayed in triplicates tanks: the FM diet, a fishmeal based control diet, in which fishmeal (59%) was the main source of protein; the VM diet, a plant-meal based diet in which the whole protein content was of plant origin, and the VM+ diet, a plant-meal based diet including 10% squid meal and 5% krill meal. VM and VM+ were supplemented with different synthetic crystalline amino acids in order to achieve optimal amino acid requirements reported for gilthead seabream juveniles (Estruch et al., 2020; J. N. Lü et al., 2012).

In the present work, a big set of proteins was observed to be under expressed in the VM group in comparison to FM and VM+ samples, affecting LFQ Intensity data and hiding the potential interesting differences between dietary groups. Accordingly, 1355 proteins were identified by MALDI-TOF-MS using MaxQuant Assay. After removing contaminants and reverse sequences, this list was reduced to 1328 proteins. 754 (56.78%) of them were found in all the samples. A summary of the proteins identified in the different groups and individual samples is shown in Table 62 (Estruch et al., 2020).

Table 62. Number of proteins identified in the different runs and experimental groups (Estruch et al., 2020) .

	FM			VM			VM+		
	FM1	**FM2**	**FM3**	**VM1**	**VM2**	**VM3**	**VM + 1**	**VM + 2**	**VM + 3**
Identifications	1233 (92.8%)	1225 (92.2%)	1244 (93.7%)	1068 (80.4%)	845 (63.6%)	1219 (91.8%)	1247 (93.9%)	1229 (92.6%)	1257 (94.7%)
Represented in the group[a]	1291 (97.2%)			1279 (96.3%)			1299 (97.8%)		
Represented in all samples	1163 (87.6%)			776 (58.4%)			1174 (88.4%)		

[a] Proteins represented in the group were identified in at least one run of the group.

Samples from the VM group, especially sample VM2 (63.6%), conveyed lower percentages of identifications in comparison to the total amount. In consequence, the represented protein population in VM group was lower (776) than the other groups, FM and VM+ (1163 and 1174, respectively). Under these circumstances, the label-free quantification (LFQ) intensity was discarded for subsequent analyses. Also, the total fishmeal replacement without marine ingredients inclusion conveyed a negative impact in the growth and biometric parameters, which resulted in an altered gut mucosa proteome. Nevertheless, it was found that the inclusion of a low percentage of marine ingredients in plant protein-based diets allowed to maintain the growth, biometrics parameters and gut mucosa proteome with similar values to FM group (Estruch et al., 2020).

Similarly, the total fishmeal replacement induced a big set of underrepresented proteins which were associated as several biological processes such as intracellular transport, assembly of cellular macrocomplex, protein localization and protein catabolism. Also, several molecular functions were detected and these were mainly related with binding to different molecules and the maintenance of the cytoskeleton structure. The set of downregulated proteins also included molecules which have a crucial role in the maintenance of the normal function of the enterocytes, and therefore, of the epithelium, including permeability, immune and inflammatory response regulation and nutritional absorption. In addition, the authors of this work indicated that the amino acid imbalance presented in VM diet, in a long-term feeding, could be the major reason of these alterations, which could be prevented by the inclusion of 15% of alternative marine sources.

In conclusion, the long-term feeding with plant protein based diets may be considered as a stress factor and lead to a negative impact on digestive and immune system mechanisms at the gut, that can become apparent in a reduced (Estruch et al., 2020).

6.6. Effects of Chronic High Stocking Density on Liver Proteome of Rainbow Trout (*Oncorhynchus mykiss*)

This study main goal was to assess the effects of chronic high stocking density on the liver proteome of rainbow trout. Rainbow trout juveniles (42.6 ± 2.3 g average body weight) were randomly distributed into six tanks at two stocking densities (low stocking density (LD) = 20 kg m^{-3} and high stocking density (HD) = 80 kg m^{-3}) (Naderi et al., 2017).

It is well known that high stocking density are responsible for the reduction of the growth performance compared to the LD fish. Hence, the lysozyme activity increased with the stocking density, while the serum complement activity decreased. In addition, it was established that the serum cortisol and total protein levels did not show significant differences ($P > 0.05$) between experimental groups (Naderi et al., 2017).

The fish reared at high stocking density showed significantly lower osmolality and globulin values but higher albumin level. The HD group had significantly higher activities of catalase, glutathione peroxidase and superoxide dismutase, and malondialdehyde content in the liver when compared to the LD group (Naderi et al., 2017).

Comparative proteomics was used to determine the proteomic responses in livers of rainbow trout reared at high stocking density for 60 days. Out of nine protein spots showing altered abundance (>1.5- folds, $P < 0.05$), eight spots were successfully identified. Two proteins including apolipoprotein A-I-2 precursor and mitochondrial stress-70 protein were found to increase in HD group. The spots found to decrease in the HD group were identified as follows: 2-peptidylprolyl isomerase A, two isoforms of glyceraldehydes-3-phosphate dehydrogenase, an unnamed protein product similar to fructosebisphosphate aldolase, 78 kDa glucose-regulated protein, and serum albumin 1 protein (Naderi et al., 2017).

Table 63. Protein spots with significantly altered abundance between liver from low density (LD) and high density (HD) groups of rainbow trout (Naderi et al., 2017).

Spot number	Accession number[a]	Protein identification (species)	Fold change[b]	MS/MS score	SC[c] (%)	PM[d]
Proteins increased in abundance in the HD group						
1	gi|185132822	Apolipoprotein A-I-2 precursor (*Oncorhynchus mykiss*)	+1.5	227	11	4
2	gi|929089754	Stress-70 protein, mitochondrial (*Salmo salar*)	+1.5	764	13	7
Proteins decreased in abundance in the HD group						
3	gi|213,514,672	2-peptidylprolyl isomerase A (*Salmo salar*)	−3.4	422	42	6
4	gi|185135354	Glyceraldehyde 3-phosphate dehydrogenase (*Oncorhynchus mykiss*)	−1.9	539	20	6

5	gi|185135354	Glyceraldehyde 3-phosphate dehydrogenase (*Oncorhynchus mykiss*)	−1.5	724	27	8
6	gi|642050237	Unnamed protein product similar to fructose-bis-phosphate aldolase (*Oncorhynchus mykiss*)	−1.6	692	21	7
7	gi|60223019	Glucose-regulated protein 78 kDa (*Oncorhynchus mykiss*)	−1.5	771	12	7
8	gi|295419235	Serum albumin 1 protein (*Oncorhynchus mykiss*)	−1.6	564	29	5
9	–	Not identified	−1.5	–	–	–

[a] NCBInr ID accession number
[b] Change in abundance in HD group relative to LD group
[c] Percentage of sequence coverage
[d] Number of peptides matched

6.7. **Proteome Modifications of Fingerling rainbow Trout (*Oncorhynchus mykiss*) Muscle as An Efect of Dietary Nucleotides**

A feeding study was conducted to determine the effect of the dietary nucleotides (NT) on the growth performance and muscle proteome profile of rainbow trout fingerlings. In this study, five experimental diets were chosen using different levels of supplemented nucleotides (0, 0.05, 0.1, 0.15 and 0.2%) in the rainbow trout for 8 weeks. Each diet was randomly allocated to triplicate groups of fish with initial average weight of approximately 23 g. The authors reported that the percentage of body weight gain (WG) and feed efficiency (FE) of the fish, were better when the fish were fed 0.15–0.2% diets (Keyvanshokooh & Tahmasebi-Kohyani, 2012).

Based on growth measurements (Table 64), fish fed diets with 0 and 0.2% NT were selected for proteomic analysis. Muscle tissue samples were taken from behind the head and above the lateral line. In order to minimize the effects of individual variation, the muscle tissues of (each) three individuals were mixed before proteome extraction so that three pools were prepared for each experimental group (Keyvanshokooh & Tahmasebi-Kohyani, 2012).

Table 64. Final weight, weight gain and feed efficiency (FE) of rainbow trout fed different levels of dietary nucleotides for 8 weeks (Keyvanshokooh & Tahmasebi-Kohyani, 2012).

Experimental diets (%)	Final weight (g)	Weight gain (%)	Feed efficiency (FE)
0	46 ± 0.7[a]	98 ± 8[a]	0.62 ± 0.21[a]
0.05	46 ± 0.5[a]	99 ± 6[a]	0.73 ± 0.18 [b]
0.1	58 ± 0.4[b]	151 ± 9[b]	0.76 ± 0.24 [b]
0.15	66 ± 0.7[c]	187 ± 7[c]	0.85 ± 0.26 [c]
0.2	67 ± 0.8[c]	192 ± 5[c]	0.95 ± 0.17[d]

Values are mean ± S.E.M. of three replicate groups. Mean values with different superscripts are significantly different from each other (significance level is defined as $P < 0.05$).

Muscles of control and treated groups were subjected to proteome analysis by 2-DE. Using the spot finding protocol of PG200 software, an average of 710 protein spots per gel were observed, with Mr ranging between 10 and 250 kDa and pI between 3.5 and 9.5. Most protein spots were located in the pI range between 5 and 8 (Figure 96) (Keyvanshokooh & Tahmasebi-Kohyani, 2012).

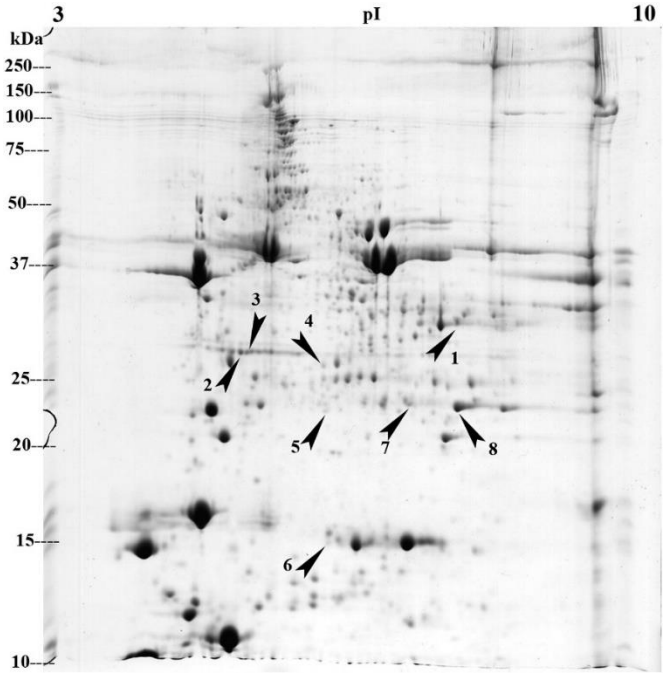

Figure 96. 2-DE map of muscle proteins of rainbow trout (Oncorhynchus mykiss), prepared by linear wide-range immobilized pH gradients (pH 3–10, 17 cm; BioRad, USA) in the first dimension and on 12% SDS-PAGE for the second dimension. Proteins were stained with colloidal Coomassie brilliant blue G-250. Labeled spots indicate proteins with significant altered expression profile after dietary nucleotides treatment (see Table 64) (Keyvanshokooh & Tahmasebi-Kohyani, 2012).

At the end of the feeding trial, fish fed the basal and 0.2% diets were subjected to proteomic analysis. Accordingly, the proteins of the muscle tissues were analyzed using two-dimensional electrophoresis, tryptic enzyme digestion and MALDI-TOF-MS (Keyvanshokooh & Tahmasebi-Kohyani, 2012).

It was found that the dietary NT caused differential expression of the muscle metabolic proteins. These included glyceraldehyde-3-phosphate dehydrogenase, creatine kinase, adenylate kinase,

nucleoside diphosphate kinase, and triosephosphate isomerase. Additionally to metabolic enzymes, troponin-T-1 as a structural protein was found to increase in abundance in the treated fish. Dietary NT caused differential expression of muscle metabolic proteins including glyceraldehyde-3-phosphate dehydrogenase, creatine kinase, adenylate kinase, nucleoside diphosphate kinase A, and triosephosphate isomerase. In addition to metabolic enzymes, troponin-T-1 as a structural protein was found to increase in abundance in the treated fish (Table 65) (Keyvanshokooh & Tahmasebi-Kohyani, 2012).

Table 65. Identification of differentially expressed proteins in the muscle tissue of rainbow trout fed dietary nucleotides (NT) for 8 weeks (Keyvanshokooh & Tahmasebi-Kohyani, 2012).

Spot number	Protein name	Accession number	Ms/Ms score	Organism	Expression	IF[a]	RF[a]	Mean NV	CV (%)
								NT/control	NT/control
1	Glyceraldehyde-3-phosphate dehydrogenase-1	gi|197632425	47	*Salmo salar*	Overexpressed	2.64*		0.127/0.048	15/23
2	Fast myotomal muscle troponin-T-1	gi|197632601	125	*S. salar*	Overexpressed	2.60*		0.138/0.053	8/21
3	Fast myotomal muscle troponin-T-1	gi|197632601	113	*S. salar*	Overexpressed	2.06*		0.066/0.032	20/16
4	Creatine kinase	gi|197632231	96	*S. salar*	Overexpressed	2.52*		0.043/0.017	5/9
5	Adenylate kinase	gi|213511412	107	*S. salar*	Underexpressed		2*	0.013/0.026	23/23
6	Nucleoside diphosphate kinase A	gi|213511196	106	*S. salar*	Overexpressed	1.7*		0.041/0.024	16/13
7	Triosephosphate isomerase 1b	gi|213515400	336	*S. salar*	Underexpressed		1.46*	0.097/0.142	21/10
8	Triosephosphate isomerase 1b	gi|213515400	500	*S. salar*	Overexpressed	1.55*		0.502/0.323	14/17

* $P < 0.05$.
[a] The induction (IF) and repression (RF) factors are the ratios between normalized volumes in treated and control.

This study suggested that the altered expression of both metabolic and structural proteins in fish fed NT could be related to higher growth rate in rainbow trout. These findings provide basic information to understand possible mechanisms of dietary NT contribution to better growth in rainbow trout (Keyvanshokooh & Tahmasebi-Kohyani, 2012).

6.8. Impact of Three Commercial Feed Formulations on Farmed Gilthead Seabream (*Sparus aurata,* L.) Metabolism as Inferred from Liver and Blood Serum Proteomics

This study examined the zootechnical performance of three different commercial feeds and their impact on the liver and serum proteins of gilthead sea bream (*Sparus aurata, L.*) during 12 week feeding trial. The authors specified that feed B was higher in fish-derived lipids and proteins,

whereas, feeds C and A were higher in vegetable components. However, the largest proportion of feed C proteins was represented by pig hemoglobin (see following Figure 97) (Ghisaura et al., 2014).

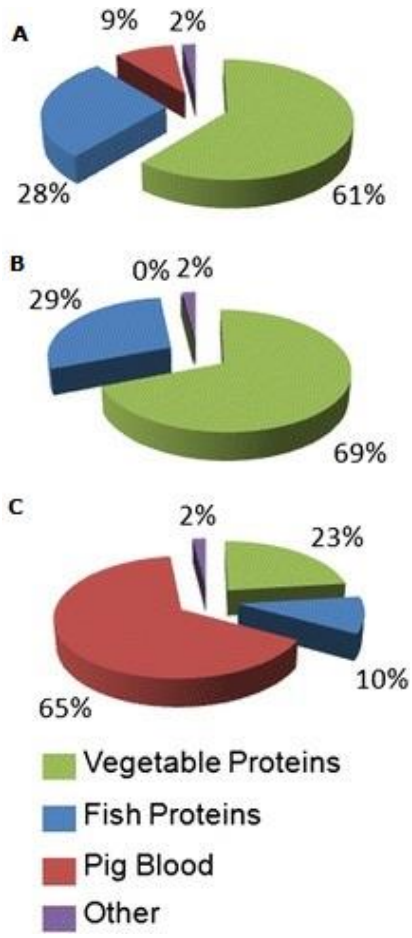

Figure 97. Protein sources in feeds. Pie charts illustrating the distribution of proteins according to their source in the three feeds used for this study and named A, B, and C. Protein sources are classified according to LC-MS/MS protein identification and ontology attributio (Ghisaura et al., 2014).

The biometric measurements have shown that the feeds had significantly different impacts on fish growth, producing a higher average weight gain and a lower liver somatic index in feed B overfeeds A and C, respectively. The following figure indicates that the biometric scale of the three feeds produced differences in growth efficiency and liver somatic index, advantaging Feed B vs

Feeds A and C (Table 66). In addition, the characterization of feeds revealed a higher amount of fish-derived lipids and proteins in Feed B when compared to Feeds A and C (Ghisaura et al., 2014).

Table 66.Biometrical results obtained on gilthead sea breams in the 12 week feeding trial (Ghisaura et al., 2014).

	Feed A	Feed B	Feed C
IW (g)	268.54 ± 27.04	294.82 ± 28.05	276.61 ± 46.14
FW (g)	376.43 ± 45.09[a]	416.01 ± 47.65[b]	373.17 ± 55.28[a]
AWG (g)	107.89 ± 7.71[b]	121.19 ± 5.17[a]	96.56 ± 7.21[b]
LSI (%)	1.00 ± 0.17[a]	0.86 ± 0.11[b]	0.96 ± 0.11[a]

Values are reported as means ± S.E. (number of fish analyzed n = 45/feed for IW, FW, and AWG; n = 9/feed for LSI); a, b, and c indicate statistically different values ($p < 0.05$, Student's t-test). IW: initial weight; FW: final weight; AWG: average weight gain; LSI: liver somatic index.

Thus, in order to assess the variation of serum protein levels following changes in feeding formulations, fish were sampled at T0 and at T12A, T12B, and T12C. Proteins from all samples were then compared for protein levels by 2D DIGE. As a result, 14, 13 and 8 differential spots were detected at T12A, T12B, and T12C, when compared to T0, respectively. The three feeds, named A, B, and C, were subjected to lipid and protein characterization by proteomics analysis using 2D DIGE and MS/MS analysis of liver tissue and of the ingenuity pathways analysis (IPA) highlighted differential changes in proteins involved in key metabolic pathways of liver, spanning carbohydrate, lipid, protein, and oxidative metabolism (Ghisaura et al., 2014).

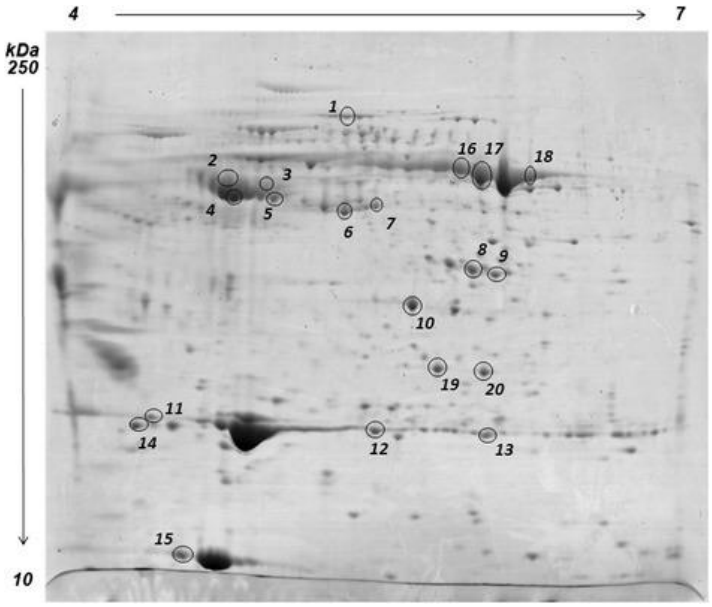

Figure 98. Representative 2D PAGE of gilthead sea bream serum proteins in the 4 to 7 pH range. Spots showing a differential abundance in T12A and T12B and a valid protein identification are circled in the map, and information on their changes and identity is reported in Table 67 (Ghisaura et al., 2014).

The proteomic analysis of liver and serum of gilthead sea breams carried out at the end of the feeding trial highlighted a higher divergence of T12B from T12A and T12C, in agreement with the biometric observations. In addition, T12C fish diverged less from T0. Concerning this latter observation, it should be considered that all sea breams had been administered Feed C during the acclimation period preceding the trial, and therefore this group did probably undergo lesser metabolic changes when compared to T12A and T12B. As a further observation, T12A behavior was closer to T12C than to T12B, both in terms of growth and proteomic results. This is also consistent with the feed formulation, which was more similar for Feeds A and C in terms of lipid and protein composition (Ghisaura et al., 2014).

Table 67. Protein spots showing statistically significant differences in expression between T12A and T12B (Ghisaura et al., 2014).

Spot	Av. ratio T12A/T12B	Protein name
1	1.59	Complement component c3
2	3.14	Alpha 1 antitrypsin
		Warm temperature acclimation-related 65 kDa protein
3	1.51	Warm temperature acclimation-related 65 kDa protein
4	2.96	Warm temperature acclimation-related 65 kDa protein
		Alpha 1 antitrypsin
5	1.5	Warm temperature acclimation-related 65 kDa protein
		Alpha 1 antitrypsin
6	1.87	Alpha 1 antitrypsin
7	3.86	Alpha 1 antitrypsin
8	−1.86	Transferrin (fragments)
9	−2.25	Transferrin (fragments)
10	−2.72	Fibrinogen beta chain
11	1.93	Apolipoprotein A-1
12	4.73	Apolipoprotein A-1
13	4.19	Apolipoprotein A-1
14	2.54	Apolipoprotein A-IV4
15	−3.3	14 kDa apolipoprotein
16	1.57	Transferrin
17	1.57	Transferrin
18	2.49	Transferrin
19	−1.77	F-type lectin 2
20	2.14	F-type lectin 2

Spots are numbered according to Figure 98.

Similar changes in lipid metabolism were observed from T0 to T12 in all sea bream groups, although with few interesting differences induced by the three feed formulations investigated in this study. In liver, all three feeds induced a consistent and concerted overexpression of apolipoprotein A1 (APOA1) and 14 kDa apolipoprotein (apo-14), which is the fish homologue of apolipoprotein A2 (APOA2) (Choudhury et al., 2009). This was also supported by the increase seen in serum apolipoprotein. The following Table 6 indicate the protein identities and their respective abundance changes (Ghisaura et al., 2014).

This study presents a comprehensive evaluation of the impact of three commercial feeds, designated as A, B, and C, on gilthead sea bream growth and metabolism, carried out by assessing protein abundance changes in liver tissue and blood serum at the end of a 12 week feeding trial (T0 vs T12A, T12B, and T12C, respectively). In addition, serum proteomics revealed interesting changes in apolipoproteins, transferrin, warm temperature acclimation-related 65 kDa protein (Wap65), fibrinogen, F-type lectin, and alpha-1-antitrypsin (Ghisaura et al., 2014).

In this work, the MS/MS identification of differential spots in liver and serum maps provided useful insights into the influence of the different feed formulation on the lipid, carbohydrate, aminoacid and small molecule pathways, as well as on their impact on oxidative stress. In general, liver proteomics can help elucidate the pathways affected by feed substitutions and offers hints to improve quality, AWG and production yield. On the other hand, serum proteomics can become a useful tool for the rapid monitoring of changes occurring in metabolism along farming. In addition, the information gathered can be used for valorization of high quality products (Ghisaura et al., 2014).

In conclusion, this study highlights the contribution of proteomics for understanding and improving the metabolic compatibility of feeds for marine aquaculture, and opens new perspectives for its monitoring with serological tests (Ghisaura et al., 2014).

6.9. **Differential Proteome Profile of Skin Mucus of Gilthead Seabream (*Sparus aurata* L) after Probiotic Intake and/or Overcrowding Stress**

The Gilthead seabream (*Sparus aurata* L.) is the major cultured fish species in the Mediterranean area. It is well known that aquaculture high density stocking causes stress and increases the impact of diseases leading to economic losses. It has been proposed that feed probiotics could represent a solution to prevent diseases through several mechanisms such as

improving the immune status and/or mucosal microbiota or competing with pathogens (Cordero et al., 2016b).

Recently, the probiotic *Shewanella putrefaciens*, (Pdp11), was isolated from the skin of healthy gilthead seabream. In this study, the authors have studied the possibility of using the skin mucus proteome of the Gilthead seabream (*Sparus aurata* L as a dietary probiotic Pdp11 intake, for fish maintained under normal or overcrowding conditions (Cordero et al., 2016b).

For this reason, the authors studied analysis the differentially expressed proteins present in skin mucus after probiotic feeding under overcrowding stress, This study was performed by proteomic analysis using 2-DE followed by LC–MS/MS. They also evaluated the changes of transcript levels of four the following four molecules: c3, nkefb, nccrp1 and lyz present in skin of gilthead seabream. In addition, this effort will contribute to better understand the changes in mucosal immunity The 2-DE showed a range of 31-452 spots well resolved. good resolution for comparatives studies (Cordero et al., 2016b).

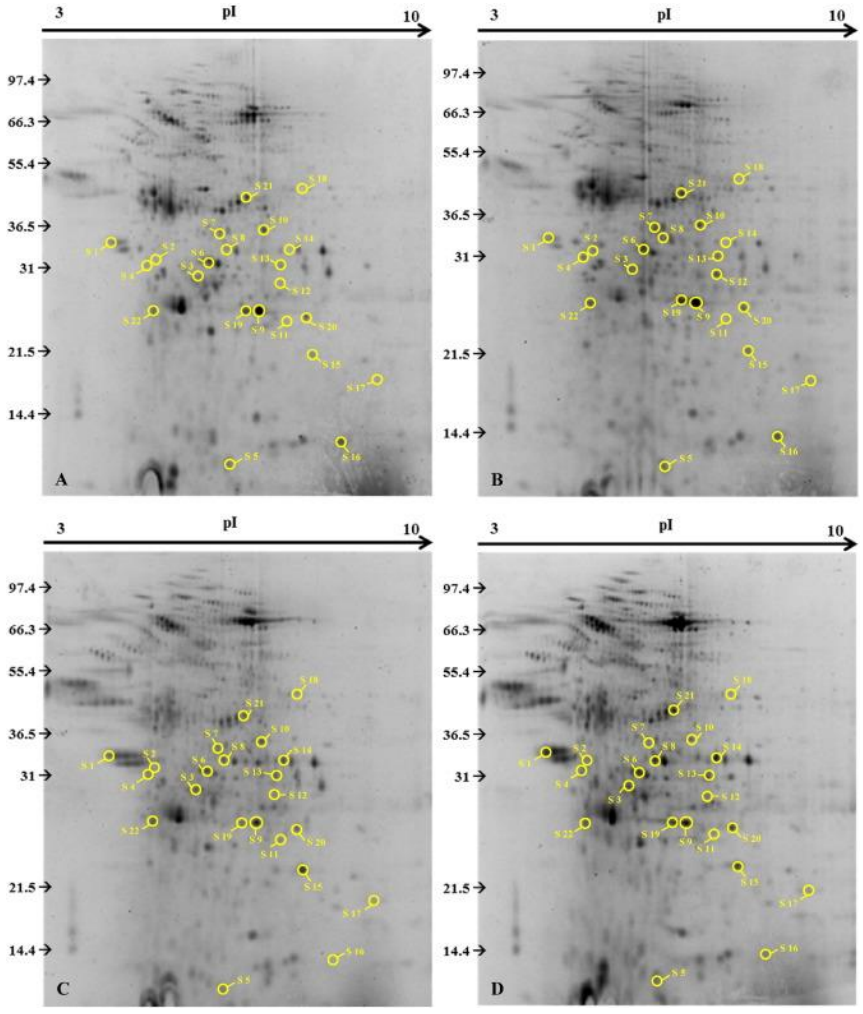

Figure 99. Representative 2-DE gels of skin mucus of S. aurata for each experimental group: commercial diet (A), probiotic diet (B), overcrowding stress (C) and overcrowding stress and probiotic diet (D). All the four gels were generated from samples at 30 days of treatment in triplicates. Skin mucus proteins were isoelectrically focused on 17 cm IPG strips (pI 3–10) and subjected to 12.5% SDS-PAGE. The 2DE gels were stained with SYPRO® Ruby protein gel stain and the spots identified in (A–D) were annotated using the data from LC–MS/MS. The spot numbers represented in gels correspond to the protein identities mentioned in Table 68 (Cordero et al., 2016b) .

This was followed by LC–ESI-MS/MS analysis which provided good resolution for comparatives studies and produced an exhaustive analysis, which allowed adjusting and optimizing the quantification of spots, and discarding spots that were not consistent, was carried out (See following Table 68) (Cordero et al., 2016b).

Table 68. Details of the differentially expressed protein spots in skin mucus of S. aurata after dietary probiotic administration and/or overcrowding stress (Cordero et al., 2016b).

SN[a]	Protein name	Organism AN[b]	pI/MW[c]	S/C[d]	M_p/U_p[e]	Peptide sequence and e-value[f]
S1	C-type lectin	*S. aurata* CB177017	7.2/28.8	59/3	1/1	**CFFMTPDK** ($4.9*10^{-2}$)
S2	Leukocyte elastase inhibitor	*S. aurata* FM146914	8.8/28.3	80/12	2/2	**ADAPYALSVANR** ($7.7*10^{-3}$) **DVQDDVHSSFAQLLGELNK** ($5.2*10^{2}$)
S3	Nonspecific cytotoxic cell receptor protein-1	*S. aurata* AAT66406	5.0/26.6	59/12	2/2	**DTPPPEPQLSDVPR** (3.2*10) **EVSYVFSGYGPGVR** (1.2*10)
S4	Apolipoprotein A1	*S. aurata* O42175	5.2/29.6	50/13	3/3	**IQANVEETK** ($1.2*10^{2}$) **TLLTPIYNDYK** (1.7*10) **AVNQLDDPQYAEFK** (3.0*10)
S5	Profilin	*S. aurata* FM146227	9.6/21.3	337/46	7/7	**EGGIWSASDMFK** (1.8) **GITPDEIK** (9.8*10) **ALYAGTEGPGNGSIVNLAGIK** ($1.7*10^{-4}$) **VITLVTMK** (1.3*10) **NTVMSESSPLVIGFFK** ($4.3*10^{-6}$) **TGLVIGLGKPGFR** (3.5*10) **SVGVTVESTTSQLK** (5.8)
S6	Inositol monophosphate	*Oreochromis mossambicus* AFY10067	5.3/31.2	284/30	7/1	**SSTVDLVTK** ($2.9*10^{-2}$) EEFGEGTHCFIGEESVAK ($1.8*10^{-4}$) EAGGILLDVDGGPFDLMSR ($1.5*10^{-3}$) IFSTMQK (5.2) IIIGSLKEEFGEGTHCFIGEESVAK($1.8*10^{2}$) ELEFGVVYSCLEDK ($1.3*10^{-2}$) SIIISEHGTDR (9.0)
S7	Beta actin	*O. mossambicus* P68143	5.3/42.1	176/15	5/5	**SYELPDGQVITIGNER** ($1.5*10^{-9}$) **QEYDESGPSIVHR** ($2.1*10^{-3}$) **EITALAPSTMK** ($3.4*10^{-4}$) **GYSFTTTAER** ($6.9*10^{-4}$) **DLTDYLMK** ($1.5*10^{-2}$)
S8	F-type lectin	*Oplegnathus fasciatus* BAK38714	5.7/31.0	144/8	2/2	**APTGENLALQGK** ($5*10^{-7}$) **IGDSLENNGNNNPR** ($1.4*10^{-2}$)

S9	Triose phosphate isomerase A	*Danio rerio* Q1MTI4	4.9/29.2	33/5	1/1	**GAFTGEISPAMIK** ($3.9*10^{-3}$)
S10	Predicted: aldose reductase-like	*Haplochromis burtoni* XP_005915666	6.2/36.0	201/13	6/5	**AAISAGYR** (4.6) **TILGFNR** (1.8) **TPAQVLIR** ($2.8*10^{-3}$) **AIGISNFNK** ($9.7*10^{-1}$) **KTPAQVLIR** (8.1) REDLFIVSK ($1.1*10^{-1}$)
S11	Peroxiredoxin 2	*Oncorhynchus mykiss* Q91191	7.0/22.3	46/5	1/1	**QITINDLPVGR** ($1.9*10^{-4}$)
S12	Complement c3	*S. aurata* ADM13620	8.1/187	138/2	5/5	**LPYSAVR** (2.8) **SVPFIIIPMK** (3.0*10) **DSSLNDGIMR** ($1.1*10^{-1}$) **VVPQGVLIK** ($3.5*10^{-1}$) **IVTLDPANK** (2.4*10)
S13	Complement c3	*S. aurata* ADM13620	8.1/187	110/1	3/3	**DSSLNDGIMR** ($2.3*10^{-2}$) **VVPQGVLIK** (5.0) **IVTLDPANK** ($1.1*10^{-1}$)
S14	Keratin, type I cytoskeletal 50 kDa	*Carassius auratus* Q90303	5.1/49.7	34/6	2/2	**SQMTGTVNVEVDAAPQEDLSR** (2.4) **ATMQNLNDR** ($3.0*10^{-3}$)
S15	Lysozyme	*S. aurata* CAO78618	6.9/20.3	217/31	4/4	**SDGLGYTGVK** ($1.3*10^{-2}$) **YGIDPAIIAAIISR** ($1.6*10^{-7}$) **GGIAAYNFGVK** ($2.8*10^{-1}$) **NVQTVAGVDVGTNHGDYSNDVVAR** ($9.1*10^{-1}$)
S16	ADP-ribosylation factor GTPase-activating protein	*Carassius auratus* AM930069	9.4/23.6	60/9	1/1	**GMDTAITKQISGADGGASR** ($2.0*10^{-2}$)
S17	Glutathione S-transferase	*S. aurata* AAQ56182	8.5/24.8	120/11	3/3	**LAAYYNR** (1.8) **MWEGYLQK** (8.0) **MFEGLTLQQK** ($4.5*10^{-4}$)
S18	NADP-dependent isocitrate dehydrogenase	*S. aurata* AGU38793	7.2/38.1	79/10	3/3	**AGSVVEMQGDEMTR** (1.2) **ATDFVVPGPGK** ($5.2*10^{-1}$) **LIDDMVAQAMK** ($1.4*10^{-2}$)
S19	PREDICTED: peroxiredoxin-6-like	*Astyanax mexicanus* XP_007259536	5.8/24.8	59/4	1/1	**VIDSLQLTAKK** ($1.3*10^{-3}$)
S20	Glutathione S-transferase	*S. aurata* AFV39802	6.9/25.5	286/31	6/4	**FTGILGDFR** ($4.1*10^{-2}$) **MTEIPAVNR** ($3.4*10^{-2}$) **TVMEVFDIK** ($3.5*10^{-2}$) **LLSDGDLMFQQVPMVEIDGMK** ($2.6*10^{-1}$) AILNYIAEK (2.5) VLSGQIYLVGGK ($4.5*10^{-6}$)
S21	Beta actin	*Morone saxatilis* AAA53024	5.1/31.7	92/15	3/3	**VAPEEHPVLLTEAPLNPK** ($1.6*10^{-2}$) **GYSFTTTAER** ($3.3*10^{-1}$) **SYELPDGQVITIGNER** ($4.2*10^{-2}$)
S22	14-3-3 protein	*S. aurata* AM957903	4.6/26.9	114/9	2/2	**DSTLIMQLLR** ($6.7*10^{-1}$) **EVLGLLDDYLIPK** ($2.3*10^{-3}$)

[a] Spot number.
[b] Accession number according to NCBI and SwissProt databases.
[c] Theoretical isoelectric point and molecular weight (kDa).
[d] Total score and coverage (%).
[e] Total matched peptides (Mp)/total unique peptides (Up).
[f] Unique peptides are in bold. Expect value (e-value) is noted for each peptide sequence.

This present study shows several differentially expressed proteins (through 22 identified spots) in the skin mucus from gilthead seabream specimens (Table 68 and 69): fed with commercial diet and non-stressed (control, Figure 99A), fed with probiotic and non-stressed (Figure 99B), fed commercial diet and stressed by overcrowding (Figure 99c), fed probiotic diet and stressed by overcrowding (Figure 99D). The intra-group variability of differentially expressed spots was in a range between 0.5% and 9.3% (Table 69) (Cordero et al., 2016b).

Table 69. List of proteins that are differentially expressed in skin mucus of S. aurata *after dietary probiotic administration and/or overcrowding stress for 15 and 30 days. ↑ and ↓ indicate over- and under-expression of the proteins at p < 0.01, respectively. Coefficient of variation (CV) in percentage (%) from different pools (n = 3) is represented in brackets (Cordero et al., 2016b).*

pot	Protein name	Fold change relative to control group + CV intra-groups		
		Probiotic	Overcrowding	Probiotic + overcrowding
Fifteen days				
S12	Complement c3 (C3)	↑ 1.95 (2.8%)		↑ 1.6 (3.9%)
S19	Peroxiredoxin 6-like (PRDX6)		↓ 0.63 (1.8%)	
S20	Glutathione S-transferase (GST)	↑ 1.97 (6.3%)		↑ 4.20 (3.3%)
S21	Beta-actin (ACTB)		↓ 0.56 (2.1%)	
S22	14–3-3 (YWHAB)	↑ 1.58 (5.2%)	↓ 0.55 (3.3%)	↓ 0.38 (1.7%)
Thirty days				
S1	C-type lectin (CLEC)		↑ 1.58 (3.6%)	↑ 2.63 (3.2%)
S2	Leucocyte elastase inhibitor (LEI)	↑ 2.18 (4.1%)	↓ 0.64 (1.4%)	↑ 2.36 (1.9%)
S3	Nonspecific cytotoxic cell receptor protein 1 (NCCRP-1)	↑ 3.27 (0.8%)	↑ 2.56 (5.8%)	↑ 2.05 (2.8%)
S4	Apolipoprotein A-1 (APOA1)	↑ 2.31 (1.6%)		↑ 1.67 (2.5%)
S5	Profilin (PFN)			↑ 1.85 (8.2%)
S6	Inositol monophosphate (IMPA)		↓ 0.39 (3.7%)	↓ 0.51 (4.9%)
S7	Actin beta (ACTB)	↑ 1.95 (7.2%)		
S8	F-type lectin (FBL)	↑ 1.54 (4.3%)	↑ 1.59 (2.1%)	↑ 2.79 (3.6%)
S9	Triose phosphate isomerase A (TPIA)		↓ 0.43 (1.9%)	↓ 0.57 (3.4%)
S10	Aldose reductase-like (AR)			↓ 0.41 (0.5%)
S11	Natural killer cell enhancing factor b (NKEF2)		↑ 9.69 (3.9%)	↑ 4.79 (5.6%)
S13	Complement c3 (C3)	↑ 1.74 (2.3%)	↑ 1.52 (3.5%)	↑ 1.64 (2.5%)
S14	Keratin, type I cytoskeletal 50 kDa (KRT1)		↑ 3.40 (5.0%)	↑ 4.31 (4.8%)
S15	Lysozyme (LYZ)	↑ 1.27 (6.1%)	↑ 4.58 (2.3%)	↑ 2.80 (1.8%)
S16	ADP-ribosylation factor GTPase-activating protein (ARFGAP)	↑ 1.39 (5.5%)	↓ 0.01 (2.7%)	↓ 0.14 (9.3%)
S17	Glutathione S-transferase (GST)		↑ 1.54 (3.1%)	↑ 1.58 (4.2%)
S18	NADP-dependent isocitrate dehydrogenase (IDH)		↑ 5.12 (4.4%)	↑ 5.20 (3.9%)

As a result, a series of differentially expressed proteins were identified. These results showed that some proteins were differentially expressed. This was true for the proteins especially involved in immune processes, such as lysozyme, complement C3, natural killer cell enhancing factor and nonspecific cytotoxic cell receptor protein 1. Their transcript profiles were also studied by qPCR. Moreover, a consistency between lysozyme protein levels in the mucus and lysozyme mRNA levels in the skin was found. It has been concluded that further research was necessary to unravel the implications of the mucosal skin immunity on fish welfare and disease (Cordero et al., 2016b).

In conclusion, the present work allowed the measuring of the proteomic changes, which were taking place in the skin mucus of stressed and non-stressed gilthead seabream after Pdp11 probiotic intake. The study contributes to improving the knowledge on skin mucosal immunology of this relevant farmed fish species (Cordero et al., 2016b).

6.10. Effect of Phosphorus Supplementation on Cell Viability, Anti-Oxidative Capacity and Comparative Proteomic Profiles of Puffer Fish (*Takifugu obscurus*) Under Low Temperature Stress

Phosphorus (P) is an essential nutrient for fish, and its concentration is low in both freshwater and seawater. P has a wide range of functions in animal metabolism. It has been reported that P deficiency signs of fish include poor growth, reduced feed efficiency,
poor bone mineralization, skeletal deformities, low ash and high lipid content in the whole body(Lall, 2002). Nevertheless, the roles of dietary P on cell structure and energy production have not been reported in fish. Also, phospholipids are the main structural components of all cellular membranes and all living cells also use phosphate to transport cellular energy in the form of adenosine triphosphate (ATP) (Ye et al., 2016).

The obscure puffer, *Takifugu obscurus* (Abe 1949), is an anadromous species and one of the newest cultured fish species in South China. The annual production of the fish has continued to rise owing to the large body size, rapid growth, and high market value (Ye et al., 2016).
Nevertheless, the information of nutrition and the response of puffer fish under environmental stress is very limited. It is important to know that the low-temperature challenge is the most serious threat for aquaculture, resulting in immune defence suppression and disease resistance (Ye et al., 2016) .

In the present study, the authors investigated the effects of dietary P supplements on blood cell counts, respiratory burst activity, antioxidant enzyme activities and plasma Malondialdehyde (MDA) level of puffer fish under low-temperature stress. They also analyzed by using the proteomics approach the differentially expressed proteins of puffer fish between P deficient and adequate groups. In addition, the authors investigated the effects of dietary P supplements. For this reason, six diets were supplemented with graded levels (0, 0.2, 0.4, 0.6, 0.8, 1.2%) of P from mono-calcium phosphate. The analyzed total P contents of the six diets were 0.40, 0.60, 0.81, 0.98, 1.19 and 1.55% respectively. Additionally, differentially expressed proteins of puffer fish between P deficient and adequate group were investigated through a proteomic approach (Ye et al., 2016).

The isolated liver tissues of the obscure puffer were homogenized and the protein was quantified. The differentially expressed protein spots were excised manually from the 2-DE gels and protein was digested and subjected to MALDI-TOF-MS analysis (Ye et al., 2016).

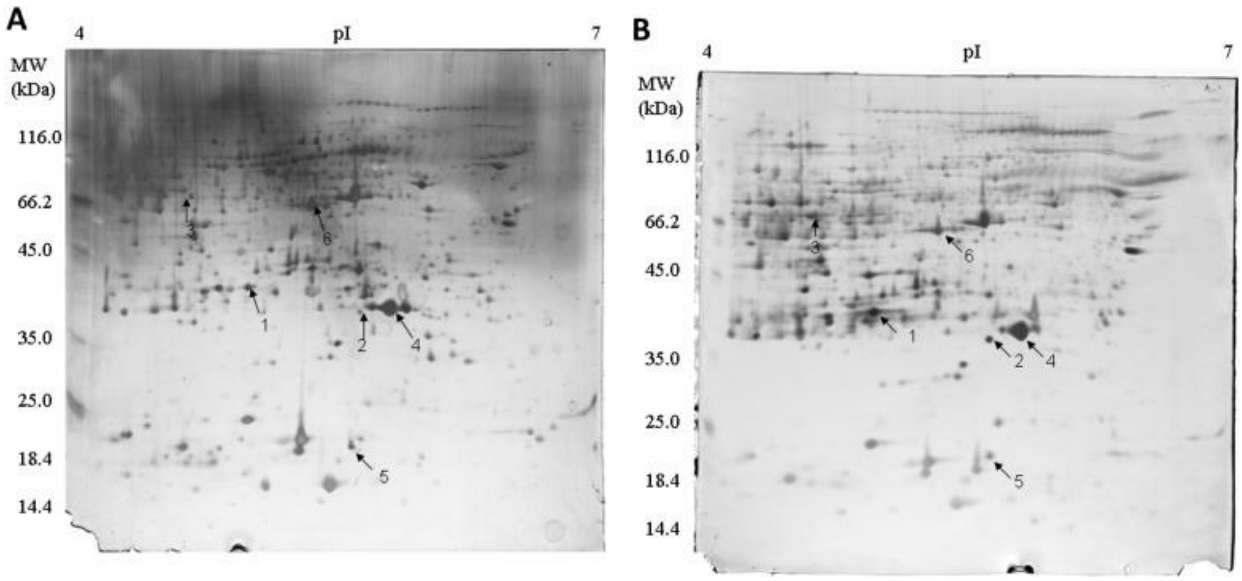

Figure 100. Silver-stained 2-D acrylamide gel of proteins in liver of puffer fish exposed to 12 ± 2 °C for 12 h. Dietary P deficient group (A); and dietary P adequate group(B).Differentially expressed proteins are labeled with numbers, which correspond to the numbers present in Table 70 (Ye et al., 2016).

The proteomic approach was used to investigate the series of altered proteins between P deficient (P=0) and adequate (P=0.8%) groups in liver of puffer fish during cold stress treatment. MALDI-TOF-MS analysis revealed that adequate P diet significantly up-regulated three energy

generation related enzymes (ribose-5-phosphate isomerase-like 5, ribulose-phosphate 3-epimerase-like and alpha-enolase-like isoform 2) and two lipid transport proteins (ApoA-I and FABP), and down-regulated an intermediate filament protein (keratin type I cytoskeletal 13-like) of puffer fish during cold stress (Ye et al., 2016).

Table 70. The altered proteins identified by MALDI-TOF/TOF MS in the liver of puffer fish fed P deficient and adequate diet under low temperature stress (Ye et al., 2016).

Spot number	MW(Kda)/PI	Sequence coverage(%)/score	Peptides matched	Accession number/species	Homologous protein
Significantly up-regulated spots by adequate P supplement					
1	17.24/7.85	16/147	1	gi | 410926779/*Takifugu rubripes*	Ribose-5-phosphate isomerase-like5
2	25.10/5.32	31/426	4	gi | 410896754/*Takifugu rubripes*	Ribulose-phosphate 3-epimerase-like
3	47.46/6.15	19/567	5	gi | 410899356/*Takifugu rubripes*	Alpha-enolase-like isoform 2
4	29.57/5.39	40/186	2	gi | 118344628/*Takifugu rubripes*	Apolipoprotein A-I precursor
5	14.88/6.59	46/515	6	gi | 410898184/*Takifugu rubripes*	Fatty acid-binding protein
Significantly down-regulated spots by adequate P supplement					
6	45.91/5.46	26/489	6	gi | 410918145/*Takifugu rubripes*	Keratin, type I cytoskeletal 13-like

This study results indicated that fish-fed diets supplemented with 0 and 0.2% P had significantly lower weight gain, feed efficiency and feed intake than the fish-fed diets supplemented with 0.6, 0.8 and 1.2% P (Ye et al., 2016).

After the 8-week feeding trial, the puffer fish were exposed to acute low-temperature challenge (12 ± 2 °C) and sampled at different time points (0, 3, 6, 12, 24, 48 h). The blood cell numbers were significantly higher in fish-fed diets supplemented with 0.6, 0.8 and 1.2% P than in fish-fed diets without P supplement at 6, 12, 24 and 48 h. The highest rate of viable blood cells was observed in fish-fed diets supplemented with 0.6 or 0.8% P at 3 and 6 h (Ye et al., 2016).

Furthermore, the respiratory burst activities after 6, 24 and 48 h tended to decrease with increasing dietary P supplement up to 0.6, 1.2 or 0.8%, respectively. At 12, 24 and 48 h, the plasma CAT activity increased with increasing dietary P supplement up to 0.8%. The highest plasma SOD activity was in fish fed diets supplemented with 0.6 and 0.8% P at 6 h (Ye et al., 2016).

At 3, 6, 12, 24 and 48 h, liver GPx activity increased significantly with the increase of dietary P supplement, and GPx activity in the 0.8% feed group achieved the highest. Fish fed diet

without P supplement showed the highest plasma MDA level at 3 h and 6 h, highest liver MDA level at 12 h and 24 h (Ye et al., 2016).

In conclusion, this study showed that the dietary P supplement could improve cell viability, anti-oxidative capacity, energy generation and lipid transportation of puffer fish under cold stress. Three energy generation related enzymes (ribose-5-phosphate isomerase-like 5, ribulose-phosphate 3-epimerase-like and alpha-enolase-like isoform2) and two lipid transport proteins (ApoA-I and FABP) were significantly up-regulated by adequate dietary P supplement. When fish was fed a P deficient diet, an intermediate filament protein (keratin type I cytoskeletal 13-like) of puffer fish was up-regulated, which may be related to P-deficient induced hepatocellular injury. These results clearly indicated that dietary P supplement could improve cell viability, anti-oxidative capacity, energy generation and lipid transportation of puffer fish under cold stress (Ye et al., 2016).

6.11. **Proteomic Sensitivity to Dietary Manipulations in Rainbow Trout**

As already mentioned before, the changes in dietary protein sources due to the substitution of fish meal by other protein sources are responsible for some metabolic consequences.

In this study, the proteomics approach was used to study the protein profiles of livers of rainbow trout that have been fed two diets containing different proportions of plant ingredients. Thus, both diets control (C) and soy (S) contained fish meal and plant ingredients and synthetic amino acids. However, diet S had a greater proportion of soybean meal. A feeding trial was performed for 12 weeks at the end of which growth and protein metabolism parameters were measured (Table 71) (Martin, Vilhelmsson, Médale, et al., 2003).

Table 71. Composition of the experimental diets used for rearing rainbow trout (Martin, Vilhelmsson, Médale, et al., 2003).

Ingredients (g/kg)	Diet S	Diet C
Fish meal (CP 70%)	389.9	316.4
Wheat gluten (Amylum, Holland)	71.4	0
Extruded whole wheat	135.7	71.8
Extruded peas (Aquatex, France)	215.1	56.8
Soybean meal (CP 42%)	25.3	331.3
Fish oil	101.6	109.5
Binder, Na alginate	10.0	10.0
Mineral mix[a]	10.0	10.0
Vitamin mix[a]	10.0	10.0
$CaHPO_4.2H_2O$ (18%)	10.9	16.1
l-amino acid mixture	20.1	68.2
Proximate composition		

Dry matter (DM, %)	90.5	92.2
Proteins (% DM)	46.3	45.1
Lipids (% DM)	16.4	15.6
Gross energy (kJ/g DM)	22.1	22.4

CP: crude protein.
[a] According to Ref. (Council, 1993).

It was observed that the protein growth rates were not different in fish fed different diets; however, the authors found that the protein consumption and protein synthesis rates were higher in the fish fed the diet S. Moreover. fish fed diet S had lower efficiency of retention of the synthesized protein. Furthermore, it was established that ammonia excretion was increased as well as the activities of hepatic glutamate dehydrogenase and aspartate amino transferase (ASAT) (Martin, Vilhelmsson, Médale, et al., 2003).

No differences were found in free amino acid pools in either liver or muscle between diets. The proteomic approach used consisted of protein extraction form the two-dimensional electrophoresis, coupled with gel image analysis, followed by identification of hundreds of protein by MS/MS (Martin, Vilhelmsson, Médale, et al., 2003).

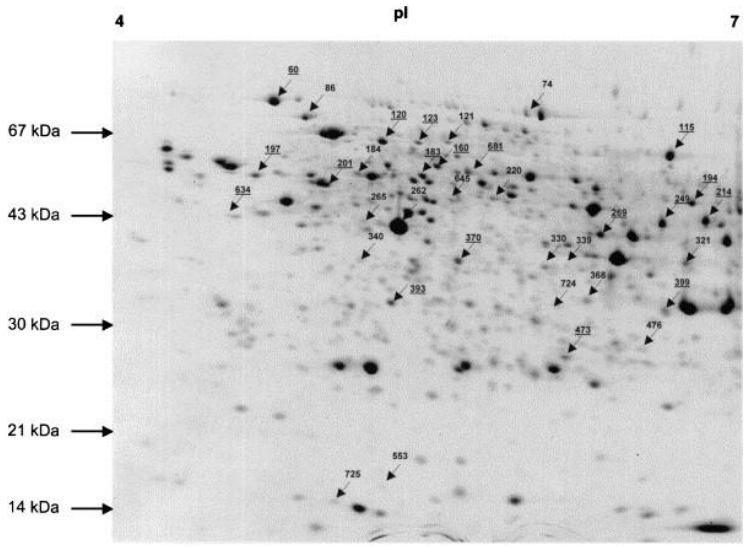

Figure 101. Two-dimensional gel of rainbow trout liver proteins (fish S3). A total liver protein extract was separated by charge between pI 4 and 7, second dimension was by size on a gradient 10–15% gel. The proteins were located by staining with colloidal coomassie blue G250. Proteins marked by arrows were found to be differentially expressed as a result of dietary manipulation, the corresponding number is the spot reference number. Underlined protein numbers were positively identified by trypsin digest fingerprinting (Martin, Vilhelmsson, Médale, et al., 2003).

During this study, around. 800 liver proteins were analyzed for expression pattern, of which 33 were found to be differentially expressed between diets C and S. Also, seventeen proteins were positively identified after database searching. Proteins were identified from diverse metabolic pathways, demonstrating the complex nature of gene expression responses to dietary manipulation revealed by proteomic characterization (Supplementary Table S15) (Martin, Vilhelmsson, Médale, et al., 2003).

6.12. Dietary Creatine Supplementation in Gilthead Seabream (*Sparus aurata*): Comparative Proteomics Analysis on Fish Allergens, Muscle Quality, and Liver

The quality of fish flesh hinge on the skeletal muscle's energetic state. Delaying the energy depletion, through diets supplementation contributes to the preservation of muscle's quality traits and reduce the modulation of fish allergens. Needless to repeat that one of the major food allergens which represent a serious public health problem worldwide is parvalbumins (Schrama et al., 2018).

In this study, the authors attempted to produce a low allergenic farmed fish, with improved muscle quality under controlled artificial conditions, by supplementing a commercial fish diet with different creatine percentages. The supplementation of the fish diets with specific nutrients was aimed at reducing the expression of parvalbumin. Accordingly, the effects of these supplemented diets on fish growth, physiological stress, fish muscle status and parvalbumin modulation, were investigated (Schrama et al., 2018, Table 72).

Data from zootechnical parameters were used to evaluate fish growth, food conversion ratios and hepatosomatic index. Physiological stress responses were assessed by measuring cortisol releases and muscle quality analyzed by *rigor mortis* and pH. Parvalbumin, creatine, and glycogen concentrations in muscle were also determined (Schrama et al., 2018, Table 72).

Table 72. Fish performance parameters (Schrama et al., 2018) .

Diet	IBW (g fish^{-1})	FBW (g fish^{-1})	%IBW/day Weight Gain[a]	%/day SGR[b]	TGC[c] (10^{-3} g$^{1/3}$°C^{-1} day^{-1})	FCR[d]	FE[e]
Ctrl	172 ± 3	278 ± 3	0.89 ± 0.01	0.69 ± 0.01	0.20 ± 0.001	1.66 ± 0.03	0.60 ± 0.01
Creatine2	171 ± 2	278 ± 4	0.91 ± 0.05	0.71 ± 0.03	0.20 ± 0.009	1.63 ± 0.10	0.61 ± 0.04
Creatine5	172 ± 2	285 ± 10	0.95 ± 0.06	0.73 ± 0.04	0.21 ± 0.012	1.58 ± 0.07	0.64 ± 0.03
Creatine8	175 ± 1	286 ± 12	0.91 ± 0.09	0.71 ± 0.06	0.21 ± 0.018	1.66 ± 0.08	0.60 ± 0.03

Table with initial body weight (IBW), final body weight (FBW), weight gain per day, specific growth rate (SGR) per day, thermal growth coefficient (TGC), feed conversion rate (FCR) and feed efficiency (FE) calculated per treatment (n = 72) at the end of the trial (69 days). Values are expressed as mean ± standard deviation. Statistics by ANOVA show no significant differences ($p > 0.05$).

[a]Weight gain per day, calculated as $[(BM_f BM_i) * 100]/(BM_i * t_f)$, where BM_f and BM_i are the final and initial biomass, respectively, and t_f are the days of the trial.

[b]Specific growth rate, calculated as SGR (% per day) = $100 * [(\text{Ln (FBW)}–\text{Ln (IBW)}]/t_f)$, where FBW and IBW are the final and initial fish body weight, respectively, and t_f are the days of the trial.

[c]Thermal growth coefficient, calculated as TGC (10^{-3} g$^{1/3}$ °C^{-1} day^{-1}) = $[(\sqrt[3]{\text{FBW}}–\sqrt[3]{\text{IBW}})/(T \times t)] \times 1{,}000$, where FBW and IBW are the final and initial fish body weight, respectively, T is the mean temperature and t are total days of the trial.

[d]Feed conversion ratio, calculated as FCR = $FC/(BM_f–BM_i)$, where FC is the feed consumption and BM_f and BM_i are the final and initial biomass, respectively.

[e]Feed efficiency, calculated as FE = (BM_f–BM_i)/FC, where BM_f and BM_i are the final and initial biomass and FC is the feed consumption.

Comparative proteomics was used to look into changes in muscle and liver tissues at protein level. The results obtained for this study suggested that the supplementation of commercial fish diets with creatine does not affect farmed fish productivity parameters, or either muscle quality (Schrama et al., 2018).

As well, the effect of higher concentrations of creatine supplementation revealed a minor influence on the fish physiological welfare. Differences at the proteome level were detected among fish fed with different diets. Differential muscle proteins expressions were identified as tropomyosins, beta enolase, and creatine kinase among others, whether in liver several proteins involved in the immune system, cellular processes, stress, and inflammation response were modulated. Regarding parvalbumin modulation, the tested creatine percentages added to the commercial diet had also no effect in the expression of this protein (Schrama et al., 2018).

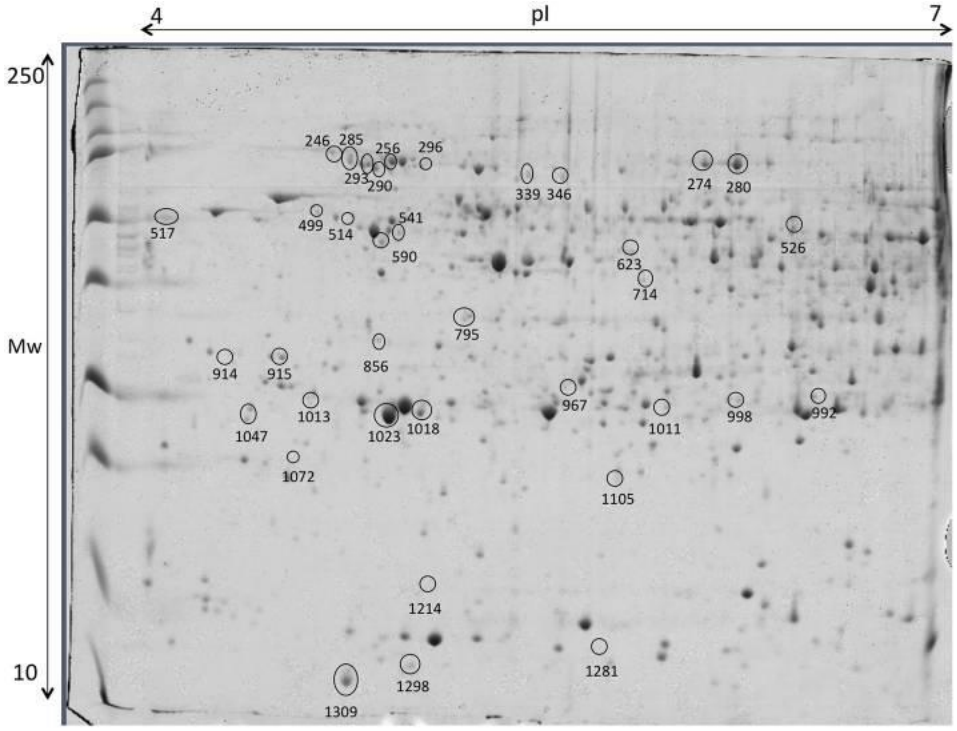

Figure 102. Representative 2-DGE gel of liver of gilthead seabream in a pH range of 4–7 on a 12.5% polyacrylamide gel. Protein identifications of significantly different spots (one-way ANOVA and post-hoc Tukey $p < 0.05$) are shown in SupplementaryTable S16.

In conclusion, the use of proteomics tools showed to be sensitive to infer about changes of the underlying molecular mechanisms regarding fish responses to external stimulus, providing a holistic and unbiased view on fish allergens and muscle quality (Schrama et al., 2018).

6.13. Effects of Genotype and Dietary Fish Oil Replacement with Vegetable Oil on the Intestinal Transcriptome and Proteome of Atlantic Salmon (*Salmo salar*)

Expansion of the aquaculture ventures requires alternative feeds and breeding strategies to reduce fish diet dependency on fish oil (FO) and improved utilization of dietary vegetable oil (VO) (S. Morais et al., 2012).

Despite the central role of intestine in maintaining body homeostasis and health, its molecular response to replacement of dietary FO by VO has been little investigated. The present study employed transcriptomic and proteomic analyses to study effects of dietary VO of two family groups of Atlantic salmon selected for flesh lipid content, 'Lean' or 'Fat'. It was established that lipid and energy metabolisms were the functional categories that were most affected by the diet (S. Morais et al., 2012).

The authors noted a series of important effects, when they measured the ribosomal proteins and signaling. They found that the long-chain polyunsaturated fatty acid (LC-PUFA) biosynthesis pathway was influenced by the fish genotype. This finding was assessed by measuring the fatty acid composition and the gene expression (S. Morais et al., 2012, Table 83).

Moreover, the intestinal tissue contents measured as docosahexaenoic acid unit, indicated that Lean salmon fed either a FO or VO diet were equivalent; however, the expression of LC-PUFA biosynthesis genes was up-regulated in VO-fed fish in Fat salmon (S. Morais et al., 2012).

The dietary VO increased lipogenesis in Lean fish was assessed by the expression of the FAS ligand, which is a homotrimeric type II transmembrane protein expressed on cytotoxic T lymphocytes. While no effect was observed on the β-oxidation, it was noted that transcripts of the mitochondrial respiratory chain were down-regulated; this suggests a less active energetic metabolism in fish fed VO (S. Morais et al., 2012).

In contrast, it was suggested that the dietary VO up-regulated genes and proteins, which were involved in the detoxification, antioxidant defense and apoptosis, were also associated with the higher levels of polycyclic aromatic hydrocarbons in this diet (S. Morais et al., 2012).

With respect of the genotype, the following pathways were identified as being differentially affected: proteasomal proteolysis, response to oxidative and cellular stress (xenobiotic and oxidant metabolism and heat shock proteins), apoptosis and structural proteins particularly associated with tissue contractile properties. This indicate that genotype effects were accentuated by dietary VO (S. Morais et al., 2012).

This study showed that the intestinal metabolism was affected by diet and genotype. Lean fish may have higher responsiveness to low dietary n-3 LC-PUFA, up-regulating the biosynthetic pathway when fed dietary VO (Table 73). As global aquaculture searches for alternative oils for feeds, this study alerts to the potential of VO introducing contaminants and demonstrates the detoxifying role of intestine. Finally, data indicate genotype-specific responses in the intestinal transcriptome and proteome to dietary VO, including possibly structural properties of the intestinal layer and defense against cellular stress, with Lean fish being more susceptible to diet-induced oxidative stress (S. Morais et al., 2012).

Table 73. Proteins differentially regulated by genotype (S. Morais et al., 2012).

Spot No	Protein ID	Accession No. (NCBInr)	Theoretical Mw (KDa)/pI	Protein Score[a]	No. Matched peptides (MS/MS)[b]	Best score peptide	Lean/Fat FO	Lean/Fat VO	p-value
1148	Hemopexin-like protein* (HPX)	emb|CAA92147.1|	50.4/5.61	169	1	VHLDAITSDDAGNIYAFR	−1.09	−1.29	0.0270
1389	Calreticulin precursor (CALR)	gb|ACI32936.1|	47.6/4.33	81	2	FEPFSNEGK	−1.28	−1.33	0.0026
1441	Alpha-enolase (ENO1)	ref|NP_001133366.1|	47.0/5.91	405	3	AAVPSGASTGIYEALELR	1.28	1.2	0.0066
1714	Heat shock protein 70 (HSP70)	ref|NP_990334.1|	70.8/5.47	111	1	IINEPTAAAIAYGLDKK	1.16	1.77	0.0260
2134	Heterogeneous nuclear ribonucleoprotein A0 (HNRNPA0)	gb|ACI67551.1|	28.8/9.10	235	2	LFVGGLNVDTDDDGLRK	−1.19	−1.09	0.0460
2154	Calponin 1 (CNN1)	ref|NP_001139857.1|	33.2/8.56	565	4	KINTSPQNWHQLENIGNFVR	−1.34	−1.51	0.0350
2157	Calponin 1*** (CNN1)	ref|NP_001139857.1|	33.2/8.56	43	1	YDPQKEEELR	−1.34	−1.47	0.0240
2213	Caspase 3 (CASP3)	ref|NP_001133393.1|	31.0/5.97	254	2	IPVEADFLYAYSTAPGYYSWR	−1.15	−1.24	0.0300
2215	Caspase 3 (CASP3)	ref|NP_001133393.1|	31.0/5.97	279	2	VANDQTVQQIQQLLSK	−1.14	−1.31	0.0130
2282	Voltage-dependent anion channel 2–2 (VDAC2)	gb|ACH71030.1|	30.1/8.85	214	1	VNNNSLVGVGYTQTLRPGVK	−1.24	−1.19	0.0160
2458	Annexin A4 (ANXA4)	gb|ACI69495.1|	28.4/5.22	218	3	NHLLQVFK	−1.14	−1.11	0.0300
2487	Dihydropteridine reductase (DHPR)	gb|ACI67281.1|	15.7/8.46	81	1	QSVWTSTISSHLATR	−1.14	−1.11	0.0300
2499	Pancreatic alpha-amylase precursor (AMY2)	ref|NP_001036176.1|	57.4/6.89	86	1	ALVFVDNHDNQR	−1.37	−1.27	0.0021
2522	Triosephosphate isomerase 1b (TPI1)	ref|NP_001133174.1|	26.6/7.63	336	2	LDPNTEVVCGAPSIYLEFAR	1.26	1.16	0.0009
2527	Histone cluster 1 (H2A)	ref|NP_001086775.1|	14.0/10.88	94	1	AGLQFPVGR	1.12	1.11	0.0074
2677	Transgelin (TAGLN)	gb|ACM09025.1|	21.7/7.69	219	1	DGCVLSELINSLHK	−1.61	−1.35	0.0350
2717	Proteasome beta 1 subunit (PSMB1)	ref|NP_001003889.1|	26.1/6.32	87	1	GAVYSFDPVGSYQR	−1.29	−1.12	0.0140
2903	Peroxiredoxin-1(PRDX1)	gb|ACI67145.1|	22.0/6.42	115	1	QITINDLPVGR	−1.62	−1.99	0.0069
3345	Retinol-binding protein II, cellular (RBP2)	ref|NP_001139954.1|	15.6/5.44	70	2	AIDIDFATR	−1.32	−1.1	0.0330
3457	Alpha globin (HBA)	emb|CAA65949.1|	15.1/9.19	170	2	TYFSHWADLSPGSAPVK	1.03	2.09	0.0320

[a]The protein score probability limit (where $P < 0.05$) is 73.
[b] Peptides with confidence interval above 95% were considered.
* Equivalent to warm-temperature-acclimation-related-65 kDa-protein.
*** Same protein identification obtained by MS/PMF (peptide mass fingerprinting): Score = 193; 27 peptides matched. Only reliable identifications of Actinopterygii, obtained by mass spectrometry (MALDI-TOF-MS/MS) analysis and searches in MASCOT, NCBI and ExPASy (Mw/pI) databases are shown.
Expression ratios between Lean and Fat family groups are given for each dietary treatment, as well as p-value for genotype (two-way ANOVA, DeCyder V7.0)

6.14. **Protein Changes as Robust Signatures of Fish Chronic Stress: A Proteomics Approach to Fish Welfare Research**

The welfare and environmental impact studies have become of extreme importance when dealing with the aquaculture industry. For these reasons, it is important to prevents the stress associated with common aquaculture practices, and to optimize the fish stress response by quantification of the stress level (Raposo De Magalhães et al., 2020).

Stress is characterized by a cascade of physiological responses, which in-turn, induce further changes at the whole animal level. These can either increase either fitness or impair welfare. Nevertheless, monitoring of this dynamic process has, up until now, relied on indicators that are only a snapshot of the stress level experienced. Promising technological tools, such as proteomics, allow an unbiased approach for the discovery of potential biomarkers for stress monitoring (Raposo De Magalhães et al., 2020).

This study examines the Gilthead seabream (*Sparus aurata*) as a model for three chronic stress conditions namely overcrowding, handling and hypoxia. These chronic stress conditions were employed to evaluate the potential of the fish protein-based adaptations as reliable diagnostic signatures of chronic stress. It is important to mention that this proteomics approach is completely different from the commonly used hormonal and metabolic indicators (Raposo De Magalhães et al., 2020) .

This study also established that that there were broad spectrum of biological variations concerning the cortisol and glucose levels. The values of which rose higher in the net-handled fish. This suggested that the potential pattern of stressor was specifically clear, as the level of response varied markedly between a persistent (crowding) and a repetitive stressor (handling). Unfortunately, the variability in the response levels of cortisol, glucose and lactate, in fish from the same groups, alongside the possible adaptation, suggested by the results, demonstrate that these indicators may not be the most robust in case of chronic stress monitoring (Raposo De Magalhães et al., 2020).

On the other hand, proteomics analysis of the plasma revealed that net-handled fish had the highest number of differential proteins, compared to the other trials. Mass spectrometric analysis, followed by gene ontology enrichment and protein-protein interaction analyses, characterized those as humoral components of the innate immune system and key elements of the response to stimulus (Raposo De Magalhães et al., 2020).

It is evident that plasma proteomics allowed the detection of a cohesive network of protein changes associated with essential immunological pathways in stressed fish. Certainly, these proteins will be useful in understanding the biological processes behind protein-based stress adaptation in fish and may, therefore, represent the first screening for potential biomarker candidates of chronic stress in gilthead seabream (Raposo De Magalhães et al., 2020).

Overall, this study represents the first screening of more reliable signatures of physiological adaptation to chronic stress in fish, allowing the future development of novel biomarker models to monitor fish welfare (Raposo De Magalhães et al., 2020).

In summary, the overall results suggest that physiological changes were higher in fish exposed to repeated handling, while mild and permanent stressors may allow the fish to refine their physiological processes and adapt to certain challenges. This work was suggested to be the first step for a more scientific and reliable assessment of fish welfare. Hence, this multidisciplinary approach, and the study of the stress response from the molecular to the behavioral level, might just be the holistic approach needed to achieve such a goal (Raposo De Magalhães et al., 202).

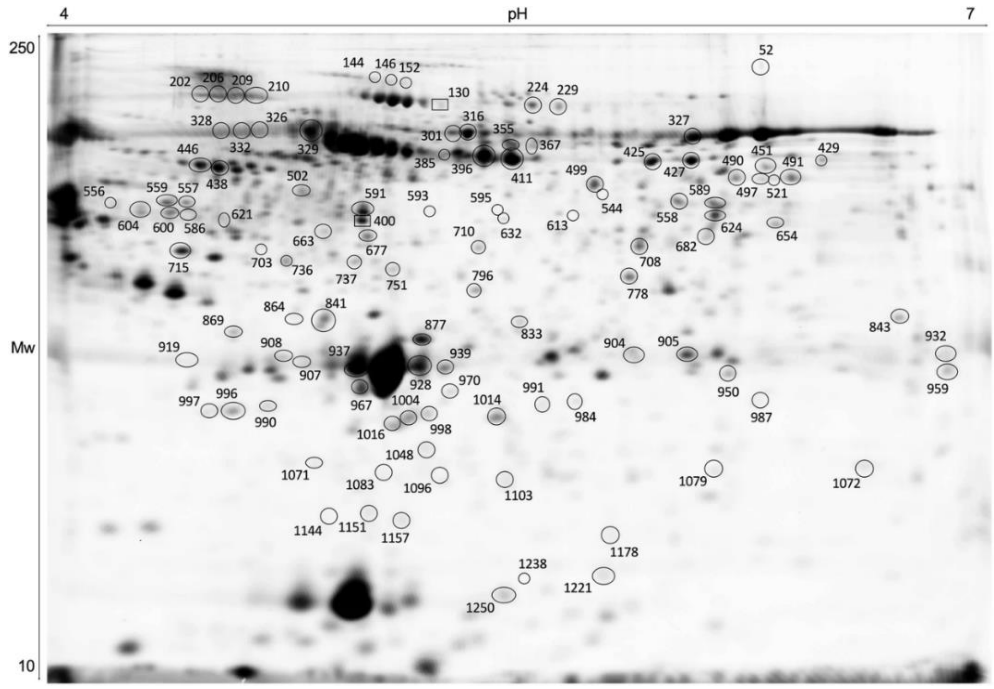

Figure 103. Representative pattern of gilthead seabream (Sparus aurata) blood plasma on a 12.5% polyacrylamide 2D gel. Black circles represent the 107 proteins identified by MALDI-TOF/TOF MS with significant differences in abundance in NET groups and black squares the 2 proteins with significant differences in abundance in HYP groups ($P < 0.05$) (Raposo De Magalhães et al., 2020).

Table 74. String annotations and fold-changes of the proteins in the PPI network. Bold lettering in the "FC" column indicates significant fold-changes (> 1.0 and < − 1.0). List is given in ascending order of spot number (Raposo De Magalhães et al., 2020).

Spot[a]	Accession no.[b]	Protein ID[c]	FC[d]		*Danio rerio* homolog (UniprotKB identifier)	String annotation
			NET2	NET4		
152	XP_008277007.1	PREDICTED: complement factor B-like [*Stegastes partitus*]	**1.72**	**2.54**	F1QFT0	zgc:158446
202	XP_010753395.2	PREDICTED: antithrombin-III [*Larimichthys crocea*]	−0.36	**−1.61**	Q8AYE3	serpinc1
209	XP_019111370.1	PREDICTED: inter-alpha-trypsin inhibitor heavy chain H3-like [Larimichthys crocea]	−0.49	**−1.76**	F1QTF9	zgc:110377
224	XP_017260893.1	alpha-2-macroglobulin, partial [Kryptolebias marmoratus]	−0.62	**−1.74**	A0A0R4IDD1	a2ml
316	AWP20152.1	putative apolipoprotein B-100-like isoform 2 [*Scophthalmus maximus*]	−0.88	**−1.46**	Q5TZ29	apobb
367	XP_023285742.1	alpha-1-antitrypsin homolog [*Seriola lalandi* dorsalis]	1.17	**2.78**	Q6P5I9	serpina1
544	KKF22678.1	Fibrinogen alpha chain [Larimichthys crocea]	1.33	**2.26**	B8A5L6	fga
556	XP_018550494.1	PREDICTED: leucine-rich alpha-2-glycoprotein-like [*Lates calcarifer*]	0.51	**1.20**	Q5RHE5	LRG1
558	AEA41139.1	transferrin [*Sparus aurata*]	−0.46	**−2.18**	A0A2R8RRA6	tfa
595	ADM13620.1	complement component c3 [Sparus aurata]	1.08	**2.06**	Q3MU74	c3b
710	ARI46218.1	haptoglobin [Sparus aurata]	**1.39**	**1.53**	F8W5P2	ENSDARG00000051890
736	AJW65884.1	Hyaluronic acid binding protein 2 [Sparus aurata]	−0.33	**−1.53**	Q1JQ29	habp2
796	ACN54269.1	warm temperature acclimation-related 65 kDa protein [Sparus aurata]	0.85	**1.13**	Q6PHG2	hpx
877	BAM36361.1	pentraxin [*Oplegnathus fasciatus*]	**−1.24**	−0.73	Q7SZ53	crp2
	XP_022604055.1	kininogen-1-like [*Seriola dumerili*]	**−1.24**	−0.73	Q5XJ76	kng1
996	APO15792.1	apolipoprotein Eb [Sparus aurata]	−0.10	**−3.04**	O42364	apoeb
997	XP_010742296.3	apolipoprotein A-I [Larimichthys crocea]	−0.92	**−4.04**	O42363	apoa1a
1072	XP_020489366.1	fetuin-B-like [*Labrus bergylta*]	−0.47	**−1.07**	E7FE90	fetub

[a] Spot no. – number of the spot in the 2D gel (Figure 102), attributed by the SameSpots software
[b] Accession number – NCBI accession number
[c] Protein ID – protein identification by MALDI-TOF/TOF MS
[d] FC - Log2(fold-change) - significant changes in protein abundance (treated/control). Bold lettering indicates significant fold-changes (> 1.0 and < − 1.0)

6.15. Extensive *De Novo* Sequencing of New Parvalbumin Isoforms Using a Novel Combination of Bottom-Up proteomics, Accurate Molecular Mass Measurement by FTICR-MS

In this work, a novel strategy was developed for the extensive characterization of the major fish allergen parvalbumins (PRVB) (11.20-11.55 kDa) and associated isoforms. This strategy consisted on the integration of a classical bottom-up proteomics approach with accurate *M*r determination by FTICR-MS of intact proteins and selected MS/MS ion monitoring (SMIM) of peptide mass gaps (Carrera et al., 2010b).

Two tryptic digests (trypsin, Glu-C) were analyzed with electrospray ionization -ion trap-tandem mass spectrometer (LC-ESI-MS/MS). The two digests were *de novo* sequenced manually with help of two programs (PEAKS, DeNovoX). The deduced peptide sequences were arranged and the theoretical *M*r for the resulting sequences was calculated. The experimental *M*r for each PRVB was measured with high mass accuracy by FTICR-MS (0.05-4.47 ppm). The ESI-MS were searched using SEQUEST (Bioworks 3.1 package, ThermoFisher) against the complete and general database UniProtKB release 15.0 (Carrera et al., 2010b).

The *de novo* sequencing was performed by manual interpretation of the product ion series of the spectra with aid of the software packages: DeNovoX (Thermo Fisher) and PEAKS Studio 4.2. It should be noted that all the peptide sequences obtained, were meticulously ordered by overlapping the results obtained with both enzymatic digests and by comparison, using BLAST, with the proteins included in the UniProtKB database. In those cases where a complete PRVB sequence was obtained, the theoretical *M*r was calculated using the Molecular Weight Calculator program (Carrera et al., 2010b).

The intact PRVBs from each species were purified by treatment with heat. Measurements of *M*r of intact PRVBs were performed on a 7T FTICR mass spectrometer (APEXIII, Bruker Daltonics) (Carrera et al., 2010b). The masses of several missing peptide gaps were estimated by comparing the theoretical and experimental*M*r, and the MS/MS spectra corresponding to these ions were obtained by LC-ESI-IT-MS/MS in the SMIM scanning mode (Carrera et al., 2010b) .

The following figure indicate the analytical scheme of the three sequential proteomics approaches employed for the complete *de novo* sequencing of new proteins: (a) classical “Bottom-Up” proteomics approach, (b) accurate *M*r determination of intact protein by FTICR-MS and (c) monitoring of peptide mass gaps by Selected MS/MS Ion Monitoring (SMIM) (Carrera et al., 2010b).

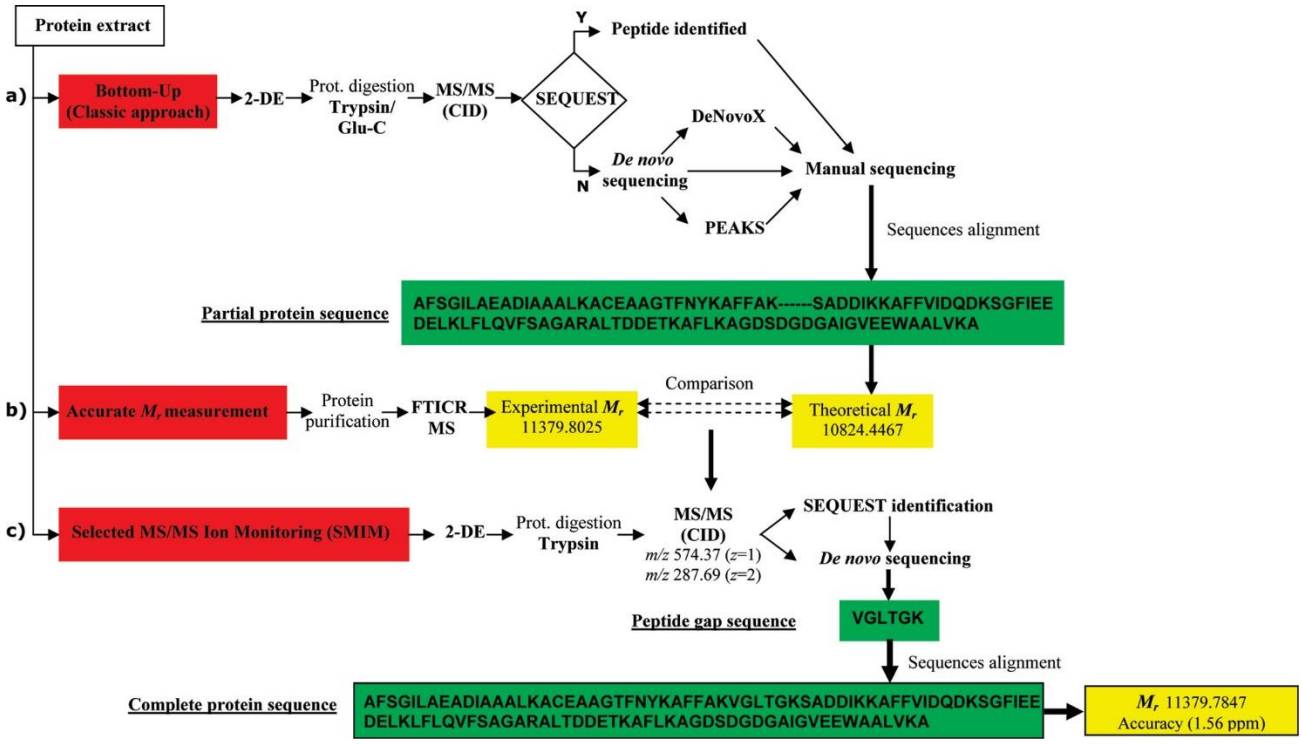

Figure 104. Analytical scheme of the three sequential proteomics approaches employed for the complete de novo sequencing of new proteins: (a) classical Bottom-Up proteomics approach, (b) accurate Mr determination of intact protein by FTICR-MS and (c) monitoring of peptide mass gaps by Selected MS/MS Ion Monitoring (SMIM) (Carrera et al., 2010b).

Finally, all peptide sequences were combined to generate the final protein sequences. This approach allowed the complete *de novo* MS-sequencing of 25 new PRVB isoforms. These new sequences obtained appeared to belong to 11 different species of the *Merlucciidae* family, organisms for which genomes remain unsequenced. This study constitutes the report accounting for the higher number of new proteins completely sequenced making use of MS-based techniques only (Table 75) (Carrera et al., 2010b).

Table 75. Isoelectric Point and Molecular Weight for All of the PRVB Spots Studied (Carrera et al., 2010b).

species[a]/subspecies	PRVB spot number	p*I*	M_r (kDa)	species[a]/subspecies	PRVB spot number	p*I*	M_r (kDa)
M. merluccius	P1	4.53	11.30		P21	4.20	11.20
	P2	4.19	11.38		P22	3.78	11.33
	P3	4.02	11.39	*M. australis polylepis*	P23	4.30	11.30
M. capensis	P4	4.55	11.30		P24	4.14	11.55
	P5	4.20	11.38		P25	3.98	11.33
	P6	3.95	11.39	*M. australis australis*	P26	4.51	11.25

M. senegalensis	P7	4.55	11.30		P27	4.30	11.30
	P8	4.20	11.38		P28	4.14	11.53
	P9	3.92	11.37		P29	3.98	11.33
M. polli	P10	4.51	11.30	*M. productus*	P30	4.51	11.37
	P11	4.19	11.35		P31	4.29	11.50
	P12	3.84	11.35		P32	4.23	11.35
M. paradoxus	P13	4.51	11.35	*M. bilinearis*	P33	4.23	11.35
	P14	4.16	11.35		P34	3.98	11.27
	P15	3.79	11.32	*Ma. novaezelandiae novaezelandiae*	P35	4.51	11.25
M. hubbsi	P16	4.57	11.30		P36	4.05	11.35
	P17	4.30	11.55		P37	3.75	11.35
	P18	4.09	11.35	*Ma. novaezelandiae magellanicus*	P38	4.51	11.25
M. gayi	P19	4.56	11.30		P39	4.05	11.35
	P20	4.27	11.53		P40	3.75	11.35

[a] *M.* (*Merluccius* genus); *Ma.* (*Macruronus* genus).

7. Climate Change, Fish Proteomics and Marine Organisms

The vital role of fish proteomics in studying the influence of climate change on fish biology is explained in the following section. Climate change stands for the expected seasonal changes and it relates quite closely to the sun variation. It is a natural process that takes place simultaneously on various timescales. Many studies on climate change' were evoted to understand its influence on the oceans. The majority of these studies were focused on predicting the physical, chemical, geographical, sociological and economic consequences of this reality, which appears to be unstoppable. However, only a few studies focused on the effects of climate change on the quality of both aquacultured cultivated and wild seafood products. Climate change is one of several unresolved issues that affect the marine environment (Piñeiro et al., 2010a). The increase in the emission of anthropogenic gases to the atmosphere is mainly caused by man-made activities which provoks global warming. This latter impose significant consequences to the marine ecosystems, which are translated into sea warming, and ocean acidification that have many deleterious effects on the entire trophic web. Also, it is well knowm that changes in temperature is an important aquaculture driver, and that the climate-driven temperature change can influence aquaculture in many ways (Reid et al., 2019., Boyd et al., 2019) .

Climate change causes stress in marine organisms, which is reflected at the cell molecular level, affecting the metabolite concentration, proteins expression, and modifications. Proteins expression and quantity vary between different types of cells in the same organism and the same

type of cells in response to diverse stimuli and environmental factors. Climate change effects cause specific protein modifications in marine organisms (Ph. Garrigues, H. Barth, C.H. Walker, 2001).

Few studies were devoted to study the effects of climate change on the proteome levels of marie organisms . In general these studies studied were effected on fish otrganisms exposed to climate change stresses. The most common techniques used in this type of study involved the proteomics approach using state-of-the art techniques such as 2DE and protein characterization by mass spectrometry (Barrera & Gómez Ariza, 2017).

Proteomics is an indispensable scientific set of methodologies with enormous potential to evaluate climate change effects on food production, specifically, wild and cultivated seafood Production. Proteomics study using MS/MS is the fast analytical methodology capable of identifying hundreds of seafood proteins in parallel, with various post-translation modifications at different expression levels (Piñeiro et al., 2010a; X. Zhang et al., 2008).

7.1. **The proteomic Response of the Mussel Congeners Mytilus galloprovincialis and M. trossulus to Acute Heat Stress**

The mussel congeners *Mytilus galloprovincialis* and *M. trossulus* acclimated to 13°C for four weeks and exposed to acute heat stress (24°C, 28°C and 32°C) for one hour and returned to 13°C to recover for 24 h after which was analyzed by the conventional Proteomics Approach.

The proteome response to acute heat stress appeared to produce higher levels of Hsp70 (Hsp 70) isoforms and Hsp families in both congeners. The abundance of proteasome subunits was greater in *M . trossulus* but lower in *M. galloprovincialis* in response to heat. Furthermore, the levels of several NADH-metabolizing proteins, which possibly are linked to the generation of reactive oxygen species (ROS), were found in higher concentrations in both species. Whereas the NADH-metabolizing proteins were lower at 32°C in the cold-adapted *M. trossulus*. At 32°C, the oxidative stress proteins abundance was lower in *M. trossulus* only, indicating that its ability to combat heat-induced oxidative stress was limited to lower temperatures. Levels of NAD-dependent deacetylase (sirtuin 5) were lower in M. *trossulus* in response to heat stress. The expression patterns of proteins showed a lower sensitivity to high-temperature damage in the warm-adapted *M. galloprovincialis*, consistent with its expanding range in warmer waters.(Barrera & Gómez Ariza, 2017; Tomanek & Zuzow, 2010).

7.2. **Proteomic Responses of the Brain of Juvenile Coral Reef Fish to Ocean Acidification**

To understand the responses to acidification of Juvenile Coral Reef Fish, Tsang and et al. exposed adult *A. polyacanthus* pairs to elevated CO_2 (754 ± 92 µatm), consistent with average atmospheric CO_2 predicted by the end of the century according to the RCP6 emissions trajectory. After a seven-day elevated CO2 exposure, they tested the reaction toward chemical alarm cues (CAC) in adults. Then Proteins from whole brain tissue were extracted along with DNA and RNA with a Qiagen AllPrep DNA/RNA Mini Kit. The samples were analyzed through three technical replicates using a Q Exactive HF mass spectrometer (Thermo Scientific) coupled with an UltiMateTM 3000 UHPLC (Thermo Scientific). Introduction of the sample into the mass spectrometer through a Nanospray Flex (Thermo Scientific) (Tsang et al., 2020).

Measuring brain proteome accumulation of organisms exposed to elevated CO_2 conditions for different durations, within and between generations, can explain how ocean acidification affects biological processes over relevant timescales. The authors found that the differential accumulation of critical proteins, were related to the stress response and epigenetic markers with elevated CO_2 exposure. Proteins related to neurological development and glucose metabolism were also differentially accumulated mainly in the long-term developmental treatment, which might be critical for juvenile development. On the other hand, the exposure to elevated CO_2 of the parental generation led to only three differentially accumulated proteins in the offspring.

This result revealed the potential for inter-generational acclimation. Lastly, we found a distinct proteomic pattern in juveniles due to the behavioural sensitivity of parents to elevated CO2, even though the behaviour of the juvenile fish was impaired regardless of parental phenotype. Our data shows that developing juveniles are affected in their brain protein accumulation by elevated CO2. However, the effect varies with the length of exposure and due to variation of parental phenotypes in the population (Tsang et al., 2020).

7.3. **The Response of the Proteome During Early Development of *Babylonia areolata* to Acidification**

Ocean acidification (OA) affects the proteome of *Babylonia areolata*. Guilan Di *et al.* used label-free proteomics to study protein changes in response to acidified (pH 7.6) or ambient seawater (pH 8.1) during three larvae developmental stages of *B. areolata*, namely, the veliger larvae before

attachment (E1), veliger larvae after attachment (E2), and carnivorous juvenile snail (E3).The veliger is the planktonic larva of many kinds of sea snails and freshwater snails, as well as most bivalve molluscs and tusk shells

The authors examined every development stage by microscopic analysis. After extracting the total protein from each stage, they separated the sample by the two-dimensional sample using Nanoacquity ultraperformance liquid chromatography. The samples were analyzed using tandem mass spectrometry label-free analysis on a Q-Exactive mass spectrometer (Thermo Fisher Scientific).

The authors identified 720 proteins. This result indicated that acidification seriously affects the late veliger stage after attachment (E2). Differentially expressed proteins important for understanding the molecular mechanisms underlying pH reduction. These proteins include glutaredoxin, heat-shock protein 70, thioredoxin, catalase, cytochrome-c-oxidase, peroxiredoxin 6, troponin T CaM kinase II alpha, proteasome subunit N3 and cathepsin L (Di et al., 2019).

7.4. **Proteomic Responses of the Marine Diazotroph *Trichodesmium* to Ocean Acidification**

Response of the globally crucial N_2-fixing marine cyanobacterium *T. erythraeum* strain IMS101 to both Fe-replete and Fe-limited concentrations under ambient and acidified conditions through Proteomic analysis by separating Peptides using an LC-20AD nano HPLC followed by tandem mass spectrometry in an Orbitrap mass spectrometer.

Proteomic analysis indicated that OA affected a more comprehensive range of proteins under Fe-limited conditions than Fe-replete conditions. OA also intensifies Fe deficiency in vital cellular processes such as photosystem I and chlorophyll-a synthesis in already Fe-limited T. erythraeum. A result of reallocating Fe from these processes to Fe-rich nitrogenase to compensate for the suppressed N2 fixation. The diazotroph adopts a series of Fe-based economic strategies to alleviate the Fe shortage, such as upregulating Fe acquisition systems for organically complexed Fe and particulate Fe and using alternative electron flow pathways to produce ATP. Under Fe-limited-OA conditions, the diazotroph adaptation strategies were more pronounced than under Fe limitation only. Consequently, OA resulted in a further decrease of N2- and carbon-fixation rates in Fe-limited T. erythraeum. In contrast, Fe-replete T. erythraeum induced photosystem I (PSI) expression to potentially enhance the PSI cyclic flow for ATP production to meet the higher demand for energy to cope with the stress caused by OA (F. Zhang et al., 2019).

8. Additional Fish Proteomic Applications

In our review, we have comprehensively gathered vast literature on some proteomic applications to Fisheries Biology Research. However, it is practically impossible to present all the examples published in the vast literature on Fish Proteomics, this is why we have included in this section 9 some additional references that were not covered by our review. The following section will introduce each proteomics approach and its fundamental principles, so that readers with no prior knowledge of proteomics can also follow how the information is obtained for the various examples listed in the following Tables 9.1 to 9.3.

8.1. Fish Health and Immunology Proteomics

Fish	Treatment Or infection	Tissue	Analytical techniques	Number of regulated proteins	Names or functions of regulated proteins	Ref
Zebrafish	Antimicrobial peptide epinecidin-1	Whole body	Bottom-up 2-DE- LC-MS/MS	18	Structural proteins, especially the cytoskeleton proteins.	(T. C. Huang & Chen, 2013)
Atlantic salmon (Salmo salar)	Amoebic gill disease (AGD)	Gill and skin mucus	Bottom-up 2-DE- LC-MS/MS	Gill: 52 Skin mucus: 42	Cell to cell signalling and inflammation pathways.	(Valdenegro-Vega et al., 2014)
Yellow catfish (*Pelteobagrus fulvidraco)*	*Edwardsiella ictalurid* infection	Skin mucus	Bottom-up gel-free approach (LC-MS/MS)	133	Structural, metabolic, signal transduction-related and immune-related proteins.	(Y. Xiong et al., 2020c)
Zebrafish	Spring viremia of carp virus infection (1, 2 and 5 days post infection)	Plasma	Bottom-up gel-free approach (LC-MS/MS)	1 day:137 2 days:63 5 days:31	Proteins of the vitellogenin family (Vtg) and the grass carp reovirus-induced gene (Gig) proteins	(Medina-Gali et al., 2019)
Rainbow trout (*Oncorhynchus mykiss*)	Skeletal deformity in diploid and triploid larvae (Note: Triploidy was induced by a heat shock)	Larvae	Bottom-up 2DE-MALDI-TOF/TOF-MS	Diploid normal larvae (DNL) Vs. Diploid deformed larvae (DDL): 5 heat-shocked normal larvae (HNL) Vs.	In Diploid deformed fish: creatine kinase was while apolipoprotein A-I-2, apolipoprotein A-II and calmodulin were down regulated. In heat shocked fish: apolipoprotein A-I-2, apolipoprotein A-II,	(Babaheydari et al., 2016)

				heat-shocked deformed larvae (HDL): 7	parvalbumin, myosin light chain 1-1 and nucleoside diphosphate kinase were downregulated	
Sea urchin *Paracentrotus lividus* coelomocytes	The bacterial lipopolysaccharide LPS injection (1, 3, 6 and 24 hours after treatment)	Coelomocytes	Bottom-up gel-free approach (LC-MS/MS)	Not specified	Cytoskeleton reorganisation, the appearance of clusters of heat shock proteins (Hsp) and histone proteins and the activation of the endocytic and phagocytic pathways	(Inguglia et al., 2020)
Zebrafish (Danio rerio)	Infectious spleen and kidney necrosis virus	Spleen	Bottom-up 2DE-MALDI-TOF/TOF-MS	35	Cytoskeletal protein, stress response, lipoprotein metabolism, ubiquitin–proteasome pathway, carbohydrate metabolism, signal transduction, proteolysis, ion binding, transport, metabolic process, catabolic process, biosynthesis, and oxidation reduction	(X. P. Xiong et al., 2011)
Japanese flounder (*Paralichthys olivaceus*)	*Edwardsiella tarda (pathogen)*	Liver	Bottom-up quantitative iTRAQ LC-MS/MS	206	Complement and coagulation cascades pathway, Mineral absorption pathway, biosynthesis and metabolism, Cytoskeleton-related proteins	(L. Wang et al., 2017)
Zebrafish	Spring Viremia of Carp Virus (24 and 96 h postinfection)	Skin	Bottom-up quantitative iTRAQ LC-MS/MS	24h: 320 96 h: 181	Differentially expressed proteins were significantly associated with complement, inflammation, and antiviral response	(R. Liu et al., 2020)
The grass carp (Ctenopharyngodon idella)	Grass carp reovirus (GCRV)	Kidney	dimethylation labeling-based quantitative LC-MS/MS (identification and quantification of lysine acetylated sites and proteins)	363	Regulated lysine acetylated proteins were highly correlated with protein processing and metabolism.	(Guo et al., 2017)

Zebrafish	Aeromonas hydrophila	Gill	Bottom-up quantitative iTRAQ LC-MS/MS	82	Stress and immune responses	(A. Lü et al., 2014)
Rainbow trout (Oncorhynchus mykiss)	Aeromonas salmonicida, the causative agent of furunculosis	Liver	Bottom-up 1-DE- LC-MS/MS	109	Upregulated complement system and acute phase response proteins	(Causey et al., 2018)

8.2. **Fish Ecotoxicological Proteomics**

Fish	**Environmental Stress**	**Tissue**	**Analytical Technique**	**No. of Regulated proteins**	**Names and/or functions of regulated proteins**	**Ref.**
Zebrafish (Danio rerio)	Aniline pesticide: 3,4-dichloroaniline (DCA)	Whole body (Larvae)	Bottom-up gel-free approach (LC-MS/MS)	24	DCA affected proteins involved in Metabolic and developmental processes	(Vieira et al., 2020)
Zebrafish (Danio rerio)	Hypoxia	Skeletal muscles	Bottom-up 2D-DIGE- MALDI-TOF/TOF	77	Hypoxia was faced by the enhancement of anaerobic metabolism and oxygen transport to tissues with a simultaneous suppression in mitochondrial metabolism.	(de Vareilles et al., 2012)
Atlantic Cod (Gadus morhua)	Polycyclic aromatic hydrocarbon (PAH) and	Plasma	Bottom-up Shotgun proteomics (LC-MS/MS)	12	Significant increase in immunoglobulins (Immune response)	(Skogland Enerstvedt et al., 2017)
Sockeye salmon	diluted bitumen	Serum	Bottom-up gel-free quantitative iTRAQ LC-MS/MS	24	Proteins involved in immune and inflammatory responses, coagulation, and iron homeostasis are significantly regulated	(Alderman et al., 2017)

Medaka (Oryzias melastigma)	acute inorganic mercury	Liver and brain	Bottom-up 2DE-MALDI-TOF/TOF	20 for brain and 27 for liver	Proteins involved in oxidative stress, cytoskeletonal assembly, signal transduction, protein modification, metabolism and other related functions are regulated (Complex and diverse effects).	(M. Wang et al., 2011)
Atlantic Cod (Gadus morhua)	Methylmercury	Liver	Bottom-up 2DE-MALDI-TOF/TOF	35	Proteins involved in oxidative stress responses, cytoskeletonal assembly, protein synthesis, protein folding, and energy metabolism are regulated. Also, levels of hemoglobin and hemopexin are highly altered	(Karlsen et al., 2014)
Channa striatus	High Temperature	Liver	Bottom-up 2DE-MALDI-TOF/TOF-MS	23	Increased abundance of two sets of proteins, the antioxidative enzymes superoxide dismutase (SOD), ferritin, cellular retinol binding protein (CRBP), glutathione- *S*-transferase (GST), and the chaperones HSP60 and protein disulfide isomerase	(Mahanty et al., 2016)
Zebrafish (Danio rerio)	Atrazine (ATZ)	Hepatic tissue	Bottom-up 2DE-MALDI-TOF/TOF-MS	7 upregulated and 6 downregulated proteins	Proteins associated with a variety of cellular biological processes, such as response to oxidative stress, oncogenesis are regulated.	(Jin et al., 2012)
European sea bass, *Dicentrarchus labrax L.*	Salinity	Gill and intestine epithelia	Bottom-up 2DE-MALDI-TOF/TOF-MS	362	Gill cells (seawater): several cytoskeleton proteins are over expressed. - Gill cells (freshwater): the prolactin receptor and the	(Ky et al., 2007)

					major histocompatibility complex class II b-antigen are over expressed. -Intestinal cells (freshwater): the Iroquois homeobox protein Ziro5 was significantly upregulated with respect to saltwater conditions.	
Spiny damselfish, *Acanthochromis polyacanthus*	Elevated CO_2	Brain of Juveniles from two different parental behavioral phenotypes exposed to short-term, long-term and inter-generational elevated CO2.	Bottom-up quantitative iTRAQ LC-MS/MS	Different numbers of regulated proteins based on the term of exposure and parental phenotype.	Proteins related to stress response and epigenetic markers are regulated.	(Madeira et al., 2017; Tsang et al., 2020)
Atlantic cod (Gadus morhua)	Hydraulic drilling fluid 200 (HDF 200) or Benzo[a]pyrene (BaP)	Bile	Bottom-up gel-free approach LC-MS/MS	2 (HDF200) and 9 (BaP)	In case of HDF200, Serotransferrin and myeloperoxidase homolog proteins are downregulated. In case of BaP, Hemoglobin alpha chain and an uncharacterized protein are upregulated, while Saxitoxin, tetrodotoxin-binding protein, Alpha-2 macroglobulin-like, Pleiotopic regulator 1, No homolog, predicted protein, Serotransferrin, Actin beta are downregulated.	(Pampanin et al., 2014)
European whitefish (Coregonus lavaretus)	Salinity	Larvae	Bottom-up gel-free approach LC-MS/MS	73	Osmotic stress which causes several proteins involved in osmoregulation to be	(Papakostas et al., 2012)

					regulated for salinity adaptation.	
Fathead minnows *(Pimephales promelas)*	Pesticides: permethrin, terbufos and a binary mixture of both	Brain	Bottom-up 2D-DIGE- LC-MS/MS	24	Proteins associated with the ubiquitin–proteasome system, glycolysis, the cytoskeleton, and hypoxia were upregulated.	(Biales et al., 2011)
Danio Rerio Fish Embryos	Phosphatidylcholine-based nanoparticles with C60 fullerenes	Embryos	Bottom-up 2DE-MALDI-TOF/TOF-MS	Out of the Total 52 proteins identified, only 24 proteins were common between the control and the exposed samples	The content of vitellogenins changed after exposure	(Barrera & Gómez Ariza, 2017).
Goldfish (Carassius auratus)	Multiple stress: pesticide mixtures and temperature increase	Liver	Bottom-up 2DE-LC-MS/MS	56	Several proteins associated with cell death control and cancer development are regulated	(Gandar et al., 2017)
Atlantic herring *(Clupea harengus L.)*	Elevated pCO_2	Whole Larvae	Bottom-up 2DE-MALDI-TOF/TOF-MS	19 proteins (slightly regulated)	No significant difference in the protein expression pattern between the control and elevated pCO2 larvae.	(Maneja et al., 2014)
Sentinel Fish Species, Cottus gobio	Cadmium	liver and gills	Bottom-up 2D-DIGE- LC-MS/MS	54 hepatic proteins and 37 branchial proteins	Proteins related to metabolic process, stress response, protein fate, and cell structure are regulated.	(Dorts et al., 2011)
Gilt-head sea bream Sparus aurata	Ocean Warming (18,24, 30 °C)	Muscles	Bottom-up 2DE-MALDI-TOF/TOF-MS	52 (exposure for 14 days) and 40 (exposure for 21 days)	The majority of proteins regulated were involved in energetic metabolism and chaperoning.	(Madeira et al., 2017)
Soles (Solea senegalensis)	Combination treatment with cadmium and benzo[a]pyrene	Liver	Bottom-up 2DE-MALDI-TOF/TOF-MS	24	Upregulation of different anti-oxidative enzymes	(P. M. Costa et al., 2010)
Puffer fish *Takifugu rubripes*	Excessive fluoride	Kidney	Bottom-up 2DE-MALDI-TOF/TOF-MS	32	Proteins involved in the biological functions associated with fluorosis are regulated	(J. Lu et al., 2010)

Eurythermal goby fish Gillichthys mirabilis	Temperature	Cardiac tissue	Bottom-up 2DE-MALDI-TOF/TOF-MS	122	Proteins involved in energy metabolism, mitochondrial regulation, iron homeostasis, cytoprotection against hypoxia, and cytoskeletal organization are regulated	(Jayasundara et al., 2015)
Teleost fish, ayu (Plecoglossus altivelis)	Cadmium	Liver	Bottom-up 2DE-MALDI-TOF/TOF-MS	23	Proteins involved in oxidative stress response, metal metabolism, methylation are regulated.	(X. J. Lu et al., 2012)
Bream Sparus aurata	Ocean warming	Larvae	Bottom-up 2DE-MALDI-TOF/TOF-MS	23	Proteins involved in folding and degradation, cytoskeletal reorganization, transcriptional regulation and the growth hormone are upregulated while proteins involved in cargo transporting and porphyrin metabolism are downregulated.	(Madeira et al., 2016)
Atlantic halibut (Hippoglossus hippoglossus)	High CO_2 at 12 and 18 °C	Gill and Plasma	Bottom-up 2DE-LC-MS/MS	Gills: 6 at 12 °C and 10 at 18 °C Plasma: 26 at 12 °C and 4 at 18 °C	Immune system-related proteins were upregulated	(K. B. de Souza et al., 2014)
Female fathead minnows	Fadrozole, a potent inhibitor of estrogen synthesis (0.04 and 1.0 µg/L treatment)	Liver	Bottom-up gel-free approach (LC-MS/MS)	-0.04 µg/L FAD: 312 proteins -1.0 µg/L FAD: 206 proteins	Vitellogenin and other proteins associated with endocrine function and cholesterol synthesis are downregulated	(Ralston-Hooper et al., 2013)
Medaka fish (Oryzias latipes)	Toxic cyanobacterial bloom (Planktothrix agardhii)	Liver	Bottom-up gel-free quantitative iTRAQ LC-MS/MS	15	Proteins involved in lipid metabolism, cell redox balance regulation and the detoxification of free radical damages are upregulated	(Sotton et al., 2017)
Medaka fish (Oryzias melastigma)	A sodium channel activator neurotoxin, brevetoxin-1	Gills and brains	Bottom-up 2DE-MALDI-TOF/TOF-MS	Gills: 14 Brain: 24	Proteins with various functional classes such as cell structure, macromolecule metabolism, signal	(Tian et al., 2011)

					transduction and neurotransmitter release are regulated	
Medaka fish *(Oryzias latipes)*	Microcystin-LR (toxin)	Liver	Bottom-up 2DE-LC-MS/MS	17	Eight proteins were reported for the first time to be regulated by MC-LR: prohibitin, fumarylacetoacetase, protein disulfide isomerase A4 and A6, glucose regulated protein 78 kDa, 40S ribosomal protein SA, cytochrome b5, and ATP synthase mitochondrial d subunit.	(Malécot et al., 2009)

8.3. **Aquaculture Applications**

Fish	**Diet or stress (treatment)**	**Tissue**	**Analytical Method**	**Number of regulated proteins**	**Names and/or functions of regulated proteins**	**Ref**
Gilthead sea bream (*Sparus aurata*)	Cold stress	Liver	Bottom-up gel-free LC-MS/MS	42	Proteins associated to cellular stress and to protein and lipid degradation processes are upregulated while proteins related to protein synthesis, actin- binding activity, amino acid metabolism, and protection from oxidative stress are downregulated.	(Ghisaura et al., 2019)
Rainbow trout (*Oncorhynchus mykiss*)	Dietary β-glucan	Muscle	Bottom-up 2DE-MALDI-TOF/TOF-MS	8	Tropomyosin alpha-1 chain and slow myotomal muscle tropomyosin were upregulated while different forms of myosin were down regulated.	(Ghaedi et al., 2016)
Rainbow trout (*Oncorhynchus mykiss*)	Vegetable based fish feed	Muscle	Bottom-up 2DE-MALDI or LC-MS/MS	39	Muscle proteins involved in lipid binding/transport, protein turnover, and binding of different ions are regulated	(Jessen et al., 2012)

rainbow trout (Oncorhynchus mykiss, Walbaum)	Probiotics in diets	Serum	Bottom-up 2DE-MALDI-TOF/TOF-MS	3	NADH dehydrogenase, dystrophin and mKIAA0350 proteins were upregulated	(Brunt et al., 2008)
Zebrafish (Danio rerio)	Dietary Lysine Imbalance (Lys(−) and Lys(+) treatments)	Muscle	Bottom-up 2D-DIGE-MALDI-TOF/TOF-MS	52	Proteins involved in the cytoskeletal network and the contractile apparatus of skeletal muscle, energy metabolism, and signal mediation in various cellular processes are regulated.	(de Vareilles et al., 2012)
gilthead seabream (Sparus aurata, L.)	High dietary plant protein without or with marine ingredients (VM and VM+) with respect to normal fishmeal (FM)	Gut mucosa	Bottom-up gel-free LC-MS/MS	Generally, the Whole set of proteins are upregulated in case of FM and VM+ with respect to VM.	Plant based diet (VM) caused the downregulation of several proteins such as those related to intracellular transport, assembly of cellular macrocomplex, protein localization and protein catabolism, maintenance of the cytoskeleton structure.	(Estruch et al., 2020)
Rainbow trout (Oncorhynchus mykiss)	High stocking density (HD)	Liver	Bottom-up 2DE-MALDI-TOF/TOF-MS	9	Two proteins including apolipoprotein A-I-2 precursor and mitochondrial stress-70 protein were upregulated, while, 2-peptidylprolyl isomerase A, two isoforms of glyceraldehydes-3-phosphate dehydrogenase, an unnamed protein product similar to fructosebisphosphate aldolase, 78 kDa glucose-regulated protein, and serum albumin 1 protein were downregulated.	(Naderi et al., 2017)
Rainbow trout (Oncorhynchus mykiss)	Dietary nucleotides	Muscles	Bottom-up 2DE-MALDI-TOF/TOF-MS	8	Muscle metabolic proteins and metabolic enzymes were regulated.	(Keyvanshokooh & Tahmasebi-Kohyani, 2012)
Farmed gilthead sea bream (Sparus aurata, L.)	Three commercial feed formulations (A, B and C)	Liver and blood serum	Bottom-up 2-DIGE-LC-MS/MS	A: 21 B:24 C:11	Proteins involved in metabolic pathways of liver were regulated in addition to the serum apolipoproteins, transferrin, warm temperature acclimation-related 65 kDa protein (Wap65), fibrinogen, F-type lectin, and alpha-1-antitrypsin.	(Ghisaura et al., 2014)

Gilthead seabream (Sparus aurata)	Probiotic intake and/or overcrowding stress	Skin mucus	Bottom-up 2-DE- LC-MS/MS	22	Proteins involved in immune processes were regulated	(Cordero et al., 2016b)
Puffer fish (Takifugu obscurus)	Phosphorus supplementation and low temp stress	Liver	Bottom-up 2DE-MALDI-TOF/TOF-MS	6	Three energy generation related enzymes and two lipid transport proteins were upregulated while intermediate filament protein (keratin type I cytoskeletal 13-like) were downregulated.	(Ye et al., 2016)
Rainbow trout	Two diets: diet C (control) and diet S (contains more soybean meal)	Liver	Bottom-up 2DE-MALDI-TOF/TOF-MS	33	Heat shock proteins, enzymes, fatty acid binding proteins and structural proteins were differentially regulated.	(Martin, Vilhelmsson, Médale, et al., 2003)
Gilthead seabream (Sparus aurata)	High stocking density (Chronic stress)	Liver	Bottom-up 2-DE- LC-MS/MS	280	Proteins involved in lipid transport and antioxidant role, chaperoning, Ca2+ signaling, lipid oxidation, ammonia metabolism, cytoskeleton, and carbohydrate metabolism were differentially expressed	(Alves et al., 2010)
Gilthead seabream (Sparus aurata)	Three chronic stresses (overcrowding, handling and hypoxia)	plasma	Bottom-up 2DE-MALDI-TOF/TOF-MS	Overcrowding: 19 Handling: 360 Hypoxia: 34	Protein associated with essential immunological pathways were regulated.	(Raposo De Magalhães et al., 2020)
Farmed gilthead sea breams (Sparus aurata, L.)	Moraxella sp. colonization	kidney	Bottom-up 2DE-MALDI-TOF/TOF-MS	10	Upregulation of several mitochondrial enzymes	(Addis et al., 2010)

9. Conclusion

n the last two decades great scientific strides were made to fish physiology and toxicology fields permitting to integrate genomic, proteomic, and metabolomic data sets. This integration will allow us to better understand the underlying physiology and how the animals interact with their environment. Certainly, fishery research studies are beginning to characterize the proteome of animal tissues such as liver for further study (Martyniuk & Denslow, 2009a; N. Wang et al., 2007).

Although the capability to study few proteomic responses in fish, is possible by using antiquated methodologies, many of which do not utilize non-gel based approaches for quantitative proteomics. These old methods only offered, limited information on post-translational modifications; which are essential in order to understand the protein function. Post-genome technologies will allow fisheries scientists to work beyond the reduction models of classic biology. Therefore, there is a constant need in fish, shellfish and seafood/seafood products to examine the various protein functions and cellular mechanisms at the molecular levels. With the availability of proteome techniques in marine wildlife, these goals can be achieved by determining which proteins interact with a given biological phenomena in a specific manner. For this reason, most of the recent published reports using the proteomic techniques that have been associated with the physiological function, relevant molecules and mechanisms, biomarkers for aquatic organism welfare. These proteomic techniques will also allow the tracking of quality changes and to study the allergies caused by seafood and seafood products, and impact the evaluations between aquatic organisms and environmental pollution.

Yet, the use of proteomics in aquaculture has been limited to date, although some of the biological questions have been addressed well using proteomics in aquaculture. Indeed, questions regarding which approach is best suited for the analysis of proteomes in samples of fish, shellfish and seafood/seafood product remained to be answered. This is needed in order to verify the associated results, determined by different laboratories using current proteomic technologies.

In future, it is anticipated that the development of more cost-effective and sensitive technologies, such as meta-proteomics and multi-dimensional liquid chromatography, will further enhance the value of proteomics to the field of aquaculture, allowing routine use of this approach.

As discussed earlier, proteomics has moved on from technical issues related to protein separation and protein identity to highly reproducible gel-based or gel-free systems. This increased ability to separate proteins and to perform peptide sequence analysis by mass spectrometry has

meant that the volume of data that is produced and the rate of identification of proteins is orders of magnitude greater than only a few years ago (Seidler et al., 2010; Simpson, 2012).

The road ahead appears to be full of promise, as the databases of proteomic information increase, and more efficient updated proteome techniques become available, thus presenting us with new opportunities to improve, increase and even create related products in the field of aquaculture. This will require interdisciplinary collaborations between a broad range of sciences, including those of physiology, cell biology and computer sciences, as well as from the aquaculture and food industries. For these reasons, bioinformatics approaches such as pathway analysis will continue to be important in providing functional insight into genomics and proteomics. The application of proteomics to the response of fish tissues to steroids must consider the various proteomic techniques are complementary, but will yield different information, due to separation and fractionation protocols, label-free or label methods MS/MS approaches, and database construction and search engines.

On the other hand, directly related to the increased volume of data generated, entails that extracting the relevant information, is no longer a simple matter of discussing a list of protein identities, and especially as interpretation of the proteins and their function is central to any medium- to large-scale proteome study (Malik et al., 2010; Sveinsdóttir et al., 2012).

In genetics, an expressed sequence tag (EST) is a short sub-sequence of a cDNA sequence, which can be used to identify gene transcripts, and EST were instrumental in gene discovery and in gene-sequence determination. The number of expressed sequence tags related to salmonid fish is currently in the order of 800,000 sequences, representing mRNAs encoding about 30–40,000 different proteins. Other commercial species including cod, sea bass, sea bream, and catfish amongst others are quickly catching up (Martin et al., 2008). These EST sequence tags can be used to help identify amino acid sequences generated during proteomics studies, which means that now the majority of proteins can be identified.

There is around 30,000 fish species, which include bony, jawless and cartilaginous fish, that constitute the largest vertebrate group. Despite their critical roles in many ecosystems, fish genomics is lagging behind work on birds and mammals. Contiguously, this also explains why fish proteomics is a very young research field that was born in the last few decades. There are now a considerable number of fish species whose whole genome is completely sequenced; zebrafish, two species of puffer fish, and stickleback have their genomes sequenced.

As more and more genes and protein sequences are deposited in databases, they are automatically annotated; and the quality of these annotations is probably one of the greatest hurdles in fully interpreting the output of either a transcriptomic study or proteomic studies. Currently, annotations include the nucleotide sequence, protein sequence, tissue distribution abundance of mRNA, gene ontology (GO) (Gaudet et al. 2009), and Kyoto Encyclopedia of Genes and Genomes (KEGG) (Okuda et al., 2008) pathways.

In future studies, data from other "omic" platforms should be combined, that is, incorporating transcriptomic data from microarray and deep sequencing and from metabolomic data. The complementary techniques, although performed often in different laboratories, do ask the same questions and one of the future steps will be to perform meta-analysis across these high throughput technologies.

To conclude this review article, we can say that the utilization of proteomics to DFO fisheries research will allow to improve our understanding of evolution and also enhance the progress of conservation and sustainable utilization of fish. To sum up, proteomics fisheries research has emerged as a powerful tool for the study of biological systems and their dynamics in different conditions, and this new fisheries technology has been increasingly used during the last years to address different questions related to fish biology.

10. References

Abbott, A. (1999). A post-genomic challenge: learning to read patterns of protein synthesis. *Nature*, *402*(6763), 715–720.

Abram, Q., Dixon, B., & Katzenback, B. (2017). Impacts of Low Temperature on the Teleost Immune System. *Biology*, *6*(4), 39. https://doi.org/10.3390/biology6040039

Adams, M. B., & Nowak, B. F. (2003). Amoebic gill disease: sequential pathology in cultured Atlantic salmon, Salmo salar L. *Journal of Fish Diseases*, *26*(10), 601–614. https://doi.org/10.1046/j.1365-2761.2003.00496.x

Adams, M. B., & Nowak, B. F. (2004). Sequential pathology after initial freshwater bath treatment for amoebic gill disease in cultured Atlantic salmon, Salmo salar L. *Journal of Fish Diseases*, *27*(3), 163–173. https://doi.org/10.1111/j.1365-2761.2004.00531.x

Addis, M. F., Cappuccinelli, R., Tedde, V., Pagnozzi, D., Viale, I., Meloni, M., Salati, F., Roggio, T., & Uzzau, S. (2010). Influence of Moraxella sp. colonization on the kidney proteome of farmed gilthead sea breams (Sparus aurata, L.). *Proteome Science*, *8*, 1–8. https://doi.org/10.1186/1477-5956-8-50

Aebersold, R., Bensimon, A., Collins, B. C., Ludwig, C., & Sabido, E. (2016). Applications and Developments in Targeted Proteomics: From SRM to DIA/SWATH. *Proteomics*, *16*(15–16), 2065–2067. https://doi.org/10.1002/pmic.201600203

Aegerter, S., & Jalabert, B. (2004). Effects of post-ovulatory oocyte ageing and temperature on egg quality and on the occurrence of triploid fry in rainbow trout, Oncorhynchus mykiss. *Aquaculture*, *231*(1–4), 59–71. https://doi.org/10.1016/j.aquaculture.2003.08.019

Agulleiro, M. J., Anguis, V., Cañavate, J. P., Martínez-Rodríguez, G., Mylonas, C. C., & Cerdà, J. (2006). Induction of spawning of captive-reared Senegal sole (Solea senegalensis) using different administration methods for gonadotropin-releasing hormone agonist. *Aquaculture*, *257*(1–4), 511–524. https://doi.org/10.1016/j.aquaculture.2006.02.001

Agulleiro, M. J., Scott, A. P., Duncan, N., Mylonas, C. C., & Cerdà, J. (2007). Treatment of GnRHa-implanted Senegalese sole (Solea senegalensis) with 11-ketoandrostenedione stimulates spermatogenesis and increases sperm motility. *Comparative Biochemistry and Physiology - A Molecular and Integrative Physiology*, *147*(4), 885–892. https://doi.org/10.1016/j.cbpa.2007.02.008

Akaike, T. (2015). Springer Handbook of Marine Biotechnology. In *Springer Handbook of Marine Biotechnology*.

Alberts, B., Johnson, A., Lewis, J., Raff, M., Roberts, K., & Walter, P. (2002). *The Shape and Structure of Proteins*. https://www.ncbi.nlm.nih.gov/books/NBK26830/

Alderman, S. L., Dindia, L. A., Kennedy, C. J., Farrell, A. P., & Gillis, T. E. (2017). Proteomic analysis of sockeye salmon serum as a tool for biomarker discovery and new insight into the sublethal toxicity of diluted bitumen. *Comparative Biochemistry and Physiology - Part D: Genomics and Proteomics*, *22*(March), 157–166. https://doi.org/10.1016/j.cbd.2017.04.003

Allfrey, V. G., Faulkner, R., & Mirsky, A. E. (1964). Acetylation and methylation of histones and their possible role in the regulation of rna synthesis. *Proceedings of the National Academy of Sciences*, *51*(5), 786–794. https://doi.org/10.1073/pnas.51.5.786

Alves, R. N., Cordeiro, O., Silva, T. S., Richard, N., de Vareilles, M., Marino, G., di Marco, P., Rodrigues, P. M., & Conceição, L. E. C. (2010). Metabolic molecular indicators of chronic stress in gilthead seabream (Sparus aurata) using comparative proteomics. *Aquaculture*, *299*(1–4), 57–66. https://doi.org/10.1016/j.aquaculture.2009.11.014

Andersen, H. R., Andersson, A. M., Arnold, S. F., Autrup, H., Barfoed, M., Beresford, N. A., Bjerregaard, P., Christiansen, L. B., Gissel, B., Hummel, R., Jørgensen, E. B., Korsgaard, B., le Guevel, R., Leffers, H., McLachlan, J., Møller, A., Nielsen, J. B., Olea, N., Oles-Karasko, A., … Grandjean, P. (1999). Comparison of short-term estrogenicity tests for identification of hormone-disrupting chemicals. *Environmental Health Perspectives*, *107*(SUPPL. 1), 89–108. https://doi.org/10.1289/ehp.99107s189

Andersen, J. S., & Mann, M. (2006). Organellar proteomics: Turning inventories into insights. *EMBO Reports*, *7*(9), 874–879. https://doi.org/10.1038/sj.embor.7400780

Ángeles Esteban, M. (2012). An Overview of the Immunological Defenses in Fish Skin. *ISRN Immunology*, *2012*, 1–29. https://doi.org/10.5402/2012/853470

Anguis, V., & Cañavate, J. P. (2005). Spawning of captive Senegal sole (Solea senegalensis) under a naturally fluctuating temperature regime. *Aquaculture*, *243*(1–4), 133–145. https://doi.org/10.1016/j.aquaculture.2004.09.026

Ao, J., Mu, Y., Xiang, L. X., Fan, D. D., Feng, M. J., Zhang, S., Shi, Q., Zhu, L. Y., Li, T., Ding, Y., Nie, L., Li, Q., Dong, W. ren, Jiang, L., Sun, B., Zhang, X. H., Li, M., Zhang, H. Q., Xie, S. B., … Chen, X. (2015). Genome Sequencing of the Perciform Fish Larimichthys crocea Provides Insights into Molecular and Genetic Mechanisms of Stress Adaptation. *PLoS Genetics*, *11*(4), 1–25. https://doi.org/10.1371/journal.pgen.1005118

Arizza, V., Giaramita, F. T., Parrinello, D., Cammarata, M., & Parrinello, N. (2007). Cell cooperation in coelomocyte cytotoxic activity of Paracentrotus lividus coelomocytes. *Comparative*

Biochemistry and Physiology Part A: Molecular & Integrative Physiology, *147*(2), 389–394. https://doi.org/10.1016/j.cbpa.2007.01.022

Babaheydari, S. B., Keyvanshokooh, S., Dorafshan, S., & Johari, S. A. (2016). Proteomic analysis of skeletal deformity in diploid and triploid rainbow trout (Oncorhynchus mykiss) larvae. *Comparative Biochemistry and Physiology - Part D: Genomics and Proteomics*, *19*, 1–7. https://doi.org/10.1016/j.cbd.2016.05.001

Balasubramanian S., Baby Rani P., Arul Prakash A., Prakash M.*, S. P. and G. G., & Department. (2012). Antimicrobial properties of skin mucus from four freshwater cultivable Fishes (Catla catla, Hypophthalmichthys molitrix, Labeo rohita and Ctenopharyngodon idella). *Asian J Biol Sci*, *24*(6), 5110–5120.

Baldwin, D. H., Spromberg, J. A., Collier, T. K., & Scholz, N. L. (2009). A fish of many scales: extrapolating sublethal pesticide exposures to the productivity of wild salmon populations. *Ecological Applications*, *19*(8), 2004–2015. https://doi.org/10.1890/08-1891.1

Balestrieri, M., Giovane, A., Mancini, F., & Napoli, C. (2008). Proteomics and Cardiovascular Disease: An Update. *Current Medicinal Chemistry*, *15*(6), 555–572. https://doi.org/10.2174/092986708783769713

Banoub, J., Cohen, A., Mansour, A., & Thibault, P. (2004). Characterization and de novo sequencing of Atlantic salmon vitellogenin protein by electrospray tandem and matrix-assisted laser desorption/ionization mass spectrometry. *European Journal of Mass Spectrometry*, *10*(1), 121–134. https://doi.org/10.1255/ejms.588

Banoub, J., Thibault, P., Mansour, A., Cohen, A., Heeley, D. H., & Jackman, D. (2003). Characterisation of the intact rainbow trout vitellogenin protein and analysis of its derived tryptic and cyanogen bromide peptides by matrix-assisted laser desorption/ionisation time-of-flight-mass spectrometry and electrospray ionisation quadrupole/time. *European Journal of Mass Spectrometry*, *9*(5), 509–524. https://doi.org/10.1255/ejms.572

Barrera, T. G., & Gómez Ariza, J. L. (2017). Environmental problems in marine biology: Methodological aspects and applications. In *Environmental Problems in Marine Biology: Methodological Aspects and Applications*. https://doi.org/10.1201/9781315119113

Bartel, M., Hartmann, S., Lehmann, K., Postel, K., Quesada, H., Philipp, E. E. R., Heilmann, K., Micheel, B., & Stuckas, H. (2012). Identification of sperm proteins as candidate biomarkers for the analysis of reproductive isolation in Mytilus: A case study for the enkurin locus. *Marine Biology*, *159*(10), 2195–2207. https://doi.org/10.1007/s00227-012-2005-7

Baumann, H., & Gauldie, J. (1994). The acute phase response. In *NeuroImmune Biology* (Vol. 3, Issue C, pp. 463–494). https://doi.org/10.1016/S1567-7443(03)80059-5

Baumann, K., Casewell, N. R., Ali, S. A., Jackson, T. N. W., Vetter, I., Dobson, J. S., Cutmore, S. C., Nouwens, A., Lavergne, V., & Fry, B. G. (2014). A ray of venom: Combined proteomic and transcriptomic investigation of fish venom composition using barb tissue from the blue-spotted stingray (Neotrygon kuhlii). *Journal of Proteomics*, *109*, 188–198. https://doi.org/10.1016/j.jprot.2014.06.004

Bayne, C. J., & Gerwick, L. (2001). The acute phase response and innate immunity of fish. *Developmental and Comparative Immunology*, *25*(8–9), 725–743. https://doi.org/10.1016/S0145-305X(01)00033-7

Bayne, C. J., Gerwick, L., Fujiki, K., Nakao, M., & Yano, T. (2001). Immune-relevant (including acute phase) genes identified in the livers of rainbow trout, Oncorhynchus mykiss, by means of suppression subtractive hybridization. *Developmental and Comparative Immunology*, *25*(3), 205–217. https://doi.org/10.1016/S0145-305X(00)00057-4

Bayram, H. L., Claydon, A. J., Brownridge, P. J., Hurst, J. L., Mileham, A., Stockley, P., Beynon, R. J., & Hammond, D. E. (2016). Cross-species proteomics in analysis of mammalian sperm proteins. *Journal of Proteomics*, *135*, 38–50. https://doi.org/10.1016/j.jprot.2015.12.027

Ben-Nissan, G., & Sharon, M. (2014). Regulating the 20S proteasome ubiquitin-independent degradation pathway. *Biomolecules*, *4*(3), 862–884. https://doi.org/10.3390/biom4030862

Beretta, L. (2009). Comparative analysis of the liver and plasma proteomes as a novel and powerful strategy for hepatocellular carcinoma biomarker discovery. *Cancer Letters*, *286*(1), 134–139. https://doi.org/10.1016/j.canlet.2009.01.025

Berthelot, C., Brunet, F., Chalopin, D., Juanchich, A., Bernard, M., Noël, B., Bento, P., da Silva, C., Labadie, K., Alberti, A., Aury, J. M., Louis, A., Dehais, P., Bardou, P., Montfort, J., Klopp, C.,

Cabau, C., Gaspin, C., Thorgaard, G. H., … Guiguen, Y. (2014). The rainbow trout genome provides novel insights into evolution after whole-genome duplication in vertebrates. *Nature Communications*, *5*. https://doi.org/10.1038/ncomms4657

Biales, A. D., Bencic, D. C., Flick, R. L., Blocksom, K. A., Lazorchak, J. M., & Lattier, D. L. (2011). Proteomic analysis of a model fish species exposed to individual pesticides and a binary mixture. *Aquatic Toxicology*, *101*(1), 196–206. https://doi.org/10.1016/j.aquatox.2010.09.019

Billard, R. (1992). Reproduction in rainbow trout: sex differentiation, dynamics of gametogenesis, biology and preservation of gametes. *Aquaculture*, *100*(1–3), 263–298. https://doi.org/10.1016/0044-8486(92)90385-X

Billard R., Cosson J., Perchec G., & Linhart O. (1995). Biology of sperm and artificial reproduction in carp. *Aquaculture*, *129*, 95–112.

Bird, S., Zou, J., & Secombes, C. (2007). Advances in Fish Cytokine Biology Give Clues to the Evolution of a Complex Network. *Current Pharmaceutical Design*, *12*(24), 3051–3069. https://doi.org/10.2174/138161206777947434

Blackstock, W. P., & Weir, M. P. (1999). Proteomics: Quantitative and physical mapping of cellular proteins. *Trends in Biotechnology*, *17*(3), 121–127. https://doi.org/10.1016/S0167-7799(98)01245-1

Bobe, J., & William Goetz, F. (2001). An Ovarian Progastricsin Is Present in the Trout Coelomic Fluid after Ovulation1. *Biology of Reproduction*, *64*(4), 1048–1055. https://doi.org/10.1095/biolreprod64.4.1048

Bogyo, M., & Cravatt, B. F. (2007). Genomics and proteomics. *Current Opinion in Chemical Biology*, *11*(1), 1–3. https://doi.org/10.1016/j.cbpa.2006.12.029

Boonmee, A., Heude Berthelin, C., Kingtong, S., Pauletto, M., Bernay, B., Adeline, B., Suquet, M., Sourdaine, P., & Kellner, K. (2016). Differential protein expression during sperm maturation and capacitation in an hermaphroditic bivalve, Pecten maximus (Linnaeus, 1758). *Journal of Molluscan Studies*, *82*(4), 575–584. https://doi.org/10.1093/mollus/eyw028

Borges, M. H., Andrich, F., Lemos, P. H., Soares, T. G., Menezes, T. N., Campos, F. v., Neves, L. X., Castro-Borges, W., & Figueiredo, S. G. (2018). Combined proteomic and functional analysis

reveals rich sources of protein diversity in skin mucus and venom from the Scorpaena plumieri fish. *Journal of Proteomics*, *187*(June), 200–211. https://doi.org/10.1016/j.jprot.2018.08.002

Borràs, E., & Sabidó, E. (2017). What is targeted proteomics? A concise revision of targeted acquisition and targeted data analysis in mass spectrometry. *Proteomics*, *17*(17–18), 17–18. https://doi.org/10.1002/pmic.201700180

Børresen, T. (1992). Quality aspects of wild and reared fish. *Quality Assurance in the Fish Industry*, 1–17.

Boshra, H., Li, J., & Sunyer, J. O. (2006). Recent advances on the complement system of teleost fish. *Fish and Shellfish Immunology*, *20*(2), 239–262. https://doi.org/10.1016/j.fsi.2005.04.004

Bossart, G. D., Baden, D. G., Ewing, R. Y., Roberts, B., & Wright, S. D. (1998). Brevetoxicosis in Manatees (Trichechus manatus latirostris) from the 1996 Epizootic: Gross, Histologic, and Immunohistochemical Features. *Toxicologic Pathology*, *26*(2), 276–282. https://doi.org/10.1177/019262339802600214

Boyd, I., Hanson, N., & Tynan, C. T. (2019). Effects of climate change on marine mammals. *Encyclopedia of Ocean Sciences, January*, 416–419. https://doi.org/10.1016/B978-0-12-409548-9.11627-6

Brewis, I. A., & Gadella, B. M. (2010). Sperm surface proteomics: from protein lists to biological function. *Molecular Human Reproduction*, *16*(2), 68–79. https://doi.org/10.1093/molehr/gap077

Bridle, A. R., Morrison, R. N., Cupit Cunningham, P. M., & Nowak, B. F. (2006). Quantitation of immune response gene expression and cellular localisation of interleukin-1β mRNA in Atlantic salmon, Salmo salar L., affected by amoebic gill disease (AGD). *Veterinary Immunology and Immunopathology*, *114*(1–2), 121–134. https://doi.org/10.1016/j.vetimm.2006.08.002

Bridle, A. R., Morrison, R. N., & Nowak, B. F. (2006). The expression of immune-regulatory genes in rainbow trout, Oncorhynchus mykiss, during amoebic gill disease (AGD). *Fish and Shellfish Immunology*, *20*(3), 346–364. https://doi.org/10.1016/j.fsi.2005.05.014

Brinchmann, M. F. (2016). Immune relevant molecules identified in the skin mucus of fish using -omics technologies. *Molecular BioSystems*, *12*(7), 2056–2063. https://doi.org/10.1039/c5mb00890e

Brunt, J., Hansen, R., Jamieson, D. J., & Austin, B. (2008). Proteomic analysis of rainbow trout (Oncorhynchus mykiss, Walbaum) serum after administration of probiotics in diets. *Veterinary Immunology and Immunopathology*, *121*(3–4), 199–205. https://doi.org/10.1016/j.vetimm.2007.09.010

Buckley, K. M., & Rast, J. P. (2012). Dynamic Evolution of Toll-Like Receptor Multigene Families in Echinoderms. *Frontiers in Immunology*, *3*. https://doi.org/10.3389/fimmu.2012.00136

Cabrita, E., Soares, F., & Dinis, M. T. (2006). Characterization of Senegalese sole, Solea senegalensis, male broodstock in terms of sperm production and quality. *Aquaculture*, *261*(3), 967–975. https://doi.org/10.1016/j.aquaculture.2006.08.020

Campana, S. E., & Thorrold, S. R. (2001). Otoliths, increments, and elements: keys to a comprehensive understanding of fish populations? *Canadian Journal of Fisheries and Aquatic Sciences*, *58*(1), 30–38.

Campos, A., Tedesco, S., Vasconcelos, V., & Cristobal, S. (2012). Proteomic research in bivalves. *Journal of Proteomics*, *75*(14), 4346–4359. https://doi.org/10.1016/j.jprot.2012.04.027

Carrera, M., Cañas, B., & Gallardo, J. M. (2013). Proteomics for the assessment of quality and safety of fishery products. *Food Research International*, *54*(1), 972–979. https://doi.org/10.1016/j.foodres.2012.10.027

Carrera, M., Cañas, B., Piñeiro, C., Vázquez, J., & Gallardo, J. M. (2007). De novo mass spectrometry sequencing and characterization of species-specific peptides from nucleoside diphosphate kinase B for the classification of commercial fish species belonging to the family merlucciidae. *Journal of Proteome Research*, *6*(8), 3070–3080. https://doi.org/10.1021/pr0701963

Carrera, M., Cañas, B., Vázquez, J., & Gallardo, J. M. (2010a). Extensive de Novo sequencing of new parvalbumin isoforms using a novel combination of bottom-up proteomics, accurate molecular mass measurement by FTICR-MS, and selected MS/MS ion monitoring. *Journal of Proteome Research*, *9*(9), 4393–4406. https://doi.org/10.1021/pr100163e

Carrera, M., Cañas, B., Vázquez, J., & Gallardo, J. M. (2010b). Extensive de Novo sequencing of new parvalbumin isoforms using a novel combination of bottom-up proteomics, accurate molecular

mass measurement by FTICR-MS, and selected MS/MS ion monitoring. *Journal of Proteome Research*, *9*(9), 4393–4406. https://doi.org/10.1021/pr100163e

Carrera, M., Ezquerra-Brauer, J. M., & Aubourg, S. P. (2020). Characterization of the jumbo squid (dosidicus gigas) skin by-product by shotgun proteomics and protein-based bioinformatics. *Marine Drugs*, *18*(1). https://doi.org/10.3390/md18010031

Carrera, M., Piñeiro, C., & Martinez, I. (2020). Proteomic Strategies to Evaluate the Impact of Aquaculture Products. *Foods*, *9*.

Casewell, N. R., Wüster, W., Vonk, F. J., Harrison, R. A., & Fry, B. G. (2013). Complex cocktails: The evolutionary novelty of venoms. *Trends in Ecology and Evolution*, *28*(4), 219–229. https://doi.org/10.1016/j.tree.2012.10.020

Causey, D. R., Pohl, M. A. N., Stead, D. A., Martin, S. A. M., Secombes, C. J., & Macqueen, D. J. (2018). High-throughput proteomic profiling of the fish liver following bacterial infection. *BMC Genomics*, *19*(1), 1–17. https://doi.org/10.1186/s12864-018-5092-0

Chaurand, P., Friedman, D. B., & Caprioli, R. M. (2008). Mass Spectrometry in Cancer Biology. *The Molecular Basis of Cancer*, 293–307. https://doi.org/10.1016/B978-141603703-3.10022-6

Chen, C., Hou, J., Tanner, J. J., & Cheng, J. (2020). Bioinformatics methods for mass spectrometry-based proteomics data analysis. *International Journal of Molecular Sciences*, *21*(8). https://doi.org/10.3390/ijms21082873

Chen, J., Wu, H. Q., Shi, Y. H., Li, C. H., & Li, M. Y. (2009). The effects of environmental salinity on trunk kidney proteome of juvenile ayu (Plecoglossus altivelis). *Comparative Biochemistry and Physiology Part D: Genomics and Proteomics*, *4*(4), 263–267.

Chen, L. L., Xie, J., Cao, D. D., Jia, N., Li, Y. J., Sun, H., Li, W. F., Hu, B., Chen, Y., & Zhou, C. Z. (2018). The pore-forming protein Aep1 is an innate immune molecule that prevents zebrafish from bacterial infection. *Developmental and Comparative Immunology*, *82*, 49–54. https://doi.org/10.1016/j.dci.2018.01.003

Chiaramonte, M., Arizza, V., & Russo, R. (2019). Evolutionary conserved pathway of the innate immune response after a viral insult in Paracentrotus lividus sea urchin. *International Journal of Immunogenetics*, *46*(3), 192–202. https://doi.org/10.1111/iji.12424

Chiaramonte, M., & Russo, R. (2015). The echinoderm innate humoral immune response. *Italian Journal of Zoology*, *82*(3), 300–308. https://doi.org/10.1080/11250003.2015.1061615

Cho, W. C. S. (2007). Proteomics Technologies and Challenges From Genomics to Proteomics. *Genomics, Proteomics & Bioinformatics*, *5*(2), 77–85.

Choudhury, M., Yamada, S., Komatsu, M., Kishimura, H., & Ando, S. (2009). Homologue of mammalian apolipoprotein A-II in non-mammalian vertebrates. *Acta Biochimica et Biophysica Sinica*, *41*(5), 370–378. https://doi.org/10.1093/abbs/gmp015

Chu, W., Li, Y., Wu, P., Chen, D., Chen, J., Shi, J., & Zhang, J. (2014). Characterization and expression analysis of myogenin gene in white muscle of Chinese mandarin fish, Siniperca chuatsi. *Journal of Proteomics and Bioinformatics*, *7*(3), 71–76. https://doi.org/10.4172/jpb.1000304

Ciereszko, A. (2008). Chemical composition of seminal plasma and its physiological relationship with sperm motility, fertilizing capacity, and cryopreservation success. In K. C. and G. R. S. M. H. Alavi, J. Cosson (Ed.), *fish. In: Fish Spermatology* (1st ed.). Alpha Science International Ltd. Oxford.

Ciereszko, A., Dietrich, M. A. A., & Nynca, J. (2017a). Fish semen proteomics — New opportunities in fish reproductive research. *Aquaculture*, *472*, 81–92. https://doi.org/10.1016/j.aquaculture.2016.03.005

Ciereszko, A., Dietrich, M. A., & Nynca, J. (2012). The identification of seminal proteins in fish: From a traditional approach to proteomics. *Journal of Applied Ichthyology*, *28*(6), 865–872. https://doi.org/10.1111/jai.12052

Ciereszko, A., Dietrich, M. A., & Nynca, J. (2017b). Fish semen proteomics — New opportunities in fish reproductive research. *Aquaculture*, *472*, 81–92. https://doi.org/10.1016/j.aquaculture.2016.03.005

Ciereszko, A.; Glogowski, J.; Dabrowski, K. (2011). Biochemical characteristics of seminal plasma and spermatozoa of freshwater fish and the relation to semen biology, quality and cryopreservation. In T. R. T. and C. C. Green (Ed.), *Cryopreservation in Aquatic Species* (2nd ed., pp. 46–79). World Aquaculture Society, Baton Rouge.

Ciereszko, A., Liu, L., & Dabrowski, K. (1996). Effects of season and dietary ascorbic acid on some biochemical characteristics of rainbow trout (Oncorhynchus mykiss) semen. *Fish Physiology and Biochemistry*, *15*(1), 1–10. https://doi.org/10.1007/BF01874832

Ciereszko, A., Wlasow, T., Dobosz, S., Goryczko, K., & Glogowski, J. (2004). Blood cells in rainbow trout Oncorhynchus mykiss milt: Relation to milt collection method and sampling period. *Theriogenology*, *62*(7), 1353–1364. https://doi.org/10.1016/j.theriogenology.2004.02.003

Clauser, K. R., Baker, P., & Burlingame, A. L. (1999). Role of accurate mass measurement (±10 ppm) in protein identification strategies employing MS or MS/MS and database searching. *Analytical Chemistry*, *71*(14), 2871–2882.

Cohen, A. M., Jahouh, F., Sioud, S., Rideout, R. M., Morgan, M. J., & Banoub, J. H. (2009a). Quantification of Greenland halibut serum vitellogenin: a trip from the deep sea to the mass spectrometer. *Rapid Communications in Mass Spectrometry*, *23*(7), 1049–1060. https://doi.org/10.1002/rcm.3966

Cohen, A. M., Jahouh, F., Sioud, S., Rideout, R. M., Morgan, M. J., & Banoub, J. H. (2009b). Quantification of Greenland halibut serum vitellogenin: a trip from the deep sea to the mass spectrometer. *Rapid Communications in Mass Spectrometry*, *23*(7), 1049–1060. https://doi.org/10.1002/rcm.3966

Cohen, A. M., Mansour, A. A. H., & Banoub, J. H. (2005a). “De novo” sequencing of Atlantic cod vitellogenin tryptic peptides by matrix-assisted laser desorption/ionization quadrupole time-of-flight tandem mass spectrometry: Similarities with haddock vitellogenin. *Rapid Communications in Mass Spectrometry*, *19*(17), 2454–2460. https://doi.org/10.1002/rcm.2084

Cohen, A. M., Mansour, A. A. H., & Banoub, J. H. (2005b). “De novo” sequencing of Atlantic cod vitellogenin tryptic peptides by matrix-assisted laser desorption/ionization quadrupole time-of-flight tandem mass spectrometry: Similarities with haddock vitellogenin. *Rapid Communications in Mass Spectrometry*, *19*(17), 2454–2460. https://doi.org/10.1002/rcm.2084

Cohen, A. M., Mansour, A. A. H., & Banoub, J. H. (2006a). Absolute quantification of Atlantic salmon and rainbow trout vitellogenin by the “signature peptide” approach using electrospray ionization

QqToF tandem mass spectrometry. *Journal of Mass Spectrometry*, *41*(5), 646–658. https://doi.org/10.1002/jms.1023

Cohen, A. M., Mansour, A. A. H., & Banoub, J. H. (2006b). Absolute quantification of Atlantic salmon and rainbow trout vitellogenin by the “signature peptide” approach using electrospray ionization QqToF tandem mass spectrometry. *Journal of Mass Spectrometry*, *41*(5), 646–658. https://doi.org/10.1002/jms.1023

Cole, A. M., Weis, P., & Diamond, G. (1997). Isolation and characterization of pleurocidin, an antimicrobial peptide in the skin secretions of winter flounder. *Journal of Biological Chemistry*, *272*(18), 12008–12013. https://doi.org/10.1074/jbc.272.18.12008

Conibear, A. C. (2020). Deciphering protein post-translational modifications using chemical biology tools. *Nature Reviews Chemistry*, *4*(12), 674–695. https://doi.org/10.1038/s41570-020-00223-8

Corbett-Detig, R. B., Zhou, J., Clark, A. G., Hartl, D. L., & Ayroles, J. F. (2013). Genetic incompatibilities are widespread within species. *Nature*, *504*(7478), 135–137. https://doi.org/10.1038/nature12678

Cordero, H., Brinchmann, M. F., Cuesta, A., & Esteban, M. A. (2017). Chronic wounds alter the proteome profile in skin mucus of farmed gilthead seabream. *BMC Genomics*, *18*(1), 1–14. https://doi.org/10.1186/s12864-017-4349-3

Cordero, H., Brinchmann, M. F., Cuesta, A., Meseguer, J., & Esteban, M. A. (2015a). Skin mucus proteome map of European sea bass (Dicentrarchus labrax). *Proteomics*, *15*(23–24), 4007–4020. https://doi.org/10.1002/pmic.201500120

Cordero, H., Brinchmann, M. F., Cuesta, A., Meseguer, J., & Esteban, M. A. (2015b). Skin mucus proteome map of European sea bass (Dicentrarchus labrax). *PROTEOMICS*, *15*(23–24), 4007–4020. https://doi.org/10.1002/pmic.201500120

Cordero, H., Morcillo, P., Cuesta, A., Brinchmann, M. F., & Esteban, M. A. (2016a). Differential proteome profile of skin mucus of gilthead seabream (Sparus aurata) after probiotic intake and/or overcrowding stress. *Journal of Proteomics*, *132*, 41–50. https://doi.org/10.1016/j.jprot.2015.11.017

Cordero, H., Morcillo, P., Cuesta, A., Brinchmann, M. F., & Esteban, M. A. (2016b). Differential proteome profile of skin mucus of gilthead seabream (Sparus aurata) after probiotic intake and/or overcrowding stress. *Journal of Proteomics*, *132*, 41–50. https://doi.org/10.1016/j.jprot.2015.11.017

Costa, P. M., Chicano-Gálvez, E., López Barea, J., Delvalls, T. A., & Costa, M. H. (2010). Alterations to proteome and tissue recovery responses in fish liver caused by a short-term combination treatment with cadmium and benzo[a]pyrene. *Environmental Pollution*, *158*(10), 3338–3346. https://doi.org/10.1016/j.envpol.2010.07.030

Costes, B., Raj, † V Stalin, Michel, † B, Fournier, G., Thirion, M., Gillet, L., Mast, J., Lieffrig, F., Bremont, M., & Vanderplasschen, A. (2009). The Major Portal of Entry of Koi Herpesvirus in Cyprinus carpio Is the Skin. *JOURNAL OF VIROLOGY*, *83*(7), 2819–2830. https://doi.org/10.1128/JVI.02305-08

Council, N. R. (1993). *Nutrient requirements of fish*. National Academies Press.

Cox, J., & Mann, M. (2008). MaxQuant enables high peptide identification rates, individualized p.p.b.-range mass accuracies and proteome-wide protein quantification. *Nature Biotechnology*, *26*(12), 1367–1372. https://doi.org/10.1038/nbt.1511

Cox, J., Neuhauser, N., Michalski, A., Scheltema, R. A., Olsen, J. v., & Mann, M. (2011). Andromeda: A peptide search engine integrated into the MaxQuant environment. *Journal of Proteome Research*, *10*(4), 1794–1805. https://doi.org/10.1021/pr101065j

da Costa, J. P., Carvalhais, V., Ferreira, R., Amado, F., Vilanova, M., Cerca, N., & Vitorino, R. (2015). Proteome signatures—how are they obtained and what do they teach us? *Applied Microbiology and Biotechnology*, *99*(18), 7417–7431. https://doi.org/10.1007/s00253-015-6795-7

Dawar, F. U., Tu, J., Xiong, Y., Lan, J., Dong, X. X., Liu, X., Khattak, M. N. K., Mei, J., & Lin, L. (2016). Chemotactic activity of cyclophilin a in the skin mucus of yellow catfish (Pelteobagrus fulvidraco) and its active site for chemotaxis. *International Journal of Molecular Sciences*, *17*(9). https://doi.org/10.3390/ijms17091422

Dayhoff, M. O., Barker, W. C., & Hunt, L. T. (1983). [47] Establishing homologies in protein sequences. In *Human Immunology* (Vol. 73, Issue 4, pp. 524–545). https://doi.org/10.1016/S0076-6879(83)91049-2

de Francesco, M., Parisi, G., Médale, F., Lupi, P., Kaushik, S. J., & Poli, B. M. (2004). Effect of long-term feeding with a plant protein mixture based diet on growth and body/fillet quality traits of large rainbow trout (Oncorhynchus mykiss) Matilde de Francescoa, Giuliana Parisia, Françoise Médaleb, Paola Lupia, Sadasivam J. Kaushikb and Bi. *Aquaculture*, *236*(June), 7–12.

de Souza, A. G., MacCormack, T. J., Wang, N., Li, L., & Goss, G. G. (2009). Large-scale proteome profile of the zebrafish (Danio rerio) gill for physiological and biomarker discovery studies. *Zebrafish*, *6*(3), 229–238. https://doi.org/10.1089/zeb.2009.0591

de Souza, K. B., Jutfelt, F., Kling, P., Förlin, L., & Sturve, J. (2014). Effects of increased CO2on fish gill and plasma proteome. *PLoS ONE*, *9*(7). https://doi.org/10.1371/journal.pone.0102901

de Vareilles, M., Conceição, L. E. C., Gómez-Requeni, P., Kousoulaki, K., Richard, N., Rodrigues, P. M., Fladmark, K. E., & Rønnestad, I. (2012). Dietary Lysine Imbalance Affects Muscle Proteome in Zebrafish (Danio rerio): A Comparative 2D-DIGE Study. *Marine Biotechnology*, *14*(5), 643–654. https://doi.org/10.1007/s10126-012-9462-3

Denslow, N. D., Chow, M. C., Kroll, K. J., & Green, L. (1999). Vitellogenin as a biomarker of exposure for estrogen or estrogen mimics. *Ecotoxicology*, *8*(5), 385–398. https://doi.org/10.1023/A:1008986522208

Dheilly, N. M., Raftos, D. A., Haynes, P. A., Smith, L. C., & Nair, S. v. (2013). Shotgun proteomics of coelomic fluid from the purple sea urchin, Strongylocentrotus purpuratus. *Developmental and Comparative Immunology*, *40*(1), 35–50. https://doi.org/10.1016/j.dci.2013.01.007

Di, G., Li, Y., Zhu, G., Guo, X., Li, H., Huang, M., Shen, M., & Ke, C. (2019). Effects of acidification on the proteome during early development of Babylonia areolata. *FEBS Open Bio*, *9*(9), 1503–1520. https://doi.org/10.1002/2211-5463.12695

Diamond, G., Beckloff, N., Weinberg, A., & Kisich, K. (2009). The Roles of Antimicrobial Peptides in Innate Host Defense. *Current Pharmaceutical Design*, *15*(21), 2377–2392. https://doi.org/10.2174/138161209788682325

Dietrich, M. A., Adamek, M., Bilińska, B., Hejmej, A., Steinhagen, D., & Ciereszko, A. (2014). Characterization, expression and antibacterial properties of apolipoproteins A from carp (Cyprinus carpio L.) seminal plasma. *Fish and Shellfish Immunology*, *41*(2), 389–401. https://doi.org/10.1016/j.fsi.2014.09.020

Dietrich, M. A., Arnold, G. J., Fröhlich, T., & Ciereszko, A. (2014). In-depth proteomic analysis of carp (Cyprinus carpio L) spermatozoa. *Comparative Biochemistry and Physiology - Part D: Genomics and Proteomics*, *12*, 10–15. https://doi.org/10.1016/j.cbd.2014.09.003

Dietrich, M. A., Arnold, G. J., Nynca, J., Fröhlich, T., Otte, K., & Ciereszko, A. (2014). Characterization of carp seminal plasma proteome in relation to blood plasma. *Journal of Proteomics*, *98*, 218–232. https://doi.org/10.1016/j.jprot.2014.01.005

Dietrich, M. A., Nynca, J., & Ciereszko, A. (2019). Proteomic and metabolomic insights into the functions of the male reproductive system in fishes. *Theriogenology*, *132*, 182–200. https://doi.org/10.1016/j.theriogenology.2019.04.018

Diwan, A. D. (2021). Basics of Proteomics in Shrimp. In *Biotechnology of Penaeid Shrimps* (pp. 43–67). CRC Press. https://doi.org/10.1201/9781003155966-3

Diz, A. P., Dudley, E., & Skibinski, D. O. F. (2012). Identification and characterization of highly expressed proteins in sperm cells of the marine mussel Mytilus edulis. *Proteomics*, *12*(12), 1949–1956. https://doi.org/10.1002/pmic.201100500

DIZ, A. P., MARTÍNEZ-FERNÁNDEZ, M., & ROLÁN-ALVAREZ, E. (2012). Proteomics in evolutionary ecology: linking the genotype with the phenotype. *Molecular Ecology*, *21*(5), 1060–1080. https://doi.org/10.1111/j.1365-294X.2011.05426.x

Domon, B., & Aebersold, R. (2006). Mass spectrometry and protein analysis. *Science*, *312*(5771), 212–217. https://doi.org/10.1126/science.1124619

Dong, X., Qin, Z., Hu, X., Lan, J., Yuan, G., Asim, M., Zhou, Y., Ai, T., Mei, J., & Lin, L. (2015). Molecular cloning and functional characterization of cyclophilin A in yellow catfish (Pelteobagrus fulvidraco). *Fish and Shellfish Immunology*, *45*(2), 422–430. https://doi.org/10.1016/j.fsi.2015.04.002

Dorts, J., Kestemont, P., Dieu, M., Raes, M., & Silvestre, F. (2011). Proteomic response to sublethal cadmium exposure in a sentinel fish species, Cottus gobio. *Journal of Proteome Research*, *10*(2), 470–478. https://doi.org/10.1021/pr100650z

Dowling, V. A., & Sheehan, D. (2006a). Proteomics as a route to identification of toxicity targets in environmental toxicology. *Proteomics*, *6*(20), 5597–5604. https://doi.org/10.1002/pmic.200600274

Dowling, V. A., & Sheehan, D. (2006b). Proteomics as a route to identification of toxicity targets in environmental toxicology. *PROTEOMICS*, *6*(20), 5597–5604. https://doi.org/10.1002/pmic.200600274

Drabik, A., Bierczynska-Krzysik, A., Bodzon-Kulakowska, A., Suder, P., Kotlinska, J., & Silberring, J. (2007). Proteomics in neurosciences. *Mass Spectrometry Reviews*, *26*(3), 432–450. https://doi.org/10.1002/mas.20131

Dun, M. D., Smith, N. D., Baker, M. A., Lin, M., John Aitken, R., & Nixon, B. (2011). The chaperonin containing TCP1 complex (CCT/TRiC) is involved in mediating sperm-oocyte interaction. *Journal of Biological Chemistry*, *286*(42), 36875–36887. https://doi.org/10.1074/jbc.M110.188888

Dutta, H. M., Misquitta, D., & Khan, S. (2006). The effects of endosulfan on the testes of bluegill fish, Lepomis macrochirus: A histopathological study. *Archives of Environmental Contamination and Toxicology*, *51*(1), 149–156. https://doi.org/10.1007/s00244-005-1061-0

Easy, R. H., & Ross, N. W. (2009). Changes in Atlantic salmon (Salmo salar) epidermal mucus protein composition profiles following infection with sea lice (Lepeophtheirus salmonis). *Comparative Biochemistry and Physiology - Part D: Genomics and Proteomics*, *4*(3), 159–167. https://doi.org/10.1016/j.cbd.2009.02.001

Education, J. S. D. (2021). *Whole-Mount In Situ Hybridization*. Developmental Biology. https://www.jove.com/v/5330/whole-mount-in-situ-hybridization

Einen, O., Mørkøre, T., Rørå, A. M. B., & Thomassen, M. S. (1999). Feed ration prior to slaughter—a potential tool for managing product quality of Atlantic salmon (Salmo salar). *Aquaculture*, *178*(1–2), 149–169.

Ellis, A. E. (2001). Innate host defense mechanisms of fish against viruses and bacteria. *Developmental and Comparative Immunology*, *25*(8–9), 827–839. https://doi.org/10.1016/S0145-305X(01)00038-6

Eng, J. K., McCormack, A. L., & Yates, J. R. (1994). An approach to correlate tandem mass spectral data of peptides with amino acid sequences in a protein database. *Journal of the American Society for Mass Spectrometry*, *5*(11), 976–989. https://doi.org/10.1016/1044-0305(94)80016-2

Estruch, G., Martínez-Llorens, S., Tomás-Vidal, A., Monge-Ortiz, R., Jover-Cerdá, M., Brown, P. B., & Peñaranda, D. S. (2020). Impact of high dietary plant protein with or without marine ingredients in gut mucosa proteome of gilthead seabream (Sparus aurata, L.). *Journal of Proteomics*, *216*(September 2019), 103672. https://doi.org/10.1016/j.jprot.2020.103672

Fæste, C. K., Moen, A., Schniedewind, B., Haug Anonsen, J., Klawitter, J., & Christians, U. (2016). Development of liquid chromatography-tandem mass spectrometry methods for the quantitation of Anisakis simplex proteins in fish. *Journal of Chromatography A*, *1432*, 58–72. https://doi.org/10.1016/j.chroma.2016.01.002

Fæste, C. K., Tartor, H., Moen, A., Kristoffersen, A. B., Dhanasiri, A. K. S., Anonsen, J. H., Furmanek, T., & Grove, S. (2020). Proteomic profiling of salmon skin mucus for the comparison of sampling methods. *Journal of Chromatography B*, *1138*(November 2019), 121965. https://doi.org/10.1016/j.jchromb.2019.121965

Fast, M. D., Sims, D. E., Burka, J. F., Mustafa, A., & Ross, N. W. (2002). Skin morphology and humoral non-specific defence parameters of mucus and plasma in rainbow trout, coho and Atlantic salmon. *Comparative Biochemistry and Physiology - A Molecular and Integrative Physiology*, *132*(3), 645–657. https://doi.org/10.1016/S1095-6433(02)00109-5

Firth, K. J., Johnson, S. C., & Ross, N. W. (2000). Characterization of proteases in the skin mucus of Atlantic salmon (Salmo salar) infected with the salmon louse (Lepeophtheirus salmonis) and in whole-body louse homogenate. *The Journal of Parasitology*, *86*(6), 1199–1205. https://doi.org/10.1645/0022-3395(2000)086[1199:COPITS]2.0.CO;2

Fletcher, T. C., & White, A. (1972). Antibody production in the plaice (Pleuronectes platessa L.) after oral and parenteral immunization with Vibrio anguillarum antigens. *Aquaculture*, *1*, 417–428. https://doi.org/10.1016/0044-8486(72)90045-2

Fletcher, T. C., & White, A. (1973). Lysozyme activity in the plaice (Pleuronectes platessa L.). *Experientia*, *29*(10), 1283–1285. https://doi.org/10.1007/BF01935119

Flewelling, L. J., Naar, J. P., Abbott, J. P., Baden, D. G., Barros, N. B., Bossart, G. D., Bottein, M.-Y. D., Hammond, D. G., Haubold, E. M., Heil, C. A., Henry, M. S., Jacocks, H. M., Leighfield, T. A., Pierce, R. H., Pitchford, T. D., Rommel, S. A., Scott, P. S., Steidinger, K. A., Truby, E. W., … Landsberg, J. H. (2005). Brevetoxicosis: red tides and marine mammal mortalities. *Nature*, *435*(7043), 755–756. https://doi.org/10.1038/nature435755a

Foegeding, E. A. (1996). Characteristics of edible muscle tissues. *Food Chemistry*.

Forné, I., Abián, J., & Cerdà, J. (2010). Fish proteome analysis: Model organisms and non-sequenced species. *Proteomics*, *10*(4), 858–872. https://doi.org/10.1002/pmic.200900609

Forné, I., María, J. A., Esther Asensio, Joaquín Abián, & Cerdà, J. (2009). 2-D DIGE analysis of Senegalese sole (Solea senegalensis) testis proteome in wild-caught and hormone-treated F1 fish. *Proteomics*, *9*(8), 2171–2181. https://doi.org/10.1002/pmic.200800696

Franco, C. F., Santos, R., & Coelho, A. v. (2011). Proteome characterization of sea star coelomocytes - The innate immune effector cells of echinoderms. *PROTEOMICS*, *11*(17), 3587–3592. https://doi.org/10.1002/pmic.201000745

Fry, B. G., Roelants, K., Champagne, D. E., Scheib, H., Tyndall, J. D. A., King, G. F., Nevalainen, T. J., Norman, J. A., Lewis, R. J., Norton, R. S., Renjifo, C., & Rodríguez De La Vega, R. C. (2009). The toxicogenomic multiverse: Convergent recruitment of proteins into animal venoms. *Annual Review of Genomics and Human Genetics*, *10*, 483–511. https://doi.org/10.1146/annurev.genom.9.081307.164356

Gandar, A., Laffaille, P., Marty-Gasset, N., Viala, D., Molette, C., & Jean, S. (2017). Proteome response of fish under multiple stress exposure: Effects of pesticide mixtures and temperature increase. *Aquatic Toxicology*, *184*, 61–77. https://doi.org/10.1016/j.aquatox.2017.01.004

Gao, Y., & Yates, J. R. (2019). Protein analysis by shotgun proteomics. *Mass Spectrometry-Based Chemical Proteomics*, 1–38. https://doi.org/10.1002/9781118970195.ch1

Gaspar, M. B., Barracha, I., Carvalho, S., & Vasconcelos, P. (2013). Clam fisheries worldwide: main species, harvesting methods and fishing impacts. In *Clam fisheries and aquaculture* (pp. 291–327). Nova Science Publishers, Inc.

Gay, N. J., & Gangloff, M. (2007). Structure and Function of Toll Receptors and Their Ligands. *Annual Review of Biochemistry*, *76*(1), 141–165. https://doi.org/10.1146/annurev.biochem.76.060305.151318

Ghaedi, G., Keyvanshokooh, ;, Azarm, M., & Akhlaghi, M. (2016). *Proteomic analysis of muscle tissue from rainbow trout (Oncorhynchus mykiss) fed dietary β-glucan*. *17*(3), 184–189.

Ghahremani, M., Stigter, K. A., & Plaxton, W. (2016). Extraction and characterization of extracellular proteins and their post-translational modifications from Arabidopsis thaliana suspension cell cultures and seedlings: A critical review. *Proteomes*, *4*(3), 14–20. https://doi.org/10.3390/proteomes4030025

Ghisaura, S., Anedda, R., Pagnozzi, D., Biosa, G., Spada, S., Bonaglini, E., Cappuccinelli, R., Roggio, T., Uzzau, S., & Addis, M. F. (2014). Impact of three commercial feed formulations on farmed gilthead sea bream (Sparus aurata, L.) metabolism as inferred from liver and blood serum proteomic. *Proteome Science*, *12*(1). https://doi.org/10.1186/s12953-014-0044-3

Ghisaura, S., Pagnozzi, D., Melis, R., Biosa, G., Slawski, H., Uzzau, S., Anedda, R., & Addis, M. F. (2019). Liver proteomics of gilthead sea bream (Sparus aurata) exposed to cold stress. *Journal of Thermal Biology*, *82*(April), 234–241. https://doi.org/10.1016/j.jtherbio.2019.04.005

Giacometti, J., Tomljanović, A. B., & Josić, D. (2013). Application of proteomics and metabolomics for investigation of food toxins. *Food Research International*, *54*(1), 1042–1051. https://doi.org/10.1016/j.foodres.2012.10.019

Glencross, B. D., Booth, M., & Allan, G. L. (2007). A feed is only as good as its ingredients ? a review of ingredient evaluation strategies for aquaculture feeds. *Aquaculture Nutrition*, *13*(1), 17–34. https://doi.org/10.1111/j.1365-2095.2007.00450.x

Glickman, M. H., & Ciechanover, A. (2002). The ubiquitin-proteasome proteolytic pathway: Destruction for the sake of construction. *Physiological Reviews*, *82*(2), 373–428. https://doi.org/10.1152/physrev.00027.2001

Gombar, R., Pitcher, T. E., Lewis, J. A., Auld, J., & Vacratsis, P. O. (2017). Proteomic characterization of seminal plasma from alternative reproductive tactics of Chinook salmon (Oncorhynchus tswatchysha). *Journal of Proteomics*, *157*, 1–9. https://doi.org/10.1016/j.jprot.2017.01.019

Gomes, T., Albergamo, A., Costa, R., Mondello, L., & Dugo, G. (2017a). Potential Use of Proteomics in Shellfish Aquaculture: from Assessment of Environmental Toxicity to Evaluation of Seafood Quality and Safety. *Current Organic Chemistry*, *21*(5), 402–425. https://doi.org/10.2174/1385272820666161102121232

Gomes, T., Albergamo, A., Costa, R., Mondello, L., & Dugo, G. (2017b). Potential Use of Proteomics in Shellfish Aquaculture: from Assessment of Environmental Toxicity to Evaluation of Seafood Quality and Safety. *Current Organic Chemistry*, *21*(5), 402–425. https://doi.org/10.2174/1385272820666161102121232

Gomes, T., Albergamo, A., Costa, R., Mondello, L., & Dugo, G. (2017c). Potential Use of Proteomics in Shellfish Aquaculture: from Assessment of Environmental Toxicity to Evaluation of Seafood Quality and Safety. *Current Organic Chemistry*, *21*(5), 402–425. https://doi.org/10.2174/1385272820666161102121232

Gomez, D., Sunyer, J. O., & Salinas, I. (2013). The mucosal immune system of fish: The evolution of tolerating commensals while fighting pathogens. *Fish and Shellfish Immunology*, *35*(6), 1729–1739. https://doi.org/10.1016/j.fsi.2013.09.032

Gómez-Requeni, P., de Vareilles, M., Kousoulaki, K., Jordal, A.-E. O., Conceição, L. E. C., & Rønnestad, I. (2011). Whole body proteome response to a dietary lysine imbalance in zebrafish Danio rerio. *Comparative Biochemistry and Physiology Part D: Genomics and Proteomics*, *6*(2), 178–186. https://doi.org/10.1016/j.cbd.2011.02.002

Görg, A., Obermaier, C., Boguth, G., Harder, A., Scheibe, B., Wildgruber, R., & Weiss, W. (2000). The current state of two-dimensional electrophoresis with immobilized pH gradients.

Electrophoresis, *21*(6), 1037–1053. https://doi.org/10.1002/(SICI)1522-2683(20000401)21:6<1037::AID-ELPS1037>3.0.CO;2-V

Görg, A., Weiss, W., & Dunn, M. J. (2004). Current two-dimensional electrophoresis technology for proteomics. *PROTEOMICS*, *4*(12), 3665–3685. https://doi.org/10.1002/pmic.200401031

Graves, P. R., & Haystead, T. A. J. (2002). Molecular Biologist's Guide to Proteomics. *Microbiology and Molecular Biology Reviews*, *66*(1), 39–63. https://doi.org/10.1128/mmbr.66.1.39-63.2002

Gronen, S., Denslow, N., Manning, S., Barnes, S., Barnes, D., & Brouwer, M. (1999). Serum vitellogenin levels and reproductive impairment of male Japanese Medaka (Oryzias latipes) exposed to 4-tert-octylphenol. *Environmental Health Perspectives*, *107*(5), 385–390. https://doi.org/10.1289/ehp.99107385

Guardiola, F. A., Cuesta, A., Arizcun, M., Meseguer, J., & Esteban, M. A. (2014). Comparative skin mucus and serum humoral defence mechanisms in the teleost gilthead seabream (Sparus aurata). *Fish and Shellfish Immunology*, *36*(2), 545–551. https://doi.org/10.1016/j.fsi.2014.01.001

Guo, H., Zhang, J., Wang, Y., Bu, C., Zhou, Y., & Fang, Q. (2017). Comparative Proteomic Analysis of Lysine Acetylation in Fish CIK Cells Infected with Aquareovirus. *International Journal of Molecular Sciences*, *18*(11), 2419. https://doi.org/10.3390/ijms18112419

Gupta, Y. R., Sellegounder, D., Kannan, M., Deepa, S., Senthilkumaran, B., & Basavaraju, Y. (2016). Effect of copper nanoparticles exposure in the physiology of the common carp (Cyprinus carpio): Biochemical, histological and proteomic approaches. *Aquaculture and Fisheries*, *1*, 15–23. https://doi.org/10.1016/j.aaf.2016.09.003

Gur, Y., & Breitbart, H. (2008). Protein synthesis in sperm: Dialog between mitochondria and cytoplasm. *Molecular and Cellular Endocrinology*, *282*(1–2), 45–55. https://doi.org/10.1016/j.mce.2007.11.015

Gutiérrez, J. L., Jones, C. G., Strayer, D. L., & Iribarne, O. O. (2003). Mollusks as ecosystem engineers: the role of shell production in aquatic habitats. *Oikos*, *101*(1), 79–90. https://doi.org/10.1034/j.1600-0706.2003.12322.x

Hamre, L. A., Eichner, C., Caipang, C. M. A., Dalvin, S. T., Bron, J. E., Nilsen, F., Boxshall, G., & Skern-Mauritzen, R. (2013). The Salmon Louse Lepeophtheirus salmonis (Copepoda: Caligidae)

Life Cycle Has Only Two Chalimus Stages. PLoS ONE, 8(9), 1–9. https://doi.org/10.1371/journal.pone.0073539

Han, X., Aslanian, A., & Yates, J. R. (2008). Mass spectrometry for proteomics. *Current Opinion in Chemical Biology*, *12*(5), 483–490. https://doi.org/10.1016/j.cbpa.2008.07.024

Hancock, R. E. W., & Lehrer, R. (1998). Cationic peptides: A new source of antibiotics. *Trends in Biotechnology*, *16*(2), 82–88. https://doi.org/10.1016/S0167-7799(97)01156-6

Hancock, R. E. W., & Scott, M. G. (2000). The role of antimicrobial peptides in animal defenses. *Proceedings of the National Academy of Sciences of the United States of America*, *97*(16), 8856–8861. https://doi.org/10.1073/pnas.97.16.8856

Haenen, O. L. M., Way, K., Bergmann, S. M., & Ariel, E. (2004). The emergence of koi herpesvirus and its significance to European aquaculture. *Bulletin of the European Association of Fish Pathologists*, *24*(6), 293–307.

Hartman, K. H., Yanong, R. P., Pouder, D. B., Petty, B. D., Francis-Floyd, R., Riggs, A. C., & Waltzek, T. B. (2013). Koi Herpesvirus Disease (KHVD). *EDIS*, *2013*(5). https://doi.org/10.32473/edis-vm113-2013

Hedrick, R. P., Gilad, O., Yun, S., Spangenberg, J. v, Marty, G. D., Nordhausen, R. W., Kebus, M. J., Bercovier, H., & Eldar, A. (2000). A herpesvirus associated with mass mortality of juvenile and adult koi, a strain of common carp. *Journal of Aquatic Animal Health*, *12*(1), 44–57.

He, J. G., Deng, M., Weng, S. P., Li, Z., Zhou, S. Y., Long, Q. X., Wang, X. Z., & Chan, S. M. (2001). Complete genome analysis of the mandarin fish infectious spleen and kidney necrosis iridovirus. *Virology*, *291*(1), 126–139. https://doi.org/10.1006/viro.2001.1208

He, P., Matich, E. K., Yonkos, L. T., Friedman, A. E., Ekin Atilla-Gokcumen, G., & Aga, D. S. (2019). Mass spectrometry based detection of common vitellogenin peptides across fish species for assessing exposure to estrogenic compounds in aquatic environments. *Science of the Total Environment*, *646*, 400–408. https://doi.org/10.1016/j.scitotenv.2018.07.252

Heller, R. A., Schena, M., Chai, A., Shalon, D., Bedilion, T., Gilmore, J., Woolley, D. E., & Davis, R. W. (1997). Discovery and analysis of inflammatory disease-related genes using cDNA

microarrays. *Proceedings of the National Academy of Sciences*, *94*(6), 2150–2155. https://doi.org/10.1073/pnas.94.6.2150

Hellio, C., Pons, A. M., Beaupoil, C., Bourgougnon, N., & Gal, Y. le. (2002). Antibacterial, antifungal and cytotoxic activities of extracts from fish epidermis and epidermal mucus. *International Journal of Antimicrobial Agents*, *20*(3), 214–219. https://doi.org/10.1016/S0924-8579(02)00172-3

Hirano, M. (2016). Echinoderm immunity: is the larval immune system immature? *Immunology & Cell Biology*, *94*(9), 809–811. https://doi.org/10.1038/icb.2016.67

Hoffmann, R., & Valencia, A. (2004). A gene network for navigating the literature [2]. *Nature Genetics*, *36*(7), 664. https://doi.org/10.1038/ng0704-664

Hogstrand, C., Balesaria, S., & Glover, C. N. (2002). Application of genomics and proteomics for study of the integrated response to zinc exposure in a non-model fish species, the rainbow trout. *Comparative Biochemistry and Physiology - B Biochemistry and Molecular Biology*, *133*(4), 523–535. https://doi.org/10.1016/S1096-4959(02)00125-2

Holmes, P., Humfrey, C., & Scullion, M. (1997). *OECD Environmental Health and Safety Publications*. Paris, France.

Huang, T. C., & Chen, J. Y. (2013). Proteomic and functional analysis of zebrafish after administration of antimicrobial peptide epinecidin-1. *Fish and Shellfish Immunology*, *34*(2), 593–598. https://doi.org/10.1016/j.fsi.2012.11.032

Huang, Y., Huang, J., & Chen, Y. (2010). Alpha-helical cationic antimicrobial peptides: Relationships of structure and function. *Protein and Cell*, *1*(2), 143–152. https://doi.org/10.1007/s13238-010-0004-3

Hui, Y. H., Nip, W. K., Nollet, L. M. L., Paliyath, G., & Simpson, B. K. (2006). Food Biochemistry and Food Processing. In Y. H. Hui (Ed.), *Food Biochemistry and Food Processing*. Blackwell Publishing. https://doi.org/10.1002/9780470277577

Ibarz, A., Beltrán, M., Fernández-Borràs, J., Gallardo, M. A., Sánchez, J., & Blasco, J. (2007). Alterations in lipid metabolism and use of energy depots of gilthead sea bream (Sparus aurata) at

low temperatures. *Aquaculture*, *262*(2–4), 470–480. https://doi.org/10.1016/j.aquaculture.2006.11.008

Ibarz, A., Blasco, J., Beltrán, M., Gallardo, M. A., Sánchez, J., Sala, R., & Fernández-Borràs, J. (2005). Cold-induced alterations on proximate composition and fatty acid profiles of several tissues in gilthead sea bream (Sparus aurata). *Aquaculture*, *249*(1–4), 477–486. https://doi.org/10.1016/j.aquaculture.2005.02.056

Ibarz, A., Fernández-Borràs, J., Blasco, J., Gallardo, M. A., & Sánchez, J. (2003). Oxygen consumption and feeding rates of gilthead sea bream (Sparus aurata) reveal lack of acclimation to cold. *Fish Physiology and Biochemistry*, *29*(4), 313–321. https://doi.org/10.1007/s10695-004-3321-8

Ibarz, A., Martín-Pérez, M., Blasco, J., Bellido, D., de Oliveira, E., & Fernández-Borràs, J. (2010). Gilthead sea bream liver proteome altered at low temperatures by oxidative stress. *PROTEOMICS*, *10*(5), 963–975. https://doi.org/10.1002/pmic.200900528

Ibarz, A., Padrós, F., Gallardo, M. Á., Fernández-Borràs, J., Blasco, J., & Tort, L. (2010). Low-temperature challenges to gilthead sea bream culture: review of cold-induced alterations and 'Winter Syndrome.' *Reviews in Fish Biology and Fisheries*, *20*(4), 539–556. https://doi.org/10.1007/s11160-010-9159-5

Ikonomou, G., Samiotaki, M., & Panayotou, G. (2009). Proteomic methodologies and their application in colorectal cancer research. *Critical Reviews in Clinical Laboratory Sciences*, *46*(5–6), 319–342. https://doi.org/10.3109/10408360903375277

Ingolfsdottir, S., Stefänsson, G., & Kristbergsson, K. (1998). Seasonal Variations in Physicochemical and Textural Properties of North Atlantic Cod (Gadus morh. ua) Mince. *Journal of Aquatic Food Product Technology*, *7*(3), 39–61.

Ingram, G. A. (1980). Substances involved in the natural resistance of fish to infection–a review. *Journal of Fish Biology*, *16*(1), 23–60.

Inguglia, L., Chiaramonte, M., Arizza, V., Turiák, L., Vékey, K., Drahos, L., Pitonzo, R., Avellone, G., & di Stefano, V. (2020). Changes in the proteome of sea urchin Paracentrotus lividus coelomocytes in response to LPS injection into the body cavity. *PLoS ONE*, *15*(2), 1–17. https://doi.org/10.1371/journal.pone.0228893

Issaq, H. J., & Veenstra, T. D. (2008). Two-dimensional polyacrylamide gel electrophoresis (2D-PAGE): Advances and perspectives. *BioTechniques*, *44*(5), 697–700. https://doi.org/10.2144/000112823

Jamieson, B. G. M. (1991). *Fish Evolution and Systematics: Evidence From Spermatozoa*. Cambridge University Press, Cambridge.

Jayasundara, N., Tomanek, L., Dowd, W. W., & Somero, G. N. (2015). Proteomic analysis of cardiac response to thermal acclimation in the eurythermal goby fish Gillichthys mirabilis. Journal of Experimental Biology, 218(9), 1359–1372. https://doi.org/10.1242/jeb.118760

Jensen, L. E., Hiney, M. P., Shields, D. C., Uhlar, C. M., Lindsay, A. J., & Whitehead, A. S. (1997). Acute phase proteins in salmonids: evolutionary analyses and acute phase response. *Journal of Immunology (Baltimore, Md. : 1950)*, *158*(1), 384–392. http://www.ncbi.nlm.nih.gov/pubmed/8977214

Jessen, F., Wulff, T., Mikkelsen, J. B., Hyldig, G., & Nielsen, H. (2012). Vegetable based fish feed changes protein expression in muscle of rainbow trout (Oncorhynchus mykiss). *Farm Animal Proteomics*, 134–137. https://doi.org/10.3920/978-90-8686-751-6_31

Jin, Y., Zhang, X., Lu, D., & Fu, Z. (2012). Proteomic analysis of hepatic tissue in adult female Zebrafish (Danio rerio) exposed to atrazine. *Archives of Environmental Contamination and Toxicology*, *62*(1), 127–134. https://doi.org/10.1007/s00244-011-9678-7

Johnson, S. C., & Brown, L. L. (2011). The Application of Genomics, Proteomics, and Metabolomics to Studies of Fish Health. In G. L. F. and M. L. Rise. C (Ed.), *Aquaculture Biotechnology* (1st ed., pp. 81–104). Wiley-Blackwell. https://doi.org/10.1002/9780470963159.ch6

Johnston, L. D., Brown, G., Gauthier, D., Reece, K., Kator, H., & van Veld, P. (2008). Apolipoprotein A-I from striped bass (Morone saxatilis) demonstrates antibacterial activity in vitro. *Comparative Biochemistry and Physiology - B Biochemistry and Molecular Biology*, *151*(2), 167–175. https://doi.org/10.1016/j.cbpb.2008.06.011

Jones, S. R. M. (2001). The occurrence and mechanisms of innate immunity against parasites in fish. *Developmental and Comparative Immunology*, *25*(8–9), 841–852. https://doi.org/10.1016/S0145-305X(01)00039-8

Jorrín-Novo, J. v., Maldonado, A. M., Echevarría-Zomeño, S., Valledor, L., Castillejo, M. A., Curto, M., Valero, J., Sghaier, B., Donoso, G., & Redondo, I. (2009). Plant proteomics update (2007–2008): Second-generation proteomic techniques, an appropriate experimental design, and data analysis to fulfill MIAPE standards, increase plant proteome coverage and expand biological knowledge. *Journal of Proteomics*, *72*(3), 285–314. https://doi.org/10.1016/j.jprot.2009.01.026

Jurado, J., Fuentes-Almagro, C. A., Guardiola, F. A., Cuesta, A., Esteban, M. Á., & Prieto-Álamo, M. J. (2015**a**). Proteomic profile of the skin mucus of farmed gilthead seabream (Sparus aurata). *Journal of Proteomics*, *120*, 21–34. https://doi.org/10.1016/j.jprot.2015.02.019

Jurado, J., Fuentes-Almagro, C. A., Guardiola, F. A., Cuesta, A., Esteban, M. Á., & Prieto-Álamo, M. J. (2015**b**). Proteomic profile of the skin mucus of farmed gilthead seabream (Sparus aurata). *Journal of Proteomics*, *120*, 21–34. https://doi.org/10.1016/j.jprot.2015.02.019

Käll, L., Canterbury, J. D., Weston, J., Noble, W. S., & MacCoss, M. J. (2007). Semi-supervised learning for peptide identification from shotgun proteomics datasets. *Nature Methods*, *4*(11), 923–925. https://doi.org/10.1038/nmeth1113

Karim, M., Puiseux-Dao, S., & Edery, M. (2011). Toxins and stress in fish: Proteomic analyses and response network. *Toxicon*, *57*(7–8), 959–969. https://doi.org/10.1016/j.toxicon.2011.03.018

Karlsen, O. A., Sheehan, D., & Goksøyr, A. (2014). Alterations in the atlantic COD (Gadus morhua) hepatic thiol-proteome after methylmercury exposure. *Journal of Toxicology and Environmental Health - Part A: Current Issues*, *77*(9–11), 650–662. https://doi.org/10.1080/15287394.2014.887427

Karr, T. L. (2007). Fruit flies and the sperm proteome. *Human Molecular Genetics*, *16*(R2), 124–133. https://doi.org/10.1093/hmg/ddm252

Kennedy, S. (2002). The role of proteomics in toxicology: identification of biomarkers of toxicity by protein expression analysis. *Biomarkers*, *7*(4), 269–290. https://doi.org/10.1080/13547500210127318

Keyvanshokooh, S., Kalbassi, M. R., Hosseinkhani, S., & Vaziri, B. (2009). Comparative proteomics analysis of male and female Persian sturgeon (Acipenser persicus) gonads. *Animal Reproduction Science*, *111*(2–4), 361–368. https://doi.org/10.1016/j.anireprosci.2008.03.005

Keyvanshokooh, S., & Tahmasebi-Kohyani, A. (2012). Proteome modifications of fingerling rainbow trout (Oncorhynchus mykiss) muscle as an effect of dietary nucleotides. *Aquaculture*, *324–325*, 79–84. https://doi.org/10.1016/j.aquaculture.2011.10.013

Kingtong, S., Kellner, K., Bernay, B., Goux, D., Sourdaine, P., & Berthelin, C. H. (2013). Proteomic identification of protein associated to mature spermatozoa in the Pacific oyster Crassostrea gigas. *Journal of Proteomics*, *82*, 81–91. https://doi.org/10.1016/j.jprot.2013.02.009

Klinovska, K., Sebkova, N., & Dvorakova-Hortova, K. (2014). Sperm-egg fusion: A molecular enigma of mammalian reproduction. *International Journal of Molecular Sciences*, *15*(6), 10652–10668. https://doi.org/10.3390/ijms150610652

Kossinova, O. A., Malygin, A. A., Babailova, E. S., & Karpova, G. G. (2008). Binding of human ribosomal protein p40 and its truncated mutants to the small ribosomal subunit. *Molecular Biology*, *42*(6), 911–916. https://doi.org/10.1134/S0026893308060125

Krishna, R. G., & Wold, F. (1993). Post-Translational Modifications of Proteins. In *Methods in Protein Sequence Analysis* (pp. 167–172). Springer US. https://doi.org/10.1007/978-1-4899-1603-7_21

Kuhl, H., Beck, A., Wozniak, G., Canario, A. V. M., Volckaert, F. A. M., & Reinhardt, R. (2010). The European sea bass Dicentrarchus labrax genome puzzle: comparative BAC-mapping and low coverage shotgun sequencing. *Bmc Genomics*, *11*(1), 1–13.

Kulichkova, V. A., Artamonova, T. O., Lyublinskaya, O. G., Khodorkovskii, M. A., Tomilin, A. N., & Tsimokha, A. S. (2017). Proteomic analysis of affinity-purified extracellular proteasomes reveals exclusively 20S complexes. *Oncotarget*, *8*(60), 102134–102149. https://doi.org/10.18632/oncotarget.22230

Kültz, D., Fiol, D., Valkova, N., Gomez-Jimenez, S., Chan, S. Y., & Lee, J. (2007). Functional genomics and proteomics of the cellular osmotic stress response in `non-model' organisms. *Journal of Experimental Biology*, *210*(9), 1593–1601. https://doi.org/10.1242/jeb.000141

Kumar, G., Hummel, K., Noebauer, K., Welch, T. J., Razzazi-Fazeli, E., & El-Matbouli, M. (2018). Proteome analysis reveals a role of rainbow trout lymphoid organs during Yersinia ruckeri infection process. *Scientific Reports*, *8*(1), 1–13. https://doi.org/10.1038/s41598-018-31982-6

Kwan, S. H., & Ismail, M. N. (2018). Identification of the Potential Bio-active Proteins Associated with Wound Healing Properties in Snakehead Fish (Channa striata) Mucus. *Current Proteomics*, *15*(4), 299–312. https://doi.org/10.2174/1570164615666180717143418

Ky, C. L., de Lorgeril, J., Hirtz, C., Sommerer, N., Rossignol, M., & Bonhomme, F. (2007). The effect of environmental salinity on the proteome of the sea bass (Dicentrarchus labrax L.). *Animal Genetics*, *38*(6), 601–608. https://doi.org/10.1111/j.1365-2052.2007.01652.x

Lacerda, C. M. R., & Reardon, K. F. (2009). Environmental proteomics: Applications of proteome profiling in environmental microbiology and biotechnology. *Briefings in Functional Genomics and Proteomics*, *8*(1), 75–87. https://doi.org/10.1093/bfgp/elp005

Ladrat, C., Chaplet, M., Verrez-Bagnis, V., Noël, J., & Fleurence, J. (2000). Neutral calcium-activated proteases from European sea bass (Dicentrarchus labrax L.) muscle: polymorphism and biochemical studies. *Comparative Biochemistry and Physiology Part B: Biochemistry and Molecular Biology*, *125*(1), 83–95.

Lahnsteiner, F. (2003). Morphology, fine structure, biochemistry, and function of the spermatic ducts in marine fish. *Tissue and Cell*, *35*(5), 363–373. https://doi.org/10.1016/S0040-8166(03)00057-0

Lahnsteiner, F., Berger, B., Weismann, T., & Patzner, R. (1995). Fine structure and motility of spermatozoa and composition of the seminal plasma in the perch. *Journal of Fish Biology*, *47*(3), 492–508. https://doi.org/10.1111/j.1095-8649.1995.tb01917.x

Lahnsteiner, F., Patzner, R. A., & Welsmann, T. (1993). The spermatic ducts of salmonid fishes (Salmonidae, Teleostei). Morphology, histochemistry and composition of the secretion. *Journal of Fish Biology*, *42*(1), 79–93. https://doi.org/10.1111/j.1095-8649.1993.tb00307.x

Lahnsteiner, F., Weismann, T. & Patzner, R. (1999). Physiological and biochemical parameters for egg quality determination in lake trout, Salmo trutta lacustris. *Fish Physiology and Biochemistry*, *20*, 375–388. https://doi.org/https://doi.org/10.1023/A:1007715621550

Lai, Y., & Gallo, R. L. (2009). AMPed up immunity: how antimicrobial peptides have multiple roles in immune defense. *Trends in Immunology*, *30*(3), 131–141. https://doi.org/10.1016/j.it.2008.12.003

Lall, S. P. (2002). The minerals. In *Fish nutrition* (pp. 469–554). Elsevier.

Lam, M. P. Y., Lau, E., Ng, D. C. M., Wang, D., & Ping, P. (2016). Cardiovascular proteomics in the era of big data: Experimental and computational advances. *Clinical Proteomics*, *13*(1), 1–14. https://doi.org/10.1186/s12014-016-9124-y

Lange, V., Picotti, P., Domon, B., & Aebersold, R. (2008). Selected reaction monitoring for quantitative proteomics: A tutorial. *Molecular Systems Biology*, *4*(222). https://doi.org/10.1038/msb.2008.61

Latterich, M., Abramovitz, M., & Leyland-Jones, B. (2008). Proteomics: New technologies and clinical applications. *European Journal of Cancer*, *44*(18), 2737–2741. https://doi.org/10.1016/j.ejca.2008.09.007

Lee, B. H., & Nagamune, T. (2004). Protein microarrays and their applications. *Biotechnology and Bioprocess Engineering*, *9*(2), 69–75. https://doi.org/10.1007/BF02932987

Lessios, H. A. (2011). Speciation genes in free-spawning marine invertebrates. *Integrative and Comparative Biology*, *51*(3), 456–465. https://doi.org/10.1093/icb/icr039

Li, H., Luo, W., Ji, R., Xu, Y., Xu, G., Qiu, S., & Tang, H. (2021). A comparative proteomic study of cold responses in potato leaves. *Heliyon*, *7*(2), e06002. https://doi.org/10.1016/j.heliyon.2021.e06002

Li, P., Hulak, M., Koubek, P., Sulc, M., Dzyuba, B., Boryshpolets, S., Rodina, M., Gela, D., Manaskova-Postlerova, P., Peknicova, J., & Linhart, O. (2010). Ice-age endurance: The effects of cryopreservation on proteins of sperm of common carp, Cyprinus carpio L. *Theriogenology*, *74*(3), 413–423. https://doi.org/10.1016/j.theriogenology.2010.02.024

Li, P., Hulak, M., Li, Z. H., Sulc, M., Psenicka, M., Rodina, M., Gela, D., & Linhart, O. (2013). Cryopreservation of common carp (Cyprinus carpio L.) sperm induces protein phosphorylation in tyrosine and threonine residues. *Theriogenology*, *80*(2), 84–89. https://doi.org/10.1016/j.theriogenology.2013.03.021

Li, P., Hulak, M., & Linhart, O. (2009). Sperm proteins in teleostean and chondrostean (sturgeon) fishes. *Fish Physiology and Biochemistry*, *35*(4), 567–581. https://doi.org/10.1007/s10695-008-9261-y

Li, P., Hulak, M., Rodina, M., Sulc, M., Li, Z. H., & Linhart, O. (2010). Comparative protein profiles: Potential molecular markers from spermatozoa of Acipenseriformes (Chondrostei, Pisces).

Comparative Biochemistry and Physiology - Part D: Genomics and Proteomics, *5*(4), 302–307. https://doi.org/10.1016/j.cbd.2010.08.003

Li, P., Li, Z. H., Dzyuba, B., Hulak, M., Rodina, M., & Linhart, O. (2010). Evaluating the impacts of osmotic and oxidative stress on common carp (Cyprinus carpio, L.) sperm caused by cryopreservation techniques. *Biology of Reproduction*, *83*(5), 852–858. https://doi.org/10.1095/biolreprod.110.085852

Li, S., Zhang, Y., Cao, Y., Wang, D., Liu, H., & Lu, T. (2017). Trancriptome profiles of Amur sturgeon spleen in response to Yersinia ruckeri infection. *Fish and Shellfish Immunology*, *70*, 451–460. https://doi.org/10.1016/j.fsi.2017.09.033

Lin, Y., Chen, Y., Yang, X., Xu, D., & Liang, S. (2009). Proteome analysis of a single zebrafish embryo using three different digestion strategies coupled with liquid chromatography-tandem mass spectrometry. *Analytical Biochemistry*, *394*(2), 177–185. https://doi.org/10.1016/j.ab.2009.07.034

Link, V., Shevchenko, A., & Heisenberg, C.-P. (2006). Proteomics of early zebrafish embryos. *BMC Developmental Biology*, *6*(1), 1. https://doi.org/10.1186/1471-213X-6-1

Lipton, M. S., Pää-Toli, L., Anderson, G. A., Anderson, D. J., Auberry, D. L., Battista, J. R., Daly, M. J., Fredrickson, J., Hixson, K. K., Kostandarithes, H., Masselon, C., Markillie, L. M., Moore, R. J., Romine, M. F., Shen, Y., Stritmatter, E., Tolić, N., Udseth, H. R., Venkateswaran, A., … Smith, R. D. (2002). Global analysis of the Deinococcus radiodurans proteome by using accurate mass tags. *Proceedings of the National Academy of Sciences of the United States of America*, *99*(17), 11049–11054. https://doi.org/10.1073/pnas.172170199

Liu, R., Hu, X., Lü, A., Song, Y., Lian, Z., Sun, J., & Sung, Y. Y. (2020). Proteomic Profiling of Zebrafish Challenged by Spring Viremia of Carp Virus Provides Insight into Skin Antiviral Response. *Zebrafish*, *17*(2), 91–103. https://doi.org/10.1089/zeb.2019.1843

Liu, T., Zhang, L., Joo, D., & Sun, S. C. (2017). NF-κB signaling in inflammation. *Signal Transduction and Targeted Therapy*, *2*(March). https://doi.org/10.1038/sigtrans.2017.23

Lødemel, J. B., & Olsen, R. L. (2003). Gelatinolytic activities in muscle of Atlantic cod (Gadus morhua), spotted wolffish (Anarhichas minor) and Atlantic salmon (Salmo salar). *Journal of the Science of Food and Agriculture*, *83*(10), 1031–1036. https://doi.org/10.1002/jsfa.1501

Loir, M., Labbé, C., Maisse, G., Pinson, A., Boulard, G., Mourot, B., & Chambeyron, F. (1990). Proteins of seminal fluid and spermatozoa in the trout (Oncorhynchus mykiss): Partial characterization and variations. *Fish Physiology and Biochemistry*, *8*(6), 485–495. https://doi.org/10.1007/BF00003405

López, J. L. (2007). Two-dimensional electrophoresis in proteome expression analysis. *Journal of Chromatography B: Analytical Technologies in the Biomedical and Life Sciences*, *849*(1–2), 190–202. https://doi.org/10.1016/j.jchromb.2006.11.049

López, J. L., Marina, A., Álvarez, G., & Vázquez, J. (2002). Application of proteomics for fast identification of species-specific peptides from marine species. *Proteomics*, *2*(12), 1658–1665. https://doi.org/10.1002/1615-9861(200212)2:12<1658::AID-PROT1658>3.0.CO;2-4

López-Barea, J., & Gómez-Ariza, J. L. (2006). Environmental proteomics and metallomics. *Proteomics*, *6*(S1), S51–S62.

López-Ferrer, D., Ramos-Fernández, A., Martínez-Bartolomé, S., García-Ruiz, P., & Vázquez, J. (2006). Quantitative proteomics using 16O/18O labeling and linear ion trap mass spectrometry. *Proteomics*, *6 Suppl 1*, 4–11. https://doi.org/10.1002/pmic.200500375

López-Pedrouso, M., Varela, Z., Franco, D., Fernández, J. A., & Aboal, J. R. (2020). Can proteomics contribute to biomonitoring of aquatic pollution? A critical review. *Environmental Pollution*, *267*. https://doi.org/10.1016/j.envpol.2020.115473

Lorscheider, F. L., Vimy, M. J., & Summers, A. O. (1995). Mercury exposure from "silver" tooth fillings: emerging evidence questions a traditional dental paradigm. *The FASEB Journal*, *9*(7), 504–508. https://doi.org/10.1096/fasebj.9.7.7737458

Love, R. M. (1997). Biochemical dynamics and the quality of fresh and frozen fish. In *Fish Processing Technology* (pp. 1–31). Springer US. https://doi.org/10.1007/978-1-4613-1113-3_1

Love, R. M., Robertson, I., Smith, G. L., & Whittle, K. J. (1974). The texture of cod muscle. *Journal of Texture Studies*, *5*(2), 201–212.

Lü, A., Hu, X., Wang, Y., Shen, X., Li, X., Zhu, A., Tian, J., Ming, Q., & Feng, Z. (2014). ITRAQ analysis of gill proteins from the zebrafish (Danio rerio) infected with Aeromonas hydrophila. *Fish and Shellfish Immunology*, *36*(1), 229–239. https://doi.org/10.1016/j.fsi.2013.11.007

Lu, J., Chen, H., Xu, Q., Zheng, J., Liu, H., Li, J., & Chen, K. (2010). Comparative proteomics of kidney samples from puffer fish Takifugu rubripes exposed to excessive fluoride: An insight into molecular response to fluorosis. *Toxicology Mechanisms and Methods*, *20*(6), 345–354. https://doi.org/10.3109/15376516.2010.490967

Lü, J. N., Chen, J., Lu, X. J., & Shi, Y. H. (2012). Identification of α1-antitrypsin as a positive acute phase protein in ayu (Plecoglossus altivelis) associated with Listonella anguillarum infection. *Fish & Shellfish Immunology*, *32*(1), 237–241.

Lu, X. J., Chen, J., Huang, Z. A., Zhuang, L., Peng, L. Z., & Shi, Y. H. (2012). Influence of acute cadmium exposure on the liver proteome of a teleost fish, ayu (Plecoglossus altivelis). *Molecular Biology Reports*, *39*(3), 2851–2859. https://doi.org/10.1007/s11033-011-1044-3

Ma, B., Zhang, K., Hendrie, C., Liang, C., Li, M., Doherty-Kirby, A., & Lajoie, G. (2003). PEAKS: Powerful software for peptide de novo sequencing by tandem mass spectrometry. *Rapid Communications in Mass Spectrometry*, *17*(20), 2337–2342. https://doi.org/10.1002/rcm.1196

Mackie, I. M., Pryde, S. E., Gonzales-Sotelo, C., Medina, I., Peréz-Martín, R., Quinteiro, J., Rey-Mendez, M., & Rehbein, H. (1999). Challenges in the identification of species of canned fish. *Trends in Food Science and Technology*, *10*(1), 9–14. https://doi.org/10.1016/S0924-2244(99)00013-8

Maclatchy, D. L., & van der kraak, G. J. (1995). The phytoestrogen β-sitosterol alters the reproductive endocrine status of goldfish. In *Toxicology and Applied Pharmacology* (Vol. 134, Issue 2, pp. 305–312). https://doi.org/10.1006/taap.1995.1196

Madeira, D., Araújo, J. E., Vitorino, R., Capelo, J. L., Vinagre, C., & Diniz, M. S. (2016). Ocean warming alters cellular metabolism and induces mortality in fish early life stages: A proteomic approach. Environmental Research, 148, 164–176. https://doi.org/10.1016/j.envres.2016.03.030

Madeira, D., Araújo, J. E., Vitorino, R., Costa, P. M., Capelo, J. L., Vinagre, C., & Diniz, M. S. (2017). Molecular Plasticity under Ocean Warming: Proteomics and Fitness Data Provides Clues for a Better Understanding of the Thermal Tolerance in Fish. *Frontiers in Physiology*, *8*. https://doi.org/10.3389/fphys.2017.00825

Magnadóttir, B. (2006). Innate immunity of fish (overview). *Fish and Shellfish Immunology*, *20*(2), 137–151. https://doi.org/10.1016/j.fsi.2004.09.006

Mahaffey, K. R. (2004). Fish and shellfish as dietary sources of methylmercury and the ω-3 fatty acids, eicosahexaenoic acid and docosahexaenoic acid: Risks and benefits. *Environmental Research*, *95*(3), 414–428. https://doi.org/10.1016/j.envres.2004.02.006

Mahanty, A., Purohit, G. K., Banerjee, S., Karunakaran, D., Mohanty, S., & Mohanty, B. P. (2016). Proteomic changes in the liver of Channa striatus in response to high temperature stress. *Electrophoresis*, *37*(12), 1704–1717. https://doi.org/10.1002/elps.201500393

Mak, M., Mak, P., Olczak, M., Szalewicz, A., Glogowski, J., Dubin, A., Wątorek, W., & Ciereszko, A. (2004). Isolation, characterization, and cDNA sequencing of α-1- antiproteinase-like protein from rainbow trout seminal plasma. *Biochimica et Biophysica Acta - General Subjects*, *1671*(1–3), 93–105. https://doi.org/10.1016/j.bbagen.2004.02.001

Mak, M., Mak, P., Olczak, M., Szalewicz, A., Glogowski, J., Dubin, A., Wątorek, W., & Ciereszko, A. (2004). Isolation, characterization, and cDNA sequencing of α-1-antiproteinase-like protein from rainbow trout seminal plasma. *Biochimica et Biophysica Acta (BBA) - General Subjects*, *1671*(1–3), 93–105. https://doi.org/10.1016/j.bbagen.2004.02.001

Malécot, M., Mezhoud, K., Marie, A., Praseuth, D., Puiseux-Dao, S., & Edery, M. (2009). Proteomic study of the effects of microcystin-LR on organelle and membrane proteins in medaka fish liver. *Aquatic Toxicology*, *94*(2), 153–161. https://doi.org/10.1016/j.aquatox.2009.06.012

Malik, R., Dulla, K., Nigg, E. A., & Körner, R. (2010). From proteome lists to biological impact–tools and strategies for the analysis of large MS data sets. *Proteomics*, *10*(6), 1270–1283.

Malmström, J., Lee, H., & Aebersold, R. (2007). Advances in proteomic workflows for systems biology. *Current Opinion in Biotechnology*, *18*(4), 378–384. https://doi.org/10.1016/j.copbio.2007.07.005

Mamone, G., Picariello, G., Caira, S., Addeo, F., & Ferranti, P. (2009). Analysis of food proteins and peptides by mass spectrometry-based techniques. *Journal of Chromatography A*, *1216*(43), 7130–7142. https://doi.org/10.1016/j.chroma.2009.07.052

Maneja, R. H., Dineshram, R., Thiyagarajan, V., Skiftesvik, A. B., Frommel, A. Y., Clemmesen, C., Geffen, A. J., & Browman, H. I. (2014). The proteome of Atlantic herring (Clupea harengus L.) larvae is resistant to elevated pCO2. *Marine Pollution Bulletin*, *86*(1–2), 154–160. https://doi.org/10.1016/j.marpolbul.2014.07.030

Manzoni, C., Kia, D. A., Vandrovcova, J., Hardy, J., Wood, N. W., Lewis, P. A., & Ferrari, R. (2018). Genome, transcriptome and proteome: The rise of omics data and their integration in biomedical sciences. *Briefings in Bioinformatics*, *19*(2), 286–302. https://doi.org/10.1093/BIB/BBW114

Martin, S. A. M., Collet, B., MacKenzie, S., Evensen, O., & Secombes, C. J. (2008). Genomic tools for examining immune gene function in salmonid fish. *Reviews in Fisheries Science*, *16*(sup1), 112–118.

Martin, S. A. M., Vilhelmsson, O., & Houlihan, D. F. (2003). Rainbow trout liver proteome-dietary manipulation and protein metabolism. *PUBLICATION-EUROPEAN ASSOCIATION FOR ANIMAL PRODUCTION*, *109*, 57–60.

Martin, S. A. M., Vilhelmsson, O., Médale, F., Watt, P., Kaushik, S., & Houlihan, D. F. (2003). Proteomic sensitivity to dietary manipulations in rainbow trout. *Biochimica et Biophysica Acta (BBA) - Proteins and Proteomics*, *1651*(1–2), 17–29. https://doi.org/10.1016/S1570-9639(03)00231-0

Martinez, I., Aursand, M., Erikson, U., Singstad, T. E., Veliyulin, E., & van der Zwaag, C. (2003). Destructive and non-destructive analytical techniques for authentication and composition analyses of foodstuffs. *Trends in Food Science & Technology*, *14*(12), 489–498.

Martinez, I., Friis, T. J., & Seppola, M. (2001). Requirements for the application of protein sodium dodecyl sulfate-polyacrylamide gel electrophoresis and randomly amplified polymorphic DNA analyses to product speciation. *Electrophoresis*, *22*(8), 1526–1533.

Martinez, I., & Jakobsen Friis, T. (2004). Application of proteome analysis to seafood authentication. *Proteomics*, *4*(2), 347–354.

Martinez, I., Ofstad, R., & Olsen, R. L. (1990). Electrophoretic study of myosin isoforms in white muscles of some teleost fishes. *Comparative Biochemistry and Physiology -- Part B: Biochemistry And*, *96*(2), 221–227. https://doi.org/10.1016/0305-0491(90)90366-2

Martyniuk, C. J., & Denslow, N. D. (2009a). Towards functional genomics in fish using quantitative proteomics. *General and Comparative Endocrinology*, *164*(2–3), 135–141.

Martyniuk, C. J., & Denslow, N. D. (2009b). Towards functional genomics in fish using quantitative proteomics. *General and Comparative Endocrinology*, *164*(2–3), 135–141. https://doi.org/10.1016/j.ygcen.2009.01.023

Mateos, J., Landeira-Abia, A., Fafián-Labora, J. A., Fernández-Pernas, P., Lesende-Rodríguez, I., Fernández-Puente, P., Fernández-Moreno, M., Delmiro, A., Martín, M. A., Blanco, F. J., & Arufe, M. C. (2015). iTRAQ-based analysis of progerin expression reveals mitochondrial dysfunction, reactive oxygen species accumulation and altered proteostasis. *Stem Cell Research and Therapy*, *6*(1), 1–17. https://doi.org/10.1186/s13287-015-0110-5

Matranga, V., Pinsino, A., Celi, M., Natoli, A., Bonaventura, R., Schröder, H. C., & Müller, W. E. G. (2005). Monitoring Chemical and Physical Stress Using Sea Urchin Immune Cells. In *Echinodermata* (pp. 85–110). Springer-Verlag. https://doi.org/10.1007/3-540-27683-1_5

Mazzeo, M. F., & Siciliano, R. A. (2016). Proteomics for the authentication of fish species. *Journal of Proteomics*, *147*, 119–124. https://doi.org/10.1016/j.jprot.2016.03.007

McDonough, C. E., Whittington, E., Pitnick, S., & Dorus, S. (2016a). Proteomics of reproductive systems: Towards a molecular understanding of postmating, prezygotic reproductive barriers. *Journal of Proteomics*, *135*, 26–37. https://doi.org/10.1016/j.jprot.2015.10.015

McDonough, C. E., Whittington, E., Pitnick, S., & Dorus, S. (2016b). Proteomics of reproductive systems: Towards a molecular understanding of postmating, prezygotic reproductive barriers. *Journal of Proteomics*, *135*, 26–37. https://doi.org/10.1016/j.jprot.2015.10.015

McNamara, L. E., Dalby, M. J., Riehle, M. O., & Burchmore, R. (2010). Fluorescence two-dimensional difference gel electrophoresis for biomaterial applications. *Journal of the Royal Society Interface*, *7*(SUPPL. 1). https://doi.org/10.1098/rsif.2009.0177.focus

Medina-Gali, R., Belló-Pérez, M., Ciordia, S., Mena, M. C., Coll, J., Novoa, B., Ortega-Villaizán, M. del M., & Perez, L. (2019). Plasma proteomic analysis of zebrafish following spring viremia of carp virus infection. *Fish and Shellfish Immunology*, *86*(October 2018), 892–899. https://doi.org/10.1016/j.fsi.2018.12.035

Meyer, A., & Málaga-Trillo, E. (1999). Vertebrate genomics: More fishy tales about Hox genes. *Current Biology*, *9*(6), 210–213. https://doi.org/10.1016/S0960-9822(99)80131-6

Mezhoud, K., Bauchet, A. L., Château-Joubert, S., Praseuth, D., Marie, A., François, J. C., Fontaine, J. J., Jaeg, J. P., Cravedi, J. P., Puiseux-Dao, S., & Edery, M. (2008). Proteomic and phosphoproteomic analysis of cellular responses in medaka fish (Oryzias latipes) following oral gavage with microcystin-LR. *Toxicon*, *51*(8), 1431–1439. https://doi.org/10.1016/j.toxicon.2008.03.017

Mogensen, T. H. (2009). Pathogen Recognition and Inflammatory Signaling in Innate Immune Defenses. *Clinical Microbiology Reviews*, *22*(2), 240–273. https://doi.org/10.1128/CMR.00046-08

Monsinjon, T., & Knigge, T. (2007). Proteomic applications in ecotoxicology. *Proteomics*, *7*(16), 2997–3009. https://doi.org/10.1002/pmic.200700101

Morais, S., Silva, T., Cordeiro, O., Rodrigues, P., Guy, D. R., Bron, J. E., Taggart, J. B., Bell, J. G., & Tocher, D. R. (2012). Effects of genotype and dietary fish oil replacement with vegetable oil on the intestinal transcriptome and proteome of Atlantic salmon (Salmo salar). *BMC Genomics*, *13*(1). https://doi.org/10.1186/1471-2164-13-448

Morais, T., Inácio, A., Coutinho, T., Ministro, M., Cotas, J., Pereira, L., & Bahcevandziev, K. (2020). Seaweed potential in the animal feed: A review. *Journal of Marine Science and Engineering*, *8*(8), 1–24. https://doi.org/10.3390/JMSE8080559

Moreira, M., Schrama, D., Farinha, A. P., Cerqueira, M., de Magalhães, C. R., Carrilho, R., & Rodrigues, P. (2021). Fish pathology research and diagnosis in aquaculture of farmed fish; a proteomics perspective. *Animals*, *11*(1), 1–25. https://doi.org/10.3390/ani11010125

Morrison, R. N., Cooper, G. A., Koop, B. F., Rise, M. L., Bridle, A. R., Adams, M. B., & Nowak, B. F. (2006). Transcriptome profiling the gills of amoebic gill disease (AGD)-affected Atlantic salmon (Salmo salar L.): A role for tumor suppressor p53 in AGD pathogenesis? *Physiological Genomics*, *26*(1), 15–34. https://doi.org/10.1152/physiolgenomics.00320.2005

Morrison, R. N., & Nowak, B. F. (2008). Immunohistochemical detection of anterior gradient-2 in the gills of amoebic gill disease-affected Atlantic salmon, Salmo salar L. *Journal of Fish Diseases*, *31*(9), 699–705. https://doi.org/10.1111/j.1365-2761.2008.00934.x

Morrison, R. N., Zou, J., Secombes, C. J., Scapigliati, G., Adams, M. B., & Nowak, B. F. (2007). Molecular cloning and expression analysis of tumour necrosis factor-α in amoebic gill disease (AGD)-affected Atlantic salmon (Salmo salar L.). *Fish and Shellfish Immunology*, *23*(5), 1015–1031. https://doi.org/10.1016/j.fsi.2007.04.003

Moseley, F. L., Bicknell, K. A., Marber, M. S., & Brooks, G. (2010). The use of proteomics to identify novel therapeutic targets for the treatment of disease. *Journal of Pharmacy and Pharmacology*, *59*(5), 609–628. https://doi.org/10.1211/jpp.59.5.0001

Mueller, L. N., Rinner, O., Schmidt, A., Letarte, S., Bodenmiller, B., Brusniak, M. Y., Vitek, O., Aebersold, R., & Müller, M. (2007). SuperHirn - A novel tool for high resolution LC-MS-based peptide/protein profiling. *Proteomics*, *7*(19), 3470–3480. https://doi.org/10.1002/pmic.200700057

Naderi, M., Keyvanshokooh, S., Salati, A. P., & Ghaedi, A. (2017). Effects of chronic high stocking density on liver proteome of rainbow trout (Oncorhynchus mykiss). *Fish Physiology and Biochemistry*, *43*(5), 1373–1385. https://doi.org/10.1007/s10695-017-0378-8

Nakachi, M., Nakajima, A., Nomura, M., Yonezawa, K., Ueno, K., Endo, T., & Inaba, K. (2011). Proteomic profiling reveals compartment-specific, novel functions of ascidian sperm proteins. *Molecular Reproduction and Development*, *78*(7), 529–549. https://doi.org/10.1002/mrd.21341

Nathan, L. R., Jerde, C. L., Budny, M. L., & Mahon, A. R. (2015). The use of environmental DNA in invasive species surveillance of the Great Lakes commercial bait trade. *Conservation Biology*, *29*(2), 430–439. https://doi.org/10.1111/cobi.12381

Natnan, M. E., Low, C. F., Chong, C. M., Bunawan, H., & Baharum, S. N. (2021). Integration of Omics Tools for Understanding the Fish Immune Response Due to Microbial Challenge. *Frontiers in Marine Science*, *8*(June). https://doi.org/10.3389/fmars.2021.668771

Nesatyy, V. J., & Suter, M. J.-F. (2008). Analysis of environmental stress response on the proteome level. *Mass Spectrometry Reviews*, *27*(6), 556–574. https://doi.org/10.1002/mas.20177

Nessen, M. A., van der Zwaan, D. J., Grevers, S., Dalebout, H., Staats, M., Kok, E., & Palmblad, M. (2016). Authentication of Closely Related Fish and Derived Fish Products Using Tandem Mass Spectrometry and Spectral Library Matching. *Journal of Agricultural and Food Chemistry*, *64*(18), 3669–3677. https://doi.org/10.1021/acs.jafc.5b05322

Nesvizhskii, A. I., & Aebersold, R. (2005). Interpretation of shotgun proteomic data: The protein inference problem. *Molecular and Cellular Proteomics*, *4*(10), 1419–1440. https://doi.org/10.1074/mcp.R500012-MCP200

Nomura M, Sakai K, T. F. (1974). The over-ripening phenome- non of rainbow trout. (I. Changes in the percentage of eyed eggs, hatching rate and incidence of abnormal alevins during the process of over-ripening. *Bull Jap Soc Science Fish*, *41*, 855–860.

Nowak, B., Cadoret, K., Feist, S. W., & Bean, T. P. (2013). Laser-capture dissection and immunohistochemistry reveals chloride and mucous-cell specific gene expression in gills of seawater acclimated Atlantic salmon Salmo salar. *Journal of Fish Biology*, *83*(5), 1459–1467. https://doi.org/10.1111/jfb.12235

Nynca, J., Arnold, G., Fröhlich, T., & Ciereszko, A. (2017). Proteomic identification of rainbow trout blood plasma proteins and their relationship to seminal plasma proteins. *Proteomics*, *17*(11), 1–41. https://doi.org/10.1002/pmic.201600460

Nynca, J., Arnold, G. J., Fröhlich, T., & Ciereszko, A. (2015a). Cryopreservation-induced alterations in protein composition of rainbow trout semen. *Proteomics*, *15*(15), 2643–2654. https://doi.org/10.1002/pmic.201400525

Nynca, J., Arnold, G. J., Fröhlich, T., & Ciereszko, A. (2015b). Shotgun proteomics of rainbow trout ovarian fluid. *Reproduction, Fertility and Development*, *27*(3), 504–512. https://doi.org/10.1071/RD13224

Nynca, J., Arnold, G. J., Fröhlich, T., Otte, K., & Ciereszko, A. (2014). Proteomic identification of rainbow trout sperm proteins. *Proteomics*, *14*(12), 1569–1573. https://doi.org/10.1002/pmic.201300521

Nynca, J., Arnold, G. J., Fröhlich, T., Otte, K., Flenkenthaler, F., & Ciereszko, A. (2014). Proteomic identification of rainbow trout seminal plasma proteins. *Proteomics*, *14*(1), 133–140. https://doi.org/10.1002/pmic.201300267

Nynca, J., Dietrich, M. A., Bilińska, B., Kotula-Balak, M., Kiełbasa, T., Karol, H., & Ciereszko, A. (2011a). Isolation of lipocalin-type protein from rainbow trout seminal plasma and its localisation in the reproductive system. *Reproduction, Fertility and Development*, *23*(2), 381. https://doi.org/10.1071/RD10118

Nynca, J., Dietrich, M. A., Bilińska, B., Kotula-Balak, M., Kiełbasa, T., Karol, H., & Ciereszko, A. (2011b). Isolation of lipocalin-type protein from rainbow trout seminal plasma and its localisation in the reproductive system. *Reproduction, Fertility and Development*, *23*(2), 381. https://doi.org/10.1071/RD10118

Nynca, J., Dietrich, M. A., Bilińska, B., Kotula-Balak, M., Kiełbasa, T., Karol, H., & Ciereszko, A. (2011c). Isolation of lipocalin-type protein from rainbow trout seminal plasma and its localisation in the reproductive system. *Reproduction, Fertility and Development*, *23*(2), 381–389. https://doi.org/10.1071/RD10118

Nynca, J., Dietrich, M. A., Karol, H., & Ciereszko, A. (2010). Identification of apolipoprotein C-I in rainbow trout seminal plasma. *Reproduction, Fertility and Development*, *22*(8), 1183–1187. https://doi.org/10.1071/RD10066

Nynca, J., Słowińska, M., Dietrich, M. A., Bilińska, B., Kotula-Balak, M., & Ciereszko, A. (2011). Isolation and identification of fetuin-B-like protein from rainbow trout seminal plasma and its localization in the reproductive system. *Comparative Biochemistry and Physiology Part B: Biochemistry and Molecular Biology*, *158*(1), 106–116. https://doi.org/10.1016/j.cbpb.2010.10.002

Ogata, H., Aranishi, F., Hara, K., Osatomi, K., & Ishihara, T. (1998). Proteolytic degradation of myofibrillar components by carp cathepsin L. *Journal of the Science of Food and Agriculture*, *76*(4), 499–504. https://doi.org/10.1002/(SICI)1097-0010(199804)76:4<499::AID-JSFA980>3.0.CO;2-W

Okuda, S., Yamada, T., Hamajima, M., Itoh, M., Katayama, T., Bork, P., Goto, S., & Kanehisa, M. (2008). KEGG Atlas mapping for global analysis of metabolic pathways. *Nucleic Acids Research*, *36*(Web Server issue), 423–426. https://doi.org/10.1093/nar/gkn282

Oliva, R., de Mateo, S., & Estanyol, J. M. (2009). Sperm cell proteomics. *Proteomics*, *9*(4), 1004–1017. https://doi.org/10.1002/pmic.200800588

Ong, S. E., Blagoev, B., Kratchmarova, I., Kristensen, D. B., Steen, H., Pandey, A., & Mann, M. (2002). Stable isotope labeling by amino acids in cell culture, SILAC, as a simple and accurate approach to expression proteomics. *Molecular & Cellular Proteomics : MCP*, *1*(5), 376–386. https://doi.org/10.1074/mcp.M200025-MCP200

Orr, H. A., & Presgraves, D. C. (2000). Speciation by postzygotic isolation: Forces, genes and molecules. *BioEssays*, *22*(12), 1085–1094. https://doi.org/10.1002/1521-1878(200012)22:12<1085::AID-BIES6>3.0.CO;2-G

Ortea, I., Cañas, B., & Gallardo, J. M. (2009). Mass spectrometry characterization of species-specific peptides from arginine kinase for the identification of commercially relevant shrimp species. *Journal of Proteome Research*, *8*(11), 5356–5362. https://doi.org/10.1021/pr900663d

Paerl, H. W., & Otten, T. G. (2013). Harmful Cyanobacterial Blooms: Causes, Consequences, and Controls. *Microbial Ecology*, *65*(4), 995–1010. https://doi.org/10.1007/s00248-012-0159-y

Palmer, M. R., Mcdowall, M. H., Stewart, L., Ouaddi, A., Maccoss, M. J., & Swanson, W. J. (2013). Mass spectrometry and next-generation sequencing reveal an abundant and rapidly evolving abalone sperm protein. *Molecular Reproduction and Development*, *80*(6), 460–465. https://doi.org/10.1002/mrd.22182

Palumbi, S. R. (1994). Genetic divergence, reproductive isolation, and marine speciation. *Annual Review of Ecology and Systematics*, *25*, 547–572. https://doi.org/10.1146/annurev.es.25.110194.002555

Pampanin, D. M., Larssen, E., Øysæd, K. B., Sundt, R. C., & Sydnes, M. O. (2014). Study of the bile proteome of Atlantic cod (Gadus morhua): Multi-biological markers of exposure to polycyclic aromatic hydrocarbons. *Marine Environmental Research*, *101*(1), 161–168. https://doi.org/10.1016/j.marenvres.2014.10.002

Pan, C.-Y., Chen, J.-Y., Cheng, Y.-S. E., Chen, C.-Y., Ni, I.-H., Sheen, J.-F., Pan, Y.-L., & Kuo, C.-M. (2007). Gene Expression and Localization of the Epinecidin-1 Antimicrobial Peptide in the Grouper (Epinephelus coioides), and Its Role in Protecting Fish Against Pathogenic Infection. *DNA and Cell Biology*, *26*(6), 403–413. https://doi.org/10.1089/dna.2006.0564

Pan, C.-Y., Huang, T.-C., Wang, Y.-D., Yeh, Y.-C., Hui, C.-F., & Chen, J.-Y. (2012). Oral administration of recombinant epinecidin-1 protected grouper (Epinephelus coioides) and zebrafish (Danio rerio) from Vibrio vulnificus infection and enhanced immune-related gene expressions. *Fish & Shellfish Immunology*, *32*(6), 947–957. https://doi.org/10.1016/j.fsi.2012.01.023

Panicker, G., Ye, Y., Wang, D., & Unger, E. R. (2010). Characterization of the human cervical mucous proteome. *Clinical Proteomics*, *6*(1–2), 18–28. https://doi.org/10.1007/s12014-010-9042-3

Papa, I., Alvarez, C., Verrez-Bagnis, V., Fleurence, J., & Benyamin, Y. (1996). Post mortemRelease of Fish White Muscle α-Actinin as a Marker of Disorganisation. *Journal of the Science of Food and Agriculture*, *72*(1), 63–70.

Papakostas, S., Vasemägi, A., Vähä, J. P., Himberg, M., Peil, L., & Primmer, C. R. (2012). A proteomics approach reveals divergent molecular responses to salinity in populations of European whitefish (Coregonus lavaretus). *Molecular Ecology*, *21*(14), 3516–3530. https://doi.org/10.1111/j.1365-294X.2012.05553.x

Papini, R., Pellegrini, O., Rossini, C., & Guidi, G. (2004). Anticardiolipin antibodies in dogs. *Veterinary Research Communications*, *28*(SUPPL. 1), 355–357. https://doi.org/10.1023/B:VERC.0000045445.89096.f4

Pappin, D. J. C., Creasy, D. M., Perkins, D. N., & S., C. J. (1999). Probability-based protein identification by searching sequence databases using mass spectrometry data. *Electrophoresis*, *20*, 3551–3567.

Parrington, J., & Coward, K. (2002). Use of emerging genomic and proteomic technologies in fish physiology. *Aquatic Living Resources*, *15*(3), 193–196. https://doi.org/10.1016/S0990-7440(02)01172-5

Patel, D. M., & Brinchmann, M. F. (2017). Skin mucus proteins of lumpsucker (Cyclopterus lumpus). *Biochemistry and Biophysics Reports*, *9*(August 2016), 217–225. https://doi.org/10.1016/j.bbrep.2016.12.016

Paz, M., Morín, M., & del Mazo, J. (2006). Proteome profile changes during mouse testis development. *Comparative Biochemistry and Physiology - Part D: Genomics and Proteomics*, *1*(4), 404–415. https://doi.org/10.1016/j.cbd.2006.10.002

Peng, J., Schwartz, D., Elias, J. E., Thoreen, C. C., Cheng, D., Marsischky, G., Roelofs, J., Finley, D., & Gygi, S. P. (2003). A proteomics approach to understanding protein ubiquitination. *Nature Biotechnology*, *21*(8), 921–926. https://doi.org/10.1038/nbt849

Pennacchi, Y., Leef, M. J., Crosbie, P. B. B., Nowak, B. F., & Bridle, A. R. (2014). Evidence of immune and inflammatory processes in the gills of AGD-affected Atlantic salmon, Salmo salar L. *Fish and Shellfish Immunology*, *36*(2), 563–570. https://doi.org/10.1016/j.fsi.2013.12.013

Pérez-Sánchez, J., Terova, G., Simó-Mirabet, P., Rimoldi, S., Folkedal, O., Calduch-Giner, J. A., Olsen, R. E., & Sitjà-Bobadilla, A. (2017). Skin mucus of gilthead sea bream (sparus aurata l.). protein mapping and regulation in chronically stressed fish. *Frontiers in Physiology*, *8*(February), 1–18. https://doi.org/10.3389/fphys.2017.00034

Perkins, D. N., Pappin, D. J. C., Creasy, D. M., & Cottrell, J. S. (1999). Probability-based protein identification by searching sequence databases using mass spectrometry data. *Electrophoresis*, *20*(18), 3551–3567. https://doi.org/10.1002/(SICI)1522-2683(19991201)20:18<3551::AID-ELPS3551>3.0.CO;2-2

Ph. Garrigues, H. Barth, C.H. Walker, J.-F. (2001). *Biomarkers in Marine Organisms. A Practical Approach* (1st ed.). Elsevier Publishing. https://www.elsevier.com/books/biomarkers-in-marine-organisms/garrigues/978-0-444-82913-9

Pierce, R. H., & Henry, M. S. (2008). Harmful algal toxins of the Florida red tide (Karenia brevis): natural chemical stressors in South Florida coastal ecosystems. *Ecotoxicology*, *17*(7), 623–631. https://doi.org/10.1007/s10646-008-0241-x

Pierrard, M. A., Kestemont, P., Phuong, N. T., Tran, M. P., Delaive, E., Thezenas, M. L., Dieu, M., Raes, M., & Silvestre, F. (2012). Proteomic analysis of blood cells in fish exposed to

chemotherapeutics: Evidence for long term effects. *Journal of Proteomics*, *75*(8), 2454–2467. https://doi.org/10.1016/j.jprot.2012.02.028

Piñeiro, C., Barros-Velázquez, J., Sotelo, C. G., & Gallardo, J. M. (1999). The use of two-dimensional electrophoresis in the characterization of the water-soluble protein fraction of commercial flat fish species. *Zeitschrift FÜr Lebensmitteluntersuchung Und - Forschung A*, *208*(5–6), 342–348. https://doi.org/10.1007/s002170050427

Piñeiro, C., Barros-Velázquez, J., Sotelo, C. G., Pérez-Martín, R. I., & Gallardo, J. M. (1998). Two-dimensional electrophoretic study of the water-soluble protein fraction in white muscle of gadoid fish species. *Journal of Agricultural and Food Chemistry*, *46*(10), 3991–3997.

Piñeiro, C., Barros-Velázquez, J., Vázquez, J., Figueras, A., & Gallardo, J. M. (2003). Proteomics as a tool for the investigation of seafood and other marine products. *Journal of Proteome Research*, *2*(2), 127–135. https://doi.org/10.1021/pr0200083

Piñeiro, C., Cañas, B., & Carrera, M. (2010a). The role of proteomics in the study of the influence of climate change on seafood products. *Food Research International*, *43*(7), 1791–1802. https://doi.org/10.1016/j.foodres.2009.11.012

Piñeiro, C., Cañas, B., & Carrera, M. (2010b). The role of proteomics in the study of the influence of climate change on seafood products. *Food Research International*, *43*(7), 1791–1802. https://doi.org/10.1016/j.foodres.2009.11.012

Piñeiro, C., Vázquez, J., Marina, A. I., Barros-Velázquez, J., & Gallardo, J. M. (2001). Characterization and partial sequencing of species-specific sarcoplasmic polypeptides from commercial hake species by mass spectrometry following two-dimensional electrophoresis. *ELECTROPHORESIS*, *22*(8), 1545–1552. https://doi.org/10.1002/1522-2683(200105)22:8<1545::AID-ELPS1545>3.0.CO;2-5

Pinsino, A., & Matranga, V. (2015). Sea urchin immune cells as sentinels of environmental stress. *Developmental & Comparative Immunology*, *49*(1), 198–205. https://doi.org/10.1016/j.dci.2014.11.013

Porta, J., Porta, J. M., Martínez-Rodríguez, G., & Alvarez, M. C. (2006). Genetic structure and genetic relatedness of a hatchery stock of Senegal sole (Solea senegalensis) inferred by microsatellites. *Aquaculture*, *251*(1), 46–55. https://doi.org/10.1016/j.aquaculture.2005.05.019

Prasanna-Mohanty, B., Mohanty, S., Mitra, T., Mahanty, A., Ganguly, S., & Singh Sivadhar. (2019). Omics Technology in Fisheries and Aquaculture. *Advances in Fish Research*, *December 2018*, 1–30. https://www.researchgate.net/publication/329830959

Premsler, T., Zahedi, R., Lewandrowski, U., & Sickmann, A. (2009). Recent advances in yeast organelle and membrane proteomics. *Proteomics*, *9*(20), 4731–4743. https://doi.org/10.1002/pmic.200900201

Pridgeon, J. W., & Klesius, P. H. (2013). Apolipoprotein A1 in channel catfish: Transcriptional analysis, antimicrobial activity, and efficacy as plasmid DNA immunostimulant against Aeromonas hydrophila infection. *Fish and Shellfish Immunology*, *35*(4), 1129–1137. https://doi.org/10.1016/j.fsi.2013.07.028

Priyadharshini, V. S., & Teran, L. M. (2020). Role of respiratory proteomics in precision medicine. In *Precision Medicine for Investigators, Practitioners and Providers* (pp. 255–261). Elsevier. https://doi.org/10.1016/B978-0-12-819178-1.00024-1

Provan, F., Jensen, L. B., Uleberg, K. E., Larssen, E., Rajalahti, T., Mullins, J., & Obach, A. (2013). Proteomic analysis of epidermal mucus from sea lice-infected Atlantic salmon, Salmo salar L. *Journal of Fish Diseases*, *36*(3), 311–321. https://doi.org/10.1111/jfd.12064

Qiao, Q., le Manach, S., Sotton, B., Huet, H., Duvernois-Berthet, E., Paris, A., Duval, C., Ponger, L., Marie, A., Blond, A., Mathéron, L., Vinh, J., Bolbach, G., Djediat, C., Bernard, C., Edery, M., & Marie, B. (2016). Deep sexual dimorphism in adult medaka fish liver highlighted by multi-omic approach. *Scientific Reports*, *6*(August), 1–12. https://doi.org/10.1038/srep32459

Rabilloud, T., & Lelong, C. (2011). Two-dimensional gel electrophoresis in proteomics: A tutorial. *Journal of Proteomics*, *74*(10), 1829–1841. https://doi.org/10.1016/j.jprot.2011.05.040

Rajan, B., Fernandes, J. M. O., Caipang, C. M. A., Kiron, V., Rombout, J. H. W. M., & Brinchmann, M. F. (2011). Proteome reference map of the skin mucus of Atlantic cod (Gadus morhua) revealing

immune competent molecules. *Fish and Shellfish Immunology*, *31*(2), 224–231. https://doi.org/10.1016/j.fsi.2011.05.006

Rajan, B., Lokesh, J., Kiron, V., & Brinchmann, M. F. (2013). Differentially expressed proteins in the skin mucus of Atlantic cod (Gadus morhua) upon natural infection with Vibrio anguillarum. *BMC Veterinary Research*, *9*. https://doi.org/10.1186/1746-6148-9-103

Ralston-Hooper, K. J., Turner, M. E., Soderblom, E. J., Villeneuve, D., Ankley, G. T., Moseley, M. A., Hoke, R. A., & Ferguson, P. L. (2013). Application of a label-free, gel-free quantitative proteomics method for ecotoxicological studies of small fish species. *Environmental Science and Technology*, *47*(2), 1091–1100. https://doi.org/10.1021/es303170u

Ramos, A. D., Conceição, K., Silva, P. I., Richardson, M., Lima, C., & Lopes-Ferreira, M. (2012). Specialization of the sting venom and skin mucus of Cathorops spixii reveals functional diversification of the toxins. *Toxicon*, *59*(6), 651–665. https://doi.org/10.1016/j.toxicon.2012.02.002

Raposo de Magalhães, C. S. F., Cerqueira, M. A. C., Schrama, D., Moreira, M. J. V., Boonanuntanasarn, S., & Rodrigues, P. M. L. (2020). A Proteomics and other Omics approach in the context of farmed fish welfare and biomarker discovery. *Reviews in Aquaculture*, *12*(1), 122–144. https://doi.org/10.1111/raq.12308

Raposo De Magalhães, C., Schrama, D., Farinha, A. P., Revets, D., Kuehn, A., Planchon, S., Rodrigues, P. M., & Cerqueira, M. (2020). Protein changes as robust signatures of fish chronic stress: A proteomics approach to fish welfare research. *BMC Genomics*, *21*(1), 1–16. https://doi.org/10.1186/s12864-020-6728-4

Redgrove, K. A., Anderson, A. L., Dun, M. D., McLaughlin, E. A., O'Bryan, M. K., Aitken, R. J., & Nixon, B. (2011). Involvement of multimeric protein complexes in mediating the capacitation-dependent binding of human spermatozoa to homologous zonae pellucidae. *Developmental Biology*, *356*(2), 460–474. https://doi.org/10.1016/j.ydbio.2011.05.674

Reid, G. K., Gurney-Smith, H. J., Flaherty, M., Garber, A. F., Forster, I., Brewer-Dalton, K., Knowler, D., Marcogliese, D. J., Chopin, T., Moccia, R. D., Smith, C. T., & de Silva, S. (2019). Climate

change and aquaculture: Considering adaptation potential. *Aquaculture Environment Interactions*, *11*, 603–624. https://doi.org/10.3354/AEI00333

Rime, H., Guitton, N., Pineau, C., Bonnet, E., Bobe, J., & Jalabert, B. (2004). Post-ovulatory ageing and egg quality: A proteomic analysis of rainbow trout coelomic fluid. *Reproductive Biology and Endocrinology*, *2*, 1–10. https://doi.org/10.1186/1477-7827-2-26

Rippey, S. R. (1994). Infectious diseases associated with molluscan shellfish consumption. *Clinical Microbiology Reviews*, *7*(4), 419–425. https://doi.org/10.1128/CMR.7.4.419

Robinson-Rechavi, M., Marchand, O., Escriva, H., & Laudet, V. (2001). An ancestral whole-genome duplication may not have been responsible for the abundance of duplicated fish genes. *Current Biology*, *11*(12), R458–R459. https://doi.org/10.1016/S0960-9822(01)00280-9

Robotti, E., & Marengo, E. (2018). *2D-DIGE and Fluorescence Image Analysis* (pp. 25–39). https://doi.org/10.1007/978-1-4939-7268-5_3

Rodrigues, P. M., Silva, T. S., Dias, J., & Jessen, F. (2012). Proteomics in aquaculture: applications and trends. *Journal of Proteomics*, *75*(14), 4325–4345.

Romero, A., Novoa, B., & Figueras, A. (2016). Cell mediated immune response of the Mediterranean sea urchin Paracentrotus lividus after PAMPs stimulation. *Developmental & Comparative Immunology*, *62*, 29–38. https://doi.org/10.1016/j.dci.2016.04.018

Romero, M. R., Pérez-Figueroa, A., Carrera, M., Swanson, W. J., Skibinski, D. O. F., & Diz, A. P. (2019). RNA-seq coupled to proteomic analysis reveals high sperm proteome variation between two closely related marine mussel species. *Journal of Proteomics*, *192*(June), 169–187. https://doi.org/10.1016/j.jprot.2018.08.020

Ross, N. W., Firth, K. J., Wang, A., Burka, J. F., & Johnson, S. C. (2000). Changes in hydrolytic enzyme activities of naive Atlantic salmon Salmo salar skin mucus due to infection with the salmon louse Lepeophtheirus salmonis and cortisol implantation. *Diseases of Aquatic Organisms*, *41*(1), 43–51. https://doi.org/10.3354/dao041043

Russell, F. E. (1965). Marine Toxins and Venomous and Poisonous Marine Animals. *Advances in Marine Biology*, *3*(C), 255–384. https://doi.org/10.1016/S0065-2881(08)60398-3

Saleh, M., Kumar, G., Abdel-Baki, A. A., Dkhil, M. A., El-Matbouli, M., & Al-Quraishy, S. (2018). Quantitative shotgun proteomics distinguishes wound-healing biomarker signatures in common carp skin mucus in response to Ichthyophthirius multifiliis. *Veterinary Research*, *49*(1), 1–12. https://doi.org/10.1186/s13567-018-0535-9

Salles, C. M. C., De-Simone, S. G., Leitão, S. A. T., Salles, J. B., Guedes, H. L. M., Cassano, V. P. F., & De-Simone, S. G. (2007). Identification and characterization of proteases from skin mucus of tambacu, a Neotropical hybrid fish. *Fish Physiology and Biochemistry*, *33*(2), 173–179. https://doi.org/10.1007/s10695-007-9128-7

Sanahuja, I., Fernández-Alacid, L., Sánchez-Nuño, S., Ordóñez-Grande, B., & Ibarz, A. (2019). Chronic Cold Stress Alters the Skin Mucus Interactome in a Temperate Fish Model. *Frontiers in Physiology*, *9*. https://doi.org/10.3389/fphys.2018.01916

Sanahuja, I., & Ibarz, A. (2015a). Skin mucus proteome of gilthead sea bream: A non-invasive method to screen for welfare indicators. *Fish and Shellfish Immunology*, *46*(2), 426–435. https://doi.org/10.1016/j.fsi.2015.05.056

Sanahuja, I., & Ibarz, A. (2015b). Skin mucus proteome of gilthead sea bream: A non-invasive method to screen for welfare indicators. *Fish and Shellfish Immunology*, *46*(2), 426–435. https://doi.org/10.1016/j.fsi.2015.05.056

Sánchez, A., Recillas, S., Font, X., Casals, E., González, E., & Puntes, V. (2011). Ecotoxicity of, and remediation with, engineered inorganic nanoparticles in the environment. *TrAC - Trends in Analytical Chemistry*, *30*(3), 507–516. https://doi.org/10.1016/j.trac.2010.11.011

Sánchez-Nuño, S., Eroldogan, O., Sanahuja, I., Özşahniğlu, I., Blasco, J., Fernández-Borràs, J., Fontanillas, R., Guerreiro, P., & Ibarz, A. (2018). Cold-induced growth arrest in gilthead sea bream Sparus aurata: metabolic reorganisation and recovery. *Aquaculture Environment Interactions*, *10*, 511–528. https://doi.org/10.3354/aei00286

Sánchez-Nuño, S., Sanahuja, I., Fernández-Alacid, L., Ordóñez-Grande, B., Fontanillas, R., Fernández-Borràs, J., Blasco, J., Carbonell, T., & Ibarz, A. (2018). Redox Challenge in a Cultured Temperate Marine Species During Low Temperature and Temperature Recovery. *Frontiers in Physiology*, *9*. https://doi.org/10.3389/fphys.2018.00923

Sanni, S., Øysæd, K. B., Høivangli, V., & Gaudebert, B. (1998). A Continuous Flow System (CFS) for chronic exposure of aquatic organisms. *Marine Environmental Research*, *46*(1–5), 97–101. https://doi.org/10.1016/S0141-1136(97)00086-X

Santos, G. A., Schrama, J. W., Mamauag, R. E. P., Rombout, J. H. W. M., & Verreth, J. A. J. (2010). Chronic stress impairs performance, energy metabolism and welfare indicators in European seabass (Dicentrarchus labrax): The combined effects of fish crowding and water quality deterioration. *Aquaculture*, *299*(1–4), 73–80. https://doi.org/10.1016/j.aquaculture.2009.11.018

Satake, H., & Sekiguchi, T. (2012). Toll-Like Receptors of Deuterostome Invertebrates. *Frontiers in Immunology*, *3*. https://doi.org/10.3389/fimmu.2012.00034

Sawyer, J. G., Martin, N. L., & Hancock, R. E. (1988). Interaction of macrophage cationic proteins with the outer membrane of Pseudomonas aeruginosa. *Infection and Immunity*, *56*(3), 693–698. https://doi.org/10.1128/iai.56.3.693-698.1988

Schena, M., Heller, R. A., Theriault, T. P., Konrad, K., Lachenmeier, E., & Davis, R. W. (1998). Microarrays: Biotechnology's discovery platform for functional genomics. *Trends in Biotechnology*, *16*(7), 301–306. https://doi.org/10.1016/S0167-7799(98)01219-0

Schrama, D., Cerqueira, M., Raposo, C. S., Rosa da Costa, A. M., Wulff, T., Gonçalves, A., Camacho, C., Colen, R., Fonseca, F., & Rodrigues, P. M. (2018). Dietary Creatine Supplementation in Gilthead Seabream (Sparus aurata): Comparative Proteomics Analysis on Fish Allergens, Muscle Quality, and Liver. *Frontiers in Physiology*, *9*. https://doi.org/10.3389/fphys.2018.01844

Schulz-Knappe, P., Hans-Dieter, Z., Heine, G., Jurgens, M., Hess, R., & Schrader, M. (2001). Peptidomics The Comprehensive Analysis of Peptides in Complex Biological Mixtures. *Combinatorial Chemistry & High Throughput Screening*, *4*(2), 207–217. https://doi.org/10.2174/1386207013331246

Scott, A. P., & Baynes, S. M. (1980). A review of the biology, handling and storage of salmonid spermatozoa. *Journal of Fish Biology*, *17*(6), 707–739. https://doi.org/10.1111/j.1095-8649.1980.tb02804.x

Secombes, C. J. (2016). What's new in fish cytokine research? *Fish and Shellfish Immunology*, *53*, 1–3. https://doi.org/10.1016/j.fsi.2016.03.035

Seidler, J., Zinn, N., Boehm, M. E., & Lehmann, W. D. (2010). De novo sequencing of peptides by MS/MS. *Proteomics*, *10*(4), 634–649. https://doi.org/10.1002/pmic.200900459

Seo, J. K., Lee, M. J., Jung, H. G., Go, H. J., Kim, Y. J., & Park, N. G. (2014). Antimicrobial function of SHβAP, a novel hemoglobin β chain-related antimicrobial peptide, isolated from the liver of skipjack tuna, Katsuwonus pelamis. *Fish and Shellfish Immunology*, *37*(1), 173–183. https://doi.org/10.1016/j.fsi.2014.01.021

Shaliutina, A., Hulak, M., Dzuyba, B., & Linhart, O. (2012). Spermatozoa motility and variation in the seminal plasma proteome of Eurasian perch (Perca fluviatilis) during the reproductive season. *Molecular Reproduction and Development*, *79*(12), 879–887. https://doi.org/10.1002/mrd.22126

Shao, C., Bao, B., Xie, Z., Chen, X., Li, B., Jia, X., Yao, Q., Ortí, G., Li, W., Li, X., Hamre, K., Xu, J., Wang, L., Chen, F., Tian, Y., Schreiber, A. M., Wang, N., Wei, F., Zhang, J., … Chen, S. (2017). The genome and transcriptome of Japanese flounder provide insights into flatfish asymmetry. *Nature Genetics*, *49*(1), 119–124. https://doi.org/10.1038/ng.3732

Shekhar, H. U. (2017). Applications of Mass-Spectrometry Based Quantitative Proteomics to Understand Complex Cellular Functions and Cell Fate Decisions. *Biomedical Journal of Scientific & Technical Research*, *1*(1), 169–171. https://doi.org/10.26717/bjstr.2017.01.000144

Shevchenko, A., Wilm, M., & Mann, M. (1997). Peptide sequencing by mass spectrometry for homology searches and cloning of genes. *Journal of Protein Chemistry*, *16*(5), 481–490. https://doi.org/10.1023/A:1026361427575

Silk, E., Zhao, H., Weng, H., & Ma, D. (2017). The role of extracellular histone in organ injury. *Cell Death and Disease*, *8*(5), 1–11. https://doi.org/10.1038/cddis.2017.52

Simmons, D. B. D., Miller, J., Clarence, S., McCallum, E. S., Balshine, S., Chandramouli, B., Cosgrove, J., & Sherry, J. P. (2017). Altered expression of metabolites and proteins in wild and caged fish exposed to wastewater effluents in situ. *Scientific Reports*, *7*(1), 1–14. https://doi.org/10.1038/s41598-017-12473-6

Simon, R., Jubeaux, G., Chaumot, A., Lemoine, J., Geffard, O., & Salvador, A. (2010). Mass spectrometry assay as an alternative to the enzyme-linked immunosorbent assay test for biomarker quantitation in ecotoxicology: Application to vitellogenin in Crustacea (Gammarus fossarum).

Journal of Chromatography A, *1217*(31), 5109–5115. https://doi.org/10.1016/j.chroma.2010.06.015

Simpson, B. K. (2012). *Food Biochemistry and Food Processing* (L. M. L. Nollet, F. Toldr´a, S. Benjaku, G. Paliyath, & Y. H. Hui, Eds.; 2nd ed.). Wiley-Blackwell. https://doi.org/10.1002/9781118308035

Sivaperumal, P., Sankar, T. v., & Viswanathan Nair, P. G. (2007). Heavy metal concentrations in fish, shellfish and fish products from internal markets of India vis-a-vis international standards. *Food Chemistry*, *102*(3), 612–620. https://doi.org/10.1016/j.foodchem.2006.05.041

Skogland Enerstvedt, K., Sydnes, M. O., & Pampanin, D. M. (2017). Study of the plasma proteome of Atlantic cod (Gadus morhua): Effect of exposure to two PAHs and their corresponding diols. *Chemosphere*, *183*, 294–304. https://doi.org/10.1016/j.chemosphere.2017.05.111

Smith, A. G., & Gangolli, S. D. (2002). Organochlorine chemicals in seafood: Occurrence and health concerns. *Food and Chemical Toxicology*, *40*(6), 767–779. https://doi.org/10.1016/S0278-6915(02)00046-7

Smith, L. C., Rast, J. P., Brockton, V., Terwilliger, D. P., Nair, S. v., Buckley, K. M., & Majeske, A. J. (2006). The sea urchin immune system. *Invertebrate Survival Journal*, *3*(1), 25–39.

Smith, M. P. W., Banks, R. E., Wood, S. L., Lewington, A. J. P., & Selby, P. J. (2009). Application of proteomic analysis to the study of renal diseases. *Nature Reviews Nephrology*, *5*(12), 701–712. https://doi.org/10.1038/nrneph.2009.183

Sokolowska, I., Wetie, A. G. N., Woods, A. G., & Darie, C. C. (2013). Applications of Mass Spectrometry in Proteomics. *Australian Journal of Chemistry*, *66*(7), 721. https://doi.org/10.1071/CH13137

Song, Y., Salbu, B., Teien, H. C., Evensen, Ø., Lind, O. C., Rosseland, B. O., & Tollefsen, K. E. (2016). Hepatic transcriptional responses in Atlantic salmon (Salmo salar) exposed to gamma radiation and depleted uranium singly and in combination. *Science of the Total Environment*, *562*, 270–279. https://doi.org/10.1016/j.scitotenv.2016.03.222

Sotelo, C. G., Piñeiro, C., Gallardo, J. M., & Pérez-Martin, R. I. (1993). Fish species identification in seafood products. *Trends in Food Science & Technology*, *4*(12), 395–401.

Sotton, B., Paris, A., le Manach, S., Blond, A., Lacroix, G., Millot, A., Duval, C., Huet, H., Qiao, Q., Labrut, S., Chiapetta, G., Vinh, J., Catherine, A., & Marie, B. (2017). Metabolic changes in Medaka fish induced by cyanobacterial exposures in mesocosms: An integrative approach combining proteomic and metabolomic analyses. *Scientific Reports*, *7*(1), 1–13. https://doi.org/10.1038/s41598-017-04423-z

Springate, J. R. C., Bromage, N. R., Elliott, J. A. K., & Hudson, D. L. (1984). The timing of ovulation and stripping and their effects on the rates of fertilization and survival to eying, hatch and swim-up in the rainbow trout (Salmo gairdneri R.). *Aquaculture*, *43*(1–3), 313–322. https://doi.org/10.1016/0044-8486(84)90032-2

Stentiford, G. D., Viant, M. R., Ward, D. G., Johnson, P. J., Martin, A., Wenbin, W., Cooper, H. J., Lyons, B. P., & Feist, S. W. (2005). Liver tumors in wild flatfish: A histopathological, proteomic, and metabolomic study. *OMICS A Journal of Integrative Biology*, *9*(3), 281–299. https://doi.org/10.1089/omi.2005.9.281

Stryiński, R., Mateos, J., Pascual, S., González, Á. F., Gallardo, J. M., Łopieńska-Biernat, E., Medina, I., & Carrera, M. (2019). Proteome profiling of L3 and L4 Anisakis simplex development stages by TMT-based quantitative proteomics. *Journal of Proteomics*, *201*(April), 1–11. https://doi.org/10.1016/j.jprot.2019.04.006

Sumpter, J. P., & Jobling, S. (1995). Vitellogenesis as a biomarker for estrogenic contamination of the aquatic environment. *Environmental Health Perspectives*, *103*(SUPPL. 7), 173–178. https://doi.org/10.1289/ehp.95103s7173

Sunyer, J. O., & Lambris, J. D. (1998). Evolution and diversity of the complement system of poikilothermic vertebrates. *Immunological Reviews*, *166*, 39–57. https://doi.org/10.1111/j.1600-065X.1998.tb01251.x

Sveinsdóttir, H., Martin, S. A. M., & Vilhelmsson, O. T. (2012). Application of Proteomics to Fish Processing and Quality. In *Food Biochemistry and Food Processing* (pp. 406–424). Wiley-Blackwell. https://doi.org/10.1002/9781118308035.ch22

Sveinsdóttir, H., Vilhelmsson, O., & Gudmundsdóttir, Á. (2008). Proteome analysis of abundant proteins in two age groups of early Atlantic cod (Gadus morhua) larvae. *Comparative*

Biochemistry and Physiology - Part D: Genomics and Proteomics, *3*(3), 243–250. https://doi.org/10.1016/j.cbd.2008.06.001

Swanson, W. J., & Vacquier, V. D. (2002). The rapid evolution of reproductive proteins. *Nature Reviews Genetics*, *3*(2), 137–144. https://doi.org/10.1038/nrg733

Taylor, R. S., Crosbie, P. B., & Cook, M. T. (2010). Amoebic gill disease resistance is not related to the systemic antibody response of Atlantic salmon, Salmo salar L. *Journal of Fish Diseases*, *33*(1), 1–14. https://doi.org/10.1111/j.1365-2761.2009.01108.x

Thorarinsdottir, K. A., Arason, S., Geirsdottir, M., Bogason, S. G., & Kristbergsson, K. (2002). Changes in myofibrillar proteins during processing of salted cod (Gadus morhua) as determined by electrophoresis and differential scanning calorimetry. *Food Chemistry*, *77*(3), 377–385.

Tian, L., Wang, M., Li, X., Lam, P. K. S., Wang, M., Wang, D., Chou, H. N., Li, Y., & Chan, L. L. (2011). Proteomic modification in gills and brains of medaka fish (Oryzias melastigma) after exposure to a sodium channel activator neurotoxin, brevetoxin-1. *Aquatic Toxicology*, *104*(3–4), 211–217. https://doi.org/10.1016/j.aquatox.2011.04.019

Tine, M., Kuhl, H., Gagnaire, P. A., Louro, B., Desmarais, E., Martins, R. S. T., Hecht, J., Knaust, F., Belkhir, K., Klages, S., Dieterich, R., Stueber, K., Piferrer, F., Guinand, B., Bierne, N., Volckaert, F. A. M., Bargelloni, L., Power, D. M., Bonhomme, F., … Reinhardt, R. (2014). European sea bass genome and its variation provide insights into adaptation to euryhalinity and speciation. *Nature Communications*, *5*(May), 5770. https://doi.org/10.1038/ncomms6770

Tomanek, L. (2011). Environmental proteomics: Changes in the proteome of marine organisms in response to environmental stress, pollutants, infection, symbiosis, and development. *Annual Review of Marine Science*, *3*(January), 373–399. https://doi.org/10.1146/annurev-marine-120709-142729

Tomanek, L., & Zuzow, M. J. (2010). The proteomic response of the mussel congeners Mytilus galloprovincialis and M. trossulus to acute heat stress: Implications for thermal tolerance limits and metabolic costs of thermal stress. *Journal of Experimental Biology*, *213*(20), 3559–3574. https://doi.org/10.1242/jeb.041228

Tomanek, L., Zuzow, M. J., Ivanina, A. v., Beniash, E., & Sokolova, I. M. (2011). Proteomic response to elevated PCO2 level in eastern oysters, Crassostrea virginica: Evidence for oxidative stress. *Journal of Experimental Biology*, *214*(11), 1836–1844. https://doi.org/10.1242/jeb.055475

TORT, L., PADRÓS, F., ROTLLANT, J., & CRESPO, S. (1998). Winter syndrome in the gilthead sea breamSparus aurata. Immunological and histopathological features. *Fish & Shellfish Immunology*, *8*(1), 37–47. https://doi.org/10.1006/fsim.1997.0120

Toshio, N. (1992). Nerve membrane Na+ channels as targets of insecticides. *Trends in Pharmacological Sciences*, *13*(C), 236–241. https://doi.org/10.1016/0165-6147(92)90075-H

Tsang, H. H., Welch, M. J., Munday, P. L., Ravasi, T., & Schunter, C. (2020). Proteomic Responses to Ocean Acidification in the Brain of Juvenile Coral Reef Fish. *Frontiers in Marine Science*, *7*(July), 1–12. https://doi.org/10.3389/fmars.2020.00605

Ullal, A. J., Wayne Litaker, R., & Noga, E. J. (2008). Antimicrobial peptides derived from hemoglobin are expressed in epithelium of channel catfish (Ictalurus punctatus, Rafinesque). *Developmental and Comparative Immunology*, *32*(11), 1301–1312. https://doi.org/10.1016/j.dci.2008.04.005

Ünlü, M., Morgan, M. E., & Minden, J. S. (1997). Difference gel electrophoresis: A single gel method for detecting changes in protein extracts. *Electrophoresis*, *18*(11), 2071–2077. https://doi.org/10.1002/elps.1150181133

Urdaneta, V., Camafeita, E., Poleo, G., Guerrero, H., Bernal, C., Galindo, I., & Diez, N. (2018). Proteomic characterization of vitellogenins from three species of South American fresh water fish. *Latin American Journal of Aquatic Research*, *46*(1), 187–196. https://doi.org/10.3856/vol46-issue1-fulltext-18

Uttakleiv Ræder, I. L., Paulsen, S. M., Smalås, A. O., & Willassen, N. P. (2007**a**). Effect of fish skin mucus on the soluble proteome of Vibrio salmonicida analysed by 2-D gel electrophoresis and tandem mass spectrometry. *Microbial Pathogenesis*, *42*(1), 36–45. https://doi.org/10.1016/j.micpath.2006.10.003

Uttakleiv Ræder, I. L., Paulsen, S. M., Smalås, A. O., & Willassen, N. P. (2007**b**). Effect of fish skin mucus on the soluble proteome of Vibrio salmonicida analysed by 2-D gel electrophoresis and

tandem mass spectrometry. *Microbial Pathogenesis*, *42*(1), 36–45. https://doi.org/10.1016/j.micpath.2006.10.003

Vacquier, V. D., & Swanson, W. J. (2011). Selection in the rapid evolution of gamete recognition proteins in marine invertebrates. *Cold Spring Harbor Perspectives in Biology*, *3*(11), 1–18. https://doi.org/10.1101/cshperspect.a002931

Valdenegro-Vega, V. A., Crosbie, P., Bridle, A., Leef, M., Wilson, R., & Nowak, B. F. (2014). Differentially expressed proteins in gill and skin mucus of Atlantic salmon (Salmo salar) affected by amoebic gill disease. *Fish and Shellfish Immunology*, *40*(1), 69–77. https://doi.org/10.1016/j.fsi.2014.06.025

van Vliet, E. (2014). Omics and Related Recent Technologies. In *Encyclopedia of Toxicology: Third Edition* (Third Edit, Vol. 3). Elsevier. https://doi.org/10.1016/B978-0-12-386454-3.01056-3

Vasta, G. R., Nita-Lazar, M., Giomarelli, B., Ahmed, H., Du, S., Cammarata, M., Parrinello, N., Bianchet, M. A., & Amzel, L. M. (2011). Structural and functional diversity of the lectin repertoire in teleost fish: Relevance to innate and adaptive immunity. *Developmental and Comparative Immunology*, *35*(12), 1388–1399. https://doi.org/10.1016/j.dci.2011.08.011

Vastrik, I., D'Eustachio, P., Schmidt, E., Joshi-Tope, G., Gopinath, G., Croft, D., de Bono, B., Gillespie, M., Jassal, B., Lewis, S., Matthews, L., Wu, G., Birney, E., & Stein, L. (2007). Reactome: A knowledge base of biologic pathways and processes. *Genome Biology*, *8*(3). https://doi.org/10.1186/gb-2007-8-3-r39

Verrez-Bagnis, V., Noel, J., Sautereau, C., & Fleurence, J. (1999). Desmin degradation in postmortem fish muscle. *Journal of Food Science*, *64*(2), 240–242. https://doi.org/10.1111/j.1365-2621.1999.tb15873.x

Vieira, L. R., Hissa, D. C., de Souza, T. M., Chayenne A., S., Evaristo, J. A. M., Nogueira, F. C. S., Carvalho, A. F. U., & Farias, D. F. (2020). Proteomics analysis of zebrafish larvae exposed to 3,4-dichloroaniline using the fish embryo acute toxicity test. *Environmental Toxicology*, *35*(8), 849–860. https://doi.org/10.1002/tox.22921

Vilhelmsson, O. T., Martin, S. A. M., Médale, F., Kaushik, S. J., & Houlihan, D. F. (2004). Dietary plant-protein substitution affects hepatic metabolism in rainbow trout (Oncorhynchus mykiss) . *British Journal of Nutrition*, *92*(1), 71–80. https://doi.org/10.1079/bjn20041176

Vilhelmsson, O. T., Martin, S. A. M., Poli, B. M., & Houlihan, D. F. (2007). Proteomics: Methodology and Application in Fish Processing. In *Food Biochemistry and Food Processing* (pp. 401–422). Blackwell Publishing. https://doi.org/10.1002/9780470277577.ch18

Villavedra, M., To, J., Lemke, S., Birch, D., Crosbie, P., Adams, M., Broady, K., Nowak, B., Raison, R. L., & Wallach, M. (2010). Characterisation of an immunodominant, high molecular weight glycoprotein on the surface of infectious Neoparamoeba spp., causative agent of amoebic gill disease (AGD) in Atlantic salmon. *Fish and Shellfish Immunology*, *29*(6), 946–955. https://doi.org/10.1016/j.fsi.2010.07.036

Vincent, B. N., Adams, M. B., Nowak, B. F., & Morrison, R. N. (2009). Cell-surface carbohydrate antigen(s) of wild-type Neoparamoeba spp. are immunodominant in sea-cage cultured Atlantic salmon (Salmo salar L.) affected by amoebic gill disease (AGD). *Aquaculture*, *288*(3–4), 153–158. https://doi.org/10.1016/j.aquaculture.2008.11.036

Vincent, B. N., Nowak, B. F., & Morrison, R. N. (2008). Detection of serum anti-Neoparamoeba spp. antibodies in amoebic gill disease-affected Atlantic salmon Salmo salar. *Journal of Fish Biology*, *73*(2), 429–435. https://doi.org/10.1111/j.1095-8649.2008.01891.x

Wade, M. G., Desaulniers, D., Leingartner, K., & Foster, W. G. (1997). Interactions between endosulfan and dieldrin on estrogen-mediated processes in vitro and in vivo. *Reproductive Toxicology*, *11*(6), 791–798. https://doi.org/10.1016/S0890-6238(97)00062-2

Wang, J., Li, D., Dangott, L. J., & Wu, G. (2006). Recent Advances in Nutritional Sciences Proteomics and Its Role in. *Journal Of Chromatography*, 1759–1762.

Wang, L., Shao, C., Xu, W., Zhou, Q., Wang, N., & Chen, S. (2017). Proteome profiling reveals immune responses in Japanese flounder (Paralichthys olivaceus) infected with Edwardsiella tarda by iTRAQ analysis. *Fish and Shellfish Immunology*, *66*, 325–333. https://doi.org/10.1016/j.fsi.2017.05.022

Wang, M., Wang, Y., Wang, J., Lin, L., Hong, H., & Wang, D. (2011). Proteome profiles in medaka (Oryzias melastigma) liver and brain experimentally exposed to acute inorganic mercury. *Aquatic Toxicology*, *103*(3–4), 129–139. https://doi.org/10.1016/j.aquatox.2011.02.020

Wang, N., MacKenzie, L., de Souza, A. G., Zhong, H., Goss, G., & Li, L. (2007). Proteome profile of cytosolic component of zebrafish liver generated by LC− ESI MS/MS combined with trypsin digestion and microwave-assisted acid hydrolysis. *Journal of Proteome Research*, *6*(1), 263–272.

Wasinger, V. C., Cordwell, S. J., Cerpa-Poljak, A., Yan, J. X., Gooley, A. A., Wilkins, M. R., Duncan, M. W., Harris, R., Williams, K. L., & Humphery-Smith, I. (1995). Progress with gene-product mapping of the Mollicutes:Mycoplasma genitalium. *Electrophoresis*, *16*(1), 1090–1094. https://doi.org/10.1002/elps.11501601185

Welford, S. M., Gregg, J., Chen, E., Garrison, D., Sorensen, P. H., Denny, C. T., & Nelson, S. F. (1998). Detection of differentially expressed genes in primary tumor tissues using representational differences analysis coupled to microarray hybridization. *Nucleic Acids Research*, *26*(12), 3059–3065. https://doi.org/10.1093/nar/26.12.3059

Westermeier, R., & Marouga, R. (2005). Protein detection methods in proteomics research. *Bioscience Reports*, *25*(1–2), 19–32. https://doi.org/10.1007/s10540-005-2845-1

Wilburn, D. B., & Swanson, W. J. (2016). From molecules to mating: Rapid evolution and biochemical studies of reproductive proteins. *Journal of Proteomics*, *135*, 12–25. https://doi.org/10.1016/j.jprot.2015.06.007

Wilkins, M. R., Sanchez, J. C., Gooley, A. A., Appel, R. D., Humphery-Smith, I., Hochstrasser, D. F., & Williams, K. L. (1996**a**). Progress with proteome projects: Why all proteins expressed by a genome should be identified and how to do it. *Biotechnology and Genetic Engineering Reviews*, *13*(1), 19–50. https://doi.org/10.1080/02648725.1996.10647923

Wilkins, M. R., Sanchez, J. C., Gooley, A. A., Appel, R. D., Humphery-Smith, I., Hochstrasser, D. F., & Williams, K. L. (1996**b**). Progress with proteome projects: Why all proteins expressed by a genome should be identified and how to do it. *Biotechnology and Genetic Engineering Reviews*, *13*(1), 19–50. https://doi.org/10.1080/02648725.1996.10647923

Williams, T. D., Gensberg, K., Minchin, S. D., & Chipman, J. K. (2003). A DNA expression array to detect toxic stress response in European flounder (Platichthys flesus). *Aquatic Toxicology*, *65*(2), 141–157. https://doi.org/10.1016/S0166-445X(03)00119-X

Wilm, M. (2009). Quantitative proteomics in biological research. *Proteomics*, *9*(20), 4590–4605. https://doi.org/10.1002/pmic.200900299

Woessner, J. F. (1991). Matrix metalloproteinases and their inhibitors in connective tissue remodeling. *The FASEB Journal*, *5*(8), 2145–2154. https://doi.org/10.1096/fasebj.5.8.1850705

Wojtczak, M., Całka, J., Glogowski, J., & Ciereszko, A. (2007**a**). Isolation and characterization of α1-proteinase inhibitor from common carp (Cyprinus carpio) seminal plasma. *Comparative Biochemistry and Physiology - B Biochemistry and Molecular Biology*, *148*(3), 264–276. https://doi.org/10.1016/j.cbpb.2007.06.004

Wojtczak, M., Całka, J., Glogowski, J., & Ciereszko, A. (2007**b**). Isolation and characterization of α1-proteinase inhibitor from common carp (Cyprinus carpio) seminal plasma. *Comparative Biochemistry and Physiology Part B: Biochemistry and Molecular Biology*, *148*(3), 264–276. https://doi.org/10.1016/j.cbpb.2007.06.004

Wojtczak, M., Dietrich, G. J., & Ciereszko, A. (2005). Transferrin and antiproteases are major proteins of common carp seminal plasma. *Fish and Shellfish Immunology*, *19*(4), 387–391. https://doi.org/10.1016/j.fsi.2005.01.009

Wojtczak, M., Dietrich, G. J., Irnazarow, I., Jurecka, P., Słowińska, M., & Ciereszko, A. (2007). Polymorphism of transferrin of carp seminal plasma: Relationship to blood transferrin and sperm motility characteristics. *Comparative Biochemistry and Physiology - B Biochemistry and Molecular Biology*, *148*(4), 426–431. https://doi.org/10.1016/j.cbpb.2007.07.011

Wolters, D. A., Washburn, M. P., & Yates, J. R. (2001). An automated multidimensional protein identification technology for shotgun proteomics. *Analytical Chemistry*, *73*(23), 5683–5690. https://doi.org/10.1021/ac010617e

Wu, L., & Han, D. K. (2006). Overcoming the dynamic range problem in mass spectrometry-based shotgun proteomics. *Expert Review of Proteomics*, *3*(6), 611–619. https://doi.org/10.1586/14789450.3.6.611

Wulff, T., Petersen, J., Nørrelykke, M. R., Jessen, F., & Nielsen, H. H. (2012). Proteome analysis of pyloric Ceca: A methodology for fish feed development? *Journal of Agricultural and Food Chemistry*, *60*(34), 8457–8464. https://doi.org/10.1021/jf3016943

Wunschel, D., Schultz, I., Skillman, A., & Wahl, K. (2005). Method for detection and quantitation of fathead minnow vitellogenin (Vtg) by liquid chromatography and matrix-assisted laser desorption/ionization mass spectrometry. *Aquatic Toxicology*, *73*(3), 256–267. https://doi.org/10.1016/j.aquatox.2005.03.015

Xiong, X. P., Dong, C. F., Xu, X., Weng, S. P., Liu, Z. Y., & He, J. G. (2011). Proteomic analysis of zebrafish (Danio rerio) infected with infectious spleen and kidney necrosis virus. *Developmental and Comparative Immunology*, *35*(4), 431–440. https://doi.org/10.1016/j.dci.2010.11.006

Xiong, Y., Dan, C., Ren, F., Su, Z. H., Zhang, Y., & Mei, J. (2020**a**). Proteomic profiling of yellow catfish (Pelteobagrus fulvidraco) skin mucus identifies differentially-expressed proteins in response to Edwardsiella ictaluri infection. In *Fish and Shellfish Immunology* (Vol. 100). Elsevier Ltd. https://doi.org/10.1016/j.fsi.2020.02.059

Xiong, Y., Dan, C., Ren, F., Su, Z. H., Zhang, Y., & Mei, J. (2020**b**). Proteomic profiling of yellow catfish (Pelteobagrus fulvidraco) skin mucus identifies differentially-expressed proteins in response to Edwardsiella ictaluri infection. *Fish & Shellfish Immunology*, *100*, 98–108. https://doi.org/10.1016/j.fsi.2020.02.059

Xiong, Y., Dan, C., Ren, F., Su, Z. H., Zhang, Y., & Mei, J. (2020**c**). Proteomic profiling of yellow catfish (Pelteobagrus fulvidraco) skin mucus identifies differentially-expressed proteins in response to Edwardsiella ictaluri infection. *Fish and Shellfish Immunology*, *100*(December 2019), 98–108. https://doi.org/10.1016/j.fsi.2020.02.059

Xu, C., Wang, Y., Bryngelson, P., Sosic, Z., Dalton, D., & Dithiothreitol, D. T. T. (2019). Advancements of Mass Spectrometry in Biomedical Research. In *Advancements of mass spectrometry in biomedical research* (Vol. 1140). http://link.springer.com/10.1007/978-3-030-15950-4

Xu, P., Zhang, X., Wang, X., Li, J., Liu, G., Kuang, Y., Xu, J., Zheng, X., Ren, L., Wang, G., Zhang, Y., Huo, L., Zhao, Z., Cao, D., Lu, C., Li, C., Zhou, Y., Liu, Z., Fan, Z., … Sun, X. (2014). Genome

sequence and genetic diversity of the common carp, Cyprinus carpio. *Nature Genetics*, *46*(11), 1212–1219. https://doi.org/10.1038/ng.3098

Xu, R., Sheng, J., Bai, M., Shu, K., Zhu, Y., & Chang, C. (2020). A Comprehensive Evaluation of MS/MS Spectrum Prediction Tools for Shotgun Proteomics. *Proteomics*, *20*(21–22), 1–21. https://doi.org/10.1002/pmic.201900345

Xu, Z., Parra, D., Gómez, D., Salinas, I., Zhang, Y. A., von Gersdorff Jørgensen, L., Heinecke, R. D., Buchmann, K., LaPatra, S., & Oriol Sunyer, J. (2013). Teleost skin, an ancient mucosal surface that elicits gut-like immune responses. *Proceedings of the National Academy of Sciences of the United States of America*, *110*(32), 13097–13102. https://doi.org/10.1073/pnas.1304319110

Yang, F., Huang, W., Xie, W., Lu, C., & Liu, W. (2015). Targeted analytical toxicology: Simultaneous determination of 17α-ethynylestradiol and the estrogen-induced vitellogenin biomarker. *Environment International*, *74*, 119–124. https://doi.org/10.1016/j.envint.2014.10.015

Yang, H., Sturmer, L. N., & Baker, S. (2016). Molluscan Shellfish Aquaculture and Production 1 Molluscan Shellfish Aquaculture in the United States. *UNIVERSITY OF FLORIDA, IFAS Extension*, 1–8.

Ye, C. X., Wan, F., Sun, Z. Z., Cheng, C. H., Ling, R. Z., Fan, L. F., & Wang, A. L. (2016). Effect of phosphorus supplementation on cell viability, anti-oxidative capacity and comparative proteomic profiles of puffer fish (Takifugu obscurus) under low temperature stress. *Aquaculture*, *452*, 200–208. https://doi.org/10.1016/j.aquaculture.2015.10.039

Young, N. D., Cooper, G. A., Nowak, B. F., Koop, B. F., & Morrison, R. N. (2008). Coordinated down-regulation of the antigen processing machinery in the gills of amoebic gill disease-affected Atlantic salmon (Salmo salar L.). *Molecular Immunology*, *45*(9), 2581–2597. https://doi.org/10.1016/j.molimm.2007.12.023

Yu, L. R., Stewart, N. A., & Veenstra, T. D. (2010). Proteomics. The Deciphering of the Functional Genome. *Essentials of Genomic and Personalized Medicine*, 89–96. https://doi.org/10.1016/B978-0-12-374934-5.00008-8

Zhang, F., Hong, H., Kranz, S. A., Shen, R., Lin, W., & Shi, D. (2019). Proteomic responses to ocean acidification of the marine diazotroph Trichodesmium under iron-replete and iron-limited conditions. *Photosynthesis Research*, *142*(1), 17–34. https://doi.org/10.1007/s11120-019-00643-8

Zhang, X., Yap, Y., Wei, D., Chen, G., & Chen, F. (2008). Novel omics technologies in nutrition research. *Biotechnology Advances*, *26*(2), 169–176. https://doi.org/10.1016/j.biotechadv.2007.11.002

Zhang, Y., Mu, H., Lau, S. C. K., Zhang, Z., & Qiu, J. W. (2015). Sperm proteome of Mytilus galloprovincialis: Insights into the evolution of fertilization proteins in marine mussels. *Proteomics*, *15*(23–24), 4175–4179. https://doi.org/10.1002/pmic.201500066

Zhou, T., Liu, S., Geng, X., Jin, Y., Jiang, C., Bao, L., Yao, J., Zhang, Y., Zhang, J., Sun, L., Wang, X., Li, N., Tan, S., & Liu, Z. (2017). GWAS analysis of QTL for enteric septicemia of catfish and their involved genes suggest evolutionary conservation of a molecular mechanism of disease resistance. *Molecular Genetics and Genomics*, *292*(1), 231–242. https://doi.org/10.1007/s00438-016-1269-x

Zilli, L., Schiavone, R., Storelli, C., & Vilella, S. (2008**a**). Molecular mechanisms determining sperm motility initiation in two sparids (Sparus aurata and Lithognathus mormyrus). *Biology of Reproduction*, *79*(2), 356–366. https://doi.org/10.1095/biolreprod.108.068296

Zilli, L., Schiavone, R., Storelli, C., & Vilella, S. (2008**b**). Molecular mechanisms determining sperm motility initiation in two sparids (Sparus aurata and Lithognathus mormyrus). *Biology of Reproduction*, *79*(2), 356–366. https://doi.org/10.1095/biolreprod.108.068296

Zilli, L., Schiavone, R., & Vilella, S. (2017). Role of protein phosphorylation/dephosphorylation in fish sperm motility activation: State of the art and perspectives. *Aquaculture*, *472*, 73–80. https://doi.org/10.1016/j.aquaculture.2016.03.043

Zilli, L., Schiavone, R., Zonno, V., Rossano, R., Storelli, C., & Vilella, S. (2005). Effect of cryopreservatron on sea bass sperm proteins. *Biology of Reproduction*, *72*(5), 1262–1267. https://doi.org/10.1095/biolreprod.104.036202

Zissler, A., Stoiber, W., Steinbacher, P., Geissenberger, J., Monticelli, F. C., & Pittner, S. (2020). Postmortem protein degradation as a tool to estimate the PMI: A systematic review. *Diagnostics*, *10*(12). https://doi.org/10.3390/diagnostics10121014

Ziv, T., Gattegno, T., Chapovetsky, V., Wolf, H., Barnea, E., Lubzens, E., & Admon, A. (2008). Comparative proteomics of the developing fish (zebrafish and gilthead seabream) oocytes. *Comparative Biochemistry and Physiology - Part D: Genomics and Proteomics*, *3*(1), 12–35. https://doi.org/10.1016/j.cbd.2007.06.004

Zou, J., & Secombes, C. J. (2016). The function of fish cytokines. *Biology*, *5*(2). https://doi.org/10.3390/biology5020023

Zybailov, B., Mosley, A. L., Sardiu, M. E., Coleman, M. K., Florens, L., & Washburn, M. P. (2006). Statistical Analysis of Membrane Proteome Expression Changes in Saccharomyces c erevisiae. *Journal of Proteome Research*, *5*(9), 2339–2347. https://doi.org/10.1021/pr060161n

11. LIST OF LEGENDS

Figure 12. Cross-reactivity between polyclonal antibodies against (A) transferrin, (B) prostaglandin D. synthase and (C) a1-antiproteinase and ovarian fluid samples (OF1, OF2, OF3). M, molecular mass marker (202.403–6.026 kDa)

Figure 13. Two-dimensional gel of rainbow trout coelomic fluid Silver stained 2D-PAGE of coelomic fluid 21 days (D21) after ovulation. Proteins (40 µg) were loaded. Protein spots marked with arrows were excised from 2D gels for MALDI-TOF-MS analysis (the numbering of spots corresponds to table 6) (Rime et al., 2004).

Figure 14. Two-dimensional gel analysis of rainbow trout coelomic fluid during post-ovulatory ageing Two-dimensional gel of rainbow trout coelomic fluid pools originating from 17 females sampled at the time of ovulation (A) and on day 7 (B), day 14 (C) and day 21 (D) after ovulation. Each sample (40 µg) was separated by IEF using a non linear immobilized pH 3–10 gradient for separation in the first dimension combined with SDS-PAGE 12% – 14% gradient gel in the second dimension. Optic density (OD, arbitrary units) of spots shown on the left panel is plotted on the graph (E). OD was arbitrarily set to 1 at 7 days postovulation (Rime et al., 2004).

Figure 15. Two-dimensional gel analysis of rainbow trout coelomic fluid at 5 and 16 days post-ovulation Two-dimensional gel of rainbow trout coelomic fluid pools originating from 22 females sampled on day 5 (A) and day 16 (B) after ovulation. Each sample (40 µg) was separated by IEF using a non linear immobilized pH 3–10 gradient for separation in the first dimension com- bined with SDS-PAGE 12 – 14% gradient gel in the second dimension. Optic density (OD, arbitrary units) of spots shown on the left panel is plotted on the graph (C). OD was arbitrarily set to 1 at 5 days post-ovulation (Nomura M, Sakai K, 1974).

Figure 16. 2D gels of Atlantic cod skin mucosal proteins. (1A) 15% 2D reference gel (17 cm) stained with Coomassie blue G. The circled portion within the gel shows galectin-1 isoforms. (1b) 10% 2D gel (17 cm) stained with Coomassie blue G. The circled portions within the gels show serpin isoforms (br-64, br-65, br-66, br-67) and 14-3-3 isoforms (br-27, br-28, br- 55, br-56). Molecular weight is indicated in kDa (Rajan et al., 2011).

Figure 17. Classification of protein spots from the mucus of Atlantic cod identified through LC-ESI-MS/MS. The spots identified were clustered into different categories based on gene ontology category: biological process (Rajan et al., 2011).

Figure 18. Functional analysis of identified proteins enriched in SP. (A) Ontology analysis. (B) STRING protein-protein interaction network. The figure was produced using STRING evidence view. Proteins in the black, blue and red circles belong to the ubiquitination, cell cycle damage checkpoint regulation and acute phase response signalling pathways, respectively. (C) Signalling

pathways and functions of proteins enriched in SP (Ingenuity Pathway Analysis) (Nynca et al., 2017).

Figure 19. Schematic studies of seminal plasma proteome for Chinook salmon alternative reproductive tactics (Gombar et al., 2017).

Figure 20. Schematic workflow of seminal plasma sample preparation and proteomic analysis. Seminal plasma was extracted from milt by centrifugation, and proteins were prepared for mass spectrometry analysis using RapiGest solubilization and in-solution trypsin digestion (Steps 1–5). Label-free internal standards (Hi3) were added to each sample for absolute quantitation (Step 6). Samples were analyzed by UPLC ion-mobility data-independent mass spectrometry (Step 7), and the data was processed using Progenesis-QI (Step 8). Statistical analysis was performed to determine significant differences in protein abundance (Step 8) (Gombar et al., 2017).

Figure 21. Gene ontology of seminal plasma proteins identified in Chinook salmon (Oncorhynchus tswatchysha) jack and hooknose seminal plasma. A) Gene ontology mapped for seminal plasma proteins in relation to biological processes. B) Gene ontology mapped for seminal plasma proteins concerning molecular function. Gene ontology terms are shown in adjacent legend with a corresponding number of matching proteins (Gombar et al., 2017).

Figure 22. (A) Venn diagram showing shared and specific proteins obtained by the three sampling methods; (B) Complete protein set (1192) with mean normalized TIC and regression line for each sampling method, sorted by increasing variation coefficient (%CV) of TIC values between the methods; (C) Scatterplot showing significant and insignificant differences in the mean normalized TIC obtained by absorbed vs wiped, (D) wiped vs scraped, and (E) absorbed vs scraped sampling methods for all detected proteins. Proteins described in more detail in Fig. 23 are boxed (Fæste et al., 2020).

Figure 23. Examples for proteins detected (A) with comparable abundance by all sampling methods (serum albumin); (B) only in scraped samples (disulphide-isomerase A3); (C) both in scraped and wiped samples with insignificant %CV (60S acidic ribosomal protein P2); both in absorbed and wiped samples with insignificant %CV (ester hydrolase C1) (Fæste et al., 2020).

Figure 24. The complete sequence of rainbow trout vitellogenin, entry Q92093 on the Swiss Prot database (Banoub et al., 2003).

Figure 25. Venn Diagram. Number of proteins found in extracts from the venomous apparatus (Sp-VAe) and from the skin mucus (Sp-SMe). Proteins found exclusively in Sp-VAe were named Sp-VP: S. plumieri Venom Proteins (Borges et al., 2018).

Figure 26. Distribution of identified proteins. Proteins were manually clustered into ten groups (1−10) according to similarities found through blast analysis in Uniprot/SwissProt. (1) Sp-VP (S. plumieri Venom Proteins): proteins found exclusively in Sp-VAe; (2) Sp-SMe: skin mucus proteins, including those also found in Sp-VAe (patterned area) (Borges et al., 2018).

Figure 27. 1D and 2D SDS-PAGE gel profiles of N. kuhlii barb venom protein extract. A) 1D SDS-PAGE gel profile highlighting the bands that were selected for in-gel digestion and protein identification. B) 2D SDS-PAGE gel profile highlighting the spots that were selected for in-gel digestion and protein identification. The numbers in each gel refer to the proteins displayed in Table 15. The gels were stained with Colloidal Coomassie Brilliant Blue G250(K. Baumann et al., 2014).

Figure 28. GO-term classification of the assembled and annotated N. kuhlii venom gland transcriptome. A) Level 2 and B) level 3 GO-term analysis of the annotated contigs. C) The relative abundance of proteins in the N. kuhlii venome (venom proteome) is calculated by transcriptomic expression levels (K. Baumann et al., 2014).

Figure 29. Differentially expressed proteins in the testis of wild-caught Senegalese sole during spermiation (F0Mat) and in the F1 testis after treatment of fish with saline (F1C), GnRHa (F1GnRHa), or GnRHa 1 OA (F1GnRHa 1 OA).Proteins were classified into six groups according to the expression pattern. The figure shows the first three groups. Values are the mean 6 SEM of the standardized abundance of each spot. Values with different superscript are significantly different (ANOVA, p,0.05).

Figure 30. Workflow for LC-MS/MS analysis of epidermal mucus samples and multivariate analysis of normalized spectral count data (Provan et al., 2013).

Figure 31. PCA score plot of samples from controls (CC, green circles), low lice levels (LL, blue squares) and high lice levels (HL, red triangles) (Provan et al., 2013).

Figure 32. NF-κB target genes involved in inflammation development and progression. NF-κB is an inducible transcription factor. After its activation, it can activate transcription of various genes and thereby regulate inflammation. NF-κB targets inflammation not only directly by increasing the production of inflammatory cytokines, chemokines and adhesion molecules but also by regulating the cell proliferation, apoptosis, morphogenesis and differentiation (T. Liu et al., 2017).

Figure 33. Proteomic analysis showing alterations in the protein profile of epinecidine-1- treated zebrafish(T. C. Huang & Chen, 2013).

Figure 34. Network analysis of differentially expressed proteins was performed using the Ingenuity Pathways Analysis (IPA) software. Proteins highlighted in red were identified as up-regulated, and those highlighted in green were found to be down-regulated in epinecidine-1 treated zebrafish(T. C. Huang & Chen, 2013).

Figure 35. Gene ontology (GO) analysis of proteins differentially expressed in epinecidine-1-treated zebrafish. The GO (A) cellular component, (B) biological process, and (C) molecular function annotations were classified using STRAP software. The percentage of proteins for each class is shown as represented in the pie chart (T. C. Huang & Chen, 2013).

Figure 36. Protein extractions from Atlantic salmon (Salmo salar) gill mucus resolved by Bis-Tris 4e12% NuPAGE and silver stained. Each lane contains a similar protein yield amount (~4 mg per lane) after dialysis and lyophilisation. Lane 1 MWM, lanes 2e6: gill mucus samples from AGD-naïve fish, lanes 7e10: gill mucus from AGD- affected fish. Stars indicate bands that were excised and subjected to in-gel digestion for identification by nanoLC/MS (Valdenegro-Vega et al., 2014).

Figure 37. Summary information of the skin mucus proteome analysis. (A) Statistics of proteomic sequencing and annotation. Total spectra: the number of the mass spectra; Spectra: the number of mass spectra after quality control; Unique peptide: specific peptide in a group of proteins. (B) VENN diagram illustrating the number of standard and unique proteins per group. C1, C2 and C3 indicate three control groups, and E. ictaluri-infected groups are indicated by P1, P2, P3. Total number of proteins of each group is shown(Y. Xiong et al., 2020c).

Figure 38. Protein classes identified by mass spectrometry. Proteins identified by Mass Spectrometry were examined using Panther (Protein Analysis Through Evolutionary Relationships, Version 13.1). A total of 137 protein was recognized and divided into eighteen classes: calcium-binding protein, cell adhesion molecule, chaperone, cytoskeletal protein, enzyme modulator, hydrolase, isomerase, ligase, lyase, membrane traffic protein, nucleic acid binding, oxidoreductase, receptor, a signalling molecule, transcription factor, transfer/carrier protein, transferase, transporter (Inguglia et al., 2020).

Figure 39. Proteome-wide identification of lysine acetylation sites and proteins in CIK cells in response to grass carp reovirus (GCRV) infection. (A) Lysine acetylation in GCRV infected or mock-infected cells as analyzed by Western blotting, β-actin was used as loading control; (B) Experimental strategy used to identify and quantify acetylated lysine sites in CIK cells in response to GCRV infection; (C) Number of identified and quantified lysine-acetylated sites and proteins. The up-regulated and down-regulated sites and proteins were also indicated. The number of proteins was shown in brackets; (D) Distribution of acetylated proteins based on their number of acetylation sites (Guo et al., 2017).

Figure 40. Gene ontology (GO) analysis of differentially expressed proteins in gills. A total of 82 proteins were identified as differentially expressed by iTRAQ analysis. Shown above is the classification of these proteins in different categories based on biological processes (A. Lü et al., 2014).

Figure 41. Summary of experimental study design (Causey et al., 2018).

Figure 42. The protein-protein interaction network of 38 up-regulated spleen proteins excluding uncharacterized proteins (Kumar et al., 2018).

Figure 43. 2-D PAGE map of Moraxella spp. positive (A) and negative (B) kidney tissue. Circled, numbered spots indicate all spots identified in this work, ordered following the increase in expression upon Moraxella sp. colonization. The ten spots most significantly upregulated in positive kidney are indicated in white. Protein identifications corresponding to spot numbers are reported in Table 30 (Addis et al., 2010).

Figure 44. D. labrax skin mucus 2DE map. Two hundred µg of proteins were loaded on 17 cm, 3–10 nonlinear IPG strips. Second dimension was a 12.5% polyacrylamide vertical gel. Red circles and numbers show analysed protein spots (Cordero et al., 2015b).

Figure 45. 2-DE image of the total soluble protein extract of V. salmonicida LFI 315. The protein extract was separated on a 13 cm nonlinear pH 3–10 IPG strip, followed by separation on 12% SDS-polyacrylamide gel. Numbers indicate annotated protein spots (see Supplementary Table S9). The protein load was 200 mg (Uttakleiv Ræder et al., 2007b).

Figure 46. Advantages and drawbacks of pollution biomonitoring from a proteomic point of view (López-Pedrouso et al., 2020).

Figure 47. Representative two-dimensional electrophoresis gels of common carp liver (n = 3) following exposure to Cu-NPs for 7 days. (Note: The spots chosen for MALDI-TOF/TOF) (a) Control and (b) Cu-NPs 100mM exposed groups. The coomassie stained 2D-gels from control and treated groups were compared with the Image Master 2D Platinum (GE-Healthcare) system. Spots indicated by circles were found to be up-regulated (U) and down-regulated (D) across the two groups. Spots were: Selenide, water dikinase 1 (UR1), ferritin heavy chain (DR1), rho guanine nucleotide exchange factor 17-like (DR2), Cytoglobin-1 (DR3) and Diphosphomevalonate decarboxylase (DR4) (Gupta et al., 2016).

Figure 48. Overview of the plasma protein profile of female Atlantic cod (gonad somatic index < 1, n = 51) identified by shotgun mass spectrometry analysis. Protein relative abundance was

calculated according to (Zybailov et al., 2006) and is reported as %. The 10 most abundant proteins are reported individually, while the remaining proteins are grouped as the top 11 to 20 most abundant proteins (top 11–20), the top 21 to 50 most abundant proteins (top 21–50) and the remaining proteins numbered 51 to 369 (other proteins) (Skogland Enerstvedt et al., 2017).

Figure 49. Characteristics of the top 20 high abundant proteins in plasma of Atlantic cod females (gonad somatic index < 1, n = 51). Gene ontology distribution according to: biological processes (A), molecular functions (B) and cellular components (C), results based on the UniProt homolog search (Skogland Enerstvedt et al., 2017).

Figure 50. Gels comparison of controls and treated samples. (A and B) Gels from control samples were stained respectively for phosphorylated and all proteins. (C and D) Gels from treated samples were stained respectively for phosphorylated and all proteins. On the four gels are indicated the spots corresponding to identified proteins. Spots numbered with letters are spots with significant statistical phosphorylation variations, and spots with numbers have significant statistical expression variations (Malécot et al., 2009).

Figure 51. Venn diagram of the chemodiversityrevealed by LC-ESI-Q-TOF-MS and MALDI-TOF in experimental cyanobacterial strains(Sotton et al., 2017) .

Figure 52. Proteome dysregulations of fish exposed to MCs producing and non-producing strains of cyanobacteria were revealed by iTRAQ proteomic analysis. The dysregulated proteins (log2 (|fold-change|) > 0.3 compared to control fish) were shown. The red and green arrows correspond to up and down-regulated proteins, respectively (Sotton et al., 2017).

Figure 53. Serial detection of phosphoproteins and total proteins from medaka hepatocyte cytosolic fraction in a 2-DE gel using sequential staining. (A) Gel stained with Pro-Q Diamond phosphoprotein dye. (B) The same gel was stained with Sypro Ruby dye. Protein spots selected for identification were discriminated by the Student t-test and Mann–Whitney test (pp0.05). Numbers inside circles; spots selected from Student t-test only; numbers inside squares; spots selected from Mann–Whitney test only (Mezhoud et al., 2008).

Figure 54. Representative 2-DE gels of brain proteins in the medaka fish after 2 d exposure to PbTx-1. (A) Control and (B) 6 μg/L. The soluble proteins from medaka fish brains were separated using 2-DE and visualized with colloidal Coomassie G-250 staining. The protein spots altered by PbTx-1 exposure are labelled with numbers. The molecular weights (MW) and pI scales are indicated. Each gel is representative of three independent replicates (Tian et al., 2011).

Figure 55. Representative 2-DE protein profiles resolved from hepatic tissues of control adult female zebrafish (a), adult female zebrafish exposed to 10 lg/l ATZ (b), and adult female zebrafish

exposed to 1000 lg/l ATZ (c) for 14 days. Proteins were solubilized from zebrafish livers and separated in the first dimension by IEF using Immobiline Dry strips (24 cm), pH 3–10. Separation in the second dimension was performed using 12.5% constant gels, followed by silver staining. Differentially expressed proteins (upregulated: 1, 3, 4, 5, 6, 8, 11; downregulated: 2, 7, 9, 10, 12, 13) were excised from gels and identified by MALDI-TOF-MS (Jin et al., 2012).

Figure 56. Sliver-stained spot no. excised and destained, followed by enzymatic digestion. Peptides were analyzed with MALDI-TOFMS. After baseline correction, peak deisotoping, and peak detection, the spot was identified as the protein of 4-Hydroxyphenylpyruvate dioxygenase. The fragments of m/z 1071.5283 (FGFEPLAYK), 1217.6082 (QIHTEYSALR), 1309.5852 (NNHFGFGAGNFK), 1324.7352 (EPLFRDPLLPK), 1395.7068 (SIVVTNYEETIK), 1521.7402 (SLFEAIEKDQDAR), 1745.8834 (GAAVLKEPWVEQDAGGK), 1873.8875 (GLEFLSAPDNYYESLR),2109.0183 (FWSIDDKQIHTEYSALR), 2131.0193 (GLEFLSAPDNYYESLREK), and 2566.2371 (YAIVQTYGDTTHTFVEYLGPYK) are included in the identification (Jin et al., 2012).

Figure 57. Scatter plots showing the distribution of the protein expression measurements for the 1500 quantified proteins in the two whitefish populations, according to the -log2 P value of the ANOVA test and the -log2 fold change in expression between the 0 ppt and 10 ppt salinities. Dark circles indicate proteins with P < 0.01, and positive fold changes represent upregulation in higher salinity. (A) In the brackishwater whitefish, 34 proteins were significantly upregulated and eight significantly downregulated in 10 ppt salinity. (B) Likewise, freshwater whitefish had 61 and 12 proteins significantly up- and downregulated in 10 ppt salinity, respectively (Papakostas et al., 2012).

Figure 58. Venn diagram of differentially expressed proteins. Proteins were identified as differentially expressed relative to control through a Dunnett's test ($p \leq 0.05$)(Biales et al., 2011).

Figure 59. List of proteins with symbol, name, function (if known), fold change ($log_2(FC)$), and p-value that were differentially expressed in goldfish plasma for each caging location in CPM compared to expression at the reference site, JH. Red bars indicate increased expression while green bars indicate decreased expression. The size of the bar represents the magnitude of the difference(Simmons et al., 2017).

Figure 60. Effects of pesticide exposure and rising temperature on liver proteome response of an aquatic fish species, Carassius auratus: experimental design. (A) Timeline of the experiment: fish were acclimated during 15 days to experimental temperature in collective tanks, and then exposed to pesticides for 96 h in 30L individual aquaria. Fish wereeuthanized and liver collected at the end of the experiment. (B) Experimental design: fish were exposed at two temperatures (22 and 32◦C) to a mixture of seven commonpesticides at different concentrations: CONTROL (total concentration = 0 _g L−1), Low Dose (total concentration = 8.4 _g L−1) and High Dose (total

concentration = 42 _g L−1).N = 12 fish for each thermal × exposure condition. (C) Measures of some water physico-chemical parameters in each thermal condition: water temperature (◦C), dissolvedoxygen (%), pH and conductivity (_S). Measures were realized daily in each aquarium. Mean ± SD (Gandar et al., 2017).

Figure 61. Representative 2D gels showing the protein expression profiles obtained from (top) liver and (bottom) gills of C. gobio exposed for 4 days to Cd. Proteins of the samples obtained for the different experimental conditions were differentially labeled with Cy3 and Cy5. An internal standard composed of equal amounts of each sample and labeled with Cy2 was added.Labeled samples (25 μg of each of the Cy3 and Cy5 labeled samples and of the Cy2 labeled internal standard) were loaded on 24 cm pH 4-7 IPG strips and subjected to IEF. Proteins were further separated by SDS-PAGE (10%) in the second dimension. Numbers allocated by the DeCyder software indicate spots with significant changes in intensity ($p < 0.05$) (n) 3) (Dorts et al., 2011).

Figure 62. PMF of K2 protein spot (Unknown protein, gi|4633116) (J. Lu et al., 2010).

Figure 63. PMF of K4 protein (ATP synthase, H^+ transporting, mitochondrial F0 complex, sub-unit b, isoform 1, gi|54400426) (J. Lu et al., 2010).

Figure 64. PMF of K12 protein spot (eukaryotic translation initiation factor 3, sub-unit 6, gi|37681791)(J. Lu et al., 2010).

Figure 65. The protein quantities of the spots in Cd-treated and healthy control groups. The total integrated optical density was calculated by PDQuest software, and proteins were identified by matrix assisted laser desorption ionization time-of-flight tandem mass spectrometry (MALDI-TOF–MS/MS). Each bar represents the mean ± SEM of the results from four ayu (X. J. Lu et al., 2012).

Figure 66. (A) Product ion spectra of doubly charged ALHPELR at m/z 418 by targeted analysis using LC-MS/MS, the Y_2^+, Y_4^+, and Y_5^{2+} were used as diagnostic ions; (B) Product ion spectra of doubly charged FIELIQLLR at m/z 573 by targeted analysis using LC-MS/MS, the Y_5^+, Y_6^+, and Y_7^+ were used as diagnostic ions (P. He et al., 2019).

Figure 67. Schematic of experimental design from wild adult fish collection, behavioural testing, environmental CO_2 exposure treatments and Proteome iTraq experimental design (Tsang et al., 2020).

Figure 68. Functional proteome response to varying length of elevated CO_2 exposure in fish brains (Tsang et al., 2020).

Figure 69. A typical proteome map of the Atlantic herring (Clupea harengus L.) larvae obtained from standard 2-DE analysis. The marked protein spots were identified using MALDI-TOF-MS and MS/MS analyses (Maneja et al., 2014).

Figure 70. Schematic summary about analyzed gills and blood plasma of Atlantic halibut (Hippoglossus hippoglossus) exposed to temperatures of 12°C (control) and 18°C (impaired growth) in combination with control (400 µatm) or high-CO_2 water (1000 µatm) for 14 weeks. The proteome analysis was performed using (2DE) followed by Nanoflow LC-MS/MS. The main systems affected are listed. Green arrows represent up-regulation, red arrows represent down-regulation, and black dashes represent no protein regulation (K. B. de Souza et al., 2014).

Figure 71. A composite gel image (or proteome map) of twenty 2-D gel images of eastern oyster (Crassostrea virginica) mantle tissue exposed to normal and elevated CO_2 levels for 2 weeks. The image represents the mean pixel volume for each of the 456 detected protein spots. The numbers correspond to proteins that significantly changed in abundance in response to treatment conditions and identified by tandem mass spectrometry (Tomanek et al., 2011).

Figure 72. An example of protein analysis using SELDI. Protein peaks from zinc-exposed gills (A) are compared to identically processed samples from control gills (B). Subtraction of commonly occurring peaks reveals uniquely induced (present in zinc-exposed gills only) or repressed (present in control gills only) proteins (C). Quantitative analysis of exposed vs. control gills reveals proteins with altered expression levels (D). The example shown is a composite analysis of proteins with mass between 5 and 10 kDa occurring on immobilized metal affinity, weak cationic exchange, and strong anionic exchange surface affinity chips after 24 h of zinc exposure (Hogstrand et al., 2002).

Figure 73. (A) Venn diagrams of the total number of proteins identified by a nonlabeled, gel-free proteomics method (LC-ESI-MS^e). (B−D) Principal component analysis (PCA) to visualize treatment effects as well as biological variability of (B) control vs low dose,(C) control vs high dose, and (D)all treatments (Ralston-Hooper et al., 2013).

Figure 74. Scatter plot of the log transformed HPLC-MS peak areas of tryptic peptides from proteins of Fathead minnows exposed to 1.0 µg/L fadrozole (y-axis) versus control (x-axis). Red crosses (+) indicate peptides associated with proteins that did not show significant change in expression whereas dark blue crosses (+) indicate those proteins that were up-regulated (greater than 2.0 fold mean change) in fadrozole-exposed fish relative to control. Green crosses (+) represent proteins that were down-regulated in the fadrozole-exposed fish. Extracted ion chromatograms are shown for selected peptides to illustrate the reproducibility and alignment of peptides that are expressed at high (C − Predicted protein LOC 100126107) and low levels (A−

Vitellogenin 6) in the fadrozole-exposed fish (light blue peaks) relative to controls (magenta peaks), as well as peptides that that did not show changes in expression (B − 40 S ribosomal protein S8) (Ralston-Hooper et al., 2013).

Figure 75. Representative 2D gels showing the protein expression profiles obtained from PBMC isolated from Pangasianodon hypophthlmus in vivo exposed to the classic MG treatment. Proteins were separated by 24 cm 4–7 NL IPG-Strips and loaded on SDS-PAGE (8–13% acrylamid) gels. Identified spots allocated by the De Cyder software showed significant changes in intensity (Anova 2 condition 1 value, $p<0.05$; interactions value, $1\leq p\geq 0.05$) that are common for both sampling times (Pierrard et al., 2012).

Figure 76. Schematic summary about evaluating the impact of malachite green (MG) treatment in peripheral blood mononuclear cells (PBMC) of the Asian catfish, Pangasianodon hypophthalmus (Pierrard et al., 2012).

Figure 77. Workflow of proteomics: discovery and targeted proteomics (Carrera, Piñeiro, et al., 2020).

Figure 78. Genomic structure of S. chuatsi myogenin gene which contains 3 exons separated by 2 introns. The conserved basic Helix-loop-helix domain is located in the exon 1. The two putative E-boxes, the MEF2 and MEF3 binding sites are indicated in the promoter. The two E-boxes are located at 170 and 184 bp, while the MEF2 and MEF3 binding sites are located at 238 and 259 bp upstream from the ATG start codon. The full-length open reading frame is 735 bp with deduced amino acids of 250 AA (Gene bank accession # HQ724299) (Chu et al., 2014).

Figure 79. Comparison of the S. chuatsi myogenin promoter sequences with other fish species, Sparus aurata (EF462192) and Epinephelus coioides (HM190251). The two E-boxes, E-box 1 (CAGTTG) and E-box 2 (CAGTTG), MEF2 (CTAAATTTAA) and MEF3 (CAGGGTTT) binding sites are underlined. The nucleotide sequence and location of the regulatory elements are highly conserved among the three fish species (Chu et al., 2014).....

Figure 80. Protein sequence comparison of myogenin from 16 vertebrates. The highly conserved basic helix-loop-helix domains are underlined, and the basic regions are marked in square box. The conserved residues are indicated by dots. The Gene bank accession number for the selected vertebrate myogenin proteins are: Epinephelus coioides (HM190251), Sparus aurata (EF462192), Oreochromis niloticus (GU246725), Paralichthys olivaceus (EF144128), Takifugu rubripes (AY566282), Danio rerio (CAQ14920), Xenopus (Silurana) tropicalis (CAJ82458), Taeniopygia guttata (XP_002195870), Salmo salar (NP_001117072), Pelodiscus sinensis (BAJ53267), Oryctolagus cuniculus (ACN53836), Mus musculus (NP_112466), Meleagris gallopavo

(AAT39143), Anas platyrhynchos (ADG85647), Bos Taurus (BAE93440), and Homo sapiens (NP_002470) (Chu et al., 2014).

Figure 81. Phylogenetic analysis of the S. chuatsi myogenin gene sequence relative to myogenin genes from other vertebrates. The deduced protein sequences were searched from Gene bank same as in Figure 80 and the phylogenetic tree was constructed with the neighbor-joining method in MEGA version 3.0 based on Poisson-corrected pairwise distances between protein sequences. Note S. chuatsi, Epinophelus coioides, Sparus aurata and Taklfugu rubripos are in the same branch (Chu et al., 2014).

Figure 82. A trypsin digest mass spectrometry fingerprint of a rainbow trout liver protein spot, identified as apolipoprotein A I-1 (S. Martin, unpublished). The open arrows indicate mass peaks corresponding to trypsin self-digestion products and were, therefore, excluded from the analysis. The solid arrows indicate the peaks that were found to correspond to expected apolipoprotein A I-1 peptides (Vilhelmsson et al., 2007).

Figure 83. 2DE liver proteome maps of four salmonid fish (S. Martin and O. Vilhelmsson, unpublished). Running conditions are as in Figure 18.2. ***A****. Brown trout (Salmo trutta),* ***B****. Arctic charr (Salvelinus alpinus),* ***C****. rainbow trout (Oncorhynchus mykiss),* ***D****. Atlantic salmon (Salmo salar)(Hui et al., 2006).*

Figure 84. Two-dimensional gel of rainbow trout liver proteins (fish S3). A total liver protein extract was separated by charge between pI 4 and 7, second dimension was by size on a gradient 10–15% gel. The proteins were located by staining with colloidal coomassie blue G250. Proteins marked by arrows were found to be differentially expressed as a result of dietary manipulation, the corresponding number is the spot reference number. Underlined protein numbers were positively identified by trypsin digest fingerprinting (Martin, Vilhelmsson, Médale, et al., 2003).

Figure 85. Comparison of protein identification results from three digestion methods. (A) In total, 509 proteins were identified in the single zebrafish embryo proteome at 72 hpf (379, 378, and 181 proteins from the urea-, SDC-, and PA-assisted digests, respectively). (B) In total, 210 proteins were identified at 120 hpf (153, 147, and 127 proteins from the urea-, 0.5% SDC-, and 1% SDC-assisted digests, respectively) (Lin et al., 2009).

Figure 86. LC–ESI-MS/MS spectra of the tryptic peptide IEDEQSLGAQLQK (precursor m/z 729.9, 2+) identified in the samples prepared by three different digestion methods: (A) urea assisted tryptic digestion; (B) SDC-assisted tryptic digestion; (C) PA-assisted digestion (Lin et al., 2009).

Figure 87. Average gels of protein extracts from 6 dph and 24 dph cod larvae showing temporal expression of proteins during early larval development. The spots circled (white) on the protein profile from 6 dph larvae were only detected in this age group whereas circled spots (black) on the protein profile from 24 dph larvae were only expressed in that group (Sveinsdóttir et al., 2008).

Figure 88. 2-DE map of muscle proteins of rainbow trout (Oncorhynchus mykiss), prepared by linear wide-range immobilized pH gradients (pH = 3-10, 17 cm; BioRad, USA) in the first dimension and on 12% SDS-PAGE for the second dimension. Proteins were stained with colloidal coomassie brilliant blue G-250. Labeled spots indicate identified proteins with significant altered expression profile after dietary β-glucan treatment . (Ghaedi et al., 2016).

Figure 89. Muscle protein expression differences in rainbow trout fed the two type of feed. Proteins(39) of interest based on Student t-test ($P<0.05$) are marked. The 2-DE gel is a representative gel of water soluble proteins from rainbow trout muscle. Mw is given i kDa (Jessen et al., 2012).

Figure 90. Two-dimensional PAGE of serum taken from a rainbow trout before stimulus (control, left) and of serum from the same rainbow trout after treatment with probiotic GC2 for 14 days (right). Presumptive acute phase response in fish is indicated by arrows (Brunt et al., 2008).

Figure 91. Changes in normalised spot volumes of Pt1, Pt2 and Pt3 preand post-stimulus with probiotic GC2 after 14 days (Brunt et al., 2008).

Figure 92. Two-dimensional PAGE of serum taken from a rainbow trout before stimulus (control, left) and of serum from the same rainbow trout after treatment with probiotic JB-1 for 14 days (right). Presumptive acute phase response in fish is indicated by arrows (Brunt et al., 2008).

Figure 93. Changes in normalised spot volumes of Pta and Ptb pre- and post-stimulus with probiotic JB-1 after 14 days (Brunt et al., 2008).

Figure 94. 2-D PAGE of 300 μg skeletal muscle protein (whole extraction) from a mix of zebrafish fed lysine deficient and lysine enriched experimental diets, performed on 11 cm ImmobilineTM Drystrip pH 4–7 (GE Healthcare) and 13.3×8.7 cm 12 % Bis–Tris Criterion™ XT Precast Gels (Bio-Rad), and stained with Colloidal Coomassie Blue, G-250. Numbered spots represent significantly differentially expressed protein spots ($p<0.05$, Student's t test; $|fold\text{-}change|>1.2$) between treatments, selected for sequencing. Light grey circles are positively identified spots. Black circles are unidentified protein spots (de Vareilles et al., 2012).

Figure 95. Heat map showing relative abundance of identified proteins for all samples. Spots were grouped using Euclidian distance by agglomerative hierarchical clustering (complete linkage method). Only spots present in more than 80 % of spot maps and with p value lower than 0.05 (Student's t test) were included. Light shades indicate a lower than average expression of protein spots and dark shades indicate a higher than average expression. Samples from Lys(+) treatment are labelled in light grey and from Lys(−) treatment in black. Numbers refer to spot IDs (de Vareilles et al., 2012).

Figure 96. 2-DE map of muscle proteins of rainbow trout (Oncorhynchus mykiss), prepared by linear wide-range immobilized pH gradients (pH 3–10, 17 cm; BioRad, USA) in the first dimension and on 12% SDS-PAGE for the second dimension. Proteins were stained with colloidal Coomassie brilliant blue G-250. Labeled spots indicate proteins with significant altered expression profile after dietary nucleotides treatment (see Table 64) (Keyvanshokooh & Tahmasebi-Kohyani, 2012).

Figure 97. Protein sources in feeds. Pie charts illustrating the distribution of proteins according to their source in the three feeds used for this study and named A, B, and C. Protein sources are classified according to LC-MS/MS protein identification and ontology attributio (Ghisaura et al., 2014).

Figure 98. Representative 2D PAGE of gilthead sea bream serum proteins in the 4 to 7 pH range. Spots showing a differential abundance in T12A and T12B and a valid protein identification are circled in the map, and information on their changes and identity is reported in Table 67 (Ghisaura et al., 2014).

Figure 99. Representative 2-DE gels of skin mucus of S. aurata for each experimental group: commercial diet (A), probiotic diet (B), overcrowding stress (C) and overcrowding stress and probiotic diet (D). All the four gels were generated from samples at 30 days of treatment in triplicates. Skin mucus proteins were isoelectrically focused on 17 cm IPG strips (pI 3–10) and subjected to 12.5% SDS-PAGE. The 2DE gels were stained with SYPRO® Ruby protein gel stain and the spots identified in (A–D) were annotated using the data from LC–MS/MS. The spot numbers represented in gels correspond to the protein identities mentioned in Table 68 (Cordero et al., 2016b) .

Figure 100. Silver-stained 2-D acrylamide gel of proteins in liver of puffer fish exposed to 12 ± 2 °C for 12 h. Dietary P deficient group (A); and dietary P adequate group(B).Differentially expressed proteins are labeled with numbers, which correspond to the numbers present in Table 70 (Ye et al., 2016).

Figure 101. Two-dimensional gel of rainbow trout liver proteins (fish S3). A total liver protein extract was separated by charge between pI 4 and 7, second dimension was by size on a gradient

10–15% gel. The proteins were located by staining with colloidal coomassie blue G250. Proteins marked by arrows were found to be differentially expressed as a result of dietary manipulation, the corresponding number is the spot reference number. Underlined protein numbers were positively identified by trypsin digest fingerprinting (Martin, Vilhelmsson, Médale, et al., 2003).

Figure 102. Representative 2-DGE gel of liver of gilthead seabream in a pH range of 4–7 on a 12.5% polyacrylamide gel. Protein identifications of significantly different spots (one-way ANOVA and post-hoc Tukey $p < 0.05$) are shown in SupplementaryTable S16.

Figure 103. Representative pattern of gilthead seabream (Sparus aurata) blood plasma on a 12.5% polyacrylamide 2D gel. Black circles represent the 107 proteins identified by MALDI-TOF/TOF MS with significant differences in abundance in NET groups and black squares the 2 proteins with significant differences in abundance in HYP groups ($P < 0.05$) (Raposo De Magalhães et al., 2020).

Figure 104. Analytical scheme of the three sequential proteomics approaches employed for the complete de novo sequencing of new proteins: (a) classical Bottom-Up proteomics approach, (b) accurate Mr determination of intact protein by FTICR-MS and (c) monitoring of peptide mass gaps by Selected MS/MS Ion Monitoring (SMIM) (Carrera et al., 2010b).

Table 1. Transcripts (loci) showing significant differences (FDR 1% at isotig level) in expression of mature male gonad tissue between Mytilus edulis (mussels from Swansea, E) and M. galloprovincialis (mussels from Vigo, G), with GO or protein name terms associated with the search term string "SPERM" OR "FERT*" and a prediction that they have a signal peptide (SP) or a transmembrane (TM) domain in their sequences, this later information coming from SignalP 4.1, TMHMM 2.0 and InterProScan 5.0 analysis. Transcripts were functionally annotated using Blast2GO against UniProt-SwissProt database [all organisms], but protein names below are derived by checking against the nrNCBI[Mollusca] protein database. The numbers of significant isotigs from each locus (FDR 1%) with higher expression levels in M. edulis compared to M. galloprovincialis (E < G) and vice-versa (G > E) are also displayed (M. R. Romero et al., 2019).*

Table 2. Proteomic studies of fish semen(Ciereszko et al., 2012).

Table 3. The most abundant seminal plasma proteins in carp (Dietrich, Arnold, Nynca, et al., 2014)) and rainbow trout (Ciereszko et al., 2017a; Nynca, Arnold, Fröhlich, Otte, Flenkenthaler, et al., 2014).

Table 4. The most abundant sperm proteins in carp (Dietrich, Arnold, Fröhlich, et al., 2014) and rainbow trout (Ciereszko et al., 2017a; Nynca, Arnold, Fröhlich, Otte, Flenkenthaler, et al., 2014).

Table 5. Proteins common for carp seminal plasma and spermatozoa (Dietrich, Arnold, Fröhlich, et al., 2014).

Table 6. List of proteins identified in coelomic fluid during post ovulation ageing. The spot identification # corresponds to Figure 13. SwissProt accession numbers and corresponding protein names are shown (Rime et al., 2004).

Table 7. Unique proteins identified from the 2D gels of the mucus of Atlantic cod - a literature-based distinction of their immune potential, secretory nature and affiliation to mucosa (Rajan et al., 2011).

Table 8. Significant seminal plasma proteins list, that may serve as future biomarkers for Chinook salmon fertility and sperm competition (Gombar et al., 2017).

Table 9. Number (N) of identified proteins and spectra in salmon skin mucus samples collected by different sampling methods (Fæste et al., 2020).

Table 10. Most abundant proteins in salmon skin mucus samples, ranked according to their relative mean normalized TICprotein,total (Fæste et al., 2020).¤

Table 11. Typical peptide markers differentiating between mucus sampling methods (Fæste et al., 2020).

Table 12. Proteins in the skin mucus of S. aurata identified by tandem MS. MS/MS-derived peptide sequence data were used for a BLAST analysis in which the search was restricted to the class Actinopterygii. Proteins are shown match completely with the sequenced peptide (Jurado et al., 2015b).

Table 13. Proteins identified by coupled PMF and MS/MS (Jurado et al., 2015b).

Table 14. Summary information on potentially interesting toxins/proteins found in Sp-VP and Sp-SMe (Borges et al., 2018).

Table 15. Protein types identified in the barb venom gland extract of N. kuhlii (K. Baumann et al., 2014).

Table 16. Selected proteins with SR values above the statistical boundary selected by the DIVA test. Samples from control (CC) vs low lice levels (LL) (Provan et al., 2013).

Table 17. Selected proteins with SR values above the statistical boundary selected by the DIVA test. Samples from control (CC) vs high lice levels (HL) (Provan et al., 2013).

Table 18. Selected proteins with SR values above the statistical boundary selected by the DIVA test. Samples from low lice levels (LL) vs high lice levels (HL) (Provan et al., 2013).

Table 19. Proteins differentially expressed upon epinecidine-1 treatment in zebrafish, as identified by LC-ESI-MS/MS(T. C. Huang & Chen, 2013).

Table 20. Proteins significantly and differentially abundant in the skin mucus of AGD-affected Atlantic salmon. NanoLC-MS/MS identified proteins. Proteins with $P < 0.05$ and fold change >2.0 are in bold letters. SPC C, Spectral count Control group; SPC D, spectral count diseased (AGD) group; FC, fold change (Valdenegro-Vega et al., 2014).

Table 21. Detailed up-regulated proteins in response to E. ictaluri infection (Y. Xiong et al., 2020c).

Table 22. Detailed down-regulated proteins in response to E. ictaluri infection (Y. Xiong et al., 2020c) .

Table 23. List of the top 20 most abundant proteins detected in the plasma of zebrafish control. The average value and standard deviation of % emPAI values are indicated concerning the total protein of the sample (n=5). UNIPROT(Medina-Gali et al., 2019).

Table 24. Protein spots with significantly altered abundance between diploid normal larvae (DNL) and diploid deformed larvae (DDL) of rainbow trout(Babaheydari et al., 2016).

Table 25. Differentially expressed protein spots in ISKNV-infected zebrafish identified by MALDI-TOF or MALDI-TOF/TOF(X. P. Xiong et al., 2011).

Table 26. Differentially expressed proteins are associated with the immune response and other biological processes (L. Wang et al., 2017).

Table 27. Representative immune-related differentially expressed proteind proteinpressed proteinpressed proteinpressed proteins in the skin of zebrafish infected with spring viremia of carp virus (R. Liu et al., 2020).

Table 28. List of top up- and down-regulated spleen proteins of rainbow trout in response to Yersinia ruckeri strains. (Full table is presented in Supplementary Table S7) (Kumar et al., 2018).

Table 29. Simplex peptides were detected in fractions of HILIC-LC-MS/MS (Fæste et al., 2016).

Table 30. Proteins identified in sea bream kidney tissue (Addis et al., 2010).

Table 31. List of identified protein spots from liver tissue of common carp (Gupta et al., 2016).

Table 32. Top 20 high abundant proteins identified in plasma of Atlantic cod females (gonad somatic index < 1, n = 51), calculated according to Zybailov et al. (2006). Proteins are ranked according to their relative abundance, and their respective gene ontology (GO) information of biological processes and molecular function, and the cellular component which they are derived from is reported. The accession numbers behind the protein homolog identities and GO information is given as Supplementary material (Table S10) (Skogland Enerstvedt et al., 2017).

Table 33. Differentially Expressed Hepatic Thiol-Proteins Identified With MALDI-ToF MS and MS/MS (Karlsen et al., 2014).

Table 34. Selected proteins with selectivity ratio (SR) values above the statistical boundary selected by the DIVA test (Pampanin et al., 2014).

Table 35. Chemodiversity of the experimental cyanobacterial strains revealed by LC-ESI-Q-TOF-MS and MALDI-TOF analyses(Sotton et al., 2017).

Table 36. Proteins identified in the liver proteome of Channa striatus by MALDI-TOF/TOF-MS Spot (Mahanty et al., 2016).

Table 37. Protein spots isolated from 2-D gels identified by MALDI-TOF mass spectrometry combined with searches in the MASCOT database restrained to Actinopterygii (Ky et al., 2007).

Table 38. Functional annotation clusters for identified proteins calculated using DAVID software (Biales et al., 2011).

Table 39. Sea bream liver proteins undergoing significant changes along the whole trial (t_2 vs t0). RNSAF > 0.5 or < −0.5; p value < 0.05; FDR multiple comparison test <0.1 (Ghisaura et al., 2019).

Table 40. Composition and characteristics of the two mixtures of pesticides: LD and HD for total concentrations of 8.4 $\mu g\ L^{-1}$ and 42 $\mu g\ L^{-1}$, respectively. $LC_{50\text{-}96h}$: concentration which causes 50% mortality at 96 h of exposure. CLP classification of chemical risk in aquatic system (CE 1272/2008): C1 = very toxic; C2 = toxic; ND = no data; NC = not concerned (Gandar et al., 2017).

Table 41. Detailed List of Protein Identified by Nano LC−MS/MS Differentially Expressed in Liver of C. gobio Following Cd Treatment (Dorts et al., 2011).

Table 42. Protein identification summary after de novo sequencing using ESI-ITMS/MS and peptide sequence database search with Protein–Protein Blast plus relative regulation factors over control (± standard deviation) for each identified protein (P. M. Costa et al., 2010).

Table 43. The list of up-and down-regulated proteins in the fluoride-treated group (group A) compared with the control group (group B) (J. Lu et al., 2010).

Table 44. Common VTG peptides present in fathead minnow, largemouth bass, and killifish, identified using non-targeted analysis by LC-Q-TOF/MS/MS (P. He et al., 2019).

Table 45. List of identified and differentially expressed protein of the Atlantic herring larvae (Clupea harengus L.) in response to elevated pCO_2 (Maneja et al., 2014).

Table 46. Protein identifications and fold changes with hypercapnia treatment in mantle tissue of the eastern oyster, Crassostrea virginica (Tomanek et al., 2011).

Table 47. Unique and differentially expressed proteins in rainbow trout gill upon exposure to zinc, as determined by SELDI analysis (Hogstrand et al., 2002).

Table 48. Differentially Expressed Hepatic Proteinsa between Control and Fadrozole-Exposed Female Fathead Minnows (Ralston-Hooper et al., 2013).

Table 49. Detailed list of protein spots identified by nano LC-MS/MS differentially expressed in PBMC of P. hypophthalmus following 0.1 ppm MG treatment (T1) and after one month of decontamination (T2), selected following an ANOVA 2 filter (MG treatment $p \leq 0.05$; no interaction between MG treatment and sampling time $p \geq 0.05$) (Pierrard et al., 2012).

Table 50. Commercially or Scientifically Important Fish and Seafood Species and the Availability of Protein and Nucleotide Sequence Data as of June 7, 2004, (Vilhelmsson et al., 2007).

Table 51. Protein Spots Affected by Dietary Plant Protein Substitution in Rainbow Trout as Judged by 2DE and Their Identities as Determined by Trypsin Digest Mass Fingerprinting (Vilhelmsson et al., 2007).

Table 52. Main Protein Source and Proximate Composition and Energy Content of the Five Types of Fish Feed (Wulff et al., 2012).

Table 53. Proteins differentially regulated by diet (S. Morais et al., 2012).

Table 54. Results from peptide mass fingerprinting of protein spots excised from the 2DE gels (Martin, Vilhelmsson, Médale, et al., 2003).

Table 55. Main identified proteins by LC–MS/MS. The identification was made by peptide fragment fingerprinting (PFF) in the option MS/MS Ion Search from the bioinformatics application Mascot. The PFF was made in the non redundant NCBInr data base for the Actinopterygii taxonomic level (p-valueb1E−05) (Alves et al., 2010).

Table 56. Identification of abundant protein spots showing constant expression during the early larval period (Sveinsdóttir et al., 2008).

Table 67. Protein spots showing statistically significant differences in expression between T12A and T12B (Ghisaura et al., 2014).

Table 68. Details of the differentially expressed protein spots in skin mucus of S. aurata after dietary probiotic administration and/or overcrowding stress (Cordero et al., 2016b).

Table 69. List of proteins that are differentially expressed in skin mucus of S. aurata after dietary probiotic administration and/or overcrowding stress for 15 and 30 days. ↑ and ↓ indicate over- and under-expression of the proteins at $p < 0.01$, respectively. Coefficient of variation (CV) in percentage (%) from different pools ($n = 3$) is represented in brackets (Cordero et al., 2016b).

Table 70. The altered proteins identified by MALDI-TOF/TOF MS in the liver of puffer fish fed P deficient and adequate diet under low temperature stress (Ye et al., 2016).

Table 71. Composition of the experimental diets used for rearing rainbow trout (Martin, Vilhelmsson, Médale, et al., 2003).

Table 72. Fish performance parameters (Schrama et al., 2018.

Table 73. Proteins differentially regulated by genotype (S. Morais et al., 2012).

Table 74. String annotations and fold-changes of the proteins in the PPI network. Bold lettering in the "FC" column indicates significant fold-changes (> 1.0 and < − 1.0). List is given in ascending order of spot number (Raposo De Magalhães et al., 2020).

Table 75. Isoelectric Point and Molecular Weight for All of the PRVB Spots Studied (Carrera et al., 2010b).

12. ANNEX 1

Supplementary Materials

Table S 1. Proteins identified in rainbow trout ovarian fluid by sodium dodecyl sulphate-polyacrylamide gel electrophoresis and liquid chromatography—tandem mass spectrometry. ECM, extracellular matrix (Nynca et al., 2015b).

Protein	Accession no.	Molecular mass (kDa)	No. unique peptides	Quantitative value	Biological process	Molecular function	Sequence source organism
Binding							
Lipid binding and metabolism							
Apolipoprotein Al-1 precursor	80686384 (+2)	30	19	450	Lipid transport, cholesterol metabolic process	Lipid binding	*Oncorhynchuss mykiss*
Apolipoprotein A1-2 precursor	gib 185132822 (+2)	30	13	188	Lipid transport, cholesterol Metabolic process	Lipid binding	*O. mykiss*
Apolipoprotein All	g029890014 (+1)	16	5	85			*O. mykiss*
Apolipoprotein E precursor	8085133428 (+1)	31	14	85	Lipid transport	Lipid binding	*O. mykiss*
Prostaglandin D synthase	gill 1095799	19	3	21	Lipid metabolic preens	Transporter activity, small molecule binding	*O. mykiss*
Serum albumin I protein	0295419235	31	9	70	Transport	Lipid and metal binding	*O. mykiss*
Serum albumin	gq95931876	19	6	65	Transport		*O. mykiss*
Sex hormone-binding globulin precursor	gib 185132366 (+I)	44	9	49	Primary spermatocyte growth	Steroid binding	*O. mykiss*
Sex hormone-binding globulin a	g012420009	44	8	37	Primary spermatocyte growth	Steroid binding	*Oncorhynchus tshamytscha*
Vitellogenin. short (= VTG)	80123011 (+1)	183	82	2392		Lipid transporter activity, nutrient reservoir activity	*O. mykiss*
Vitellogenin, partial	80066855 (+1)	50	3	313		Lipid transporter activity	*O. mykiss*
Vitellogenin	80894096	34	3	456		Lipid transporter activity	*O. mykiss*
Vitellogcnin As	8i1522209345	183	*7*	1667		Lipid transporter activity	*O. clarkii*
Vitellogenin C	gi1522209364	143	16	46		Lipid transporter activity	*Oncorhynchus clarkii*

Carbohydrate binding								
	C-Type lectin receptor B	giI223049425 (+I)	27	5	45		Carbohydrate binding	*O. mykiss*

Mannan-binding lectin H3 precursor	gil159147215 (+I)	26	3	9		Carbohydrate	*O. mykiss*
C-Type mannose-binding lectin precursor	8085132516 (+1)	21	2	5		Carbohydrate binding	*O. mykiss*
Mannan-binding lectin H2 precursor	gi1159147213 (+1)	26	6	II		Carbohydrate binding	*O. mykiss*
Ion transport							
Cobalamin-binding protein, partial giI400364966		46	3	4		Cobalamin binding	*O. mykiss*
Heme-binding protein 2	gil225705018 (+1)	25	2	2			*O. mykiss*
Hcmopexin-like protein	gill848139	50	8	36		Metal ion binding	*O. mykiss*
1-lemopexin-like protein variant I	gill 1095771	13	3	9		Metal ion binding	*O. mykiss*
Lymphocyte cytosolic protein I precursor	gi1134285833	55	2	2		Calcium ion binding	*O. mykiss*
Transferrin precursor	gil218931236 (+1)	75	22	112	Iron ion transport and homeostasis	Ferric iron binding	*O. mykiss*
Immune response							
Complement C3	gi11352103	182	19	28	Complement activation, inflammatory response	Endopeptidase inhibitor activity	*O. mykiss*
Complement component C3, partial	gi1431608	180	5	5	Complement activation, inflammatory response	Endopeptidase inhibitor activity	*O. mykiss*
Complement component 4 precursor	gil185135626 (+I)	193	3	9		Endopeptidase inhibitor activity	*O. mykiss*
Complement component C6 precursor	gil185133413 (+1)	106	2	2	Immune response		*O. mykiss*

Complement component C7-2 precursor	gill85132432 (+I)	94	2	2	Immune response		*O. mykiss*
Complement component C9 precursor	gi1185133255 (+1)	67	6	25	Immune response		*O. mykiss*
Complement component C9	gill 16616	64	5	11	Complement activation, classical pathway		*O. mykiss*
Complement factor Bf-2	gi13982895	85	5	8	Complement activation	Stripe-type endopeptidase activity	*O. mykiss*
Complement factor H precursor	gil 185132505 (+1)	93	3	3	Regulation of complement activation	Heparin binding	*O. mykiss*
Immunoglobulin mu heavy chain secretory form	gil58201845	65	7	17			*O. mykiss*
IgM heavy chain	gi19256318	65	6	14			*O. mykiss*
Ig light chain-fragment	gii345556 (+1)	25	2	3			*O. mykiss*
Lysozyme C II	gil266485 (+4)	16	2	2	Cell wall macromolecule catabolic process	Lysozyme activity	*O. mykiss*
Precerebellin-like protein precursor	gi1185133875 (+1)	20	2	15			*O. mykiss*
Cell structure, shape							*O. mykiss*
13-Actin	gill 9309743 (+2)	42	7	24		ATP binding	*O. mykiss*
Collagen ot-1(V) chain-like, partial	gil551527443	170	5	9		ECM structural constituent	*Xiphophorus maculams*
Keratin S8 type I	gil15028982 (+1)	48	2	4		Structural molecule activity	*O. mykiss*
Keratin El type II	gi115028976 (+1)	62	2	5		Structural molecule *activity*	*O. mykiss*
PREDICTED: low-quality protein: thin	gi1528490869	3922	5	8	Cell morphogenesis, regulation of Rho protein signal transduction; sarcomere organisation	ATP binding, Rab GTPase activator activity, structural constituent of muscle	*Dania rerio*

PREDICTED: titin isoform X7	gi1528510293	1933	*5*	8			*Danio rerio*
Vitelline envelope protein gamma precursor	gi1185134311 (+1)	50	12	50			*O. mykiss*
Zona pellucida 2.3 precoursor	gi1185132234 (+1)	58	4	4			*O. mykiss*
Proteolysis							
α-Antiproteinase-like protein precursor	gi1185132174 (+1)	48	10	81	Proteolysis	Serine-type endopeptie inhibitor activity	*O. mykiss*
Cathepsin D precursor	gi1185132376 (+1)	43	4	12	Proteolysis	Aspartic-type endopeptidase activity	*O. mykiss*
Coagulation factor II precursor	gill85135584 (+I)	71	2	5	Blood coagulation, proteolysis	Serine-type endopeptidasc activity	*O. mykiss*
Cysteine proteinase inhibitor	gil54300680	15	3	8		Cysteine-type peptidase activity	*O. mykiss*
Matrix metalloproteinase-2 precursor	gill 85134355 (+1)	74	2	3	Proteolysis	Metalloendopee activity	*O. mykiss*
Myeloid cell lineage chitinase	0195954322	51	3	6	Chitinase activity	Chitin catabolic process: carbohydrate metabolic process	*O. mykiss*
Other							
UPF0762 protein aorf58 homologue	gi156310256 (+2)	40	3	11			*O. mykiss*
Triose-phosphate om erase	gi134221914	22	2	2	Gluconeogenesis	Triose-phosphate isomerase activity	*O. mykiss*

Table S 2. The protein spots from 2D gels of Atlantic cod skin mucus: Information on details retrieved from databases along with physical characteristics inferred from the gel, NA: Not applicable.[a] Isoelectric point/Molecular weight. (Rajan et al., 2011).

Spot no.	Protein name (Species)	Acc. No	Theoretical PI/MW	Actual PI/MW	Score Protein/EST	Cod EST Acc. no
Immune-related proteins						
br−2	Galectin-1 (*Hippoglossus hippoglossus*)	ABJ80692	5.91/14.3	6.3/12.2	NA[a]/82	GW858786
br-3	Galectin-1 (*Salmo salar*)	ACMO8580	5.27/13.3	5.8/13.5	NA/157	EX727594
br-4	Galectin-1 (*S. salar*)	ACMO8580	5.27/13.3	5.60/13.5	NA/264	EX727594
br-5	Galectin-1 (*S. salar*)	ACMO8580	5.27/13.3	5.3/13.1	NA/299	EX727594
br-30	Galectin-1 (*S. salar*)	ACMO8580	5.27/13.3	5.1/14.0	NA/337	EX727594
br-31	Galectin-1 (*S. salar*)	ACMO8580	5.27/13.3	4.8/14.6	NA/226	EX727594
br-7	g-type Lysozyme (*Gadus morhua*)	AY614594	7.88/20.80	7.50/23.0	502/NA	NA
br-58	g-type Lysozyme (*G. morhua*)	AY614594	7.88/20.80	8.40/23.0	943/NA	NA
br-19	FK-506 binding protein (*Danio rerio*)	NP_956239	7.78/11.6	7.2/13.5	NA/119	ES244445
br-21	CyclophilinA (*Ictalurus punctatus*)	ABO15709	8.84/17.4	8.55/18.2	NA/287	CO541665
br-24	Cystatin B (*Anoplopoma fimbria*)	ACQ58093	7.16/12.7	6.6/13.5	NA/297	EG643140
br-25	Mannan binding lectin (*Esox lucius*)	ACO14169	6.4/12.3	6.7/12.2	NA/142	Es469752
br-40	Leukocyte elastase inhibitor (*S. salar*)	ACI33239	6.37/42.88	5.2/41.2	NA/443	Ex723245
br-60	Leukocyte elastase inhibitor (*S. salar*)	ACI33239	6.37/42.88	7.6/39.3	NA/232	Ex723245
br-64	Leukocyte elastase inhibitor (*S. salar*)	ACI33239	6.37/42.88	7.60/43.9	NA/220	Ex723245
br-65	Leukocyte elastase inhibitor (*S. salar*)	ACI33239	6.37/42.88	6.9/43.7	NA/295	Ex723245
br-66	Leukocyte elastase inhibitor (*S. salar*)	ACI33239	6.37/42.88	6.50/43.4	NA/163	Ex723245
br-67	Leukocyte elastase inhibitor (*S. salar*)	ACI33239	6.37/42.88	6.3/43.5	NA/229	Ex723245
br-59	Glutathione s transferase Pi (*D. rerio*)	NP_571809	8.17/23.5	7.70/28.3	NA/785	Ex724703
Proteins in protein metabolism						
br-1	Ubiquitin (*Salmo* sp.)	0412265A	6.56/8.5	6.75/6.70	NA/77	NA
br-10	Cofilin-2 (*Osmerus mordax*)	ACO10161	6.75/18.9	6.0/21.2	311/813	ES470174
br-38	S formyl glutathione hydrolase (*O. mordax*)	ACO09141	6.06/31.1	5.6/38.4	NA/549	EX184764
br-46	Proteasome subunit alpha type 3 (*O. mordax*)	ACO09997	4.96/28.5	4.9/34.1	NA/301	CO542197
br-48	Protein disulfide isomerase (*D. rerio*)	NP_998529	4.55/56.6	4.60/60.5	NA/349	EX73895
br-49	Calreticulin precursor (*S. salar*)	ACI32936	4.33/47.6	4.30/59.9	NA/285	EX722975
br-52	Calreticulin (*Paralichthys olivaceous*)	ABG00263	4.38/49.276	4.50/49.8	NA/259	EY975743
br-53	Calreticulin precursor (*S. salar*)	ACI32936	4.33/47.5	4.40/55.5	NA/243	ES782005
br-54	Cytosolic nonspecific dipeptidase (*Oreochromis niloticus*)	BAE45263	5.54/52.807	4.6/54.3	NA/454	GO379362
br-62	Proteasome subunit alpha type 7 (*E. lucius*)	ACO13646	8.51/36	7.732.9/	273/NA	NA
Proteins in carbohydrate metabolism						
br-11	6-Phosphogluconate dehydrogenase (*O. mordax*)	ACO090011	6.25/53.2	6.60/47.8	233/322	FF410818
br-12	Citrate synthase precursor (*D. rerio*)	NP_955892	7.69/51.8	6.6/44.7	160/NA	NA

br-13	Alpha enolase (*Acipenser baerii*)	ABF6006	5.91/47.03	5.5/49	NA/532	EX739365
br-14	Alpha enolase (*A. baerii*)	ABF6006	5.91/47.03	5.48/48.8	NA/485	EX739365
br-50	Alpha enolase (*A. baerii*)	ABF6006	5.91/47.03	5.6/54.1	NA/675	EX739365
br-51	Alpha enolase (*A. baerii*)	ABF6006	5.91/47.03	5.6/54.5	NA/908	EX739365
br-20	Triose phosphate isomerase (*E. lucius*)	ACO14153	8.16/29.9	6.9/28.6	286/NA	NA
br-35	Cytoslic malate dehydrogenase (*Oryzias latipes*)	NP_001156606	7.58/36.2	6.8/40.2	NA/401	EX730034
br-36	Fructose 1,6-biphosphatase (*O. mordax*)	ACO09700	6.15/36.6	6.4/40.2	NA/382	EX189761
br-37	Transaldolase (*O. mordax*)	ACO08950	6.48/37.7	6.10/40.9	NA/343	GO394691
br-61	Triose phosphate isomerase B (*Xiphophorus maculates*)	AAK85204	7.61/26.5	7.7/31	NA/189	GO382871
br-63	Glyceraldehyde-3-phosphate dehydrogenase (*E. lucius*)	ACO13646	8.51/36.02	7.6/41	273/NA	NA
Proteins in nucleic acid metabolism						
br-6	Nucleoside diphosphate kinase (*D. rerio*)	AF202052	7.77/17.397	6.70/17.0	231/572	CO542766
br-17	Inositol monophosphatase (*O. mordax*)	ACO10012	5.05/30.52	5.3/34	NA/332	EX732594
br-57	Deoxycitydyl deaminase (*S. salar*)	ACI68336	5.93/21.9	5.34/21.9	NA/339	FF407255
br-47	Deoxycytidyl deaminase (*E. lucius*)	ACO13300	4.90/26.6	4.90/26.6	NA/481	GW854502
Proteins in cell communication						
br-15	RAB-7 like (*D. rerio*)	NP_957222	6.4/23.8	5.9/26.1	217/NA	NA
br-27	14-3-3 Protein beta/alpha-1 (*S. salar*)	ACI69428	4.56/28.3	4.60/33.1	NA/753	GO376905
br-28	14-3-3 Protein beta/alpha-1 (*S. salar*)	-do-	-do-	4.7/34.2	NA/332	-do-
br-34	Predicted: similar to 14-3-3 CG17870-PA, isoform A isoform 2 (*Apis mellifera*)	XP_623183	4.79/28.1	4.5/38	NA/584	EX740849
br-55	14-3-3 Protein beta/alpha (*S. salar*)	NP_001135087	4.6/28.2	4.7/32.9	NA/1001	EX178653
br-56	14-3-3 Protein beta/alpha-2 (*O. mordax*)	ACO09912	4.67/27.8	4.7/32	NA/659	EX740336
Cytoskeltal proteins						
br-18	Beta actin (*Rhynchocypris oxycephalus*)	AAF63689	5.29/42.06	5.2/31	342/NA	NA
br-33	Actin cytoplasmic 1 (*O. mordax*)	ACO09390	5.31/41.8	5.21/45	958/NA	NA
br-43	Keratin type 1cytoskeltal 13 (*Oncorhynchus mykiss*)	NP_001117848	5.17/52	4.9/37.3	NA/217	EX728380
br-44	Keratin type 1cytoskeltal 13 (*O. mykiss*)	NP_001117848	5.17/52	4.9/36.5	NA/325	EX735943
br-45	Tropomyosin alpha-3 chain (*S. salar*)	ACN10639	4.71/28.5	4.8/35	NA/163	CO542576
Lipid metabolism						
br-29	Preproapolipoprotein A1(*G. morhua*)	AAU87042	5.92/14.8	5.1/32.1	49/NA	NA
br-32	Fatty acid binding protein, adipocyte (*S. salar*)	NP_001134675	5.1/15.2	4.9/34	NA/355	CO541669
Phosphate metabolism						
br-39	Inorganic pyrophosphatase (*O. mordax*)	ACO09976	5.28/32.7	5.5/39.2	NA/725	EX1778389
Others						
br-8	No match- predicted superfamily Concanavalin A lectin/glucanases	NA	NA	5.5/25	NA/375	EX730599

br-9	No match- predicted superfamily Concanavalin A lectin/glucanases	NA	NA	5.6/23.10	NA/124	EX730599
br-16	No match- predicted superfamily Concanavalin A lectin/glucanases	NA	NA	6.1/26.0	NA/169	EX730599
br-22	No match	NA	NA	4.7/19.1	NA	NA
br-23	No match	NA	NA	4.8/19.1	NA	NA
br-26	No match- predicted superfamily Cytolysin/lectin	NA	NA	4.7/18	NA/524	EX725990
br-42	Unnamed protein product (*Tetradon nigroviridis*)	CAF98408	6.39/38.4	5.8/43.2	NA/611	FF415007

Table S 3. Proteins confirmed in salmon skin mucus sampled by different methods sorted in order of highest to lowest signal abundances (Fæste et al., 2020).

Protein	Accession No.*	Number of identified Peptides		
		absorbed	scraped	wiped
Deoxyribonuclease	B5XFE6	25	24	24
Actin, cytoplasmic 1	O42161	25	37	32
Serum albumin 1	P21848	34	37	38
Serotransferrin-1	B5X2B3	33	33	35
Elongation factor 2	C0H9N2	44	57	54
Keratin, type II cytoskeletal 8	B5X320	22	46	37
Gelsolin (Fragment)	C0PU67	32	35	38
Heat shock cognate 70 kDa protein	B5X3U6	32	42	32
Transketolase	B5X4R7	29	37	35
Alpha-enolase	B5X1B5	28	34	29
Major vault protein	C0HA52	35	39	40
Lysine--tRNA ligase (Fragment)	C0PUL2	24	28	28
Heat shock protein hsp90 beta	Q9W6K6	14	47	39
WD repeat-containing protein 1	B5X1Z0	28	26	30
Tubulin beta-1 chain	C0H808	22	30	25
Deoxyribonuclease	B5XGV3	12	11	12
Protein disulfide isomerase associated 3	D0QEL0	29	39	33
78 kDa glucose-regulated protein	B5X397	23	31	28
Rab GDP dissociation inhibitor beta	B5X1S6	29	28	31
Myosin-9 (Fragment)	C0PU50	22	36	30
Glutathione S-transferase P	B5XGZ2	14	14	13
Tubulin alpha chain	B5DGE8	19	25	25
Fructose-bisphosphate aldolase	C0H9I1	24	32	26
Alpha-actinin-1	C0H9I5	24	25	22
L-lactate dehydrogenase B chain	B5X4K4	20	21	19
Triosephosphate isomerase	B5DGL3	18	22	19
Transaldolase	B9EM17	19	24	21
6-phosphogluconate dehydrogenase, decarboxylating	C0H9U3	27	22	29

Disulfide-isomerase (Fragment)	C0PU58	17	30	22
Asparaginyl-tRNA synthetase, cytoplasmic	B5X340	23	29	31
Echinoderm microtubule-associated protein-like 1 (Fragment)	C0PU59	21	22	25
14-3-3 protein beta/alpha-1	B5XF08	17	24	20
SH3 domain-binding glutamic acid-rich-like protein 3	B5X6G0	12	11	11
Glyceraldehyde-3-phosphate dehydrogenase	B5X3K2	14	13	15
Tropomyosin alpha-3 chain	B5X4C0	13	26	20
Pyruvate kinase (Fragment)	C0PUK9	19	24	22
Apolipoprotein A-I-1	B5XFF2	6	28	24
Alanyl-tRNA synthetase, cytoplasmic	B5X2C6	20	36	40
Adenylyl cyclase-associated protein	B5X2E1	19	24	24
Anterior gradient protein 2 homolog	Q2V6Q8	9	13	11
Glutathione transferase omega-1	B5X9Y8	18	19	18
Annexin	B5XCU8	15	25	17
Argininosuccinate synthase	B5XAP9	11	26	24
Cofilin-2	B9ELH2	14	17	14
Adenosylhomocysteinase	B5DGE0	19	21	25
Elongation factor 1-alpha	Q9DDK2	13	24	21
Glucose-6-phosphate isomerase	C0H9M4	23	18	26
Vacuolar protein sorting-ass. prot. 26A-like	B5X0V6	38	26	46
Histone H3	B5DG71	3	8	4
Heterogeneous nuclear ribonucleoprotein A1	C0H8N3	11	18	16
GDP-mannose 4,6 dehydratase	B5XE59	19	16	18
Alpha-N-acetylgalactosaminidase	C0HAA7	17	14	15
14-3-3 protein beta/alpha-2	B5DGB9	14	18	15
Cofilin-2	B9ELX6	12	22	17
Moesin	C0HB84	17	19	26
Heat shock cognate 70 kDa protein	B5DFX7	12	19	13
Actin-related protein 2-A	C0H939	14	16	16
Nucleoside diphosphate kinase	B5XCJ8	8	12	10
Vacuolar ATP synthase catalytic subunit A	C0H9X1	22	22	24
Aldose reductase	B5X9C6	15	11	15
Goose-type lysozyme	A6PZ97	13	16	13
Disulfide-isomerase A3	B5X1H7	16	25	18
ATP-dependent RNA helicase DDX39 (Fragment)	C0PUM3	15	21	21
Vigilin	C0HA19	4	30	32
Asparagine synthetase	B5X2U4	16	22	26
T-complex protein 1 subunit beta	B5X2M8	16	26	22
Histone H2A	B9EN25	14	20	17

Thioredoxin	B5X6M7	10	10	10
Malate dehydrogenase	C0H820	12	13	15
Actin-related protein 3	C0HBE5	16	18	17
40S ribosomal protein S3a	B5DGL6	10	15	16
Proteasome activator complex subunit 1	B9EPW1	16	21	20
Actin related protein 2/3 complex subunit 2	B5DGD5	17	12	15
Peptidyl-prolyl cis-trans isomerase	B5XAR1	8	14	11
Peptidyl-prolyl cis-trans isomerase	B9EPT4	7	10	8
FAM139A (Fragment)	C0PUF6	9	26	24
Chaperonin containing TCP1, subunit 3 (Fragment)	B5RI17	14	20	21
Beta-hexosaminidase beta chain	B5X1T5	18	16	18
Guanine nucleotide bind. prot. (G protein) beta polypeptide 2-like 1	B5DFX3	16	18	17
Rho GDP-dissociation inhibitor 1	B5X0W2	12	10	11
60S ribosomal protein L4-A	B5X3Q6	9	23	19
Profilin	B5X5I8	6	11	8
ATP synthase subunit beta (Fragment)	B5RI36	10	30	24
Proteasome subunit alpha type	B5X5N7	13	10	12
40S ribosomal protein S2	B5DGA8	13	15	13
Sialic acid synthase	B5X2G1	11	15	15
Adenosine kinase a	B5DGF0	16	16	14
Tropomyosin alpha-3 chain	C0H9C0	9	14	10
Fast myotomal muscle actin 2	B5DG40	11	7	7
Calpastatin 2	K4LAG6	14	11	14
Betaine-homocysteine methyltransferase	B5DGE7	14	16	14
Cystathionine gamma-lyase	B5X1V6	18	13	16
14-3-3 protein beta/alpha-1	B5XCY4	15	13	15
Transgelin	B5X8M6	15	18	18
T-complex protein 1 subunit theta	B5X4M2	15	21	23
Coatomer subunit alpha	B5X3T4	5	29	30
Calpastatin	C0HA95	18	16	16
Prolyl endopeptidase	C0HBI8	19	15	22
Alcohol dehydrogenase class 3	C0H868	15	12	16
Peptidyl-prolyl cis-trans isomerase	B5DG94	5	7	5
Ras GTPase-activating-like protein IQGAP1 (Fragment)	C0PUU6	5	25	27
Glutathione S-transferase P	B5XC10	11	12	11
Staphylococcal nuclease domain-containing protein 1 (Fragment)	C0PUJ3	8	25	23
Proteasome subunit alpha type	B5DGU6	13	13	13

F-actin-capping protein subunit beta	B5X3R3	13	15	12
Creatine kinase B-type	B5X0S0	15	16	15
T-complex protein 1 subunit delta	B5X1Z2	9	18	20
40S ribosomal protein S4 (Fragment)	B5RI97	11	15	17
Galectin-3	B5X815	7	9	9
Glutamate dehydrogenase	C0HA51	15	24	16
Peroxiredoxin-1	B5XBY3	11	9	13
26S proteasome non-ATPase regulatory subunit 2	C0H8V2	4	20	17
Fructose-bisphosphate aldolase	O73866	13	11	16
Glucose-6-phosphate 1-dehydrogenase	B5X1I3	17	18	21
T-complex protein 1 subunit alpha	C0HA30	9	19	22
Aldehyde dehydrogenase family 9 member A1-A	B5X2H6	15	14	16
Serum albumin 2	Q03156	7	5	7
Elongation factor 1-gamma	C0H7V4	10	13	16
High mobility group protein B2	B5DGK0	7	11	10
Ictacalcin	B5XGX4	3	4	4
40S ribosomal protein S3	B5X8A9	10	19	14
Proteasome subunit alpha type	B5XAL3	14	14	15
Histone H2A	B5X851	3	6	4
2,3-cyclic-nucleotide 3-phosphodiesterase	C0H9F4	8	15	17
Annexin	C0H815	10	25	14
Thimet oligopeptidase	B5X1B9	17	10	15
GDP dissociation inhibitor 2	B5DG32	16	14	15
40S ribosomal protein S8	B5DGK7	7	12	11
Hemoglobin subunit beta-1	C0H824	8	9	8
T-complex protein 1 subunit epsilon	C0HBB4	8	17	16
ATP synthase subunit alpha	B5X195	2	28	15
60 kDa heat shock protein, mitochondrial	B5X1G7	6	32	12
Glucosamine--fructose-6-phosphate aminotransferase 1	B5X3D1	0	32	27
Junction plakoglobin	B5X4L1	2	25	18
N-acylneuraminate cytidylyltransferase	B5X1H6	13	11	15
Eukaryotic translation initiation factor 3 subunit A	C0H9S0	6	13	20
ADP-ribosylation factor 1	B5X3Q1	9	12	11
Probable ATP-dependent RNA helicase DDX5	C0HB50	3	22	18
Aldehyde dehydrogenase family 7 member A1 homolog	B5X0S9	19	13	16
Lipocalin	B5XCL8	7	7	8
Calreticulin	B5X0V5	12	13	10
Proteasome activator complex subunit 2	B5X6E1	6	13	11
Hemoglobin subunit beta	B5XD42	10	12	12

40S ribosomal protein SA	B5DGB6	7	14	16
Bifunctional purine biosynthesis protein PURH	B5X2R0	14	16	17
Glutathione S-transferase A	B9ENS1	13	8	12
Leukocyte elastase inhibitor	B5X1Q8	11	14	17
Proteasome subunit beta type	B5X9D0	8	8	8
Eukaryotic translation initiation factor 5A-1	B9EL07	8	13	12
Carbonyl reductase 1	B5X931	10	14	15
SET translocation (Myeloid leukemia-associated) B	B5DFV7	11	7	10
Ubiquitin-conjugating enzyme E2 L3 (Fragment)	C0PUD2	7	9	8
Proteasome subunit alpha type	B5X9F8	11	9	10
Cold-inducible RNA-binding protein	C0H8U7	2	6	2
Phosphoglycerate kinase	B5X0U6	11	18	17
14-3-3 protein epsilon	B5DFX5	11	12	11
Proteasome subunit beta type	B5XBR9	12	11	10
Proteasome subunit alpha type	B5XGI9	8	8	8
Phosphoacetylglucosamine mutase	B5X1B2	16	10	15
Heterogeneous nuclear ribonucleoprotein A0	B5X9N1	8	13	15
Calpain small subunit 1	B5X6W1	8	10	13
Malate dehydrogenase	B5DGS4	8	21	19
Peroxiredoxin	B5XCW3	11	11	11
Myosin light polypeptide 6	B5XGW1	9	12	9
Aminopeptidase B	B5X4T6	13	13	18
Proliferation-associated protein 2G4	B5X193	15	12	15
Malate dehydrogenase	B5X2Q1	10	10	12
60S ribosomal protein L7a	B5DGW5	5	18	17
Hemoglobin subunit alpha	P11251	9	11	9
S100-A1	B5XA95	4	5	5
GTP-binding nuclear protein Ran	Q9YGC0	10	12	12
60S ribosomal protein L3	B5X7J4	8	12	12
Beta-microseminoprotein	B5XB38	6	7	6
60S ribosomal protein L7	B5X4H4	4	12	8
Proteasome subunit alpha type	B5XAG6	10	9	11
Cytosolic non-specific dipeptidase	B5X4K2	9	9	10
60S ribosomal protein L10	B5X8D0	2	15	13
Serine/threonine-protein phosphatase	C0H9N7	12	10	12
Coronin	C0H959	8	13	14
60 kDa lysophospholipase	B5X1B1	4	16	16
AMP deaminase 3	C0H8Y0	8	10	9
Phosphomannomutase 2	B5DFW8	8	8	9

Hyperosmotic glycine rich protein	Q7ZYV6	4	8	5
Vacuolar ATP synthase subunit B, brain isoform	B5X274	11	8	14
Peroxiredoxin-5, mitochondrial	B5X5Q6	8	10	8
Cystatin-B	B5XDV8	5	7	7
Ras-related protein Rab-7a	C0HBN0	9	11	9
Carbonyl reductase 1	B5XGN3	9	10	10
Phosphoglycerate mutase 1	B5X0R8	12	6	12
Glutathione reductase, mitochondrial	B5X3C0	17	10	16
Transforming protein RhoA	B5X7H3	6	11	8
Tubulin alpha chain	B5DH01	6	10	8
Hematopoietic lineage cell-specific protein	B5X4K0	9	5	10
Coatomer subunit gamma	B5X361	4	18	19
Inorganic pyrophosphatase	B5X764	10	9	11
Serine/threonine-protein phosphatase	B5X0W0	13	8	12
Cystatin-B	B5X912	4	6	5
Heterogeneous nuclear ribonucleoprotein M	B5X2U1	2	10	9
Ubiquitin carboxyl-terminal hydrolase	B5X4M3	1	15	16
Coactosin-like protein	C0H764	7	11	8
Barrier-to-autointegration factor	B5XFP1	5	8	10
Interleukin enhancer-binding factor 3 homolog	B5X1E6	4	21	17
F-actin-capping protein subunit alpha-1	B5X2H9	10	9	11
Cathepsin M	Q70SU8	9	6	11
26S protease regulatory subunit 7	B5DG36	1	16	14
Proteasome subunit beta type	C0H7E4	8	9	7
Fructose-1,6-bisphosphatase 1 (Fragment)	C0PUI9	13	11	9
Lactoylglutathione lyase	B5XCC9	10	7	10
Filamin-A (Fragment)	C0PUT2	6	17	14
Heterogeneous nuclear ribonucleoprotein U-like protein 1	C0HA39	2	9	9
Alpha-enolase	C0H878	9	12	10
RAB2A, member RAS oncogene family	B5DG90	8	11	8
Ribosomal protein L23a (Fragment)	B5RI65	4	8	9
Cysteinyl-tRNA synthetase, cytoplasmic	B5X1G4	10	10	15
Histone H1-beta, late embryonic	B5X1W1	2	14	11
Phosphotriesterase-related protein	B5X4Y9	13	4	12
Aspartyl aminopeptidase	B5X1S2	14	1	12
Serine/threonine-prot. phosphatase 2A 65 kDa reg. sub. A beta iso.	C0PUM7	1	17	15
Myosin regulatory light chain 2, smooth muscle isoform	B5XAL5	7	8	8

Annexin	B5XEI6	4	23	10
Plastin-2	B5XDI6	7	9	11
Angiotensinogen	B5X4A7	8	10	13
Annexin	B5X865	7	15	7
40S ribosomal protein S19	B5XDA8	6	7	7
Antithrombin	Q9PTA8	15	2	13
Rho GDP-dissociation inhibitor 1	B5X2E5	7	7	7
Profilin	B5X4T2	7	8	6
Thymosin beta-a	B9EPG7	2	3	3
40S ribosomal protein S13	C0H753	4	9	11
Septin-7	B5X2M3	5	6	10
Triosephosphate isomerase	B5XB51	9	8	9
C-type lectin domain family 4 member E	B5X5V9	8	5	7
Heterogeneous nuclear ribonucleoprotein Q (Fragment)	C0PU03	5	14	11
Signal transducer and activator of transcription 1-alpha/beta	B5X3E8	1	13	11
Histone H1	B9EQF7	3	3	2
40S ribosomal protein S12	B5DGG8	6	10	9
Iron-responsive element-binding protein 1	B5X348	13	6	16
GDP-L-fucose synthetase	B5XDS7	9	10	12
Ras-related protein Rab-1A	B9EN43	7	7	6
Superoxide dismutase [Cu-Zn]	B9EM68	4	5	4
Ribosomal protein S9 (Fragment)	B5RI35	8	11	9
Arginyl-tRNA synthetase, cytoplasmic	B5X4E3	4	16	17
Keratin, type I cytoskeletal 18	B5X4L3	4	9	7
Heterogeneous nuclear ribonucleoprotein K	B5X1A5	7	11	12
ADP/ATP translocase 2	B5X8C1	0	16	11
Heterogeneous nuclear ribonucleoprotein A0	B5X0T7	7	7	11
Heterogeneous nuclear ribonucleoprotein K	B5X0W3	6	7	7
Twinfilin-1	B5X2M7	8	12	14
26S proteasome non-ATPase regulatory subunit 11 (Fragment)	C0PUD4	2	13	17
L-lactate dehydrogenase B chain	C0HAI2	8	6	10
Proteasome subunit beta type	B5XFH8	8	6	8
Heterogeneous nuclear ribonucleoprotein M	B5X2U1	2	0	3
26S proteasome non-ATPase regulatory subunit 3	B5DGU9	0	13	14
Coatomer subunit beta	B5X3S5	0	10	14
AMBP protein	B5XD04	12	5	10
RCC2 homolog	B5X2E2	9	11	14

Proteasome (Prosome, macropain) 26S subunit, non-ATPase, 13	B5DGU8	3	9	8
26S protease regulatory subunit 6A	B5X5I0	5	9	13
Tropomyosin alpha-4 chain	B5X2S2	6	10	8
Actin-related protein 2/3 complex subunit 5	B5XCZ5	5	8	7
17-beta-hydroxysteroid dehydrogenase 14	B5XFG4	6	7	7
Cathepsin B	C0H850	7	8	8
Alcohol dehydrogenase	C0H826	12	3	11
Glutamine synthetase	B5XCB2	9	4	9
Apolipoprotein A-I	B5XBH3	0	16	11
Translationally-controlled tumor protein	B5XBT6	7	8	11
NG,NG-dimethylarginine dimethylaminohydrolase 2	B5X0W7	12	7	11
60S ribosomal protein L17	B5DGH7	2	11	10
Dolichyl-diphosphooligosaccharide prot. glycosyltransferase sub. 1	C0HAM9	1	26	12
Cofilin-2	B5XC25	4	4	4
Histone H1 (Fragment)	P84408	2	2	2
APEX nuclease 1	B5DG28	9	7	7
Tumor-associated calcium signal transducer 2	B5XFC3	9	11	6
6-phosphogluconolactonase	B9EPN0	10	8	9
Histone H2B	B5XEY5	1	2	1
Calpain-1 catalytic subunit	C0HAF6	2	13	9
Elongation factor 1-delta	C0HAM4	5	8	5
15-hydroxyprostaglandin dehydrogenase	B9EPG3	5	8	12
Acidic leucine-rich nuclear phosphoprotein 32 family member A	B5X6K3	4	8	6
Ribosomal protein	B5DGV1	5	10	9
Proteasome subunit alpha type	B5XGP5	9	6	9
Proteasome subunit beta type	A7KII5	9	7	8
Cathepsin D	B5DFV6	7	7	8
Thymosin beta-12	B5XAM0	3	4	3
Mitogen-activated protein kinase 3	C0H802	0	12	9
60S ribosomal protein L8	C0H8H2	3	9	8
Tripartite motif-containing protein 16	B5X415	4	9	7
Probable aminopeptidase NPEPL1	B5X304	12	8	14
Stress-induced-phosphoprotein 1 (Hsp70/Hsp90-organizing)	B5DG46	2	14	13
Non-specific cytotoxic cell receptor protein-1	B8YBH8	8	8	10
S100-A5	B5XGM0	8	8	10
Actin-related protein 2/3 complex subunit 4	B5X9U3	6	5	6

Apoptosis-associated speck-like protein containing a CARD	B5DG91	4	6	6
Ubiquitin	B9ELE8	5	5	6
Protein-arginine deiminase type-2 (Fragment)	C0PU89	4	7	6
Thymidine phosphorylase	B5X3F7	4	8	8
Proteasome subunit alpha type	B5DGU3	11	5	9
Heterogeneous nuclear ribonucleoprotein A/B	B5X3L9	2	9	6
40S ribosomal protein S5	B5DGY6	3	10	7
MHC class I (Fragment)	Q8HX48	3	15	9
26S protease regulatory subunit 4	C0HAC7	4	10	13
60S ribosomal protein L5	B5DGH0	0	13	7
Actin-related protein 2/3 complex subunit 1B	C0HBR6	8	11	11
PolyrC-binding protein 2	B5X1E2	5	11	8
Cofilin-2	B5XB84	3	3	3
40S ribosomal protein S14	C0H7E7	6	8	8
Tubulin alpha chain	B5X0S5	4	10	7
PDZ and LIM domain protein 1	B5X7N9	8	11	14
Poly synthetase 3	B5X1N3	6	7	13
Annexin	C0HAX2	1	19	5
Eukaryotic translation initiation factor 4B (Fragment)	C0PUQ2	7	5	8
Peptidyl-prolyl cis-trans isomerase	B5X469	8	9	9
Glutathione S-transferase P	B5XBZ2	6	4	7
Eukaryotic translation initiation factor 3 subunit E	B5DGH9	3	9	10
60S acidic ribosomal protein P0	B5XDP1	1	11	11
Ras-related protein Rab-11B	B5X445	7	7	7
40S ribosomal protein S11	Q9DF27	4	8	6
Lysosomal protective protein	B5X2W5	7	4	7
Xaa-Pro aminopeptidase 1	B5X374	9	7	12
40S ribosomal protein S24	B5X5I9	4	4	5
Ribosomal protein L6	B5DGJ4	3	9	10
Vacuolar protein sorting-associated protein 35	C0H9L8	6	6	14
Nuclease-sensitive element-binding protein 1	B5DH08	7	4	6
Proteasome (Prosome, macropain) 26S subunit, ATPase, 6	B5RI16	4	15	11
S100 calcium binding protein V2-like	B5DGJ9	4	7	5
Plasminogen activator inhibitor 1 RNA-binding protein	B5X326	4	3	4
Thioredoxin-like 1	B5DGD1	7	10	11
40S ribosomal protein S7	B5DGA0	4	8	8
Disulfide-isomerase A5	B5X1P6	3	11	9

26S protease regulatory subunit 6B	B9EPF8	1	11	10
Tropomodulin-3	C0HBN6	7	10	11
Non-metastatic cells 1 protein	B5DGC6	6	4	7
Adenylate kinase isoenzyme 2, mitochondrial	B9EQG9	4	7	6
Peptidyl-prolyl cis-trans isomerase	B5XCW1	7	9	8
Elongation factor 1-beta	B5XDB6	3	6	4
60S ribosomal protein L13	B5DGD9	3	6	7
Vacuolar protein sorting-associated protein 29	B5X686	6	5	5
Calreticulin (Fragment)	C0PUU5	7	8	4
Casein kinase II subunit alpha	C0HB27	5	3	9
Nascent polypeptide-associated complex subunit alpha	B5XEL8	4	6	6
Eukaryotic translation initiation factor 2 subunit 1	B5X2W6	6	10	8
40S ribosomal protein S18	A7KIL2	4	11	7
60S ribosomal protein L9	B5DG02	2	6	6
Lysozyme C II	B5XA65	3	6	7
Glutathione S-transferase	B5X779	4	3	5
Lissencephaly-1 homolog A	B5X3Z6	6	5	8
Methionine aminopeptidase	B5X2F4	3	4	5
Eukaryotic translation initiation factor 3 subunit C	C0H9I7	2	6	10
Annexin	B5X999	0	16	8
ARMET	B5XGI6	4	11	3
Fatty acid-binding protein 7	B9ELZ6	6	7	6
Myelin expression factor 2	C0HBC4	0	12	5
Splicing factor 3B subunit 3	C0H8V4	6	11	10
Nucleoside diphosphate kinase	B5XAW0	5	3	5
Proteasome subunit beta type-6-A like protein	A7KE01	8	4	7
Delta-aminolevulinic acid dehydratase	B5XEM0	8	6	7
Lumican	B5X293	9	5	10
Peroxiredoxin-6	B5X9Q1	5	9	9
Disulfide-isomerase A6	B5X4Y3	2	11	6
Complement component C6	C0H9G0	10	3	8
Ras-related protein Rab-5C	B5X0Q1	6	5	6
14-3-3 protein beta/alpha	B5XDE4	5	5	5
40S ribosomal protein S6	B5DGY8	3	6	6
Hemoglobin subunit alpha-4	B5X746	6	9	7
Cell division control protein 42 homolog	B5X2M9	2	8	6
Phosphorylase	C0H9H1	2	9	11
Heterogeneous nuclear ribonucleoprotein H	C0HAA5	1	7	4
60S ribosomal protein L18a	C0H8I0	0	9	8

NHP2-like protein 1	B5X9W9	5	5	5
Ras-related protein Rap-1b	C0H8F9	7	8	6
Eukaryotic initiation factor 4A-III	B5DG42	2	12	7
Splicing factor, proline-and glutamine-rich	B5X173	0	7	5
14-3-3 protein zeta	B5XDU3	6	7	6
THO complex subunit 4	C0H7U2	6	5	6
SH3 domain-binding glutamic acid-rich-like protein	B9EPE7	4	4	5
Alpha-1-microglobulin/bikunin, 3' end. (Fragment)	Q91484	10	4	10
Histone H2A	B5DGB8	3	5	4
60S ribosomal protein L13a	C0H7C9	3	6	5
ATP synthase subunit b, mitochondrial	B5XEN1	0	12	8
Peptidyl-prolyl cis-trans isomerase	B9ELU4	3	4	3
Proteasome subunit beta type-9	Q9DD33	7	4	7
Eukaryotic translation initiation factor 3 subunit E-interacting prot.	C0HAF2	1	9	8
Calcyclin-binding protein	B5X9E1	2	3	6
Mx3 protein	Q98992	1	11	8
Branched-chain-amino-acid aminotransferase	B5X837	7	8	4
DJ-1	B5DFV4	7	5	6
40S ribosomal protein S16	B5DG73	5	5	6
Coronin	C0HAR0	5	9	8
Ras-related C3 botulinum toxin substrate 1	B5X1F7	2	8	3
Coatomer subunit delta	B5X2H8	3	7	8
Ubiquitin-conjugating enzyme E2 N	B9EMT3	4	9	7
Actin-related protein 2/3 complex subunit 3	B9EQK6	4	3	5
Nuclear migration protein nudC	C0H9I3	5	3	7
Dipeptidyl-peptidase 3	B5X435	7	5	12
H/ACA ribonucleoprotein complex subunit 4	B5X270	0	7	5
Epididymal secretory protein E1	B5X5H1	3	5	6
Caspase 6A (Fragment)	Q4ZHV1	11	4	6
von Willebrand factor A domain containing 5A	D0QYP1	5	3	7
Stress-70 protein, mitochondrial	C0HAF8	1	15	4
RNA-binding protein 8A	B5DGI7	6	6	5
Cellular retinoic acid-binding protein	B5X8L7	5	5	6
Myotrophin	C0H9A4	4	4	5
Proteasome subunit beta type	Q9DE54	9	4	8
Muscle fatty acid binding protein	Q6R758	5	5	5
Nucleosome assembly protein 1-like 1	B9ELC3	5	4	11
DNA damage-binding protein 1	C0H989	10	1	12
Zinc finger protein 9-2	B5DH11	2	4	2

Protein mago nashi homolog	B9ENE7	4	7	5
Autophagy-related protein 7	C0H8W2	4	6	13
60S ribosomal protein L18 (Fragment)	B5RIC0	3	5	4
Cytosolic 5-nucleotidase 1A	C0H904	4	10	8
26S protease regulatory subunit 8	B5XCM1	2	7	10
Spectrin alpha chain, brain (Fragment)	C0PUV6	7	7	5
Myeloperoxidase (Fragment)	C0PU42	0	26	11
Ras-related protein Rab-14	B5X3F9	6	8	7
Heat shock protein 10	B5DGB3	2	7	6
14-3-3 protein eta	B5X330	5	7	7
26S proteasome non-ATPase regulatory subunit 6	B5XBN2	2	7	6
Caspase 3B	Q4ZHV0	2	10	8
U2 small nuclear ribonucleoprotein A	O73931	3	4	7
High choriolytic enzyme 1	B5X7S6	2	11	9
High mobility group protein B3	B9EM70	6	3	10
Vacuolar protein sorting-associating protein 4B	B5X1U4	0	8	6
40S ribosomal protein S15a	B5DGX3	4	8	5
Septin-2	B5X499	3	6	8
N-acetylglucosamine-6-sulfatase	C0HAB4	5	4	6
Elongation factor 1-delta	B9EMF8	4	10	7
Peptidyl-prolyl cis-trans isomerase	B5X8H7	6	4	5
40S ribosomal protein S25	B5XCX3	2	6	6
Ribosomal protein L15	B5XB05	2	6	7
Ran-specific GTPase-activating protein	B9EPI2	4	6	7
Cold-inducible RNA-binding protein	B5X3A3	4	4	3
Heterogeneous nuclear ribonucleoprotein G	C0H8T1	2	4	5
Beta-2-microglobulin	B9ELZ2	4	5	6
Eukaryotic translation initiation factor 3 subunit G	B5XFV7	4	6	6
26S proteasome non-ATPase regulatory subunit 14	B5XAH1	3	3	8
Apoptosis-associated speck-like protein containing a CARD	B5X786	6	8	8
Proteasome subunit beta type	B5X8C2	3	3	3
60S acidic ribosomal protein P2	B5XEB4	2	9	6
Low molecular weight phosphotyrosine protein phosphatase	B5XA56	4	4	7
Phosphoglucomutase 1	B5DG72	5	3	6
EF-hand domain-containing protein D2	C0HBT4	7	4	6
S100-A16	B5XDV1	2	6	3
Haloacid dehalogenase-like hydrolase domain-containing prot. 1A	B5XA20	8	3	6

Proteasome subunit beta type	B5X814	7	3	7
Hemoglobin subunit beta	Q91473	4	4	4
Beta-centractin	C0H9E1	3	4	7
Isocitrate dehydrogenase [NADP]	B5DGS2	4	14	3
Serine/threonine-protein phosphatase	B5X2G2	5	4	5
28 kDa heat-and acid-stable phosphoprotein	B5X267	3	2	4
60S ribosomal protein L30	B5X5W5	2	5	4
Beta-2-glycoprotein 1	C0H7U1	6	6	9
Heterogeneous nuclear ribonucleoprotein (Fragment)	Q6ZZX5	5	5	5
Elongation factor-1 delta-1	B5DGP8	3	5	4
40S ribosomal protein S10	B5XG42	3	2	4
Acidic leucine-rich nuclear phosphoprotein 32 family member E	C0HAU4	3	3	9
Histone-binding protein RBBP7	B5X3G4	5	4	8
ELAV-like protein 1	B5X1D5	1	6	5
Acyl-protein thioesterase 2	B5X0S8	2	7	6
Aspartyl-tRNA synthetase, cytoplasmic	B5X4S5	1	10	12
Trifunctional enzyme subunit alpha, mitochondrial (Fragment)	C0PU77	0	11	2
Tumor protein D52	B5XCG6	4	8	7
C-reactive protein	B5X672	6	5	7
26S proteasome subunit (Fragment)	B5RI31	3	6	10
Heterogeneous nuclear ribonucleoprotein R	C0HB71	2	6	5
Splicing factor, arginine/serine-rich 5	C0HAB7	0	7	5
Leucyl-tRNA synthetase, cytoplasmic	C0H907	0	9	5
Obg-like ATPase 1	C0H944	0	12	9
Sodium/potassium-transporting ATPase subunit alpha-1	C0H8U1	0	10	1
Thiosulfate sulfurtransferase KAT	B9EP38	4	5	5
Gastrotropin	B5X688	4	5	5
Osteoclast-stimulating factor 1	B5X958	4	6	7
Cathepsin Z (Fragment)	C0PUQ5	3	5	4
Cystatin-B	B5X6W2	3	4	4
Tumor protein D54	B5XAX0	3	6	6
Leukotriene A-4 hydrolase	B5X2K3	4	5	6
Myelin expression factor 2	C0HBC4	1	2	2
DnaJ homolog subfamily A member 2	C0HBK7	0	5	4
DNA replication licensing factor MCM3	B5X2W3	0	8	5
NMDA receptor-regulated protein 1	B5X2S1	0	10	6
High mobility group protein B3	C0HBT7	3	6	6

5-3 exoribonuclease 2 (Fragment)	C0PUI6	2	4	5
Malic enzyme	C0H987	3	12	4
Activated RNA polymerase II transcriptional coactivator p15	B9EPK7	2	4	5
Prothymosin alpha	B9EL48	3	6	6
Plastin-2	B5XFL6	3	3	5
Ribosomal protein L19	B5X7R3	3	3	3
Lactoylglutathione lyase	B5XBQ0	5	3	5
Acidic leucine-rich nuclear phosphoprotein 32 family member B	B9ELQ2	1	5	5
Phenylalanyl-tRNA synthetase beta chain	B5X0Z8	4	7	9
Heterogeneous nuclear ribonucleoprotein A3 homolog 2	B5XBH7	1	4	3
40 kDa peptidyl-prolyl cis-trans isomerase	B5X5H7	1	4	3
Trifunctional enzyme subunit beta, mitochondrial	C0H9B8	0	12	6
Glucosamine 6-phosphate N-acetyltransferase	B5X977	6	2	5
Proteasome subunit beta type	B5X6T8	4	2	3
GDP-L-fucose synthetase	B9EL11	5	5	7
Ubiquitin-conjugating enzyme E2 variant 1	A8QKW3	3	5	7
KH domain-containing, RNA-bind., signal transduction-ass. prot. 1	C0PUJ5	1	2	1
Interferon-induced guanylate-binding protein 1	C0H966	1	4	6
Retinoic acid-inducible gene-I	C7C1L7	0	5	3
Splicing factor, arginine/serine-rich 1	C0H9Z3	0	10	4
Transcription factor BTF3 homolog 4	B5XE39	5	4	7
Microtubule-associated protein RP/EB family member 1	B9EMY8	5	6	7
Vacuolar proton pump subunit G 1	B5XD10	2	3	3
60S ribosomal protein L24	B5X748	1	6	5
Far upstream element-binding protein 3	B5X224	0	10	5
Pyruvate dehydrogenase E1 component subunit beta, mitochondrial	B5X485	4	11	4
Polypyrimidine tract-binding protein 1	C0H8X4	0	10	7
40S ribosomal protein S20	B5DGK9	3	4	5
Inorganic pyrophosphatase	B5X8C7	4	4	7
Anterior gradient-2-like protein 2	Q2V6Q7	3	3	3
40S ribosomal protein S15	C0H7I9	2	5	5
40S ribosomal protein S17	B9EMI7	2	5	6
Ubiquitin carboxyl-terminal hydrolase isozyme L3	B9EPR5	4	5	5
Chromobox protein homolog 3	B9ELS6	2	5	4
Tyrosyl-tRNA synthetase, cytoplasmic	B5XCP6	5	2	4

Allograft inflammatory factor 1	B5X824	2	4	4
Glutamate--cysteine ligase catalytic subunit	B5X493	5	2	6
Sorting nexin-2	B5X3R1	2	6	9
Ribosomal protein L28	B5DGI1	3	6	5
Cysteine-rich protein 1	C0H7Q9	2	2	3
Dihydropteridine reductase	B5XEA8	3	2	3
Proteasome activator complex subunit 1	B9EPF1	5	5	6
S-phase kinase-associated protein 1	B9EQI2	2	6	5
60S ribosomal protein L21	B5DGV5	1	3	3
Natterin-like protein	B5X1I2	4	5	8
Nucleophosmin (Fragment)	C0PTY0	1	5	4
Tyrosine-protein phosphatase non-receptor type 6	B5X4B3	0	9	8
ATP synthase gamma chain	B5DGC9	0	11	6
S100-A1	B9ELE1	3	3	3
Alpha-galactosidase A	C0HA45	4	3	5
Transketolase-like protein 2 (Fragment)	C0PUI7	3	4	3
Drebrin-like protein	B5X1P0	4	5	9
CDC45-related protein	B5X2X0	1	2	1
Zinc finger protein 576	B5X202	3	1	2
Cystatin	B5X7N7	3	3	3
3-hydroxybutyrate dehydrogenase type 2	B5X8E1	6	5	5
Programmed cell death protein 5	B5XCG1	3	3	4
Proteasome subunit alpha type	B5X619	4	3	4
26S proteasome non-ATPase regulatory subunit 7 like 2	B5DH25	3	6	5
Glucosamine-6-phosphate isomerase	B5X4R2	5	1	8
60S ribosomal protein L12	C0H751	1	6	5
Proliferating cell nuclear antigen	B9EMQ6	4	3	5
ADP-ribosylarginine hydrolase	B5DG81	5	5	7
Serine/threonine-protein phosphatase	B5DG05	6	2	5
60S ribosomal protein L27	B5X8W7	3	5	6
Apoptosis inhibitor 5	B5X3S1	1	7	5
Probable saccharopine dehydrogenase	B5X147	0	10	3
NEDD8	B5XBM9	2	4	2
Prostaglandin E synthase 3	B5XCK8	2	5	4
Splicing factor U2AF 65 kDa subunit	C0HB34	2	5	4
Proactivator polypeptide	B5X4D6	2	4	4
Tubulin beta-2A chain	C0HBL4	2	2	2
Acetyl-CoA acetyltransferase, cytosolic	B5X1M6	6	2	7

Calcium/calmodulin-dependent protein kinase type II delta chain	C0PUT9	2	3	4
F-actin-capping protein subunit alpha-2 (Fragment)	C0PUH3	4	3	5
Serine/threonine-protein phosphatase (Fragment)	C0PU36	4	2	5
Aldose reductase	B5XF51	4	7	4
Splicing factor, arginine/serine-rich 9	B5X448	1	4	5
TAR DNA-binding protein 43	C0H962	0	6	4
26S proteasome non-ATPase regulatory subunit 8	B5XAB2	0	5	4
rRNA 2-O-methyltransferase fibrillarin	B5X300	0	10	7
ATP synthase subunit d, mitochondrial	C0H715	0	9	6
Proteasome subunit alpha type	B5XG15	4	3	3
F-actin-capping protein subunit alpha-1	C0H8S8	4	5	4
Mannose-binding protein C	B5XEZ1	6	3	4
Zonadhesin-like	Q5S3N1	2	2	3
Thimet oligopeptidase	C0H9W4	4	1	4
SUMO-activating enzyme subunit 1	B9END7	2	2	5
Nucleolar protein 5A	C0HAC2	0	7	3
60S ribosomal protein L14	C0H7P0	3	5	5
Proteasome subunit alpha type	B5DG53	5	2	4
L-plastin (Fragment)	C7C4W8	4	3	6
Eukaryotic translation initiation factor 2 subunit 3	C0HA50	2	5	9
Hsp90 co-chaperone Cdc37	B5X4J1	1	5	5
Platelet-activating factor acetylhydrolase IB subunit gamma	B5XAE1	4	4	5
Transmembrane emp24 domain-containing protein 10	B5XE99	1	8	6
Epithelial cadherin	C0H958	5	3	4
Plasminogen activator inhibitor 1 RNA-binding protein	B5X2G5	3	2	4
Clathrin light chain A	B5X377	1	3	2
Microtubule-associated protein RP/EB family member 1	C0H9W6	4	5	5
6-phosphofructokinase	C0HAA0	1	5	4
Isochorismatase domain-containing protein 1	B5X0W9	6	1	4
Complement C1q-like protein 4	B9EPU5	4	3	5
Vesicle-fusing ATPase	B5X134	0	4	2
Matrix metalloproteinase-9	B5X4C7	0	15	1
Peroxiredoxin-1	B5X7X7	4	3	4
Eukaryotic translation initiation factor 3 subunit I	B5X0W4	4	5	8
KIAA0174 homolog	C0HAI6	2	6	8
60S ribosomal protein L11	B5XE05	1	6	3

Catechol-O-methyltransferase domain-containing protein 1	B5XDZ7	8	1	8
EH domain-containing protein 4	B5X0R0	1	4	5
Methenyltetrahydrofolate synthetase domain-containing protein	B5X4V8	1	2	3
Proactivator polypeptide	B5X2Q8	0	6	4
Anterior gradient protein 3 homolog	B5XF60	2	7	5
Aspartate aminotransferase	B5X3Z1	3	9	5
Aldehyde dehydrogenase, mitochondrial	B5X2T3	2	10	3
40S ribosomal protein S23	C0H7K2	3	3	4
Eukaryotic translation initiation factor 2 subunit 2	B9EPN7	2	3	3
Small nuclear ribonucleoprotein Sm D2	B5XGC3	5	4	6
Eukaryotic translation initiation factor 3 subunit M	B5XBY6	1	4	4
COP9 signalosome complex subunit 4	C0HBE8	0	5	5
Lambda-crystallin	B5X6Z9	7	0	7
Splicing factor, arginine/serine-rich 5	B5X3D2	0	6	5
NADH-cytochrome b5 reductase 3	B5X1Q9	0	6	5
Calmodulin	B5XCM2	2	2	3
Homeodomain-only protein	B5XBT5	4	3	4
Glia maturation factor beta	B9EP59	5	4	6
Thioredoxin	B5XF92	5	3	5
Glyoxalase 1	B5DFZ9	4	2	4
N-acetylgalactosamine kinase	B5X1Z3	2	4	8
Elongation factor 2	B5X1W2	2	5	7
60S ribosomal protein L32	B5DG97	1	5	6
Eukaryotic translation initiation factor 4E	B9EQ27	0	4	4
Mitochondrial inner membrane protein	B5X1N7	0	11	3
Phosphoenolpyruvate carboxykinase, mitochondrial	B5X3P1	1	10	3
40S ribosomal protein S28	C0H7D5	2	5	3
Ras-related protein Rab-3D	B5X2Y7	4	3	4
Transcription elongation factor B polypeptide 2	B5XFL9	3	3	4
Vacuolar protein sorting-associated protein 26B-B	B5X1R6	5	2	6
60S acidic ribosomal protein P1	B5DH21	1	2	2
Lens epithelium-derived growth factor	B5X458	2	2	1
Fatty acyl-CoA hydrolase, medium chain (Fragment)	C0PUR6	4	3	4
SUMO-activating enzyme subunit 2	B5X383	1	4	10
Nucleobindin-1	B5X443	1	9	5
Charged multivesicular body protein 3	B5X3V9	1	2	3
Integrin beta	C0H8X0	0	8	1
60S ribosomal protein L36	B5X5S9	2	3	3

Eukaryotic translation initiation factor 4H	C0H8S0	3	3	4
Glyoxylate reductase/hydroxypyruvate reductase	B5X0R3	4	3	5
Lupus La protein homolog B	C0HAU7	1	6	8
60S ribosomal protein L35	B5DG50	0	3	5
Ester hydrolase C11orf54 homolog	B5X8V5	6	0	5
Signal recognition particle 54	B5DG49	0	6	0
Cold-inducible RNA-binding protein	B5DGC5	2	3	3
Nucleolin	B5X4X9	2	3	4
High mobility group-T protein	C0HBP8	2	3	2
SUMO-conjugating enzyme UBC9-B	B5X609	5	1	4
Barrier-to-autointegration factor	B5RI51	7	2	6
Charged multivesicular body protein 2a	B3TDD9	1	2	2
Sepiapterin reductase	B5X3E6	4	5	6
Small nuclear ribonucleoprotein-associated protein	B5XAK0	2	1	3
Intracellular hyaluronan-binding protein 4	B9EQ40	4	0	4
Guanine nucleotide-binding protein Gi, alpha-2 subunit	B5X4F0	0	6	4
Prohibitin-2	B5XEI9	0	9	7
Proteasome subunit alpha type	B5X959	3	3	3
Deoxyribonuclease	B5XFM6	3	1	4
Dihydrolipoyl dehydrogenase	B5X1V8	3	7	3
Ras-related protein Rab-1A	C0HAK6	1	2	1
Acidic leucine-rich nuclear phosphoprotein 32 family member E	B9EN91	2	1	2
60S ribosomal protein L23	C0H7M7	2	6	6
BolA-like protein 2	B9EL42	3	3	3
Leukocyte cell-derived chemotaxin 2	B5XCD7	4	3	6
Vps20-associated 1 like 1	B5DH22	2	2	4
Polypyrimidine tract-binding protein 2	B5X232	1	7	6
26S proteasome non-ATPase regulatory subunit 12	B5X386	0	6	8
SH3 domain-binding glutamic acid-rich-like protein 3	B5X4I3	2	2	2
Ubiquitin-conjugating enzyme E2 N	B5XC59	2	2	3
Phosphoglycerate kinase 1	B5DFX8	2	6	4
Pre-mRNA-processing factor 19	C0HBN2	2	4	4
ATP-dependent DNA helicase 2 subunit 1	B5X1Q2	0	2	3
Serine/threonine-prot. phosphatase 2A 56 kDa reg. sub epsilon iso.	B5X3X0	0	5	4
Proteasome subunit beta type (Fragment)	B5RI58	6	2	5
Growth factor receptor-bound protein 2	C0H8R6	2	2	4
Clathrin interactor 1	C0HAA2	0	2	2

Flotillin-2a	B5X242	0	6	2
Hydroxysteroid dehydrogenase-like protein 2	C0H8N5	0	6	2
60S ribosomal protein L6	C0H7M0	2	3	3
N-acetylneuraminate lyase	B5X130	5	2	5
Legumain	C0H9C5	1	2	4
Prefoldin subunit 6	B5XFC5	2	4	4
Eukaryotic translation initiation factor 3 subunit H	B5RI54	1	4	5
Cathepsin H	B5X7N5	7	4	4
Deoxyhypusine synthase	B5X252	4	1	5
Inositol-3-phosphate synthase A	B5X3P3	4	2	5
Phenylalanyl-tRNA synthetase alpha chain	B5X2Q7	2	2	5
Cystatin	B5XF86	3	1	4
THO complex subunit 4	B9EQ17	1	2	2
SH2/SH3 adaptor crk	C0H993	5	0	4
Twinfilin-1	C0HBN3	3	1	3
Vacuolar proton pump subunit E 1	B5XBK1	0	4	5
Flotillin-1	B5X3E3	0	6	1
Actin-related protein 2/3 complex subunit 5	C0H8E0	2	2	2
Cofilin-2	B9EM12	1	3	2
ADP-ribosylation factor 4	B5X1K6	2	4	4
Hsc70-interacting protein	B5X4G1	0	6	6
Inosine-5'-monophosphate dehydrogenase	C0H976	0	2	3
Cystatin	B5X5W9	3	2	3
Tubulin beta-2C chain	C0H8A6	3	3	3
Heterogeneous nuclear ribonucleoprotein A/B	C0H844	1	4	3
Hematological and neurological expressed 1-like protein	B5X0X5	6	1	4
Caspase-3	C0HBK4	3	3	3
UV excision repair protein RAD23 homolog A	B5X4K8	2	3	3
Zymogen granule membrane protein 16	B9EQH7	1	4	3
60S ribosomal protein L26	B5DGV7	1	4	6
60 kDa heat shock protein, mitochondrial	C0HBF1	2	11	2
Transmembrane emp24 domain-containing protein 9	B5X3D5	0	8	2
Annexin	B5X1W5	0	11	1
Hypoxanthine phosphoribosyltransferase 1	B5DFU2	3	4	5
Histone H1.0	C0H823	1	4	1
Splicing factor, arginine/serine-rich 2	B5XDF3	0	2	2
Syntenin-1	B5X137	1	3	3
Nitrilase homolog 2	B5X7A6	5	0	4
Nucleolar protein 5	B5X218	0	6	4

Protein arginine methyltransferase 1	B5DGE3	0	7	2
T-complex protein 1 subunit gamma	B5X3E4	0	2	1
Ribosomal protein L22 (Fragment)	B5RI62	2	5	4
40S ribosomal protein S27	B5DGY0	2	3	3
Ribulose-phosphate 3-epimerase	B5XGT2	2	1	3
60S ribosomal protein L38	C0H7L4	1	4	4
Transcription elongation factor B polypeptide 1	B9EN56	2	2	3
Thioredoxin domain-containing protein 17	B5X9Q5	4	4	5
Serine/threonine-protein phosphatase	B5X934	3	3	3
Stathmin	B5X953	2	2	1
Granulins	C0HA53	2	3	3
Macrophage migration inhibitory factor	Q0ZBS0	4	2	3
Basic transcription factor 3-1	B5DGN4	3	6	6
Epoxide hydrolase 2	B5X3M6	3	7	4
Methionine aminopeptidase	B5X372	7	1	5
FAM49B	B5X1W0	0	3	2
ADP/ATP translocase 2	B5X6K4	0	3	2
Endonuclease domain-containing 1 protein	B5XG37	7	0	4
B-cell receptor-associated protein 31	B5X317	0	4	3
Small ubiquitin-related modifier 3	B9EMA2	2	2	2
Myosin-11 (Fragment)	C0PU27	2	2	3
Proteasome subunit beta type	C0H856	2	1	2
COP9 signalosome complex subunit 6	B9EPB6	0	4	5
3,2-trans-enoyl-CoA isomerase, mitochondrial	C0HAW6	4	4	2
Ezrin-radixin-moesin-binding phosphoprotein 50	C0H943	1	1	5
Ubiquitin carboxyl-terminal hydrolase isozyme L5	B5X5H3	0	4	5
Dolichyl-diphosphooligosaccharide prot. glycosyltransf. sub. STT3A	C0H9J5	0	5	2
Voltage-dependent anion channel 2-3	B5DH07	0	9	1
Profilin	B5X5R2	1	3	3
Nicotinamide phosphoribosyltransferase (Fragment)	C0PU79	1	1	2
Palmitoyl-protein thioesterase 1	B5XEC6	2	4	3
FACT complex subunit SSRP1	C0HB78	1	3	3
Uroporphyrinogen decarboxylase	B5X376	2	0	4
Phospholipase A-2-activating protein	B5X4A4	1	3	5
RNA-binding protein 39	B5X379	0	2	1
Keratin, type I cytoskeletal 20	B5X588	2	4	1
Interferon-induced guanylate-binding protein 1 (Fragment)	C0PU99	0	2	0
Cathepsin B	B5X4P4	3	4	2

Sorting nexin-12	B9EP10	2	3	4
Clathrin light chain B	B9EQ28	1	1	2
40S ribosomal protein S21	B5XGU1	2	3	3
Aminoacylase-1	B5X1P3	5	0	3
Flavin reductase	B5XA45	1	4	4
Integrin beta	C0HBK5	1	1	2
P38b1 mitogen activated protein kinase	A1ED58	0	4	5
Histone deacetylase	B5X2E0	1	1	3
Enolase 3-2	B5DGQ7	2	0	2
Glutamate dehydrogenase (Fragment)	Q7T1N7	0	6	1
RuvB-like 1	B5X3S2	0	4	2
Prohibitin	B5X2M2	0	8	6
Collagenase 3	B5X4P7	0	11	1
Proliferation-associated protein 2G4	B5X3I7	1	1	4
CTLA-2-beta	B5XBI7	3	3	3
Vesicle-associated membrane protein-associated protein A	B9EMQ9	1	4	4
Ubiquitin-fold modifier-conjugating enzyme 1	B9EM04	3	2	3
Dynactin subunit 2	B5X3R2	2	3	6
60S acidic ribosomal protein P2	B9EQJ1	1	4	3
Casein kinase II subunit beta	B5X2D0	4	1	4
Adenylosuccinate synthetase	B5X373	3	3	7
Caprin-1	C0HBQ7	2	2	5
Splicing factor 3 subunit 1	B5X263	1	4	3
Tripeptidyl-peptidase 1	B5X2E6	1	7	7
Vacuolar protein sorting 28	B5DG99	2	2	2
60S ribosomal protein L31	C0H7F9	0	2	2
ATP-binding cassette sub-family F member 1	C0H9P3	0	2	2
Glutamate decarboxylase-like protein 1	C0HA17	0	4	0
Beta-2-microglobulin	B5X5Y2	1	3	3
Beta-hexosaminidase alpha chain	B5X4C8	2	1	1
Cytosolic purine 5-nucleotidase	B5X1K3	1	3	2
Cytosolic sulfotransferase 3	B5XDY6	1	4	6
Arfaptin-1	C0H909	0	2	2
Serine/threonine-protein kinase VRK1	B5X850	1	3	6
Pyridoxal kinase	B5X1E5	7	0	7
Calcium/calmodulin-dependent protein kinase type 1	B5X2V5	0	4	6
Alpha amylase	A0SEG1	3	0	2
Far upstream element (FUSE) binding protein 3 (Fragment)	B5RI78	0	4	4

DNA replication licensing factor mcm5	C0HAG8	0	4	0
Vimentin	B5X4G3	0	6	2
60S ribosomal protein L37a	B5DGW2	1	3	4
Ras-related C3 botulinum toxin substrate 2	B5X2S9	1	4	3
Thymidylate kinase	B5X868	4	3	4
Eukaryotic translation initiation factor 3 subunit K	B5X5X0	2	3	4
Tubulin-specific chaperone A	B5X9U4	4	3	4
Galactonate dehydratase	B5X4N7	4	4	5
Microtubule-associated protein, RP/EB family member 1	B5DG69	2	1	4
Hemoglobin subunit alpha-4	C0H789	2	3	2
Ras-related protein Rab-35	B5XAZ2	2	2	3
Pyruvate dehydrogenase E1 comp. sub. alpha, somatic form, mitoch.	B5X4R5	3	10	2
Ras-related protein Rab-18	B5X0U0	1	6	4
Calcium-binding mitochondrial carrier protein SCaMC-1	B5X2X8	0	5	3
Transmembrane 9 superfamily member 2	B5X419	0	8	3
Interleukin enhancer-binding factor 2 homolog	B5X1U2	0	2	0
Galectin-8	B5X3K3	1	2	2
Phosphatase 1G	B5X3X4	1	3	4
Retinoblastoma-binding protein 9	B5XBC8	4	4	6
Hydroxyacylglutathione hydrolase	B5XA69	4	2	3
60S ribosomal protein L34	C0H7M9	1	3	2
Helicase MOV-10	C0HAB8	1	3	1
Leukocyte elastase inhibitor	B5X4J0	1	0	7
Metalloproteinase inhibitor 2	B5X8G7	5	0	5
Proteasome subunit alpha type	B9EM89	3	2	2
Gamma-interferon-inducible lysosomal thiol reductase	B5X8K4	2	2	1
Troponin C-akin-1 protein	B5XEV0	4	3	3
Cold-inducible RNA-binding protein	E0R8Z1	1	2	2
Prostaglandin E synthase 3	B9ELX0	1	3	4
Prefoldin subunit 3	B5XA06	2	3	2
40S ribosomal protein S26	C0H7R8	2	3	3
Lipocalin	B5XGC5	2	1	2
Transcriptional activator protein Pur-beta	B5X2A4	0	2	3
60S ribosomal protein L27a	B5X6U7	0	3	4
Dual specificity mitogen-activated protein kinase kinase 2	B5X0Y3	1	3	4
TANK-binding kinase 1	H5ZTW4	0	5	2

ADP-ribosylation factor GTPase-activating protein 3	C0H9V0	1	0	3
Eukaryotic translation initiation factor 2A	B5X2E8	3	0	2
Electron-transfer-flavoprotein alpha polypeptide (Fragment)	B5RI57	0	8	2
Ubiquitin-conjugating enzyme E2 D2	B9EP40	2	2	2
Peptide methionine sulfoxide reductase	B5X8R5	5	2	4
SAPK substrate protein 1	C0H8H7	5	4	3
Histidine triad nucleotide-binding protein 1	B5XBP3	1	4	3
Cathepsin S	B5X3V4	2	2	5
Adenylate kinase	B5DGM6	0	4	4
Mitochondrial 2-oxoglutarate/malate carrier protein	B5XBE3	5	2	5
Vacuolar ATP synthase catalytic subunit A	B5X161	2	3	3
Cytochrome c oxidase subunit 5B, mitochondrial	B5X6C6	0	4	3
CD2 antigen cytoplasmic tail-binding protein 2	B9EQK1	0	0	6
Acyl-CoA-binding protein	B5X5W4	1	5	4
Interferon-induced 35 kDa protein homolog	B5X4Y5	3	2	3
Cytochrome c oxidase subunit 4 isoform 1, mitochondrial	B9EM26	0	3	2
Src-family tyrosine kinase SCK	Q9DDK6	1	4	3
Carbonic anhydrase	B5X3I8	4	3	4
Aspartate aminotransferase	B5X2F0	0	4	0
Succinate dehydrogenase complex subunit A flavoprotein	B5DFZ8	0	4	0
Alpha-endosulfine	B5XE27	4	1	3
Creatine kinase, testis isozyme	B5X6F1	1	3	3
Twinfilin-1	C0H986	1	3	4
C7orf57 homolog	B5X365	4	0	3
Mannose-1-phosphate guanyltransferase alpha-A	B5X2A9	4	4	4
Small inducible cytokine subfamily E, member 1-like	B5RI76	1	3	1
Heterogeneous nuclear ribonucleoproteins C1/C2	B5X3G1	0	1	3
Nucleolysin TIAR	B5X439	0	3	3
Ubiquilin-4	B5X126	0	5	5
Bactericidal permeability-increasing protein	B5X1K1	0	6	2
Eukaryotic translation initiation factor 3 subunit J	B9ENH4	2	2	3
Proteasome subunit beta type	B5XD66	4	1	3
Prefoldin subunit 5	B9EMI8	2	2	2
Polyadenylate-binding protein 2	C0HAW0	2	2	2
Profilin	B5XDX4	2	2	2
Plasma retinol-binding protein 1	B5XCH7	2	2	2
Receptor expression-enhancing protein 5	B5X9E9	0	4	2

Dynein light chain Tctex-type 3	B5XGQ0	2	0	2
Complement C1q subcomponent subunit C	B5X3K9	1	1	3
Ribose-phosphate pyrophosphokinase 2	B5XFY7	0	5	5
Spermatogenesis-associated serine-rich protein 2	B9EM25	0	2	2
FADD	B5XB08	0	4	4
mRNA turnover protein 4 homolog	B5X724	2	3	1
Serine/threonine-protein kinase MST4	B5X318	0	3	3
Eukaryotic translation initiation factor 5	B5X401	1	1	4
Anamorsin-A	B5XEX1	2	0	5
Actin, adductor muscle	B5XFZ3	0	4	0
Ras-related protein Rab-10	B9ELM7	1	2	1
Ictacalcin	B5X7A4	1	2	2
Eukaryotic translation initiation factor 1A, X-chromosomal	B5X726	2	1	3
Tyrosine phosphatase type IVA 2	B5X2I4	2	1	3
Proteasome subunit alpha type	B5DGU4	3	1	2
Charged multivesicular body protein 5	B9ELB6	2	3	4
AP-2 complex subunit beta-1 (Fragment)	C0PUP3	1	2	4
Ras-related protein ralB-B	B5X6D9	2	3	3
Nuclear receptor coactivator 5	B5X1C7	0	2	2
C14orf166	B9EPN8	1	3	3
Selenide, water dikinase 1	C0HA78	3	2	3
Eukaryotic peptide chain release factor GTP-binding subunit ERF3B	B5X2S5	0	1	2
Methylcrotonoyl-CoA carboxylase subunit alpha, mitochondrial	B5X404	0	2	1
PRA1 family protein 3	B9ELK3	0	4	3
Costars family protein ABRACL	B5X8A5	1	2	2
S-adenosylmethionine synthase	B5X1I0	2	2	4
COP9 signalosome complex subunit 7a	B5X7V8	1	2	3
Alpha-aspartyl dipeptidase	B5XC91	5	2	2
Small nuclear ribonucleoprotein Sm D3	B5XBB1	2	2	3
Coiled-coil domain-containing protein 6 (Fragment)	C0PUR1	0	2	3
Regucalcin	B5XEE5	3	0	3
Proteasome activator complex subunit 2	B9EML6	1	0	2
Sorbitol dehydrogenase	B5XFZ2	3	1	2
H-2 class II histocompatibility antigen gamma chain	B5XH65	0	4	3
Guanine nucleotide-binding protein GI/GS/GT subunit beta-1	B5X1F5	0	5	3
DNA replication licensing factor mcm2	C0H9U0	0	2	0

Annexin	B5RI22	0	1	2
Vasodilator-stimulated phosphoprotein	B5X8V4	3	2	3
Serine/threonine-protein phosphatase	B5X1D2	2	1	2
Macrosialin	C0H9A0	0	4	3
cAMP-dependent protein kinase catalytic subunit beta	C0HBG9	0	4	1
Death-associated protein 1	B5XGR4	3	1	3
S-formylglutathione hydrolase	B5XG47	2	1	3
AP-1 complex subunit mu-2	C0H8J4	0	3	2
Endothelial differentiation-related factor 1-1	B5DGP6	1	1	4
Splicing factor, arginine/serine-rich 3	B5XAU0	0	5	4
Methylmalonate-semialdehyde dehydrogenase	B5X4I4	0	3	0
Flavin reductase	B5XFB2	0	2	3
Anterior gradient protein 3 homolog	B5X704	0	2	1
CASC4	C0H956	0	5	0
Vacuolar protein-sorting-associated protein 36	C0HAY1	1	2	1
Plectin 1 (Fragment)	B5RI77	0	4	2
Sorcin	B9EMB8	0	7	2
60S ribosomal protein L5	B5X413	0	5	2
Collectrin	B5X131	1	2	1
Leukocyte common antigen (Fragment)	C0PUA6	0	3	0
3-ketoacyl-CoA thiolase, mitochondrial	B5X2A5	0	4	1
SH3 and PX domain-containing protein 2A	B5X4S7	0	2	0
Prefoldin subunit 2	B5X9Z0	2	2	2
Regulator of chromosome condensation	C0HAF1	0	3	4
Peptidyl-prolyl cis-trans isomerase	B9EL76	1	3	2
Glutathione peroxidase (Fragment)	B5RI90	3	1	3
Sperm acrosome membrane-associated protein 4	B5XER6	1	2	2
Probable thiopurine S-methyltransferase	B5XCX0	3	1	4
Ras-related protein Rab-25	B9EPR0	0	4	2
Apolipoprotein D	B5XEY8	0	4	2
Na,K-ATPase alpha subunit isoform 1c/i (Fragment)	Q5IR98	0	3	1
Signal peptidase complex catalytic subunit SEC11A	B5XDQ9	0	4	2
Ubiquinol-cytochrome c reductase core protein 2	B5DGG6	0	2	1
26S proteasome non-ATPase regulatory subunit 7	B9EMK0	1	2	1
Interleukin enhancer-binding factor 2 homolog	B5X2K6	0	5	3
Vacuolar protein sorting-associated protein 26A	B5X0V6	3	0	6
BCCIP homolog	B5XCY8	0	2	4
Cell division control protein 42 homolog	B5X466	0	5	3
Proteasome activator complex subunit 3	B9EP79	1	2	3

Actin-like protein 6B	B5X0S6	1	2	1
Complement component 1 Q subcomponent-bind. prot., mitochond.	B5XAU5	1	5	2
ATP-binding cassette sub-family E member 1	B5X0Q5	0	2	1
Inosine-5'-monophosphate dehydrogenase	B5DG43	1	5	2
Hypoxia up-regulated protein 1 (Fragment)	C0PUQ0	1	3	1
ATP synthase subunit O, mitochondrial	B5XDM0	0	5	2
Splicing factor 3A subunit 3	B5X1D0	0	2	2
Apoptosis inhibitor 5 (Fragment)	C0PUV2	0	1	2
Polypeptide N-acetylgalactosaminyltransferase 2	C0HA92	0	3	0
Ubiquitin-fold modifier 1	B9ENM6	2	1	4
Pentraxin	P79905	3	1	2
Eukaryotic translation initiation factor 1b	B5X7T5	4	2	3
Inositol polyphosphate 1-phosphatase	C0H8H4	1	2	2
Junction plakoglobin	B5X1P2	0	4	2
Splicing factor, arginine/serine-rich 7	B9EMR5	0	3	3
Small nuclear ribonucleoprotein E	B5X6H9	1	1	2
Coactosin-like protein	B9ENI2	1	2	2
60S ribosomal protein L35a	C0H7D2	1	5	4
Heterogeneous nuclear ribonucleoprotein A1	B5X7A3	1	1	2
Digestive cysteine proteinase 2	B5X4D9	0	2	4
Glycylpeptide N-tetradecanoyltransferase (Fragment)	C0PUR8	1	1	3
Vesicle-trafficking protein SEC22b-B	B9ENR6	0	5	5
Estradiol 17-beta-dehydrogenase 12-B	B5X3S0	0	3	3
Leucine-rich repeat-containing protein 47 (Fragment)	C0PUH1	1	0	2
MACRO domain-containing protein 1	B5X8D5	0	5	1
Vesicle-associated membrane protein-associated protein B/C	B5X1V1	2	2	0
NDRG1	B5X292	0	2	3
Coagulation factor XIII A chain	C0H9Z9	0	3	0
Prefoldin subunit 4	B5X6D2	2	1	1
60S acidic ribosomal protein P2	B5DGW8	0	2	2
Tubulin, alpha 8 like 3-2	B5DH02	1	2	2
Cysteine and glycine-rich protein 1	B9EMK9	1	1	5
ATP synthase subunit alpha	B5DG78	0	3	2
Lipocalin	B5X598	2	1	3
Probable saccharopine dehydrogenase	C0HAR9	0	3	2
GTP cyclohydrolase 1 feedback regulatory protein	B5XC31	2	0	2
Nardilysin (Fragment)	C0PUK2	1	1	3
Kunitz-type protease inhibitor 1	C0H9F6	3	1	2

Syntenin-1	B5XEZ7	0	4	1
Band 4.1-like protein 2 (Fragment)	C0PUS5	1	0	3
Translation machinery-associated protein 20	B5XEV2	0	2	2
Cytochrome c oxidase subunit VIb isoform 1	B5X6N6	0	4	4
Hemoglobin subunit beta	B5X8L0	1	2	1
Transcription factor BTF3 homolog 4	B5XDZ0	2	2	2
Pre-mRNA branch site protein p14	B5X662	1	1	2
Interferon-induced protein 44	B5X426	0	3	2
Peptidyl-prolyl cis-trans isomerase	B5X5R4	2	2	2
3-hydroxyacyl-CoA dehydrogenase type-2	B5XGY1	1	5	1
Calcyphosin-like protein	B5XGN9	1	2	2
Heat shock 70 kDa protein 4 (Fragment)	C0PUG5	2	2	4
Cytochrome c oxidase subunit 2	Q37677	0	3	2
TAR DNA-binding protein 43	B5X2Z5	0	1	2
Methylcrotonoyl-CoA carboxylase beta chain, mitochondrial	C0HAQ0	1	2	2
Ras-related protein Rab-6C	B5X1I9	0	5	2
Delta-1-pyrroline-5-carboxylate synthetase	C0HBA2	0	4	0
Disulfide-isomerase A6	B5X291	0	6	1
Serine/threonine-protein phosphatase 2A 65 kDa reg. sub. A beta iso.	C0PUA0	1	3	2
Finkel-Biskis-Reilly murine sarcoma virus ribosomal protein S30	B5DGJ7	2	0	4
MHC class I (Fragment)	Q8HX43	1	3	1
Beta-catenin-like protein 1	B5X4Y0	0	2	2
Galectin-9	B5X2C9	1	5	3
Autophagy-related protein 3	B9EN22	0	2	1
ATP synthase-coupling factor 6, mitochondrial	B5X4S6	0	4	3
NEDD8-conjugating enzyme Ubc12	C0HBK6	0	2	2
Cytochrome c1, heme protein, mitochondrial	B9EN90	0	4	1
Solute carrier family 25 member 3	B5DG35	0	4	0
Calcium-binding mitochondrial carrier protein Aralar1	B5X446	0	2	1
U4/U6 small nuclear ribonucleoprotein Prp31	C0HBK9	0	2	1
Fibronectin (Fragment)	C0PUB2	1	6	2
Phosphorylase (Fragment)	C0PUK4	0	2	2
6-phosphofructo-2-kinase/fructose-2, 6-biphosphatase 4	B5X4R9	0	4	0
Connective tissue growth factor	B5X1X2	0	2	1
Band 3 anion exchange protein (Fragment)	C0PUF0	0	4	0

Ras-related protein Rab-7a	B5X431	2	2	1
Annexin	B5XAE0	1	2	1
40S ribosomal protein S3	B5DGY5	1	2	2
40S ribosomal protein S3	B5XAC5	3	3	3
Abhydrolase domain-containing protein 14B	B5X8P9	2	2	2
Kunitz-type protease inhibitor 1	C0HAY4	2	1	1
ADP-ribosylation factor-like protein 1	B5XET7	0	3	1
High mobility group protein B1	B9ELI1	0	1	4
Superoxide dismutase	C0H894	2	3	2
U5 small nuclear ribonucleoprotein 200 kDa helicase (Fragment)	C0PTY9	0	3	3
Enoyl Coenzyme A hydratase short chain 1 mitochondrial	B5DG66	1	3	1
Translocon-associated protein subunit delta	B5XBL0	0	4	2
Mitochondrial carrier homolog 2	B9EPN2	0	4	1
Transmembrane emp24 domain-containing protein 2	B5X6M4	0	2	1
Transmembrane 9 superfamily member 3	B5X1L2	0	4	1
Dehydrogenase/reductase SDR family member 13	B5XAB1	0	3	1
Proteasome subunit alpha type	B5XCL4	1	1	2
Calpain small subunit 1	B5X856	1	3	2
N-acetyltransferase NAT13	B5XA07	0	2	3
Ubiquitin-conjugating enzyme E2 variant 1	B5X8I8	1	2	2
Arginine N-methyltransferase 5 (Fragment)	C0PUL6	1	2	3
COP9 constitutive photomorphogenic homolog subunit 5	B5DFV3	1	2	5
Catechol O-methyltransferase	B5XD19	0	7	2
Cytochrome c oxidase subunit 5A, mitochondrial	B9ENR4	0	3	1
Small ubiquitin-related modifier 1	B5XGQ7	2	0	1
Small glutamine-rich tetratricopeptide repeat-containing protein A	B5X4G2	0	1	3
N-terminal acetyltransferase complex ARD1 subunit homolog A	B9ENY3	0	2	3
Uridine 5-monophosphate synthase	C0HBQ0	0	2	3
MHC class I antigen (Fragment)	Q2QF03	0	4	5
3-hydroxyisobutyrate dehydrogenase, mitochondrial	B5X3N8	1	3	0
Cysteine desulfurase, mitochondrial	B5X101	0	3	0
Tubulin alpha-1C chain (Fragment)	C0PU76	2	2	2
Cell division control protein 42 homolog	B5XE81	1	3	2
Annexin	B5XCE7	1	2	1
Isoamyl acetate-hydrolyzing esterase 1 homolog	B5X7K9	3	2	3

Homeobox protein Nkx-2.3	C0HAS1	1	2	2
60S ribosomal protein L35	B5X6R2	0	3	3
Farnesyl pyrophosphate synthetase	B5X3Y4	3	0	3
Apolipoprotein C-I	B5XE16	1	3	1
LYRIC	B5X3H6	1	2	2
COP9 signalosome complex subunit 3	B5X4W9	1	4	2
Galectin-9	B5X9R4	0	3	2
Integrin beta-1 (Fragment)	C0PUP8	1	2	0
WD repeat-containing protein 57	B5X8U2	0	2	2
Histone deacetylase complex subunit SAP18	B9EQ87	0	2	2
Acetyl-CoA acetyltransferase, mitochondrial	B5X3B8	0	2	0
Pyrroline-5-carboxylate reductase 3	B5XC04	2	1	0
Transgelin	B5X7F2	1	3	3
Plastin-2	B9EQN9	1	2	2
TUBB	A7KIJ4	1	3	2
Casein kinase II subunit alpha	B9EMZ5	2	2	2
DJ-1	B9EN63	4	0	3
Tripartite motif-containing protein 25	B5XBH9	0	1	3
Beta-galactoside-binding lectin	B9ELC5	1	3	2
Sulfotransferase 6B1	B5X5I2	1	2	1
Phosphoribosyl pyrophosphate synthetase-associated protein 1	B5XFK7	0	3	3
14 kDa phosphohistidine phosphatase	B5X7K4	1	1	2
RNA-binding protein 4B	B5X4H7	0	3	1
Cytochrome b-c1 complex subunit 1, mitochondrial (Fragment)	C0PUA8	0	3	1
ATP synthase-coupling factor 6, mitochondrial	B5X626	0	4	2
NADH dehydrogenase iron-sulfur protein 3, mitochondrial	B5XG99	0	3	1
Developmentally-regulated GTP-binding protein 1	B5XBM0	1	2	2
Calponin-2	B5X3R8	0	4	1
FAM3C	B5X1E3	0	3	2
Complement C1q subcomponent subunit B	C0HBS7	2	0	2
Ganglioside GM2 activator	B5X3U1	0	4	2
Grancalcin	B5X944	0	2	0
Aflatoxin B1 aldehyde reductase member 2	B5RI21	1	0	2
Adenylate kinase 2, mitochondrial	B5XCA1	0	2	1
Annexin	B5XF75	0	4	0
Actin-related protein 2/3 complex subunit 3	B5X8R6	1	1	3
Phosphoserine phosphatase	B5X9K1	2	1	1

Type-4 ice-structuring protein LS-12	B5XDA4	0	4	3
Type-4 ice-structuring protein	B5X6Y1	0	4	3
ATP synthase subunit f, mitochondrial	C0H7D0	0	2	1
Lissencephaly-1 homolog B	B5X3C4	2	1	1
PolyADP-ribose glycohydrolase ARH3	B5XG88	5	0	3
Cleavage and polyadenylation specificity factor subunit 5	B5XBB9	1	3	2
Proline synthetase co-transcribed bacterial homolog protein	B5XEC5	2	0	3
Succinyl-CoA ligase subunit alpha, mitochondrial (Fragment)	C0PU29	0	5	1
NADH dehydrogenase 1 alpha subcomplex sub. 10, mitochondrial	B5XCJ3	0	2	1
Ribosomal protein S29	B5DFW3	0	2	0
Cathepsin K	B5X425	2	0	2
Transport-associated protein	P79908	0	3	1
Ornithine decarboxylase 1	B5X2J4	0	2	1
Erlin-2	C0H9J4	0	4	1
FK506-binding protein 10	C0HAV9	0	2	1
Ecto-ADP-ribosyltransferase 4	B5XBZ1	2	0	1
DNA replication licensing factor mcm7-A (Fragment)	C0PUG8	0	2	0
Syntaxin-7	B5X671	1	1	2
Proliferation-associated protein 2G4 (Fragment)	C0PTY4	1	1	2
60S ribosomal protein L7	B5DGW4	1	2	1
HN1 protein	I7LSU2	2	0	2
ATP synthase protein 8	P68529	0	2	1
Translocon-associated protein subunit alpha	C0HAK7	0	2	1
Ependymin	B5XDG6	1	2	2
Retinol dehydrogenase 12	B5XB52	0	3	1
Hydroxyacyl-coenzyme A dehydrogenase, mitochondrial	B5XDQ2	0	5	1
Acyl-Coenzyme A dehydrogenase C-4 to C-12 straight chain	B5DG29	0	4	1
NADH dehydrogenase iron-sulfur protein 8, mitochondrial	B5XEV5	0	2	2
Phospholipase B-like 1	B5X2C7	3	0	2
Cytidine deaminase	B9EPM5	3	5	3
MHC class I (Fragment)	Q8HX50	0	4	0
Cathepsin S	C0HDJ6	2	1	2
Actin-related protein 2/3 complex subunit 5	B9EMH3	2	0	1
Small nuclear ribonucleoprotein Sm D3	B5X738	1	1	2

Cytochrome c oxidase copper chaperone	B5X6H1	1	2	1
N-lysine methyltransferase setd6	C0H8I2	1	1	2
Thioredoxin domain-containing protein 12	B9ELD9	1	3	2
ATP synthase subunit g, mitochondrial	B5XF93	0	3	2
Ubiquinol-cytochrome c reductase iron-sulfur subunit	B5XAY2	0	3	0
Complement C1q subcomponent subunit C	C0HB93	3	0	2
Glutathione S-transferase theta-1	B5X8W2	0	4	0
Vacuolar proton pump subunit H	B5X3Z9	0	2	2
Nedd8 activating enzyme E1 subunit 1	B5DFY9	2	0	0
Small nuclear ribonucleoprotein G	B5XB66	2	2	2
U1 small nuclear ribonucleoprotein A	B5XCU4	0	2	2
ISG15-like protein	Q29W12	1	2	2
ADP-sugar pyrophosphatase	B5XAK9	2	1	2
Histone H2A	B5X351	1	2	1
Serine hydroxymethyltransferase, mitochondrial	B5X423	2	4	1
Nuclear protein Hcc-1	B5X8Q7	1	0	2
Mitochondrial 2-oxoglutarate/malate carrier protein	B5X7D7	0	3	1
Signal peptidase complex subunit 3	B5X6E9	0	3	1
Voltage-dependent anion-selective channel protein 2	B5X2M6	0	3	0
Mps one binder kinase activator-like 1A	B5X3D8	0	2	2
Core-binding factor beta subunit	Q0H914	0	1	2
Tyrosine-protein kinase SRK2	B5X5P2	0	3	0
Ras-related protein Rap-1b	B9EM10	3	2	1
Copper transport protein ATOX1	B5X5H6	0	2	2
RING finger protein 181	B5XCA0	2	0	2
Polypeptide N-acetylgalactosaminyltransferase 6 (Fragment)	C0PUL4	1	2	1
Nuclear protein Hcc-1	B9EM58	0	2	3
GTP-binding protein SAR1a	B5X110	0	4	1
FUS-interacting serine-arginine-rich protein 1	B5X1S5	0	2	2
BMP and activin membrane-bound inhibitor homolog	B5XEJ0	2	0	1
Hydroxymethylglutaryl-CoA lyase, mitochondrial	B5X4F3	0	3	0
Nck-associated protein 1 (Fragment)	C0PUT7	0	2	0
Tubulin alpha chain	C0HA00	0	2	1
Programmed cell death protein 10	B9EN83	0	2	3
Pre-mRNA-processing factor 39	C0H9W3	0	2	3
Nicotinamide mononucleotide adenylyltransferase 1	B5X0T2	0	1	2
THO complex subunit 4	B5XE82	2	0	1
Lipocalin	B5X6W0	1	0	2
Casein kinase II subunit alpha	C0HB89	0	2	1

V-type proton ATPase subunit F	B5XCI2	2	1	2
Calcineurin subunit B isoform 1 (Fragment)	C0PU72	2	0	1
Calumenin-A	B5X186	1	2	0
Coatomer subunit zeta-1	B5X8E4	0	1	2
Thioredoxin-dependent peroxide reductase, mitochondrial	B5X6K7	0	2	1
Guanylate kinase	B5X4R6	0	2	1
Galectin-4	B9EPI0	0	3	1
Complement component 1 Q subcomponent-bind. prot., mitochon.	B5XBX7	0	4	0
GTPase HRas	B5X1B6	0	2	1
E2-induced gene 5 protein homolog	C0HBN8	0	2	0
Zymogen granule membrane protein 16	B9EPC9	0	2	1
Phosphatidylethanolamine-binding protein 1	B9EQ08	2	1	2
Septin-8	C0HAT5	0	1	3
Dihydrolipoyl dehydrogenase, mitochondrial (Fragment)	C0PUP1	0	3	1
Churchill protein	B5XGR1	2	0	1
Serine/threonine-protein phosphatase	B5DG88	2	2	0
TFG	C0HB49	1	0	0
NADH dehydrogenase 1 beta subcomplex subunit 3	B9EMN2	0	2	0
Heterogeneous nuclear ribonucleoprotein A/B	B5X2K8	0	2	2
60S acidic ribosomal protein P2	B9ELM2	0	2	1
NADPH oxidase 1	B8YQA0	0	2	0
Angiogenin-1	B5XAZ0	4	0	0
TFG	C0HB49	0	0	2
Inducible nitric oxide synthase (Fragment)	Q9YHU8	0	3	1
MHC class I (Fragment)	Q8HX47	0	3	0
Neutrophil cytosol factor 2	C0H9S3	0	2	0
Sodium/potassium-transporting ATPase subunit alpha-1 (Fragment)	C0PUF8	0	2	1
MHC class II (Fragment)	Q31589	0	3	0
MHC class I antigen (Fragment)	G5D5C9	0	5	0
C10	B9EL19	0	3	1
ATP synthase subunit delta, mitochondrial	B5XDU6	0	3	1
H/ACA ribonucleoprotein complex subunit 2-like protein	B5X7M4	0	2	2
Trafficking protein particle complex subunit 3	B9ENY9	0	2	2
Glutaredoxin-related protein 5	B5XCG9	0	2	1
Transmembrane emp24 domain-containing protein 7	B5XDR9	0	2	1

Y-box-binding protein 2-A	B5X2B2	1	0	2
Collagen alpha-1I chain (Fragment)	C0PUP9	2	0	0
MHC class I antigen (Fragment)	Q2QF05	0	1	2
Brain protein 44	B5DG58	0	2	0
Acyl-CoA-binding protein	B5X9M2	0	0	2
Rho-related GTP-binding protein RhoG	B5XDC3	0	2	0
Complement factor D	B5XEN8	0	3	0
Galectin-9	B5X7H8	0	3	0
Disulfide-isomerase A3	B5X4S3	0	2	0
DNA-directed RNA polymerase II subunit RPB4	B9EP00	0	2	1
S100-A14	C0H880	0	2	1
Translocon-associated protein subunit alpha	B9EL33	0	2	0

Table S 4. Representative immune-related differentially expressed proteind proteinpressed proteinpressed proteinpressed proteins in the skin of zebrafish infected with spring viremia of carp virus (R. Liu et al., 2020).

Accession	*Protein*	*Score*	*Coverage*	*Fold chant old than, (24/96 h \) (24/96 h)rage*	*Fold than, (24/96 h)rage*	*Fold than, (24/96 h)rage*	*Fold change (24/96 h)*	*MW/kDa*	*p1*	*Peptide sequence*
Q7ZUQO	[Actin-related] protein 2/3 complex Subunit 1A	35.60	8.65	1.29/1.04 1.29/1.046 5	1.29/1. 0465	1.29/1.0465	1.29/1.04	15.25	5.45	TLESSIQGLR, WSPLENK, VFSAYIK, NAYVWSQK
Q6POV8	Annexin 5b	733.1 3	48.26	0.57/0.81 0.57/0.81 26	0.57/0. 8126	0.57/0.8126	0.57/0.81	35.07	5.64	YGTDEGQFITILGNR, LSGFEIEESIQR, VPGYFADSLYAAMK
042363	Apolipoprotein A-	1156.	55.73	0.59/0.94	0.59/0.	0.59/0.9473	0.59/0.94	140.12	5.06	ALDNLDGTDYEQYK,
Q6PH54	Arginase 2	42.20	3.46	1.60/0.80	1.60/0.	1.60/0.8646	1.60/0.80	37.75	6.73	VMEVTLDHLLAR
Q7ZUJ4	B cell receptor-associated protein	22.40	6.48	0.79/1.06 0.79/1.06	0.79/1. 0648	0.79/1.0648	0.79/1.06	26.19	4.46	VDLSNNPVAIEHIHMK
E9QG20	Calcineurin subunit B type 1	46.00	12.94	0.80/1.25 0.80/1.25	0.80/1. 2594	0.80/1.2594	0.80/1.25	16.11	4.68	DTQLQQIVDK, EFIEGVSQFSVK
Q6PHF1	Calcium-regulated heat stable protein 1	79.20	18.06	1.11/1.65 1.11/1.65 06	1.11/1. 6506	1.11/1.6506	1.11/1.65	16.51	8.05	IQAVEVTITHLAPGTK, AAEGPVFSGVCK
A0JMP4	Calcium-transporting	1739. 42	34.51	0.62/0.92 0.62/0.92	0.62/0. 9251	0.62/0.9251	0.62/0.92	67.47	7.46	ANACCSVVK, KNFTLEFSR, SMSVYCTPVKGDAGSK
Q7SXP1	Capping protein muscle Z-line beta	246.0 7	34.43	1.39/1.05 1.39/1.054 3	1.39/1. 0543	1.39/1.0543	1.39/1.05	27.05	7.36	TGSGTMNLGGSLTR, QMEKDETVSESSPHIANIGR
A0A0G2L2 I4	C-C motif chemokine	32.92	23.66	2.18/1.72 2.18/1.72	2.18/1. 7266	2.18/1.7266	2.18/1.72	10.56	8.85	TIQIIDDR, VDCTLPGVIFVTQK
A9ZPF5	C-C motif chemokine 19a	37.96	20.17	1.32/1.60 1.32/1.661	1.32/1. 6017	1.32/1.6017	1.32/1.60	13.42	8.97	GLNLCAPPASEELWVR, DAVIFITR
A9ZPF2	Chemokine CCL25b/CCL-	37.19	23.58	2.96/1.03 2.96/1.03	2.96/1. 0358	2.96/1.0358	2.96/1.03	12.23	9.58	DWVQAIIK, QLTDGGCNIPAVVFK
A9ZPF8	Chemokine CXCL-C lc	43.50	11.40	1.38/1.15 1.38/1.15	1.38/1. 1540	1.38/1.1540	1.38/1.15	13.03	8.69	TTASGQLCLNPQK
Q8AYE0	Coagulation factor V	41.56	2.21	2.07/1.06 2.07/1.062	2.07/1. 0621	2.07/1.0621	2.07/1.06	46.7	7.87	IELLGCDFE
BOS5I1	Complement	78.87	5.83	0.73/0.90	0.73/0.	0.73/0.9083	0.73/0.90	33.33	7.96	QNILVEGHNLAK

Q6NY70	Epithelial cell	205.2	23.84	0.81/1.44	0.81/1.	0.81/1.4484	0.81/1.44	34.20	8.05	CEPAETYWVR,
Q7ZTX5	Exocyst complex component 7	35.80	1.49	2.64/1.54 2.64/1.54	2.64/1. 5449	2.64/1.5449	2.64/1.54	76.9	6.44	LDEYLACIAK
Q7SXJ0	Galectin 2b	72.37	33.61	0.70/2.25 0.70/2.256	0.70/2.2 561	0.70/2.2561	0.70/2.25	64.06	9.45	FNAHGDSNTIVCNSK, EHCFPFQQGEEFK
F1Q6K5	Galectin-3-binding protein B	47.28	5.42	1.26/1.17 1.26/1.17.42	1.26/1.17. 42	1.26/1.17.42	1.26/1.17	64.9	5.97	NQNNVFHVQDFK
A0A0R4IAU8	Heat repeat-containing protein 1	28.60	1.07	2.77/1.20 2.77/1.260	2.77/1.2 607	2.77/1.2607	2.77/1.20	241.92	6.35	MPAVLDTLK, ALPQNDSSLLGR
Q5RG12	Heat shock protein 90-alpha 2	674.27	18.80	1.42/1.15 1.42/1.1580	1.42/1.1 580	1.42/1.1580	1.42/1.15	84.6	5.01	HLEINPDHPIVETLR
Q6NX86	High-mobility group box 1	91.25	24.88	0.83/1.27 0.83/1.27.88	0.83/1.27. 88	0.83/1.27.88	0.83/1.27	45.32		KHPEATVNFSEFSK, GKFEDMAK, VKEETPGLSIGDVAK
A7MBY4	Histone H2B	561.16	65.67	0.62/2.55 0.62/2.5567	0.62/2.5 567	0.62/2.5567	0.62/2.55	7.39	9.88	AVSEGTK, LLPGELAK, AVSEGTK, INSFVNDIFER, LLLPGELAK, AGEASR, IQTAVR
QILV17	Interferon regulatory factor 2-binding protein 1	31.60	1.49	1.27/1.04 1.27/1.0449	1.27/1.0 449	1.27/1.0449	1.27/1.04	842.97	6.11	IELLIDTAR
A2BHB8	Interferon-stimulated gene 15	44.27	19.11	1.72/1.29 1.72/1.29111	1.72/1.29 111	1.72/1.29111	1.72/1.29	222.64	5.68	TYDVDANETVDQLQTK, QLESGMK, LLGGDVK
B3DH90	Interferon-induced GTP-	159.11	17.82	1.81/1.39 1.81/1.3982	1.81/1.3 982	1.81/1.3982	1.81/1.39	62.93	5.06	LRGQPENIGDQIK, LYEEGFATIPK, KLYEEGFATIPK, LLEEPALK, LSFFIDK, LEEQIQTK
Q802V0	LIM domain binding 3b	68.90	14.04	0.64/0.86 0.64/0.8604	0.64/0.8 604	0.64/0.8604	0.64/0.86	118.40	7.81	MDSPMPVIPHQ, DSALSTHKPIEVK
AOAOKOK5Q0	Melanoma differentiation-associated	39.20	1.61	1.54/1.01 1.54/1.0161	1.54/1.0 161	1.54/1.0161	1.54/1.01	22.67	4.98	FLQALEDTEHR
Q31359	MHC class II alpha chain	91.54	15.68	0.24/1.39 0.24/1.39.68	0.24/1.39. 68	0.24/1.3968	0.24/1.39	26.12	4.42	TPAEGDIYSTVK, IQGQPNTK, TPAEGDISTVK, NSDGTFNMFSALK
Q24JW9	MHC II dab protein	132.31	27.05	0.98/1.26 0.98/1.2605	0.98/1.2 605	0.98/1.2605	0.98/1.26	27.68	7.15	DQAYLHQLK, AQVDTFCR, DKAVLPEVTIK, IQCLVEHASLTQPLTK
Q6VN46	Myoglobin	324.55	64.63	0.44/0.42 0.44/0.4263	0.44/0.4 263	0.44/0.4263	0.44/0.42	15.6	7.55	FSGISQGDLAGSPAVAAHGATVLK, GDHAALLKPLANTHANIHK
Q7T2Y I	Myosin light chain 2	69.31	42.44	0.20/0.21 0.20/0.2144	0.20/0.2 144	0.20/0.2144	0.20/0.21	18.99	4.82	EAFGCIDQNR, ETYAQLGK, LNGTDPEETILAAFK

Accession	*Protein*	*Score*	*Coverage*	*(24/96 h)*	*MW/kDa*	*pl*	*Peptide sequence*
Q918V0	Parvalbumin 2	983.73	58.72	0.53/0.96	11.61	4.68	LFLQNFSAGAR, AFLSAGDSDGDGK
LFLQNFSAGAR,	Parvalbumin 3	658.18	37.61	0.52/0.88	11.54	4.64	LFLQNFSAGAR, IGVDEFASLVKA
LFLQNFSAGAR, IGVDEFASLVKA	Parvalbumin 4	897.92	33.94	0.60/0.83	57.79	7.03	AFAIIDQDK, LFLQNFK, IGIDEFAALVKA, AADSFNHK
AFAIIDQDK,	Phospholipid-transporting	30.22	1.85	3.14/1.97	126.51	6.80	NLLLLGATAIEDR, IWVLTGDK
NLLLLGATAIEDR,	Ras-related protein Rab-13	163.14	14.50	1.84/1.61	22.44	9.38	LLIIGDSGVGK, LQVWDTAGQER, FFETSAK
LLIIGDSGVGK,	Rh type C glycoprotein2b	22.86	1.43	1.38/1.75	53.61	5.67	GFWCGPK
GFWCGPK	RNA-binding motif protein	48.60	2.87	1.88/2.65	58.29		LLGVPI
LLGVPIIVQASQAE K	Serpin peptidase inhibitor Glade B member 1	36.25	2.63	1.12/1.36	103.18	7.90	VQVLELPYVK
VQVLELPYVK	Signal transducer and activator of transcription la	167.87	12.82	1.22/1.02	86.80	5.87	AASDPEAQIPWNR
AASDPEAQIPWNR	Sodium channel protein type 4 subunit alpha B	41.72	0.78	0.65/0.83	56.92	4.65	FMGNLRQK, ERPCPPGWYK
FMGNLRQK,	Sodium/potassium-	715.22	26.24	2.21/1.05	112.67	5.35	VFLAEQTDVPILK
VFLAEQTDVPILK	ATPase subunit alpha						
VFILGDQETK,	Solute carrier family 12	74.33	1.93	2.19/1.12	21.10	8.54	VFILGDQETK, FEDTITPFR
DFLAGGVAAAISK, TAVAPIER,	Solute carrier family 25 member 4	441.73	30.87	0.59/0.91	32.67	9.7	DFLAGGVAAAISK, TAVAPIER, EFTGLGNCVAK, AAYFGIYDTAK
LLTAEEVATK,	Tropomyosin 1	1290.62	30.99	1.14/1.18	125.85	9.03	LLTAEEVATK, RIQLVEEELDRAQER, AADESER
SLVLSITK,	Troponin I skeletal fast 2a.3	70.74	13.64	0.52/0.90	19.72	9.22	SLVLSITK, EVVDTAAAK, VVDLQGK
ALSNGSQYSSYLQK ,	Troponin T 3b	75.33	25.88	0.37/0.75	27.27		ALSNGSQYSSYLQK, ALSNMGSQYSSYLQK, PDGDKVDFDDIQKK
ICDGINK	Tumor necrosis factor alpha-induced protein 8-like protein 3	21.29	3.47	0.56/1.02	23.19	5.77	ICDGINK
LGISPLSEIK,	Tumor protein D52-like 2a	28.75	9.09	1.29/1.08	112.88	6.34	LGISPLSEIK, HAAELK
IEEAGGATAAQIE	Uncharacterized protein	2952.19	27.12	0.27/0.26	223.24	5.67	IEEAGGATAAQIEMNK, QADSVAELGEQIDNLQR,
EPEVLSTMATIVN	Uncharacterized protein	37.27	2.80	1.76/1.71	123.07	6.19	EPEVLSTMATIVNK
TASPQVSLLQK, TSTLNVKPEEWK,	Zgc:111997	45.50	11.01	1.51/2.03	38.71	5.55	TASPQVSLLQK, TSTLNVKPEEWK, ESGIVPVFK

Table S 5. List of identified lysine acetylated proteins and sites--4-10-Comparative Proteomic Analysis of Lysine Acetylation in Fish CIK Cells Infected with Aquareovirus. (Guo et al., 2017).

Protein accession	Position	Protein names	Gene names	Score	Modified sequence	Mass error [ppm]	Ratio H/L
carp-female_000000000_00957794_00974051	106	Histidyl-tRNA synthetase, cytoplasmic	hars	104.17	_ETLTGK(ac)YGEDSK_	0.32864	
carp-female_000000000_01904551_01911645	153	Ribosomal protein L26	rpl26	70.056	_GHYK(ac)GQQIGK_	0.27473	1.063
carp-female_000000000_01904551_01911645	167	Ribosomal protein L26	rpl26	138.98	_K(ac)YVIYIER_	-0.79625	0.954
carp-female_000000000_03663588_03683915	75	Catenin (Cadherin-associated protein), alpha	ctnna1	120.4	_AHVLAASVETATQNFLDK(ac)GEK_	1.4013	0.652
carp-female_000000000_03663588_03683915	306	Catenin (Cadherin-associated protein), alpha	ctnna1	103.44	_DVHHK(ac)DQMAAAR_	-0.91305	0.977
carp-female_000000000_03663588_03683915	340	Catenin (Cadherin-associated protein), alpha	ctnna1	118.16	_ACLQHPDVAAYK(ac)ANR_	-0.31885	1.114
carp-female_000000000_04019072_04022985	140	Ppp2ca protein	ppp2ca	54.982	_K(ac)YGNANVWK_	0.60914	1.416
carp-female_000000000_04027941_04033360	55	Sideroflexin 1	sfxn1	130.75	_QIIQDYK(ac)K_	0.097239	0.866
carp-female_000000000_04027941_04033360	72	Sideroflexin 1	sfxn1	132.51	_AK(ac)YVFDSAFHPDTGEK_	0.13868	0.646
carp-female_000000000_04576065_04586515	37	Electron transfer flavoprotein-ubiquinone oxidoreductase, mitochondrial	ETFD	69.03	_QLANQHEK(ac)ELR_	-0.39665	0.949
carp-female_000000000_04576065_04586515	87	Electron transfer flavoprotein-ubiquinone oxidoreductase, mitochondrial	ETFD	82.859	_GAPLNTPVTEDK(ac)FSILTEK_	0.62798	

carp-female_000000000_05488574_05498163	221	NMDA receptor-regulated gene 1a	naa15a	64.82	_GELLLK(ac)LDR_	0.36774	1.755
carp-female_000000000_05488574_05498163	404	NMDA receptor-regulated gene 1a	naa15a	52.579	_IYK(ac)HAGNIR_	0.028031	3.152
carp-female_000000000_05488574_05498163	485	NMDA receptor-regulated gene 1a	naa15a	107.09	_SLNK(ac)YGEALK_	1.0107	1.998
carp-female_000000000_05728315_05737603	34	Zgc:171967 protein	zgc:171967	86.014	_TCDQSAFCK(ac)R_	-1.24	0.861
carp-female_000000000_05728315_05737603	457	Zgc:171967 protein	zgc:171967	85.493	_VDSGYK(ac)IHNEITTK_	-0.43392	0.599
carp-female_000000000_07608372_07615419	148	Tetraspanin 7	tspan7	138.98	_AVLQEGYK(ac)K_	-0.26292	0.077
carp-female_000000000_08962721_08970678	54	Glutathione reductase, mitochondrial	GSHR	78.939	_AHFSWQLIK(ac)R_	-0.56883	0.28
carp-female_000000000_08962721_08970678	350	Glutathione reductase, mitochondrial	GSHR	80.165	_TWGK(ac)DNVK_	0.35373	4.139
carp-female_000000000_10351921_10370020	324	Atlastin 3	atl3	125.75	_DQYYK(ac)NMEK_	-0.21534	0.555
carp-female_000000000_10351921_10370020	345	Atlastin 3	atl3	114.99	_VCGGDLPYVAPDSLEEK(ac)HR_	-0.38654	1.057
carp-female_000000000_10351921_10370020	694	Atlastin 3	atl3	93.839	_FVK(ac)MLPPNDCR_	-0.55806	1.067
carp-female_000000000_10351921_10370020	753	Atlastin 3	atl3	108.6	_FTGIK(ac)HEWQVNGLEDIK_	0.68011	1.204
carp-female_000000000_10857057_10861468	243	Fhla protein	fhl1a	64.522	_FTAHEDQFYCVDCYK(ac)TDVAK_	0.42095	
carp-female_000000000_10984317_10995531	226	Transmembrane 9 superfamily member 2	TM9S2	96.82	_LVAATVEPK(ac)SIK_	0.51605	0.461

carp-female_000000000_11600258_11602519	163	Solute carrier family 25 alpha, member 5	slc25a5	131.72	_YFPTQALNFAFK(ac)DK_	1.0973	0.876
carp-female_000000000_11600258_11602519	176	Solute carrier family 25 alpha, member 5	slc25a5	47.302	_VFLDGVDK(ac)R_	0.82451	0.87
carp-female_000000000_11600258_11602519	330	Solute carrier family 25 alpha, member 5	slc25a5	134.06	_GADIMYSGTIDCWK(ac)K_	0.31424	1.034
carp-female_000000000_11600258_11602519	343	Solute carrier family 25 alpha, member 5	slc25a5	173.76	_AFFK(ac)GAWSNVLR_	-0.42298	0.849
carp-female_000000000_13046905_13057421	273	Clathrin interactor 1	clint1a	80.236	_GVPSK(ac)TIDLGAAAHYTGDK_	-0.094545	1.095
carp-female_000000000_14860321_14870819	403	Acsl4a protein	acsl4a	85.554	_LAYDYK(ac)LEQIK_	0.39085	0.778
carp-female_000000000_15829395_15841876	20	Neuroblast differentiation-associated protein AHNAK	UY3_04292	100.53	_EVLFPQWMGADK(ac)HGLTIEQK_	1.0967	0.705
carp-female_000000000_15829395_15841876	36	Neuroblast differentiation-associated protein AHNAK	UY3_04292	129.37	_GQGEIFVK(ac)EVK_	0.022378	0.32
carp-female_000000000_15829395_15841876	1091	Neuroblast differentiation-associated protein AHNAK	UY3_04292	77.14	_FK(ac)MPSFGLK_	-0.65478	0.478
carp-female_000000000_15829395_15841876	2228	Neuroblast differentiation-associated protein AHNAK	UY3_04292	77.062	_SK(ac)TFDGDMK_	0.44344	0.305
carp-female_000000000_15829395_15841876	2569	Neuroblast differentiation-associated protein AHNAK	UY3_04292	110.31	_SK(ac)SASLDLFK_	0.92653	0.987
carp-female_000000000_15829395_15841876	2577	Neuroblast differentiation-associated protein AHNAK	UY3_04292	66.056	_SASLDLFK(ac)K_	-0.18037	0.925
carp-female_000000000_15875749_15884489	315	Elongation factor 1-gamma	eef1g	82.279	_K(ac)FAEMQPK_	-0.28507	1.028
carp-female_000000000_15875749_15884489	396	Elongation factor 1-gamma	eef1g	123.51	_SSFVMDEFK(ac)R_	-0.52204	0.746

carp-female_000000000_16066787_16081915	683	Lectin, mannose-binding 2	lman2	79.875	_VSHAK(ac)YMVTDR_	-0.30823	0.801
carp-female_000000000_17574594_17582809	148	Stanniocalcin 2	stc2a	101.75	_ECYMK(ac)HNLCSAAK_	0.25836	0.608
carp-female_000000000_18618397_18645425	584	Menkes disease ATPase	atp7a	57.434	_AHVK(ac)YDPEVTGPR_	0.36623	0.975
carp-female_000000001_02057429_02071506	103	Cytoskeleton-associated LIM domain protein	lima1	40.098	_MMFEK(ac)GETIHNVSR_	-0.026338	1.592
carp-female_000000001_02057429_02071506	278	Cytoskeleton-associated LIM domain protein	lima1	130.05	_GNYDEGFGHRPHK(ac)ELWETR_	-1.3324	0.952
carp-female_000000001_02141590_02142836	29	Nonclathrin coat protein zeta1-COP	copz1	109.83	_LYAK(ac)YYDDTYPTVK_	0.66787	0.886
carp-female_000000001_02141590_02142836	51	Nonclathrin coat protein zeta1-COP	copz1	59.35	_NIFNK(ac)THR_	0.58286	0.825
carp-female_000000001_02166796_02171151	48	Cbx5 protein	cbx5	102.9	_GFTDK(ac)HNTWEPEK_	0.91956	4.341
carp-female_000000001_02547325_02557711	186	Tubulin alpha chain	TBA	195.77	_GDDSFNTFFSETGAGK(ac)HVPR_	-0.012144	1.151
carp-female_000000001_02547325_02557711	520	Tubulin alpha chain	TBA	127.56	_LDHK(ac)FDLM(ox)YAK_	-0.065103	1.433
carp-female_000000001_02547325_02557711	527	Tubulin alpha chain	TBA	150.05	_FDLM(ox)YAK(ac)R_	-0.089874	1.204
carp-female_000000001_03402460_03453617	220	Coiled-coil-helix-coiled-coil-helix domain-containing protein 6	CHCH6	91.313	_EQITNLEK(ac)K_	0.51885	1.131
carp-female_000000001_03455306_03461493	510	Seryl-tRNA synthetase	sars	76.759	_FVK(ac)PAPIDLEATK_	0.071843	1.059
carp-female_000000001_03482362_03485979	145	Chromosome undetermined SCAF7862, whole genome shotgun sequence. (Fragment)	GSTENG00005343001	74.533	_DK(ac)LTELQLR_	-0.59184	1.013

carp-female_000000001_03482362_03485979	217	Chromosome undetermined SCAF7862, whole genome shotgun sequence. (Fragment)	GSTENG00005343001	85.212	_SFFEAK(ac)K_	1.1499	0.728
carp-female_000000001_03515448_03525499	241	Citrate synthase	cs	125.75	_AYSEGVNK(ac)AK_	1.02	0.22
carp-female_000000001_03515448_03525499	416	Citrate synthase	cs	98.421	_EFALK(ac)HLPNDPMFK_	-0.24124	1.021
carp-female_000000001_04378975_04384527	216	Sdcbp protein	sdcbp2	105.58	_DSSGHVGFIFK(ac)SGR_	0.07704	0.806
carp-female_000000001_04465168_04466295	161	Cell division cycle 42 like 2	cdc42l2	174.39	_AVK(ac)YVECSALTQK_	0.0851	0.572
carp-female_000000001_04950531_04960550	867	Nascent polypeptide-associated complex alpha polypeptide (Fragment)	unknown	153.72	_IEDLSQQAQLAAAEK(ac)FK_	0.45958	0.691
carp-female_000000001_05205733_05220435	315	unknown	unknown	57.034	_AVEYFSAASK(ac)PR_	-0.44858	0.923
carp-female_000000001_05295894_05308912	646	NF-kappaB essential modulator	ikbkg	128.45	_GQDVGK(ac)YQVSWSVPHK_	-0.20368	0.96
carp-female_000000001_05803416_05809184	276	Sarcolemma associated protein	slmapb	78.932	_TQVDLEK(ac)R_	1.2453	0.092
carp-female_000000001_05933655_05938581	128	Chromosome undetermined SCAF10501, whole genome shotgun sequence. (Fragment)	GSTENG00008691001	57.175	_EIGEHLVNIK(ac)K_	-0.077972	0.796
carp-female_000000001_05933655_05938581	711	Chromosome undetermined SCAF10501, whole genome shotgun sequence. (Fragment)	GSTENG00008691001	79.614	_VPCEEILVK(ac)HLGNR_	0.37333	0.775
carp-female_000000001_06126262_06133051	121	Tkt protein	tktb	47.187	_YFDK(ac)SSYR_	0.85114	0.813

carp-female_000000001_06126262_06133051	467	Tkt protein	tktb	80.994	_TSRPDTAVLYDAEEK(ac)FEIGK_	4.5304	0.377
carp-female_000000001_06884020_06889266	281	Chromosome 9 SCAF14710, whole genome shotgun sequence	GSTENG00022548001	49.483	_GQVVTK(ac)TSLLK_	0.14786	1.032
carp-female_000000001_07577777_07584809	79	Enolase	eno1a	143.93	_GNPTVEVDLYTK(ac)K_	-0.2551	1.887
carp-female_000000001_09147684_09162673	162	unknown	unknown	120.4	_AASTHLQTLTFTK(ac)VDLGDR_	-0.58983	0.91
carp-female_000000001_09147684_09162673	183	unknown	unknown	133.23	_AYTEYDK(ac)R_	-0.37478	1.024
carp-female_000000001_09147684_09162673	327	unknown	unknown	74.987	_DNYMK(ac)GIISGK_	-1.9247	0.923
carp-female_000000001_09147684_09162673	333	unknown	unknown	118.51	_GIISGK(ac)SDPYAVLR_	1.2611	1.461
carp-female_000000001_09147684_09162673	617	unknown	unknown	60.436	_SDPYVK(ac)IR_	-4.9026	0.176
carp-female_000000001_09147684_09162673	816	unknown	unknown	200.76	_ELLNEK(ac)DLVLDR_	0.37277	0.912
carp-female_000000001_09147684_09162673	842	unknown	unknown	60.305	_AELK(ac)LLDSK_	-0.25906	0.5
carp-female_000000001_09147684_09162673	971	unknown	unknown	130.56	_FDFDMSLEEAK(ac)QK_	-1.0911	0.848
carp-female_000000001_09228393_09265951	1143	unknown	unknown	44.425	_IQNFCAK(ac)HLK_	1.8035	0.882
carp-female_000000001_09228393_09265951	1489	unknown	unknown	68.355	_ADK(ac)HTCYEYR_	-0.32122	1.228
carp-female_000000001_09524946_09530660	97	GDP dissociation inhibitor 1	gdi1	50.314	_VVEGSFVYK(ac)GGK_	-0.11605	0.78

carp-female_000000001_09540982_09554063	104	Teleost complement regulatory membrane protein	tecrem	220.52	_SCGSPPDFLHGK(ac)YEITGISFGDK_	-0.41099	0.805
carp-female_000000001_10141190_10146911	116	Prostaglandin E synthase 3 (Cytosolic)	ptges3a	80.117	_LDFSCVGGTDNMK(ac)HHNEVELFESIDPNESK_	0.20762	1.176
carp-female_000000001_11099313_11137500	2272	Putative e3 ubiquitin-protein ligase huwe1	unknown	46.704	_ALGMAEGTEK(ac)HAR_	-3.0273	
carp-female_000000001_11677994_11680279	104	6-phosphogluconate dehydrogenase, decarboxylating	pgd	131.61	_TVSK(ac)VHDFLNNEAK_	-0.026765	0.878
carp-female_000000001_11677994_11680279	117	6-phosphogluconate dehydrogenase, decarboxylating	pgd	109.04	_GTK(ac)VIGAESLEDMVSK_	0.40077	0.651
carp-female_000000001_11802690_11807444	203	Nicotinamide mononucleotide adenylyltransferase 1	NMNA1	101.89	_FINQSDVLYK(ac)HR_	-1.3261	0.811
carp-female_000000003_00538178_00547944	283	Prohibitin 2	phb2a	125.75	_AQFYVEK(ac)AK_	0.11527	0.869
carp-female_000000003_01632757_01671893	489	Epidermal growth factor receptor	egfra	79.659	_VFK(ac)SDEQSVR_	0.086648	0.979
carp-female_000000003_01969544_01973134	57	Zgc:103652	cope	122.18	_K(ac)YAVVLDEIKPSSSEELQAVR_	-0.42002	0.906
carp-female_000000004_01302094_01304391	35	Natural killer cell enhancing factor	nkef	182.64	_DLSLSEYK(ac)GK_	-0.36879	1.523
carp-female_000000004_01859136_01861721	32	Vesicle-trafficking protein SEC22b-A	sec22ba	133.89	_NLQK(ac)YQSQAK_	-0.086159	0.54
carp-female_000000004_01937296_01943730	285	AP-2 complex subunit mu-1-A	ap2m1a	91.076	_LNYSDHDVIK(ac)WVR_	0.80224	1.139
carp-female_000000004_01946043_01954044	39	Zgc:110237	pcyt1aa	163.18	_CTVGLK(ac)YPAPYADQLESMEDKPYQR_	0.34665	1.587
carp-female_000000004_01946043_01954044	236	Zgc:110237	pcyt1aa	65.88	_K(ac)YNLQER_	0.39363	1.073

carp-female_000000004_02245903_02355814	2063	Chromosome 15 SCAF14992, whole genome shotgun sequence. (Fragment)	GSTENG00028349001	123.67	_ESEHEQEWK(ac)FR_	-0.63368	0.971
carp-female_000000004_02245903_02355814	3118	Chromosome 15 SCAF14992, whole genome shotgun sequence. (Fragment)	GSTENG00028349001	151.38	_EVVDK(ac)TAQSQGHISK_	-0.11588	0.747
carp-female_000000004_02245903_02355814	3140	Chromosome 15 SCAF14992, whole genome shotgun sequence. (Fragment)	GSTENG00028349001	96.143	_DVPQDQVLVSLK(ac)TEDSK_	1.0078	1.14
carp-female_000000004_02777722_02810321	478	Cdc73 protein	cdc73	71.524	_AFHLK(ac)YDEAR_	1.9453	1.184
carp-female_000000004_03267663_03271388	77	60S ribosomal protein L5	RL5	70.525	_NK(ac)YNTPK_	-1.5816	0.811
carp-female_000000004_04557685_04579456	943	Zgc:158450	zgc:158450	86.488	_LLK(ac)NHDEESLECLCR_	-0.52444	1.223
carp-female_000000004_05373464_05376608	4	Calponin 3, acidic b	cnn3b	87.519	_IAQK(ac)YDLQK_	0.40731	1.303
carp-female_000000004_05373464_05376608	124	Calponin 3, acidic b	cnn3b	54.005	_VDIGVK(ac)YADK_	-1.2385	0.692
carp-female_000000004_05942638_05967553	701	LOC571089 protein (Fragment)	LOC571089	86.772	_GQVSDLLSQK(ac)AK_	0.55479	0.466
carp-female_000000004_07024832_07032532	385	Si:ch211-12e1.4 protein	afg3l2	63.998	_HLSDAINQK(ac)HFEQAIER_	2.0068	0.703
carp-female_000000004_07784930_07788318	24	Calponin 2	cnn2	58.32	_IAQK(ac)YDPQREEELR_	0.28795	0.415
carp-female_000000004_07784930_07788318	144	Calponin 2	cnn2	68.845	_GIHSNVDIGVK(ac)YAER_	-0.16395	0.932
carp-female_000000004_07784930_07788318	271	Calponin 2	cnn2	60.305	_QIYDAK(ac)YCPK_	1.6758	2.791

carp-female_000000004_08861514_08864815	299	Acyl-Coenzyme A dehydrogenase, C-4 to C-12 straight chain	acadm	127.71	_ALEEATK(ac)YALER_	1.2015	0.732
carp-female_000000004_13211489_13233786	371	unknown	unknown	133.23	_DLEFLK(ac)QAAK_	-1.0453	
carp-female_000000004_14864427_14865483	3	Novel protein similar to human candidate tumor suppressor p33 ING1 (Inhibitor of growth 1)	ing5b	112.85	_(ac)AK(ac)GMYLEHYLDSIEGLPCELQR_	0.34167	
carp-female_000000004_15237719_15253901	32	Cotamer alpha	copa	69.111	_MCTLIDK(ac)FDEHDGPVR_	-1.9655	0.921
carp-female_000000004_15237719_15253901	47	Cotamer alpha	copa	66.636	_GIDFHK(ac)QQPLFVSGGDDYK_	1.1507	0.858
carp-female_000000004_15237719_15253901	588	Cotamer alpha	copa	103.08	_K(ac)YEEVLHMVR_	-0.83237	0.906
carp-female_000000004_15237719_15253901	624	Cotamer alpha	copa	81.526	_GYPEVALHFVK(ac)DEK_	0.62075	0.909
carp-female_000000004_15291659_15296777	48	Putative translocation protein (Fragment)	unknown	100.93	_AVDCLLDSK(ac)WAK_	0.23999	0.804
carp-female_000000004_16079875_16086958	656	LOC559360 protein (Fragment)	acin1a	109.24	_TPELAAQK(ac)HAPQEEEK_	-0.23917	0.993
carp-female_000000004_16221780_16232426	330	Proteasome subunit beta type-5	D623_10009442	77.899	_VSQEDVLQLHLK(ac)YQSEK_	-0.031331	0.935
carp-female_000000004_16626200_16639382	317	Coatomer protein complex, subunit beta 2	copb2	135.02	_IIWAK(ac)HSEIQQANLK_	0.012509	0.913
carp-female_000000005_01305536_01308522	28	Zgc:113369 protein	zgc:113369	174.22	_YEWQK(ac)HGTCAAQAESLNSEHK_	0.22022	1.109
carp-female_000000005_01677318_01687512	256	Mitochondrial calcium uniporter	mcu	57.885	_QYLLFFHK(ac)GAK_	-1.5195	0.781
carp-female_000000005_01677318_01687512	267	Mitochondrial calcium uniporter	mcu	157.91	_FDIEK(ac)YNK_	0.88884	0.917

carp-female_000000005_02867301_02880721	409	Adipocyte plasma membrane-associated protein	apmap	66.004	_SPYLCK(ac)LDLSK_	-0.37624	1.119
carp-female_000000005_05092459_05121594	262	Interferon gamma receptor 1-2	unknown	57.347	_YTITHDQK(ac)K_	-0.37766	1.253
carp-female_000000005_05343556_05395924	1824	Dystonin	DST	70.552	_DK(ac)YQATDR_	-0.49757	1.128
carp-female_000000005_05935743_05940360	117	Gclc protein	gclc	45.565	_EFVAK(ac)HPQYK_	0.073062	1.087
carp-female_000000005_06693330_06699068	29	Degenerative spermatocyte homolog 1, lipid desaturase (Drosophila)	degs1	83.182	_EILAK(ac)YPEIK_	0.54999	1.111
carp-female_000000005_07593934_07596058	104	Zgc:66168	rps27a	71.501	_LAVLK(ac)YYK_	0.1604	1.101
carp-female_000000006_00488543_00492255	96	40S ribosomal protein S14 (Fragment)	unknown	103.43	_ELGITALHIK(ac)LR_	-0.6676	1.108
carp-female_000000006_00946696_00969588	673	Glucosamine--fructose-6-phosphate aminotransferase 1	unknown	126.77	_SLADELHHQK(ac)SLLVMGR_	-0.35346	1
carp-female_000000006_01695152_01695781	171	Ras homolog gene family, member Gb	rhogb	115.57	_QIHAVK(ac)YMECSALSQDGIK_	1.5251	0.733
carp-female_000000006_01712959_01738587	50	unknown	unknown	55.353	_EDLK(ac)YNDPK_	-0.54129	1.284
carp-female_000000006_01897638_01904724	598	Solute carrier family 7 (Cationic amino acid transporter, y+ system), member 3	slc7a3a	80.755	_K(ac)YEPPLQNK_	0.40269	0.297
carp-female_000000006_01964013_01964347	47	LOC495350 protein	grpel2	73.881	_LHDVFTK(ac)HGLEK_	0.80266	0.805
carp-female_000000006_01965496_01966308	66	H/ACA ribonucleoprotein complex subunit 2-like protein	nhp2	100.02	_EVQK(ac)FINK_	0.24052	0.764

carp-female_000000006_03571836_03607035	460	Pyruvate carboxylase	pcxb	88.596	_K(ac)YSLDYYLK_	-0.025296	0.953
carp-female_000000006_03571836_03607035	882	Pyruvate carboxylase	pcxb	91.961	_VFQEFK(ac)EFTR_	-0.7231	3.312
carp-female_000000006_03631937_03713404	318	Pyruvate carboxylase	pcxa	177.6	_QVNYENAGTVEFLVDK(ac)HGK_	-0.23408	0.937
carp-female_000000006_03721474_03728658	183	Zgc:55813	slc3a2b	159.64	_EAGNADQFTK(ac)LIQAAHR_	-0.84816	0.692
carp-female_000000006_03721474_03728658	404	Zgc:55813	slc3a2b	86.014	_SFFK(ac)TVSEK_	0.26123	0.547
carp-female_000000006_03721474_03728658	436	Zgc:55813	slc3a2b	82.452	_K(ac)WDQNER_	-0.40456	0.615
carp-female_000000006_03721474_03728658	533	Zgc:55813	slc3a2b	246.95	_EAFSLFDK(ac)DGDGTITTK_	0.23335	0.981
carp-female_000000006_05903309_05926132	492	Retinoblastoma 1	rb1	210.34	_GLATISK(ac)DVGTLAAK_	-0.48534	1.061
carp-female_000000006_07757777_07795187	109	Nicotinamide nucleotide transhydrogenase	nnt	75.911	_FSDDMYTK(ac)AGATIK_	0.040423	0.608
carp-female_000000006_07757777_07795187	118	Nicotinamide nucleotide transhydrogenase	nnt	145.43	_DVK(ac)DVFSSDVLLK_	0.01	1.01
carp-female_000000006_07757777_07795187	431	Nicotinamide nucleotide transhydrogenase	nnt	56.548	_GSVVMK(ac)DGK_	0.54885	0.744
carp-female_000000006_07879567_07902271	812	LOC794796 protein	rai14	53.756	_TLLIEK(ac)YK_	-0.49949	1.331
carp-female_000000006_08153453_08156753	54	60S ribosomal protein L17	RL17	103.91	_DVMVK(ac)HQCVPFR_	0.066238	1.389
carp-female_000000006_09004949_09014310	361	Gsna protein (Fragment)	gsna	95.502	_TADEFIK(ac)K_	-0.26638	3.048

carp-female_000000006_09282220_09315540	226	unknown	unknown	69.639	_VDQSILTGESVSVIK(ac)HTDPVPDPR_	-1.1021	0.845
carp-female_000000006_09282220_09315540	568	unknown	unknown	47.361	_K(ac)EFTLEFSR_	0.013697	0.532
carp-female_000000006_09282220_09315540	600	unknown	unknown	78.401	_MFVK(ac)GAPEGVIDR_	0.57788	0.285
carp-female_000000006_09282220_09315540	1079	unknown	unknown	58.815	_NYLDK(ac)PK_	0.32788	0.808
carp-female_000000006_09326410_09330229	68	Actin related protein 2/3 complex, subunit 3	arpc3	56.295	_ANVFFK(ac)NYEIK_	-2.2671	
carp-female_000000006_09326410_09330229	73	Actin related protein 2/3 complex, subunit 3	arpc3	76.332	_NYEIK(ac)NEADR_	0.28079	
carp-female_000000006_10137964_10143809	122	Isocitrate dehydrogenase [NAD] subunit beta, mitochondrial'	IDH3B	97.502	_IHTPMEYK(ac)GELASYEMR_	0.2062	0.7
carp-female_000000006_10137964_10143809	218	Isocitrate dehydrogenase [NAD] subunit beta, mitochondrial'	IDH3B	53.567	_VTAVHK(ac)ANIMK_	0.94736	0.935
carp-female_000000006_10152518_10154866	242	Glutathione S-transferase (Fragment)	gstT	77.058	_MEPLK(ac)PK_	0.025169	0.5
carp-female_000000006_11704767_11714559	96	Zgc:171284 protein (Fragment)	dync2i1	80.229	_VEQK(ac)YNK_	0.19499	0.28
carp-female_000000006_11704767_11714559	107	Zgc:171284 protein (Fragment)	dync2i1	80.462	_QPFFQK(ac)R_	-0.3215	1.028
carp-female_000000006_11704767_11714559	178	Zgc:171284 protein (Fragment)	dync2i1	83.229	_VLSK(ac)EFHLNESGDPSSK_	0.49181	1.033
carp-female_000000006_11704767_11714559	196	Zgc:171284 protein (Fragment)	dync2i1	66.073	_STEIK(ac)WK_	1.3528	1.124
carp-female_000000006_12348300_12348961	34	Glrx protein	glrx	63.565	_DVLSK(ac)YR_	1.2922	0.03

carp-female_000000006_12808989_12841786	452	unknown	unknown	51.864	_QK(ac)YDYFR_	0.1961	0.288
carp-female_000000008_02003944_02085183	127	Chromosome undetermined SCAF14764, whole genome shotgun sequence. (Fragment)	GSTENG00025154001	54.343	_GVNLADGK(ac)WHR_	0.31313	0.334
carp-female_000000009_00179808_00221387	189	unknown	unknown	66.215	_EFNTFHK(ac)VLSER_	0.77572	0.54
carp-female_000000009_00179808_00221387	233	unknown	unknown	125.97	_STEYK(ac)AVDDTQVK_	0.2039	0.475
carp-female_000000009_00179808_00221387	941	unknown	unknown	88.338	_DK(ac)HSVLQLAQR_	0.49279	0.602
carp-female_000000009_00541592_00545933	156	Protein CMSS1	cmss1	63.673	_EVCPK(ac)WAK_	0.92313	1.188
carp-female_000000009_01981245_01988092	237	60 kDa heat shock protein	hsp60	105.28	_TLHDELEIIEGMK(ac)FDR_	-0.64667	0.937
carp-female_000000009_01981245_01988092	378	60 kDa heat shock protein	hsp60	163.32	_DDTMLLK(ac)GR_	-0.3252	1.096
carp-female_000000009_01990700_01991267	63	Heat shock 10 protein 1 (Chaperonin 10)	hspe1	63.091	_VTPVCVK(ac)VGDK_	-0.53786	1
carp-female_000000009_02228671_02232977	249	Dnajb11 protein	dnajb11	88.392	_VLK(ac)HPVFER_	-1.2804	0.969
carp-female_000000009_02233367_02235148	202	Rab-like protein 3	rabl3	58.699	_FFDK(ac)VIEK_	0.70497	0.516
carp-female_000000009_02591882_02593586	46	60S ribosomal protein L8	rpl8	133.16	_GIVK(ac)DIIHDPGR_	0.18438	1.097
carp-female_000000009_03591700_03598877	105	Solute carrier family 25 (Mitochondrial carrier adenine nucleotide translocator), member 6	slc25a6	181.72	_QVFLGGVDK(ac)HTQFWR_	-0.18573	0.937

carp-female_000000009_03633868_03640910	461	Cell division cycle 16	cdc16	42.976	_K(ac)YEQALEYHR_	0.62827	1.279
carp-female_000000009_12715240_12852745	6889	Titin (Fragment)	UY3_16565	56.404	_GIIPK(ac)DEAK(ac)K_	0.31661	0.96
carp-female_000000009_12715240_12852745	6893	Titin (Fragment)	UY3_16565	56.404	_GIIPK(ac)DEAK(ac)K_	0.31661	0.96
carp-female_000000009_13549003_13580198	199	unknown	unknown	46.844	_YSPDLK(ac)HVHR_	1.1824	0.908
carp-female_000000009_13884165_13939556	166	Nck-associated protein 1	nckap1	83.758	_AKPSYLIDK(ac)NLESAVK_	0.78682	1.338
carp-female_000000009_13884165_13939556	1213	Nck-associated protein 1	nckap1	97.767	_TSFDK(ac)PDHMAALFK_	-1.014	1.13
carp-female_000000010_00924389_00928340	42	DnaJ (Hsp40) homolog, subfamily C, member 5aa	dnajc5aa	59.163	_LALK(ac)YHPDKNPDNPEAADK_	-0.019358	0.847
carp-female_000000010_01239096_01245966	532	Fance protein	fance	142.39	_AAELPHMDIEALK(ac)K_	0.5483	0.994
carp-female_000000010_01239096_01245966	547	Fance protein	fance	143.93	_K(ac)YDAFLASESLIK_	0.28589	1.235
carp-female_000000010_01645158_01697110	631	Succinyl-CoA:3-ketoacid-coenzyme A transferase (Fragment)	unknown	74.841	_AVFDVDK(ac)DK_	-0.044785	0.899
carp-female_000000010_01970506_01976694	278	U5 small nuclear ribonucleoprotein 200 kDa helicase	unknown	51.567	_TIHK(ac)YVHQFPK_	1.6736	0.858
carp-female_000000010_02218611_02222195	433	Cpt2 protein	cpt2	67.385	_LTIDAMEFK(ac)K_	-0.68431	0.818
carp-female_000000010_02261725_02262989	252	Zgc:112962	zgc:112962	89.266	_YCDHENAAYK(ac)K_	0.18785	0.994
carp-female_000000010_02669932_02681563	359	Zgc:136639	zgc:136639	91.549	_GK(ac)SETQEVK_	0.028107	1.406

carp-female_000000010_03033615_03059357	1087	Notch homolog 2 (Fragment)	notch2	113.4	_GVTVDMVCK(ac)HAGTCK_	-0.31804	0.904
carp-female_000000010_03033615_03059357	1474	Notch homolog 2 (Fragment)	notch2	93.345	_TSTNTCK(ac)YDK_	-0.45796	0.789
carp-female_000000010_03532494_03537374	305	Coproporphyrinogen oxidase	cpox	46.844	_HHPK(ac)YYPDFK_	1.1549	0.759
carp-female_000000010_03532494_03537374	311	Coproporphyrinogen oxidase	cpox	47.082	_YYPDFK(ac)K_	0.69504	0.728
carp-female_000000010_04374856_04376532	159	Centromere protein h	cenph	108.7	_AEAVLQK(ac)YQK_	-0.11923	4.925
carp-female_000000010_04614357_04631136	830	DEP domain containing 1a	depdc1a	73.887	_LEHPAGGYK(ac)K_	-0.14724	0.81
carp-female_000000010_04640858_04683752	439	Oxysterol-binding protein	osbpl9	67.234	_TSAVTHK(ac)DSTVLK_	0.472	1.329
carp-female_000000010_04686730_04692395	160	Calreticulin, like 2	calrl2	68.847	_NHLINK(ac)DIR_	-1.7993	0.773
carp-female_000000010_04686730_04692395	287	Calreticulin, like 2	calrl2	86.879	_QIDNPAYK(ac)GK_	0.20695	0.614
carp-female_000000010_04686730_04692395	289	Calreticulin, like 2	calrl2	104.18	_GK(ac)WVHPEIDNPEYTADNEIYK_	0.074588	
carp-female_000000010_07320443_07334877	251	ATPase, Ca++ transporting, cardiac muscle, slow twitch 2a	atp2a2a	79.492	_MFIIDK(ac)AEGEK_	-1.0366	0.525
carp-female_000000010_08694007_08717153	72	Novel protein similar to vertebrate caldesmon 1 (CALD1)	bcap31	61.962	_K(ac)YSVSEK_	0.43784	0.709
carp-female_000000010_08694007_08717153	94	Novel protein similar to vertebrate caldesmon 1 (CALD1)	bcap31	71.376	_VDLSNNPVAIEHIHMK(ac)LFR_	-0.79632	0.643
carp-female_000000010_08694007_08717153	148	Novel protein similar to vertebrate caldesmon 1 (CALD1)	bcap31	111.46	_K(ac)YMEENEK_	-0.55914	0.601

carp-female_000000010_09130092_09150003	692	Zgc:172102 protein	abcd1	53.237	_FEK(ac)LDASTR_	0.75968	0.73
carp-female_000000010_09607487_09613991	265	Zgc:153440	zgc:153440	60.301	_EHQVK(ac)YAQTSR_	-1.2476	0.507
carp-female_000000010_11271806_11312993	689	Novel protein similar to human general control of amino-acid synthesis 1-like 1 (Yeast) (GCN1) (Fragment)	gcn1l1	93.243	_MNPAEFIDK(ac)HLEK_	0.31974	0.824
carp-female_000000010_11911112_11920158	67	Zgc:56036	acaa2	149.04	_TPFGTYGGVLK(ac)DHSATDLAEHAAK_	-0.23395	0.899
carp-female_000000010_11921730_11928107	120	60S ribosomal protein L6 (Fragment)	unknown	48.998	_TLTDAYFK(ac)K_	-0.43396	1.237
carp-female_000000010_11921730_11928107	141	60S ribosomal protein L6 (Fragment)	unknown	126.71	_EK(ac)YQLTEQR_	-0.27446	1.641
carp-female_000000010_12052231_12055493	22	Voltage-dependent anion channel 3	vdac3	152.7	_AAGNLEVK(ac)YK_	-0.28807	1.303
carp-female_000000010_12187469_12200431	115	Citrate transporter (Precursor)	ctp	54.486	_MQGLEAHK(ac)YK_	0.17763	0.971
carp-female_000000012_02549682_02550094	76	Aspartate aminotransferase	got1	78.342	_VLSQMEK(ac)IVR_	-0.19061	0.408
carp-female_000000012_05177587_05180517	22	Splicing factor, arginine/serine-rich 5	srsf5a	91.853	_DVEK(ac)FFK_	-0.70739	0.898
carp-female_000000012_05262254_05301347	478	Alpha-actinin-1	GW7_03701	92.051	_LDHLAEK(ac)FR_	0.94732	0.375
carp-female_000000012_05262254_05301347	762	Alpha-actinin-1	GW7_03701	69.812	_SIVNYK(ac)PK_	-0.018498	0.845
carp-female_000000012_07092852_07097731	66	Ephx1 protein (Fragment)	ephx1l	185.67	_FVVK(ac)TSVEEIEDLHR_	-0.63226	0.945
carp-female_000000012_07092852_07097731	383	Ephx1 protein (Fragment)	ephx1l	77.058	_FYK(ac)ENLK_	-0.36141	0.88

carp-female_000000012_07429147_07434790	472	Golgin subfamily A member 5	golga5	91.095	_QELQDYK(ac)NK_	0.4496	
carp-female_000000012_07441851_07459661	61	Chromosome 10 SCAF14487, whole genome shotgun sequence. (Fragment)	GSTENG00013722001	41.695	_TLLQQK(ac)EVEISHLK_	-4.3135	
carp-female_000000012_08629488_08631884	106	Phosphoglycerate mutase 1a	pgam1a	101.2	_AETAAK(ac)HGEAQVK_	-0.57182	1.081
carp-female_000000012_09358336_09370502	370	Pyroglutamylated RFamide peptide receptor	QRFPR	99.815	_ATVPK(ac)TEIR_	0.29996	1.474
carp-female_000000012_09894361_09922003	281	unknown	unknown	82.01	_K(ac)WLLLSDPDDSISGAR_	2.3019	0.193
carp-female_000000012_09894361_09922003	520	unknown	unknown	212.32	_KVEDISNDDILVAQK(ac)YQR_	-0.43115	1.816
carp-female_000000012_09894361_09922003	762	unknown	unknown	126.02	_VPANQVLYSTHSDQAIGK(ac)YCGR_	-0.63416	1.082
carp-female_000000012_09894361_09922003	838	unknown	unknown	85.963	_HK(ac)FSDVTGK_	0.3706	1.723
carp-female_000000012_09894361_09922003	1075	unknown	unknown	124.67	_FDK(ac)SFIYHLR_	-1.274	0.958
carp-female_000000012_09894361_09922003	1392	unknown	unknown	150.39	_FYASINEHEK(ac)CGPYLQK_	-0.70819	1.038
carp-female_000000012_09894361_09922003	1762	unknown	unknown	132.5	_EHFWSLDK(ac)TEFR_	-0.12383	0.857
carp-female_000000012_09894361_09922003	1828	unknown	unknown	68.856	_NLAPTSLFSQK(ac)SVR_	-0.34422	0.401
carp-female_000000012_10993043_10996095	23	unknown	unknown	108.63	_AEALVSK(ac)HMAEMAQR_	0.056833	0.72
carp-female_000000012_12087234_12088283	237	Calcium homeostasis modulator 2	calhm2	99.055	_TAEVHAK(ac)YHAAECVK_	0.090556	1.077

carp-female_000000012_12138610_12140673	201	Zgc:92254	gsto1	119.54	_K(ac)WTEHMLEDPTVK_	0.57341	3.856
carp-female_000000012_12505469_12509093	222	Erlin-1	erlin1	98.062	_MAQVAEIHFQQK(ac)VMEK_	0.46616	1.003
carp-female_000000012_12592469_12594321	186	Echs1 protein (Fragment)	echs1	52.424	_AVGK(ac)SLAMEMVLTGDR_	0.041575	
carp-female_000000012_12832011_12865894	29	Polypeptide N-acetylgalactosaminyltransferase 2	GALT2	67.385	_NK(ac)FNQVESDK_	-0.63035	0.75
carp-female_000000012_13404454_13437477	2143	Putative hexokinase HKDC1	Hkdc1	180.85	_GIFETK(ac)FLSQIESDR_	-0.39133	0.288
carp-female_000000012_13445338_13452629	148	Hexokinase 1	hk1	139.86	_ASGVEGMDVVK(ac)LLNK_	-0.30385	0.463
carp-female_000000012_13445338_13452629	298	Hexokinase 1	hk1	60.157	_IETK(ac)HVSAIEK_	0.23147	1.626
carp-female_000000012_13445338_13452629	379	Hexokinase 1	hk1	104.84	_TTVGIDGSLYK(ac)MHPQYSR_	-0.13341	1.16
carp-female_000000012_13445338_13452629	449	Hexokinase 1	hk1	58.699	_DQLLEVK(ac)K_	-1.2166	0.408
carp-female_000000012_13619458_13633023	70	Glutamate dehydrogenase	glud1a	119.45	_GASIVEDK(ac)LVHDLK_	0.5223	0.884
carp-female_000000012_13619458_13633023	76	Glutamate dehydrogenase	glud1a	105.52	_LVHDLK(ac)TR_	0.88295	0.792
carp-female_000000012_13619458_13633023	177	Glutamate dehydrogenase	glud1a	118.24	_INPK(ac)NYSDTELEK_	0.66575	3.188
carp-female_000000012_13619458_13633023	443	Glutamate dehydrogenase	glud1a	86.794	_LTFK(ac)YER_	0.3791	1.249
carp-female_000000012_13619458_13633023	466	Glutamate dehydrogenase	glud1a	90.718	_FGK(ac)HGGAIPIVPTSEFQDR_	-0.5366	0.453

carp-female_000000012_17780876_17799709	143	LETM1 and EF-hand domain-containing protein 1, mitochondrial	letm1	66.989	_VVDEVK(ac)HYYHGFR_	0.52485	0.662
carp-female_000000012_18748607_18750946	236	Novel protein similar to vertebrate mitochondrial ribosomal protein S26 (MRPS26)	mrps26	95.138	_NYNFAIDK(ac)EGR_	-0.23304	0.522
carp-female_000000012_19046728_19054341	72	Zgc:158660	sfxn3	212.9	_AK(ac)YIYDSAFHPDTGEK_	-0.10544	0.952
carp-female_000000012_19046728_19054341	183	Zgc:158660	sfxn3	99.055	_ELK(ac)FGIPITDAEGK_	1.3505	0.761
carp-female_000000012_19522328_19527955	20	Mitochondrial voltage-dependent anino channel protein 2	VDAC2	88.101	_DIFNK(ac)GYGFGMVK_	4.2402	0.085
carp-female_000000012_19522328_19527955	42	Mitochondrial voltage-dependent anino channel protein 2	VDAC2	170.61	_SASGVEFK(ac)TSGSSNTDTSK_	-1.2513	0.908
carp-female_000000012_19522328_19527955	61	Mitochondrial voltage-dependent anino channel protein 2	VDAC2	110.39	_VVGSLETK(ac)YK_	0.37866	0.952
carp-female_000000012_19522328_19527955	224	Mitochondrial voltage-dependent anino channel protein 2	VDAC2	105.03	_FGIAAK(ac)YQLDK_	-0.26685	0.782
carp-female_000000012_20234722_20248949	272	Annexin	anxa11a	62.088	_VPLLVSYK(ac)TAYGK_	0.1345	0.947
carp-female_000000012_20234722_20248949	284	Annexin	anxa11a	68.972	_DLK(ac)SELSGNFEK_	-0.25195	1.311
carp-female_000000012_20234722_20248949	311	Annexin	anxa11a	85.28	_TLAQYDAYELK(ac)EAIK_	1.5134	
carp-female_000000012_20234722_20248949	344	Annexin	anxa11a	102.87	_EINQLFK(ac)AENK_	-0.32685	0.927
carp-female_000000012_20234722_20248949	546	Annexin	anxa11a	102.98	_NYGK(ac)SLYTAISGDTSGDYK_	-0.49856	0.949
carp-female_000000012_20234722_20248949	561	Annexin	anxa11a	249.6	_SLYTAISGDTSGDYK(ac)K_	1.0357	0.341

carp-female_000000012_20754285_20759850	138	Apoptosis-inducing factor-like mitochondrion-associated inducer of death	AMID	120.4	_HNCVDTYQSAIQK(ac)YDDFVK_	-0.76516	0.726
carp-female_000000012_21187697_21196881	413	Atl2 protein (Fragment)	atl2	44.395	_YHEEFK(ac)K_	0.45114	0.162
carp-female_000000012_21483320_21497939	358	Calpain 2a	unknown	64.827	_HWSTCK(ac)FDGTWR_	0.32691	1.536
carp-female_000000012_21765410_21774464	446	Eukaryotic translation initiation factor 3 subunit L	eif3l	64.841	_IQLLVFK(ac)HK_	0.11726	0.692
carp-female_000000012_21765410_21774464	501	Eukaryotic translation initiation factor 3 subunit L	eif3l	92.943	_QIHK(ac)FEELNR_	1.1176	3.005
carp-female_000000012_22587640_22593945	64	Khdrbs1 protein	khdrbs1a	142.57	_KESETYLDLFTAK(ac)NVR_	0.056907	1.007
carp-female_000000012_22806547_22808313	42	Microsomal glutathione S-transferase 3	unknown	113.24	_YGIK(ac)YPTMYSDK_	-0.22758	0.708
carp-female_000000012_23159794_23216057	413	Leucine-rich PPR-motif containing	LRPPRC	96.745	_HCVNMDK(ac)SVEK_	0.30281	0.98
carp-female_000000012_23159794_23216057	686	Leucine-rich PPR-motif containing	LRPPRC	102.4	_TLAELK(ac)AEGK_	0.29664	4.262
carp-female_000000012_23159794_23216057	764	Leucine-rich PPR-motif containing	LRPPRC	110.12	_KDSEVALDAQK(ac)YVALVR_	0.76161	0.833
carp-female_000000012_23159794_23216057	1106	Leucine-rich PPR-motif containing	LRPPRC	145.46	_EATVEDYK(ac)LK_	0.55829	1.089
carp-female_000000012_23650982_23653947	86	Prdx3 protein	prdx3	118.28	_EISLEDFK(ac)GK_	-0.63591	0.265
carp-female_000000012_23650982_23653947	248	Prdx3 protein	prdx3	46.426	_EYFEK(ac)VN_	0.65406	1.026
carp-female_000000012_23665403_23670928	45	Eukaryotic translation initiation factor 3 subunit A	eif3a	88.075	_TWQK(ac)IHEPIMLK_	-0.16069	1.112

carp-female_000000012_23665403_23670928	351	Eukaryotic translation initiation factor 3 subunit A	eif3a	95.264	_LLDMDGIIVEK(ac)HR_	-0.42625	1.598
carp-female_000000013_00508109_00511120	135	Signal peptidase complex catalytic subunit SEC11A	SC11A	60.102	_QGQHWLEK(ac)K_	0.13916	0.482
carp-female_000000013_00862608_00869073	208	Isocitrate dehydrogenase [NADP]	idh2	101.54	_VEEFNLK(ac)K_	0.47676	1.833
carp-female_000000013_00862608_00869073	234	Isocitrate dehydrogenase [NADP]	idh2	106.18	_EPIICK(ac)NIPR_	-0.68962	1.086
carp-female_000000013_00862608_00869073	259	Isocitrate dehydrogenase [NADP]	idh2	94.281	_HAHGDQYK(ac)ATDFVVSQPGK_	-0.84497	0.976
carp-female_000000013_00862608_00869073	322	Isocitrate dehydrogenase [NADP]	idh2	57.174	_K(ac)WPLYMSTK_	-0.49556	0.978
carp-female_000000013_00862608_00869073	354	Isocitrate dehydrogenase [NADP]	idh2	71.614	_NYK(ac)PEFDK_	0.63377	10.514
carp-female_000000013_00862608_00869073	359	Isocitrate dehydrogenase [NADP]	idh2	75.739	_NYKPEFDK(ac)LK_	0.082858	3.714
carp-female_000000013_00862608_00869073	361	Isocitrate dehydrogenase [NADP]	idh2	86.67	_LK(ac)IWYEHR_	0.84256	0.93
carp-female_000000013_00870861_00871425	33	Isocitrate dehydrogenase [NADP]	unknown	108.71	_LDGNPDLIK(ac)FSQTLER_	0.058125	1.929
carp-female_000000013_02666598_02669821	23	Cleavage and polyadenylation specificity factor subunit 5	CPSF5	123.29	_GVNQFGNK(ac)YISQPAK_	0.2102	1.072
carp-female_000000013_02912132_02916617	634	CCCTC-binding factor	ctcf	119.54	_THTGEK(ac)PYACNQCEK_	0.0063928	1.112
carp-female_000000013_03897674_03902314	118	Acylglycerol kinase, mitochondrial	agk	77.597	_IVK(ac)TDYEGQAK_	0.85008	
carp-female_000000013_04557732_04560627	104	Ribosomal protein L4	rpl4	92.732	_MFAPTK(ac)TWR_	0.25879	1.683

carp-female_000000013_04557732_04560627	160	Ribosomal protein L4	rpl4	75.064	_IEEIPEVPVVVDDKVEGYK(ac)K_	-0.19662	1.386
carp-female_000000013_04557732_04560627	170	Ribosomal protein L4	rpl4	80.438	_EAVLLLK(ac)K_	0.64926	1.586
carp-female_000000013_04557732_04560627	179	Ribosomal protein L4	rpl4	65.252	_AWNDIK(ac)K_	0.36757	2.768
carp-female_000000013_04557732_04560627	237	Ribosomal protein L4	rpl4	54.729	_LDLLK(ac)LAPGGHVGR_	-0.31435	1.324
carp-female_000000013_04557732_04560627	292	Ribosomal protein L4	rpl4	77.662	_IIK(ac)SEEVQK_	0.30731	0.789
carp-female_000000013_04869003_04877964	486	Aars protein	aars	149.23	_GVAATDDSPK(ac)YK_	0.44172	
carp-female_000000013_04916607_04940299	101	Splicing factor 3B subunit 3	sf3b3	67.102	_NMFEK(ac)IHQETFGK_	0.087846	0.943
carp-female_000000013_04916607_04940299	109	Splicing factor 3B subunit 3	sf3b3	45.28	_IHQETFGK(ac)SGCR_	-0.67368	0.851
carp-female_000000013_08098898_08099508	91	Cytochrome b-c1 complex subunit Rieske, mitochondrial	UCRI	101.3	_LSDIPEGK(ac)NMTFK_	0.55999	0.26
carp-female_000000013_11614279_11620769	364	U3 small nucleolar RNA-associated protein 15 homolog	utp15	76.064	_LHLQK(ac)YDK_	1.5023	1.089
carp-female_000000014_00080838_00088866	38	Mitochondrial voltage-dependent anino channel protein 1	VDAC1	96.171	_VAGTLETK(ac)YK_	0.3971	2.042
carp-female_000000014_00080838_00088866	40	Mitochondrial voltage-dependent anino channel protein 1	VDAC1	150.34	_YK(ac)WAEHGLTFTEK_	0.38363	1.111
carp-female_000000015_00790715_00793401	187	COMM domain containing 2	commd2	63.401	_ALAELK(ac)SNHCR_	1.0329	0.997
carp-female_000000015_02490998_02495641	93	Zgc:152810	ncl	72.2	_SAISK(ac)FFSK_	2.2976	1.569

carp-female_000000015_02490998_02495641	97	Zgc:152810	ncl	153.09	_FFSK(ac)EGLEIQDVR_	0.75925	0.728
carp-female_000000015_02490998_02495641	112	Zgc:152810	ncl	95.067	_K(ac)FGYVDFSSEEELQK_	-0.33696	0.999
carp-female_000000015_02490998_02495641	288	Zgc:152810	ncl	142.39	_AK(ac)GFAFLEFESMEDAK_	-0.52551	1.865
carp-female_000000015_02490998_02495641	345	Zgc:152810	ncl	151.41	_TLFVK(ac)GLSEETTDQTLK_	-0.3624	1.192
carp-female_000000015_02490998_02495641	414	Zgc:152810	ncl	76.943	_VTLDYAK(ac)PK_	0.080453	1.095
carp-female_000000015_02889661_02904599	215	Psmd1 protein (Fragment)	Psmd1	70.089	_VINDK(ac)HDDVMAK_	-0.28378	0.09
carp-female_000000015_03373445_03409681	553	Putative phospholipid-transporting ATPase IF (Fragment)	Anapl_03201	55.04	_VHVDEFALK(ac)GLR_	1.6341	0.564
carp-female_000000015_05170340_05172275	130	Zgc:153327	manf	117.79	_DSQICELK(ac)YDK_	-0.45424	
carp-female_000000015_06326563_06350822	15	Smc3 protein	smc3	167.32	_VIGAK(ac)K(ac)DQYFLDK_	-0.10605	0.72
carp-female_000000015_06326563_06350822	16	Smc3 protein	smc3	167.32	_VIGAK(ac)K(ac)DQYFLDK_	-0.10605	0.72
carp-female_000000015_06326563_06350822	50	Smc3 protein	smc3	74.392	_SNPYYIVK(ac)QGK_	-2.4555	0.684
carp-female_000000015_07985112_08038559	230	Aryl hydrocarbon receptor 2	AhR2	53.756	_LK(ac)YLHGQNK_	-0.17181	1.301
carp-female_000000015_07985112_08038559	276	Aryl hydrocarbon receptor 2	AhR2	80.755	_TLLFQTK(ac)HK_	0.24795	1.366
carp-female_000000016_01122656_01129008	151	Source of immunodominant MHC-associated peptides	SIMP	128.88	_NQGNLYDK(ac)AGK_	-1.838	0.836

carp-female_000000016_01122656_01129008	422	Source of immunodominant MHC-associated peptides	SIMP	74.92	_QALDHK(ac)LR_	-0.32113	1.992
carp-female_000000016_01509959_01560806	149	Eukaryotic translation initiation factor 3 subunit E-A	eif3ea	87.624	_MLFDYLADK(ac)HGFR_	-0.38502	0.935
carp-female_000000016_02568824_02575674	259	2,4-dienoyl-CoA reductase, mitochondrial	DECR	72.478	_FEK(ac)AMFER_	-2.2613	0.935
carp-female_000000016_02817855_02829699	830	LOC570454 protein (Fragment)	LOC570454	56.632	_K(ac)YFLHSER_	0.041809	1.999
carp-female_000000016_03050072_03055313	450	CTP synthase	ctps1b	72.315	_FEVNPELK(ac)HHFEDR_	0.058152	1.445
carp-female_000000016_04193887_04198494	97	Tubulin, beta 5	tubb5	101.9	_ISVYYNEATGGK(ac)YVPR_	-1.2716	0.559
carp-female_000000016_05192890_05204267	89	Triosephosphate isomerase B	tpi1b	78.69	_DCGVK(ac)WVILGHSER_	0.23026	0.472
carp-female_000000016_08752386_08753821	18	60S ribosomal protein L18	rpl18	62.338	_EPK(ac)SQDIYLR_	0.25276	0.935
carp-female_000000016_09240403_09243601	110	Chromosome 8 SCAF15044, whole genome shotgun sequence	GSTENG00033986001	73.834	_SIK(ac)YATGGIHLSK_	-0.85081	0.23
carp-female_000000016_10760640_10783664	589	Anoctamin	ano10a	55.755	_LDKLEFDSLEALK(ac)K_	0.53763	1.69
carp-female_000000017_00033075_00042320	115	Transaldolase	taldo1	47.606	_LSFDK(ac)DAMVSR_	-0.49462	0.938
carp-female_000000017_00033075_00042320	279	Transaldolase	taldo1	58.981	_IYNYYK(ac)K_	0.58162	1.06
carp-female_000000018_00029420_00038887	94	Phosphoenolpyruvate carboxylase	unknown	109.66	_TVIVTK(ac)NQR_	0.49882	0.964
carp-female_000000018_00029420_00038887	122	Phosphoenolpyruvate carboxylase	unknown	119.46	_SQLGSWMSEADFQK(ac)AR_	0.73308	1.068

carp-female_000000018_00029420_00038887	315	Phosphoenolpyruvate carboxylase	unknown	134.34	_VECVGDDIAWMK(ac)FDSQGK_	1.0189	0.961
carp-female_000000018_00029420_00038887	387	Phosphoenolpyruvate carboxylase	unknown	73.273	_LTDWHGK(ac)SWK_	2.2114	0.922
carp-female_000000018_00029420_00038887	390	Phosphoenolpyruvate carboxylase	unknown	149.86	_SWK(ac)YGDSTLCAHPNSR_	-0.75741	0.91
carp-female_000000018_01815173_01819759	153	TIM21-like protein, mitochondrial	TI21L	70.089	_ENPETGK(ac)YEFR_	-0.9667	0.957
carp-female_000000018_02072273_02080049	275	Chaperonin containing TCP1, subunit 5 (Epsilon)	cct5	111.31	_LDVTSVEDYK(ac)ALQK_	0.1864	1.068
carp-female_000000018_02072273_02080049	284	Chaperonin containing TCP1, subunit 5 (Epsilon)	cct5	83.456	_DK(ac)FAEMIR_	0.23369	0.991
carp-female_000000018_02072273_02080049	529	Chaperonin containing TCP1, subunit 5 (Epsilon)	cct5	47.228	_MILK(ac)IDDIR_	0.88245	2.433
carp-female_000000018_02338151_02342822	435	Pdia4 protein	pdia4	187.37	_DDYK(ac)FMHTFNNEVAK_	0.31002	0.388
carp-female_000000018_02338151_02342822	462	Pdia4 protein	pdia4	95.662	_ASPGQVVMLHSEK(ac)FR_	-0.51953	0.78
carp-female_000000018_02338151_02342822	466	Pdia4 protein	pdia4	79.036	_SK(ac)YEPASHSLTIK_	0.46703	1.554
carp-female_000000018_02338151_02342822	633	Pdia4 protein	pdia4	134.14	_VVVGK(ac)TFDDIVMDAK_	-1.0219	0.128
carp-female_000000018_02338151_02342822	733	Pdia4 protein	pdia4	61.56	_FVEK(ac)HATK_	0.55691	0.709
carp-female_000000018_04234688_04235225	91	LOC100170534 protein	cstb	52.185	_LELHGIQTSK(ac)AHHDAIEYF_	-1.0869	1.186
carp-female_000000018_04237268_04237554	46	Zgc:56530	zgc:56530	74.611	_SYK(ac)TQVVAGR_	0.3498	0.733

carp-female_000000018_04378035_04382378	56	N-alpha-acetyltransferase 50	naa50	115.91	_FYK(ac)DVLEVGELAK_	0.25046	1.5
carp-female_000000018_04817413_04821724	48	Acyl-CoA thioesterase 9	acot9.1	184.1	_EK(ac)YLNYHNSVR_	0.23001	0.899
carp-female_000000018_05985767_05990055	207	Hgd protein	hgd	183	_TVATGYTIVNK(ac)YQGK_	-0.92229	0.936
carp-female_000000018_05985767_05990055	384	Hgd protein	hgd	86.014	_NYYK(ac)CWEALK_	-1.8967	1.2
carp-female_000000019_00473844_00491139	12	Chromosome undetermined SCAF14629, whole genome shotgun sequence. (Fragment)	GSTENG00019846001	75.819	_VK(ac)WNQSTAAK_	-0.035252	0.862
carp-female_000000019_01740386_01743210	5	ATP synthase subunit gamma	ATPG	76.927	_ATLK(ac)DITLR_	-0.31241	0.899
carp-female_000000019_01740386_01743210	31	ATP synthase subunit gamma	ATPG	101.72	_MVAAAK(ac)YAR_	0.17669	1.03
carp-female_000000019_01740386_01743210	55	ATP synthase subunit gamma	ATPG	112.34	_VYGTGAMALYEK(ac)AEIK_	0.3529	0.873
carp-female_000000019_01740386_01743210	66	ATP synthase subunit gamma	ATPG	98	_NK(ac)HLIIGVSSDR_	-0.27718	0.838
carp-female_000000019_01740386_01743210	91	ATP synthase subunit gamma	ATPG	46.334	_AMK(ac)NEIAK_	-0.78929	1.599
carp-female_000000019_03742708_03772620	2483	Chromosome 19 SCAF14731, whole genome shotgun sequence. (Fragment)	GSTENG00023829001	72.898	_K(ac)HNESLAALEQER_	-1.7628	1.105
carp-female_000000019_03742708_03772620	2966	Chromosome 19 SCAF14731, whole genome shotgun sequence. (Fragment)	GSTENG00023829001	89.484	_MLEQLHLQK(ac)SELDR_	0.40911	0.942
carp-female_000000019_03742708_03772620	3314	Chromosome 19 SCAF14731, whole genome shotgun sequence. (Fragment)	GSTENG00023829001	109.29	_GFGGK(ac)YGVQK_	0.40677	0.839

carp-female_000000019_04220012_04222822	183	Ribosomal protein S16	rps16	179.56	_ALVAYYQK(ac)YVDEASK_	0.026229	1.156
carp-female_000000019_04220012_04222822	194	Ribosomal protein S16	rps16	45.28	_EIK(ac)DILIQYDR_	-0.39776	1.727
carp-female_000000019_05450121_05452246	86	Fibrinogen-like 2	fgl2	121.68	_ELQSLK(ac)ETVNR_	-0.47299	1.092
carp-female_000000020_00631105_00635541	304	Malonyl CoA:ACP acyltransferase (Mitochondrial)	mcat	41.427	_YMHDK(ac)HVR_	0.963	1.125
carp-female_000000020_02113206_02120765	290	L-lactate dehydrogenase B chain	ldhb	105.03	_MVVDSAYEVIK(ac)LK_	0.10825	0.098
carp-female_000000020_02113206_02120765	375	L-lactate dehydrogenase B chain	ldhb	184.76	_SSADTLWGIQK(ac)DLK_	-0.72473	0.907
carp-female_000000020_02386014_02399244	226	Decorin variant 1	DCN	58.885	_EVPANIPK(ac)SLQELR_	0.48176	0.814
carp-female_000000020_02638385_02646586	175	Coatomer subunit gamma-2	copg2	97.635	_MSFDVVK(ac)R_	0.83429	0.068
carp-female_000000020_02638385_02646586	262	Coatomer subunit gamma-2	copg2	66.613	_NK(ac)HEMVVYEAASAIVHMPNCTAR_	-0.62763	1.315
carp-female_000000020_02638385_02646586	471	Coatomer subunit gamma-2	copg2	70.056	_TPTPSK(ac)YIR_	0.66827	1.052
carp-female_000000020_02638385_02646586	572	Coatomer subunit gamma-2	copg2	81.01	_SLHQYTLEPSEK(ac)PFDMK_	0.23858	1.007
carp-female_000000020_02865197_02919405	147	Chchd3 protein	chchd3	86.488	_VTNENYHK(ac)AADEVNAK_	0.55467	
carp-female_000000020_02865197_02919405	155	Chchd3 protein	chchd3	94.363	_AADEVNAK(ac)FK_	-0.47136	0.492
carp-female_000000020_03304491_03309596	80	Ubiquitin-conjugating enzyme E2 H	PAL_GLEAN10019139	44.543	_VDLPDK(ac)YPFK_	0.63502	0.877

carp-female_000000020_03393384_03396967	110	26S protease regulatory subunit 7	PRS7	58.98	_IINADSEDPK(ac)YIINVK_	0.91324	1.468
carp-female_000000020_04220852_04223533	108	Calumenin-A	calua	121.61	_K(ac)YIYDNVER_	0.86098	0.616
carp-female_000000020_04713721_04722425	177	LEM domain containing 3	lemd3	81.904	_GK(ac)SSGLEETER_	0.0020673	0.917
carp-female_000000020_05475873_05481460	48	Cytochrome b5 reductase 3	cyb5r3	113.47	_RPAITLEDPNVK(ac)YPLR_	0.79141	1.165
carp-female_000000020_05475873_05481460	56	Cytochrome b5 reductase 3	cyb5r3	88.075	_LVDK(ac)EIISHDTR_	-0.37141	0.892
carp-female_000000020_05475873_05481460	121	Cytochrome b5 reductase 3	cyb5r3	56.258	_IYYK(ac)NVHPK_	0.76942	0.895
carp-female_000000020_05475873_05481460	126	Cytochrome b5 reductase 3	cyb5r3	55.258	_NVHPK(ac)FPEGGK_	0.98535	
carp-female_000000020_05716873_05721297	97	GDP dissociation inhibitor 2	unknown	47.971	_VIEGSFVYK(ac)K_	-0.52469	0.809
carp-female_000000020_05716873_05721297	254	GDP dissociation inhibitor 2	unknown	118.87	_VVGVK(ac)SEGEIAR_	0.20951	0.792
carp-female_000000020_06590953_06644378	44	Protein Flnc	Flnc	131.09	_DLAEDAPWK(ac)K_	-0.8477	0.679
carp-female_000000020_06590953_06644378	2475	Protein Flnc	Flnc	43.05	_FDDK(ac)HIAGSPFTAK_	0.25806	1.11
carp-female_000000020_06802059_06808618	75	Heat shock protein	Hsp90	106.32	_AEK(ac)HVFQAEVNR_	0.41224	0.311
carp-female_000000020_06802059_06808618	161	Heat shock protein	Hsp90	136.3	_EELVK(ac)NLGTIAK_	0.889	0.406
carp-female_000000020_06802059_06808618	357	Heat shock protein	Hsp90	197.07	_EVEEDEYK(ac)AFYK_	1.2442	1.45

carp-female_000000020_06802059_06808618	456	Heat shock protein	Hsp90	152.7	_ETLQQHK(ac)LLK_	-1.2482	0.316
carp-female_000000020_06802059_06808618	494	Heat shock protein	Hsp90	51.942	_EFGTNIK(ac)LGVIEDHSNR_	-0.17714	0.446
carp-female_000000020_06802059_06808618	629	Heat shock protein	Hsp90	90.906	_ALK(ac)DNIEK_	1.46	0.307
carp-female_000000021_01299101_01305083	101	ARD1 homolog a, N-acetyltransferase	naa10	176.67	_FQISEVEPK(ac)YYADGEDAYAMK_	-0.31108	2.365
carp-female_000000021_01307370_01312008	241	Glucose-6-phosphate 1-dehydrogenase	g6pd	43.592	_VQPNEAIYAK(ac)MMSK_	0.33194	
carp-female_000000021_01307370_01312008	336	Glucose-6-phosphate 1-dehydrogenase	g6pd	94.09	_GPAEADELVQK(ac)VGFR_	-0.7218	0.983
carp-female_000000021_02290326_02297117	108	Elongation factor 1-alpha	eef1a2	121.02	_FEK(ac)EAAEMGK_	0.17145	2.066
carp-female_000000021_03319954_03323293	193	LOC553479 protein (Fragment)	LOC553479	53.756	_VELISLK(ac)K_	0.38577	0.969
carp-female_000000021_03324720_03328120	111	Keratin, type I cytoskeletal 18	krt18	115.12	_FLEQANSK(ac)LELK_	0.54446	0.829
carp-female_000000021_03324720_03328120	240	Keratin, type I cytoskeletal 18	krt18	135.99	_VK(ac)YESELSIR_	-0.77966	1.467
carp-female_000000021_03324720_03328120	331	Keratin, type I cytoskeletal 18	krt18	73.248	_YEK(ac)MALK_	-0.29314	0.148
carp-female_000000021_03324720_03328120	335	Keratin, type I cytoskeletal 18	krt18	130.98	_M(ox)ALK(ac)NQEELK_	0.47977	3.308
carp-female_000000021_03324720_03328120	390	Keratin, type I cytoskeletal 18	krt18	59.227	_NLK(ac)GSLEATLR_	0.31861	0.841
carp-female_000000021_03324720_03328120	443	Keratin, type I cytoskeletal 18	krt18	205.24	_NNIQHQTQEYEALLNIK(ac)MK_	0.33311	0.787

carp-female_000000021_03324720_03328120	463	Keratin, type I cytoskeletal 18	krt18	163.18	_LLDGGDFK(ac)LQDALDEQK_	0.58538	0.949
carp-female_000000021_03382666_03386768	12	Keratin, type II cytoskeletal 8	krt8	196.95	_TSYTVK(ac)SSSSGSVPR_	-0.56442	0.95
carp-female_000000021_03382666_03386768	142	Keratin, type II cytoskeletal 8	krt8	243.9	_M(ox)LETK(ac)WSLLQNQTATR_	0.21771	0.983
carp-female_000000021_03382666_03386768	178	Keratin, type II cytoskeletal 8	krt8	177.1	_QLDSLGNDK(ac)MK_	0.85097	0.703
carp-female_000000021_03382666_03386768	196	Keratin, type II cytoskeletal 8	krt8	202.6	_LEADLHNMQGLVEDFK(ac)NK_	-0.46581	0.991
carp-female_000000021_03382666_03386768	217	Keratin, type II cytoskeletal 8	krt8	189.3	_TECENEFVLIK(ac)K_	0.47817	9.22
carp-female_000000021_03382666_03386768	227	Keratin, type II cytoskeletal 8	krt8	204.82	_KDVDEAYMNK(ac)VELEAK_	0.10664	0.938
carp-female_000000021_03382666_03386768	303	Keratin, type II cytoskeletal 8	krt8	134.13	_AEAEMWYK(ac)SK_	0.64293	0.987
carp-female_000000021_03382666_03386768	305	Keratin, type II cytoskeletal 8	krt8	194.12	_SK(ac)YEEM(ox)QTSATK_	0.0084938	0.8
carp-female_000000021_03382666_03386768	315	Keratin, type II cytoskeletal 8	krt8	352.72	_YEEMQTSATK(ac)YGDDLR_	-0.68968	1.032
carp-female_000000021_03382666_03386768	324	Keratin, type II cytoskeletal 8	krt8	265.72	_STK(ac)TEIADLNR_	0.20885	0.971
carp-female_000000021_03382666_03386768	345	Keratin, type II cytoskeletal 8	krt8	71.176	_LQSEIDAVK(ac)GQR_	-1.4094	1.013
carp-female_000000021_03382666_03386768	507	Keratin, type II cytoskeletal 8	krt8	136.96	_SVVIK(ac)M(ox)IETK_	-0.45521	0.924
carp-female_000000021_03902018_03931315	118	unknown	unknown	43.501	_EAHVPSFEK(ac)YK_	-1.1124	1.681

carp-female_000000021_03902018_03931315	489	unknown	unknown	51.359	_LLMK(ac)YGSEPVQK_	0.43965	0.976
carp-female_000000021_04897640_04911504	157	TM9SF4	tm9sf4	125.84	_DTLK(ac)DIQFEHGYR_	-0.50128	0.956
carp-female_000000021_04897640_04911504	210	TM9SF4	tm9sf4	65.278	_FEVMPK(ac)SVK_	-0.78823	0.799
carp-female_000000021_06941580_06949099	314	T-complex protein 1 subunit alpha	tcp1	91.62	_VCDDELILVK(ac)NTK_	-0.38164	0.346
carp-female_000000024_00161629_00165522	76	Proteasome subunit beta type	PSB3	93.345	_LNLYELK(ac)EGR_	-0.5869	1.064
carp-female_000000024_01882305_01892725	405	Mcm6 protein	mcm6	96.673	_SQFLK(ac)HVEEFSPR_	0.92701	1.399
carp-female_000000024_03134270_03139565	190	Obg-like ATPase 1	ola1	71.159	_IK(ac)SWVVDEK_	-0.19332	0.791
carp-female_000000024_03134270_03139565	209	Obg-like ATPase 1	ola1	85.493	_YYHDWNDK(ac)EIEVLNK_	-0.36494	1.133
carp-female_000000024_03686761_03707792	207	Ribosome biogenesis protein wdr12	wdr12	44.44	_IVTDNLVYCK(ac)TVR_	-1.4018	0.885
carp-female_000000024_03686761_03707792	277	Ribosome biogenesis protein wdr12	wdr12	87.184	_TQLYDYLK(ac)NR_	-0.059998	0.977
carp-female_000000024_03964560_03976364	645	MGC162584 protein	vps16	41.825	_QFCK(ac)HQEQETLK_	0.78562	0.7
carp-female_000000024_04216574_04234623	498	Chromosome 3 SCAF14639, whole genome shotgun sequence	GSTENG00020067001	69.846	_ISTK(ac)IVSQEQR_	1.2052	
carp-female_000000024_04713262_04732736	499	unknown	unknown	140.14	_K(ac)FDQMLAEEK_	-0.046985	1.717
carp-female_000000024_04736967_04751675	52	Tetratricopeptide repeat protein 26	ttc26	62.466	_SDGVYIINLK(ac)K_	1.3028	1.033

carp-female_000000024_06867041_06878399	26	Reticulon	rtn4a	116.98	_ADK(ac)HVNSLQDEAADFSIR_	0.92641	1.052
carp-female_000000024_06867041_06878399	230	Reticulon	rtn4a	74.853	_SEDGHPFK(ac)MYLDK_	-1.0115	0.637
carp-female_000000024_06867041_06878399	235	Reticulon	rtn4a	67.646	_MYLDK(ac)DIAIPTEMVHK_	1.9185	0.489
carp-female_000000024_06867041_06878399	260	Reticulon	rtn4a	86.453	_YSDTALGHINAVVK(ac)ELR_	-0.74925	0.892
carp-female_000000026_00720139_00726461	336	Matrix metalloproteinase 14 (Membrane-inserted) alpha	mmp14a	94.309	_SDGK(ac)FVFFK_	0.25528	0.833
carp-female_000000026_00720139_00726461	344	Matrix metalloproteinase 14 (Membrane-inserted) alpha	mmp14a	110.38	_GDK(ac)YWVFNEAK_	0.75819	0.913
carp-female_000000026_00720139_00726461	437	Matrix metalloproteinase 14 (Membrane-inserted) alpha	mmp14a	149	_GAFMSEDGAHTYFYK(ac)ANK_	0.1088	0.948
carp-female_000000026_02198750_02225249	430	Proline-, glutamic acid- and leucine-rich protein 1 (Fragment)	PELP1	75.018	_QIILTSGTLLK(ac)EDLHK_	0.020391	0.635
carp-female_000000026_02583583_02589420	174	Eukaryotic translation initiation factor 4A, isoform 1A	eif4a1a	57.59	_YLSPK(ac)YIK_	1.0708	3.482
carp-female_000000026_02583583_02589420	306	Eukaryotic translation initiation factor 4A, isoform 1A	eif4a1a	72.928	_DIIMK(ac)EFR_	-2.8517	
carp-female_000000026_02633084_02640164	150	Phospholipid scramblase 1	PLS1	75.109	_SFDMK(ac)IK_	0.34749	0.894
carp-female_000000026_02947832_02950047	99	Chromosome undetermined SCAF7485, whole genome shotgun sequence	RPS13	145.69	_GLAPDLPEDLYHLIK(ac)K_	0.36662	1.184
carp-female_000000026_03554511_03560631	48	R-ras	unknown	111.33	_GSFEEIYK(ac)FQR_	-0.25526	1.148
carp-female_000000026_04367338_04389547	249	Serine/threonine-protein kinase VRK3	VRK3	78.324	_YSGAK(ac)WSEGVR_	0.71282	0.799

carp-female_000000026_04974839_04980270	190	LOC407663 protein (Fragment)	LOC407663	44.44	_VVNVSSLAHEK(ac)GK_	0.78334	6.667
carp-female_000000026_04974839_04980270	259	LOC407663 protein (Fragment)	LOC407663	47.894	_HFLPTLPLWK(ac)R_	1.693	1.527
carp-female_000000026_06844800_06874226	40	CD81 antigen	cd81	43.761	_HDTK(ac)TSSLLDLR_	0.56997	0.846
carp-female_000000026_08501499_08526463	717	unknown	unknown	96.113	_LDEDLHVK(ac)YPR_	0.12105	0.803
carp-female_000000026_10762484_10769015	67	Mitochondrial carrier homolog 2	mtch2	114.89	_TDGK(ac)SGLFK_	0.033436	0.862
carp-female_000000026_10770581_10774331	58	26S protease regulatory subunit 6A	PRS6A	63.091	_VTHELQAMK(ac)DK_	-0.46453	1.139
carp-female_000000026_11488673_11493122	127	GrpE protein homolog	grpel1	119.68	_ATESVPK(ac)TEVSAANPHLK_	0.22591	0.901
carp-female_000000026_13019100_13028307	106	Alanine aminotransferase 2-like	gpt2	220.21	_CLEEGGTK(ac)PFSEVIK_	0.24203	0.542
carp-female_000000026_13033698_13034704	29	DnaJ (Hsp40) homolog, subfamily A, member 2	dnaja2	101.38	_QIVVK(ac)YPAGK_	-0.50705	0.829
carp-female_000000027_01204940_01206121	117	Zgc:171577 protein	rpz5	58.829	_FQDFVNAK(ac)PK_	0.74953	0.536
carp-female_000000027_03524553_03546701	62	Smarcc1 protein (Fragment)	smarcc1a	75.088	_K(ac)YVQTDSPTSK_	-2.1356	
carp-female_000000027_03524553_03546701	909	Smarcc1 protein (Fragment)	smarcc1a	94.45	_QAFHMEQLK(ac)YAEMK_	0.51538	0.615
carp-female_000000027_04777135_04777760	47	S100 calcium binding protein A10b	s100a10b	96.946	_ELSSFLK(ac)SQK_	0.95446	0.785
carp-female_000000027_05461577_05471900	157	Tyrosine 3-monooxygenase/tryptophan 5-monooxygenase activation protein, beta polypeptide like	ywhabl	82.77	_DAFEISK(ac)AEMQPTHPIR_	-1.0572	1.045

carp-female_000000027_05864281_05866629	130	Zgc:136493 protein (Fragment)	im:7137941	42.629	_IVEGHNFSK(ac)FR_	-0.55378	1.958
carp-female_000000027_06832316_06840375	112	Thioredoxin domain containing 4 (Endoplasmic reticulum)	erp44	63.624	_TIIGYFEK(ac)K_	1.127	0.704
carp-female_000000027_06832316_06840375	246	Thioredoxin domain containing 4 (Endoplasmic reticulum)	erp44	95.582	_GSINFLHADCDK(ac)FR_	0.79146	1.774
carp-female_000000027_06832316_06840375	298	Thioredoxin domain containing 4 (Endoplasmic reticulum)	erp44	120.6	_QFVLDLHSGK(ac)LHR_	0.021037	0.753
carp-female_000000027_06951132_06956691	152	Golgi-associated plant pathogenesis-related protein 1	GAPR1	70.47	_LFCEEVLK(ac)THNEYR_	0.0597	0.905
carp-female_000000027_06951132_06956691	190	Golgi-associated plant pathogenesis-related protein 1	GAPR1	83.045	_ILK(ac)HSAESSR_	-0.15426	0.636
carp-female_000000027_06975907_06983141	392	Chromosome 8 SCAF15044, whole genome shotgun sequence. (Fragment)	GSTENG00034057001	85.355	_GEEFYQK(ac)VHK_	0.79871	0.839
carp-female_000000027_07947743_07951397	44	Cathepsin K	unknown	134.49	_GYK(ac)EIPQGNER_	-0.76067	1.113
carp-female_000000027_08422679_08426771	67	Chaperonin containing TCP1, subunit 3 (Gamma)	cct3	84.166	_EIQVQHPAAK(ac)SMIEISR_	-1.6509	1.969
carp-female_000000027_08429132_08434558	347	Zgc:77086	zgc:77086	164.59	_TTAGHK(ac)YSM(ox)QEEFTR_	-0.1357	0.831
carp-female_000000027_08429132_08434558	371	Zgc:77086	zgc:77086	110.88	_FLEDYFAK(ac)R_	-0.86609	0.569
carp-female_000000027_08429132_08434558	427	Zgc:77086	zgc:77086	70.525	_NLEPK(ac)YK_	0.76899	0.063
carp-female_000000027_08483034_08503082	111	Nuclear lamin A	lmna	85.355	_VREDYK(ac)ELK_	-0.3381	0.418
carp-female_000000027_08483034_08503082	198	Nuclear lamin A	lmna	77.776	_IQTLK(ac)EELEFQK_	-1.8948	1.179

carp-female_000000027_08483034_08503082	267	Nuclear lamin A	lmna	87.184	_TYNSK(ac)LENAR_	0.48619	0.538
carp-female_000000027_08483034_08503082	471	Nuclear lamin A	lmna	167.32	_VTVDEVDM(ox)EGK(ac)YVR_	1.202	0.738
carp-female_000000027_08483034_08503082	478	Nuclear lamin A	lmna	168.69	_LCNK(ac)SDQDQTLGHWQVK_	-0.77311	0.459
carp-female_000000027_08483034_08503082	491	Nuclear lamin A	lmna	178.67	_SDQDQTLGHWQVK(ac)R_	-0.1722	0.596
carp-female_000000027_09068632_09069609	84	unknown	unknown	162.31	_VTLEDGTK(ac)WLVHK_	-0.43383	0.199
carp-female_000000027_09147371_09202288	989	Chromosome 8 SCAF14543, whole genome shotgun sequence. (Fragment)	GSTENG00015321001	54.772	_ADVFK(ac)HMPSK_	0.4652	1.004
carp-female_000000027_09210702_09220403	141	Cdc42l protein	cdc42l	99.161	_EK(ac)WVPEISHHCPR_	0.52691	1.096
carp-female_000000027_09210702_09220403	198	Cdc42l protein	cdc42l	182.33	_AVK(ac)YVECSALTQR_	-0.10409	1.055
carp-female_000000027_09294505_09295818	11	40S ribosomal protein s9	RS9	104.41	_SWVCSK(ac)TYVTPR_	0.77117	0.823
carp-female_000000027_09349353_09352981	96	Lysophospholipid acyltransferase 7	mboat7	139.08	_MVSLANEVQSFHLEK(ac)K_	-0.67634	0.315
carp-female_000000027_10437783_10448105	222	Chromosome undetermined SCAF14292, whole genome shotgun sequence	GSTENG00013080001	74.428	_DEPWHK(ac)ECFVCTSCK_	-0.98438	1.138
carp-female_000000027_10437783_10448105	274	Chromosome undetermined SCAF14292, whole genome shotgun sequence	GSTENG00013080001	111.97	_CEACNKPITGFGGGK(ac)YISFEDR_	-0.065968	1.117
carp-female_000000027_10574326_10578596	583	unknown	unknown	54.393	_SK(ac)HQEQHSAPLQIK_	0.79848	1.566

carp-female_000000028_02441408_02445596	11	Ribosomal protein L35a	unknown	127.84	_AIFAGYK(ac)R_	0.22381	1.202
carp-female_000000028_02441408_02445596	41	Ribosomal protein L35a	unknown	87.568	_TEVDFYLGK(ac)R_	-0.63954	16.262
carp-female_000000028_02441408_02445596	91	Ribosomal protein L35a	unknown	72.34	_SNLPAK(ac)AIGHR_	2.2207	1.631
carp-female_000000028_03083682_03096529	317	Zgc:123303	arfgap2	94.767	_LAYK(ac)ELEIDR_	1.1244	0.785
carp-female_000000028_03097428_03106553	106	Chromosome undetermined SCAF14620, whole genome shotgun sequence. (Fragment)	GSTENG00019549001	64.654	_YK(ac)NELEQR_	0.27795	0.731
carp-female_000000028_03194134_03203570	166	N-ethylmaleimide sensitive fusion protein attachment protein alpha	napa	61.344	_YSAK(ac)DYFFK_	0.23332	0.741
carp-female_000000028_03208231_03214842	368	EH-domain containing 2	ehd2	116.78	_MQEQLMAHDFSK(ac)FK_	-0.013703	1.32
carp-female_000000028_09771470_09791854	78	Cox4 neighbor	emc8	48.288	_ENK(ac)YVIAGYYQANER_	0.46664	
carp-female_000000028_09798069_09800552	123	Cytochrome c oxidase subunit IV isoform 1	cox4i1	139.88	_K(ac)YVYGDVPHTFDPEYK_	-0.73581	0.853
carp-female_000000028_09798069_09800552	138	Cytochrome c oxidase subunit IV isoform 1	cox4i1	169.64	_YVYGDVPHTFDPEYK(ac)QK_	0.54319	0.794
carp-female_000000029_02054840_02058175	120	Clusterin	clu	52.167	_TCVK(ac)YYSR_	-1.0544	1.302
carp-female_000000029_02976262_03013586	405	Chromosome 14 SCAF15120, whole genome shotgun sequence. (Fragment)	GSTENG00035449001	79.474	_FTHDPK(ac)YR_	0.48748	0.893
carp-female_000000029_03976118_03980629	80	Sorting nexin	DKEYP-70E6.2-001	49.934	_YK(ac)HFDWLYER_	1.1278	0.568

carp-female_000000029_05421189_05424167	74	Tmed10 protein	tmed10	72.642	_ITDSSGHILYVK(ac)EDATK_	-0.47478	0.703
carp-female_000000029_05421189_05424167	130	Tmed10 protein	tmed10	60.509	_NYEEIAK(ac)VEK_	0.27043	0.495
carp-female_000000029_05421189_05424167	135	Tmed10 protein	tmed10	83.862	_LK(ac)PLEVELR_	-0.82414	0.722
carp-female_000000029_06824397_06831521	379	Lysine-specific demethylase NO66	no66	49.269	_DK(ac)FTAHIQGLIK_	-1.0717	0.613
carp-female_000000029_07365981_07371241	243	Heat shock cognate protein HSP 90-beta-like isoform 3	CB1_001402089	91.752	_APFDLFENK(ac)K_	0.4867	1.77
carp-female_000000029_07365981_07371241	286	Heat shock cognate protein HSP 90-beta-like isoform 3	CB1_001402089	77.062	_EMLQQSK(ac)ILK_	0.10326	1.182
carp-female_000000029_07365981_07371241	446	Heat shock cognate protein HSP 90-beta-like isoform 3	CB1_001402089	114.89	_AK(ac)FENLCK_	0.41852	0.902
carp-female_000000029_08759743_08761002	33	40S ribosomal protein S29	GW7_12197	47.082	_K(ac)YGLNMCR_	-0.83496	0.57
carp-female_000000030_00023913_00029855	234	Basic leucine zipper and W2 domain-containing protein 1-A	bzw1a	162.7	_SCEHFSK(ac)YFTDAGLK_	0.30037	1.666
carp-female_000000030_00023913_00029855	393	Basic leucine zipper and W2 domain-containing protein 1-A	bzw1a	98.156	_GK(ac)SVFLEQMK_	-2.6437	
carp-female_000000030_02911153_02916952	271	5A11/Basigin-2	bsg	101.05	_VSPHVAAYK(ac)HSESANEK_	-2.9324	0.941
carp-female_000000030_03565934_03569916	626	Elongation factor 2	EF2	111.83	_YLADK(ac)YEWEVTEAR_	-0.515	1.115
carp-female_000000030_05772694_05782541	203	Ubiquitin carboxyl-terminal hydrolase L5	uchl5	62.166	_IQK(ac)YSEGEIR_	-2.1896	0.125
carp-female_000000030_05840894_05884329	464	unknown	unknown	106.42	_FLAHSVTAAGDGYK(ac)GK_	-0.50531	0.456

carp-female_000000030_06351767_06357107	116	DnaJ (Hsp40) homolog, subfamily A, member 3B	dnaja3b	54.09	_K(ac)YHPDTNPDDPEAK_	0.81292	1.341
carp-female_000000030_06658256_06687802	1577	unknown	unknown	109.1	_FVYTCNECK(ac)HHVETR_	0.29522	3.174
carp-female_000000030_08101126_08107526	68	Pyruvate dehydrogenase (Lipoamide) beta	pdhb	152.59	_VFLLGEEVAQYDGAYK(ac)VSR_	0.30134	0.607
carp-female_000000030_08543066_08553404	450	Striatin-interacting protein 1 homolog	strip1	81.632	_QHK(ac)YVSIAEVQIAK_	1.2335	1.411
carp-female_000000030_10605608_10626845	105	LAG1 homolog, ceramide synthase 5 (S. cerevisiae)	cers5	54.09	_HLEGLSK(ac)QLDWDVR_	2.3388	0.655
carp-female_000000030_10635543_10640525	173	Keratin type IIs	krt1	96.668	_YEDEINK(ac)R_	-0.59827	1.163
carp-female_000000030_10664189_10683103	1143	Mcm2 protein	mcm2	64.121	_SQFLK(ac)YVEK_	-1.194	10.947
carp-female_000000030_11047852_11057798	783	Cherp protein	cherp	54.776	_DK(ac)WDQYK_	-2.0173	
carp-female_000000032_01179180_01182878	43	Magnesium transporter protein 1	magt1	106.26	_VSQMMEWASK(ac)R_	0.24917	0.95
carp-female_000000032_01218926_01234833	625	Plastin 3 (T isoform)	pls3	181.61	_LDNAK(ac)YAVSMAR_	-0.51057	1.037
carp-female_000000032_01218926_01234833	649	Plastin 3 (T isoform)	pls3	66.989	_VYALPDDLVEVK(ac)PK_	1.2579	0.989
carp-female_000000032_02253454_02272958	96	Heat shock protein 9	hspa9	73.248	_NVPYK(ac)IVR_	0.98506	1.292
carp-female_000000032_02253454_02272958	187	Heat shock protein 9	hspa9	147.25	_VINEPTAAALAYGLDK(ac)TQDK_	1.2096	0.798
carp-female_000000032_02253454_02272958	237	Heat shock protein 9	hspa9	131.82	_STNGDTFLGGEDFDQHLLK(ac)HIVK_	-1.2696	1.163

carp-female_000000032_02253454_02272958	241	Heat shock protein 9	hspa9	81.296	_HIVK(ac)EFK_	-0.031839	0.681
carp-female_000000033_01312689_01320687	57	unknown	unknown	78.69	_ESGQHFAMK(ac)ILDK_	2.529	0.249
carp-female_000000034_00520790_00525323	57	DEAD-box RNA-dependent helicase p68	unknown	88.385	_FEK(ac)NFYQEHHEVSR_	-0.25523	1.123
carp-female_000000034_02010544_02026521	1495	Procollagen type I alpha 1 chain (Fragment)	col1a1a	112.13	_TVIDYK(ac)TTK_	0.23386	1.968
carp-female_000000034_02712912_02755978	915	unknown	unknown	52.255	_SYK(ac)SVDGR_	0.09349	1.64
carp-female_000000034_04019323_04045212	141	Chromosome 3 SCAF14700, whole genome shotgun sequence. (Fragment)	GSTENG00022074001	72.898	_VYDDQDLCAK(ac)SYR_	0.072137	1.702
carp-female_000000034_04019323_04045212	664	Chromosome 3 SCAF14700, whole genome shotgun sequence. (Fragment)	GSTENG00022074001	72.096	_VFHAGALEK(ac)R_	-0.47451	0.96
carp-female_000000034_04019323_04045212	965	Chromosome 3 SCAF14700, whole genome shotgun sequence. (Fragment)	GSTENG00022074001	106.66	_STWETASK(ac)TCLTHK_	0.63986	1.253
carp-female_000000034_04019323_04045212	1063	Chromosome 3 SCAF14700, whole genome shotgun sequence. (Fragment)	GSTENG00022074001	57.792	_CDAEK(ac)HGFICMK_	-2.0073	1.35
carp-female_000000034_04222777_04228601	121	Gcat protein (Fragment)	gcat	55.011	_FICGTQSLHK(ac)NLEEK_	-1.1233	4.268
carp-female_000000034_04222777_04228601	126	Gcat protein (Fragment)	gcat	120.9	_NLEEK(ac)LAQFHER_	-0.80793	0.847
carp-female_000000034_04222777_04228601	185	Gcat protein (Fragment)	gcat	132.97	_YK(ac)HMDLNDLEEK_	0.072896	2.989
carp-female_000000034_04376314_04386958	13	Protein KRI1 homolog	kri1	51.346	_FAEK(ac)YEK_	0.096413	0.749

carp-female_000000034_04997343_04999344	95	Ribosomal protein S2	rps2	44.847	_DEVLK(ac)IMPVQK_	1.1588	1.542
carp-female_000000034_04997343_04999344	280	Ribosomal protein S2	rps2	191.37	_ETVFTK(ac)SPYQEFTDHLAK_	-0.43235	1.482
carp-female_000000034_04997343_04999344	292	Ribosomal protein S2	rps2	81.157	_SPYQEFTDHLAK(ac)THTR_	-0.064246	1.391
carp-female_000000034_05236100_05264059	489	ATP citrate lyase	aclya	110.04	_EFLYK(ac)HICTTAAVQNR_	-0.59163	1.396
carp-female_000000035_00189960_00203394	630	Major vault protein	mvp	89.484	_GAVASVQFDDFHK(ac)NSIR_	-0.2851	0.793
carp-female_000000035_00351582_00363838	135	Lim and sh3 domain protein 1	LASP1	136.66	_TQDQISNIK(ac)YHEDFEK_	-0.51579	
carp-female_000000036_00322865_00441961	354	Chromosome 2 SCAF14781, whole genome shotgun sequence. (Fragment)	GSTENG00026046001	92.19	_ESPSIHLLK(ac)LQR_	0.030569	0.709
carp-female_000000036_00322865_00441961	365	Chromosome 2 SCAF14781, whole genome shotgun sequence. (Fragment)	GSTENG00026046001	52.576	_LLPEDSGK(ac)YICR_	1.4131	6.23
carp-female_000000036_00975332_00984107	161	Zgc:154056	dars	94.122	_LEYK(ac)EGVAMLR_	0.21497	0.619
carp-female_000000036_00975332_00984107	195	Zgc:154056	dars	97.797	_EK(ac)YDTDFYVLDK_	-1.6009	1.109
carp-female_000000036_01860986_01862809	30	Transmembrane protein 41A-A	tmem41aa	86.772	_LK(ac)FPSDLDELK_	1.1566	0.661
carp-female_000000037_00633378_00678193	130	Spectrin SH3 domain-binding protein 1-like protein	unknown	115.57	_MESSINHISQTVDIHK(ac)EK_	-0.53002	1.667
carp-female_000000037_01538390_01570296	173	Fn1 protein	fn1a	86.772	_GEWTCK(ac)PVAER_	-0.21123	1.106
carp-female_000000037_02293318_02298524	11	Four and half LIM domains protein 2 isoform a	fhl2a	101.3	_YDCHYCK(ac)ESLFGK_	-0.043102	1.407

carp-female_000000037_03989733_04001865	300	Cystathionine beta-synthase	cbsb	74.611	_FLSDK(ac)WMCEK_	-0.23334	0.706
carp-female_000000039_02350391_02384148	68	unknown	unknown	99.855	_EK(ac)YYSVER_	-0.080497	1.377
carp-female_000000039_04594487_04612622	1183	Transitional endoplasmic reticulum ATPase	UY3_03327	78.342	_K(ac)DHFEEAMR_	0.28863	0.663
carp-female_000000039_04594487_04612622	1204	Transitional endoplasmic reticulum ATPase	UY3_03327	73.415	_K(ac)YEMFAQTLQQSR_	-0.32637	0.555
carp-female_000000039_04824285_04826474	67	SUB1 homolog (S. cerevisiae)	sub1b	141.54	_NSDDNMFQIGK(ac)LR_	-0.289	1.043
carp-female_000000039_05808392_05814950	144	Anthrax toxin receptor 2a	antxr2a	55.261	_LEK(ac)YIHQLTK_	-0.0945	1.075
carp-female_000000039_07474049_07478088	314	Tagln2 protein	tagln2	58.699	_GDPSWFHK(ac)K_	-0.42762	1.946
carp-female_000000039_07936605_07947802	463	Myosin-Ic	Myo1c	111.63	_IICDLVEEK(ac)HK_	-0.53086	1.952
carp-female_000000039_07936605_07947802	822	Myosin-Ic	Myo1c	75.109	_IQPEWK(ac)K_	-1.1489	
carp-female_000000040_00810717_00829640	441	Procollagen-proline, 2-oxoglutarate 4-dioxygenase (Proline 4-hydroxylase), alpha polypeptide 2	p4ha2	151.95	_VSK(ac)SAWLEGEDDPVIAR_	-0.016684	0.901
carp-female_000000040_00810717_00829640	594	Procollagen-proline, 2-oxoglutarate 4-dioxygenase (Proline 4-hydroxylase), alpha polypeptide 2	p4ha2	44.612	_WVSNK(ac)WIHER_	0.64232	0.891
carp-female_000000040_01296612_01311591	161	Septin-8-A	sept8a	117.7	_SLDLVTMK(ac)K_	-0.8412	0.787
carp-female_000000040_01296612_01311591	181	Septin-8-A	sept8a	85.813	_ADTISK(ac)SELHK_	0.78701	0.162

carp-female_000000040_01296612_01311591	357	Septin-8-A	sept8a	78.136	_ELHEK(ac)FEQLK_	1.0603	2.913
carp-female_000000040_01604128_01609619	59	Dyskeratosis congenita 1, dyskerin	dkc1	48.794	_NFDK(ac)LNIR_	-0.28219	0.674
carp-female_000000040_01876498_01878546	134	Zgc:103627	fundc2	64.266	_FNEVQVFVK(ac)K_	-0.61842	0.569
carp-female_000000040_04971645_04995685	343	Zgc:112061 protein	kif20a	48.568	_LSDDK(ac)HGNPYVK_	1.9065	1.139
carp-female_000000041_00424049_00434384	414	Aldehyde dehydrogenase	aldh3a2b	44.44	_YHGK(ac)YGFDHLSHLR_	-0.4119	0.977
carp-female_000000041_00527357_00541059	37	Splicing factor, arginine/serine-rich 1B	sfrs1b	143.31	_DVEDVFYK(ac)YGAIR_	-0.32191	1.093
carp-female_000000041_00527357_00541059	254	Splicing factor, arginine/serine-rich 1B	sfrs1b	82.279	_DIAAYIK(ac)K_	0.40066	0.58
carp-female_000000041_00542726_00548455	8	Zgc:152927	pigs	90.15	_AALQLEK(ac)QR_	0.64282	1.064
carp-female_000000041_01328043_01337229	227	Phosphoglycerate kinase	pgk1	130.27	_VLK(ac)NMEIGTSLYDEEGAK_	0.19181	0.695
carp-female_000000043_00930835_00959810	22	DEAH (Asp-Glu-Ala-His) box polypeptide 15	unknown	41.429	_YYEILK(ac)K_	-1.219	2.366
carp-female_000000043_02252982_02264248	156	CTD nuclear envelope phosphatase 1B	ctdnep1b	45.598	_VVIDK(ac)HPVR_	0.27241	1
carp-female_000000043_03539141_03543311	82	60S ribosomal protein L13	LOC100712089	226.59	_GFSLEELK(ac)AAGINK_	0.22727	1.752
carp-female_000000043_03548130_03586519	1827	Lysine--tRNA ligase	kars	58.246	_FTDK(ac)HEWVR_	1.1077	3.114
carp-female_000000043_04168896_04172758	108	40S ribosomal protein S17	RS17	86.882	_VVIEK(ac)YYTR_	0.14963	0.668

carp-female_000000043_04746456_04753978	360	7-dehydrocholesterol reductase	dhcr7	85.813	_STNHQK(ac)DLFR_	0.066021	1.865
carp-female_000000043_05025912_05042461	236	Importin 7	ipo7	61.691	_VLYQYK(ac)EK_	-0.075179	0.924
carp-female_000000046_02451052_02454565	240	Transcription factor mafK	mafk	96.82	_AK(ac)YEALQCFAR_	0.62291	0.285
carp-female_000000046_03080433_03083966	112	Eukaryotic translation initiation factor 3 subunit B	eif3ba	68.786	_NADGYK(ac)LDK_	-1.056	2.145
carp-female_000000046_03635227_03641081	307	Actin related protein 2/3 complex, subunit 1B	arpc1b	93.374	_FQNLDK(ac)K_	-0.82205	1.12
carp-female_000000046_03761959_03768003	226	Fascin	fscn1a	67.645	_DCTGK(ac)YLAPSGPSGTMK_	0.40242	1.241
carp-female_000000046_03761959_03768003	466	Fascin	fscn1a	78.113	_STEGK(ac)YLK_	-0.71798	0.093
carp-female_000000046_03794654_03799486	375	Beta-actin	unknown	128.71	_MQK(ac)EITSLAPSTMK_	-0.086048	1.268
carp-female_000000046_03943890_03945302	4	Mitochondrial ATP synthase subunit f	ATPK	87.667	_ADK(ac)PVALAQK_	0.37447	0.754
carp-female_000000046_03943890_03945302	49	Mitochondrial ATP synthase subunit f	ATPK	138.4	_YYNK(ac)YINVK_	1.0956	0.905
carp-female_000000046_04352237_04355463	161	Fructose-bisphosphate aldolase	aldoaa	107.21	_DGADFAK(ac)WR_	0.026239	0.355
carp-female_000000046_04352237_04355463	344	Fructose-bisphosphate aldolase	aldoaa	122.96	_ACQEEFIK(ac)R_	0.47842	0.634
carp-female_000000046_04352237_04355463	356	Fructose-bisphosphate aldolase	aldoaa	102.39	_ALNNSLACVGK(ac)YVSSGDK_	-0.59445	0.261
carp-female_000000046_05274523_05275700	15	Ribosomal protein S11	unknown	118.67	_QPTIFQNK(ac)K_	-0.72139	2.124

carp-female_000000046_05746299_05753388	309	26S proteasome regulatory subunit S9	EGM_07598	95.5	_EYK(ac)AELQDDPIISTHLTK_	-0.44811	1.927
carp-female_000000046_05775279_05805016	1006	Integrin alpha 3 protein	itga3b	90.696	_ELYEAK(ac)AQK_	-4.086	0.874
carp-female_000000046_06077232_06091190	891	Retinoblastoma binding protein 6 (Fragment)	unknown	51.495	_CAEK(ac)YGHLHVNTTGAAR_	0.032438	1.571
carp-female_000000047_00082013_00099032	305	Chromosome undetermined SCAF15013, whole genome shotgun sequence. (Fragment)	GSTENG00031571001	81.784	_K(ac)YEQLCR_	0.37792	0.064
carp-female_000000047_02602977_02614833	137	MYST histone acetyltransferase 2	kat7	56.708	_CPTPGCNSLGHLTGK(ac)HER_	-0.82619	1.514
carp-female_000000047_04285605_04286644	44	Cytochrome c oxidase assembly factor 3 homolog, mitochondrial	coa3	107.95	_QVELAQWK(ac)K_	-0.059832	0.666
carp-female_000000047_06519975_06552961	1058	Chromosome undetermined SCAF9304, whole genome shotgun sequence. (Fragment)	GSTENG00006854001	44.246	_LHSSQK(ac)YTQANVNR_	0.1623	
carp-female_000000049_01956684_01959474	63	Zgc:153651	nt5c2b	106.26	_TVENLEK(ac)YVVK_	-3.8992	0.178
carp-female_000000049_03864331_03867898	84	Translationally-controlled tumor protein homolog	tpt1	102.52	_LQETSFDK(ac)K_	-0.60129	0.923
carp-female_000000049_05514862_05516656	58	Zgc:123215	hmgb2a	90.15	_GK(ac)FEEMAK_	-0.3391	1.589
carp-female_000000049_05910501_05913204	105	Signal peptidase complex subunit 3 homolog (S. cerevisiae)	spcs3	83.692	_SK(ac)YFFFDDGNGLR_	0.026778	0.415
carp-female_000000049_07441504_07445621	252	Low density lipoprotein receptor-related protein associated protein 1	lrpap1	43.761	_EHVLHQK(ac)HADLK_	0.23006	0.634
carp-female_000000049_07441504_07445621	319	Low density lipoprotein receptor-related protein associated protein 1	lrpap1	121.73	_HFETK(ac)VEK_	0.14882	2.086

carp-female_000000049_07441504_07445621	355	Low density lipoprotein receptor-related protein associated protein 1	lrpap1	83.045	_EK(ac)YNTLAEK_	-0.35293	0.576
carp-female_000000049_07860522_07873182	73	Ssrp1b protein (Fragment)	ssrp1b	59.728	_LCTSTGHIYK(ac)YDGFK_	3.8491	0.747
carp-female_000000049_08056071_08059039	57	Mitochondrial import inner membrane translocase subunit Tim10	timm10	103.76	_CVAK(ac)YLDLHER_	-0.68766	0.55
carp-female_000000049_08452153_08453389	72	CDGSH iron sulfur domain-containing protein 2	cisd2	108.43	_DSLINLK(ac)IQK_	-0.028593	
carp-female_000000049_08454444_08471856	49	Succinate-CoA ligase, GDP-forming, alpha subunit	suclg1	114.4	_NLYINK(ac)NTK_	0.33297	1.151
carp-female_000000049_08789547_08818204	502	Catenin alpha-2	Ctnna2	155.97	_ASYVASTK(ac)YQK_	0.78925	1.519
carp-female_000000050_00560254_00585128	872	Bromodomain-and PHD finger-containing 1	brpf1	74.173	_TSVLFSK(ac)K_	0.16451	1.429
carp-female_000000050_00770066_00782851	411	Zgc:101589	cdk11b	59.709	_ISADEALK(ac)HEYFR_	0.077552	0.865
carp-female_000000050_01715475_01720169	93	Mitochondrial 28S ribosomal protein s25	RT25	73.138	_FYLDDGEQVLVDVEGK(ac)HHK_	-0.56143	0.806
carp-female_000000050_02328316_02331115	58	Tubulin beta-1 chain	TBB1	188.44	_INVYYNEASGGK(ac)YVPR_	-0.85902	1.115
carp-female_000000050_02328316_02331115	297	Tubulin beta-1 chain	TBB1	123.32	_SLTVPELTQQMFDAK(ac)NMMAACDPR_	-0.76931	1.391
carp-female_000000050_02328316_02331115	324	Tubulin beta-1 chain	TBB1	56.339	_MSMK(ac)EVDEQMLNVQNK_	-0.77315	1.765
carp-female_000000050_02697366_02720081	116	Zgc:112450	dbnlb	43.042	_ASGANYSFHK(ac)ESNR_	0.20784	0.759
carp-female_000000050_03306831_03324064	249	Basic fibroblast growth factor receptor 1-A	fgfr1a	119.34	_VFSDSQPHIQWLK(ac)HIEVDGSR_	-0.60593	1.079

carp-female_000000050_05881217_05905972	558	Chromosome undetermined SCAF9708, whole genome shotgun sequence	MFN2	55.064	_VYK(ac)NELHR_	0.36219	0.194
carp-female_000000051_04165819_04167331	102	Proteasome subunit alpha type	PSMA6	80.916	_YEAANWK(ac)YK_	-0.16605	0.607
carp-female_000000051_05406563_05413826	206	26S protease regulatory subunit s10b	PRS10	136.34	_VVSSSIVDK(ac)YIGESAR_	-1.4071	1.373
carp-female_000000051_06052696_06090422	217	Si:dkey-30h14.2	lpgat1	48.561	_DHLDK(ac)YYYSR_	0.88408	0.996
carp-female_000000051_07259968_07261598	125	Btf3l4 protein	btf3l4	48.794	_K(ac)LAEQFPR_	0.22141	1.125
carp-female_000000051_07367270_07370738	239	ATP synthase subunit beta	LOC101164037	128.38	_DTTSK(ac)VALVYGQMNEPPGAR_	-0.84186	1.162
carp-female_000000051_07611022_07612093	54	unknown	unknown	44.426	_EMQTLTVK(ac)HDK_	-0.50652	1.332
carp-female_000000051_07611022_07612093	64	unknown	unknown	100.19	_VVWVK(ac)NQR_	-0.34343	1.056
carp-female_000000052_01698030_01702872	226	ATP synthase, H+ transporting, mitochondrial F0 complex, subunit b, isoform 1	atp5f1	135.83	_HMLFDAK(ac)R_	-0.16383	0.938
carp-female_000000052_01896445_01921839	309	Adenosylhomocysteinase	ahcyl1	67.08	_QK(ac)FDNLYCCR_	-0.81957	1.046
carp-female_000000052_02327973_02342338	140	Mitogen-activated protein kinase 14A	mapk14a	78.401	_GLK(ac)YIHSADIIHR_	-0.019942	1.153
carp-female_000000053_00296442_00323444	301	Mitochondrial import inner membrane translocase subunit TIM50	timm50	44.318	_K(ac)WDGNSEDR_	0.043845	1.979
carp-female_000000053_00390989_00410148	187	Transcription elongation factor SPT5	supt5h	64.841	_EVTNLK(ac)PK_	0.5047	1.304

carp-female_000000053_02250774_02319459	559	S-adenosyl-L-methionine-dependent tRNA 4-demethylwyosine synthase	tyw1	53.1 68	_GGCYK(ac)HTFYGIESHR_	-0.28434	1.03
carp-female_000000053_02645463_02689522	828	unknown	unknown	118. 24	_QQIGGDK(ac)YDVFK_	-1.0693	0.82 2
carp-female_000000053_03227130_03234740	105	CD151 antigen, like	cd151l	80.5 85	_NTMVQK(ac)YHQPEQEHVTK_	-0.19733	1.12 4
carp-female_000000053_04450920_04470110	292	Sodium-dependent Vitamin C transporter 2	slc23a2	58.9 81	_DK(ac)YGFYAR_	-0.14296	0.68
carp-female_000000054_01227110_01229796	119	Elongation factor 1-alpha	unknown	66.2 7	_EVSAYIK(ac)K_	0.14511	1.13 3
carp-female_000000054_01227110_01229796	379	Elongation factor 1-alpha	unknown	132. 06	_QTVAVGVIK(ac)SVEK_	0.28988	1.75
carp-female_000000054_01307641_01325658	800	Pumilio1	pum1	91.6 2	_FISAAPGAEAK(ac)YR_	-0.60002	1.20 8
carp-female_000000054_01307641_01325658	1174	Pumilio1	pum1	57.0 47	_LEK(ac)YYMK_	1.193	1.06 4
carp-female_000000054_01358110_01360645	82	Fatty-acid binding protein 3b	FABP3b	74.9 87	_VK(ac)SLITLDGDK_	-0.34515	0.97 8
carp-female_000000054_01358110_01360645	97	Fatty-acid binding protein 3b	FABP3b	54.7 84	_LVHVQK(ac)WDGK_	-0.75442	0.5
carp-female_000000054_01550659_01554963	51	Cartilage associated protein	crtap	132. 32	_HALDK(ac)YSEEK_	-0.57641	1.24 3
carp-female_000000054_01550659_01554963	140	Cartilage associated protein	crtap	48.0 73	_ETIEEFEK(ac)R_	-4.2974	0.94 5
carp-female_000000054_01550659_01554963	170	Cartilage associated protein	crtap	93.7 76	_AVSAAHTFLLK(ac)HPDDEMMQR_	0.80025	0.99 4
carp-female_000000054_01550659_01554963	185	Cartilage associated protein	crtap	75.5 35	_NMNYYK(ac)SLPGAEEHMK_	0.27359	0.95 1

carp-female_000000054_01556797_01565522	127	FK506 binding protein 9	fkbp9	112.11	_MVK(ac)SGDFVR_	-2.5224	0.661
carp-female_000000054_02529145_02537881	899	Collagen, type I, alpha 2	col1a2	102.65	_HTGQWSK(ac)TVIEYR_	-0.39743	1.929
carp-female_000000054_02999099_03015534	637	Si:ch211-173p18.1 protein	zmym4	78.342	_SLFEHDLVK(ac)R_	1.3289	1.053
carp-female_000000054_02999099_03015534	1208	Si:ch211-173p18.1 protein	zmym4	80.245	_FFNYK(ac)TVEQHR_	1.0081	1.214
carp-female_000000054_05696772_05708538	151	Dystonin	D623_10026671	88.37	_TFTK(ac)WVNK_	0.35153	0.884
carp-female_000000054_07006908_07009054	26	Ribosomal protein L30	unknown	76.228	_SGK(ac)YVLGYK_	0.53903	1.516
carp-female_000000054_07006908_07009054	32	Ribosomal protein L30	unknown	115.7	_YVLGYK(ac)QSQK_	-0.34367	1.216
carp-female_000000054_07006908_07009054	87	Ribosomal protein L30	unknown	108.25	_TGVHHYSGNNIELGTACGK(ac)YYR_	0.82031	1.95
carp-female_000000054_08013660_08018583	82	Histone-binding protein RBBP4	rbb4	84.479	_VINEEYK(ac)IWK_	-0.018677	9.579
carp-female_000000054_08091223_08096443	491	Yars protein	yars	53.034	_VFEK(ac)LQVDLK_	0.14521	0.766
carp-female_000000054_08353876_08358232	283	Si:ch211-215a10.4 protein	si:ch211-215a10.4	50.484	_LTK(ac)HPEDGSIK_	1.1775	0.611
carp-female_000000054_08704697_08709175	16	Eukaryotic translation initiation factor 3 subunit I	eif3i	137.69	_SITQIK(ac)YNR_	-0.40014	0.91
carp-female_000000054_08710955_08718087	32	Histone deacetylase	hdac1	65.598	_VCYYYDGDVGNYYYGQGHPMK(ac)PHR_	-0.96409	0.996
carp-female_000000054_08710955_08718087	67	Histone deacetylase	hdac1	151.04	_ANAEEMTK(ac)YHSDDYIK_	-0.95115	1.127

carp-female_000000054_08710955_08718087	221	Histone deacetylase	hdac1	164.64	_GK(ac)YYAVNYPLR_	0.21569	0.833
carp-female_000000054_09686420_09705911	80	tRNA (Cytosine(34)-C(5))-methyltransferase	NSUN2	50.108	_ITGYK(ac)SHAK_	0.7263	1.427
carp-female_000000054_10096838_10110282	90	Phosphatidylinositide phosphatase SAC1-B	sacm1lb	103.44	_AVEFDVISYK(ac)K_	-0.6876	0.801
carp-female_000000054_10096838_10110282	380	Phosphatidylinositide phosphatase SAC1-B	sacm1lb	116.63	_IEEQADFEK(ac)IYK_	0.90961	0.892
carp-female_000000054_10096838_10110282	383	Phosphatidylinositide phosphatase SAC1-B	sacm1lb	142.45	_IYK(ac)NAWADNANACAK_	0.58072	0.744
carp-female_000000054_10215898_10219704	150	CK2 beta subunit	CK2-b	78.903	_CMDVYTPK(ac)SSR_	-0.33943	0.87
carp-female_000000054_11564820_11568338	109	S100v2 protein	s100v2	85.536	_SDHFGEVLK(ac)QMGVK_	0.33222	1.193
carp-female_000000055_00969852_00973229	196	Mitochondrial import inner membrane translocase subunit Tim23	timm23	70.256	_DMPWSK(ac)PR_	0.47462	0.766
carp-female_000000055_01852604_01874289	2510	Chromosome undetermined SCAF12412, whole genome shotgun sequence. (Fragment)	GSTENG00010858001	146.19	_ASSEYGDGLGSDYK(ac)LHEVCDGK_	-0.97765	68.75
carp-female_000000055_03795753_03805149	39	Aldh18a1 protein	aldh18a1	98.048	_AHGK(ac)SFAHR_	-0.73843	
carp-female_000000055_04653437_04666121	403	Zgc:158610 protein	brd1b	73.927	_RPLTIYEDSK(ac)PK_	0.11021	1.321
carp-female_000000055_04938635_04945021	84	Sb:cb825 protein (Fragment)	pdia3	119.38	_VDCTANSNVCSK(ac)YGVSGYPTLK_	-1.0175	0.423
carp-female_000000055_04938635_04945021	137	Sb:cb825 protein (Fragment)	pdia3	130.2	_SQAEFEK(ac)FIGDR_	-0.82372	0.695

carp-female_000000055_04938635_04945021	184	Sb:cb825 protein (Fragment)	pdia3	98.105	_FAHTNVEDLLK(ac)K_	0.63534	0.354
carp-female_000000055_04938635_04945021	211	Sb:cb825 protein (Fragment)	pdia3	138.02	_FEDGSVK(ac)FSEDK_	0.51699	0.838
carp-female_000000055_04938635_04945021	216	Sb:cb825 protein (Fragment)	pdia3	106.16	_FSEDK(ac)FTSGK_	0.91298	0.349
carp-female_000000055_04938635_04945021	325	Sb:cb825 protein (Fragment)	pdia3	91.853	_GDK(ac)YVMK_	-0.52964	0.223
carp-female_000000055_04938635_04945021	329	Sb:cb825 protein (Fragment)	pdia3	77.744	_YVMK(ac)EEFSR_	0.81223	0.755
carp-female_000000055_04938635_04945021	350	Sb:cb825 protein (Fragment)	pdia3	127.17	_FLQDYFDGK(ac)LK_	0.17372	0.437
carp-female_000000055_04938635_04945021	405	Sb:cb825 protein (Fragment)	pdia3	75.109	_SLEPK(ac)YK_	-0.3722	1.57
carp-female_000000055_04938635_04945021	471	Sb:cb825 protein (Fragment)	pdia3	59.155	_EVSDFISYLK(ac)R_	1.6351	
carp-female_000000055_05614889_05616453	50	Caveolin	cav1	151.49	_TLQDVHTK(ac)EIDLVNR_	-0.22287	1.077
carp-female_000000055_05614889_05616453	60	Caveolin	cav1	130.36	_EIDLVNRDPK(ac)HLNDNVVK_	0.10433	0.639
carp-female_000000055_05693578_05697926	167	unknown	unknown	53.981	_IK(ac)NMESDLCHVHTER_	-0.40786	0.972
carp-female_000000055_05993097_06007190	3375	LOC100151220 protein (Fragment)	map1aa	104.39	_NVDQEFFK(ac)R_	0.55928	0.952
carp-female_000000056_00349501_00362980	86	RAB7, member RAS oncogene family	rab7	97.798	_K(ac)FSNQYK_	0.70272	1.247
carp-female_000000056_01804273_01835065	374	DEC-205/CD205	unknown	51.009	_GFCYK(ac)LHSTTESK_	0.32579	0.858

carp-female_000000057_00132905_00133478	32	Protein DJ-1	park7	90.759	_MMAGDHYK(ac)YSEAR_	-0.4668	1.043
carp-female_000000057_00388747_00398161	286	Delta-1-pyrroline-5-carboxylate dehydrogenase, mitochondrial	aldh4a1	92.939	_VAGECGGK(ac)NFHFVHK_	-0.11208	1.132
carp-female_000000057_00713870_00835798	2334	unknown	unknown	100.02	_ADK(ac)YVGGDMK_	1.2446	3.077
carp-female_000000057_02656843_02688559	1796	Protein polybromo-1 (Fragment)	Anapl_05039	55.105	_LASK(ac)TVESYTK_	1.1031	2.329
carp-female_000000057_03611693_03627832	136	Exportin-2	cse1l	110.51	_HEFK(ac)SNELWSEIK_	0.51427	0.172
carp-female_000000057_04560576_04573644	31	Cat eye syndrome chromosome region, candidate 5	CECR5	79.07	_AFQK(ac)LVDAK_	2.4505	1.371
carp-female_000000057_04560576_04573644	109	Cat eye syndrome chromosome region, candidate 5	CECR5	73.294	_YHDK(ac)YVLVSGQGPVLDIAK_	0.51168	1.718
carp-female_000000057_04560576_04573644	377	Cat eye syndrome chromosome region, candidate 5	CECR5	65.374	_DANQCIK(ac)ETVFHGHR_	0.79126	1.915
carp-female_000000057_04755505_04764341	276	Sp1-like protein	sp1	222.57	_GETGK(ac)PFQNMSSDNR_	-0.070637	0.866
carp-female_000000057_04755505_04764341	484	Sp1-like protein	sp1	61.593	_VYGK(ac)TSHLR_	0.37604	0.774
carp-female_000000057_04781699_04785615	261	Melanocyte proliferating gene 1	MYG1	57.225	_EHLFALEK(ac)EMK_	0.38452	0.464
carp-female_000000057_05849700_05856513	104	unknown	unknown	89.355	_DK(ac)YGPPVR_	0.027519	0.866
carp-female_000000057_05849700_05856513	146	unknown	unknown	48.391	_QAGEVTYADAHK(ac)ER_	0.34012	0.183
carp-female_000000058_00252333_00267027	387	Ribophorin II	rpn2	127.56	_NLYK(ac)FELDTAER_	0.36597	0.925

carp-female_000000058_01957358_02009847	743	Plasma membrane calcium ATPase 4	atp2b4	86.114	_SSPTDK(ac)HTLVK_	0.155	0.924
carp-female_000000058_01957358_02009847	1032	Plasma membrane calcium ATPase 4	atp2b4	49.081	_FLK(ac)EAGHGIPK_	0.41624	3.12
carp-female_000000058_03950901_03956376	162	Proteasome (Prosome, macropain) 26S subunit, non-ATPase, 6	psmd6	84.753	_AK(ac)SLIEEGGDWDR_	2.7264	2.755
carp-female_000000059_01227965_01233051	167	Solute carrier family 25 member 46	slc25a46	49.715	_ELSHK(ac)WNPK_	-1.2062	0.41
carp-female_000000059_02287710_02308577	266	Protein phosphatase 2A regulatory subunit A alpha isoform	unknown	91.62	_YMVADK(ac)FSDLQK_	-0.054379	14.502
carp-female_000000059_03121584_03134563	587	Nucleoporin 88	nup88	51.979	_LADK(ac)YEDAK_	1.126	1.088
carp-female_000000059_03244884_03286756	247	Ras GTPase-activating protein 4-like protein	unknown	90.498	_SK(ac)HSEYEGTLGSLR_	0.58256	6.994
carp-female_000000059_03244884_03286756	387	Ras GTPase-activating protein 4-like protein	unknown	99.568	_K(ac)YVELDPSK_	2.0795	1.123
carp-female_000000059_03244884_03286756	599	Ras GTPase-activating protein 4-like protein	unknown	57.888	_K(ac)YYVTLSK_	0.2769	1.513
carp-female_000000059_04558576_04590484	107	Bckdk protein	bckdk	58.592	_YLHK(ac)ELPVR_	1.5115	0.055
carp-female_000000059_05730384_05743892	366	Stress-induced-phosphoprotein 1 (Hsp70/Hsp90-organizing protein)	stip1	106.14	_EAIQFFNK(ac)SLTEHR_	0.18049	0.916
carp-female_000000059_06668658_06675615	86	Zgc:86898	slc25a11	105.28	_EYK(ac)TSLHAVASILR_	0.37476	1.01
carp-female_000000059_07418303_07423995	89	S-adenosylmethionine synthase	mat2ab	57.288	_DTIK(ac)HIGYDDSSK_	2.4484	0.14
carp-female_000000059_07418303_07423995	98	S-adenosylmethionine synthase	mat2ab	61.409	_HIGYDDSSK(ac)GFDYK_	0.30776	0.032

carp-female_000000059_07418303_07423995	323	S-adenosylmethionine synthase	mat2ab	129.89	_TEQELLK(ac)IVK_	0.12801	0.394
carp-female_000000059_07889086_07901638	495	ATP-dependent RNA helicase	ddx54	81.565	_HVSENAYK(ac)HYLK_	1.8031	
carp-female_000000059_08294949_08306238	30	unknown	unknown	98.048	_GK(ac)SIETQK_	-0.69051	0.166
carp-female_000000059_10326476_10348260	477	Aldh2b protein	aldh2.2	62.732	_FK(ac)SLEEVIER_	0.68858	0.709
carp-female_000000060_00057848_00094445	403	Dynein cytoplasmic 1 heavy chain 1	dync1h1	49.536	_NTK(ac)YPIQR_	0.46952	2.551
carp-female_000000060_00057848_00094445	1145	Dynein cytoplasmic 1 heavy chain 1	dync1h1	60.161	_YDSWHK(ac)EVLSK_	1.6473	1.099
carp-female_000000060_00057848_00094445	2985	Dynein cytoplasmic 1 heavy chain 1	dync1h1	45.825	_K(ac)YTGEDFDEDLR_	-0.4809	1.038
carp-female_000000060_00057848_00094445	3244	Dynein cytoplasmic 1 heavy chain 1	dync1h1	78.342	_IK(ac)SQELEVK_	-0.32156	1.23
carp-female_000000060_00057848_00094445	4212	Dynein cytoplasmic 1 heavy chain 1	dync1h1	76.302	_K(ac)YEFGESDLR_	-0.1669	0.942
carp-female_000000060_00057848_00094445	4413	Dynein cytoplasmic 1 heavy chain 1	dync1h1	83.573	_TVENIK(ac)DPLFR_	0.4366	0.906
carp-female_000000062_01419375_01443524	553	Zgc:158138 protein	hadhab	69.825	_MFEK(ac)IEK_	1.0086	1.695
carp-female_000000063_02329534_02344024	411	Zinc finger CCCH domain-containing protein 7B	ZC3H7B	66.19	_SSDDPTWK(ac)R_	0.54136	1.352
carp-female_000000063_02362425_02374879	68	Aconitase 2, mitochondrial	aco2	92.295	_FEPSSYVNYDK(ac)LR_	-1.039	0.878
carp-female_000000063_03667811_03688065	651	N-ethylmaleimide-sensitive factor b	nsfb	103.67	_EEGAFGSAK(ac)HGAI_	0.73869	0.663

carp-female_000000063_03832086_03844644	155	Capg protein (Fragment)	capgb	176.43	_GVSYK(ac)EGGVESGFR_	1.0664	3.433
carp-female_000000063_04026940_04034428	48	RAB18A, member RAS oncogene family	rab18a	105.46	_VK(ac)TLAVDGNR_	0.27743	0.771
carp-female_000000063_04544999_04552162	666	Chromosome undetermined SCAF14565, whole genome shotgun sequence. (Fragment)	GSTENG00016560001	151.04	_TVVQHDNQNLLK(ac)TSSK_	0.19171	1.284
carp-female_000000063_04633004_04663849	77	Proteasome activator complex subunit 4B	psme4b	69.864	_FSK(ac)EDHVLFIK_	-4.128	21.181
carp-female_000000063_05070661_05081280	64	F-box protein 11	FBXO11	120.56	_VSGK(ac)SQDLPAAPAEQYLQEK_	-0.23387	0.915
carp-female_000000063_05597755_05613489	511	Glutamate dehydrogenase	glud1b	157.5	_TANK(ac)YNLGLDLR_	-1.0984	
carp-female_000000063_05922194_05935361	607	Integrin beta	itgb3b	61.161	_DCVECK(ac)HFK_	-0.078593	1.258
carp-female_000000063_07147043_07192035	995	Chromosome 2 SCAF1692, whole genome shotgun sequence. (Fragment)	GSTENG00036729001	50.354	_VATLECLK(ac)GQR_	0.11127	1.739
carp-female_000000063_07678778_07683475	108	Palmitoyltransferase	zdhhc6	48.423	_LCQGYK(ac)APR_	0.21416	0.718
carp-female_000000065_00076766_00091631	48	NADH dehydrogenase (Ubiquinone) 1 beta subcomplex 9	ndufb9	52.49	_FDENK(ac)HEK_	0.82239	0.907
carp-female_000000065_04723206_04763909	661	Plectin	UY3_13696	96.82	_GLHQSIEDFK(ac)AK_	-0.99199	0.774
carp-female_000000065_04723206_04763909	931	Plectin	UY3_13696	95.815	_SVIQLK(ac)PR_	0.76718	
carp-female_000000065_04723206_04763909	1095	Plectin	UY3_13696	61.265	_DYK(ac)ETTQHFDNLLR_	-0.89821	

carp-female_000000065_04723206_04763909	2569	Plectin	UY3_13696	76.326	_AIADLENEK(ac)AK_	-0.64302	5.742
carp-female_000000065_04723206_04763909	2728	Plectin	UY3_13696	92.939	_VTQEIHIQTEYK(ac)K_	-0.25489	0.572
carp-female_000000065_04723206_04763909	2882	Plectin	UY3_13696	137.8	_AVTGYK(ac)DPYTEAK_	-0.29708	1.679
carp-female_000000065_04723206_04763909	3111	Plectin	UY3_13696	122.81	_GQLLVK(ac)DVSEMEHVR_	-0.46055	0.987
carp-female_000000065_04723206_04763909	3209	Plectin	UY3_13696	117.93	_AVTGYK(ac)DPYTGK_	1.3625	9.02
carp-female_000000065_04723206_04763909	3263	Plectin	UY3_13696	73.294	_IPNDIACMK(ac)GSFDDATHK_	-0.82961	1.533
carp-female_000000065_04723206_04763909	3452	Plectin	UY3_13696	85.376	_NSSVNK(ac)YLQGSESIAGVYLEPTK_	0.85865	0.145
carp-female_000000065_04723206_04763909	3540	Plectin	UY3_13696	139.3	_AVTGYK(ac)DPFTGNK_	-0.23915	1.046
carp-female_000000065_04723206_04763909	3609	Plectin	UY3_13696	84.68	_QLASSIAESK(ac)YFSDPASDENISYK_	0.031153	1.102
carp-female_000000065_04723206_04763909	4018	Plectin	UY3_13696	112.74	_K(ac)YLEGSSCIAGVYVESSK_	-0.43847	0.637
carp-female_000000065_04723206_04763909	4525	Plectin	UY3_13696	105.65	_DVSGYTK(ac)YLTCPK_	-0.17384	1.227
carp-female_000000066_01245954_01257380	553	Lipase maturation factor 2	unknown	113.76	_AK(ac)LYNYHFTDPAK_	0.087884	0.959
carp-female_000000066_01453501_01454593	74	Single-stranded DNA-binding protein	ssbp1	82.287	_DVAYQYVK(ac)K_	0.20658	0.949
carp-female_000000066_01713419_01715550	74	CD9 antigen	unknown	200.48	_DFYTQTFDNYK(ac)STQQEALK_	1.3153	1.223

carp-female_000000066_02395532_02401122	70	Nucleosome assembly protein 1-like 1	NAP1L1	75.589	_K(ac)YAALYQPLFDK_	-1.6762	
carp-female_000000066_02644148_02648505	72	Zgc:110731	bcap29	98.048	_K(ac)YSNADQAK_	0.48201	0.516
carp-female_000000066_02644148_02648505	149	Zgc:110731	bcap29	93.345	_K(ac)YMEDNEMLK_	-0.62806	0.669
carp-female_000000066_02644148_02648505	202	Zgc:110731	bcap29	83.045	_SK(ac)SDLDAMK_	-2.2021	9.467
carp-female_000000066_03664429_03674503	190	Anoctamin	ano6	89.468	_LLSGGVYK(ac)DAYPLHDCR_	-0.13837	1.048
carp-female_000000069_00041648_00043198	216	EH domain-containing protein 3	EHD3	113.52	_FYLSK(ac)ADEAGGESDR_	-2.1241	
carp-female_000000069_00147622_00154047	181	40S ribosomal protein S15a (Fragment)	Anapl_00970	113.62	_SINNAEK(ac)R_	0.09526	1.417
carp-female_000000069_00147622_00154047	246	40S ribosomal protein S15a (Fragment)	Anapl_00970	71.888	_FDVQLK(ac)DLEK_	-0.29681	1.024
carp-female_000000069_00147622_00154047	250	40S ribosomal protein S15a (Fragment)	Anapl_00970	79.885	_DLEK(ac)WQNNLLPSR_	-1.282	0.729
carp-female_000000069_00932460_00950854	945	Ubiquitin carboxyl-terminal hydrolase	usp7	41.695	_EEEITLYPDK(ac)HGCVR_	-0.15866	0.935
carp-female_000000069_01052717_01076129	409	4-aminobutyrate aminotransferase, mitochondrial	GABT	117.14	_DELQADK(ac)PYR_	0.17264	1.141
carp-female_000000069_01661474_01662461	88	Galectin	lgals2a	130.44	_YK(ac)YMHFDGEAK_	0.30471	2.186
carp-female_000000069_02033431_02040119	159	Eukaryotic translation initiation factor 3 subunit D	eif3d	93.649	_SQAQLK(ac)PR_	0.27857	0.685
carp-female_000000069_02033431_02040119	513	Eukaryotic translation initiation factor 3 subunit D	eif3d	77.533	_YLILK(ac)DPNK_	1.999	0.887

carp-female_000000069_02192462_02226350	1337	RUN domain-containing protein 1	RUND1	158.67	_AVIVK(ac)NIDDGTADRPYSHALVAGIDR_	-1.0314	1.668
carp-female_000000069_02192462_02226350	1383	RUN domain-containing protein 1	RUND1	165.49	_AFVK(ac)VFNYNHLMPTR_	-1.1026	1.137
carp-female_000000069_02192462_02226350	1403	RUN domain-containing protein 1	RUND1	47.774	_YSVDIPLDK(ac)TVVNK_	1.065	1.054
carp-female_000000069_02192462_02226350	1438	RUN domain-containing protein 1	RUND1	80.462	_NK(ac)WFFQK_	1.0665	1.144
carp-female_000000069_02234713_02242090	144	Branched-chain-amino-acid aminotransferase	bcat2	151.42	_GGVGEYK(ac)MGGNYGPTIAVQSEAAK_	1.2167	0.984
carp-female_000000069_02234713_02242090	289	Branched-chain-amino-acid aminotransferase	bcat2	81.676	_FHK(ac)ELTDIQYGR_	0.92299	0.534
carp-female_000000069_02801133_02811021	247	Protein serine/threonine phosphatase-1 alpha isoform	unknown	72.891	_FLHK(ac)HDMDLICR_	-0.44166	1.645
carp-female_000000069_02801133_02811021	269	Protein serine/threonine phosphatase-1 alpha isoform	unknown	123.29	_AHQVVEDGYEFFAK(ac)R_	-0.6001	1.46
carp-female_000000069_02934862_02943383	94	ADP-ribosylation factor-like 6 interacting protein	arl6ip1	142.45	_VFGSNK(ac)WTTEQQQR_	0.10873	1.209
carp-female_000000069_02934862_02943383	112	ADP-ribosylation factor-like 6 interacting protein	arl6ip1	73.877	_FHEICGNLVK(ac)TQR_	-0.11577	0.79
carp-female_000000069_03027056_03028752	140	Chromosome 3 SCAF14700, whole genome shotgun sequence	GSTENG10015593001	96.82	_EMYYQK(ac)NQQGFVR_	0.25749	0.774
carp-female_000000069_03027056_03028752	177	Chromosome 3 SCAF14700, whole genome shotgun sequence	GSTENG10015593001	73.632	_AIVK(ac)LEVWDK_	0.35126	
carp-female_000000069_03032171_03032924	124	Chromosome 2 SCAF14705, whole genome shotgun sequence	GSTENG00022310001	147.91	_ALYK(ac)HMYEGK_	0.21588	1.053

carp-female_000000069_03298533_03302831	288	Coiled-coil domain-containing protein 47	ccdc47	43.861	_EMQDLSEFCGDK(ac)PK_	-0.28073	0.644
carp-female_000000069_03474790_03478425	214	Ring finger protein 113A	rnf113a	64.441	_SDYK(ac)HGWQIER_	0.67832	0.481
carp-female_000000069_03739653_03764284	473	unknown	unknown	113.22	_SLLHGK(ac)CYDR_	1.5211	0.791
carp-female_000000069_03839830_03843013	98	Related RAS viral (R-ras) oncogene homolog	rras	132.32	_EIQK(ac)FHTQILR_	0.84103	1.347
carp-female_000000069_03939251_03942780	138	Reticulocalbin 3, EF-hand calcium binding domain	rcn3	71.176	_YIEENVDK(ac)HWK_	0.32191	7.89
carp-female_000000069_04160575_04161329	7	unknown	unknown	97.452	_(ac)SAHELK(ac)EVK_	0.013561	
carp-female_000000070_00459578_00466849	323	DnaJ homolog subfamily C member 13	DNAJC13	55.776	_EMMLEHFK(ac)QQK_	-0.56985	1.251
carp-female_000000070_00473257_00476675	186	DnaJ homolog subfamily C member 13	DNAJC13	53.493	_FLK(ac)YTHLK_	0.36124	0.866
carp-female_000000070_02197425_02225261	428	Chromosome undetermined SCAF14565, whole genome shotgun sequence. (Fragment)	GSTENG00016608001	65.232	_SFENNLK(ac)TYK_	-0.23856	1.006
carp-female_000000070_02197425_02225261	491	Chromosome undetermined SCAF14565, whole genome shotgun sequence. (Fragment)	GSTENG00016608001	103.13	_MFAVNDGFEGFHK(ac)GQIK_	0.37832	0.248
carp-female_000000070_03092541_03098473	82	Endozepine	unknown	89.698	_AK(ac)WDAWK_	0.61495	0.169
carp-female_000000070_03366543_03369831	41	Cyb5a protein	cyb5a	73.448	_VYDVTK(ac)FLEEHPGGEEVLR_	0.50519	2.577
carp-female_000000071_00631956_00662208	136	FCH domain only protein 2 (Fragment)	fcho2	70.089	_ATESYK(ac)SYVEK_	0.26515	1

carp-female_000000071_00631956_00662208	141	FCH domain only protein 2 (Fragment)	fcho2	111.63	_SYVEK(ac)YATAK_	1.6043	0.371
carp-female_000000071_01380924_01388813	207	Ranbp1 protein	ranbp1	82.452	_MK(ac)FDECK_	0.20269	0.905
carp-female_000000071_01443137_01445109	64	Bri3bp protein (Fragment)	bri3bp	70.747	_FFSK(ac)TTER_	-0.70156	0.682
carp-female_000000071_02960341_02966088	78	Ubiquinone biosynthesis methyltransferase COQ5, mitochondrial	coq5	115.56	_K(ac)YDVMNDAMSLGIHR_	-1.8972	0.863
carp-female_000000072_00146339_00152728	39	Transgelin	tagln	92.939	_IEQK(ac)YDTELEAR_	-0.44307	2.099
carp-female_000000072_00146339_00152728	169	Transgelin	tagln	67.414	_GDPNWFFK(ac)K_	-0.40889	0.7
carp-female_000000072_04818513_04830986	1165	Pre-mRNA-processing-splicing factor 8	D623_10015723	61.958	_LMK(ac)HDVNLGR_	1.7872	
carp-female_000000072_04818513_04830986	2353	Pre-mRNA-processing-splicing factor 8	D623_10015723	97.904	_HDPNMK(ac)YDLQLSNPK_	-0.41012	1.02
carp-female_000000072_04861662_04880150	492	Unconventional myosin-Ic	myo1c	60.598	_IICDLVEEK(ac)FK_	-1.1256	6.771
carp-female_000000072_04861662_04880150	955	Unconventional myosin-Ic	myo1c	48.527	_NINPEWK(ac)HQLEQK_	0.94662	0.414
carp-female_000000075_00015676_00016381	8	Ubiquitin-60S ribosomal protein L40	TREES_T100014679	107.09	_MQIFVK(ac)TLTGK_	-0.53488	0.99
carp-female_000000075_00015676_00016381	65	Ubiquitin-60S ribosomal protein L40	TREES_T100014679	200.48	_TLSDYNIQK(ac)ESTLHLVLR_	-0.48206	1.188
carp-female_000000075_00015676_00016381	90	Ubiquitin-60S ribosomal protein L40	TREES_T100014679	85.813	_QLAQK(ac)YNCEK_	0.46988	
carp-female_000000077_00373304_00376103	47	unknown	unknown	40.496	_YTEK(ac)HIESR_	-0.68379	1.402

carp-female_000000080_02890744_02893801	34	RAB14, member RAS oncogene family	rab14	78.903	_SCLLHQFTEK(ac)K_	0.85653	0.86
carp-female_000000080_04261007_04369108	1815	Probable E3 ubiquitin-protein ligase MYCBP2	MYCBP2	63.216	_ENVK(ac)YAVR_	1.4543	10.401
carp-female_000000082_00006949_00016121	629	Transferrin receptor 1b	tfr1b	72.898	_LVHDHILK(ac)LDVTK_	0.25495	1.372
carp-female_000000082_00006949_00016121	634	Transferrin receptor 1b	tfr1b	110.92	_LDVTK(ac)YSSVINK_	0.76512	0.954
carp-female_000000082_00139607_00140545	43	Zgc:123339	zgc:123339	118.9	_YLGK(ac)WYEIEK_	0.47855	0.494
carp-female_000000082_00226881_00228115	69	Eukaryotic translation initiation factor 5A	unknown	108.47	_K(ac)YEDICPSTHNMDVPNTK_	0.13787	0.842
carp-female_000000082_01976234_01986067	486	Asparaginyl-tRNA synthetase, cytoplasmic	SYNC	106.26	_IWDSEELLEGYK(ac)R_	-0.0062799	1.997
carp-female_000000082_02041993_02050233	447	Asparagine synthetase	asns	64.121	_APTDGVEK(ac)YLLR_	0.29468	1.56
carp-female_000000082_02762419_02777589	190	ATP-binding cassette, sub-family D (ALD), member 3a	abcd3a	73.082	_LTK(ac)HLYDEYLK_	1.1211	0.832
carp-female_000000082_02762419_02777589	290	ATP-binding cassette, sub-family D (ALD), member 3a	abcd3a	139.3	_MTVTEQK(ac)YEGEYR_	-0.30608	1.027
carp-female_000000082_03226861_03235247	282	Vimentin	vim	122.97	_SK(ac)FADLSEAAAR_	-0.77091	0.868
carp-female_000000082_04619826_04620686	134	CCAAT/enhancer binding protein (C/EBP), delta	cebpd	78.552	_LQHQEGGFGK(ac)GAFYAPIK(ac)R_	-1.3107	1.915
carp-female_000000082_04619826_04620686	142	CCAAT/enhancer binding protein (C/EBP), delta	cebpd	78.552	_LQHQEGGFGK(ac)GAFYAPIK(ac)R_	-1.3107	1.915
carp-female_000000083_00399987_00419892	837	Chromosome undetermined SCAF13628, whole genome shotgun sequence. (Fragment)	GSTENG00011544001	89.506	_K(ac)FAHLLEFGDNDIR_	-0.18712	1.355

carp-female_000000086_01069219_01094068	291	Protein argonaute-3	ago3a	74.267	_EK(ac)YNLQLK_	0.37636	1.726
carp-female_000000086_01852638_01897719	1074	Ubr5 protein (Fragment)	ubr5	102.4	_ELQNK(ac)YTPGR_	1.0414	1.014
carp-female_000000086_02335074_02346679	32	Zgc:158642 protein	zgc:158642	142.08	_AAEFDIISYK(ac)K_	-0.99541	0.788
carp-female_000000086_02335074_02346679	273	Zgc:158642 protein	zgc:158642	53.377	_YIAFDFHK(ac)ECSR_	-0.25011	0.822
carp-female_000000086_02335074_02346679	363	Zgc:158642 protein	zgc:158642	103.76	_IEDQADFEK(ac)IYK_	-0.43508	0.051
carp-female_000000086_02335074_02346679	366	Zgc:158642 protein	zgc:158642	142.45	_IYK(ac)NAWADNANACAK_	0.58072	0.744
carp-female_000000086_02335074_02346679	414	Zgc:158642 protein	zgc:158642	48.822	_YYK(ac)NNFSDGFR_	-0.65245	1.197
carp-female_000000086_02807666_02845401	211	Zgc:85680	ethe1	49.418	_LYESIHK(ac)K_	0.34803	1.727
carp-female_000000090_01171518_01175745	62	Voltage-dependent anion-selective channel protein 2	VDAC2	90.05	_VIGNLETK(ac)YK_	-0.099222	2.107
carp-female_000000090_01171518_01175745	64	Voltage-dependent anion-selective channel protein 2	VDAC2	80.632	_YK(ac)WAEYGLTFTEK_	0.21025	0.811
carp-female_000000091_00522844_00581962	388	NADPH--cytochrome P450 reductase	zgc:63480	105.14	_TYEHYNATGK(ac)YVDK_	0.47815	0.689
carp-female_000000092_04545522_04550438	148	Zgc:92746	srprb	105.52	_VQIVEK(ac)YK_	0.62983	0.831
carp-female_000000092_04545522_04550438	231	Zgc:92746	srprb	196.11	_GK(ac)DFEFSQLPAR_	-0.069645	0.814
carp-female_000000095_04358210_04362581	47	Ribosomal protein S5	rps5	71.153	_YAK(ac)YLPHSSGR_	-0.20879	1.075

carp-female_000000098_03141120_03176025	374	Extended synaptotagmin-2-B	ESYT2-B	59.013	_VYTENVDK(ac)R_	0.38738	0.171
carp-female_000000098_03141120_03176025	721	Extended synaptotagmin-2-B	ESYT2-B	79.88	_DDK(ac)HECSLGTVSFPLSK_	-0.72269	1.294
carp-female_000000105_01425923_01437380	398	Arih1 protein	arih1	48.998	_FEHK(ac)LYAQVK_	0.71251	0.966
carp-female_000000105_03373989_03376492	185	Htatip2 protein	htatip2	68.044	_VDHDYVLK(ac)SAELAK_	-0.41483	0.765
carp-female_000000106_00524817_00538057	46	SRA stem-loop-interacting RNA-binding protein, mitochondrial	SLIRP	149.23	_CLLPFDK(ac)ETGFHR_	0.43344	0.876
carp-female_000000106_02381743_02392106	339	Procollagen-proline, 2-oxoglutarate 4-dioxygenase (Proline 4-hydroxylase), alpha polypeptide I	p4ha1b	106.75	_ISK(ac)SAWLSGYEHSTIER_	0.12642	2.009
carp-female_000000106_02381743_02392106	467	Procollagen-proline, 2-oxoglutarate 4-dioxygenase (Proline 4-hydroxylase), alpha polypeptide I	p4ha1b	143.93	_HAACPVLVGNK(ac)WVSNK_	-0.38331	1.186
carp-female_000000106_02381743_02392106	472	Procollagen-proline, 2-oxoglutarate 4-dioxygenase (Proline 4-hydroxylase), alpha polypeptide I	p4ha1b	44.612	_WVSNK(ac)WIHER_	0.64232	0.891
carp-female_000000107_00032791_00078820	92	Chromosome 2 SCAF15088, whole genome shotgun sequence. (Fragment)	GSTENG00034621001	54.276	_VFTAITK(ac)HPDEK_	-2.2869	0.91
carp-female_000000110_00479846_00482461	297	Tubulin beta 1	unknown	58.812	_ALTVPELTQQMFDAK(ac)NMMAACDPR_	-0.83403	4.976
carp-female_000000110_03605251_03608582	36	GTP-binding nuclear protein Ran	ran	117.02	_HLTGEFEK(ac)K_	-0.051383	5.017
carp-female_000000110_03605251_03608582	59	GTP-binding nuclear protein Ran	ran	176.56	_GAIK(ac)YNVWDTAGQEK_	0.97371	1.134

carp-female_000000110_03605251_03608582	98	GTP-binding nuclear protein Ran	ran	77.062	_VTYK(ac)NVPNWHR_	-1.0769	1.163
carp-female_000000110_03669983_03685620	95	Structure specific recognition protein 1a	ssrp1a	69.276	_FSK(ac)QSVVYK_	1.2579	1.232
carp-female_000000110_03669983_03685620	141	Structure specific recognition protein 1a	ssrp1a	69.485	_LATSTGHIYK(ac)YDGFK_	-1.9256	0.507
carp-female_000000112_00655682_00669456	69	Chromosome 18 SCAF14786, whole genome shotgun sequence. (Fragment)	GSTENG00026385001	97.631	_AAGMLK(ac)AEGSDIR_	0.61659	1.004
carp-female_000000112_00655682_00669456	161	Chromosome 18 SCAF14786, whole genome shotgun sequence. (Fragment)	GSTENG00026385001	94.122	_QADDIVNWLK(ac)K_	0.13072	
carp-female_000000112_00655682_00669456	302	Chromosome 18 SCAF14786, whole genome shotgun sequence. (Fragment)	GSTENG00026385001	111.86	_DFQDK(ac)MDQFK_	-0.37467	0.546
carp-female_000000112_00655682_00669456	339	Chromosome 18 SCAF14786, whole genome shotgun sequence. (Fragment)	GSTENG00026385001	90.15	_ILEFFGLK(ac)K_	0.074594	0.416
carp-female_000000112_00655682_00669456	383	Chromosome 18 SCAF14786, whole genome shotgun sequence. (Fragment)	GSTENG00026385001	51.089	_LK(ac)PHLMSQDIPEDWDK_	0.18034	0.493
carp-female_000000112_00655682_00669456	406	Chromosome 18 SCAF14786, whole genome shotgun sequence. (Fragment)	GSTENG00026385001	62.861	_VLVGK(ac)NFEEVAFNPAK_	1.3248	0.687
carp-female_000000112_00655682_00669456	491	Chromosome 18 SCAF14786, whole genome shotgun sequence. (Fragment)	GSTENG00026385001	80.361	_VHSFPTLK(ac)FFPAGDDHK_	1.0941	0.566
carp-female_000000112_00655682_00669456	515	Chromosome 18 SCAF14786, whole genome shotgun sequence. (Fragment)	GSTENG00026385001	87.863	_TLDGFTK(ac)FLESGGK_	1.09	0.828
carp-female_000000112_00924047_00930234	43	UTP6, small subunit (SSU) processome	utp6	71.03	_STALEYK(ac)LHR_	0.83666	0.767

		component, homolog (Yeast)					
carp-female_000000112_01324078_01345821	86	Sept9b protein	sept9b	45.452	_TIEIK(ac)SISHDIEEK_	-0.60025	2.679
carp-female_000000112_02565726_02573879	151	Tissue inhibitor of metalloproteinase 2	timp2	97.734	_MIQYDIK(ac)QMK_	1.0308	0.42
carp-female_000000112_03291919_03299963	84	Ras-related C3 botulinum toxin substrate 1	RAC1	117.89	_AK(ac)WYPEVR_	-0.079402	1.29
carp-female_000000112_03291919_03299963	141	Ras-related C3 botulinum toxin substrate 1	RAC1	153.22	_EIGAVK(ac)YLECSALTQR_	-0.36214	1.058
carp-female_000000112_04289359_04311224	229	Coagulation factor X	FA10	54.343	_K(ac)YSDFQVAVGK_	-1.6314	1.377
carp-female_000000113_00107024_00115240	491	Protein kinase C substrate 80K-H	prkcsh	44.238	_YLVMK(ac)YEHGTGCWQGPSR_	-0.94441	0.648
carp-female_000000113_00593453_00601556	82	Eukaryotic translation initiation factor 3 subunit G	eif3g	83.204	_TVTEYK(ac)LEDDGQK_	0.70225	0.843
carp-female_000000113_01259501_01275141	1024	Bromodomain-containing protein 4	GW7_16018	107.99	_GPSALGGIK(ac)EEK_	2.115	0.639
carp-female_000000113_02193825_02200601	85	Elongation factor Tu	tufm	191.96	_YK(ac)TYEDIDNAPEEK_	0.33032	0.838
carp-female_000000113_02300492_02320320	650	Interleukin enhancer-binding factor 3 homolog	ilf3	44.662	_GLK(ac)YELISETGGSHDK_	-0.33263	1.429
carp-female_000000113_02348726_02354574	152	Gcdhl protein	gcdhl	80.165	_AK(ac)YNPSSR_	0.53938	0.838
carp-female_000000116_00209891_00223730	382	Inner membrane protein, mitochondrial (Mitofilin)	immt	148.48	_VVTK(ac)VQTAQSEAK_	0.80708	2.977
carp-female_000000116_00209891_00223730	549	Inner membrane protein, mitochondrial (Mitofilin)	immt	71.853	_EEAQEILTSK(ac)MMEQETHYR_	-0.41877	0.972
carp-female_000000116_00225280_00235127	83	Pentatricopeptide repeat domain-containing protein 3, mitochondrial	ptcd3	71.524	_NTAK(ac)YFINK_	0.36985	0.883

carp-female_000000116_00225280_00235127	236	Pentatricopeptide repeat domain-containing protein 3, mitochondrial	ptcd3	111.86	_GMVK(ac)YGAYSK_	-0.44387	0.957
carp-female_000000116_00262015_00271161	208	PRP19/PSO4 homolog (S. cerevisiae)	prp19	86.136	_AEDLSK(ac)YR_	0.95624	0.707
carp-female_000000116_00352111_00358611	106	Calnexin 2	canx2	62.055	_KDGIDEEIAK(ac)YDGK_	0.13982	1.54
carp-female_000000116_00352111_00358611	110	Calnexin 2	canx2	169.37	_YDGK(ac)WEVEEMQNTK_	0.012397	0.682
carp-female_000000116_00352111_00358611	206	Calnexin 2	canx2	116.24	_CGEDYK(ac)LHFIFR_	-0.0086944	0.91
carp-female_000000116_00352111_00358611	224	Calnexin 2	canx2	76.927	_TGEFEEK(ac)HAK_	0.052228	1.529
carp-female_000000116_00352111_00358611	465	Calnexin 2	canx2	45.829	_WAADSWGLK(ac)K_	-1.4992	0.934
carp-female_000000118_00188890_00207435	435	Chromosome 15 SCAF14992, whole genome shotgun sequence	GSTENG00028441001	134.88	_NVMTK(ac)VEEMSSVQK_	-0.78336	1.053
carp-female_000000118_00380301_00394726	325	Presequence protease, mitochondrial	pitrm1	41.242	_VQHYFK(ac)NNTHR_	1.2944	0.774
carp-female_000000119_01640048_01644501	111	1-acylglycerol-3-phosphate O-acyltransferase 3 (Fragment)	agpat3	42.336	_VLAK(ac)HELLK_	-0.52322	0.876
carp-female_000000119_02372562_02375184	18	Trafficking protein particle complex 5	trappc5	88.495	_GK(ac)SAILER_	0.49166	2.056
carp-female_000000127_01668221_01681515	515	Solute carrier family 25 (Mitochondrial carrier phosphate carrier), member 3	slc25a3b	81.771	_LQVDPAK(ac)YK_	0.15387	2.066
carp-female_000000127_02089452_02099016	31	Fatty acid desaturase 2	fads2	94.781	_HTK(ac)SGDQWIVVER_	0.76738	1.506

carp-female_000000127_02089452_02099016	409	Fatty acid desaturase 2	fads2	132.01	_ALCDK(ac)YGVK_	-0.26408	1.849
carp-female_000000127_02089452_02099016	413	Fatty acid desaturase 2	fads2	48.091	_YGVK(ac)YQEK_	-0.4228	1.157
carp-female_000000129_00693094_00699399	152	Enolase 1, (Alpha)	eno3	83.862	_K(ac)FSVVDQEK_	-0.23831	1.074
carp-female_000000129_00693094_00699399	163	Enolase 1, (Alpha)	eno3	80.632	_IDK(ac)FMLELDGTENK_	0.9648	1.151
carp-female_000000129_00693094_00699399	197	Enolase 1, (Alpha)	eno3	114.87	_AGAAEK(ac)GVPLYR_	0.85141	0.756
carp-female_000000129_00693094_00699399	477	Enolase 1, (Alpha)	eno3	74.376	_LAK(ac)YNQLMR_	-0.22496	1.008
carp-female_000000129_00704022_00707344	106	Profilin-1	PROF1	117.08	_TSEKEPDPFSFTIGK(ac)SHK_	0.21646	0.806
carp-female_000000129_01012551_01019774	421	Plod3 protein	plod3	73.834	_FLK(ac)DYIAPVTEK_	0.59988	0.676
carp-female_000000129_01540888_01544378	149	High-mobility group box 2	hmgb2b	61.78	_APFEQK(ac)AMK_	-0.40114	0.915
carp-female_000000130_00988310_01050753	281	Protein kinase C	prkca	160.52	_STDELYAIK(ac)ILK_	-0.0074272	0.896
carp-female_000000130_00988310_01050753	555	Protein kinase C	prkca	109	_GAENFDK(ac)FFTR_	0.28825	0.212
carp-female_000000131_00456911_00474451	313	Acyl-coenzyme A oxidase	acox1	73.885	_ENMLMK(ac)YAK_	1.0793	0.804
carp-female_000000131_00456911_00474451	484	Acyl-coenzyme A oxidase	acox1	63.565	_YLVK(ac)SYK_	-1.0012	0.71
carp-female_000000131_00510014_00530671	136	Signal recognition particle subunit SRP68	LOC100145378	82.494	_AAK(ac)HGEQLEK_	0.96963	0.125

carp-female_000000132_00080174_00107410	941	Chromosome 19 SCAF14240, whole genome shotgun sequence	GSTENG00012993001	47.849	_NFAK(ac)AAR_	0.32287	0.723
carp-female_000000133_01184002_01190221	44	Transmembrane protein 19	tmem19	51.726	_QIDSDYK(ac)EGGQR_	-0.1538	0.794
carp-female_000000133_01377791_01389245	279	Nucleoporin 50	nup50	74.475	_K(ac)YGSGTSDGGVEK_	-0.12996	0.514
carp-female_000000133_01377791_01389245	474	Nucleoporin 50	nup50	106.86	_VK(ac)TAEDADELHQILQEK_	1.5334	0.014
carp-female_000000133_01765414_01769257	7	Zgc:154045	zgc:154045	145.46	_(ac)AAAGGK(ac)TYSFK_	0.35351	
carp-female_000000138_00577298_00578788	310	unknown	unknown	81.625	_ELEQLK(ac)GNEK_	0.052148	1.213
carp-female_000000138_00924279_00926623	197	Heterogeneous nuclear ribonucleoprotein A/B	hnrnpaba	57.174	_K(ac)YHNVSGSK_	2.2515	7.908
carp-female_000000139_00003689_00012005	242	Proteasome subunit alpha type	psma4	80.245	_VLNK(ac)TMDVSK_	1.0809	1.017
carp-female_000000139_00191792_00193181	169	Peptidyl-prolyl cis-trans isomerase	ppib	97.431	_GFGYK(ac)GSK_	-0.099013	0.551
carp-female_000000139_00191792_00193181	196	Peptidyl-prolyl cis-trans isomerase	ppib	45.438	_GDGTGGK(ac)SIYGDR_	0.41271	0.316
carp-female_000000139_00374723_00396949	481	Chondroitin sulfate proteoglycan 4	UY3_15682	62.466	_IK(ac)YLHDGNEK_	-0.41424	0.872
carp-female_000000139_00374723_00396949	847	Chondroitin sulfate proteoglycan 4	UY3_15682	62.005	_VFAK(ac)DQYSR_	-0.045949	0.83
carp-female_000000139_00374723_00396949	908	Chondroitin sulfate proteoglycan 4	UY3_15682	53.756	_ITQDPK(ac)HGR_	0.2047	0.7
carp-female_000000139_00850906_00856949	475	Catalase	cat	119.86	_GAQLFIQK(ac)R_	-0.60252	0.703

carp-female_000000139_00850906_00856949	498	Catalase	cat	64.104	_VQALLDK(ac)HNAEGK_	1.3877	1.537
carp-female_000000140_00043760_00065477	364	Aryl hydrocarbon receptor repressor	AHRR	75.043	_YAHYGK(ac)PYR_	0.75787	13.363
carp-female_000000140_01510401_01511471	33	Chaperonin containing TCP1, subunit 2 (Beta)	cct2	99.013	_EAELLIAK(ac)K_	0.030899	0.917
carp-female_000000140_01510401_01511471	90	Chaperonin containing TCP1, subunit 2 (Beta)	cct2	56.205	_LLTHHK(ac)DHFAR_	0.86216	0.921
carp-female_000000140_01550712_01553934	206	Chromosome 19 SCAF14691, whole genome shotgun sequence. (Fragment)	GSTENG00021560001	71.03	_YK(ac)SDLHELK_	-0.69874	0.554
carp-female_000000140_01550712_01553934	213	Chromosome 19 SCAF14691, whole genome shotgun sequence. (Fragment)	GSTENG00021560001	112.71	_SDLHELK(ac)AR_	0.21426	0.924
carp-female_000000140_01550712_01553934	376	Chromosome 19 SCAF14691, whole genome shotgun sequence. (Fragment)	GSTENG00021560001	87.352	_LNALESK(ac)YESHENSLSGCR_	-0.10097	
carp-female_000000140_01550712_01553934	402	Chromosome 19 SCAF14691, whole genome shotgun sequence. (Fragment)	GSTENG00021560001	75.197	_HDLEGMK(ac)SR_	0.95136	
carp-female_000000145_00778798_00788562	472	Kelch domain-containing protein 4 (Fragment)	Anapl_14365	62.466	_TEK(ac)YWLGLAR_	-0.85654	
carp-female_000000145_00865582_00897632	588	Septin 7b	sept7b	89.859	_THMQDLK(ac)DVTNNVHYENYR_	1.1342	0.919
carp-female_000000146_00148692_00155571	157	14-3-3 protein beta/alpha-B	ywhabb	76.073	_AYQDAFEISK(ac)K_	1.4168	0.892
carp-female_000000146_00318124_00367183	662	2-oxoglutarate dehydrogenase, mitochondrial	OGDH	123.86	_GVLQK(ac)YAEK_	0.67916	1.319
carp-female_000000146_00318124_00367183	1078	2-oxoglutarate dehydrogenase, mitochondrial	OGDH	115.29	_NQGYYDYVK(ac)PR_	1.0872	0.944

carp-female_000000146_00318124_00367183	1115	2-oxoglutarate dehydrogenase, mitochondrial	OGDH	84.882	_NTHLLELK(ac)R_	0.093279	1.062
carp-female_000000146_01217156_01270130	422	Mystique	pdlim2	148.52	_TTSSVAGVQK(ac)YHTCEK_	-0.32593	1.342
carp-female_000000149_00354217_00363368	14	Proteasome (Prosome, macropain) 26S subunit, non-ATPase, 2	psmd2	64.52	_VPDDIYK(ac)THLENNR_	0.8978	1.277
carp-female_000000150_00468237_00474865	24	Addicsin	arl6ip5b	112.44	_FSK(ac)PDVSDLSK_	1.44	0.793
carp-female_000000150_00468237_00474865	32	Addicsin	arl6ip5b	114.54	_FSKPDVSDLSK(ac)WNNR_	-0.76242	2.302
carp-female_000000150_00468237_00474865	187	Addicsin	arl6ip5b	72.705	_IQDFLESK(ac)LKD_	0.0065752	0.946
carp-female_000000152_01375796_01378931	40	Succinate dehydrogenase cytochrome b560 subunit, mitochondrial	C560	99.568	_EEMNK(ac)YWTK_	-0.083142	0.203
carp-female_000000152_01375796_01378931	141	Succinate dehydrogenase cytochrome b560 subunit, mitochondrial	C560	47.302	_HLMWDVGK(ac)GFK_	-0.82686	0.57
carp-female_000000152_01709186_01746164	113	unknown	unknown	99.498	_SDPSVFNHPAIK(ac)R_	-0.20748	0.988
carp-female_000000155_00168729_00179474	118	Chromosome 12 SCAF7567, whole genome shotgun sequence	GSTENG00004749001	57.288	_LEDPDGTVLYK(ac)EMK_	1.0874	1.195
carp-female_000000158_00319279_00329560	25	Annexin	unknown	92.8	_GTVTEASGFK(ac)PEEDAQK_	0.59064	0.809
carp-female_000000158_00319279_00329560	139	Annexin	unknown	66.568	_EIIATYK(ac)R_	0.43465	0.988
carp-female_000000158_00319279_00329560	294	Annexin	unknown	159.22	_AEIDMLDIK(ac)AEFLK_	-0.55524	1.041
carp-female_000000158_00319279_00329560	299	Annexin	unknown	47.732	_AEFLK(ac)MYGK_	0.66983	1.187

carp-female_000000158_00319279_00329560	310	Annexin	unknown	142.57	_TLHSFIK(ac)GDTSGDYR_	-0.93372	1.038
carp-female_000000160_01265833_01272452	1396	unknown	unknown	40.377	_EANDPVFYFEK(ac)K_	0.77745	0.168
carp-female_000000161_00165383_00166503	59	Zgc:56141 protein	rbm4.3	94.281	_NLHLYK(ac)LHGTPINVEASR_	0.51598	1.291
carp-female_000000161_01403705_01410179	158	Neighbor of COX4	CX4NB	108.3	_DK(ac)HTIMLR_	0.68806	1.371
carp-female_000000161_01484780_01492989	6	Protein pelota homolog	pelo	54.066	_LVHK(ac)DIEK_	0.49286	0.606
carp-female_000000161_02960226_02975776	343	DNA topoisomerase 2	top2a	58.123	_VPPLITDYK(ac)EYHTDTTVR_	-0.61815	1.164
carp-female_000000161_02960226_02975776	396	DNA topoisomerase 2	top2a	88.338	_K(ac)YESVQDILK_	0.69655	1.06
carp-female_000000161_02960226_02975776	476	DNA topoisomerase 2	top2a	68.846	_AWK(ac)QAQEK_	0.70007	1.25
carp-female_000000161_02983912_02988556	15	DNA topoisomerase 2 (Fragment)	top2a	129.82	_SLFENK(ac)ALSK_	-0.41288	
carp-female_000000165_00466508_00475942	280	Pyruvate kinase	TREES_T100018937	146.1	_K(ac)FDEIMEASDGIMVAR_	-0.39937	0.946
carp-female_000000168_01162239_01166570	79	Transmembrane emp24 domain trafficking protein 2	tmed2	94.387	_ESSGK(ac)YSVAAHM(ox)DGTYK_	-0.56853	0.813
carp-female_000000168_01222730_01228035	228	Voltage-dependent anion-selective channel protein 2	VDAC2	116.19	_YQLDK(ac)DASLSAK_	0.73857	0.876
carp-female_000000168_01229271_01241592	269	LOC795332 protein (Fragment)	slc25a1b	114.7	_VK(ac)FIHDQSSANPK_	-0.11886	0.867
carp-female_000000168_01229271_01241592	280	LOC795332 protein (Fragment)	slc25a1b	146.79	_FIHDQSSANPK(ac)YR_	0.41926	0.952

carp-female_000000168_01229271_01241592	330	LOC795332 protein (Fragment)	slc25a1b	108.47	_NWYK(ac)GDNPNK_	0.5731	2.068
carp-female_000000171_00788022_00797188	175	Serrate RNA effector molecule homolog	srrt	59.739	_YNEYK(ac)IDFR_	0.54821	
carp-female_000000174_00044448_00050068	158	Cytochrome P450 3A	unknown	70.089	_EMFGIMK(ac)THSK_	-1.1341	0.894
carp-female_000000174_00372791_00383900	323	unknown	unknown	82.831	_AAMNLEK(ac)LK_	0.69714	1.116
carp-female_000000178_00030615_00052103	821	Nucleoporin 155	nup155	85.554	_K(ac)YHTEAQAYEK_	0.72502	1.432
carp-female_000000178_01024387_01058511	473	Phosphatidylinositol 4-kinase III alpha	pi4kaa	86.772	_LYK(ac)YHSQYTTGTGEIK_	0.24327	0.687
carp-female_000000178_01024387_01058511	1289	Phosphatidylinositol 4-kinase III alpha	pi4kaa	59.198	_SK(ac)YINLSEK_	-0.63543	0.914
carp-female_000000179_00597117_00615140	242	Glucose-6-phosphate isomerase	unknown	70.056	_EWFLK(ac)SAK_	0.88628	0.779
carp-female_000000179_01205188_01208430	19	Histone H4	GW7_16515	89.08	_K(ac)QLATK(ac)AAR_	0.31803	0.617
carp-female_000000179_01205188_01208430	24	Histone H4	GW7_16515	99.136	_QLATK(ac)AAR_	0.23045	0.539
carp-female_000000179_01205188_01208430	57	Histone H4	GW7_16515	89.266	_YQK(ac)STELLIR_	-0.47181	0.89
carp-female_000000179_01205188_01208430	80	Histone H4	GW7_16515	174.72	_EIAQDFK(ac)TDLR_	0.12217	0.808
carp-female_000000179_01205188_01208430	123	Histone H4	GW7_16515	113.24	_VTIMPK(ac)DIQLAR_	-0.28646	0.826
carp-female_000000180_00304724_00306941	103	Translocon-associated protein subunit gamma	SSRG	69.812	_K(ac)LSEADNR_	0.13875	0.851

carp-female_000000180_01055277_01064217	292	Bckdha protein	bckdha	86.8	_SVDEVNYWDK(ac)QDHPISR_	0.13699	
carp-female_000000181_00246986_00251367	58	Tubulin beta 1	unknown	136.34	_ISVYYNEASGGK(ac)YVPR_	-0.018492	0.624
carp-female_000000181_00625945_00634539	16	Glycoprotein, synaptic 2	tecrb	78.191	_SMFHK(ac)SHPQWYPAR_	-0.46522	0.691
carp-female_000000184_00289439_00299590	887	Probable 2-oxoglutarate dehydrogenase E1 component DHKTD1, mitochondrial	dhtkd1	117.89	_FEK(ac)QLACK_	0.15936	0.782
carp-female_000000186_00000433_00010367	259	Lon protease homolog, mitochondrial	LONM	74.841	_K(ac)YLLQEQLK_	0.48606	0.56
carp-female_000000186_00016608_00025920	269	Lamin B2	LamB2	120.54	_AELQQTFMAK(ac)LDNAK_	0.24415	0.595
carp-female_000000186_00016608_00025920	486	Lamin B2	LamB2	85.469	_QIGDEEEITYK(ac)FSPK_	-0.61891	0.816
carp-female_000000186_00796544_00798374	202	Transmembrane protein 43	TMM43	76.759	_EHQLNAMK(ac)TWALR_	0.86253	1.139
carp-female_000000187_00277107_00282018	181	ATP synthase subunit alpha	LOC101169376	103.13	_QTGK(ac)TAIAIDTIINQK_	-0.095921	0.858
carp-female_000000187_00277107_00282018	279	ATP synthase subunit alpha	LOC101169376	265.77	_HALIIYDDLSK(ac)QAVAYR_	-2.3273	0.928
carp-female_000000187_00277107_00282018	461	ATP synthase subunit alpha	LOC101169376	102.4	_GHLDK(ac)MEPSK_	0.67572	2.466
carp-female_000000187_00566186_00582768	697	Leucine rich repeat containing 8 family, member A	lrrc8a	81.918	_IETLPPELFQCK(ac)K_	-0.34427	1.079
carp-female_000000189_00448469_00457564	29	Protein Jade-1	jade1	56.688	_VPSTSEDSDNGSISTSWSQHSNSK(ac)HR_	0.092667	0.831
carp-female_000000189_00859327_00862617	411	YTH domain family 2	yth2	101.3	_VFIIK(ac)SYSEDDIHR_	-1.3687	0.858

carp-female_000000189_03335757_03343285	329	Isovaleryl Coenzyme A dehydrogenase	ivd	117	_EAFGQK(ac)IGHFQLMQGK_	3.306	0.388
carp-female_000000191_00583563_00584824	101	Zgc:77235	rpl27a	90.412	_INFDK(ac)YHPGYFGK_	-0.63189	1.799
carp-female_000000192_00356629_00371326	90	Zgc:101621 protein	scp2b	93.345	_LHEDGEQFVK(ac)K_	0.40261	11.921
carp-female_000000193_00380544_00386196	46	Glutathione peroxidase (Fragment)	gpx7	69.598	_LVSLDK(ac)YR_	0.17566	0.795
carp-female_000000196_00285736_00311003	10	Microphthalmia-associated transcription factor b	mitfb	91.547	_VQTHLENPTK(ac)YHIQQAQR_	-0.70843	0.512
carp-female_000000197_00285680_00299823	607	Integral membrane protein 1	itm1	55.297	_HIK(ac)EHDYYTPTGEFR_	-1.1853	1.108
carp-female_000000204_00150174_00152745	31	Peptidyl-prolyl cis-trans isomerase	ppiab	122.39	_ADVVPK(ac)TAENFR_	0.18117	1.244
carp-female_000000204_00150174_00152745	44	Peptidyl-prolyl cis-trans isomerase	ppiab	156.36	_ALCTGEK(ac)GFGYK_	-0.33119	1.185
carp-female_000000204_00150174_00152745	49	Peptidyl-prolyl cis-trans isomerase	ppiab	184.24	_GFGYK(ac)GSGFHR_	-0.00781 15	0.939
carp-female_000000204_00150174_00152745	82	Peptidyl-prolyl cis-trans isomerase	ppiab	136.34	_SIYGNK(ac)FADENFTLK_	-0.16657	0.808
carp-female_000000204_00150174_00152745	91	Peptidyl-prolyl cis-trans isomerase	ppiab	134.68	_FADENFTLK(ac)HGGK_	0.77801	1.377
carp-female_000000204_00380801_00383770	64	Homeobox protein Ved	ved	86.014	_PENTEVQEK(ac)R_	4.233	7.184
carp-female_000000205_00671471_00689416	74	Chromosome 7 SCAF14557, whole genome shotgun sequence. (Fragment)	GSTENG00016274001	119.21	_GFEQK(ac)WYK_	-0.53741	0.148
carp-female_000000205_00671471_00689416	584	Chromosome 7 SCAF14557, whole genome shotgun sequence. (Fragment)	GSTENG00016274001	203.11	_TVLQNYHSVFDQK(ac)R_	-1.2982	0.962

carp-female_000000205_00796795_00868691	1418	Citron Rho-interacting kinase	CIT	45.433	_K(ac)YVVLDGTK_	1.3755	1.199
carp-female_000000205_00910423_00913491	130	Heat shock protein 5	hspa5	59.198	_VM(ox)EHFIK(ac)LYK_	0.11697	0.355
carp-female_000000205_00910423_00913491	188	Heat shock protein 5	hspa5	194.12	_AK(ac)FEELNMDLFR_	1.0699	0.405
carp-female_000000205_00910423_00913491	244	Heat shock protein 5	hspa5	123.67	_EFFNGK(ac)EPSR_	1.9127	0.209
carp-female_000000206_00146077_00161479	323	Chromosome 2 SCAF15032, whole genome shotgun sequence	GSTENG00033110001	174.42	_EFNK(ac)YDTDGSK_	0.80337	0.833
carp-female_000000213_00139715_00141676	79	Ribosomal protein S20	rps20	89.507	_TPCGEGSK(ac)TWDR_	0.24387	0.47
carp-female_000000213_00248134_00255298	240	LOC559236 protein (Fragment)	LOC559236	66.486	_VHYGFILK(ac)SENK_	0.48284	0.839
carp-female_000000220_00225403_00280238	750	Structural maintenance of chromosomes protein	smc1al	92.039	_LK(ac)YSQSDLEQTK_	-0.64004	1.898
carp-female_000000221_00058565_00083388	674	Tyrosine-protein kinase receptor	pdgfrb	91.307	_NK(ac)HSFLQNYADK_	-0.31965	0.969
carp-female_000000222_00101592_00162405	572	Myosin-9	I79_023145	61.127	_NLVNNPLAQADWATK(ac)K_	0.296	1.604
carp-female_000000222_00101592_00162405	855	Myosin-9	I79_023145	139.46	_SELCLEGYSK(ac)YR_	-0.17549	1.614
carp-female_000000222_00101592_00162405	1344	Myosin-9	I79_023145	93.424	_NK(ac)HEAMITDLEDR_	0.90209	1.783
carp-female_000000222_00101592_00162405	1565	Myosin-9	I79_023145	93.237	_QLSTMQAQLVDMK(ac)K_	-0.14787	1.321
carp-female_000000223_00012179_00015305	111	Rpl14 protein	rpl14	82.417	_K(ac)WEESSWAK_	-2.0565	1.216

carp-female_000000223_00440611_00441315	57	Nucleoside diphosphate kinase	nme2b.2	99.392	_QHYIDLK(ac)DRPFYPGLVK_	0.85518	0.91
carp-female_000000223_00474988_00494760	919	Importin subunit beta-1	PAL_GLEAN10019656	101.57	_TLATWATK(ac)ELR_	0.71589	0.784
carp-female_000000242_00409651_00424172	126	Zgc:158605	prss16	103.39	_FYGK(ac)SHPTEDLSTANLR_	0.3833	0.744
carp-female_000000256_00002980_00015567	292	Zgc:92481	zgc:92481	67.136	_EVLDLVK(ac)SHVYSHR_	1.1509	1.18
carp-female_000000256_00057624_00060277	29	40S ribosomal protein s17	RS17	123.75	_VIIEK(ac)YYTR_	-0.043623	0.818
carp-female_000000270_00153297_00160675	89	WD repeat domain 1	wdr1	85.909	_EHLLK(ac)YEYQPFGGK_	0.018245	1.011
carp-female_000000270_00153297_00160675	98	WD repeat domain 1	wdr1	107.06	_YEYQPFGGK(ac)IK_	0.39164	1.153
carp-female_000000270_00153297_00160675	482	WD repeat domain 1	wdr1	95.264	_VVTVFTVADGYK(ac)EK_	-0.78485	1.01
carp-female_000000299_04645836_04651938	486	ATPase, Na+/K+ transporting, alpha 1 polypeptide	atp1a1a.1	145.43	_IAEIPFNSTNK(ac)YQLSIHK_	0.2654	0.837
carp-female_000000299_04645836_04651938	493	ATPase, Na+/K+ transporting, alpha 1 polypeptide	atp1a1a.1	110.25	_YQLSIHK(ac)NINTNK_	0.15526	0.83
carp-female_000000299_04645836_04651938	499	ATPase, Na+/K+ transporting, alpha 1 polypeptide	atp1a1a.1	136.39	_NINTNK(ac)TETNHLLVMK_	-0.22366	0.767
carp-female_000000299_04645836_04651938	509	ATPase, Na+/K+ transporting, alpha 1 polypeptide	atp1a1a.1	124.29	_TETNHLLVMK(ac)GAPER_	0.5926	0.964
carp-female_000000299_06532144_06534604	10	60S ribosomal protein L24	rpl24	121.82	_VELCSFSGYK(ac)IYPGHGR_	0.02239	1.137
carp-female_000000299_06532144_06534604	41	60S ribosomal protein L24	rpl24	133.23	_CESAFLSK(ac)R_	-0.48423	1.036

carp-female_000000300_01513060_01515885	77	Eukaryotic translation initiation factor 3 subunit F	EIF3F	40.724	_NMYELHK(ac)K_	0.071576	0.618
carp-female_000000300_02738497_02743503	61	Zgc:77126	nans	88.495	_SELEYK(ac)FNK_	0.3627	1.168
carp-female_000000300_07721516_07724293	167	C-4 methylsterol oxidase	sc4mol	55.676	_IYK(ac)YIHK_	0.77557	4.069
carp-female_000000300_07721516_07724293	280	C-4 methylsterol oxidase	sc4mol	125.5	_LFNTDSQYNK(ac)HYTHQK_	0.73348	4.833
carp-female_000000300_08567722_08574695	7	Annexin	anxa5b	201.61	_GTVK(ac)PHSGFNANNDAEVLYK_	0.12052	0.897
carp-female_000000300_08567722_08574695	137	Annexin	anxa5b	44.863	_K(ac)FATSLHK_	0.68354	1.114
carp-female_000000300_08567722_08574695	144	Annexin	anxa5b	42.066	_FATSLHK(ac)MIQGDTSGDYR_	-0.068635	0.931
carp-female_000000300_08929738_08949191	161	unknown	unknown	133.86	_VDK(ac)WWGNR_	-0.23838	1.543
carp-female_000000300_08929738_08949191	223	unknown	unknown	109.79	_NFLGEK(ac)YIR_	2.0106	1.851
carp-female_000000300_09658054_09661559	28	40S ribosomal protein S3a	rps3a	65.224	_K(ac)DWYDVK_	-0.26652	1.213
carp-female_000000300_09658054_09661559	182	40S ribosomal protein S3a	rps3a	237.21	_EVQTNDLK(ac)EVVNK_	0.6591	1.706
carp-female_000000301_00614925_00640312	24	Pdcd11 protein (Fragment)	pdcd11	52.527	_VK(ac)THDVDNLFENR_	1.2227	2.29
carp-female_000000301_00614925_00640312	1297	Pdcd11 protein (Fragment)	pdcd11	40.493	_VEFQHATK(ac)YFMDDPK_	0.31897	0.996
carp-female_000000301_01016615_01022349	109	Malate dehydrogenase	MDH	89.624	_ANVAIFK(ac)TQGEALEK_	1.0057	0.832

carp-female_000000301_01016615_01022349	117	Malate dehydrogenase	MDH	130.1	_TQGEALEK(ac)YAK_	0.25351	8.852
carp-female_000000301_01178856_01184335	298	Zgc:66241 protein (Fragment)	esf1	102.73	_ATDVDYGSYK(ac)PK_	0.043111	1.388
carp-female_000000302_00694445_00698613	151	Elmod2 protein (Fragment)	elmod2	40.693	_EVFDPENEK(ac)HETMLLK_	-1.9799	0.316
carp-female_000000304_01365055_01365447	11	Receptor expression-enhancing protein 5	REEP5	94.309	_FDK(ac)FLYEK_	0.12422	0.828
carp-female_000000304_01439737_01500518	2300	Talin-1 (Fragment)	TLN1	122.53	_AIADMLHSCK(ac)QAAFHPEVNR_	-0.026234	0.861
carp-female_000000304_01560571_01565345	331	3-hydroxy-3-methylglutaryl-Coenzyme A synthase 1 (Soluble)	hmgcs1	107.09	_ASSELFENK(ac)TK_	-0.85312	5.29
carp-female_000000304_02066780_02080386	72	Serine palmitoyltransferase 1 (Fragment)	Anapl_16186	121.9	_K(ac)YGVGTCGPR_	0.11017	1.002
carp-female_000000304_02066780_02080386	155	Serine palmitoyltransferase 1 (Fragment)	Anapl_16186	98.942	_YFK(ac)HNDMEDLER_	0.81867	0.855
carp-female_000000304_05363977_05376993	489	Chromosome 4 SCAF14752, whole genome shotgun sequence. (Fragment)	GSTENG00024727001	48.527	_HPNEDYK(ac)SHFPNR_	-0.14916	1.426
carp-female_000000304_05880320_05907760	684	Annexin	anxa3b	94.09	_QTLVEYK(ac)SLSGK_	0.92537	1.084
carp-female_000000304_06480836_06483554	125	Activated RNA polymerase II transcriptional coactivator p15	TCP4	186.74	_NDNMFQIGK(ac)MR_	-0.81747	1.115
carp-female_000000304_07288867_07299197	212	Developmentally regulated GTP binding protein 1	drg1	84.403	_SILSEYK(ac)IHNADITLR_	1.1859	1.514
carp-female_000000304_08864119_08871322	129	LOC100006201 protein (Fragment)	letm2	64.224	_VLDELK(ac)HYYHGFR_	0.030093	0.874

carp-female_000000304_11308263_11317998	239	Voltage-sensing phosphoinositide phosphatase	tpte	83.182	_FLDTK(ac)HLDHYK_	0.38984	1.965
carp-female_000000304_11665326_11670757	291	Cct8 protein	cct8	65.276	_IADMALHYANK(ac)YK_	0.94113	0.991
carp-female_000000304_11665326_11670757	424	Cct8 protein	cct8	91.62	_K(ac)FAEAFEAVPR_	0.35099	1.284
carp-female_000000304_14304022_14317252	157	Hypoxia up-regulated protein 1	hyou1	74.364	_TADNPQVAQYLK(ac)HFPEHQLHR_	0.43273	0.245
carp-female_000000304_14304022_14317252	341	Hypoxia up-regulated protein 1	hyou1	81.09	_DHLAK(ac)LFNEQK_	0.2504	1.729
carp-female_000000304_14330462_14330842	16	Histone H2B 3	hist2h2l	80.688	_K(ac)AVTK(ac)TQK_	-0.4441	2.215
carp-female_000000304_14330462_14330842	20	Histone H2B 3	hist2h2l	80.688	_K(ac)AVTK(ac)TQK_	-0.4441	2.215
carp-female_000000304_14352375_14355516	71	Heat shock cognate 70	hsc70	184.99	_NQVAMNPTNTVFDAK(ac)R_	0.23189	0.754
carp-female_000000304_14352375_14355516	108	Heat shock cognate 70	hsc70	130.1	_VQVEYK(ac)GETK_	-0.33935	0.975
carp-female_000000304_14352375_14355516	187	Heat shock cognate 70	hsc70	80.585	_IINEPTAAAIAYGLDK(ac)K_	0.23253	2.755
carp-female_000000304_14352375_14355516	246	Heat shock cognate 70	hsc70	88.24	_MVNHFITEFK(ac)R_	-0.32516	0.772
carp-female_000000304_14352375_14355516	328	Heat shock cognate 70	hsc70	93.776	_MDK(ac)AQIHDIVLVGGSTR_	-1.7534	0.615
carp-female_000000304_14352375_14355516	524	Heat shock cognate 70	hsc70	148.32	_MVQEAEK(ac)YK_	0.24616	0.198
carp-female_000000304_14352375_14355516	557	Heat shock cognate 70	hsc70	102.06	_STVEDEK(ac)LK_	-0.52516	0.789

carp-female_000000304_16132778_16137222	285	Malate dehydrogenase	mdh2	186.75	_SEETECK(ac)YFSTPLLLGK_	-0.16438	0.957
carp-female_000000304_16132778_16137222	300	Malate dehydrogenase	mdh2	62.338	_NGIEK(ac)NLGLGK_	-0.38373	0.821
carp-female_000000304_16754929_16761111	99	Alg5 protein	alg5	137.89	_TTEVAMK(ac)YTK_	-0.079533	0.032
carp-female_000000304_16889868_16901389	226	NADPH--cytochrome P450 reductase	por	112.17	_TYEHYNATGK(ac)YTDK_	0.7486	1.312
carp-female_000000304_16889868_16901389	590	NADPH--cytochrome P450 reductase	por	111.95	_AWQK(ac)DQGK_	0.51473	0.319
carp-female_000000304_17584110_17585466	58	High-mobility group box 1	hmgb1a	81.972	_GK(ac)FEDMAK_	1.1039	3.913
carp-female_000000304_17584110_17585466	156	High-mobility group box 1	hmgb1a	46.844	_YEK(ac)DIAAYR_	0.17828	1.146
carp-female_000000304_18586781_18591200	186	HSP47	unknown	140.45	_HYNYEHSK(ac)INFR_	-0.71968	0.619
carp-female_000000304_18586781_18591200	205	HSP47	unknown	137.8	_AINEWASK(ac)STDGK_	0.19481	
carp-female_000000304_18586781_18591200	345	HSP47	unknown	142.23	_VSMEVSHNLQK(ac)HLAELGLTEAVDK_	-0.96466	0.693
carp-female_000000305_00047422_00063362	523	Puromycin-sensitive aminopeptidase (Fragment)	Npepps	60.621	_MAAEVK(ac)SFFESHHAPAAER_	-1.2724	2.158
carp-female_000000306_00482506_00494090	646	6-phosphofructokinase	LOC570106	76.586	_IEISQHAK(ac)YTCSFCGK_	0.58163	0.858
carp-female_000000306_00482506_00494090	654	6-phosphofructokinase	LOC570106	80.014	_YTCSFCGK(ac)TK_	-0.80721	0.363
carp-female_000000306_01627469_01632656	244	Replication factor C subunit RFC4	rfc4	68.108	_GAFEK(ac)LELAVK_	0.18999	1.116

carp-female_000000306_02664578_02669105	40	Cytochrome b5 reductase 1	cyb5r1	76.358	_KPQITLIDPSEK(ac)YK_	0.61471	1.048
carp-female_000000306_02664578_02669105	58	Cytochrome b5 reductase 1	cyb5r1	55.258	_NVHPK(ac)FPEGGK_	0.98535	
carp-female_000000306_02672497_02676431	97	Adiponectin receptor protein 1	ADR1	59.248	_MEEFVHK(ac)VWEGR_	-0.027695	0.97
carp-female_000000306_03666143_03671601	62	Cpne1 protein	cpne1	102.98	_NCQDPEFSTK(ac)LHIDYHFEK_	0.76838	1.031
carp-female_000000306_03666143_03671601	71	Cpne1 protein	cpne1	95.417	_LHIDYHFEK(ac)VQK_	-0.51206	0.96
carp-female_000000306_03666143_03671601	123	Cpne1 protein	cpne1	83.204	_AVVMEVEAK(ac)NLDK_	0.3951	0.995
carp-female_000000306_03666143_03671601	139	Cpne1 protein	cpne1	98.048	_NNLNPSWK(ac)K_	0.31284	0.918
carp-female_000000306_03814414_03823373	57	Zgc:136367	acad9	83.623	_DLFLGK(ac)VNK_	0.22172	0.854
carp-female_000000306_04342831_04359440	569	Constitutive coactivator of PPAR-gamma-like protein 1-like protein (Fragment)	fam120a	50.04	_EWAAYK(ac)GK_	-1.3475	
carp-female_000000306_05452986_05453456	76	Zgc:123327	rpl22	88.163	_ITVTSEVPFSK(ac)R_	0.021828	0.829
carp-female_000000306_05891607_05897232	215	Peroxisomal trans-2-enoyl-CoA reductase	pecr	64.385	_TAMENYK(ac)EHGPTMFK_	-0.3011	1.993
carp-female_000000306_08284059_08286677	109	Guanine nucleotide-binding protein G(I), alpha-2 subunit	PAL_GLEAN10009213	99.688	_SK(ac)FEDLNK_	0.85057	0.356
carp-female_000000306_08710919_08824478	75	Inositol 1,4,5-trisphosphate receptor type 1'	ITPR1	70.942	_SNK(ac)YLTVNK_	0.14571	1.017
carp-female_000000306_08710919_08824478	1345	Inositol 1,4,5-trisphosphate receptor type 1'	ITPR1	41.242	_VVTHK(ac)DCIPEVK_	-0.3848	0.732

carp-female_000000306_09851578_09857742	168	Histone H1-beta, late embryonic	H1B	64.82	_K(ac)YPSVEMDK_	-0.64891	0.572
carp-female_000000306_10564069_10568262	96	Ras-like protein Cdc42a	cdc42	82.925	_EK(ac)WVPEITHHCPK_	-1.0494	1.048
carp-female_000000308_01138943_01149474	371	Neutral amino acid transporter SLC1A5	slc1a5	76.358	_CVEENNGVSK(ac)HISR_	-1.0014	
carp-female_000000310_01926369_01934665	245	Zgc:92013	fuca2	74.987	_HK(ac)WENCMTIDQK_	-0.16559	1.019
carp-female_000000310_03165171_03170431	35	26S protease regulatory subunit 4 (Fragment)	PSMC1	52.6	_K(ac)YEPPIPTR_	0.66304	1.419
carp-female_000000310_04996555_05001479	52	Peptidyl-prolyl cis-trans isomerase E	ppie	45.853	_CLCTHEK(ac)GFGFK_	0.21349	0.756
carp-female_000000311_00736206_00746958	102	CTAGE family, member 5	ctage5	78.342	_VAELLDEK(ac)CK_	0.22137	0.795
carp-female_000000311_01757309_01763347	152	UPF0568 protein C14orf166 homolog	zgc:56576	81.92	_HDDYLVMLK(ac)AIR_	0.34011	0.829
carp-female_000000311_02050746_02051239	83	Glucosamine 6-phosphate N-acetyltransferase	GNA1	114.31	_VTLECAPK(ac)NVEFYK_	0.43264	0.994
carp-female_000000312_00891245_00904711	246	Pleckstrin homology domain containing, family A (Phosphoinositide binding specific) member 1	plekha1	45.357	_VQECK(ac)HGEIMMR_	-0.77947	0.92
carp-female_000000312_00909410_00935747	280	Htra1 protein	htra1	94.09	_YK(ac)YNFIADVVEK_	0.67816	1.561
carp-female_000000313_01688067_01703991	1196	Novel protein similar to human rearranged L-myc fusion sequence (RLF) (Fragment)	CH211-154E15.8-001	51.03	_LSSK(ac)SELPQTHDHIK_	0.38323	2.237
carp-female_000000313_01706521_01713398	61	Novel protein (Zgc:55655)	zmpste24	67.997	_IMDSETFEK(ac)SR_	-0.11021	1.655

carp-female_000000313_01716967_01719318	35	Ribosomal protein L13a	rpl13a	78.377	_LK(ac)YLAFLR_	0.085418	0.797
carp-female_000000313_01716967_01719318	116	Ribosomal protein L13a	rpl13a	69.176	_K(ac)FALLGR_	0.26705	1.562
carp-female_000000313_01716967_01719318	130	Ribosomal protein L13a	rpl13a	157.98	_LAHEVGWK(ac)YQAITATLEEK_	-0.50711	0.915
carp-female_000000313_01716967_01719318	173	Ribosomal protein L13a	rpl13a	74.841	_IAK(ac)YTEVLK_	0.020996	1.71
carp-female_000000316_00044342_00056629	307	Dihydrolipoyllysine-residue succinyltransferase component of 2-oxoglutarate dehydrogenase complex, mitochondrial (Fragment)	DLST	67.334	_QYK(ac)DAFLK_	0.49685	0.863
carp-female_000000316_00684198_00693179	261	NS1-associated protein 1	syncripl	187.75	_GFCFLEYEDHK(ac)TAAQAR_	-0.52415	0.978
carp-female_000000316_00918602_00975911	185	Fermitin family like protein 2	UY3_09763	89.506	_THWTLDK(ac)YGIQADAR_	-0.46839	0.778
carp-female_000000319_02680296_02690985	158	Casein kinase II subunit alpha	CSK21	119.45	_DVK(ac)PHNVMIDHEHR_	0.53457	0.967
carp-female_000000319_05636576_05647010	284	Novel protein similar to vertebrate zinc finger protein 384 (ZNF384)	znf384l	100.18	_IHSGAK(ac)PYTCSYCQK_	0.02143	1.993
carp-female_000000319_05963499_05970334	312	Succinate dehydrogenase [ubiquinone] flavoprotein subunit, mitochondrial	sdha	161.21	_GQVITHK(ac)DGEDK_	-0.45338	1.392
carp-female_000000319_05963499_05970334	433	Succinate dehydrogenase [ubiquinone] flavoprotein subunit, mitochondrial	sdha	113.76	_MDSIYK(ac)SLDDIK_	-0.13899	0.977
carp-female_000000319_05963499_05970334	505	Succinate dehydrogenase [ubiquinone] flavoprotein subunit, mitochondrial	sdha	47.603	_K(ac)PFEQHWR_	0.55684	0.947
carp-female_000000319_06117943_06124770	105	Chromosome 21 SCAF14577, whole	GSTENG00017380001	65.232	_SFAK(ac)HTQGYGR_	0.35081	0.851

		genome shotgun sequence					
carp-female_000000319_06305440_06313717	1279	Impa1 protein (Fragment)	znf687b	101.61	_RFDK(ac)TSDLNTHFR_	-0.096219	0.758
carp-female_000000320_00316109_00326335	78	Poly A binding protein, cytoplasmic 1 b	pabpc1b	69.92	_ALDTMNFDVIK(ac)GR_	-0.78271	
carp-female_000000320_00331521_00343779	177	Ywhai protein	ywhaz	102.64	_NTSPAESQVFYLK(ac)MK_	0.592	0.729
carp-female_000000320_00331521_00343779	214	Ywhai protein	ywhaz	147	_SQEGYQAAFDISK(ac)DNMQPTHPIR_	-1.3069	1.054
carp-female_000000320_00596242_00605090	69	mRNA cap guanine-N7 methyltransferase	rnmt	44.342	_LVTEESLHSQK(ac)VATHYNK_	1.6301	0.815
carp-female_000000320_03644131_03647944	5	Ribosomal protein L15	rpl15	101.56	_GAYK(ac)YMQELWR_	-0.080858	1.738
carp-female_000000320_03644131_03647944	153	Ribosomal protein L15	rpl15	65.043	_NPDTQWITK(ac)AVHK_	-0.28994	0.857
carp-female_000000321_01734972_01738515	117	RAB5A, member RAS oncogene family	rab5aa	111.17	_NWVK(ac)ELQR_	0.56617	0.941
carp-female_000000321_01789650_01796167	364	CNDP dipeptidase 2 (Metallopeptidase M20 family)	cndp2	136.81	_QVMTHLESK(ac)FAELK_	-0.18451	0.577
carp-female_000000321_01789650_01796167	369	CNDP dipeptidase 2 (Metallopeptidase M20 family)	cndp2	72.434	_FAELK(ac)SPNK_	2.4556	0.916
carp-female_000000321_02433523_02469055	344	Nuclear factor of activated T-cells calcineurin-dependent 1	unknown	109.5	_ETYCSGFLDVPQHPYWSK(ac)PK_	0.92846	1.779
carp-female_000000321_02522945_02541898	214	Epiplakin	UY3_08593	147.73	_GLYDK(ac)DLFR_	0.080515	1.287
carp-female_000000321_02522945_02541898	415	Epiplakin	UY3_08593	45.829	_ELIVK(ac)EHGIR_	0.24765	0.991
carp-female_000000321_02522945_02541898	741	Epiplakin	UY3_08593	125.68	_DLIVK(ac)DHGIR_	-1.0302	1.047

carp-female_000000321_02522945_02541898	938	Epiplakin	UY3_08593	86.898	_TYK(ac)NVIQGK_	0.6325	1.359
carp-female_000000321_02522945_02541898	1469	Epiplakin	UY3_08593	46.73	_EPLTYHQLMK(ac)K_	0.5335	1.33
carp-female_000000321_02522945_02541898	1641	Epiplakin	UY3_08593	183.08	_QTMSISEAK(ac)NK_	0.11326	6.44
carp-female_000000321_02522945_02541898	1689	Epiplakin	UY3_08593	202.81	_LSVEQAVAEGIVGTEWK(ac)NK_	0.17223	1.293
carp-female_000000321_02550520_02559309	50	unknown	unknown	52.576	_QIILVK(ac)EAAQK_	-0.97528	0.87
carp-female_000000321_02550520_02559309	170	unknown	unknown	194.24	_QEADAEMAK(ac)YK_	0.19257	0.806
carp-female_000000321_02550520_02559309	451	unknown	unknown	78.326	_EADDLHK(ac)AIAELEK_	-1.9349	1.016
carp-female_000000321_02550520_02559309	686	unknown	unknown	151.26	_GK(ac)TTLQELSK_	0.81894	0.72
carp-female_000000321_02550520_02559309	694	unknown	unknown	84.352	_TTLQELSK(ac)HDK_	1.927	7.621
carp-female_000000321_02550520_02559309	775	unknown	unknown	62.203	_DTLIGPELHTK(ac)LLSAER_	0.49995	0.942
carp-female_000000321_02550520_02559309	998	unknown	unknown	121.82	_SSVPASELLEAK(ac)VINK_	0.79241	1.099
carp-female_000000321_02550520_02559309	1002	unknown	unknown	48.998	_VINK(ac)DLFNK_	1.3525	1.015
carp-female_000000321_02550520_02559309	1114	unknown	unknown	145.31	_AVCGYK(ac)DPYTGK_	-0.88451	0.601
carp-female_000000321_02550520_02559309	1167	unknown	unknown	76.345	_ITPDIAYK(ac)R_	0.14278	1.079

carp-female_000000321_02550520_02559309	1327	unknown	unknown	145.44	_GPVPASSLLESK(ac)IIDK_	-0.15817	1.122
carp-female_000000321_02550520_02559309	1336	unknown	unknown	111.12	_IIDKDTYDK(ac)IQQGK_	0.36722	0.819
carp-female_000000321_02550520_02559309	1441	unknown	unknown	187.11	_AVTGYK(ac)DPYTGNK_	1.7024	1.084
carp-female_000000321_02550520_02559309	1500	unknown	unknown	132.88	_GYFSK(ac)QLAK_	-0.61379	1.143
carp-female_000000321_02550520_02559309	1774	unknown	unknown	170.66	_AVTGYK(ac)DPYSGK_	0.28646	21.602
carp-female_000000321_02550520_02559309	1865	unknown	unknown	72.638	_LSYALLLK(ac)R_	-0.51958	0.907
carp-female_000000321_02550520_02559309	1986	unknown	unknown	111.94	_NLK(ac)MNVIEAVK_	-0.35486	5.778
carp-female_000000321_02550520_02559309	2038	unknown	unknown	107.21	_GLILK(ac)DHGIR_	-0.75073	1.979
carp-female_000000321_02550520_02559309	2436	unknown	unknown	150.22	_DVSGYSK(ac)YLTCPK_	-1.1772	0.955
carp-female_000000321_02563851_02571773	70	unknown	unknown	131.08	_GLHQSIEEFK(ac)SK_	-0.14832	0.739
carp-female_000000321_02563851_02571773	97	unknown	unknown	98.942	_EYLGK(ac)LDLQYAK_	0.91507	0.975
carp-female_000000321_02563851_02571773	104	unknown	unknown	72.321	_LDLQYAK(ac)LLNSSK_	0.36923	0.745
carp-female_000000321_02563851_02571773	279	unknown	unknown	89.468	_EQLNEFK(ac)THLEGLNR_	-0.27125	1.096
carp-female_000000321_02563851_02571773	296	unknown	unknown	48.157	_TIIQLK(ac)PR_	0.052472	0.895

carp-female_000000321_02563851_02571773	415	unknown	unknown	40.645	_LQAENSYSK(ac)ATQHYDNLLR_	0.56583	1.212
carp-female_000000321_02563851_02571773	562	unknown	unknown	184.32	_STQGAEDILNK(ac)YENQLR_	-0.75139	1.008
carp-female_000000321_02656580_02666438	148	Chromosome undetermined SCAF6308, whole genome shotgun sequence. (Fragment)	GSTENG00002836001	86.548	_SK(ac)SASGDVLDPAER_	-1.03	0.744
carp-female_000000321_03749658_03759359	379	U2 small nuclear RNA auxiliary factor 2b	u2af2b	112.13	_EECSK(ac)YGQVK_	0.13527	
carp-female_000000321_03749658_03759359	433	U2 small nuclear RNA auxiliary factor 2b	u2af2b	131.35	_VVVTK(ac)YCDPDAYHR_	-0.55444	0.526
carp-female_000000321_04231825_04233006	182	unknown	unknown	52.891	_VSIAK(ac)SSDGTPK_	-0.59908	1.519
carp-female_000000321_04328519_04356924	2200	unknown	unknown	113.61	_YVTIQPGSK(ac)PK_	0.13823	1.184
carp-female_000000325_00825806_00831039	54	Nucleoporin 43	nup43	57.788	_AHK(ac)YSCDNAPCTAIVCR_	-0.57229	0.902
carp-female_000000325_01616569_01620109	172	Brain-subtype creatine kinase	ckbb	100.19	_GK(ac)YYALK_	0.64605	1.484
carp-female_000000325_04752520_04771216	425	Exocyst complex component 1	exoc1	58.246	_EK(ac)YEGLSR_	-0.11169	0.797
carp-female_000000325_06977607_06980313	70	Cardiac muscle actin	OlMA1	162.65	_GILTLK(ac)YPIEHGIITNWDDM(ox)EK_	1.196	3.439
carp-female_000000325_07482540_07486516	121	40S ribosomal protein S7	rps7	79.059	_SFQK(ac)IQVR_	0.53278	4.236
carp-female_000000325_07775362_07777824	45	Superoxide dismutase	unknown	110.4	_HHATYVNNLNVTEEK(ac)YQEALAK_	0.25445	1.008
carp-female_000000325_07775362_07777824	107	Superoxide dismutase	unknown	87.806	_DFGSFQK(ac)MK_	-0.98248	0.611

carp-female_000000325_07911751_07918447	352	Protein disulfide isomerase-related protein P5 (Precursor)	pdip5	67.981	_MMAEK(ac)YK_	-0.46291	0.405
carp-female_000000325_09092472_09100223	154	ATP-dependent RNA helicase DDX1	DDX1	109.04	_GK(ac)YYYEVACHDQGLCR_	0.022547	1.341
carp-female_000000325_09641427_09644339	269	Prostaglandin G/H synthase 2b	ptgs2b	59.733	_VCDILK(ac)QEHPDWDDER_	2.3029	
carp-female_000000325_09999928_10011153	385	Calcium-binding mitochondrial carrier protein SCaMC-1	slc25a24	114.4	_FMAYEQYK(ac)K_	-0.07547	2.077
carp-female_000000327_00230933_00241220	309	Annexin	anxa13	209.13	_SEIDLETIK(ac)DMYLEK_	-0.082211	0.741
carp-female_000000327_00230933_00241220	315	Annexin	anxa13	113.99	_DMYLEK(ac)YDVPLK_	0.0027876	0.716
carp-female_000000327_00230933_00241220	333	Annexin	anxa13	129.34	_EAISSECGGDFK(ac)R_	-0.56069	1.059
carp-female_000000327_01488446_01507644	143	Polymerase I and transcript release factor	ptrfb	158.3	_GNLEK(ac)QAGQIK_	0.22473	0.338
carp-female_000000327_01488446_01507644	497	Polymerase I and transcript release factor	ptrfb	132.21	_VVK(ac)SFTPDHTIYAR_	0.29528	1.267
carp-female_000000327_01698739_01714392	118	Thioredoxin domain-containing protein 5	TXNDC5	77.288	_LFK(ac)PEQEAVK_	-0.21363	
carp-female_000000327_01698739_01714392	125	Thioredoxin domain-containing protein 5	TXNDC5	154.69	_LFKPEQEAVK(ac)YQGPR_	-0.18662	0.575
carp-female_000000327_01698739_01714392	389	Thioredoxin domain-containing protein 5	TXNDC5	100.11	_DLESLHSFVMK(ac)QAR_	-0.048988	0.505
carp-female_000000329_00329479_00338686	434	Mitochondrial Rho GTPase 2	rhot2	40.211	_QHHGMSPSEFCYK(ac)HR_	-0.56126	0.84
carp-female_000000329_00342487_00345301	43	Histone H1.0	H10	112.44	_ATSHPK(ac)YSEMIK_	0.093782	1.049

carp-female_000000329_00342487_00345301	68	Histone H1.0	H10	109.29	_QSIQK(ac)YVK_	0.089844	1.027
carp-female_000000329_00342487_00345301	75	Histone H1.0	H10	84.173	_NHYK(ac)VGDNADSQIK_	1.5269	1.272
carp-female_000000329_01159915_01166616	280	Major facilitator superfamily domain-containing protein 1	MFSD1	117.93	_FIQDK(ac)YSGYSQK_	-0.26195	0.679
carp-female_000000330_01043094_01051071	74	L-lactate dehydrogenase	ldha	124.46	_GEAMDLQHGSLFLK(ac)THK_	-0.47514	0.879
carp-female_000000330_01043094_01051071	319	L-lactate dehydrogenase	ldha	206.2	_QLVK(ac)SAETLWGVQK_	0.92923	0.743
carp-female_000000330_02102781_02112531	112	Sulfide quinone reductase-like (Yeast)	sqrdl	102.07	_SK(ac)VAEFDPENNTVHTDSGK_	-0.36608	0.973
carp-female_000000330_02102781_02112531	172	Sulfide quinone reductase-like (Yeast)	sqrdl	218.6	_TVEK(ac)TWNALR_	0.10831	0.971
carp-female_000000330_02102781_02112531	236	Sulfide quinone reductase-like (Yeast)	sqrdl	125.53	_K(ac)YADALWEIVK_	0.27103	1.006
carp-female_000000330_02102781_02112531	246	Sulfide quinone reductase-like (Yeast)	sqrdl	108.56	_YADALWEIVK(ac)K_	-0.26057	0.431
carp-female_000000330_02102781_02112531	315	Sulfide quinone reductase-like (Yeast)	sqrdl	236.96	_GSTLDDADGWLDVNK(ac)HNLQHK_	-0.32927	1.194
carp-female_000000330_03172826_03180813	142	Annexin	anxa2a	166.69	_STAELM(ox)EIK(ac)K_	-1.8245	2.305
carp-female_000000330_03172826_03180813	146	Annexin	anxa2a	67.981	_VYK(ac)EFFK_	-0.13741	1.228
carp-female_000000330_03172826_03180813	188	Annexin	anxa2a	99.092	_RDEPSSVVDYQK(ac)IDEDAR_	0.098101	1.22
carp-female_000000330_03172826_03180813	225	Annexin	anxa2a	61.48	_SVPHLQK(ac)VFDR_	-0.20481	0.968

carp-female_000000330_03172826_03180813	231	Annexin	anxa2a	152.95	_YK(ac)SYSPYDMQESIR_	-0.24724	0.956
carp-female_000000330_03172826_03180813	306	Annexin	anxa2a	103.26	_QEFK(ac)AHHGK_	0.60282	1.161
carp-female_000000330_03700374_03704847	193	Isocitrate dehydrogenase 3 (NAD+) alpha	idh3a	111.63	_EVAENFK(ac)DVK_	0.16368	1.012
carp-female_000000330_03771375_03773835	195	ATP synthase oligomycin sensitivity conferral protein	atp5o	100.92	_GETIK(ac)LETK_	-0.35928	0.766
carp-female_000000330_04088457_04094656	8	Dihydrolipoyl dehydrogenase	dldh	114.96	_NQVTAK(ac)TADGEQVINTK_	-1.3074	
carp-female_000000330_04088457_04094656	259	Dihydrolipoyl dehydrogenase	dldh	135.23	_TEEQLKEEGVPYK(ac)VGK_	0.081782	0.864
carp-female_000000334_00236949_00244162	183	Mitochondrial ribosomal protein L12	mrpl12	42.785	_THFTVK(ac)LTELK_	-0.19554	1.025
carp-female_000000335_01029328_01043603	365	Zgc:171553 protein	cald1l	154.88	_LEQYTTAVQSHK(ac)EVR_	0.32898	0.945
carp-female_000000335_01029328_01043603	481	Zgc:171553 protein	cald1l	130.1	_SLWENK(ac)GSSATK_	0.41558	0.576
carp-female_000000337_00802749_00845010	899	Tenascin	TREES_T100003780	122.49	_IK(ac)YGPIAGGAHGEDMFPR_	1.1833	2.126
carp-female_000000339_01103817_01114804	169	Radixin	msna	77.894	_IQVWHEEHK(ac)GMLR_	0.28645	1
carp-female_000000339_01103817_01114804	242	Radixin	msna	51.528	_NISFNDK(ac)K_	0.30582	0.581
carp-female_000000339_01670839_01675182	196	Phosphoribosyl pyrophosphate synthetase 1A	prps1a	71.506	_LNVDFALIHK(ac)ER_	-0.85585	0.65
carp-female_000000339_01876789_01880422	180	CWC15 homolog	CWC15	54.157	_FMEK(ac)YVK_	-1.0397	1.176

carp-female_000000339_01891016_01895840	153	Zgc:110752	htatip	133.23	_GK(ac)TLPTPK(ac)R_	0.42559	1.794
carp-female_000000339_01891016_01895840	159	Zgc:110752	htatip	133.23	_GK(ac)TLPTPK(ac)R_	0.42559	1.794
carp-female_000000339_02175273_02183024	273	Pdha1 protein	pdha1a	66.299	_ADQLYK(ac)QK_	0.27442	0.304
carp-female_000000339_02175273_02183024	457	Pdha1 protein	pdha1a	145.14	_EATK(ac)FAADHCR_	0.11706	0.779
carp-female_000000339_02175273_02183024	503	Pdha1 protein	pdha1a	117.09	_SK(ac)SDPISMLK_	0.9017	0.925
carp-female_000000339_02175273_02183024	511	Pdha1 protein	pdha1a	84.507	_SDPISMLK(ac)DR_	-0.028502	1.159
carp-female_000000339_02304879_02319859	417	Eukaryotic translation initiation factor 4A, isoform 1B	eif4a1b	45.368	_NVDIFQK(ac)K_	0.69136	
carp-female_000000339_03080476_03083283	152	Annexin	anxa1a	85.744	_QVFK(ac)QDYK_	-2.3396	1.315
carp-female_000000339_03080476_03083283	240	Annexin	anxa1a	56.258	_YSK(ac)VDVAK_	0.058973	1.264
carp-female_000000339_03080476_03083283	245	Annexin	anxa1a	83.692	_VDVAK(ac)AIDLELK_	0.53083	1.497
carp-female_000000339_03080476_03083283	269	Annexin	anxa1a	66.989	_CAGNK(ac)SAFFAEK_	-1.2939	0.319
carp-female_000000339_03080476_03083283	307	Annexin	anxa1a	40.727	_SEIDLAK(ac)IK_	1.0323	0.812
carp-female_000000339_03080476_03083283	315	Annexin	anxa1a	112.36	_QEYQSK(ac)FGK_	1.0488	1.167
carp-female_000000339_03816552_03828805	135	Serine/threonine protein kinase ARAF	araf	65.231	_CQTCGYK(ac)FHQHCSSK_	-0.050478	1.28

carp-female_000000339_04915744_04930094	459	Si:dkey-286j20.1 protein (Fragment)	fam129bb	107.06	_K(ac)FDYDSSTVR_	-0.34955	1.253
carp-female_000000339_05038610_05044559	176	unknown	unknown	58.427	_GYK(ac)DYAWGHDELKPISK_	1.0833	1.026
carp-female_000000339_05414625_05415394	71	LOC100135331 protein	LOC100135331	112.71	_NCYYK(ac)TEDK_	0.44117	1.439
carp-female_000000339_05932828_05933256	130	Histone H2A.x	h2afx	72.662	_TGQAVASSGK(ac)SGK(ac)K_	0.10255	0.307
carp-female_000000339_05932828_05933256	133	Histone H2A.x	h2afx	61.265	_TGQAVASSGK(ac)SGK(ac)K_	0.10255	1.232
carp-female_000000339_06823472_06827590	17	Protein phosphatase 6, catalytic subunit	ppp6c	99.5	_QCK(ac)YLPENDLK_	0.21033	
carp-female_000000339_07254028_07258117	284	Carnitine O-acetyltransferase	UY3_08269	99.568	_AYNNLIK(ac)DK_	-1.1417	3.511
carp-female_000000339_07289908_07291636	41	Ribosomal protein L12	unknown	63.076	_ATGDWK(ac)GLR_	-0.47233	1.304
carp-female_000000339_07374562_07376423	58	Putative tubulin beta-2c chain-like protein	unknown	80.719	_INVYYNEATGGK(ac)YVPR_	-0.35159	1.709
carp-female_000000340_02172629_02189732	201	High density lipoprotein-binding protein (Vigilin)	hdlbpa	50.452	_FVIGK(ac)SGEK_	0.0056939	0.979
carp-female_000000340_03342324_03363204	497	Translocase of outer mitochondrial membrane 70 homolog A (Yeast)	tomm70a	145.6	_GNLDK(ac)AIDMFNK_	-0.18999	0.919
carp-female_000000340_03853070_03866459	401	Zgc:86841	phb2b	58.63	_AQFFVEK(ac)AK_	-0.35829	0.352
carp-female_000000340_06260156_06263609	97	LOC100135318 protein	LOC100135318	66.299	_NEDFK(ac)YVR_	0.51441	0.996
carp-female_000000340_06695274_06700680	287	SERPINE1 mRNA binding protein 1	serbp1a	54.486	_ANEGTDWK(ac)K_	-0.35802	0.683

carp-female_000000340_07651745_07673195	302	Dynamin-like 120 kDa protein, mitochondrial	opa1	56.547	_TQMK(ac)YQR_	0.18861	
carp-female_000000340_08050696_08058355	303	Phf16 protein	phf16	84.759	_MEPITK(ac)VSHIPPSR_	0.25572	1.002
carp-female_000000340_08150345_08170718	420	Cytoplasmic FMR1-interacting protein 1 homolog	cyfip1	78.548	_LVHPTDK(ac)YSNK_	0.32306	0.984
carp-female_000000340_08150345_08170718	592	Cytoplasmic FMR1-interacting protein 1 homolog	cyfip1	102.29	_SSLEGPTILDIEK(ac)FHR_	-1.0131	10.235
carp-female_000000340_09015910_09020996	245	Krt4 protein	krt4	271.45	_M(ox)LETK(ac)WSLLQEQTTTR_	-1.1382	1.065
carp-female_000000340_09015910_09020996	299	Krt4 protein	krt4	179.35	_NMQGLVEDFK(ac)NK_	-0.74585	1.105
carp-female_000000340_09015910_09020996	320	Krt4 protein	krt4	60.157	_ASVENEFVLLK(ac)K_	-0.5018	0.661
carp-female_000000340_09015910_09020996	456	Krt4 protein	krt4	161.48	_STK(ac)AEIAELNR_	-0.085947	1.147
carp-female_000000340_09053887_09057663	136	Zgc:77517	zgc:77517	208.68	_DYSK(ac)YNAILDDLR_	-0.13576	0.921
carp-female_000000340_09053887_09057663	175	Zgc:77517	zgc:77517	172.61	_VK(ac)FENELAIR_	-0.59444	0.859
carp-female_000000340_09053887_09057663	194	Zgc:77517	zgc:77517	190.03	_QSVEGDIAGLK(ac)K_	-0.53192	0.794
carp-female_000000340_09053887_09057663	222	Zgc:77517	zgc:77517	161.08	_LNVEGEIESLKEELLFLK(ac)K_	-0.34253	0.775
carp-female_000000340_09053887_09057663	266	Zgc:77517	zgc:77517	125.75	_ANYEK(ac)QALK_	0.52656	1.725
carp-female_000000340_09053887_09057663	270	Zgc:77517	zgc:77517	121.96	_QALK(ac)NAEELK_	0.64909	0.888

carp-female_000000340_09053887_09057663	378	Zgc:77517	zgc:77517	342.85	_SNITEQGHEYEALLNMK(ac)MK_	-1.2773	0.875
carp-female_000000340_09053887_09057663	389	Zgc:77517	zgc:77517	67.385	_LEAEISTYK(ac)K_	0.071066	0.731
carp-female_000000340_09207912_09220198	40	La-related protein 4 (Fragment)	unknown	68.536	_VVQTK(ac)YVEAK_	0.27914	0.534
carp-female_000000340_09305181_09322207	55	Putative chromatin remodeling factor subunit	unknown	92.247	_K(ac)YIQAEPPTNK_	-0.13757	0.806
carp-female_000000340_09751682_09758397	440	Alpha-enolase	ENOA	78.516	_LAK(ac)YNQILR_	0.42691	1.02
carp-female_000000340_10497000_10501726	29	Poly (ADP-ribose) polymerase family, member 3	parp3	52.482	_DK(ac)FTSVK_	0.90328	1.006
carp-female_000000340_10497000_10501726	340	Poly (ADP-ribose) polymerase family, member 3	parp3	83.194	_IIEK(ac)YLNATGR_	-0.54352	0.819
carp-female_000000340_13748766_13759247	97	Capping protein (Actin filament) muscle Z-line, alpha 1	capza1a	86.898	_QSFK(ac)FDHLR_	0.79393	1.108
carp-female_000000340_14515689_14516087	28	ATP synthase epsilon chain, mitochondrial	ATP5E	75.738	_AALK(ac)PQIK_	0.016399	0.862
carp-female_000000340_14517102_14542988	357	Adenosylhomocysteinase	ahcy	169.64	_GISEETTTGVHNLYK(ac)MLK_	1.1234	1.034
carp-female_000000340_14517102_14542988	379	Adenosylhomocysteinase	ahcy	94.767	_SK(ac)FDNLYGCR_	-1.0283	1.382
carp-female_000000340_14517102_14542988	549	Adenosylhomocysteinase	ahcy	56.937	_K(ac)LDEEVAAAHLDK_	0.91803	
carp-female_000000340_14517102_14542988	575	Adenosylhomocysteinase	ahcy	84.522	_QAK(ac)YLGLPR_	1.3546	1.767
carp-female_000000340_15609967_15613588	157	14-3-3 protein beta/alpha-1	ywhab1	103.14	_AYQDAFEISK(ac)R_	0.032349	1.04

carp-female_000000340_15624650_15626023	88	Cytochrome c oxidase subunit 6C-1	unknown	157.66	_QAYADFYK(ac)R_	0.22365	0.996
carp-female_000000340_15624650_15626023	94	Cytochrome c oxidase subunit 6C-1	unknown	66.953	_YDAMK(ac)EFNAMR_	0.12774	1.252
carp-female_000000340_15636352_15665196	173	unknown	unknown	137.69	_GSSTHLQTLSFTK(ac)IDFGGK_	0.067114	2.185
carp-female_000000340_15636352_15665196	361	unknown	unknown	54.772	_SK(ac)HLDNTLNPK_	-0.32511	1.444
carp-female_000000340_15636352_15665196	413	unknown	unknown	69.825	_LDLGIVK(ac)K_	0.17393	0.866
carp-female_000000340_15636352_15665196	582	unknown	unknown	95.502	_GK(ac)SDPYVK_	-0.15914	0.39
carp-female_000000340_15636352_15665196	943	unknown	unknown	55.437	_SDPYVK(ac)IHIGDTTFK_	0.88949	0.659
carp-female_000000340_15636352_15665196	952	unknown	unknown	62.287	_IHIGDTTFK(ac)SHVIK_	0.31657	0.962
carp-female_000000340_15636352_15665196	1119	unknown	unknown	106.93	_STSPQWSEAFHFLVHK(ac)PR_	-0.41793	0.946
carp-female_000000340_15636352_15665196	1177	unknown	unknown	88.596	_AQLK(ac)ILDSR_	0.11916	
carp-female_000000340_15636352_15665196	1462	unknown	unknown	151.04	_TQYNDEWFTLNDIK(ac)HGR_	0.70695	0.863
carp-female_000000340_16006372_16024582	177	Guanine nucleotide binding protein (G protein), alpha inhibiting activity polypeptide 2	gnai2b	214.82	_TTGIVETHFTFK(ac)DLHFK_	-0.83477	0.933
carp-female_000000340_16006372_16024582	182	Guanine nucleotide binding protein (G protein), alpha inhibiting activity polypeptide 2	gnai2b	115.24	_DLHFK(ac)MFDVGGQR_	-0.50702	0.861
carp-female_000000340_16540718_16544143	66	40S ribosomal protein S10	rps10	67.136	_DVHLAK(ac)HPELADK_	-0.0059677	3.876

carp-female_000000340_17309025_17311551	155	Probable N-acetyltransferase camello	CML	41.652	_K(ac)YGEVYR_	2.1121	0.975
carp-female_000000340_18706881_18719031	78	Serine hydroxymethyltransferase	SHMT2	175.56	_AALEAQGSCLNNK(ac)YSEGYPGK_	-0.48397	3.09
carp-female_000000340_18706881_18719031	167	Serine hydroxymethyltransferase	SHMT2	99.93	_AVPSPFEHADLVTSTTHK(ac)SLR_	0.023245	1.083
carp-female_000000340_18706881_18719031	253	Serine hydroxymethyltransferase	SHMT2	42.336	_AMADALLK(ac)K_	0.21939	0.885
carp-female_000000340_19142339_19149140	92	Dynactin subunit 2	dctn2	74.376	_ETPQQK(ac)YQR_	-0.56807	0.775
carp-female_000000341_00000685_00019677	253	Dynactin 1a	dctn1a	61.11	_IQLEQLQEWK(ac)NK_	0.24718	1.083
carp-female_000000342_00072012_00080301	39	Zgc:55733	zgc:55733	88.163	_ADVEAIFSK(ac)YGK_	-0.5021	1.715
carp-female_000000343_00778098_00784667	117	Microfibrillar-associated protein 3-like	MFA3L	93.228	_GK(ac)YTCVASNAHGK_	-0.94238	1.092
carp-female_000000343_00778098_00784667	201	Microfibrillar-associated protein 3-like	MFA3L	79.469	_AFEIAK(ac)R_	0.45281	0.129
carp-female_000000344_00960146_00977733	300	Chromosome undetermined SCAF8631, whole genome shotgun sequence. (Fragment)	GSTENG00006157001	81.799	_GSGIK(ac)WDLR_	-0.060046	
carp-female_000000344_02065294_02066962	46	Mitochondrial fission 1 protein	FIS1	124.67	_SK(ac)YTNDIVK_	0.63684	0.73
carp-female_000000345_01145593_01151483	74	40S ribosomal protein S4, X isoform	rps4x	56.205	_VAAPK(ac)HWMLDK_	-0.024288	1.521
carp-female_000000345_01145593_01151483	111	40S ribosomal protein S4, X isoform	rps4x	133.32	_LK(ac)YALTGDEVK_	0.013306	1.252
carp-female_000000345_01145593_01151483	129	40S ribosomal protein S4, X isoform	rps4x	58.981	_FIK(ac)IDGK_	0.34003	1.081

carp-female_000000345_01145593_01151483	258	40S ribosomal protein S4, X isoform	rps4x	95.264	_EK(ac)HPGSFDVVHVK_	-0.047091	1.326
carp-female_000000345_01145593_01151483	291	40S ribosomal protein S4, X isoform	rps4x	78.342	_GNK(ac)PWVSLPR_	0.27776	0.985
carp-female_000000345_01217590_01224829	71	Aspartate aminotransferase	got2b	111.12	_DDSGK(ac)PYVLSCVR_	-0.99312	0.907
carp-female_000000345_01217590_01224829	88	Aspartate aminotransferase	got2b	160.38	_AEALIASK(ac)MLDK_	0.25485	2.088
carp-female_000000345_01217590_01224829	131	Aspartate aminotransferase	got2b	79.492	_FHSVAK(ac)DVYLPK_	0.43464	0.638
carp-female_000000345_01217590_01224829	341	Aspartate aminotransferase	got2b	105.98	_EMLVTNLK(ac)K_	0.13051	1.053
carp-female_000000345_01642976_01686749	832	IQ motif containing GTPase activating protein 1	IQGAP1	40.941	_LQYFK(ac)DHINDVVK_	-0.57688	1.05
carp-female_000000345_01642976_01686749	1475	IQ motif containing GTPase activating protein 1	IQGAP1	113.24	_K(ac)YQDLINDIAK_	-0.057151	0.891
carp-female_000000345_01827847_01847374	206	LOC100127828 protein	LOC100127828	151.13	_DIESK(ac)YNVETK_	-0.59048	1.453
carp-female_000000345_01827847_01847374	365	LOC100127828 protein	LOC100127828	115.78	_GLDAEYK(ac)SK_	0.10209	1.053
carp-female_000000347_00458821_00461991	7	Chromosome 9 SCAF14729, whole genome shotgun sequence	GSTENG00023474001	123.76	_EYK(ac)LVVLGSGGVGK_	-0.19049	1.182
carp-female_000000347_00513340_00517929	77	Tubulin, alpha 2	tuba8l	111.11	_TIGGGDDSFNTFFSETGSGK(ac)HVPR_	0.29889	1.152
carp-female_000000347_01374388_01398191	352	Chromosome 12 SCAF14999, whole genome shotgun sequence. (Fragment)	GSTENG00029616001	67.685	_SDGQVYHTVHK(ac)DSGLYK_	0.46772	0.666
carp-female_000000348_01025883_01047204	279	PRP40 pre-mRNA processing factor 40 homolog A (Yeast)	prpf40a	74.789	_FLENHEK(ac)MTSTTR_	-1.0413	

carp-female_000000351_00655091_00691711	366	Rho GDP-dissociation inhibitor 1	UY3_10413	72.321	_EIVSGLK(ac)YVQQTFR_	0.65414	1.105
carp-female_000000353_00609948_00648017	469	Agps protein	agps	99.069	_VLQHEK(ac)QVYDIAAK_	0.37194	0.973
carp-female_000000353_00609948_00648017	609	Agps protein	agps	121.82	_GLSDPVHVYEK(ac)VEHAAR_	-0.48113	1.107
carp-female_000000353_01429207_01429677	52	Endozepine	unknown	105.46	_AK(ac)WDAWEAK_	-0.93343	0.056
carp-female_000000355_00973054_01017573	445	DNA topoisomerase 2	top2b	49.715	_AQTQLNK(ac)K_	0.6515	2.731
carp-female_000000355_00973054_01017573	631	DNA topoisomerase 2	top2b	63.419	_TWHIK(ac)YYK_	0.59943	1.188
carp-female_000000355_00973054_01017573	634	DNA topoisomerase 2	top2b	61.235	_YYK(ac)GLGTSTSK_	0.053257	1.968
carp-female_000000357_00814871_00820100	110	Zgc:153569	glg1b	131.96	_CLFNHK(ac)YEESMSDK_	-1.0763	
carp-female_000000365_00378042_00430372	3707	Mesothelin	UY3_05875	53.756	_K(ac)QILLNSAR_	-0.088569	0.601
carp-female_000000370_00067012_00068544	55	Zgc:92406	cyp8b1	57.249	_DTAK(ac)FLQR_	1.4924	1.947
carp-female_000000375_00085107_00092079	473	Short/branched chain specific acyl-CoA dehydrogenase, mitochondrial '	ACADSB	55.084	_DYPIEK(ac)YYR_	-0.41879	1.412
carp-female_000000375_00113722_00118085	65	Fumarate hydratase, mitochondrial	fh	59.709	_VPSDK(ac)YYGAQTVR_	0.70871	1.351
carp-female_000000375_00113722_00118085	99	Fumarate hydratase, mitochondrial	fh	41.892	_AFGILK(ac)K_	0.84611	0.818
carp-female_000000375_00179393_00187228	222	Annexin	anxa11b	74.537	_VPLLAAYK(ac)TTYGK_	0.33063	0.757

carp-female_000000375_00179393_00187228	299	Annexin	anxa11b	194.77	_ADYGK(ac)SLEDAITSDTSGHFR_	-0.52378	1.086
carp-female_000000375_00179393_00187228	406	Annexin	anxa11b	230.93	_ETSGDLESGMVAVVK(ac)CIK_	-0.79639	1.1
carp-female_000000375_00179393_00187228	458	Annexin	anxa11b	177.08	_QFGK(ac)SLYTHISGDTSGDYK_	-0.53701	0.978
carp-female_000000375_00179393_00187228	473	Annexin	anxa11b	203.99	_SLYTHISGDTSGDYK(ac)K_	-1.1006	0.514
carp-female_000000395_00108634_00111326	69	Reticulon	rtn4a	56.514	_SNEGHPFK(ac)WFLEK_	-0.61096	0.743
carp-female_000000416_00043923_00061851	36	Endonuclease-reverse transcriptase	unknown	65.252	_SLDWPK(ac)K_	-0.0055824	1.542
carp-female_000000422_00059759_00061263	9	GF20391	Dana\GF20391	90.913	_GGK(ac)GLGK(ac)GGAK_	0.67984	2.569
carp-female_000000422_00059759_00061263	13	GF20391	Dana\GF20391	95.502	_GLGK(ac)GGAK(ac)R_	0.53646	0.993
carp-female_000000422_00059759_00061263	17	GF20391	Dana\GF20391	95.502	_GLGK(ac)GGAK(ac)R_	0.53646	0.476
carp-female_000000422_00059759_00061263	32	GF20391	Dana\GF20391	143.31	_DNIQGITK(ac)PAIR_	-0.17641	0.991
carp-female_000000422_00059759_00061263	128	GF20391	Dana\GF20391	158.56	_AVTK(ac)TAGK(ac)GGK_	-0.19619	0.658
carp-female_000000422_00059759_00061263	132	GF20391	Dana\GF20391	158.56	_AVTK(ac)TAGK(ac)GGK_	-0.19619	0.843
carp-female_000000422_00059759_00061263	151	GF20391	Dana\GF20391	170.04	_ESYAIYVYK(ac)VLK_	0.0048004	0.941
carp-female_000000422_00059759_00061263	154	GF20391	Dana\GF20391	90.966	_VLK(ac)QVHPDTGISSK_	-1.3468	1.252

carp-female_000000422_00059759_00061263	193	GF20391	Dana\GF20391	58.167	_LAHYNK(ac)R_	0.25729	0.848
carp-female_000000422_00059759_00061263	216	GF20391	Dana\GF20391	186.97	_LLLPGELAK(ac)HAVSEGTK_	-0.10054	1.173
carp-female_000000422_00059759_00061263	224	GF20391	Dana\GF20391	76.826	_HAVSEGTK(ac)AVTK(ac)YTSSK_	0.31103	0.789
carp-female_000000422_00059759_00061263	228	GF20391	Dana\GF20391	148.32	_HAVSEGTK(ac)AVTK(ac)YTSSK_	0.31103	0.928
carp-female_000000574_00003096_00007559	264	unknown	unknown	77.744	_TIHSGEYK(ac)LK_	-0.061783	0.416
carp-female_000000602_00002028_00004616	186	Zgc:112350	ddx47	77.894	_ALK(ac)YLVMDEADR_	1.2407	1.465
carp-female_000000652_00003283_00003514	70	unknown	unknown	101.64	_LVQNLNK(ac)R_	-0.025373	0.873
carp-female_000002562_00000078_00000729	7	Annexin	anxa5b	145	_DLVDDLK(ac)SELGGK_	0.42011	0.755
carp-female_000002562_00000078_00000729	63	Annexin	anxa5b	156.2	_SANEINEIK(ac)SLYK_	0.23194	0.89
carp-female_000002562_00000078_00000729	67	Annexin	anxa5b	147.26	_SLYK(ac)QEHNDDLEEDVTGDTAGHFK_	0.03686	0.876
carp-female_000002562_00000078_00000729	87	Annexin	anxa5b	76.492	_QEHNDDLEEDVTGDTAGHFK(ac)R_	-0.050391	0.966
carp-female_000019400_00000333_00000700	19	Chromosome undetermined SCAF9415, whole genome shotgun sequence. (Fragment)	GSTENG00006971001	71.806	_IMK(ac)HEGPAAFYK_	0.3327	0.951
carp-female_000030818_00001287_00001442	28	TNF receptor-associated protein 1	trap1	103.08	_YVAQAHDK(ac)PR_	-1.0007	0.245
carp-female_000030837_00000001_00001695	26	TNF receptor-associated protein 1	trap1	118.72	_LISAETDIVVDHYK(ac)EEK_	-1.4435	0.932

carp-female_000032378_00001877_00002196	84	Zgc:171897 protein	zgc:171897	115.34	_TTETDHTGEYK(ac)LK_	0.67606	0.907
carp-female_000057495_00000122_00001392	14	LOC100145057 protein (Fragment)	LOC100145057	118.9	_QLLSLK(ac)AEYK_	-0.3099	0.669
carp-female_000057495_00000122_00001392	91	LOC100145057 protein (Fragment)	LOC100145057	156.48	_TLLELK(ac)GQYK_	1.0707	0.615
carp-female_000058005_00000989_00003423	37	Xrcc5 protein	xrcc5	93.623	_IVGYK(ac)AVTEEK_	-1.9211	22.147
carp-female_000058005_00000989_00003423	57	Xrcc5 protein	xrcc5	52.576	_SWAVVDAQSHK(ac)R_	-0.25124	0.936
carp-female_000058005_00000989_00003423	104	Xrcc5 protein	xrcc5	90.827	_VDEDQMK(ac)YK_	-1.9327	1.111
carp-female_000058169_00000393_00004695	40	Actin related protein 2/3 complex, subunit 2	arpc2	171.26	_FFK(ac)ELQEHGADELLK_	-0.13991	0.879
carp-female_000060758_00000076_00000796	186	unknown	unknown	74.392	_STNTSAK(ac)YSK_	1.0257	29.124
carp-female_000062162_00000443_00007828	284	Supervillin	svila	132.51	_AAELATFVQTK(ac)HDLGCR_	-0.24005	1.844
carp-female_000066018_00001031_00003361	113	Sorting and assembly machinery component 50 homolog A	samm50	78.225	_ETSYGLSFFK(ac)PQPGHFER_	-0.69641	1.067
carp-female_000067678_00003958_00004350	90	Cellular nucleic acid-binding protein	CNBP	85.362	_ASEVNCYNCGK(ac)SGHVAK_	-0.34984	
carp-female_000069478_00000229_00003699	141	Eukaryotic translation elongation factor 2	eef2b	54.871	_FSK(ac)SANGPDGK_	0.77581	1.774
carp-female_000070885_00000516_00001006	78	Collagen alpha-4(VI) chain (Fragment)	Col6a4	46.462	_QVINNIK(ac)QR_	0.68929	0.066
carp-female_000075362_00002177_00008138	265	unknown	unknown	67.997	_AK(ac)YQYGGVSSGR_	-0.26633	1.082

carp-female_000075562_00000295_00000925	83	60S ribosomal protein L11	rpl11	64.224	_AEEILEK(ac)GLK_	0.14021	0.783
carp-female_000083949_00001258_00001844	11	LOC100145220 protein	LOC100145220	50.392	_ISNVK(ac)PADLGVDVTSR_	-0.12934	0.858
carp-female_000088672_00000545_00001833	118	Carnitine O-acetyltransferase (Fragment)	C9JBD1	81.92	_FVK(ac)AMDDPAK_	-0.338	1.281
carp-female_000094154_00000222_00003211	31	ATP synthase, H+ transporting, mitochondrial F0 complex, subunit d	atp5h	126.03	_AGMVDEFEK(ac)K_	-0.8581	1.163
carp-female_000094154_00000222_00003211	32	ATP synthase, H+ transporting, mitochondrial F0 complex, subunit d	atp5h	106.93	_K(ac)FAALTVPEPVDTQTAK_	1.2919	0.955
carp-female_000094154_00000222_00003211	58	ATP synthase, H+ transporting, mitochondrial F0 complex, subunit d	atp5h	55.705	_IDAQEQESNK(ac)TAAAYLEASK_	2.2846	
carp-female_000094154_00000222_00003211	68	ATP synthase, H+ transporting, mitochondrial F0 complex, subunit d	atp5h	111.31	_TAAAYLEASK(ac)AR_	-0.056976	0.73
carp-female_000094154_00000222_00003211	108	ATP synthase, H+ transporting, mitochondrial F0 complex, subunit d	atp5h	77.42	_AK(ac)YPYWPHKPIADL_	1.91	0.902
carp-female_000110191_00000120_00000494	19	Histone H2B	LOC570661	142.83	_AVTK(ac)TAGK(ac)SGK_	-0.317	0.658
carp-female_000110191_00000120_00000494	23	Histone H2B	LOC570661	142.83	_AVTK(ac)TAGK(ac)SGK_	-0.317	0.678
carp-female_000110191_00000120_00000494	115	Histone H2B	LOC570661	76.826	_HAVSEGTK(ac)AVTK(ac)YTSSK_	0.31103	0.789
carp-female_000112197_00000940_00002638	221	Myosin-9	PAL_GLEAN10015410	105.65	_VDYK(ac)ADEWLMK_	-0.21303	1.433
carp-female_000112324_00000597_00001020	98	unknown	unknown	76.573	_AETQVQELQVK(ac)HAESER_	0.24863	1.685

carp-female_000116705_00002576_00003046	12	Zgc:110216 protein (Fragment)	zgc:110216	67.095	_ALAAGGYDVEK(ac)NNSR_	-0.89429	3.848
carp-female_000118762_00000124_00000435	82	unknown	unknown	55.37	_AFHTGK(ac)YK_	0.93776	0.275
carp-female_000151529_00000375_00001559	118	Pbx2 (Fragment)	pbx2	53.013	_K(ac)FSSIQTQLK_	0.018091	0.989
carp-female_000154339_00007781_00010254	74	60S ribosomal protein L18a (Fragment)	unknown	52.495	_IFAPNHVVAK(ac)SR_	0.20393	0.974
carp-female_000154339_00007781_00010254	176	60S ribosomal protein L18a (Fragment)	unknown	71.176	_RPAIK(ac)QFHDSK_	-0.05468	1.546
carp-female_000154339_00007781_00010254	184	60S ribosomal protein L18a (Fragment)	unknown	75.738	_IK(ac)FPLPHR_	0.041497	1.357

Table S 6. roteins showing significantly differential abundance between AS-challenged and control fish, given in descending order of Log2 fold-change (Causey et al., 2018).

NCBI accession	Protein product	Fold-change (Log2)
XP_021480534	Complement c1q-like protein 2	3.917
XP_021446773	Eosinophil peroxidase	3.915
XP_021438648	Leukocyte cell-derived chemotaxin-2-like	2.837
XP_021466891	Cerebellin-2-like	2.756
XP_021441170	High choriolytic enzyme 1	2.565
XP_021417046	Sequestosome-1	2.417
XP_021442122	Ferritin heavy subunit	2.411
XP_021462825	Haptoglobin-like	2.359
XP_021451323	Microfibril-associated glycoprotein 4-like	2.133
XP_021417220	Complement C3	2.054
XP_021439265	SIL1 nucleotide exchange factor	1.992
XP_021441697	Haptoglobin-like	1.979
XP_021417240	Complement C3	1.917
XP_021469499	Catechol O-methyltransferase domain-containing protein 1-like	1.698
XP_021475009	ATP-binding cassette sub-family A member 1-like	1.446
XP_021436350	Uncharacterized LOC106608805	1.350
XP_021474674	Histone H2AX	1.291
XP_021431988	Angiotensinogen (serpin peptidase inhibitor, clade A, member 8)	1.273
XP_021449457	Probable C-mannosyltransferase DPY19L1	1.263
XP_021417877	C-type lectin domain family 4 member E-like	1.199
XP_021454428	Nucleobindin-2-like	1.183
XP_021458892	Ribosomal protein L28	1.148
XP_021475868	Complement c1q-like protein 3	1.133
XP_021413091	Metalloreductase STEAP4	1.069
XP_021416974	Mannosyl-oligosaccharide 1,2-alpha-mannosidase IC-like	1.061
XP_021454217	L-threonine 3-dehydrogenase, mitochondrial-like	0.996
XP_021474489	Complement factor B-like	0.979
XP_021442709	Alpha-2-macroglobulin-like	0.966
XP_021423951	Uncharacterized LOC106611396	0.962
XP_021423876	Complement C3-like	0.935
XP_021467115	Actin, alpha cardiac	0.923
XP_021445885	Complement factor B-like	0.882
XP_021480047	Apolipoprotein A-IV-like	0.858
XP_021464723	Nuclear factor of kappa light polypeptide gene enhancer in B-cells 2, p49/p100	0.853
XP_021467190	Leucine-rich alpha-2-glycoprotein-like	0.811
XP_021481050	Probable ATP-dependent RNA helicase DDX5	0.772
XP_021460419	Ceruloplasmin (ferroxidase)	0.757
XP_021479504	Hypoxia up-regulated protein 1-like	0.715
XP_021430114	Fibrinogen-like protein 1-like protein	0.714
XP_021417252	Complement C3	0.680
XP_021425166	Carboxylesterase 5A	0.662

XP_021481346	ATP-dependent Clp protease proteolytic subunit, mitochondrial-like	0.662
XP_021451946	Complement C4-like	0.650
XP_021479838	Transcription factor BTF3 homolog 4	0.637
XP_021462359	Complement component 5	0.625
XP_021442137	Complement C4-like	0.591
XP_021453075	Dnaj homolog subfamily B member 11-like	0.581
XP_021480381	Eukaryotic translation initiation factor 1	0.575
XP_021475794	Thioredoxin domain-containing protein 5-like	0.569
XP_021464769	Microtubule-associated protein 1 light chain 3 alpha	0.563
XP_021461669	Family with sequence similarity 160, member B1	0.558
XP_021428745	Neutral cholesterol ester hydrolase 1-like	0.537
XP_021454752	Vesicle-trafficking protein SEC22b-B-like	0.513
XP_021446601	78 kda glucose-regulated protein	0.511
XP_021476867	Endoplasmic reticulum mannosyl-oligosaccharide 1,2-alpha-mannosidase-like	0.481
XP_021481745	Reticulocalbin 3, EF-hand calcium binding domain	0.478
XP_021478379	Golgi phosphoprotein 3	0.477
XP_021441988	Furin-1-like	0.454
XP_021473449	Glutathione S-transferase kappa 1-like	0.437
XP_021460947	Endoplasmin-like	0.418
XP_021438958	Transmembrane emp24 domain-containing protein 9-like	0.403
XP_021421845	Tyrosine-protein phosphatase non-receptor type 1-like	0.398
XP_021455883	Calreticulin-like	0.381
XP_021434540	DEAD (Asp-Glu-Ala-Asp) box helicase 3, X-linked	0.378
XP_021456822	Transmembrane protein 214-like	0.376
XP_021420055	C4b-binding protein alpha chain-like	0.365
XP_021439514	Transmembrane 9 superfamily member 2-like	0.354
XP_021429629	Sec23 homolog A, COPII coat complex component	0.323
XP_021412244	Ethanolamine-phosphate cytidylyltransferase	0.315
XP_021437539	NADPH--cytochrome P450 reductase	0.306
XP_021451429	ATP synthase, H+ transporting, mitochondrial Fo complex, subunit F2	−0.257
XP_021472646	Alpha-enolase	−0.286

XP_021463425	Regulator of microtubule dynamics protein 2-like	−0.298
XP_021414705	Brain-specific angiogenesis inhibitor 1-associated protein 2-like	−0.331
XP_021418673	Thimet oligopeptidase	−0.333
XP_021458913	Proteasome 26S subunit, non-atpase 5	−0.362
XP_021419800	APEX nuclease (multifunctional DNA repair enzyme) 1	−0.366
XP_021469331	Niemann-Pick C1 protein-like	−0.366
XP_021472978	Dynein light chain 2, cytoplasmic	−0.378
XP_021419888	Inter-alpha-trypsin inhibitor heavy chain H2-like	−0.378
XP_021430578	ATP synthase, H+ transporting, mitochondrial Fo complex, subunit s (factor B)	−0.379
XP_021439703	Nuclear cap-binding protein subunit 1-like	−0.382
XP_021424380	Inter-alpha-trypsin inhibitor heavy chain H3-like	−0.403
XP_021425476	Uncharacterized LOC106565741	−0.405
XP_021459433	Basigin (Ok blood group)	−0.425
XP_021439789	Tryptophan 2,3-dioxygenase A-like	−0.426
XP_021474939	Acid ceramidase-like	−0.438
XP_021461466	WD repeat domain 11	−0.439
XP_021421009	C-reactive protein, pentraxin-related	−0.480
XP_021458562	Phosphatidylinositol transfer protein beta isoform-like	−0.482
XP_021439959	Tripeptidyl peptidase I	−0.482
XP_021433346	High mobility group protein B3-like	−0.495
XP_021479945	Beta-glucuronidase-like	−0.522
XP_021478259	Lysosome membrane protein 2-like	−0.525
XP_021412279	Arylformamidase	−0.526
XP_021444801	Phosphotriesterase related	−0.531
XP_021461213	Lysosome membrane protein 2-like	−0.573
XP_021478257	Lysosome membrane protein 2-like	−0.582
XP_021481136	Serine protease hepsin-like	−0.584
XP_021453070	Isocitrate dehydrogenase [NADP] cytoplasmic-like	−0.593
XP_021469787	Eukaryotic translation initiation factor 2B, subunit 5 epsilon, 82kda	−0.594
XP_021470341	Serum albumin 1	−0.649
XP_021460202	ATP-binding cassette, sub-family C (CFTR/MRP), member 2	−0.665

XP_021420795	Family with sequence similarity 234, member A	−0.688
XP_021466049	Neurofascin	−0.718
XP_021440760	Apolipoprotein B-100-like	−0.738
XP_021419747	Prestin-like	−0.810
XP_021445727	Transferrin receptor protein 1-like	−0.881
XP_021467201	Apolipoprotein B-100	−0.883

*Table S 7. A complete list of differentially expressed proteins of spleen of rainbow trout in response to Yersinia ruckeri strains. Fold change (infected vs control) was statistically analysed in Y. ruckeri CSF007-82 (biotype 1) and 7959-11 (biotype 2) infected and control rainbow trout samples (n = 27). *denotes statistically significant difference according to both* ANOVA *and post hoc Tukey's HSD with FDR-adjusted* p-*value <0.05 and fold change < −2 or > +2 (Kumar et al., 2018).*

Accession	Protein	No. of quantified peptides	FDR-adjusted p-value ANOVA (3 dpe)	FDR-adjusted p-value ANOVA (9 dpe)	FDR-adjusted p-value ANOVA (28 dpe)	Spleen control in response to strain	Fold change 3 dpe	Fold change 9 dpe	Fold change 28 dpe
LYSC2_ONCMY	Lysozyme C II	6	0.04	0.16	0.42	CSF007-82	**4.6***	11.8	3.7
						7959-11	**3.0***	6.6	3.5
W8W0Y8_ONCMY	Glutathione peroxidase	5	0.03	0.05	0.12	CSF007-82	1.9	1.3	1.6
						7959-11	**2.2***	1.9	1.4
Q60FB5_ONCMY	NADPH oxidase cytosolic protein p67phox	4	0.03	0.22	0.76	CSF007-82	**2.7***	2.2	-1.3
						7959-11	**3.1***	2.1	-1.4
Q60FB6_ONCMY	NADPH oxidase cytosolic protein p40phox	6	0.03	0.14	0.05	CSF007-82	**3.0***	2.6	1.5
						7959-11	**3.0***	2.2	1.3
C1BHL9_ONCMY	Ras-related C3 botulinum toxin substrate 2	2	0.00	0.01	0.14	CSF007-82	**7.3***	**5.4***	3.6
						7959-11	**5.2***	**4.9***	3.4
C1BFF6_ONCMY	Thioredoxin	4	0.03	0.03	0.10	CSF007-82	1.8	**2.3***	2.0
						7959-11	1.6	2.0	1.8
C1BH85_ONCMY	Thioredoxin	5	0.02	0.07	0.10	CSF007-82	**3.3***	4.8	3.6
						7959-11	**2.8***	2.6	3.1
B5X4P4_SALSA	Cathepsin B	2	0.12	0.02	0.05	CSF007-82	2.3	**3.8***	**2.6***
						7959-11	1.5	**2.9***	**2.6***
Q9DFJ1_ONCMY	Chemotaxin (Fragment)	5	0.03	0.05	0.63	CSF007-82	**4.9***	3.6	1.5
						7959-11	**4.2***	3.0	1.3
Q92004_ONCMY	Beta-2-microglobulin	4	0.13	0.05	0.35	CSF007-82	2.2	**4.1***	2.0
						7959-11	1.7	**3.0***	2.1
A0A060VM33_ONCMY	Metalloendopeptidase	6	0.05	0.35	0.05	CSF007-82	4.0	-1.3	**3.1***

						7959-11	4.7	1.5	1.7
C0HBR8_SALSA	Metalloreductase STEAP4	2	0.35	0.02	0.78	CSF007-82	2.2	**3.7***	1.2
						7959-11	2.6	**2.2***	1.4
B5X1B5_SALSA	Alpha-enolase	2	0.01	0.01	0.05	CSF007-82	**3.1***	**3.0***	**2.4***
						7959-11	**3.2***	**2.9***	1.8
A0A060VVF4_ONCMY	Transgelin	2	0.16	0.03	0.07	CSF007-82	2.9	**2.4***	2.5
						7959-11	2.5	1.6	1.8
B9EM17_SALSA	Transaldolase	2	0.04	0.35	0.40	CSF007-82	**2.5***	1.6	1.3
						7959-11	**2.6***	1.6	1.3
A0A060X145_ONCMY	Tetraspanin	2	0.02	0.02	0.04	CSF007-82	**4.0***	**4.5***	**3.7***
						7959-11	**2.9***	**5.2***	**3.2***
C0PUI9_SALSA	Fructose-1,6-bisphosphatase 1 (Fragment)	6	0.03	0.35	0.04	CSF007-82	**3.6***	1.5	**2.5***
						7959-11	**4.0***	1.9	1.7
A0A060XEX6_ONCMY	Glucose-6-phosphate 1-dehydrogenase	6	0.05	0.30	0.40	CSF007-82	**2.3***	1.5	1.3
						7959-11	**3.0***	1.4	1.0
B5X4R9_SALSA	6-phosphofructo-2-kinase/fructose-2,6-biphosphatase 4	2	0.04	0.71	0.93	CSF007-82	1.5	1.1	1.0
						7959-11	**2.0***	1.2	1.1
C0H8V3_SALSA	Pyruvate kinase	3	0.23	0.03	0.66	CSF007-82	1.8	1.8	1.3
						7959-11	1.9	**2.2***	1.2
A0A060Y7U5_ONCMY	Aminomethyltransferase	2	0.89	0.37	0.01	CSF007-82	1.5	-1.5	**17.8***
						7959-11	2.2	1.3	**10.3***
B5X1B2_SALSA	Phosphoacetylglucosamine mutase	3	0.66	0.03	0.65	CSF007-82	1.2	**2.1***	1.1
						7959-11	1.2	1.9	1.1
B5X0W0_SALSA	Serine/threonine-protein phosphatase	3	0.14	0.01	0.34	CSF007-82	1.7	1.9	1.4
						7959-11	1.5	**2.0***	1.2
C1BHY0_ONCMY	Epididymal secretory protein E1	4	0.10	0.04	0.57	CSF007-82	2.3	**4.9***	1.6
						7959-11	1.8	**3.0***	1.8
C1BEX7_ONCMY		2	0.30	0.03	0.09	CSF007-82	2.3	**2.7***	3.0

	Hemoglobin subunit alpha-4					7959-11	1.5	1.7	2.3
B5XAH0_SALSA	Fatty acid-binding protein intestinal	5	0.02	0.29	0.87	CSF007-82	-1.3	1.2	-1.1
						7959-11	**-2.9***	-1.4	1.1
C0HBS0_SALSA	ADP/ATP translocase 2	5	0.66	0.03	0.35	CSF007-82	1.3	**2.0***	1.0
						7959-11	1.3	1.8	1.2
B9ENC0_SALSA	Cellular nucleic acid-binding protein	5	0.02	0.00	0.03	CSF007-82	**5.4***	**7.2***	**5.7***
						7959-11	**4.5***	**7.1***	**4.3***
F8RP06_ONCMA	Ribosomal protein S5	5	0.01	0.00	0.05	CSF007-82	**3.6***	**3.7***	**3***
						7959-11	**3.2***	**3.2***	**2.7***
B5DGY1_SALSA	Ribosomal protein S27-3	2	0.39	0.03	0.52	CSF007-82	1.8	**2.7***	1.7
						7959-11	1.2	1.8	1.6
C1BHQ0_ONCMY	60S ribosomal protein L36	4	0.11	0.03	0.35	CSF007-82	1.5	**2.2***	1.3
						7959-11	1.3	1.8	1.4
B5DGG8_SALSA	40S ribosomal protein S12	3	0.02	0.03	0.09	CSF007-82	**2.1***	**2.7***	1.7
						7959-11	1.6	2.0	1.7
B9EL24_SALSA	Small nuclear ribonucleoprotein F	2	0.02	0.03	0.02	CSF007-82	**2.1***	**2.7***	**2.4***
						7959-11	**2.2***	**2.6***	**2.8***
Q8UUJ3_ONCKE	Type I collagen alpha 2 chain (Fragment)	6	0.04	0.10	0.18	CSF007-82	-1.7	-2.0	-2.1
						7959-11	**-2.0***	-1.7	-1.5
B5X1G4_SALSA	Cysteinyl-tRNA synthetase, cytoplasmic	6	0.55	0.03	0.48	CSF007-82	1.5	**3.5***	1.2
						7959-11	1.8	**2.7***	1.7
C0HB50_SALSA	Probable ATP-dependent RNA helicase DDX5	5	0.03	0.05	0.79	CSF007-82	1.9	2.3	1.1
						7959-11	**2.6***	2.0	1.2
Q9I9G8_ONCMY	B-actin (Fragment)	2	0.02	0.04	0.19	CSF007-82	**2.1***	1.9	1.6
						7959-11	**2.1***	1.8	1.5
C1BH21_ONCMY	Dynein light chain 1, cytoplasmic	3	0.06	0.01	0.04	CSF007-82	2.0	**2.9***	**2.4***
						7959-11	1.7	**2.9***	**2.1***
B5X1V0_SALSA	Erythrocyte band 7 integral membrane protein	2	0.47	0.02	0.82	CSF007-82	1.2	**2.9***	1.1
						7959-11	1.5	**2.6***	1.0

C1BGJ3_ONCMY	Transmembrane emp24 domain-containing protein 7	2	0.05	0.02	0.33	CSF007-82	2.9	**2.6***	1.6
						7959-11	2.5	**2.2***	1.5
K1C18_ONCMY	Keratin. type I cytoskeletal 18	6	0.02	0.10	0.34	CSF007-82	-1.4	-1.1	-1.6
						7959-11	**-2.0***	-1.4	-1.2
A0A060Z9I8_ONCMY	Protein S100	3	0.01	0.07	0.53	CSF007-82	-1.7	-1.4	-1.5
						7959-11	**-3.2***	-1.8	-1.1
C1BHS7_ONCMY	Protein S100	2	0.04	0.09	0.10	CSF007-82	-1.3	-1.5	-1.1
						7959-11	**-2.4***	-1.4	1.2
C1BEZ5_ONCMY	C6orf115	2	0.02	0.03	0.03	CSF007-82	**3.0***	**4.0***	**2.8***
						7959-11	**2.5***	**2.5***	**2.2***
A0A060Y668_ONCMY	Caveolin	2	0.68	0.69	0.01	CSF007-82	1.4	-1.8	**-7.8***
						7959-11	-1.1	-1.3	1.4
B5X242_SALSA	Flotillin-2a	3	0.90	0.03	0.52	CSF007-82	-1.2	-1.2	1.2
						7959-11	-1.0	**2.1***	1.5
A0A060YAR2_ONCMY	Uncharacterized protein	4	0.03	0.13	0.45	CSF007-82	**5.8***	7.7	1.6
						7959-11	**5.4***	5.3	2.5
A0A060YML0_ONCMY	Uncharacterized protein	4	0.13	0.03	0.17	CSF007-82	2.9	**2.7***	1.5
						7959-11	2.1	**2.3***	1.4
A0A060YTX4_ONCMY	Uncharacterized protein (Fragment)	2	0.14	0.03	0.19	CSF007-82	1.9	**4.7***	2.0
						7959-11	1.3	**2.7***	1.9
A0A060YV33_ONCMY	Uncharacterized protein (Fragment)	5	0.04	0.24	0.80	CSF007-82	**2.3***	1.0	1.4
						7959-11	**2.7***	1.5	1.0
A0A060WK59_ONCMY	Uncharacterized protein	4	0.55	0.05	0.65	CSF007-82	2.3	**2.5***	1.5
						7959-11	2.0	1.6	1.2
A0A060YMT8_ONCMY	Uncharacterized protein	6	0.05	0.64	0.44	CSF007-82	**2.5***	1.2	1.5
						7959-11	**3.1***	1.7	1.3
A0A060WLD1_ONCMY	Uncharacterized protein	6	0.03	0.20	0.61	CSF007-82	**2.1***	2.4	1.4
						7959-11	**2.4***	1.5	1.3
A0A060YHU0_ONCMY	Uncharacterized protein	4	0.24	0.02	0.45	CSF007-82	1.7	**3.0***	1.4

						7959-11	1.6	**2.3***	1.4
A0A060XQJ4_ONCMY	Uncharacterized protein	3	0.03	0.06	0.76	CSF007-82	**2.1***	1.7	1.2
						7959-11	**2.3***	1.6	1.1
A0A060Z016_ONCMY	Uncharacterized protein (Fragment)	3	0.03	0.97	0.04	CSF007-82	**3.1***	-1.3	**2.0***
						7959-11	**3.2***	-1.2	1.6
A0A060YZE3_ONCMY	Uncharacterized protein	2	0.05	0.02	0.78	CSF007-82	3.6	**4.4***	1.0
						7959-11	2.2	**2.5***	-1.7
A0A060Y8K0_ONCMY	Uncharacterized protein (Fragment)	2	0.02	0.08	0.57	CSF007-82	**4.4***	5.8	1.4
						7959-11	**3.3***	2.5	1.6
A0A060XSB4_ONCMY	Uncharacterized protein	3	0.23	0.03	0.04	CSF007-82	3.0	**2.9***	**4.4***
						7959-11	2.1	**2.3***	**2.9***
A0A060W2V1_ONCMY	Uncharacterized protein	4	0.02	0.05	0.07	CSF007-82	**2.4***	2.1	2.1
						7959-11	**2.5***	1.8	1.9
A0A060ZFF1_ONCMY	Uncharacterized protein	2	0.13	0.03	0.18	CSF007-82	1.8	**3.1***	1.7
						7959-11	2.6	**2.4***	1.4
A0A060XU19_ONCMY	Uncharacterized protein	2	0.02	0.22	0.18	CSF007-82	**2.2***	2.1	2.1
						7959-11	**2.8***	2.1	1.9
A0A060XFS7_ONCMY	Uncharacterized protein (Fragment)	4	0.02	0.04	0.49	CSF007-82	**2.1***	**2.3***	1.7
						7959-11	1.8	1.9	3.7
A0A060YG41_ONCMY	Uncharacterized protein	2	0.08	0.03	0.23	CSF007-82	3.2	**4.9***	3.0
						7959-11	1.9	**3.3***	2.1
A0A060ZAC8_ONCMY	Uncharacterized protein (Fragment)	2	0.04	0.13	0.36	CSF007-82	**2.3***	1.5	1.8
						7959-11	**3.0***	1.8	1.3
A0A060YMH1_ONCMY	Uncharacterized protein	3	0.09	0.03	0.35	CSF007-82	1.8	**2.1***	1.5
						7959-11	1.8	**2.3***	1.4
A0A060YIL0_ONCMY	Uncharacterized protein (Fragment)	4	0.23	0.02	0.50	CSF007-82	1.9	**2.3***	1.6
						7959-11	1.9	1.9	1.4
A0A060Z4D4_ONCMY	Uncharacterized protein (Fragment)	4	0.46	0.03	0.73	CSF007-82	1.5	**2.8***	-1.1
						7959-11	1.6	1.9	1.1

A0A060WA19_ONCMY	Uncharacterized protein	2	0.03	0.13	0.32	CSF007-82	**2.7***	2.3	1.9
						7959-11	1.8	1.8	1.1
A0A060Y9N6_ONCMY	Uncharacterized protein (Fragment)	2	0.65	0.06	0.04	CSF007-82	1.6	2.8	**3.8***
						7959-11	1.4	2.2	**2.3***
A0A060YQ22_ONCMY	Uncharacterized protein (Fragment)	2	0.03	0.14	0.37	CSF007-82	1.6	1.8	1.5
						7959-11	**2.5***	1.2	1.3
A0A060Y7T4_ONCMY	Uncharacterized protein	2	0.45	0.03	0.35	CSF007-82	1.8	**2.3***	1.3
						7959-11	1.8	1.6	1.1
A0A060YXS6_ONCMY	Uncharacterized protein	4	0.84	0.03	0.34	CSF007-82	1.2	**2.2***	1.6
						7959-11	-1.1	1.7	1.6
A0A060VQZ6_ONCMY	Uncharacterized protein	6	0.04	0.08	0.12	CSF007-82	**-2.4***	-2.9	-3.2
						7959-11	**-2.4***	-2.5	-2.4
A0A060W754_ONCMY	Uncharacterized protein	6	0.45	0.37	0.04	CSF007-82	-1.4	-1.7	**-2.1***
						7959-11	-1.1	-1.1	-1.7
A0A060W4N0_ONCMY	Uncharacterized protein	6	0.02	0.60	0.39	CSF007-82	**-4.8***	-3.3	-1.5
						7959-11	**-3.8***	-2.1	-1.3
A0A060YPN6_ONCMY	Uncharacterized protein	6	0.09	0.01	0.22	CSF007-82	-2.0	-1.9	-2.2
						7959-11	-2.2	**-2.0***	-1.5
A0A060WT62_ONCMY	Uncharacterized protein	4	0.61	0.01	0.65	CSF007-82	-1.8	**-4.9***	-1.3
						7959-11	-1.1	-1.0	1.2
A0A060YPS5_ONCMY	Uncharacterized protein	6	0.02	0.22	0.95	CSF007-82	-1.8	-1.3	1.0
						7959-11	**-2.7***	-1.2	-1.0
A0A060X9U4_ONCMY	Uncharacterized protein	2	0.04	0.24	0.81	CSF007-82	-1.8	-1.5	-1.2
						7959-11	**-3.0***	-1.9	-1.2
A0A060YYU3_ONCMY	Uncharacterized protein	2	0.02	0.72	0.37	CSF007-82	**-6.0***	-1.5	-2.0
						7959-11	**-3.5***	1.0	-1.1
A0A060WR72_ONCMY	Uncharacterized protein	2	0.05	0.09	0.35	CSF007-82	-1.8	-1.6	-1.5
						7959-11	**-2.1***	-1.5	-1.3
A0A060XIH9_ONCMY	Uncharacterized protein	2	0.90	0.94	0.01	CSF007-82	-1.6	-1.2	**-3.0***

						7959-11	-1.6	-1.1	**-2.4***
A0A060WP40_ONCMY	Uncharacterized protein	2	0.02	0.59	0.72	CSF007-82	-1.2	-2.2	-1.1
						7959-11	**-4.9***	-1.1	-1.4
A0A060XNH5_ONCMY	Uncharacterized protein	2	0.03	0.02	0.35	CSF007-82	**-2.1***	-1.9	-1.5
						7959-11	-1.9	-2.0	-1.5

Table S 8. Identified proteins from D. labrax skin mucus grouped into biological groups (Cordero et al., 2015b)

SN [a]	Protein	Symbol [b]	Species	ID/Database [c]	p*I*/MW [d]	S/C [e]	U/T [f]
	Structural proteins						
39	Actin beta	ACTB	*Dicentrarchus labrax*	CAD60932/NCBI	5.29/42.1	51/2	1/1
66	Actin, cytoplasmic 1	ACTB	*Ctenopharyngodon idella*	P83751/Sprot	5.30/42.1	20/4	1/1
79	Actin, cytoplasmic 1	ACTB	*Oreochromis mossambicus*	P68143/Sprot	5.30/42.1	856/40	7/16
85	Actin, cytoplasmic 1	ACTB	*Oreochromis mossambicus*	P68143/Sprot	5.30/42.1	266/20	7/7
95	Alpha actinin-4 isoform X1	ACTN	*Stegastes partitus*	XP_008281276/NCBI	4.90/103.2	578/14	1/7
6	Coactosin-likeprotein-like	COTL1	*Oryzias latipes*	XP_004069874/NCBI	4.83/16.2	141/19	1/2
5	Cofilin-2	COF2	*Dicentrarchus labrax*	FM006818/EST	8.38/28.2	167/16	5/5
84	F-actin-capping protein subunit alpha-2	CAPZA2	*Salmo salar*	ACN58682/NCBI	5.84/32.3	131/11	1/2
65	F-actin-capping protein subunit alpha-1	CAPZA1	*Dicentrarchus labrax*	CBN80762/NCBI	5.42/32.8	80/14	2/2
60	Gelsolin-like	GSNL1	*Oreochromis mossambicus*	ABE98236/NCBI	5.96/42.9	66/5	3/3
89	Gelsolin-like	GSNL1	*Stegastes partitus*	XP_008276815/NCBI	6.54/79.8	159/6	1/4
92	Gelsolin-like	GSNL1	*Xiphophorus maculatus*	XP_005802408/NCBI	6.28/79.6	241/7	6/6
100	Gelsolin-like	GSNL1	*Oreochromis mossambicus*	ABE98236/NCBI	5.96/42.9	87/5	2/2
7	Keratin type II cytoskeletal 8-like	KRT8	*Maylandia zebra*	XP_004545214/NCBI	5.03/62.2	104/5	1/3
26	Keratin, type I cytoskeletal 17-like	KRT17	*Stegastes partitus*	XP_008298721/NCBI	5.22/48.3	128/3	3/3
90	Keratin, type II cytoskeletal 8-like	KRT8	*Stegastes partitus*	XP_008303627/NCBI	5.97/50.3	82/7	2/2
93	Keratin, type I cytoskeletal 13-like	KRT13	*Lepisosteus oculatus*	XP_006638395/NCBI	5.05/49.7	63/2	1/6
47	Microfibril-associatedglycoprotein 4	MFAP4	*Dicentrarchus labrax*	FM019963/NCBI	5.88/30.0	95/12	2/2
3	Myosin light polypeptide 6	MYL6	*Anoplopoma fimbria*	ACQ58516/NCBI	4.41/17.1	61/17	2/2
88	Scinderin-likeprotein	SCINL	*Paralichthys olivaceus*	AFQ38973/NCBI	6.54/80	120/4	1/3
28	Type II keratin E3-like protein	KRT	*Sparus aurata*	AAT44423/NCBI	4.89/38.6	71/6	1/2
78	Type II keratin E3	KRT	*Oncorhynchus mykiss*	NP_001123458/NCBI	5.32/55.3	509/20	1/12
63	Tropomyosin alpha-1 chain	TPM1	*Liza aurata*	P84335/Sprot	4.69/32.8	24/4	1/1
55	Vimentin	VIM	*Cynoglossus semilaevis*	XP_008332705/NCBI	5.26/52.8	47/3	1/2
76	Vimentin	VIM	*Cyprinus carpio*	1807305A/NCBI	5.07/52.6	49/3	1/2
18	Profilin	PFN1	*Dicentrarchus labrax*	FM000924/EST	7.74/23.5	280/16	4/4
	Protein metabolism						
54	40S ribosomalprotein S18	40S	*Ictalurus punctatus*	Q90YQ5/Sprot	10.99/17.7	19/5	1/1

41	60S ribosomalprotein L15	60S	*Carassius auratus*	Q7T3N9/Sprot	11.53/24.1	13/3	1/1
87	Alcohol dehydrogenase	ADH	*Salmo salar*	ACN10195/NCBI	6.32/37.2	99/6	1/2
24	Anterior gradient protein 2 homolog	AGR2	*Maylandia zebra*	XP_004561006/NCBI	8.87/19.1	136/22	2/4
22	Cyclin-dependent kinase 7	CDK7	*Carassius auratus*	P51953/Sprot	8.98/38.6	19/4	1/1
82	Elogantion factor 1-alpha	EF1A	*Oryzias latipes*	Q9YIC0/Sprot	9.23/50.6	24/6	1/1
9	Golgi-associated plant pathogenesis-related protein 1-like	GAPR1	*Maylandia zebra*	XP_004576580/NCBI	5.38/18.7	62/6	1/1
45	Progonadoliberin-2	GNRH2	*Clarias gariepinus*	P43306/Sprot	9.27/10	19/10	1/1
34	Secretagogin	SCGN	*Astyanax mexicanus*	XP_007256889	5/31.7	117/8	2/2
8	SH3 domain-binding glutamic acid-rich-like protein	SH3BGRL	*Osmerus mordax*	ACO10145/NCBI	4.78/13.1	68/21	2/2
27	Translationally-controlled tumor protein	TCTP	*Dicentrarchus labrax*	FM000425/EST	5.91/31.8	73/11	3/3
	Carbohydrate metabolism						
59	Deoxycytidylate deaminase	DCTD	*Dicentrarchus labrax*	FM019776/NCBI	8.60/31.7	67/3	1/1
75	Enolase A	ENOA	*Acipenser baerii*	ABF60006/NCBI	5.98/47.5	125/10	3/3
58	Fructose-bisphosphatealdolase B	ALDOB	*Sparus aurata*	P53447/Sprot	8.43/40.2	17/4	1/1
50	Glyceraldehyde-3-phosphate dehydrogenase	GAPDH	*Oncorhynchus mykiss*	O42259/Sprot	6.37/36.6	18/5	1/1
86	Inosine-uridine preferring nucleoside hydrolase-like	IUNH	*Maylandia zebra*	XP_004575422/NCBI	6.88/35.4	63/5	2/2
11	Inositol monophosphatase	IMPA	*Dicentrarchus labrax*	CBN82127/NCBI	5.47/28.9	403/29	4/6
20	Nucleoside diphosphate kinase	NDK	*Siniperca chuatsi*	AAY79301/NCBI	5.86/13	107/37	2/4
44	Phosphatidylethanolamine binding protein	PEBP	*Ictalurus punctatus*	NP_001187975/NCBI	6.82/21.2	92/13	3/3
4	Phosphatidylinositol 3,4,5-trisphosphate 5-phosphatase 2B	INPPL1	*Sparus aurata*	FM148029/NCBI	4.54/13.2	54/8	1/1
71	Transaldolase-like	TALDO	*Oryzias latipes*	XP_004066906/NCBI	6.69/37.8	163/9	3/3
68	Triosephosphate isomerase B	TPI1B	*Oreochromis niloticus*	XP_003450633/NCBI	6.9/26.9	151/14	3/3
69	Triosephosphate isomerase B	TPI1B	*Oryzias latipes*	BAD17901/NCBI	6.14/23	182/24	1/4
	RNA/DNA metabolism						
51	Heterogeneous nuclear						
	ribonucleoprotein A0	HNRNPA0	*Salmo salar*	ACI67551/NCBI	9.1/29.4	119/6	1/1
61	Homeobox protein HMX3-B	HMX3B	*Oryzias latipes*	Q90XN9/Sprot	6.42/32.6	13/2	1/1
35	Protein SET-like	SEPSIP	*Oreochromis niloticus*	XP_003439510/NCBI	4.15/31.1	93/8	2/2
94	RNA-bindingprotein 12	RBP12	*Stegastes partitus*	XP_008296875/NCBI	9.24/95.5	45/1	1/1
52	Transducin-like enhancer protein 1	TLE1	*Oryzias latipes*	XP_004072378/NCBI	8.08/69.5	45/1	1/1

73	Histone H1	H1	*Astyanax fasciatus*	AEC13086/NCBI	11.05/20.8	46/5	1/1
81	Histone H4	H4	*Oncorhynchus mykiss*	P62797/Sprot	11.36/113.6	25/11	1/1
	Signal transduction						
23	14-3-3 protein epsilon-like isoform X1	14-3-3	*Poecilia formosa*	XP_007563007/NCBI	5.02/36.9	153/10	3/3
30	14-3-3 protein beta/alpha-A-like	14-3-3	*Astyanax mexicanus*	XP_007230880/NCBI	4.65/28	178/15	2/4
31	14-3-3 protein beta/alpha-1-like	14-3-3	*Xiphophorus maculatus*	XP_005805709/NCBI	4.62/27.7	291/21	3/6
32	14-3-3 protein epsilon-like isoform X1	14-3-3	*Stegastes partitus*	XP_008291071/NCBI	4.74/30	116/10	1/2
21	S100-A6	S100A6	*Anoplopoma fimbria*	ACQ58920/NCBI	5.08/13	74/11	1/1
80	Rab GDP dissociation inhibitor beta-like	GDI2	*Astyanax mexicanus*	XP_007252464/NCBI	5.6/50.8	368/16	2/6
19	Rho GDP-dissociation inhibitor 1	GDI1	*Dicentrarchus labrax*	FM018448/EST	5.36/32.4	88/11	1/2
37	Rho GDP-dissociation inhibitor 1-like	GDI1	*Oryzias latipes*	XP_004071582/NCBI	5.01/23.5	178/16	4/4
	Immune-related protein						
17	Antifreeze protein	AFP	*Dicentrarchus labrax*	FN565768/EST	6.47/21.8	88/14	2/2
16	Apolipoprotein A-1	APOA1	*Morone saxatilis*	ACH90227/NCBI	4.75/20.6	300/31	4/7
33	Apolipoprotein A-1	APOA1	*Morone saxatilis*	ACH90229/NCBI	5.09/16.1	434/35	5/8
64	Apoptosis-associated speck-like protein containing a CARD	ASC	*Dicentrarchus labrax*	FM020581/EST	5.85/28.5	196/11	2/2
1	Calmodulin	CALM	*Electrophorus electricus*	P02594/Sprot	4.6/16.8	96/7	2/2
2	Calmodulin	CALM	*Electrophorus electricus*	P02594/Sprot	4.09/16.8	118/11	1/1
72	Calreticulin precursor	CALR	*Dicentrarchus labrax*	AGI60286/NCBI	4.37/49.4	258/17	2/5
48	Caspase-1	CASP1	*Dicentrarchus labrax*	AM984268/EST	8.57/24.5	293/32	5/5
15	Caspase-6	CASP6	*Cynoglossus semilaevis*	XP_008315389/NCBI	6.02/34.5	84/5	1/1
36	C1q family protein	C1Q	*Dicentrarchus labrax*	FM002850/EST	8.64/19.4	100/15	1/3
38	C1q-like protein	C1Q	*Dicentrarchus labrax*	FM000708/EST	5.77/25.4	143/9	2/2
42	C1q tumor necrosis factor-related protein 3-like	C1Q	*Dicentrarchus labrax*	FL487070/EST	8.03/20.2	278/45	2/7
77	Complement component 3	C3	*Solea senegalensis*	ACR20030/NCBI	6.04/6.5	69/17	1/1
83	Complement component 3	C3	*Epinephelus coioides*	ADU33222/NCBI	6.07/186.2	62/1	2/2
102	Complement component 3	C3	*Larimichthys crocea*	AHZ41228/NCBI	6.15/186.8	108/2	2/3
101	Complement component 3	C3	*Sparus aurata*	ADM13620/NCBI	8.08/186.9	67/1	1/2
25	Cyclophilin A	CyPA	*Gadus morhua*	AEK21703/NCBI	8.51/18	48/5	1/1
74	Endoplasmic reticulum p57	PDIA3	*Dicentrarchus labrax*	AGI60170/NCBI	5.39/56.3	256/18	5/7
97	Endoplasmic reticulum p57	PDIA3	*Dicentrarchus labrax*	AGI60170/NCBI	5.39/56.3	122/8	4/4

13	Fucose-binding lectin	FBL	*Dicentrarchus labrax*	ACF94293/NCBI	6.08/34.8	317/29	6/6
14	Fucose-binding lectin	FBL	*Dicentrarchus labrax*	ACF94293/NCBI	6.08/34.8	212/13	5/5
43	Fucose binding protein precursor	FBL	*Morone chrysops*	ABB29990/NCBI	6.21/34.7	115/7	2/2
46	Glutathione S-transferase omega-1	GST	*Anoplopoma fimbria*	ACQ58017/NCBI	7.01/27.8	47/3	1/1
49	Glutathione S-transferase mu	GST	*Takifugu obscurus*	ABV24049/NCBI	5.47/26.4	124/11	1/3
91	Heat shock protein 70 kDa	HSP70	*Dicentrarchus labrax*	AAR01102/NCBI	5.31/71.6	52/5	2/2
29	Leukocyte elastase inhibitor	LEI	*Dicentrarchus labrax*	CBN81773/NCBI	4.9/44.7	205/14	5/5
67	Lysozyme	LYZ	*Paralichthys olivaceus*	Q90VZ3/NCBI	8.69/21.4	86/14	2/2
70	Lysozyme g protein	LYZ	*Dicentrarchus labrax*	CBJ56263/NCBI	8.53/20.4	58/9	1/1
6	Natural killer cell enhancing factor	NKEF	*Anoplopoma fimbria*	ACQ58049/NCBI	6.3/22.2	212/18	3/4
104	Protein disulphide isomerase precursor	PDI1	*Dicentrarchus labrax*	AGI60172/NCBI	4.54/57.2	323/11	6/7
12	Superoxide dismutase Cu/Zn	SOD	*Dicentrarchus labrax*	FM000596/EST	6.18/22.0	99/6	1/1
98	Transferrin	TF	*Dicentrarchus labrax*	ACN80997/NCBI	5.93/76	1103/38	21/23
99	Transferrin	TF	*Dicentrarchus labrax*	ACN80997/NCBI	5.93/76	69/2	1/1
96	Warm temperature acclimation protein 65-1	WAP65A	*Dicentrarchus labrax*	DAA12503/NCBI	5.45/49.7	423/26	1/11
103	Warm temperature acclimation protein 65-2	WAP65B	*Dicentrarchus labrax*	DAA12504/NCBI	5.47/49.3	948/50	19/20

[a] SN: spot number in reference 2DE gel.
[b] Protein symbol according to Uniprot database.
[c] Identification or accession number according to the corresponding database.
[d] Theoretical *pI* and mass (kDa) for each identified protein.
[e] Total protein score (S) and percentage of coverage (C) for each identified protein.
[f] Total unique peptides (U) against total matched peptides (T).

Table S 9. Identification of protein species differing in spot intensity as an effect of growth in the presence of skin mucus proteins (Uttakleiv Ræder et al., 2007b).

Spot no.	Protein	MS[a]	Matched peptides	SC[b]	MW Teor./ Obs.	PI Teor./ Obs.	Function
Heat shock proteins and chaperones							
2701	DnaK	196	IINEPTAAALAYGLDK	11	68379/65000	4.59/4.90	Member of the 70-kDa heat shock protein (HSP70) family
			AKLESLVEDLVVR				
			SLGQFNLEGIQAAPR				
			ITIQASGGLTDEEIEAMVQEAEANKDADK				
2702	GroEL	36	SFGAPTITK	12	57651/50000	4.68/4.95	The GroEL chaperonin system, molecular chaperone similar to HSP60.
			ELLPTLEAVAK				
			MLEGVNVLADAVK				
			AAVEEGVVAGGGVALIR				
1002[c]	CsaA	45	METIAYGDFAK	10	12568/12000	4.79/4.80	Chaperone like protein, part of csa operon in *E. coli*
Cell mobility							
1502	FlaC	36	EAIQQEVGALNDELNR	4	39776/37000	4.67/4.80	Flagellin subunits including flaA, flaB, flaC, flaD and flaE.
2501	FlaD	43	AVAILDSAMQYVDSNR	4	40000/37000	4.90/4.95	Flagellin subunits including flaA, flaB, flaC, flaD and flaE.
1501	FlaE	96	SFQVGADSGEAVMLTLNNLR	18	41715/37000	4.65/4.70	Flagellin subunits including flaA, flaB, flaC, flaD and flaE.
			AGDDIEEVATYINGQTDK				
			VSASVGEDGK				
			TVGNIDVTTVAGSQNAVAVVDAAMK				
Antioxidant protein							
2401	Thiol peroxidase-glutaredoxin fusion peroxidase (TPx·Grx)	131	EGQSVPQVTFPTR	15	27018/23000	5.60/ 5.20	Lipid hydroperoxide reductase, AhpC/TSA subfamily
			GLNYEEVVLGK				
			TTVPQVFIGGK				
2202	AhpC	150	NTAIEDGGIGQVK,	17	22394/19000	4.72/5.00	Alkyl hydroperoxide reductase, AhpC/TSA family
			GSFLIDADGLVR				
			HQVVNDLPLGR				
Energy metabolism							
3405	Malate dehydrogenase	140	GYCGEDPTPALEGADVVLISAGVAR	8	32517/28000	4.83/5.40	Catalyzes the reversible oxidation of malate to oxaloacetate: (S)-malate+NAD(+)=oxaloacetate+NADH.
6401	6-phosphofructo-kinase	96	EALIQNIQDGIAK	4	34897/27000	5.62/5.80	Catalyzes the formation of D-fructose 1,6-bisphosphate from D-fructose 6-phosphate in glycolysis
5603		117	AQVVVLGAGPAGYSAAFR	13	52630/46000	5.97/5.70	

	Pyruvate/2-oxoglutarate dehydrogenase complex, dihydrolipoamide dehydrogenase component		CADLGLDTVLIER				Reaction: Protein N(6)-(dihydrolipoyl)lysine+NAD(+)=protein N(6)-(lipoyl)lysine+NADH
			YNTLGGVCLNVGCIPSK				
			VIPSIAYTEPEVAWVGK				
4601	Glycerol kinase	356	YIVALDQGTTSSR	17	55817/44000	5.17/5.50	Catalyzes the formation of glycerol 3-phosphate: ATP+glycerol=ADP+sn-glycerol 3-phosphate
			ENTGLVVDPYFSGTKELDIPLSMMPEVKIPI				
			DQQAALYGQMCVEQGQAKATLESIAYQTR				
			DVIDAMQADSGIK				
2602	ATP synthase beta chain	86	LVLEVQQQLGGGVVR	12	50862/47000	4.82/5.10	F-type H+-transporting ATPase beta chain
			YTLAGTEVSALLGR				
			DIIAILGMDELSEEDKQVVSR				
Transport							
4301	ABC-type amino acid transport.	78	IVAQDWDGIIPSLLAR	16	28684/21000	6.08/5.50	ABC-type amino acid transport/signal transduction systems, periplasmic component/domain
			KYDAIIAAMSITEER				
			YGSFDEAYLDLK				
1602	ABC-type uncharacterised transport system	20	MMCHR EPQHEYTK ERQMQRIR	4	60000/45000	4.80/4.6	Duplicated ATPase component
2301[c]	ABC-type sugar transport system	52	AILINPTDSDAVSNAIR	5	30860/21000	5.25/5.10	Periplasmic binding proteins and sugar binding domain of the LacI family
Metabolism of cofactors/amino acid metabolism/Lipid metabolism/Nucleoside metabolism							
3105	6,7-dimethyl-8-ribityllumazine synthase	327	MNVIEGGVAAPNAK	33	16542/14000	5.17/5.40	Catalyzes the condensation of 5-amino-6-(1′-D)-ribityl-amino-2,4(1 H,3 H)-pyrimidinedione with L-3,4-dihydrohy-2-butanone-4-phosphate yielding 6,7-dimethyl-8-lumazine
			FGQVSEENITVVR				
			CPGAVELPLVAQR				
			YDAIVSLGSVIR				
5401	Cysteine synthase	160	IYEDNSQTIGNTPLVR	36	34753/26000	5.37/5.70	Pyridoxal-phosphate dependent enzyme, catalysing the O3-acetyl-L-serine+hydrogen sulfide=L-cysteine+acetate
			LTLTMPASMSLER				
			YLLLQQFNNPANPAIHEK				
			AVLSVAVEPAESPVIAQALAGEEIKPAPHK				
			IQGIGAGFIPGNLDLTLIDR				
			LMEEEGILAGISSGAAVVAANR				
4503	Alanine dehydrogenase	348	LPLLAPMSEVAGR	21	39705/38000	5.69/5.50	Alanine dehydrogenase catalyzes the NAD-dependent reversible reductive amination of pyruvate into alanine
			MSIQAGAQTLEK				

			GLLLGGVPGVEPAK				
			VVIVGGGVVGANAAR				
			VVYSTVDAIEK				
			TSTFALNNATLPYIIK				
3504[c]	3-oxoacyl-[acyl-carrier-protein] synthase I/II	42	TGIVAGSGGASSLNQVNAVDILR	11	42576/37000	5.08/5.40	Reaction: acyl-ACP+malonyl-ACP=3-oxoacyl-ACP+CO2+ACP
			MAMQNVDSVDYVNTHGTSTPVGDAK				
5201	Purine nucleoside phosphorylase	63	LMDVVIGMGASTDSK	12	25723/20000	5.37/5.75	purine nucleoside+phosphate=purine+alpha-D-ribose 1-phosphate
			SFNDMMTVALETAIK				
Genetic Information Processing							
6101	Ribosomal protein L10	78	AAAFEGAVTDADVLATLPTYDEAIAR	20	13983/14500	5.89/5.85	LSU ribosomal protein L10P
8403	Ribosomal protein S2	90	TVPMFNEALAELAK	5	26791/24000	8.59/8.90	30S ribosomal protein S2
6104[d]	Arginine repressor	60	QIDHLTKVRRTMR LURAFKALLK	13	20000/14000	6.00/6.80	Transcription factor
Unclassified/hyphotetical							
3104[d]	Predicted O-methyltransferase	22	SPLDHDCPRWR	23	31000/16000	5.40/5.40	O-methyltransferase possibly involved in polyketide biosynthesis
			TRFYRLDNGRCR				
			DHDCPRWRSWQRWIAR				
			IPSELLQPLWLRSR				
			WRSWQR				
			LDTRFYR				
			NGRCRWFELDTDENLLWRER				
5103[d]	Uncharacterized membrane-associated protein	15	GRYSRYFRAMRYRLLTNPYFRQVRRRLLA	20	22000/13000	5.75/5.50	DedA family
			RPFIN-LFTIR				
5202[d]	Predicted sulfurtransferase	61	EKHHIR	10	37000/21000	5.75/5.50	Member of the Rhodanese Homology Domain
			RFREREKKCHGKHSEEQVE				
			RFRERNRTKVKLKK				
			QVERFRER				

Protein spot identity is based on MS/MS product ion data searched by the MASCOT search engine and peptide de novo sequencing. The spot numbers correlate with the numbers indicated in Figure 45.

[a] Mascot score. [b] Sequence coverage (SC) in percentage. [c] Proteins displaying reduced spot intensity as function of mucus proteins in the growth media. [d] De novo sequenced.

Table S 10. Complete list of all detected proteins by shotgun MS in plasma of Atlantic cod (with gonad somatic index < 1). Proteins are listed according to their relative abundance in % (calculated according to Zybailov et al. 2006), and are presented with their Gadus morhua EST identification (ID) and the respective identified protein homolog and its homolog accession (acc.) and e-value from the NCBI BLASTp non-redundant search (Skogland Enerstvedt et al., 2017).

	Rel. abnd., %	*Gadus morhua* EST ID	Homolog acc.	Protein homolog	E-value
1	41,60	GENSCAN00000016011	AEB31264	14 kDa apolipoprotein, partial [Epinephelus bruneus]	2,0E-53
2	9,33	GENSCAN00000035282	XP_010792180	PREDICTED: apolipoprotein A-I [Notothenia coriiceps]	3,0E-83
3	3,10	GENSCAN00000059677	XP_005752392	PREDICTED: alpha-2-macroglobulin-like, partial [Pundamilia nyererei]	5,0E-20
4	2,06	GENSCAN00000035270	Q56TU0	RecName: Full=Type-4 ice-structuring protein; AltName: Full=Antifreeze protein type IV; Flags: Precursor [Gadus morhua]	9,0E-81
5	1,67	GENSCAN00000019236	Q92079	RecName: Full=Serotransferrin, partial [Gadus morhua]	1,0E-173
6	1,50	GENSCAN00000017833	AAG13324	hemopexin-like protein, partial [Gillichthys mirabilis]	1,0E-58
7	1,37	GENSCAN00000020822	CBX31964	fibrinogen beta chain precursor [Plecoglossus altivelis]	2,0E-155
8	1,36	GENSCAN00000026416	XP_010901644	PREDICTED: hemopexin-like [Esox lucius]	3,0E-22
9	1,16	GENSCAN00000026760	ABA03142	liver angiotensinogen [Rhabdosargus sarba]	0,0E+00
10	1,12	GENSCAN00000019012	XP_014045532	PREDICTED: alpha-2-macroglobulin-like protein 1 [Salmo salar]	1,0E-21
11	0,91	GENSCAN00000032266	XP_008430852	PREDICTED: hemopexin [Poecilia reticulata]	9,0E-38
12	0,85	GENSCAN00000014629	AAD19585	immunoglobulin light chain L1 region J-C 10.3, partial [Gadus morhua]	5,0E-41
13	0,84	GENSCAN00000056826		No homolog	
14	0,80	GENSCAN00000013380	XP_006807286	PREDICTED: alpha-2-macroglobulin-like [Neolamprologus brichardi]	6,0E-22
15	0,77	GENSCAN00000008741	XP_005752387	PREDICTED: alpha-2-macroglobulin-like [Pundamilia nyererei]	5,0E-61
16	0,76	GENSCAN00000060214	XP_017288315	PREDICTED: hemopexin [Austrofundulus limnaeus]	5,0E-169
17	0,74	GENSCAN00000016018	XP_004550997	PREDICTED: apolipoprotein C-I-like [Maylandia zebra]	4,0E-18
18	0,74	GENSCAN00000074793	XP_018542557	PREDICTED: complement C1q-like protein 2 [Lates calcarifer]	8,0E-62
19	0,73	GENSCAN00000059408	XP_011611035	PREDICTED: complement C3-like [Takifugu rubripes]	7,0E-03
20	0,72	GENSCAN00000001502	XP_010740565	PREDICTED: apolipoprotein A-IV-like [Larimichthys crocea]	1,0E-55
21	0,71	GENSCAN00000030172	XP_004568432	PREDICTED: pleiotropic regulator 1-like [Maylandia zebra]	0,0E+00
22	0,61	GENSCAN00000021623	XP_008430852	PREDICTED: hemopexin [Poecilia reticulata]	5,0E-38
23	0,57	GENSCAN00000042176	ACU86959	warm temperature acclimation-related 65 kDa protein [Paralichthys olivaceus]	3,0E-14
24	0,55	GENSCAN00000021070	AAF72568	immunoglobulin D heavy chain constant region variant b [Gadus morhua]	5,0E-48
25	0,55	GENSCAN00000003371	XP_010738618	PREDICTED: alpha-2-macroglobulin-like isoform X1 [Larimichthys crocea]	0,0E+00

26	0,55	GENSCAN00000008521	CAA10691	MHC class I [Gadus morhua]	3,0E-38
27	0,50	GENSCAN00000007861	CAA12451	immunoglobulin light chain [Gadus morhua]	2,0E-13
28	0,48	GENSCAN00000076544	CAB91906	immunoglobulin heavy chain variable region [Gadus morhua]	3,0E-42
29	0,48	GENSCAN00000061534	XP_007573447	PREDICTED: alpha-2-macroglobulin-like [Poecilia formosa]	8,0E-15
30	0,48	GENSCAN00000029118	XP_005158243	PREDICTED: uncharacterized protein LOC101883708 [Danio rerio]	7,0E-11
31	0,47	GENSCAN00000015937	Q1AGS6	RecName: Full=Hemoglobin subunit beta-2; AltName: Full=Beta-2-globin; AltName: Full=Hemoglobin beta-2 chain [Boreogadus saida]	6,0E-48
32	0,40	GENSCAN00000020825	XP_006806674	PREDICTED: fibrinogen alpha chain-like [Neolamprologus brichardi]	0,0E+00
33	0,39	GENSCAN00000035313	XP_008296526	PREDICTED: alpha-2-macroglobulin-like [Stegastes partitus]	4,0E-109
34	0,38	GENSCAN00000035372	AKC43351	hemoglobin alpha 2 [Gadus macrocephalus]	4,0E-18
35	0,37	GENSCAN00000042806	A46538	Ig heavy chain, secreted form - Atlantic codemb|CAA41680.1| immunoglobulin heavy chain secretory form [Gadus morhua]	8,0E-31
36	0,34	GENSCAN00000026022	XP_009298112	PREDICTED: stonustoxin subunit beta-like [Danio rerio]	9,0E-25
37	0,34	GENSCAN00000057822	XP_007573447	PREDICTED: alpha-2-macroglobulin-like [Poecilia formosa]	2,0E-20
38	0,34	GENSCAN00000035308	AAR06589	alpha-2-macroglobulin, partial [Sparus aurata]	0,0E+00
39	0,33	GENSCAN00000013150	XP_008278356	PREDICTED: hemopexin [Stegastes partitus]	3,0E-25
40	0,33	GENSCAN00000073084	ACV69847	hemoglobin beta 3 [Gadus morhua]	3,0E-105
41	0,32	GENSCAN00000035493	XP_010754728	PREDICTED: cytosolic phospholipase A2 gamma-like [Larimichthys crocea]	6,0E-22
42	0,32	GENSCAN00000054274	KKF26544	Cytosolic phospholipase A2 gamma [Larimichthys crocea]	6,0E-22
43	0,32	GENSCAN00000003855	CCF55068	putative male specific protein [Oreochromis niloticus]	3,0E-33
44	0,30	GENSCAN00000044314	XP_008303501	PREDICTED: inter-alpha-trypsin inhibitor heavy chain H2 [Stegastes partitus]	0,0E+00
45	0,29	GENSCAN00000062295	XP_005748435	PREDICTED: protein NLRC3-like [Pundamilia nyererei]	3,0E-39
46	0,29	GENSCAN00000018172	CAA12426	immunoglobulin light chain [Gadus morhua]	9,0E-31
47	0,28	GENSCAN00000074120		No homolog	
48	0,28	GENSCAN00000037558	XP_008303267	PREDICTED: ceruloplasmin-like [Stegastes partitus]	0,0E+00
49	0,27	GENSCAN00000022169	A46538	Ig heavy chain, secreted form - Atlantic codemb|CAA41680.1| immunoglobulin heavy chain secretory form [Gadus morhua]	2,0E-47
50	0,27	GENSCAN00000041819	A46538	Ig heavy chain, secreted form - Atlantic codemb|CAA41680.1| immunoglobulin heavy chain secretory form [Gadus morhua]	1,0E-46
51	0,26	GENSCAN00000072422	XP_010750598	PREDICTED: complement factor H-like [Larimichthys crocea]	2,0E-18
52	0,25	GENSCAN00000001239	CAC03754	immunoglobulin light chain, isotype 2 [Gadus morhua]	1,0E-27
53	0,25	GENSCAN00000073133	XP_007234889	PREDICTED: fibronectin-like [Astyanax mexicanus]	2,0E-12
54	0,25	GENSCAN00000068455	XP_005755860	PREDICTED: inter-alpha-trypsin inhibitor heavy chain H3-like [Pundamilia nyererei]	7,0E-71
55	0,25	GENSCAN00000042257	ABV66068	leukocyte cell-derived chemotaxin 2 [Lates calcarifer]	2,0E-53

56	0,24	GENSCAN00000001674	ACJ66344	hemoglobin beta 2 chain [Gadus morhua]	9,0E-88
57	0,24	GENSCAN00000061942	ACV69839	hemoglobin beta 1 [Gadus morhua]	2,0E-40
58	0,23	GENSCAN00000043334	XP_010892316	PREDICTED: roundabout homolog 4 isoform X3 [Esox lucius]	5,0E-04
59	0,22	GENSCAN00000016731	CAA12426	immunoglobulin light chain [Gadus morhua]	1,0E-50
60	0,22	GENSCAN00000038564	XP_008330695	PREDICTED: roundabout homolog 4 isoform X2 [Cynoglossus semilaevis]	3,0E-05
61	0,22	GENSCAN00000016726	XP_010781926	PREDICTED: leucine-rich alpha-2-glycoprotein-like [Notothenia coriiceps]	1,0E-145
62	0,21	GENSCAN00000053540	P84609	RecName: Full=Hemoglobin subunit alpha-1; AltName: Full=Alpha-1-globin; AltName: Full=Hemoglobin alpha-1 chain [Gadus morhua]	2,0E-26
63	0,21	GENSCAN00000043611	CBN81064	Inter-alpha-trypsin inhibitor heavy chain H3 [Dicentrarchus labrax]	0,0E+00
64	0,21	GENSCAN00000016019	ACF21982	apolipoprotein E [Oplegnathus fasciatus]	3,0E-121
65	0,20	GENSCAN00000035310	KKF21587	Alpha-2-macroglobulin [Larimichthys crocea]	3,0E-63
66	0,20	GENSCAN00000011924	XP_009298112	PREDICTED: stonustoxin subunit beta-like [Danio rerio]	5,0E-26
67	0,20	GENSCAN00000054746	XP_009298112	PREDICTED: stonustoxin subunit beta-like [Danio rerio]	1,0E-25
68	0,20	GENSCAN00000055022	XP_009297830	PREDICTED: NACHT, LRR and PYD domains-containing protein 12-like isoform X3 [Danio rerio]	8,0E-21
69	0,20	GENSCAN00000069758	XP_009298112	PREDICTED: stonustoxin subunit beta-like [Danio rerio]	6,0E-25
70	0,20	GENSCAN00000070135	XP_009297830	PREDICTED: NACHT, LRR and PYD domains-containing protein 12-like isoform X3 [Danio rerio]	1,0E-24
71	0,20	GENSCAN00000038298	AGV52721	truncated MHC class I antigen, partial [Gadus morhua]	6,0E-96
72	0,19	GENSCAN00000031696	XP_009298124	PREDICTED: stonustoxin subunit beta-like [Danio rerio]	3,0E-22
73	0,19	GENSCAN00000070772	CAA12439	immunoglobulin light chain [Gadus morhua]	2,0E-55
74	0,19	GENSCAN00000059918	ADR78295	heparin cofactor II [Oplegnathus fasciatus]	0,0E+00
75	0,18	GENSCAN00000008600	ACJ66341	hemoglobin alpha 1 chain [Gadus morhua]	2,0E-98
76	0,18	GENSCAN00000025838	XP_009298124	PREDICTED: stonustoxin subunit beta-like [Danio rerio]	2,0E-23
77	0,18	GENSCAN00000005553	XP_008401449	PREDICTED: protein NLRC3-like [Poecilia reticulata]	1,0E-20
78	0,18	GENSCAN00000003582	XP_010865229	PREDICTED: stonustoxin subunit beta-like [Esox lucius]	6,0E-58
79	0,18	GENSCAN00000077088	XP_010903592	PREDICTED: stonustoxin subunit beta-like [Esox lucius]	1,0E-20
80	0,17	GENSCAN00000064047	XP_010882881	PREDICTED: complement C4-like [Esox lucius]	5,0E-19
81	0,17	GENSCAN00000075804	XP_010867115	PREDICTED: stonustoxin subunit beta-like [Esox lucius]	1,0E-57
82	0,17	GENSCAN00000049453	XP_005459133	PREDICTED: inter-alpha-trypsin inhibitor heavy chain H3-like [Oreochromis niloticus]	0,0E+00
83	0,16	GENSCAN00000071569	ABV21479	hemoglobin alpha chain [Gadus morhua]	2,0E-73
84	0,16	GENSCAN00000043676	CAA12443	immunoglobulin light chain [Gadus morhua]	7,0E-68
85	0,16	GENSCAN00000074612	XP_010866491	PREDICTED: protein NLRC3-like [Esox lucius]	9,0E-44
86	0,16	GENSCAN00000070187	CAA12432	immunoglobulin light chain [Gadus morhua]	5,0E-64
87	0,15	GENSCAN00000019231	XP_008304816	PREDICTED: eukaryotic translation initiation factor 4 gamma 1-like, partial [Stegastes partitus]	0,0E+00

88	0,15	GENSCAN00000030127	XP_010892316	PREDICTED: roundabout homolog 4 isoform X3 [Esox lucius]	2,0E-08
89	0,15	GENSCAN00000059488		No homolog	
90	0,14	GENSCAN00000029706	XP_010892316	PREDICTED: roundabout homolog 4 isoform X3 [Esox lucius]	2,0E-10
91	0,14	GENSCAN00000060487	XP_010892316	PREDICTED: roundabout homolog 4 isoform X3 [Esox lucius]	2,0E-10
92	0,14	GENSCAN00000072880	XP_010892316	PREDICTED: roundabout homolog 4 isoform X3 [Esox lucius]	1,0E-08
93	0,14	GENSCAN00000019025	CAA12454	immunoglobulin light chain [Gadus morhua]	3,0E-68
94	0,14	GENSCAN00000026384	XP_010892314	PREDICTED: roundabout homolog 4 isoform X1 [Esox lucius]	4,0E-10
95	0,14	GENSCAN00000018903	ACV69839	hemoglobin beta 1 [Gadus morhua]	4,0E-28
96	0,14	GENSCAN00000072954	XP_008319581	PREDICTED: catechol O-methyltransferase domain-containing protein 1-like [Cynoglossus semilaevis]	3,0E-56
97	0,13	GENSCAN00000056830	XP_010903592	PREDICTED: stonustoxin subunit beta-like [Esox lucius]	6,0E-57
98	0,13	GENSCAN00000063461	CAA12448	immunoglobulin light chain [Gadus morhua]	4,0E-67
99	0,12	GENSCAN00000068838	XP_010899734	PREDICTED: NACHT, LRR and PYD domains-containing protein 12-like, partial [Esox lucius]	3,0E-51
100	0,12	GENSCAN00000026062	XP_010768624	PREDICTED: fibronectin-like, partial [Notothenia coriiceps]	5,0E-21
101	0,12	GENSCAN00000040303	CAB91929	immunoglobulin heavy chain variable region [Gadus morhua]	1,0E-42
102	0,12	GENSCAN00000078428	XP_010892316	PREDICTED: roundabout homolog 4 isoform X3 [Esox lucius]	7,0E-09
103	0,12	GENSCAN00000065225	XP_005930069	PREDICTED: Fc receptor-like protein 5-like [Haplochromis burtoni]	4,0E-50
104	0,11	GENSCAN00000004569	XP_010787469	PREDICTED: kininogen-1 [Notothenia coriiceps]ref|XP_010787470.1| PREDICTED: kininogen-1 [Notothenia coriiceps]	3,0E-49
105	0,11	GENSCAN00000016721	XP_010739017	PREDICTED: apolipoprotein B-100-like [Larimichthys crocea]	0,0E+00
106	0,11	GENSCAN00000057737	ACJ26846	tributyltin binding protein type 2-like protein [Epinephelus coioides]	2,0E-08
107	0,11	GENSCAN00000049458	XP_005741573	PREDICTED: inter-alpha-trypsin inhibitor heavy chain H3-like [Pundamilia nyererei]	6,0E-15
108	0,11	GENSCAN00000074492	XP_010869354	PREDICTED: NACHT, LRR and PYD domains-containing protein 4-like [Esox lucius]	2,0E-56
109	0,10	GENSCAN00000032571	XP_010867115	PREDICTED: stonustoxin subunit beta-like [Esox lucius]	4,0E-59
110	0,10	GENSCAN00000065585		No homolog	
111	0,10	GENSCAN00000069898	AGV52700	MHC class I antigen, partial [Gadus morhua]	4,0E-27
112	0,10	GENSCAN00000061684	CAB91971	immunoglobulin heavy chain variable region [Gadus morhua]	6,0E-63
113	0,10	GENSCAN00000023430	XP_010869354	PREDICTED: NACHT, LRR and PYD domains-containing protein 4-like [Esox lucius]	4,0E-68
114	0,10	GENSCAN00000029239	CDQ96126	unnamed protein product [Oncorhynchus mykiss]	2,0E-61
115	0,10	GENSCAN00000022778	XP_016401454	PREDICTED: apolipoprotein A-I-like [Sinocyclocheilus rhinocerous]	6,0E-60
116	0,10	GENSCAN00000008933	XP_007541445	PREDICTED: prothrombin [Poecilia formosa]	0,0E+00
117	8,8E-02	GENSCAN00000041463	AAA58483	fibronecton type III, partial [Homo sapiens]	4,0E-29

118	8,8E-02	GENSCAN00000064459	XP_012988514	PREDICTED: stonustoxin subunit beta-like [Esox lucius]	4,0E-66
119	8,6E-02	GENSCAN00000042397	XP_010869276	PREDICTED: protein NLRC3-like [Esox lucius]	2,0E-55
120	8,4E-02	GENSCAN00000056898	AAF72568	immunoglobulin D heavy chain constant region variant b [Gadus morhua]	0,0E+00
121	8,2E-02	GENSCAN00000018597	XP_008299939	PREDICTED: secreted phosphoprotein 24-like [Stegastes partitus]	1,0E-39
122	8,0E-02	GENSCAN00000010572	XP_005816673	PREDICTED: complement C5-like, partial [Xiphophorus maculatus]	2,0E-14
123	7,9E-02	GENSCAN00000039611	XP_003964733	PREDICTED: galectin-3-binding protein [Takifugu rubripes]	7,0E-67
124	7,7E-02	GENSCAN00000065473	XP_008281044	PREDICTED: zinc finger and BTB domain-containing protein 4 [Stegastes partitus]	3,0E-172
125	7,6E-02	GENSCAN00000005382	CAG11529	unnamed protein product, partial [Tetraodon nigroviridis]	3,0E-156
126	7,3E-02	GENSCAN00000069510	CDQ90783	unnamed protein product [Oncorhynchus mykiss]	7,0E-58
127	7,3E-02	GENSCAN00000064709	XP_005724821	PREDICTED: uncharacterized protein LOC102203498 [Pundamilia nyererei]	3,0E-25
128	7,2E-02	GENSCAN00000052607	XP_008336748	PREDICTED: histidine-rich glycoprotein-like [Cynoglossus semilaevis]	8,0E-12
129	7,0E-02	GENSCAN00000033418	XP_010870818	PREDICTED: fetuin-B-like [Esox lucius]	2,0E-95
130	7,0E-02	GENSCAN00000003369	XP_010738618	PREDICTED: alpha-2-macroglobulin-like isoform X1 [Larimichthys crocea]	2,0E-48
131	6,9E-02	GENSCAN00000020727	CAB91897	immunoglobulin heavy chain variable region [Gadus morhua]	8,0E-61
132	6,8E-02	GENSCAN00000023150	NP_001134717	microfibrillar-associated protein 4 precursor [Salmo salar]	4,0E-81
133	6,5E-02	GENSCAN00000074972	CAA10685	MHC class I [Gadus morhua]	6,0E-21
134	6,4E-02	GENSCAN00000075115	CAA12427	immunoglobulin light chain [Gadus morhua]	6,0E-31
135	6,3E-02	GENSCAN00000029439	CAA12454	immunoglobulin light chain [Gadus morhua]	4,0E-51
136	6,2E-02	GENSCAN00000011606	XP_008413267	PREDICTED: cytosolic phospholipase A2 gamma [Poecilia reticulata]	6,0E-141
137	6,1E-02	GENSCAN00000024304	CAB91929	immunoglobulin heavy chain variable region [Gadus morhua]	8,0E-33
138	6,0E-02	GENSCAN00000072808	XP_010792411	PREDICTED: layilin-like [Notothenia coriiceps]	9,0E-167
139	6,0E-02	GENSCAN00000077599	BAM36372	pentraxin-2 [Oplegnathus fasciatus]	5,0E-60
140	5,9E-02	GENSCAN00000024891	XP_009298124	PREDICTED: stonustoxin subunit beta-like [Danio rerio]	2,0E-21
141	5,7E-02	GENSCAN00000078264	BAA86878	complement component C9 [Paralichthys olivaceus]	7,0E-73
142	5,7E-02	GENSCAN00000077281	CDQ99070	unnamed protein product, partial [Oncorhynchus mykiss]	7,0E-63
143	5,6E-02	GENSCAN00000026691	KKF20783	hypothetical protein EH28_03857 [Larimichthys crocea]	4,0E-59
144	5,6E-02	GENSCAN00000043615	CBN81064	Inter-alpha-trypsin inhibitor heavy chain H3 [Dicentrarchus labrax]	0,0E+00
145	5,5E-02	GENSCAN00000060806	CAA10761	beta2-microglobulin [Gadus morhua]	2,0E-74
146	5,5E-02	GENSCAN00000008392		No homolog	
147	5,4E-02	GENSCAN00000014765	XP_005468660	PREDICTED: cytosolic phospholipase A2 zeta-like [Oreochromis niloticus]	3,3E-01
148	5,4E-02	GENSCAN00000037316	XP_004568710	PREDICTED: cytosolic phospholipase A2 gamma-like [Maylandia zebra]	3,4E-01
149	5,2E-02	GENSCAN00000034908	CAA12438	immunoglobulin light chain [Gadus morhua]	2,0E-69

150	5,0E-02	GENSCAN00000006175	AAL14541	MHC class Ia antigen [Gadus morhua]	1,0E-34
151	5,0E-02	GENSCAN00000045095	AFV91208	MHC class I antigen, partial [Gadus morhua]	4,0E-31
152	4,9E-02	GENSCAN00000074863	XP_008283052	PREDICTED: fibronectin-like isoform X3 [Stegastes partitus]	0,0E+00
153	4,9E-02	GENSCAN00000030418	XP_005473942	PREDICTED: hyaluronan-binding protein 2-like isoform X1 [Oreochromis niloticus]	1,0E-14
154	4,9E-02	GENSCAN00000059193	CDQ99767	unnamed protein product, partial [Oncorhynchus mykiss]	4,0E-61
155	4,8E-02	GENSCAN00000069106	AAD19584	immunoglobulin light chain L1 region leader-V 10.3, partial [Gadus morhua]	8,0E-28
156	4,8E-02	GENSCAN00000061683	CAB91968	immunoglobulin heavy chain variable region [Gadus morhua]	4,0E-56
157	4,8E-02	GENSCAN00000076846	CAA10692	MHC class I [Gadus morhua]	1,0E-22
158	4,7E-02	GENSCAN00000054467	XP_011601975	PREDICTED: cytosolic phospholipase A2 zeta-like [Takifugu rubripes]	2,0E-144
159	4,7E-02	GENSCAN00000025405	ADP76803	plasminogen [Epinephelus coioides]	0,0E+00
160	4,6E-02	GENSCAN00000063609	KKF25679	Acidic mammalian chitinase [Larimichthys crocea]	0,0E+00
161	4,4E-02	GENSCAN00000072753	XP_009298124	PREDICTED: stonustoxin subunit beta-like [Danio rerio]	5,0E-22
162	4,3E-02	GENSCAN00000025383	XP_008299098	PREDICTED: complement C5 [Stegastes partitus]	4,0E-37
163	4,3E-02	GENSCAN00000013144	AFV91271	MHC class I antigen, partial [Gadus morhua]	1,0E-26
164	4,1E-02	GENSCAN00000070513	XP_010740565	PREDICTED: apolipoprotein A-IV-like [Larimichthys crocea]	3,0E-11
165	4,0E-02	GENSCAN00000044949	KKF13765	Ig kappa chain V region 3368 [Larimichthys crocea]	2,0E-40
166	4,0E-02	GENSCAN00000003727	AAL14536	MHC class Ia antigen [Gadus morhua]	1,0E-42
167	3,9E-02	GENSCAN00000049647	CAF88872	unnamed protein product, partial [Tetraodon nigroviridis]	9,0E-16
168	3,8E-02	GENSCAN00000019500	XP_004569367	PREDICTED: alpha-2-HS-glycoprotein-like isoform X2 [Maylandia zebra]	5,0E-47
169	3,8E-02	GENSCAN00000035094	XP_007254941	PREDICTED: uncharacterized protein LOC103027637 [Astyanax mexicanus]	2,0E-103
170	3,7E-02	GENSCAN00000069855	AFV91209	MHC class I antigen, partial [Gadus morhua]	1,0E-42
171	3,7E-02	GENSCAN00000007407	AFZ93920	complement component 1qB like-protein [Oplegnathus fasciatus]	9,0E-66
172	3,6E-02	GENSCAN00000073085	ABV21423	hemoglobin beta chain [Gadus morhua]	6,0E-72
173	3,6E-02	GENSCAN00000010585	KKX04153	asparaginase-like isoform X4, partial [Scleropages formosus]	1,0E-34
174	3,3E-02	GENSCAN00000065811		No homolog	
175	3,2E-02	GENSCAN00000008800	CAA12454	immunoglobulin light chain [Gadus morhua]	1,0E-57
176	3,2E-02	GENSCAN00000040396	AFE88226	warm-temperature-acclimation-related 65-kDa protein [Oplegnathus fasciatus]	6,0E-06
177	3,1E-02	GENSCAN00000025491	XP_005752421	PREDICTED: olfactory receptor 2AT4-like [Pundamilia nyererei]	5,0E-142
178	3,1E-02	GENSCAN00000033787	XP_008281691	PREDICTED: 60 kDa lysophospholipase isoform X3 [Stegastes partitus]	3,0E-14
179	3,0E-02	GENSCAN00000066784	XP_007256953	PREDICTED: uncharacterized protein LOC103025530 [Astyanax mexicanus]	7,0E-44
180	3,0E-02	GENSCAN00000013095	ABW74636	immunoglobulin light chain [Epinephelus coioides]	1,0E-39
181	2,8E-02	GENSCAN00000057622	XP_005755860	PREDICTED: inter-alpha-trypsin inhibitor heavy chain H3-like [Pundamilia nyererei]	1,0E-34

182	2,8E-02	GENSCAN00000014161	XP_008284485	PREDICTED: plasma protease C1 inhibitor isoform X2 [Stegastes partitus]	7,0E-110
183	2,7E-02	GENSCAN00000050112	KKF31817	Apolipoprotein A-IV [Larimichthys crocea]	2,0E-21
184	2,6E-02	GENSCAN00000062102	NP_001117857	complement component 4 precursor [Oncorhynchus mykiss]	0,0E+00
185	2,4E-02	GENSCAN00000016009	XP_005736206	PREDICTED: apolipoprotein C-II-like [Pundamilia nyererei]	8,0E-39
186	2,3E-02	GENSCAN00000014813	AHG06617	caspase 1 [Miichthys miiuy]	7,0E-49
187	2,3E-02	GENSCAN00000024340	CAA12435	immunoglobulin light chain [Gadus morhua]	1,0E-69
188	2,1E-02	GENSCAN00000069517	XP_005473942	PREDICTED: hyaluronan-binding protein 2-like isoform X1 [Oreochromis niloticus]	0,0E+00
189	2,1E-02	GENSCAN00000022985	ABW74636	immunoglobulin light chain [Epinephelus coioides]	1,0E-39
190	2,1E-02	GENSCAN00000000273	XP_010746866	PREDICTED: protein NLRC3-like [Larimichthys crocea]	0,0E+00
191	2,0E-02	GENSCAN00000040980	XP_005853119	PREDICTED: tankyrase-1 [Myotis brandtii]	1,0E-25
192	2,0E-02	GENSCAN00000053979	XP_008291739	PREDICTED: fibronectin-like [Stegastes partitus]	8,0E-09
193	2,0E-02	GENSCAN00000049381	KKF16592	Proteasome subunit beta type-4 [Larimichthys crocea]	1,0E-176
194	2,0E-02	GENSCAN00000075026	AGV52645	MHC class I antigen, partial [Gadus morhua]	1,0E-88
195	1,9E-02	GENSCAN00000071105	AAL05892	glyceraldehyde 3-phosphate dehydrogenase [Gadus morhua]	0,0E+00
196	1,9E-02	GENSCAN00000060988	ADN65119	ceruloplasmin [Carassius auratus]	5,0E-10
197	1,9E-02	GENSCAN00000078118	XP_005455016	PREDICTED: Ig heavy chain Mem5-like [Oreochromis niloticus]	5,0E-31
198	1,8E-02	GENSCAN00000030583	CBN81064	Inter-alpha-trypsin inhibitor heavy chain H3 [Dicentrarchus labrax]	8,0E-12
199	1,8E-02	GENSCAN00000036255	KKF26541	Cytosolic phospholipase A2 gamma [Larimichthys crocea]	2,0E-09
200	1,8E-02	GENSCAN00000042955	XP_008283653	PREDICTED: inter-alpha-trypsin inhibitor heavy chain H3 [Stegastes partitus]	8,0E-14
201	1,8E-02	GENSCAN00000004171		No homolog	
202	1,8E-02	GENSCAN00000060393		No homolog	
203	1,8E-02	GENSCAN00000009858	XP_010784023	PREDICTED: cytidine deaminase [Notothenia coriiceps]	1,0E-63
204	1,8E-02	GENSCAN00000060543	BAC81202	Immunoglobulin light chain [Cyprinus carpio]	2,0E-18
205	1,7E-02	GENSCAN00000006486	XP_010728839	PREDICTED: insulin-like growth factor-binding protein complex acid labile subunit [Larimichthys crocea]	0,0E+00
206	1,7E-02	GENSCAN00000078025	BAC81202	Immunoglobulin light chain [Cyprinus carpio]	2,0E-18
207	1,7E-02	GENSCAN00000027009	XP_008429577	PREDICTED: complement C3-like [Poecilia reticulata]	0,0E+00
208	1,7E-02	GENSCAN00000034910	ACQ58496	Ig kappa chain V region 3547 [Anoplopoma fimbria]	4,0E-39
209	1,7E-02	GENSCAN00000053905	AIN76766	complement component 4 [Oplegnathus fasciatus]	2,0E-11
210	1,7E-02	GENSCAN00000039585	XP_005946820	PREDICTED: PR domain zinc finger protein 12-like isoform X1 [Haplochromis burtoni]	1,0E-165
211	1,7E-02	GENSCAN00000052806	XP_008291776	PREDICTED: zinc finger BED domain-containing protein 4-like, partial [Stegastes partitus]	0,0E+00
212	1,6E-02	GENSCAN00000001677	ABV21491	hemoglobin alpha chain [Gadus morhua]	1,0E-04
213	1,6E-02	GENSCAN00000012892	CAB91970	immunoglobulin heavy chain variable region [Gadus morhua]	7,0E-65
214	1,6E-02	GENSCAN00000012712		No homolog	
215	1,6E-02	GENSCAN00000029092	XP_004078952	PREDICTED: alpha-2-HS-glycoprotein [Oryzias latipes]	2,0E-44

216	1,6E-02	GENSCAN00000056739	XP_007566589	PREDICTED: saxitoxin and tetrodotoxin-binding protein 1-like isoform X2 [Poecilia formosa]	1,0E-07
217	1,5E-02	GENSCAN00000075867		No homolog	
218	1,5E-02	GENSCAN00000056897	CAB91957	immunoglobulin heavy chain variable region [Gadus morhua]	4,0E-74
219	1,5E-02	GENSCAN00000062106	XP_005738670	PREDICTED: complement C4-B-like [Pundamilia nyererei]	0,0E+00
220	1,5E-02	GENSCAN00000007673	XP_007231638	PREDICTED: stonustoxin subunit beta-like isoform X3 [Astyanax mexicanus]	3,0E-99
221	1,5E-02	GENSCAN00000029710	XP_011616382	PREDICTED: alpha-2-macroglobulin-like protein 1 [Takifugu rubripes]	5,0E-04
222	1,5E-02	GENSCAN00000043057	XP_010751312	PREDICTED: protein NLRC3-like [Larimichthys crocea]	0,0E+00
223	1,4E-02	GENSCAN00000054660	CAQ53699	warm temperature acclimation-related protein [Plecoglossus altivelis]	2,0E-27
224	1,4E-02	GENSCAN00000037636	XP_010864119	PREDICTED: microfibril-associated glycoprotein 4-like [Esox lucius]	1,0E-113
225	1,4E-02	GENSCAN00000034996	XP_005814198	PREDICTED: alpha-2-macroglobulin-like protein 1-like [Xiphophorus maculatus]	2,3E-01
226	1,3E-02	GENSCAN00000050455	CAB91895	immunoglobulin heavy chain variable region [Gadus morhua]	3,0E-65
227	1,3E-02	GENSCAN00000063244	KKF19508	Beta-microseminoprotein, partial [Larimichthys crocea]	1,0E-31
228	1,3E-02	GENSCAN00000053043	KKF29532	Nuclear receptor subfamily 5 group A member 2 [Larimichthys crocea]	0,0E+00
229	1,3E-02	GENSCAN00000027904		No homolog	
230	1,2E-02	GENSCAN00000067572	XP_006801498	PREDICTED: complement C4-B-like [Neolamprologus brichardi]	1,0E-33
231	1,2E-02	GENSCAN00000023169	XP_010746866	PREDICTED: protein NLRC3-like [Larimichthys crocea]	0,0E+00
232	1,2E-02	GENSCAN00000017046	XP_011473574	PREDICTED: inter-alpha-trypsin inhibitor heavy chain H3 [Oryzias latipes]	1,0E-12
233	1,2E-02	GENSCAN00000056253	XP_010746866	PREDICTED: protein NLRC3-like [Larimichthys crocea]	0,0E+00
234	1,2E-02	GENSCAN00000057946	AGR75380	DNA methylase [Mannheimia haemolytica USMARC_2286]	4,0E-09
235	1,2E-02	GENSCAN00000023935	XP_008278409	PREDICTED: complement C1r subcomponent [Stegastes partitus]	0,0E+00
236	1,1E-02	GENSCAN00000063370	XP_010785445	PREDICTED: glypican-6-like, partial [Notothenia coriiceps]	3,0E-64
237	1,1E-02	GENSCAN00000052393	ACN10482	Fatty aldehyde dehydrogenase [Salmo salar]	6,0E-132
238	1,1E-02	GENSCAN00000021496	XP_008400708	PREDICTED: phospholipid transfer protein isoform X2 [Poecilia reticulata]	1,0E-160
239	1,0E-02	GENSCAN00000076881	XP_005814989	PREDICTED: uncharacterized protein LOC102223852 [Xiphophorus maculatus]	0,0E+00
240	1,0E-02	GENSCAN00000041679	XP_004575713	PREDICTED: protein NLRC3-like [Maylandia zebra]	0,0E+00
241	9,9E-03	GENSCAN00000028670	XP_013870955	PREDICTED: voltage-dependent T-type calcium channel subunit alpha-1I [Austrofundulus limnaeus]	7,0E-65
242	9,7E-03	GENSCAN00000073250	XP_008298530	PREDICTED: cadherin-2-like [Stegastes partitus]	0,0E+00
243	9,5E-03	GENSCAN00000002769	XP_005458607	PREDICTED: LOW QUALITY PROTEIN: nodal modulator 1-like [Oreochromis niloticus]	0,0E+00
244	9,4E-03	GENSCAN00000040728	AGV52682	MHC class I antigen, partial [Gadus morhua]	5,0E-125
245	9,2E-03	GENSCAN00000054351	XP_014012459	PREDICTED: serine/threonine-protein kinase BRSK2-like isoform X1 [Salmo salar]	8,0E-14

246	9,2E-03	GENSCAN00000006577	XP_008286532	PREDICTED: ectonucleotide pyrophosphatase/phosphodiesterase family member 2-like isoform X2 [Stegastes partitus]	0,0E+00
247	9,1E-03	GENSCAN00000035135	XP_010755429	PREDICTED: collagenase 3-like [Larimichthys crocea]	1,0E-180
248	8,5E-03	GENSCAN00000045587	XP_010769296	PREDICTED: complement C3-like, partial [Notothenia coriiceps]	3,0E-59
249	8,4E-03	GENSCAN00000029672	XP_008401074	PREDICTED: uncharacterized protein LOC103460609 [Poecilia reticulata]	2,0E-12
250	8,2E-03	GENSCAN00000023753	CAA12428	immunoglobulin light chain [Gadus morhua]	2,0E-42
251	8,1E-03	GENSCAN00000008416	XP_008396009	PREDICTED: NHS-like protein 1 isoform X7 [Poecilia reticulata]	1,0E-08
252	7,7E-03	GENSCAN00000043587	ADX97142	beta-2-glycoprotein 1, partial [Perca flavescens]	4,0E-172
253	7,7E-03	GENSCAN00000011544	XP_010791917	PREDICTED: creatine kinase M-type [Notothenia coriiceps]	0,0E+00
254	7,4E-03	GENSCAN00000067468	XP_010889908	PREDICTED: fibrinogen gamma chain [Esox lucius]	3,0E-43
255	6,8E-03	GENSCAN00000033480	XP_008281295	PREDICTED: uncharacterized protein C1orf21 homolog [Stegastes partitus]	3,0E-47
256	6,6E-03	GENSCAN00000064299	XP_008295593	PREDICTED: creatine kinase M-type [Stegastes partitus]	0,0E+00
257	6,4E-03	GENSCAN00000071718	XP_006788145	PREDICTED: lactose-binding lectin l-2-like [Neolamprologus brichardi]	1,0E-37
258	6,3E-03	GENSCAN00000037782	XP_003439569	PREDICTED: cholesteryl ester transfer protein-like isoform X1 [Oreochromis niloticus]	4,0E-171
259	6,1E-03	GENSCAN00000078334	KKF17367	Lumican [Larimichthys crocea]	0,0E+00
260	6,0E-03	GENSCAN00000071821	XP_005752387	PREDICTED: alpha-2-macroglobulin-like [Pundamilia nyererei]	2,0E-54
261	5,9E-03	GENSCAN00000056740	XP_005463637	PREDICTED: pogo transposable element with ZNF domain-like [Oreochromis niloticus]	1,0E-43
262	5,8E-03	GENSCAN00000052600	XP_008299098	PREDICTED: complement C5 [Stegastes partitus]	4,0E-33
263	5,5E-03	GENSCAN00000063361	KKF27380	Glypican-6 [Larimichthys crocea]	2,0E-49
264	5,5E-03	GENSCAN00000067551	XP_008275082	PREDICTED: glutaminyl-peptide cyclotransferase [Stegastes partitus]	2,0E-168
265	5,3E-03	GENSCAN00000009109	CAB91897	immunoglobulin heavy chain variable region [Gadus morhua]	8,0E-60
266	4,8E-03	GENSCAN00000003291	KKF17378	Collagen alpha-2(VIII) chain [Larimichthys crocea]	8,0E-55
267	4,6E-03	GENSCAN00000071799		No homolog	
268	4,5E-03	GENSCAN00000052973	XP_008329364	PREDICTED: palmitoyl-protein thioesterase 1 [Cynoglossus semilaevis]	0,0E+00
269	4,4E-03	GENSCAN00000038315	XP_008289550	PREDICTED: plexin domain-containing protein 2 [Stegastes partitus]	9,0E-148
270	4,4E-03	GENSCAN00000072320	XP_010746598	PREDICTED: cytosolic non-specific dipeptidase-like [Larimichthys crocea]	0,0E+00
271	4,2E-03	GENSCAN00000018563	XP_006130617	PREDICTED: fatty acyl-CoA hydrolase precursor, medium chain-like isoform X3 [Pelodiscus sinensis]	5,0E-157
272	4,1E-03	GENSCAN00000010101	XP_010776898	PREDICTED: uncharacterized protein LOC104951859 [Notothenia coriiceps]	1,0E-10
273	3,8E-03	GENSCAN00000041895		No homolog	
274	3,6E-03	GENSCAN00000070228	AFJ05590	immmunoglobulin light chain [Epinephelus coioides]	3,0E-40
275	3,5E-03	GENSCAN00000060216	XP_005477033	PREDICTED: 60 kDa lysophospholipase-like isoform X2 [Oreochromis niloticus]	0,0E+00
276	3,4E-03	GENSCAN00000039122	KKF28544	Vitamin K-dependent protein C [Larimichthys crocea]	0,0E+00

277	3,4E-03	GENSCAN00000027585		No homolog	
278	3,2E-03	GENSCAN00000066727	AFC89899	complement component C3 [Miichthys miiuy]	0,0E+00
279	3,0E-03	GENSCAN00000062108	AJA33608	complement component 4 [Larimichthys crocea]	9,0E-88
280	3,0E-03	GENSCAN00000003612	NP_001133464	Para-nitrobenzyl esterase [Salmo salar]	2,0E-86
281	2,9E-03	GENSCAN00000027158	XP_008286089	PREDICTED: protein ACN9 homolog, mitochondrial [Stegastes partitus]	2,0E-58
282	2,6E-03	GENSCAN00000040778	XP_010887435	PREDICTED: integrin alpha-D-like isoform X3 [Esox lucius]	8,0E-31
283	2,5E-03	GENSCAN00000040267	XP_004539242	PREDICTED: complexin-1-like [Maylandia zebra]	5,0E-28
284	2,4E-03	GENSCAN00000060815	XP_006796662	PREDICTED: cell adhesion molecule 2-like isoform X2 [Neolamprologus brichardi]	1,0E-123
285	2,3E-03	GENSCAN00000051925	XP_008284618	PREDICTED: coagulation factor XIII A chain-like isoform X1 [Stegastes partitus]	0,0E+00
286	2,2E-03	GENSCAN00000001493	KKF31814	Protein misato [Larimichthys crocea]	0,0E+00
287	2,1E-03	GENSCAN00000035666	NP_001290561	alpha-1-microglobulin/bikunin precursor [Esox lucius]	2,0E-07
288	1,9E-03	GENSCAN00000061679	CAB91889	immunoglobulin heavy chain variable region [Gadus morhua]	2,0E-63
289	1,9E-03	GENSCAN00000021653	CAC03754	immunoglobulin light chain, isotype 2 [Gadus morhua]	3,0E-62
290	1,9E-03	GENSCAN00000012301	XP_005923480	PREDICTED: di-N-acetylchitobiase-like [Haplochromis burtoni]	0,0E+00
291	1,8E-03	GENSCAN00000025408	XP_008279839	PREDICTED: cation-independent mannose-6-phosphate receptor [Stegastes partitus]	0,0E+00
292	1,8E-03	GENSCAN00000065760	XP_010901660	PREDICTED: diacylglycerol kinase delta isoform X1 [Esox lucius]	0,0E+00
293	1,8E-03	GENSCAN00000075013	XP_010755425	PREDICTED: sialate O-acetylesterase [Larimichthys crocea]	3,0E-148
294	1,7E-03	GENSCAN00000064718	XP_006791692	PREDICTED: Ig heavy chain Mem5-like [Neolamprologus brichardi]	3,0E-86
295	1,6E-03	GENSCAN00000044124	XP_011476888	PREDICTED: zinc finger protein Gfi-1-like isoform X1 [Oryzias latipes]	3,1E-02
296	1,6E-03	GENSCAN00000064580		No homolog	
297	1,6E-03	GENSCAN00000041922	XP_004574497	PREDICTED: complement C3-like [Maylandia zebra]	0,0E+00
298	1,6E-03	GENSCAN00000062215	XP_008401766	PREDICTED: uncharacterized protein LOC103461223 [Poecilia reticulata]	3,0E-67
299	1,6E-03	GENSCAN00000033414	XP_006803405	PREDICTED: sulfhydryl oxidase 1-like [Neolamprologus brichardi]	1,0E-158
300	1,6E-03	GENSCAN00000028112	XP_013983971	PREDICTED: V-type proton ATPase 116 kDa subunit a isoform 2-like [Salmo salar]	0,0E+00
301	1,5E-03	GENSCAN00000026666	NP_001080249	26S protease regulatory subunit 6A-A [Xenopus laevis]	7,0E-159
302	1,5E-03	GENSCAN00000041541	XP_010753985	PREDICTED: coagulation factor V [Larimichthys crocea]	0,0E+00
303	1,5E-03	GENSCAN00000072675	ACV89350	complement factor D/adipsin and kallikrein-like serine protease [Paralichthys olivaceus]	1,0E-121
304	1,4E-03	GENSCAN00000069956	XP_005449635	PREDICTED: cAMP-specific 3',5'-cyclic phosphodiesterase 7B isoform X3 [Oreochromis niloticus]	8,0E-39
305	1,3E-03	GENSCAN00000016016	ACI67068	Apolipoprotein A-IV precursor [Salmo salar]	1,0E-134
306	1,3E-03	GENSCAN00000066485	XP_019131431	PREDICTED: cleft lip and palate transmembrane protein 1-like protein [Larimichthys crocea]	2,0E-118
307	1,3E-03	GENSCAN00000061215	XP_015815293	PREDICTED: ER membrane protein complex subunit 3 [Nothobranchius furzeri]	0,0E+00

308	1,3E-03	GENSCAN00000034246	XP_010743323	PREDICTED: exportin-5 isoform X1 [Larimichthys crocea]	0,0E+00
309	1,2E-03	GENSCAN00000038323	XP_008315543	PREDICTED: scavenger receptor cysteine-rich type 1 protein M130-like [Cynoglossus semilaevis]	4,0E-39
310	1,2E-03	GENSCAN00000068628	XP_010865125	PREDICTED: pre-B-cell leukemia transcription factor 1-like [Esox lucius]	0,0E+00
311	1,1E-03	GENSCAN00000024437	AIT83017	wntless-like protein [Sparus aurata]	0,0E+00
312	1,0E-03	GENSCAN00000054771	XP_018526100	PREDICTED: keratinocyte differentiation factor 1-like isoform X1 [Lates calcarifer]	4,0E-56
313	9,8E-04	GENSCAN00000073972	ADX97064	mitochondrial 2-oxoglutarate/malate carrier protein, partial [Perca flavescens]	0,0E+00
314	9,7E-04	GENSCAN00000045181	XP_008284750	PREDICTED: phosphatidylcholine-sterol acyltransferase [Stegastes partitus]	0,0E+00
315	9,7E-04	GENSCAN00000017661	XP_008297618	PREDICTED: merlin-like [Stegastes partitus]	0,0E+00
316	9,6E-04	GENSCAN00000018084	XP_008281712	PREDICTED: kinesin-like protein KIF26A [Stegastes partitus]	0,0E+00
317	8,9E-04	GENSCAN00000015858	XP_010746595	PREDICTED: apolipoprotein B-100-like [Larimichthys crocea]	0,0E+00
318	8,8E-04	GENSCAN00000012304	BAM22586	vitellogenin A [Gadus chalcogrammus]	0,0E+00
319	8,7E-04	GENSCAN00000045346	XP_012722299	PREDICTED: GPI ethanolamine phosphate transferase 2 isoform X2 [Fundulus heteroclitus]	2,0E-146
320	8,6E-04	GENSCAN00000073009	XP_018551181	PREDICTED: myozenin-2-like isoform X1 [Lates calcarifer]	7,0E-107
321	8,0E-04	GENSCAN00000041455	XP_010781251	PREDICTED: 26S protease regulatory subunit 6A [Notothenia coriiceps]	0,0E+00
322	7,9E-04	GENSCAN00000025724	XP_004544204	PREDICTED: A disintegrin and metalloproteinase with thrombospondin motifs 13-like [Maylandia zebra]	0,0E+00
323	7,7E-04	GENSCAN00000002368	XP_004084996	PREDICTED: leukotriene A-4 hydrolase [Oryzias latipes]	0,0E+00
324	7,7E-04	GENSCAN00000074812		No homolog	
325	7,6E-04	GENSCAN00000072090	AFK76487	toll-like receptor 22c [Gadus morhua]	0,0E+00
326	7,6E-04	GENSCAN00000043638	XP_008300098	PREDICTED: HSPB1-associated protein 1 [Stegastes partitus]	0,0E+00
327	7,5E-04	GENSCAN00000008305	XP_007564438	PREDICTED: glyceraldehyde-3-phosphate dehydrogenase-like [Poecilia formosa]	0,0E+00
328	7,3E-04	GENSCAN00000077068	XP_008296086	PREDICTED: tankyrase-1-like isoform X1 [Stegastes partitus]	0,0E+00
329	6,9E-04	GENSCAN00000012312	AAK15157	vitellogenin B [Melanogrammus aeglefinus]	0,0E+00
330	6,8E-04	GENSCAN00000002128	XP_014060371	PREDICTED: collagen alpha-1(XII) chain isoform X6 [Salmo salar]	0,0E+00
331	6,4E-04	GENSCAN00000012286	BAM22587	vitellogenin B [Gadus chalcogrammus]	0,0E+00
332	6,3E-04	GENSCAN00000062892	XP_018541161	PREDICTED: T-complex protein 11-like protein 2 [Lates calcarifer]	0,0E+00
333	6,3E-04	GENSCAN00000046878	XP_010776732	PREDICTED: death ligand signal enhancer isoform X1 [Notothenia coriiceps]	6,0E-117
334	6,3E-04	GENSCAN00000018698	XP_010897801	PREDICTED: otopetrin-3 [Esox lucius]	0,0E+00
335	6,3E-04	GENSCAN00000014217	XP_010736908	PREDICTED: galectin-3-binding protein [Larimichthys crocea]	5,0E-171
336	6,2E-04	GENSCAN00000000922	XP_011616871	PREDICTED: phosphatidate phosphatase LPIN1-like isoform X1 [Takifugu rubripes]	0,0E+00
337	5,6E-04	GENSCAN00000002746	KKF18596	Zinc finger protein 436 [Larimichthys crocea]	0,0E+00
338	5,4E-04	GENSCAN00000041585	XP_008301209	PREDICTED: MAGUK p55 subfamily member 5-A-like isoform X2 [Stegastes partitus]	0,0E+00

339	5,1E-04	GENSCAN00000024607	XP_004553637	PREDICTED: NK1 transcription factor-related protein 1 [Maylandia zebra]	2,0E-98
340	5,0E-04	GENSCAN00000057913	XP_005463022	PREDICTED: sphingomyelin phosphodiesterase 4 isoform X3 [Oreochromis niloticus]	0,0E+00
341	5,0E-04	GENSCAN00000055854	CBN80793	Protein-glutamine gamma-glutamyltransferase 5 [Dicentrarchus labrax]	0,0E+00
342	4,6E-04	GENSCAN00000041425	KKF28128	Synaptotagmin-7 [Larimichthys crocea]	0,0E+00
343	4,5E-04	GENSCAN00000008801	XP_011600879	PREDICTED: FYVE, RhoGEF and PH domain-containing protein 3 isoform X2 [Takifugu rubripes]	0,0E+00
344	4,2E-04	GENSCAN00000018296	KKF12851	Phosphatidylinositol 4-kinase alpha [Larimichthys crocea]	0,0E+00
345	4,2E-04	GENSCAN00000065124	XP_005949040	PREDICTED: olfactomedin-like [Haplochromis burtoni]	4,0E-134
346	4,0E-04	GENSCAN00000055988	XP_016861103	PREDICTED: cytosolic 10-formyltetrahydrofolate dehydrogenase isoform X3 [Homo sapiens]	0,0E+00
347	4,0E-04	GENSCAN00000051779	XP_018534970	PREDICTED: NADPH oxidase 5 isoform X2 [Lates calcarifer]	0,0E+00
348	3,8E-04	GENSCAN00000035058	XP_018532096	PREDICTED: 5'-AMP-activated protein kinase subunit gamma-1-like isoform X2 [Lates calcarifer]	0,0E+00
349	3,8E-04	GENSCAN00000006287	XP_015765475	PREDICTED: uncharacterized protein LOC107344333 [Acropora digitifera]	0,0E+00
350	3,6E-04	GENSCAN00000013357	XP_018530652	PREDICTED: nephrocystin-4 isoform X2 [Lates calcarifer]	1,0E-106
351	3,2E-04	GENSCAN00000034603	XP_008304081	PREDICTED: uncharacterized protein C10orf71 homolog [Stegastes partitus]	0,0E+00
352	3,1E-04	GENSCAN00000037089	XP_018545279	PREDICTED: disks large homolog 1 isoform X7 [Lates calcarifer]	0,0E+00
353	3,0E-04	GENSCAN00000021297	XP_013984287	PREDICTED: armadillo repeat protein deleted in velo-cardio-facial syndrome-like [Salmo salar]	0,0E+00
354	2,9E-04	GENSCAN00000059537	XP_006804907	PREDICTED: ADAMTS-like protein 4-like [Neolamprologus brichardi]	0,0E+00
355	2,9E-04	GENSCAN00000004611	XP_010738923	PREDICTED: thrombospondin-1-like [Larimichthys crocea]	0,0E+00
356	2,9E-04	GENSCAN00000072410	XP_018553974	PREDICTED: oxysterol-binding protein-related protein 7-like isoform X1 [Lates calcarifer]	0,0E+00
357	2,8E-04	GENSCAN00000047600	XP_005798563	PREDICTED: delta-type opioid receptor-like [Xiphophorus maculatus]	0,0E+00
358	2,7E-04	GENSCAN00000033700	XP_003439438	PREDICTED: troponin I, cardiac muscle [Oreochromis niloticus]	7,0E-121
359	2,6E-04	GENSCAN00000043076	XP_018558087	PREDICTED: phospholipid-transporting ATPase IC [Lates calcarifer]	0,0E+00
360	2,6E-04	GENSCAN00000019921	XP_008398271	PREDICTED: kinesin-like protein KIF15 isoform X2 [Poecilia reticulata]	0,0E+00
361	2,4E-04	GENSCAN00000015256	XP_008306095	PREDICTED: traf2 and NCK-interacting protein kinase-like isoform X11 [Cynoglossus semilaevis]	0,0E+00
362	2,4E-04	GENSCAN00000062750	KKF26902	putative serine protease 56 [Larimichthys crocea]	0,0E+00
363	2,3E-04	GENSCAN00000035866	XP_017590224	PREDICTED: armadillo repeat protein deleted in velo-cardio-facial syndrome [Corvus brachyrhynchos]	0,0E+00
364	2,2E-04	GENSCAN00000043563	XP_016116662	PREDICTED: LOW QUALITY PROTEIN: general transcription factor 3C polypeptide 1 [Sinocyclocheilus grahami]	0,0E+00
365	2,1E-04	GENSCAN00000016705	KKF23121	Apolipoprotein B-100 [Larimichthys crocea]	0,0E+00
366	2,0E-04	GENSCAN00000015229	XP_008294564	PREDICTED: tyrosine-protein phosphatase non-receptor type 4 [Stegastes partitus]	0,0E+00
367	1,5E-04	GENSCAN00000063989	XP_018542839	PREDICTED: CAD protein [Lates calcarifer]	0,0E+00

368	1,2E-04	GENSCAN00000034599	XP_008418011	PREDICTED: matrix-remodeling-associated protein 5-like [Poecilia reticulata]	0,0E+00
369	1,2E-04	GENSCAN00000057322	XP_016319659	PREDICTED: myosin-IIIb-like [Sinocyclocheilus anshuiensis]	0,0E+00

Table S 11. Quantification of 513 identified proteins in juvenile sockeye salmon serum (Alderman et al., 2017).

	Accession	Coverage (%)	#Peptides	# Unique	Description	C1S	C1NS	H1S	H1NS	C4NS	C4S	H4S	H4NS	Sum (C1NS + C4NS)
TOP 30 ABUNDANT PROTEINS	gi|185132771	84	88	51	apolipoprotein A-I-1 precursor [Oncorhynchus mykiss]gi|6686384|sp|O57523.1|APA11_ONCMY RecName: Full=Apolipoprotein A-I-1; Short=Apo-AI-1; Short=ApoA-I-1; AltName: Full=Apolipoprotein A1-1; Contains: RecName: Full=Proapo...	1.48E+09	1.97E+09	1.39E+09	2.36E+09	1.64E+09	2.09E+09	1.41E+09	2.13E+09	**4.06E+09**
	gi|5837767	84	110	38	transferrin [Oncorhynchus nerka]	4.18E+08	5.43E+08	3.69E+08	5.43E+08	3.71E+08	4.48E+08	3.25E+08	5.26E+08	**9.92E+08**
	gi|185132822	84	57	24	apolipoprotein A-I-2 precursor [Oncorhynchus mykiss]gi|6686385|sp|O57524.1|APA12_ONCMY RecName: Full=Apolipoprotein A-I-2; Short=Apo-AI-2; Short=ApoA-I-2; AltName: Full=Apolipoprotein A1-2; Contains: RecName: Full=Proapo...	4.08E+08	5.46E+08	3.70E+08	5.99E+08	3.71E+08	4.30E+08	2.89E+08	4.64E+08	**9.76E+08**
	gi|185139	69	70	49	hemopexin-like protein [Oncorhynchus mykiss]	3.31E+08	4.44E+08	3.09E+08	4.16E+08	4.29E+08	4.59E+08	3.58E+08	4.81E+08	**9.03E+08**
	gi|95931876	77	22	12	serum albumin [Oncorhynchus mykiss]	7.39E+07	9.71E+07	6.89E+07	1.31E+08	1.11E+08	1.22E+08	7.62E+07	1.16E+08	**2.19E+08**
	gi|617439215	6	10	8	PREDICTED: collagen alpha-1(VII) chain-like isoform X12 [Poecilia formosa]	8.19E	1.01E	7.64E	1.13E	7.85E	1.15E	6.76E	1.14E	**2.16E+08**

					+07	+08	+07	+08	+07	+08	+07	+08	
gi|642094847	18	9	8	alpha-2-HS-glycoprotein-like	6.57E+07	9.58E+07	6.28E+07	1.02E+08	7.46E+07	8.61E+07	6.16E+07	7.91E+07	**1.82E+08**
gi|642099235	47	22	14	warm-temperature-acclimation-related 65-kDa	6.20E+07	8.61E+07	6.55E+07	9.74E+07	7.91E+07	8.82E+07	5.39E+07	7.75E+07	**1.74E+08**
gi|1352103	79	184	58	RecName: Full=Complement C3; Contains: RecName: Full=Complement C3 beta chain; Contains: RecName: Full=Complement C3 alpha chain; Contains: RecName: Full=C3a anaphylatoxin; Contains: RecName: Full=Complement C3b alpha' ch...	3.48E+07	5.49E+07	4.18E+07	6.38E+07	4.85E+07	6.06E+07	3.57E+07	5.94E+07	**1.16E+08**
gi|185132174	53	45	44	alpha-1-antiproteinase-like protein precursor [Oncorhynchus mykiss]gi|30519704|emb|CAD90255.1| alpha-1-antiproteinase-like protein [Oncorhynchus mykiss]gi|642082949|emb|CDQ85260.1| unnamed protein product [Oncorhynchus ...	4.23E+07	5.90E+07	4.41E+07	6.56E+07	5.06E+07	5.47E+07	3.66E+07	5.54E+07	**1.14E+08**
gi|642093623	45	20	8	salarin precursor	3.91E+07	4.83E+07	3.64E+07	4.79E+07	4.07E+07	4.19E+07	3.16E+07	4.11E+07	**9.02E+07**
gi|642116634	42	31	28	complement C3-like	3.50E+07	4.39E+07	3.69E+07	4.50E+07	3.94E+07	4.43E+07	3.72E+07	4.44E+07	**8.82E+07**
gi|642086397	68	9	5	apolipoprotein C-I-like	2.53E	3.65E	2.80E	5.88E	2.91E	3.93E	2.61E	3.29E	**7.57E+07**

					+07	+07	+07	+07	+07	+07	+07	+07	
	gi|642076289	34	18	17	antihemorrhagic factor cHLP-B-like	1.99E+07	3.34E+07	2.36E+07	3.50E+07	2.21E+07	3.20E+07	1.97E+07	3.88E+07	**6.54E+07**
	gi|74096001	18	7	5	hemopexin precursor [Takifugu rubripes]gi|47076410|dbj|BAD18109.1| warm-temperature-acclimation-related-65kDa- protein [Takifugu rubripes]	2.40E+07	2.80E+07	2.53E+07	2.69E+07	3.14E+07	3.47E+07	2.33E+07	3.00E+07	**6.28E+07**
	gi|64194996 2	54	19	3	14 kDa partial	1.86E+07	2.36E+07	2.13E+07	3.20E+07	2.36E+07	2.85E+07	2.00E+07	2.71E+07	**5.21E+07**
	gi|64198565 5	55	62	4	complement C3	1.44E+07	2.14E+07	1.23E+07	2.02E+07	1.90E+07	2.42E+07	1.11E+07	1.77E+07	**4.56E+07**
	gi|64212335 2	39	79	48	apolipoprotein B-100-like	1.59E+07	2.06E+07	1.53E+07	2.25E+07	1.72E+07	2.39E+07	1.55E+07	2.19E+07	**4.44E+07**
	gi|35053731 5	26	20	16	complement factor B/C2 precursor [Oncorhynchus mykiss]gi|324983881|gb|ADY68777.1| complement factor B/C2 [Oncorhynchus mykiss]	1.48E+07	2.11E+07	1.32E+07	2.01E+07	1.81E+07	2.09E+07	1.39E+07	1.97E+07	**4.20E+07**
	gi|64211663 5	46	34	28	complement C3-like	1.51E	1.86E	1.57E	2.15E	1.58E	1.82E	1.60E	2.09E	**3.68E+07**

						+07	+07	+07	+07	+07	+07	+07	+07	
	gi|185133875	55	14	13	precerebellin-like protein precursor [Oncorhynchus mykiss]gi|38000006|gb|AAF04305.2|AF192969_1 precerebellin-like protein [Oncorhynchus mykiss]gi|642115944|emb|CDQ67808.1| unnamed protein product [Oncorhynchus mykiss]	1.18E+07	1.82E+07	1.15E+07	1.77E+07	1.21E+07	1.71E+07	9.78E+06	1.55E+07	**3.52E+07**
	gi|742106867	11	25	13	PREDICTED: complement C3-like [Esox lucius]	1.06E+07	2.00E+07	9.95E+06	1.24E+07	1.07E+07	1.45E+07	8.38E+06	1.08E+07	**3.45E+07**
	gi|642075161	28	14	10	complement component C8 beta chain	1.27E+07	1.77E+07	1.33E+07	1.68E+07	1.32E+07	1.46E+07	1.23E+07	1.57E+07	**3.23E+07**
	gi|642123102	53	28	20	carboxylesterase 5A-like	1.25E+07	1.64E+07	1.26E+07	1.64E+07	1.36E+07	1.43E+07	1.22E+07	1.47E+07	**3.07E+07**
	gi|185133428	67	22	8	apolipoprotein E precursor [Oncorhynchus mykiss]gi|6688890|emb|CAB65320.1| apolipoprotein E [Oncorhynchus mykiss]	8.87E+06	1.45E+07	8.79E+06	1.38E+07	1.00E+07	1.42E+07	9.01E+06	1.33E+07	**2.87E+07**
	gi|642170226	30	10	2	alpha-2-macroglobulin 1	1.08E+07	1.47E+07	1.10E+07	1.43E+07	1.00E+07	1.41E+07	9.84E+06	1.69E+07	**2.87E+07**
	gi|742122380	20	15	7	PREDICTED: serum albumin 2-like [Esox lucius]	8.58E	1.72E	1.51E	8.69E	8.66E	1.02E	8.25E	8.94E	**2.75E+07**

						+06	+07	+07	+06	+06	+07	+06	+06	
	gi|642048510	51	7	4	apolipoprotein C-I	8.47E+06	1.37E+07	1.00E+07	1.16E+07	9.13E+06	1.31E+07	6.72E+06	1.02E+07	**2.68E+07**
	gi|642097655	41	17	8	haptoglobin-like	8.66E+06	1.30E+07	1.06E+07	1.46E+07	1.12E+07	1.24E+07	9.26E+06	1.22E+07	**2.53E+07**
	gi|1105532 6	47	6	6	chemotaxin [Oncorhynchus mykiss]gi|642125108|emb|CDQ61744.1| unnamed protein product [Oncorhynchus mykiss]	9.06E+06	1.34E+07	9.42E+06	1.66E+07	9.17E+06	1.16E+07	7.57E+06	1.15E+07	**2.51E+07**
TOP 100 ABUNDANT PROTEINS	gi|742105007	3	9	8	PREDICTED: ubiquitin carboxyl-terminal hydrolase 24 [Esox lucius]	8.43E+06	1.17E+07	8.85E+06	1.20E+07	1.14E+07	1.33E+07	6.64E+06	1.05E+07	**2.50E+07**
	gi|642114463	46	63	11	alpha-2-macroglobulin-like	9.96E+06	1.26E+07	9.49E+06	1.44E+07	1.10E+07	1.15E+07	1.02E+07	1.25E+07	**2.40E+07**
	gi|642120787	29	27	9	plasminogen	9.20E+06	1.17E+07	9.05E+06	1.26E+07	1.02E+07	1.22E+07	8.68E+06	1.10E+07	**2.40E+07**
	gi|315131458	23	14	13	complement factor I [Oncorhynchus mykiss]	5.80E	1.17E	7.96E	1.08E	8.46E	1.22E	5.71E	1.02E	**2.39E+07**

						+06	+07	+06	+07	+06	+07	+06	+07	
	gi|642085863	41	28	22	coagulation factor VII-like	7.67E+06	1.14E+07	8.89E+06	1.28E+07	9.51E+06	1.20E+07	8.45E+06	1.01E+07	**2.34E+07**
	gi|642083649	48	25	2	serum albumin 2	7.76E+06	1.05E+07	8.26E+06	1.43E+07	1.19E+07	1.30E+07	7.12E+06	1.19E+07	**2.34E+07**
	gi|642037772	15	4	4	complement factor H-related 2 isoform X3	6.54E+06	9.93E+06	6.60E+06	9.72E+06	8.92E+06	1.28E+07	6.32E+06	8.99E+06	**2.27E+07**
	gi|642096909	35	17	12	vitamin K-dependent C	9.88E+06	1.20E+07	1.03E+07	1.25E+07	9.07E+06	1.06E+07	1.03E+07	1.17E+07	**2.27E+07**
	gi|642061820	30	12	10	unnamed protein product	7.47E+06	1.04E+07	9.17E+06	1.32E+07	9.36E+06	1.21E+07	8.57E+06	1.07E+07	**2.25E+07**
	gi|642029044	37	26	13	inter-alpha-trypsin inhibitor heavy chain H3-like isoform X2	9.47E+06	1.23E+07	8.77E+06	1.47E+07	8.90E+06	9.81E+06	8.16E+06	1.13E+07	**2.21E+07**
	gi|642120266	46	24	9	antithrombin-III isoform X2	6.22E	1.05E	8.00E	1.08E	8.23E	1.15E	8.46E	1.30E	**2.20E+07**

						+06	+07	+06	+07	+06	+07	+06	+07	
	gi|642109357	41	27	20	kininogen 1 precursor	8.21E+06	1.09E+07	8.10E+06	1.32E+07	9.79E+06	1.09E+07	8.52E+06	1.10E+07	**2.18E+07**
	gi|238231567	32	8	5	C type lectin receptor B [Oncorhynchus mykiss]gi|223049425|gb|ACM80352.1| C type lectin receptor B [Oncorhynchus mykiss]	8.76E+06	1.12E+07	8.88E+06	1.37E+07	8.90E+06	1.01E+07	8.47E+06	1.01E+07	**2.14E+07**
	gi|642123356	36	103	68	apolipo B-100-like	6.76E+06	1.22E+07	6.75E+06	1.12E+07	6.65E+06	9.08E+06	7.93E+06	8.79E+06	**2.13E+07**
	gi|185132366	52	22	19	sex hormone-binding globulin precursor [Oncorhynchus mykiss]gi|82941397|dbj|BAE48779.1| sex hormone-binding globulin [Oncorhynchus mykiss]gi|642097615|emb|CDQ78569.1| unnamed protein product [Oncorhynchus mykiss]	8.21E+06	1.08E+07	8.33E+06	1.20E+07	9.65E+06	1.02E+07	8.35E+06	9.71E+06	**2.10E+07**
	gi|642093095	31	14	14	complement component C8 alpha chain	7.82E+06	1.14E+07	8.70E+06	1.05E+07	8.20E+06	9.37E+06	7.52E+06	1.03E+07	**2.08E+07**
	gi|642009198	47	26	6	alpha-2-macroglobulin- partial	7.85E+06	1.16E+07	7.43E+06	1.04E+07	9.90E+06	9.21E+06	8.32E+06	9.75E+06	**2.08E+07**
	gi|742213767	3	3	3	PREDICTED: trichohyalin-like [Esox lucius]	6.66E	8.77E	1.18E	1.16E	1.06E	1.16E	5.97E	9.32E	**2.04E+07**

					+06	+06	+07	+07	+07	+07	+06	+06	
	gi|64212335 4	48	28	10	apolipo B-100-like	7.01E+06	1.01E+07	7.24E+06	9.20E+06	7.50E+06	1.02E+07	7.02E+06	8.40E+06	**2.03E+07**
	gi|64211382 7	46	14	12	hibernation-specific plasma HP-55-like	7.20E+06	9.15E+06	6.71E+06	9.66E+06	7.90E+06	1.11E+07	7.03E+06	1.05E+07	**2.02E+07**
	gi|60490 11	50	49	3	transferrin [Oncorhynchus kisutch]	7.67E+06	9.77E+06	6.87E+06	1.11E+07	8.20E+06	1.02E+07	5.96E+06	9.76E+06	**2.00E+07**
	gi|64212212 7	43	18	13	angiotensinogen precursor	7.28E+06	1.05E+07	9.04E+06	1.15E+07	7.87E+06	9.42E+06	6.79E+06	9.03E+06	**1.99E+07**
	gi|19458011 1	55	20	3	complement component C3 [Salmo marmoratus]	5.72E+06	8.56E+06	6.12E+06	1.01E+07	8.52E+06	1.12E+07	4.95E+06	9.47E+06	**1.97E+07**
	gi|64200935 6	51	13	4	alpha-2-macroglobulin-like isoform X1	7.43E+06	9.55E+06	7.40E+06	1.01E+07	8.45E+06	8.99E+06	6.04E+06	8.42E+06	**1.85E+07**
	gi|49895296 1	6	25	15	PREDICTED: sacsin-like isoform X1 [Maylandia zebra]	5.76E	8.55E	6.53E	1.14E	4.27E	9.87E	2.04E	7.28E	**1.84E+07**

					+06	+06	+06	+07	+06	+06	+07	+06	
	gi|238814310	68	19	2	apolipoprotein A-II precursor [Oncorhynchus mykiss]gi|229890014|dbj|BAH58380.1| apolipoprotein A-II [Oncorhynchus mykiss]	6.33E+06	8.84E+06	7.22E+06	1.02E+07	7.62E+06	9.39E+06	6.12E+06	8.19E+06	**1.82E+07**
	gi|642097292	13	6	5	saxitoxin and tetrodotoxin-binding 1-like	6.57E+06	8.72E+06	7.51E+06	9.93E+06	7.46E+06	9.24E+06	5.68E+06	9.33E+06	**1.80E+07**
	gi|642116654	30	10	9	zinc-binding A33-like	6.45E+06	1.00E+07	6.83E+06	9.07E+06	5.43E+06	7.81E+06	4.62E+06	5.89E+06	**1.79E+07**
	gi|642106250	43	38	8	alpha-2-macroglobulin-like	6.56E+06	8.10E+06	6.47E+06	9.10E+06	7.98E+06	9.61E+06	6.99E+06	8.73E+06	**1.77E+07**
	gi|642112120	24	24	19	hyaluronan-binding 2	6.31E+06	8.58E+06	6.10E+06	7.04E+06	6.98E+06	8.96E+06	5.50E+06	7.36E+06	**1.75E+07**
	gi|742132676	11	38	11	PREDICTED: apolipoprotein B-100 [Esox lucius]	3.25E+06	1.49E+07	1.05E+07	2.70E+06	1.86E+06	2.47E+06	1.93E+06	2.53E+06	**1.74E+07**
	gi|642092661	35	54	31	complement C5	6.08E	8.74E	6.86E	8.07E	6.77E	8.47E	5.51E	7.05E	**1.72E+07**

					+06	+06	+06	+06	+06	+06	+06	+06	
	gi|597792168	12	3	3	PREDICTED: hemopexin-like isoform X1 [Astyanax mexicanus]	6.56E+06	9.03E+06	7.03E+06	9.27E+06	6.66E+06	7.93E+06	6.85E+06	7.13E+06	**1.70E+07**
	gi|642048509	62	15	4	apolipo Eb-like	5.79E+06	8.51E+06	5.60E+06	8.42E+06	6.55E+06	8.37E+06	6.39E+06	8.39E+06	**1.69E+07**
	gi|526253032	40	12	5	trout C-polysaccharide binding protein 2 precursor [Oncorhynchus mykiss]gi|432177701|emb|CCO02601.1| trout C-polysaccharide binding protein 2 [Oncorhynchus mykiss]	7.09E+06	9.50E+06	7.58E+06	1.17E+07	6.55E+06	7.11E+06	5.62E+06	8.68E+06	**1.66E+07**
	gi|642084202	32	20	13	vitronectin isoform X1	6.74E+06	8.61E+06	5.74E+06	8.52E+06	6.79E+06	7.80E+06	5.95E+06	7.39E+06	**1.64E+07**
	gi|642092626	17	6	5	venom factor-like	6.19E+06	8.25E+06	6.59E+06	9.40E+06	7.16E+06	7.52E+06	4.90E+06	1.01E+07	**1.58E+07**
	gi|185133413	28	24	22	complement component C6 precursor [Oncorhynchus mykiss]gi|55725598|emb|CAF22026.2| complement component C6 [Oncorhynchus mykiss]	4.94E+06	8.28E+06	6.53E+06	7.19E+06	6.01E+06	7.44E+06	5.19E+06	7.14E+06	**1.57E+07**
	gi|641931803	26	5	4	zinc-binding A33-like	4.94E	9.64E	6.51E	7.57E	3.09E	5.93E	3.76E	3.76E	**1.56E+07**

						+06	+06	+06	+06	+06	+06	+06	+06	
	gi|642033098	51	23	8	beta-2-glyco 1-like	5.29E+06	7.47E+06	5.76E+06	8.16E+06	6.02E+06	7.58E+06	5.00E+06	6.49E+06	**1.51E+07**
	gi|185135433	56	26	7	C1 inhibitor [Oncorhynchus mykiss]gi|40217254|emb|CAD58653.1| C1 inhibitor [Oncorhynchus mykiss]	4.67E+06	6.61E+06	5.27E+06	7.56E+06	6.13E+06	8.26E+06	5.00E+06	7.38E+06	**1.49E+07**
	gi|3982895	28	21	12	complement factor Bf-2 [Oncorhynchus mykiss gairdneri]	4.55E+06	6.44E+06	4.75E+06	1.05E+07	5.80E+06	8.43E+06	5.47E+06	7.04E+06	**1.49E+07**
	gi|64213318 2	50	35	7	prothrombin precursor	5.18E+06	7.32E+06	5.80E+06	7.90E+06	6.44E+06	7.49E+06	5.52E+06	6.97E+06	**1.48E+07**
	gi|64212260 2	31	22	13	complement factor B-like	5.02E+06	7.04E+06	5.37E+06	7.99E+06	6.14E+06	7.66E+06	4.96E+06	7.34E+06	**1.47E+07**
	gi|64212335 5	14	22	5	apolipo B-100	4.86E+06	7.22E+06	4.61E+06	6.79E+06	5.18E+06	7.12E+06	7.35E+06	5.78E+06	**1.43E+07**
	gi|642099368	36	14	6	inter-alpha-trypsin inhibitor heavy chain H3-like isoform X2	4.71E	6.75E	4.73E	7.06E	5.09E	7.04E	5.78E	6.58E	**1.38E+07**

						+06	+06	+06	+06	+06	+06	+06	+06	
	gi|642128069	31	86	69	apolipo B-100-like	5.09E+06	7.00E+06	5.00E+06	6.25E+06	4.67E+06	6.57E+06	5.42E+06	5.34E+06	**1.36E+07**
	gi|185134285	24	15	13	FBPL4 [Oncorhynchus mykiss]gi|78191586|gb|ABB29988.1| FBPL4 [Oncorhynchus mykiss]	5.42E+06	7.00E+06	4.80E+06	5.94E+06	3.20E+06	6.44E+06	3.65E+06	7.08E+06	**1.34E+07**
	gi|642045087	10	18	13	coagulation factor V	4.76E+06	7.39E+06	5.64E+06	6.78E+06	4.70E+06	5.99E+06	4.57E+06	6.11E+06	**1.34E+07**
	gi|642079848	61	12	2	apolipo B-100	4.84E+06	6.96E+06	4.36E+06	6.84E+06	4.44E+06	6.41E+06	4.32E+06	5.85E+06	**1.34E+07**
	gi|642113141	49	23	10	antithrombin-III isoform X2	4.18E+06	7.27E+06	4.03E+06	5.47E+06	4.63E+06	6.00E+06	3.62E+06	4.73E+06	**1.33E+07**
	gi|642102573	31	16	8	heparin cofactor 2	4.41E+06	5.93E+06	5.61E+06	8.76E+06	5.60E+06	6.91E+06	4.40E+06	5.83E+06	**1.28E+07**
	gi|209737406	72	34	2	Apolipoprotein A-I-1 precursor [Salmo salar]	5.44E	5.90E	5.65E	7.31E	5.70E	6.89E	4.97E	6.05E	**1.28E+07**

					+06	+06	+06	+06	+06	+06	+06	+06	
gi|642045735	25	11	6	fibrinogen alpha chain-like	4.50E+06	7.14E+06	5.42E+06	7.55E+06	4.26E+06	5.58E+06	4.00E+06	4.71E+06	**1.27E+07**
gi|642119413	65	8	4	Nucleoside diphosphate kinase A	6.10E+06	6.83E+06	6.59E+06	8.28E+06	4.98E+06	5.86E+06	5.06E+06	6.67E+06	**1.27E+07**
gi|736191546	7	23	12	PREDICTED: apolipoprotein B-100 [Notothenia coriiceps]	3.67E+06	8.65E+06	7.13E+06	3.68E+06	2.43E+06	3.86E+06	4.00E+06	3.16E+06	**1.25E+07**
gi|642008118	33	15	8	apolipo B-100-like	4.57E+06	6.32E+06	4.41E+06	6.23E+06	4.49E+06	6.03E+06	4.99E+06	5.15E+06	**1.24E+07**
gi|642122678	29	21	6	plasminogen precursor	4.51E+06	6.36E+06	4.64E+06	5.43E+06	5.19E+06	5.95E+06	4.10E+06	5.22E+06	**1.23E+07**
gi|642124443	25	10	6	LEG1 homolog	5.33E+06	7.22E+06	4.72E+06	6.55E+06	4.13E+06	4.93E+06	3.32E+06	4.57E+06	**1.22E+07**
gi|597760976	4	131	58	PREDICTED: titin-like [Astyanax mexicanus]	4.44E	6.82E	4.52E	5.42E	4.29E	5.34E	3.82E	4.51E	**1.22E+07**

						+06	+06	+06	+06	+06	+06	+06	+06	
	gi|642106148	27	10	9	coagulation factor IX-like	4.60E+06	6.28E+06	4.82E+06	6.37E+06	4.74E+06	5.82E+06	4.59E+06	6.34E+06	**1.21E+07**
	gi|642094497	60	114	16	complement C3-like	4.04E+06	5.88E+06	4.89E+06	5.86E+06	3.43E+06	6.18E+06	3.40E+06	5.67E+06	**1.21E+07**
	gi|185134784	17	12	10	complement factor B/C2-B precursor [Oncorhynchus mykiss]gi|11990428|dbj|BAB19788.1| complement factor B/C2-B [Oncorhynchus mykiss]	4.12E+06	7.17E+06	5.81E+06	5.07E+06	3.41E+06	4.64E+06	3.35E+06	4.27E+06	**1.18E+07**
	gi|642058544	32	15	13	myosin-2 heavy chain-like	4.44E+06	6.43E+06	4.68E+06	6.61E+06	4.03E+06	5.27E+06	3.12E+06	3.80E+06	**1.17E+07**
	gi|642087780	15	3	2	fucolectin-6-like	3.36E+06	6.82E+06	6.14E+06	3.91E+06	4.65E+06	4.62E+06	5.99E+06	4.64E+06	**1.14E+07**
	gi|185135501	30	12	9	chitinase precursor [Oncorhynchus mykiss]gi|56713231|emb|CAD59687.1| chitinase [Oncorhynchus mykiss]	3.70E+06	5.92E+06	5.38E+06	6.65E+06	4.37E+06	5.39E+06	4.12E+06	6.23E+06	**1.13E+07**
	gi|224613330	51	29	10	Fibronectin [Salmo salar]	4.14E	5.97E	4.45E	6.10E	3.89E	5.30E	3.98E	5.29E	**1.13E+07**

						+06	+06	+06	+06	+06	+06	+06	+06	
	gi|642040877	37	12	3	lumican precursor	4.69E+06	5.98E+06	4.38E+06	6.53E+06	4.74E+06	5.21E+06	4.04E+06	5.07E+06	**1.12E+07**
	gi|308322391	5	2	2	coagulation factor VII [Ictalurus furcatus]	2.94E+06	5.39E+06	3.65E+06	4.94E+06	4.40E+06	5.77E+06	3.44E+06	5.29E+06	**1.12E+07**
	gi|185135668	21	7	5	protein AMBP precursor [Oncorhynchus mykiss]gi|59796517|emb|CAD66667.1| alpha-1-microglobulin/bikunin precursor [Oncorhynchus mykiss]	3.93E+06	5.48E+06	4.09E+06	5.39E+06	4.41E+06	5.40E+06	3.44E+06	4.28E+06	**1.09E+07**
	gi|642114487	26	19	6	alpha-2-macroglobulin-like isoform X2	4.10E+06	5.86E+06	3.98E+06	5.54E+06	4.18E+06	4.97E+06	3.79E+06	4.48E+06	**1.08E+07**
	gi|658911471	3	10	7	PREDICTED: apolipoprotein B-100-like [Poecilia reticulata]	2.27E+06	5.50E+06	2.90E+06	3.58E+06	3.03E+06	5.17E+06	2.40E+06	3.12E+06	**1.07E+07**
	gi|808884183	7	17	8	Myosin-7 [Larimichthys crocea]	2.51E+06	4.77E+06	3.28E+06	4.95E+06	3.22E+06	5.73E+06	8.44E+06	4.26E+06	**1.05E+07**
	gi|642018013	47	12	5	complement factor D	3.71E	5.15E	3.92E	5.67E	3.90E	5.32E	3.06E	4.22E	**1.05E+07**

						+06	+06	+06	+06	+06	+06	+06	+06	
	gi|551503634	4	9	7	PREDICTED: ATP-binding cassette sub-family C member 8-like [Xiphophorus maculatus]	1.62E+06	9.64E+06	8.69E+06	1.30E+06	6.09E+05	7.44E+05	5.03E+05	6.30E+05	**1.04E+07**
	gi|642089067	28	6	3	ceruloplasmin isoform X1	4.00E+06	5.44E+06	3.64E+06	5.74E+06	3.59E+06	4.93E+06	3.43E+06	5.42E+06	**1.04E+07**
	gi|584003084	3	12	9	death-inducer obliterator 1 isoform X1	3.37E+06	6.01E+06	5.46E+06	4.50E+06	3.59E+06	4.35E+06	2.71E+06	4.20E+06	**1.04E+07**
	gi|642076990	38	9	6	Apolipo B-100	4.31E+06	5.70E+06	4.06E+06	5.34E+06	3.95E+06	4.58E+06	3.40E+06	4.04E+06	**1.03E+07**
	gi|642030929	13	5	5	complement C1q 2	3.75E+06	4.72E+06	3.72E+06	5.75E+06	5.03E+06	5.56E+06	4.00E+06	5.46E+06	**1.03E+07**
	gi|642106109	51	9	8	type-4 ice-structuring LS-12-like	4.61E+06	5.73E+06	4.17E+06	5.27E+06	3.66E+06	4.46E+06	3.04E+06	4.15E+06	**1.02E+07**
	gi|642027913	40	7	4	complement C3-like	3.92E	5.14E	3.94E	5.90E	4.34E	4.76E	3.54E	4.69E	**9.90E+06**

						+06	+06	+06	+06	+06	+06	+06	+06	
	gi|642127797	51	35	8	prothrombin-like isoform X1	3.94E+06	5.30E+06	3.73E+06	4.74E+06	3.70E+06	4.56E+06	3.78E+06	3.88E+06	**9.85E+06**
	gi|64219461	15	9	5	sulfhydryl oxidase 1-like	3.63E+06	5.13E+06	3.73E+06	4.43E+06	3.75E+06	4.64E+06	3.46E+06	4.54E+06	**9.76E+06**
	gi|226823296	12	3	3	leukolectin protein precursor [Salmo salar]gi|223016919|gb|ACM77812.1| leukolectin [Homo sapiens]gi|223016921|gb|ACM77813.1| leukolectin [Danio rerio]gi|226434249|emb|CAX65106.1| leukolectin protein [Salmo salar]	3.82E+06	5.68E+06	4.14E+06	4.28E+06	3.33E+06	3.95E+06	3.21E+06	3.97E+06	**9.63E+06**
	gi|64206708 7	40	15	5	complement C1q tumor necrosis factor-related 3-like	3.32E+06	4.75E+06	3.35E+06	5.27E+06	3.65E+06	4.80E+06	3.07E+06	4.58E+06	**9.56E+06**
	gi|64210517 1	43	21	3	complement component C9	3.29E+06	5.09E+06	3.86E+06	5.59E+06	3.83E+06	4.45E+06	3.03E+06	4.66E+06	**9.54E+06**
	gi|64212986 0	62	44	2	complement C3	3.00E+06	4.21E+06	3.36E+06	4.82E+06	3.74E+06	5.07E+06	3.06E+06	4.70E+06	**9.28E+06**
	gi|11095759	61	6	6	biotinidase fragment 2 [Oncorhynchus mykiss]	3.48E	5.43E	3.74E	5.04E	3.13E	3.84E	2.70E	3.90E	**9.27E+06**

						+06	+06	+06	+06	+06	+06	+06	+06	
	gi|642027912	40	19	11	complement C3-like	3.89E+06	5.05E+06	3.85E+06	4.85E+06	3.64E+06	4.22E+06	3.51E+06	3.98E+06	**9.27E+06**
	gi|642121560	46	21	7	beta-2-glyco 1-like	3.60E+06	4.93E+06	3.65E+06	4.39E+06	3.43E+06	4.28E+06	3.37E+06	4.22E+06	**9.22E+06**
	gi|642087097	32	62	5	complement C3-like	3.29E+06	4.76E+06	3.44E+06	4.90E+06	3.33E+06	4.39E+06	3.61E+06	4.22E+06	**9.16E+06**
	gi|641989771	52	8	4	alpha-2-macroglobulin- partial	3.46E+06	4.53E+06	3.52E+06	4.40E+06	3.91E+06	4.51E+06	3.36E+06	4.33E+06	**9.04E+06**
	gi|185132505	14	15	2	complement factor H precursor [Oncorhynchus mykiss]gi|86990283|emb|CAF25505.1| complement factor H precursor [Oncorhynchus mykiss]	3.99E+06	4.93E+06	3.84E+06	5.60E+06	4.01E+06	4.10E+06	3.99E+06	3.77E+06	**9.03E+06**
	gi|449885122	37	14	13	peptidoglycan recognition protein L2 [Oncorhynchus mykiss]gi|449885176|gb|AGF29406.1| peptidoglycan recognition protein L2 [Oncorhynchus mykiss]	3.30E+06	4.51E+06	3.81E+06	4.32E+06	3.57E+06	4.51E+06	3.38E+06	5.00E+06	**9.02E+06**
	gi|642087040	29	13	10	Z-dependent protease inhibitor	3.06E	4.31E	3.15E	5.33E	3.07E	4.65E	2.92E	4.32E	**8.96E+06**

						+06	+06	+06	+06	+06	+06	+06	+06	
	gi|185134355	14	10	8	matrix metalloproteinase-2 precursor [Oncorhynchus mykiss]gi|4996455|dbj|BAA78479.1| matrix metalloproteinase-2 [Oncorhynchus mykiss]	2.79E+06	5.39E+06	3.09E+06	3.78E+06	2.64E+06	3.49E+06	3.36E+06	3.81E+06	**8.88E+06**
	gi|185133340	9	4	3	complement factor H1 protein precursor [Oncorhynchus mykiss]gi|77362542|emb|CAJ01769.2| complement factor H1 protein [Oncorhynchus mykiss]	2.57E+06	4.60E+06	3.03E+06	4.23E+06	2.72E+06	4.26E+06	3.08E+06	3.53E+06	**8.86E+06**
	gi|642119594	4	79	47	titin-like isoform X12	8.83E+05	4.95E+06	1.31E+06	1.08E+06	9.68E+05	3.83E+06	1.25E+06	1.04E+06	**8.78E+06**
	gi|642091667	15	7	5	hibernation-specific plasma HP-55-like	3.68E+06	4.70E+06	3.11E+06	3.82E+06	2.79E+06	3.85E+06	3.06E+06	3.50E+06	**8.55E+06**
	gi|642080218	40	21	9	inter-alpha-trypsin inhibitor heavy chain H2	2.89E+06	4.44E+06	3.08E+06	4.41E+06	3.21E+06	3.97E+06	3.44E+06	3.62E+06	**8.41E+06**
	gi|642114347	18	7	7	carboxypeptidase N subunit 2-like	3.29E+06	4.38E+06	3.18E+06	4.00E+06	3.48E+06	3.98E+06	3.34E+06	3.79E+06	**8.36E+06**
	gi|528504300	17	2	2	PREDICTED: uncharacterized protein LOC101883708 [Danio rerio]	2.59E	4.26E	3.08E	3.53E	2.45E	4.04E	2.07E	3.12E	**8.30E+06**

						+06	+06	+06	+06	+06	+06	+06	+06	
	gi|642120853	30	5	5	prostaglandin-H2 D-isomerase-like	3.16E+06	4.46E+06	3.59E+06	4.00E+06	3.33E+06	3.84E+06	3.10E+06	3.85E+06	**8.29E+06**
	gi|551530433	6	5	4	PREDICTED: complement C5-like partial [Xiphophorus maculatus]	2.78E+06	4.30E+06	3.55E+06	4.62E+06	3.22E+06	3.89E+06	3.53E+06	3.71E+06	**8.19E+06**
	gi|213511196	66	9	5	Nucleoside diphosphate kinase A [Salmo salar]gi|209735398|gb|ACI68568.1| Nucleoside diphosphate kinase A [Salmo salar]gi|223647142|gb|ACN10329.1| Nucleoside diphosphate kinase A [Salmo salar]gi|223673015|gb|ACN12689.1|...	3.85E+06	4.63E+06	4.04E+06	4.76E+06	3.22E+06	3.51E+06	3.15E+06	3.75E+06	**8.14E+06**
	gi|642077823	14	4	2	complement factor H-like	3.22E+06	4.87E+06	3.15E+06	3.97E+06	2.67E+06	3.22E+06	2.99E+06	3.27E+06	**8.08E+06**
	gi|742251821	22	23	3	PREDICTED: inter-alpha-trypsin inhibitor heavy chain H3-like [Esox lucius]	2.96E+06	3.55E+06	2.85E+06	4.85E+06	3.39E+06	4.35E+06	2.73E+06	3.90E+06	**7.90E+06**
	gi|742179653	9	35	16	PREDICTED: apolipoprotein B-100-like [Esox lucius]	4.70E+06	4.09E+06	2.91E+06	5.04E+06	2.90E+06	3.80E+06	2.96E+06	3.66E+06	**7.90E+06**
	gi|642051686	22	13	7	inter-alpha-trypsin inhibitor heavy chain H3	3.13E	4.73E	2.76E	4.36E	2.18E	3.08E	2.85E	3.39E	**7.81E+06**

						+06	+06	+06	+06	+06	+06	+06	+06	
	gi|641931516	39	10	7	inter-alpha-trypsin inhibitor heavy chain H3-like isoform X2	3.21E+06	4.00E+06	3.14E+06	4.10E+06	2.50E+06	3.76E+06	2.87E+06	3.54E+06	**7.77E+06**
	gi|209736396	55	10	3	Catechol-O-methyltransferase domain-containing protein 1 [Salmo salar]	2.89E+06	3.72E+06	3.06E+06	5.14E+06	2.83E+06	4.01E+06	3.15E+06	3.94E+06	**7.73E+06**
	gi|47213186	17	7	5	warm temperature acclimation-related 65 kDa	2.56E+06	4.12E+06	3.06E+06	4.19E+06	3.10E+06	3.60E+06	2.81E+06	3.41E+06	**7.73E+06**
	gi|642114970	22	5	3	complement C1q 4	2.62E+06	3.76E+06	2.87E+06	4.02E+06	3.26E+06	3.96E+06	3.43E+06	3.70E+06	**7.72E+06**
	gi|642091496	29	10	7	alpha-2-antiplasmin-like isoform X3	3.14E+06	4.29E+06	3.29E+06	4.00E+06	3.00E+06	3.37E+06	2.54E+06	2.84E+06	**7.66E+06**
	gi|642098841	20	18	11	complement C4-like	2.96E+06	3.93E+06	3.58E+06	3.58E+06	3.03E+06	3.72E+06	3.22E+06	4.26E+06	**7.65E+06**
	gi|742166032	23	7	5	PREDICTED: coagulation factor VII-like [Esox lucius]	2.46E	3.55E	2.17E	3.05E	3.03E	4.03E	1.91E	2.84E	**7.58E+06**

						+06	+06	+06	+06	+06	+06	+06	+06	
	gi|742160240	9	19	3	PREDICTED: complement C4-like [Esox lucius]	3.11E+06	3.87E+06	2.77E+06	3.77E+06	2.98E+06	3.58E+06	2.83E+06	3.36E+06	**7.45E+06**
	gi|642101908	33	10	6	serine (or cysteine) peptidase clade member 2 precursor	2.71E+06	3.71E+06	2.95E+06	3.91E+06	2.88E+06	3.38E+06	2.15E+06	2.67E+06	**7.08E+06**
	gi|742081634	19	26	3	PREDICTED: alpha-2-macroglobulin-like isoform X1 [Esox lucius]	6.08E+06	3.87E+06	3.22E+06	3.70E+06	3.10E+06	3.13E+06	3.04E+06	3.74E+06	**6.99E+06**
	gi|642091137	41	23	7	inter-alpha-trypsin inhibitor heavy chain H3-like isoform X1	2.86E+06	3.76E+06	2.76E+06	3.43E+06	2.43E+06	3.22E+06	2.86E+06	3.35E+06	**6.99E+06**
	gi|642130235	29	49	10	myosin-6 isoform X1	2.61E+06	3.91E+06	2.45E+06	3.32E+06	3.12E+06	3.05E+06	2.74E+06	3.05E+06	**6.95E+06**
	gi|642089068	8	3	3	ceruloplasmin	2.77E+06	3.75E+06	2.74E+06	3.57E+06	2.37E+06	3.17E+06	2.43E+06	3.08E+06	**6.92E+06**
	gi|642109461	33	14	4	insulin-like growth factor-binding complex acid labile subunit	2.51E	3.47E	2.52E	3.32E	2.42E	3.45E	2.62E	3.81E	**6.92E+06**

						+06	+06	+06	+06	+06	+06	+06	+06	
	gi|658846088	4	20	7	PREDICTED: dynein heavy chain 8 axonemal [Poecilia reticulata]	5.02E+05	1.71E+06	5.64E+05	1.19E+06	1.40E+06	5.15E+06	1.59E+07	4.48E+06	**6.86E+06**
	gi|642048493	36	15	12	Pancreatic alpha-amylase	2.41E+06	3.49E+06	2.89E+06	3.55E+06	2.69E+06	3.34E+06	2.44E+06	3.21E+06	**6.83E+06**
	gi|742106233	7	5	4	PREDICTED: alpha-2-HS-glycoprotein-like [Esox lucius]	2.40E+06	3.54E+06	2.48E+06	3.20E+06	2.87E+06	3.26E+06	2.19E+06	2.91E+06	**6.80E+06**
	gi|528512584	2	7	6	PREDICTED: apolipoprotein B-100 [Danio rerio]	2.25E+06	3.36E+06	2.37E+06	3.16E+06	2.09E+06	3.33E+06	2.16E+06	2.95E+06	**6.69E+06**
	gi|642122677	60	6	3	plasminogen precursor	3.17E+06	3.38E+06	2.71E+06	2.95E+06	2.83E+06	3.15E+06	1.98E+06	2.82E+06	**6.53E+06**
	gi|213513658	12	7	5	Galectin-3-binding protein precursor [Salmo salar]gi|209155534|gb|ACI33999.1| Galectin-3-binding protein precursor [Salmo salar]gi|223648342|gb|ACN10929.1| Galectin-3-binding protein precursor [Salmo salar]	2.43E+06	3.38E+06	2.48E+06	2.88E+06	2.62E+06	3.11E+06	2.56E+06	3.09E+06	**6.49E+06**
	gi|185134392	19	6	6	sex hormone-binding globulin beta form precursor [Oncorhynchus mykiss]gi|146771518|gb|ABQ45411.1| sex hormone-binding globulin beta form [Oncorhynchus mykiss]	2.98E	4.01E	2.81E	2.92E	1.71E	2.45E	2.55E	2.62E	**6.46E+06**

						+06	+06	+06	+06	+06	+06	+06	+06	
	gi|642033097	17	5	3	Beta-2-glyco 1 precursor	2.57E+06	3.26E+06	2.69E+06	3.82E+06	2.82E+06	3.15E+06	2.90E+06	3.64E+06	**6.40E+06**
	gi|642095786	33	22	10	complement C4-B-like	3.71E+06	3.16E+06	3.01E+06	2.98E+06	2.44E+06	3.15E+06	2.33E+06	2.79E+06	**6.31E+06**
	gi|642098176	28	14	6	plastin-2	2.55E+06	3.62E+06	2.73E+06	2.77E+06	2.42E+06	2.59E+06	2.32E+06	2.76E+06	**6.21E+06**
	gi|642084496	38	23	3	alpha-2-macroglobulin-like isoform X1	2.06E+06	3.06E+06	2.17E+06	3.20E+06	2.51E+06	3.01E+06	1.99E+06	2.51E+06	**6.08E+06**
	gi|642085716	18	5	5	complement C1s subcomponent-like	2.20E+06	3.27E+06	2.40E+06	2.85E+06	2.29E+06	2.76E+06	1.86E+06	2.45E+06	**6.02E+06**
	gi|185133660	32	2	2	apolipoprotein CII precursor [Oncorhynchus mykiss]gi|9992871|gb|AAG11410.1|AF140783_1 apolipoprotein CII [Oncorhynchus mykiss]gi|642000858|emb|CDQ98000.1| unnamed protein product [Oncorhynchus mykiss]	2.31E+06	3.16E+06	2.07E+06	3.22E+06	2.43E+06	2.86E+06	1.94E+06	2.80E+06	**6.02E+06**
	gi|642105269	28	6	2	plasma protease C1 inhibitor-like	1.94E	2.95E	2.05E	2.68E	2.29E	3.01E	2.09E	2.48E	**5.97E+06**

						+06	+06	+06	+06	+06	+06	+06	+06	
	gi|642123347	25	8	6	leucine-rich alpha-2-glyco -like	2.81E+06	3.10E+06	2.26E+06	3.59E+06	2.32E+06	2.80E+06	2.07E+06	2.79E+06	**5.90E+06**
	gi|642110737	16	16	3	Epithelial cadherin precursor	2.35E+06	3.21E+06	2.30E+06	2.68E+06	2.59E+06	2.66E+06	2.31E+06	2.94E+06	**5.86E+06**
	gi|213512923	19	6	5	Carboxypeptidase N catalytic chain precursor [Salmo salar]gi|209153960|gb|ACI33212.1| Carboxypeptidase N catalytic chain precursor [Salmo salar]	2.26E+06	4.06E+06	3.42E+06	2.26E+06	1.49E+06	1.75E+06	1.45E+06	1.85E+06	**5.81E+06**
	gi|238231541	45	12	2	mannan-binding lectin H3 precursor [Oncorhynchus mykiss]gi|159147215|gb|ABW91002.1| mannan-binding lectin H3 precursor [Oncorhynchus mykiss]	1.96E+06	2.88E+06	1.86E+06	2.68E+06	2.37E+06	2.70E+06	2.43E+06	2.53E+06	**5.58E+06**
	gi|583990154	4	10	8	PREDICTED: protein furry homolog-like isoform X4 [Neolamprologus brichardi]	1.65E+06	3.46E+06	2.36E+06	2.64E+06	1.54E+06	2.11E+06	1.52E+06	1.73E+06	**5.56E+06**
	gi|209155350	14	8	7	Epoxide hydrolase 2 [Salmo salar]	2.36E+06	3.01E+06	2.40E+06	2.51E+06	2.17E+06	2.51E+06	2.17E+06	2.49E+06	**5.52E+06**
	gi|642108905	21	8	8	phospholipid transfer -like	2.40E	2.87E	2.46E	2.75E	2.38E	2.62E	2.59E	2.55E	**5.49E+06**

						+06	+06	+06	+06	+06	+06	+06	+06	
	gi|439850	49	23	4	IgM heavy chain membrane bound form [Oncorhynchus mykiss]	1.79E+06	2.41E+06	1.73E+06	2.44E+06	3.06E+06	3.07E+06	2.62E+06	4.13E+06	**5.48E+06**
	gi|197632385	36	11	2	creatine kinase-3 [Salmo salar]	2.17E+06	2.64E+06	3.27E+06	2.79E+06	1.87E+06	2.82E+06	2.51E+06	2.94E+06	**5.46E+06**
	gi|642097131	19	10	10	atrial natriuretic peptide-converting enzyme-like	1.98E+06	2.91E+06	2.63E+06	2.39E+06	2.29E+06	2.48E+06	1.77E+06	2.45E+06	**5.39E+06**
	gi|641950286	40	2	2	inter-alpha-trypsin inhibitor heavy chain H3-like isoform X2	1.74E+06	2.95E+06	2.28E+06	2.55E+06	1.95E+06	2.44E+06	1.81E+06	2.13E+06	**5.39E+06**
	gi|642132215	21	7	3	apolipo Eb-like	2.24E+06	2.98E+06	1.95E+06	2.80E+06	1.65E+06	2.38E+06	2.11E+06	3.08E+06	**5.36E+06**
	gi|657738164	10	5	2	PREDICTED: antithrombin-III [Cynoglossus semilaevis]	2.23E+06	2.86E+06	2.38E+06	2.77E+06	1.76E+06	2.43E+06	1.97E+06	2.23E+06	**5.29E+06**
	gi|64211917 2	37	11	2	C1 inhibitor	2.04E	2.72E	2.03E	2.71E	2.20E	2.56E	1.98E	2.70E	**5.28E+06**

						+06	+06	+06	+06	+06	+06	+06	+06	
	gi|641949433	18	3	3	inter-alpha-trypsin inhibitor heavy chain H2	1.87E+06	2.67E+06	1.97E+06	2.43E+06	1.81E+06	2.59E+06	1.77E+06	2.11E+06	**5.26E+06**
	gi|171544935	11	8	2	serotransferrin precursor [Oryzias latipes]gi|158138479|dbj|BAF81983.1| transferrin [Oryzias latipes]	1.64E+06	2.60E+06	1.92E+06	2.35E+06	1.99E+06	2.62E+06	1.09E+06	1.93E+06	**5.22E+06**
	gi|642016083	14	3	3	Transaldolase	2.73E+06	2.94E+06	2.61E+06	3.19E+06	2.34E+06	2.28E+06	2.76E+06	2.78E+06	**5.22E+06**
	gi|642065539	41	13	6	alpha-2-macroglobulin- partial	1.96E+06	2.55E+06	2.06E+06	2.53E+06	2.09E+06	2.67E+06	1.69E+06	2.40E+06	**5.22E+06**
	gi|499032797	17	5	5	PREDICTED: apolipoprotein A-I-like [Maylandia zebra]	2.17E+06	2.73E+06	2.10E+06	2.80E+06	2.36E+06	2.47E+06	2.10E+06	2.58E+06	**5.20E+06**
	gi|224587882	42	7	6	Calcium/calmodulin-dependent protein kinase type II delta chain [Salmo salar]	1.93E+06	2.72E+06	1.88E+06	2.41E+06	2.03E+06	2.47E+06	1.80E+06	2.36E+06	**5.19E+06**
	gi|47224327	3	2	2	EFR3 homolog B isoform X3	8.15E	4.23E	2.84E	1.18E	8.15E	9.52E	9.13E	1.12E	**5.18E+06**

						+05	+06	+06	+06	+05	+05	+05	+06	
	gi|642031521	53	27	6	fibronectin isoform X2	2.49E+06	2.63E+06	2.02E+06	2.99E+06	1.82E+06	2.53E+06	1.80E+06	2.12E+06	**5.16E+06**
	gi|213512537	34	8	5	betaine--homocysteine S-methyltransferase 1 [Salmo salar]gi|197632195|gb|ACH70821.1| betaine-homocysteine methyltransferase [Salmo salar]	3.20E+06	2.59E+06	2.50E+06	2.87E+06	2.08E+06	2.53E+06	2.11E+06	2.81E+06	**5.12E+06**
	gi|642077821	19	18	3	complement factor H-like	1.78E+06	2.93E+06	1.97E+06	2.54E+06	1.76E+06	2.19E+06	1.62E+06	1.86E+06	**5.11E+06**
	gi|498949194	3	8	2	PREDICTED: fibronectin-like isoform X1 [Maylandia zebra]	1.51E+06	2.57E+06	1.87E+06	2.48E+06	1.67E+06	2.43E+06	1.54E+06	1.87E+06	**5.00E+06**
	gi|642084217	25	10	5	aminopeptidase	2.11E+06	2.61E+06	1.87E+06	2.20E+06	1.88E+06	2.37E+06	1.88E+06	2.40E+06	**4.98E+06**
	gi|11613556	30	58	3	complement component C3-3 [Oncorhynchus mykiss]	1.69E+06	2.39E+06	1.87E+06	2.55E+06	2.16E+06	2.58E+06	1.61E+06	2.11E+06	**4.97E+06**
	gi|642117475	6	12	9	rootletin isoform X3	1.19E	2.69E	1.18E	1.07E	1.05E	2.25E	9.70E	1.36E	**4.93E+06**

						+06	+06	+06	+06	+06	+06	+05	+06	
	gi|742119387	6	6	2	PREDICTED: thrombospondin-4 [Esox lucius]	2.01E+06	2.39E+06	1.72E+06	2.31E+06	1.97E+06	2.47E+06	1.84E+06	2.50E+06	**4.85E+06**
	gi|642099637	11	4	4	Ependymin precursor	1.76E+06	2.53E+06	1.41E+06	1.76E+06	1.68E+06	2.27E+06	1.52E+06	1.80E+06	**4.80E+06**
	gi|657528227	3	12	9	PREDICTED: vacuolar protein sorting-associated protein 13B [Stegastes partitus]	6.27E+05	4.35E+06	1.21E+06	4.79E+05	3.26E+05	4.43E+05	4.63E+05	5.15E+05	**4.79E+06**
	gi|224487706	45	10	4	RecName: Full=L-rhamnose-binding lectin CSL1 [Oncorhynchus keta]	1.80E+06	2.35E+06	1.92E+06	2.57E+06	2.26E+06	2.44E+06	1.97E+06	2.98E+06	**4.79E+06**
	gi|736300249	4	8	3	PREDICTED: complement C4-like [Notothenia coriiceps]	2.00E+06	2.45E+06	2.05E+06	2.50E+06	1.97E+06	2.33E+06	2.04E+06	2.02E+06	**4.77E+06**
	gi|765163024	6	25	17	PREDICTED: apolipoprotein B-100-like isoform X1 [Oryzias latipes]	1.74E+06	2.49E+06	2.26E+06	2.49E+06	1.52E+06	2.25E+06	1.80E+06	2.05E+06	**4.74E+06**
	gi|197632581	14	5	4	solute carrier family 25-1 [Salmo salar]gi|209733508|gb|ACI67623.1| ADP/ATP translocase 2 [Salmo salar]gi|223646686|gb|ACN10101.1| ADP/ATP translocase 2 [Salmo salar]gi|223672535|gb|ACN12449.1| ADP/ATP translocase 2 [Salmo ...	2.07E	2.64E	1.67E	2.07E	2.50E	2.03E	1.75E	1.95E	**4.67E+06**

						+06	+06	+06	+06	+06	+06	+06	+06	
	gi|51949771	7	17	6	fibronectin 1b [Danio rerio]	1.75E+06	2.60E+06	2.16E+06	2.21E+06	1.74E+06	2.01E+06	1.60E+06	1.86E+06	**4.61E+06**
	gi|221221540	15	3	2	Ig kappa chain V-IV region JI precursor [Salmo salar]	9.95E+05	3.25E+06	1.24E+06	1.26E+06	1.09E+06	1.24E+06	1.21E+06	1.31E+06	**4.49E+06**
	gi|642025580	30	12	3	haptoglobin-like	1.62E+06	2.46E+06	1.93E+06	3.02E+06	1.54E+06	2.00E+06	1.57E+06	1.88E+06	**4.46E+06**
	gi|642106413	14	7	4	phosphatidylcholine-sterol acyltransferase-like	1.99E+06	2.51E+06	1.97E+06	2.28E+06	1.72E+06	1.94E+06	1.70E+06	2.11E+06	**4.44E+06**
	gi|213515556	6	7	3	glycogen phosphorylase muscle form [Salmo salar]gi|197632011|gb|ACH70729.1| glycogen phosphorylase [Salmo salar]	1.82E+06	2.47E+06	1.88E+06	2.35E+06	1.60E+06	1.91E+06	1.89E+06	1.74E+06	**4.38E+06**
	gi|742234068	10	8	2	PREDICTED: complement factor B-like [Esox lucius]	1.66E+06	2.44E+06	1.65E+06	2.04E+06	1.53E+06	1.93E+06	1.38E+06	2.16E+06	**4.38E+06**
	gi|831313718	4	113	51	PREDICTED: titin-like [Clupea harengus]	1.78E	2.19E	1.90E	2.48E	2.39E	2.18E	1.71E	2.15E	**4.37E+06**

						+06	+06	+06	+06	+06	+06	+06	+06	
	gi|658840761	4	3	2	PREDICTED: mitogen-activated protein kinase 6 [Poecilia reticulata]gi|658840763|ref|XP_008402784.1| PREDICTED: mitogen-activated protein kinase 6 [Poecilia reticulata]	1.24E+06	1.93E+06	1.82E+06	2.26E+06	1.97E+06	2.44E+06	1.36E+06	2.13E+06	**4.37E+06**
	gi|657599686	3	6	5	PREDICTED: myosin-9-like isoform X2 [Stegastes partitus]	1.47E+06	2.06E+06	1.74E+06	2.49E+06	1.95E+06	2.28E+06	1.72E+06	1.95E+06	**4.34E+06**
	gi|1109575 7	23	2	2	biotinidase fragment 1 [Oncorhynchus mykiss]	1.74E+06	2.48E+06	1.74E+06	2.83E+06	1.47E+06	1.87E+06	1.90E+06	1.79E+06	**4.34E+06**
	gi|311771746	22	9	5	serine (or cysteine) peptidase inhibitor clade F member 2 precursor [Oncorhynchus mykiss]gi|302353533|emb|CBW45296.1| serpin peptidase inhibitor clade F member 2 [Oncorhynchus mykiss]	1.60E+06	2.18E+06	1.59E+06	2.07E+06	1.55E+06	2.14E+06	2.02E+06	1.86E+06	**4.32E+06**
	gi|1542598 6	16	5	2	immunoglobulin light chain [Salmo salar]	1.55E+06	1.95E+06	1.51E+06	1.94E+06	2.18E+06	2.36E+06	2.16E+06	2.59E+06	**4.31E+06**
	gi|742219423	15	12	4	PREDICTED: ectonucleotide pyrophosphatase/phosphodiesterase family member 2-like isoform X1 [Esox lucius]	2.45E+06	2.25E+06	1.70E+06	2.07E+06	1.76E+06	2.06E+06	1.89E+06	2.41E+06	**4.31E+06**
	gi|820122492	13	10	4	serotransferrin precursor [Scleropages formosus]	1.61E	2.31E	1.77E	2.32E	1.59E	1.99E	1.49E	1.98E	**4.30E+06**

						+06	+06	+06	+06	+06	+06	+06	+06	
	gi|642106460	5	2	2	cholesteryl ester transfer	2.07E+06	2.27E+06	1.80E+06	2.45E+06	1.82E+06	2.02E+06	1.99E+06	2.44E+06	**4.29E+06**
	gi|742225458	16	3	2	PREDICTED: C-reactive protein-like [Esox lucius]	1.68E+06	2.28E+06	1.92E+06	2.77E+06	1.76E+06	1.97E+06	1.57E+06	1.99E+06	**4.25E+06**
	gi|657559544	5	6	2	PREDICTED: inter-alpha-trypsin inhibitor heavy chain H3-like isoform X2 [Stegastes partitus]	2.19E+06	2.13E+06	1.93E+06	2.74E+06	1.71E+06	2.01E+06	2.23E+06	2.52E+06	**4.14E+06**
	gi|617452509	11	10	2	PREDICTED: ectonucleotide pyrophosphatase/phosphodiesterase family member 2-like [Poecilia formosa]	1.23E+06	2.47E+06	1.33E+06	2.40E+06	1.83E+06	1.65E+06	1.84E+06	1.42E+06	**4.13E+06**
	gi|734622170	8	23	10	PREDICTED: apolipoprotein B-100-like [Larimichthys crocea]	1.49E+06	1.83E+06	1.52E+06	1.83E+06	1.69E+06	2.27E+06	1.06E+06	1.51E+06	**4.10E+06**
	gi|334883514	17	3	3	F-type lectin 2 [Oplegnathus fasciatus]	2.29E+06	2.20E+06	2.16E+06	2.34E+06	1.60E+06	1.85E+06	2.01E+06	2.04E+06	**4.05E+06**
	gi|768940388	8	3	3	PREDICTED: alpha-1-antitrypsin homolog [Takifugu rubripes]	1.69E	2.10E	1.86E	2.16E	1.61E	1.91E	1.34E	1.73E	**4.01E+06**

						+06	+06	+06	+06	+06	+06	+06	+06	
	gi|185133567	52	58	3	serum albumin 2 precursor [Salmo salar]gi|543792|sp|Q03156.1|ALBU2_SALSA RecName: Full=Serum albumin 2; Flags: Precursor [Salmo salar]gi|64350|emb|CAA43187.1| serum albumin 2 [Salmo salar]	1.28E+06	2.21E+06	1.57E+06	1.74E+06	1.55E+06	1.80E+06	1.00E+06	1.53E+06	**4.01E+06**
	gi|642014409	16	6	2	coagulation factor IX-like	1.54E+06	2.20E+06	1.41E+06	1.92E+06	1.37E+06	1.79E+06	1.58E+06	1.90E+06	**3.99E+06**
	gi|642117140	31	10	10	Z-dependent protease inhibitor-like	1.52E+06	2.14E+06	1.50E+06	1.95E+06	1.42E+06	1.85E+06	1.60E+06	2.02E+06	**3.99E+06**
	gi|432910300	8	2	2	PREDICTED: apolipoprotein A-I-like isoform X2 [Oryzias latipes]	1.47E+06	2.43E+06	1.64E+06	1.79E+06	1.02E+06	1.53E+06	1.44E+06	1.50E+06	**3.96E+06**
	gi|831280882	1	5	5	PREDICTED: SCO-spondin [Clupea harengus]	5.81E+05	2.93E+06	7.81E+05	6.01E+05	3.56E+05	1.03E+06	8.90E+05	3.41E+05	**3.96E+06**
	gi|742082238	10	14	6	PREDICTED: complement C4-A-like [Esox lucius]	1.37E+06	1.69E+06	1.19E+06	1.51E+06	1.72E+06	2.24E+06	1.30E+06	2.99E+06	**3.93E+06**
	gi|641990040	19	5	3	coagulation factor XIII A chain-like isoform X1	2.11E	2.03E	1.57E	2.11E	1.63E	1.90E	1.58E	1.94E	**3.93E+06**

						+06	+06	+06	+06	+06	+06	+06	+06	
	gi|642106337	33	22	5	integrin beta-1-like isoform X1	1.36E+06	2.28E+06	1.83E+06	1.95E+06	1.58E+06	1.59E+06	1.37E+06	1.61E+06	**3.87E+06**
	gi|820146409	4	10	3	slow myosin heavy chain 2 [Scleropages formosus]	1.54E+06	2.26E+06	1.83E+06	1.95E+06	1.42E+06	1.60E+06	1.43E+06	1.63E+06	**3.86E+06**
	gi|688540567	5	12	8	PREDICTED: uncharacterized protein LOC103910187 [Danio rerio]	1.36E+06	2.21E+06	1.31E+06	1.62E+06	1.25E+06	1.60E+06	1.21E+06	1.32E+06	**3.81E+06**
	gi|642126852	26	12	3	complement C3-like	1.46E+06	2.06E+06	1.28E+06	2.03E+06	1.42E+06	1.71E+06	1.49E+06	1.47E+06	**3.77E+06**
	gi|213512772	20	18	2	Complement component C7 precursor [Salmo salar]gi|209147494|gb|ACI32892.1| Complement component C7 precursor [Salmo salar]	1.21E+06	1.91E+06	1.35E+06	1.99E+06	1.71E+06	1.85E+06	1.96E+06	1.63E+06	**3.76E+06**
	gi|820133078	7	7	4	integrin beta-2 [Scleropages formosus]	1.30E+06	2.03E+06	1.29E+06	1.78E+06	1.41E+06	1.73E+06	1.03E+06	1.51E+06	**3.76E+06**
	gi|768942557	8	13	3	PREDICTED: complement C3-like [Takifugu rubripes]	1.33E	2.05E	1.20E	1.52E	1.37E	1.71E	1.28E	1.55E	**3.76E+06**

						+06	+06	+06	+06	+06	+06	+06	+06	
	gi|688572309	4	128	49	PREDICTED: titin isoform X5 [Danio rerio]	1.26E+06	1.94E+06	1.40E+06	1.64E+06	1.36E+06	1.82E+06	1.26E+06	1.45E+06	**3.76E+06**
	gi|675304903	9	3	3	apolipoprotein A-1 [Channa striata]	1.11E+06	2.38E+06	1.34E+06	1.25E+06	9.36E+05	1.38E+06	1.05E+06	1.10E+06	**3.75E+06**
	gi|642101935	31	10	7	Beta-Ala-His dipeptidase	1.44E+06	1.93E+06	1.47E+06	2.17E+06	1.36E+06	1.74E+06	1.74E+06	1.77E+06	**3.67E+06**
	gi|145279639	10	4	2	sulfotransferase family 2 cytosolic sulfotransferase 3 [Danio rerio]gi|688592577|ref|XP_009290901.1| PREDICTED: sulfotransferase family 2 cytosolic sulfotransferase 3 isoform X1 [Danio rerio]gi|688592581|ref|XP_009290...	1.48E+06	1.98E+06	1.81E+06	1.53E+06	1.05E+06	1.63E+06	1.53E+06	1.42E+06	**3.61E+06**
	gi|209732794	55	18	2	Apolipoprotein A-IV precursor [Salmo salar]	1.43E+06	1.79E+06	1.90E+06	1.85E+06	1.15E+06	1.78E+06	1.34E+06	1.57E+06	**3.57E+06**
	gi|742108646	9	4	4	PREDICTED: biotinidase [Esox lucius]	1.36E+06	2.12E+06	1.58E+06	1.87E+06	1.20E+06	1.44E+06	1.22E+06	1.25E+06	**3.57E+06**
	gi|185135590	16	2	2	ependymin-1 precursor [Oncorhynchus mykiss]gi|119515|sp|P28770.1|EPD1_ONCMY RecName: Full=Ependymin-1; AltName: Full=Ependymin I; Short=EPD-I; Flags:	1.76E	1.97E	1.60E	1.67E	1.42E	1.60E	1.30E	1.35E	**3.56E+06**

					Precursor [Oncorhynchus mykiss]gi|213412|gb|AAA49399.1| ependymin [On...	+06	+06	+06	+06	+06	+06	+06	+06	
	gi|642100192	15	5	4	coagulation factor IX	1.14E+06	1.75E+06	1.09E+06	1.46E+06	1.24E+06	1.81E+06	3.06E+06	1.64E+06	**3.55E+06**
	gi|736214088	9	7	2	PREDICTED: inter-alpha-trypsin inhibitor heavy chain H2 [Notothenia coriiceps]	1.52E+06	1.77E+06	1.41E+06	1.81E+06	1.28E+06	1.74E+06	1.33E+06	1.61E+06	**3.50E+06**
	gi|742248710	7	30	14	PREDICTED: apolipoprotein B-100-like [Esox lucius]	2.18E+06	1.81E+06	1.19E+06	1.70E+06	1.27E+06	1.67E+06	1.03E+06	1.25E+06	**3.48E+06**
	gi|808860225	3	98	27	Titin [Larimichthys crocea]	1.71E+06	1.81E+06	1.08E+06	1.47E+06	1.26E+06	1.62E+06	8.63E+05	2.10E+06	**3.43E+06**
	gi|185133678	38	11	2	glyceraldehyde-3-phosphate dehydrogenase [Salmo salar]gi|89143257|emb|CAJ76703.1| glyceraldehyde-3-phosphate dehydrogenase [Salmo salar]	1.17E+06	1.79E+06	1.28E+06	1.49E+06	1.03E+06	1.61E+06	1.05E+06	1.74E+06	**3.40E+06**
	gi|642001593	47	8	2	catechol O-methyltransferase domain-containing 1-like	1.39E+06	1.84E+06	1.33E+06	1.85E+06	1.29E+06	1.56E+06	1.31E+06	1.58E+06	**3.40E+06**
	gi|338808846	9	19	3	complement component C3 [Xiphophorus hellerii]	1.27E	1.64E	1.30E	1.52E	1.21E	1.72E	1.21E	1.51E	**3.36E+06**

						+06	+06	+06	+06	+06	+06	+06	+06	
	gi|185135824	17	3	2	carbonic anhydrase II [Oncorhynchus mykiss]gi|32187014|gb|AAP73748.1| erythrocyte carbonic anhydrase [Oncorhynchus mykiss]gi|61506864|dbj|BAD36836.2| carbonic anhydrase 2 [Oncorhynchus mykiss]gi|642119268|emb|CDQ65658....	1.30E+06	1.65E+06	1.12E+06	1.40E+06	1.30E+06	1.65E+06	1.18E+06	1.25E+06	**3.31E+06**
	gi|642093704	34	13	3	fibrinogen gamma chain	7.30E+05	1.16E+06	8.22E+05	2.31E+06	8.00E+05	2.14E+06	9.45E+05	2.68E+06	**3.30E+06**
	gi|64201962 3	5	2	2	unnamed protein product	1.31E+06	1.56E+06	1.22E+06	1.51E+06	1.59E+06	1.73E+06	1.28E+06	1.59E+06	**3.29E+06**
	gi|742083337	15	29	3	PREDICTED: alpha-2-macroglobulin-like [Esox lucius]	1.33E+06	1.67E+06	1.47E+06	2.09E+06	1.35E+06	1.60E+06	1.72E+06	1.79E+06	**3.27E+06**
	gi|642085862	7	3	3	coagulation factor VII-like	1.18E+06	1.85E+06	1.33E+06	1.42E+06	8.77E+05	1.41E+06	9.97E+05	1.20E+06	**3.26E+06**
	gi|642067224	34	25	3	alpha-2-macroglobulin-like isoform X1	1.32E+06	1.78E+06	1.34E+06	1.91E+06	1.28E+06	1.47E+06	1.30E+06	1.59E+06	**3.25E+06**
	gi|642129461	7	3	3	phosphoinositide 3-kinase adapter protein	1.18E	1.82E	1.17E	1.49E	1.24E	1.41E	1.19E	1.43E	**3.23E+06**

						+06	+06	+06	+06	+06	+06	+06	+06	
	gi|642083433	9	2	2	glutathione peroxidase 3-like	1.09E+06	1.62E+06	1.26E+06	1.52E+06	1.22E+06	1.59E+06	1.36E+06	1.61E+06	**3.22E+06**
	gi|237512664	18	9	3	warm temperature acclimation-related protein [Plecoglossus altivelis]	1.24E+06	1.81E+06	1.65E+06	2.56E+06	1.35E+06	1.40E+06	1.47E+06	1.59E+06	**3.21E+06**
	gi|597807117	16	13	4	PREDICTED: complement C3-like [Astyanax mexicanus]	1.17E+06	1.58E+06	1.07E+06	1.67E+06	1.23E+06	1.63E+06	1.10E+06	1.55E+06	**3.20E+06**
	gi|159132021	7	4	2	properdin P factor 3 [Oncorhynchus mykiss]gi|159132021|emb|CAP17613.1| properdin P factor 3 [Oncorhynchus mykiss]	1.26E+06	1.64E+06	1.48E+06	1.89E+06	1.47E+06	1.49E+06	1.21E+06	1.56E+06	**3.12E+06**
	gi|688568447	3	12	10	PREDICTED: hemicentin-1 [Danio rerio]	8.45E+05	1.75E+06	8.93E+05	3.06E+06	7.59E+05	1.35E+06	2.43E+06	1.06E+06	**3.10E+06**
	gi|808859822	12	10	7	NACHT LRR and PYD domains-containing protein 12 [Larimichthys crocea]	4.71E+05	2.71E+06	7.42E+05	5.02E+05	2.84E+05	3.79E+05	3.88E+05	2.66E+05	**3.09E+06**
	gi|185135614	38	3	2	toxin-1 precursor [Oncorhynchus mykiss]gi|20385167|gb|AAM21198.1|AF363273_1 toxin-1 [Oncorhynchus mykiss]	1.38E	1.98E	1.37E	1.58E	1.01E	1.10E	9.61E	9.03E	**3.08E+06**

						+06	+06	+06	+06	+06	+06	+05	+05	
	gi|617396044	3	5	4	PREDICTED: KN motif and ankyrin repeat domain-containing protein 4 isoform X1 [Poecilia formosa]gi|617396044|ref|XP_007550905.1| PREDICTED: KN motif and ankyrin repeat domain-containing protein 4 isoform X1 [Poecilia for...	9.25E+05	2.03E+06	1.76E+06	1.21E+06	8.52E+05	1.04E+06	7.75E+05	7.25E+05	**3.08E+06**
	gi|47218668	17	7	3	warm-temperature-acclimation-related 65-kDa	1.15E+06	1.59E+06	1.30E+06	1.67E+06	1.10E+06	1.43E+06	1.07E+06	1.42E+06	**3.02E+06**
	gi|209738638	48	9	2	Triosephosphate isomerase [Salmo salar]	1.93E+06	1.58E+06	1.17E+06	1.47E+06	1.17E+06	1.35E+06	1.10E+06	1.37E+06	**2.94E+06**
	gi|336087815	13	15	2	alpha-2-macroglobulin [Plecoglossus altivelis]	9.66E+05	1.32E+06	1.10E+06	1.30E+06	9.87E+05	1.60E+06	3.42E+06	1.76E+06	**2.92E+06**
	gi|213511540	15	3	3	complement C1q subcomponent subunit C precursor [Salmo salar]gi|209155316|gb|ACI33890.1| Complement C1q subcomponent subunit C precursor [Salmo salar]gi|223672577|gb|ACN12470.1| Complement C1q subcomponent subunit C pre...	1.06E+06	1.60E+06	1.23E+06	1.30E+06	1.05E+06	1.30E+06	1.33E+06	1.20E+06	**2.90E+06**
	gi|573889513	10	20	3	PREDICTED: myosin-6-like isoform X1 [Lepisosteus oculatus]	5.50E+05	2.39E+06	9.54E+05	5.45E+05	5.65E+05	4.98E+05	4.33E+05	5.06E+05	**2.89E+06**
	gi|642098216	41	5	3	mannose-specific lectin-like	1.50E	1.61E	1.29E	1.30E	1.23E	1.28E	1.13E	1.20E	**2.88E+06**

						+06	+06	+06	+06	+06	+06	+06	+06	
	gi|641931185	15	4	2	fish-egg lectin-like	1.11E+06	1.65E+06	1.19E+06	1.45E+06	1.10E+06	1.22E+06	1.52E+06	1.49E+06	**2.87E+06**
	gi|597745728	3	4	3	PREDICTED: fibronectin-like [Astyanax mexicanus]	1.14E+06	1.44E+06	1.13E+06	1.49E+06	9.41E+05	1.43E+06	1.31E+06	1.21E+06	**2.87E+06**
	gi|348527268	2	4	3	PREDICTED: histone-lysine N-methyltransferase NSD3-like [Oreochromis niloticus]	9.83E+05	1.37E+06	1.18E+06	1.39E+06	8.80E+05	1.45E+06	1.12E+06	1.23E+06	**2.82E+06**
	gi|657797976	4	138	65	PREDICTED: titin-like [Cynoglossus semilaevis]	8.90E+06	1.61E+06	1.08E+06	1.27E+06	1.19E+06	1.19E+06	9.44E+05	9.87E+05	**2.79E+06**
	gi|642098842	31	17	4	complement C4-like	9.46E+05	1.45E+06	1.08E+06	1.04E+06	8.99E+05	1.32E+06	1.17E+06	1.85E+06	**2.77E+06**
	gi|831321581	6	22	7	PREDICTED: apolipoprotein B-100-like [Clupea harengus]	9.94E+05	1.53E+06	9.33E+05	1.03E+06	8.55E+05	1.22E+06	9.41E+05	9.66E+05	**2.76E+06**
	gi|657814990	2	4	2	PREDICTED: complement C5 [Cynoglossus semilaevis]	1.13E	1.33E	1.09E	1.17E	1.26E	1.40E	1.12E	1.82E	**2.72E+06**

						+06	+06	+06	+06	+06	+06	+06	+06	
	gi|642107212	14	4	2	seleno P	5.12E+05	1.42E+06	9.56E+05	1.50E+06	1.09E+06	1.24E+06	1.08E+06	1.24E+06	**2.66E+06**
	gi|642132622	9	12	7	A disintegrin and metallo ase with thrombospondin motifs 13 isoform X2	1.03E+06	1.47E+06	9.54E+05	1.21E+06	8.65E+05	1.17E+06	1.06E+06	1.19E+06	**2.64E+06**
	gi|185135447	7	4	4	C1R/C1S subunit of Ca2+-dependent complex precursor [Oncorhynchus mykiss]gi|40217256|emb|CAD58654.1| C1R/C1S subunit of Ca2+-dependent complex [Oncorhynchus mykiss]	1.49E+06	1.44E+06	1.17E+06	1.13E+06	8.25E+05	1.20E+06	1.13E+06	1.23E+06	**2.63E+06**
	gi|642095738	6	3	2	acidic mammalian chitinase-like	1.18E+06	1.29E+06	1.42E+06	1.32E+06	1.17E+06	1.34E+06	1.34E+06	1.24E+06	**2.63E+06**
	gi|642130149	6	6	5	neuronal cell adhesion molecule-like isoform X1	9.52E+05	1.43E+06	1.19E+06	1.23E+06	9.52E+05	1.16E+06	9.06E+05	1.26E+06	**2.59E+06**
	gi|498926834	7	24	20	PREDICTED: LOW QUALITY PROTEIN: dynein heavy chain 6 axonemal-like [Maylandia zebra]	1.07E+06	1.30E+06	1.08E+06	1.28E+06	1.10E+06	1.26E+06	1.08E+06	1.21E+06	**2.56E+06**
	gi|657566884	11	5	3	PREDICTED: betaine--homocysteine S-methyltransferase 1-like [Stegastes partitus]	1.10E	1.56E	1.38E	1.54E	9.41E	9.86E	1.14E	1.26E	**2.54E+06**

						+06	+06	+06	+06	+05	+05	+06	+06	
	gi|409971023	21	12	8	warm temperature acclimation-related 65 kDa protein 1 [Plecoglossus altivelis]gi|514830679|gb|AGO59326.1| warm temperature acclimation 65 kDa protein 1 [Plecoglossus altivelis]	8.53E+05	1.48E+06	1.07E+06	1.12E+06	8.60E+05	1.07E+06	1.31E+06	9.49E+05	**2.54E+06**
	gi|642083379	12	3	2	complement C1q 2	9.57E+05	1.32E+06	9.89E+05	1.41E+06	1.03E+06	1.22E+06	7.33E+05	9.47E+05	**2.54E+06**
	gi|642117405	36	12	5	kininogen 1 precursor	9.60E+05	1.57E+06	1.03E+06	1.44E+06	9.26E+05	9.64E+05	9.29E+05	1.09E+06	**2.53E+06**
	gi|642102761	8	3	3	carboxypeptidase B2	9.81E+05	1.19E+06	9.70E+05	1.18E+06	1.05E+06	1.30E+06	8.48E+05	1.13E+06	**2.48E+06**
	gi|642116933	47	7	2	serum lectin isoform 1 precursor	9.58E+05	1.42E+06	1.17E+06	1.37E+06	1.03E+06	1.06E+06	9.51E+05	1.08E+06	**2.48E+06**
	gi|768930540	16	4	2	PREDICTED: LOW QUALITY PROTEIN: histone H3-like centromeric protein cpar-1 [Takifugu rubripes]	8.09E+05	1.24E+06	8.76E+05	1.14E+06	9.70E+05	1.24E+06	7.63E+05	1.15E+06	**2.48E+06**
	gi|528511594	6	21	15	PREDICTED: apolipoprotein Bb tandem duplicate 1 isoform X1 [Danio rerio]	8.76E	1.26E	9.78E	1.24E	8.89E	1.19E	8.87E	1.05E	**2.45E+06**

						+05	+06	+05	+06	+05	+06	+05	+06	
	gi|642129859	47	63	6	complement C3	9.30E+05	1.26E+06	1.07E+06	1.14E+06	1.00E+06	1.19E+06	9.61E+05	1.21E+06	**2.45E+06**
	gi|617471190	4	16	12	PREDICTED: apolipoprotein B-100-like isoform X1 [Poecilia formosa]	8.90E+05	1.36E+06	8.62E+05	1.10E+06	7.33E+05	1.07E+06	9.18E+05	9.72E+05	**2.43E+06**
	gi|162949444	21	3	2	nucleoside diphosphate kinase [Oncorhynchus masou formosanus]	1.12E+06	1.46E+06	1.28E+06	1.17E+06	9.10E+05	9.59E+05	9.58E+05	1.05E+06	**2.41E+06**
	gi|742238749	4	111	54	PREDICTED: titin-like [Esox lucius]	1.23E+06	1.21E+06	1.00E+06	1.27E+06	7.92E+05	1.19E+06	8.46E+05	1.16E+06	**2.40E+06**
	gi|742088854	3	6	4	PREDICTED: putative leucine-rich repeat-containing protein DDB_G0290503 isoform X1 [Esox lucius]	9.79E+05	1.30E+06	8.79E+05	1.15E+06	6.95E+05	1.02E+06	8.19E+05	8.35E+05	**2.32E+06**
	gi|185132432	23	20	4	complement component C7-2 precursor [Oncorhynchus mykiss]gi|53748602|emb|CAF22025.2| complement component C7-2 [Oncorhynchus mykiss]	1.01E+06	1.21E+06	1.04E+06	1.33E+06	1.02E+06	1.11E+06	8.15E+05	9.79E+05	**2.32E+06**
	gi|642056507	30	19	3	ectonucleotide pyrophosphatase phosphodiesterase family member 2-like	9.44E	1.15E	6.81E	1.10E	7.23E	1.17E	6.89E	1.11E	**2.32E+06**

						+05	+06	+05	+06	+05	+06	+05	+06	
	gi|342731470	10	3	2	immunoglobulin light chain [Anguilla japonica]	3.85E+05	1.76E+06	5.52E+05	5.52E+05	4.06E+05	5.38E+05	5.29E+05	3.90E+05	**2.29E+06**
	gi|808872033	10	20	6	Alpha-2-macroglobulin [Larimichthys crocea]	7.07E+05	9.58E+05	9.30E+05	9.46E+05	7.04E+05	1.32E+06	1.21E+06	1.77E+06	**2.28E+06**
	gi|734648978	10	19	6	PREDICTED: complement C3-like [Larimichthys crocea]	7.81E+05	1.30E+06	7.70E+05	9.67E+05	8.74E+05	9.62E+05	7.81E+05	9.45E+05	**2.26E+06**
	gi|642082470	17	3	2	thrombospondin-1-like	9.05E+05	1.22E+06	7.98E+05	1.04E+06	8.21E+05	1.04E+06	8.05E+05	9.70E+05	**2.26E+06**
	gi|658850956	7	6	2	PREDICTED: inter-alpha-trypsin inhibitor heavy chain H3-like [Poecilia reticulata]	7.01E+05	1.21E+06	8.43E+05	1.22E+06	8.47E+05	1.04E+06	8.27E+05	1.01E+06	**2.25E+06**
	gi|657751641	6	20	12	PREDICTED: apolipoprotein B-100-like [Cynoglossus semilaevis]	8.59E+05	1.20E+06	7.84E+05	1.30E+06	7.15E+05	1.04E+06	7.78E+05	1.62E+06	**2.24E+06**
	gi|768951276	4	4	4	PREDICTED: DEP domain-containing protein 5 isoform X5 [Takifugu rubripes]	1.08E	1.19E	7.94E	8.21E	9.55E	1.04E	6.64E	8.89E	**2.23E+06**

						+06	+06	+05	+05	+05	+06	+05	+05	
	gi|808847825	2	2	2	Protein MMS22-like protein [Larimichthys crocea]	6.94E+05	1.13E+06	8.85E+05	9.30E+05	7.45E+05	1.07E+06	7.40E+05	8.05E+05	**2.20E+06**
	gi|736192937	6	5	3	PREDICTED: fibrinogen alpha chain-like [Notothenia coriiceps]	3.90E+05	4.93E+05	3.49E+05	1.74E+06	4.30E+05	1.70E+06	4.42E+05	2.61E+06	**2.20E+06**
	gi|551507245	5	10	3	PREDICTED: complement C3-like [Xiphophorus maculatus]	8.52E+05	1.12E+06	7.98E+05	1.18E+06	9.07E+05	1.07E+06	8.07E+05	9.52E+05	**2.19E+06**
	gi|583979954	5	4	2	PREDICTED: G protein-coupled receptor kinase 6-like [Neolamprologus brichardi]	8.49E+05	1.20E+06	1.25E+06	1.00E+06	7.32E+05	9.92E+05	7.45E+05	7.82E+05	**2.19E+06**
	gi|831299943	8	7	3	PREDICTED: ectonucleotide pyrophosphatase/phosphodiesterase family member 2 isoform X1 [Clupea harengus]	7.81E+05	1.33E+06	8.58E+05	7.68E+05	6.02E+05	8.28E+05	7.02E+05	6.58E+05	**2.16E+06**
	gi|742219741	4	8	7	PREDICTED: tudor domain-containing protein 6 isoform X3 [Esox lucius]	8.50E+05	1.12E+06	7.99E+05	1.13E+06	8.67E+05	1.01E+06	7.35E+05	8.93E+05	**2.13E+06**
	gi|734624041	2	9	8	PREDICTED: protocadherin Fat 4 [Larimichthys crocea]	6.41E	1.17E	6.53E	8.95E	6.62E	9.54E	7.69E	7.62E	**2.12E+06**

						+05	+06	+05	+05	+05	+05	+05	+05	
	gi|742174310	2	7	5	PREDICTED: huntingtin [Esox lucius]	8.15E+05	1.05E+06	8.57E+05	1.08E+06	8.15E+05	1.06E+06	9.65E+05	1.14E+06	**2.11E+06**
	gi|64197084 6	42	8	4	complement C4-like	8.70E+05	1.15E+06	7.28E+05	9.61E+05	5.86E+05	9.56E+05	6.44E+05	7.39E+05	**2.11E+06**
	gi|734616630	7	5	4	PREDICTED: F-box only protein 10 [Larimichthys crocea]	3.24E+05	1.15E+06	4.28E+05	4.57E+05	2.18E+05	9.51E+05	5.37E+05	3.45E+05	**2.10E+06**
	gi|642125187	64	8	3	mannose-specific lectin-like	1.02E+06	1.16E+06	1.02E+06	1.01E+06	8.46E+05	9.16E+05	7.92E+05	7.44E+05	**2.08E+06**
	gi|642104794	13	4	2	complement C1q 2	7.11E+05	1.27E+06	7.43E+05	9.27E+05	4.61E+05	7.71E+05	6.23E+05	7.00E+05	**2.04E+06**
	gi|336087809	15	9	2	fibrinogen beta chain precursor [Plecoglossus altivelis]	4.87E+05	8.96E+05	6.66E+05	1.14E+06	5.59E+05	1.14E+06	5.62E+05	1.19E+06	**2.04E+06**
	gi|243010659	11	3	2	immunoglobulin light chain III variable region [Oncorhynchus mykiss]	6.21E	8.55E	5.12E	1.09E	1.02E	1.17E	9.17E	1.48E	**2.02E+06**

						+05	+05	+05	+06	+06	+06	+05	+06	
	gi|641999687	39	9	2	alpha-2-macroglobulin-like isoform X1	7.34E+05	1.19E+06	8.18E+05	1.13E+06	7.92E+05	8.33E+05	8.52E+05	9.89E+05	**2.02E+06**
	gi|198285477	31	12	3	ATP synthase H+ transporting mitochondrial F1 complex beta [Salmo salar]	7.61E+05	9.91E+05	7.59E+05	9.86E+05	9.84E+05	1.02E+06	6.70E+05	8.71E+05	**2.02E+06**
	gi|642085864	9	4	4	venom prothrombin activator porpharin-D-like	7.15E+05	1.14E+06	8.96E+05	9.04E+05	6.13E+05	8.19E+05	6.46E+05	8.54E+05	**1.96E+06**
	gi|734639152	3	14	6	PREDICTED: vacuolar protein sorting-associated protein 13C [Larimichthys crocea]	7.05E+05	8.99E+05	8.46E+05	1.16E+06	6.71E+05	1.06E+06	1.84E+06	1.30E+06	**1.96E+06**
	gi|742250586	23	54	3	PREDICTED: complement C3-like [Esox lucius]	6.65E+05	9.69E+05	5.08E+05	5.86E+05	6.89E+05	9.89E+05	5.79E+05	7.37E+05	**1.96E+06**
	gi|193480074	5	3	2	transferrin [Ctenopharyngodon idella]	6.77E+05	1.39E+06	7.04E+05	5.75E+05	4.59E+05	5.61E+05	5.83E+05	5.56E+05	**1.95E+06**
	gi|642116636	12	2	2	complement C3-like isoform X1	8.15E	9.84E	8.70E	9.90E	8.41E	9.52E	8.78E	9.34E	**1.94E+06**

						+05	+05	+05	+05	+05	+05	+05	+05	
	gi|224613288	25	11	4	Gelsolin precursor [Salmo salar]	9.21E+05	1.05E+06	8.03E+05	7.75E+05	7.82E+05	8.83E+05	7.58E+05	7.72E+05	**1.93E+06**
	gi|642073756	9	8	4	Proteoglycan 4	7.79E+05	1.07E+06	7.90E+05	8.61E+05	5.33E+05	8.49E+05	5.85E+05	7.96E+05	**1.92E+06**
	gi|291190410	10	3	3	Coagulation factor X precursor [Salmo salar]gi|223648910|gb|ACN11213.1| Coagulation factor X precursor [Salmo salar]	6.59E+05	1.13E+06	6.48E+05	8.50E+05	6.92E+05	7.85E+05	6.92E+05	7.44E+05	**1.92E+06**
	gi|657584724	12	15	2	PREDICTED: alpha-2-macroglobulin-P-like [Stegastes partitus]	5.31E+05	1.42E+06	1.05E+06	7.03E+05	2.79E+05	4.85E+05	5.29E+05	5.19E+05	**1.90E+06**
	gi|831326017	6	14	6	PREDICTED: fibronectin-like isoform X1 [Clupea harengus]	6.60E+05	1.08E+06	8.37E+05	1.04E+06	6.48E+05	8.21E+05	5.88E+05	7.02E+05	**1.90E+06**
	gi|657798968	15	8	4	PREDICTED: hemopexin [Cynoglossus semilaevis]	8.23E+05	9.98E+05	1.08E+06	1.13E+06	7.63E+05	8.47E+05	8.93E+05	1.10E+06	**1.85E+06**
	gi|548348354	5	2	2	PREDICTED: glycine receptor subunit beta-like [Pundamilia nyererei]	6.81E	1.04E	7.76E	8.03E	6.36E	8.03E	9.92E	8.60E	**1.84E+06**

						+05	+06	+05	+05	+05	+05	+05	+05	
	gi|188536034	3	3	2	folliculin-interacting protein 1 [Danio rerio]gi|171846455|gb|AAI61668.1| Zgc:175140 protein [Danio rerio]	9.47E+05	9.70E+05	6.39E+05	7.16E+05	1.32E+06	8.61E+05	5.83E+05	6.60E+05	**1.83E+06**
	gi|657810365	6	7	4	PREDICTED: LOW QUALITY PROTEIN: collagen alpha-1(VI) chain [Cynoglossus semilaevis]	7.25E+05	8.04E+05	6.97E+05	9.04E+05	7.69E+05	9.92E+05	5.92E+05	9.29E+05	**1.80E+06**
	gi|831296829	3	12	8	PREDICTED: nesprin-2-like [Clupea harengus]	6.35E+05	8.65E+05	7.29E+05	1.01E+06	7.26E+05	9.10E+05	6.02E+05	1.38E+06	**1.78E+06**
	gi|153792045	5	9	4	complement component c3b tandem duplicate 2 isoform 1 precursor [Danio rerio]	6.56E+05	8.36E+05	7.87E+05	8.44E+05	7.21E+05	9.37E+05	5.79E+05	7.54E+05	**1.77E+06**
	gi|641973286	19	6	2	AMBP precursor	6.18E+05	1.00E+06	6.17E+05	8.95E+05	5.84E+05	7.69E+05	7.75E+05	7.79E+05	**1.77E+06**
	gi|223649332	25	20	3	Integrin beta-1 precursor [Salmo salar]	5.39E+05	1.08E+06	8.40E+05	6.98E+05	5.86E+05	6.83E+05	5.77E+05	7.10E+05	**1.77E+06**
	gi|742183402	11	9	7	PREDICTED: liprin-beta-1 isoform X2 [Esox lucius]	6.24E	1.01E	3.77E	6.61E	5.58E	7.42E	6.67E	4.56E	**1.75E+06**

						+05	+06	+05	+05	+05	+05	+05	+06	
	gi|736162220	5	25	19	PREDICTED: LOW QUALITY PROTEIN: ryanodine receptor 2 [Notothenia coriiceps]	6.42E+05	9.47E+05	7.06E+05	8.85E+05	6.25E+05	7.93E+05	1.07E+06	1.16E+06	**1.74E+06**
	gi|528468696	4	4	4	PREDICTED: mannosyl-oligosaccharide glucosidase isoform X1 [Danio rerio]gi|528468698|ref|XP_005160134.1| PREDICTED: mannosyl-oligosaccharide glucosidase isoform X1 [Danio rerio]gi|528468700|ref|XP_005160135.1| PREDICTED...	6.84E+05	8.17E+05	5.22E+05	7.89E+05	8.25E+05	9.17E+05	6.42E+05	8.93E+05	**1.73E+06**
	gi|831292882	3	4	2	PREDICTED: calcium-dependent secretion activator 1-like [Clupea harengus]	6.73E+05	9.70E+05	8.44E+05	8.22E+05	6.94E+05	7.60E+05	6.97E+05	7.27E+05	**1.73E+06**
	gi|642123711	17	7	3	aminopeptidase	7.71E+05	8.98E+05	6.22E+05	8.34E+05	7.19E+05	8.27E+05	7.28E+05	9.52E+05	**1.73E+06**
	gi|742162575	3	8	6	PREDICTED: E3 ubiquitin-protein ligase UBR5 isoform X11 [Esox lucius]	6.23E+05	6.88E+05	7.28E+05	7.92E+05	6.61E+05	1.03E+06	7.26E+05	7.71E+05	**1.72E+06**
	gi|658839896	4	134	47	PREDICTED: titin-like [Poecilia reticulata]	4.49E+05	9.82E+05	5.91E+05	6.87E+05	6.64E+05	7.30E+05	4.66E+05	6.03E+05	**1.71E+06**
	gi|641937128	23	5	3	ceruloplasmin isoform X1	6.55E	1.05E	7.34E	7.04E	5.21E	6.62E	6.01E	7.36E	**1.71E+06**

						+05	+06	+05	+05	+05	+05	+05	+05	
	gi|688617491	2	3	3	PREDICTED: tight junction protein ZO-1 isoform X1 [Danio rerio]	6.49E+05	9.65E+05	7.33E+05	7.26E+05	5.77E+05	7.09E+05	6.02E+05	6.84E+05	**1.67E+06**
	gi|742173334	7	3	2	PREDICTED: sex hormone-binding globulin [Esox lucius]	5.72E+05	8.65E+05	7.64E+05	8.51E+05	6.64E+05	7.81E+05	4.84E+05	6.55E+05	**1.65E+06**
	gi|410917321	9	18	4	PREDICTED: complement C3-like [Takifugu rubripes]	4.05E+05	7.61E+05	4.33E+05	8.01E+05	5.81E+05	8.41E+05	5.67E+05	7.06E+05	**1.60E+06**
	gi|642106397	11	5	4	olfactomedin-4-like isoform X2	6.00E+05	7.55E+05	6.19E+05	8.24E+05	5.82E+05	8.43E+05	6.64E+05	1.06E+06	**1.60E+06**
	gi|658921430	2	10	8	PREDICTED: histone-lysine N-methyltransferase 2C isoform X11 [Poecilia reticulata]	5.58E+05	8.67E+05	6.64E+05	6.96E+05	5.14E+05	7.31E+05	4.97E+05	6.62E+05	**1.60E+06**
	gi|736198254	4	2	2	PREDICTED: LOW QUALITY PROTEIN: polyubiquitin-C-like partial [Notothenia coriiceps]	8.72E+05	7.95E+05	8.39E+05	1.12E+06	7.60E+05	7.90E+05	5.90E+05	9.04E+05	**1.58E+06**
	gi|209736842	9	2	2	Delta-aminolevulinic acid dehydratase [Salmo salar]gi|223672761|gb|ACN12562.1| Delta-aminolevulinic acid dehydratase [Salmo salar]	8.63E	1.05E	9.21E	6.20E	5.93E	5.31E	5.58E	8.08E	**1.58E+06**

						+05	+06	+05	+05	+05	+05	+05	+05	
	gi|642120767	12	6	4	Clusterin precursor	6.07E+05	8.85E+05	7.47E+05	9.05E+05	6.31E+05	6.75E+05	8.40E+05	6.62E+05	**1.56E+06**
	gi|641972240	19	2	2	alpha-2-macroglobulin- partial	5.61E+05	7.63E+05	5.43E+05	7.59E+05	9.62E+05	7.77E+05	4.58E+05	7.19E+05	**1.54E+06**
	gi|657529190	6	3	2	PREDICTED: histidine-rich glycoprotein-like [Stegastes partitus]	5.71E+05	7.77E+05	5.79E+05	6.60E+05	4.96E+05	7.51E+05	5.50E+05	6.85E+05	**1.53E+06**
	gi|657760797	10	20	6	PREDICTED: complement C3-like [Cynoglossus semilaevis]	6.43E+05	8.17E+05	7.41E+05	5.53E+05	6.55E+05	7.03E+05	6.05E+05	5.68E+05	**1.52E+06**
	gi|573894654	6	3	2	PREDICTED: complement component C8 beta chain-like [Lepisosteus oculatus]	6.34E+05	8.18E+05	6.04E+05	8.47E+05	6.60E+05	6.93E+05	6.70E+05	7.97E+05	**1.51E+06**
	gi|642128323	8	2	2	olfactomedin-4-like	6.53E+05	8.85E+05	6.17E+05	6.25E+05	5.40E+05	6.24E+05	6.40E+05	9.89E+05	**1.51E+06**
	gi|642095478	16	7	3	bleomycin hydrolase	5.34E	6.08E	4.97E	7.55E	5.08E	9.01E	6.37E	6.02E	**1.51E+06**

						+05	+05	+05	+05	+05	+05	+05	+05	
	gi|831307006	19	6	5	PREDICTED: protein lifeguard 3-like [Clupea harengus]	4.71E+05	8.06E+05	5.03E+05	6.80E+05	4.29E+05	6.84E+05	4.92E+05	7.16E+05	**1.49E+06**
	gi|47218829	19	4	3	complement C1q 2	5.59E+05	8.00E+05	7.46E+05	9.39E+05	5.35E+05	6.90E+05	4.61E+05	6.19E+05	**1.49E+06**
	gi|642006130	27	5	2	alpha-2-macroglobulin-like isoform X1	5.44E+05	7.52E+05	5.13E+05	6.83E+05	5.27E+05	7.22E+05	4.27E+05	7.26E+05	**1.47E+06**
	gi|642084841	18	8	2	glucose-6-phosphate isomerase-like	5.99E+05	7.72E+05	6.23E+05	7.59E+05	5.77E+05	6.95E+05	5.83E+05	9.05E+05	**1.47E+06**
	gi|734629206	7	6	3	PREDICTED: complement factor B-like isoform X1 [Larimichthys crocea]	5.78E+05	8.20E+05	7.19E+05	5.05E+05	4.40E+05	6.39E+05	4.66E+05	7.05E+05	**1.46E+06**
	gi|573884304	4	4	4	PREDICTED: rho guanine nucleotide exchange factor 11-like [Lepisosteus oculatus]	6.46E+05	7.36E+05	4.82E+05	7.04E+05	6.46E+05	7.10E+05	4.52E+05	5.54E+05	**1.45E+06**
	gi|363807314	6	12	3	complement component c3a precursor [Danio rerio]	5.59E	6.80E	5.91E	6.85E	5.36E	7.60E	5.62E	6.09E	**1.44E+06**

						+05	+05	+05	+05	+05	+05	+05	+05	
	gi|657567867	7	21	6	PREDICTED: LOW QUALITY PROTEIN: apolipoprotein B-100-like [Stegastes partitus]	4.64E+05	7.23E+05	5.21E+05	6.18E+05	5.02E+05	7.13E+05	4.92E+05	5.53E+05	**1.44E+06**
	gi|642068445	23	4	4	apolipo F	5.33E+05	6.43E+05	3.15E+05	5.49E+05	4.24E+05	7.67E+05	3.99E+05	5.42E+05	**1.41E+06**
	gi|573909187	10	15	6	PREDICTED: alpha-2-macroglobulin-like protein 1-like [Lepisosteus oculatus]	6.00E+05	7.99E+05	8.19E+05	9.41E+05	4.34E+05	6.02E+05	6.42E+05	5.04E+05	**1.40E+06**
	gi|742230630	5	12	11	PREDICTED: von Willebrand factor [Esox lucius]	6.90E+05	7.37E+05	6.62E+05	6.40E+05	7.62E+05	6.61E+05	7.15E+05	8.92E+05	**1.40E+06**
	gi|617299068	5	32	11	PREDICTED: plectin-like isoform X3 [Poecilia formosa]	6.03E+05	7.90E+05	8.31E+05	8.20E+05	5.93E+05	6.01E+05	5.38E+05	7.23E+05	**1.39E+06**
	gi|688572279	4	107	56	PREDICTED: titin isoform X1 [Danio rerio]	5.38E+05	7.52E+05	4.65E+05	1.12E+06	4.43E+05	6.21E+05	4.69E+05	5.88E+05	**1.37E+06**
	gi|642072263	10	6	5	sushi domain-containing 2	6.41E	8.11E	5.58E	6.69E	4.43E	5.55E	5.01E	6.66E	**1.37E+06**

						+05	+05	+05	+05	+05	+05	+05	+05	
	gi|742148851	10	8	3	PREDICTED: inter-alpha-trypsin inhibitor heavy chain H3 [Esox lucius]	5.14E+05	7.15E+05	5.23E+05	9.10E+05	5.23E+05	6.43E+05	5.08E+05	7.65E+05	**1.36E+06**
	gi|157278135	6	11	5	complement component 4 (within H-2S) precursor [Oryzias latipes]gi|7209638|dbj|BAA92287.1| Orla C4 [Oryzias latipes]	4.38E+05	6.60E+05	5.08E+05	5.72E+05	5.94E+05	6.80E+05	4.26E+05	5.31E+05	**1.34E+06**
	gi|642087021	22	8	2	pentraxin fusion -like	4.46E+05	6.78E+05	6.14E+05	7.21E+05	4.84E+05	6.39E+05	3.91E+05	4.90E+05	**1.32E+06**
	gi|642106771	10	6	4	hepatocyte growth factor	4.72E+05	6.62E+05	5.35E+05	7.02E+05	5.48E+05	6.53E+05	4.98E+05	6.04E+05	**1.32E+06**
	gi|742163864	48	5	2	PREDICTED: mannose-specific lectin-like [Esox lucius]gi|742163874|ref|XP_010883812.1| PREDICTED: mannose-specific lectin-like [Esox lucius]	1.04E+06	8.41E+05	1.01E+06	8.37E+05	9.41E+05	4.67E+05	5.96E+05	5.47E+05	**1.31E+06**
	gi|548375018	3	10	5	PREDICTED: small subunit processome component 20 homolog isoform X2 [Pundamilia nyererei]	3.87E+05	7.38E+05	5.34E+05	5.09E+05	3.67E+05	5.68E+05	8.42E+05	4.89E+05	**1.31E+06**
	gi|583977791	5	4	3	PREDICTED: tuftelin-interacting protein 11-like isoform X2 [Neolamprologus brichardi]	6.66E	6.30E	5.25E	6.11E	4.93E	6.60E	5.03E	5.30E	**1.29E+06**

						+05	+05	+05	+05	+05	+05	+05	+05	
	gi|183207561	31	28	4	transferrin [Salmo trutta]	6.89E+05	7.94E+05	4.09E+05	6.82E+05	3.48E+05	4.90E+05	4.54E+05	5.59E+05	**1.28E+06**
	gi|13591600	18	8	4	28kDa-2 apolipoprotein [Anguilla japonica]gi|76573852|dbj|BAE45335.1| apolipoprotein A-I [Anguilla japonica]	2.66E+05	1.11E+06	1.10E+06	1.72E+05	9.10E+04	1.39E+05	1.72E+05	1.77E+05	**1.25E+06**
	gi|831275359	18	30	11	PREDICTED: LOW QUALITY PROTEIN: complement C3-like [Clupea harengus]	5.09E+05	6.17E+05	4.19E+05	5.97E+05	3.92E+05	6.26E+05	4.22E+05	5.37E+05	**1.24E+06**
	gi|400131697	31	12	2	trout C-polysaccharide binding protein 1 isoform 1 [Oncorhynchus mykiss]	5.49E+05	7.11E+05	4.30E+05	5.91E+05	3.75E+05	5.30E+05	4.54E+05	7.45E+05	**1.24E+06**
	gi|1449079	36	3	3	beta-2 microglobulin [Oncorhynchus mykiss]	3.91E+05	6.24E+05	4.22E+05	6.81E+05	4.34E+05	5.99E+05	6.24E+05	5.39E+05	**1.22E+06**
	gi|657546302	18	7	5	PREDICTED: hemopexin [Stegastes partitus]	4.71E+05	7.26E+05	4.89E+05	5.87E+05	4.53E+05	4.91E+05	5.22E+05	5.88E+05	**1.22E+06**
	gi|658891316	10	5	2	PREDICTED: LOW QUALITY PROTEIN: hyaluronan-binding protein 2 [Poecilia reticulata]	4.48E	6.80E	4.21E	4.82E	3.82E	5.10E	4.56E	5.72E	**1.19E+06**

						+05	+05	+05	+05	+05	+05	+05	+05	
	gi|765111502	2	11	5	PREDICTED: ankyrin-2-like isoform X5 [Oryzias latipes]	4.90E+05	6.31E+05	5.41E+05	4.95E+05	5.59E+05	5.56E+05	3.68E+05	4.75E+05	**1.19E+06**
	gi|642123053	5	22	14	spectrin beta non-erythrocytic 5	3.54E+05	7.11E+05	3.69E+05	4.83E+05	5.88E+05	4.55E+05	4.63E+05	3.59E+05	**1.17E+06**
	gi|551490556	10	6	2	PREDICTED: insulin-like growth factor-binding protein complex acid labile subunit-like [Xiphophorus maculatus]	4.18E+05	6.81E+05	4.60E+05	4.78E+05	2.95E+05	4.78E+05	4.61E+05	5.06E+05	**1.16E+06**
	gi|820160543	14	6	4	isocitrate dehydrogenase [NADP] mitochondrial [Scleropages formosus]	3.97E+05	7.50E+05	3.36E+05	5.07E+05	5.37E+05	3.86E+05	3.44E+05	4.30E+05	**1.14E+06**
	gi|768963085	11	5	4	PREDICTED: complement C3-like partial [Takifugu rubripes]	7.66E+05	5.71E+05	3.73E+05	5.00E+05	4.19E+05	5.39E+05	3.97E+05	4.94E+05	**1.11E+06**
	gi|219798812	9	3	2	Apolipoprotein A-I precursor [Plecoglossus altivelis]	4.70E+05	5.85E+05	3.54E+05	6.99E+05	2.75E+05	5.25E+05	3.83E+05	5.37E+05	**1.11E+06**
	gi|742102412	25	13	2	PREDICTED: antithrombin-III isoform X1 [Esox lucius]	3.86E	5.76E	3.86E	4.08E	3.15E	5.18E	3.50E	4.38E	**1.09E+06**

						+05	+05	+05	+05	+05	+05	+05	+05	
	gi|185135626	41	68	3	complement component 4 precursor [Oncorhynchus mykiss]gi|40217259|emb|CAD66666.1| complement C4 [Oncorhynchus mykiss]	4.81E+05	5.61E+05	4.84E+05	4.84E+05	4.08E+05	5.31E+05	4.03E+05	4.30E+05	**1.09E+06**
	gi|808878196	5	3	2	Biotinidase [Larimichthys crocea]	4.01E+05	6.85E+05	5.28E+05	5.15E+05	3.24E+05	3.94E+05	3.63E+05	4.00E+05	**1.08E+06**
	gi|115495297	7	2	2	intelectin-like	5.18E+05	5.85E+05	5.03E+05	5.17E+05	3.71E+05	4.90E+05	4.03E+05	4.68E+05	**1.08E+06**
	gi|12802903	20	3	2	ferritin-H subunit [Oncorhynchus nerka]	3.84E+05	6.94E+05	5.85E+05	4.53E+05	3.55E+05	3.77E+05	3.52E+05	4.16E+05	**1.07E+06**
	gi|642102139	9	3	3	L-lactate dehydrogenase A chain	4.50E+05	6.25E+05	5.63E+05	5.02E+05	3.34E+05	4.39E+05	4.10E+05	4.30E+05	**1.06E+06**
	gi|736253373	18	7	2	PREDICTED: heparin cofactor 2 [Notothenia coriiceps]	3.63E+05	5.12E+05	4.02E+05	5.83E+05	4.00E+05	5.36E+05	6.55E+05	4.22E+05	**1.05E+06**
	gi|213514836	5	5	2	fibulin-1 precursor [Salmo salar]gi|209155358|gb|ACI33911.1| Fibulin-1 precursor [Salmo salar]	3.91E	5.81E	4.24E	4.83E	3.02E	4.48E	3.25E	4.80E	**1.03E+06**

						+05	+05	+05	+05	+05	+05	+05	+05	
	gi|197631777	21	6	2	malate dehydrogenase 1 [Salmo salar]	3.81E+05	6.32E+05	3.52E+05	4.23E+05	5.29E+05	3.80E+05	4.17E+05	5.20E+05	**1.01E+06**
	gi|528506730	5	18	10	PREDICTED: stAR-related lipid transfer protein 9 [Danio rerio]	3.55E+05	6.28E+05	2.58E+06	6.85E+05	2.91E+05	3.74E+05	3.21E+05	4.54E+05	**1.00E+06**
	gi|41152334	11	2	2	ATP synthase subunit d mitochondrial [Danio rerio]gi|528475049|ref|XP_005163831.1| PREDICTED: ATP synthase subunit d mitochondrial isoform X1 [Danio rerio]gi|688544355|ref|XP_009297977.1| PREDICTED: ATP synthase subunit d...	3.06E+05	6.63E+05	4.42E+05	3.04E+05	3.56E+05	3.33E+05	3.69E+05	3.06E+05	**9.96E+05**
	gi|734626267	4	15	7	PREDICTED: basement membrane-specific heparan sulfate proteoglycan core protein [Larimichthys crocea]	4.49E+05	5.76E+05	3.43E+05	5.08E+05	4.01E+05	4.11E+05	3.61E+05	4.80E+05	**9.86E+05**
	gi|573889912	1	3	2	PREDICTED: coagulation factor VIII-like [Lepisosteus oculatus]	8.33E+05	4.77E+05	3.38E+05	4.98E+05	3.60E+05	4.81E+05	3.27E+05	4.24E+05	**9.58E+05**
	gi|742191488	3	12	8	PREDICTED: uncharacterized protein KIAA1109 homolog isoform X2 [Esox lucius]	4.35E+05	4.92E+05	3.63E+05	4.65E+05	3.77E+05	4.66E+05	3.37E+05	4.64E+05	**9.58E+05**
	gi|725798572	6	8	4	alpha-2-macroglobulin-like precursor [Danio rerio]	3.64E	4.92E	3.85E	3.89E	3.55E	4.46E	3.40E	3.72E	**9.39E+05**

						+05	+05	+05	+05	+05	+05	+05	+05	
	gi|548342214	2	4	3	PREDICTED: UDP-glucose:glycoprotein glucosyltransferase 2-like isoform X4 [Pundamilia nyererei]	3.32E+05	4.90E+05	3.74E+05	4.18E+05	3.57E+05	4.45E+05	3.49E+05	3.88E+05	**9.35E+05**
	gi|742191606	7	7	2	PREDICTED: complement component C7 [Esox lucius]	3.84E+05	5.30E+05	4.60E+05	6.99E+05	3.71E+05	4.00E+05	5.29E+05	5.85E+05	**9.31E+05**
	gi|820135877	8	6	4	warm-temperature-acclimation-related-65 kDa-protein-like-protein precursor [Scleropages formosus]	3.24E+05	5.53E+05	2.99E+05	3.98E+05	2.53E+05	3.76E+05	2.88E+05	3.04E+05	**9.28E+05**
	gi|213514688	12	3	3	fibroleukin precursor [Salmo salar]gi|209155588|gb|ACI34026.1| Fibroleukin precursor [Salmo salar]	3.55E+05	5.44E+05	3.65E+05	3.77E+05	2.75E+05	3.79E+05	3.14E+05	3.64E+05	**9.22E+05**
	gi|831277266	14	4	2	PREDICTED: tropomyosin alpha-1 chain [Clupea harengus]	2.98E+05	5.43E+05	3.02E+05	5.05E+05	4.08E+05	3.72E+05	2.62E+05	3.61E+05	**9.15E+05**
	gi|642124499	16	3	3	Apolipo A-IV	2.83E+05	5.02E+05	3.44E+05	4.26E+05	2.65E+05	4.06E+05	3.38E+05	3.85E+05	**9.08E+05**
	gi|734605711	8	23	7	PREDICTED: fibronectin-like [Larimichthys crocea]	3.61E	4.45E	3.55E	5.82E	3.35E	4.54E	6.21E	3.94E	**8.98E+05**

						+05	+05	+05	+05	+05	+05	+05	+05	
	gi|736223836	2	13	8	PREDICTED: protein piccolo [Notothenia coriiceps]	1.40E+04	8.30E+05	1.19E+05	7.05E+04	5.40E+04	6.50E+04	2.22E+05	2.23E+04	**8.95E+05**
	gi|148806527	23	6	4	immunoglobulin light chain partial [Sparus aurata]	4.19E+05	4.60E+05	3.30E+05	4.97E+05	3.25E+05	4.32E+05	3.34E+05	4.48E+05	**8.92E+05**
	gi|554853527	9	4	2	PREDICTED: glucose-6-phosphate isomerase-like isoform X2 [Haplochromis burtoni]	3.03E+05	4.94E+05	2.81E+05	3.35E+05	2.87E+05	3.90E+05	4.01E+05	2.97E+05	**8.84E+05**
	gi|209155206	5	2	2	Hyaluronidase-2 precursor [Salmo salar]	4.47E+05	4.76E+05	3.71E+05	4.15E+05	2.87E+05	4.02E+05	3.40E+05	3.49E+05	**8.78E+05**
	gi|573896793	3	4	2	PREDICTED: ectonucleotide pyrophosphatase/phosphodiesterase family member 3-like [Lepisosteus oculatus]	3.26E+05	5.06E+05	2.68E+05	3.44E+05	3.15E+05	3.54E+05	3.68E+05	3.93E+05	**8.61E+05**
	gi|688571119	1	14	13	PREDICTED: collagen alpha-3(VI) chain isoform X4 [Danio rerio]	3.33E+05	4.41E+05	2.98E+05	4.14E+05	3.31E+05	4.08E+05	3.86E+05	3.51E+05	**8.49E+05**
	gi|642122351	25	9	2	C-reactive precursor	3.56E	4.72E	3.69E	4.87E	2.93E	3.75E	3.77E	3.81E	**8.47E+05**

						+05	+05	+05	+05	+05	+05	+05	+05	
	gi|185132436	7	2	2	leukocyte elastase inhibitor [Oncorhynchus mykiss]gi|51949906|gb|AAU14875.1| leukocyte elastase inhibitor [Oncorhynchus mykiss]	3.56E+05	4.89E+05	3.18E+05	2.96E+05	2.87E+05	3.52E+05	2.95E+05	2.98E+05	**8.40E+05**
	gi|213512925	7	3	2	aspartyl aminopeptidase [Salmo salar]gi|209154042|gb|ACI33253.1| Aspartyl aminopeptidase [Salmo salar]	3.85E+05	4.58E+05	3.65E+05	4.80E+05	3.83E+05	3.77E+05	4.69E+05	4.23E+05	**8.34E+05**
	gi|499047444	10	8	3	PREDICTED: ectonucleotide pyrophosphatase/phosphodiesterase family member 2-like [Maylandia zebra]	3.57E+05	4.35E+05	3.52E+05	4.21E+05	3.61E+05	3.95E+05	3.55E+05	4.68E+05	**8.30E+05**
	gi|768959936	5	12	5	PREDICTED: myosin-7B [Takifugu rubripes]	3.05E+05	4.71E+05	2.48E+05	4.32E+05	3.23E+05	3.57E+05	3.50E+05	3.55E+05	**8.28E+05**
	gi|742166262	4	3	2	PREDICTED: coagulation factor VII-like partial [Esox lucius]	2.92E+05	4.46E+05	4.27E+05	3.58E+05	2.54E+05	3.79E+05	2.58E+05	3.20E+05	**8.26E+05**
	gi|633265707	10	5	3	transferrin [Megalobrama amblycephala]	1.59E+05	5.59E+05	1.60E+05	2.74E+05	2.04E+05	2.49E+05	2.95E+05	2.39E+05	**8.08E+05**
	gi|642126851	35	43	2	complement C3-like	3.02E	4.30E	2.85E	4.36E	2.79E	3.67E	2.78E	2.98E	**7.97E+05**

						+05	+05	+05	+05	+05	+05	+05	+05	
	gi|113431906	18	3	3	lysozyme g [Salmo salar]	3.47E+05	4.37E+05	3.43E+05	2.82E+05	1.77E+05	3.53E+05	2.91E+05	2.87E+05	**7.90E+05**
	gi|1174771	34	28	3	RecName: Full=Serotransferrin-2; AltName: Full=Serotransferrin II; Short=STF II; Short=sTF2; AltName: Full=Siderophilin II; Flags: Precursor [Salmo salar]	3.77E+05	3.97E+05	3.03E+05	4.34E+05	3.51E+05	3.92E+05	3.43E+05	3.96E+05	**7.88E+05**
	gi|831311632	15	7	4	PREDICTED: fibrinogen beta chain [Clupea harengus]	1.20E+05	3.40E+05	1.70E+05	4.33E+05	1.71E+05	4.48E+05	2.14E+05	4.87E+05	**7.88E+05**
	gi|213515184	13	3	2	phosphoglycerate mutase 2-2 (muscle) [Salmo salar]gi|197632481|gb|ACH70964.1| phosphoglycerate mutase 2-2 (muscle) [Salmo salar]	2.96E+05	4.55E+05	2.80E+05	3.97E+05	3.03E+05	3.20E+05	3.21E+05	3.82E+05	**7.75E+05**
	gi|657763341	11	4	4	PREDICTED: glucose-6-phosphate 1-dehydrogenase isoform X1 [Cynoglossus semilaevis]	3.30E+05	4.53E+05	3.29E+05	3.75E+05	2.76E+05	3.20E+05	3.26E+05	3.46E+05	**7.73E+05**
	gi|642114462	33	55	3	alpha-2-macroglobulin-like	2.13E+05	3.16E+05	2.32E+05	1.96E+05	1.77E+05	4.57E+05	1.44E+05	2.57E+05	**7.73E+05**
	gi|742088005	12	7	4	PREDICTED: complement component C8 beta chain isoform X1 [Esox lucius]	3.04E	3.55E	3.54E	4.31E	3.85E	4.09E	2.52E	3.56E	**7.64E+05**

						+05	+05	+05	+05	+05	+05	+05	+05	
	gi|657559298	16	7	3	PREDICTED: antithrombin-III [Stegastes partitus]gi|657559301|ref|XP_008283572.1| PREDICTED: antithrombin-III [Stegastes partitus]	2.78E+05	4.21E+05	2.97E+05	3.42E+05	2.53E+05	3.42E+05	3.68E+05	3.96E+05	**7.63E+05**
	gi|573887935	7	16	3	PREDICTED: complement C3-like [Lepisosteus oculatus]	2.55E+05	5.01E+05	3.13E+05	3.77E+05	1.64E+05	2.56E+05	2.52E+05	2.58E+05	**7.57E+05**
	gi|642105825	18	8	2	alpha-2-macroglobulin-like isoform X2	2.95E+05	3.82E+05	3.91E+05	3.55E+05	2.32E+05	3.64E+05	2.56E+05	2.75E+05	**7.47E+05**
	gi|657752349	6	25	20	PREDICTED: LOW QUALITY PROTEIN: ryanodine receptor 3 [Cynoglossus semilaevis]	2.89E+05	4.12E+05	3.31E+05	3.17E+05	2.26E+05	3.24E+05	2.65E+05	4.35E+05	**7.35E+05**
	gi|209156172	7	5	2	Cytosolic non-specific dipeptidase [Salmo salar]	2.97E+05	3.21E+05	3.28E+05	4.15E+05	3.54E+05	4.11E+05	2.74E+05	3.30E+05	**7.32E+05**
	gi|47222714	6	5	2	plasminogen	2.84E+05	3.87E+05	2.45E+05	2.11E+05	2.44E+05	3.43E+05	1.87E+05	1.83E+05	**7.30E+05**
	gi|213514808	10	2	2	Glutathione S-transferase A [Salmo salar]gi|209737598|gb|ACI69668.1| Glutathione S-transferase A [Salmo salar]	2.76E	4.05E	2.68E	3.32E	2.30E	3.23E	2.19E	3.86E	**7.29E+05**

						+05	+05	+05	+05	+05	+05	+05	+05	
	gi|380853836	15	11	2	warm-temperature-acclimation-related 65-kDa protein [Oplegnathus fasciatus]gi|380853840|gb|AFE88227.1| warm-temperature-acclimation-related 65-kDa protein [Oplegnathus fasciatus]	2.90E+05	3.56E+05	2.59E+05	5.03E+05	2.55E+05	3.52E+05	3.50E+05	2.86E+05	**7.08E+05**
	gi|657589609	5	22	13	PREDICTED: apolipoprotein B-100-like [Stegastes partitus]	2.57E+05	3.88E+05	2.49E+05	2.15E+05	2.41E+05	2.98E+05	2.71E+05	3.21E+05	**6.86E+05**
	gi|223646832	34	8	4	Hemoglobin subunit alpha [Salmo salar]gi|223672691|gb|ACN12527.1| Hemoglobin subunit alpha [Salmo salar]	2.87E+05	3.43E+05	2.46E+05	3.89E+05	2.80E+05	3.25E+05	2.82E+05	3.07E+05	**6.68E+05**
	gi|221219416	13	2	2	Cofilin-2 [Salmo salar]gi|223646808|gb|ACN10162.1| Cofilin-2 [Salmo salar]gi|223672667|gb|ACN12515.1| Cofilin-2 [Salmo salar]	2.57E+05	4.17E+05	2.41E+05	2.64E+05	1.56E+05	2.31E+05	2.15E+05	2.70E+05	**6.48E+05**
	gi|688590496	6	17	12	PREDICTED: neurobeachin-like protein 2 isoform X1 [Danio rerio]	1.82E+05	5.47E+05	2.12E+05	1.07E+05	8.38E+04	9.35E+04	9.49E+04	9.75E+04	**6.41E+05**
	gi|742167255	26	10	4	PREDICTED: hemopexin-like [Esox lucius]	2.46E+05	2.96E+05	2.93E+05	4.39E+05	3.39E+05	3.33E+05	1.64E+05	2.44E+05	**6.30E+05**
	gi|597746045	11	10	3	PREDICTED: inter-alpha-trypsin inhibitor heavy chain H2 [Astyanax mexicanus]	2.24E	3.32E	2.00E	2.48E	2.79E	2.95E	2.16E	2.56E	**6.27E+05**

						+05	+05	+05	+05	+05	+05	+05	+05	
	gi|150551056	34	20	2	complement component C5 [Oncorhynchus mykiss]	2.63E+05	3.04E+05	2.04E+05	2.25E+05	2.19E+05	2.74E+05	2.45E+05	2.70E+05	**5.77E+05**
	gi|573880156	5	9	3	PREDICTED: complement C4-B-like [Lepisosteus oculatus]	2.21E+05	2.96E+05	2.39E+05	1.90E+05	1.59E+05	2.69E+05	2.41E+05	2.43E+05	**5.65E+05**
	gi|765129516	3	4	3	PREDICTED: probable ATP-dependent RNA helicase DHX37 isoform X1 [Oryzias latipes]gi|765129518|ref|XP_011477194.1| PREDICTED: probable ATP-dependent RNA helicase DHX37 isoform X1 [Oryzias latipes]	2.51E+05	3.10E+05	2.26E+05	3.20E+05	1.90E+05	2.53E+05	2.76E+05	2.72E+05	**5.62E+05**
	gi|642003662	15	2	2	gonadal somatic cell derived factor isoform X1	2.25E+05	2.96E+05	2.10E+05	2.68E+05	2.47E+05	2.64E+05	2.02E+05	2.37E+05	**5.59E+05**
	gi|225056702	15	11	2	transferrin [Dicentrarchus labrax]	2.12E+05	3.16E+05	2.15E+05	3.88E+05	2.15E+05	2.35E+05	1.64E+05	2.77E+05	**5.50E+05**
	gi|188586663	6	5	3	fibulin-1 precursor [Danio rerio]gi|30580409|sp|O42182.1|FBLN1_DANRE RecName: Full=Fibulin-1; Short=FIBL-1; Flags: Precursor [Danio rerio]gi|2522169|gb|AAB80944.1| fibulin-1 D [Danio rerio]	4.24E+05	3.49E+05	2.00E+05	1.91E+05	1.60E+05	1.96E+05	2.12E+05	1.73E+05	**5.45E+05**
	gi|831303918	3	14	7	PREDICTED: WD repeat and FYVE domain-containing protein 3 [Clupea harengus]	2.22E	2.91E	2.39E	1.83E	1.17E	2.50E	2.18E	2.56E	**5.41E+05**

						+05	+05	+05	+05	+05	+05	+05	+05	
	gi|498976641	9	15	2	PREDICTED: myosin heavy chain fast skeletal muscle-like [Maylandia zebra]	2.39E+05	2.42E+05	1.91E+05	4.14E+05	1.74E+05	2.98E+05	4.88E+05	3.18E+05	**5.41E+05**
	gi|657762465	13	2	2	PREDICTED: proteasome subunit beta type-3 [Cynoglossus semilaevis]	1.92E+05	2.71E+05	1.86E+05	1.78E+05	1.11E+05	2.55E+05	1.51E+05	1.91E+05	**5.26E+05**
	gi|6686389	59	38	3	RecName: Full=Apolipoprotein A-I; Short=Apo-AI; Short=ApoA-I; AltName: Full=Apolipoprotein A1; Contains: RecName: Full=Proapolipoprotein A-I; Short=ProapoA-I; Flags: Precursor [Salmo trutta]gi|1196888|gb|AAA88542.1| ap...	3.14E+05	2.42E+05	2.59E+05	3.68E+05	1.67E+05	2.83E+05	6.67E+05	3.62E+05	**5.25E+05**
	gi|47218987	9	8	2	inter-alpha-trypsin inhibitor heavy chain H3-like isoform X1	2.33E+05	2.32E+05	2.18E+05	3.78E+05	3.10E+05	2.88E+05	2.38E+05	2.82E+05	**5.21E+05**
	gi|548423295	2	3	3	PREDICTED: formin-1-like [Pundamilia nyererei]	1.39E+06	2.91E+05	2.09E+05	3.53E+05	1.84E+05	2.29E+05	2.15E+05	1.87E+05	**5.20E+05**
	gi|742093634	7	3	2	PREDICTED: coagulation factor IX [Esox lucius]	1.82E+05	2.48E+05	1.47E+05	1.92E+05	2.49E+05	2.56E+05	1.45E+05	2.18E+05	**5.03E+05**
	gi|657751734	7	7	5	PREDICTED: leucine-rich repeat protein soc-2-like [Cynoglossus semilaevis]	2.01E	2.91E	2.07E	2.03E	1.40E	2.10E	1.89E	2.34E	**5.01E+05**

						+05	+05	+05	+05	+05	+05	+05	+05	
	gi|400364966	9	3	2	cobalamin-binding protein partial [Oncorhynchus mykiss]	2.17E+05	2.83E+05	1.89E+05	2.78E+05	1.88E+05	2.05E+05	1.73E+05	2.09E+05	**4.88E+05**
	gi|291190624	15	9	5	Moesin [Salmo salar]gi|223649090|gb|ACN11303.1| Moesin [Salmo salar]	2.59E+05	3.03E+05	2.14E+05	2.21E+05	2.04E+05	1.68E+05	1.62E+05	2.27E+05	**4.71E+05**
	gi|542203128	29	15	4	PREDICTED: hemopexin-like [Oreochromis niloticus]	2.12E+05	2.38E+05	1.70E+05	2.61E+05	2.56E+05	2.29E+05	1.49E+05	2.63E+05	**4.67E+05**
	gi|658859574	2	4	3	PREDICTED: calmodulin-binding transcription activator 1-like isoform X4 [Poecilia reticulata]	2.60E+05	2.63E+05	1.63E+05	2.09E+05	1.35E+05	2.00E+05	2.09E+05	3.08E+05	**4.63E+05**
	gi|185133218	6	4	2	complement protein component C7-1 precursor [Oncorhynchus mykiss]gi|31620984|emb|CAD92841.1| complement protein component C7-1 [Oncorhynchus mykiss]	1.50E+05	2.57E+05	1.15E+05	1.52E+05	1.12E+05	2.02E+05	9.52E+04	1.63E+05	**4.59E+05**
	gi|597752622	5	6	2	PREDICTED: complement C3-like [Astyanax mexicanus]	1.24E+05	2.57E+05	1.91E+05	1.53E+05	1.16E+05	1.74E+05	1.15E+05	1.22E+05	**4.31E+05**
	gi|831286361	4	8	6	PREDICTED: eukaryotic translation initiation factor 3 subunit A [Clupea harengus]	1.53E	2.36E	1.62E	2.03E	1.14E	1.71E	1.19E	1.85E	**4.06E+05**

						+05	+05	+05	+05	+05	+05	+05	+05	
	gi|657558475	4	29	8	PREDICTED: plectin-like isoform X3 [Stegastes partitus]	1.32E+05	2.40E+05	1.60E+05	1.43E+05	9.58E+04	1.57E+05	1.19E+05	1.36E+05	**3.96E+05**
	gi|410903672	17	9	6	PREDICTED: complement component C9 [Takifugu rubripes]gi|2499468|sp|P79755.1|CO9_TAKRU RecName: Full=Complement component C9; Flags: Precursor [Takifugu rubripes]gi|1845349|gb|AAC60288.1| complement component C9 [Takifu...	1.33E+05	1.91E+05	1.52E+05	2.59E+05	1.87E+05	1.90E+05	1.13E+05	1.87E+05	**3.81E+05**
	gi|765158382	5	6	5	PREDICTED: CD109 antigen-like [Oryzias latipes]	2.65E+05	2.32E+05	2.47E+05	2.34E+05	1.44E+05	1.47E+05	2.11E+05	2.54E+05	**3.79E+05**
	gi|768955466	5	8	2	PREDICTED: alpha-2-macroglobulin-like protein 1 [Takifugu rubripes]	1.51E+05	2.03E+05	1.15E+05	1.72E+05	1.51E+05	1.58E+05	1.53E+05	1.73E+05	**3.61E+05**
	gi|742106654	7	4	2	PREDICTED: ovostatin-like partial [Esox lucius]	1.22E+05	1.78E+05	1.31E+05	2.02E+05	1.35E+05	1.82E+05	1.23E+05	1.31E+05	**3.61E+05**
	gi|742181536	3	6	4	PREDICTED: coagulation factor V [Esox lucius]	5.87E+05	1.90E+05	1.19E+05	1.72E+05	1.11E+05	1.61E+05	1.48E+05	2.08E+05	**3.51E+05**
	gi|551494873	9	3	2	PREDICTED: tubulin alpha chain-like [Xiphophorus maculatus]	1.45E	2.14E	1.49E	1.55E	1.60E	1.35E	1.12E	1.34E	**3.48E+05**

						+05	+05	+05	+05	+05	+05	+05	+05	
	gi|697870411	9	18	2	alpha-2-macroglobulin [Rachycentron canadum]	1.08E+05	1.97E+05	9.46E+04	1.36E+05	8.93E+04	1.42E+05	1.20E+05	1.30E+05	**3.38E+05**
	gi|642131130	73	31	2	LEG1 homolog	2.12E+05	1.87E+05	1.81E+05	2.26E+05	1.24E+05	1.43E+05	1.54E+05	1.89E+05	**3.30E+05**
	gi|498981474	3	3	2	PREDICTED: hephaestin-like protein 1-like isoform X1 [Maylandia zebra]	9.58E+04	8.30E+04	7.69E+04	7.28E+05	6.76E+04	2.46E+05	1.13E+06	3.48E+05	**3.29E+05**
	gi|38423491	18	9	2	salarin [Salvelinus alpinus]	1.25E+05	1.59E+05	1.19E+05	1.61E+05	1.07E+05	1.60E+05	1.08E+05	1.34E+05	**3.19E+05**
	gi|551504003	2	8	4	PREDICTED: LOW QUALITY PROTEIN: vacuolar protein sorting-associated protein 13B-like [Xiphophorus maculatus]	1.92E+05	1.70E+05	1.01E+05	1.06E+05	1.05E+05	1.45E+05	1.96E+05	1.07E+05	**3.15E+05**
	gi|742084554	4	27	16	PREDICTED: golgin subfamily B member 1-like isoform X5 [Esox lucius]	6.61E+04	6.06E+04	6.40E+04	4.92E+05	1.35E+05	2.33E+05	1.45E+05	2.46E+05	**2.94E+05**
	gi|657815896	6	6	4	PREDICTED: thrombospondin-4 [Cynoglossus semilaevis]	1.26E	1.44E	6.42E	1.39E	8.76E	1.45E	1.39E	1.66E	**2.90E+05**

						+05	+05	+04	+05	+04	+05	+05	+05	
	gi|573899332	5	20	12	PREDICTED: dynein heavy chain 3 axonemal-like [Lepisosteus oculatus]	9.15E+04	1.81E+05	1.22E+05	1.26E+05	1.04E+05	1.07E+05	8.61E+04	1.05E+05	**2.88E+05**
	gi|765156826	7	12	2	PREDICTED: complement C3-like [Oryzias latipes]	8.30E+04	1.66E+05	8.86E+04	8.36E+04	9.71E+04	1.17E+05	8.16E+04	8.11E+04	**2.83E+05**
	gi|657737950	10	8	2	PREDICTED: glycogen phosphorylase muscle form [Cynoglossus semilaevis]	1.13E+05	1.59E+05	1.33E+05	1.29E+05	1.08E+05	1.20E+05	1.24E+05	1.01E+05	**2.79E+05**
	gi|688594957	5	22	12	PREDICTED: spectrin beta chain non-erythrocytic 5 isoform X1 [Danio rerio]	1.27E+05	1.29E+05	1.15E+05	2.48E+05	1.57E+05	1.40E+05	1.48E+05	1.54E+05	**2.69E+05**
	gi|854620	25	23	4	apolipoprotein B [Salmo salar]	9.21E+04	1.61E+05	7.90E+04	1.20E+05	8.83E+04	9.32E+04	8.89E+04	1.29E+05	**2.54E+05**
	gi|617439790	5	25	19	PREDICTED: dynein heavy chain 2 axonemal [Poecilia formosa]	7.38E+04	1.26E+05	1.14E+05	1.10E+05	8.63E+04	1.15E+05	9.59E+04	8.21E+04	**2.41E+05**
	gi|498987457	9	6	2	PREDICTED: alpha-actinin-2-like [Maylandia zebra]gi|548350222|ref|XP_005727440.1| PREDICTED: alpha-actinin-2-like isoform X1 [Pundamilia	7.16E	1.51E	6.78E	1.41E	1.42E	8.06E	5.54E	7.40E	**2.32E+05**

					nyererei]gi|554806732|ref|XP_005914292.1| PREDICTED: alpha-actinin-2-like isoform ...	+04	+05	+04	+05	+05	+04	+04	+04	
	gi|641980149	12	3	3	scavenger receptor cysteine-rich type 1 M130-like	8.72E+04	1.14E+05	1.17E+05	1.54E+05	1.54E+05	1.14E+05	1.01E+05	1.55E+05	**2.28E+05**
	gi|573906258	3	5	4	PREDICTED: nuclear pore complex protein Nup214-like [Lepisosteus oculatus]	5.98E+04	1.20E+05	4.39E+04	1.07E+05	8.40E+04	1.06E+05	6.82E+04	9.30E+04	**2.26E+05**
	gi|11870062	30	51	4	complement component C3-4 [Oncorhynchus mykiss]	7.58E+04	1.06E+05	8.98E+04	1.44E+05	8.90E+04	1.08E+05	6.76E+04	8.04E+04	**2.14E+05**
	gi|573876316	5	24	15	PREDICTED: apolipoprotein B-100-like [Lepisosteus oculatus]	6.35E+04	1.05E+05	5.28E+04	1.32E+05	7.54E+04	8.73E+04	1.99E+05	8.28E+04	**1.92E+05**
	gi|528502955	16	6	3	hemopexin	1.17E+05	1.18E+05	2.24E+05	2.08E+05	9.43E+04	7.28E+04	1.13E+05	1.08E+05	**1.90E+05**
	gi|794627581	15	12	2	transferrin [Oreochromis niloticus]	7.91E+04	9.57E+04	5.51E+04	1.26E+05	8.88E+04	9.19E+04	9.40E+04	1.07E+05	**1.88E+05**
	gi|597745052	6	27	13	PREDICTED: sacsin isoform X2 [Astyanax mexicanus]	8.82E	8.36E	9.52E	1.30E	8.95E	9.49E	7.12E	1.07E	**1.78E+05**

						+04	+04	+04	+05	+04	+04	+04	+05	
	gi|472210667	6	4	3	heterogeneous nuclear ribonucleo U 1	3.41E+04	1.06E+05	2.97E+04	5.34E+04	3.04E+04	6.51E+04	6.87E+04	4.14E+04	**1.71E+05**
	gi|188496504	10	4	4	angiotensinogen [Plecoglossus altivelis]	5.35E+04	9.02E+04	6.97E+04	6.99E+04	5.98E+04	7.97E+04	6.39E+04	6.75E+04	**1.70E+05**
	gi|820110591	16	11	2	integrin beta 1a precursor partial [Scleropages formosus]	4.51E+04	6.29E+04	3.86E+04	6.76E+04	4.64E+04	6.43E+04	3.85E+04	5.42E+04	**1.27E+05**
	gi|734626935	9	4	3	PREDICTED: heat shock cognate 71 kDa protein [Larimichthys crocea]gi|734626937|ref|XP_010741634.1| PREDICTED: heat shock cognate 71 kDa protein [Larimichthys crocea]gi|808869193|gb|KKF19322.1| Heat shock cognate protein...	5.64E+04	6.33E+04	4.54E+04	7.36E+04	1.33E+05	5.24E+04	6.30E+04	9.37E+04	**1.16E+05**
	gi|157311655	10	18	4	complement component C3-1 precursor [Oryzias latipes]gi|7209634|dbj|BAA92285.1| Orla C3-1 [Oryzias latipes]	2.64E+04	6.00E+04	4.39E+04	1.68E+04	3.19E+04	3.24E+04	2.90E+04	3.52E+04	**9.24E+04**
	gi|213512270	11	5	2	pyruvate kinase [Salmo salar]gi|197632483|gb|ACH70965.1| pyruvate kinase [Salmo salar]gi|197632485|gb|ACH70966.1| pyruvate kinase [Salmo salar]	2.51E+04	4.06E+04	1.81E+04	2.53E+04	2.25E+04	3.85E+04	1.48E+04	2.12E+04	**7.91E+04**
	gi|831298016	11	9	3	PREDICTED: inter-alpha-trypsin inhibitor heavy chain H2 [Clupea harengus]	1.98E	5.36E	2.79E	2.06E	1.08E	2.06E	1.76E	2.79E	**7.42E+04**

						+04	+04	+04	+04	+04	+04	+04	+04	
	gi|267585	36	8	3	RecName: Full=Retinol-binding protein 4-B; AltName: Full=Plasma retinol-binding protein 2; Short=PRBP-2; AltName: Full=Plasma retinol-binding protein II; Short=PRBP-II [Oncorhynchus mykiss]	4.37E+04	5.09E+04	2.24E+04	4.49E+04	1.78E+04	2.19E+04	1.33E+04	3.67E+04	**7.28E+04**
	gi|657537967	4	20	9	PREDICTED: spectrin beta chain non-erythrocytic 5-like [Stegastes partitus]	1.47E+04	2.90E+04	1.03E+04	2.98E+04	1.35E+04	1.81E+04	1.23E+04	1.71E+04	**4.70E+04**
	gi|765148647	12	25	2	PREDICTED: LOW QUALITY PROTEIN: myosin-7 [Oryzias latipes]	8.27E+03	1.05E+04	1.01E+04	2.15E+04	1.07E+04	1.94E+04	7.50E+03	1.45E+04	**2.98E+04**

Column B:	Accession number
Column C:	Sequence coverage (%)
Column D:	Total number of identifying peptides
Column E:	Number of unique identifying peptides
Column F:	Protein name from NCBI non-redundant protein database (Actinopterygii). Any "unknown protein" identifications were searched using Blast2Go, and the top match is shown here (the Accession number is the original "unnamed protein")
Columns G - N:	Protein abundance, arranged by treatment (concentration, time, exercise)
Column O:	Sum of protein abundance for control + no swim. Protein list is arranged in decreasing order from this value. The top 30 (dark green) and top 100 (light green) abundant proteins are indicated.
Abbreviations:	Concentration -> C (control, TPAH 0 ug/L); DB (dilbit, TPAH 66.7 ug/L) Time -> 1 (1 wk continuous exposure); 4 (4 wk continuous exposure) Exercise -> NS (no swim); S (swim, samples collected immediately after a critical swimming speed test)

Table S 12. Protein spots identification from the gels corresponding to MC-LR- treated were digested overnight, and the desalted peptides were then analyzed by electrospray mass spectrometry (ESI-MS) (Malécot et al., 2009).

	Experimental		Theoretical		Databases	Species	Accession number	Score	Number of peptides identified
	MW (kDa)	p1	MW(kDa)	p1					
Glucose regulated protein 78 kDa	85	z 5.0	72.5	4.79	NCBInr	*Paniliclays otivaceus*	110226520	192[a]	4a
					EST	0. *latipes*	66703162	97[a]	2[a]
					NCBInr	*Tetroodon*	47218700	100%	14
					EST	*0. loupes*	112265248	502	8
					Ensembl	*0. latipes*	ENSORLP00000008651	100%	20
Phenylalanine hydroxylase	Ix 55	5.4	45.44	5.2	NCBInr	a *rerio*	32442452	99%	2
					EST	0. *latipes*	66708523/66751361	139	4
					Ensembl	*0. latipes*	ENSORLP00000020655	100%	4
Aldehyde dehydrogenase 2 mitochondria'	ar. 55	= 5.8	57.24	6.66	NCBInr	*T. nigroviridis*	472052256	100%	4
					EST	*0. loupes*	66704840	338	7
					Ensembl	0. *Intipes*	ENSORLP00000005184	100%	6
ATP synthase beta subunit mitochondria'	55	z 4.9	55.16	4.86	NCBInr	*T. nigroviridis*	47218629	100%	18
					EST	*0. !napes*	45246978	874	20
					Ensembl	*0. latipes*	ENSORLP0000004384	100%	21
Transferrin	95	6.3	74.49	625	NCBInr	*0. Wipes*	171544935	100%	2
					EST	*0. loupes*	12589105	150	2
					Ensembl	*0. latipes*	ENSORLP00000020672	100%	5
Beta tubuline 4	55	4.9	49.85/49.86	4.52/4.6	NCBInr	*Notothenia coriiceps*	10242160	100%	3
					EST	*0. !napes*	45247295	185	5
					Ensembl	*0. latipes*	ENSORLP00000020413/22197	100%	5
40S ribosomal protein	x 38	4.9	33.37/32.75	4.6/4.62	NCBInr	*Solea senegalensis*	124300851	100%	4
SA									

					EST	*0. latipes*	17356435	143	3
					Ensembl	*0. latipes*	ENSORLP00000020346/7	100%	4
Thiosulfate sulfurtransferase	34	6.3	33.15	6.23	EST	0. *latipes*	66706524	174	4
					Ensembl	*0. latipes*	ENSOL00000016910	100%	4
Apolipoprotein Al	-^e. 25	5.4	30.03	5.12	EST	0. *latipes*	187670465	438	18
					Ensembl	*0. loupes*	ENSORLP00000019715	100%	7
Cytochrome 1)5	–-.: 18	-A- 4.6	15.59	4.55	EST	*0. latipes*	17357005	116	4
					Ensembl	*0. Wipes*	ENSORLP00000004277	100%	3
Heat shock cognate	al 80	rc 5.3	71.03	5.17	EST	*0. latipes*	24977713	118	3 (2 frames)
71 kDa protein									
					EST	*0. latipes*	9933444	102	3
					Ensembl	0. *Mapes*	ENSORLP00000006701	100%	3
ATP synthase d subunit	20	–-.: 5.8	-		EST	*0. latipes*	17357311	87	2
Protein disulfide	kr. 48	5.3	48.92	4.92	EST	*0. Incepts*	141625790	72	2
					Ensembl	0. *latipes*	ENSORLP00000015908	100%	3
Fumarylacetoacetase	2-- 45	6.2	26.38	7.81	EST	0. *latipes*	112332544	298	6
					Ensembl	*0. latipes*	ENSORLP00000024229	100%	5
Prohibitin	—. 30	x,-5.3	29.92	5.04	NCBInr	*D. redo*	41152028	-	4
					EST	0. *latipes*	17358286	341	8
					Ensembl	*0. loupes*	ENSORLP00000003919	100%	4
Protein disulfide isomerase A4	85	a'' 5.0	71.9	4.69	EST	*0. latipes*	66753090	194	4
					Ensembl	0. *Mapes*	ENSORLP00000009119	100%	7

Complement C3-1	90	;t 6.4	184.8	6.45	NCBInr	*0. latipes*	157311655	100%	4
					EST	0. *latipes*	18041526	114	2
					Ensembl	*0. :wipes*	ENSORLP00000014130	100%	5

MW: molecular weight.
p*I*: isoelectric point.
Note: Theoretical molecular weights and isoelectric points are the ones for medaka's protein in the Ensembl database.
Scores for the EST database correspond to Mascot ion score and for the two other databases correspond to Scaffold probability.
[a] These peptides were identified by Mascot with tandem mass spectra produce by nanoESI-QTOF for desalted peptides so the scores correspond to Mascot ion scores.

Table S 13. The IDs, descriptions and p-values of the GO terms that were found enriched (P < 0.05) for the lists of significant proteins in freshwater and brackishwater whitefish. In light blue are the descriptions of those terms that have been identified as terminal (result not shown). UniProt identifiers correspond to Homo sapiens orthologs (Papakostas et al., 2012).

Freshwater whitefish				Brackishwater whitefish			
Biological Process							
GO-ID	*p*-value	Description	Genes in test set	GO-ID	*p*-value	Description	Genes in test set
6880	3.50E-03	intracellular sequestering of iron ion	P30626|P02794	45823	1.21E-03	positive regulation of heart contraction	P09493|P05023
42572	3.50E-03	retinol metabolic process	P02753|P09455	5977	2.93E-03	glycogen metabolic process	P62140|P11217|P62158
6816	9.12E-03	calcium ion transport	P13693|P30626|P08133	6073	2.93E-03	cellular glucan metabolic process	P62140|P11217|P62158
51651	9.12E-03	maintenance of location in cell	P30101|P30626|P02794	44042	2.93E-03	glucan metabolic process	P62140|P11217|P62158
70838	9.12E-03	divalent metal ion transport	P13693|P30626|P08133	3013	3.48E-03	circulatory system process	P09493|P80404|P05023|P05976
6449	1.01E-02	regulation of translational termination	P52758|P62495	8015	3.48E-03	blood circulation	P09493|P80404|P05023|P05976
32024	1.01E-02	positive regulation of insulin secretion	P00367|P02753	8217	4.08E-03	regulation of blood pressure	P09493|P80404|P05023
2793	1.01E-02	positive regulation of peptide secretion	P00367|P02753	44264	4.08E-03	cellular polysaccharide metabolic process	P62140|P11217|P62158
6695	1.01E-02	cholesterol biosynthetic process	P42765|P11413	70534	6.93E-03	protein K63-linked ubiquitination	Q13404|Q96LR5
90277	1.01E-02	positive regulation of peptide hormone secretion	P00367|P02753	7517	7.17E-03	muscle organ development	P09493|O43847|P14649|P05976
46887	1.01E-02	positive regulation of hormone secretion	P00367|P02753	5976	1.12E-02	polysaccharide metabolic process	P62140|P11217|P62158
51238	1.01E-02	sequestering of metal ion	P30626|P02794	6814	1.13E-02	sodium ion transport	P05023|Q16795
16126	1.01E-02	sterol biosynthetic process	P42765|P11413	5980	1.13E-02	glycogen catabolic process	P11217|P62158
70972	1.01E-02	protein localization in endoplasmic reticulum	P30101|P61011	9251	1.13E-02	glucan catabolic process	P11217|P62158
6875	1.13E-02	cellular metal ion homeostasis	P13693|P30626|P11217|P0768	44247	1.13E-02	cellular polysaccharide catabolic process	P11217|P62158
55065	1.13E-02	metal ion homeostasis	P13693|P30626|P11217|P0768	45087	1.64E-02	innate immune response	P52907|Q13404|P68371
6323	1.52E-02	DNA packaging	P55209|P41227|P07305|P4973	3015	1.66E-02	heart process	P09493|P05976
72511	1.79E-02	divalent inorganic cation transport	P13693|P30626|P08133	60048	1.66E-02	cardiac muscle contraction	P09493|P05976
33273	1.79E-02	response to vitamin	P00480|P02753|P09455	60047	1.66E-02	heart contraction	P09493|P05976
51235	1.79E-02	maintenance of location	P30101|P30626|P02794	33275	1.95E-02	actin-myosin filament sliding	P09493|P14649|P05976
30003	1.87E-02	cellular cation homeostasis	P13693|P30626|P11217|P0768	70252	1.95E-02	actin-mediated cell contraction	P09493|P14649|P05976
50801	1.91E-02	ion homeostasis	P00480|P13693|P30626|P1121	30049	1.95E-02	muscle filament sliding	P09493|P14649|P05976
2683	1.94E-02	negative regulation of immune system process	P42574|P02760	6952	2.08E-02	defense response	P52907|Q01085|Q13404|P68371
1508	1.94E-02	regulation of action potential	P30626|P07686	209	2.27E-02	protein polyubiquitination	Q13404|Q96LR5
6887	2.17E-02	exocytosis	P62937|P61006|O43852|Q9H	272	2.27E-02	polysaccharide catabolic process	P11217|P62158
48878	2.24E-02	chemical homeostasis	P00480|P13693|P30626|P027	30048	2.28E-02	actin filament-based movement	P09493|P14649|P05976
42592	2.44E-02	homeostatic process	P00480|P30101|P13693|P3062	6457	2.54E-02	protein folding	Q9H2H8|P50502|P50
55080	2.50E-02	cation homeostasis	P13693|P30626|P11217|P0768	14706	2.64E-02	striated muscle tissue development	P09493|O43847|P14649
51704	2.63E-02	multi-organism process	P62937|P35998|P13693|Q7K2	60537	2.64E-02	muscle tissue development	P09493|O43847|P14649
71103	2.70E-02	DNA conformation change	P55209|P41227|P07305|P4973	61061	2.84E-02	muscle structure development	P09493|O43847|P14649|P05976
72503	3.02E-02	cellular divalent inorganic cation homeostasis	P13693|P11217|P07686	9987	3.33E-02	cellular process	Q01085|P62750|Q131
72507	3.02E-02	divalent inorganic cation homeostasis	P13693|P11217|P07686	6936	3.43E-02	muscle contraction	P09493|P14649|P05976|P62158
6874	3.02E-02	cellular calcium ion homeostasis	P13693|P11217|P07686	3012	3.43E-02	muscle system process	P09493|P14649|P05976|P62158
55074	3.02E-02	calcium ion homeostasis	P13693|P11217|P07686	6112	3.46E-02	energy reserve metabolic process	P62140|P11217|P62158
1666	3.02E-02	response to hypoxia	P09972|O00151|P11217	10962	3.52E-02	regulation of glucan biosynthetic process	P62140

79	3.11E-02	regulation of cyclin-dependent protein kinase activity	Q9P287|P42574
33189	3.11E-02	response to vitamin A	P02753|P09455
9084	3.11E-02	glutamine family amino acid biosynthetic process	P00480|P00367
6309	3.11E-02	DNA fragmentation involved in apoptotic nuclear change	P07305|P42574
51047	3.11E-02	positive regulation of secretion	P00367|P02753
737	3.11E-02	DNA catabolic process, endonucleolytic	P07305|P42574
6776	3.11E-02	vitamin A metabolic process	P02753|P09455
5980	3.11E-02	glycogen catabolic process	P11217|P62158
9251	3.11E-02	glucan catabolic process	P11217|P62158
44247	3.11E-02	cellular polysaccharide catabolic process	P11217|P62158
6259	3.64E-02	DNA metabolic process	P62937|P23193|P55209|P073
70482	3.76E-02	response to oxygen levels	P09972|O00151|P11217
65007	3.93E-02	biological regulation	P23193|P35998|P00367|O146
8203	4.49E-02	cholesterol metabolic process	P42765|P11413
6919	4.49E-02	activation of caspase activity	P42574|P23396
6694	4.49E-02	steroid biosynthetic process	P42765|P11413
6721	4.49E-02	terpenoid metabolic process	P02753|P09455
6720	4.49E-02	isoprenoid metabolic process	P02753|P09455
6775	4.49E-02	fat-soluble vitamin metabolic process	P02753|P09455
16125	4.49E-02	sterol metabolic process	P42765|P11413
16101	4.49E-02	diterpenoid metabolic process	P02753|P09455
1523	4.49E-02	retinoid metabolic process	P02753|P09455
9583	4.49E-02	detection of light stimulus	P02753|O14610
5976	4.58E-02	polysaccharide metabolic process	P11217|P07686|P62158
9416	4.58E-02	response to light stimulus	P02753|O14610|P42574
44419	4.72E-02	interspecies interaction between organisms	P62937|P35998|Q7KZF4|P05

2228	3.52E-02	natural killer cell mediated immunity	P68371
10894	3.52E-02	negative regulation of steroid biosynthetic process	P05023
90032	3.52E-02	negative regulation of steroid hormone biosynthetic process	P05023
90030	3.52E-02	regulation of steroid hormone biosynthetic process	P05023
45939	3.52E-02	negative regulation of steroid metabolic process	P05023
32350	3.52E-02	regulation of hormone metabolic process	P05023
32351	3.52E-02	negative regulation of hormone metabolic process	P05023
32885	3.52E-02	regulation of polysaccharide biosynthetic process	P62140
32353	3.52E-02	negative regulation of hormone biosynthetic process	P05023
32881	3.52E-02	regulation of polysaccharide metabolic process	P62140
32411	3.52E-02	positive regulation of transporter activity	P62158
32414	3.52E-02	positive regulation of ion transmembrane transporter activity	P62158
61083	3.52E-02	regulation of protein refolding	P50502
61084	3.52E-02	negative regulation of protein refolding	P50502
32465	3.52E-02	regulation of cytokinesis	P62158
45989	3.52E-02	positive regulation of striated muscle contraction	P05023
10460	3.52E-02	positive regulation of heart rate	P09493
32020	3.52E-02	ISG15-protein conjugation	Q96LR5
51044	3.52E-02	positive regulation of membrane protein ectodomain proteolysis	O43847
51043	3.52E-02	regulation of membrane protein ectodomain proteolysis	O43847
43255	3.52E-02	regulation of carbohydrate biosynthetic process	P62140
3065	3.52E-02	positive regulation of heart rate by epinephrine	P09493
3062	3.52E-02	regulation of heart rate by chemical signal	P09493
31943	3.52E-02	regulation of glucocorticoid metabolic process	P05023
31946	3.52E-02	regulation of glucocorticoid biosynthetic process	P05023
31947	3.52E-02	negative regulation of glucocorticoid biosynthetic process	P05023
31944	3.52E-02	negative regulation of glucocorticoid metabolic process	P05023
7620	3.52E-02	copulation	P80404
3321	3.52E-02	positive regulation of blood pressure by epinephrine-norepinephrine	P09493
34063	3.52E-02	stress granule assembly	Q14011
60315	3.52E-02	negative regulation of ryanodine-sensitive calcium-release channel activity	P62158
60316	3.52E-02	positive regulation of ryanodine-sensitive calcium-release channel activity	P62158
46885	3.52E-02	regulation of hormone biosynthetic process	P05023
42256	3.52E-02	mature ribosome assembly	P56537
5979	3.52E-02	regulation of glycogen biosynthetic process	P62140
5981	3.52E-02	regulation of glycogen catabolic process	P62140
42267	3.52E-02	natural killer cell mediated cytotoxicity	P68371
42373	3.52E-02	vitamin K metabolic process	P16152
48148	3.52E-02	behavioral response to cocaine	P80404

1909	3.52E-02	leukocyte mediated cytotoxicity	P68371
70873	3.52E-02	regulation of glycogen metabolic process	P62140
1993	3.52E-02	regulation of systemic arterial blood pressure by norepinephrine-epinephrine	P09493
1996	3.52E-02	positive regulation of heart rate by epinephrine-norepinephrine	P09493
55001	3.72E-02	muscle cell development	P09493|O43847
55002	3.72E-02	striated muscle cell development	P09493|O43847
7519	3.72E-02	skeletal muscle tissue development	O43847|P14649
8016	3.72E-02	regulation of heart contraction	P09493|P05023
31327	3.75E-02	negative regulation of cellular biosynthetic process	Q14011|Q13185|P06733|P05023
6950	4.04E-02	response to stress	P52907|Q01085|P203
9890	4.08E-02	negative regulation of biosynthetic process	Q14011|Q13185|P06733|P05023
60538	4.55E-02	skeletal muscle organ development	O43847|P14649

Cellular component

GO-ID	*p*-value	Description	Genes in test set
16529	9.21E-03	sarcoplasmic reticulum	P30626|P11217|O43852
5850	1.02E-02	eukaryotic translation initiation factor 2 complex	Q9BY44|P05198
14069	1.02E-02	postsynaptic density	Q15417|Q9HAP6
16528	1.32E-02	sarcoplasm	P30626|P11217|O43852

GO-ID	*p*-value	Description	Genes in test set
32991	2.84E-03	macromolecular complex	Q01085|P62750|P067
34399	4.07E-03	nuclear periphery	Q9Y281|P52272|P56537
43234	5.70E-03	protein complex	P62140|O75821|P067
44430	1.05E-02	cytoskeletal part	P52907|P09493|Q131
44449	1.65E-02	contractile fiber part	P09493|P06733|P14649|P05976
10494	1.65E-02	stress granule	Q01085|Q14011
16460	1.65E-02	myosin II complex	P14649|P05976
5859	1.65E-02	muscle myosin complex	P14649|P05976
43292	1.85E-02	contractile fiber	P09493|P06733|P14649|P05976
43228	2.06E-02	non-membrane-bounded organelle	Q01085|P62140|P627
43232	2.06E-02	intracellular non-membrane-bounded organelle	Q01085|P62140|P627
16363	2.95E-02	nuclear matrix	Q9Y281|P52272
32059	3.51E-02	bleb	P09493
164	3.51E-02	protein phosphatase type 1 complex	P62140
32144	3.51E-02	4-aminobutyrate transaminase complex	P80404
31618	3.51E-02	nuclear centromeric heterochromatin	Q13185
5719	3.51E-02	nuclear euchromatin	Q13185
791	3.51E-02	euchromatin	Q13185
5638	3.51E-02	lamin filament	P56537
5678	3.51E-02	chromatin assembly complex	P55209
42587	3.51E-02	glycogen granule	P62140
5876	3.51E-02	spindle microtubule	P62158
44422	3.52E-02	organelle part	P62750|Q13185|P067
1726	3.71E-02	ruffle	P20339|P09493

				5856	4.03E-02	cytoskeleton	P52907|P09493|Q9Y2
				35770	4.54E-02	RNA granule	Q01085|Q14011
				30017	4.88E-02	sarcomere	P09493|P06733|P05976
Molecular function							
GO-ID	*p*-value	Description	Genes in test set	GO-ID	*p*-value	Description	Genes in test set
8135	2.88E-03	translation factor activity, nucleic acid binding	P23193|Q9BY44|P62495|P05	30544	1.22E-03	Hsp70 protein binding	P50502|P31948
5246	3.36E-03	calcium channel regulator activity	P30626|P02760	8307	1.14E-02	structural constituent of muscle	P09493|P14649|P05976
4518	6.82E-03	nuclease activity	Q7KZF4|P52758|Q01780|P23	19904	3.19E-02	protein domain specific binding	P52272|P50502|Q13185|P62158
43021	8.90E-03	ribonucleoprotein binding	P61011|Q9BY44|P62495|P05	4090	3.54E-02	carbonyl reductase (NADPH) activity	P16152
16247	9.71E-03	channel regulator activity	P30626|P02760	32554	3.54E-02	purine deoxyribonucleotide binding	P50502
43022	1.70E-02	ribosome binding	Q9BY44|P62495|P05198	32552	3.54E-02	deoxyribonucleotide binding	P50502
5509	1.97E-02	calcium ion binding	P13693|P30626|P20472|P095	32558	3.54E-02	adenyl deoxyribonucleotide binding	P50502
5543	2.12E-02	phospholipid binding	P00480|P09525|Q9UMY4|P0	42296	3.54E-02	ISG15 ligase activity	Q96LR5
8289	2.25E-02	lipid binding	P02689|P00480|P02753|P095	70181	3.54E-02	SSU rRNA binding	Q14011
16597	3.57E-02	amino acid binding	P00480|P00367|P54136	47298	3.54E-02	(S)-3-amino-2-methylpropionate transaminase activity	P80404
19841	4.33E-02	retinol binding	P02753|P09455	32564	3.54E-02	dATP binding	P50502
				50115	3.54E-02	myosin-light-chain-phosphatase activity	P62140
				31432	3.54E-02	titin binding	P62158
				16402	3.54E-02	pristanoyl-CoA oxidase activity	O15254
				16411	3.54E-02	acylglycerol O-acyltransferase activity	Q9NRZ7
				47021	3.54E-02	15-hydroxyprostaglandin dehydrogenase (NADP+) activity	P16152
				32145	3.54E-02	succinate-semialdehyde dehydrogenase binding	P80404
				51021	3.54E-02	GDP-dissociation inhibitor binding	P20339
				43274	3.54E-02	phospholipase binding	P62158
				31997	3.54E-02	N-terminal myristoylation domain binding	P62158
				16208	3.54E-02	AMP binding	P11217
				17018	3.54E-02	myosin phosphatase activity	P62140
				50221	3.54E-02	prostaglandin-E2 9-reductase activity	P16152
				3841	3.54E-02	1-acylglycerol-3-phosphate O-acyltransferase activity	Q9NRZ7
				3869	3.54E-02	4-nitrophenylphosphatase activity	P05023
				3867	3.54E-02	4-aminobutyrate transaminase activity	P80404
				8374	3.54E-02	O-acyltransferase activity	Q9NRZ7
				31072	4.59E-02	heat shock protein binding	P50502|P31948
				166	4.63E-02	nucleotide binding	Q01085|P62750|P522

Table S 14. KEGG pathways, GO Biological Processes, GO Molecular Functions significantly enriched (FDR<0.05) with number of proteins and identification of contributing proteins in the three trial steps: Cooling phase (t1 vs t0), Maintenance phase (t2 vs t1) and Overall (t2 vs t0). Gene ontology analysis was performed with String version 10 (Search Tool for the Retrieval of Interacting Genes/Proteins; http://string-db.org) using the Danio rerio database (Ghisaura et al., 2019).

KEGG PATHWAYS	N. of contributing proteins	FDR	IDs of contributing proteins
Cooling phase (t1 *vs* t0)			
Metabolic pathways	10	2.26E-04	ATP6,COX2,ahcy,ftcd,gapdh,got2a,hpda,lipca,me3,pgm1
Phenylalanine metabolism	2	1.69E-02	got2a,hpda
Carbon metabolism	3	2.18E-02	gapdh,got2a,me3
Ribosome	3	2.18E-02	rpl30,rps28,rpsa
Tyrosine metabolism	2	2.59E-02	got2a,hpda
Microbial metabolism in diverse environments	3	2.96E-02	gapdh,me3,pgm1
Cysteine and methionine metabolism	2	3.00E-02	ahcy,got2a
Maintenance phase (t2 *vs* t1)			
Metabolic pathways	10	2.51E-06	AMDHD1,ahcy,aldh4a1,atp5c1,bhmt,fh,g6pca.2,glud1b,pgk1,tpi1b
Glycolysis / Gluconeogenesis	3	2.32E-03	g6pca.2,pgk1,tpi1b
Carbon metabolism	3	6.40E-03	fh,pgk1,tpi1b
Ribosome	3	6.40E-03	rpl30,rpl6,rps19
Microbial metabolism in diverse environments	3	1.05E-02	fh,pgk1,tpi1b
Alanine, aspartate and glutamate metabolism	2	1.33E-02	aldh4a1,glud1b
Cysteine and methionine metabolism	2	1.33E-02	ahcy,bhmt
Arginine and proline metabolism	2	3.21E-02	aldh4a1,glud1b
Biosynthesis of amino acids	2	4.18E-02	pgk1,tpi1b
Overall (t2 *vs* t0)			
Metabolic pathways	13	6.08E-06	UROC1,ahcy,aldh4a1,fh,ftcd,g6pca.2,glud1b,got2a,hpda,hsd17b12b,me3,tpi1b,zgc:66313
Alanine, aspartate and glutamate metabolism	3	2.47E-03	aldh4a1,glud1b,got2a
Carbon metabolism	4	2.47E-03	fh,got2a,me3,tpi1b
Microbial metabolism in diverse environments	4	5.76E-03	cat,fh,me3,tpi1b
Arginine and proline metabolism	3	6.83E-03	aldh4a1,glud1b,got2a
Phenylalanine metabolism	2	9.60E-03	got2a,hpda
Histidine metabolism	2	2.10E-02	UROC1,ftcd
Tyrosine metabolism	2	2.75E-02	got2a,hpda
Cysteine and methionine metabolism	2	3.38E-02	ahcy,got2a
Starch and sucrose metabolism	2	3.38E-02	g6pca.2,zgc:66313
Pyruvate metabolism	2	3.38E-02	fh,me3

GO Biological processes	N. of contributing proteins	FDR	IDs of contributing proteins
Cooling phase (t1 *vs* t0)			
Single-organism transport	8	2.29E-06	ATP6,COX2,SLC25A24,ba1,hbaa1,ran,rps28,rpsa
rRNA-containing ribonucleoprotein complex export from nucleus	3	1.17E-05	ran,rps28,rpsa
Single-organism process	12	5.87E-05	ATP6,COX2,SLC25A24,ba1,cyp26a1,decr2,hbaa1,hpda,ran,rps28,rpsa,tmx2b
Ribonucleoprotein complex localization	3	5.87E-05	ran,rps28,rpsa
Biological_process	13	1.38E-04	ATP6,COX2,SLC25A24,ba1,cyp26a1,decr2,hbaa1,mt,pin4,ran,rps28,rpsa,tmx2b
Oxidation-reduction process	5	4.15E-04	COX2,cyp26a1,decr2,gapdh,hpda
rRNA export from nucleus	2	4.64E-04	rps28,rpsa
Single-organism intracellular transport	4	7.53E-04	SLC25A24,ran,rps28,rpsa
Cellular process	11	1.03E-03	ATP6,COX2,SLC25A24,decr2,gapdh,hpda,pin4,ran,rps28,rpsa,tmx2b
Organonitrogen compound metabolic process	5	1.05E-03	ATP6,gapdh,hpda,rps28,rpsa
Nucleobase-containing compound transport	3	1.66E-03	SLC25A24,rps28,rpsa
Ribosome biogenesis	3	4.40E-03	ran,rps28,rpsa
Oxygen transport	2	4.44E-03	ba1,hbaa1
Cellular localization	4	7.77E-03	SLC25A24,ran,rps28,rpsa
Small molecule metabolic process	4	9.53E-03	ATP6,decr2,gapdh,hpda
Hydrogen ion transmembrane transport	2	1.07E-02	ATP6,COX2
Single-organism cellular process	8	1.26E-02	ATP6,COX2,SLC25A24,decr2,gapdh,hpda,ran,tmx2b
Organic substance transport	4	1.26E-02	SLC25A24,ran,rps28,rpsa
Ion transmembrane transport	3	1.30E-02	ATP6,COX2,SLC25A24
Cellular metabolic process	8	1.36E-02	ATP6,COX2,decr2,gapdh,hpda,pin4,rps28,rpsa
Response to metal ion	2	1.55E-02	SLC25A24,mt
Carboxylic acid metabolic process	3	2.04E-02	decr2,gapdh,hpda
Metabolic process	8	3.02E-02	ATP6,COX2,cyp26a1,decr2,pin4,ran,rps28,rpsa
ATP metabolic process	2	3.02E-02	ATP6,gapdh
Single-organism metabolic process	5	3.26E-02	ATP6,COX2,cyp26a1,decr2,hpda
RNA localization	2	3.98E-02	rps28,rpsa
Maintenance phase (t2 *vs* t1)			
Carboxylic acid metabolic process	5	2.16E-05	AMDHD1,aldh4a1,bhmt,fh,tpi1b
Dicarboxylic acid metabolic process	3	3.47E-05	AMDHD1,aldh4a1,fh
Glutamate metabolic process	2	5.41E-04	AMDHD1,aldh4a1
Alpha-amino acid metabolic process	3	1.15E-03	AMDHD1,aldh4a1,bhmt
Organic substance catabolic process	4	3.19E-03	AMDHD1,aldh4a1,bhmt,tpi1b
Organonitrogen compound metabolic process	4	7.59E-03	AMDHD1,aldh4a1,bhmt,tpi1b
Single-organism catabolic process	3	1.05E-02	AMDHD1,aldh4a1,tpi1b
Alpha-amino acid catabolic process	2	1.25E-02	AMDHD1,aldh4a1
Alpha-amino acid biosynthetic process	2	1.25E-02	aldh4a1,bhmt

Cellular catabolic process	3	4.03E-02	AMDHD1,aldh4a1,bhmt
Overall (t2 *vs* t0)			
Oxidation-reduction process	8	5.69E-07	aldh4a1,aldh8a1,cat,cyp26a1,decr2,fh,hpda,hsd17b12b
Carboxylic acid metabolic process	6	1.21E-05	aldh4a1,decr2,fh,hpda,hsd17b12b,tpi1b
Single-organism metabolic process	9	7.19E-05	aldh4a1,aldh8a1,cat,cyp26a1,decr2,fh,hpda,hsd17b12b,tpi1b
Biological_process	15	2.06E-04	LOC561322,SLC25A24,aldh4a1,aldh8a1,ba1,cwc27,cyp26a1,decr2,fabp10a,fh,hbaa1,hsd17b12b,rpsa,tmem129,tpi1b
Single-organism process	13	2.34E-04	SLC25A24,aldh4a1,aldh8a1,ba1,cat,cyp26a1,decr2,fh,hbaa1,hpda,hsd17b12b,rpsa,tpi1b
Single-organism catabolic process	4	3.03E-03	aldh4a1,cat,hpda,tpi1b
Metabolic process	11	5.38E-03	aldh4a1,aldh8a1,cat,cwc27,cyp26a1,decr2,fh,hsd17b12b,rpsa,tmem129,tpi1b
Cellular process	12	5.38E-03	LOC561322,SLC25A24,aldh4a1,cat,cwc27,decr2,fh,hpda,hsd17b12b,rpsa,tmem129,tpi1b
Cellular metabolic process	10	8.33E-03	aldh4a1,cat,cwc27,decr2,fh,hpda,hsd17b12b,rpsa,tmem129,tpi1b
Monocarboxylic acid metabolic process	3	1.14E-02	decr2,hsd17b12b,tpi1b
Oxygen transport	2	1.35E-02	ba1,hbaa1
Dicarboxylic acid metabolic process	2	2.21E-02	aldh4a1,fh
Response to oxidative stress	2	3.16E-02	SLC25A24,cat
Primary metabolic process	9	3.16E-02	aldh4a1,cwc27,decr2,fh,hpda,hsd17b12b,rpsa,tmem129,tpi1b
Organic substance metabolic process	9	3.40E-02	aldh4a1,cwc27,decr2,fh,hpda,hsd17b12b,rpsa,tmem129,tpi1b
Alpha-amino acid catabolic process	2	3.77E-02	aldh4a1,hpda
Response to metal ion	2	4.26E-02	SLC25A24,cat

GO Molecular function	N. of contributing proteins	FDR	IDs of contributing proteins
Cooling phase (t1 *vs* t0)			
Molecular_function	13	7.57E-05	ATP6,COX2,SLC25A24,actb1,cyp26a1,decr2,h3f3a,hbaa1,mt,pin4,ran,rps28,rpsa
Substrate-specific transporter activity	5	7.88E-05	ATP6,COX2,SLC25A24,ba1,hbaa1
Binding	11	8.38E-05	COX2,SLC25A24,actb1,ba1,cyp26a1,h3f3a,hbaa1,hpda,mt,pin4,ran
Ion binding	9	8.38E-05	COX2,SLC25A24,actb1,ba1,cyp26a1,hbaa1,hpda,mt,ran
Oxidoreductase activity	5	1.38E-04	COX2,cyp26a1,decr2,gapdh,hpda
Heme binding	3	2.81E-04	ba1,cyp26a1,hbaa1
Iron ion binding	3	4.80E-04	ba1,cyp26a1,hbaa1
Metal ion binding	7	4.80E-04	COX2,SLC25A24,ba1,cyp26a1,hbaa1,hpda,mt

Organic cyclic compound binding	8	4.80E-04	actb1,ba1,cyp26a1,gapdh,h3f3a,hbaa1,pin4,ran
Heterocyclic compound binding	8	4.80E-04	actb1,ba1,cyp26a1,gapdh,h3f3a,hbaa1,pin4,ran
Oxygen transporter activity	2	2.06E-03	ba1,hbaa1
Oxygen binding	2	2.06E-03	ba1,hbaa1
Hydrogen ion transmembrane transporter activity	2	4.62E-03	ATP6,COX2
Ion transmembrane transporter activity	3	5.96E-03	ATP6,COX2,SLC25A24
Transition metal ion binding	4	9.20E-03	COX2,ba1,cyp26a1,hbaa1
Cold maintenance phase (t2 *vs* t1)			
Catalytic activity	6	4.98E-02	AMDHD1,aldh4a1,bhmt,fh,ola1,tpi1b
Overall (t2 *vs* t0)			
Molecular_function	17	6.38E-07	LOC561322,SLC25A24,actb1,actb2,aldh4a1,aldh8a1,cat,cwc27,cyp26a1,decr2,fh,hbaa1,hsd17b12b,krt18,rpsa,tmem129,tpi1b
Oxidoreductase activity	7	1.25E-06	aldh4a1,aldh8a1,cat,cyp26a1,decr2,hpda,hsd17b12b
Heme binding	4	8.05E-06	ba1,cat,cyp26a1,hbaa1
Ion binding	10	9.45E-05	SLC25A24,actb1,actb2,ba1,cat,cyp26a1,fabp10a,hbaa1,hpda,tmem129
Catalytic activity	10	1.06E-04	aldh4a1,aldh8a1,cat,cwc27,cyp26a1,decr2,fh,hsd17b12b,tmem129,tpi1b
Binding	11	7.95E-04	LOC561322,SLC25A24,actb1,actb2,ba1,cat,cyp26a1,fabp10a,hbaa1,hpda,tmem129
Iron ion binding	3	1.75E-03	ba1,cyp26a1,hbaa1
Metal ion binding	7	3.27E-03	SLC25A24,ba1,cat,cyp26a1,hbaa1,hpda,tmem129
Transporter activity	4	3.52E-03	SLC25A24,ba1,fabp10a,hbaa1
Oxygen transporter activity	2	3.52E-03	ba1,hbaa1
Oxidoreductase activity, acting on the aldehyde or oxo group of donors, NAD or NADP as acceptor	2	3.52E-03	aldh4a1,aldh8a1
Oxygen binding	2	3.52E-03	ba1,hbaa1
Organic cyclic compound binding	8	3.52E-03	LOC561322,actb1,actb2,ba1,cat,cyp26a1,fabp10a,hbaa1
Heterocyclic compound binding	7	1.98E-02	LOC561322,actb1,actb2,ba1,cat,cyp26a1,hbaa1
Isomerase activity	2	2.03E-02	cwc27,tpi1b
Substrate-specific transporter activity	3	3.52E-02	SLC25A24,ba1,hbaa1

Table S 15. *Results from peptide mass fingerprinting of protein spots excised from the 2DE gels (Martin, Vilhelmsson, Médale, et al., 2003).*

Reference spot	p*I*	kDa	Identities by MS-Fit followed by BLASTx					Identities by Mascot			
			Salmonid sequence	MS-Fit Mowse score	Protein	Species identified	Accession no.	Protein	Species identified	Accession no.	Mascot score
60[C]	4.9	85	BG933954	1.4×10^{-4}	HSP108	*Salmo salar*	AF387865	HSP108	*Gallus gallus*	AF387865	201
115[C]	6.8	67	CA343417	1.6×10^{5}	Transketolase	*Xenopus laevis*	AAF67194	*N*-ethylmaleimide-sensitive factor	*Homo sapiens*	15314649	82
120[C]	5.5	66	BX081803	2.3×10^{5}	HSP70	*Oncorhynchus mykiss*	P08108	HSP70	*Oncorhynchus mykiss*		108
123[C]	5.6	66	CA044261	4.6×10^{4}	HSP70	*Oncorhynchus mykiss*	P08108	HSP70	*Xiphophorus maculatus*		115
160[C]	5.7	59	AJ295231	1.3×10^{4}	Nitric oxide synthase	*Oncorhynchus mykiss*	CAC82808				
183[C]	5.7	55	AJ272373	3.0×10^{10}	Simple type II Keratin k8	*Oncorhynchus mykiss*	CAC45060	Simple type II Keratin k8	*Oncorhynchus mykiss*	CAC45060	88
194[C]	6.8	54	CA375586	3.3×10^{5}	Selenium binding protein 2	*Rattus norvegicus*	NP_543168	Occludin-like protein	*Drosophila melanogaster*		81
197[S]	4.8	53	CA386490	7.5×10^{3}	HSP108	*Xenopus laevis*	AAO21339	HSP108	*Gallus gallus*	AF387865	193
201[C]	5.2	52	CA350990	8.6×10^{7}	Beta tubulin	*Notothenia coriiceps*	AAG15317	Beta tubulin	*Haliotis discus*		95
214[C]	6.9	51	BX080834	3.5×10^{3}	Adenosylhomocysteinase 2	*Xenopus laevis*	O93477	Adenosylhomocysteinase 2	*Xenopus laevis*	O93477	85
249[C]	6.7	47	CA363453	6.6×10^{7}	Homogentisate 1,2-dioxygenase	*Mus musculus*	XP_147229	–	–		
269[C]	6.5	45	BG934321	6.4×10^{7}	Phosphogluconate dehydrogenase	*Homo sapiens*	AAH00368	–	–		
321[C]	6.8	39			–	–		–	–		
370[S]	5.6	36	CA039103	5.0×10^{4}	Hypothetical ORF	*Saccharomyces cerevisiae*	NP_014422	Protein Phosphatase 2A catalytic chain	*Xenopus laevis*		114

393^{C}	5.5	33						Apo A I-1	*Oncorhynchus mykiss*	AAB96972	148
399^{SBM}	6.8	33	AF067796	4.8×10^{4}	Aldolase B	*Salmo salar*	AAD11573	Aldolase B	*Salmo salar*	AAD11573	82
330^{SBM}	6.2	30	BG933866	2.5×10^{-3}	–	–		–	–		
473^{FM}	6.4	28	BX076136	2.5×10^{4}	Hypoxanthine guanine phosphoribosyl transferase	*Gallus gallus*	AJ697	Hypoxanthine guanine phosphoribosyl transferase	*Homo sapiens*		75
485	5.4	25	BX074107	2.8×10^{4}	Apo A I-1	*Oncorhynchus mykiss*	AAB96972				
487	5.3	25	CA386629	1.6×10^{7}	Apo A I-2	*Oncorhynchus mykiss*	AAB96973	Apo A I-2	*Oncorhynchus mykiss*	AAB96973	87
553^{SBM}	5.4	17			–	–		–	–		
634^{SBM}	4.8	42			–	–		Glucose regulated protein precursor (GRP 78)	*Gallus gallus*	Q90593	447
681^{FM}	5.9	57	CA361952	1.0×10^{5}	Pyruvate kinase	*Takifugu rubripes*	BAC02918	–	–		

The superscript following the reference spot number indicates if the spot is increased in abundance after being fed the diet. Using MS-Fit, if unannotated cDNA sequences were identified, this sequence was used to search GenBank using BLASTx to show the protein the cDNA encodes, if a significant hit is obtained. All digests were also searched using Mascot search program. (–) indicates no homology for this protein. ^{C} and ^{S} indicate which diet the protein is more abundan.

Table S 16. Protein identification of liver proteins in gilthead seabream (Schrama et al., 2018) .

Metabolism	Spot	Uniprot/NCBI	Protein name	Score	Mw T/C	pI T/C	Peptides	Coverage (%)	ANOVA	Tukey's Test (*q* value)	Fold change	Expression
Immune system	246	F8U094	Warm temperature acclimation like protein Fragment OS *Epinephelus bruneus*	990	42,159/64,966	5.46/4.8	4	7	0.001	0.0001	2.08	CTRL>CR5 > CR2>CR8
	274	F2YLA1	Transferrin OS *Sparus aurata*	31,467	74,234/63,269	5.88/5.7	36	44	0.0008	0.0004	1.62	CTRL>CR2 > CR8>CR5
	280	F2YLA1	Transferrin OS *Sparus aurata*	47,042	74,234/63,269	5.88/5.8	59	69	0.02	0.0207	1.57	CTRL>CR2 > CR8>CR5
	285	C0L788	Warm temperature acclimation related 65 kDa protein OS *Sparus aurata*	8,120	49,126/62,438	5.34/4.9	7	16	0.0006	0.0001	2.55	CTRL>CR2 > CR8>CR5
	290	C0L788	Warm temperature acclimation related 65 kDa protein OS *Sparus aurata*	11,826	49,126/61,617	5.34/4.9	12	24	0.0003	0.0000	1.94	CTRL>CR2 > CR5>CR8
	293	F8U094	Warm temperature acclimation like protein Fragment OS *Epinephelus bruneus*	2,250	42,159/62,438	5.46/4.9	8	11	0.001	0.0005	2.06	CTRL>CR2 > CR8>CR5
	339	A0FJG5	Fibrinogen beta chain OS *Larimichthys crocea*	1,013	55,585/60,807	5.89/5.2	4	8	0.002	0.0012	1.88	CTRL>CR2 > CR8>CR5
	346	A0FJG5	Fibrinogen beta chain OS *Larimichthys crocea*	978	55,585/60,008	5.89/5.3	6	9	0.002	0.0016	1.57	CTRL>CR8 > CR2>CR5

	795	Q7ZU45	Tetratricopeptide repeat protein 25 OS *Danio rerio*	134	55,545/36,781	8.70/5.1	1	2	0.002	0.0043	2.08	CR5>CR8>CR2>CTRL
Cell process/stress response	256	Q9I8F9	Heat shock 70 kDa protein 1 OS *Oryzias latipes*	1,382	70,307/63,269	5.31/4.9	2	4	0.0009	0.0034	1.72	CR5>CR2>CTRL>CR8
	296	Q90473	Heat shock cognate 71 kDa protein OS *Danio rerio* GN hspa8	266	70,930/61,617	4.99/5.0	3	6	0.03	0.0356	1.28	CR5>CR2>CR8>CTRL
	499	Q6P3H7	Histone binding protein RBBP4 OS *Danio rerio*	946	47,621/53,272	4.56/4.7	6	30	0.002	0.0015	1.42	CTRL>CR5>CR8>CR2
	514	Q0GYP4	Trypsinogen II OS *Sparus aurata*	18,962	26,240/51,881	4.98/4.8	16	49	0.016	0.0088	1.48	CTRL>CR2>CR8>CR5
	714	G3PT17	Uncharacterized protein OS *Gasterosteus aculeatus* PE 4 SV 1 [after blast on 28-04-2017 26S proteasome non-ATPase regulatory subunit 13 (*Anoplopoma fimbria*)]	2,099	43,327/41,432	5.95/5.6	14	26	0.045	0.0369	1.17	CR8>CR2>CR5>CTRL
	856	C3KGT8	Coatomer subunit epsilon OS *Anoplopoma fimbria*	2,111	34,041/33,528	4.75/4.9	10	23	0.026	0.0427	1.32	CR8>CR2>CR5>CTRL
	967	M4AWP5	Chloride intracellular channel protein [*Xiphophorus maculatus*]	327	28,409/28,988	5.84/5.3	6	30	0.044	0.0399	1.46	CR8>CR5>CR2>CTRL
	998	Q4QY74	Chymotrypsin B like protein Fragment OS *Sparus aurata*	646	23,818/27,132	7.03/5.7	5	28	0.003	0.0061	3.25	CR8>CR2>CR5>CTRL
	1,011	Q98TJ6	Glutathione S transferase Fragment OS *Platichthys flesus*	6,467	14,570/26,077	5.65/5.6	9	28	0.049	0.0247	2.63	CR2>CR8>CR5>CTRL

	1,105	G3Q5U8	Uncharacterized protein Fragment OS *Gasterosteus aculeatus* [after blast on 28-04-2017 Peroxiredoxin-1 (*Anoplopoma fimbria*)]	523	22,120/20,014	6.6/5.2	5	29	0.047	0.0278	1.27	CR5>CR2> CTRL>CR8
	1,281	F1QSJ0	Cytidine deaminase OS *Danio rerio*	3,713	14,325/10,891	7.55/5.2	2	17	0.018	0.0238	1.58	CR8>CR2> CTRL>CR5
Cytoskeleton	517	P48677	Glial fibrillary acidic protein Fragment OS *Carassius auratus*	426	42,578/51,200	4.73/4.8	1	3	0.002	0.0020	1.93	CTRL>CR2 > CR8>CR5
	526	B5DGQ7	Beta enolase OS *Salmo salar*	972	47,257/49,207	6.65/5.9	3	8	0.015	0.0103	1.44	CTRL>CR2 > CR8>CR5
	541	P18520	Intermediate filament protein ON3 OS *Carassius auratus*	1,416	57,753/49,207	4.95/4.9	16	23	0.023	0.0369	1.43	CR5>CR2> CTRL>CR8
	590	Q6NWF6	Keratin type II cytoskeletal 8 OS *Danio rerio*	3,453	57,723/47,292	4.94/4.9	19	28	0.015	0.0403	1.67	CR5>CR8> CR2>CTRL
	914	Q7T3F0	Tropomyosin 4 OS *Danio rerio*	770	28,484/30,161	4.43/4.5	10	26	0.015	0.0178	1.53	CTRL>CR2 > CR5>CR8
	915	P13104	Tropomyosin poa 1 chain OS *Danio rerio*	1,828	32,702/30,970	4.5/4.6	7	11	0.048	0.0426	1.21	CR8>CR2> CR5>CTRL
	992	P48677	Glial fibrillary acidic protein Fragment OS *Carassius auratus*	176	42,578/27,132	4.73/6.0	1	3	0.03	0.0494	1.14	CR8>CR2> CTRL>CR5
	1,072	W5N831	Uncharacterized protein OS *Lepisosteus oculatus* [after blast on 28-04-2017 Keratin, type I	327	88,937/21,668	4.67/4.6	5	4	0.003	0.0023	1.78	CTRL>CR2 > CR8>CR5

			cytoskeletal 19 (*Alligator mississippiensis*)]									
	1,298	P80972	Cytochrome c oxidase subunit 5A 1 mitochondrial Fragment OS *Thunnus obesus*	5,414	2,402/10,329	4.28/4.9	1	50	0.007	0.0097	1.53	CTRL>CR5 > CR8>CR2
Lipid metabolism	1,018	O42175	Apolipoprotein A I OS *Sparus aurata*	22,152	29,615/26,077	5.03/5.0	31	68	0.004	0.0058	1.79	CTRL>CR5 > CR2>CR8
	1,023	O42175	Apolipoprotein A I OS *Sparus aurata*	28,332	29,615/25,396	5.03/4.9	59	70	0.003	0.0081	2.12	CTRL>CR8 > CR2>CR5
	1,047	Q5KSU1	Apolipoprotein A IV4 OS *Takifugu rubripes*	2,047	28,474/25,734	4.59/4.6	4	12	0.039	0.0278	1.8	CTRL>CR2 > CR8>CR5
	1,309	Q4QY86	Putative uncharacterized protein OS *Sparus aurata* [after blast on 28-04-2017 14 kDa apolipoprotein (*Epinephelus bruneus*)]	12,510	15,857/9,797	5.03/4.8	9	48	0.006	0.0137	2.19	CTRL>CR8 > CR2>CR5
Metabolic pathway	623	Q66I24	Argininosuccinate synthase OS *Danio rerio*	504	47,099/46,671	6.46/5.5	5	7	0.01	0.0112	1.32	CR5>CR2> CR8>CTRL
	1,013	Q1MTI4	Triosephosphate isomerase A OS *Danio rerio*	2,170	26,836/26,776	4.72/4.7	6	25	0.002	0.0023	2.03	CR2>CR5> CR8>CTRL
	1,214	G3PDP5	Uncharacterized protein OS *Gasterosteus aculeatus* [after blast on 28-04-2017 bifunctional protein GlmU-like (*Salmo salar*)]	1,661	15,732/13,637	5.34/5.0	1	9	0.016	0.0462	1.73	CR8>CR2> CR5>CTRL